Matti Pajari

Prestressed hollow core slabs supported on beams

Finnish shear tests on floors in 1990–2006

ISBN 978-951-38-7495-7 (URL: http://www.vtt.fi/publications/index.jsp)
ISSN 1459-7683 (URL: http://www.vtt.fi/publications/index.jsp)

JULKAISIJA – UTGIVARE – PUBLISHER

VTT, Vuorimiehentie 5, PL 1000, 02044 VTT
puh. vaihde 020 722 111, faksi 020 722 4374

VTT, Bergsmansvägen 5, PB 1000, 02044 VTT
tel. växel 020 722 111, fax 020 722 4374

VTT Technical Research Centre of Finland, Vuorimiehentie 5, P.O. Box 1000, FI-02044 VTT, Finland
phone internat. +358 20 722 111, fax +358 20 722 4374

Series title, number and report code of publication

VTT Working Papers 148
VTT-WORK-148

Author(s)
Matti Pajari

Title

Prestressed hollow core slabs supported on beams
Finnish shear tests on floors in 1990–2006

Abstract

Arrangements and results of 20 full-scale load tests on floors, each made of eight to twelve prestressed hollow core slabs and three beams, are presented. The tests have been carried out by VTT Technical Research Centre of Finland and Tampere University of Technology.

ISBN
978-951-38-7495-7 (URL: http://www.vtt.fi/publications/index.jsp)

Series title and ISSN		Project number
VTT Working Papers 1459-7683 (URL: http://www.vtt.fi/publications/index.jsp)		
Date November 2010	Language English	Pages 674 p.
Name of project Querkraftfähigkeit von Spannbeton-Fertigdecken bei biegeweicher Lagerung	Commissioned by Institut für Massivbau der RWTH Aachen	
Keywords Prestress, hollow core slab, flexible support, shear resistance, floor test, composite construction, concrete	Publisher VTT Technical Research Centre of Finland P.O. Box 1000, FI-02044 VTT, Finland Phone internat. +358 20 722 4520 Fax +358 20 722 4374	

Preface

The reduction of the shear resistance of hollow core slabs due to deflection of the supporting beams has been studied since 1990. Despite numerous tests, theoretical and numerical analyses and international cooperation, no common European understanding about the reasons of and solutions for this phenomenon has been achieved. A German research project "*Querkrafttragfähigkeit von Spannbeton-Fertigdecken bei biegeweicher Lagerung*", recently completed at Institut für Massivbau, Rheinisch-Westfälische Technische Hochschule, Aachen, aimed to be a step to that direction. The present report has been elaborated as a part of this project.

All reported tests have been performed in confidential projects and commissions. The owners of the results mentioned in the report have permitted the publication of all relevant data and paid the costs of the information service, which is gratefully acknowledged.

The work has financially been supported by the research team in Aachen, i.e. Prof. Hegger, Dr. Roggendorf and their coworkers. Without their contribution it would not have been possible to realise the work. Special thanks are due to them for their patience in waiting for the completion of the report and for the kind and encouraging atmosphere before, during and after the project.

Contents

Meaning of abbreviations

VTT	Technical Research Centre of Finland
TUT	Tampere University of Technology
PC	Prestressed concrete beam
RC	Reinforced concrete beam
S	Steel beam
CP	Composite, prestressed beam
CR	Composite reinforced beam
WQ	Top-hat steel beam
InvT	Inverted T-beam (concrete)
Rect	Rectangular beam (concrete)
A-beam, Delta, MEK, LB, LBL, Super	Patented composite beams
Unif	Uniformly distributed load over half floor
Topp	Reinforced concrete topping
Norm	Normal support (slabs on the top of the beam)
Cont	Continuous beam

1. Introduction

The effect of flexible supports, i.e. reduction of the shear resistance of the hollow core slabs due to deflection of the supporting beams, has been experimentally studied since 1990. The results and analysis of ten tests carried out by VTT, Finland, have been published previously. Due to these tests and parallel tests performed elsewhere it has become clear that the reduction of the shear resistance has to be taken into account in design.

European standard EN 1168. *Precast concrete products. Hollow core slabs* has been amended by a sentence stating that the effect of flexible supports on the shear resistance shall be taken into account. How this can be done, is not specified. Therefore, national design rules, if any, are applied to meet this requirement. It is obvious that a European design method has to be developed, but this is not only a question of standardisation; research is also needed.

In 2005, a research project dealing with the effects of flexible supports was started at RWTH, Aachen. New floor tests were performed, but the results of the former Finnish and German tests were also considered. As a part of the project, the test arrangements and results of twenty Finnish floor tests in 1990–2006 have been elaborated and published in this report. The aim has been to provide experimental data which can be referred to when writing scientific papers or when developing and standardizing European design rules. No analysis of the results is presented. The aim has also been to make the data so complete that there is no need to read the original test reports, five of which have been written in Finnish. Some tabulated characteristics of the tests are given on the first page. The rest of the report is divided in 20 Chapters, each including the results on one floor test and the related reference tests.

The German test results are available at

http://www.imb.rwth-aachen.de/Weitere-Informationen/
(Titel „Zum Tragverhalten von Spannbeton-Fertigdecken bei biegeweicher Lagerung“)

2. Summary

Basic data about the tests are given in Table 1.

Table 1. Thickness of slabs (h_{slab}), length of core filling (L_{fill}), span of beams (L), length of slabs (L_{slab}), shear resistance / one slab in floor test (V_{obs}), mean of shear resistances observed in reference tests (V_{ref}) and last measured deflection of the middle beam before failure (δ).

Test	h_{slab} mm	L_{fill} mm	L m	L_{slab} m	V_{obs} kN	V_{ref} kN	$\frac{V_{obs}}{V_{ref}}$	δ [1] mm	L/δ
VTT.CR.Delta.265.1990	265	50	5,0	6,0	114,6	283,9	0,40	16,3	307
VTT.S.WQ.265.1990	265	50	5,0	6,0	166,1	230,5	0,72	17,6	284
VTT.PC.InvT.265.1990	265	50	5,0	6,0	103,4	230,5	0,45	9,9	505
VTT.PC.InvT.400.1992	400	**320**	5,0	7,2	252,1	490,3	0,51	5,4 [2]	926
VTT.S.WQ.400.1992	400	30	5,0	7,2	293,6	516,3	0,57	14,6	342
VTT.PC.InvT-Unif.265.1993	265	**185**	5,0	6,0	147,6	251,8	0,59	39	128
VTT.PC.InvT-Topp.265.1993	265	50	5,0	6,0	140,3	193,6	0,72	13,8	362
VTT.PC.Rect-Norm.265.1993	265	50	5,0	6,0	163,8	210,9	0,78	7,7	649
VTT.PC.InvT-Cont.265.1994	265	50	5,0	6,0	191,4	194,6	0,98	5,2	962
TUT.CR.MEK.265.1994	265	50	5,02	6,0	148,2	223,2	0,66	16,7	301
VTT.RC.Rect-Norm.265.1994	265	50	7,2	6,0	106,7	226,2	0,47	30,3	238
VTT.CP.LBL.320.1998	320	50	5,0	7,2	161,9	295,3	0,55	20,9	240
VTT.CR.Delta.400.1999	400	50	5,0	8,4	222,0	419,5	0,53	24	208
VTT.CP.Super.320.2002	320	**250**	4,8	9,6	127,5	242,8	0,53	17,5	274
TUT.CP.LB.320.2002	320	50	4,8	7,2	149,2	313,3	0,48	21,3	225
VTT.S.WQ.500.2005	500	**400**	7,2	10,0	269,6	650,7	0,41	21,2	340
VTT.PC.InvT.500.2005	500	**400**	7,2	10,0	336,4	547,1	0,61	21,8	330
VTT.CR.Delta.500.2005	500	**400**	7,2	10,0	366,9	529,4	0,69	25,7	280
VTT.PC.InvT.400.2006	400	50	4,8	9,0	282,4	332,7	0,85	6,2	774
VTT.CR.A-beam.320.2006	320	50	4,8	8,0	183,3	284,0	0,65	20,9	230

[1] Last measured deflection before failure
[2] Deflection at failure > 5,4 mm and < 7,2 mm

3. Shear tests on floors

1	**General information**
1.1 Identification and aim	**VTT.CR.Delta.265.1990** **Last update 2.11.2010** **DE265** (Internal identification) Aim of the test: To test the interaction between Delta beam and hollow core slabs.
1.2 Test type	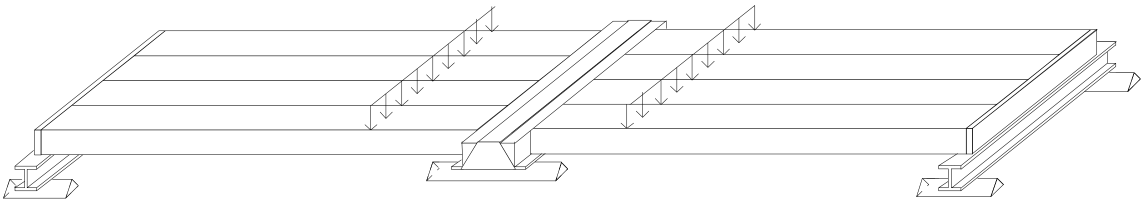 *Fig. 1. Illustration of test setup. Delta beam in the middle, steel I-beams at the ends.*
1.3 Laboratory & date of test	VTT/FI 6.9.1990
1.4 Test report (in Finnish)	Author(s): Koukkari, H. Name: *Deltapalkin ja ontelolaataston koekuormitus (Load test on Delta beam and hollow core floor) (in Finnish)* Ref. number: RAT01814/90 Date: 17.9.1990 Availability: Confidential, owner is Peikko Group Oy, P.O. Box 104, FI-15101 Lahti, Finland
2	**Test specimen and loading**
2.1 General plan	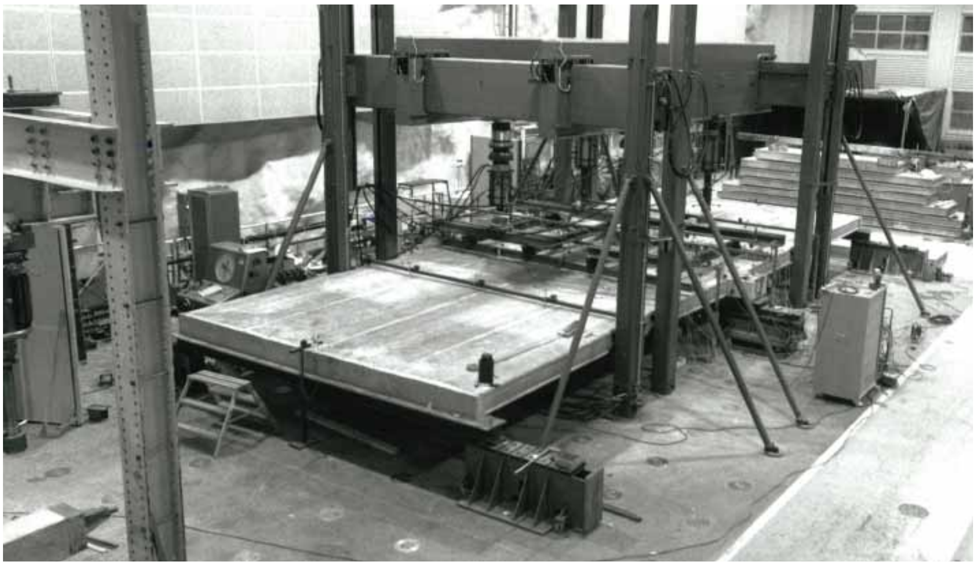 *Fig. 2. View on test arrangements.*

<table>
<tr>
<td></td>
<td>

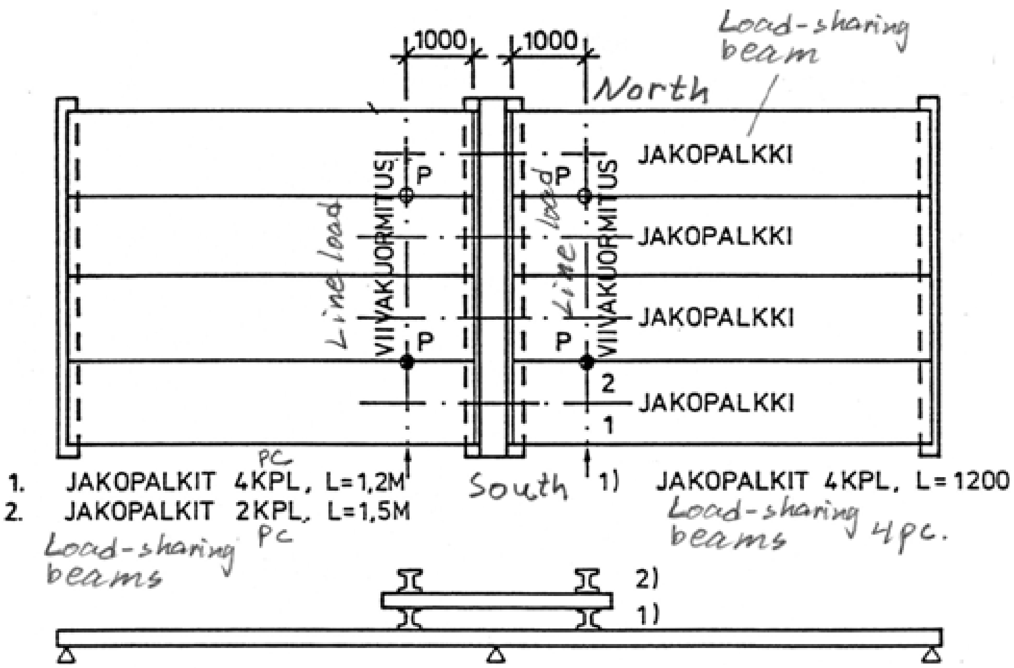

Fig. 3. Plan. Beams 1) were 1,2 m long cuts of railway rails, There was a small gap between the ends of consecutive cuts. The beams between beams 1) and 2) were also cuts of railway rails. Beams 2) were 1,5 m long steel I-profiles. Measures to eliminate the friction between the stacking steel beams were considered unnecessary.

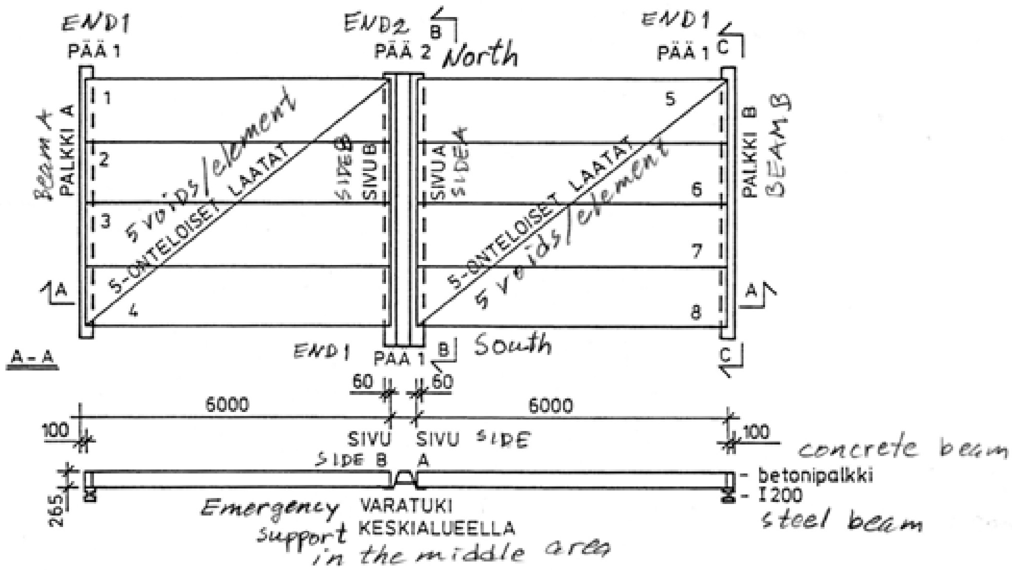

Fig. 4. Plan and section A-A.

</td>
</tr>
<tr>
<td>

2.2
End beams

</td>
<td>

HE 200 B

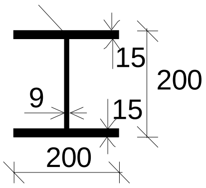

Fig. 5. End beam.

</td>
</tr>
</table>

2.3
Middle beam

The middle beam, see Figs 6–8, comprised
- a prefabricated steel component made of a top plate, bottom plate and two folded and perforated web plates
- a cast-in-situ part of concrete K30 which filled the empty space between the slab ends laying on the ledges of the web plates.

The concrete was cast by VTT in laboratory, 24.8.1990.

Structural steel: Raex, see 9.1

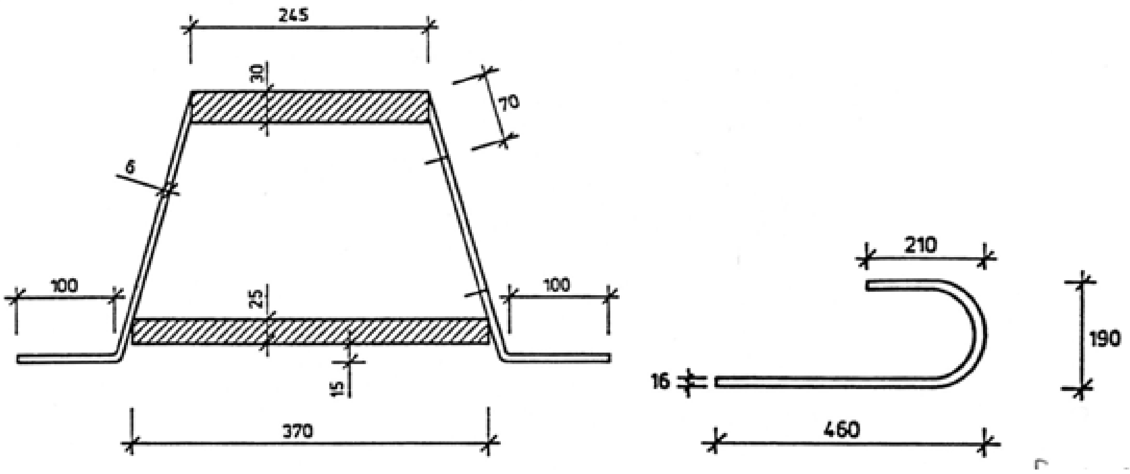

Fig. 6. Middle beam. Cross-section and tie reinforcement (hooks made of rebars T16) for anchoring of slabs to the beam. Depth of beam = 265 mm + 6 mm.

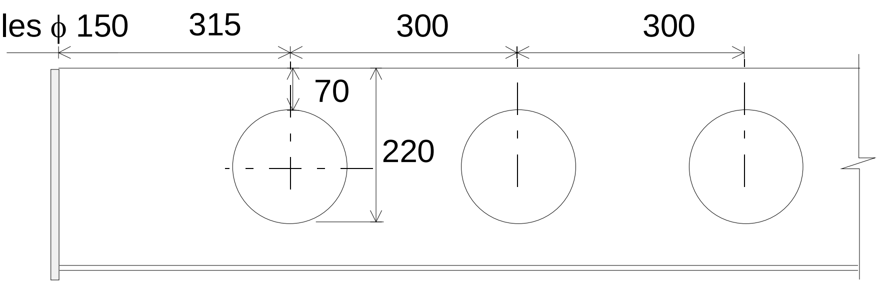

Fig. 7. Middle beam. Position of holes in the webs. South end.

2.4
Arrangements at middle beam

- Simply supported, span = 5,0 m
- Note the nonsymmetric position of the beam with respect to the supports (Fig. 7). Such a displacement was necessary because there was no web hole in the mid-point of the beam. The tie reinforcement had to be anchored both to the longitudinal joints between adjacent hollow core units and to the beam through the web holes.

Tie reinforcement:
- perpendicular to the beam: 3x(1+1) hooks T16 of the type shown in Fig. 6, anchored to the longitudinal joints of the slabs and inside the beam
- parallel to the beam: In the cast-in-situ concrete, parallel to the Delta beam and between the edges of the beam and the slab ends, there were two straight rebars T8, 4,75 m long, one on each side of the beam, see Fig. 8.

<table>
<tr>
<td></td>
<td>
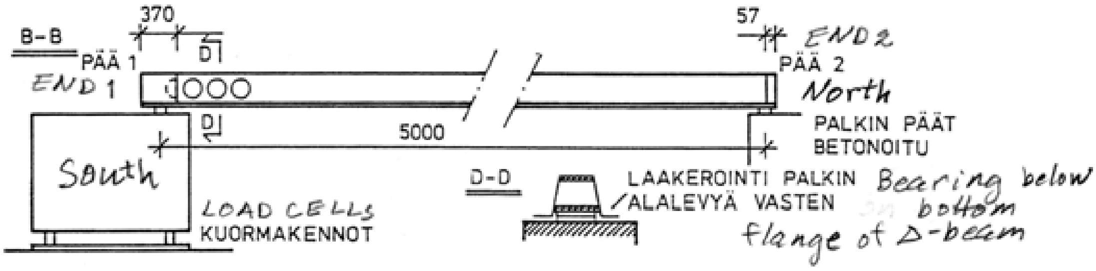

Fig. 8. Middle beam. One end of the Delta beam was free to move in beam’s direction.

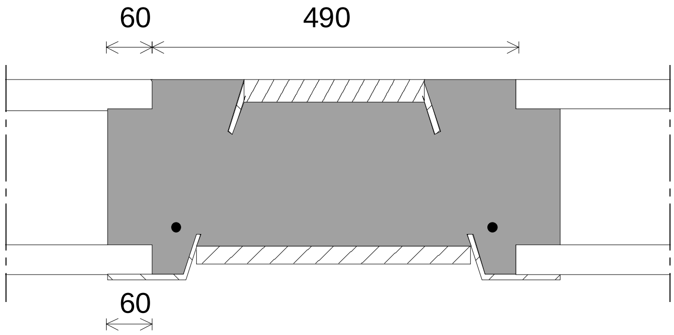

Fig. 9. Cast-in-situ concrete within and outside middle beam. Note the tie bars T8.
</td>
</tr>
<tr>
<td>2.5
Slabs</td>
<td>
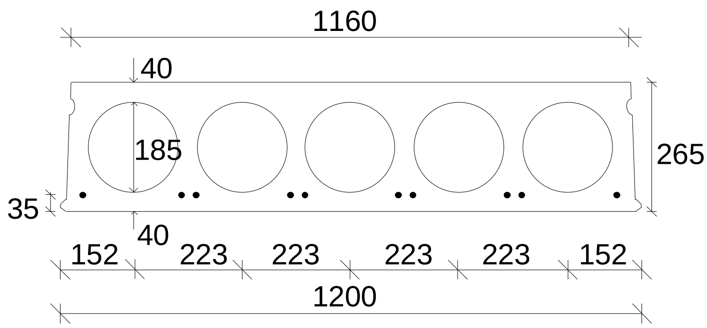

Fig. 10. Nominal geometry of slab units.

- Extruded by Partek Oy, Nastola factory, grade of concrete K60
- 10 lower strands J12,5 initial prestress 1100 MPa

J12,5: seven indented wires, ϕ =12,5 mm, A_p = 93 mm^{2}m see 9.1 for the strength.
</td>
</tr>
<tr>
<td>2.6
Temporary supports</td>
<td>No temporary supports below beams.</td>
</tr>
<tr>
<td>2.7
Loading arrangements</td>
<td>See Fig. 11. There was a gypsum layer between the tertiary beams and the top surface of the slabs. The primary spreader beams were in direct contact with the secondary spreader beams and the secondary beams with the tertiary spreader beams. No attempts were made to eliminate the friction. For this reason it is difficult to evaluate exactly, to which extent the spreader beams participated to the load-carrying mechanism.</td>
</tr>
</table>

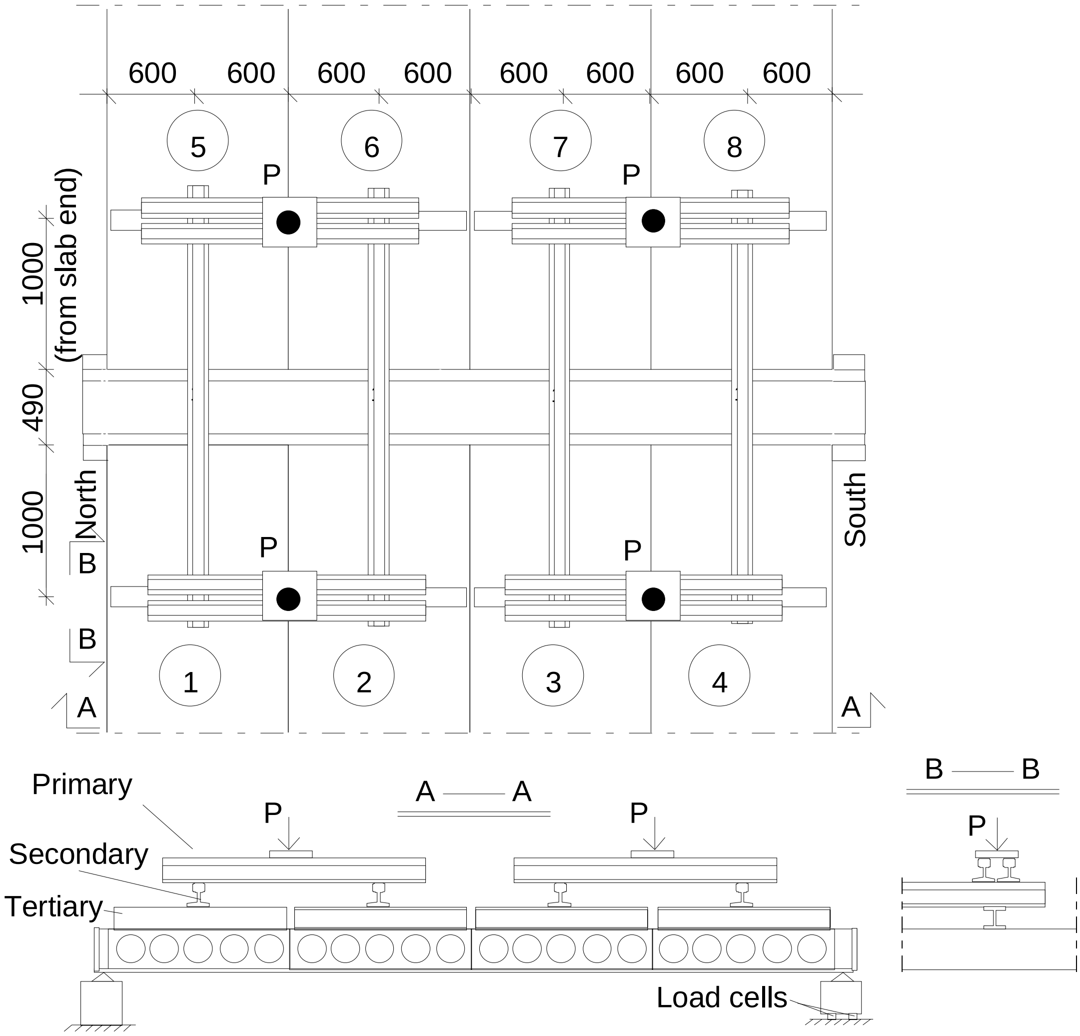

Fig. 11. Loading arrangement with three layers of spreader beams.

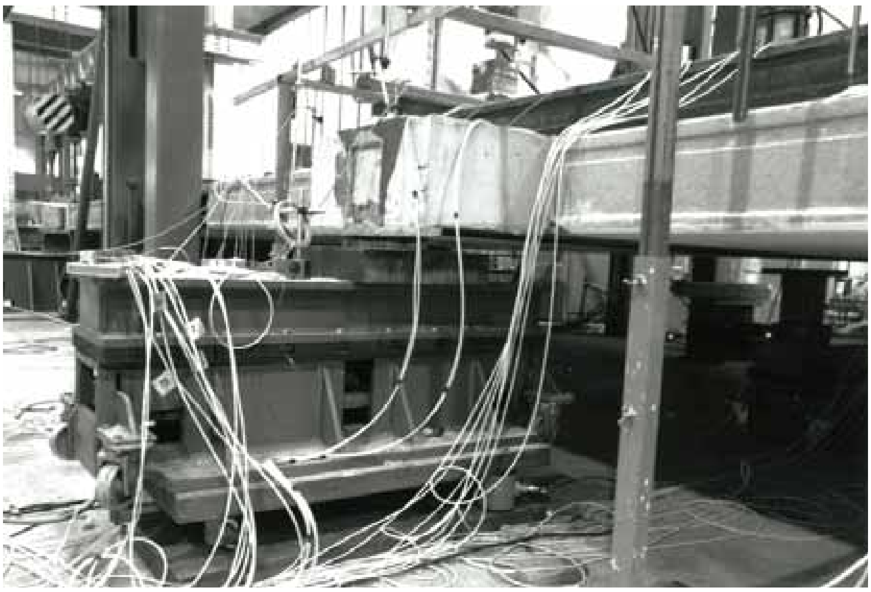

Fig. 12. Arrangements at South end of Delta beam.

3	**Measurements**
3.1 Support reactions	The support reaction of the middle beam due to the actuator loads 4*P* was measured by load cells below the South end of the middle beam. See Figs 8 and 11. Due to the eccentric position of the concrete slabs with respect to the supports of the middle beam, the support reaction below the North end was roughly = 1,08 times the support reaction below the South end where the reaction was measured.
3.2 Vertical displacement	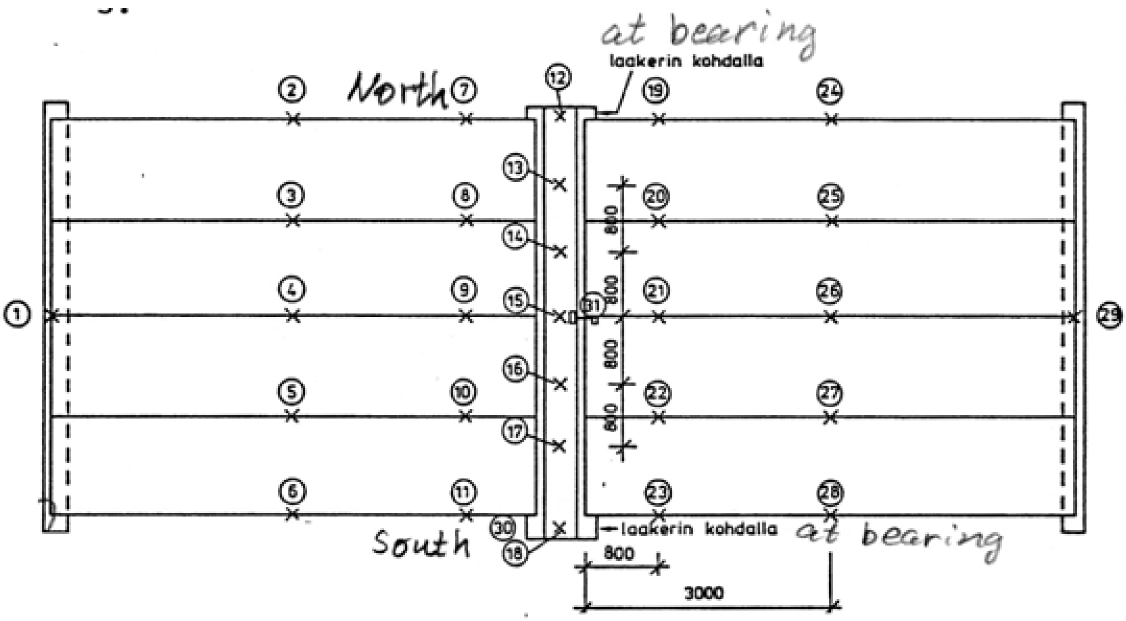 *Fig. 13. Location of transducers 1 … 29 for measuring vertical deflection as well as the location of transducers 30 (measuring differential horizontal displacement between slab edge and Delta beam) and 31 (measuring vertical diff. displacement between slab end and middle beam).*
3.3 Average strain	Not measured
3.4 Horizontal. displacements	*See Fig. 13 for the only horizontal transducer 30.*
3.5 Strain	There were strain gauges for measuring the steel strain in the Delta beam, both parallel to the beam and in transverse direction at the bottom surface of the ledges. Two strain gauges were glued to the top surface of the top plate and two to the bottom surface of the bottom plate, all four parallel to the beam. The soffit and top surface of the hollow core slabs were also provided with strain gauges in order to measure the strain parallel to the Delta beam. The position of all strain gauges is given in Fig. 14.

<table>
<tr><td></td><td>
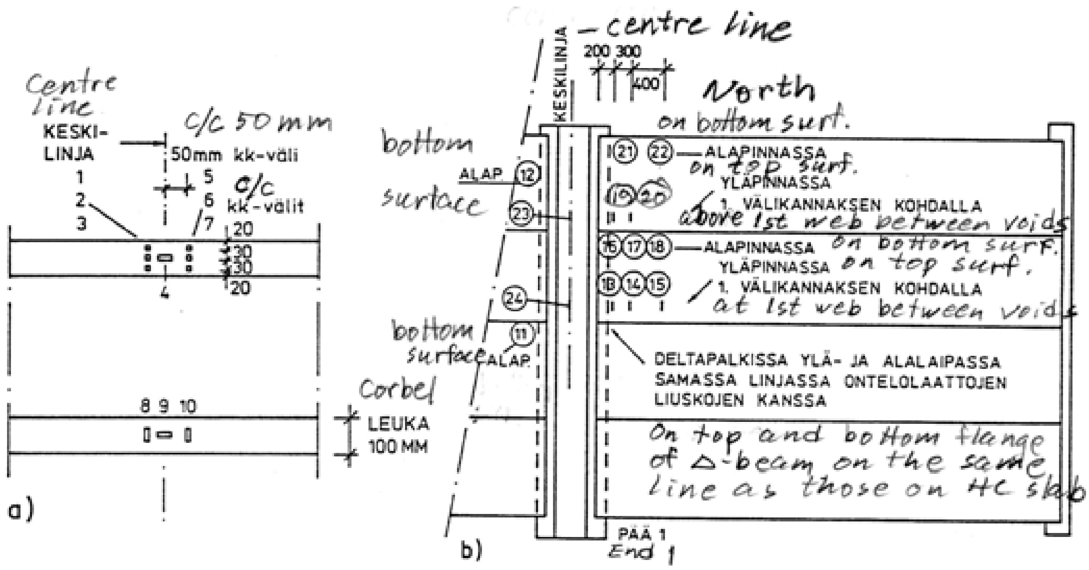

Fig. 14. Position of strain gauges. a) Bottom surface of the ledges of Delta beam, gauges 1–10. b) On the bottom and top flange of Delta beam (gauges 11, 12, 23 and 24) and on the hollow core slabs (13–22).
</td></tr>
<tr><td>4</td><td>Special arrangements

-</td></tr>
<tr><td>5</td><td>Loading strategy</td></tr>
<tr><td>5.1
Load-time relationship</td><td>Before starting the test, all measuring devices were zero-balanced. Thereafter, the actuator loads P were cyclically varied in such a way that three cycles of the type 0 → 43,2 kN → 0 were followed by two cycles of the type 0 → 86,4 kN → 0 (Stage I) wherafter P was monotonously increased to failure (Stage II).</td></tr>
<tr><td>5.2
After failure</td><td></td></tr>
<tr><td>6</td><td>Observations during loading
<table>
<tr><td>Stage I</td><td>At P = 38,8 kN longitudinal cracks appeared in the joint concrete along the Delta beam close to the supports of the beam. The cracks grew both in length and width with increasing load.</td></tr>
<tr><td>Stage II</td><td>At P = 210 kN, the first inclined crack appeared at the edge of slab 4 near the support. Before failure there was an inclined crack at the outermost edge of slabs 1, 4, 5 and 8. At P = 240 kN slab 1 failed along an inclined crack as shown in Fig. 17. This was followed by the failure of all slabs on the same side of the Delta beam. The failure patterns are illustrated in Figs 15–22.</td></tr>
<tr><td>After failure</td><td></td></tr>
</table>
</td></tr>
<tr><td>7</td><td>Cracks in concrete

In the following figures, the numbers refer to the value of the actuator loads P in kN.</td></tr>
<tr><td>7.1
Cracks at service load</td><td>See Fig. 15.</td></tr>
</table>

7.2 Cracks after failure	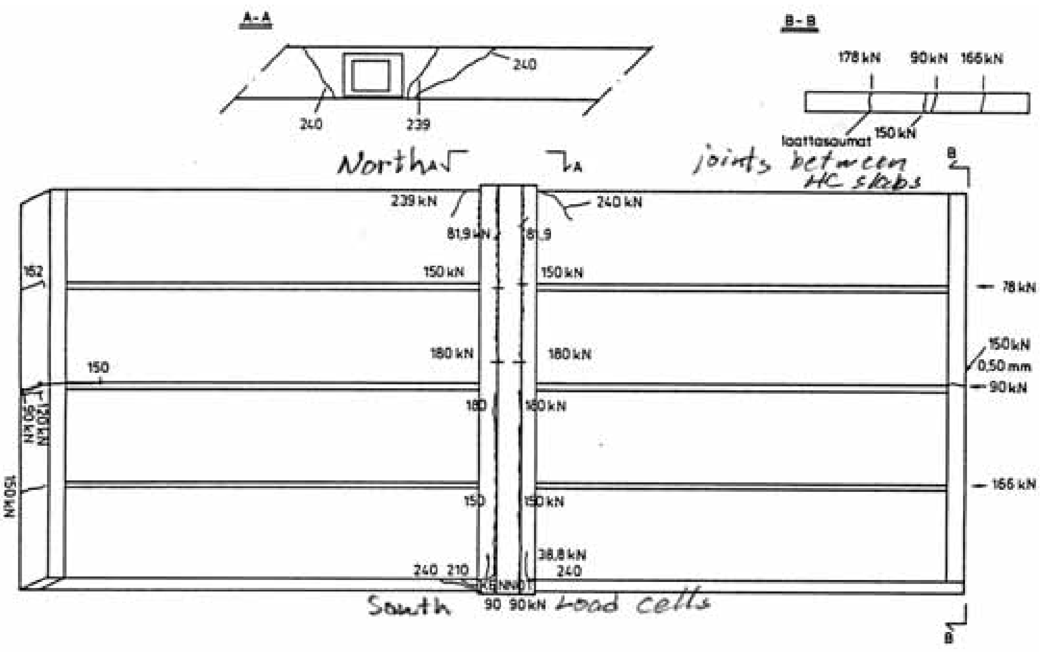 *Fig. 15. Cracks on the top and on the edges of the floor after failure.* 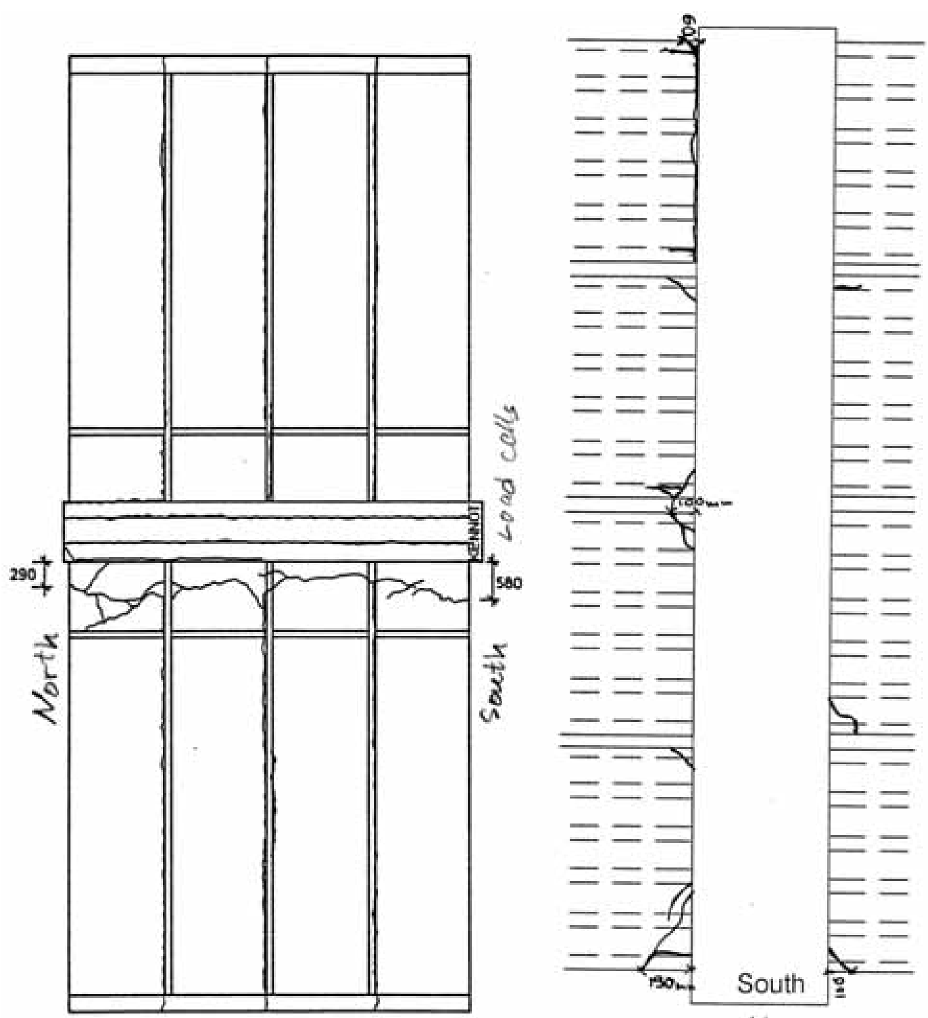 *Fig. 16. Cracks in the soffit after failure.*

Fig. 17. Slab 1 after failure.

Fig. 18. Top surface of slabs 1 (on the left), 2 and 3 after failure.

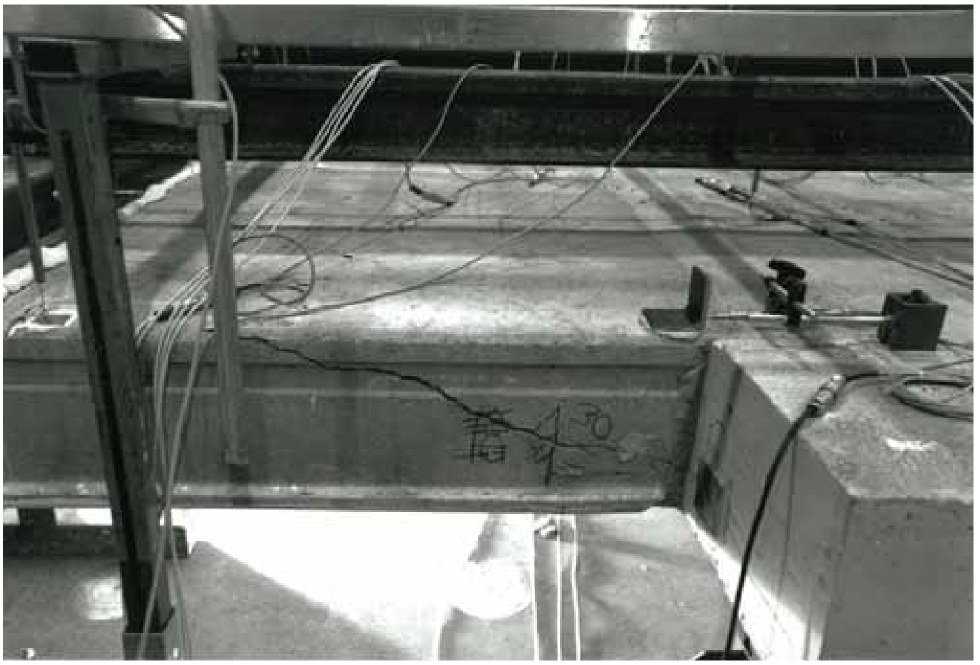

Fig. 19. Slab 4 after failure.

Fig. 20. Top surface of slabs 4 (on the right) and 3 after failure.

	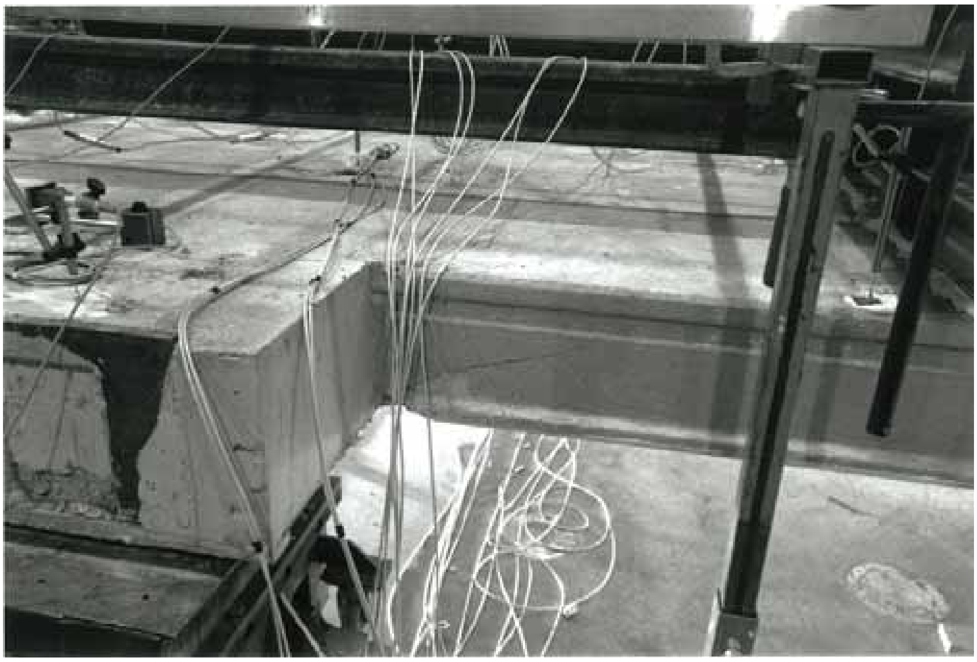 *Fig. 21. Slab 8 after failure.*  *Fig. 22. Soffit of slabs 1–4 after failure.*
8	**Observed shear resistance**
	The measured support reaction vs. the total imposed actuator load is depicted in Fig. 23. This relationship and the known eccentricity of the slabs and loads with respect to the beam supports have been used when calculating the observed shear resistance of the slabs.

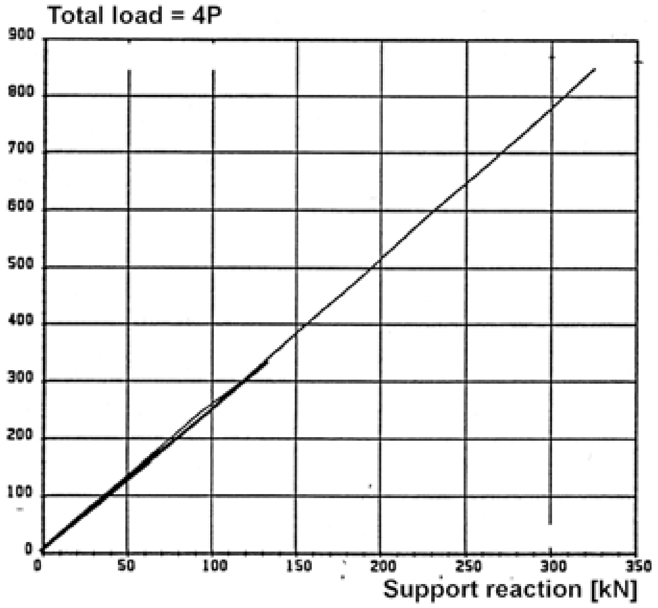

Fig. 23. Total imposed actuator load vs. support reaction of middle beam. South end.

The shear resistance of one slab end (support reaction of slab end at failure) due to different load components is given by

$$V_{obs} = V_{g,sl} + V_{g,jc} + V_{eq} + V$$

where $V_{g,sl}$, $V_{g,jc}$, V_{eq} and V_P are shear forces due to the self-weight of slab unit, weight of joint concrete, weight of loading equipment and actuator forces P, respectively. The test report does not give all these components but the sum

$$V_{eq} + V_P = 101{,}9 \text{ kN}$$

which is based on measured support reaction below one end of the middle beam and on the geometry of the test specimen. The self weight of the loading equipment was 420 kg/ one actuator. From this, V_{eq} = 1,8 kN is obtained. Hence V_P = 100,1 kN.

From the measured density of the concrete and nominal geometry

$$V_{g,sl} + V_{g,jc} = 12{,}3 + 0{,}4 \text{ kN} = 12{,}7 \text{ kN}$$

follows. The shear resistance $\boldsymbol{V_{obs}}$ **= 114,6 kN** (shear force at support) is obtained for one slab unit with width = 1,2 m. The shear resistance per unit width is $\boldsymbol{v_{obs}}$ **= 95,5 kN/m**

9 **Material properties**

9.1
Strength of steel

Component	$R_{eH}/R_{p0,2}$ MPa	R_m MPa	Note
Delta beam - web plates - top plate - bottom plate	 355 390 390		 Nominal (Raex 37-52) Nominal (Raex 423) Nominal (Raex 423)
End beams	≈ 350		Nominal (Fe52)
Slab strands J12,5	≥1570–1630	1770–1860	Nominal (no yielding in test)
Reinforcement Txy	500		Nominal value for reinforcing bars (no yielding in test)

9.2
Strength of slab concrete, floor test

#	Cores	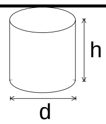	*h* mm	*d* mm	Date of test	Note
12			50	50	6.9.1990 (0 d)[1]	Upper flange of slabs 1–4. 3 from each, ρ = 2393 kg/m^3 Vertically drilled Tested as drilled[2]
Mean strength [MPa]			74,2			
St.deviation [MPa]			6,2			

9.3
Strength of slab concrete, reference tests

Not measured, assumed to be the same as that in the floor test

9.4
Strength of cast-in-situ concrete

#	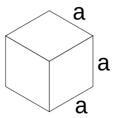	*a* mm	Date of test	Note
3		150	31.8.1990 (-6 d)[1]	Kept in laboratory in the same conditions as the floor specimen ρ = 2247 kg/m^3
Mean strength [MPa]		33,8		
St.deviation [MPa]		-		

[1] Date of material test minus date of structural test (floor test or reference test)
[2] After drilling, kept in a closed plastic bag until compression

10

Measured displacements and strains

In the following figures, *P* stands for the actuator force plus load due to loading equipment per one actuator. The cylic stage (Stage I) is not shown. The first point on each curve corresponds to the start of the monotonous loading stage (Stage II). Due to the abrupt failure, the measured results at the last load step are missing.

10.1
Deflections

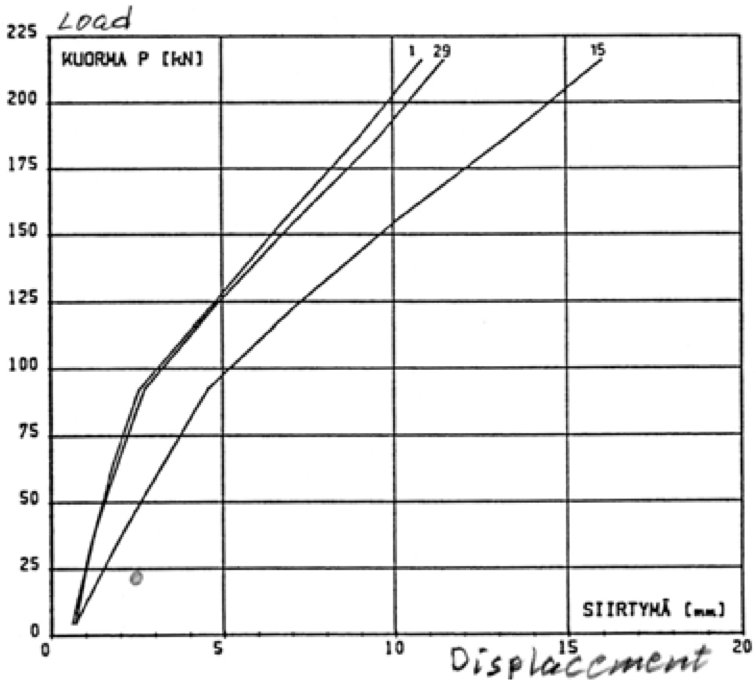

Fig. 24. Mid-point deflection of middle beam (transducer 15) and end beams (transducers 1 and 29).

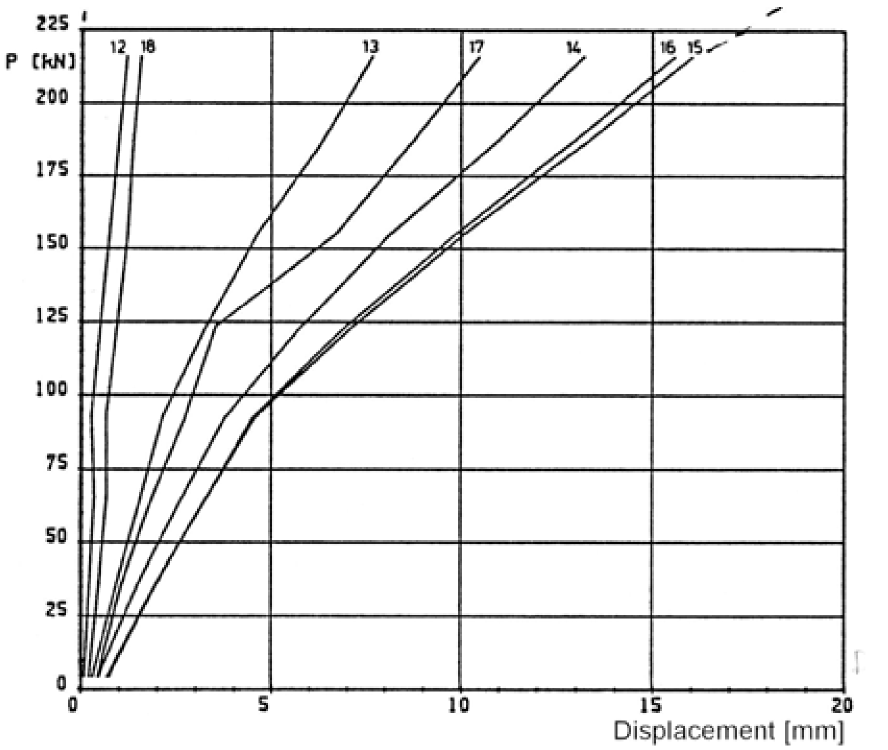

Fig. 25. Deflection of middle beam measured by transducers 12–17.

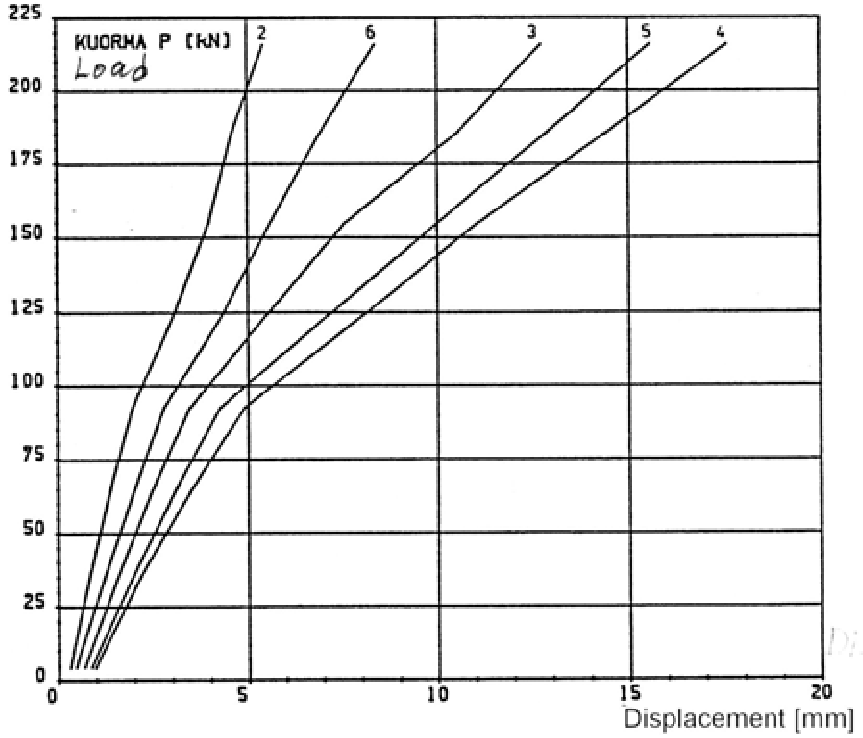

Fig. 26. Deflection of slabs 1–4 measured by transducers 2–6.

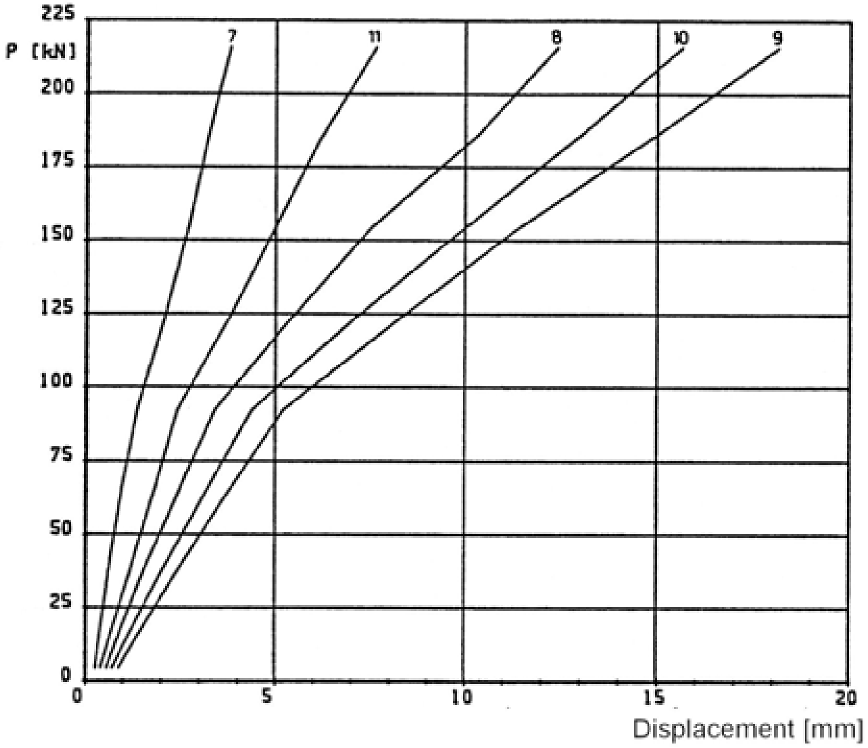

Fig. 27. Deflection of slabs 1–4 measured by transducers 7–11.

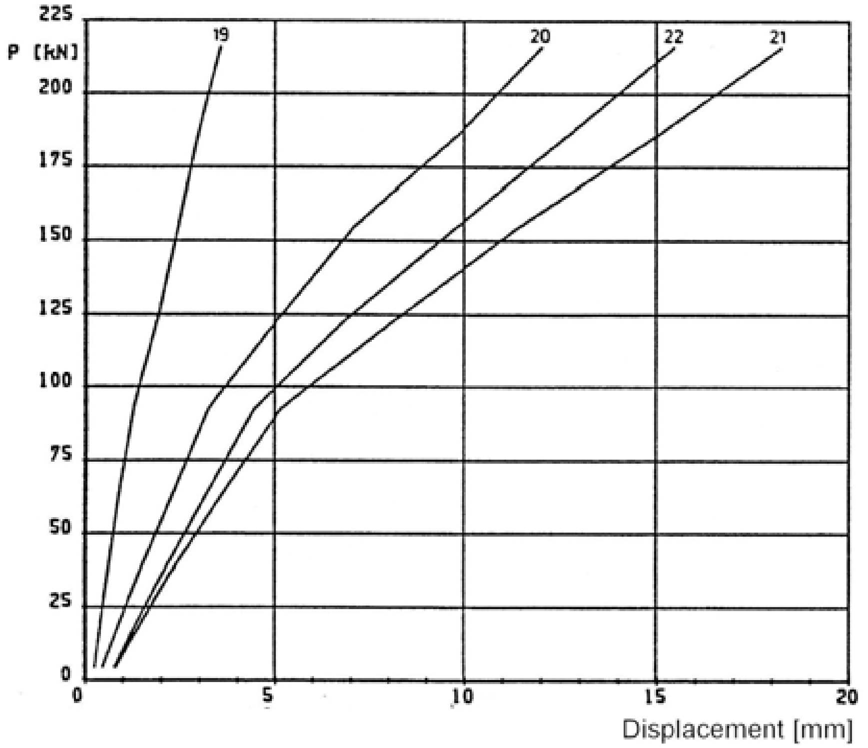

Fig. 28. Deflection of slabs 5–8 measured by transducers 19–22.

	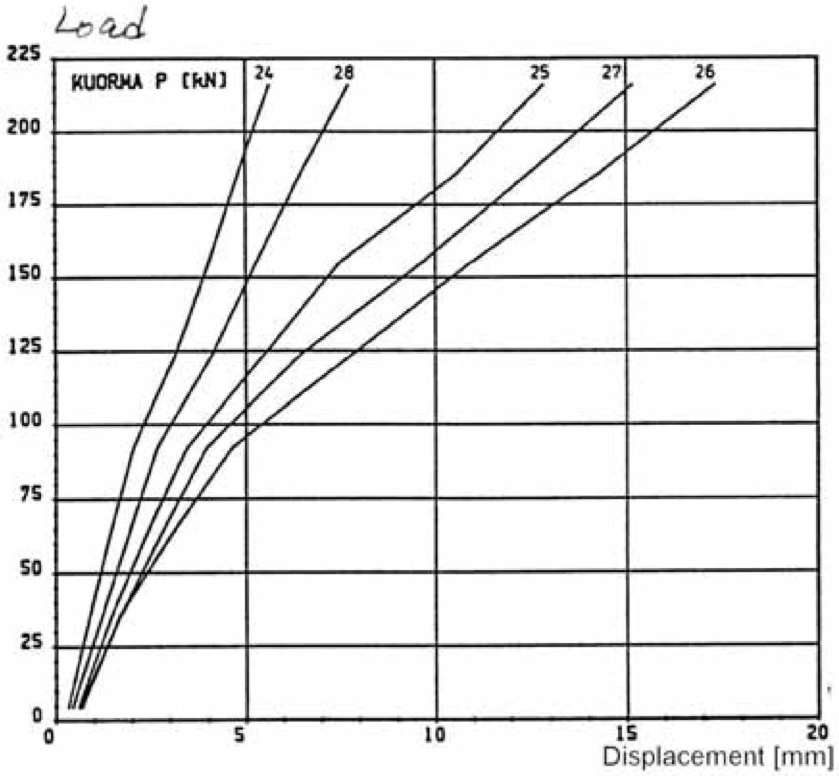 *Fig. 29. Deflection of slabs 5–8 measured by transducers 24–28.* 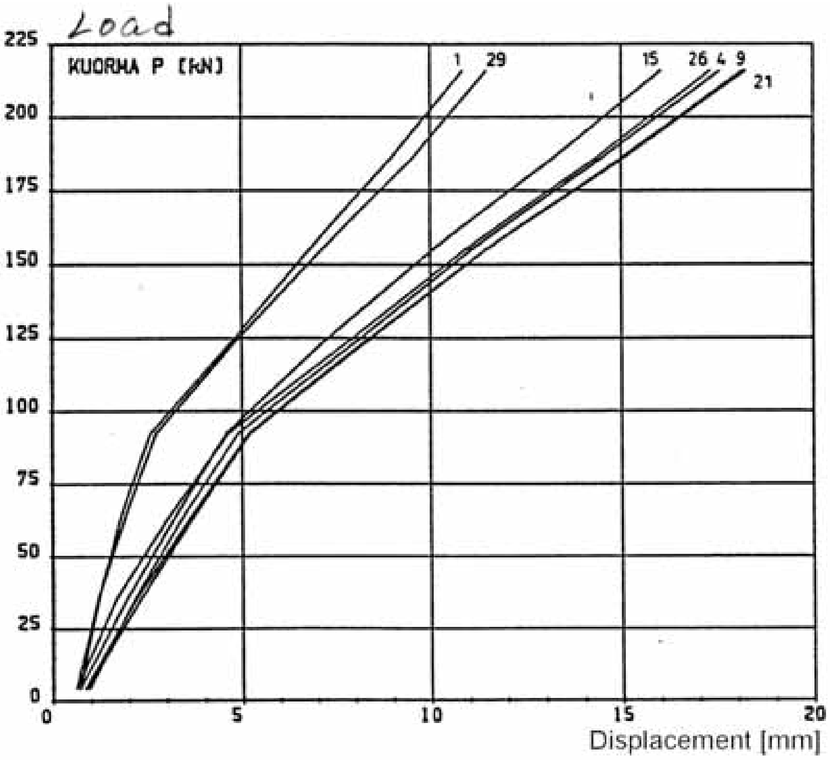 *Fig. 30. Deflection along longitudinal line of symmetry measured by transducers 1, 4, 9, 15, 21, 26 and 29.*
10.3 Average strain	-

10.4
Differential displacement

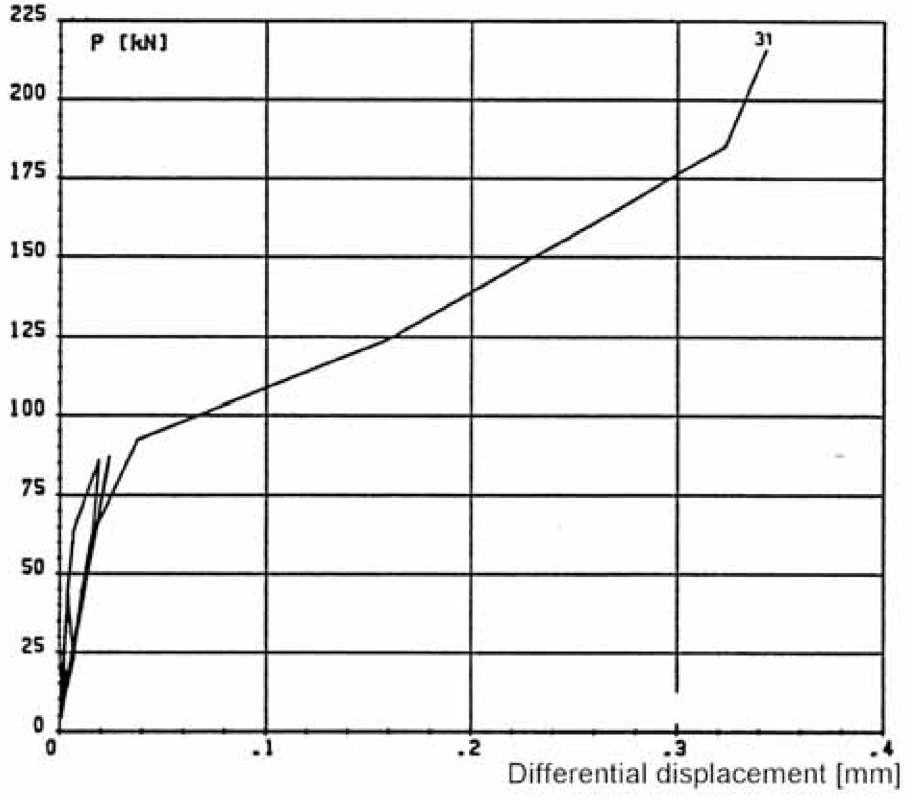

Fig. 31. Differential vertical displacement between middle beam and end of slab 7 measured by transducer 31.

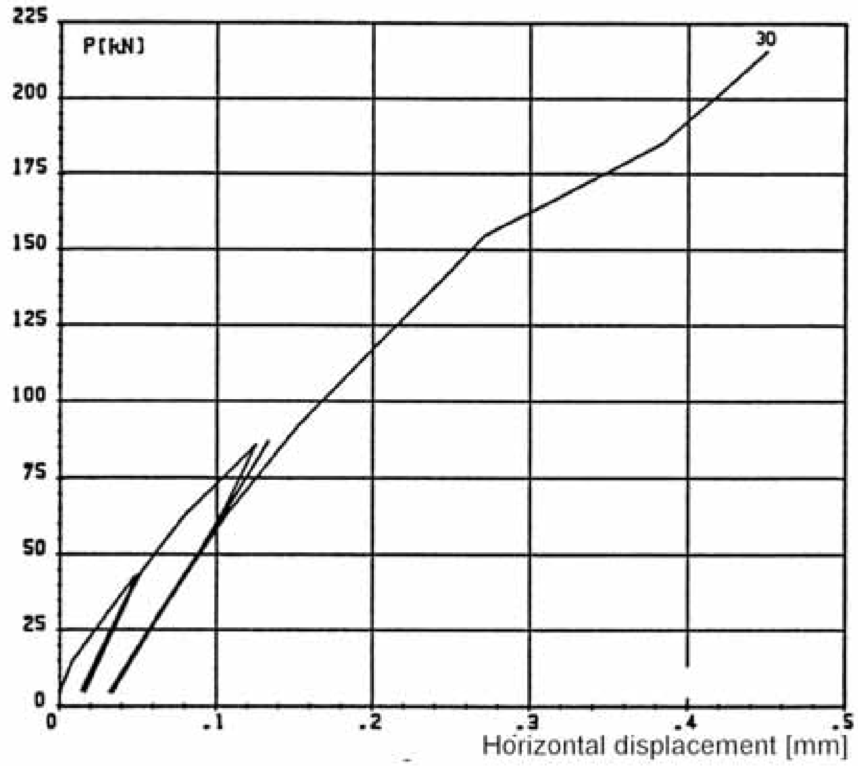

Fig. 32. Differential horizontal displacement between middle beam and edge of slab 4 measured by transducer 30.

10.5 **Strain**

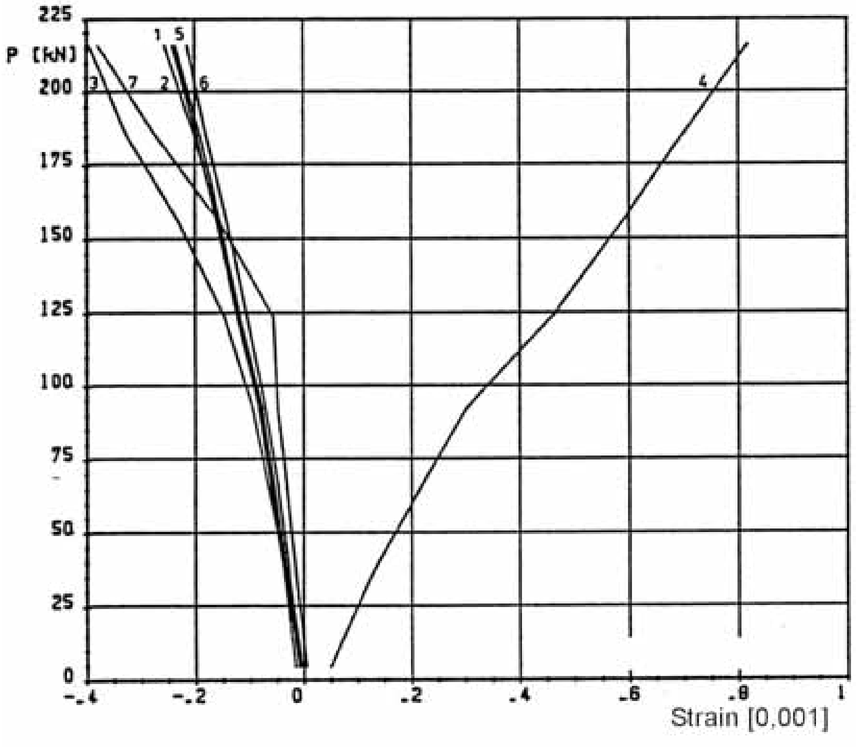

Fig. 33. Longitudinal (gauge 4) and transverse strain (gauges 1–3 and 5–7) measured at the bottom surface of the ledge of Delta beam.

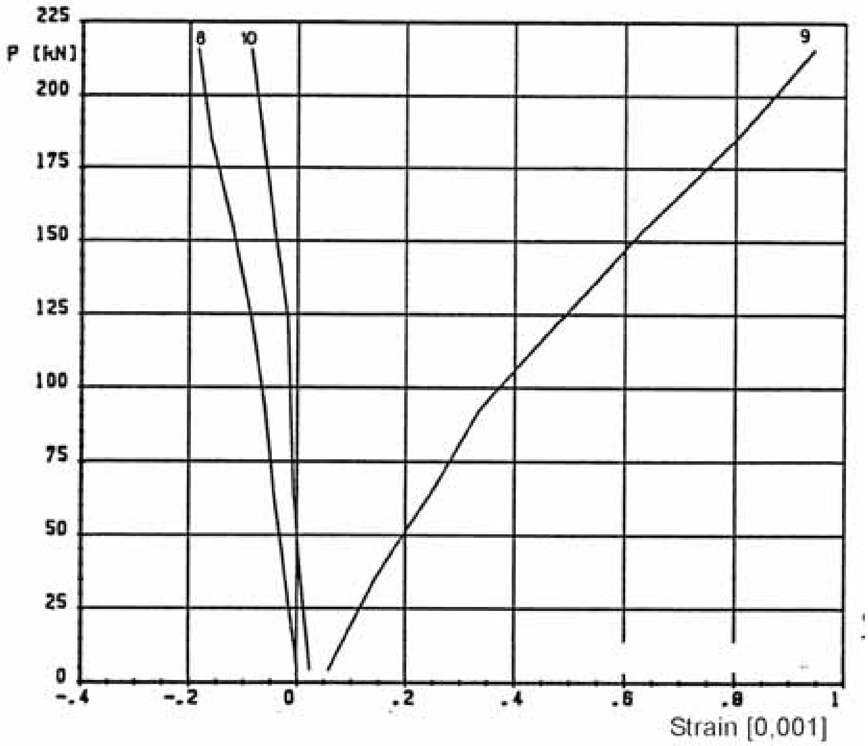

Fig. 34. Longitudinal (gauge 9) and transverse strain (gauges 8 and 10) measured at the bottom surface of the ledge of Delta beam.

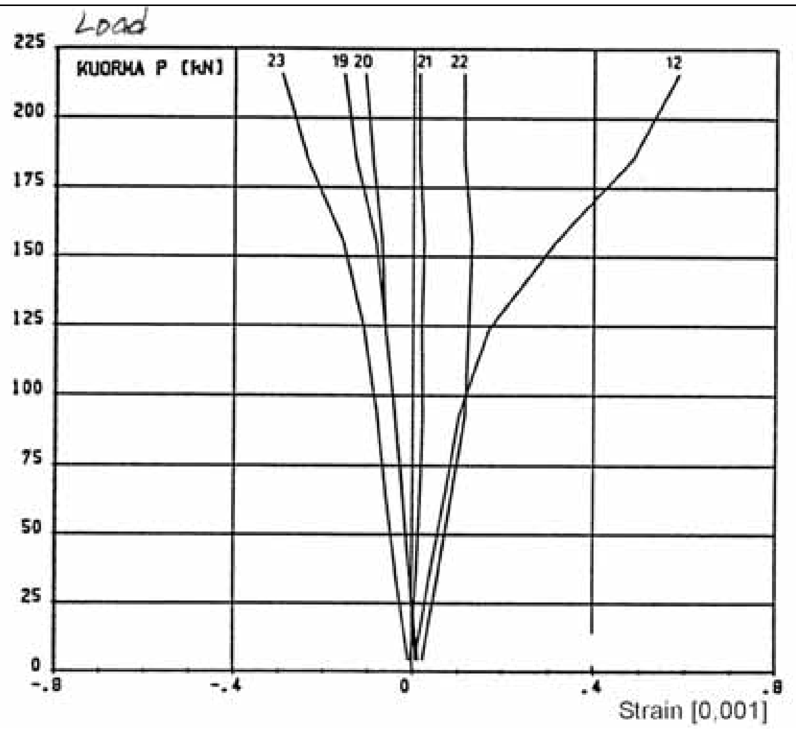

Fig. 35. Strain parallel to the beam

- *on the top surface (gauges 19 and 20) and on the bottom surface (gauges 21 and 22) of the hollow core slabs*
- *on the top surface of the top plate (gauge 23) and on the bottom surface of the bottom plate of the Delta beam (gauge 12).*

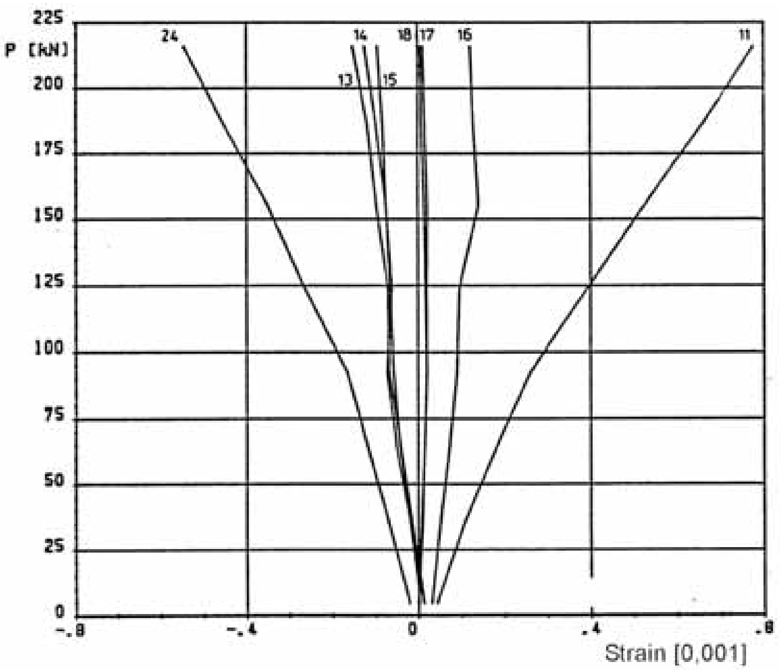

Fig. 36. Strain parallel to the beam

- *on the top surface (gauges 13–15) and on the bottom surface (gauges 16–18) of the hollow core slabs*
- *on the top surface of the top plate (gauge 24) and on the bottom surface of the bottom plate of the Delta beam (gauge 11).*

The tensile strain of the order 0,001 measured at the bottom of the bottom plate and in the ledges of the Delta beam confirm that the steel in the beam was far from yielding.

11	**Reference tests**
	After the load test on the floor, slabs 3 and 7 were taken as reference test specimens. Their ends which had been supported by the end beams, where loaded in shear as shown in Fig. 37. The concrete tie beam partly outside the slab end, partly in the hollow cores, was not removed before loading.

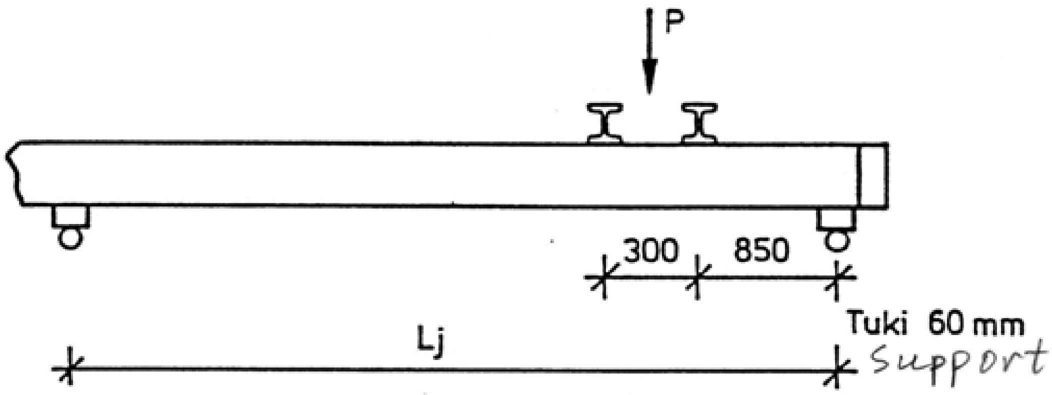

Fig. 37. Layout of reference test. For L_j, see the next table.

Table. Reference tests. Span of slab, shear force V_g at support due to the self weight of the slab, actuator force P_a at failure + weight of loading equipment P_{eq}, total shear force V_{obs} at failure and total shear force v_{obs} per unit width.

Test	Date	Span mm	V_g kN	P_a+P_{eq} kN	V_{a+eq} kN	V_{obs} kN	v_{obs} kN/m	Note
R3	>6.9.1990	4938	10,3	348,5	277,9	288,2	240,2	Web shear failure
R7	>6.9.1990	4810	10,0	340,4	269,6	279,6	233,0	Web shear failure
				Mean		**283,9**	**236,6**	

12	**Comparison: floor test vs. reference tests**
	The observed shear resistance (support reaction) of the hollow core slab in the floor test was equal to 114,6 kN per one slab unit or 95,5 kN/m. This is **40%** of the mean of the shear resistances observed in the reference tests.

13	**Discussion**
	1. The span of the middle beam was 5,0 m; that of the end beams 4,9 m. 2. The friction between the spreader beams was not intentionally eliminated, which may have affected the response of the floor test specimen to some extent. 3. The failure took place at an unexpected low load level. Therefore, the load increments applied were still relatively big and the gap between the failure load, at which no measurements were made, and the proceeding load level at which the response was measured, was big, too. The conclusions below about the strains and deflections at failure are based on the extrapolation of the measured curves. 4. At failure, the net deflection of the middle beam due to the imposed actuator loads (deflection minus settlement of supports) was 16,3 mm or *L*/307, i.e. rather small. It was 3,5–4,3 mm greater than that of the end beams. Hence, the torsional stresses due to the different deflection of the middle beam and end beams had a minor effect, if any, on the failure of the slabs. 5. The shear resistance measured in the reference tests was higher than the mean of the observed values for similar slabs given in *Pajari, M. Resistance of prestressed hollow core slab against a web shear failure. VTT Research Notes 2292, Espoo 2005.* This difference may be attributable to the concrete tie beam at the edge of the sheared end in the reference test. It prevented the deformation of the end section of the slab and thus equalized the strains in the webs of the slab, which effectively eliminated the premature failure of any individual web. 6. The beams did not yield in the floor test. 7. The failure mode was web shear failure of edge slabs close to the supports of the middle beam. Unlike in an isolated hollow core slab unit, the appearance of the first inclined crack close to the slab end did not mean failure but the loads could still be increased.

1	**General information**
1.1 Identification and aim	**VTT.S.WQ.265.1990** — **Last update 2.11.2010** WQ265 — (Internal identification). Note that the top-hat steel beam was called HQ-beam when the floor test was carried out, but later on the name has been changed. The present name WQ-beam is used in the following Aim of the test — To study whether or not the shear resistance of the hollow core slabs is reduced when supported on a WQ-beam
1.2 Test type	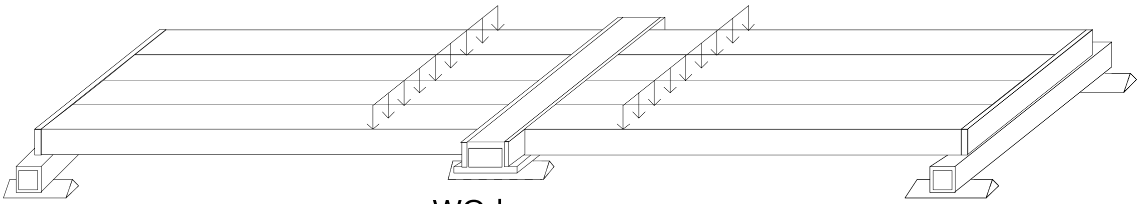 *Fig. 1. Illustration of test setup.*
1.3 Laboratory & date of test	VTT/FI 11.10.1990
1.4 Test report	Author(s): Koukkari, H. Name: *Matalien leukapalkkien ja ontelolaataston kuormituskokeet (Load tests on shallow beams and hollow core floor)*, in Finnish Ref. number: RAT01839/90 Date: 19.11.1990 Availability: Confidential, owner is Rautaruukki Oyj, P.O. Box 35, FI-01531 Vantaa, Finland

2	**Test specimen and loading**
2.1 General plan	 *Fig. 2. Overview on arrangements.*

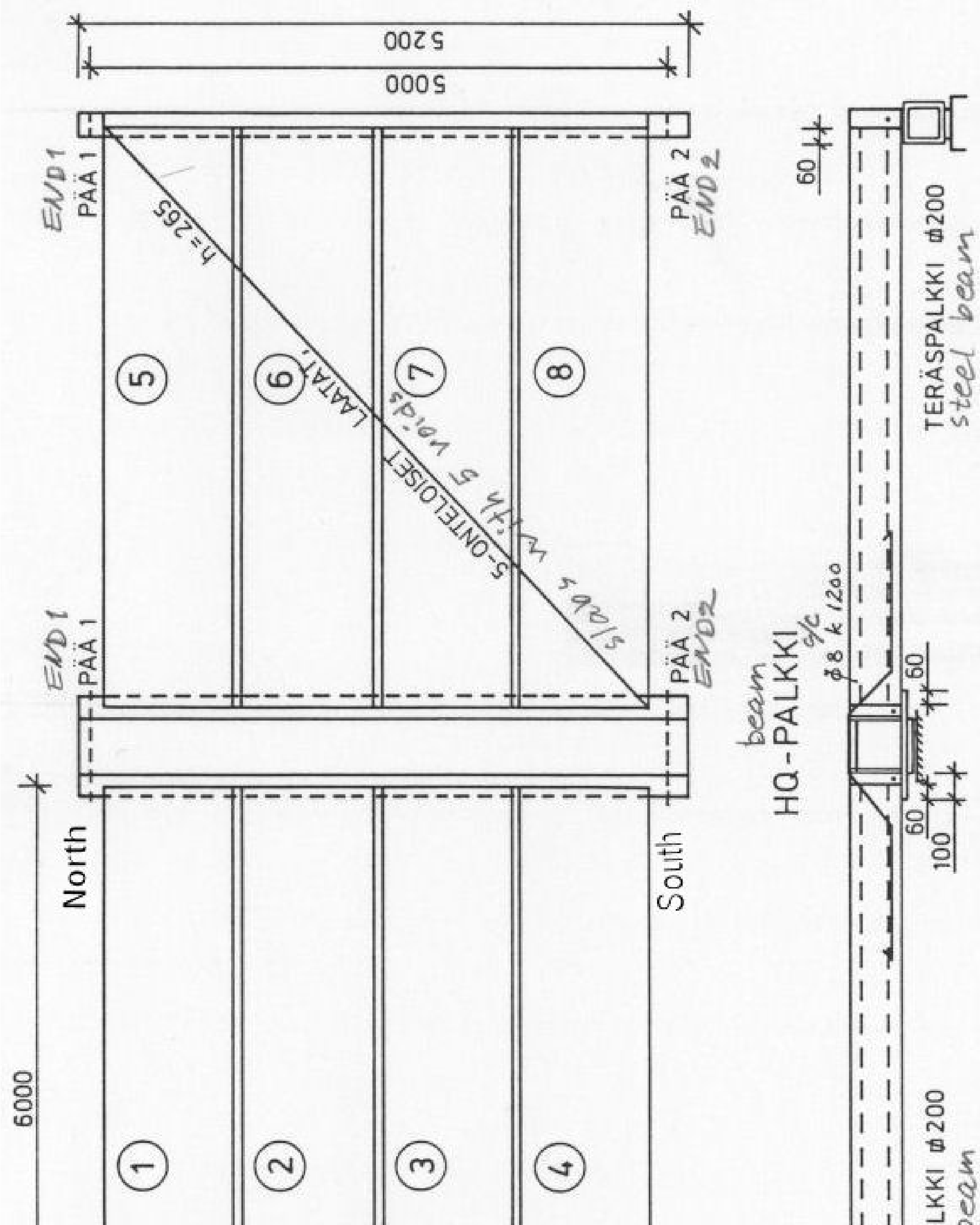

Fig. 3. Plan and longitudinal section along joint between adjacent slab units. Note the suspension reinforcement 3T8 c/c 1200 in the longitudinal joints of slabs and rebars (1+2+1)T8 tying the slab ends at the ends of the specimen and on both sides of the WQ-beam.

T8: Hot rolled, weldable rebar A500HW, ϕ = 8 mm

2.2 End beams	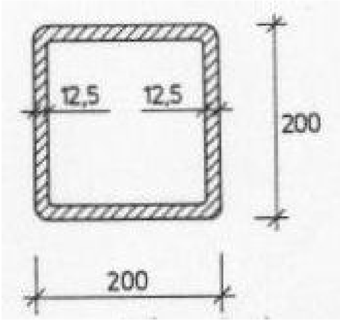 *Fig. 4. End beam.* - Simply supported, span = 5,0 m - There was plywood between the slabs and the end beam, see also Fig. 3 - Structural steel**:** Fe 52, $f_y \approx$ 350 MPa (nominal f_y)
2.3 Middle beam	The beam was designed to carry the support reactions from the slabs, slightly lower than those corresponding to the estimated shear resistance of the slab ends. The beam was made by PPTH-Teräs Oy and delivered to VTT on the 8th of August 1990. The measured camber of the beam was 12,7 mm. 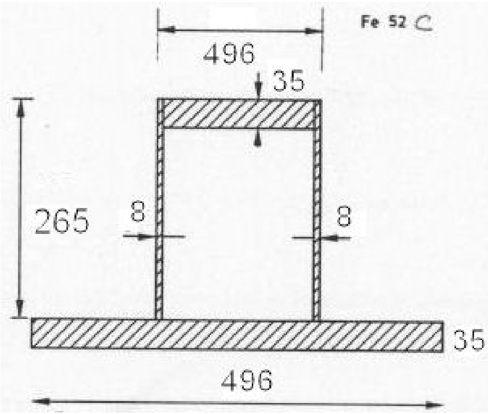 *Fig. 5. WQ-beam.* **Structural steel:** Fe 52C, $f_y \approx$ 350 MPa (nominal f_y)
2.4 Arrangements at middle beam	- Simply supported, span = 5,0 m - 4 load cells below support at South end - bearing length of slabs = 60 mm - see Fig. 3 for the bar reinforcement across the beam and parallel to it - joint concrete cast 27.9.1990

2.5 Slabs	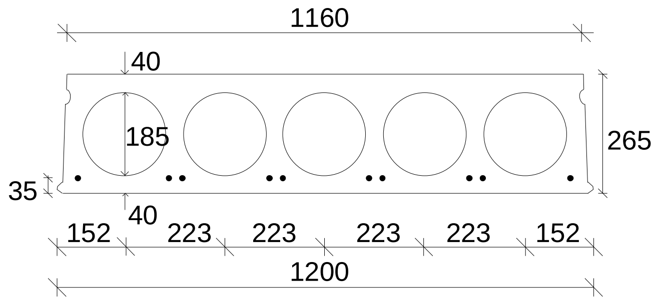 *Fig. 6. Nominal geometry of slab units.* - Extruded by Parma Oy 29.6.1990 - delivered to VTT, 12.9.1990 - grade of concrete K60 - 10 lower strands J12,5; initial prestress 1100 MPa **J12,5**: seven indented wires, ϕ =12,5 mm, A_p = 93 mm^2
2.6 Temporary supports	-
2.7 Loading arrangements	See Fig. 7. There was a gypsum layer between the tertiary beams and the top surface of the slabs. The primary spreader beams were in direct contact with the secondary spreader beams and the secondary beams with the tertiary spreader beams. No attempts were made to eliminate the friction. For this reason it is difficult to evaluate, to which extent the spreader beams participated in the load-carrying mechanism.

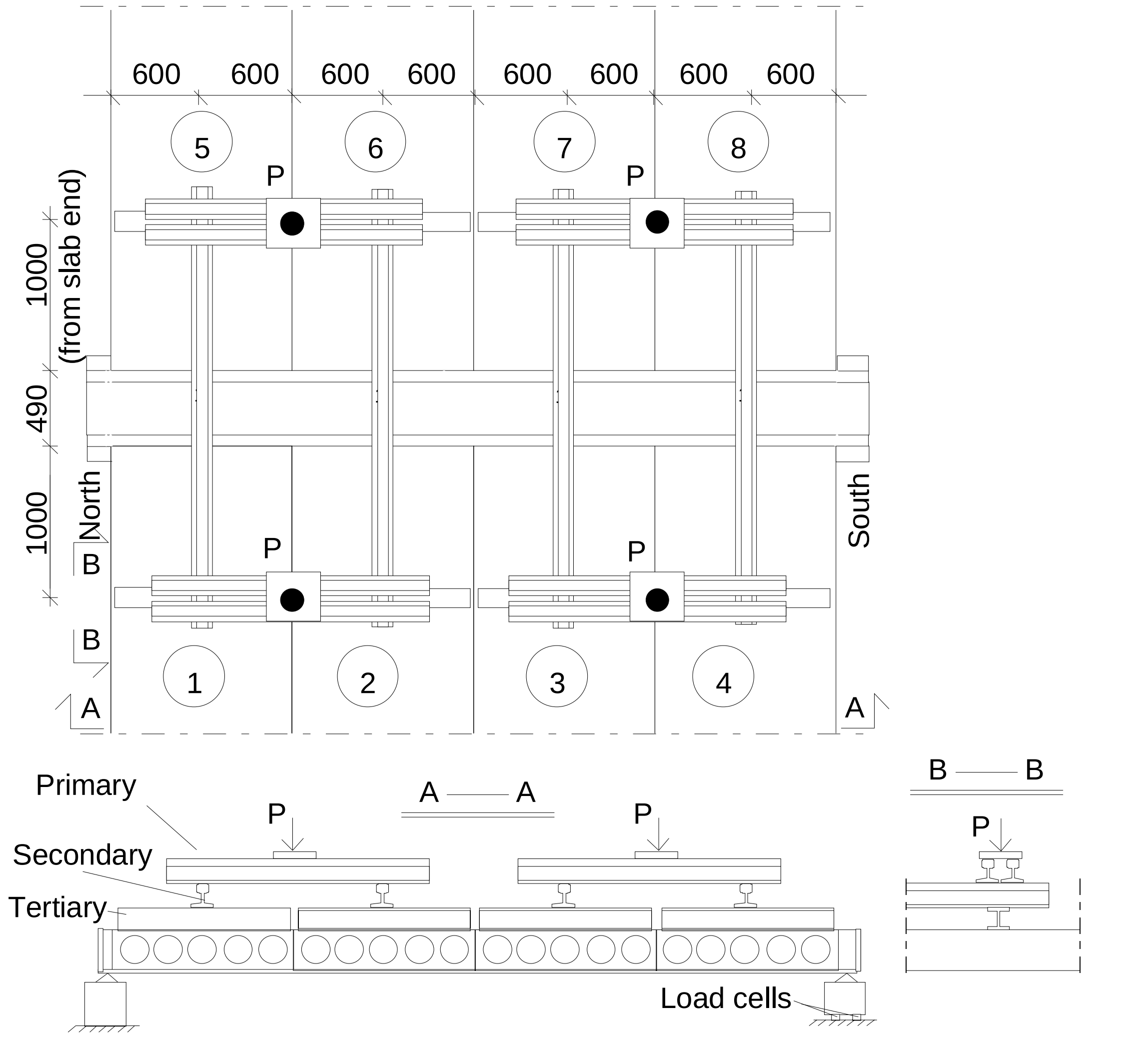

Fig. 7. Loading arrangements with three layers of spreader beams. The joint concrete between the slab ends and middle beam was extended to the ends of the WQ-beam.

3	**Measurements**
3.1 Support reactions	There were four load cells below the South end of the WQ-beam for measuring the support reaction due to the actuator loads.
3.2 Vertical displacement	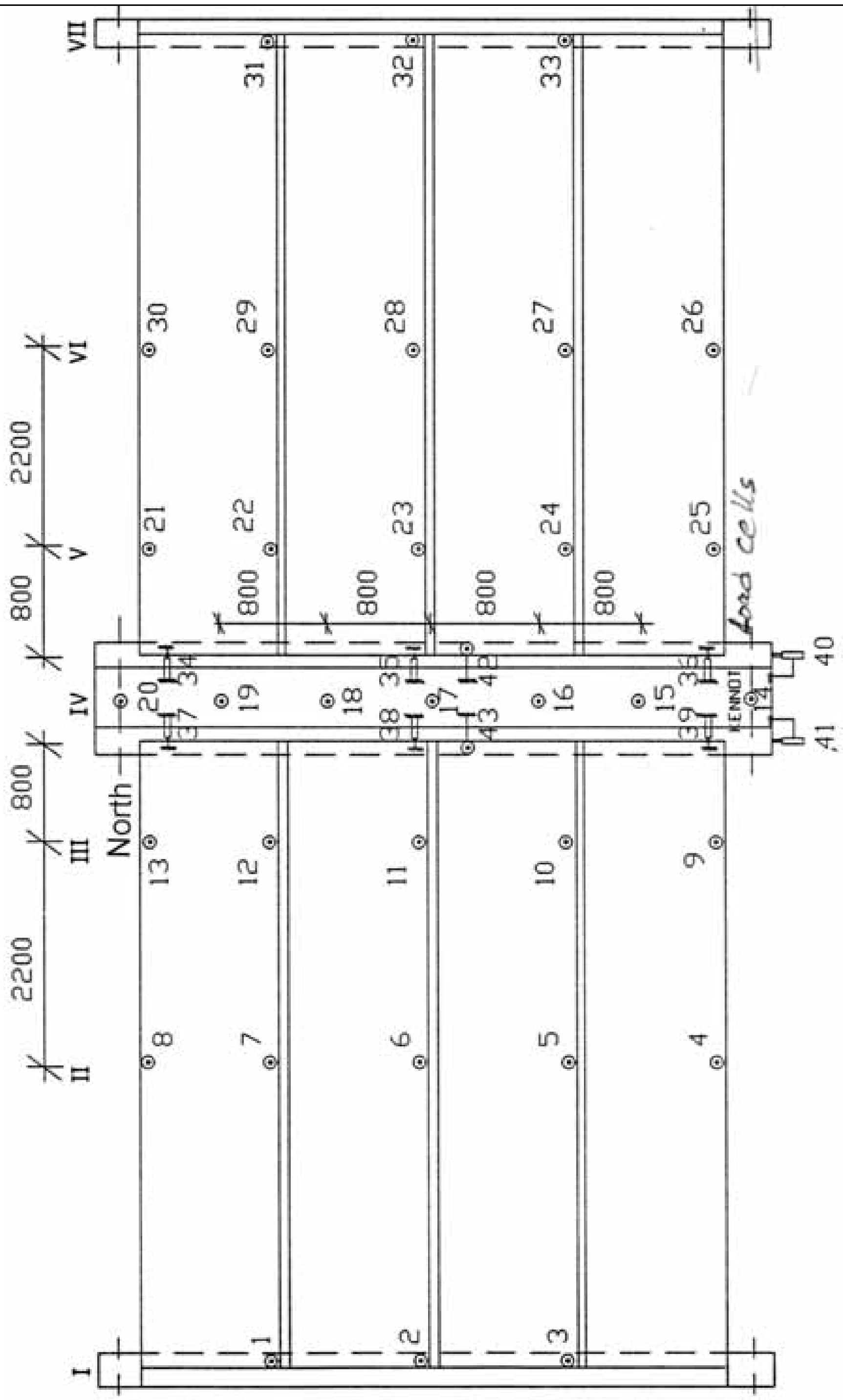 *Fig. 8. Location of transducers 1 … 33 for measuring vertical deflection, 34 … 39 for measuring the opening of cracks along the WQ-beam, 40 and 41 for measuring the differential horizontal displacement between the end of the beam and the joint concrete (see Fig. 13) and 42 & 43 for measuring differential vertical displacement between the slab end and the beam.*

3.3 Average strain	-
3.4 Horizontal displacements	*See Fig. 8, transducers 34 … 41. Transducers 40 and 41 measured the sliding of the joint concrete along the WQ-beam. Fig. 13 gives an impression of the vertical position of these transducers.*
3.5 Strain	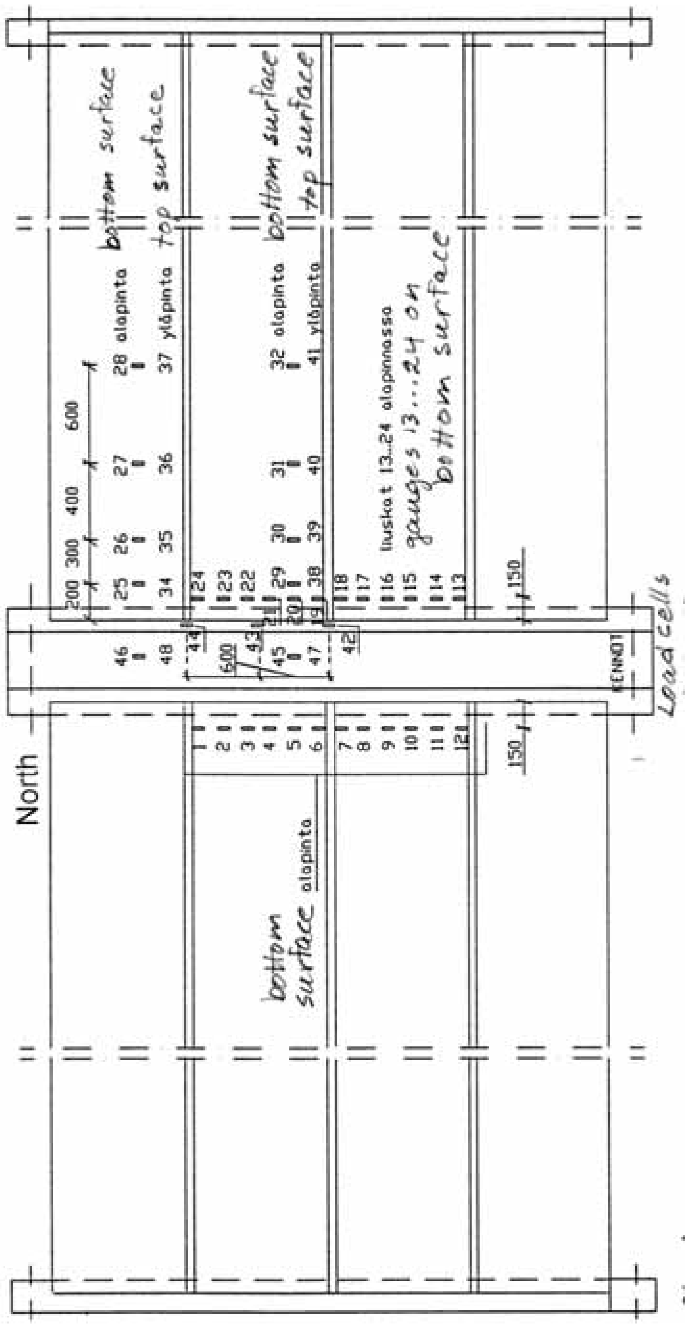 *Fig. 9. Position of strain gauges 1 … 48, all parallel to the beams.*

	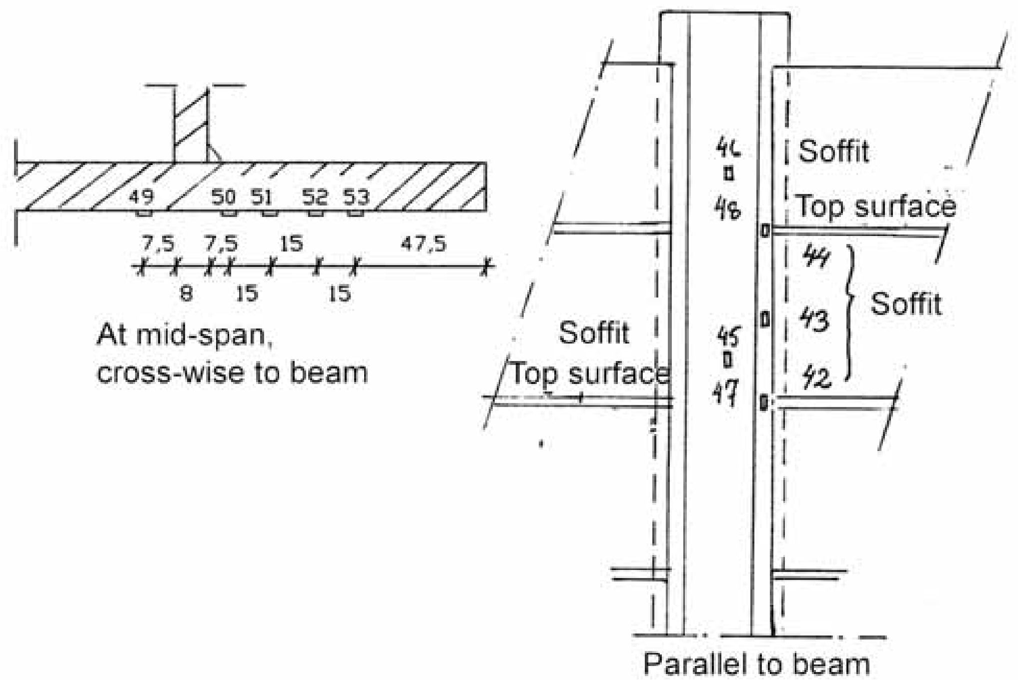 *Fig. 10. Position of strain gauges 49 … 53 below WQ-beam, all transverse to the beam, and position of strain gauges 42–48, all parallel to the beam.*
4	**Special arrangements** -
5	**Loading strategy**
5.1 Load-time relationship	Date of test was 11.10.1990 Before starting the test, all measuring devices were zero-balanced. Thereafter, the actuator loads *P* were varied in such a way that after five cycles of the type 0 → 201,6 kN → 0 (Stage I) the loads *P* were monotonously increased to 293 kN (Stage II). At this point unloading was necessary due to a leakage in the hycraulic circuit. After having fixed the leakage, loads *P* were monotonously increased to failure (Stage III).
5.2 After failure	
6	**Observations during loading** For the cracks observed during the loading and after the failure, see Figs 11–19.

Stage I	Cracks parallel to and along the edges of the WQ-beam were observed in the joint concrete. Some longitudinal cracks along the strands in the soffit of the slabs and vertical cracks in the tie beams at the ends of the floor were discovered.
Stage II	The cracks along the edges of the WQ-beam grew gradually and at *P* = 230 kN they were continuous from one beam end to the other. At *P* = 273 kN, an inclined crack, starting at the mid-depth of slab 4 next to the WQ-beam and growing upwards, appeared. At *P* = 283 kN an inclined crack also appeared at the end of slab1, and at *P* = 292 kN in slab 8.
Stage III	Right before failure, an inclined crack was observed in slab 8, and at the same time, a similar crack appeared in slab 1. At *P* = 345 kN, slabs 8 and 7 failed in shear.

7	**Cracks in concrete**
7.1 Cracks at service load	
7.2 Cracks after failure	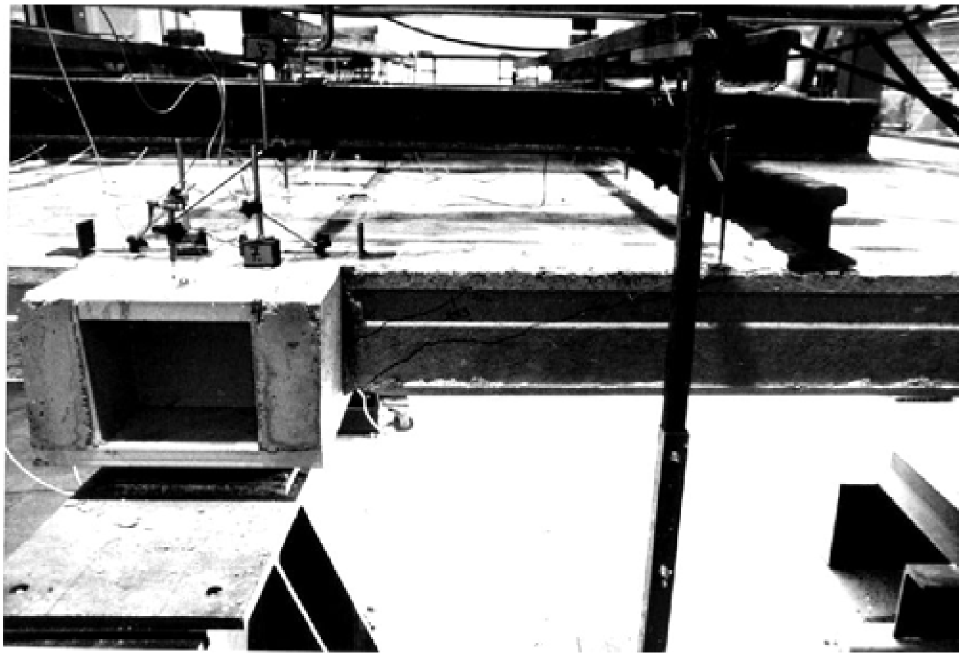 *Fig. 11. Inclined cracks in slab 1 after failure of slabs 7 and 8.* 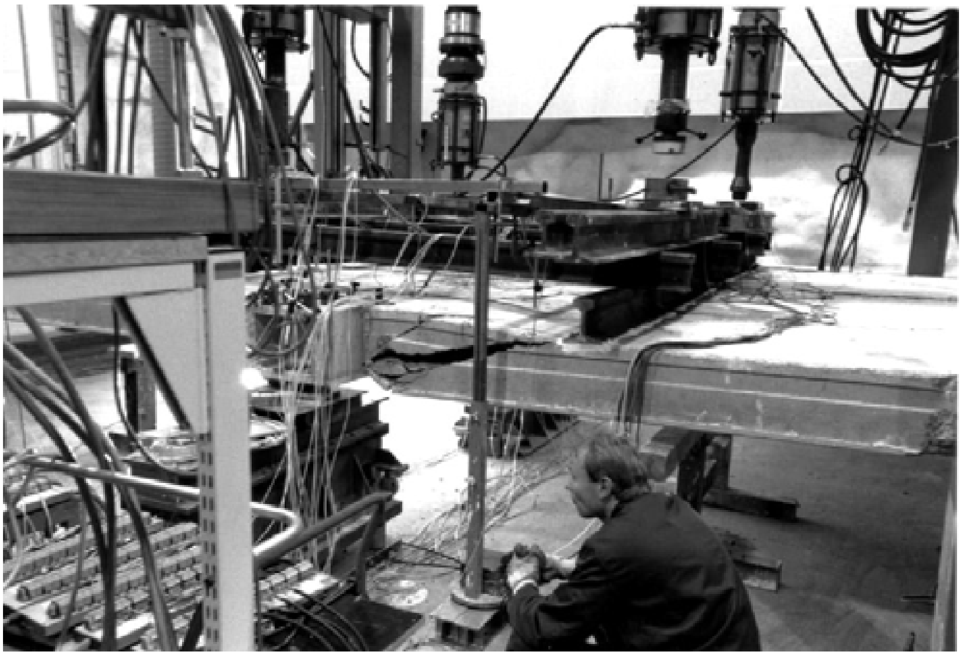 *Fig. 12. Failure of slabs 8 and 7.*

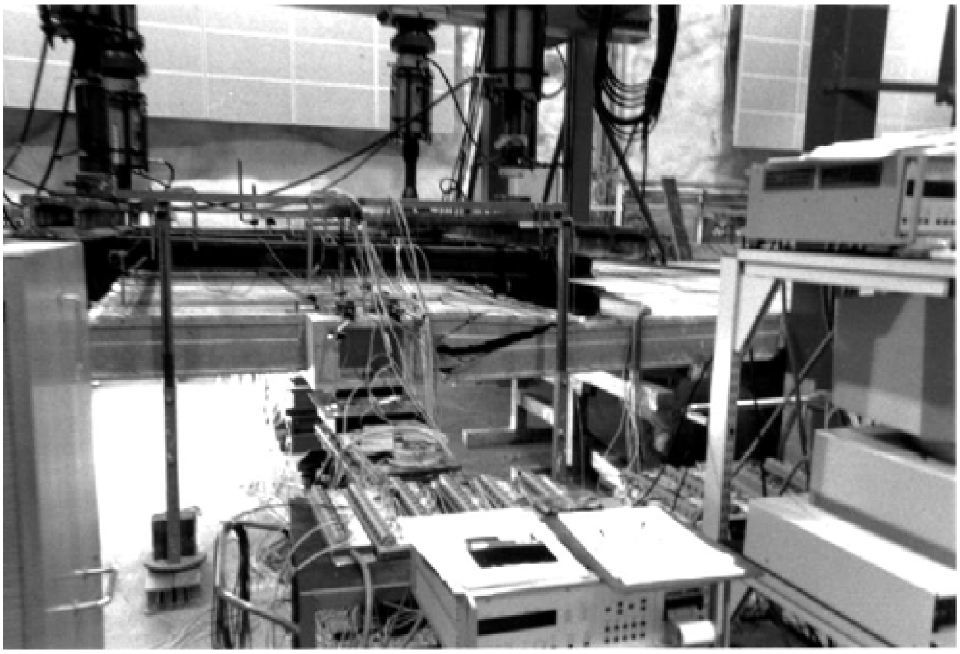

Fig. 13. Failure of slabs 8 and 7.

Fig. 14. Failure of slab 8.

Fig. 15. Failure of slab 8.

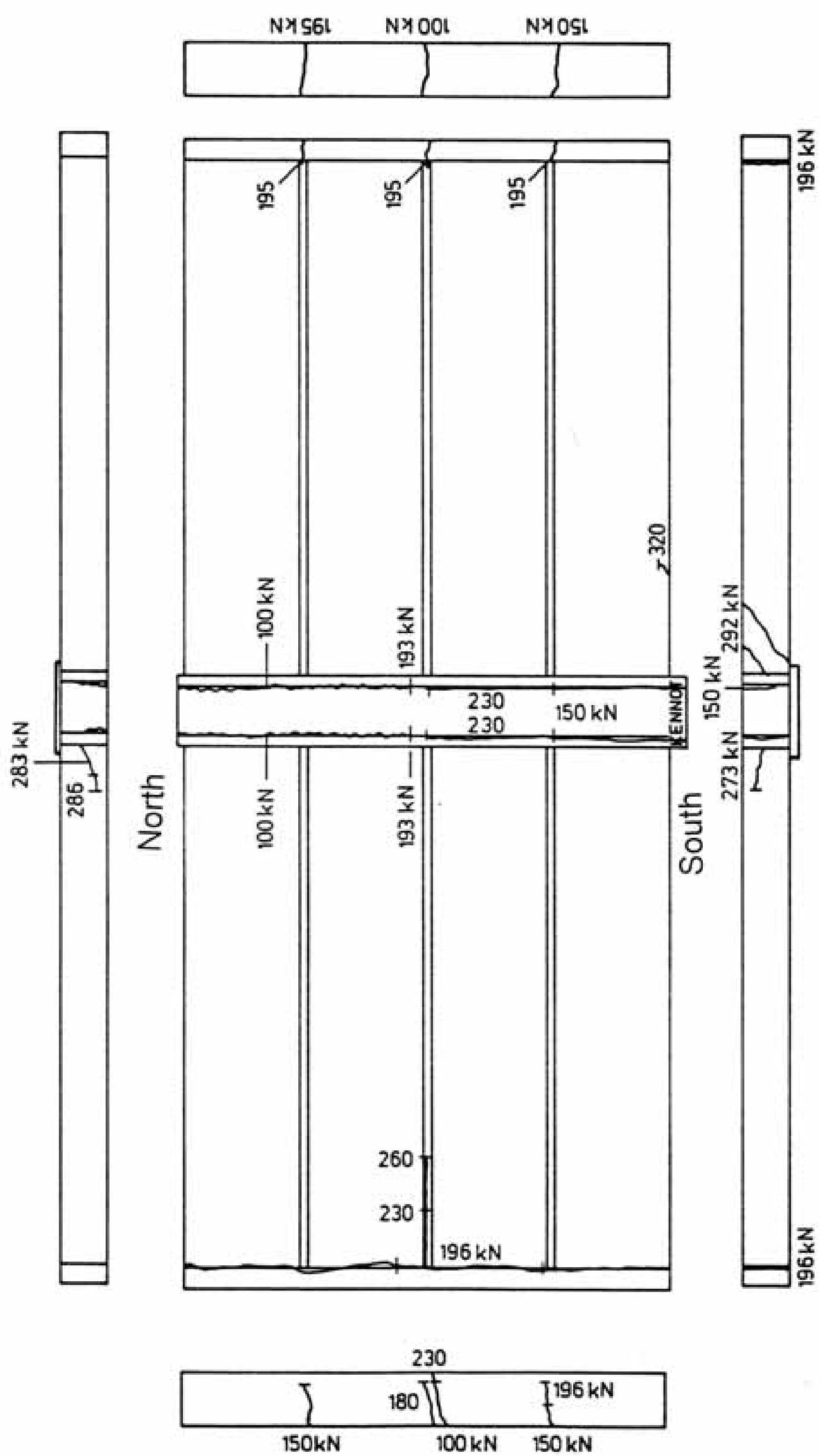

Fig. 16. Cracks on the top and at the edges of the floor after failure. The load values refer to actuator load P at which the crack was observed.

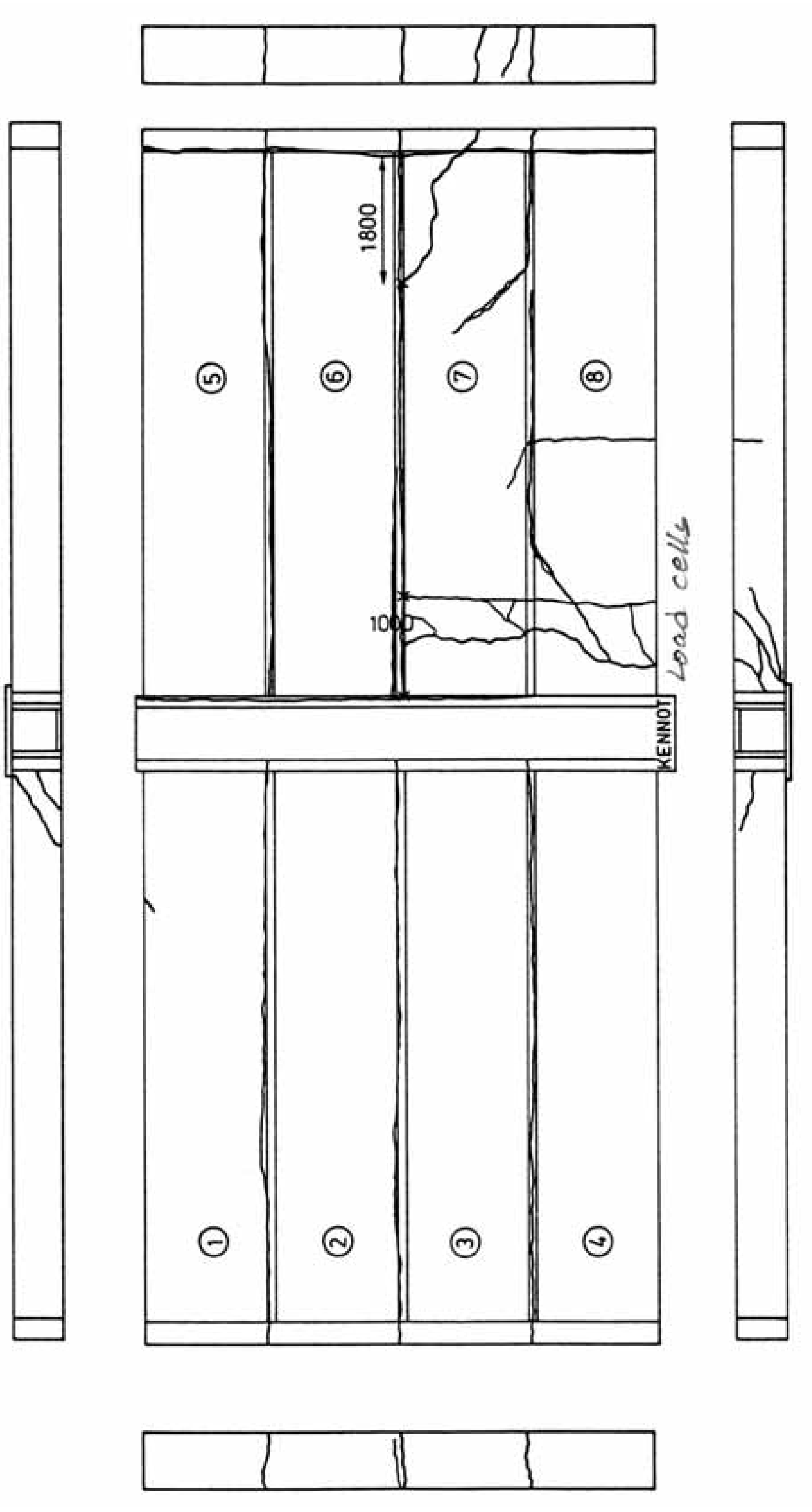

Fig. 17. Cracks on the top and at the edges of the floor after failure.

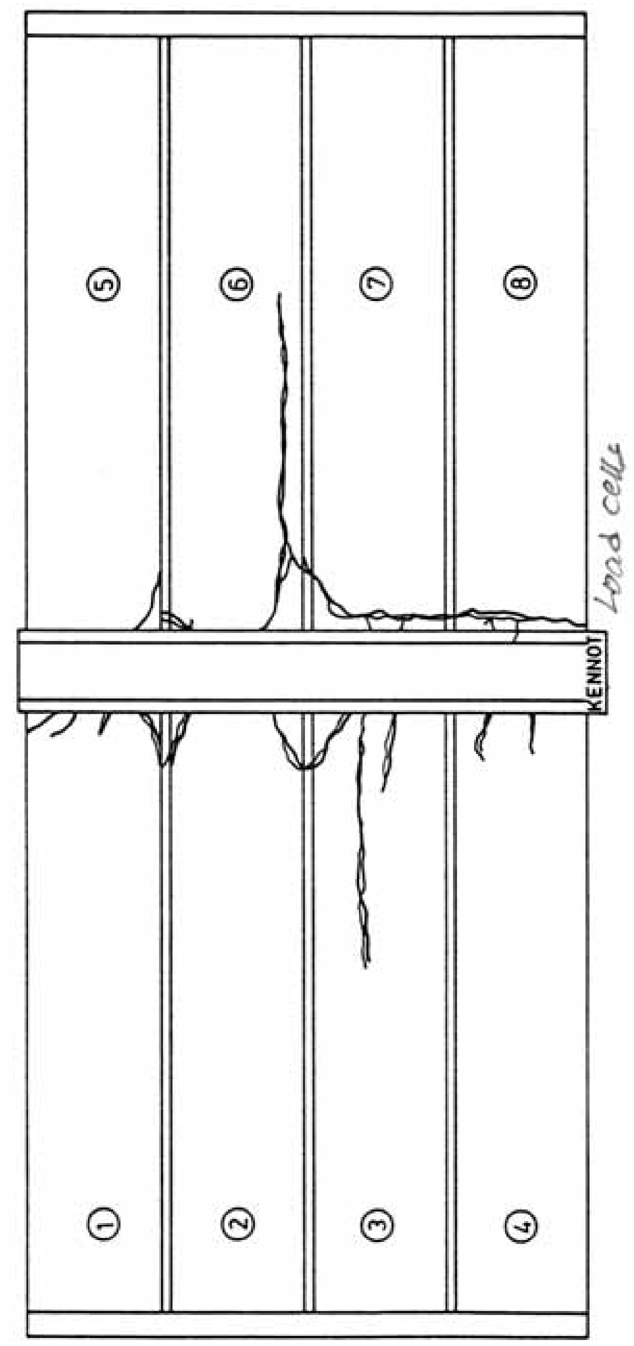

Fig. 18. Cracks after failure in the soffit.

	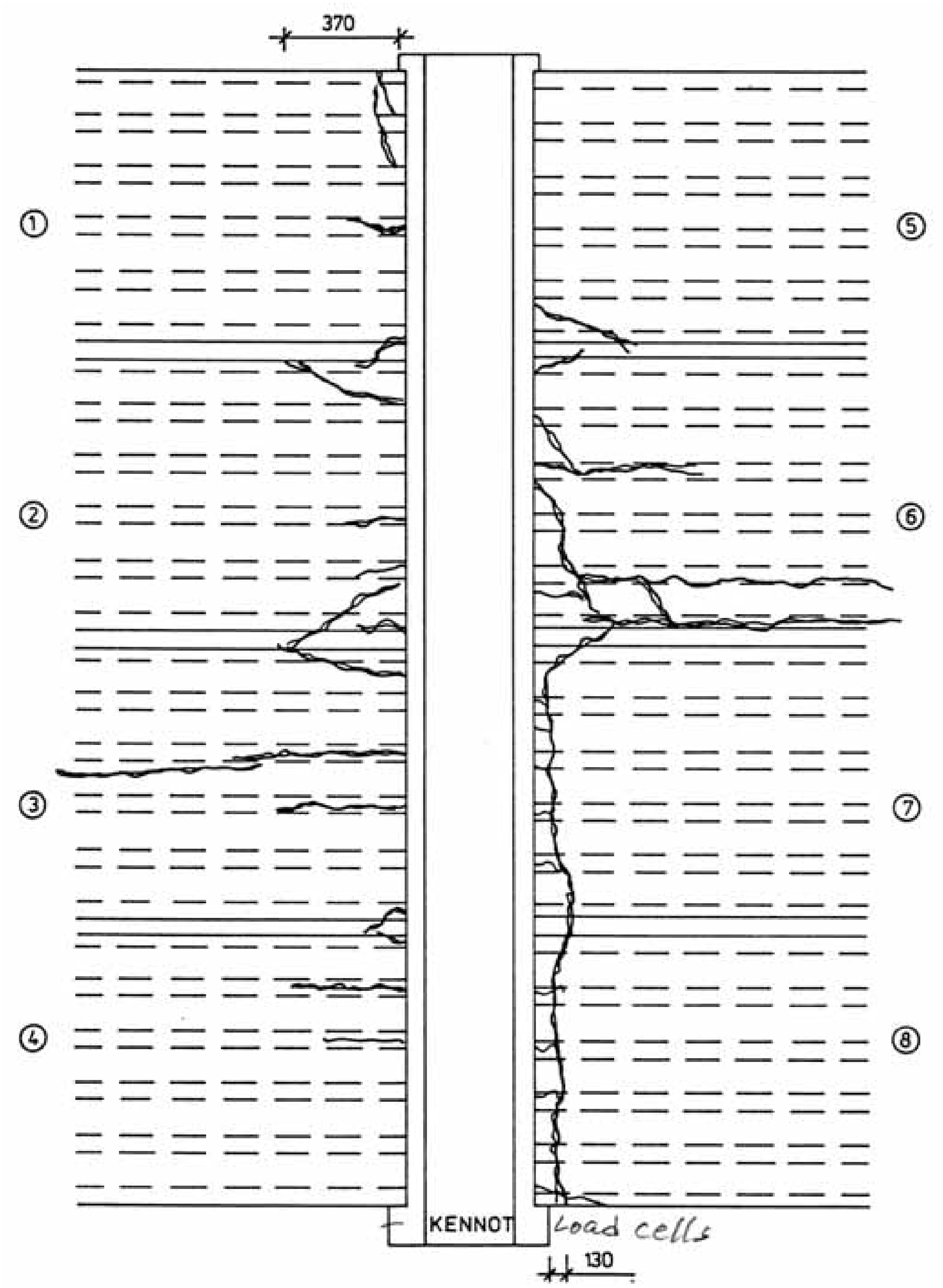 *Fig. 19. A part of the previous figure in more detail. The position of the webs in the hollow core slabs is indicated by dashed lines.*
8	**Observed shear resistance**
	The total actuator load = 4*P* vs. measured support reaction below the South end of the middle beam is shown in Fig. 20. The theoretical reaction is calculated assuming simply supported slabs. This comparison shows that the support reaction due to the actuator forces can be calculated accurately enough assuming simply supported slabs. However, the failure of the slab ends at the North end of the middle beam resulted in reduction of support reaction below that end while the actuator force could still slightly be increased. The maximum support reaction is regarded as the indicator of failure.

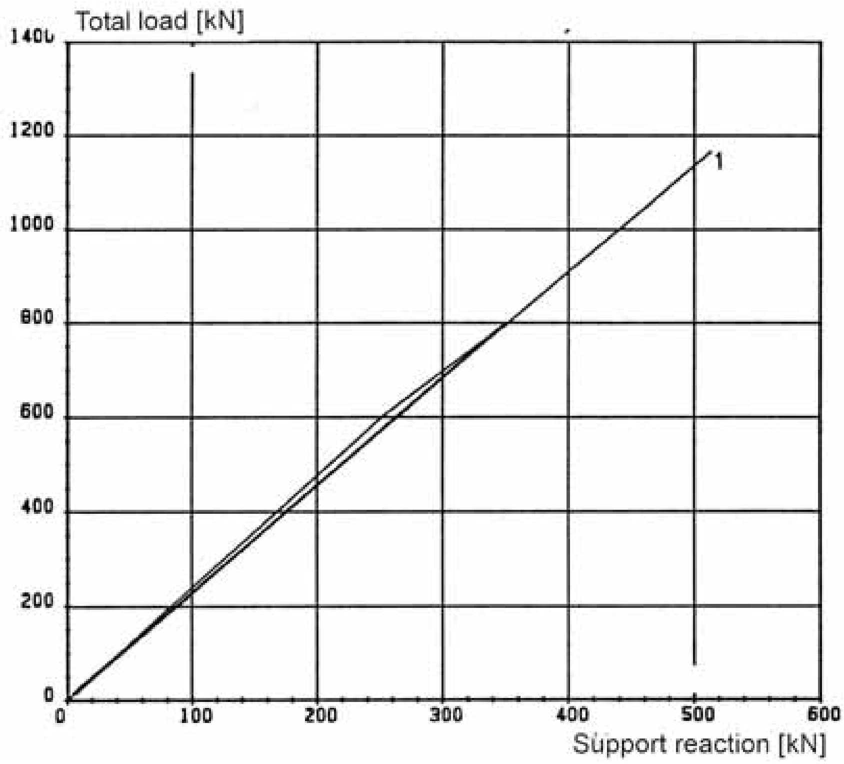

Fig. 20. Stages I and II. Measured support reaction due to total actuator load 4P.

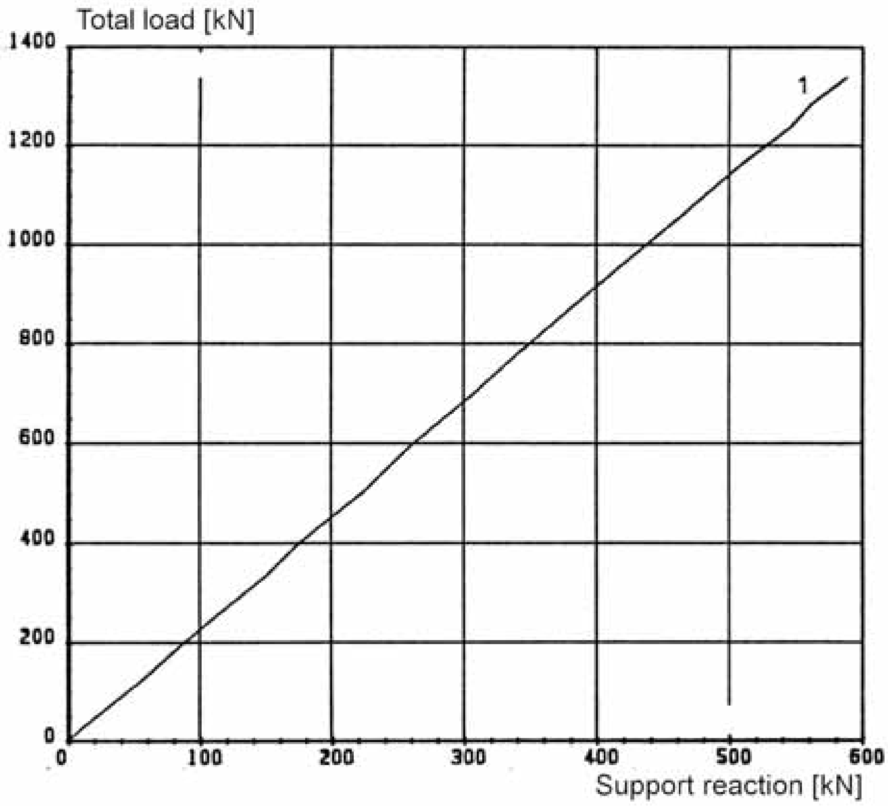

Fig. 21. Stage III. Measured support reaction due to total actuator load 4P.

The shear resistance of one slab end (support reaction of slab end at failure) due to different load components is given by

$$V_{obs} = V_{g,sl} + V_{g,jc} + V_{eq} + V_P$$

where $V_{g,sl}$, $V_{g,jc}$, V_{eq} and V_P are shear forces due to the self-weight of slab unit, weight of joint concrete, weight of loading equipment and actuator forces P, respectively. The test report does not give all these components but

$$V_P = 151{,}6 \text{ kN}$$

is obtained from the failure load P = 345 kN using the load-reaction relationship shown in Fig. 21 [reaction = 0,8844x(2P)].

In the same way

$$V_{eq} = 1{,}8 \text{ kN}$$

is obtained from the weigth of the loading equipment (= 210 kg / one slab).

From the nominal geometry and measured density of the concrete

$$V_{g,sl} + V_{g,jc} = 12{,}3+0{,}4 = 12{,}7 \text{ kN}$$

follows. The shear resistance $\boldsymbol{V_{obs}}$ **= 166,1 kN** (shear force at support) is obtained for one slab unit with width = 1,2 m. The shear force per unit width is $\boldsymbol{v_{obs}}$ **= 138,4 kN/m.**

9 **Material properties**

9.1
Strength of steel

Component	$R_{eH}/R_{p0,2}$ MPa	R_m MPa	Note
End beam	≈ 350		Nominal (Fe 52, no yielding in test)
WQ-beam	≈ 350		Nominal (Fe 52C, no yielding in test)
Slab strands J12,5	1570–1630	1770–1860	Nominal (no yielding in test)
Reinforcement Txy	500		Nominal value for reinforcing bars, (no yielding in test)

9.2
Strength of slab concrete, floor test

#	Cores	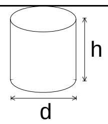	*h* mm	*d* mm	Date of test	Note
6			50	50	12.11.1990 (+1 d)[1)]	Upper flange of slabs 5 and 3 (3pc. each), ρ = 2398 kg/m^3 vertically drilled Tested as drilled[2)]
Mean strength [MPa]			65,3			
St.deviation [MPa]			4,0			

9.3
Strength of slab concrete, reference tests

Not measured, assumed to be the same as that in the floor test.

9.4 Strength of grout in joints

#	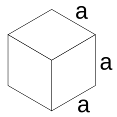	*a* mm	Date of test	Note
3		150	10.10.1990 (-1 d)[1)]	Kept in laboratory in the same conditions as the floor specimen ρ =2223 kg/m³
Mean strength [MPa]		30,5		
St.deviation [MPa]				

#	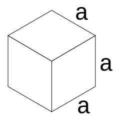	*a* mm	Date of test	Note
3		150	12.10.1990 (+1 d)[1)]	Kept in laboratory in the same conditions as the floor specimen ρ =2213 kg/m³
Mean strength [MPa]		31,7		
St.deviation [MPa]				

[1)] Date of material test minus date of structural test (floor test or reference test)
[2)] After drilling, kept in a closed plastic bag until compression

10 **Results measured during floor test**

In the following graphs, *P* is the actuator load.

10.1 Deflections

The measured deflections in Stages II and III are shown in Figs 22–39. The numbers close to the curves refer to the number of transducer, see Fig. 8.

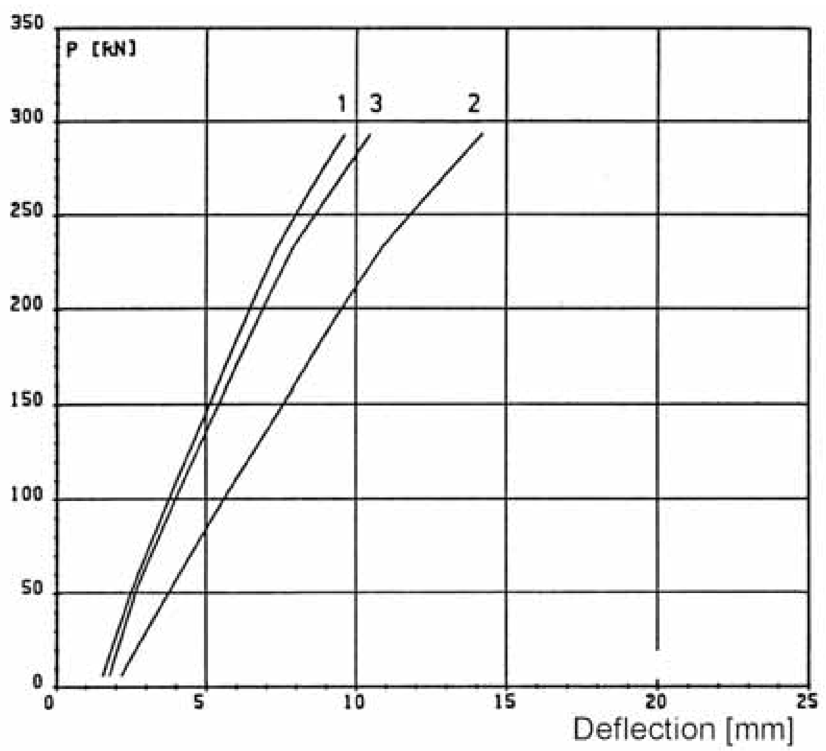

Fig. 22. Stage II.

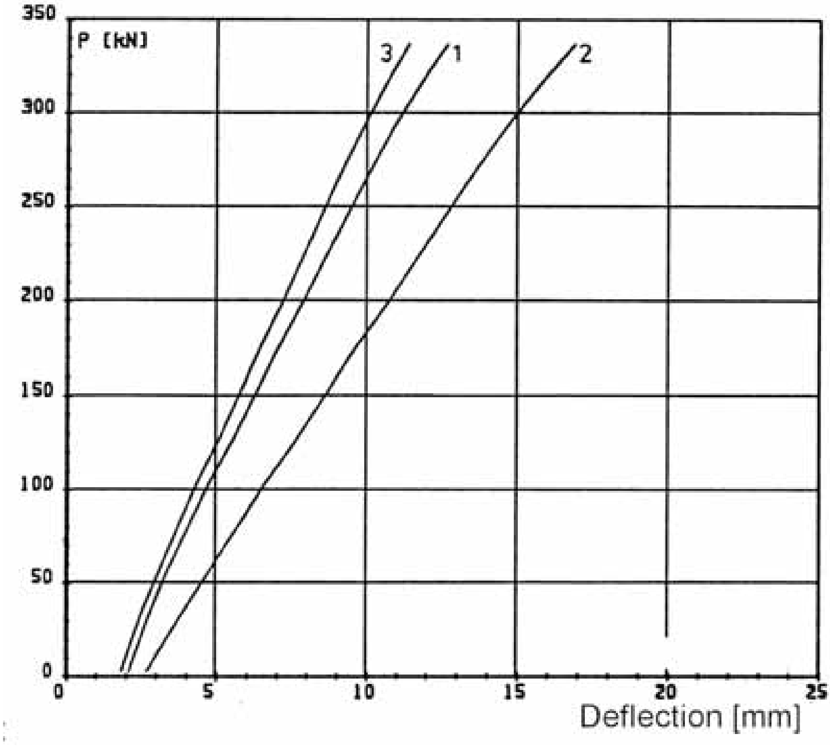

Fig. 23. Stage III.

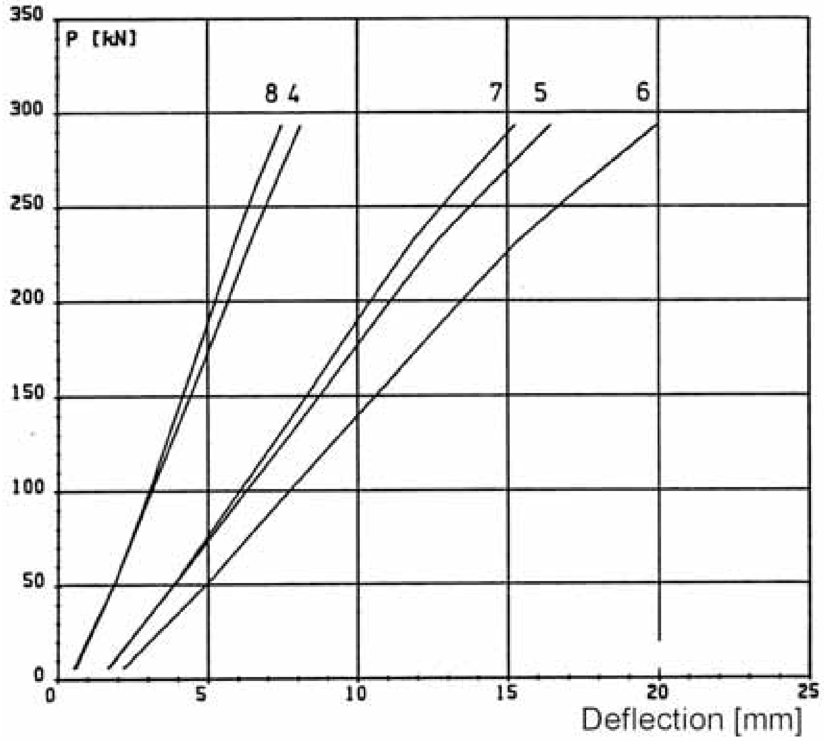

Fig. 24. Stage II.

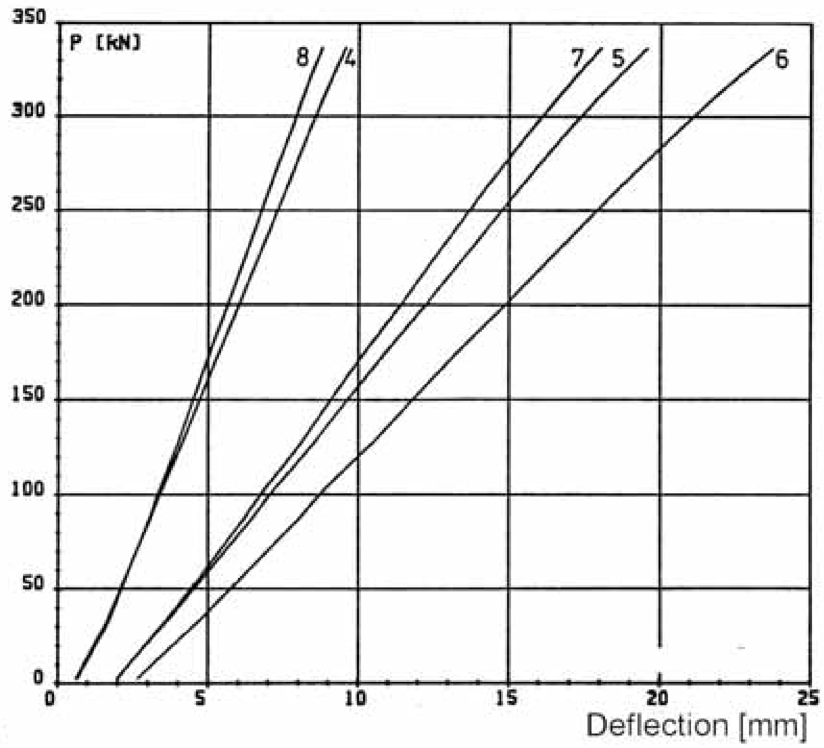

Fig. 25. Stage III.

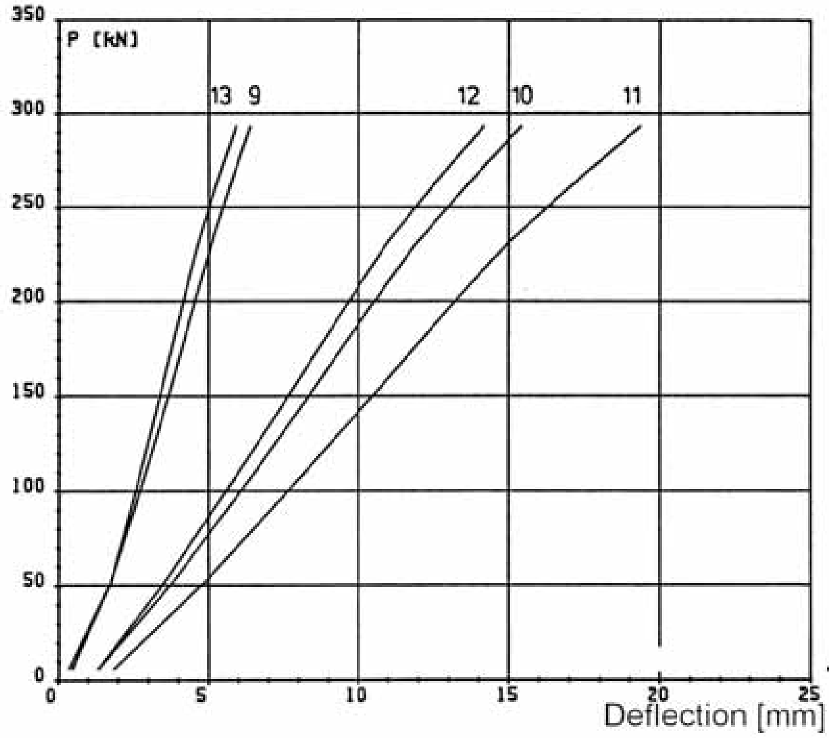

Fig. 26. Stage II.

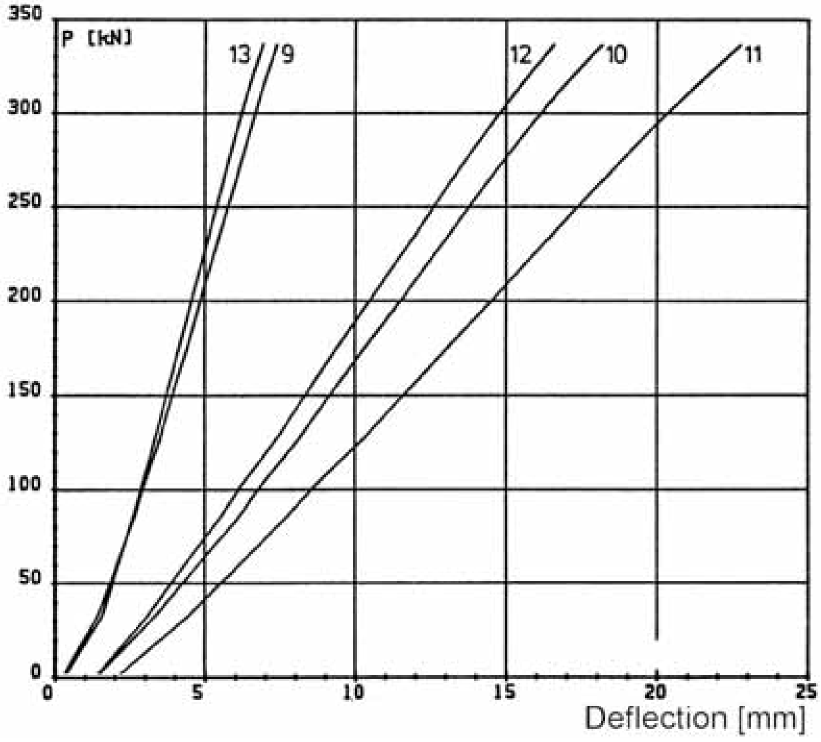

Fig. 27. Stage III.

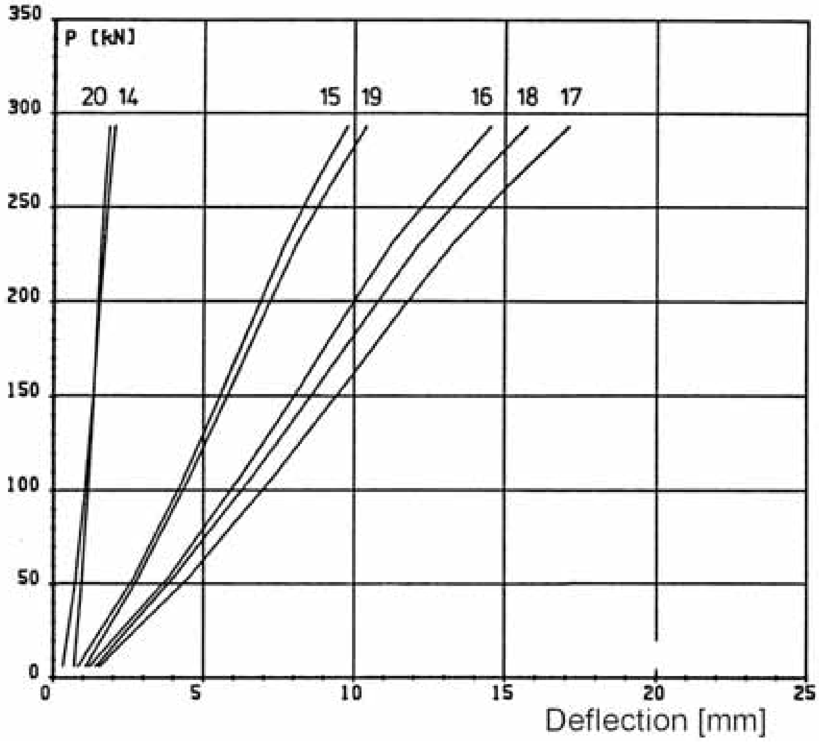

Fig. 28. Stage II.

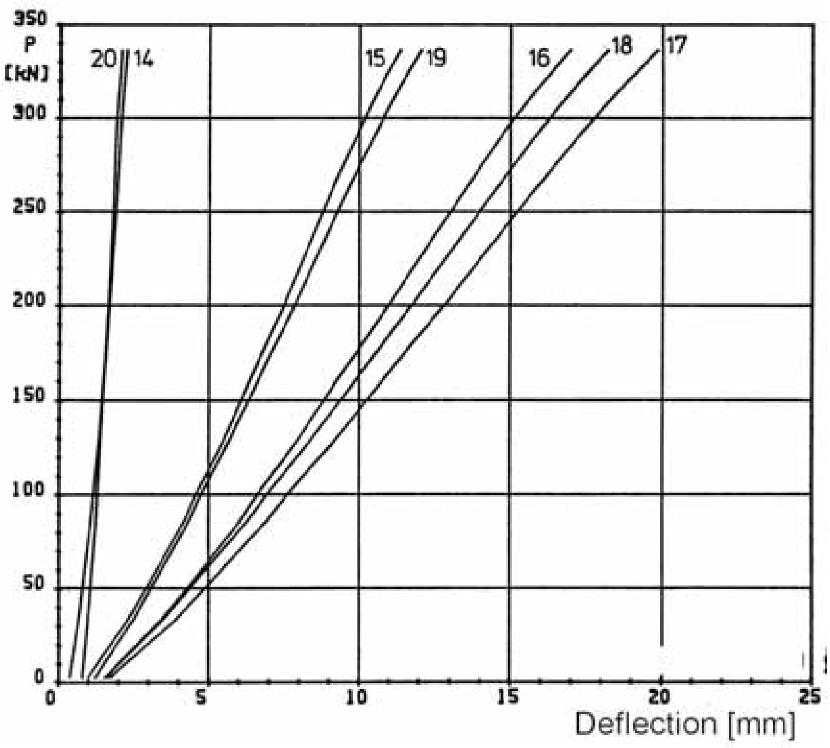

Fig. 29. Stage III.

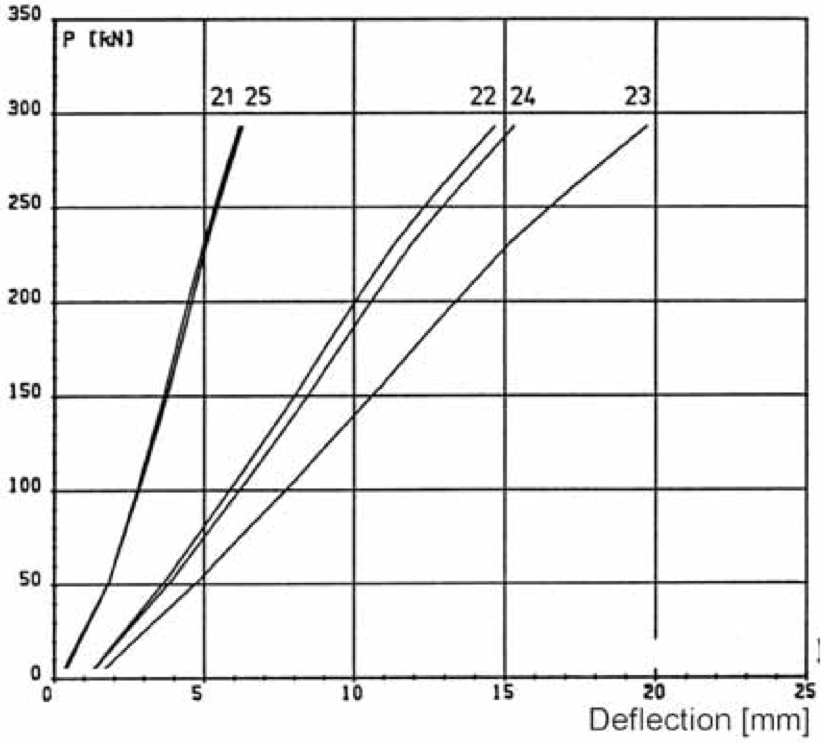

Fig. 30. Stage II.

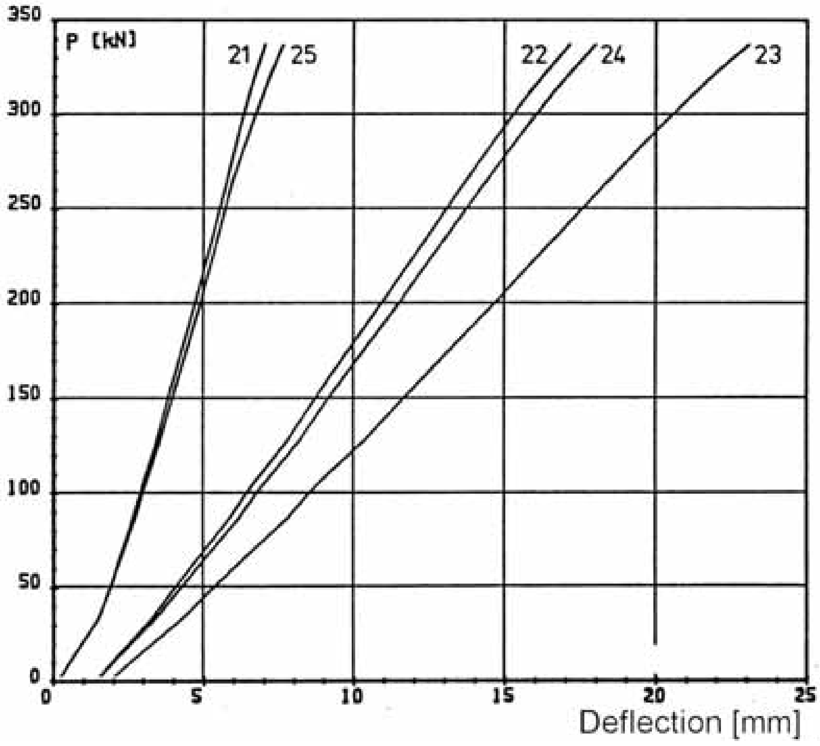

Fig. 31. Stage III.

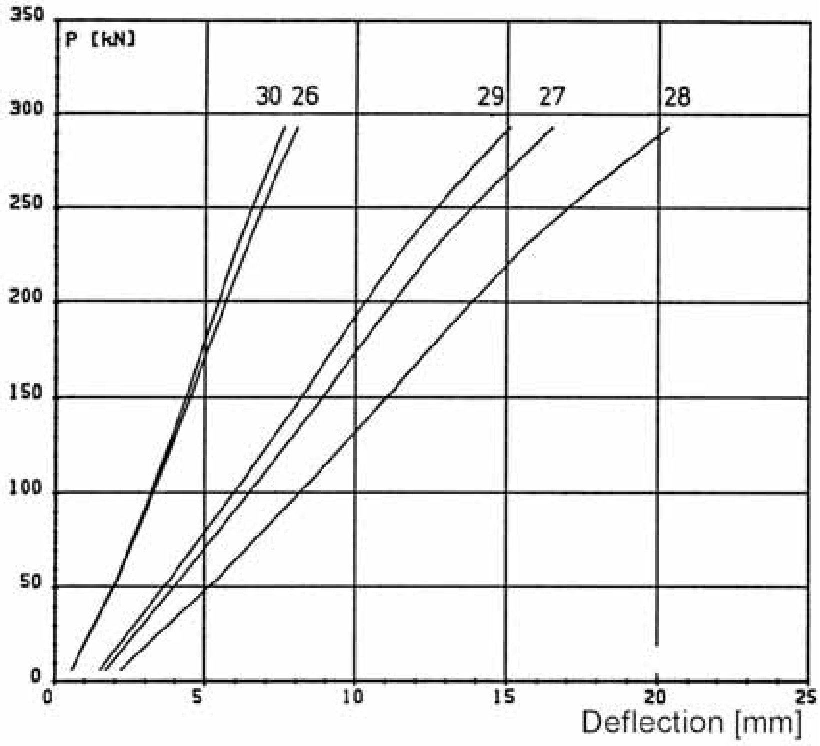

Fig. 32. Stage II.

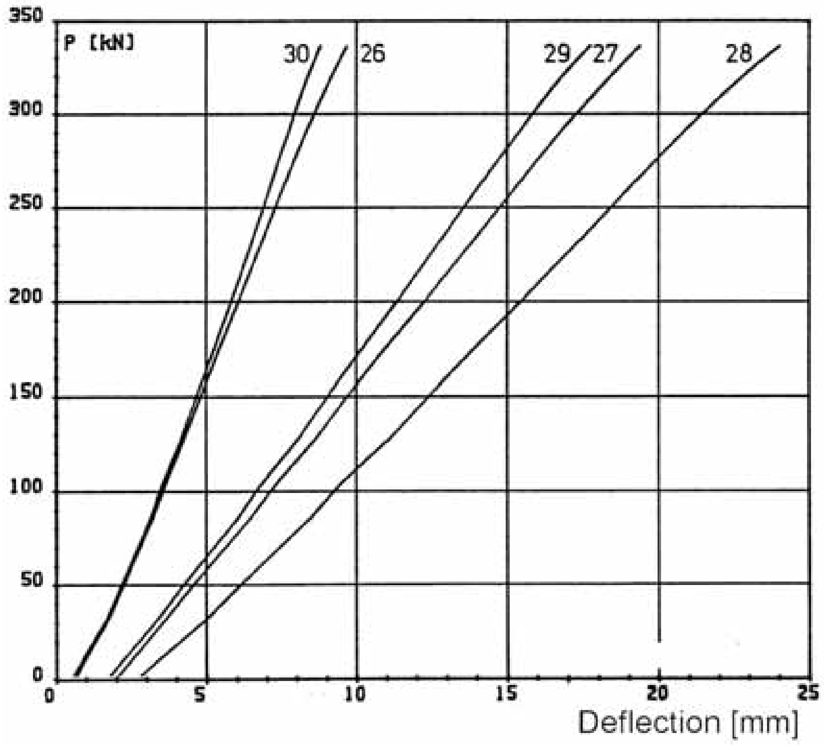

Fig. 33. Stage III.

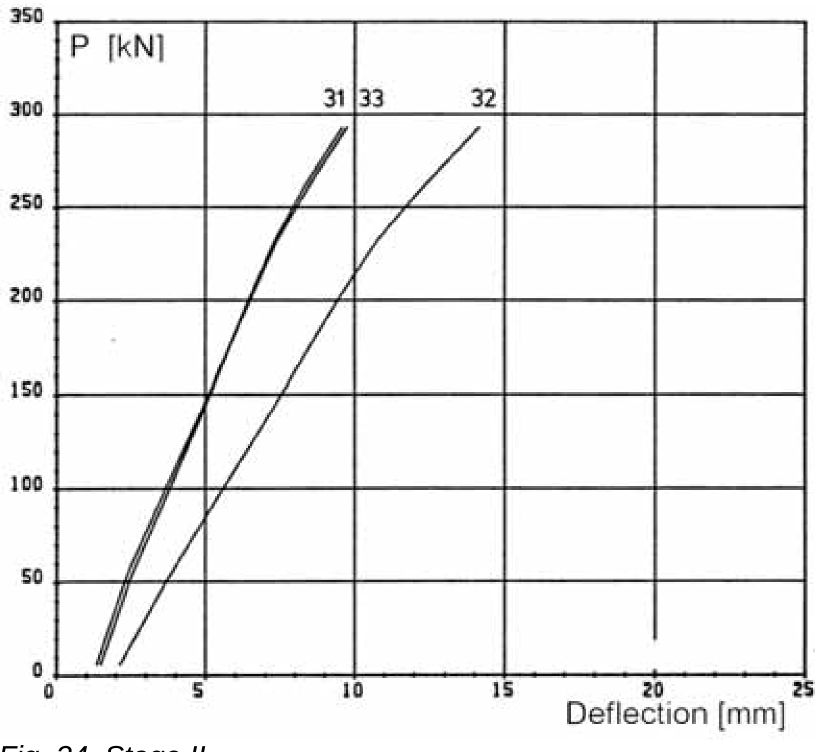

Fig. 34. Stage II.

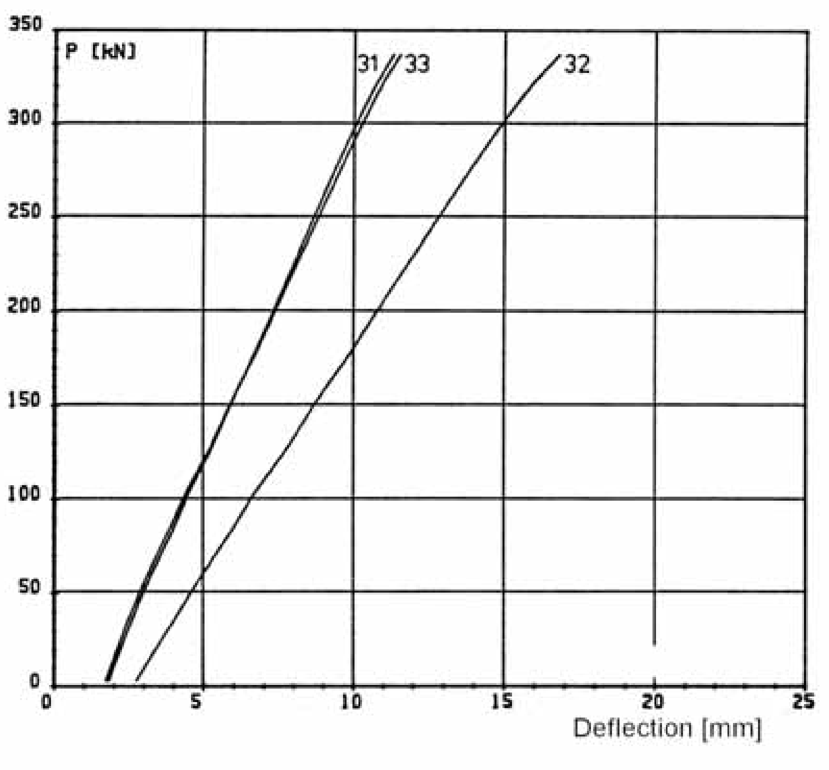

Fig. 35. Stage III.

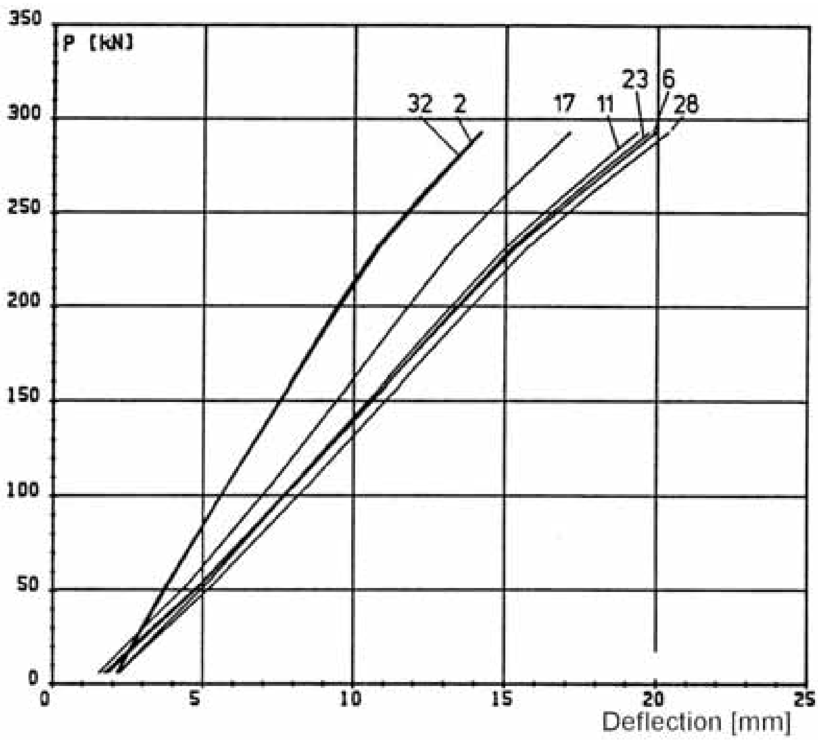

Fig. 36. Stage II.

	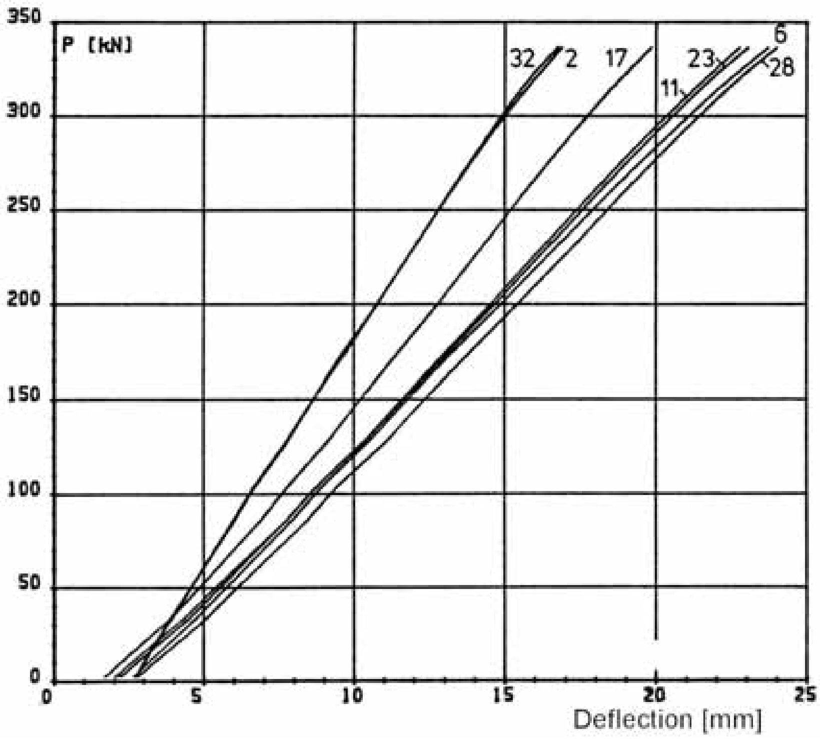 *Fig. 37. Stage III.*
10.2 Crack width	The differential displacement measured by horizontal transducers 34–39 reflect the crack width in the joint concrete next to the WQ-beam. These differential displacements in stages II and III are shown in Figs 38 and 39. 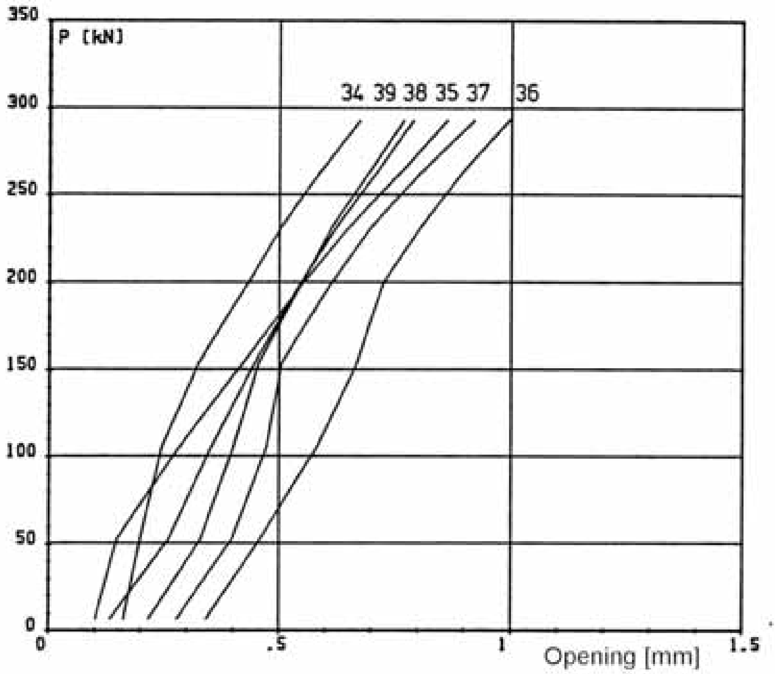 *Fig. 38. Stage II.*

	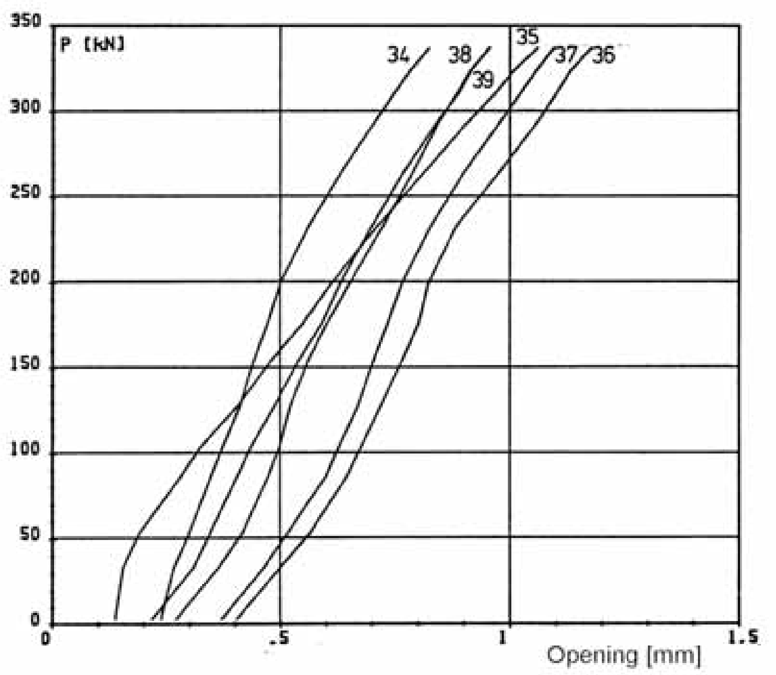 *Fig. 39. Stage III.*
10.3 Average strain	-
10.4 Differential horizontal displacement	A positive value means that the concrete is moving towards the beam end. 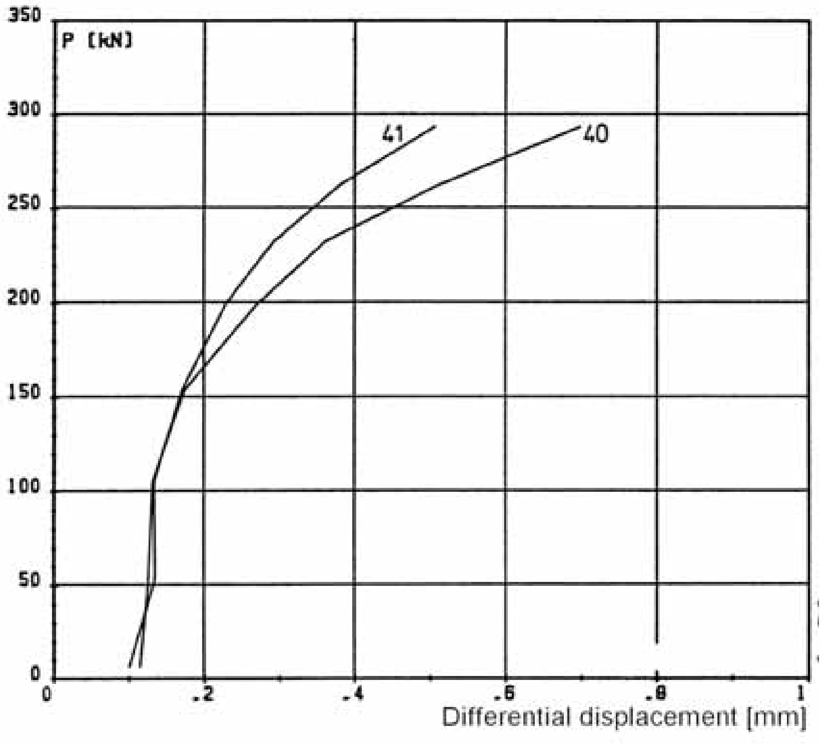 *Fig. 40. Stage II.*

	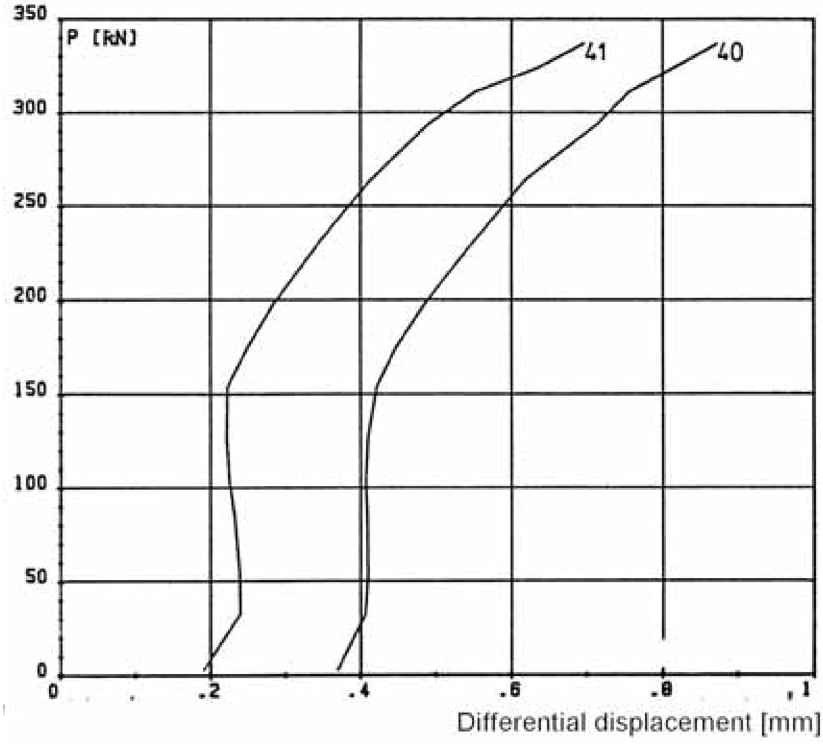 *Fig. 41. Stage III.*
10.5 Differential vertical displacement	A positive value means that the slab end is deflecting more than the beam. 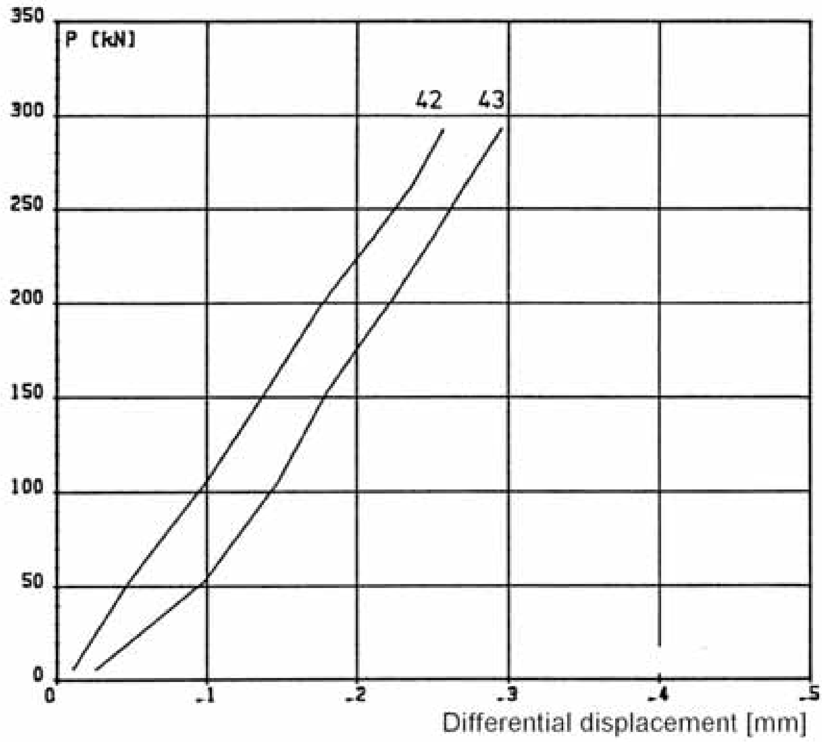 *Fig. 42. Stage II.*

	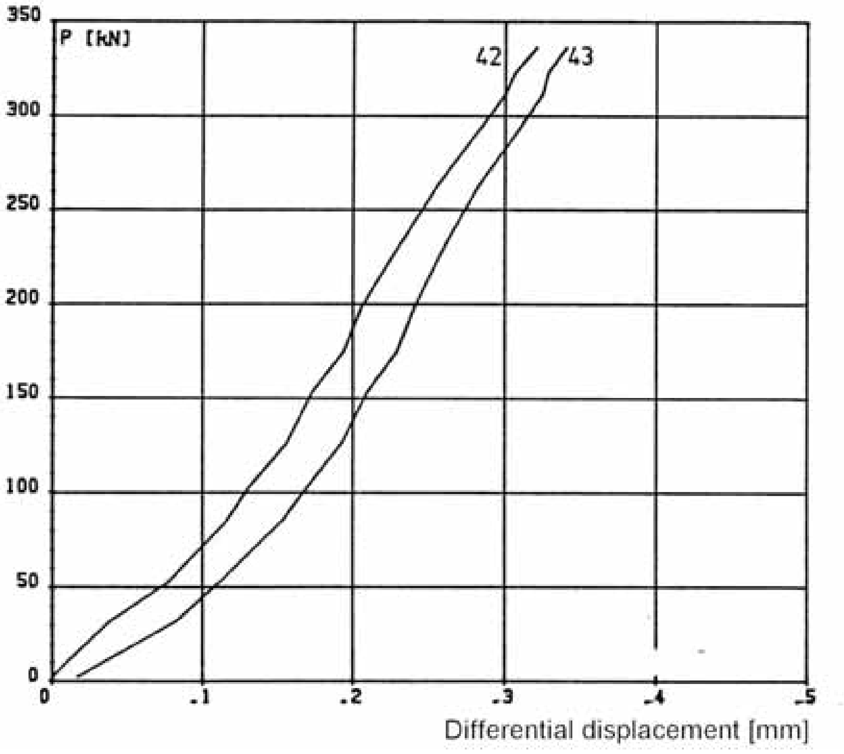 *Fig. 43. Stage III.*
10.6 Strain	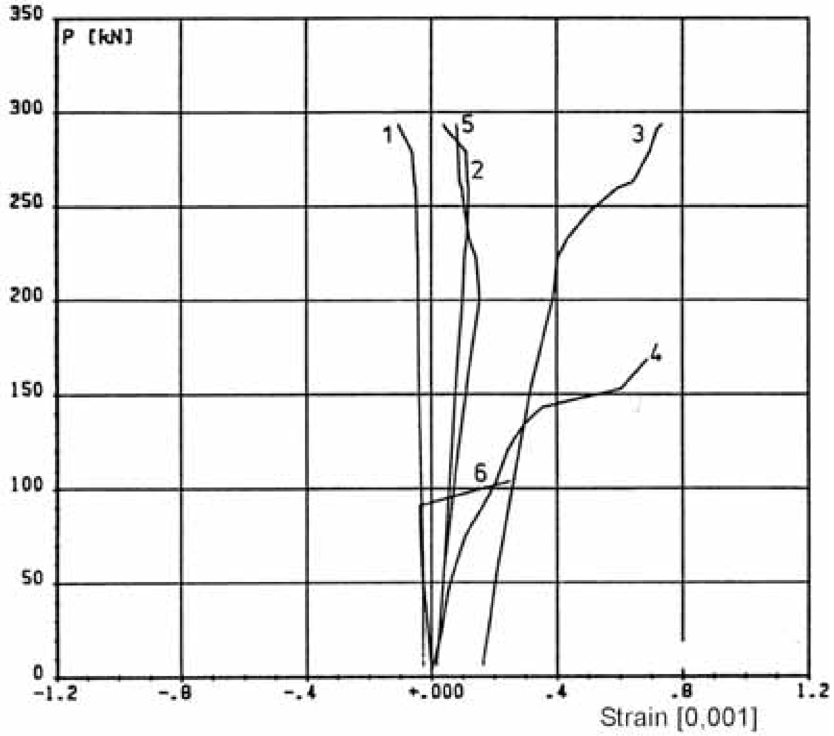 *Fig. 44. Stage II.*

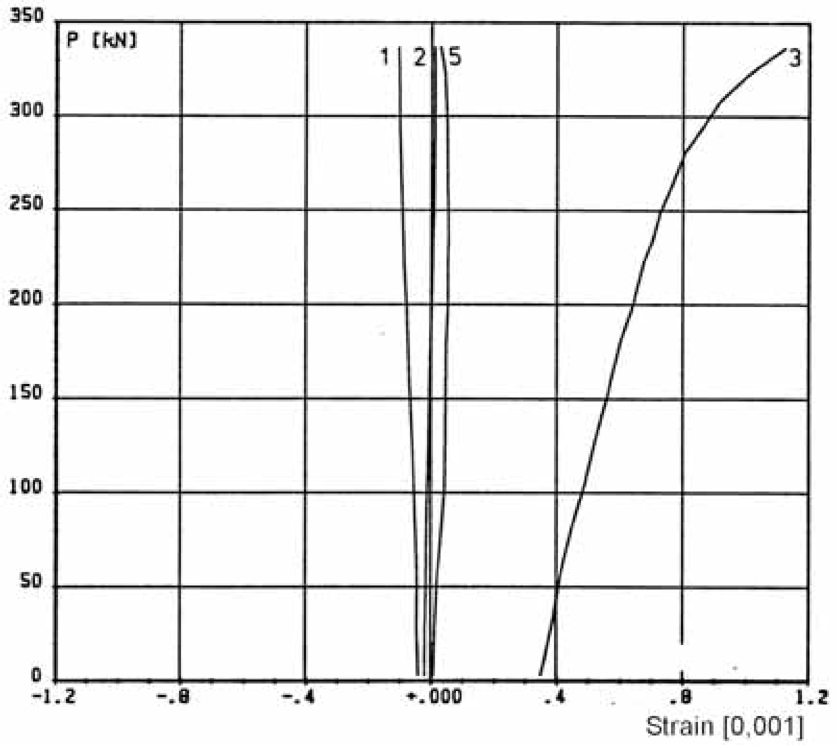

Fig. 45. Stage III.

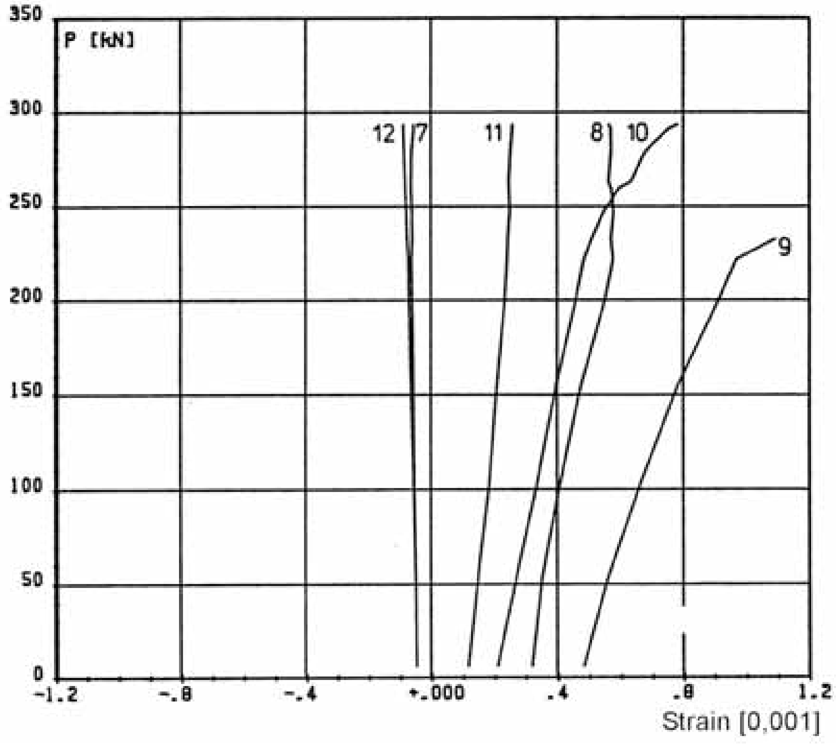

Fig. 46. Stage II.

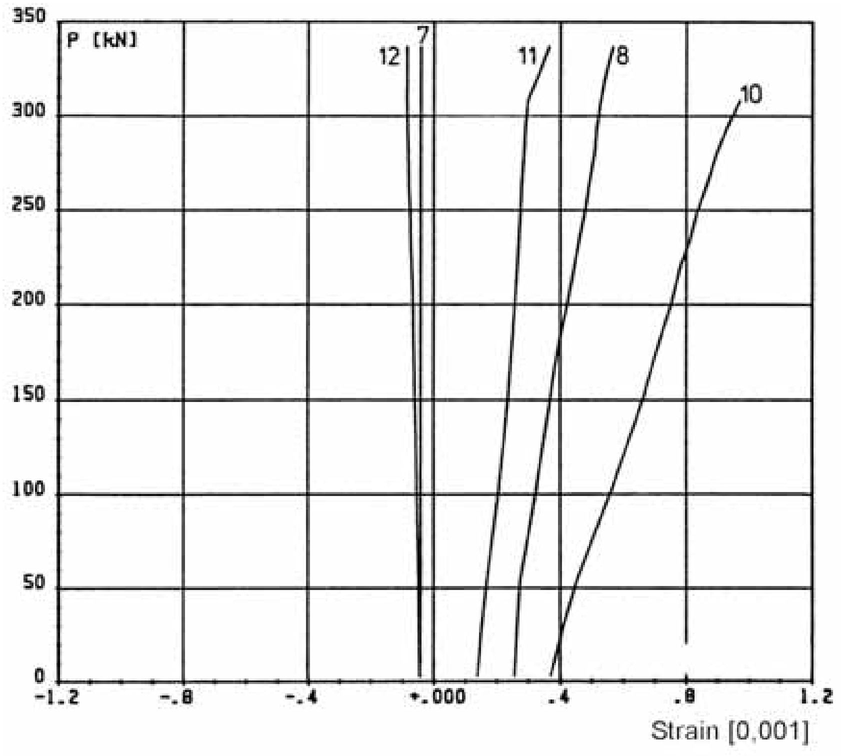

Fig. 47. Stage III.

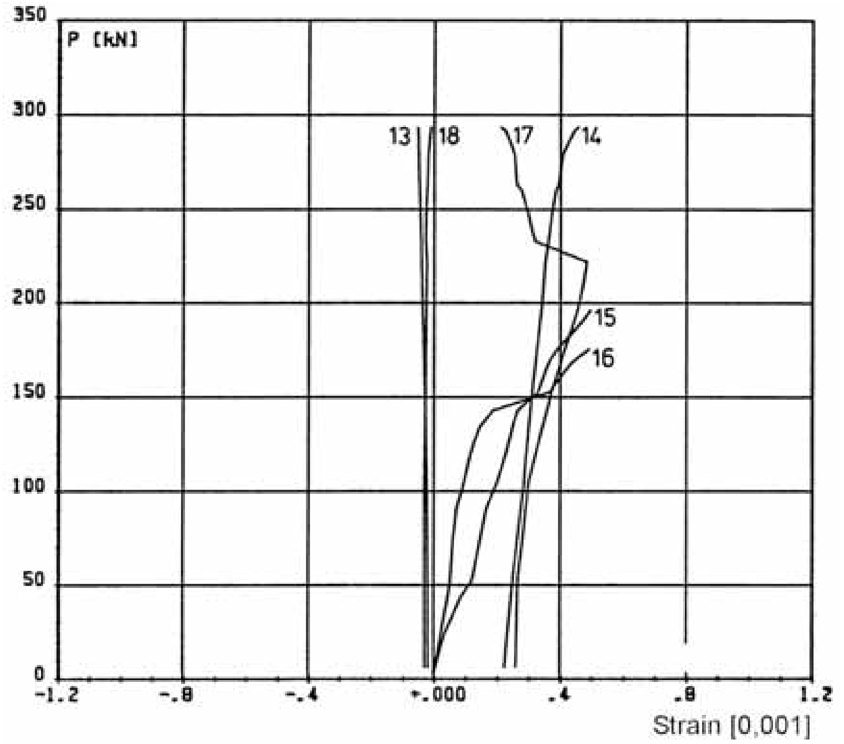

Fig. 48. Stage II.

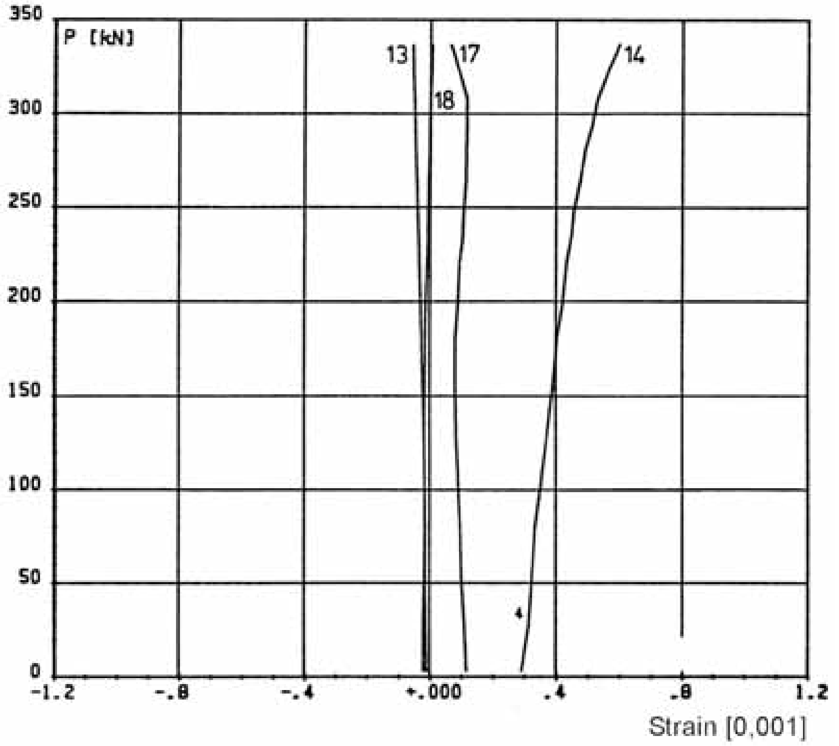

Fig. 49. Stage III.

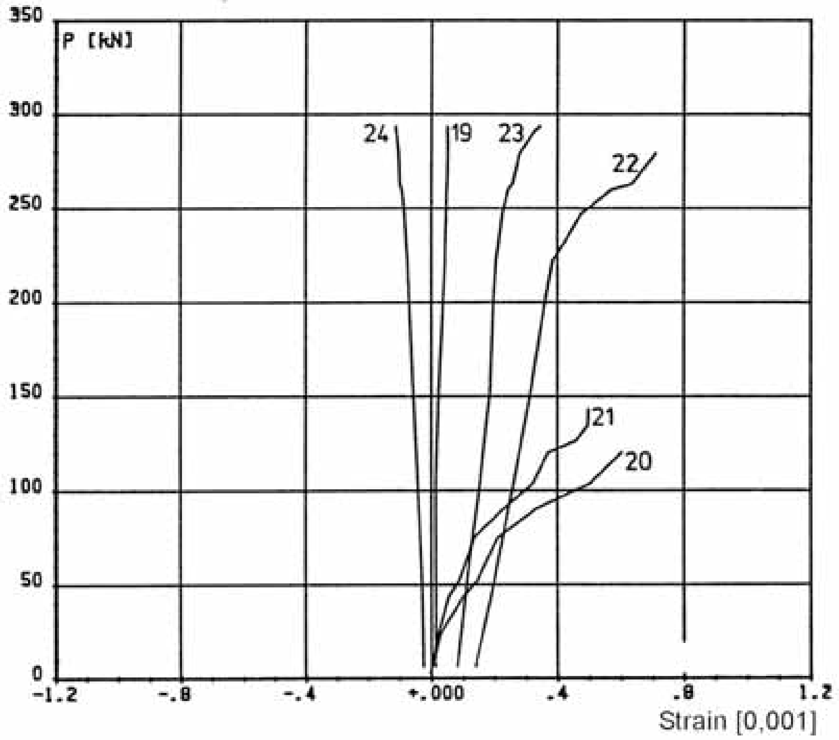

Fig. 50. Stage II.

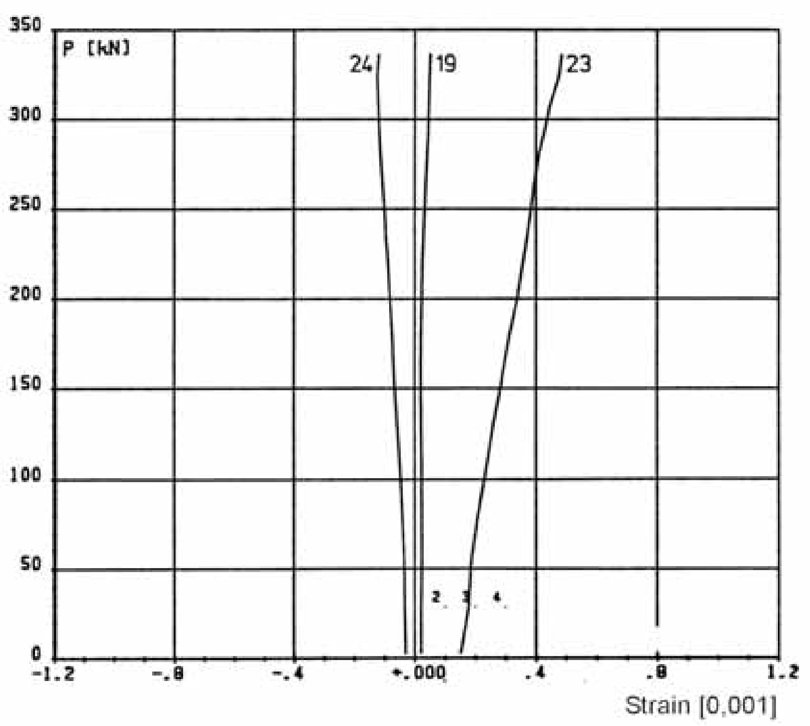

Fig. 51. Stage III.

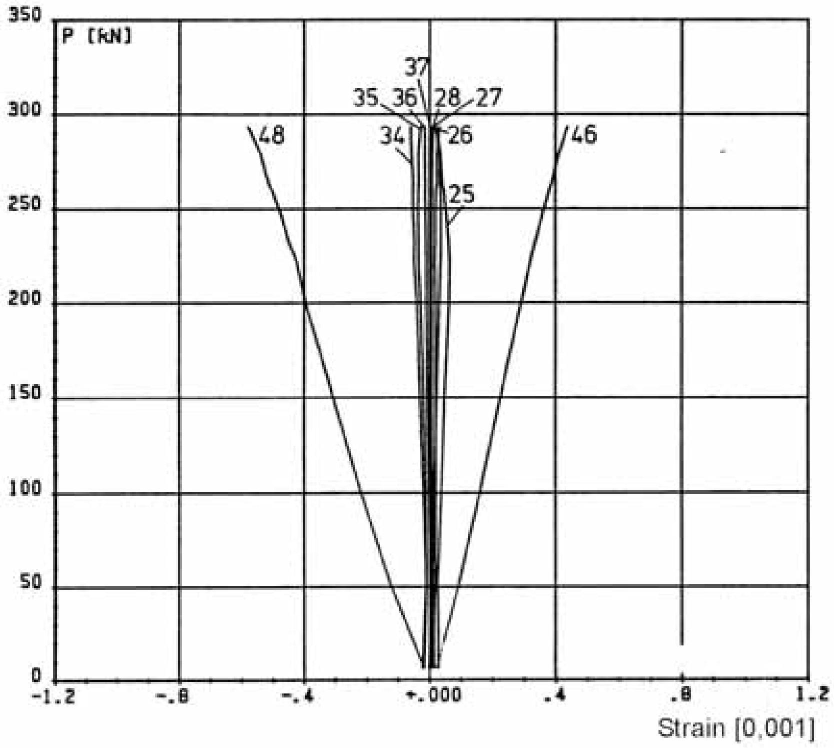

Fig. 52. Stage II.

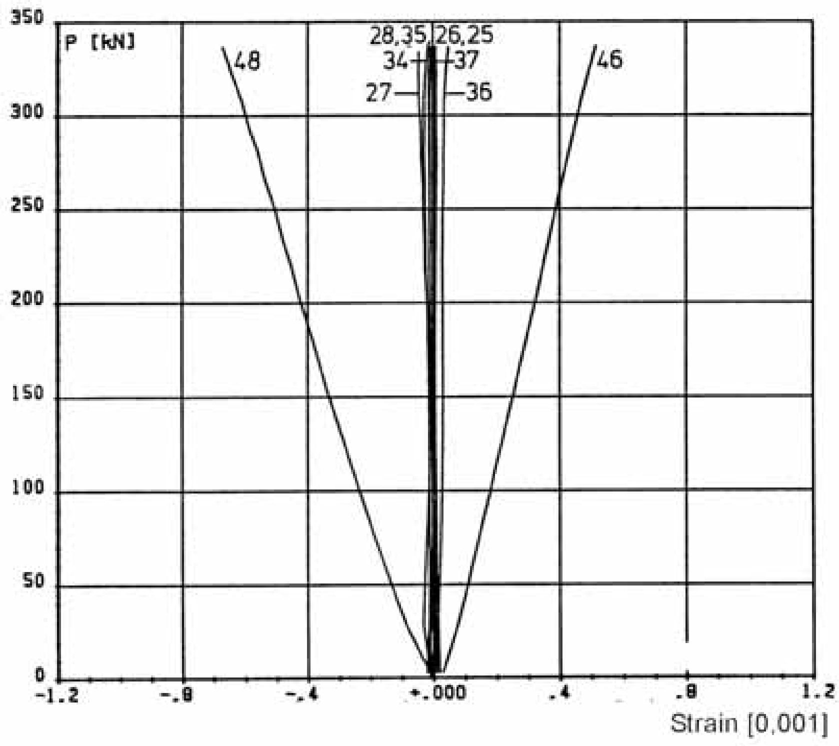

Fig. 53. Stage III.

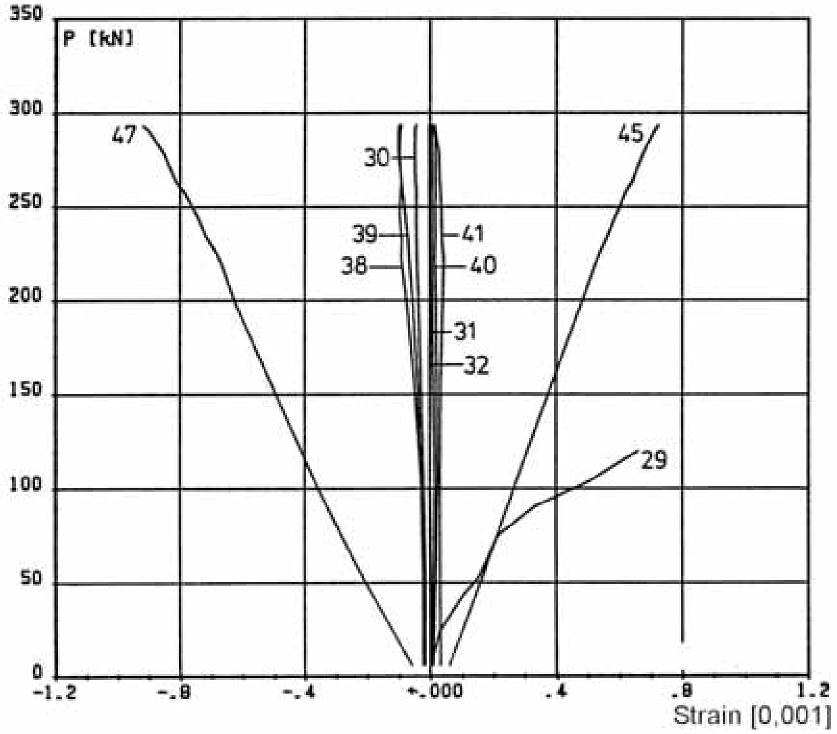

Fig. 54. Stage II.

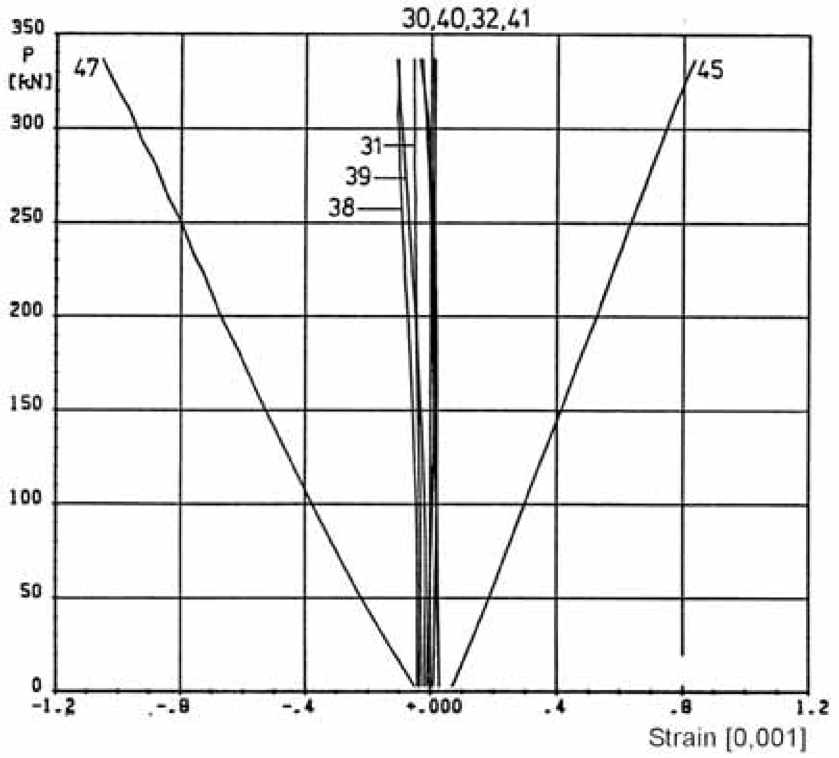

Fig. 55. Stage III.

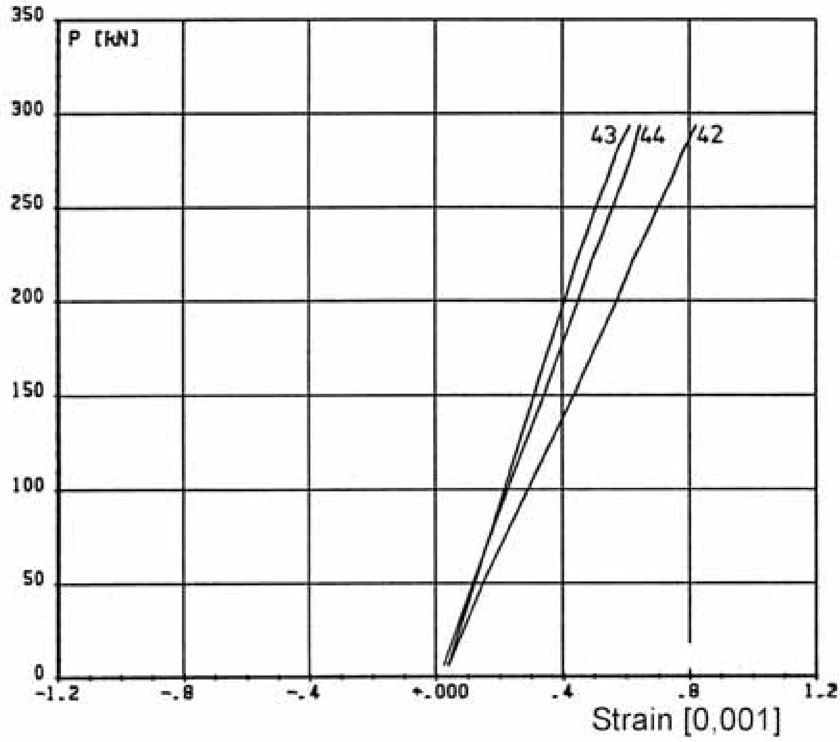

Fig. 56. Stage II.

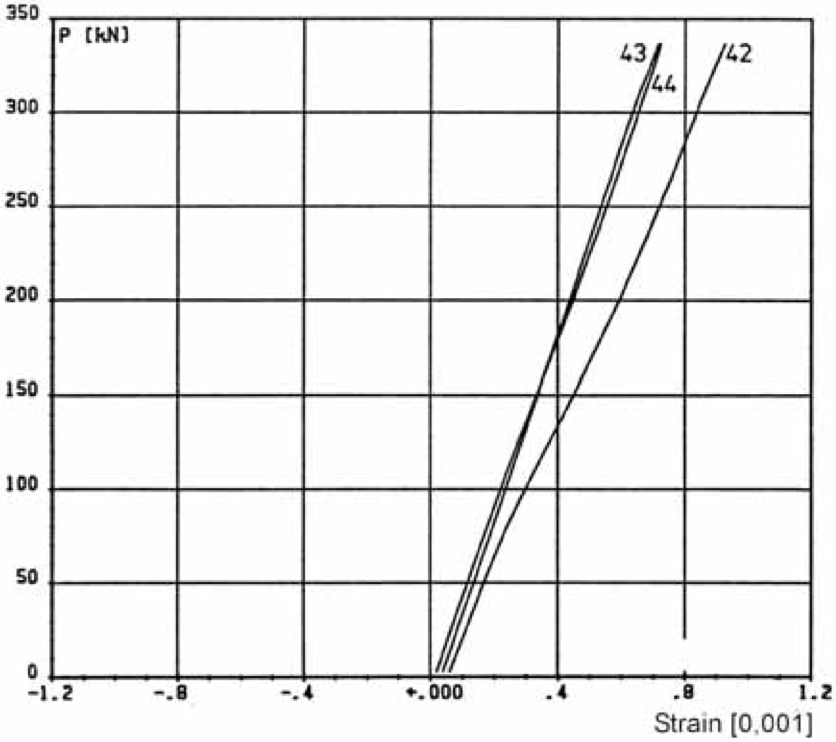

Fig. 57. Stage III.

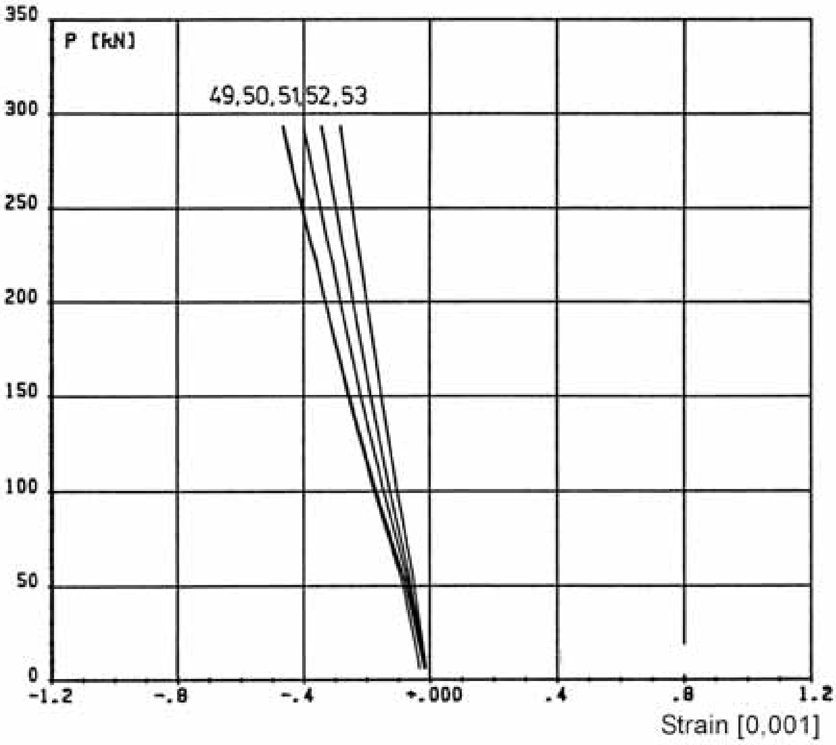

Fig. 58. Stage II.

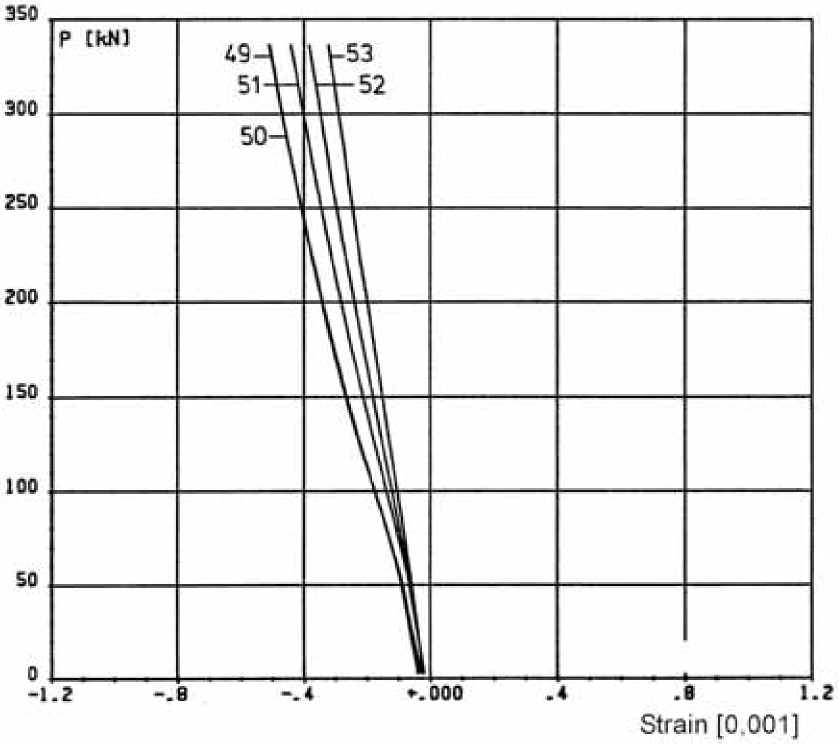

Fig. 59. Stage III.

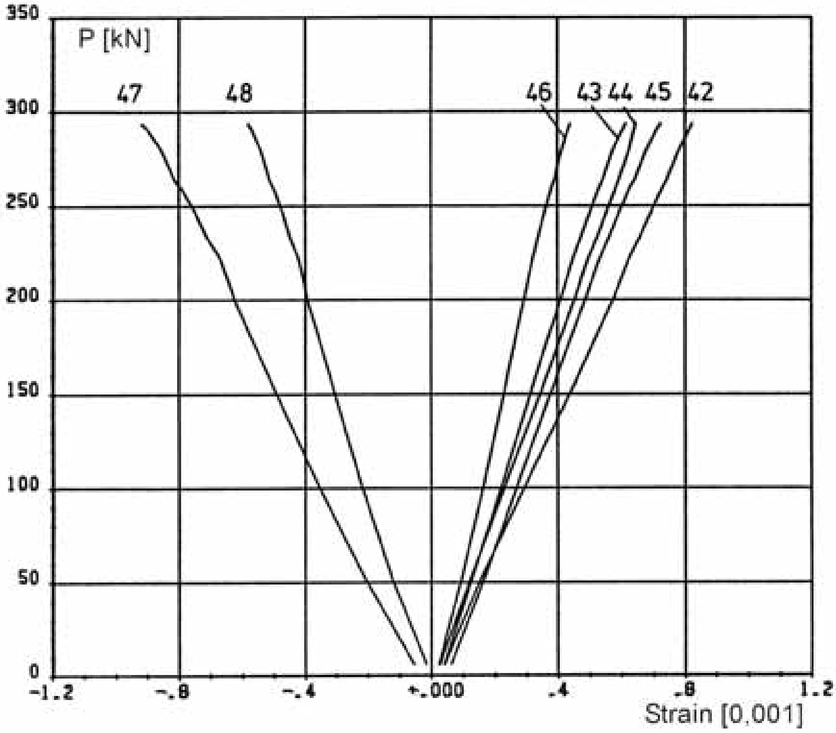

Fig. 60. Stage II.

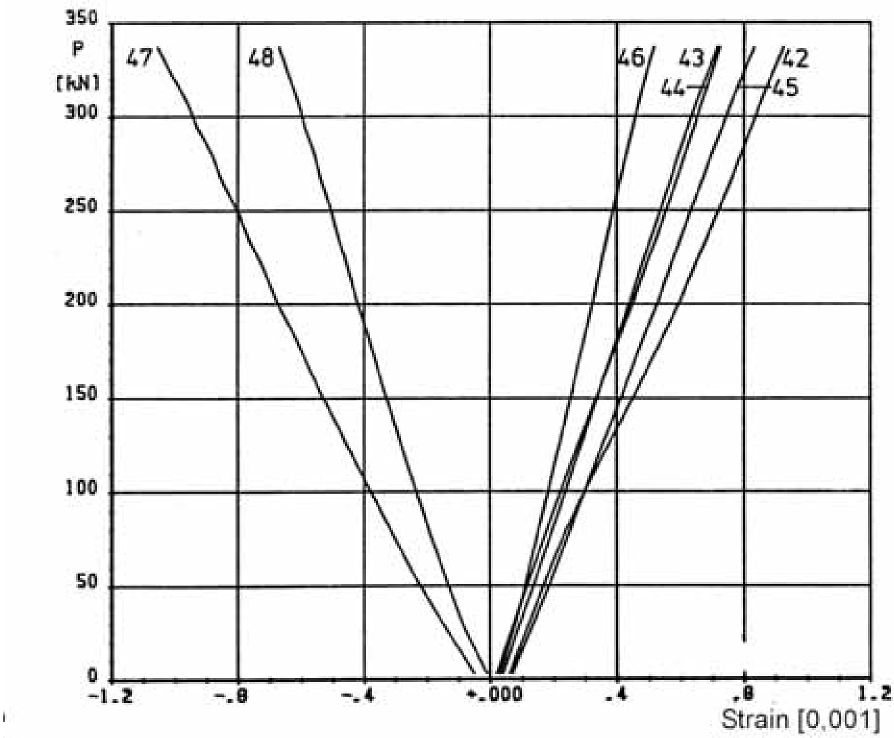

Fig. 61. Stage III.

11 Reference tests

After the floor test, slabs 3 and 5 were taken for reference test specimens. Their ends which had been supported by the end beams, were loaded in shear as shown in Fig. 62. The concrete tie beam partly outside the slab end, partly in the hollow cores, was not removed before loading.

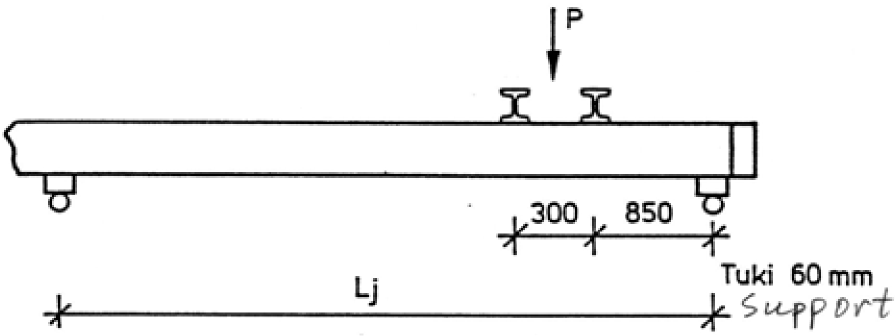

Fig. 62. Layout of reference test. For L_j, see the next table.

Table. Reference tests. Span of slab, shear force V_g at support due to the self weight of the slab, actuator force P_a at failure + weight of loading equipment P_{eq}, total shear force V_{obs} at failure and total shear force v_{obs} per unit width.

Test	Date	Span mm	V_g kN	P_a+P_{eq} kN	V_{a+eq} kN	V_{obs} kN	v_{obs} kN/m	Note
R3	12.10.1990	5940	12,3	285,5	237,4	249,6	208,0	Web shear failure
R7	12.10.1990	5950	12,3	239,5	199,2	211,4	176,2	Web shear failure
				Mean		**230,5**	**192,1**	

12	**Comparison: floor test vs. reference tests**
	The observed shear resistance (support reaction) of the hollow core slab in the floor test was equal to 166,1 kN per one slab unit or 138,4 kN/m. This is **72%** of the mean of the shear resistances observed in the reference tests.
13	**Discussion**
	1. The friction between the spreader beams was not eliminated, which may have affected the response of the floor test specimen to some extent. 2. The last measured net deflection of the middle beam due to the imposed actuator loads only (deflection minus settlement of supports) was 17,6 mm or *L*/284. It was 4,9–6,2 mm greater than that of the end beams. Hence, the torsional stresses due to the different deflection of the middle beam and end beams may have had a minor effect on the failure of the slabs. 3. The shear resistance measured in the reference tests was of the same order as or slightly higher than the mean of the observed values for similar slabs given in *Pajari, M. Resistance of prestressed hollow core slab against a web shear failure. VTT Research Notes 2292, Espoo 2005*. The concrete tie beam at the sheared end may have enhanced the resistance. It prevented the deformation of the end section of the slab and thus equalized the strains in the webs of the slab, which effectively eliminated the premature failure of any individual web. 4. The beams did not yield in the floor test. 5. The failure mode was web shear failure of edge slabs close to the supports of the middle beam. Unlike in an isolated hollow core slab unit, in the floor test the appearance of the first inclined crack close to the slab end did not mean failure but the loads could still be increased.

1	**General information**
1.1 Identification and aim	**VTT.PC.InvT.265.1990** **Last update 2.11.2010** PC265 (Internal identification). Aim of the test: To study whether or not the shear resistance of the hollow core slabs is reduced when supported on a shallow prestressed concrete beam
1.2 Test type	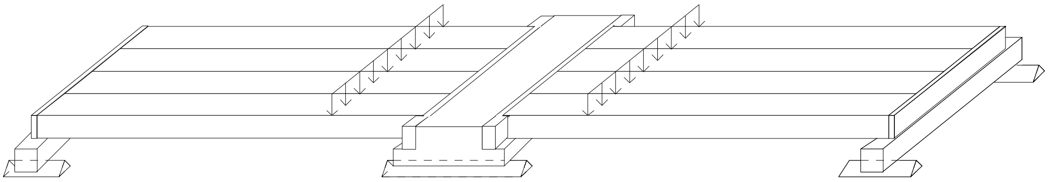 *Fig. 1. Illustration of test setup.*
1.3 Laboratory & date of test	VTT/FI 14.–19.11.1990
1.4 Test report	Author(s): Koukkari, H. Name: *Matalien leukapalkkien ja ontelolaataston kuormituskokeet (Load tests on shallow beams and hollow core floor)*, in Finnish Ref. number: RAT01854/90 Date: 28.11.1990 Availability: Confidential, owner is Rakennustuoteteollisuus RTT ry, P.O. Box 381, FI-00131 Helsinki
2	**Test specimen and loading**
2.1 General plan	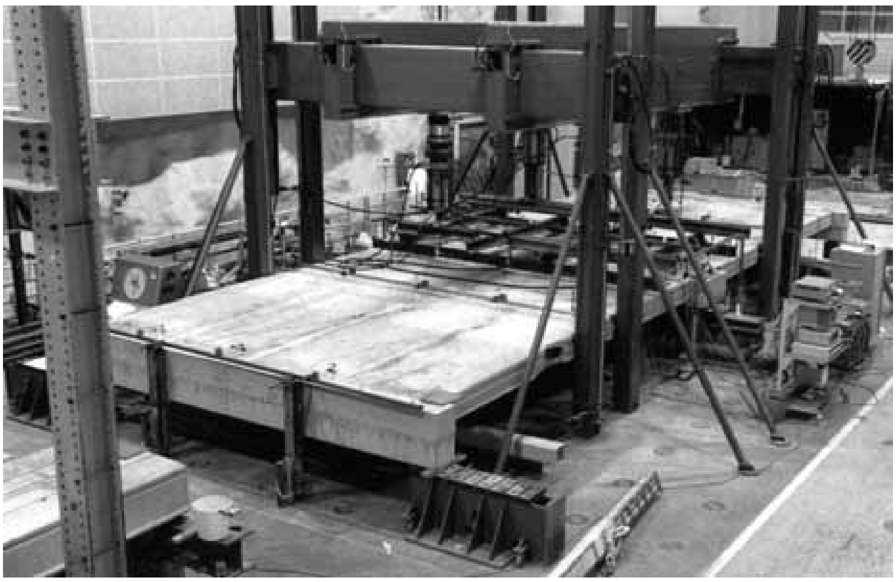 *Fig. 2. Overview on arrangements.*

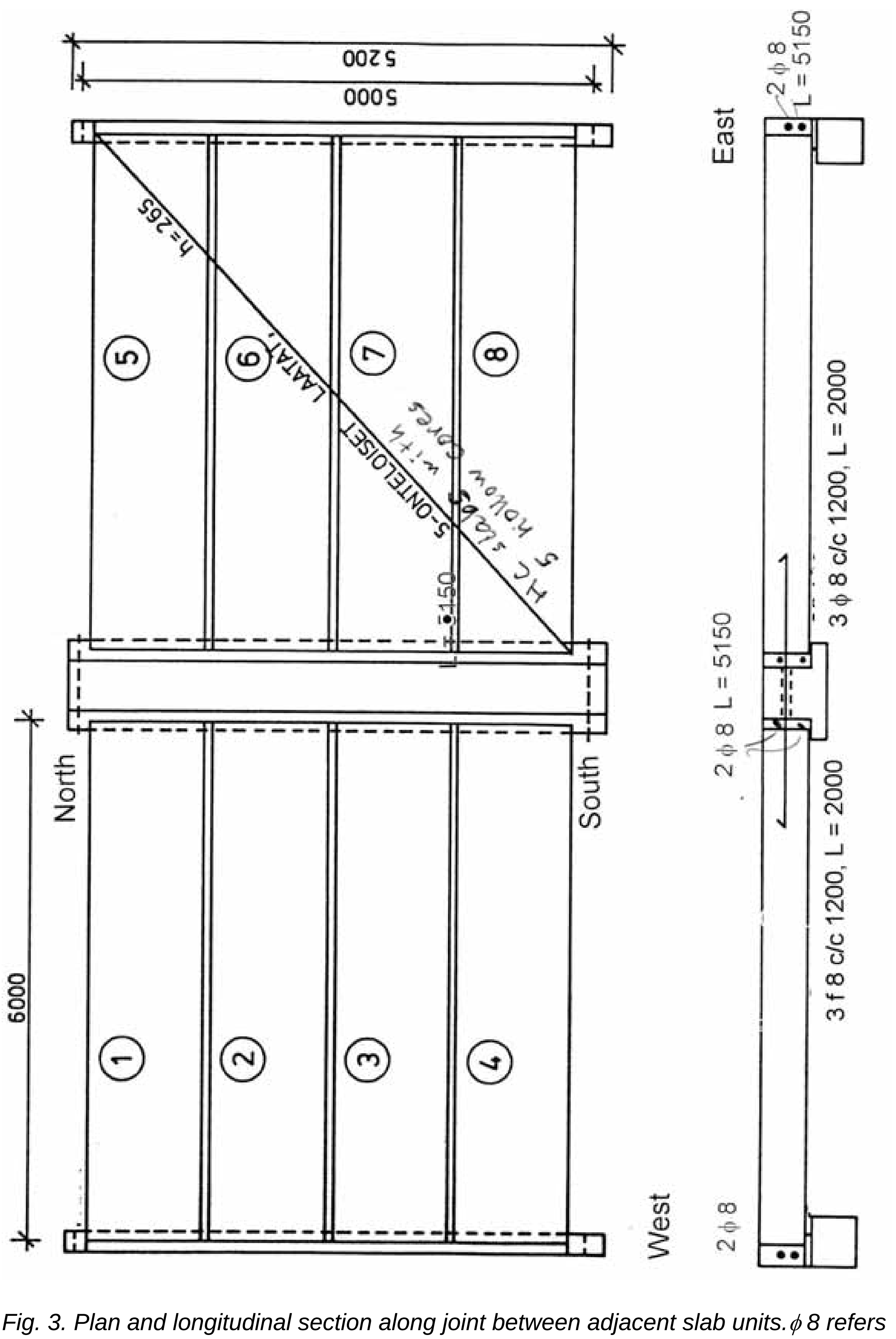

Fig. 3. Plan and longitudinal section along joint between adjacent slab units. ϕ 8 refers to rebar T8, see 9.1.Note the tie reinforcement 3T8 c/c 1200 in the longitudinal joints of slabs and rebars (1+2+1) T8 tying the slab ends at the ends of the specimen and on both sides of the PC beam.

<table>
<tr><td>2.2
End beams</td><td>
- Reinforced concrete beam
- Made by Lohja Oy, delivered to VTT on the 2nd of August 1990
- Simply supported, span = 5,0 m
- Concrete K40

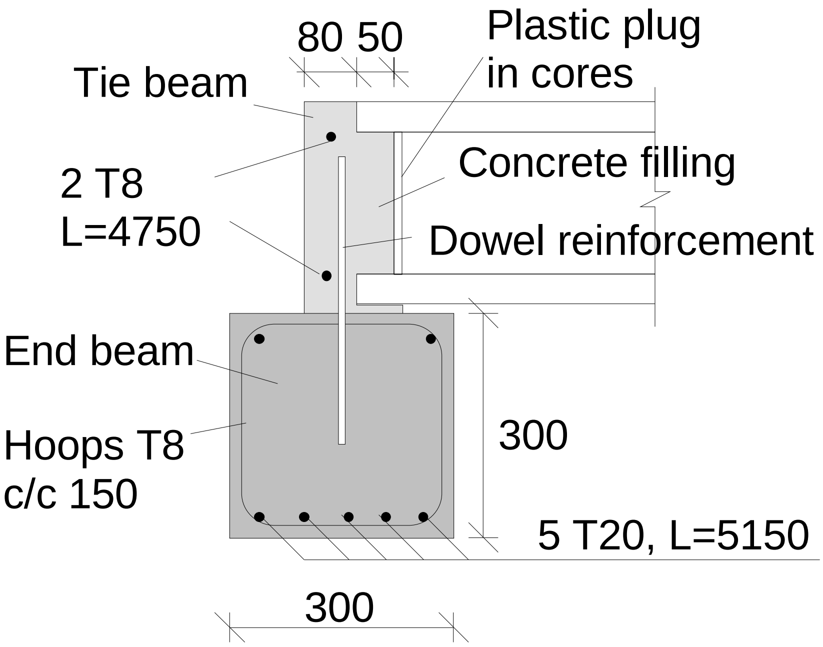

Fig. 4. Arrangements at end beam. Txy refes to a rebar with diameter xy mm, see 9.1. The size and spacing of the dowel reinforcement has not been given in the report.
</td></tr>
<tr><td>2.3
Middle beam</td><td>
The beam was designed to carry the support reactions from the slabs, somewhat lower than those corresponding to the estimated shear resistance of the slab ends on non-flexible support. The beam was manufactured by Lohja Oy in Nummela factory and it was delivered to VTT on the 2nd of August 1990. The measured camber of the beam was 20,6 mm.

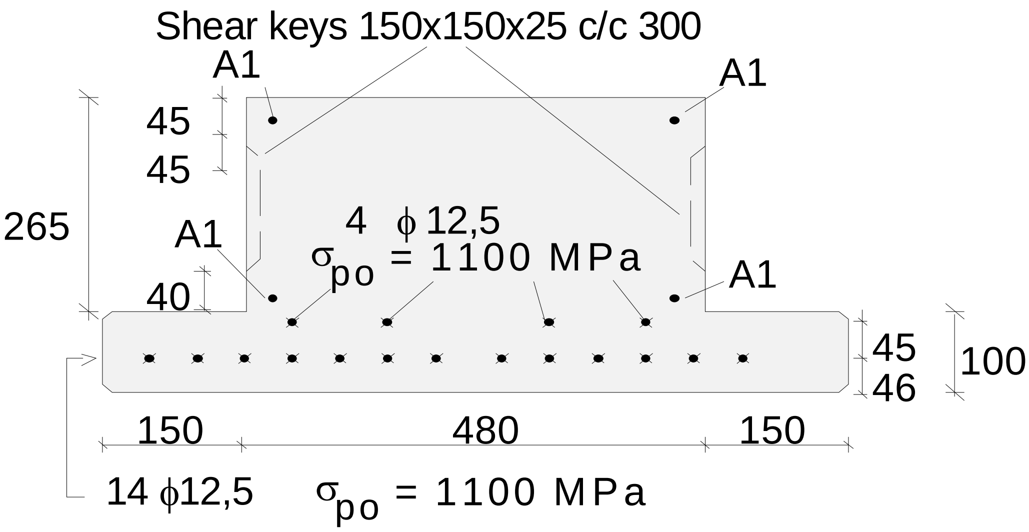

Fig. 5. Cross-section of PC beam. ϕ12,5 refers to a prestressing strand J12,5 and A1 to a rebar T12, see 9.1. Concrete K60.
</td></tr>
</table>

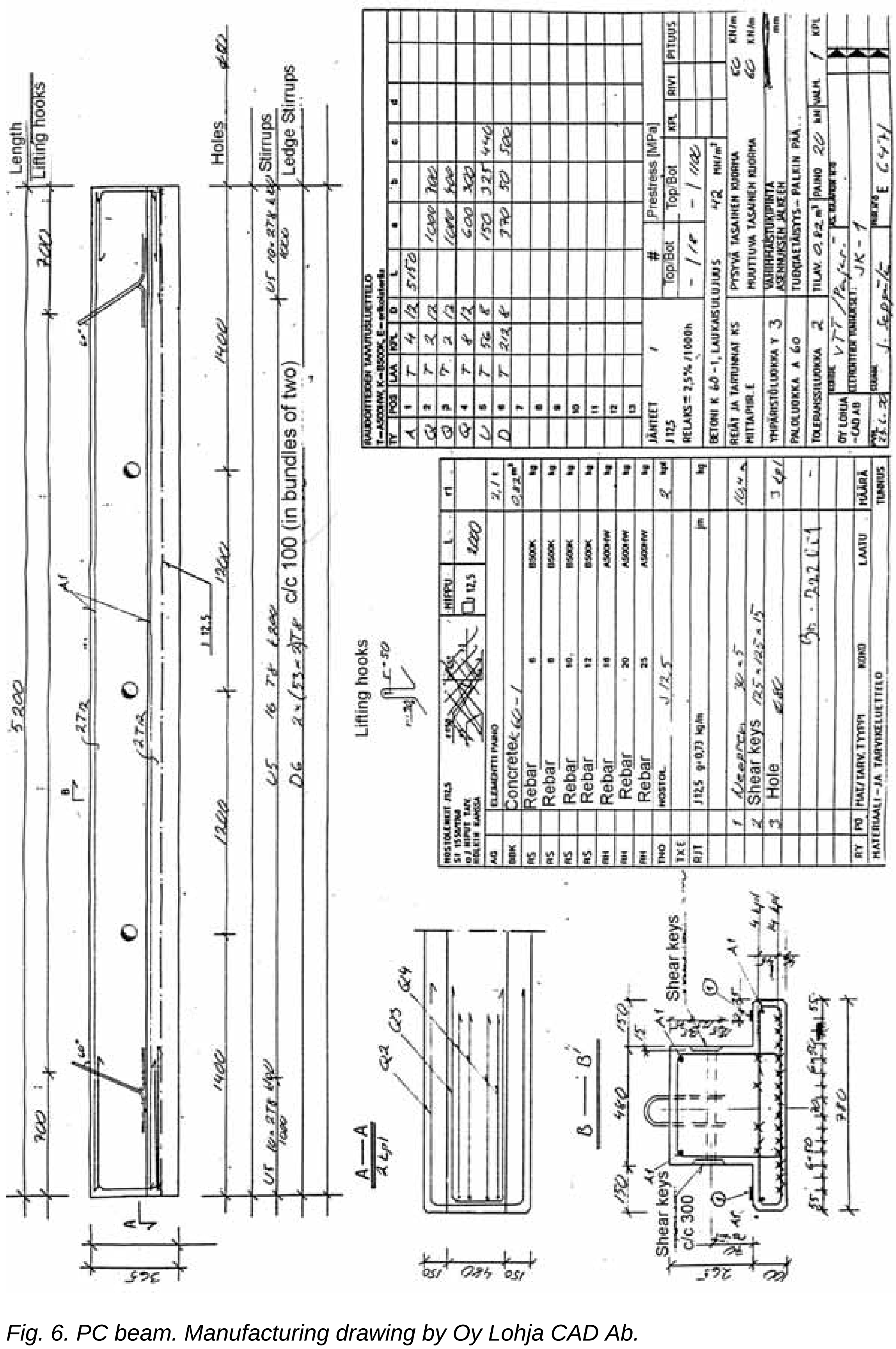

Fig. 6. PC beam. Manufacturing drawing by Oy Lohja CAD Ab.

J12,5: 7 indented wires, ϕ =12,5 mm, A_p = 93 mm^2, low relaxation (<2,5% 100 h)

2.4 Arrangements at middle beam	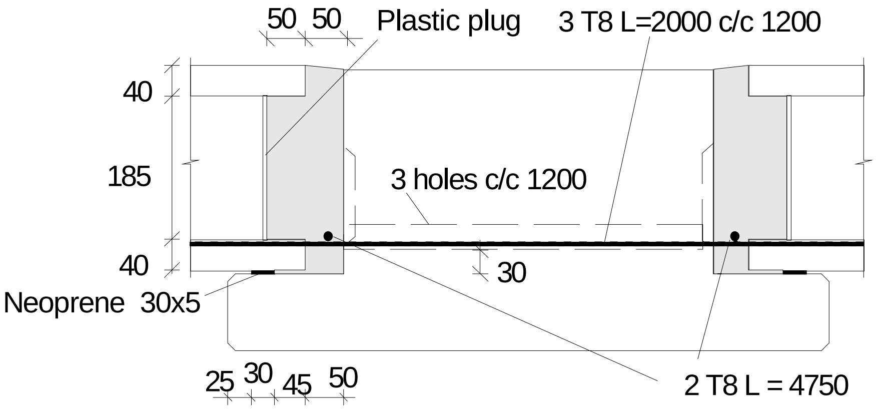 *Fig. 7. Arrangements at middle beam for T8 see 9.1.* - Simply supported, span = 5,0 m - 4 load cells below support at South end - joint concrete K30 cast 7.11.1990, maximum aggregate size 8 mm, consistency 1–2 VBs, rapidly hardening cement
2.5 Slabs	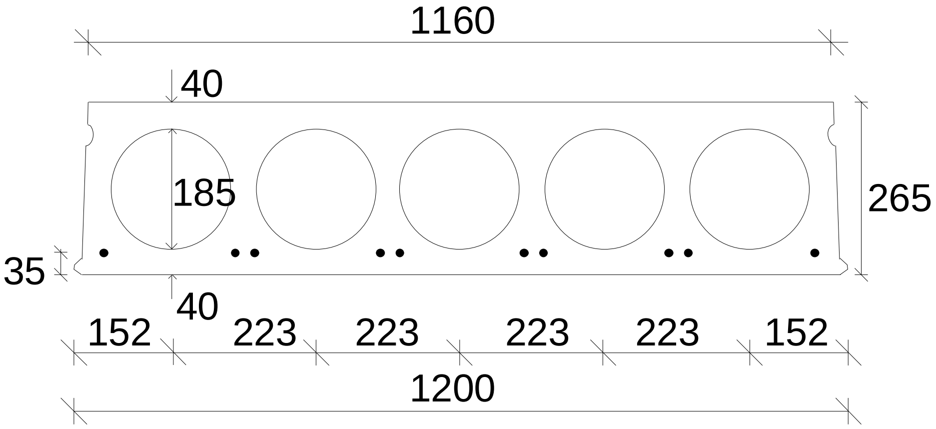 *Fig. 8. Nominal geometry of slab units.* - Extruded by Parma Oy 29.6.1990, the same bed and casting lot as for the slabs in test VTT.S.WQ.265 - delivered to VTT, 18.10.1990 - concrete K60 - 10 lower strands J12,5 initial prestress 1100 MPa **J12,5**: seven indented wires, ϕ =12,5 mm, A_p = 93 mm^2, low relaxation (<2,5% 100 h), see 9.1

2.6 Temporary supports	-
2.7 Loading arrangements	See Fig. 7. There was a gypsum layer between the tertiary beams and the top surface of the slabs. The primary spreader beams were in direct contact with the secondary spreader beams and the secondary beams with the tertiary spreader beams. No attempts were made to eliminate the friction. For this reason it is difficult to evaluate, to which extent the spreader beams participated in the load-carrying mechanism. 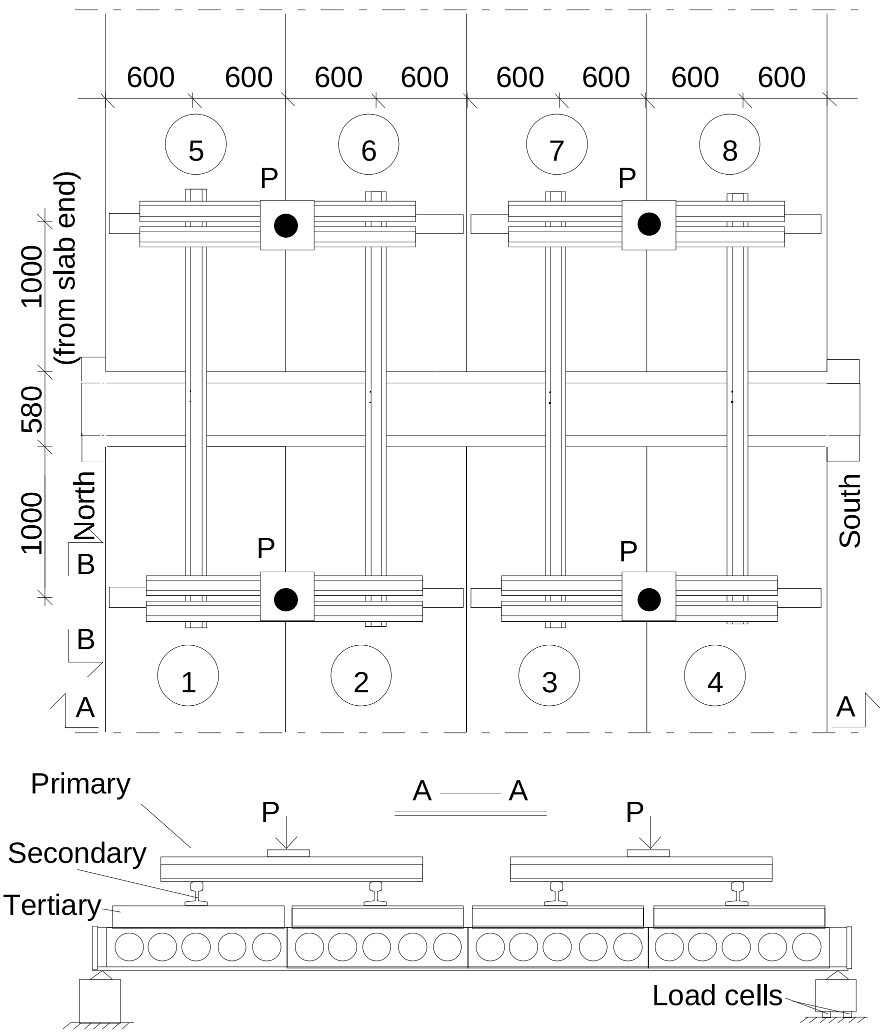 *Fig. 9. Loading arrangement with three layers of spreader beams.*

3	**Measurements**
3.1 Support reactions	There were four load cells below the South end of the PC beam for measuring the support reaction due to the actuator loads.
3.2 Vertical displacement	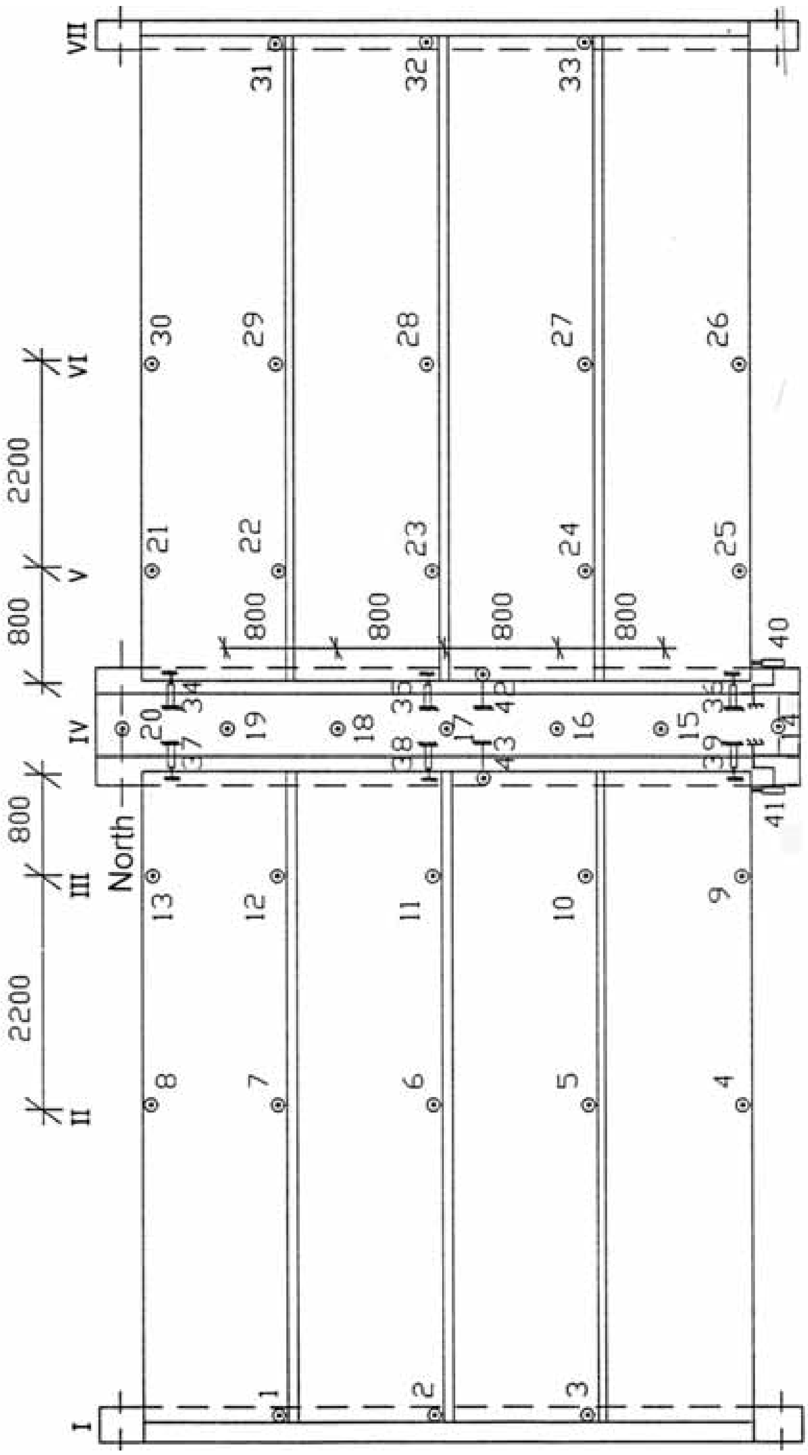 *Fig. 10. Location of transducers 1 … 33 for measuring the vertical deflection, 40 & 41 for measuring the differential horizontal displacement between the end of the beam and the joint concrete (see Figs 11 & 17) and 42 & 43 for measuring differential vertical displacement between the slab end and the beam.*

3.3 Average strain	-
3.4 Horizontal displacements	*See Fig. 8, transducers 34 … 41. Transducers 40 and 41 measured the sliding of the slab along the WQ-beam. Figs 11 and 17 give an impression of the position of these transducers.* 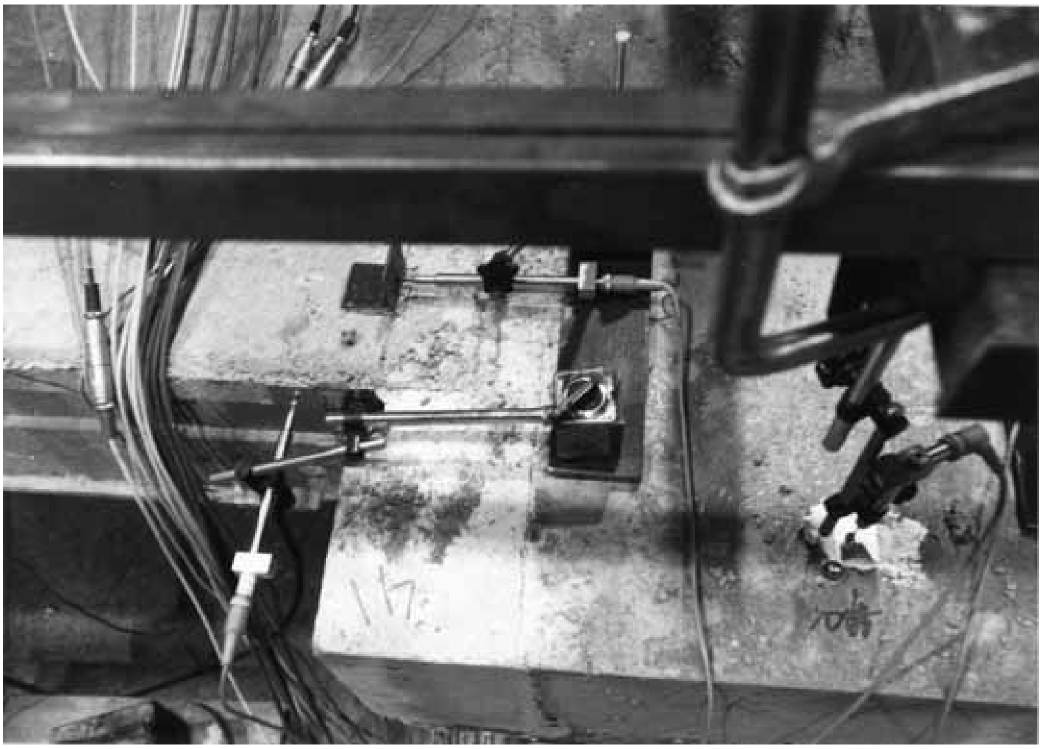 *Fig. 11. Position of horizontal transducers 39 and 41at South end of middle beam.*

3.5 Strain	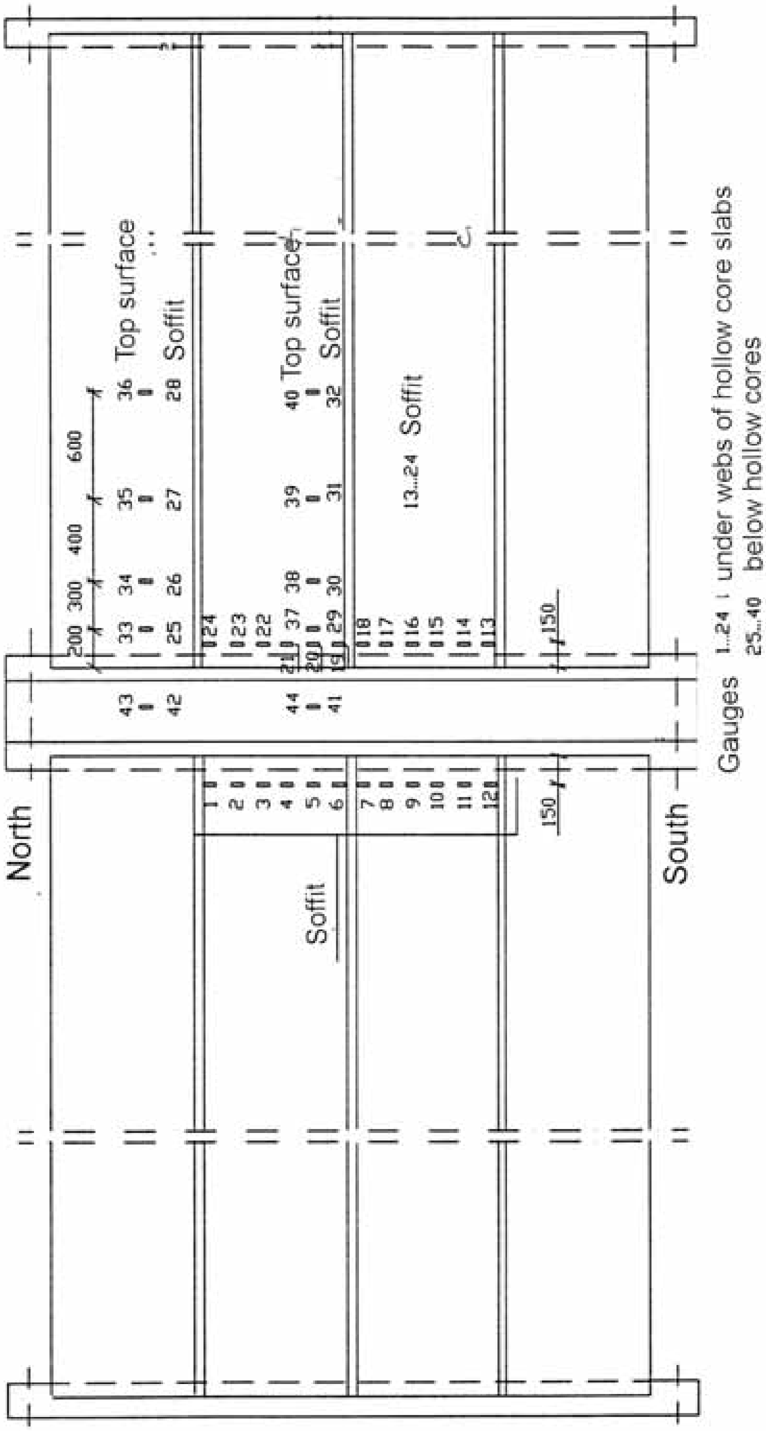 *Fig. 12. Position of strain gauges 1 … 44, all parallel to the beams.*
4	**Special arrangements** -

<table>
<tr><td>5</td><td>Loading strategy</td></tr>
<tr><td>5.1
Load-time relationship</td><td>The exact date of the floor test is not mentioned in the test report but it has been before 19.11.1990 and most likely not before 14.11.1990.

Before starting the test, all measuring devices were zero-balanced. Thereafter, the actuator loads P were varied in such a way that after five cycles of the type 0 → 185,3 kN → 0 (Stage I), loads P were monotonously increased to failure load 205,6 kN (Stage II).</td></tr>
<tr><td>5.2
After failure</td><td></td></tr>
<tr><td>6</td><td>Observations during loading

For the cracks observed during the loading and after the failure, see Figs 12–23.
<table>
<tr><td>Stage I</td><td>Cracks parallel to and along the edges of the PC beam were observed in the joint concrete. Cracks between the tie beams and the slab ends were also observed above the end beams.</td></tr>
<tr><td>Stage II</td><td>At P = 180 kN, inclined cracks appeared in the upper corners of the outermost webs of slabs 1, 4, 5 and 8 next to the supports of the middle beam. At P = 200 kN new inclined cracks below the first inclined cracks appeared and at P = 205,6 kN a failure took place along these new cracks.</td></tr>
</table></td></tr>
<tr><td>7</td><td>Cracks in concrete</td></tr>
<tr><td>7.1
Cracks at service load</td><td></td></tr>
<tr><td>7.2
Cracks after failure</td><td>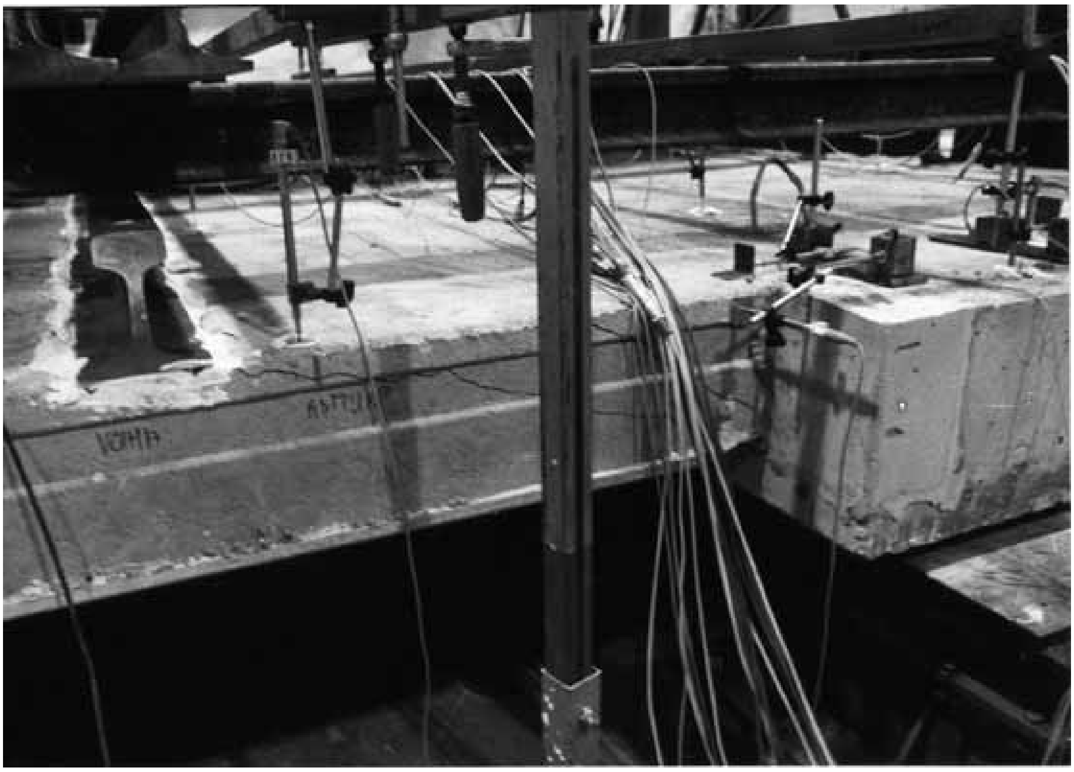

Fig. 13. Failure of slab 4.</td></tr>
</table>

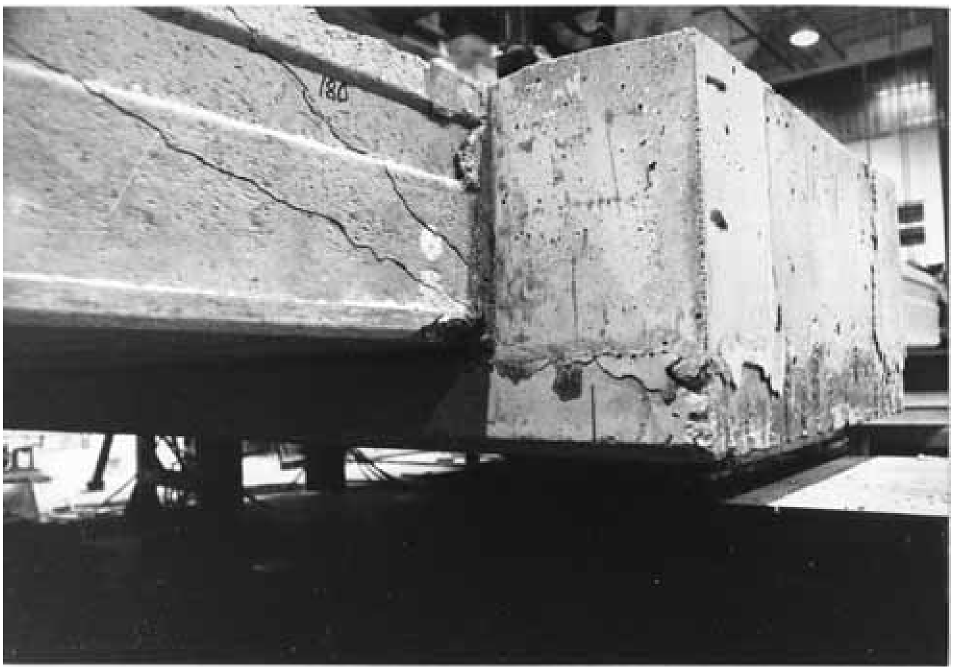

Fig. 14. Failure of slab 4.

Fig. 15. Cracks parallel to beam. South end of middle beam.

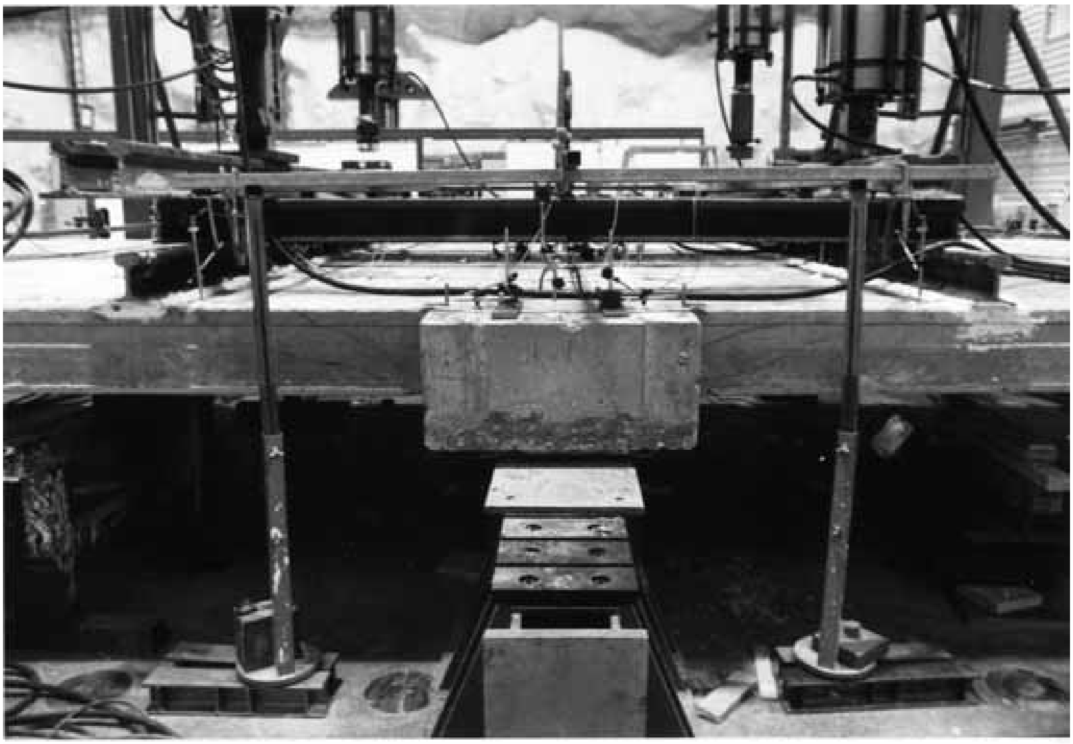

Fig. 16. Failure of slabs 1 (on the right) and 5 (on the left).

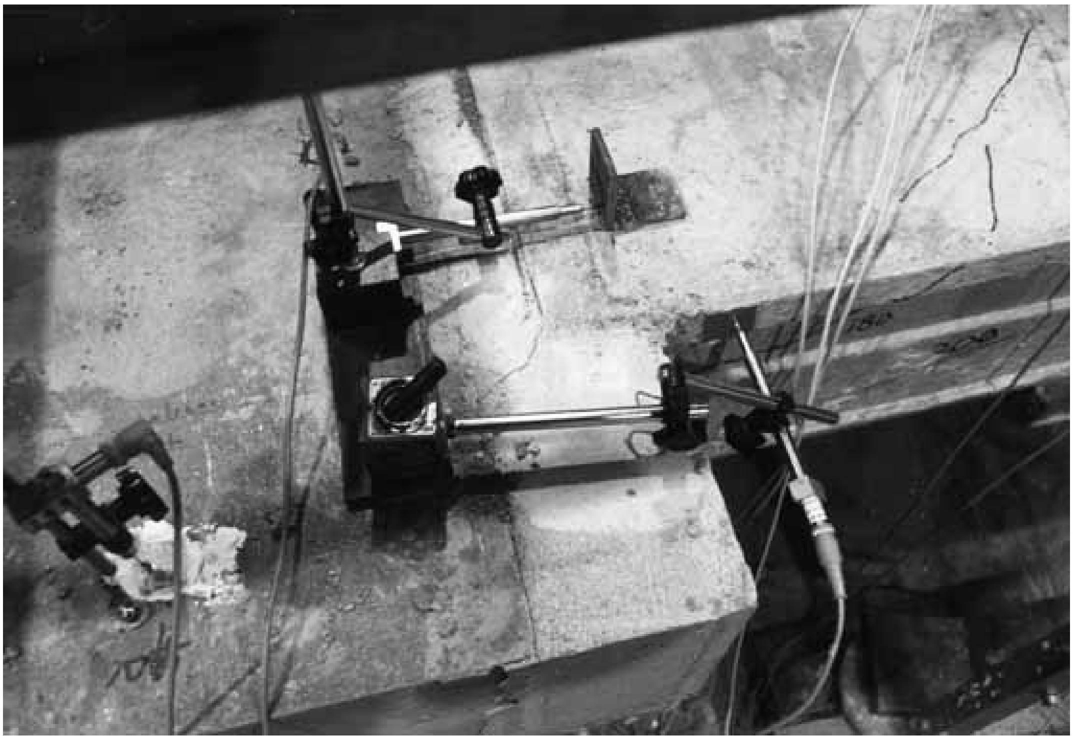

Fig. 17. Cracks after failure in slab 8 and in the joint concrete.

Fig. 18. Failure of slab 1.

Fig. 19. Failure of slab 5.

Fig. 20. Cracks parallel to beam in joint concrete. North end of middle beam.

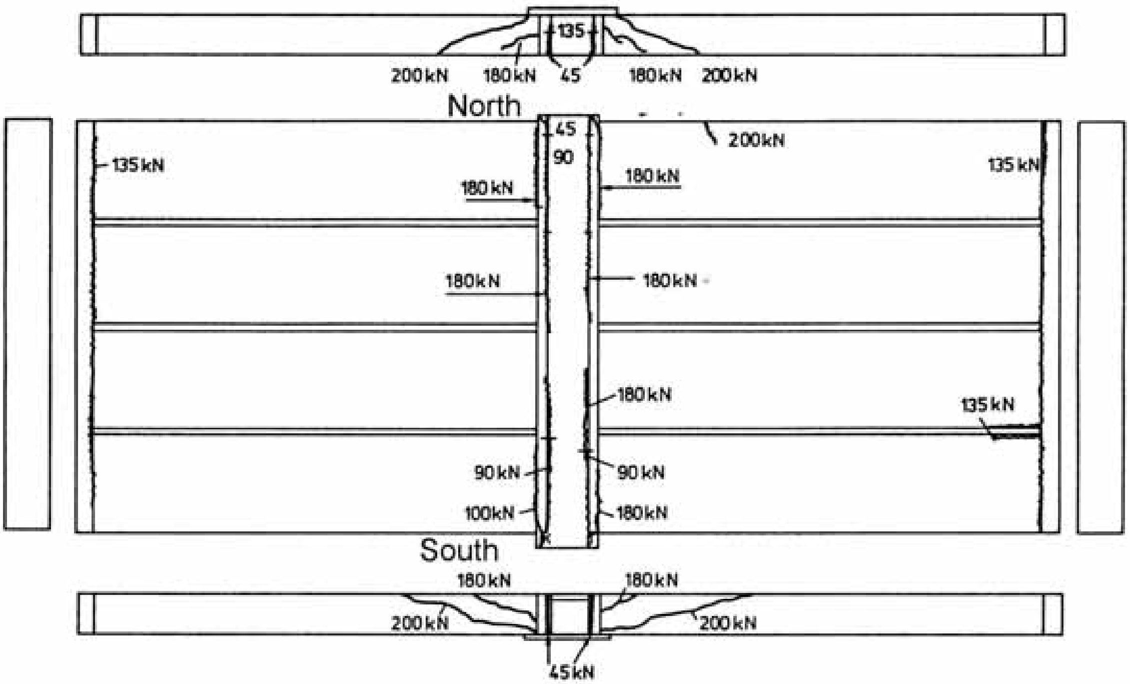

Fig. 21. Cracks on the top and at the edges of the floor after failure. The load values refer to the value of actuator load P at which the crack was observed.

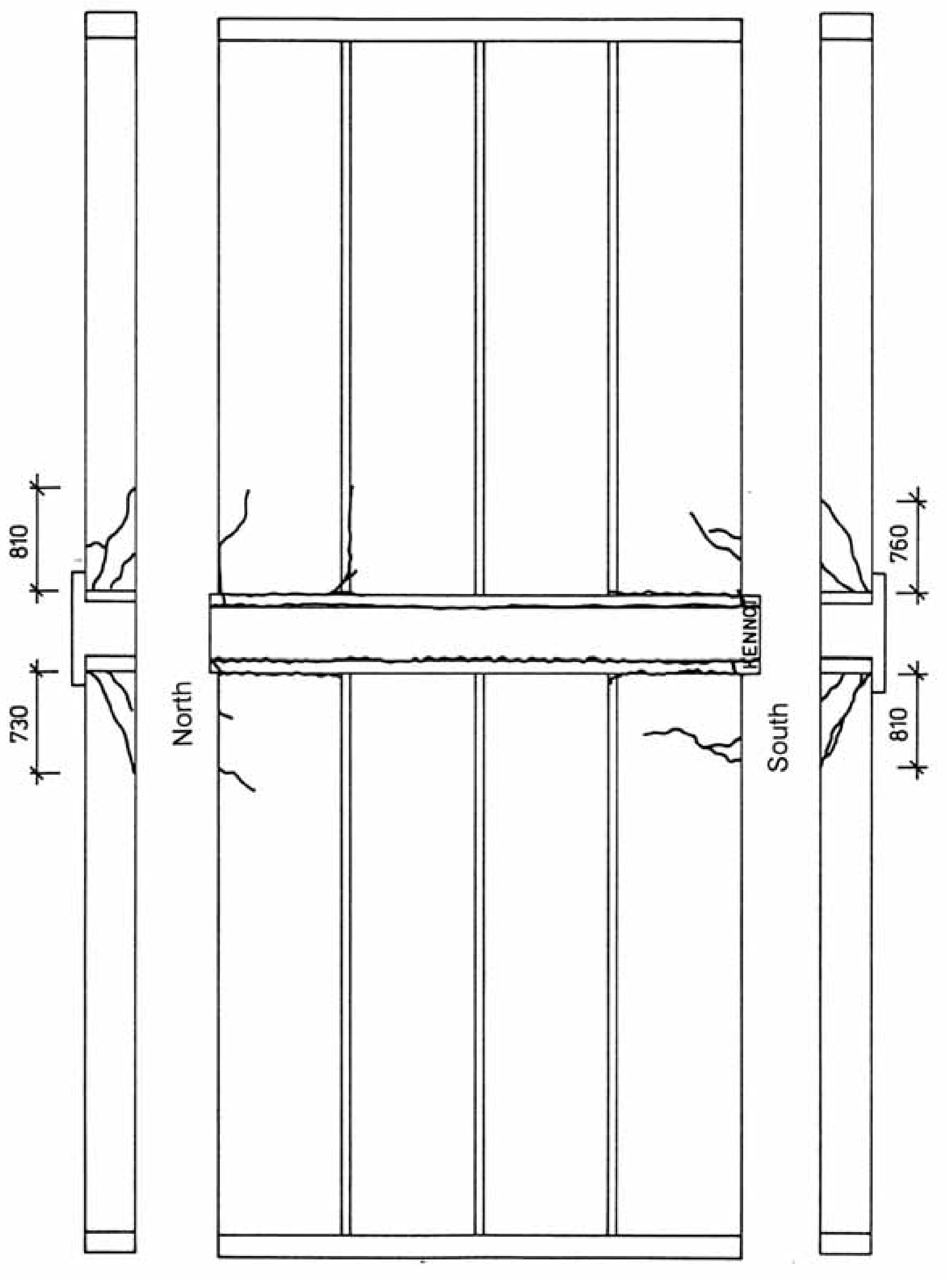

Fig. 22. Failure cracks and other major cracks on the top and at the edges of the floor after failure.

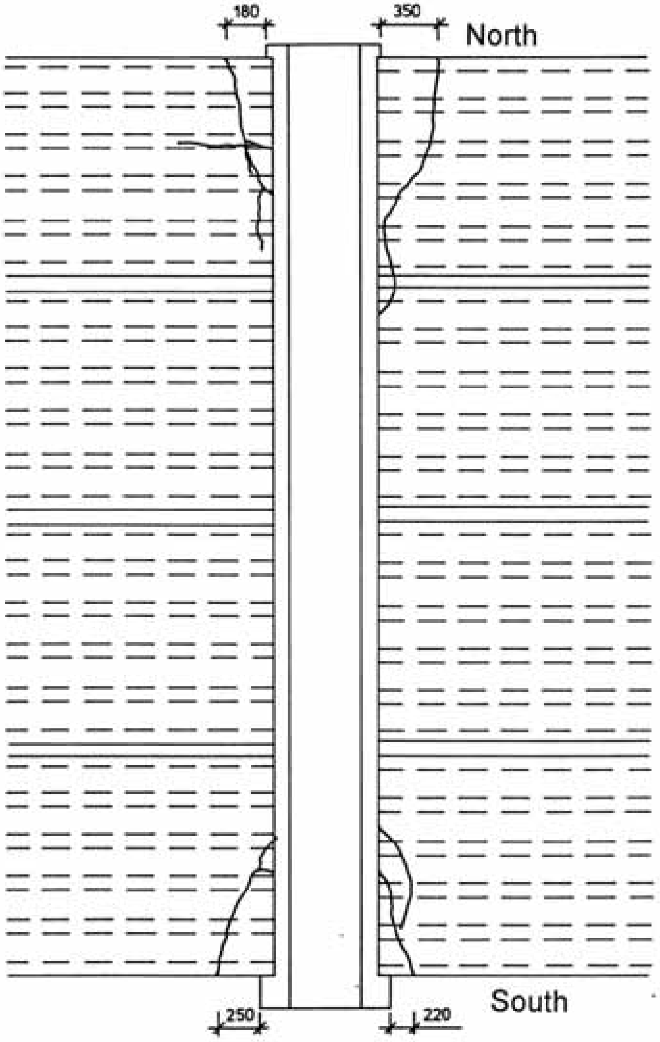

Fig. 23. Cracks in the soffit after failure.

8	**Observed shear resistance**
	The actuator load = P vs. measured support reaction below the South end of the middle beam is shown in Fig. 24.

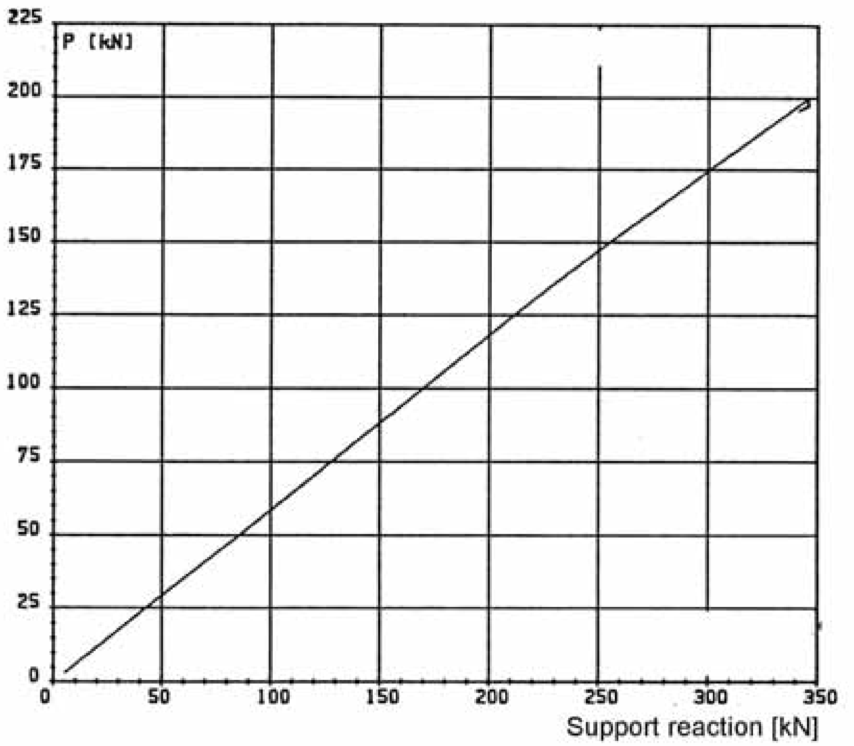

Fig. 24. Measured support reaction below South end of PC beam vs. actuator load P.

The shear resistance of one slab end (support reaction of slab end at failure) due to different load components is given by

$$V_{obs} = V_{g,sl} + V_{g,jc} + V_{eq} + V_P$$

where $V_{g,sl}$, $V_{g,jc}$, V_{eq} and V_P are shear forces due to the self-weight of slab unit, weight of joint concrete, weight of loading equipment and actuator forces P, respectively.

$$V_P = 88{,}9 \text{ kN}$$

is obtained from the failure load P = 205,6 kN using the load-reaction relationship shown in Fig. 31 [$V_P = 0{,}8645x(0{,}5P)$].

In the same way

$$V_{eq} = 1{,}8 \text{ kN}$$

is obtained from the weigth of the loading equipment (= 210 kg / one slab).

From the nominal geometry and measured density of the concrete

$$V_{g,sl} + V_{g,jc} = 12{,}3+0{,}4 = 12{,}7 \text{ kN}$$

follows. The shear resistance $\boldsymbol{V_{obs}}$ **= 103,4 kN** (shear force at support) is obtained for one slab unit with width = 1,2 m. The shear force per unit width is $\boldsymbol{v_{obs}}$ **= 86,2 kN/m.**

9	**Material properties**

9.1
Strength of steel

Component	$R_{eH}/R_{p0,2}$ MPa	R_m MPa	Note
Slab strands J12,5	1570–1630	1770–1860	Nominal (no yielding in test)
Reinforcement Txy (ϕ=xy mm)	500		Nominal value for reinforcing bars A500HW (no yielding in test)

9.2
Strength of slab concrete, floor test

#	Cores	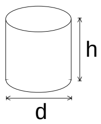	*h* mm	*d* mm	Date of test	Note
6			50	50	14.–19.11.1990?	Upper flange of slabs 4 and 8 (3pc. each), ρ = 2418 kg/m^3
Mean strength [MPa]			63,8		(? d)[1)]	vertically drilled
St.deviation [MPa]			4,6			Tested as drilled[2)]

9.3
Strength of slab concrete, reference tests

-

9.4
Strength of grout in joints

#	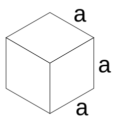	*a* mm	Date of test	Note
3		150	14.11.1990	Kept in laboratory in the same
Mean strength [MPa]		26,8	(? d)[1)]	conditions as the floor specimen
St.deviation [MPa]				ρ =2267 kg/m^3

1) Date of material test minus date of structural test (floor test or reference test)
2) After drilling, kept in a closed plastic bag until compression

10	**Results measured during floor test** In the following graphs, *P* is the actuator load.
10.1 Deflections	The measured deflections in Stage II are shown in Figs 25–41. The numbers close to the curves refer to the number of transducer, see Fig. 10. 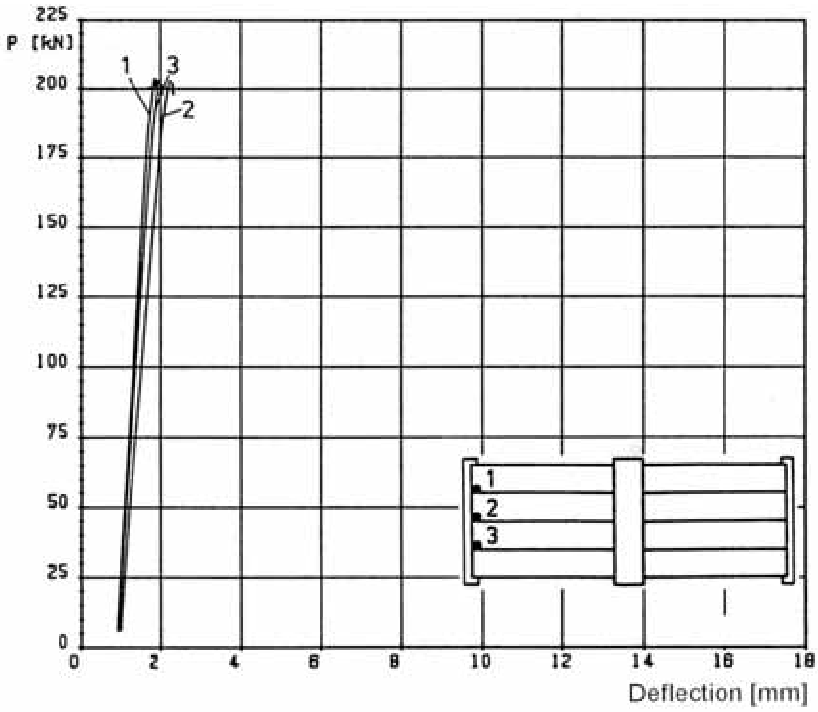 *Fig. 25. Measured deflection.* 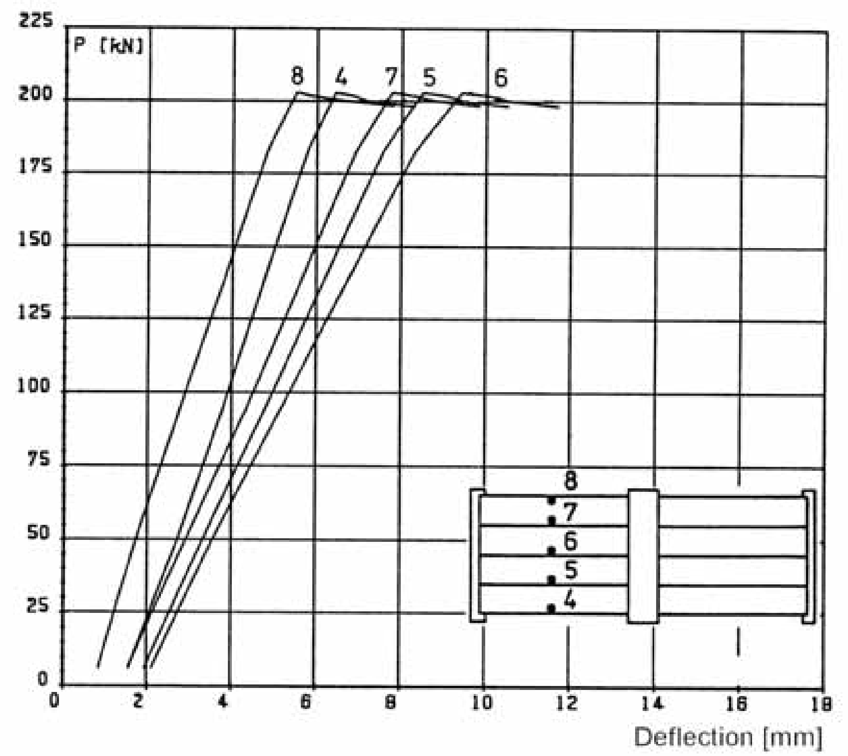 *Fig. 26. Measured deflection.*

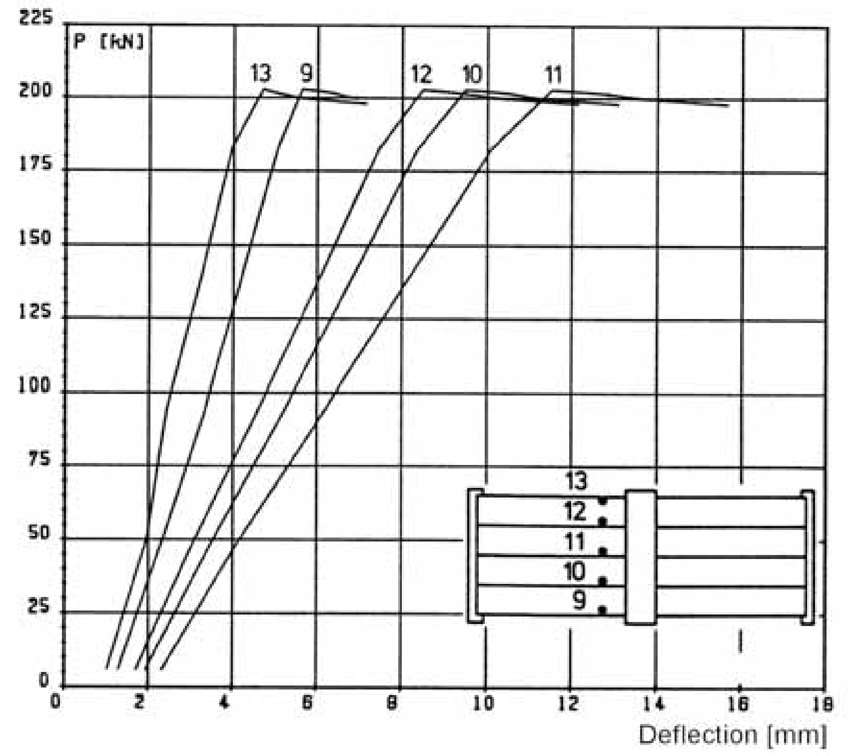

Fig. 27. Measured deflection.

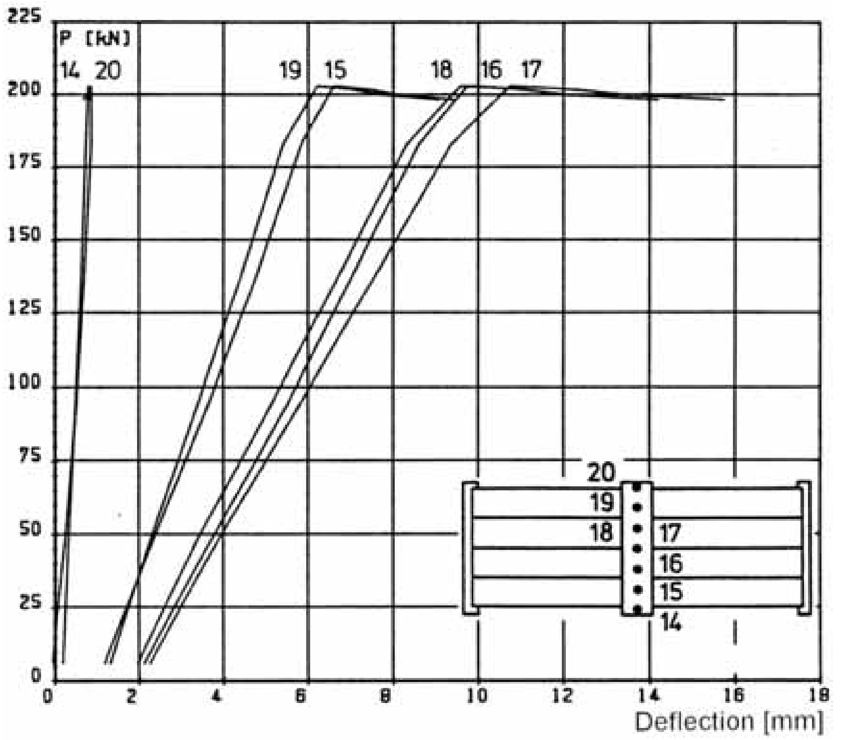

Fig. 28. Measured deflection.

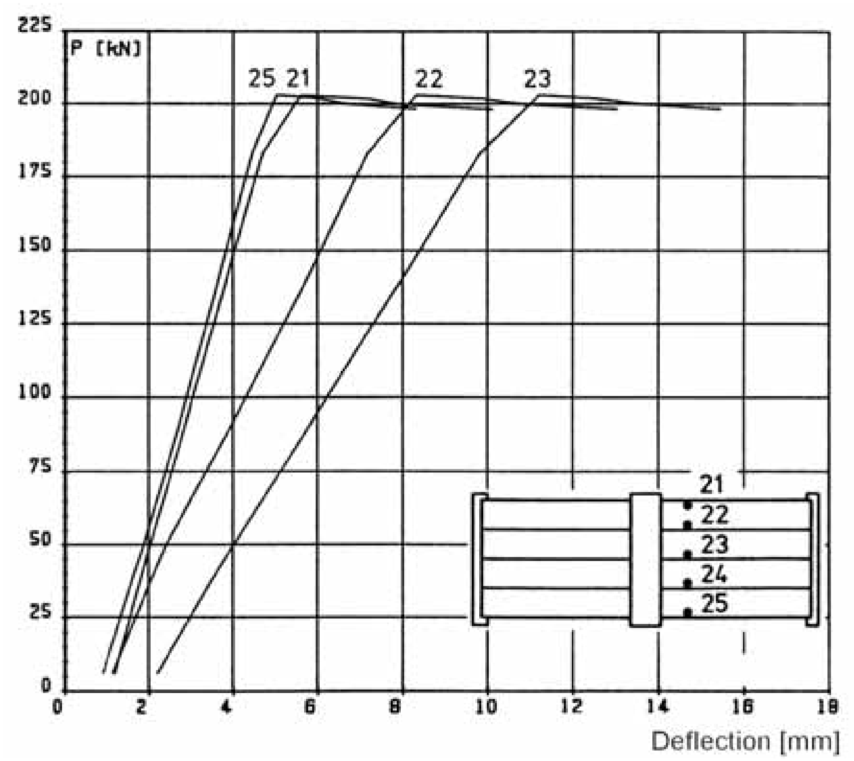

Fig. 29. Measured deflection.

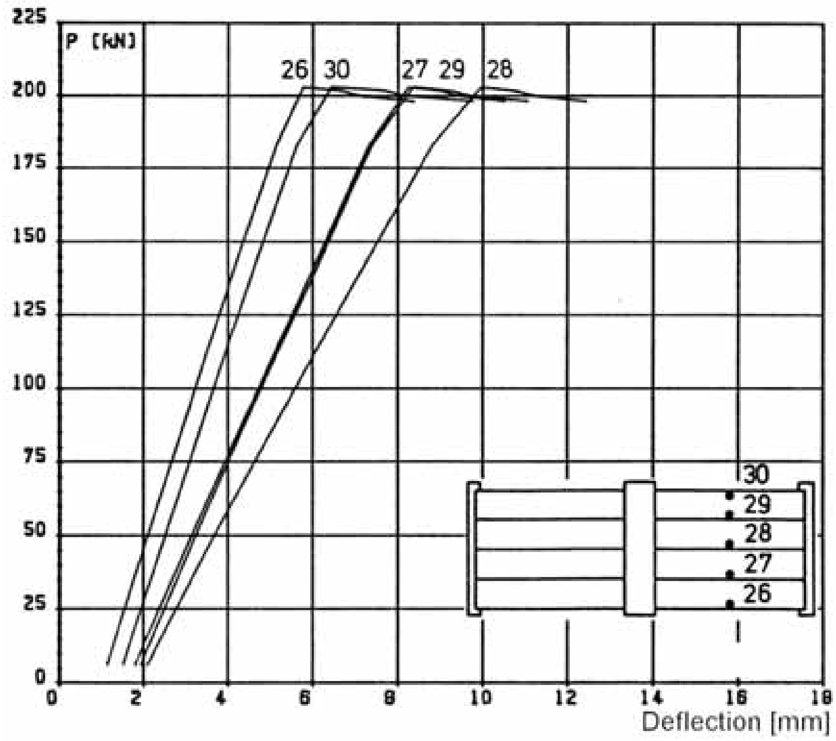

Fig. 30. Measured deflection.

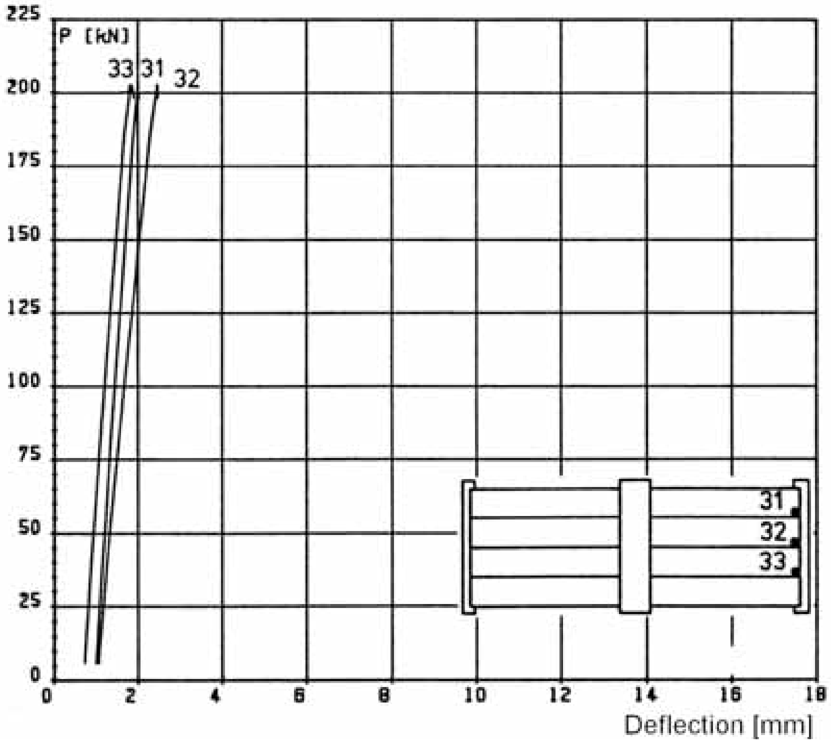

Fig. 31. Measured deflection.

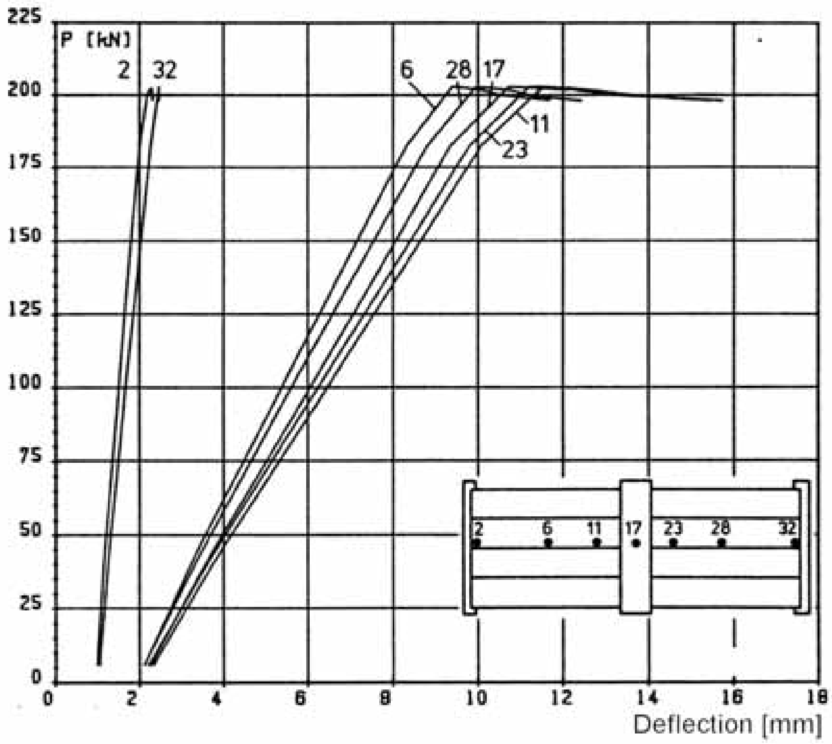

Fig. 32. Measured deflection.

10.2
Crack width

The differential displacement measured by horizontal transducers 34–39 reflect the crack width in the joint concrete next to the middle beam. These measured displacements in Stage II are shown in Fig. 33.

	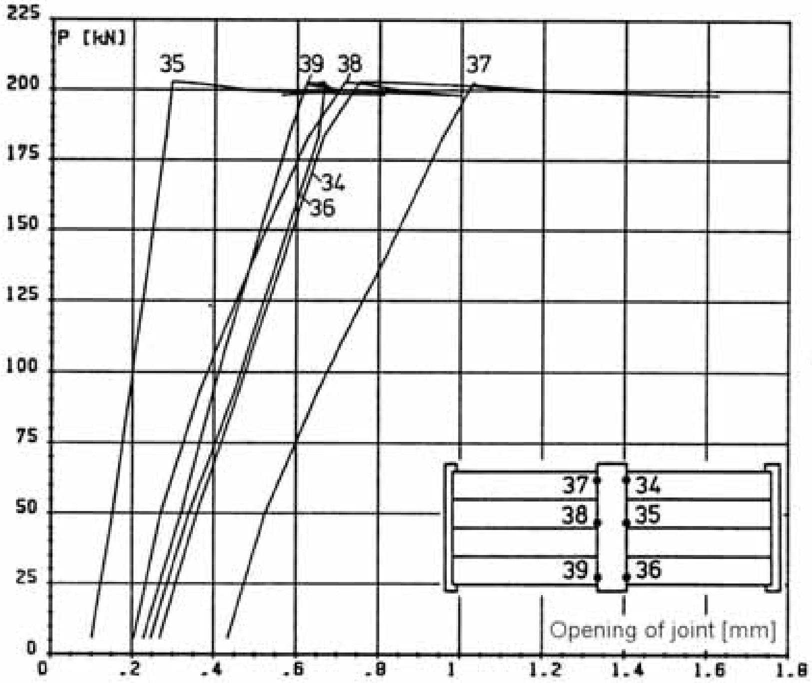 *Fig. 33. Opening of joint in Stage II.*
10.3 Average strain	-
10.4 Differential horizontal displacement	A positive value means that the concrete is moving towards the beam end. 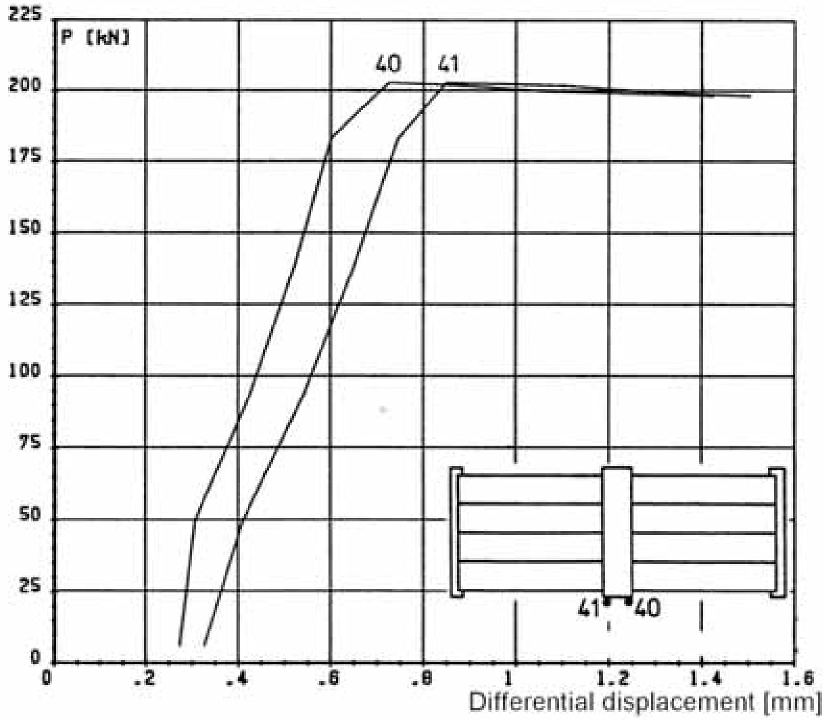 *Fig. 34. Differential horizontal displacement between South end of middle beam and edge of slab in Stage II.*

10.5 Differential vertical displacement	A positive value means that the slab end is deflecting more than the beam. 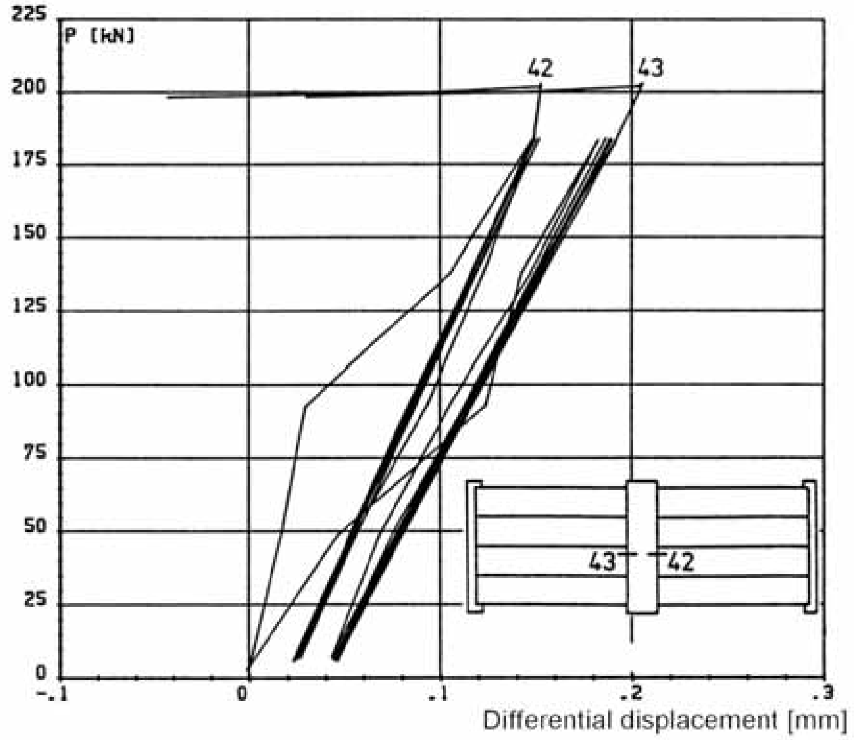 *Fig. 35. Differential vertical displacement between middle beam and slab end. Stages I and II.*
10.6 **Strain**	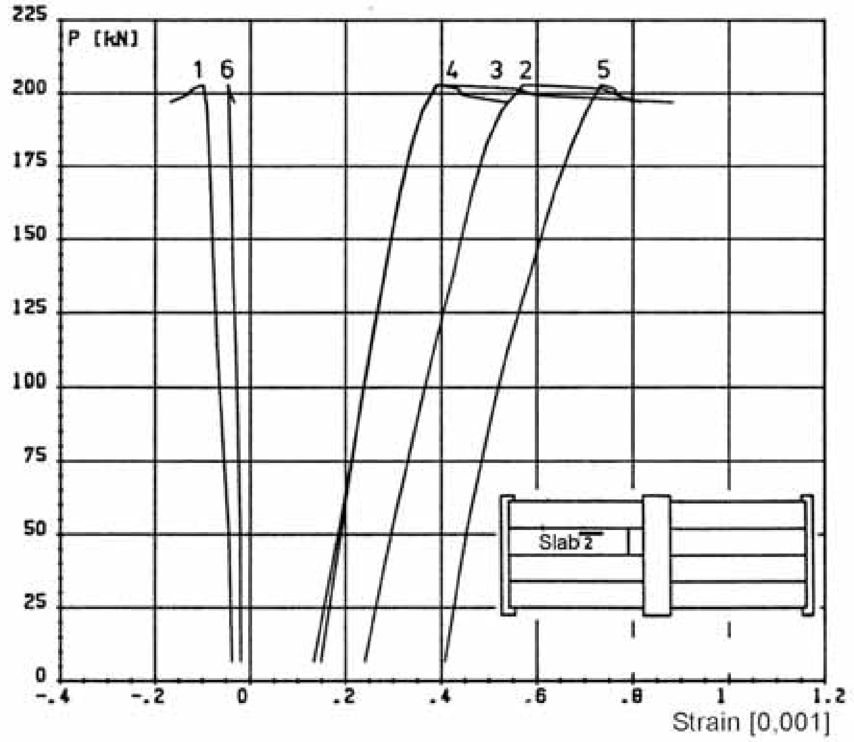 *Fig. 36. Strain measured by gauges 1–6. Stage II.*

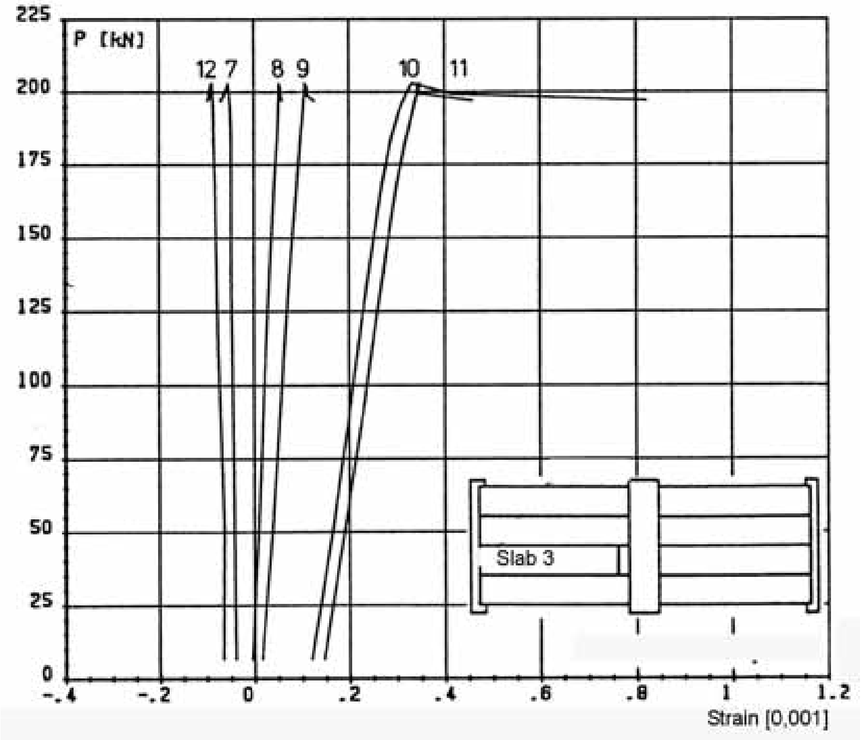

Fig. 37. Strain measured by gauges 7–12. Stage II.

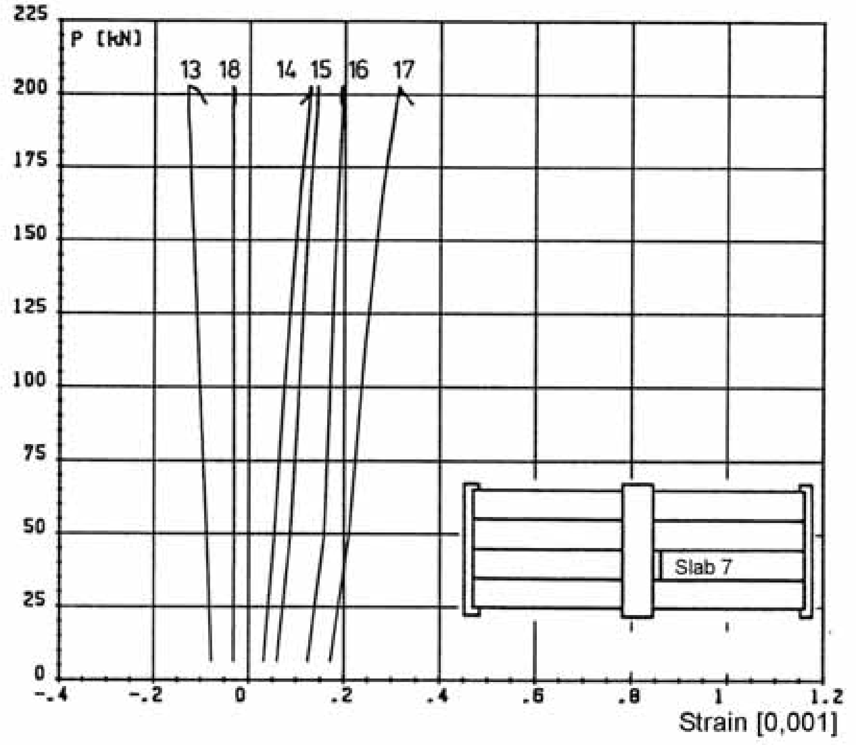

Fig. 38. Strain measured by gauges 13–18. Stage II.

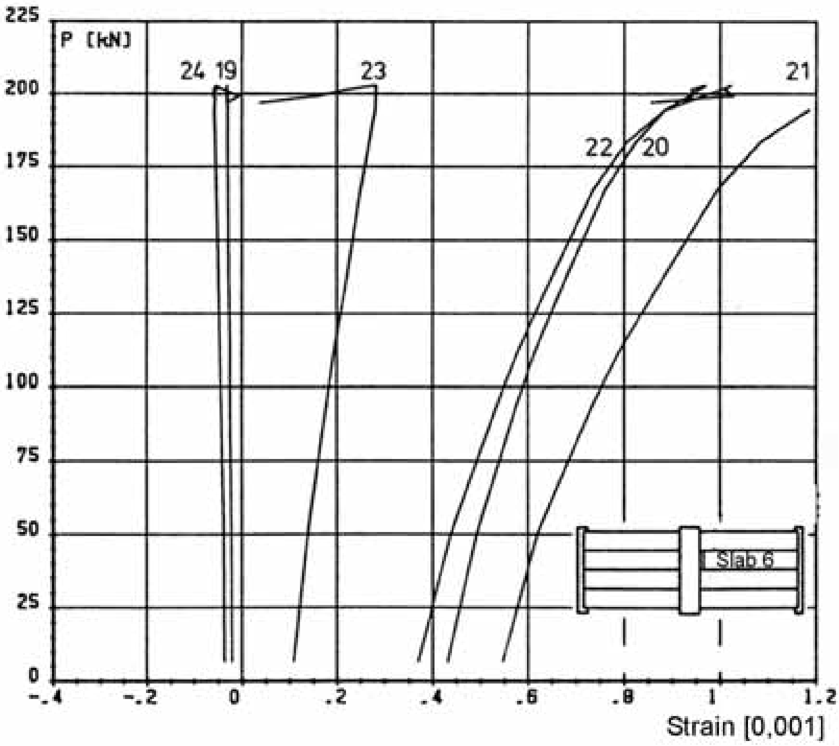

Fig. 39. Strain measured by gauges 19–24. Stage II.

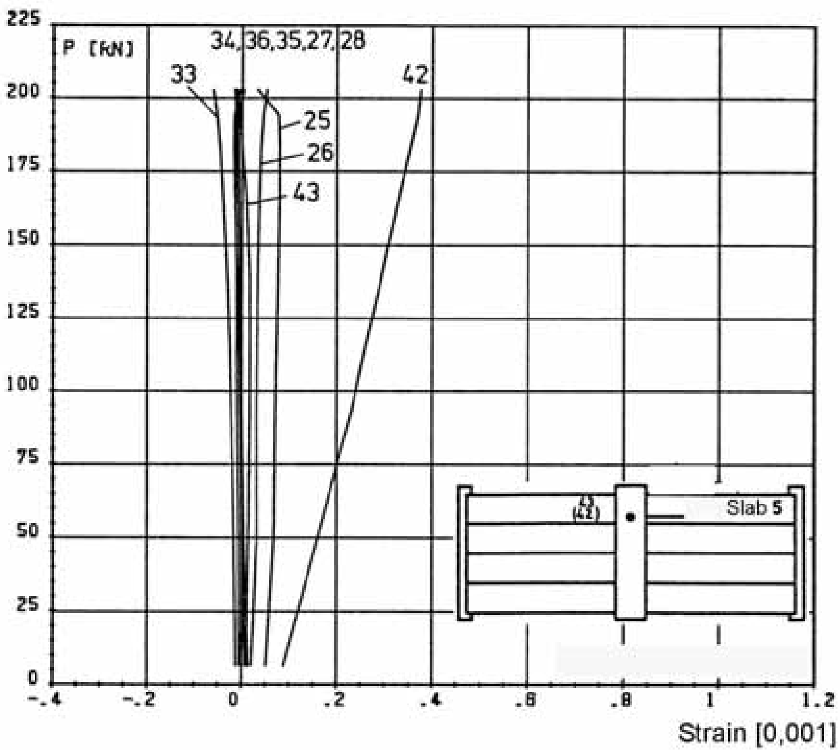

Fig. 40. Strain measured by gauges 25–28, 33–36 and 42–43. Stage II.

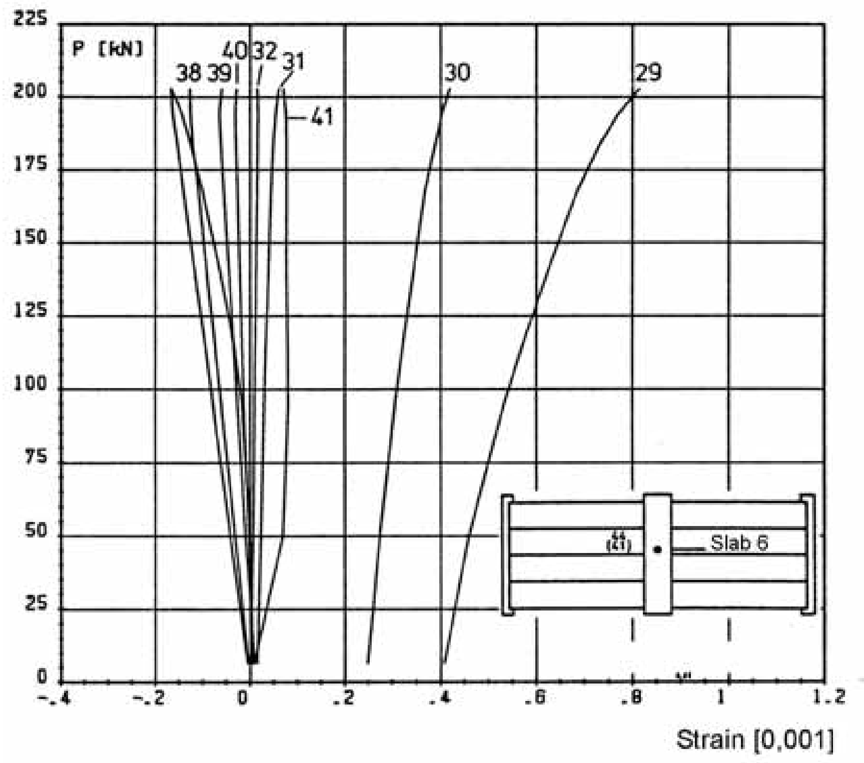

Fig. 41. Strain measured by gauges 29–32 and 38–41. Stage II.

11	**Reference tests**

No reference tests were performed for the slabs in the present floor test. Instead, the reference tests carried out for two slabs taken from floor test VTT.S.WQ.265.1990 are regarded as applicable to this case, too, because

- the slabs for these two floor tests were taken from the same casting lot and bed
- the slabs were cast as early as 29.6.1990 and the change in concrete strength must have been very small in October – November 1990 when the tests were carried out.

The results presented below are taken from report VTT.S.WQ.265.1990.

Table. Reference tests. Span of slab, shear force V_g at support due to the self weight of the slab, actuator force P_a at failure + weight of loading equipment P_{eq}, total shear force V_{obs} at failure and total shear force v_{obs} per unit width.

Test	Date	Span mm	V_g kN	P_a+P_{eq} kN	V_{a+eq} kN	V_{obs} kN	v_{obs} kN/m	Note
R3	12.10.1990	5940	12,3	285,5	237,4	249,6	208,0	Web shear failure
R7	12.10.1990	5950	12,3	239,5	199,2	211,4	176,2	Web shear failure
				Mean		**230,5**	**192,1**	

12	**Comparison: floor test vs. reference tests**
	The observed shear resistance (support reaction) of the hollow core slab in the floor test was equal to **103,4 kN** per one slab unit or **86,1 kN/m**. This is **45%** of the mean of the shear resistances observed in the reference tests.
13	**Discussion**
	1. The friction between the spreader beams was not eliminated, which may have affected the response of the floor test specimen to some extent. This additional stiffness reduced the deflection of the floor but it is difficult to evaluate whether the net effect on the observed shear resistance was positive or negative. 2. The net deflection of the end beams (deflection minus settlement of supports was very small beams, apparently < 2 mm. The original idea was to reduce the horizontal interaction between the end beam and the slab ends above it, but due to some misunderstanding, the beams were provided with dowel reinforcement which was not specified in the drawings. These dowels made the laboratory personnel believe that the slab ends and the end beam must be cast together. In this way the resulting composite beam became far too stiff to deflect like the middle beam, which was the primary design criterion for the end beam. 3. The last measured net deflection of the middle beam due to the imposed actuator loads only (deflection minus settlement of supports) was 9,9 mm or *L*/505. It was ≈8 mm greater than that of the end beams. Hence, the torsional stresses due to the different deflection of the middle beam and end beams may have had a minor effect on the failure of the slabs. On one hand, the torsion in the slab elements due to the different deflection of the middle beam and end beams reduced the deflection of the middle beam but increased the torsional shear stresses in the webs of the outermost slab elements. The net effect of the torsion on the observed shear resistance may have been positive or negative. 4. The shear resistance measured in the reference tests was of the same order as or slightly higher than the mean of the observed values for similar slabs given in *Pajari, M. Resistance of prestressed hollow core slab against a web shear failure.VTT Research Notes 2292, Espoo 2005*. The concrete tie beam at the sheared end may have enhanced the resistance in the reference tests. It prevented the deformation of the end section of the slab and thus equalized the strains in the webs of the slab, which effectively eliminated the premature failure of any individual web. 5. The beams did not yield in the floor test. 6. The failure mode was web shear failure of edge slabs close to the supports of the middle beam. Unlike in an isolated hollow core slab unit, in the floor test the appearance of the first inclined crack close to the slab end did not mean failure but the loads could still be increased. 7. The failure mode was web shear failure of edge slabs close to the supports of the middle beam. Unlike in an isolated hollow core slab unit, in the floor test the appearance of the first inclined crack close to the slab end did not mean failure but the loads could still be increased.

1 General information

1.1 Identification and aim

VTT.PC.InvT.400.1992	**Last update 2.11.2010**
PC400	(Internal identification)
Aim of the test	To study the shear resistance of thick hollow core slabs supported on beams.

1.2 Test type

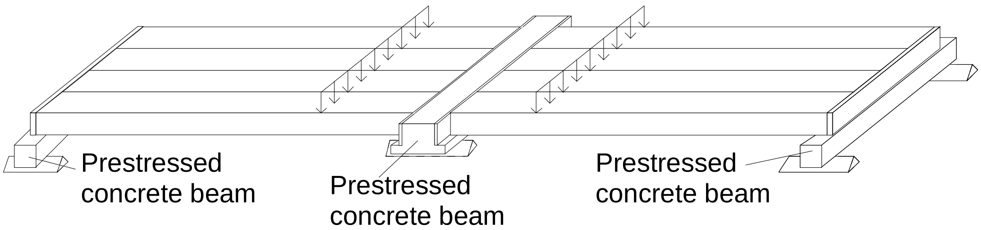

Fig. 1. Illustration of test setup.

1.3 Laboratory & date of test

VTT/FI 24.2.1992

1.4 Test report

Author(s)	Pajari, M.
Name	*Loading test for 400 mm hollow core floor supported on prestressed concrete beams*
Ref. number	RAT-IR-3/1993
Date	15.4.1993
Availability	Public, available on request from VTT Expert Services, P.O. Box 1001, FI-02044 VTT.

Financed by Lohja Oy, Finland; NCC Prefab AB, Sweden; Parma Oy, Finland; Oy Partek Concrete Ab, Finland; Skanska Prefab AB, Sweden and AB Strängbetong, Sweden. The Finnish companies were financially supported by TEKES, Finland.

2 Test specimen and loading

(see also Appendix A)

2.1 General plan

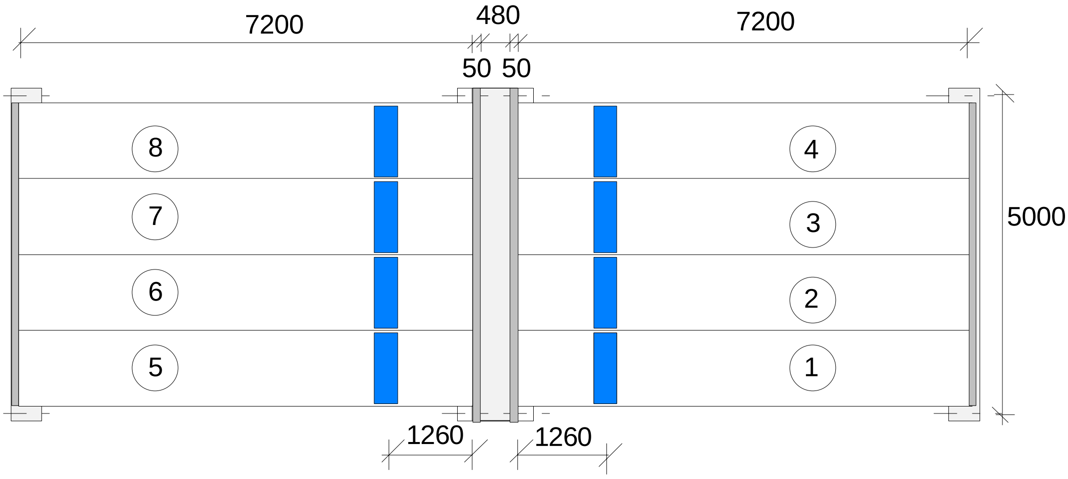

Fig. 2. Plan.

2.2
End beams

Simply supported, prestressed concrete beams. Span = 5,0 m

Concrete: K60

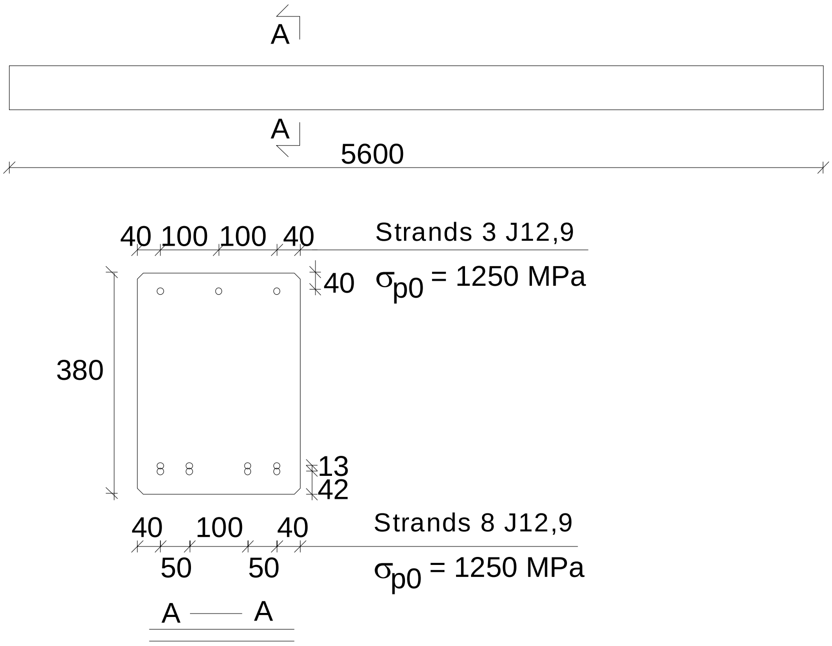

Fig. 3. End beam. For J12,9 see 2.3.

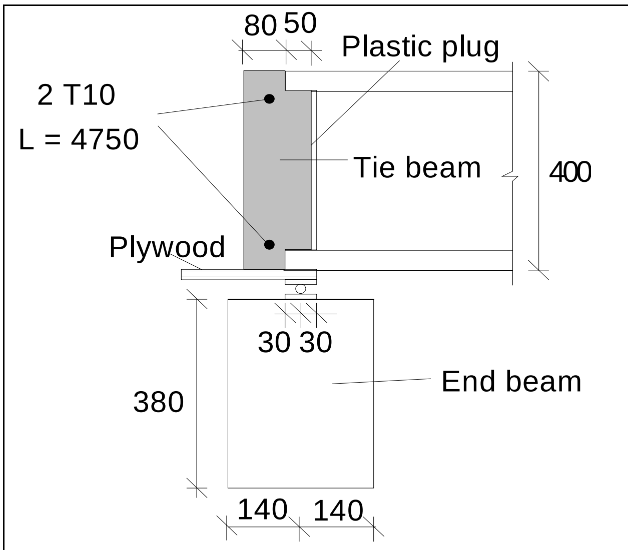

Fig. 4. Arrangements at end beam. T10 refers to a reinforcing bar, see 2.4.

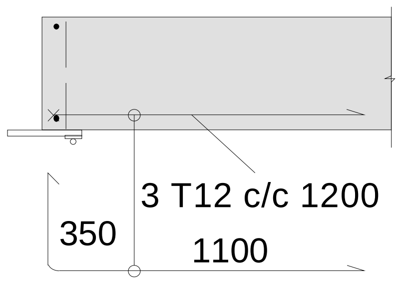

Fig. 5. Tie reinforcement in joints between adjacent slabs. T12 refers to a reinforcing bar, see 2.4.

<table>
<tr>
<td>2.3
Middle beam</td>
<td>

Concrete: K60

Tendons:
J12,9: Prestressing strand, 7 wires, ϕ =12,9 mm, A_p = 100 mm^2, see 9.1

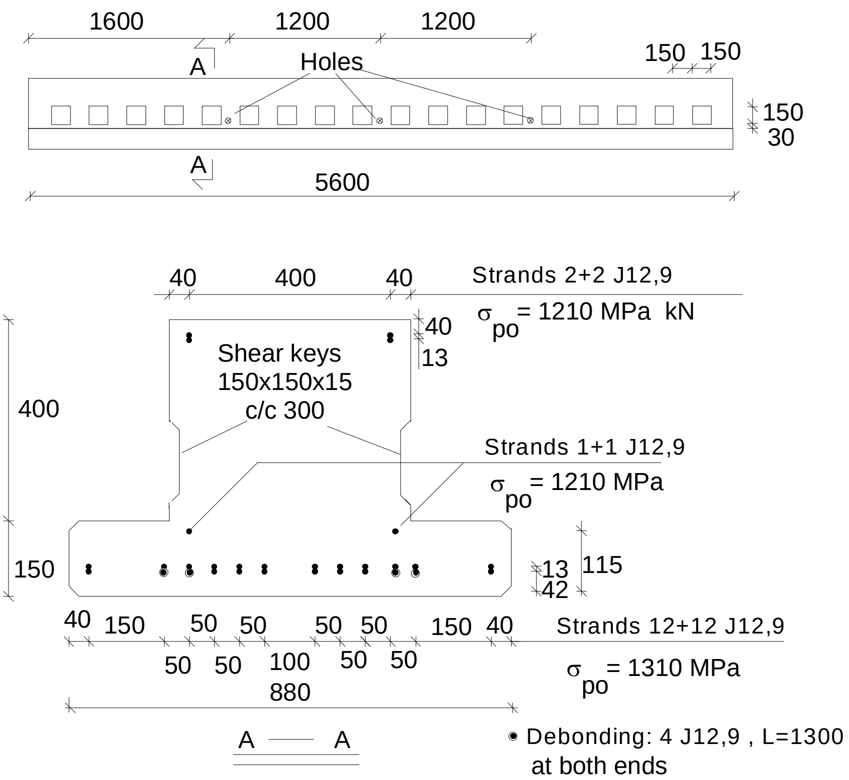

Fig. 6. Elevation and section of middle beam.

</td>
</tr>
<tr>
<td>2.4
Arrangements at middle beam</td>
<td>

320 mm of all hollow cores where filled by concrete. Neither slots nor holes were made in the hollow core slabs.

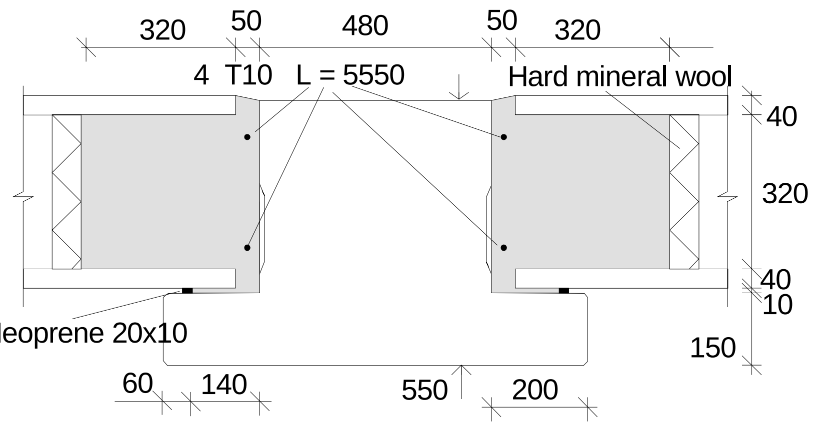

Fig. 7. Section along hollow cores.

</td>
</tr>
</table>

	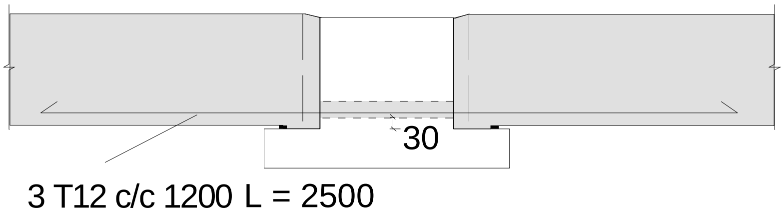 *Fig. 8. Tie reinforcement in joints between adjacent slabs.* - Simply supported, span = 5,0 m **Txy**: Hot rolled, weldable rebar A500HW, ϕ = xy mm, see 9.1.
2.5 Slabs	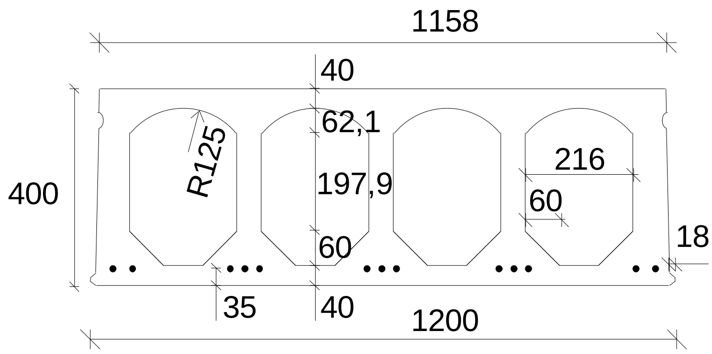 *Fig. 9. Nominal geometry of slab units (in scale).* - Extruded by Partek Betoniteollisuus Oy, Hyrylä factory 15.1.1992 - 13 lower strands J12,5 initial prestress 1100 MPa **J12,5**: seven indented wires, ϕ =12,5 mm, A_p = 93 mm^2 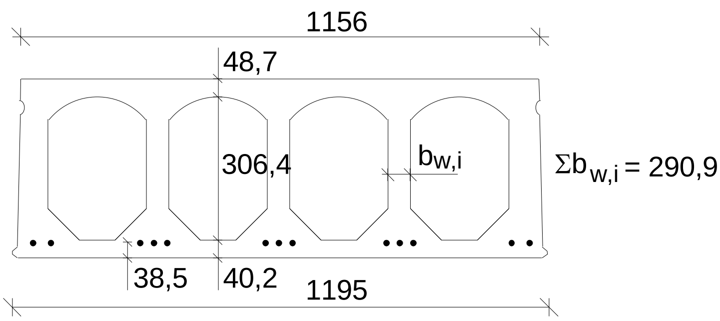 Max measured bond slips: 2,0 in slab 5; 1,4 in slab 4; 1,3 in slab 7 and 0,9 in slabs 3 and 4 Measured weight of slab units = 5,49 kN/m *Fig. 10. Mean of most relevant measured geometrical characteristics.*
2.6 Temporary supports	Temporary supports below beams (Yes/No) - No

2.7
Loading arrangements

There were two separate, manually controlled hydraulic circuits, one for actuators P_1 and the other for actuators P_2, see Fig. 11. Attempts were made to keep $P_1 \approx P_2$.

The primary spreader beams on the top of the floor were railway rails cut in pieces slightly shorter than 1,2 m. The friction between the secondary and primary spreader beams was eliminated by teflon plates.

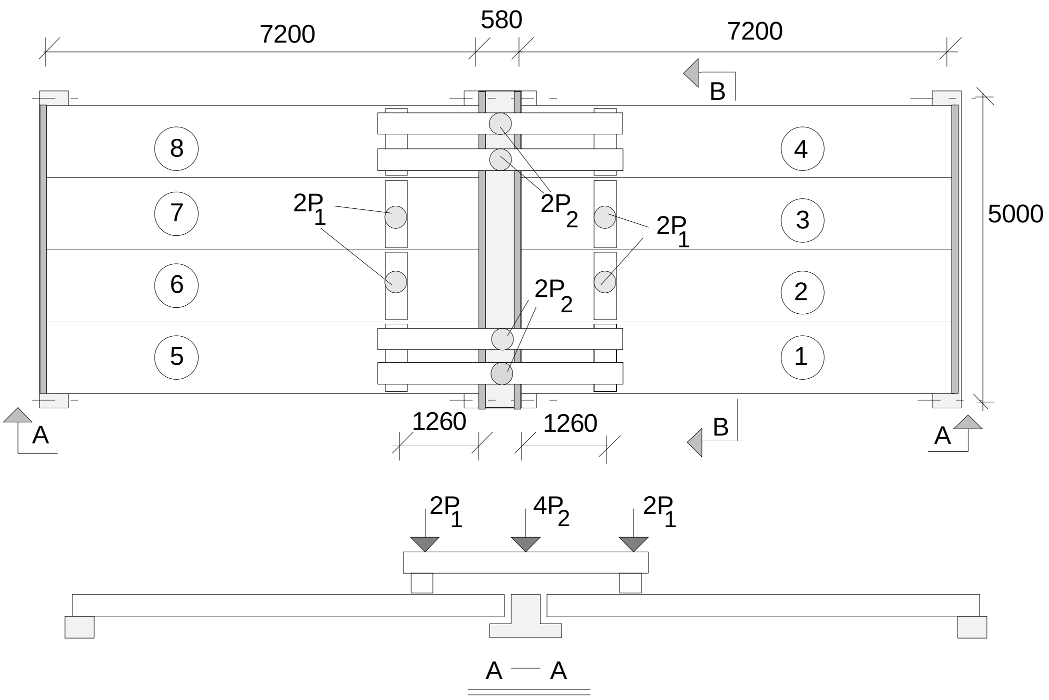

Fig. 11. Plan. P_1 and P_2 refer to vertical actuator forces.

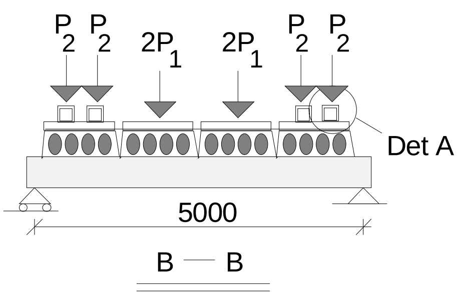

Fig. 12. Section B-B, see previous figure.

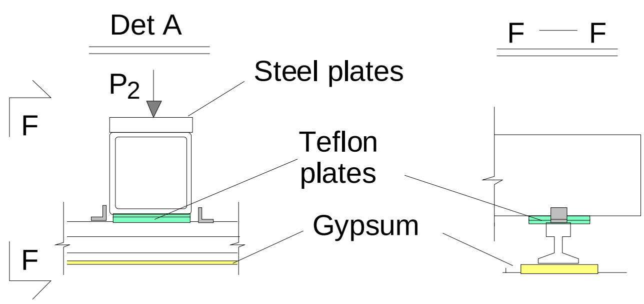

Fig. 13. Detail A, see previous figure.

3 Measurements

3.1
Support reactions

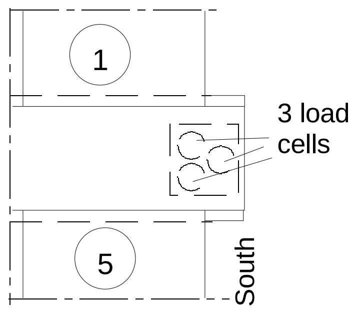

Fig. 14. Load cells below the South end of the middle beam.

3.2
Vertical displacement

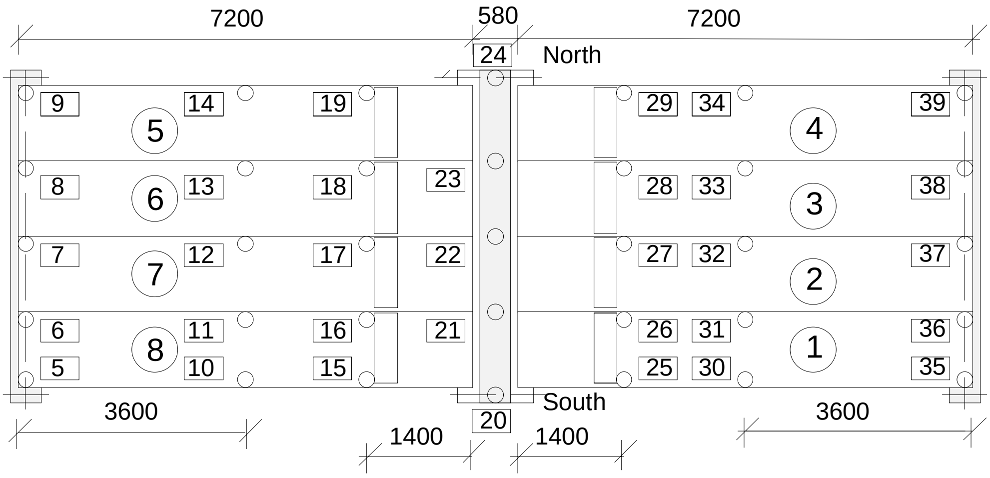

Fig. 15. Location of transducers 5 … 39 for measuring vertical deflection along lines I … VII.

3.3
Average strain

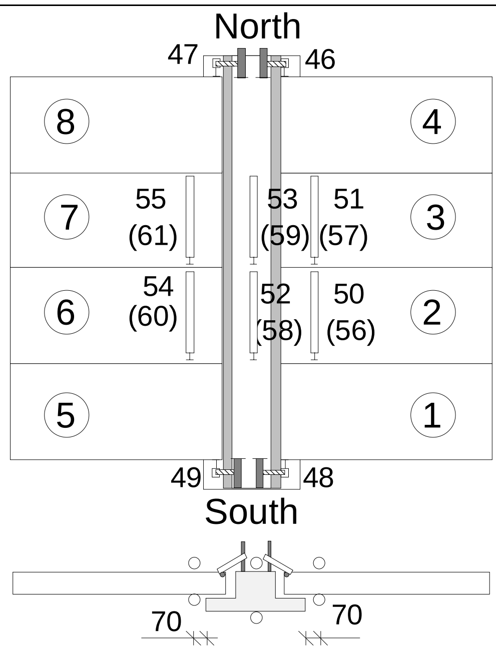

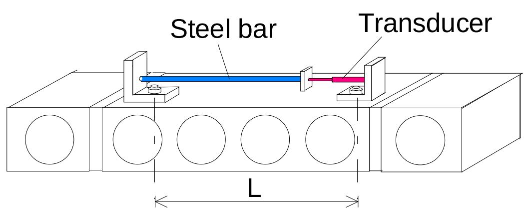

Fig. 16. Apparatus for measuring average strain. L =1120mm and 1060 mm for the bottom and top side transducers, respectively.

Fig. 17. Position of device (transducers 50–61) measuring average strain parallel to the beams. Transducers 46–49 measured the sliding of the outermost slabs along the beam. Numbers in parentheses refer to the soffit of the floor, others to the top side.

3.4 Horizontal. displacements	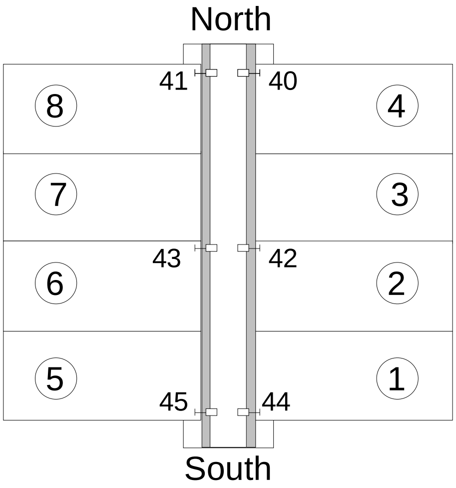 *Fig. 18. Transducers 40–45 measuring crack width on the top of the floor.*
3.5 Strain	To detect longitudinal cracks along strands, the soffit of slabs 2, 3, 6 and 7 was provided with strain gauges as shown in Figs 19 and 20. The measuring length of the gauges was 67 mm. 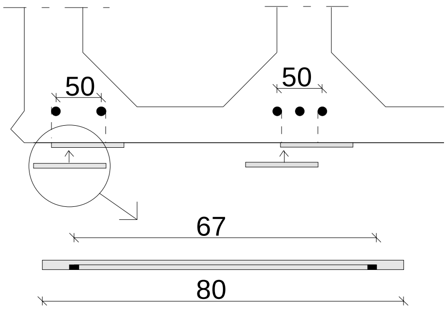 *Fig. 19. Strain gauges below strands.* 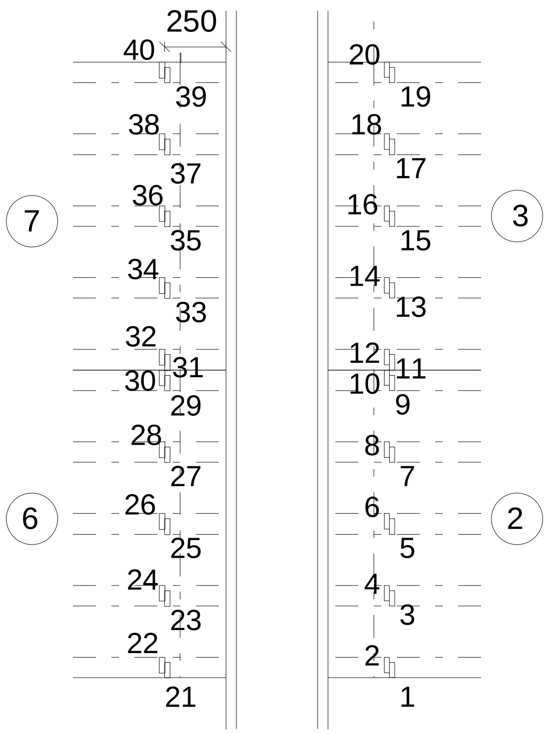 *Fig. 20. Position of strain gauges. The webs of the slabs are indicated by dot-and-dash lines below strands.*
4	**Special arrangements** -

5	**Loading strategy**
5.1 Load-time relationship	Date of the floor test was 24.2.1992 When the actuator forces P_i were equal to zero but the weight of the loading equipment was on, all measuring devices were zero-balanced. The loading history is shown in Fig.21. Note, that the number of load step, not the time, is given on the horizontal axis. In the following, the loading until failure (steps 1–29) is called Stage 1 and the post-failure stage with a support below failed slab 1 (steps 30–38) Stage 2. In Stage 3 the support was still under slab 1 and the load on slab 2 was removed. 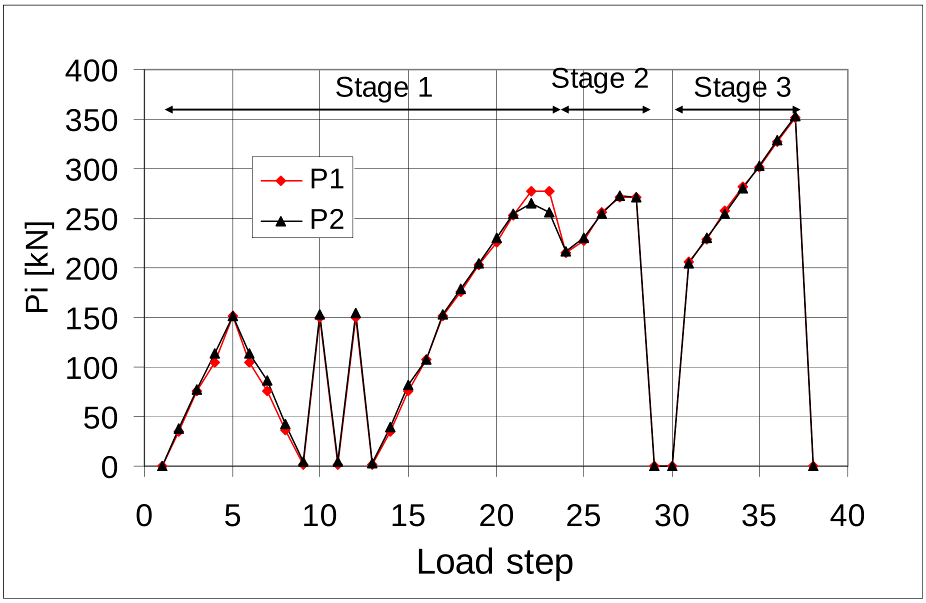 *Fig. 21. Development of actuator loads P_1 and P_2.* The weight of loading equipment per actuator was 1,2 kN and 5,6 kN for actuators P_1 and P_2, respectively. Consequently, the imposed load per slab was $F_1 = P_1 + 1{,}2$ kN for slabs 2, 3, 6 and 7 $F_2 = P_2 + 5{,}6$ kN for slabs 1, 4, 5 and 8
5.2 After failure	See Stages 2 and 3 on the next page.

6 Observations during loading

Stage 1	At P_1 = 276,8 kN, P_2 = 265,3 kN a shear failure took place in slab 1 between the line load and the support, see Appendix A, Fig. 4.
Stage 2	A support was placed below the line load F_1 on slab 1 as shown in Fig. 23. The aim was to continue the loading with seven line loads but the end of slab 2 failed shortly after the reloading was started as shown in Fig. 24. This failure was obviously due to the load transfer from slab 1 to slab 2 across the vertical joint because the support under slab 1 was not able to carry load before a certain additional deflection of slab 1 had taken place, and this deflection was not possible before slab 2 had failed.
Stage 3	After the failure of slab 2, the actuator on slab 2 was removed. Now slab 1 was tightly lying on the support below the line load. A shear failure took place in slab 5 at P_1 = 375,0 kN, P_2 = 379,0 kN, see Appendix A, Figs 5–7.
After failure	When demolishing the test specimen it was observed that the core fillings were perfect and the gap between the soffit of the slabs and the upper surface of the ledges of the middle beam was completely filled by the grout, see Appendix A, Figs 8–12. The middle beam looked intact after the failure.

7 Cracks in concrete

7.1
Cracks at service load

-

7.2
Cracks after failure

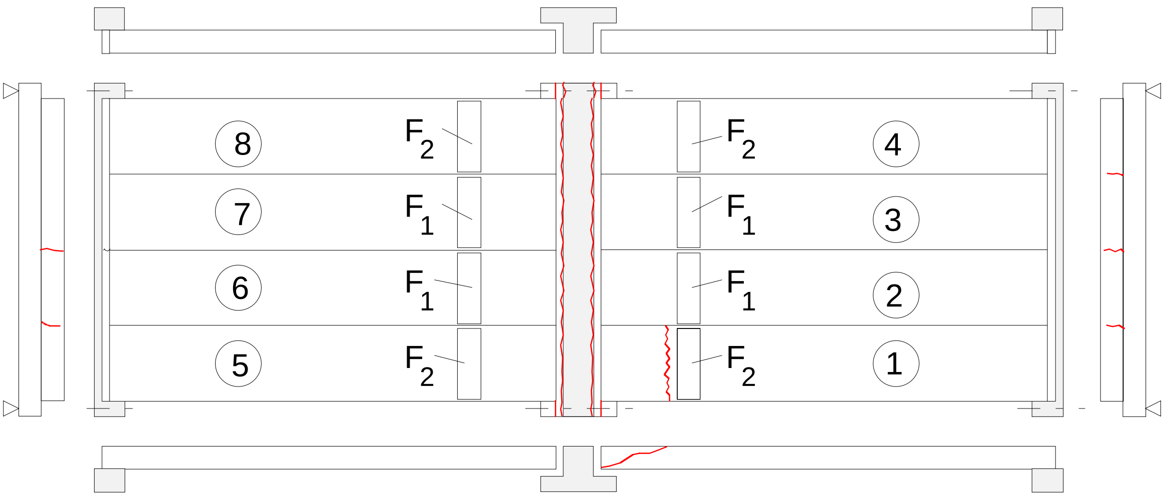

Fig. 22. Stage 1. Cracks on the top and at the edges of the floor after failure.

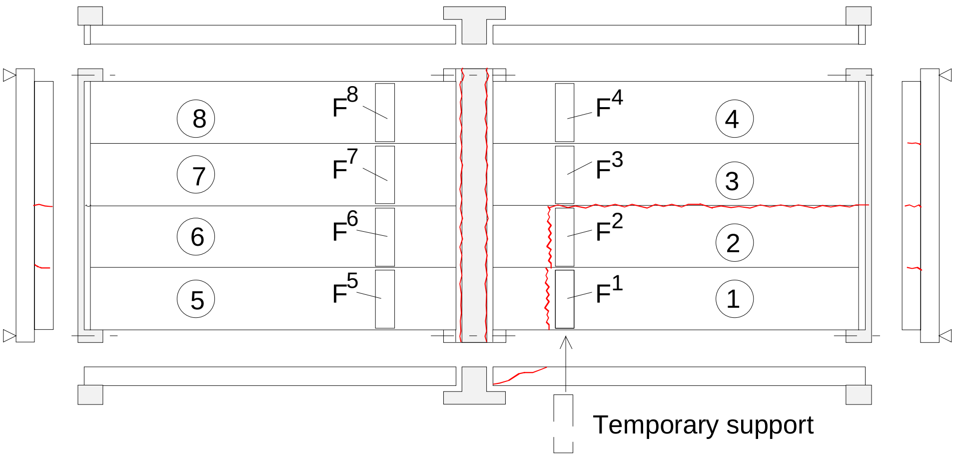

Fig. 23. Stage 2. Cracks after failure of slab 2.

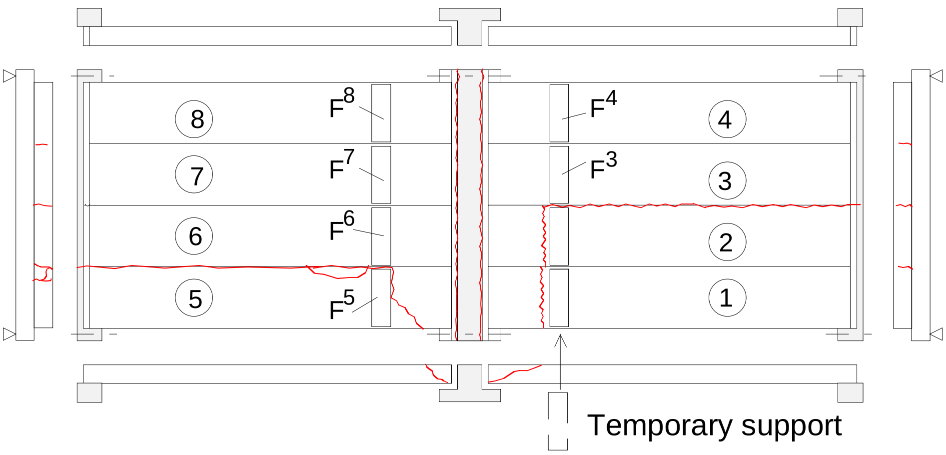

Fig. 24. Stage 3. Cracks after failure of slab 5.

8 Observed shear resistance

The maximum support reaction is regarded as the indicator of failure. The failure most likely took place before the load values P_1 = 276,8 kN, P_2 = 265,3 kN were measured and when the sum of actuator loads load on half floor was = 1085,0 kN. This is supported by the fact that the efforts to keep all actuator loads equal succeeded well except at this point. Due to the softening of slab 1 the pressure in actuators P_2 was reduced and the middle beam rose upwards, which resulted in increasing pressure in actuators P_1. This is in accordance with the difference in loads shown in Fig. 21 at steps 22 and 23. In this way the support reaction of the South end of the middle beam was reduced at the expense of increased support reaction at the North end.

Fig. 25 shows the relationship between the measured support reaction below the South end of the middle beam and the sum of actuator loads on half floor. The ratio of the reaction to the load is shown in Fig. 26 and in a larger scale in Fig. 27. Assuming simply supported slabs gives the theoretical ratio of 0,835. The measured support reaction seems to follow the theoretical value rather well until load 1015 kN at which the ratio 0,845 is obtained. The next step gives only 0,810 which suggests that slab 1 has already lost a part of its shear stiffness and the load on it is partly transferred to slab 2.

After failure of slab 1 it is unclear, how much load was transferred via slab 1 to the middle beam and how much directly to the floor of the hall. Therefore, no definite values for the shear resistance are given in Stages 2 and 3.

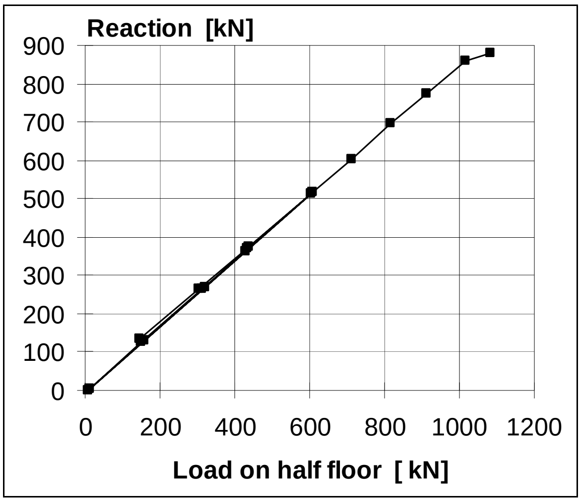

Fig. 25. Stage 1. Support reaction measured below South end of the middle beam vs. load on half floor = 2(P_1 + P_2).

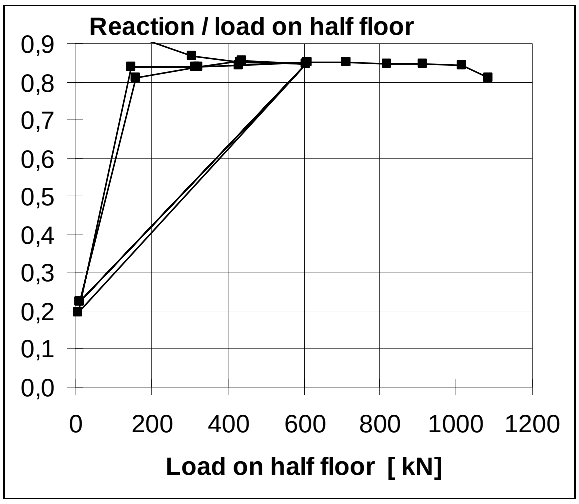

Fig. 26. Ratio of measured support reaction (below South end of the middle beam) to load on half floor.

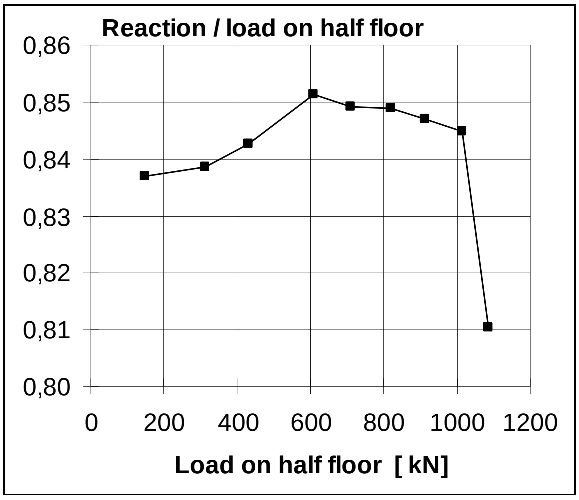

Fig. 27. A part of the previous figure in a large scale.

The observed shear resistance of one slab end (support reaction of slab end at failure) due to different load components is given by

$$V_{obs} = V_{g,sl} + V_{g,jc} + V_{eq} + V_p$$

where $V_{g,sl}$, $V_{g,jc}$, V_{eq} and V_p are shear forces due to the self-weight of slab unit, weight of joint concrete, weight of loading equipment and actuator forces P_i, respectively.

It is concluded that the maximum support reaction of the failed slab 1 has been at least V_p = 0,845 x (actuator loads on half floor) /4 = 0,845 x(276,8+265,5) /2 = 229,1 kN. In the same way, the support reaction due to the weight of the loading equipment has been 0,845x(1,2+5,6)/2 = 2,87 kN. $V_{g,jc}$ is calculated from the nominal geometry of the joints and measured density of the grout. When calculating $V_{g,sl}$, the measured weight of the slabs is used. The values of the shear force components are given in Table 1 below.

Table 1. Components of shear resistance due to different loads.

Action	Load	Shear force kN/slab
Weight of slab unit	5,49 kN/m	19,4
Weight of joint concrete	0,19 kN/m	0,7
Loading equipment	(1,2+5,6)/2 kN/slab	2,9
Actuator loads	(276,8+265,5)/2 kN /slab	229,1

The observed shear resistance $\boldsymbol{V_{obs}}$ **= 252,1 kN** (shear force at support) is obtained for one slab unit with width = 1,2 m. The shear force per unit width is $\boldsymbol{v_{obs}}$ **= 210,1 kN/m.**

9 **Material properties**

9.1 Strength of steel

Component	$R_{eH}/R_{p0,2}$ MPa	R_m MPa	Note
Slab strands J12,5	1630	1860	Nominal (no yielding in test)
Beam strands J12,5	1630	1860	Nominal (no yielding in test)
Reinforcement Txy	500		Nominal value for reinforcing bars (no yielding in test)

9.2
Strength of slab concrete, floor test

#	Cores	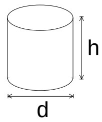	*h* mm	*d* mm	Date of test	Note
6			50	50	2.4.1992[0)]? (+? d)[1)]	Upper flange of slab 1, vertically drilled Tested as drilled[2)] Density = 2437 kg/m^3
Mean strength [MPa]			81,4			
St.deviation [MPa]			5,1			

[0)] This is the date given in the report. It is most likely too late because it is the same as the date of the core tests for VTT.S.WQ.400.1992 carried out after the present floor test

#	Cores	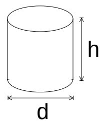	*h* mm	*d* mm	Date of test	Note
6			50	50	2.4.1992[0)]? (+? d)[1)]	Upper flange of slab 5, vertically drilled Tested as drilled[2)] Density = 2442 kg/m^3
Mean strength [MPa]			84,3			
St.deviation [MPa]			2,2			

[0)] This is the date given in the report. It is most likely too late because it is the same as the date of the core tests for VTT.S.WQ.400.1992 carried out after the present floor test

9.3
Strength of slab concrete, reference tests

The slabs for the reference tests were taken from the floor test specimen.

9.4
Strength of concrete in middle beam

#	Cores	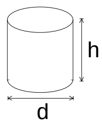	*h* mm	*d* mm	Date of test	Note
6			100	100	18.3.1992 (+22 d)[1)]	Top surface of beam, vertically drilled Tested as drilled[2)] Density = 2358 kg/m^3
Mean strength [MPa]			64,3			
St.deviation [MPa]			3,2			

9.4
Strength of grout in joints and core filling

#	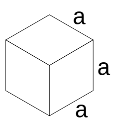	*a* mm	Date of test	Note
6		150	24.2.1992 (+0 d)[1)]	Kept in laboratory in the same conditions as the floor specimen
Mean strength [MPa]		27,8		
St.deviation [MPa]		0,58		

[1)] Date of material test minus date of structural test (floor test or reference test)
[2)] After drilling, kept in a closed plastic bag until compression

9.5
Strength of concrete in end beams

Not measured, nominal value K60

10	**Measured displacements** Note that the last points on each curve represent the post failure situation.
10.1 Deflections	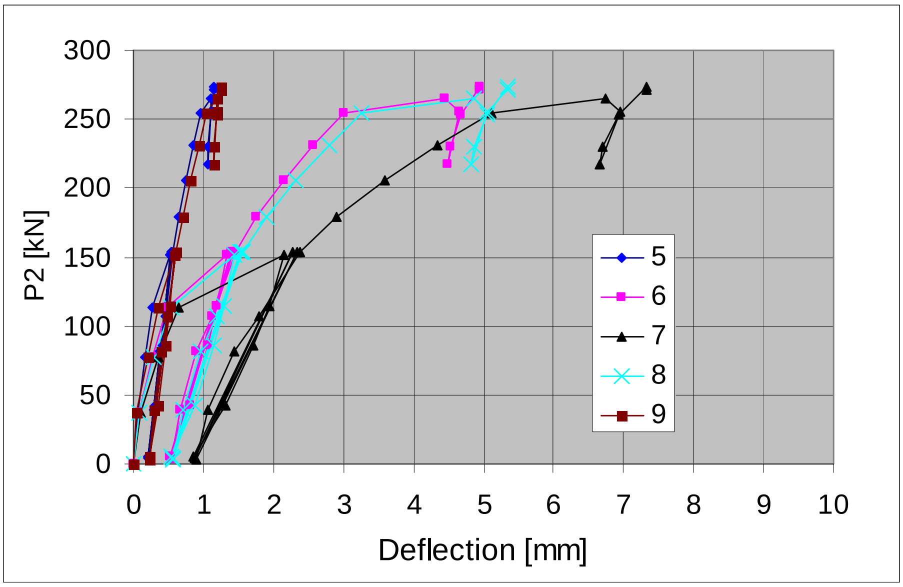 *Fig. 28. Deflection on line I, Western end beam.* 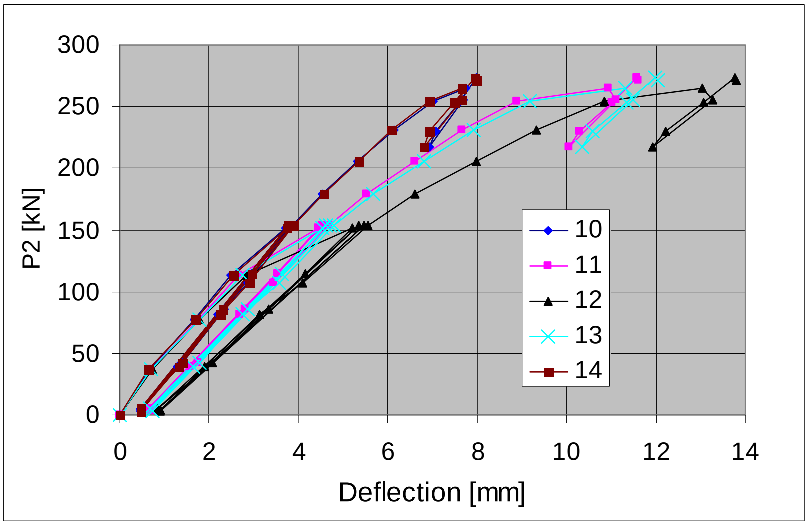 *Fig. 29. Deflection on line II.*

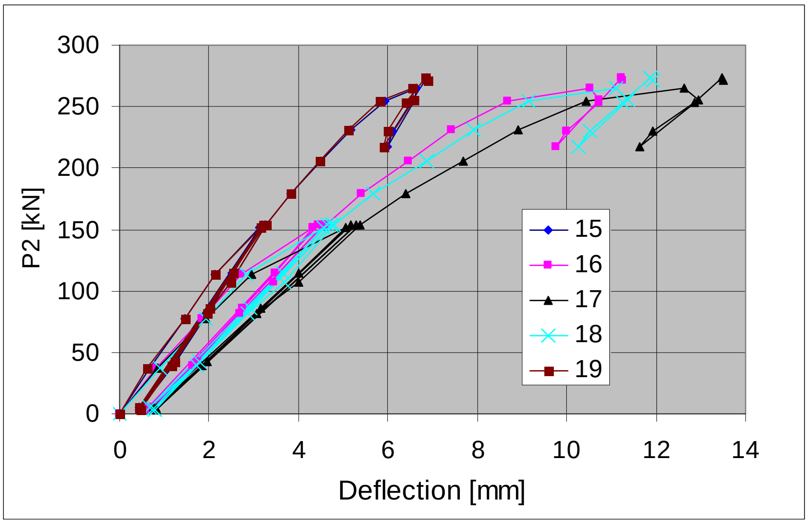

Fig. 30. Deflection on line III.

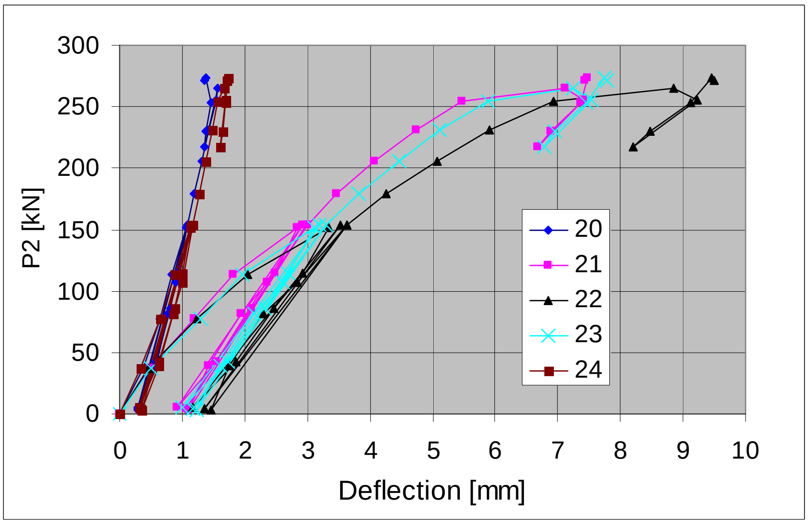

Fig. 31. Deflection on line IV, middle beam.

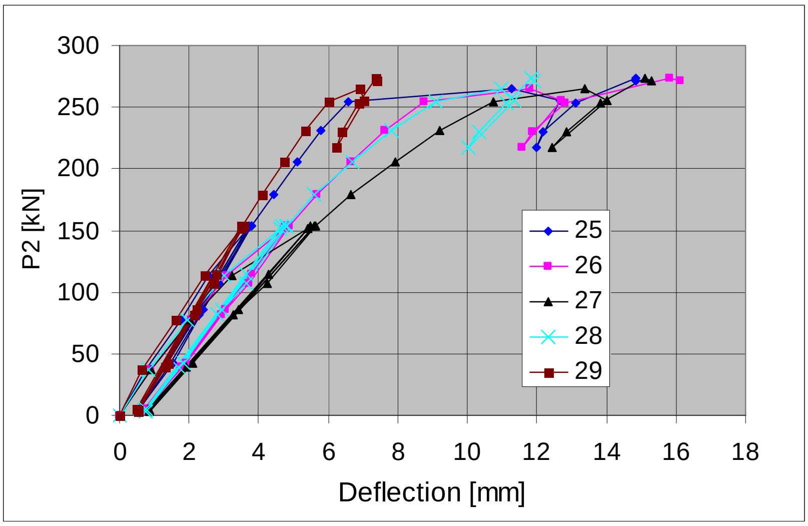

Fig. 32. Deflection on line VI.

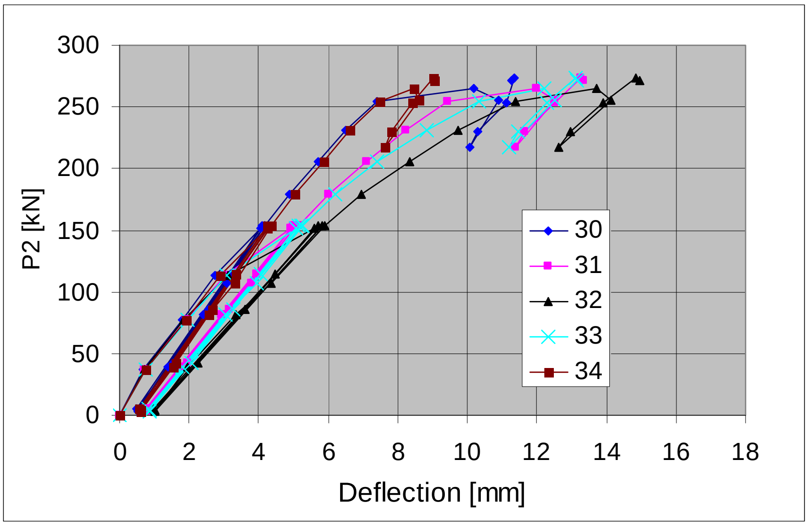

Fig. 33. Deflection on line VII.

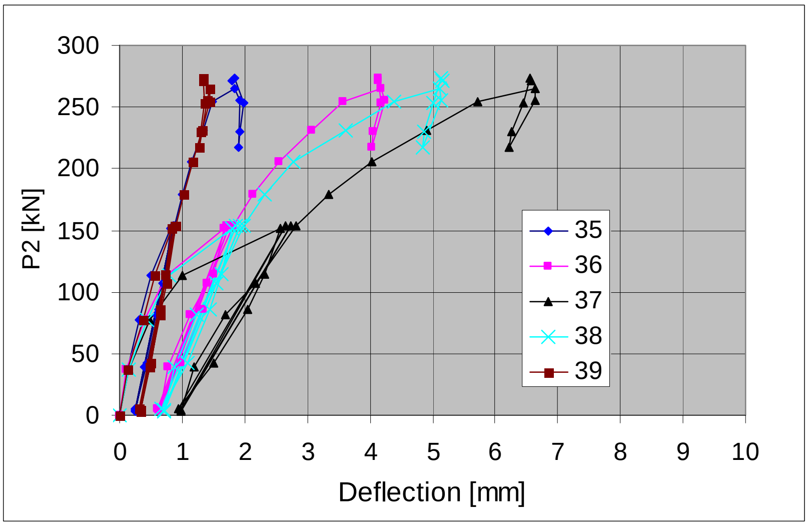

Fig. 34. Deflection on line VIII along Eastern end beam.

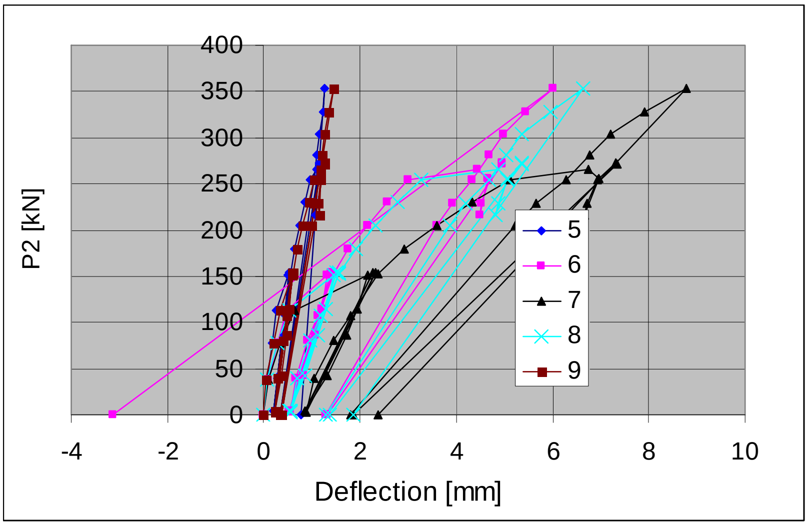

Fig. 35. Deflection on line I along Western end beam, stages 1–3.

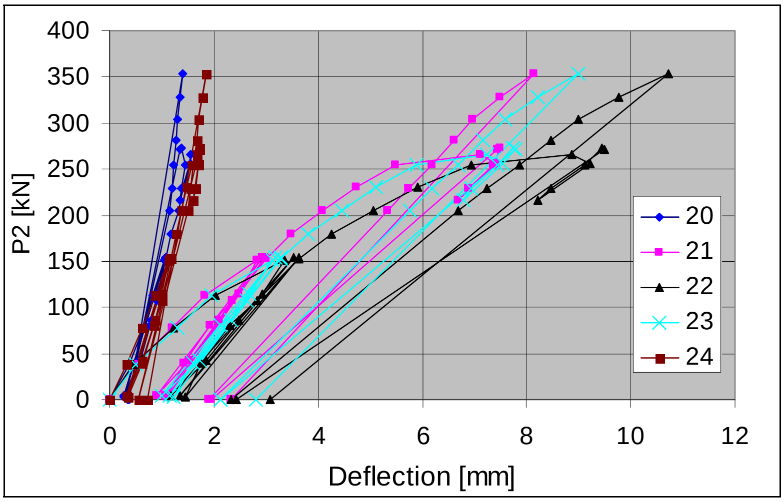

Fig. 36. Deflection on line IV along middle beam, stages 1–3.

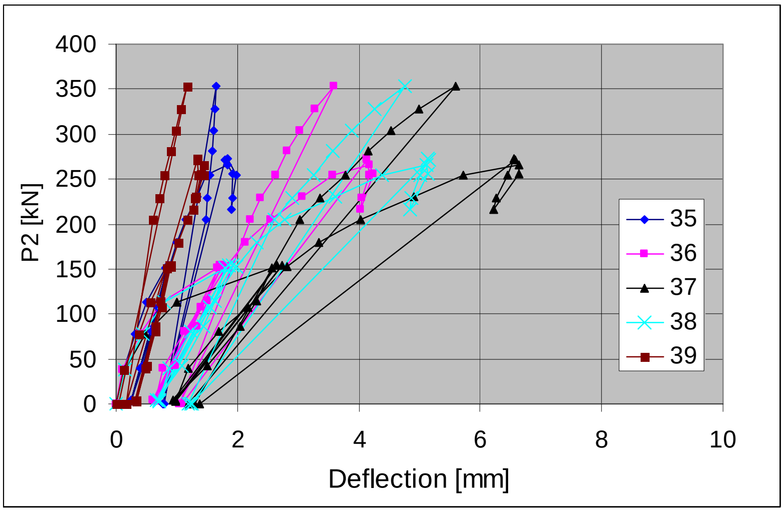

Fig. 37. Deflection on line VIII along Western end beam, stages 1–3.

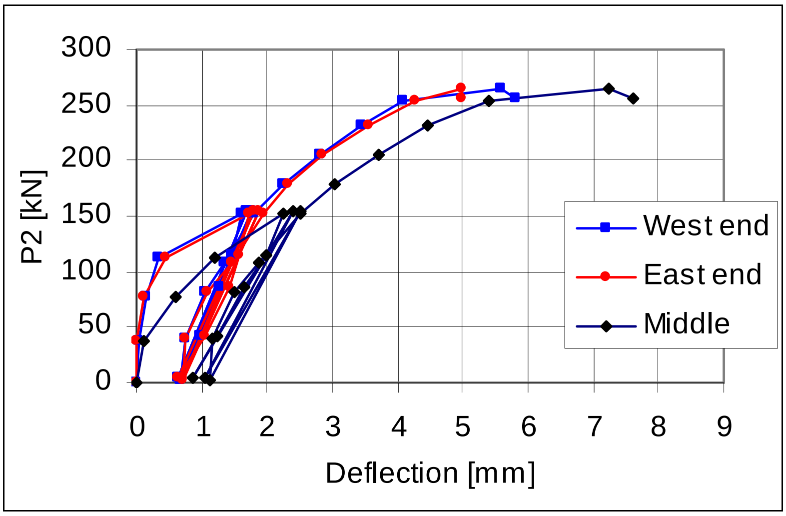

Fig. 38. Stage 1. Net deflection of mid-point of beams (rigid body motion = settlement of beam supports eliminated).

	The last measured net deflection of the middle beam was 5,4 mm before the highest load level and the first measured after it was 7,2 mm. Before failure, the net deflection of the middle beam was 1,4 mm and after the highest load level 1,7–2,2 mm greater than that of the end beams.
10.2 Crack width	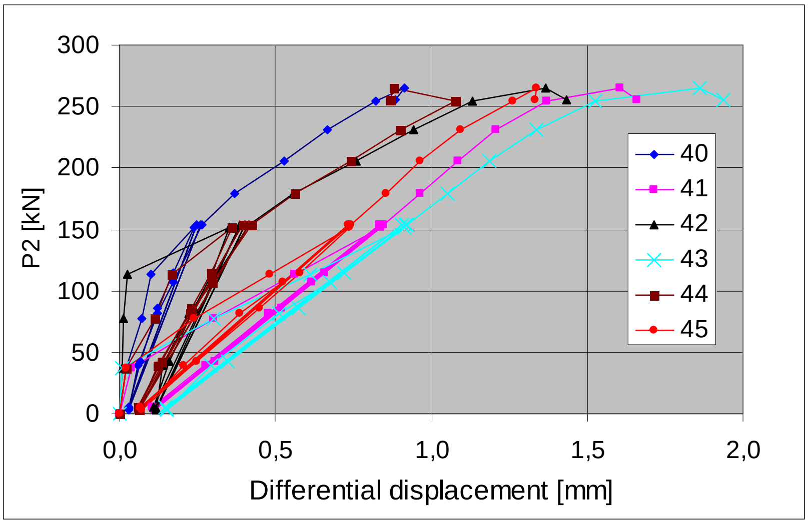 *Fig. 39. Differential displacement (≈ crack width) measured by transducers 40–46.*
10.3 Average strain (actually differential displacement)	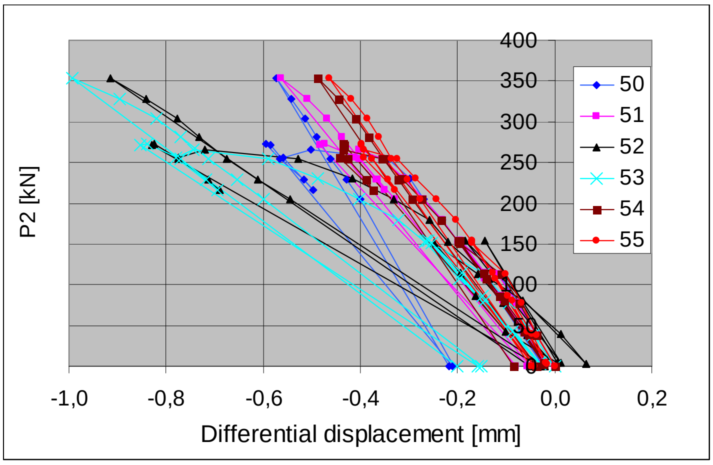 *Fig. 40. Differential displacement at top surface of floor measured by transducers 50–55.*

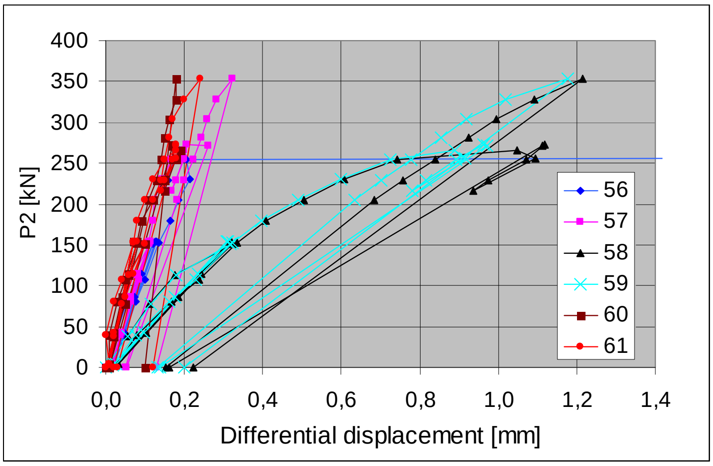

Fig. 41. Differential displacement at soffit measured by transducers 56–61.

10.4
Shear displacement

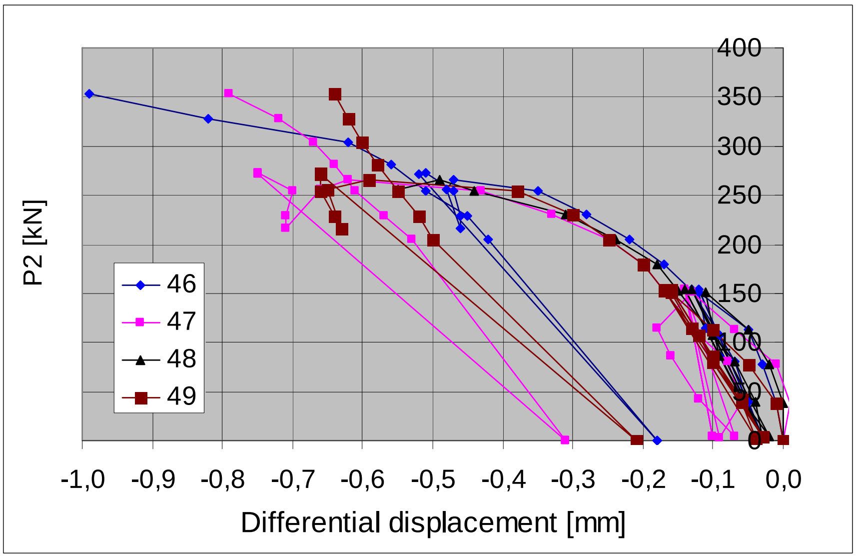

Fig. 42. Stages 1–3. Differential displacement between edge of slab and middle beam. A negative value means that the slab is moving towards the end of the beam.

10.5 Strain

A gradual growth in the measured strain means that there has been a crack, most likely attributable to the release of the prestressing force, before the loading. A sudden increase in crack width indicates a new crack. An example of the former and latter behaviour are illustrated e.g. by transducers 35 and 34, respectively, see Fig. 49.

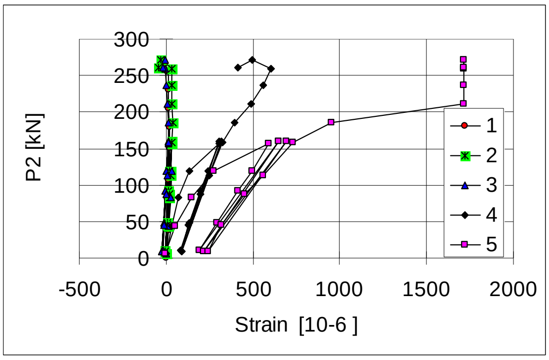

Fig. 43. Strain measured by gauges 1–5.

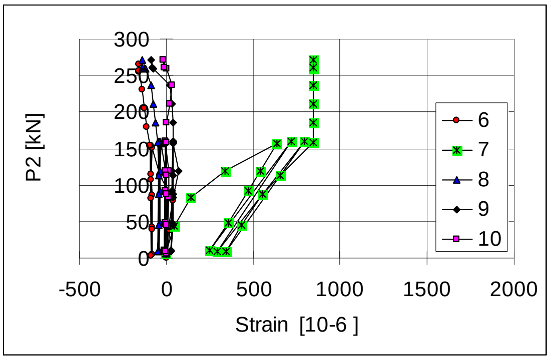

Fig. 44. Strain measured by gauges 6–10.

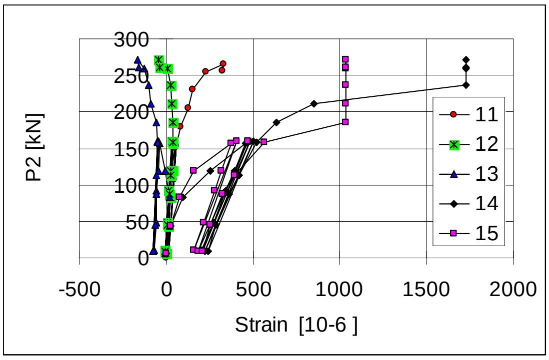

Fig. 45. Strain measured by gauges 11–15.

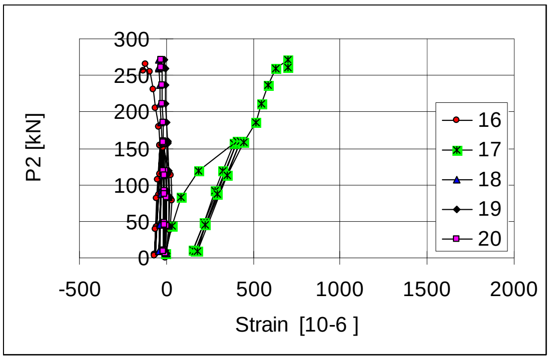

Fig. 46. Strain measured by gauges 16–20.

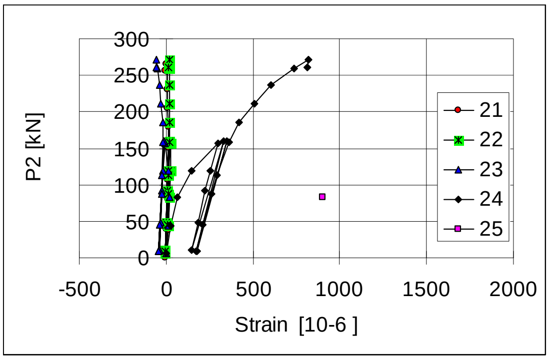

Fig. 47. Strain measured by gauges 21–25.

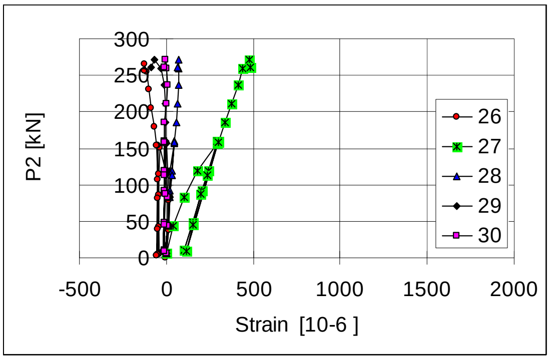

Fig. 48. Strain measured by gauges 26–30.

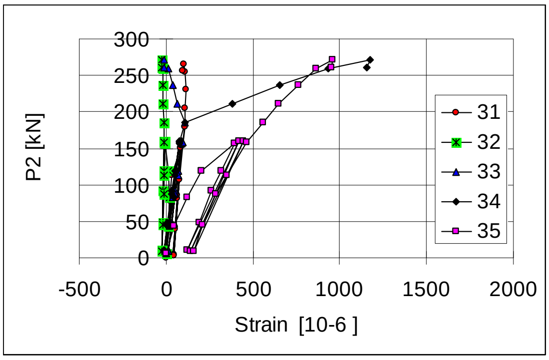

Fig. 49. Strain measured by gauges 31–35.

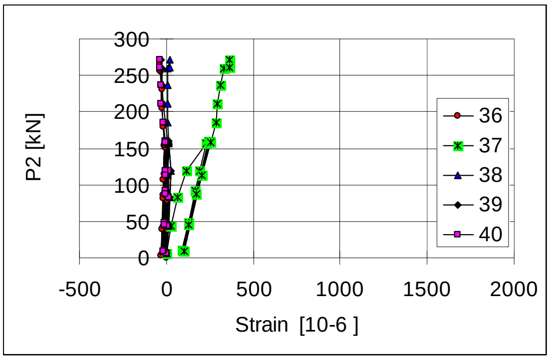

Fig. 50. Strain measured by gauges 36–40.

In Figs 51 and 52 the cracks below the soffit of slab 2, 3, 6 and 7 are shown.

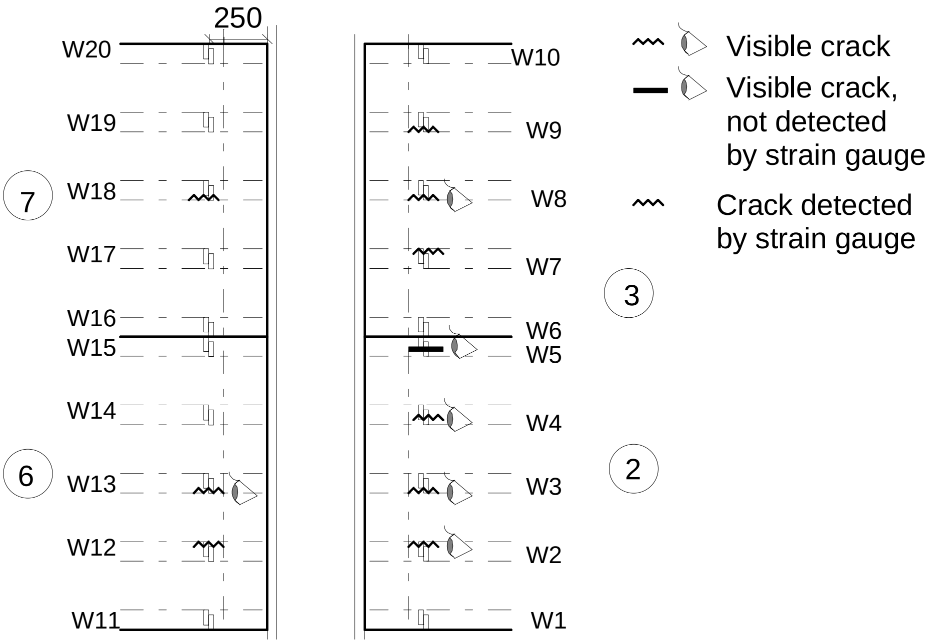

Fig. 51. Location of cracks observed visually or by strain gauges under load P_2 = 153,2 kN.

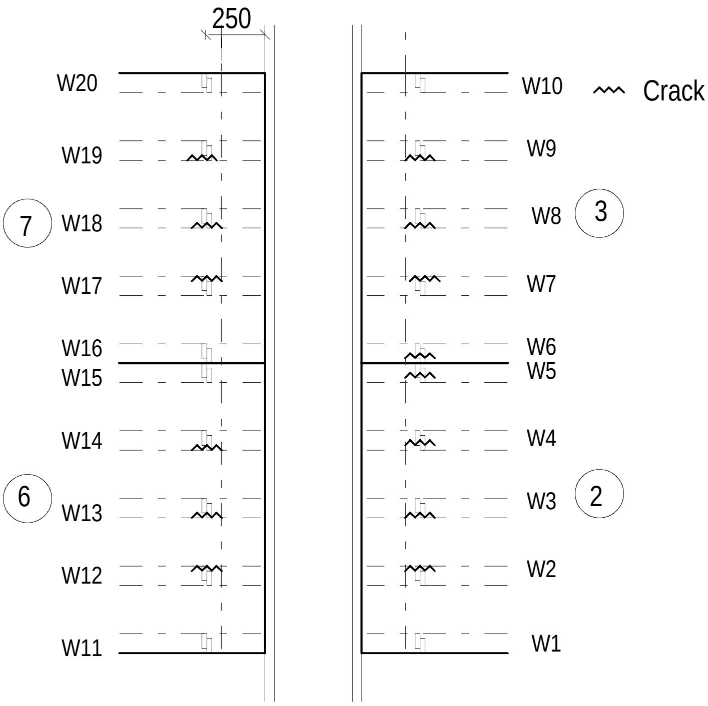

Fig. 52. Location of cracks observed visually or by strain gauges under load P_2 = 251,3 kN.

11 **Reference tests**

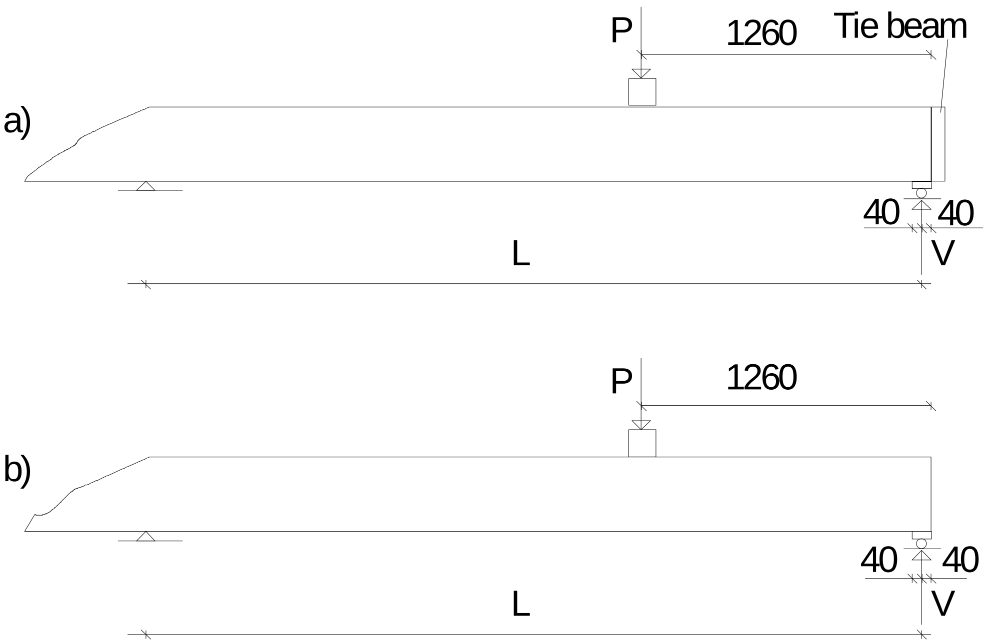

Fig. 53. Layout of reference test. a) With tie beam, slabs 1 and 5. b) Without tie beams, slabs 7 and 8. For L, see the Table 2.

Table 2. Span L, ultimate load P_{obs}, ultimate shear force V_{obs} and failure mode in reference tests. The weight of the loading equipment = 0,5 kN is included in P_{obs}.

Slab	L mm	Tie beam	P_u kN	V_u kN	Failure mode
1	5985	Yes	> 600*	> 494*	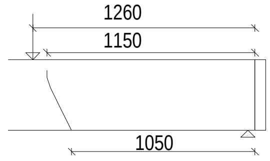
5	5000	Yes	591	461	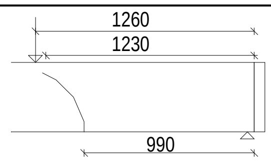 Anchorage failure
7	7110	No	564	487	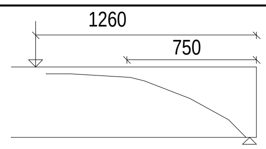 Shear tension failure
8	7115	No	568	490	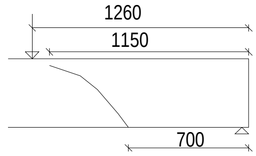 Shear tension failure
			Mean	483	

12 Comparison: floor test vs. reference tests

The observed shear resistance (support reaction) of the hollow core slab in the floor test was equal to 252,1 kN per one slab unit or 210,1 kN/m. This is **52%** of the mean of the shear resistances observed in the reference tests.

13 Discussion

1. The net deflection of the middle beam due to the imposed actuator loads only (deflection minus settlement of supports) was 5,4–7,2 mm or L/926–L/694, i.e. rather small.
2. The shear resistance measured in the reference tests was slightly higher than the mean of the observed values for similar slabs given in *Pajari, M. Resistance of prestressed hollow core slab against a web shear failure. VTT Research Notes 2292, Espoo 2005*.
3. Before failure, the net deflection of the middle beam was 1,5 mm and right after the highest load level 1,8–2,2 mm greater than that of the end beams. This is a too small difference to cause considerable torsional stresses in the slabs.

The failure mode was web shear failure of edge slab 1 close to the middle beam. The middle beam seemed to recover completely after the failure.

APPENDIX A: PHOTOGRAPHS

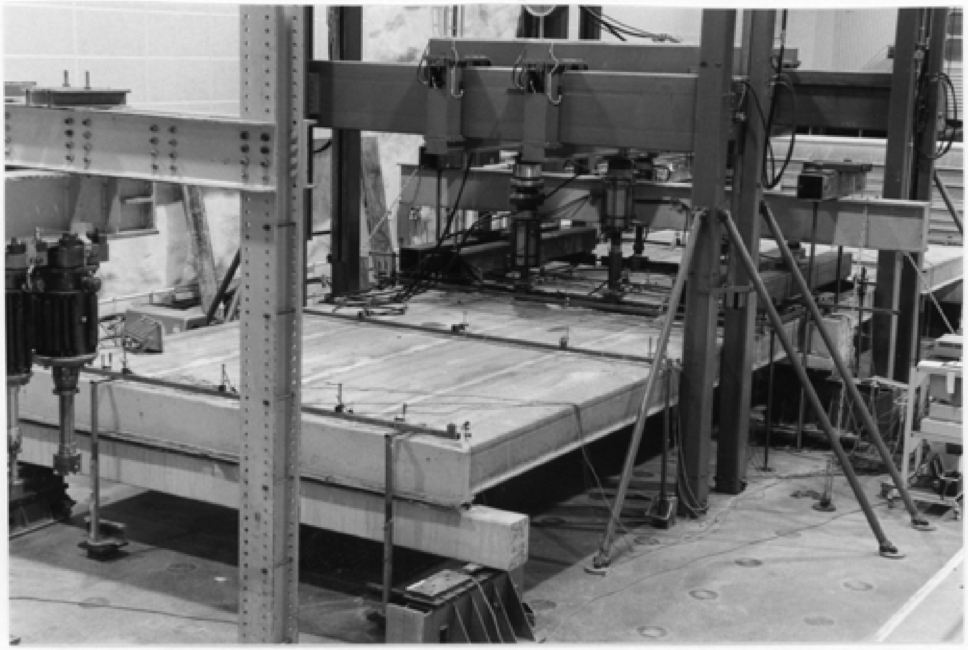

Fig. 1. Overview of floor test.

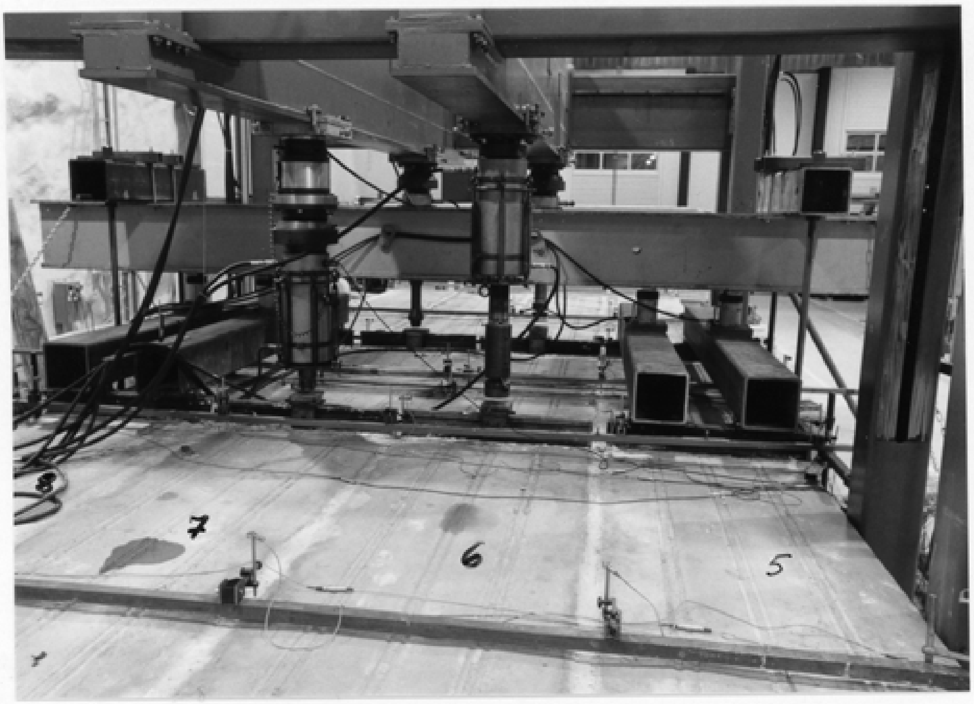

Fig. 2. Longitudinal view of floor test.

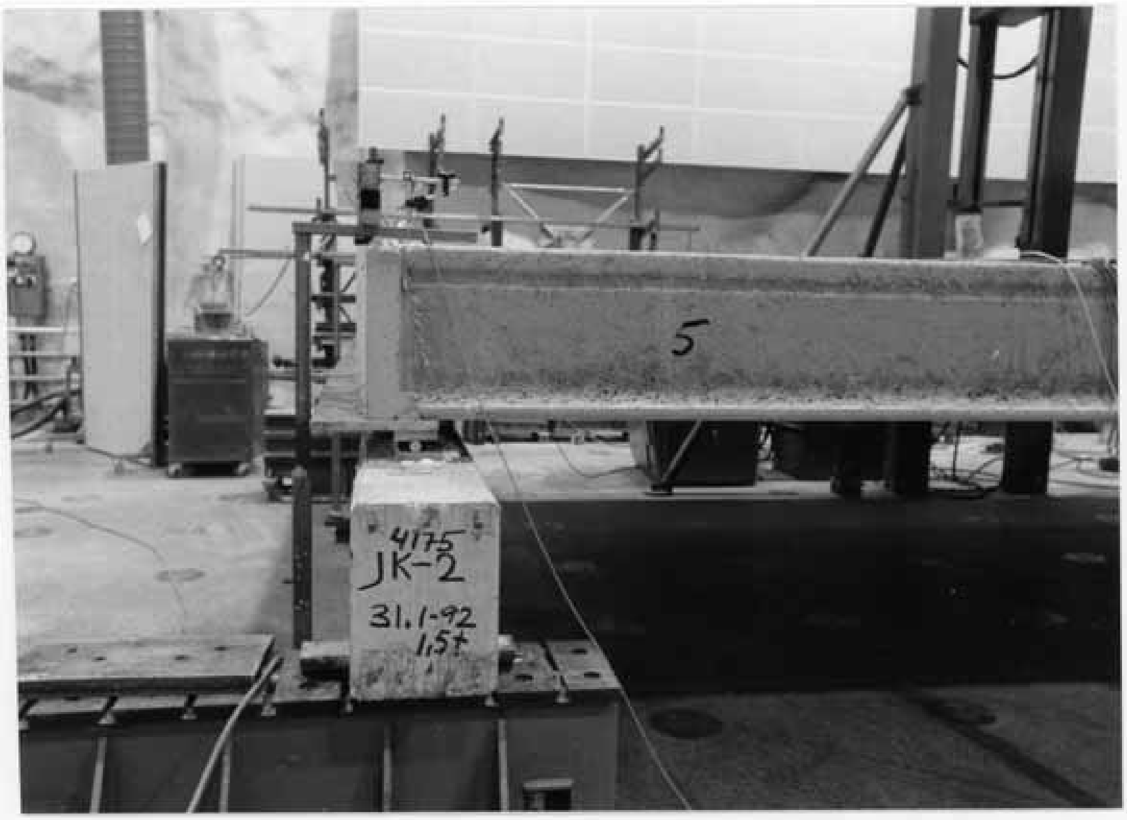

Fig. 3. End beam.

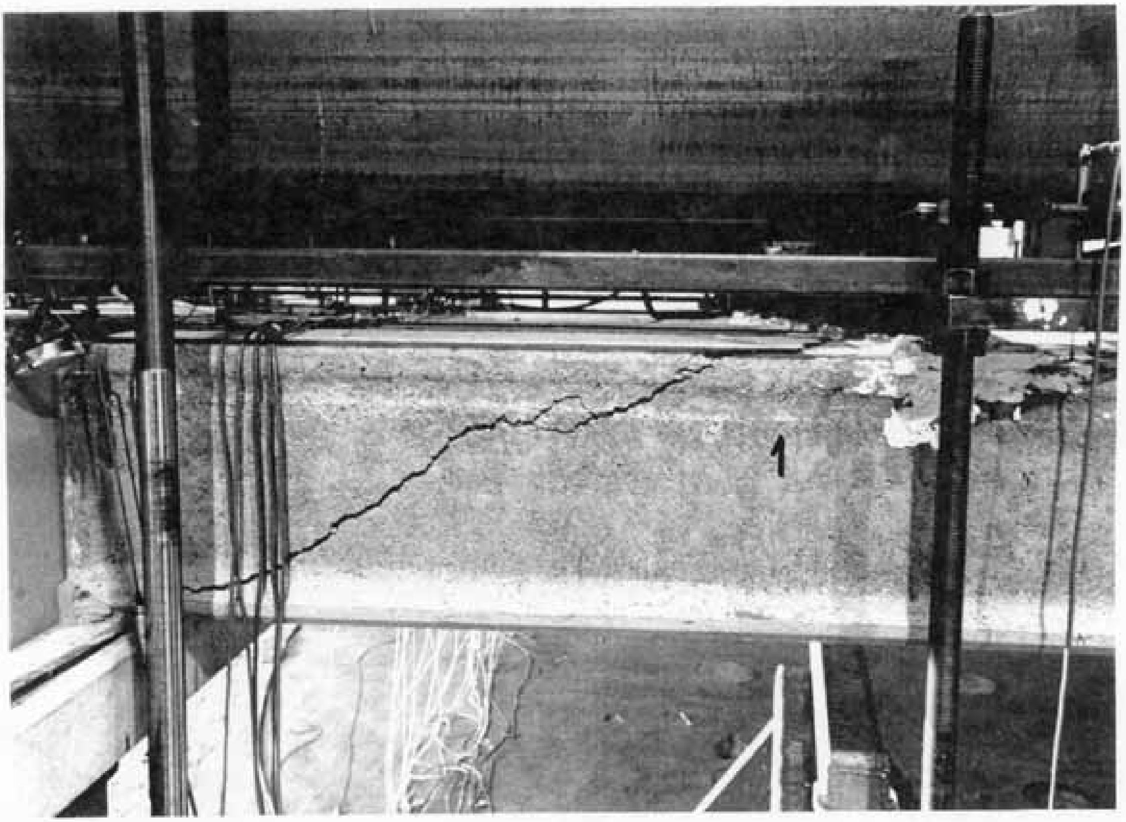

Fig. 4. Failure at stage 1.

Fig. 5. Failure at stage 3. Side view.

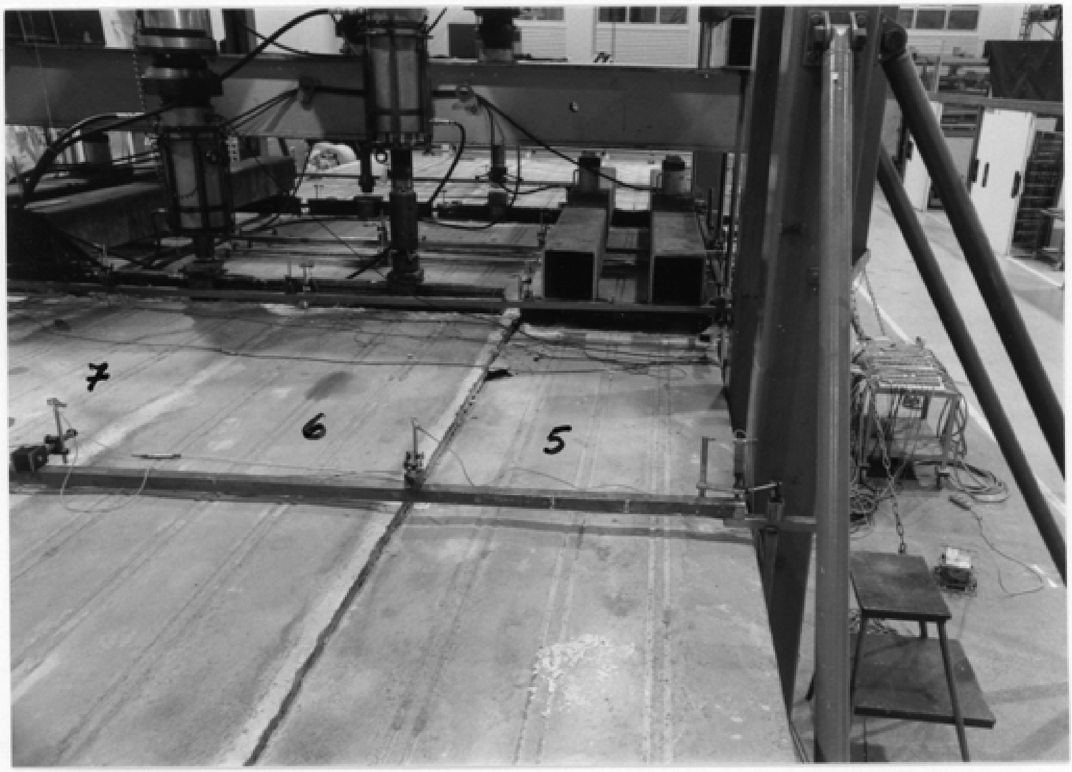

Fig. 6. Failure at stage 3 seen from above.

Fig. 7. Failure at stage 3 seen from above after removal of loading equipment.

Fig. 8. Concrete in hollow cores. Note the proper filling.

Fig. 9. Filling of outermost hollow core. Note the perfect filling on the top.

Fig. 10. End of slab unit no 3 after removal. Note the cracking of the shear keys.

Fig. 11. Cracking of joint concrete along middle beam. Note the cracking of the shear keys.

Fig. 12. Concrete filling between hollow core slab and ledger of middle beam. Note the perfect penetrationof the concrete under the end of the slab.

Fig. 13. Cracking of joint concrete along edge of middle beam.

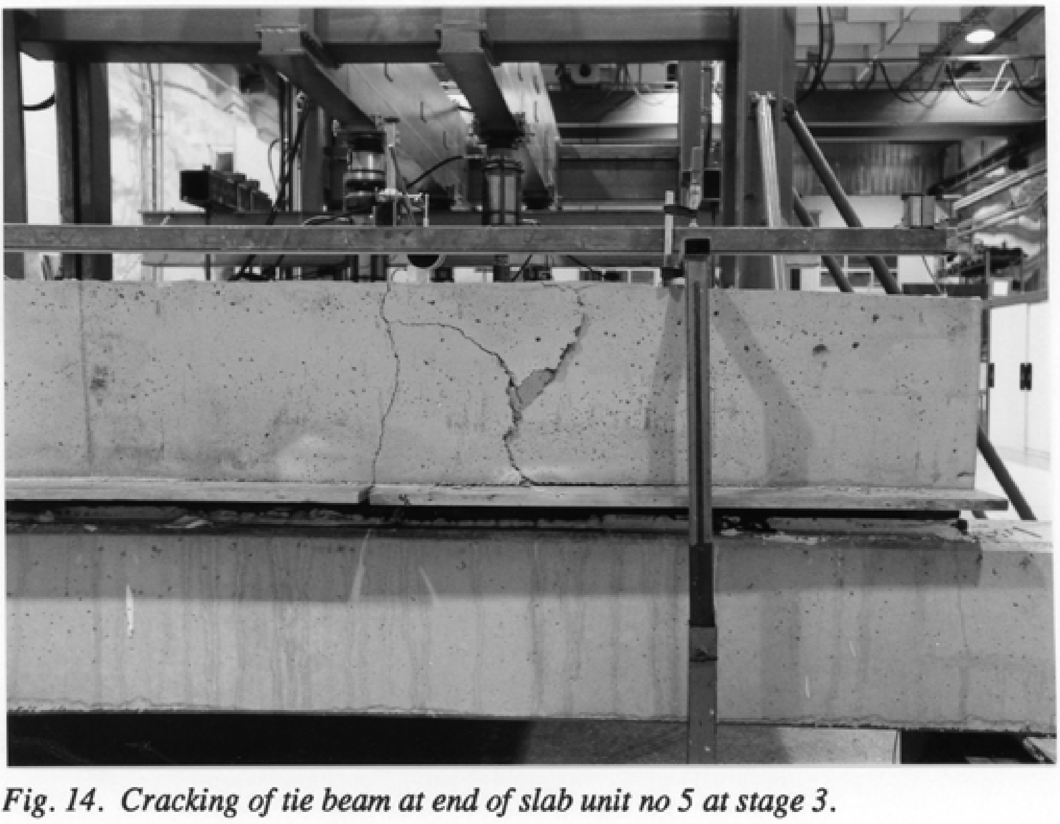

Fig. 14. Cracking of tie beam at end of slab unit no 5 at stage 3.

Fig. 15. Cracking pattern of slab unit no 1 in reference test.

Fig. 16. Failure pattern of slab unit no 5 in reference test. The strand buckled when lifting the slab unit after the test.

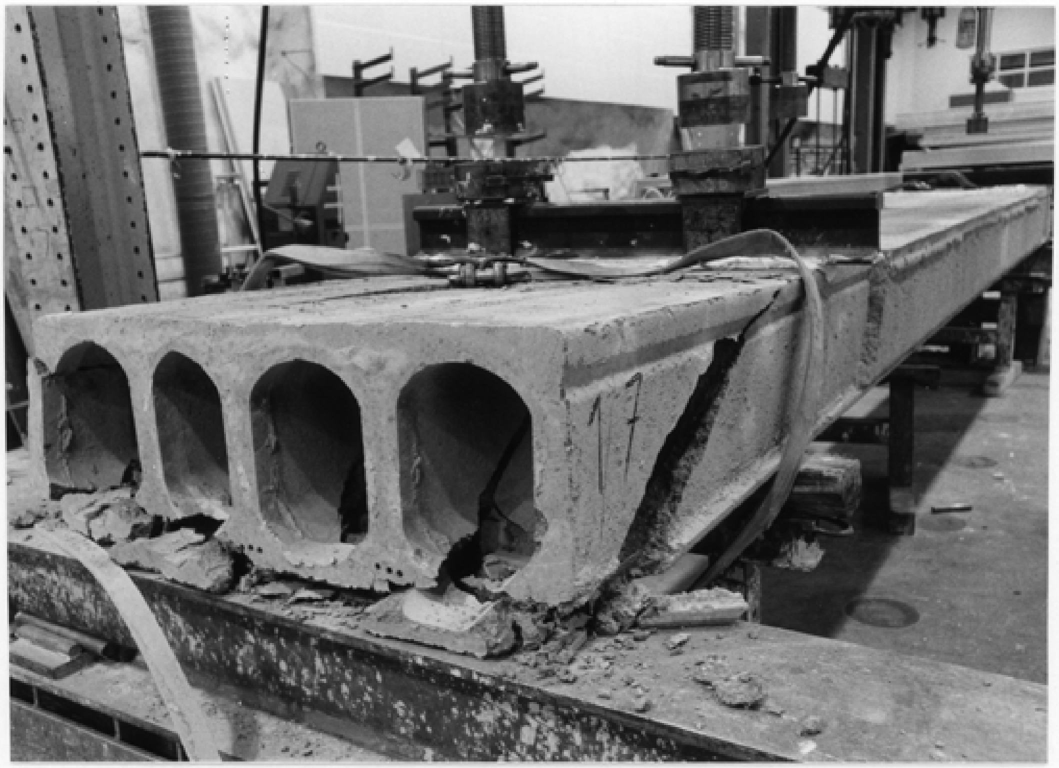

Fig. 17. Failure pattern of slab unit no 7 in reference test.

Fig. 18. Failure pattern of slab unit no 8 in reference test.

<table>
<tr><td>1</td><td>General information</td></tr>
<tr><td>1.1
Identification and aim</td><td>VTT.S.WQ.400.1992   Last update 2.11.2010
ST400   (Internal identification)
Aim of the test   To study the shear resistance of thick hollow core slabs supported on steel beams.</td></tr>
<tr><td>1.2
Test type</td><td>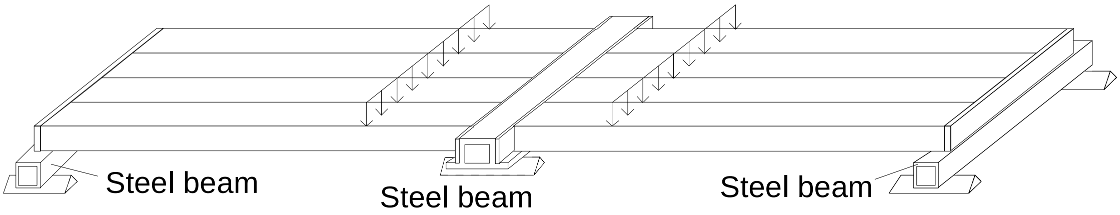

Fig. 1. Illustration of test setup.</td></tr>
<tr><td>1.3
Laboratory
& date of test</td><td>VTT/FI   25.3.1992</td></tr>
<tr><td>1.4
Test report</td><td>Author(s)   Pajari, M.
Name   Loading test for 400 mm hollow core floor supported on steel beams
Ref. number   RAT-IR-4/1993
Date   23.4.1993
Availability   Public, available on request from VTT Expert Services, P.O. Box 1001, FI-02044 VTT.
Financed by Lohja Oy, Finland; NCC Prefab AB, Sweden; Parma Oy, Finland; Oy Partek Concrete Ab, Finland; Skanska Prefab AB, Sweden and AB Strängbetong, Sweden. The Finnish companies were financially supported by TEKES, Finland.</td></tr>
<tr><td>2</td><td>Test specimen and loading
(see also Appendix A)</td></tr>
<tr><td>2.1
General plan</td><td>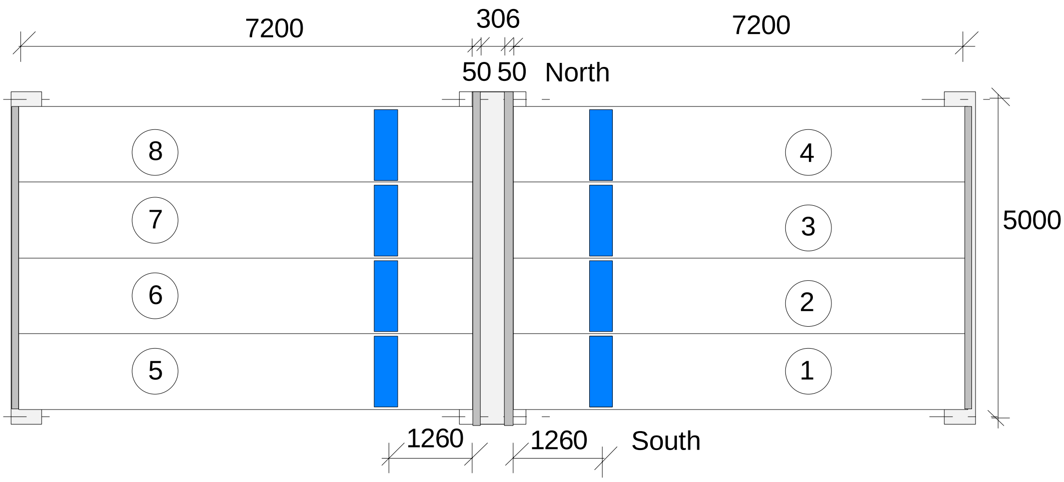

Fig. 2. Plan.</td></tr>
</table>

<table>
<tr>
<td>2.2
End beams</td>
<td>
Simply supported box girders made of steel. Span = 5,0 m

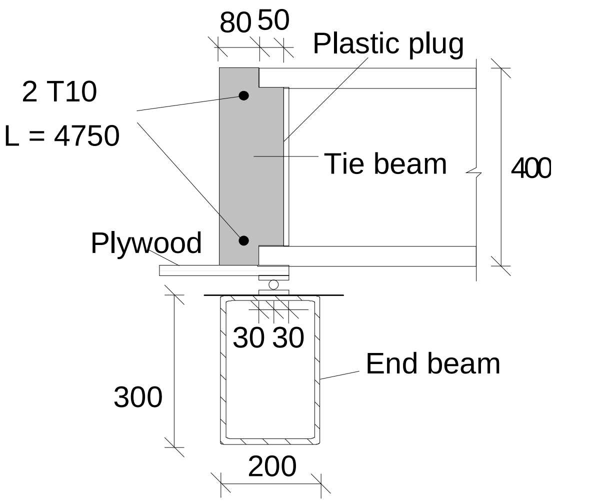

Fig. 3. Arrangements at end beam. T10 refers to a reinforcing bar, see 2.4.

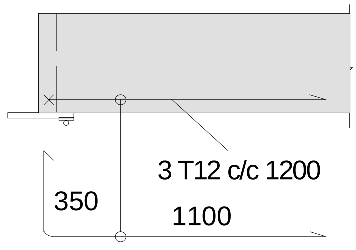

Fig. 4. Tie reinforcement in joints between adjacent slabs. T12 refers to a reinforcing bar, see 2.4.
</td>
</tr>
<tr>
<td>2.3
Middle beam</td>
<td>

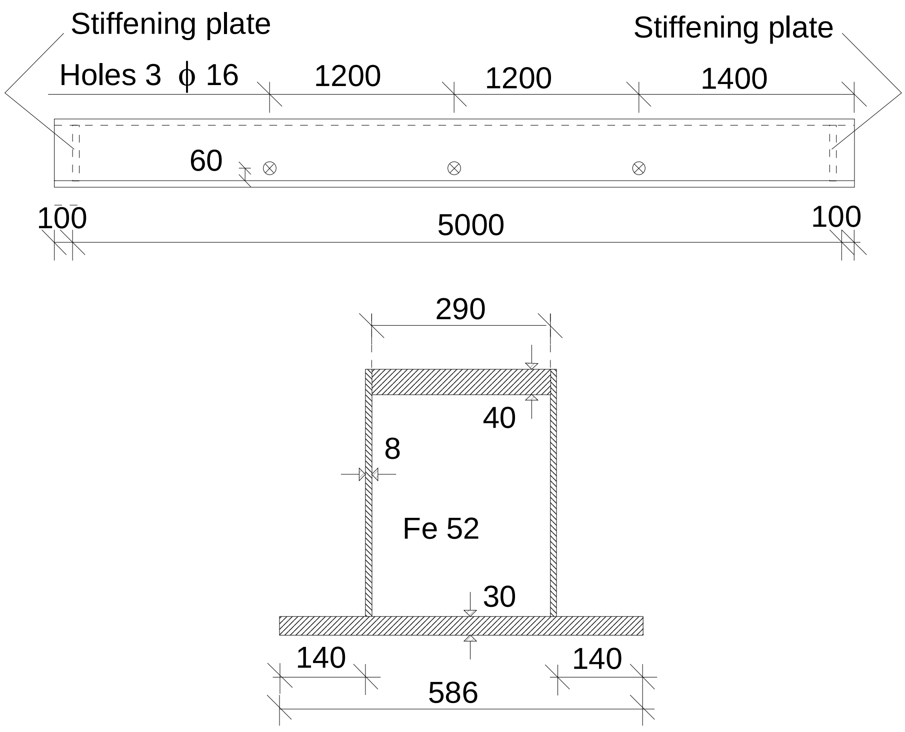

Fig. 5. Elevation and section of middle beam.
</td>
</tr>
</table>

2.4 Arrangements at middle beam	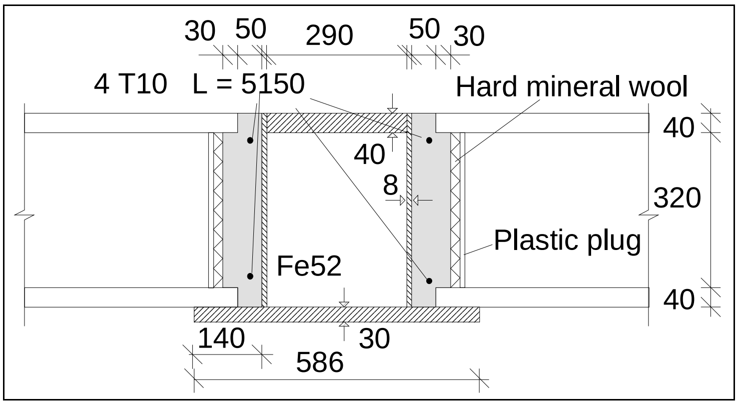 *Fig. 6. Section along hollow cores.* 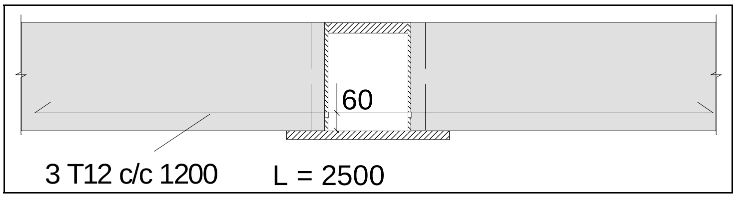 *Fig. 7. Tie reinforcement in joints between adjacent slabs.* - Simply supported, span = 5,0 m **Txy**: Hot rolled, weldable rebar A500HW, ϕ = xy mm, see 9.1.
2.5 Slabs	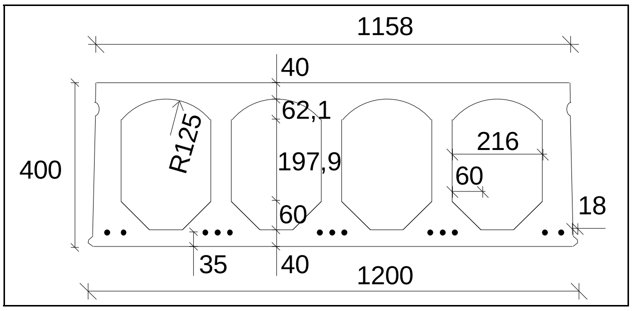 *Fig. 8. Nominal geometry of slab units (in scale).* - Extruded by Partek Betoniteollisuus Oy, Hyrylä factory 15.1.1992 - 13 lower strands J12,5 initial prestress 1100 MPa **J12,5**: seven indented wires, ϕ =12,5 mm, A_p = 93 mm^2 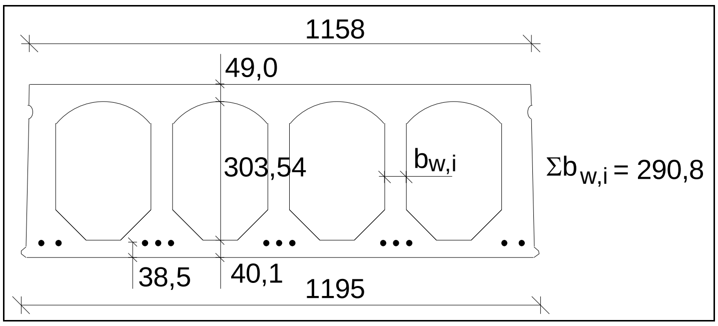 Max measured bond slips: 1,2 and 1,1 in slab 1; 1,0 in slabs 3 and 7 Measured weight of slab units = 5,51 kN/m *Fig. 9. Mean of most relevant measured geometrical characteristics.*

<table>
<tr><td>2.6
Temporary supports</td><td>Temporary supports below beams (Yes/No)
- No</td></tr>
<tr><td>2.7
Loading arrangements</td><td>
There were two separate, manually controlled hydraulic circuits, one for actuators P_1 and the other for actuators P_2, see Fig. 10. Attempts were made to keep $P_1 \approx P_2$ so as to generate two linear line loads on the floor.

The primary spreader beams on the top of the floor were railway rails cut in pieces slightly shorter than 1,2 m. The friction between the secondary and primary spreader beams was eliminated by teflon plates.

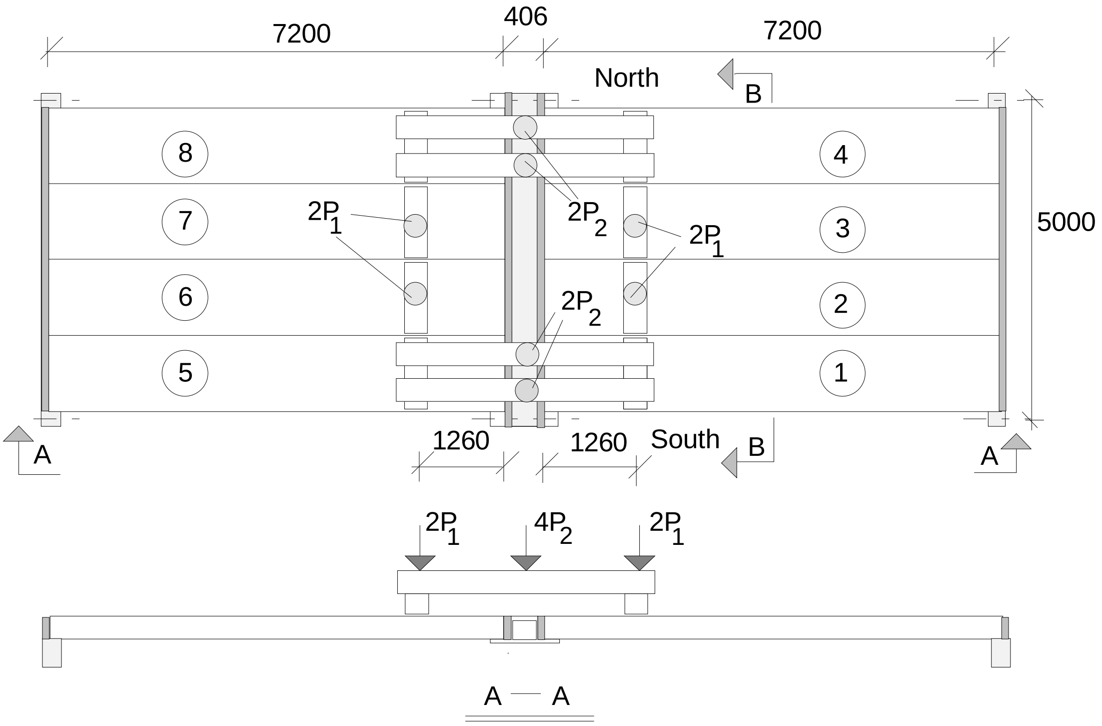

Fig. 10. Plan. P_1 and P_2 refer to vertical actuator forces.

<table>
<tr><td>
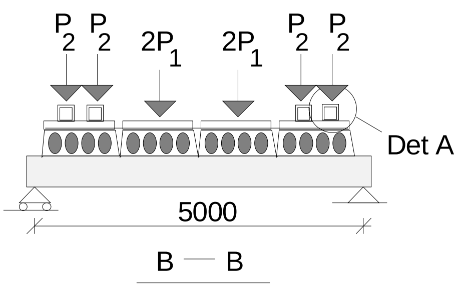

Fig. 11. Section B-B, see previous figure.
</td><td>
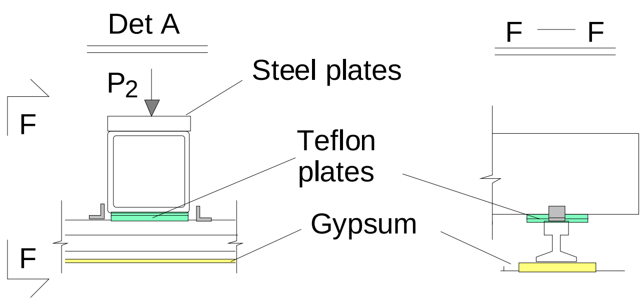

Fig. 12. Detail A, see previous figure.
</td></tr>
</table>
</td></tr>
</table>

3	**Measurements**
3.1 Support reactions	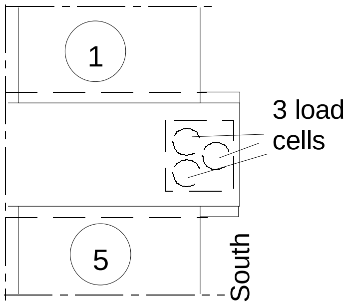 *Fig. 13. Load cells below the South end of the middle beam.*
3.2 Vertical displacement	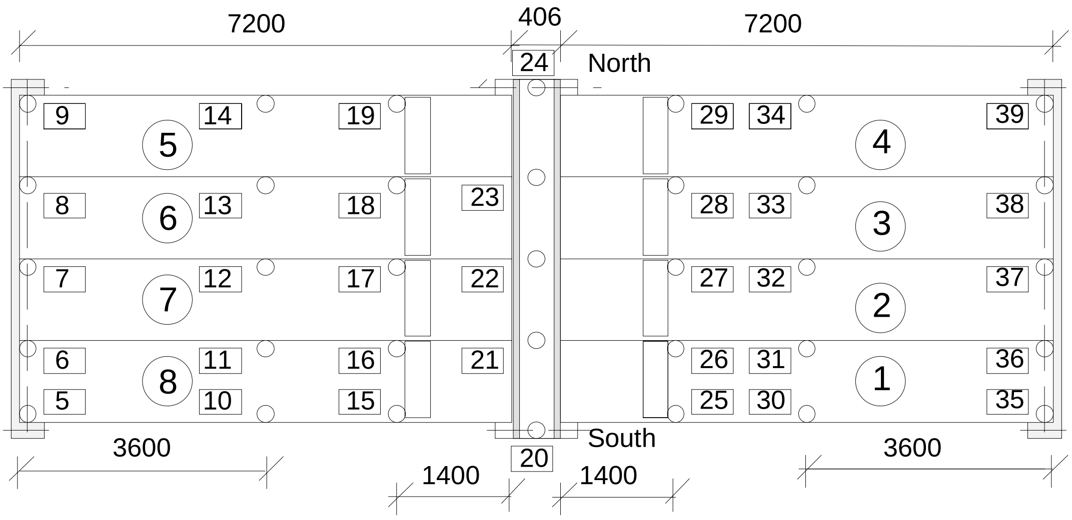 *Fig. 14. Location of transducers 5 … 39 for measuring vertical deflection.*
3.3 Average strain	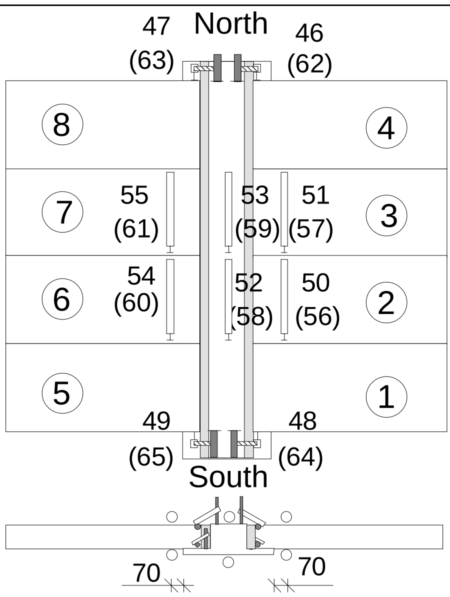 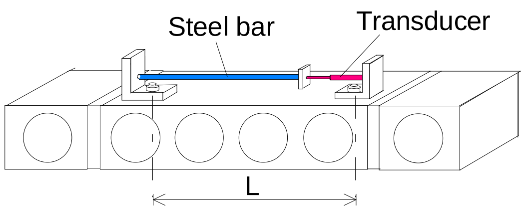 *Fig. 15. Apparatus for measuring average strain. L =1120mm and 1060 mm for the bottom and top side transducers, respectively.* *Fig. 16. Position of device (transducers 50–61) measuring average strain parallel to the beams. Transducers 46–49 and 62–65 measured the sliding of the outermost slabs along the beam. Numbers in parentheses refer to the soffit of the floor, others to the top side.*

3.4 Horizontal displacements	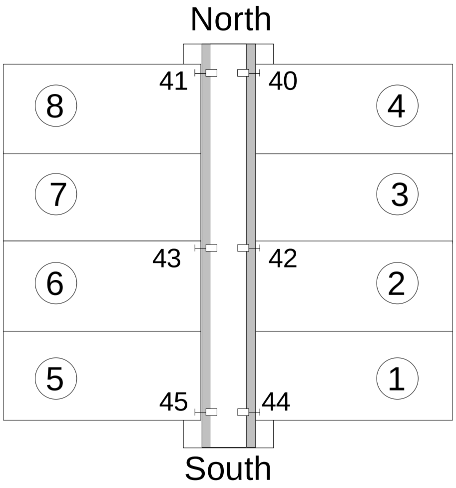 *Fig. 17. Transducers 40–45 measuring crack width on the top of the floor.*
3.5 Strain	To detect longitudinal cracks along strands, the soffit of slabs 2, 3, 6 and 7 was provided with strain gauges as shown in Figs 18 and 19. The measuring length of the gauges was 67 mm. 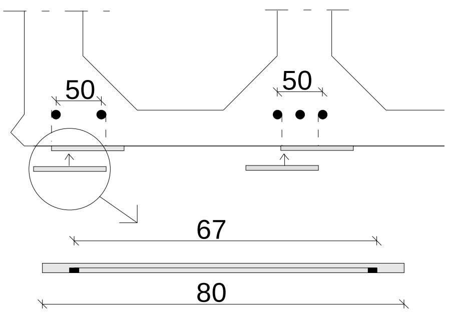 *Fig. 18. Strain gauges below strands.* 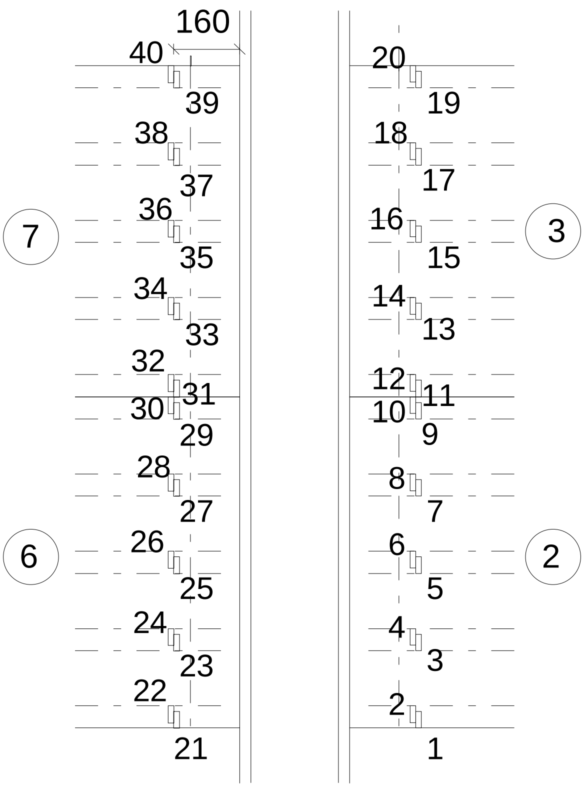 *Fig. 19. Position of strain gauges. The webs of the slabs are indicated by dot-and-dash lines below strands.*
4	**Special arrangements** -

5	**Loading strategy**
5.1 Load-time relationship	Date of the floor test was 25.3.1992 All measuring devices were zero-balanced when the actuator forces P_i were equal to zero but the weight of the loading equipment was on. The loading history is shown in Fig. 20. Note, that the number of load step, not the time, is given on the horizontal axis. In the following, the cyclic stage (steps 1–16) and the monotonous stage until failure (steps 16–41) are called Stage 1. 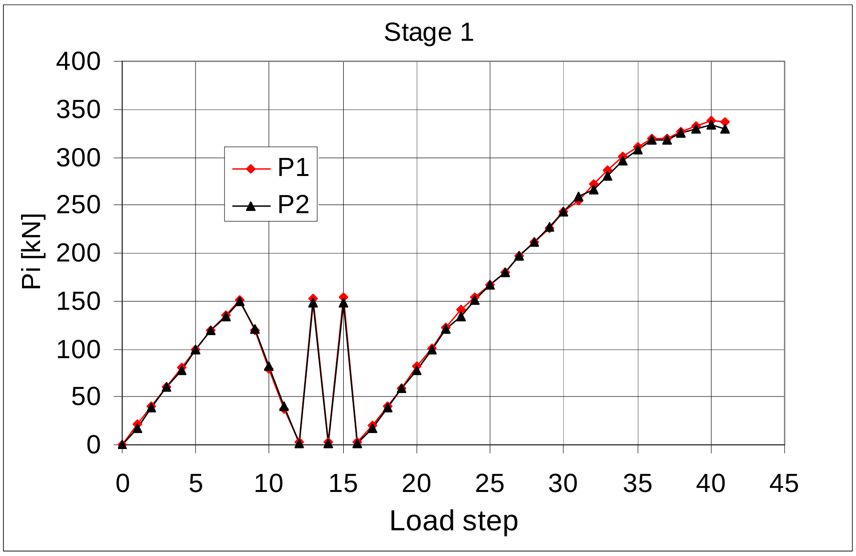 *Fig. 20. Development of actuator loads P_1 and P_2.* The weight of loading equipment per actuator was 1,2 kN and 5,6 kN for actuators P_1 and P_2, respectively. Consequently, the imposed load per slab was $F_1 = P_1 + 1{,}2$ kN for slabs 2, 3, 6 and 7 $F_2 = P_2 + 5{,}6$ kN for slabs 1, 4, 5 and 8

5.2 After failure	After failure, the failed slab 5 was temporarily supported and the load test was continued. This is called Stage 2. 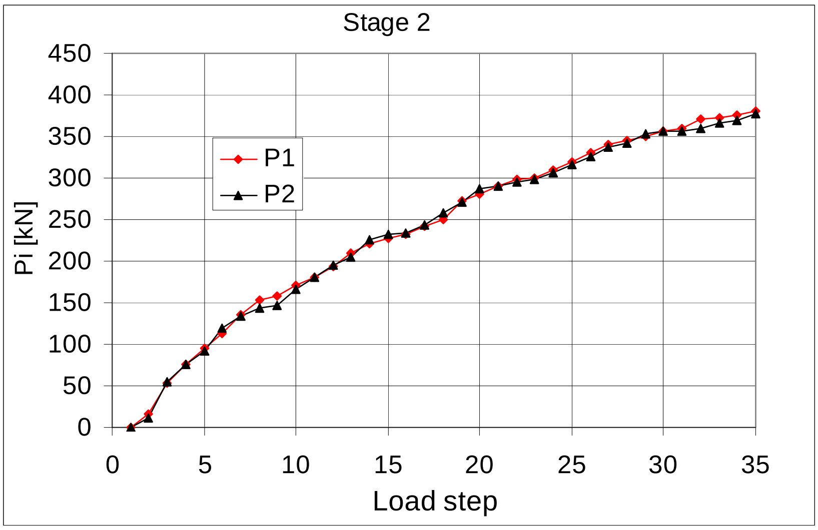 *Fig. 21. Development of actuator loads P_1 and P_2 in Stage 2.*
6	**Observations during loading**

Stage 1	At P_1 = 300,3 kN, P_2 = 297,1 corners of slabs 5 and 8 cracked next to the support of the beam. At P_1 = 319,7 kN, P_2 = 318,1 kN a narrow shear crack appeared in the web of slab 5, see Fig. 22. It grew in width and length when the loads were increased. At P_1 = 337,9 kN, P_2 = 334,2 kN a shear failure took place in slab 5 between the line load and the support, see Appendix A, Figs 3–5.
Stage 2	After the failure, a temporary support was placed below slab 5 as shown in Fig. 23. The aim was to continue the load test with seven line loads. When the loads were increased, a corner of slab 1 cracked as shown in Fig. 23. At P_1 = 381,1 kN, P_2 = 377,2 kN slabs 6 and 7 failed as shown in Fig. 23 and in Annex A, Figs 7–11.
After failure	When demolishing the test specimen it was observed that the interface between the webs of the middle beam and the slab ends had cracked neatly along the edge of the beam, see Appendix A, Fig. 6. The middle beam looked intact after the failure.

7	**Cracks in concrete**
7.1 Cracks at service load	Not documented.
7.2 Cracks after failure	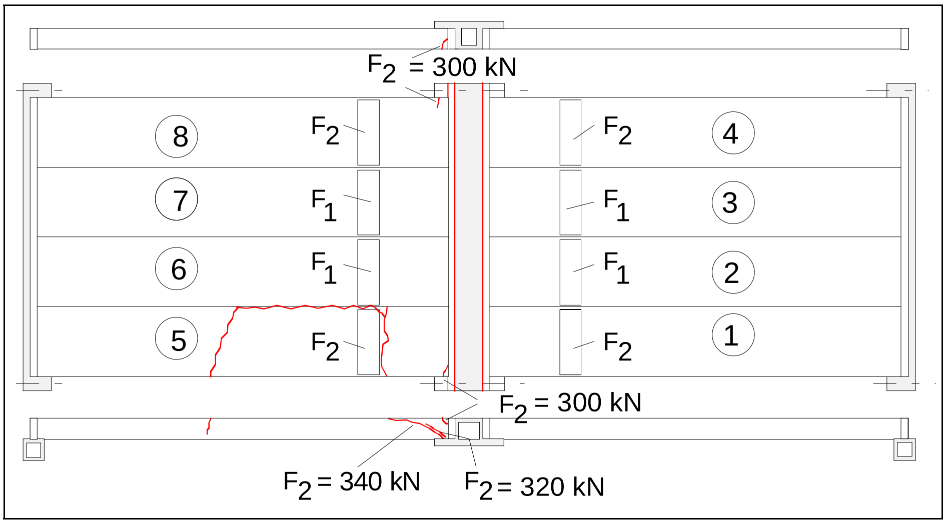 *Fig. 22. Stage 1. Cracks after failure on the top and at the edges of the floor specimen.* 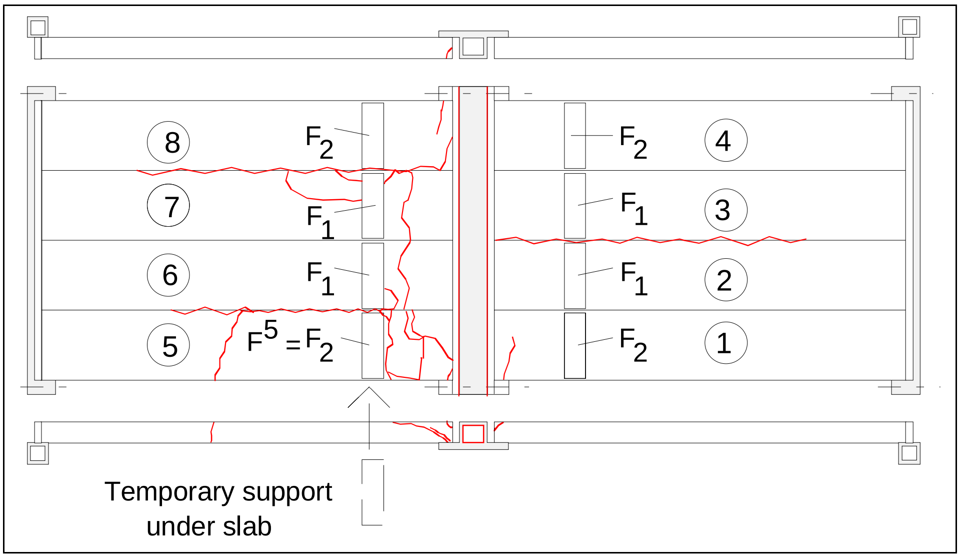 *Fig. 23. Stage 2. Cracks after failure of slabs 6 and 7.*
8	**Observed shear resistance**
	The maximum measured support reaction is regarded as the indicator of failure. The failure took place at P_1 = 337,9 kN, P_2 = 334,2 kN or F_1 = 339,1 kN, F_2 = 339,8 kN. Fig. 24 shows the relationship between the measured support reaction below the South end of the middle beam and the sum of actuator loads on half floor. The ratio of the reaction to the load is shown in Fig. 25 and in a larger scale in Fig. 26. Assuming simply supported slabs gives the theoretical ratio of 0,825. The measured support reaction seems to be ≈ 0,805 times the load before failure.

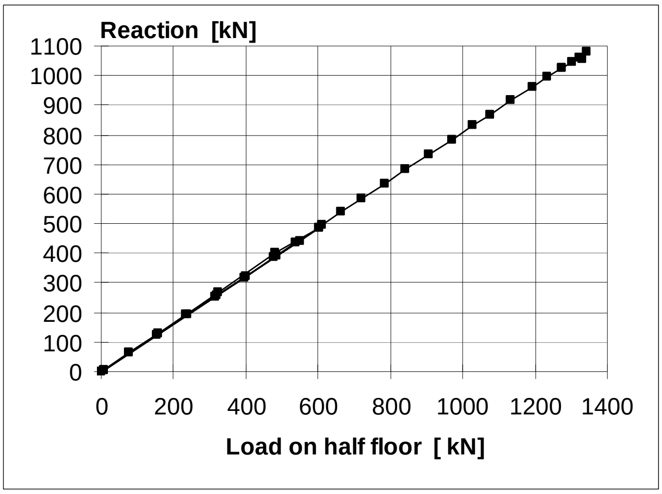

Fig. 24. Stage 1. Support reaction measured below South end of the middle beam vs. load on half floor = 2(P_1 + P_2).

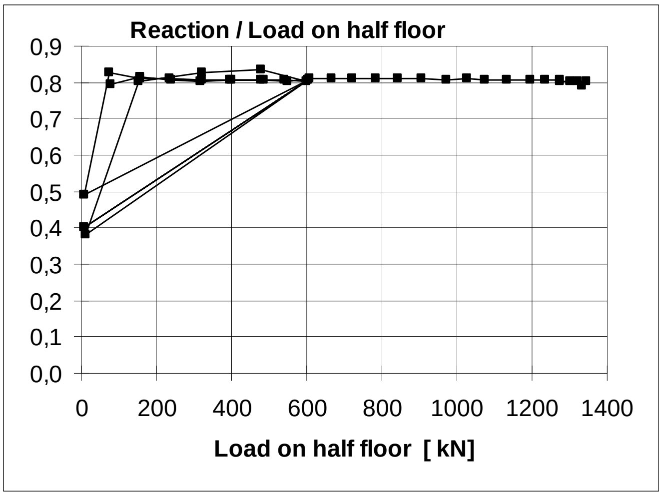

Fig. 25. Ratio of measured support reaction (below South end of the middle beam) to actuator loads on half floor.

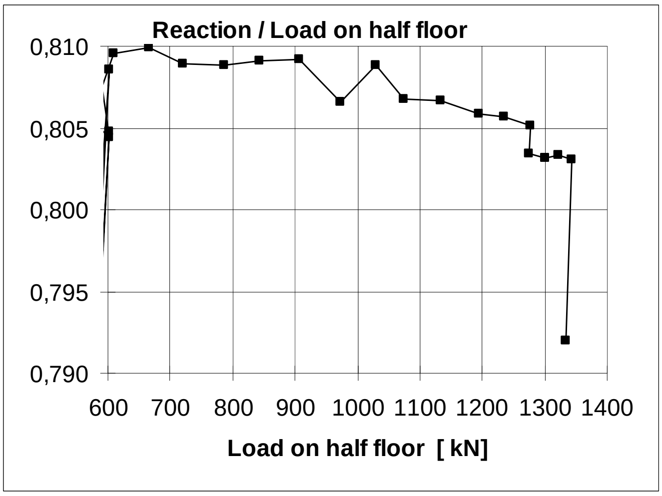

Fig. 26. A part of the previous figure in a large scale.

The observed shear resistance of one slab end (support reaction of slab end at failure) due to different load components is given by

$$V_{obs} = V_{g,sl} + V_{g,jc} + V_{eq} + V_p$$

where $V_{g,sl}$, $V_{g,jc}$, V_{eq} and V_p are shear forces due to the self-weight of slab unit, weight of joint concrete, weight of loading equipment and actuator forces P_i, respectively.

It is concluded that the maximum support reaction due to the imposed load of the failed slab 5 due has been

$$V_p = 0{,}805 \times \text{(actuator loads on half floor)} /4 = 0{,}805 \times (337{,}9+334{,}2) /2 = 270{,}5 \text{ kN.}$$

In the same way, the support reaction due to the weight of the loading equipment has been 0,805x(1,2+5,6)/2 = 2,74 kN. $V_{g,jc}$ is calculated from the nominal geometry of the joints and measured density of the grout. When calculating $V_{g,sl}$, the measured weight of the slabs is used. The values of the shear force components are given in Table 1 below.

Table 1. Components of shear resistance due to different loads.

Action	Load	Shear force kN/slab
Weight of slab unit	5,51 kN/m	19,7
Weight of joint concrete	0,19 kN/m	0,7
Loading equipment	(1,2+5,6)/2 kN/slab	2,7
Actuator loads	(337,9+334,2) /2 kN /slab	270,5

The observed shear resistance $\boldsymbol{V_{obs}}$ **= 293,6 kN** (shear force at support) is obtained for one slab unit with width = 1,2 m. The shear force per unit width is $\boldsymbol{v_{obs}}$ **= 244,7 kN/m.**

9 **Material properties**

9.1
Strength of steel

Component	$R_{eH}/R_{p0,2}$ MPa	R_m MPa	Note
Slab strands J12,5	1630	1860	Nominal (no yielding in test)
Reinforcement Txy	500		Nominal value for reinforcing bars, no yielding in test
End beams	≈ 350		Nominal value for Fe 52, no yielding in test

9.2
Strength of slab concrete, floor test

#	Cores	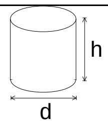	*h* mm	*d* mm	Date of test	Note
6			50	50	2.4.1992 (+8 d)[1]	Upper flange of slab 4, vertically drilled Tested as drilled[2] Density = 2425 kg/m^3
Mean strength [MPa]			77,1			
St.deviation [MPa]			5,8			

#	Cores	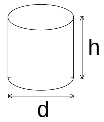	*h* mm	*d* mm	Date of test	Note
6			50	50	2.4.1992 (+8 d)[1]	Upper flange of slab 8, vertically drilled Tested as drilled[2] Density = 2425 kg/m^3
Mean strength [MPa]			81,0			
St.deviation [MPa]			6,5			

9.3
Strength of slab concrete, reference tests

The slabs for the reference tests were taken from the floor test specimen.

9.4
Strength of grout in joints and core filling

#	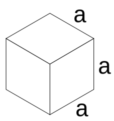	*a* mm	Date of test	Note
3		150	25.3.1992 (+0 d)[1]	Kept in laboratory in the same conditions as the floor specimen
Mean strength [MPa]		23,2		
St.deviation [MPa]		-		

9.5
Strength of concrete in end beams

-

[1] Date of material test minus date of structural test (floor test or reference test)
[2] After drilling, kept in a closed plastic bag until compression

10	**Measured displacements** Note that the last points on each curve represent the post failure situation.
10.1 Deflections	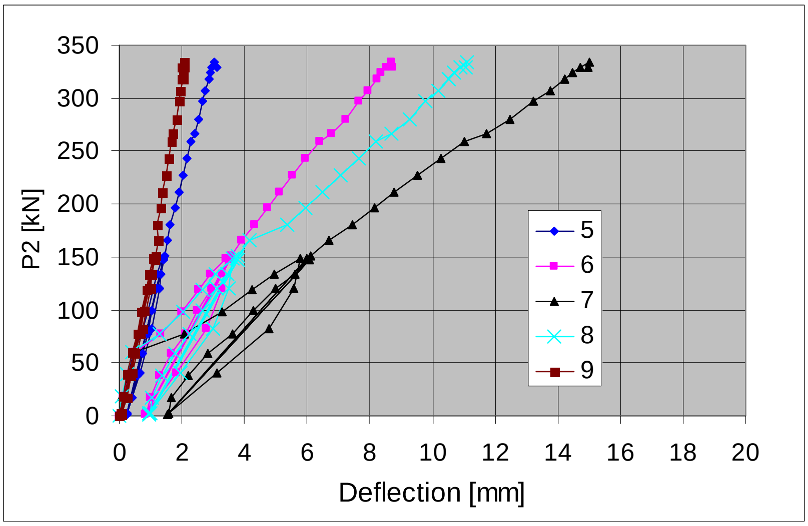 *Fig. 27. Deflection on line I, Western end beam.* 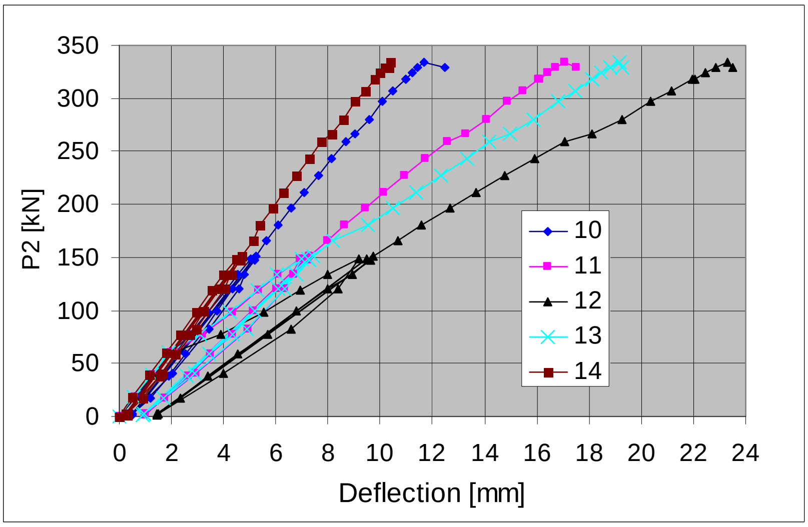 *Fig. 28. Deflection on line II.*

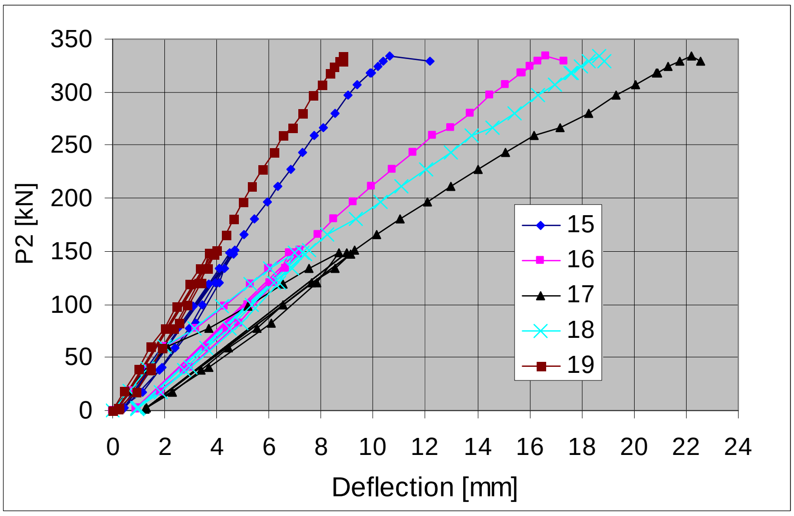

Fig. 29. Deflection on line III.

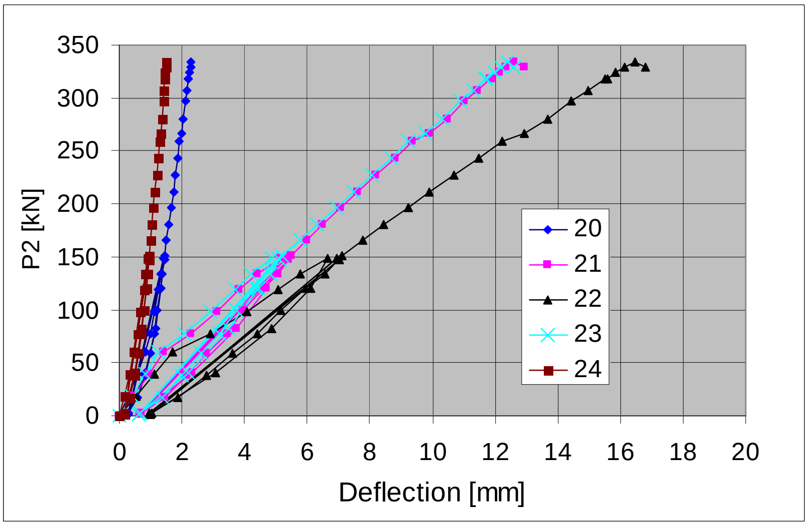

Fig. 30. Deflection on line IV, middle beam.

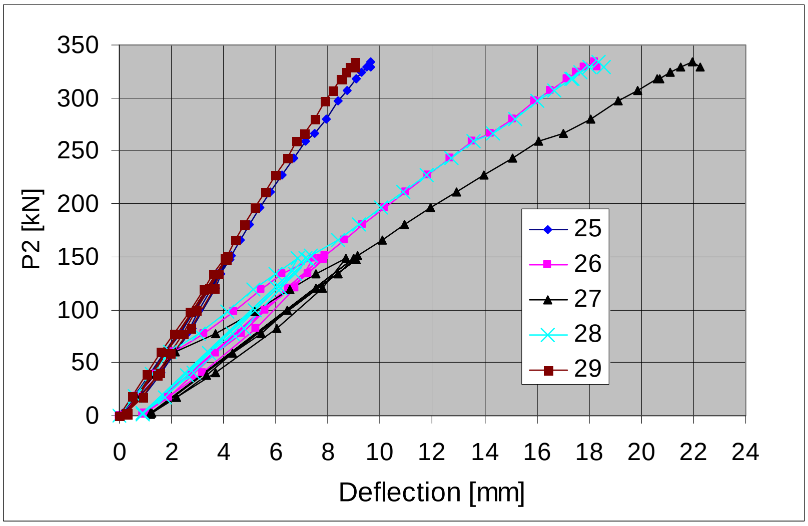

Fig. 31. Deflection on line VI.

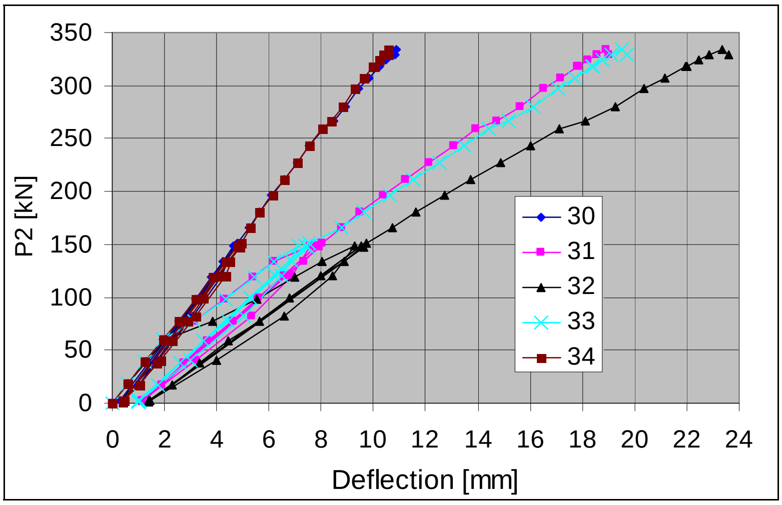

Fig. 32. Deflection on line VII.

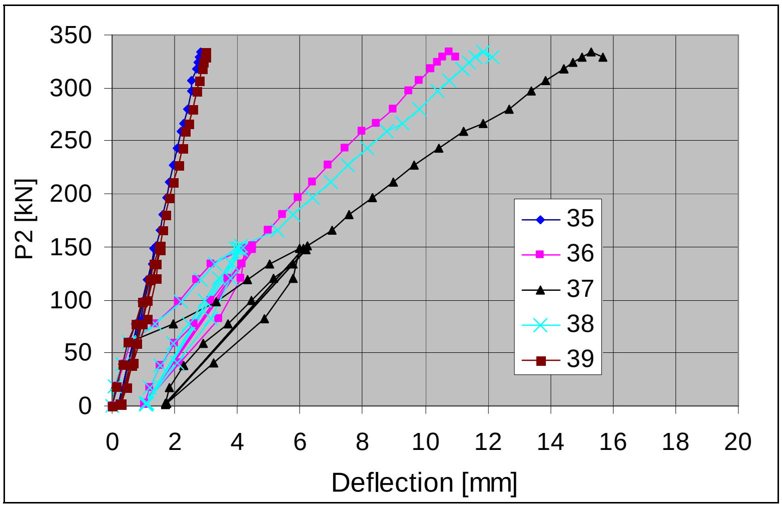

Fig. 33. Deflection on line VIII along Eastern end beam.

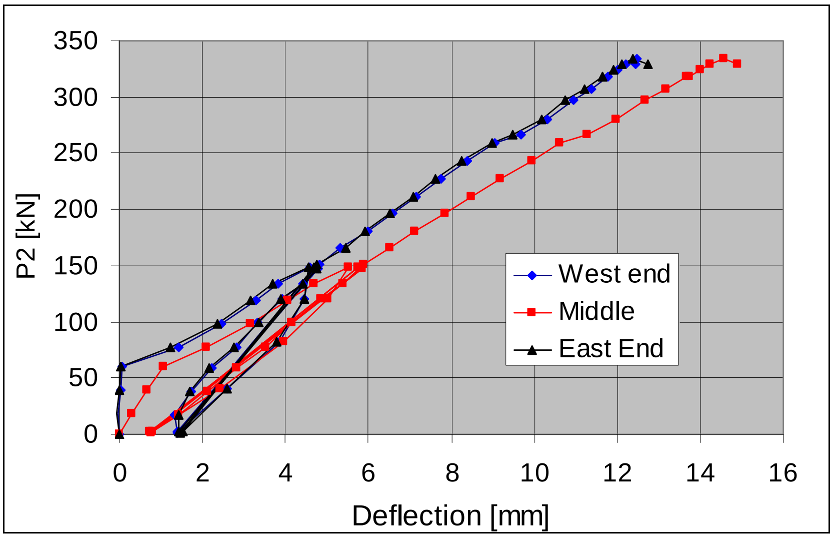

Fig. 34. Stage 1. Net deflection of mid-point of beams (rigid body motion = settlement of beam supports eliminated).

The last measured net deflection of the middle beam before failure was 14,6 mm. Before failure, the net deflection of the middle beam was 1,4 mm and after the highest load level 2,2–2,5 mm greater than that of the end beams.

10.2
Crack width

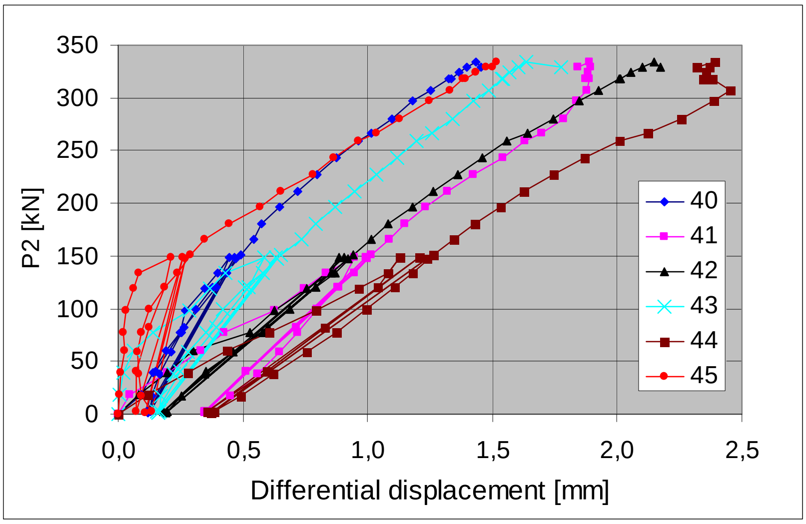

Fig. 35. Differential displacement (≈ crack width) measured by transducers 40–46.

10.3
Average strain (actually differential displacement)

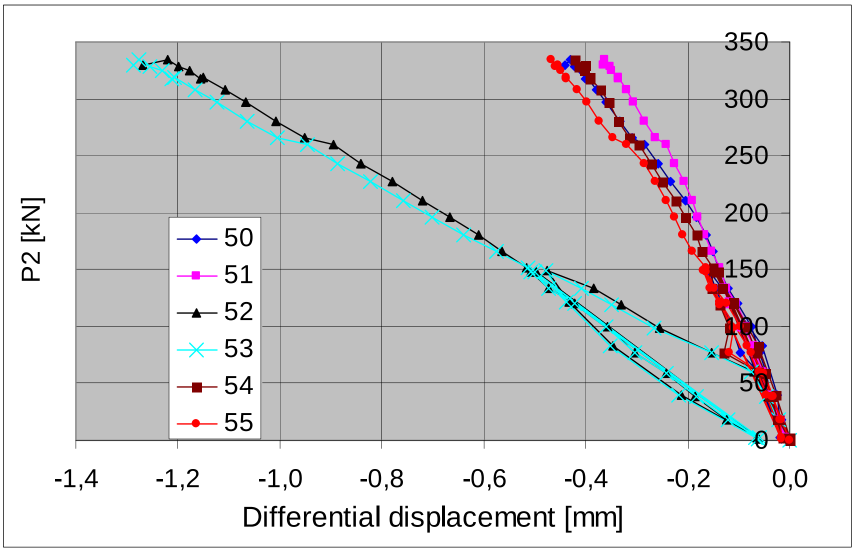

Fig. 36. Differential displacement at top surface of floor measured by transducers 50–55.

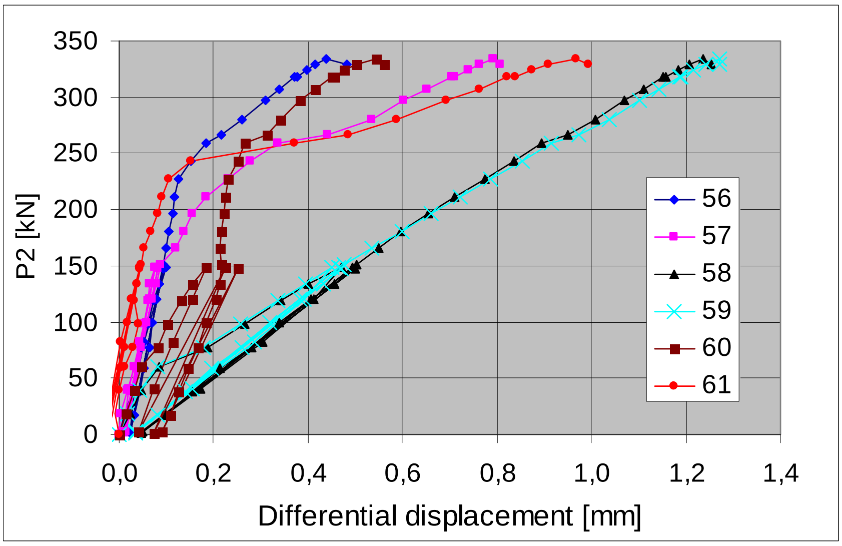

Fig. 37. Differential displacement at soffit measured by transducers 56–61.

10.4
Shear displacement

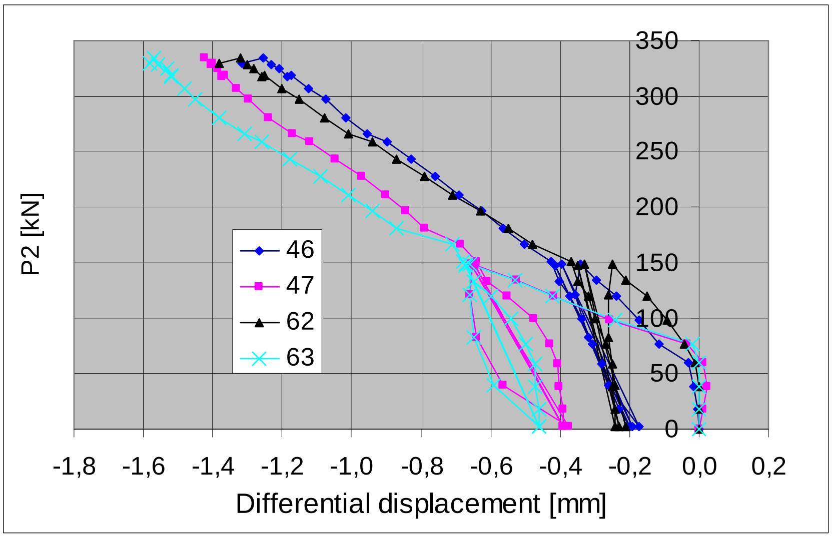

Fig. 38. North end of middle beam. Differential displacement between edge of slab and middle beam. A negative value means that the slab is moving towards the end of the beam.

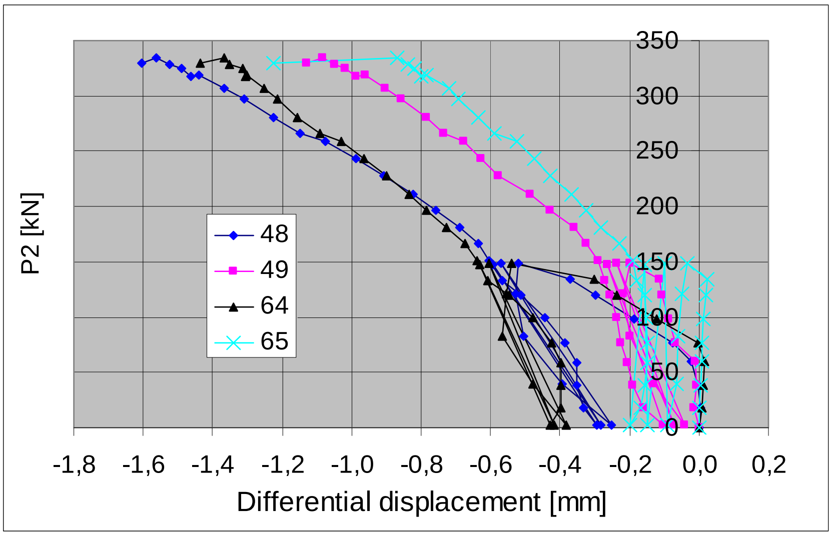

Fig. 39. South end of middle beam. Differential displacement between edge of slab and middle beam. A negative value means that the slab is moving towards the end of the beam.

10.5 Strain

A gradual growth in the measured strain means that there has been a crack before the loading, most likely attributable to the release of the prestressing force. A sudden increase in crack width indicates a new crack. An example of the former and latter behaviour are illustrated e.g. by transducers 26 and 30, respectively, see Fig. 45.

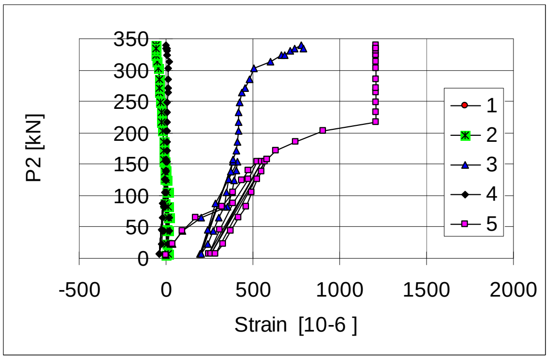

Fig. 40. Strain measured by gauges 1–5.

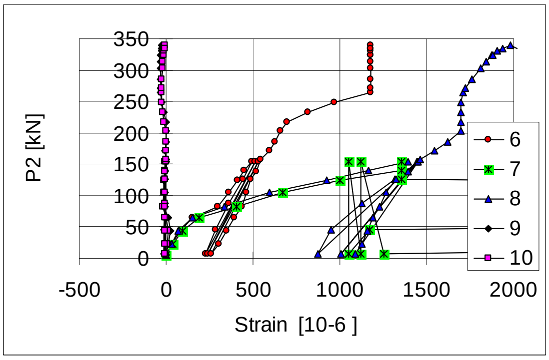

Fig. 41. Strain measured by gauges 6–10.

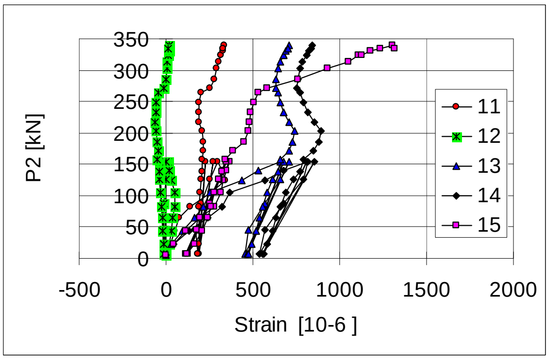

Fig. 42. Strain measured by gauges 11–15.

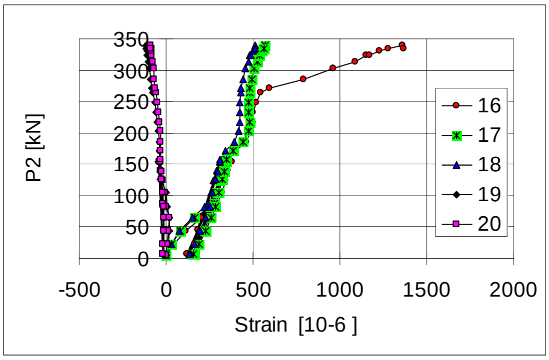

Fig. 43. Strain measured by gauges 16–20.

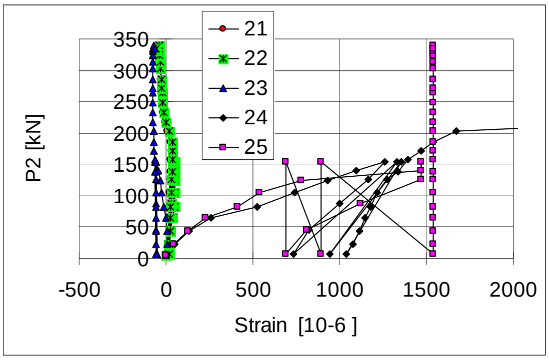

Fig. 44. Strain measured by gauges 21–25.

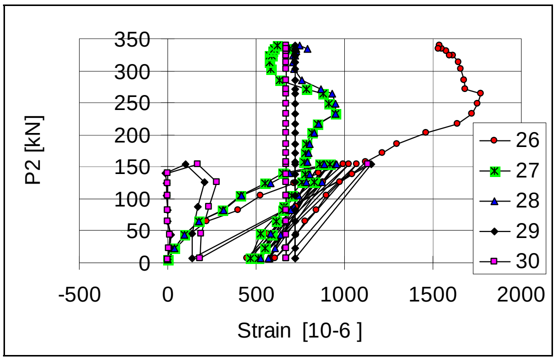

Fig. 45. Strain measured by gauges 26–30.

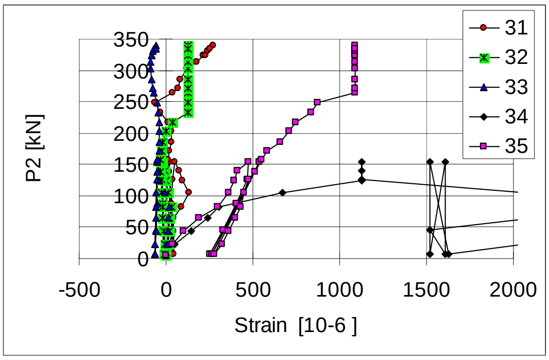

Fig. 46. Strain measured by gauges 31–35.

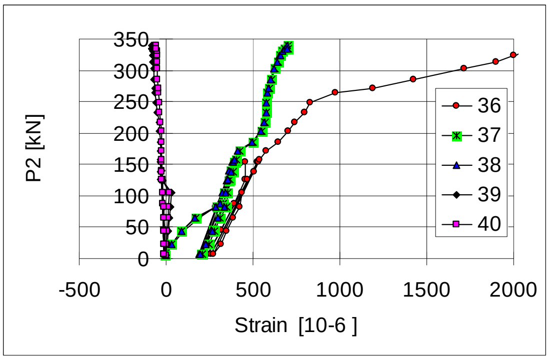

Fig. 47. Strain measured by gauges 36–40.

In Figs 48 and 49 the cracks below the soffit of slabs 2, 3, 6 and 7 are shown.

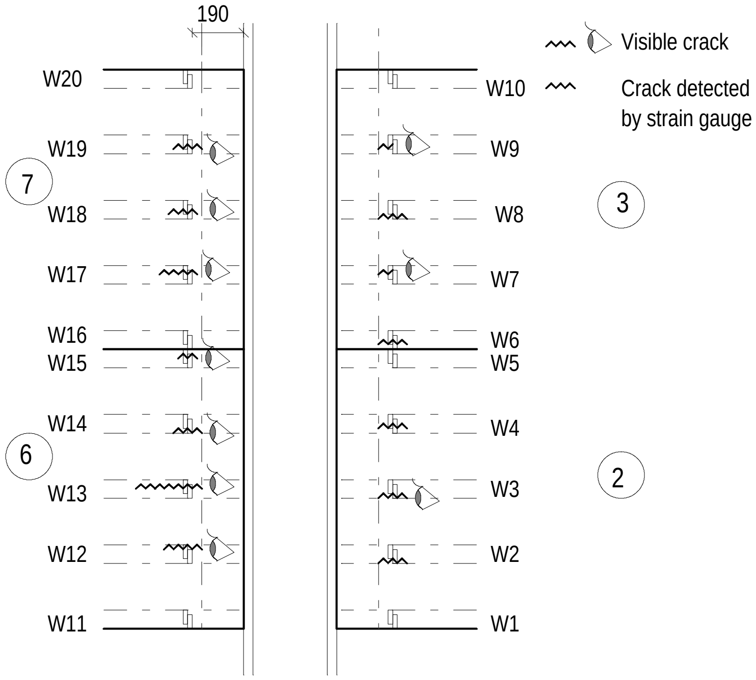

Fig 48. Cracking of bottom surface of hollow core units no 2, 3, 6 and 7 along the strands under force F_2 = 153.2 kN. The cracking limit for the strain gauge measurements is 0,03%. The length of the broken line corresponds to the length of the visible crack.

	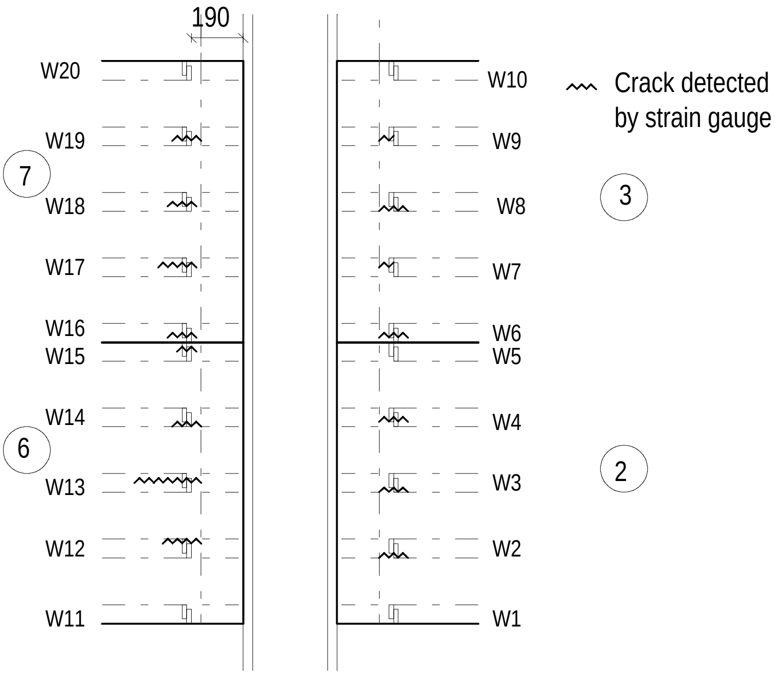 *Fig. 49. Cracking of bottom surface of hollow core units no 2, 3, 6 and 7 along the strands under force F_2 =330 kN.*
11	**Reference tests**
	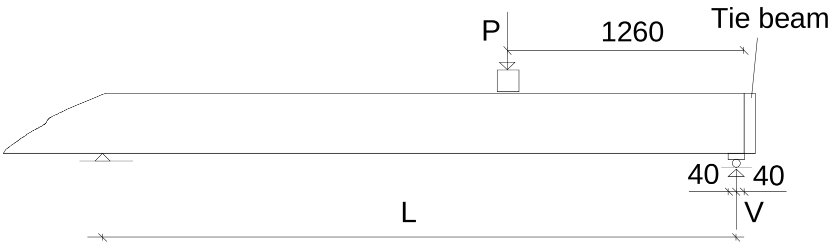 *Fig. 50. Layout of reference tests on slabs 4 and 8 taken from the floor test specimen. For L, see Table 2.*

Table 2. Span L, ultimate load P_u, ultimate shear force V_u and failure mode in reference tests. The weight of the loading equipment = 0,5 kN is included in P_u.

Slab	L mm	P_u kN	V_u kN	Failure mode
4	7000	582	499,8	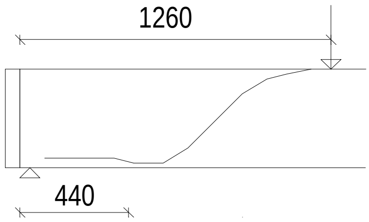 Shear tension failure
8	7000	622	532,8	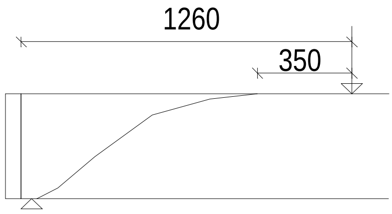 Shear tension failure
		Mean	516,3	

12	**Comparison: floor test vs. reference tests**
	The observed shear resistance (support reaction) of the hollow core slab in the floor test was equal to **293,6** kN per one slab unit or **244,7** kN/m. This is **57%** of the mean of the shear resistances observed in the reference tests.
13	**Discussion**

1. The net deflection of the middle beam due to the imposed actuator loads only (deflection minus settlement of supports) was 14,6 mm or L/342

2. The shear resistance measured in the reference tests was somewhat higher than the mean of the observed values for similar slabs given in *Pajari, M. Resistance of prestressed hollow core slab against web shear failure. VTT Research Notes 2292, Espoo 2005*. This may be due to the tie beam which made the shear stresses in the webs more uniform than those in the tests without tie beams.

3. Before failure, the net deflection of the middle beam was 2,2–2,5 mm greater than that of the end beams. This is a too small difference to cause considerable torsional stresses in the slabs.

4. The failure mode was web shear failure of edge slab 5 close to the middle beam. The middle beam seemed to recover completely after the failure.

APPENDIX A: PHOTOGRAPHS

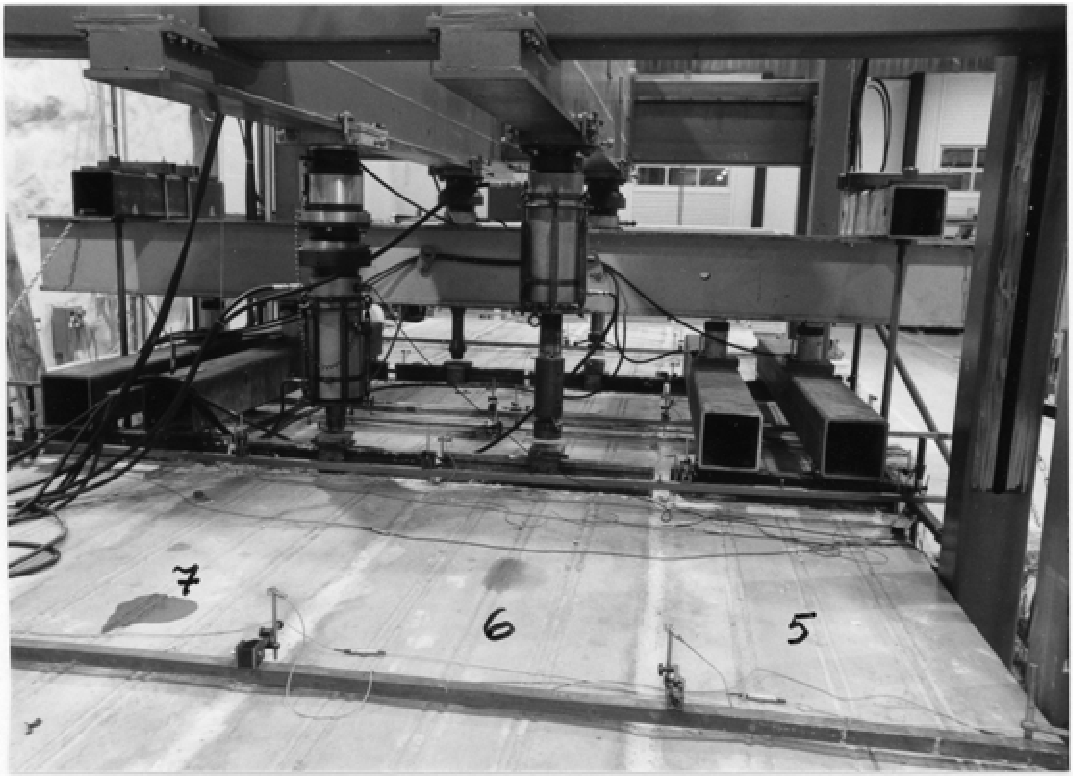

Fig. 1. Loading arrangement in floor test.

Fig. 2. Inductive transducer measuring differential horizontal displacement between top surface of beam and hollow core slab.

Fig. 3. Failure at stage 1. Side view.

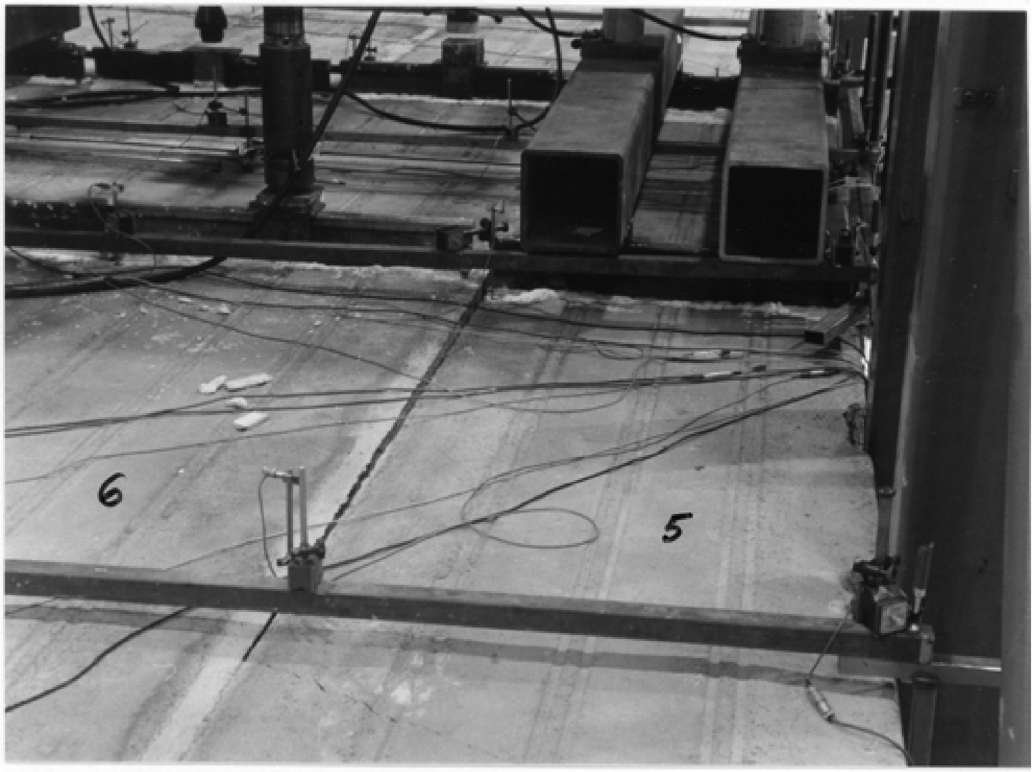

Fig. 4. Failure at stage 1 seen from above.

Fig. 5. Failure at stage 1. The narrow crack above the failure crack appeared first. Its growth could be followed visually until failure.

Fig. 6. Cracking of the joint concrete along the beam at stage 2.

Fig. 7. Failure at stage 2 seen from above after removal of loading equipment.

Fig. 8. Failure at stage 2 seen from above after removal of loading equipment.

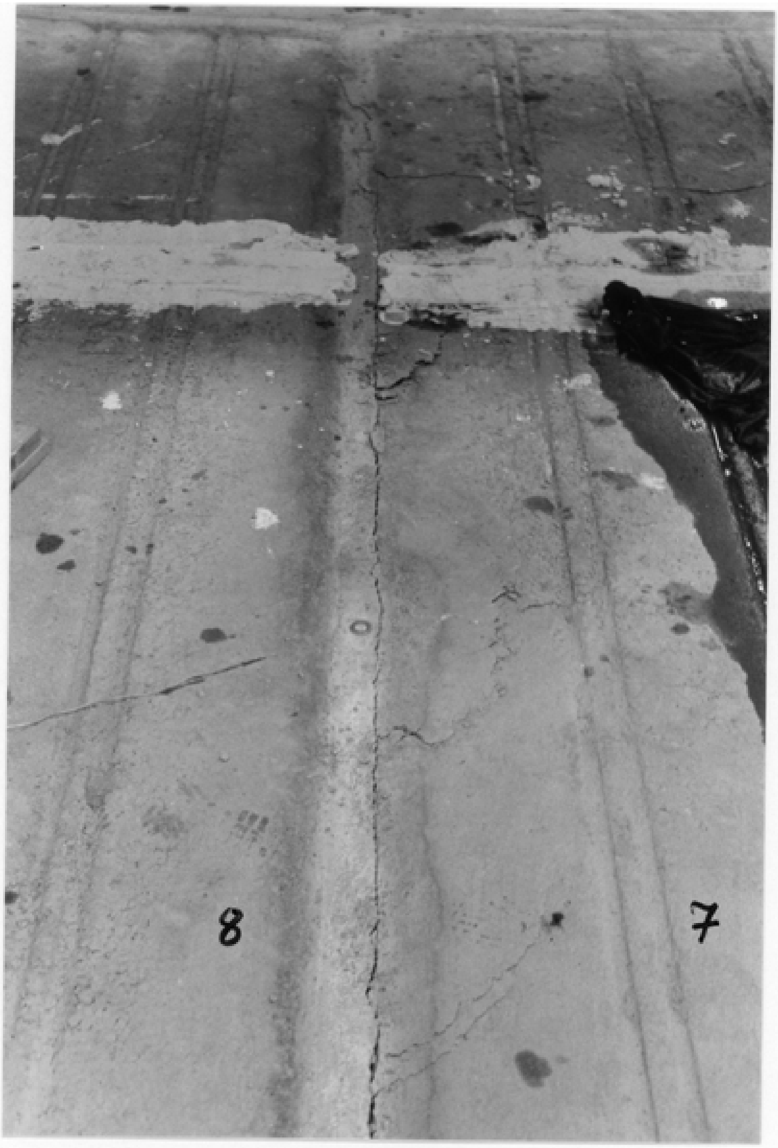

Fig. 9. Failure at stage 2 seen from above after removal of loading equipment.

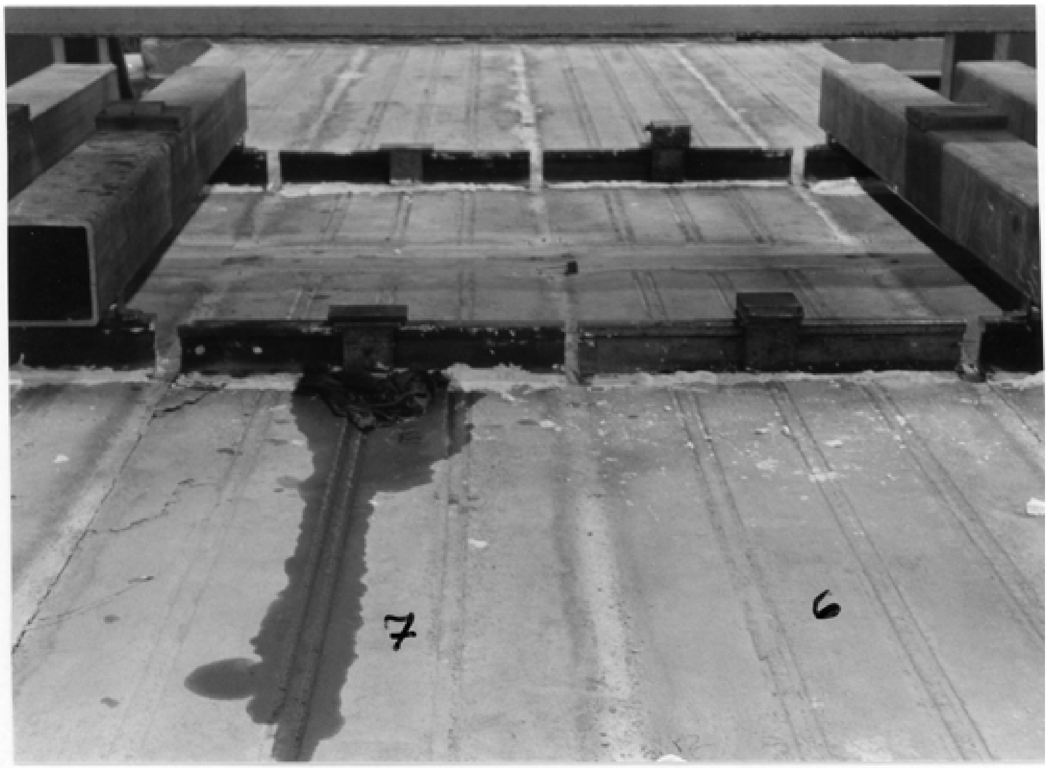

Fig. 10. Failure at stage 2 seen from above after removal of loading equipment.

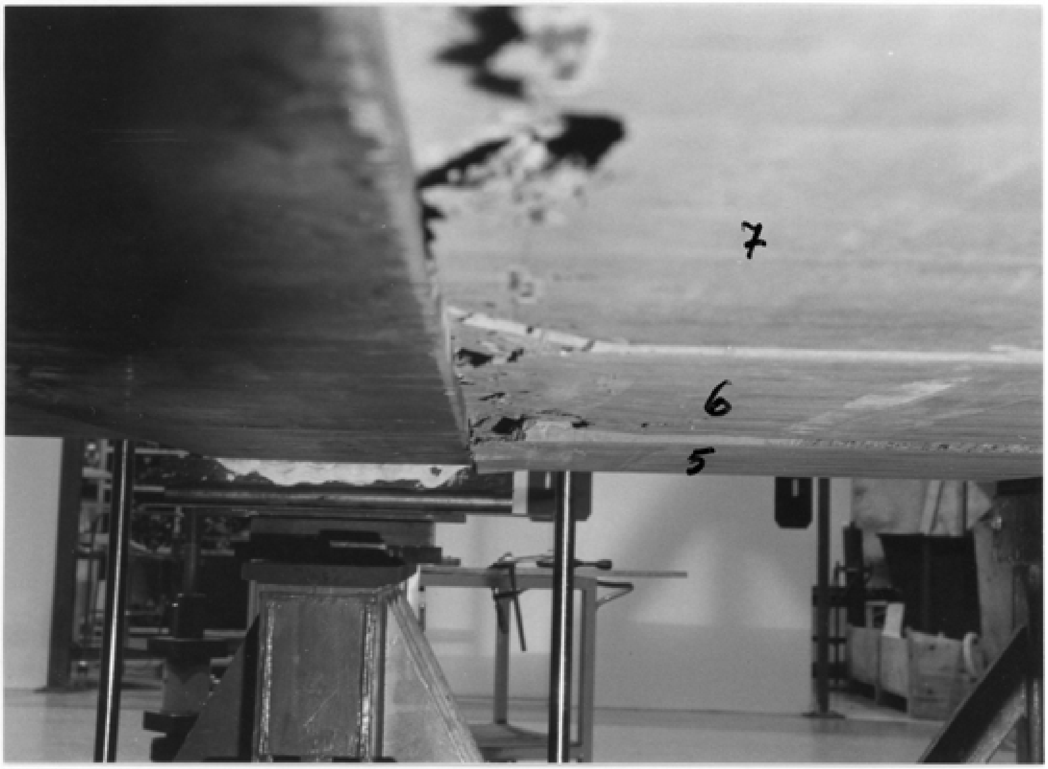

Fig. 11. Failure at stage 2 seen from below.

Fig. 12. Failure pattern of slab unit no 4 in reference test.

Fig. 13. Failure pattern of slab unit no 8 in reference test.

1	**General information**
1.1 Identification and aim	**VTT.PC.InvT-Unif.265.1993** **Last update 2.11.2010** PC265E (Internal identification) Aim of the test: To study the effect of core filling with length equal to the core height.
1.2 Test type	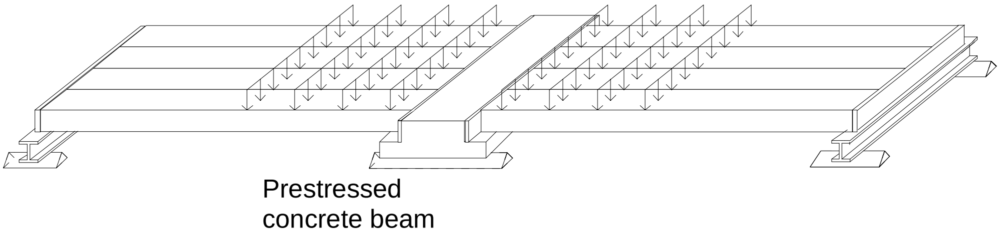 Fig. 1. *Illustration of test setup.*
1.3 Laboratory & date of test	VTT/FI 18.1.1993
1.4 Test report	Author(s): Pajari, M. Name: *265 mm hollow core floor supported on prestressed concrete beam under evenly distributed load* Ref. number: RAT-IR-5/1993 Date: 7.3.1993 Availability: Public, available on request from VTT Expert Services, P.O. Box 1001, FI-02044 VTT. Financed by Parma Oy, Finland; Oy Partek Concrete Ab, Finland; Skanska Prefab AB, Sweden and AB Strängbetong, Sweden
2	**Test specimen and loading** (see also Appendix A)
2.1 General plan	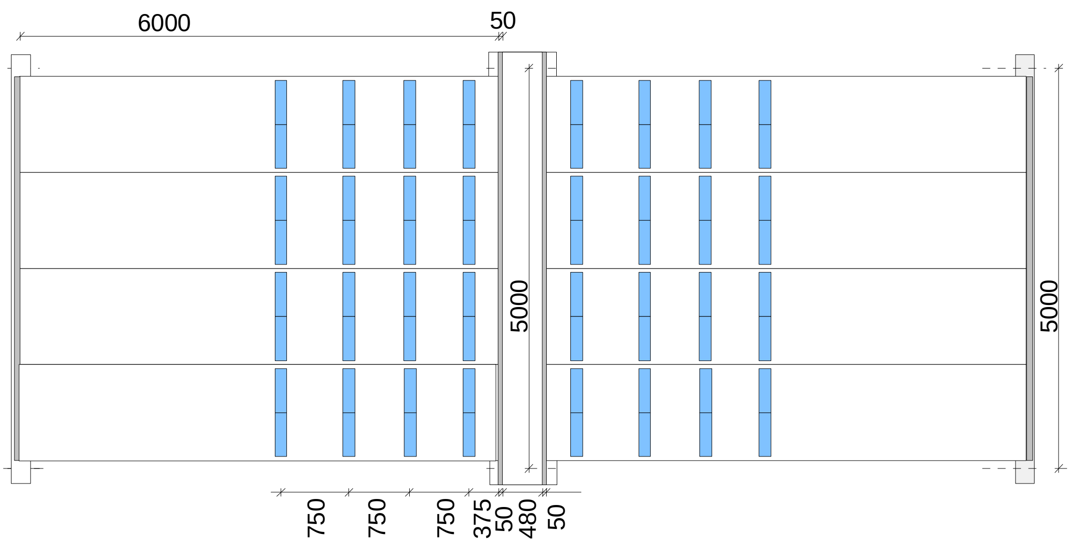 *Fig. 2. Plan.*

<table>
<tr>
<td>2.2
End beams</td>
<td>

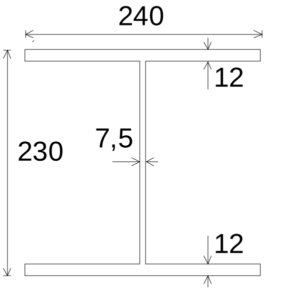

Fig. 3. Cross-section of end beam.

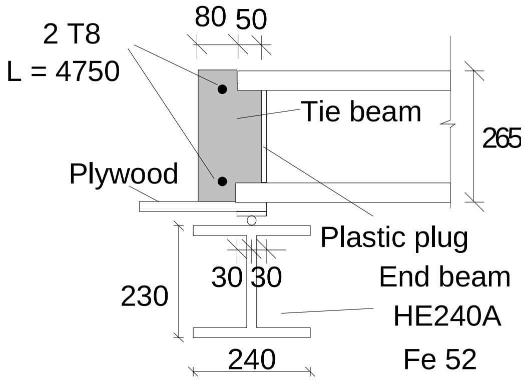

Fig. 4. Arrangements at end beam. T8 refers to a reinforcing bar with diameter 8 mm, see 2.3.

Simply supported, span = 5,0 m,
$f_y \approx$ 350 MPa (nominal f_y), did not yield in the test.

</td>
</tr>
<tr>
<td>2.3
Middle beam</td>
<td>

Prestressed concrete beam, see Figs 5–7.

Concrete: K60

Passive reinforcement and tendons:
T8: Hot rolled, weldable rebar A500HW, ϕ = 8 mm, see 9.1
J12,5: strand with 7 indented wires, ϕ =12,5 mm, A_p = 93 mm^2, see 9.1

Tie reinforcement: Straight rebars in the tie beams, across the middle beam and in the longitudinal joints of the slabs, see Figs 4 and 7.

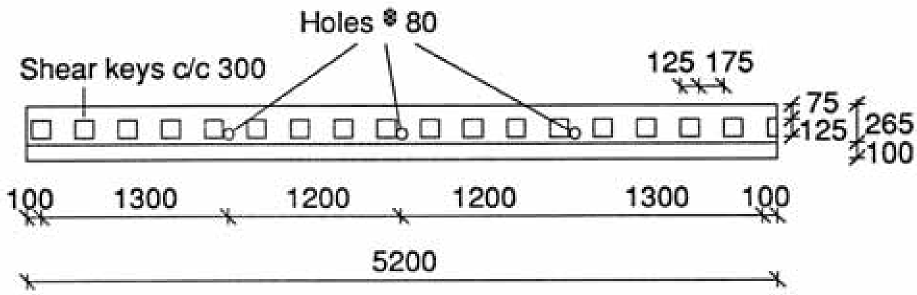

Fig. 5. Middle beam.

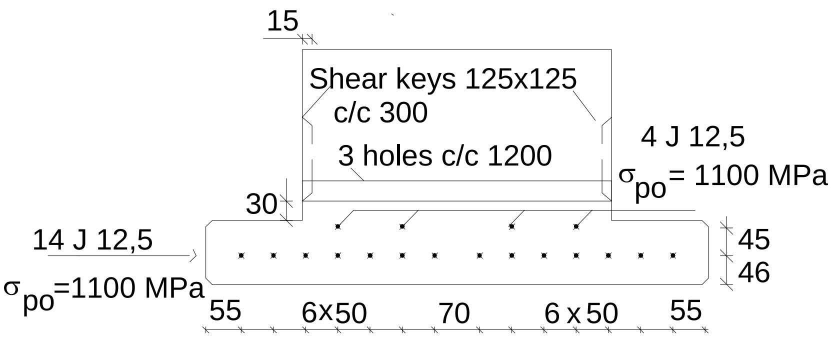

Fig. 6. Section of middle beam. See also Fig. 7.

</td>
</tr>
</table>

<table>
<tr><td>2.4
Arrangements at middle beam</td><td>

- Simply supported, span = 5,0 m
- Joints and tie beams grouted on the 17th of December 1992
- The concrete filling in the hollow cores was cast via the end of the slab; neither slots nor holes in the slab elements were made.

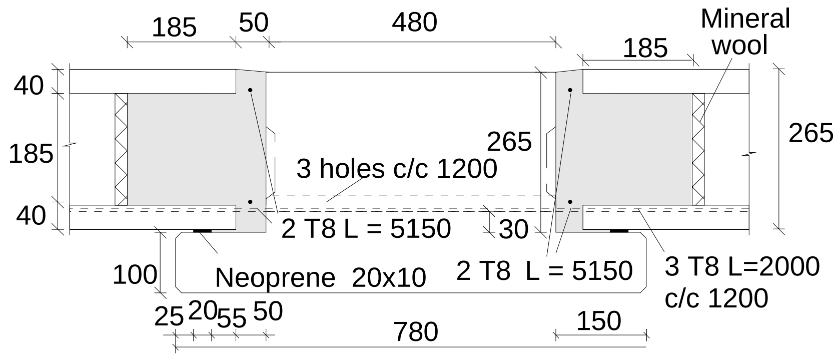

Fig. 7. Section along hollow cores.

</td></tr>
<tr><td>2.5
Slabs</td><td>

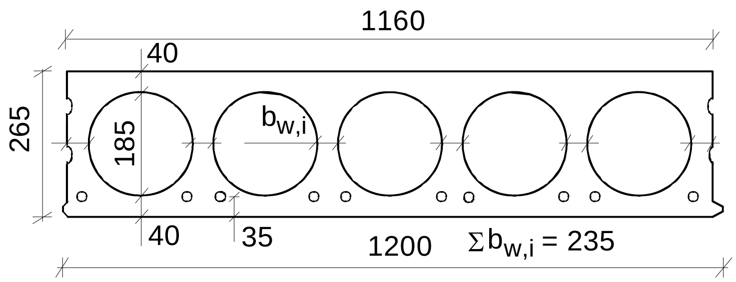

Fig. 8. Nominal geometry of slab units. Nominal length = 6000 mm.

- 10 slabs extruded 7.12.1992 by Partek Betoniteollisuus Oy, Hyrylä factory, all from the same casting bed and casting lot
- Grade of concrete K60
- 10 lower strands J12,5 initial prestress 1100 MPa
- Slabs 1–8 for floor test, slabs 9–10 for reference tests

J12,5: seven indented wires, ϕ =12,5 mm, A_p = 93 mm^2, see 9.1.

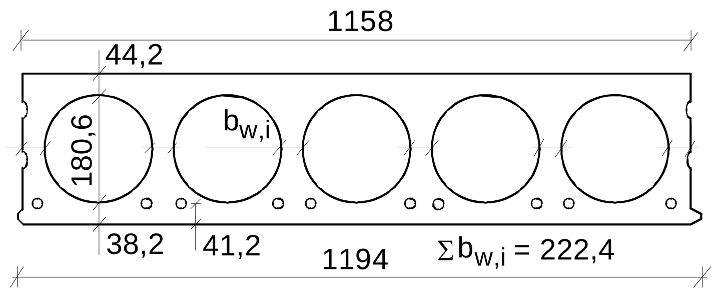

Max measured bond slips: 1,8;1,7&1,6; 1,5 and 1,4 mm in slabs 10; 3; 6 and 9, respectively

Measured weight of slab units = 4,12 kN/m

Fig. 9. Mean of most relevant measured geometrical characteristics.

</td></tr>
<tr><td>2.6
Temporary supports</td><td>

- No

</td></tr>
</table>

2.7
Loading arrangements

64 short I-beams (primary spreader beams) were placed on the floor as shown in Fig. 10. The length of these beams was 550 mm. There was gypsum mortar between the slabs and the floor to smoothe the uneven top surface of the slabs. The loads from 16 actuators were distributed to the primary beams with the aid of 16 tertiary spreader beams and 32 secondary spreader beams as shown in Fig. 10. To eliminate the contribution of the loading equipment to the load-carrying mechanism of the floor, two teflon plates were placed below one end of each secondary and tertiary beam, see Appendix A, Figs 2 and 3.

The actuators were connected to three hydraulic circuits which were controlled separately to create the same force in each actuator. Eight of them (P_1 and P_2) were of long type with a swivel at both ends, eight (P_3) were of short type with a swivel on the top. Attempts were made to keep all actuator forces equal during the test. The total imposed load due to the actuator force P_i and weight of underlying loading equipment was

$F_1 = P_1 + 1{,}4$ kN
$F_2 = P_2 + 1{,}4$ kN
$F_3 = P_3 + 1{,}8$ kN

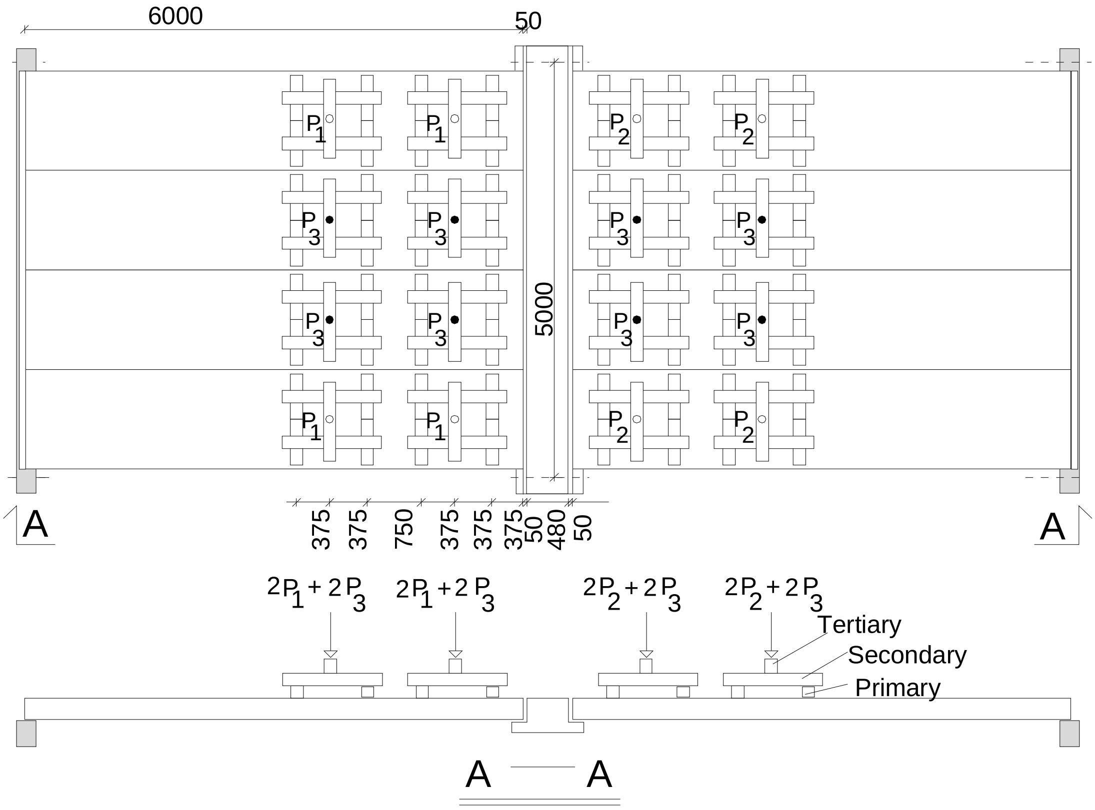

Fig. 10. Plan. P_1, P_2 and P_3 refer to vertical actuator forces.

<table>
<tr><td>3</td><td>Measurements</td></tr>
<tr><td>3.1
Support reactions</td><td>

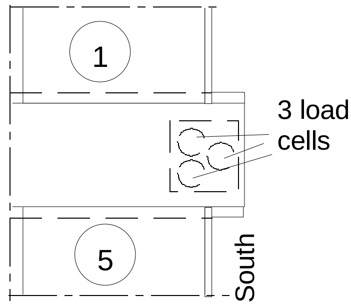

Fig. 11. Load cells below the South end of the middle beam.

</td></tr>
<tr><td>3.2
Vertical displacement</td><td>

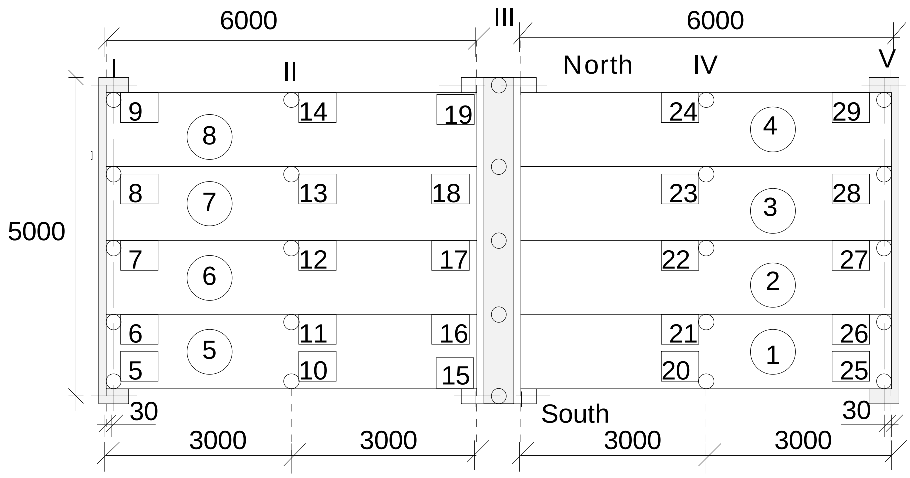

Fig. 12. Location of transducers 5 … 29 for measuring vertical deflection along lines I … V.

</td></tr>
<tr><td>3.3
Average strain</td><td>

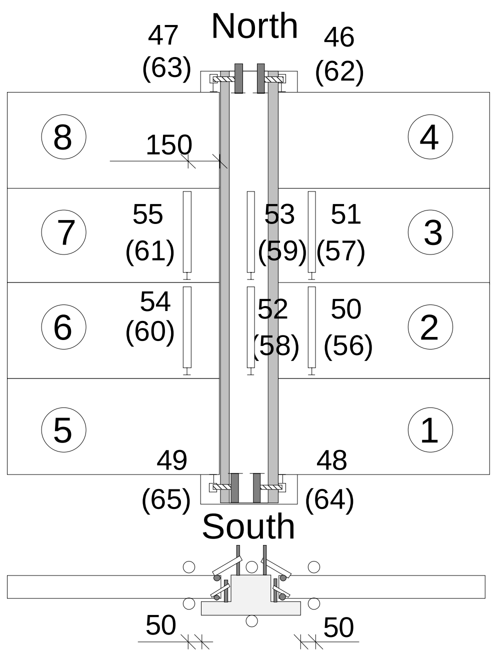

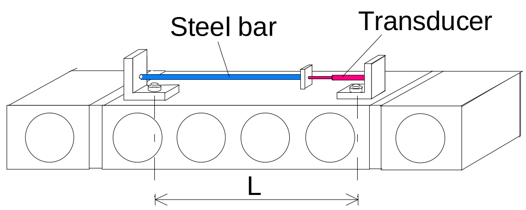

Fig. 13. Apparatus for measuring average strain. L =1120mm and 1060 mm for the bottom and top side transducers, respectively.

Fig. 14. Position of device (transducers 50–61) measuring average strain parallel to the beams. Transducers 46–49 and 62–65 measured the sliding of the outermost slabs along the beam. Numbers in parentheses refer to the soffit of the floor, others to the top.

</td></tr>
</table>

3.4 Horizontal. displacements	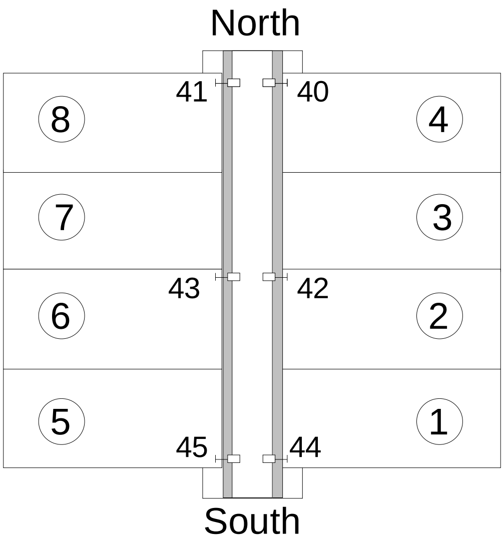 *Fig. 15. Position of transducers 40–45 measuring crack width.*
3.5 Strain	
4	**Special arrangements** -
5	**Loading strategy**
5.1 Load-time relationship	Date of test was 18.1.1993. When the actuator forces P_i were equal to zero but the weight of the loading equipment was on, all measuring devices were zero-balanced. The loading history is shown in Fig.16. Note, that the number of load step, not the time, is given on the horizontal axis. The whole load test took two hours and five minutes. In the following, the cyclic stage (steps 0–16) is called Stage I, the monotonous stage from increment 16 to failure is called Stage II. 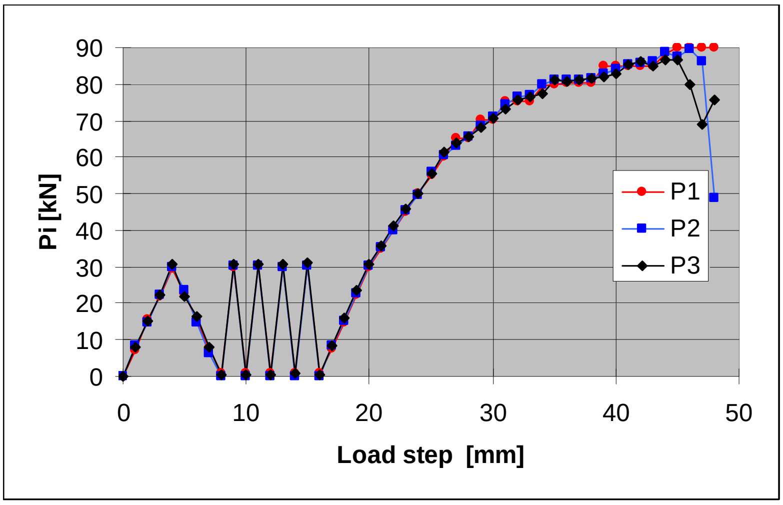 *Fig. 16. Development of actuator forces P_1, P_2 and P_3.*

5.2 After failure		
6	**Observations during loading**	
	Stage I	-
	Stage II	At P_i = 40 kN soffit of the middle beam cracked. At P_i = 45 kN cracks in the corners of slabs 2 and 7 as well as a longitudinal crack along a hollow core in the soffit of slab 3 were observed, see Figs 17 and 18. At P_i = 75 kN one corner of slab 4 cracked as shown in App. A, Fig. 6. When increasing the loads, diagonal shear cracks appeared in the webs of slab units; first in slab 4 (Figs. 7 and 8 in App. A), then in slab 8 (Figs 15 and 16 in App. A) and finally also in slab 1 (Fig. 17 in App. A). At P_1 = 90,0 kN, P_2 = 87,6 kN P_3 = 86,8 kN a web shear failure took place in slab 4 close to the middle beam. The cracking patterns after the failure are shown in Figs 17 and 18 and in App. A, Figs 9–18 and 21–23.
	After failure	When demolishing the test specimen it was observed that all core fillings were perfect, see App. A, Figs 19–20.
7	**Cracks in concrete**	
7.1 Cracks at service load		
7.2 Cracks after failure	The vertical cracking in the joint concrete next to the middle beam typically took place along the edges of the middle beam, not along the joint concrete or along the slab ends.	

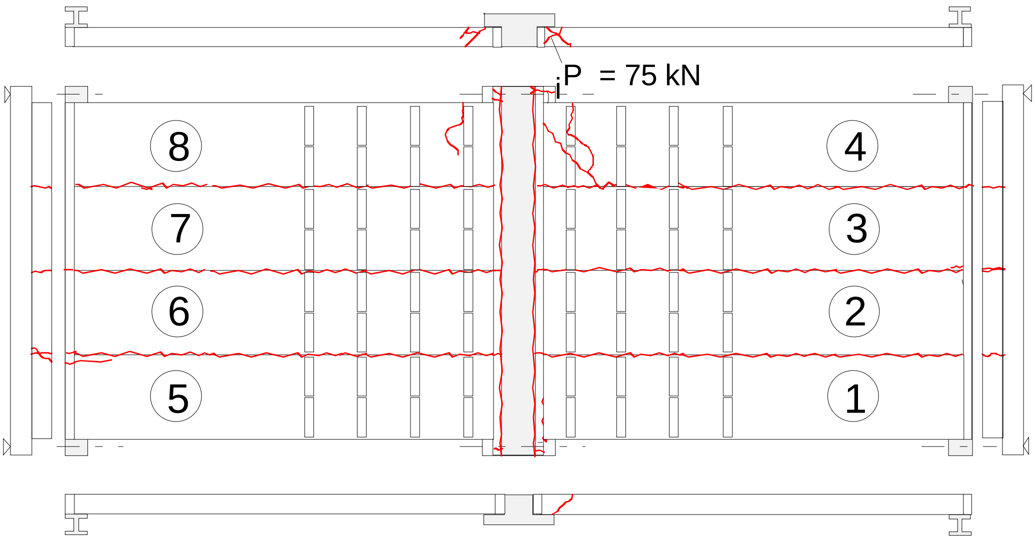

Fig. 17. Cracks after failure on the top and at the edges.

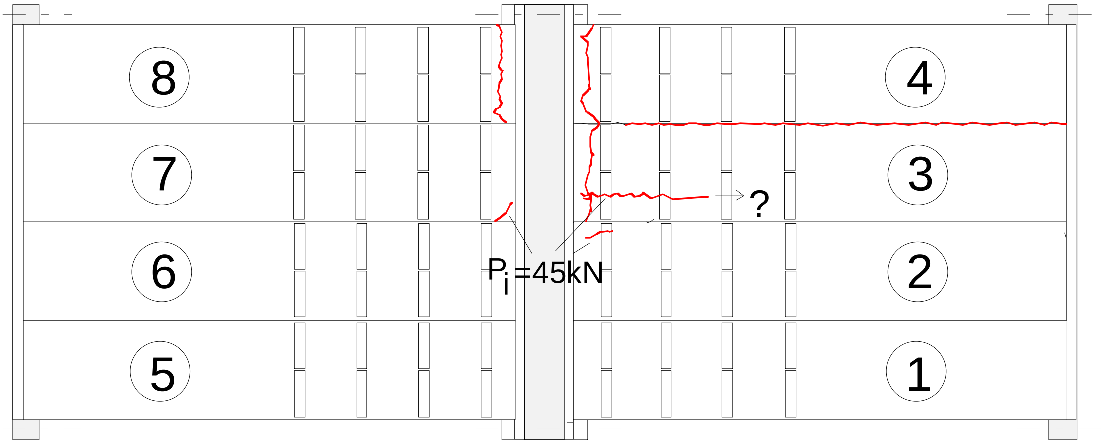

Fig. 18. Cracks after failure in the soffit.

8 Observed shear resistance

The maximum support reaction is regarded as the indicator of failure. The failure took place when P_1 = 90,0 kN, P_2 = 87,6 kN P_3 = 86,8 kN or when the sum of actuator loads load on half floor was = 702,4 kN.

Fig. 19 shows the relationship between the measured support reaction below the South end of the middle beam and the sum of actuator loads on half floor. The ratio of the reaction to the load is shown in Fig. 20 and in Fig. 21 in a larger scale. Assuming simply supported slabs the ratio = 0,756 is obtained, and the measured support reaction seems to follow this assumption well until at load 646 kN (P_i = 80 kN) the sudden softening of slab 4 at the North end of the middle beam resulted in load transfer from the North to the South end of the middle beam. At failure the ratio equalled 0,78, but the failure took place at the opposite (North) end of the beam where the support reaction must have been lower. For this reason it seems justified to use the value of 0,756 for calculation of the shear resistance.

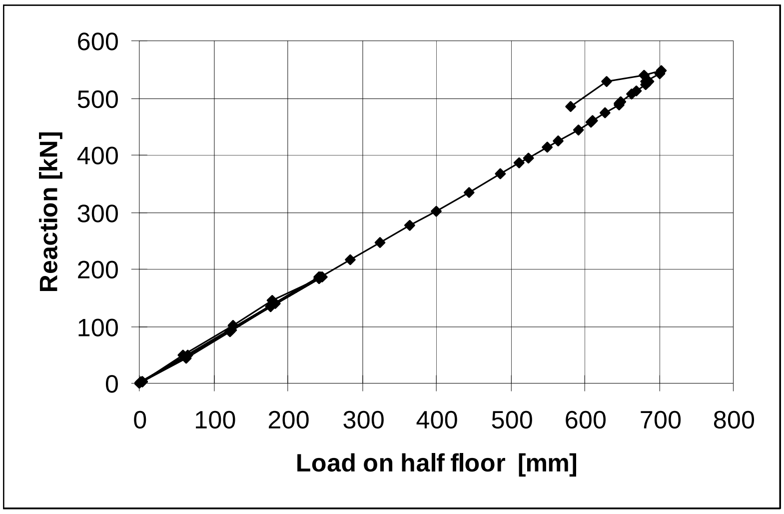

Fig. 19. Support reaction measured below South end of the middle beam vs. load on half floor = 2(P_1 + P_2) + 4 P_3.

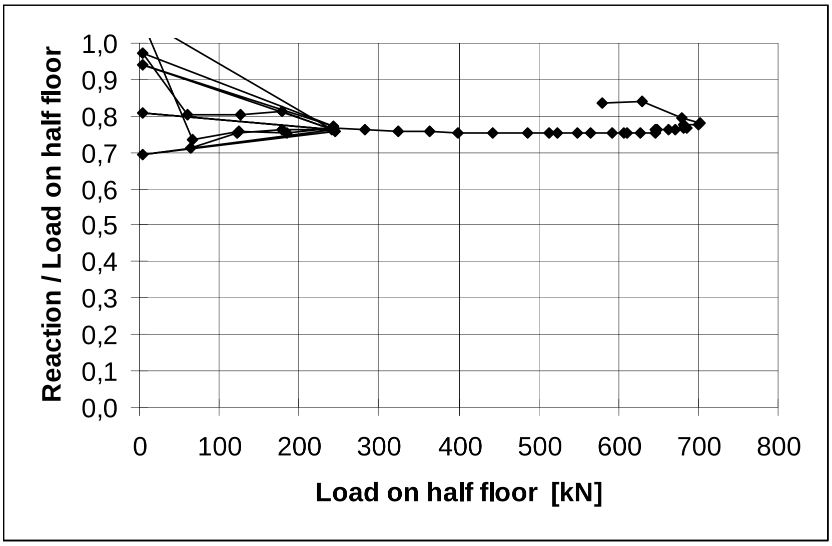

Fig. 20. Ratio of measured support reaction (below South end of the middle beam) to load on half floor.

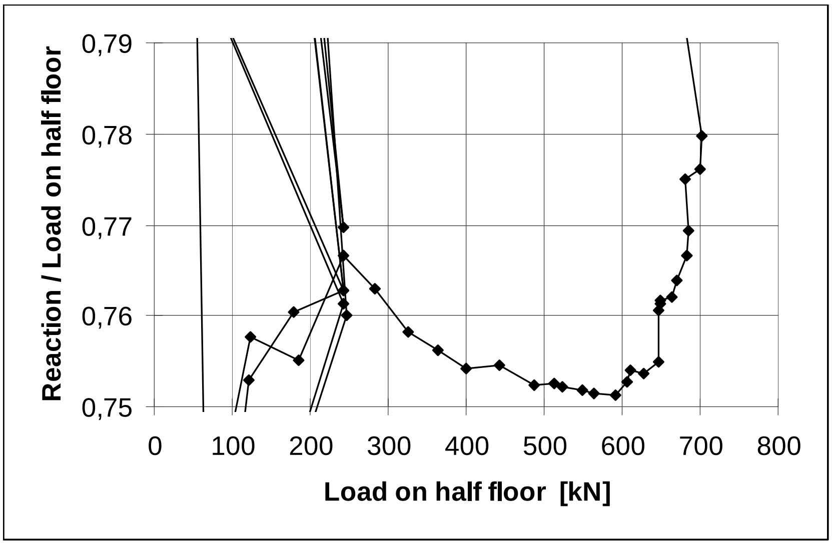

Fig. 21. A part of the previous figure in a large scale.

The shear resistance of one slab end (support reaction of slab end at failure) due to different load components is given by

$$V_{obs} = V_{g,sl} + V_{g,jc} + V_{eq} + V_p$$

where $V_{g,sl}$, $V_{g,jc}$, V_{eq} and V_p are shear forces due to the self-weight of slab unit, weight of joint concrete, weight of topping concrete, weight of loading equipment and actuator forces P_i, respectively.

The shear force at failure is calculated assuming that the slabs behave as simply supported beams. For V_{eq} and V_P this means that $V_{eq} = 0{,}756\times(8\times1{,}4 + 8\times1{,}8)/8 = 2{,}4$ kN and $V_p = 0{,}756\times(4\times P_1 + 4\times P_2 + 8\times P_3)/8$. $V_{g,jc}$ is calculated from the nominal geometry of the joints and measured density of the concrete, other components of the shear force are calculated from measured loads and weights. The values for the components of the shear force are given in Table on the next page.

Table. Components of shear resistance due to different loads.

Action	Load	Shear force kN
Weight of slab unit	4,117 kN/m	12,2
Weight of joint concrete	0,11 kN/m	0,3
Loading equipment	3,2 kN	2,4
Actuator loads	(4×90,0+4×87,6+8×86,8)/8 kN	132,7

The observed shear resistance $\boldsymbol{V_{obs}}$ **= 147,6 kN** (shear force at support) is obtained for one slab unit with width = 1,2 m. The shear force per unit width is $\boldsymbol{v_{obs}}$ **= 123,0 kN/m.**

9 Material properties

9.1
Strength of steel

Component	$R_{eH}/R_{p0,2}$ MPa	R_m MPa	Note
End beams	≈ 350		Nominal (Fe 52)
Slab strands J12,5	>1570	>1770	Nominal (no yielding in test)
Beam strands J12,5	>1570	>1770	Nominal (may have yielded in test)
Reinforcement Txy	500		Nominal value for reinforcing bars A500HW (no yielding in test)

9.2
Strength of slab concrete, floor test

#	Cores	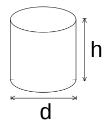	*h* mm	*d* mm	Date of test	Note
6			50	50	25.01.1993 (+7 d)[1)]	Upper flange of slab 4, tested as drilled[2)] Density = 2440 kg/m^3
Mean strength [MPa]			72,9			
St.deviation [MPa]			4,5			

9.3
Strength of slab concrete, reference tests

Not measured, assumed to be the same as that in the floor test.

9.4
Strength of grout in longitudinal joints of slab units

#	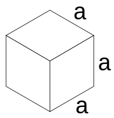	*a* mm	Date of test	Note
3		150	18.1.1993 (+0 d)[1)]	Kept in laboratory in the same conditions as the floor specimen Density = 2150 kg/m^3
Mean strength [MPa]		31,3		
St.deviation [MPa]		0,76		

9.5
Strength of concrete in the middle beam

#	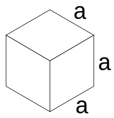	*a* mm	Date of test	Note
6		150	25.1.1993 (+0 d)[1)]	Kept in laboratory in the same conditions as the floor specimen Density = 2403 kg/m^3
Mean strength [MPa]		68,6		
St.deviation [MPa]		3,30		

1) Date of material test minus date of structural test (floor test or reference test)
2) After drilling, kept in a closed plastic bag until compression

10

Measured displacements

In the following figures, *F* stands for the average actuator load + the average weight of loading equipment per actuator.

10.1
Deflections

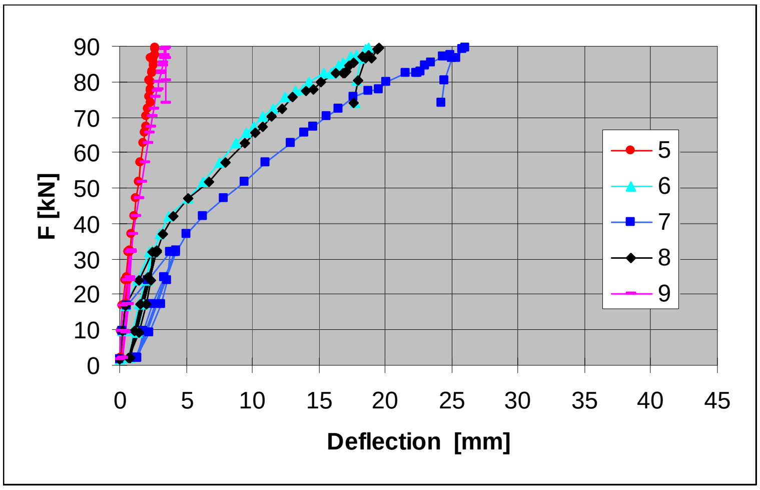

Fig. 22. Deflection measured by transducers 5–9.

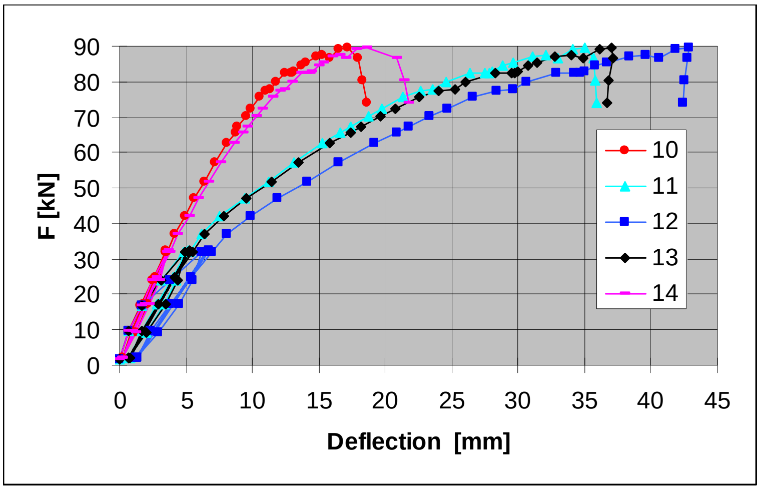

Fig. 23. Deflection measured by transducers 10–14.

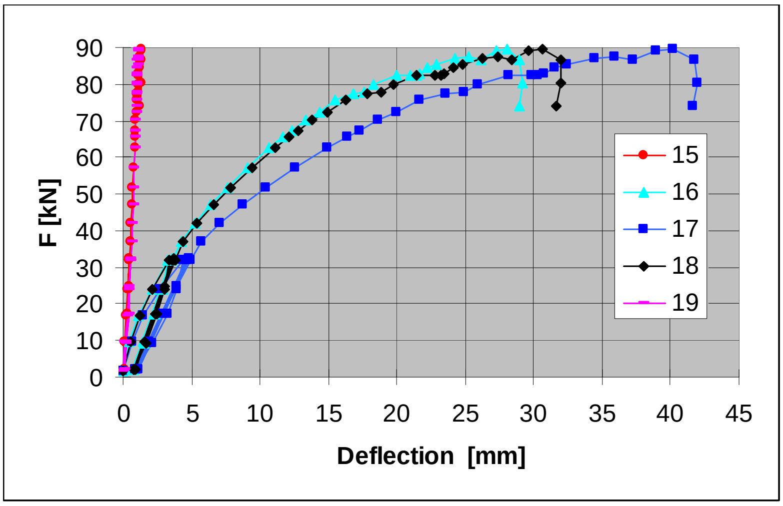

Fig. 24. Deflection measured by transducers 15–19.

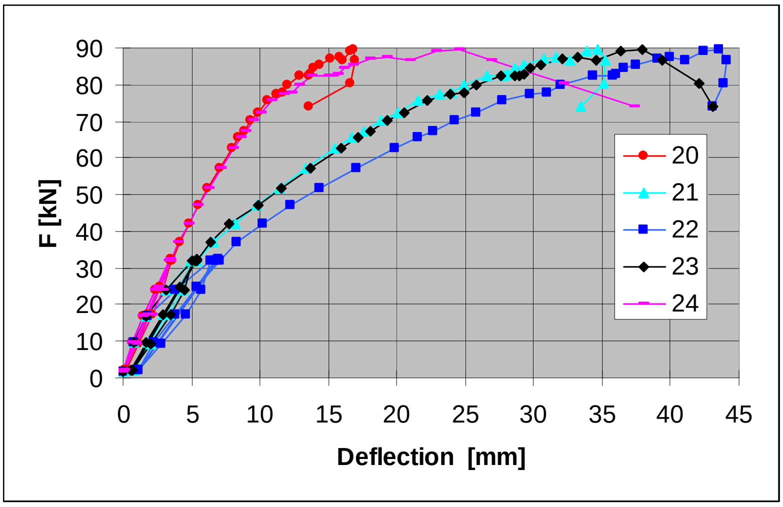

Fig. 25. Deflection measured by transducers 20–24.

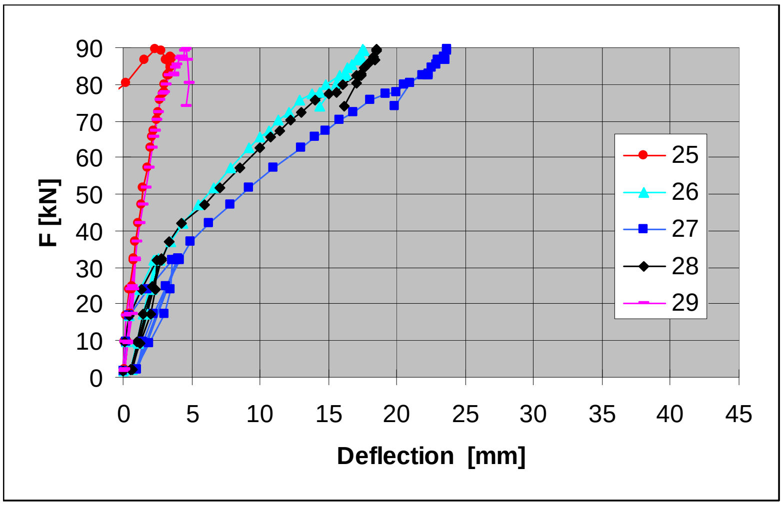

Fig. 26. Deflection measured by transducers 25–29.

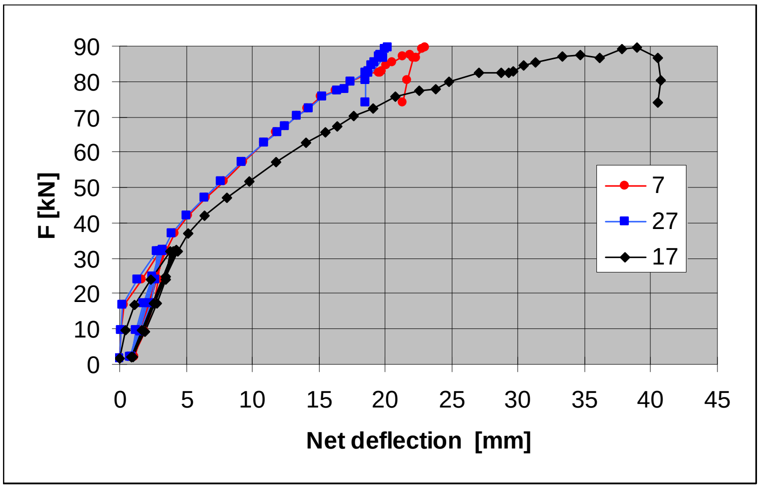

Fig. 27. Net mid-point deflection (measured deflection – settlement of supports) for end beams (7 and 27) and middle beam (17).

10.2
Crack width

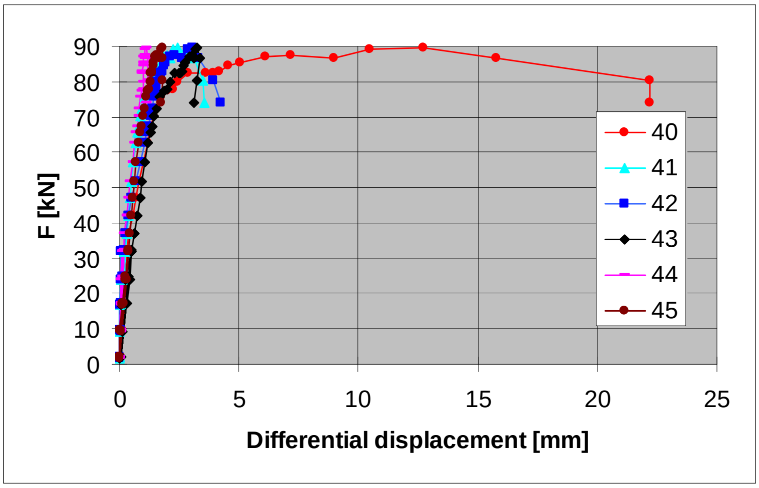

Fig. 28. Differential displacement (≈ crack width) measured by transducers 40–45, see Fig. 15.

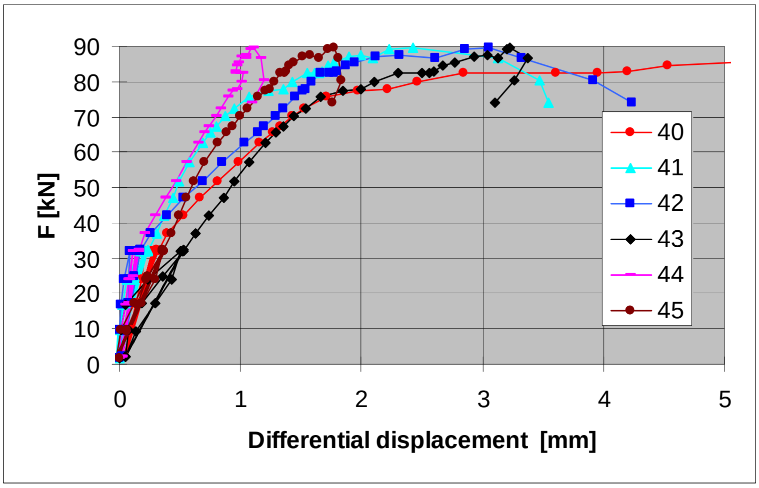

Fig. 29. A part of the previous figure in a larger scale.

10.3
Average strain (actually differential displacement)

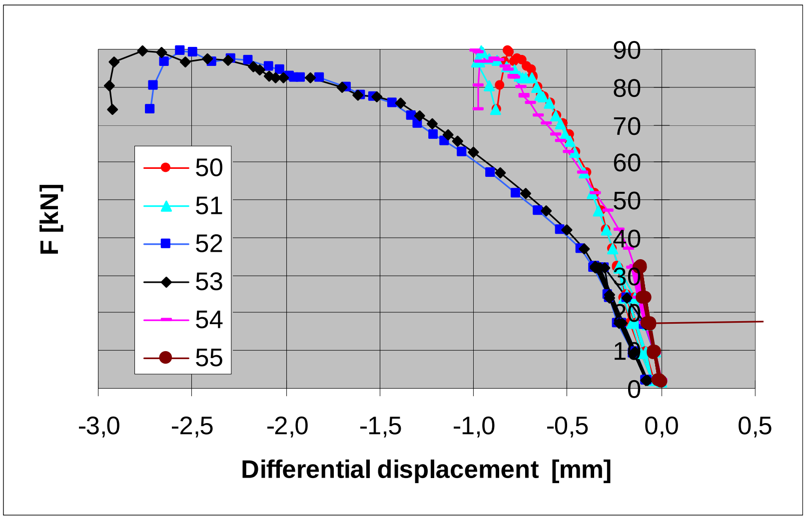

Fig. 30. Differential displacement measured by transducers 50–55, see Fig. 12.

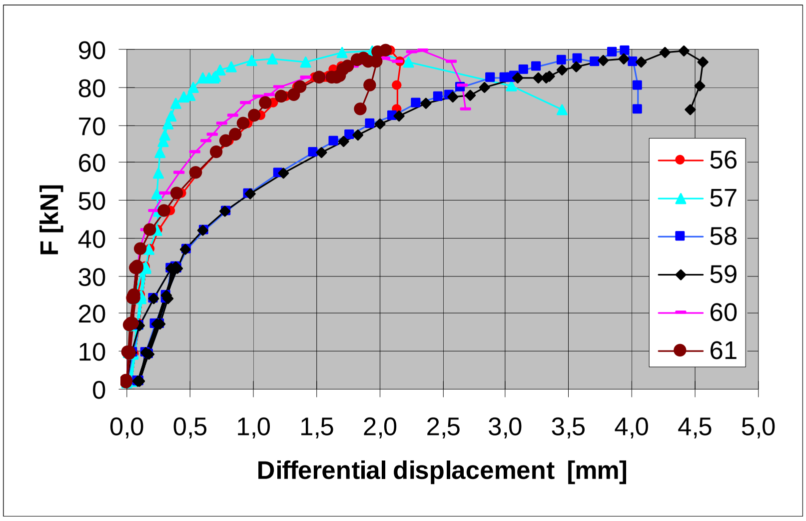

Fig. 31. Differential displacement measured by transducers 56–61, see Fig. 12.

To get a rough estimate of the strains before failure, the measured results on the top and at the bottom of the middle beam are shown in Fig. 32. The displacements were actually measured 10–20 mm outside the top and bottom surface of the floor but this is ignored in Fig. 32.

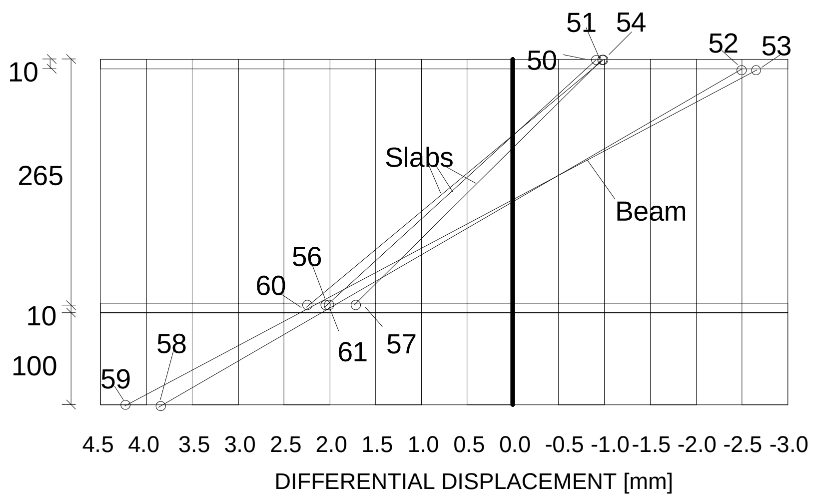

Fig. 32. Differential displacement measured by transducers 50–61 at failure. The values measured on the top and at the bottom are connected with a straight line.

Dividing the values given in Fig. 32 on the top by 1060 mm and those at the bottom by 1120, the value of average strain is obtained. Multiplying the average strain by 1,07, the strain change at the mid-section of the beam due to the actuator loads is obtained. Hence, the change in concrete strain on the top of the beam is

$$\Delta\varepsilon_c = -2{,}55 / 1060 \cdot 1{,}07 = -0{,}26\%$$

and the change in the stress of the lower tendons of the beam is

$$\Delta\sigma_p = E_p \Delta\varepsilon_p = (190GPa) \cdot 3{,}2/1120 \cdot 1{,}07 = 580MPa$$

Taking into account the low prestress level 1100 MPa, the losses of prestress, the elastic deformation due to the release of the prestressing force as well as the short span of the beam and the low self-weight of the slabs, it is clear that the stress in the lowest tendons must have been below 1000 MPa before the actuator loads were applied. This means that the stress in the tendons must have been of the order of yield stress or a bit lower. It can also be concluded that the compression zone of the beam could still carry a higher load. So, the yielding of the beam could not be the reason to the failure.

10.4 Shear displacement

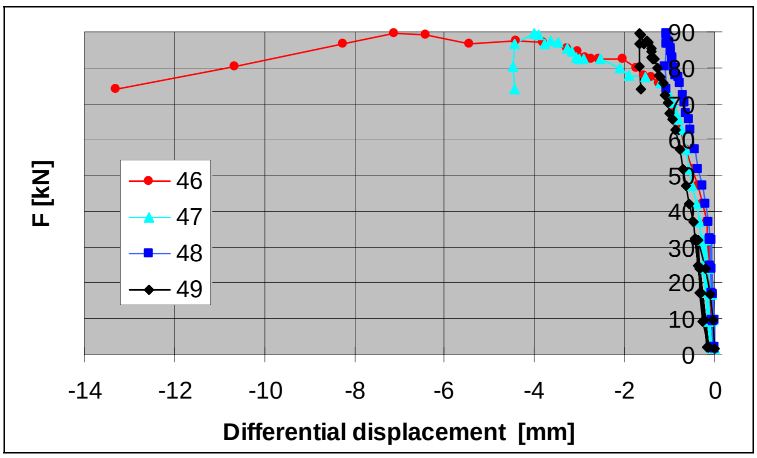

Fig. 33. Sliding of upper edge of slabs 1, 4, 5 and 8 along middle beam, see Fig. 12.

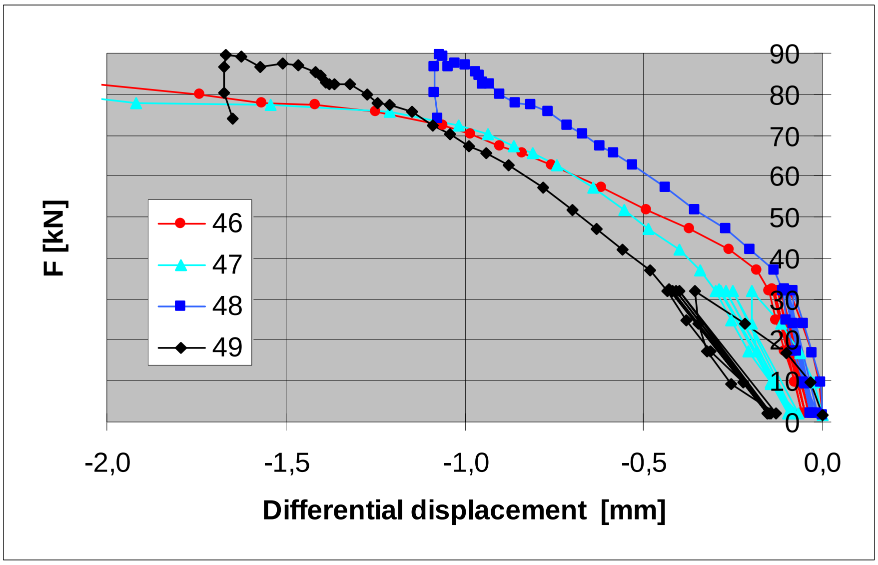

Fig. 34. A part of the previous figure in a larger scale.

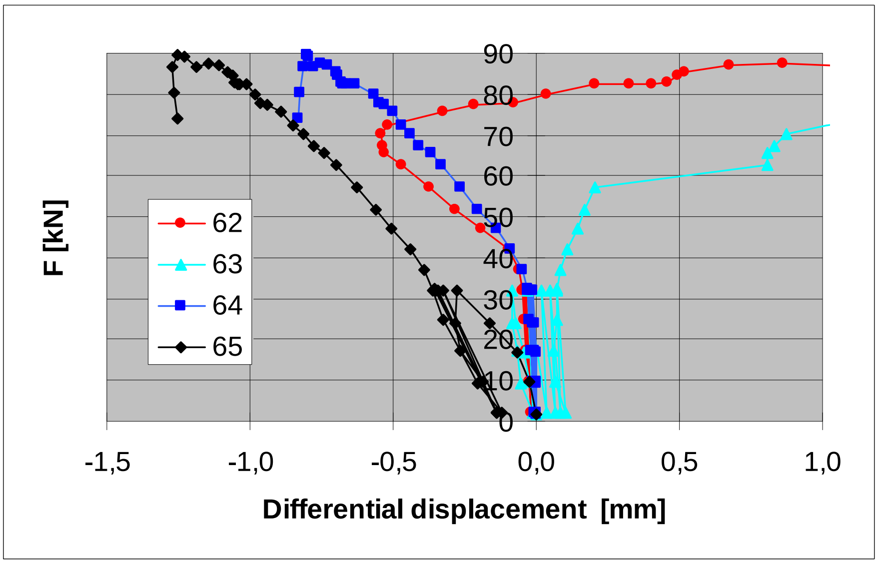

Fig. 35. Sliding of lower edge of slabs 1, 4, 5 and 8 along middle beam. Cracking of the corner of slab 4 at F = 70 kN makes the curve of transducer 62 meaningless after that point. The curve of transducer 63 seems to be incorrect from the beginning.

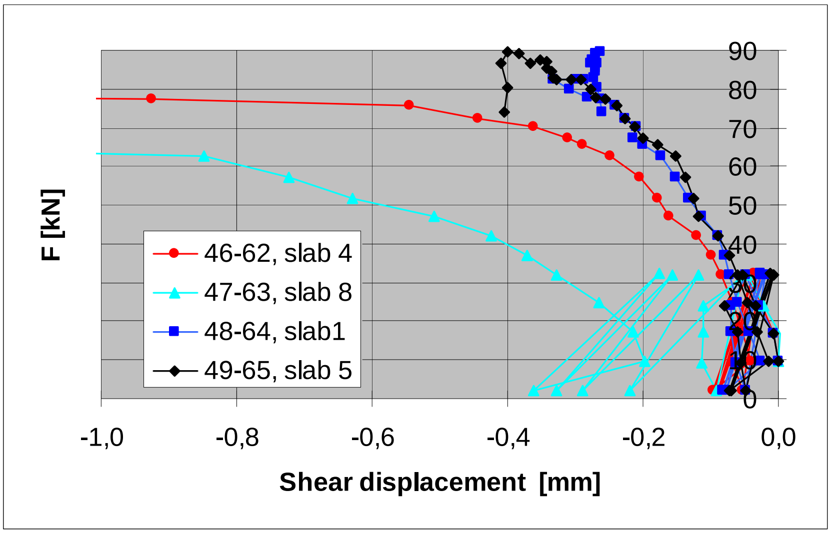

Fig. 36. Shear displacement (= differential displacement between upper and lower edge of slabs 1, 4, 5 and 8) in beam's direction, see Fig. 12. After F = 70 kN the curve for slab 4 reflects primarily the rigid body motion of a loose piece of concrete. Due to the errors in transducer 63, the curve for slab 8 has no physical meaning.

Fig. 36 shows that the core filling could not totally eliminate the transverse horizontal shear deformation of the slab ends.

10.5 Strain

-

11 Reference tests

Two tests were carried out: R9 (slab 9) and R10 (slab 10).

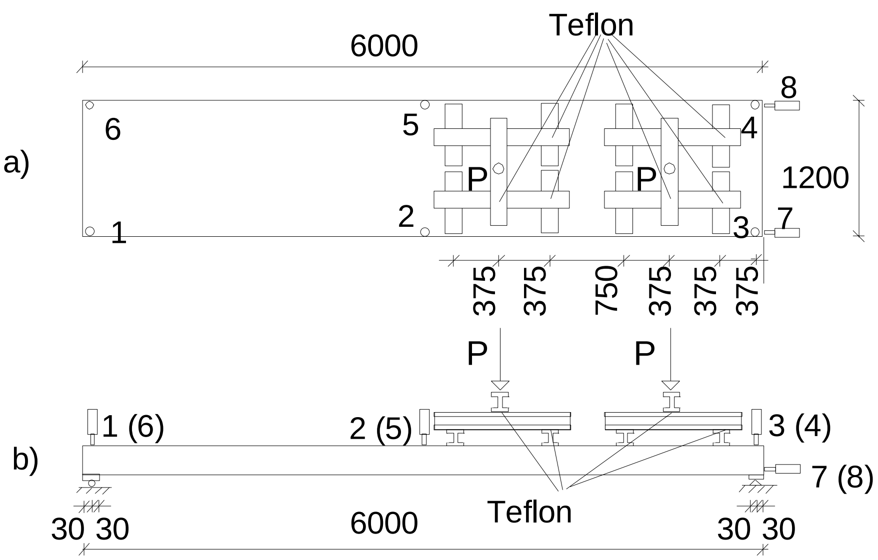

Fig. 37. Layout of reference test. a) Plan. b) Elevation. There was gypsum mortar between the lowest spreader beams ant the top surface of the slab. Transducers 1–6 measured vertical displacement of the top surface, transducers 7 and 8 the slippage of the outermost strands.

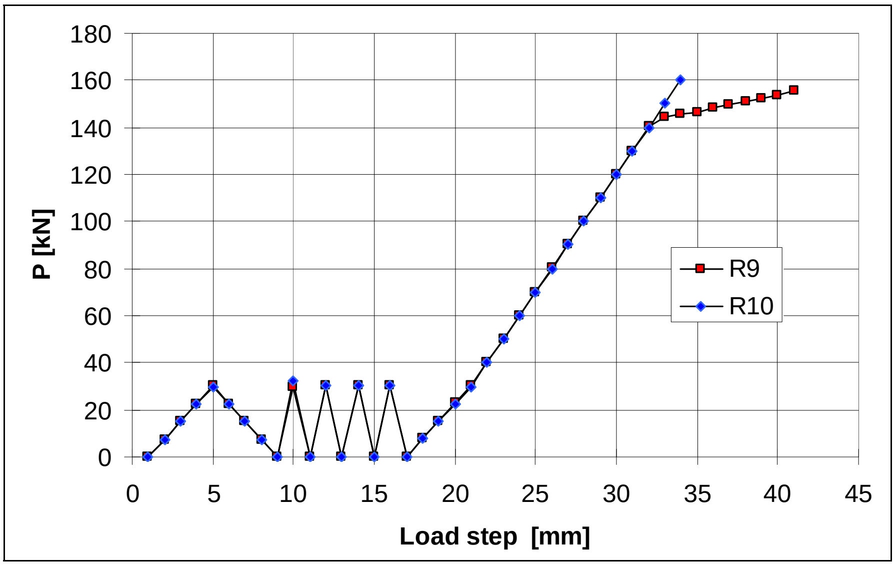

Fig. 38. Loading.

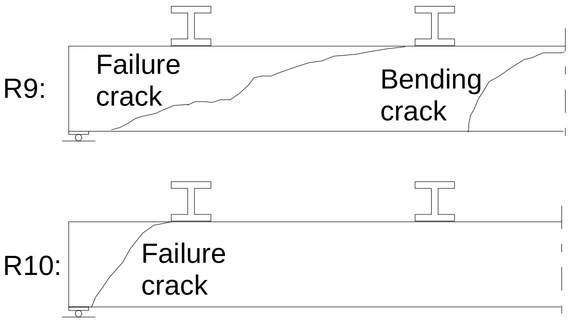

Fig. 39. Failure modes in reference tests. The bending crack in test R9 did not contribute to the actual failure. See also Appendix A, Figs 24–28.

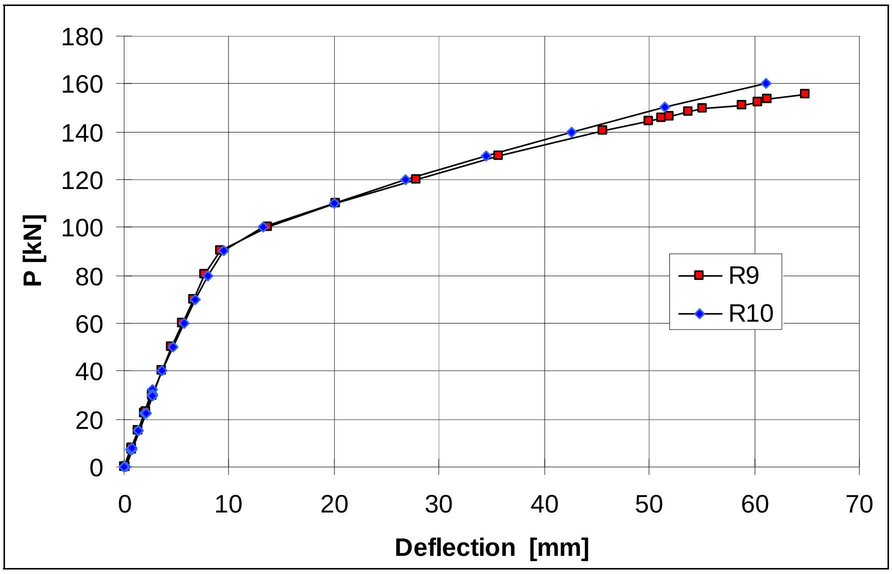

Fig. 40. Midpoint deflection from which the rigid body motion due to the settlement of the supports has been eliminated. P is the actuator force.

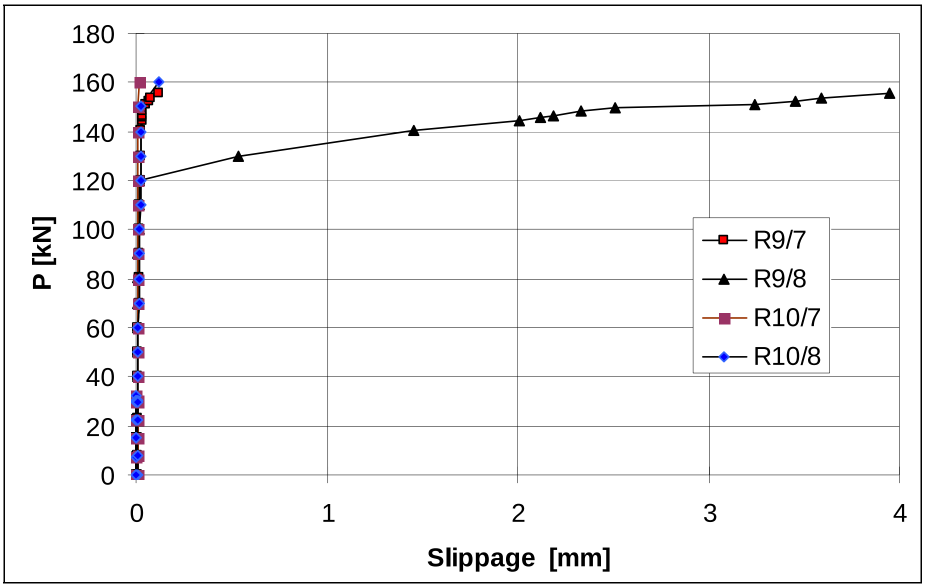

Fig. 41. Slippage of outermost strands measured by transducers 7 and 8.

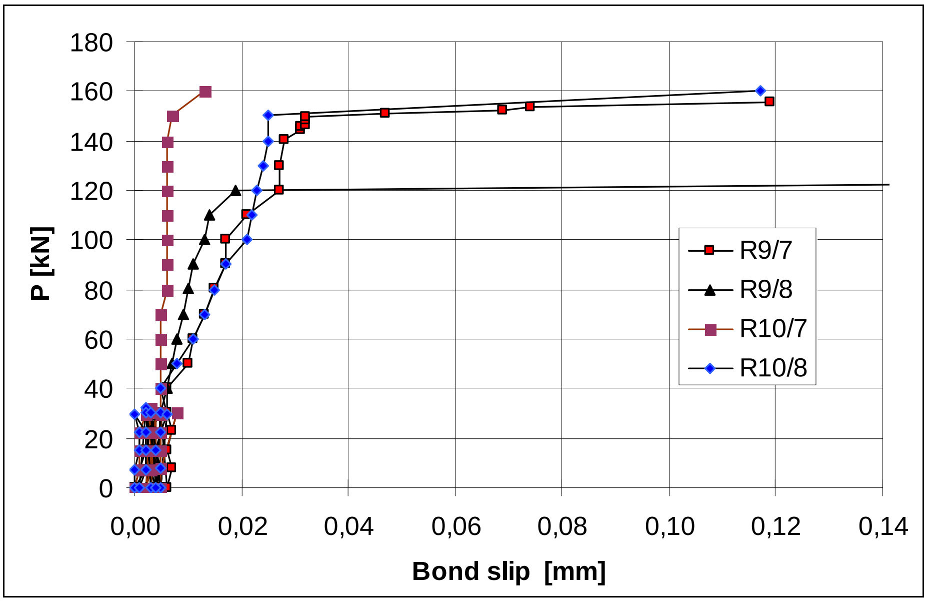

Fig. 42. A part of the previous figure in a larger scale.

Table. Reference tests. Span of slab, shear force V_g at support due to the self weight of the slab, actuator force P at failure, weight of loading equipment P_{eq}, total shear force V_{obs} at failure and total shear force v_{obs} per unit width.

Test	Date	Span mm	V_g kN	P kN	P_{eq} kN	V_{obs} kN	v_{obs} kN/m	Note
R9	22.1.2002	5940	12,2	155,6	1,4	248,5	196,9	Web shear failure
R10	22.1.2002	5940	12,2	160,0	1,4	255,1	212,5	Flexural shear failure
				Mean		**251,8**	**209,8**	

12	**Comparison: floor test vs. reference tests**
	The observed shear resistance (support reaction) of the hollow core slab in the floor test was equal to 147,6 kN per one slab unit or 123,0 kN/m. This is **59%** of the mean of the shear resistances observed in the reference tests.
13	**Discussion**
	1. The failure mode was web shear failure of edge slabs. The prestressed concrete beam seemed to recover completely after the failure. 2. The obtained shear resistance was 43% higher than that observed in test VTT.PC.InvT.265.1990. The filled hollow cores and the uniformly distributed load over half floor made the difference in the present test. It is difficult to say, to which extent the enhanced resistance was attributable to each of these differences. 3. The net deflection of the middle beam due to the imposed actuator loads (deflection minus settlement of supports) was 39 mm or *L*/128. It was 17–19 mm greater than the deflection of the end beams. Hence, the torsion due to the different deflection of the middle beam and end beams has to be taken into account when analyzing the test result. 4. The measured strains on the top and at the bottom of the middle beam suggest that the middle beam was not yielding when the failure took place.

APPENDIX A: PHOTOGRAPHS

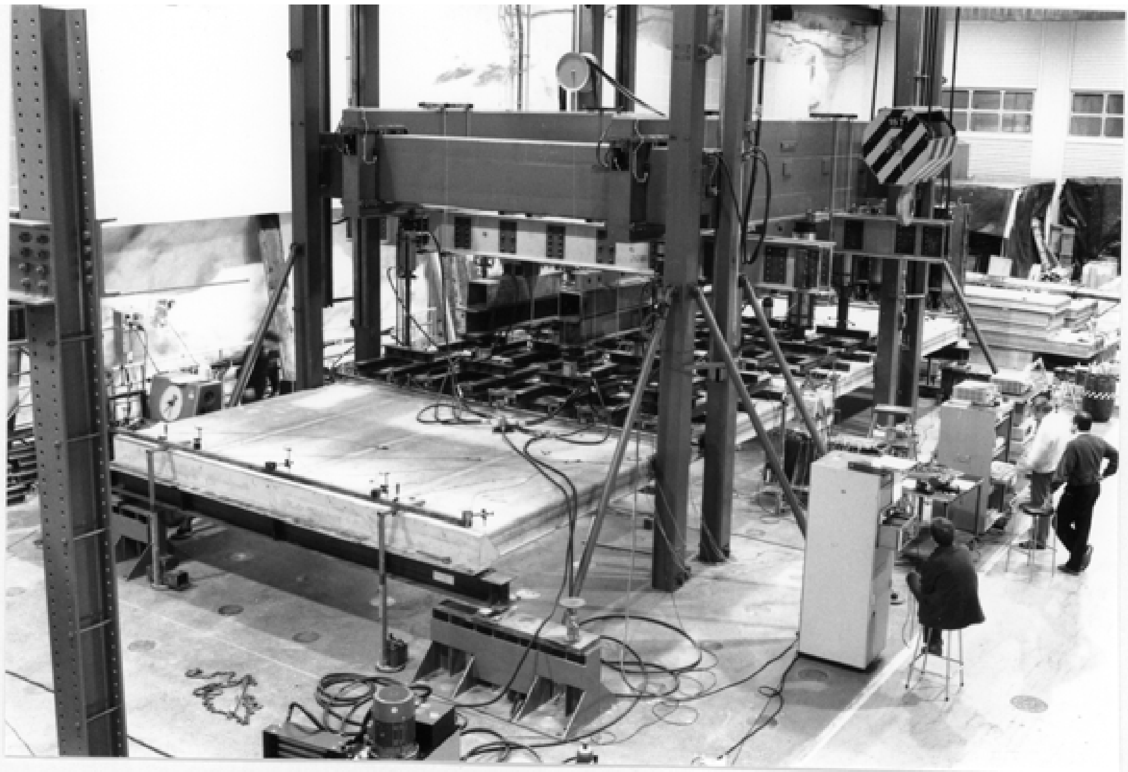

Fig. 1. Overview of test arrangement in floor test.

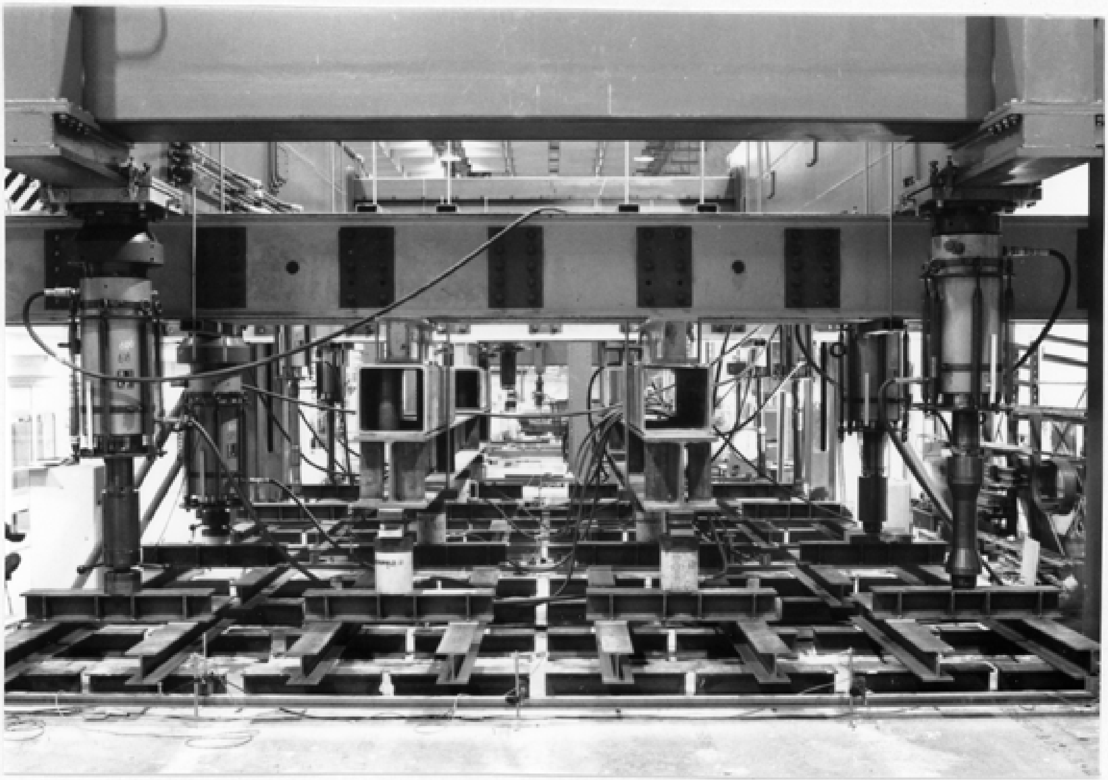

Fig. 2. Longitudinal view of loading equipment. Actuators of type 2 on the right and on the left. Actuators of type 3 in the middle.

Fig. 3. Actuators of type 3. Note the white teflon sheets between the load distributing beams and above the actuators.

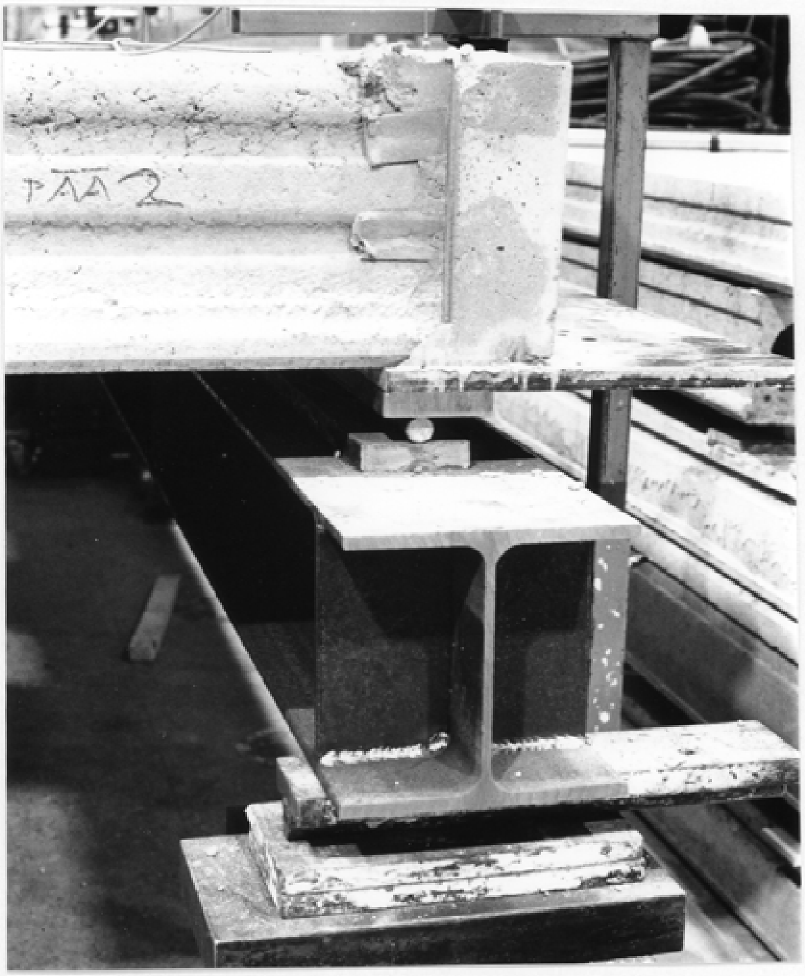

Fig. 4. View of end beam.

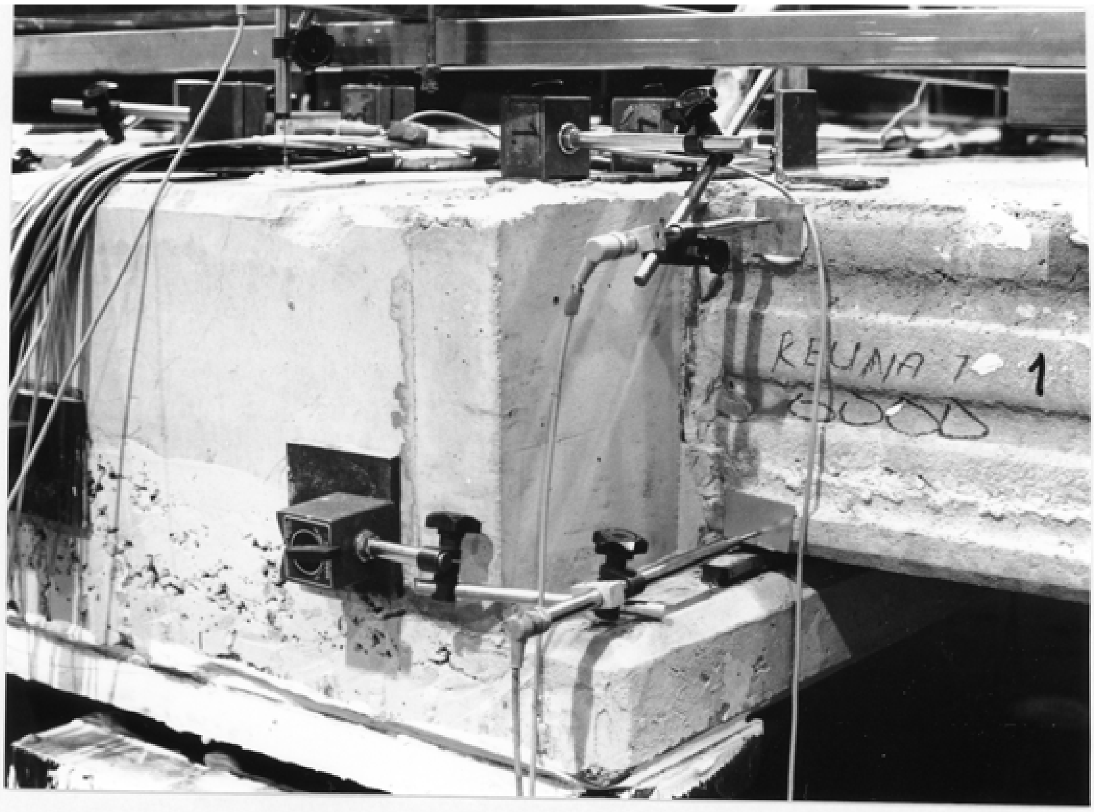

Fig. 5. Equipment for measuring transverse displacement of slab with reference to beam.

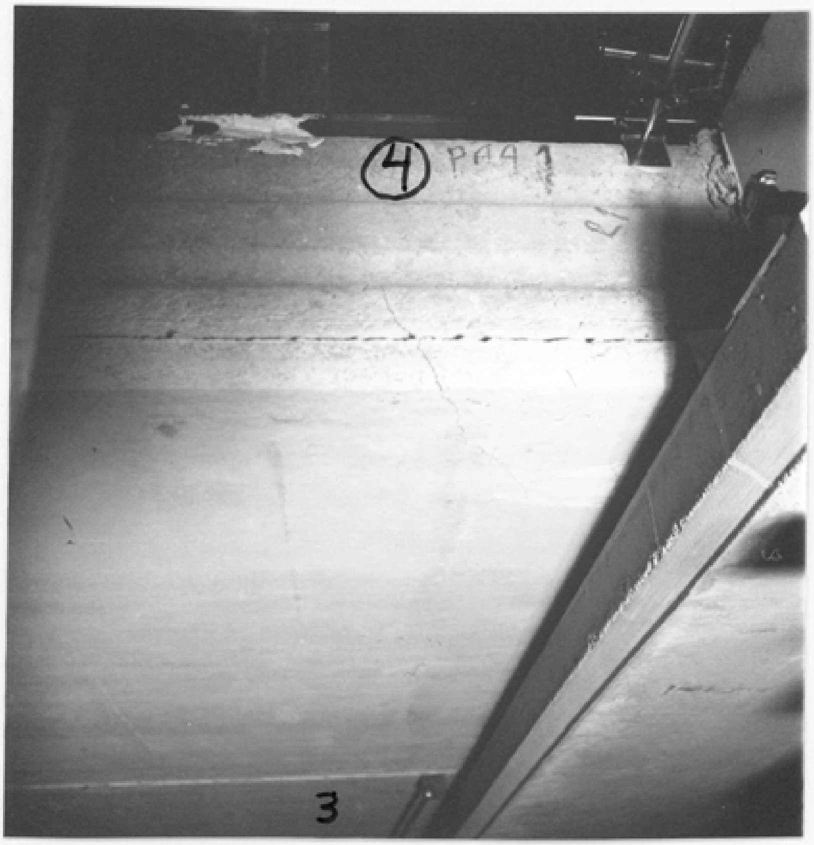

Fig. 6. Flexural cracking of slab unit no 4.

Fig. 7. Shear cracking of slab unit no. 4. Note also the growth of the flexural crack.

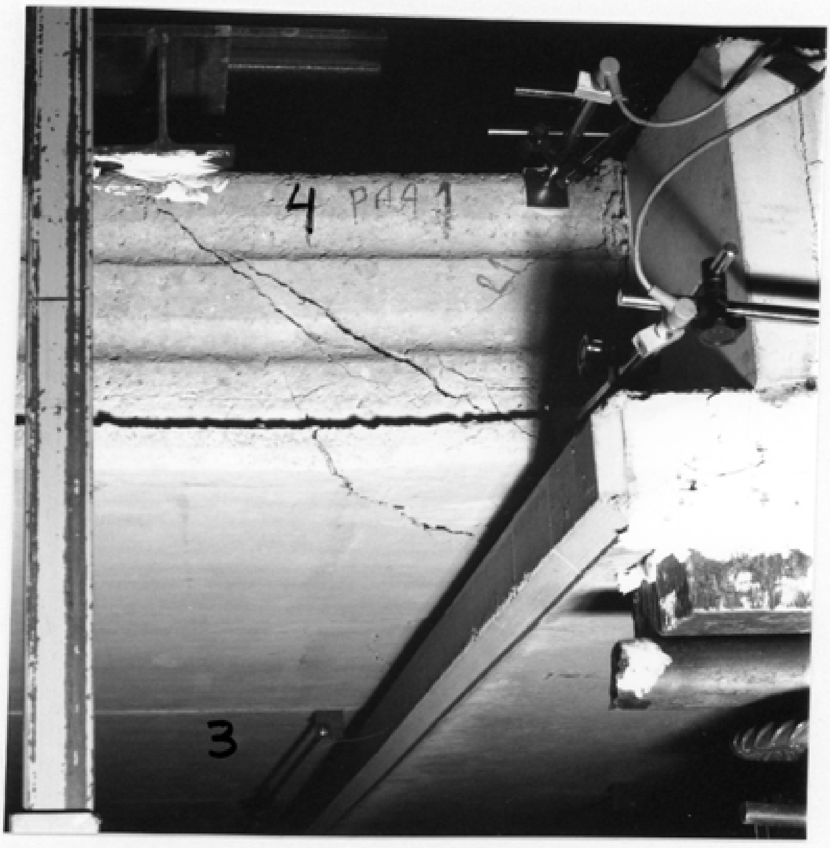

Fig. 8. Cracking pattern of slab unit no 4 before failure.

Fig. 9. Failure of slab unit no 4.

Fig. 10. Failure of slab unit no 4.

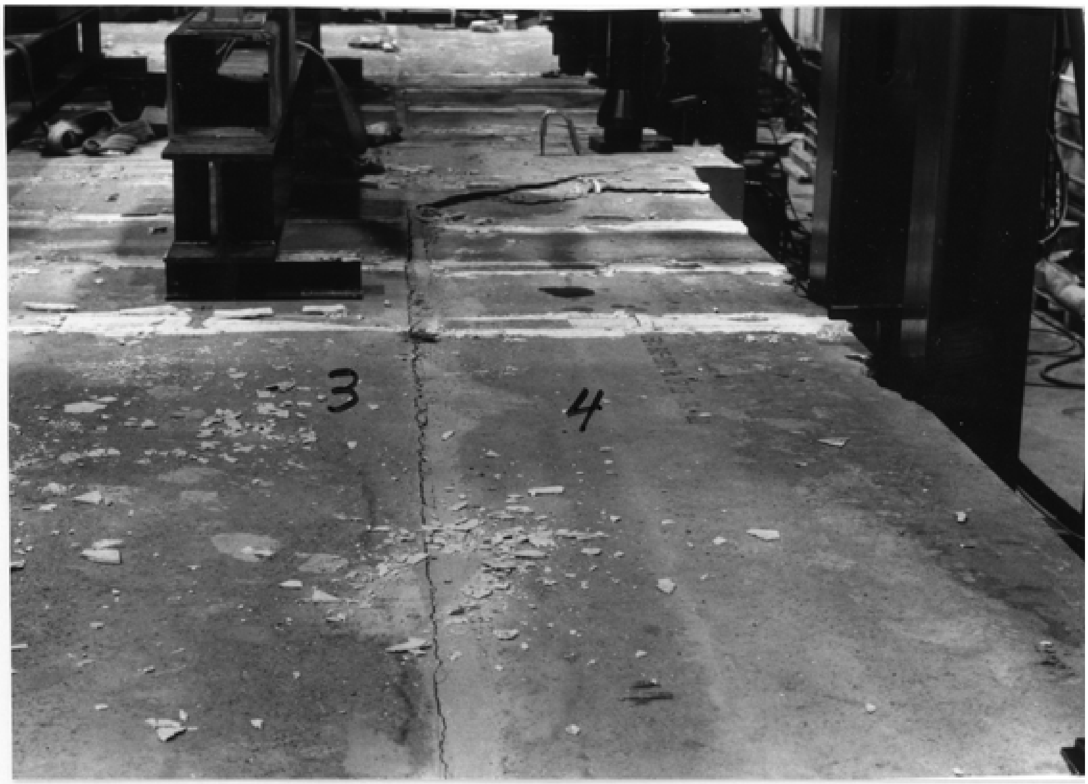

Fig. 11. Failure of slab unit no. 4 seen from above.

Fig. 12. Failure of slab unit no 4 seen from above.

Fig. 13. Failure of slab unit no 4 seen from above.

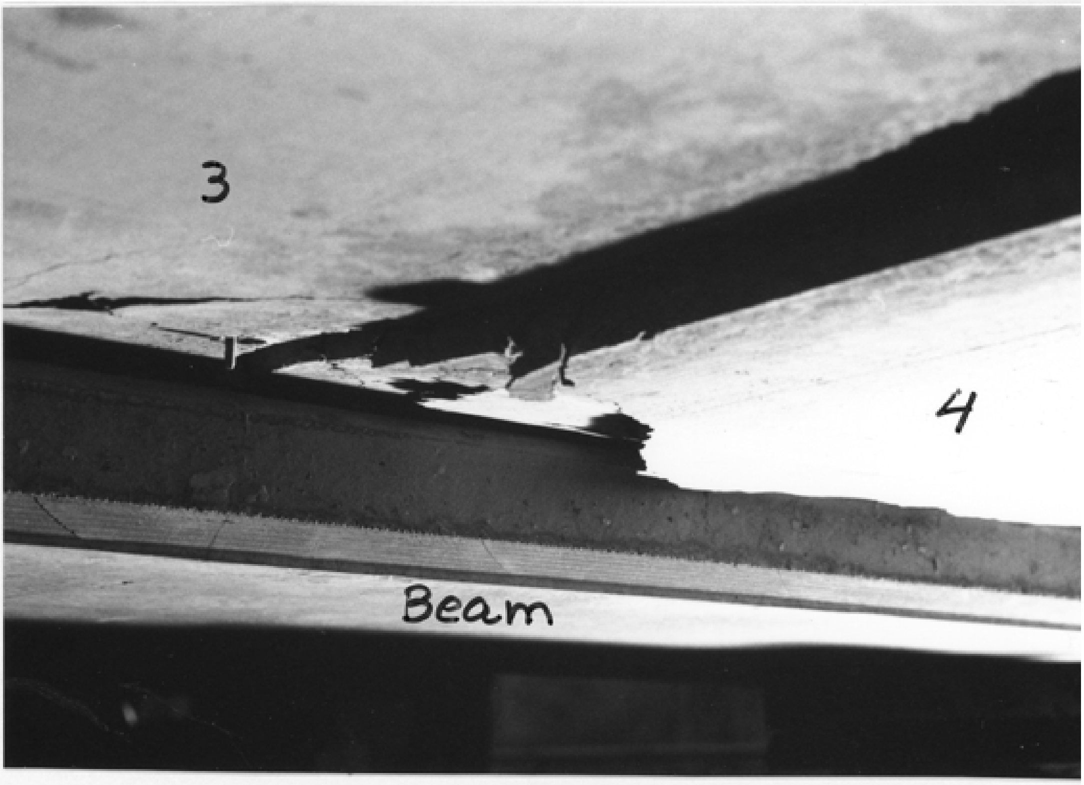

Fig. 14. Failure of slab unit no 4 seen from below after removal of loading.

Fig. 15. Failure of slab unit no 8.

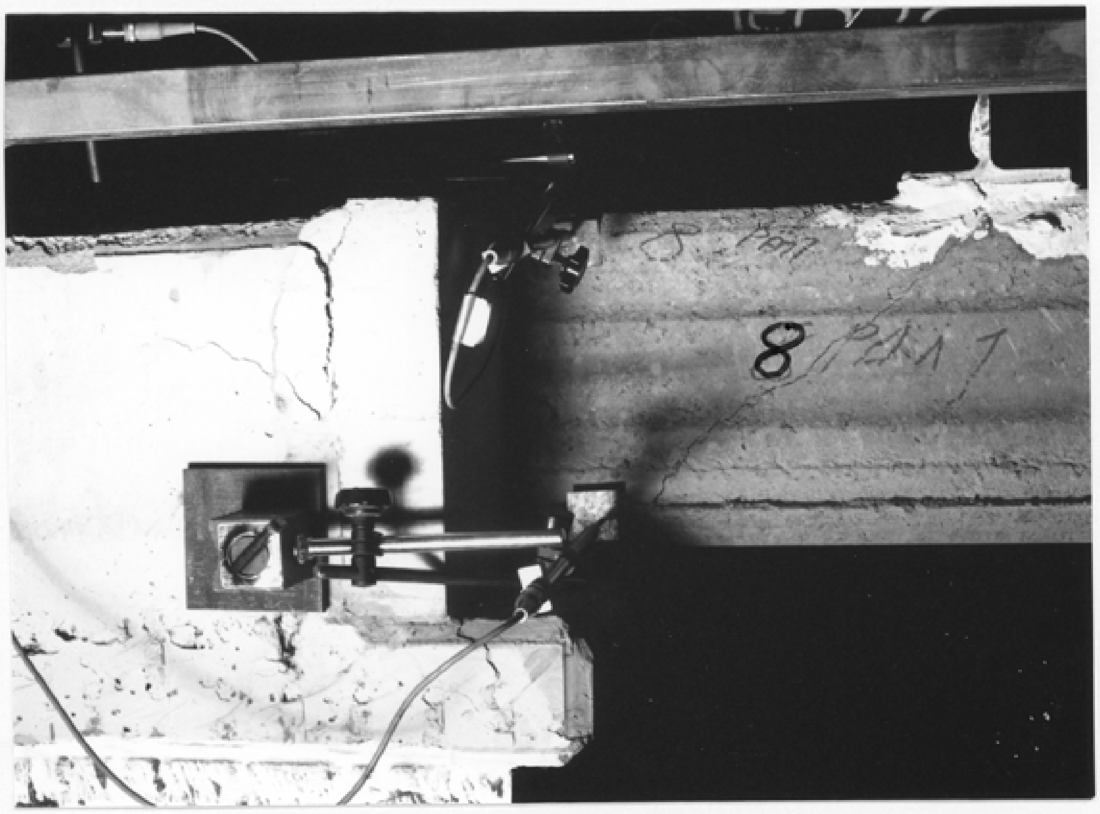

Fig. 16. Failure of slab unit no 8. Note also the cracking of the ledge of the beam.

Fig. 17. Cracking of slab unit no 1.

Fig. 18. Longitudinal and transverse cracking of slab unit no 3 seen from below.

Fig. 19. Void filling at end of slab unit no 8 (upside down).

Fig. 20. Void filling at end of slab unit no 8 (upside down). Note that the concrete has filled the void completely.

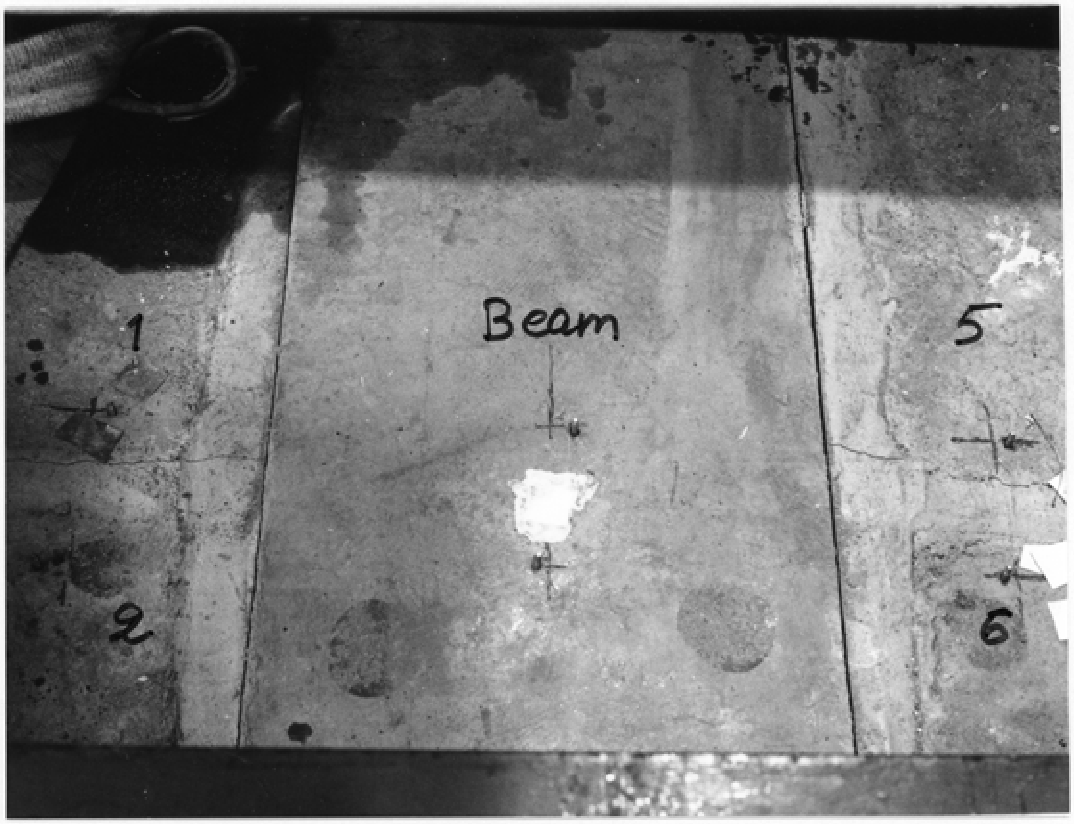

Fig. 21. Cracking of joint concrete along middle beam after removal of loading.

Fig. 22. Cracking of end 2 of middle beam. The inductive transducers no 62 and 63 were attached to the steel plates which moved with reference to the beam when the corners of the beam cracked.

Fig. 23. Cracking of end 1 of middle beam.

Fig. 24. Reference test R1. Failure pattern.

Fig. 25. Reference test R1. Failure pattern.

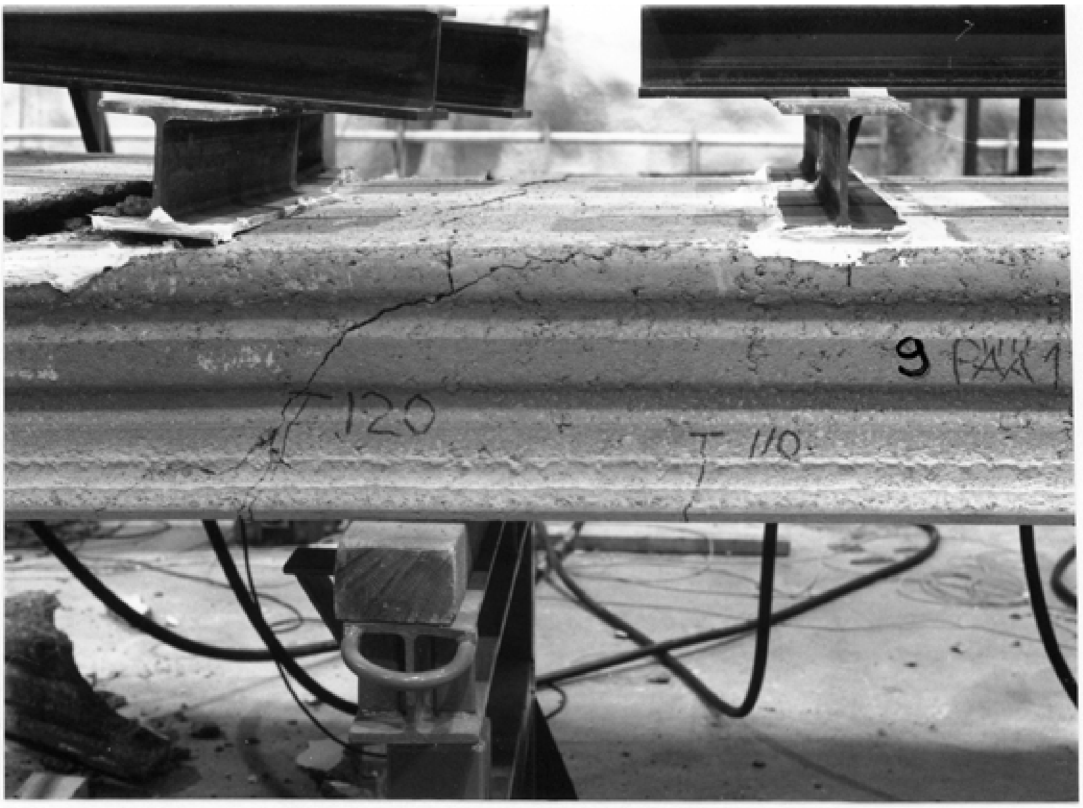

Fig. 26. Reference test R1 (photographed after the failure). The width of the diagonal crack in the figure was several millimetres before the failure took place to the left of the diagonal crack (see Figs 24 and 25).

Fig. 27. Reference test R2. Failure pattern.

Fig. 28. Reference test R2. Failure pattern.

1	**General information**
1.1 Identification and aim	**VTT.PC.InvT-Topp.265.1993** **Last update 2.11.2010** PC265T (Internal identification) Aim of the test: To study the effect of reinforced concrete topping on the shear resistance of hollow core slabs supported on a beam. A prestressed concrete beam was chosen because, according to previous tests, the interaction between the slabs and concrete beam was stronger than with steel beam.
1.2 Test type	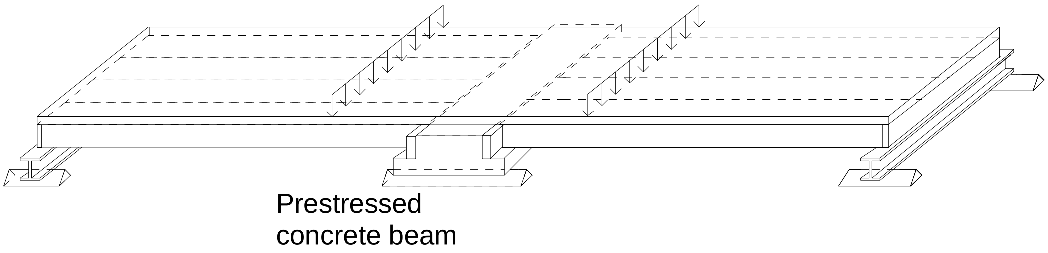 *Fig. 1. Illustration of test setup.*
1.3 Laboratory & date of test	VTT/FI 11.10.1993
1.4 Test report	Author(s): Koukkari, H. Name: *Loading test on 265 mm hollow core floor with topping supported on prestressed concrete beam* Ref. number: RAT-IR-19/1993 Date: 15.12.1993 Availability: Public, available on request from VTT Expert Services, P.O. Box 1001, FI-02044 VTT. Financed by Finnish Association of Building Industry RTT, the International Prestressed Hollow Core Association IPHA, KB Kristianstads Cementgjuteri, Sweden, Skanska Prefab AB, Sweden
2	**Test specimen and loading** (see also Appendix A)
2.1 General plan	See Figs 1 and 10 and Appendix A, Figs 3 and 4.
2.2 End beams	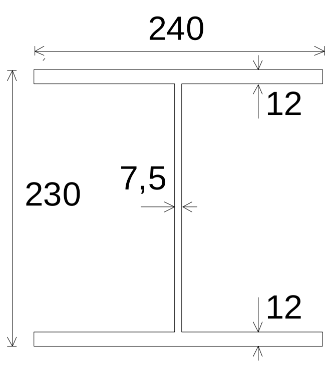 *Fig. 2. Cross-section of end beam.* 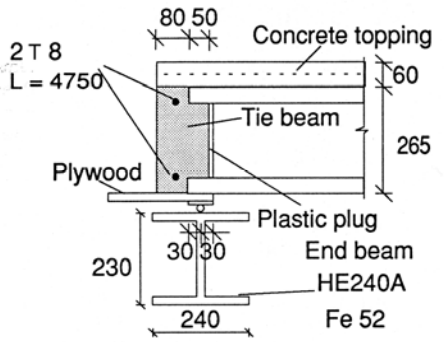 *Fig. 3. Arrangements at end beam. T8 refers to a reinforcing bar with diameter 8 mm, see 2.3.*

	Simply supported, span = 5,0 m
2.3 Middle beam	Prestressed concrete beam, see Figs 4–6 and Appendix A **Concrete**: K60 **Passive reinforcement and tendons:** **Txy**: Hot rolled, weldable rebar A500HW, ϕ = xy mm, see 9.1 **J12,5**: strand with 7 indented wires, ϕ =12,5 mm, A_p = 93 mm^2 **B5**: Cold formed rebar B500K, ϕ = 5 mm, see 9.1 **Tie reinforcement**: Straight rebars in the tie beams, across the middle beam and in the longitudinal joints of the slabs, see Figs 3 and 6. 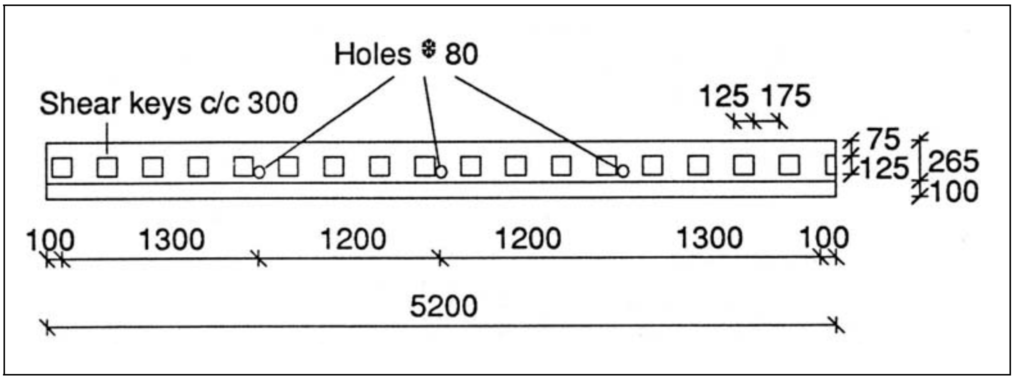 *Fig. 4. Middle beam.* 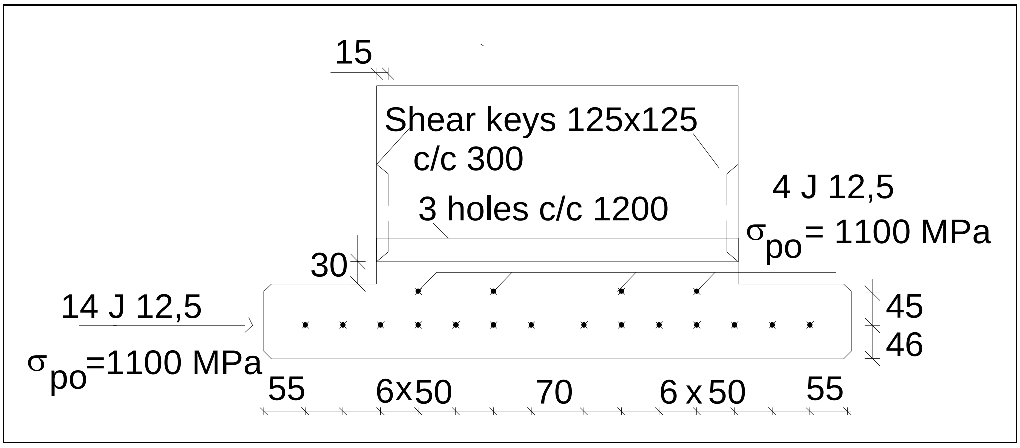 *Fig. 5. Section of middle beam. See also Fig. 6.*
2.4 Arrangements at middle beam	- Simply supported, span = 5,0 m - Joints and tie beams grouted on the 24th of September 1993 - The top surface of the slab units and the middle beam were cleaned and moistened before casting the topping concrete on the 29th of September 1993 - No special measures to enhance the bond between the topping and the underlying concrete

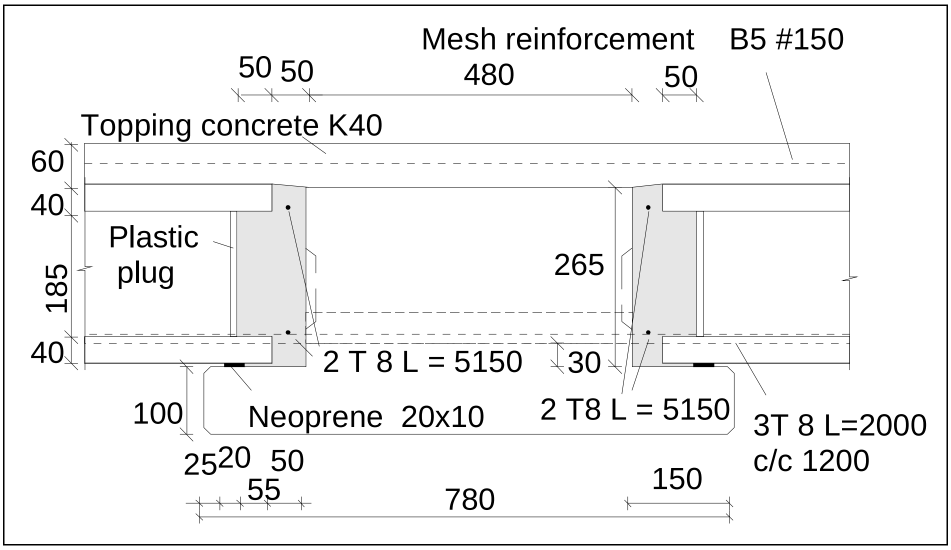

Fig. 6. Section along hollow cores.

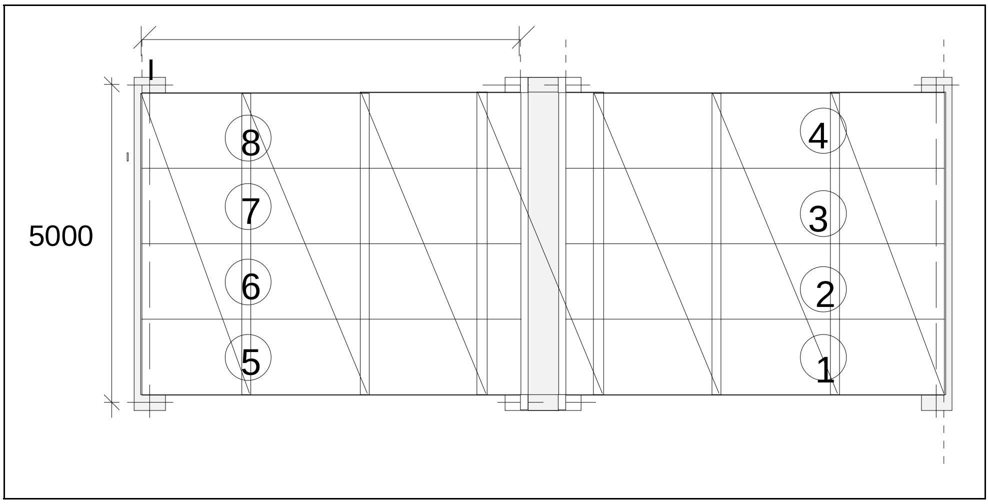

Fig. 7. Overlapping of mesh reinforcement.

2.5
Slabs

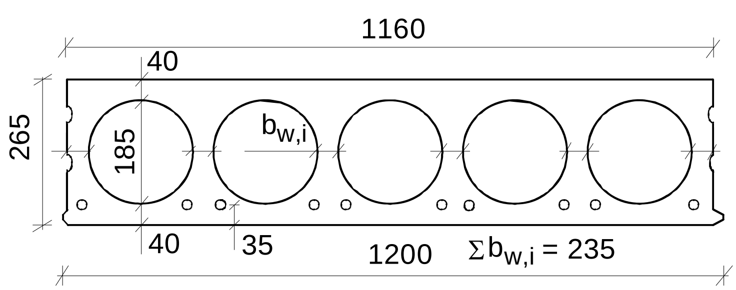

Fig. 8. Nominal geometry of slab units.

- Extruded 15.9.1993 by Partek Oy, Hyrylä factory, grade of concrete K60
- 10 lower strands J12,5 initial prestress 950 MPa

J12,5: seven indented wires, ϕ =12,5 mm, A_p = 93 mm^2, see 9.1.

	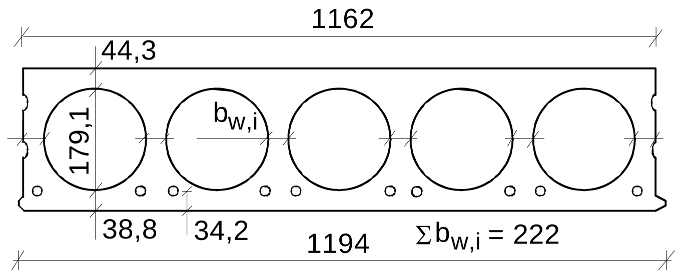 *Fig. 9. Mean of most relevant measured geometrical characteristics, slabs 1–8.*	Max measured bond slips: 2,0 in slab 7; 1,8 in slab 10 and 1,6 in slab 4, Measured weight of slab units = 4,18 kN/m
2.6 Temporary supports	-	
2.7 Loading arrangements	There were two separate hydraulic circuits, one for actuator loads P_1 and the other for actuator loads P_2. See Fig. 10 and App. A, Figs 3 and 4 for the loading arrangements. 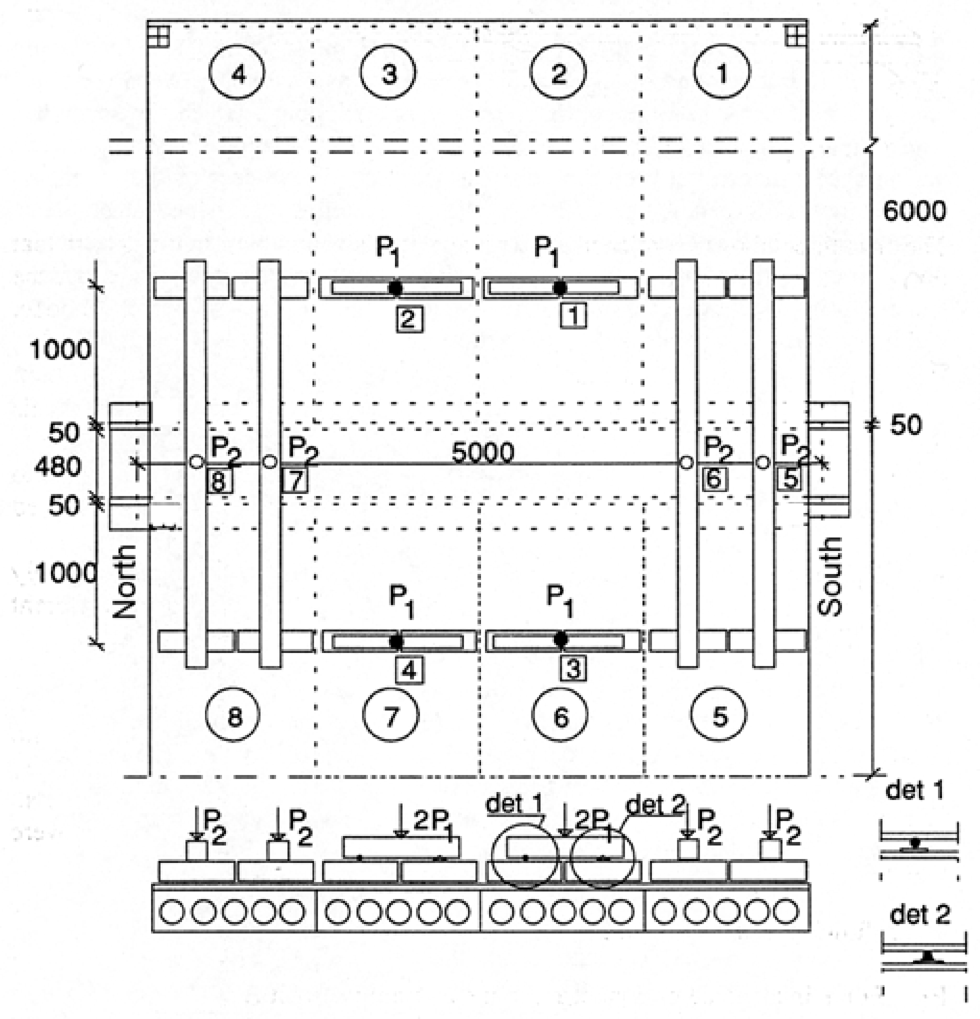 *Fig. 10. Plan. P_1 and P_2 refer to vertical actuator forces. det 1: roller bar, det 2: hinge. The thickness of the topping was 60 mm in those corners of slabs 1, 4, 5 and 8 which where on the South and North edge of the floor specimen.*	

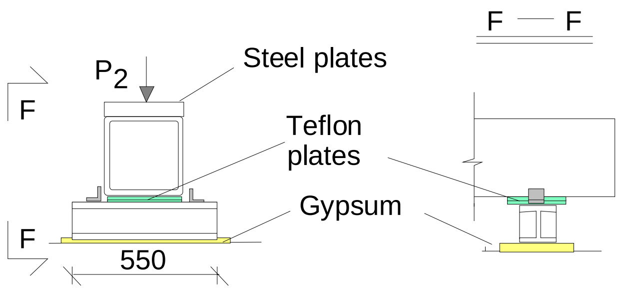

Fig. 11. Bearing above the spreader beams on slabs 1, 4, 5 and 8. The hydraulic actuators (P_2) prevented the lateral motion of the square steel tube beams (see App. 1, Figs 3 and 4) and the friction at the ends was eliminated by teflon plates.

3 Measurements

3.1 Support reactions

The support reaction due to the actuator loads below the Southern end of the middle beam was measured by three load cells, see Fig. 12.

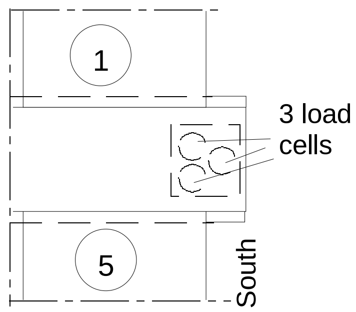

Fig. 12. Load cells below one end of the middle beam.

3.2 Vertical displacement

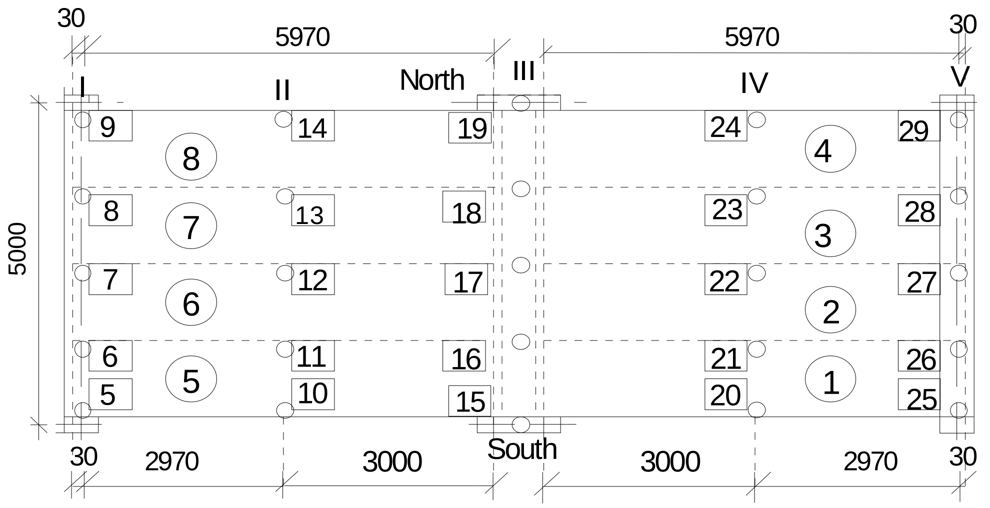

Fig. 13. Location of transducers 5–29 for measuring vertical deflection along lines I–V.

3.3 Sliding of slab (horizontal displacement)

The sliding of the slab ends along the middle beam was measured using eight transducers (46–48 & 62–65). Their position is shown in Fig. 16. See also Figs 7 and 10–13 in App. A.

<table>
<tr>
<td>3.4
Crack width (horizontal displacement)</td>
<td>The differential displacement reflecting the width of vertical cracks in the topping was measured by six transducers located as shown in Fig. 14.
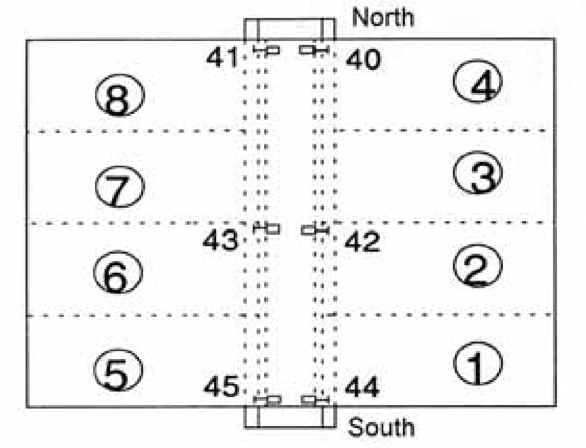

Fig. 14. Transducers (40–45) measuring crack width between the middle beam and the slab ends.</td>
</tr>
<tr>
<td>3.5
Average strain</td>
<td>Average strain was measured using 12 devices of the type shown in Fig. 15. See Fig 16 for the position of the transducers.
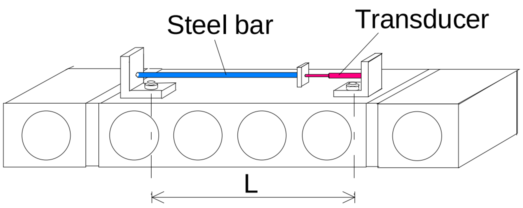

Fig. 15. Apparatus for measuring average strain. L = 1120mm and 1060 mm for the top and soffit transducers (50–55 and 56–61), respectively.
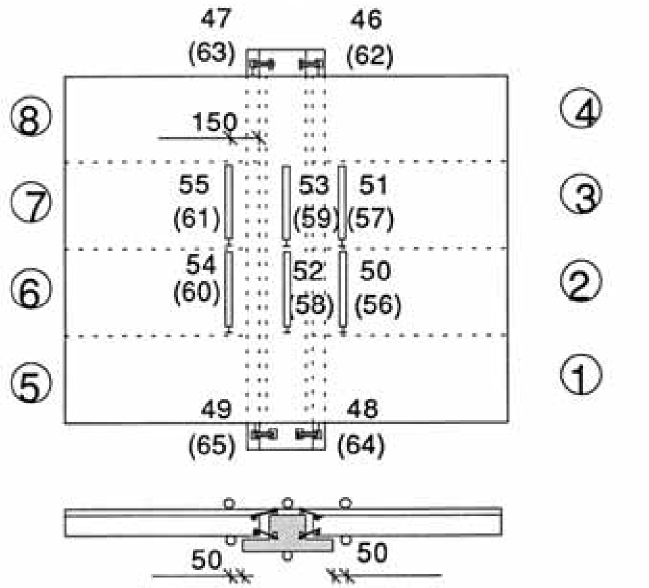

Fig. 16. Position of transducers 50–61 measuring average strain parallel to the beam and position of transducers 46–48 & 62–65 measuring sliding of slabs along the beam. The numbers in parentheses refer to lower transducers.</td>
</tr>
</table>

4	**Special arrangements** - none
5	**Loading strategy**
5.1 Load-time relationship	The date of the floor test was 11.10.1993 The imposed load F_i on each hollow core slab was equal to $P_i + P_{eq,\,i}$ where P_i is the actuator load P_1 or P_2 shown in Fig. 10 and $P_{eq,i}$ the load due to the self weight of the loading equipment. So $F_1 = P_1$ + 1,2 kN for slab units 2, 3, 6 and 7 $F_2 = P_2$ + 5,6 kN for slab units 1, 4, 5 and 8 When the actuator forces P_i were equal to zero but the weight of the loading equipment was on, all measuring devices were zero-balanced. The loading history is shown in Fig.17. Note, that the number of load increment, not the time, is given on the horizontal axis. The whole test took roughly two hours. In the following, the cyclic stage (increments 0–16) is called Stage I, the monotonous stage from increment 16 to failure is called Stage II. 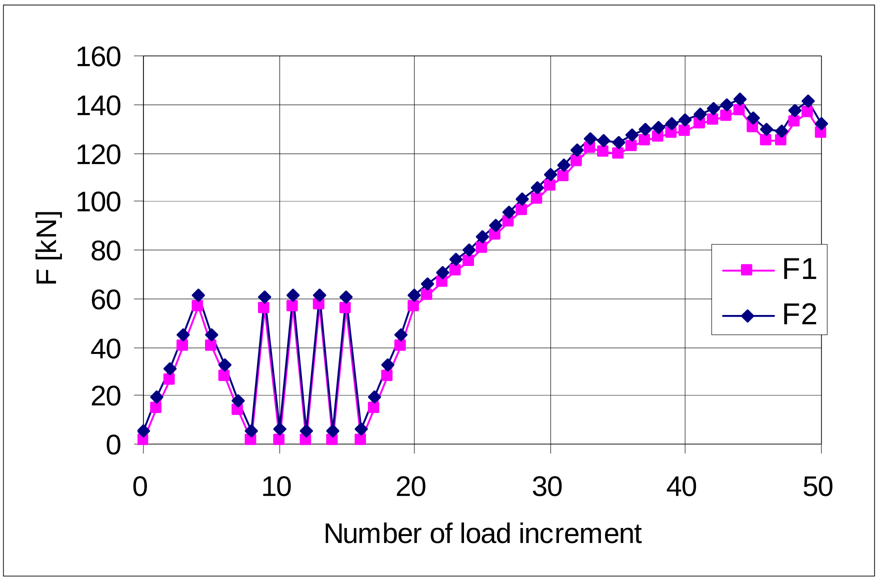 *Fig. 17. Loading history.*
5.2 After failure	

6

Observations during loading

P_i kN	Observations	Cracking pattern
55 (1)	Vertical cracks in the flange of the middle beam, under slab 6	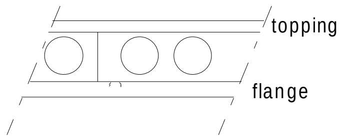
55 (1)	Vertical cracks in the longitudinal edges of the topping, above the middle beam ends	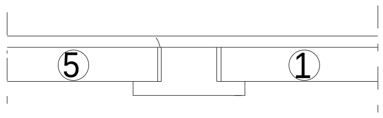
55(1)	One vertical crack in the tie beam, above the end beam	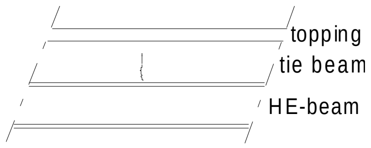
55(3)	Several vertical cracks in the middle beam ends	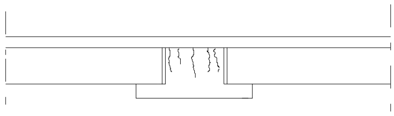
55(5)	A vertical crack in the longitudinal edge of the topping	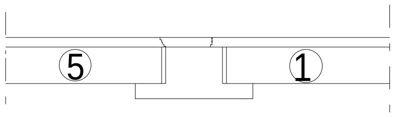
60	Cracking in the middle beam flange grew down to the bottom of the middle beam	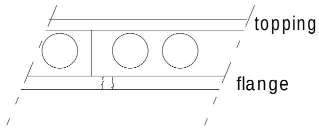
80	Cracks on the surface of the topping along the joint between the middle beam and slabs 1–4	see Fig. 18
80	A transverse crack in the soffit of the middle beam	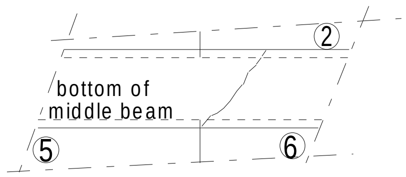
90	The cracks in the end tie beams reached the surface ot the topping	
90	A vertical crack in the longitudinal edge of the topping starting from the corner of the middle beam	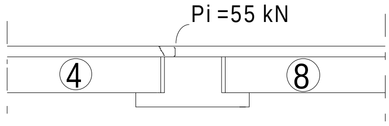
100	A vertical crack in the concrete tie beam, between slabs 5 and 6	
100	A vertical crack in the joint between slab 1 and the middle beam, next to the beam	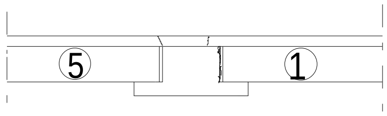

110	A vertical crack in the joint between the slab 5 and the middle beam, next to the beam	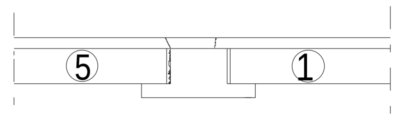
115	A vertical crack in the longitudinal edge of the topping starting from the corner of the middle beam	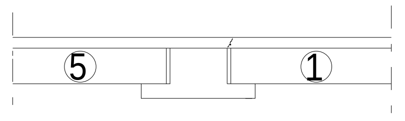
115	The concrete topping became loose above the middle beam, between slabs 1 and 5	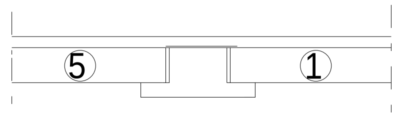
120	Diagonal cracks developed in edges of slabs 1 and 4 near the middle beam and a vertical crack along the ends of slabs 5–8 appeared in the topping. After a while diagonal cracks developed in edges of slabs 5 and 8 near the middle beam.	
135	A shear failure took place in slabs 4 and 8.	

7	**Cracks in concrete**
7.1 Cracks at service load	
7.2 Cracks after failure	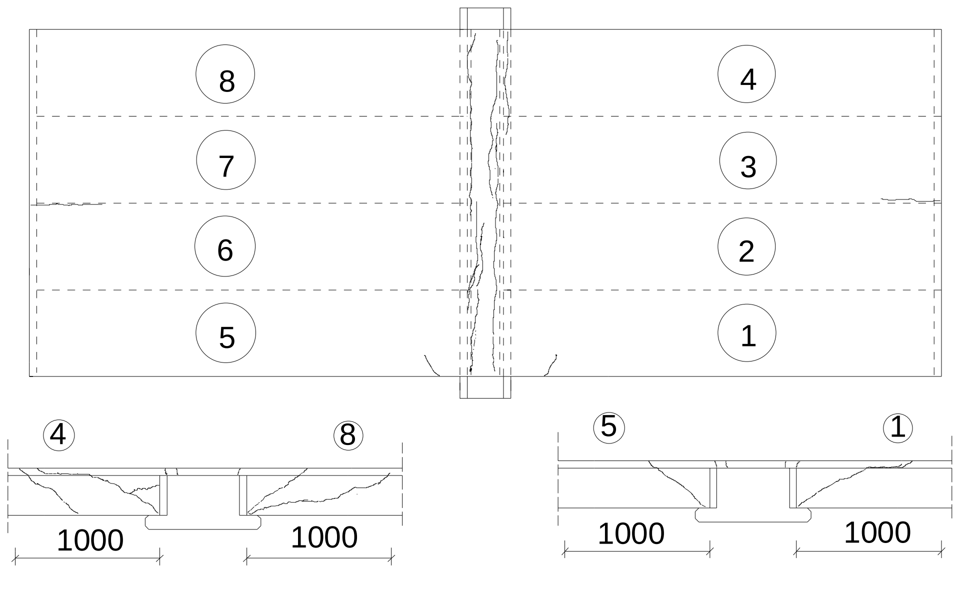 *Fig. 18. Cracks after failure on the top and at the edges.*

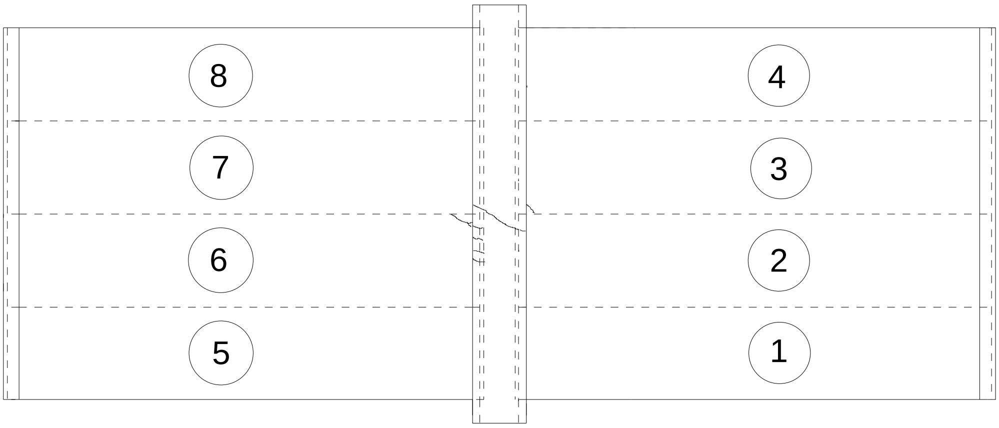

Fig. 19. Cracks after failure in the soffit.

8	**Observed shear resistance**

The maximum support reaction is regarded as the indicator of failure.

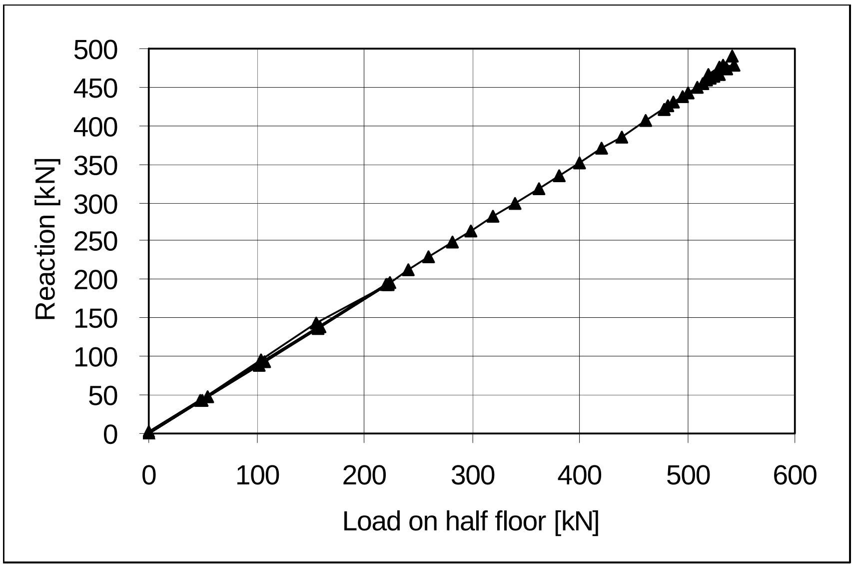

Fig. 20. Support reaction measured below South end of the middle beam vs. load on half floor = $2(P_1 + P_2)$.

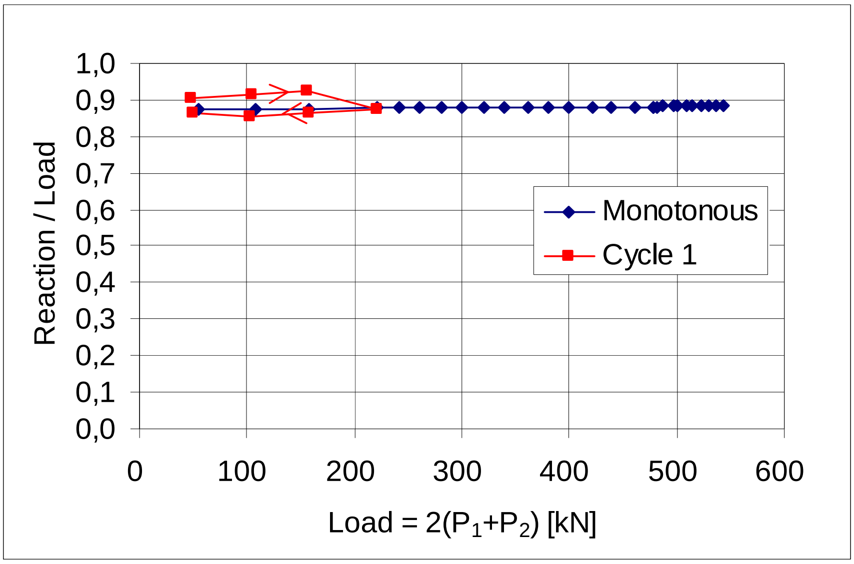

Fig. 21. Ratio of measured support reaction (below South end of the middle beam) to load on half floor = 2(P_1 + P_2).

The shear resistance of one slab end (support reaction of slab end at failure) due to different load components is given by

$$V_{obs} = V_{g,sl} + V_{g,jc} + V_{g,top} + V_{eq} + V_p$$

where $V_{g,sl}$, $V_{g,jc}$, $V_{g,top}$, V_{eq} and V_p are shear forces due to the self-weight of slab unit, weight of joint concrete, weight of topping concrete, weight of loading equipment and actuator forces P_i, respectively.

The shear force due to the the self-weight of the structure is calculated assuming that the slabs behave as simply supported beams. V_{eq} and V_P are calculated using the measured relationship between the support reaction of the beam and the loads. This means that V_{eq} = 0,883xP_{eq} and V_p = 0,883x(P_1.+ P_2)/2. $V_{g,jc}$ and $V_{g,top}$ are calculated from the nominal geometry of the joints, nominal thickness 60 mm of the topping and measured density of the concrete, other components of the shear force are calculated from measured loads and weights. The values for the components of the shear force are given in Table below.

Table. Components of shear resistance due to different loads.

Action	Load	Shear force kN
Weight of slab unit	4,18 kN/m	12,4
Weight of joint concrete	0,11 kN/m	0,3
Loading equipment	(1,2+5,6)/2 kN	3,0
Weight of topping	1,58 kN/m	4,7
Actuator loads 271,6	(135,4+136,3)/2 kN	119,9

The observed shear resistance $\boldsymbol{V_{obs}}$ **= 140,3 kN** (shear force at support) is obtained for one slab unit with width = 1,2 m. The shear force per unit width is $\boldsymbol{v_{obs}}$ **= 116,9 kN/m**

9 Material properties

9.1 Strength of steel:

Component	$R_{eH}/R_{p0,2}$ MPa	R_m MPa	Note
End eams	≈ 350		Nominal (Fe 52, no yielding in test)
Strands J12,5	>1570	>1770	Nominal (no yielding in test)
Reinforcement B5	500		Nominal (B500K)
Reinforcement T8	500		Nominal (A500HW)

9.2 Strength of slab concrete, floor test

#	Cores	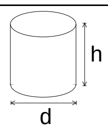	*h* mm	*d* mm	Date of test	Note
6			50	50	25.10.1993	Upper flange of slabs 1, 3 & 8, two pc. from each
Mean strength [MPa]			78,2		(+14 d)[1)]	Vertically drilled
St.deviation [MPa]			4,3			Tested as drilled[2)] Density = 2417 kg/m^3

9.3 Strength of slab concrete, reference tests

#	Cores	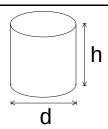	*h* mm	*d* mm	Date of test	Note
6			50	50	25.10.1993	Upper flange of slab9
Mean strength [MPa]			72,0		(+14 d)[1)]	Vertically drilled
St.deviation [MPa]			4,9			Tested as drilled[2)] Density = 2407 kg/m^3

9.4 Strength of grout in longitudinal joints of slab units and tie beams

#	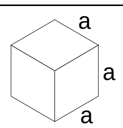	*a* mm	Date of test	Note
2		150	11.10.1993	Kept in laboratory in the same
Mean strength [MPa]		29,3	(+0 d)[1)]	conditions as the floor specimen
St.deviation [MPa]				Density = 2200 kg/m^3

#	Cores	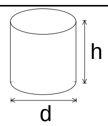	*h* mm	*d* mm	Date of test	Note
3			50	50	25.10.1993	Vertically drilled
Mean strength [MPa]			33,8		(+14 d)[1)]	Tested as drilled[2)]
St.deviation [MPa]			4,6			Density = 2147 kg/m^3

9.5
Strength of concrete in the topping

#	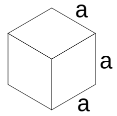	*a* mm	Date of test	Note
2		150	11.10.1993 (+0 d)[1)]	Kept in laboratory in the same conditions as the floor specimen Density = 2200 kg/m^3
Mean strength [MPa]		29,3		
St.deviation [MPa]				

#	Cores	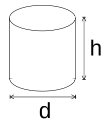	*h* mm	*d* mm	Date of test	Note
6			50	50	25.10.1993 (+14 d)[1)]	Vertically drilled Tested as drilled[2)] Density = 2200 kg/m^3
Mean strength [MPa]			34,2			
St.deviation [MPa]			1,25			

9.6
Strength of concrete in the middle beam

#	Cores	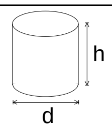	*h* mm	*d* mm	Date of test	Note
6			75	75	25.10.1993 (+14 d)[1)]	Vertically drilled Tested as drilled[2)] Density = 2387 kg/m^3
Mean strength [MPa]			62,9			
St.deviation [MPa]			3,6			

1) Date of material test minus date of structural test (floor test or reference test)
2) After drilling, kept in a closed plastic bag until compression

10 **Measured displacements**

In the following figures, $F_2 = P_2$ +5,6 kN is the line load on slabs 1, 4, 5 and 8 due to actuator force P_2 and weight of loading equipment. Note that the last six points on each curve represent the post failure situation.

10.1 Deflections	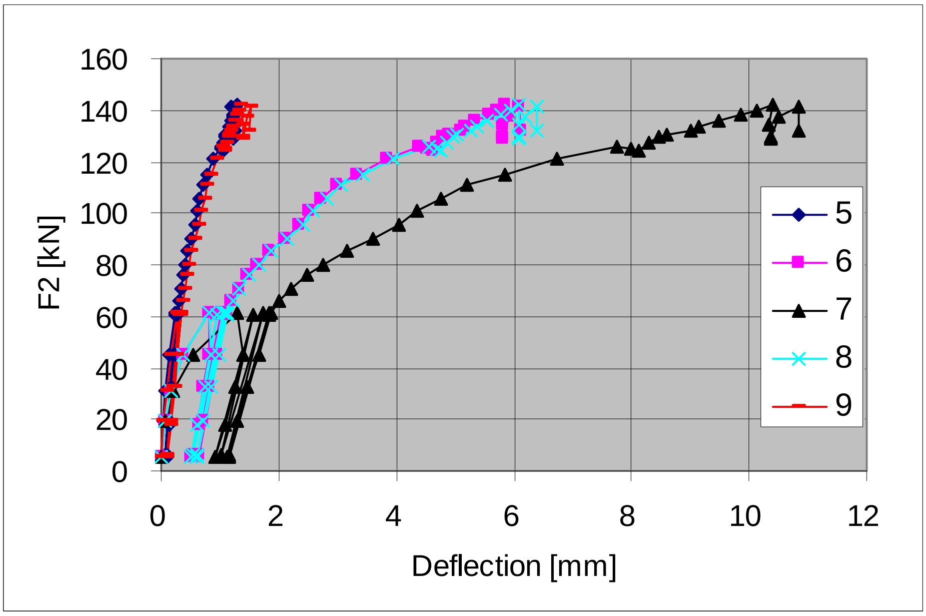 *Fig. 22. Deflection measured by transducers 5–9.* 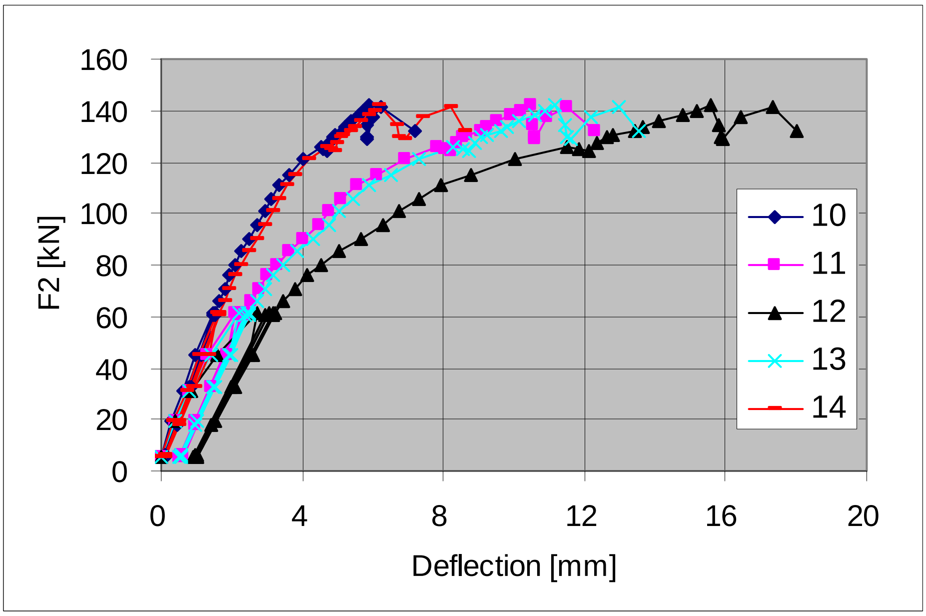 *Fig. 23. Deflection measured by transducers 10–14.*

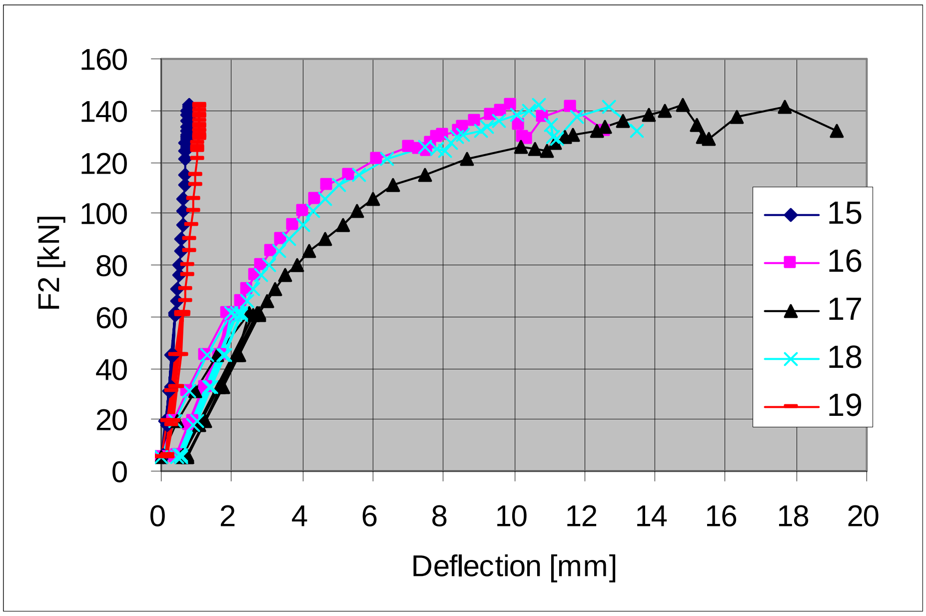

Fig. 24. Deflection measured by transducers 15–19.

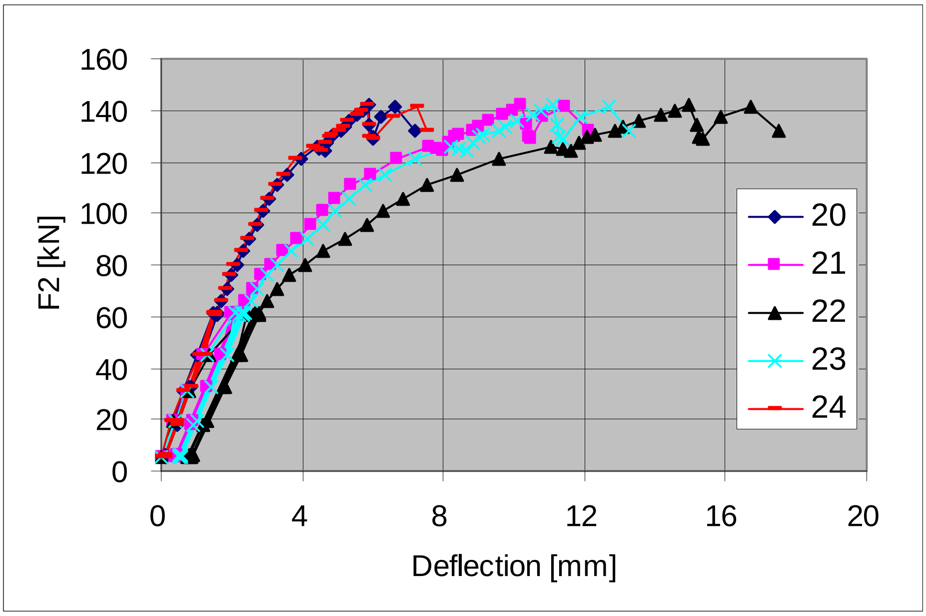

Fig. 25. Deflection measured by transducers 20–24.

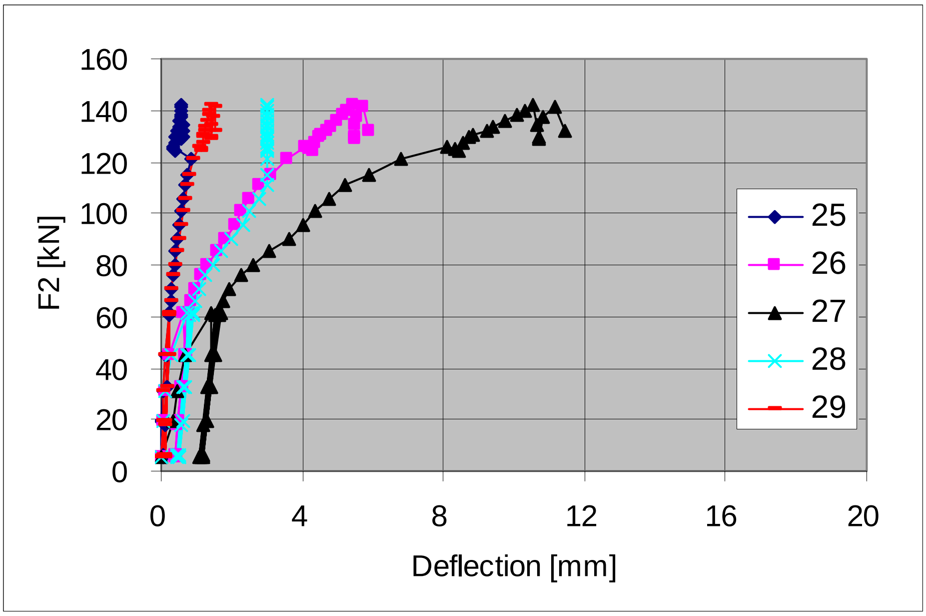

Fig. 26. Deflection measured by transducers 25–29.

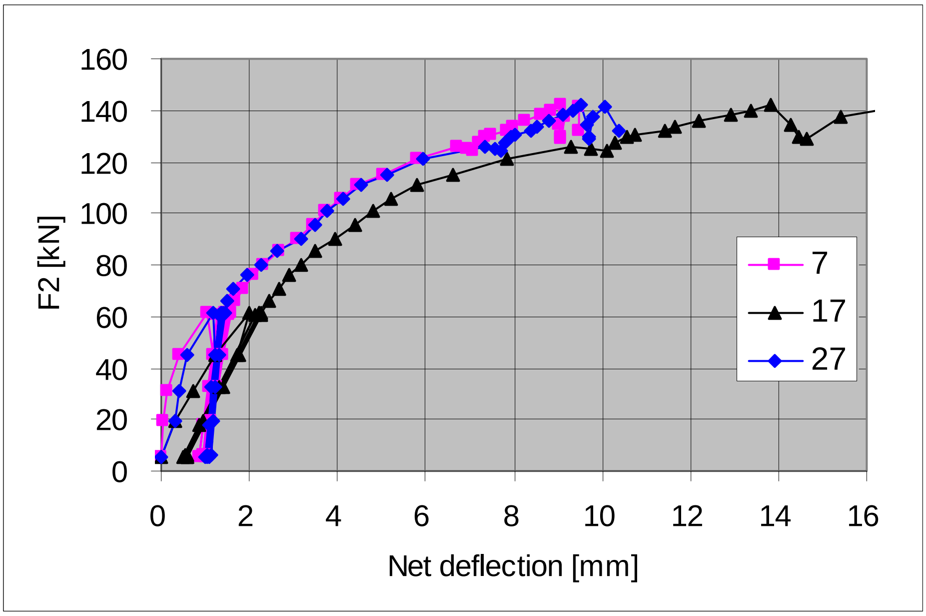

Fig. 27. Net mid-point deflection (measured deflection – settlement of supports) for end beams (7 and 27) and middle beam (17).

10.2
Crack width

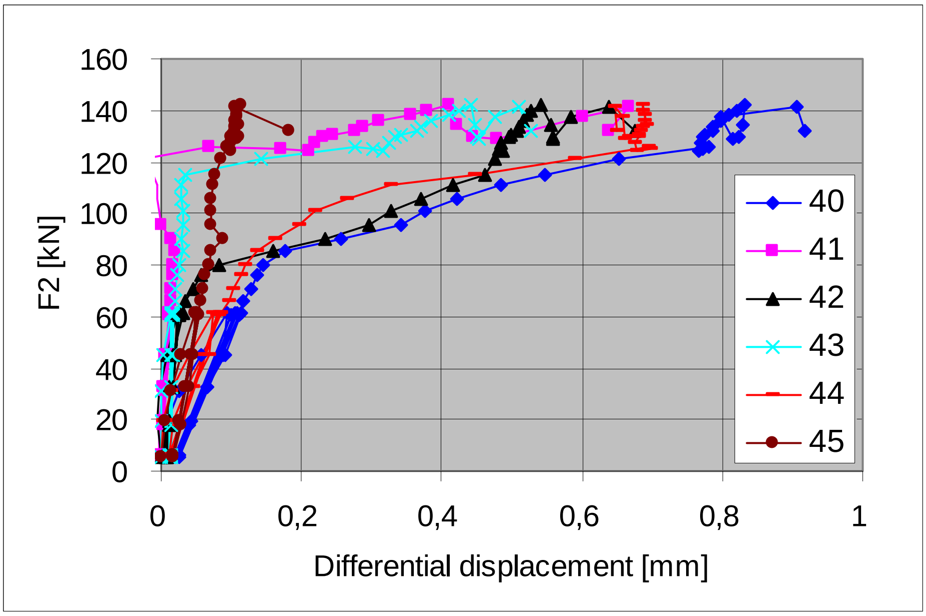

Fig. 28. Differential displacement (≈ crack width) measured by transducers 40–45, see Fig. 14.

10.3
Average strain (actually differential displacement)

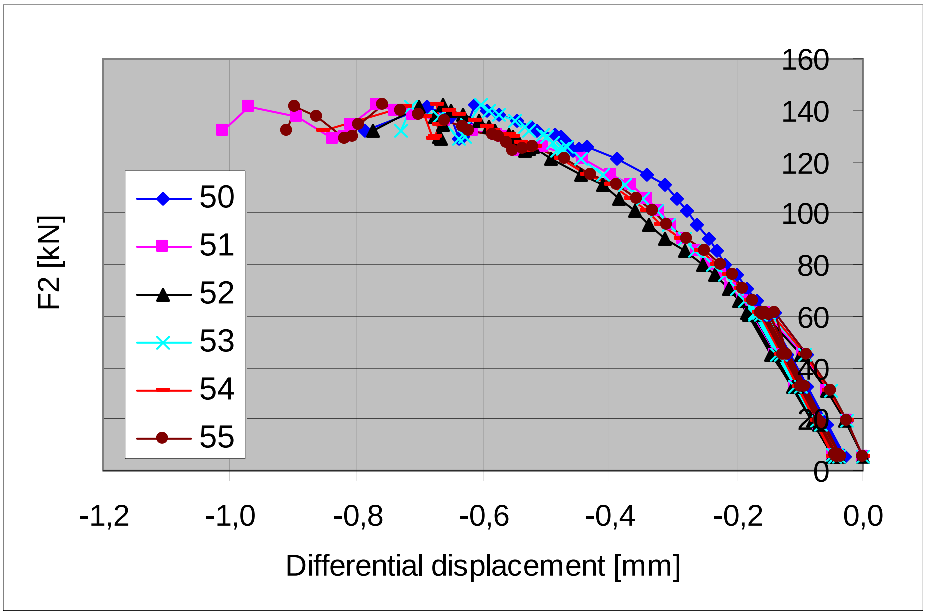

Fig. 29. Differential displacement measured by transducers 50–55, see Fig. 16.

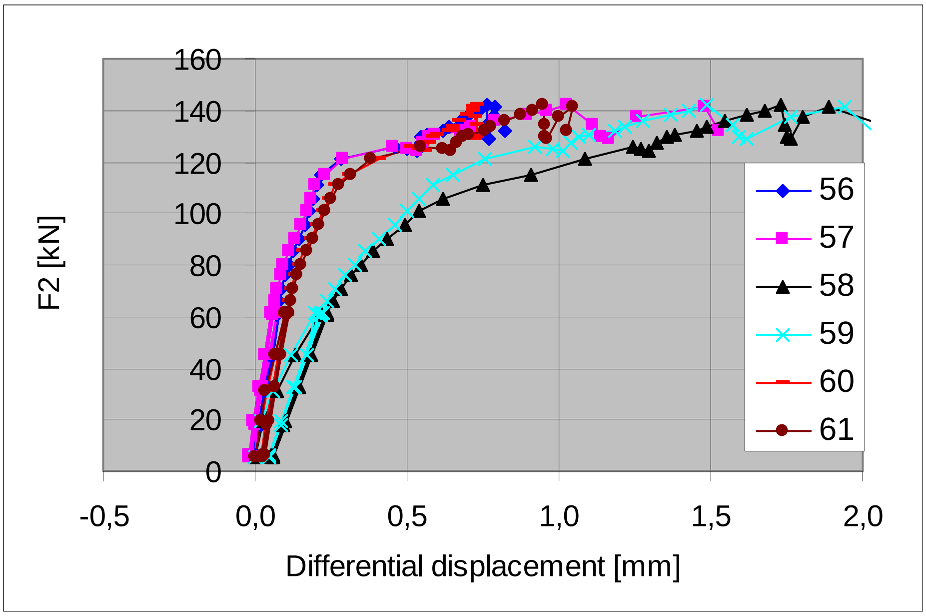

Fig. 30. Differential displacement measured by transducers 56–61, see Fig. 16.

10.4
Sliding of slab along middle beam

A negative value means that the slab is moving towards the end of the beam.

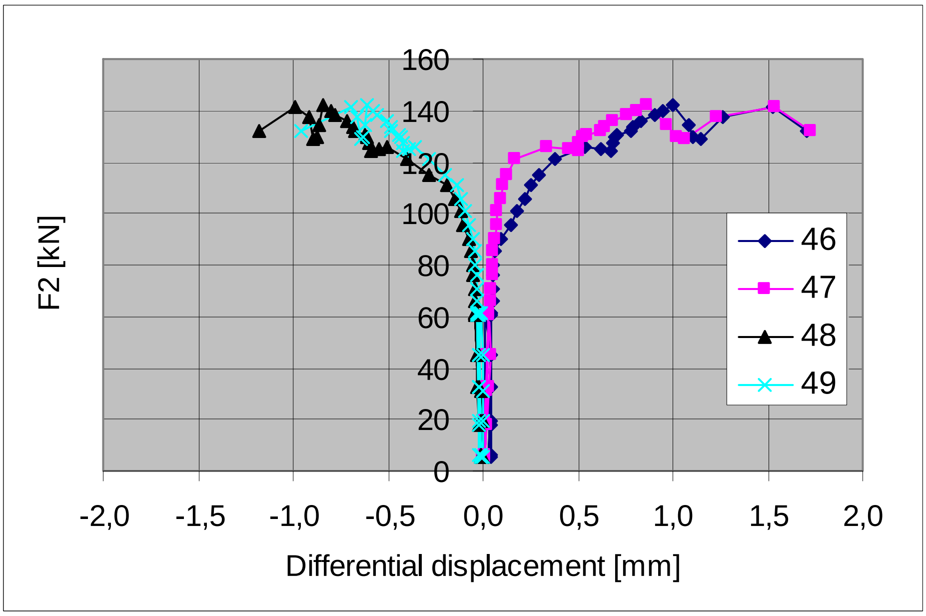

Fig. 31. Sliding of upper edge of slabs 1, 4, 5 and 8 along middle beam, see Fig. 16. No explanation for the positive values of 46 and 47 could be given after the test.

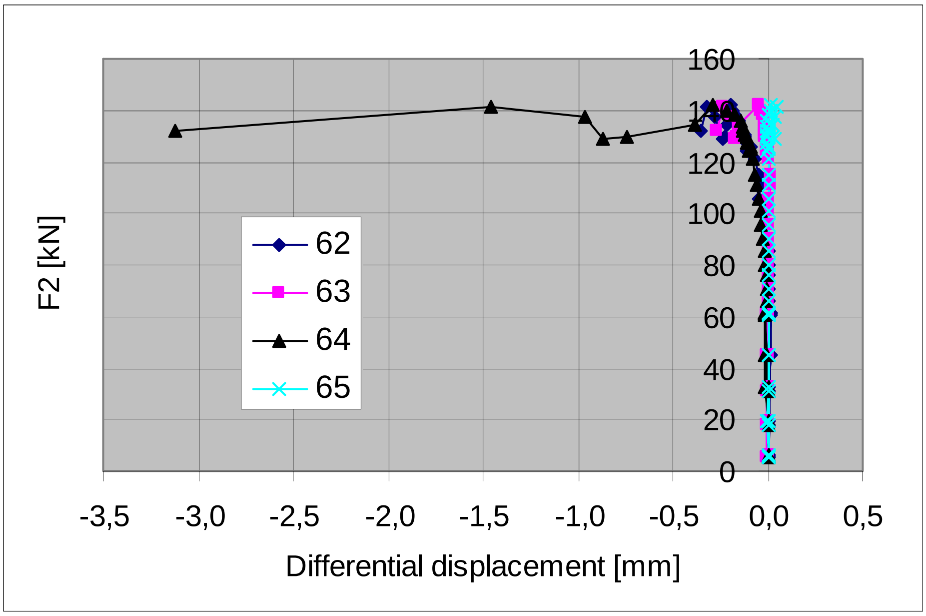

Fig. 32. Sliding of lower edge of slabs 1, 4, 5 and 8 along the middle beam, see Fig. 16.

10.5 **Strain**

-

11 **Reference tests**

Both ends of slabs 9 and 10 were loaded. The results of slab 10 have been ignored because the slab was not cast on the same bed as slabs 1–9.

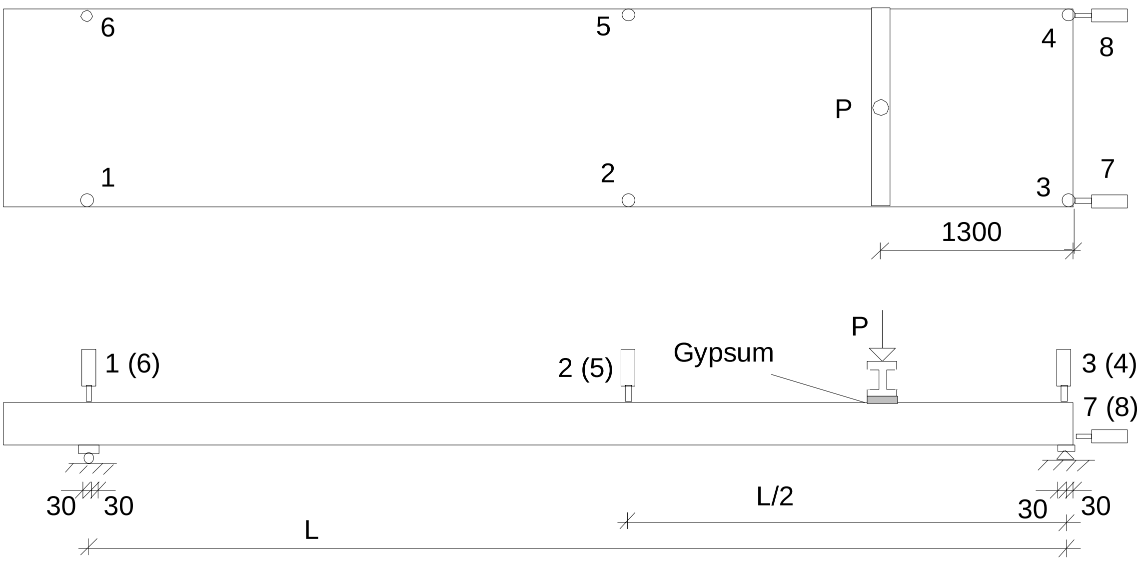

Fig. 33. Layout of reference test. a) Plan. b) Elevation. For L, see the next Table.

Table. Reference tests. Span of slab, shear force V_g at support due to the self weight of the slab, actuator force P_a at failure, weight of loading equipment P_{eq}, total shear force (support reaction) V_{obs} at failure and total shear force v_{obs} per unit width.

Test	Date	Span L mm	V_g kN	P_a kN	P_{eq} kN	V_{obs} kN	v_{obs} kN/m	Note
R9/1	19.10.1993	5940	12,4	233,7	0,7	208,5	173,8	Web shear failure
R9/2	19.10.1993	4940	9,9	209,3	0,7	178,6	148,8	Web shear failure
				Mean		**193,6**	**161,3**	

12 Comparison: Floor test vs. reference tests

The observed shear resistance (support reaction) of the hollow core slab in the floor test was equal to 140,3 kN per one slab unit or 116,9 kN/m. This is **72%** of the mean of the shear resistances observed in the reference tests.

13 Discussion

1. The failure mode was web shear failure of edge slabs. The prestressed concrete beam seemed to recover completely after the failure.

2. The net deflection of the middle beam due to the imposed actuator loads (deflection minus settlement of supports) was 13,8 mm or L/360, i.e. rather small. It was 4,3–4,8 mm greater than that of the end beams. Hence, the torsional stresses due to the different deflection of the middle beam and end beams had a minor or negligible effect on the failure of the slabs.

3. The mean of shear resistances measured in the reference tests was roughly 10% lower than the mean of the observed values for similar slabs given in *Pajari, M. Resistance of prestressed hollow core slab against a web shear failure. VTT Research Notes 2292, Espoo 2005*.

4. The topping concrete above the middle beam became loose at one end of the middle beam when the imposed load was 85% of the failure load. The failure took place at the opposite side

5. Comparing the deflection of the middle beam in the present test with that in test VTT.PC.InvT-Unif.265.1993 suggests that the middle beam was still far from yielding when the failure took place.

APPENDIX A: PHOTOGRAPHS

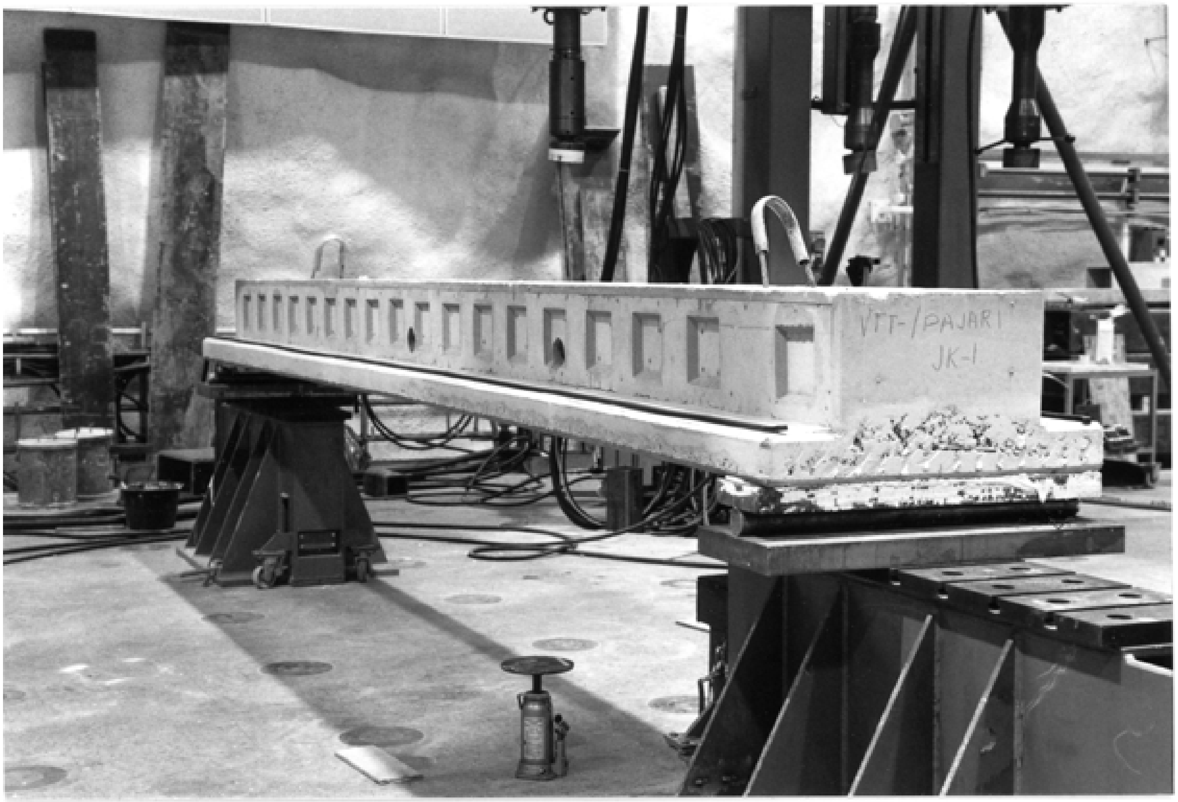

Fig 1. The prestressed concrete middle beam on the supports.

Fig. 2. A hollow core slab unit supported on the middle beam.

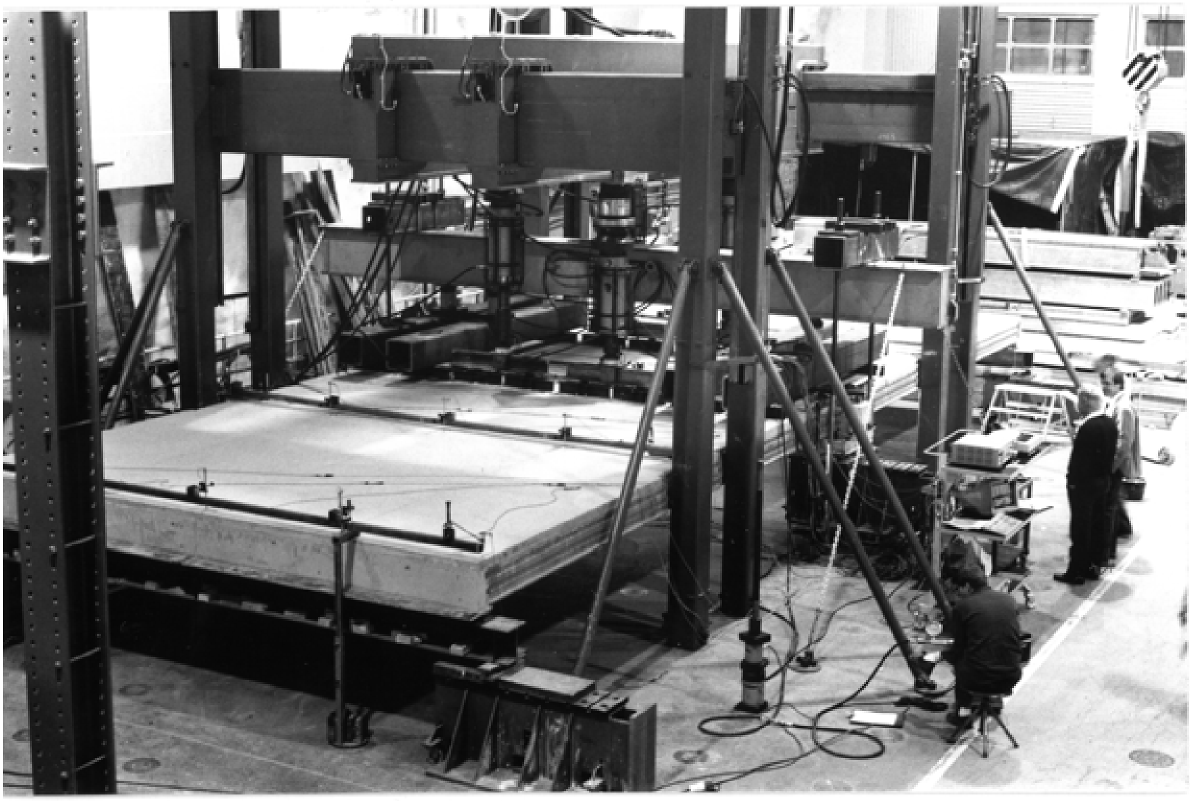

Fig. 3. Loading and measurement arrangement.

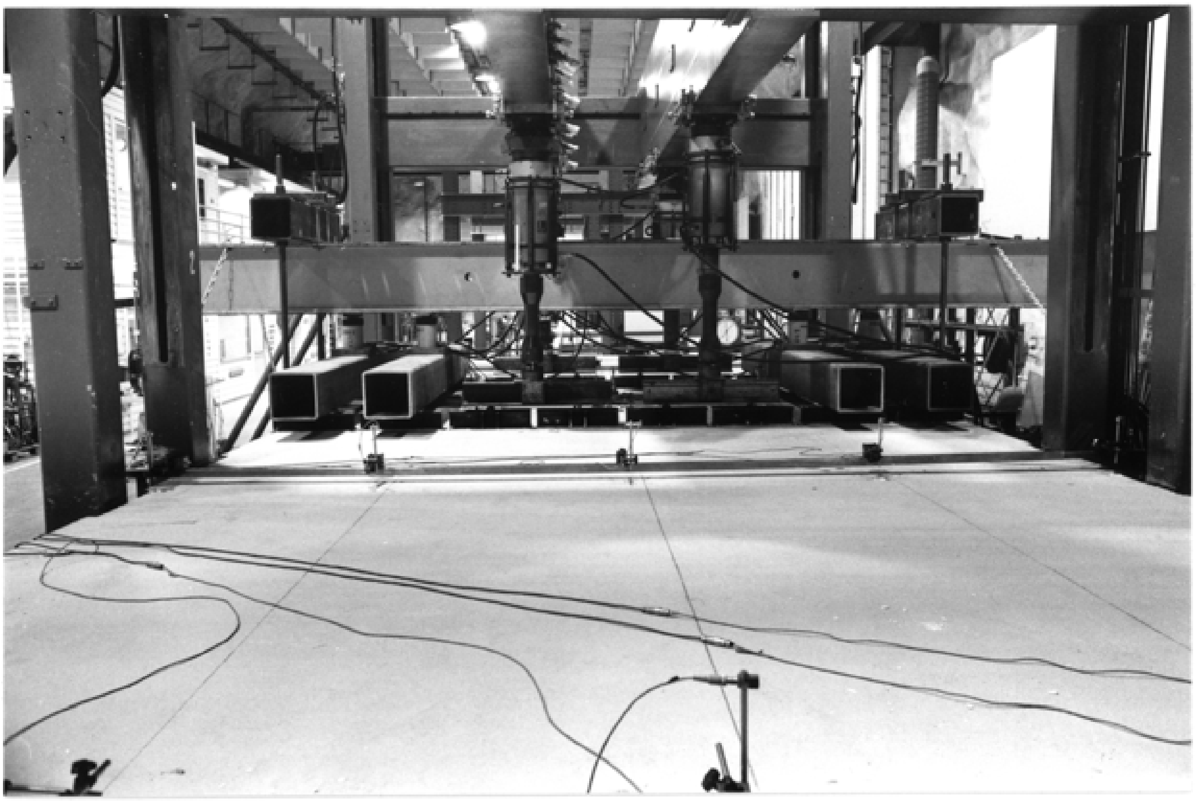

Fig. 4. Loading arrangement.

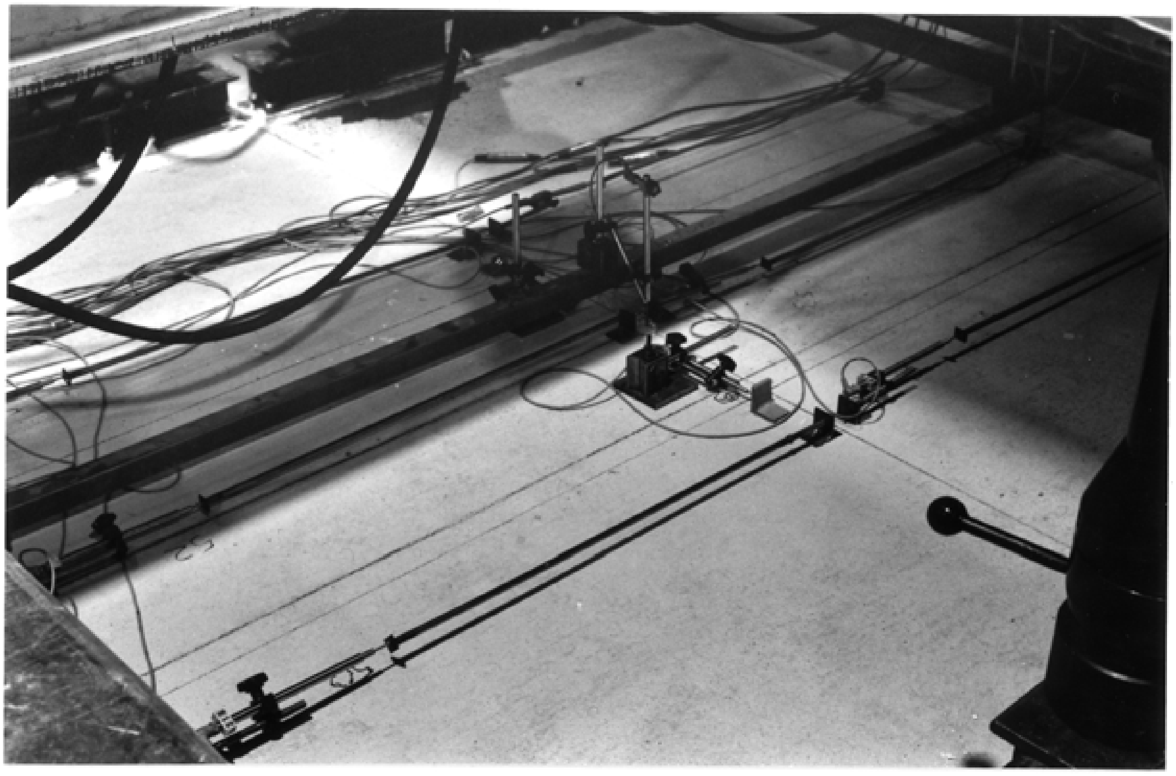

Fig. 5. Measurements for the displacement difference between the middle beam and the end of a slab unit and that one between the edges of a slab unit on the surface of the concrete topping.

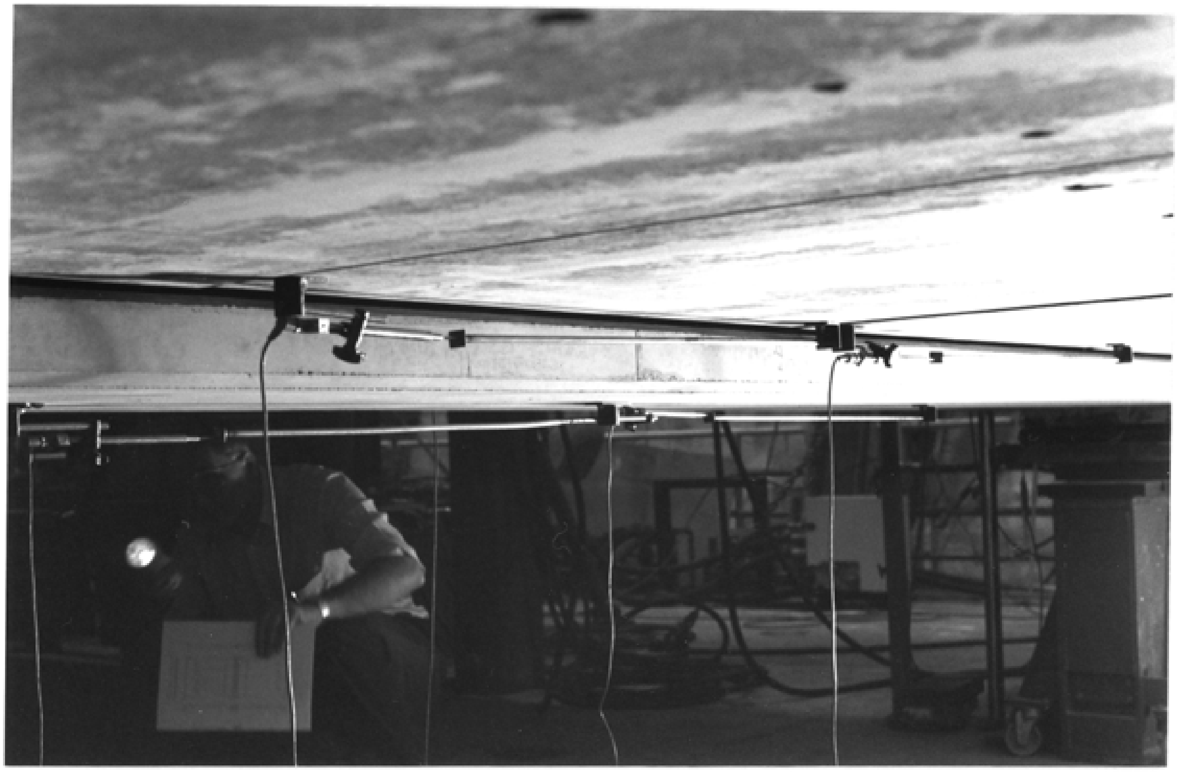

Fig. 6. Measurement for the displacement difference between the edges of a slab unit on the bottom of the slab.

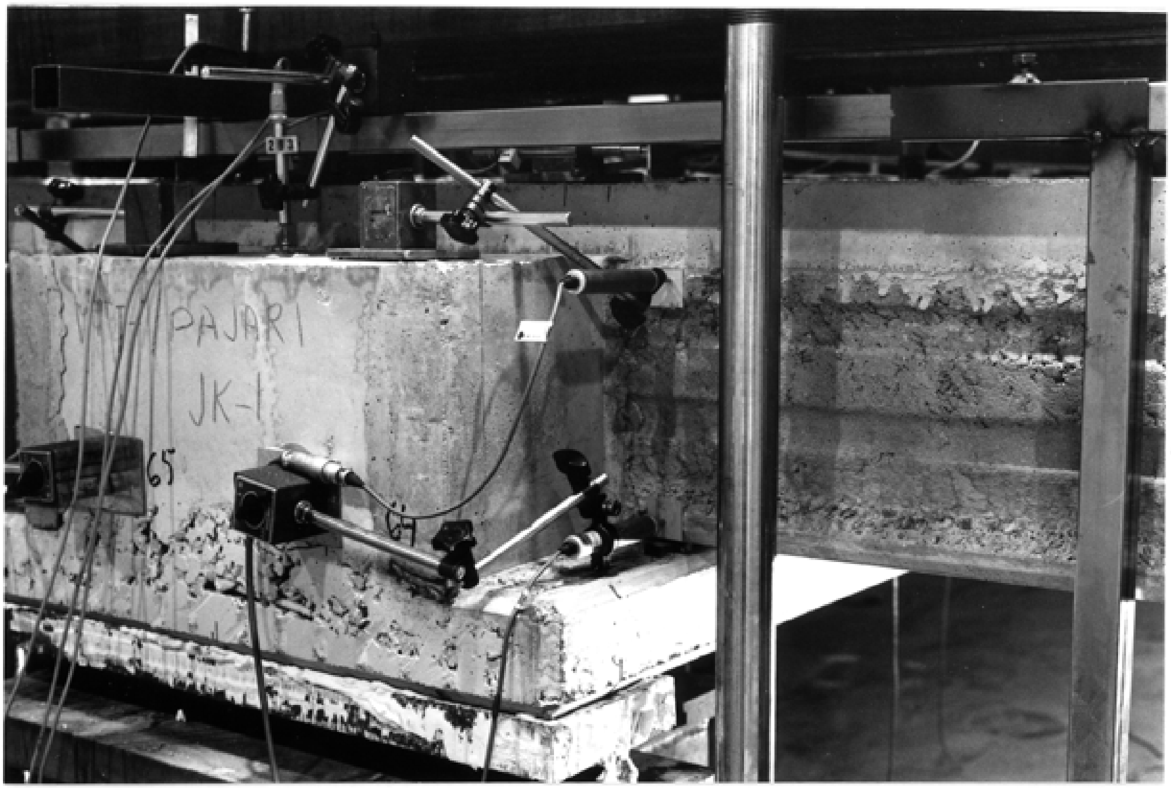

Fig. 7. Measurement for the displacement difference between the end of the middle beam and the edge of a slab unit.

Fig. 8. A crack in the middle of the concrete tie beam, between the slab unit no 2 and 3.

Fig. 9. A crack in the middle of the concrete tie beam, between the slab units no 6 and 7.

Fig. 10. The cracks in the longitudinal edge of the slab unit no 1, near the middle beam, at failure.

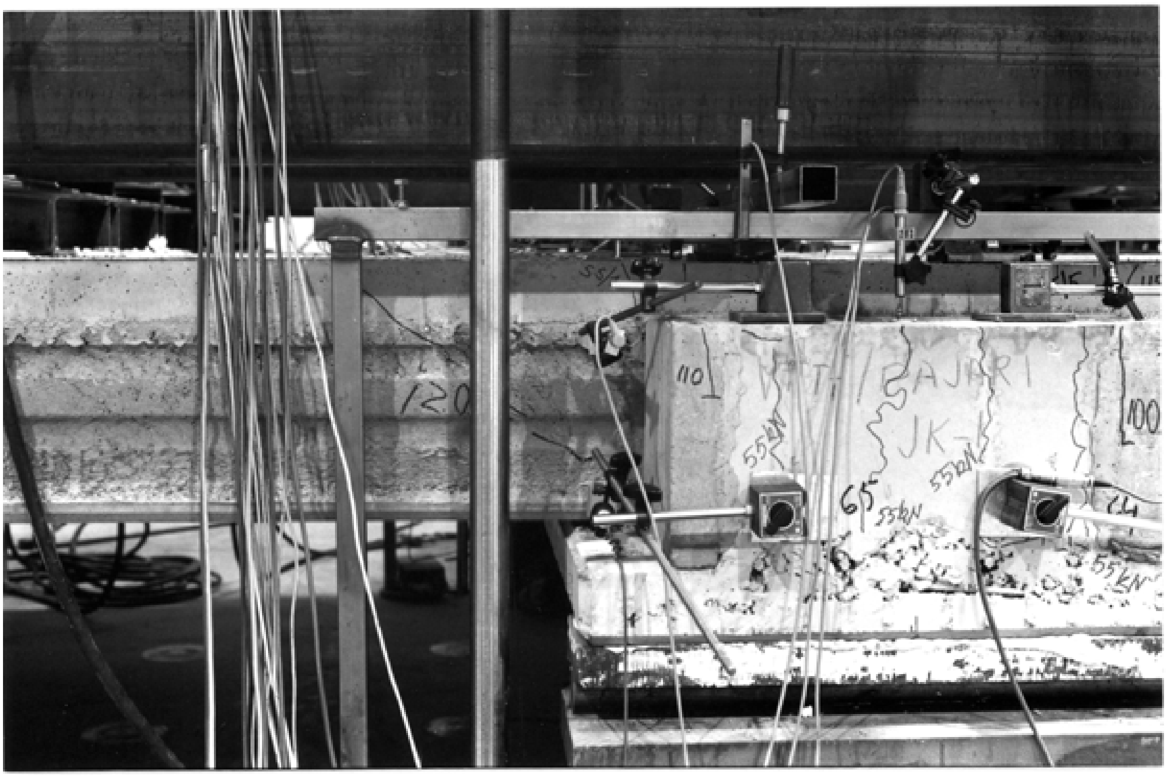

Fig. 11. The cracks in the longitudinal edge of the slab unit no 5, near the middle beam, at failure.

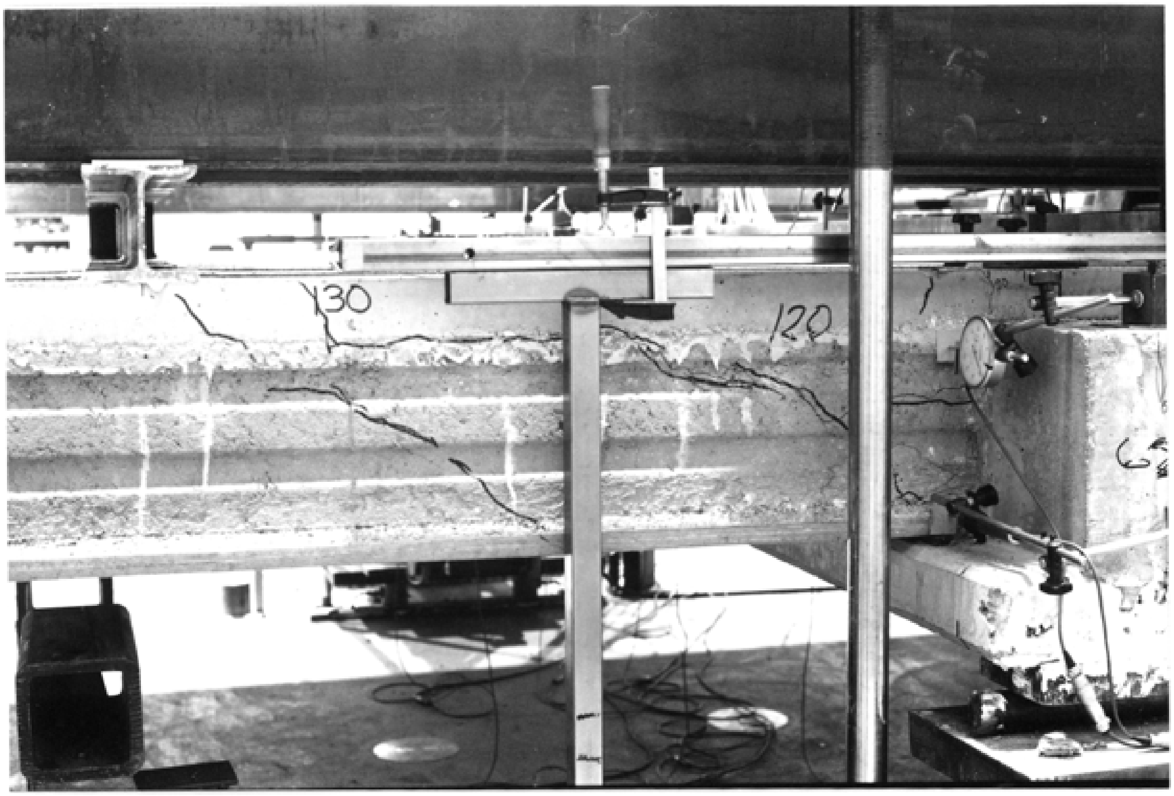

Fig. 12. The cracks in the longitudinal edge of the slab unit no 4, near the middle beam, at failure.

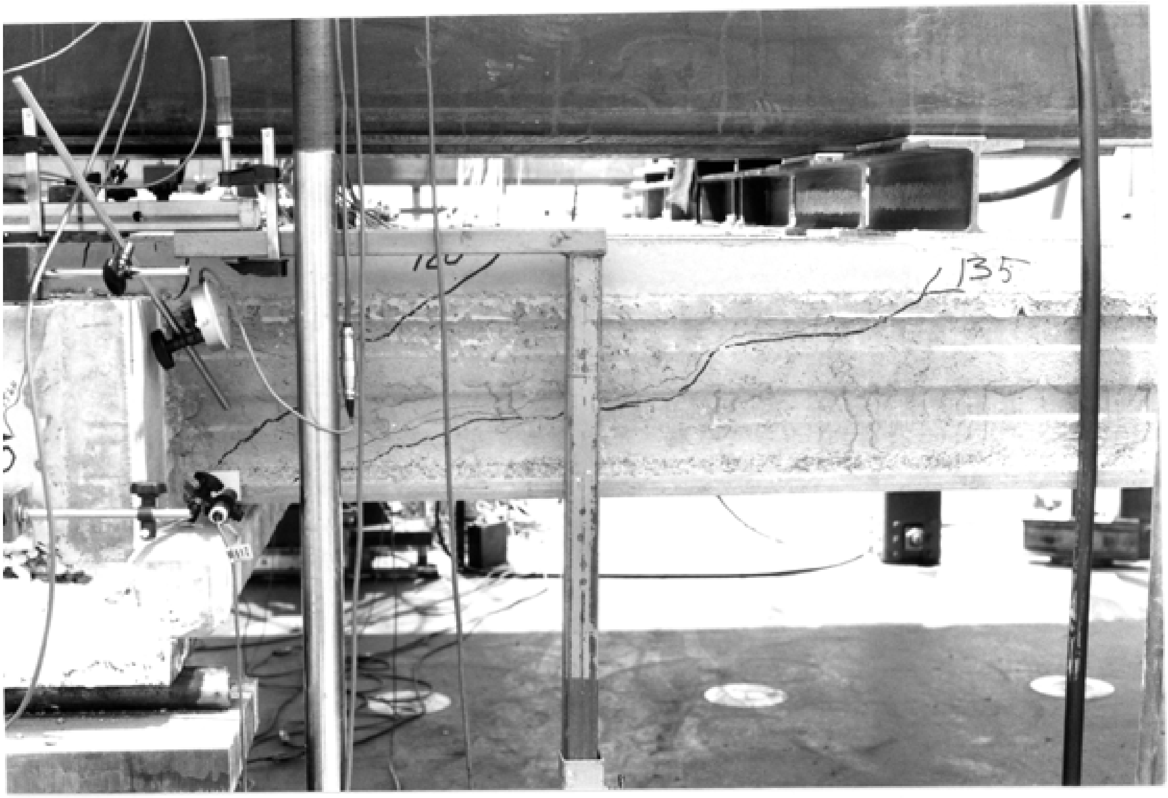

Fig. 13. The cracks in the longitudinal edge of the slab unit no 8, near the middle beam, at failure.

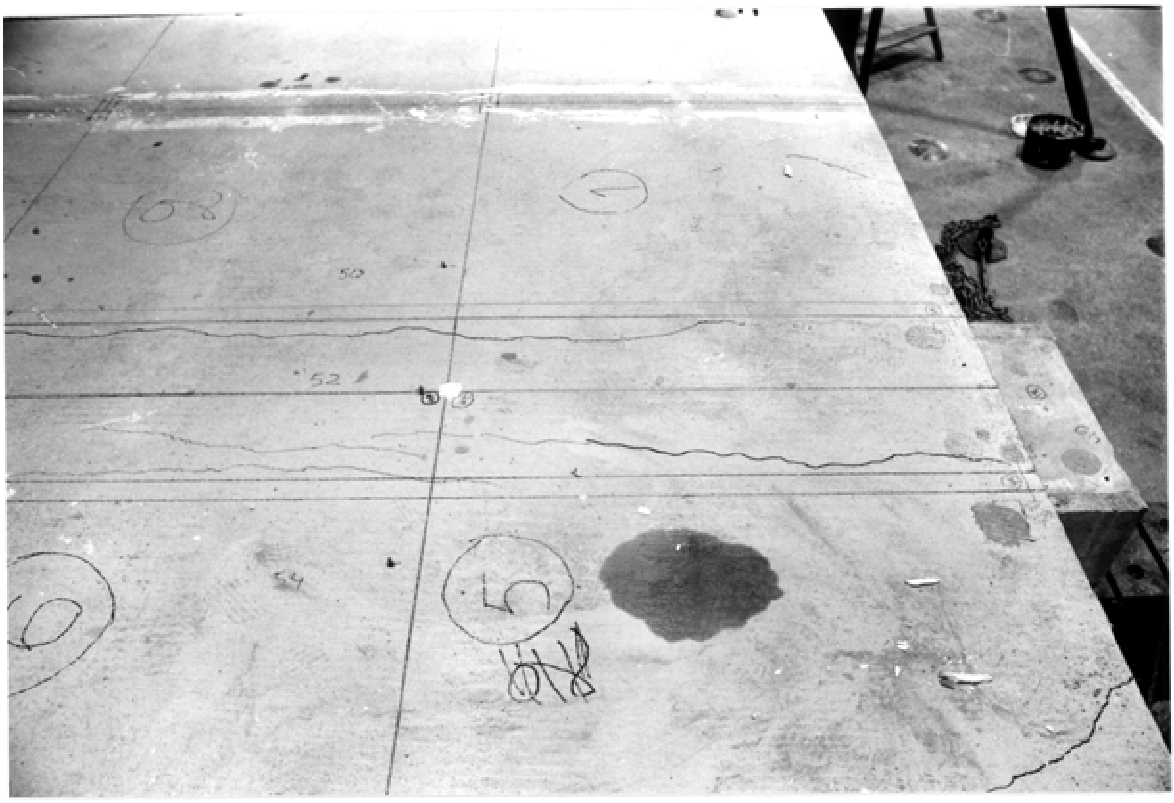

Fig. 14. The cracking of the concrete topping along the joint between the middle beam and the ends of the slab units no 1 - 2 and no 5 - 6.

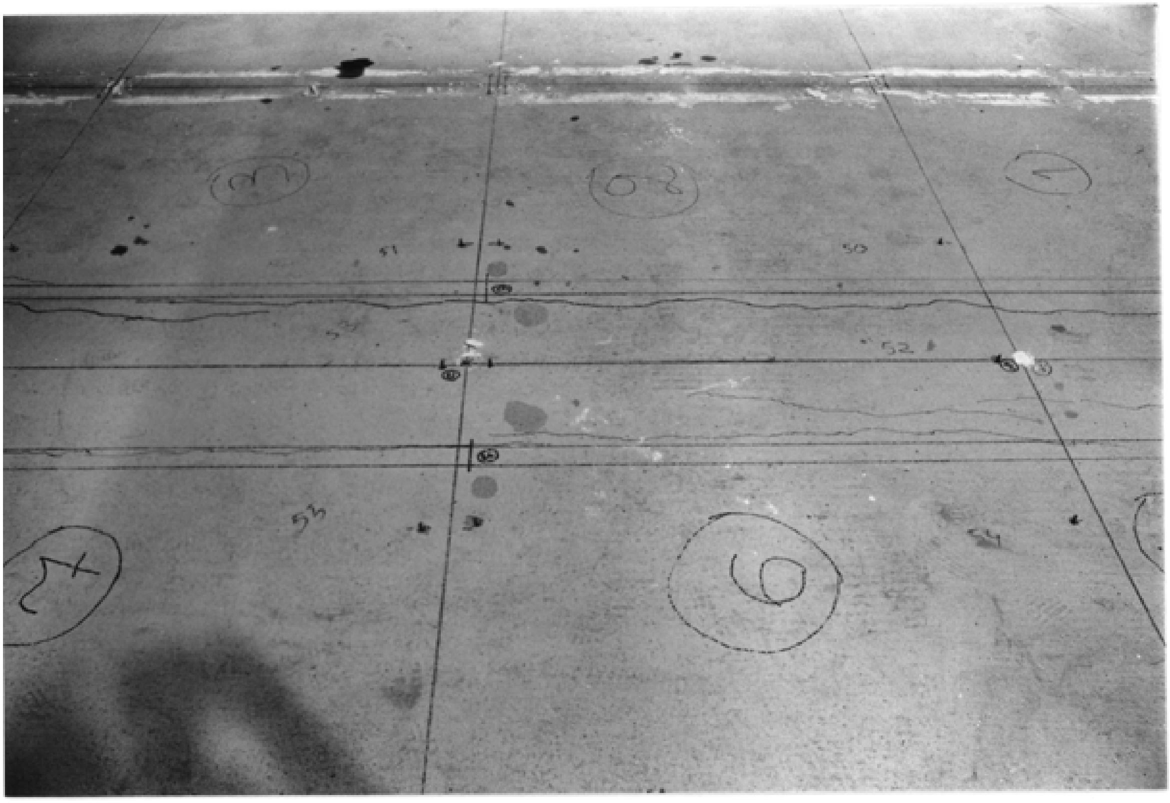

Fig. 15. The cracking of the concrete topping along the joint between the middle beam and the ends of the slab units no 1 - 3 and no 6 - 7.

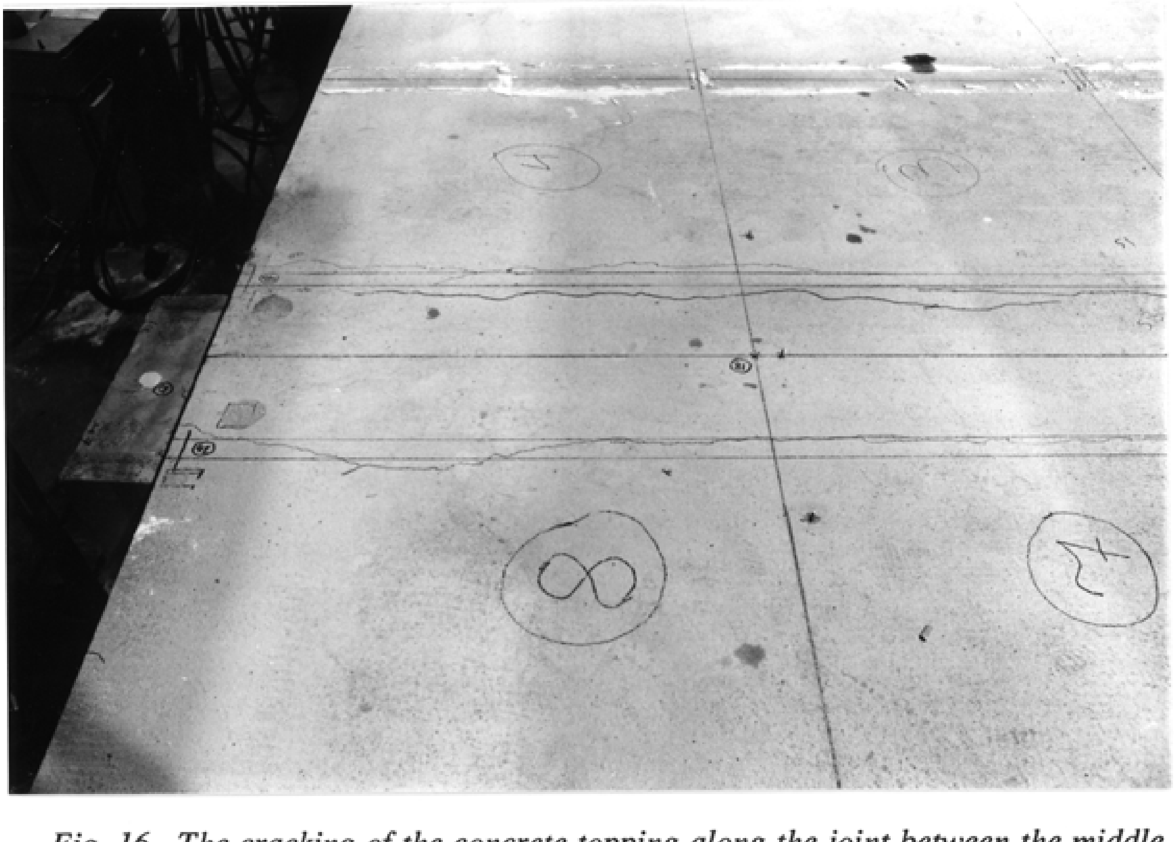

Fig. 16. The cracking of the concrete topping along the joint between the middle beam and the ends of the slab units no 3 - 4 and no 7 - 8.

Fig. 17. The cracking of the concrete topping and the tie beam between the slab units no 2 and 3.

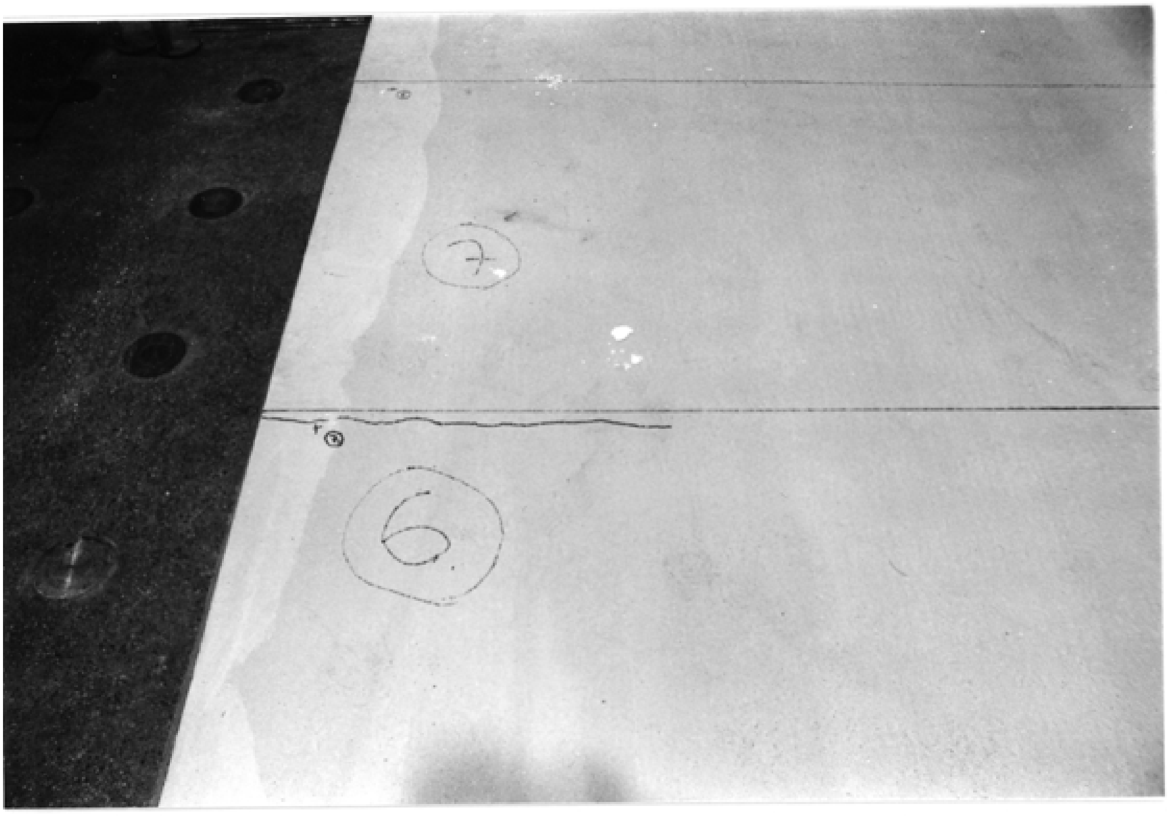

Fig. 18. The cracking of the concrete topping and the tie beam between the slab units no 6 and 7.

Fig. 19. The failure of the end 1 of the slab unit no 9 in the reference loading test.

Fig. 20. The failure of the end 2 of the slab unit no 9 in the reference loading test.

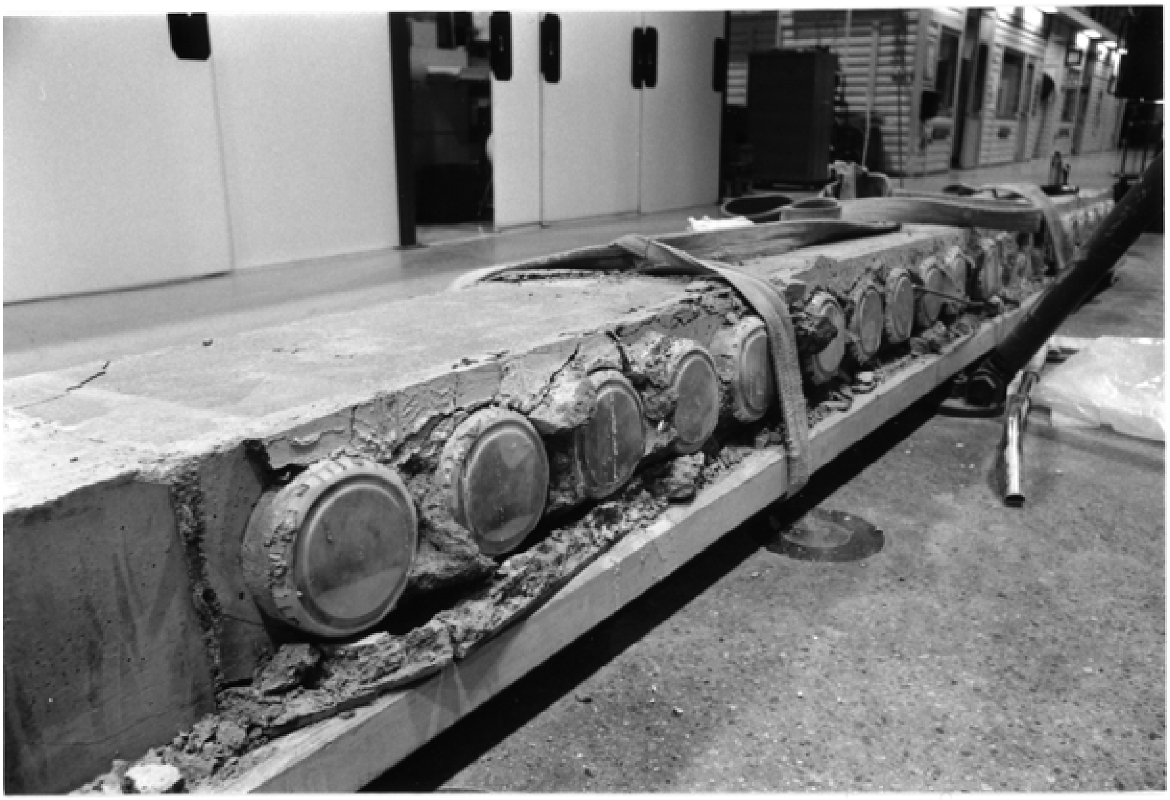

Fig. 21. The middle beam after the loading test, on the side of the slab units no 1 - 4.

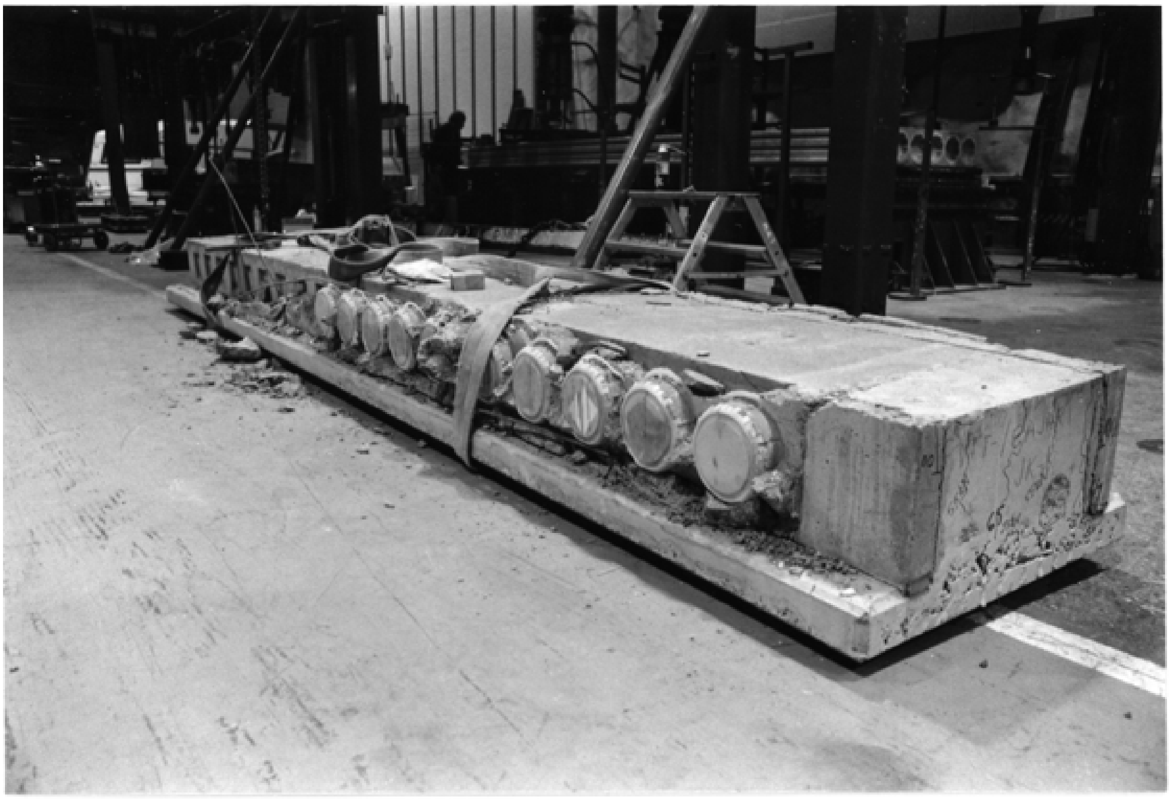

Fig. 22. The middle beam after the loading test, or the side of the slab units no 5 - 8.

1	**General information**
1.1 Identification and aim	**VTT.PC.Rect-norm.265.1993** **Last update 2.11.2010** PC265N (Internal identification) Aim of the test: To study the shear resistance of hollow core slabs supported on the top of beam.
1.2 Test type	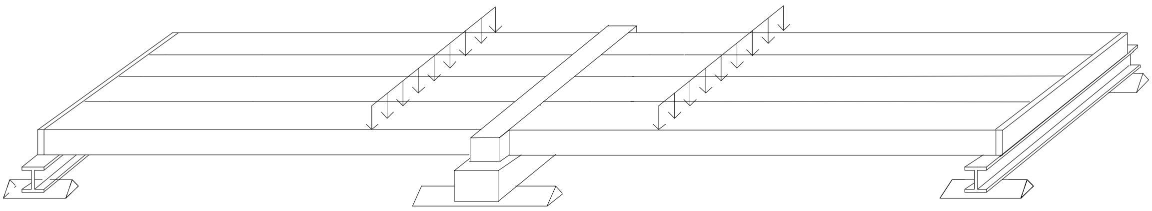 *Fig. 1. Illustration of test setup.*
1.3 Laboratory & date of test	VTT/FI 14.12.1993
1.4 Test report	Author(s): Koukkari, H. & Pajari, M. Name: *Loading test on 265 mm hollow core floor supported on prestressed concrete beam* Ref. number: RAT-IR-20/1993 Date: 15.2.1994 Availability: Public, available on request from VTT Expert Services, P.O. Box 1001, FI-02044 VTT Financed by the Finnish Association of Building Industry RTT (supported by the Technology Development Centre of Finland); the International Prestressed Hollow Core Association IPHA; KB Kristianstads Cementgjuteri, Sweden and Skanska Prefab AB, Sweden
2	**Test specimen and loading** (see also photographs in Appendix A)
2.1 General plan	

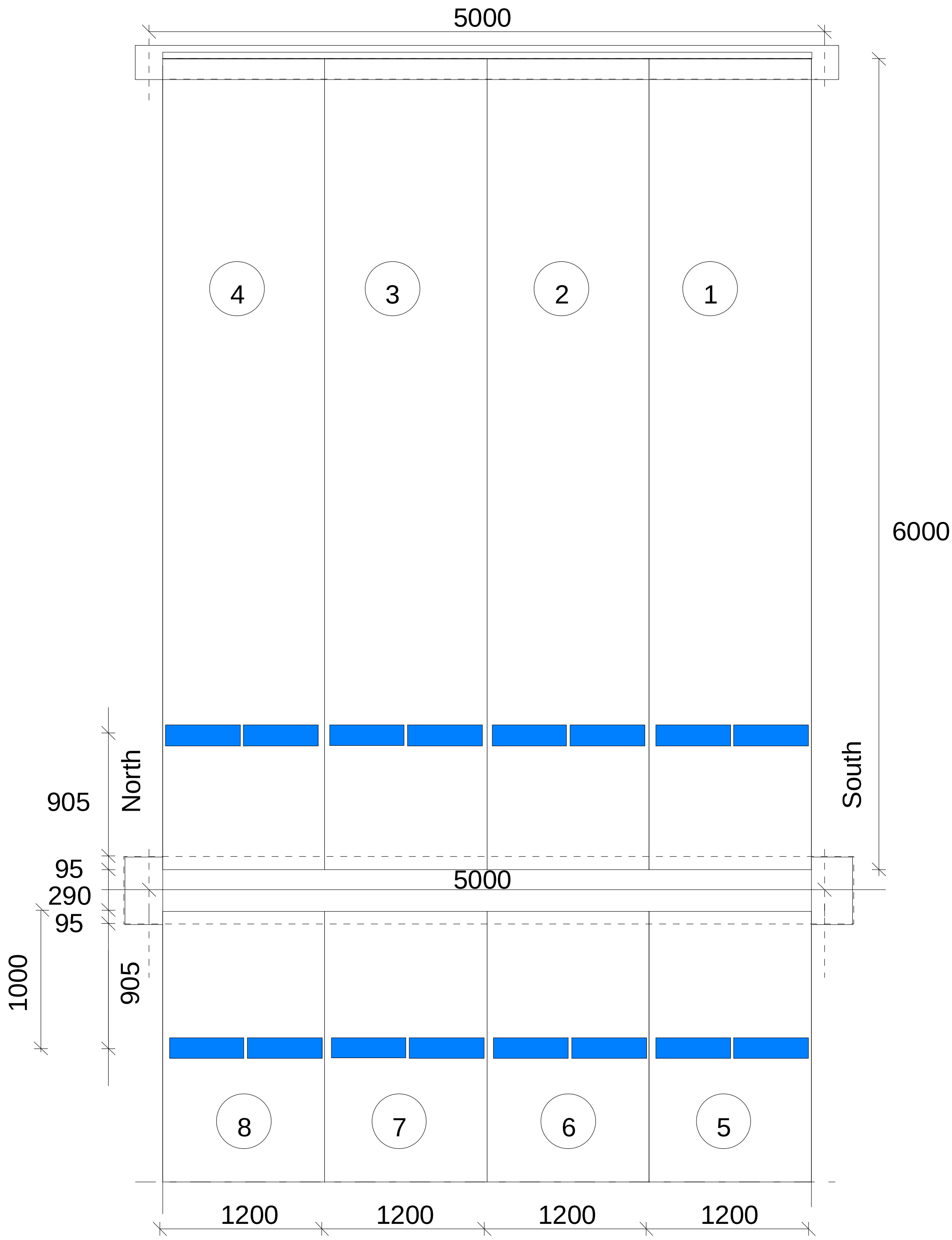
5000
4
3
2
1
6000
905
North
South
95
290
95
5000
1000
905
8
7
6
5
1200
1200
1200
1200

Fig. 2. Plan.

2.2
End beams

I-beams made of steel. Span = 5,0 m

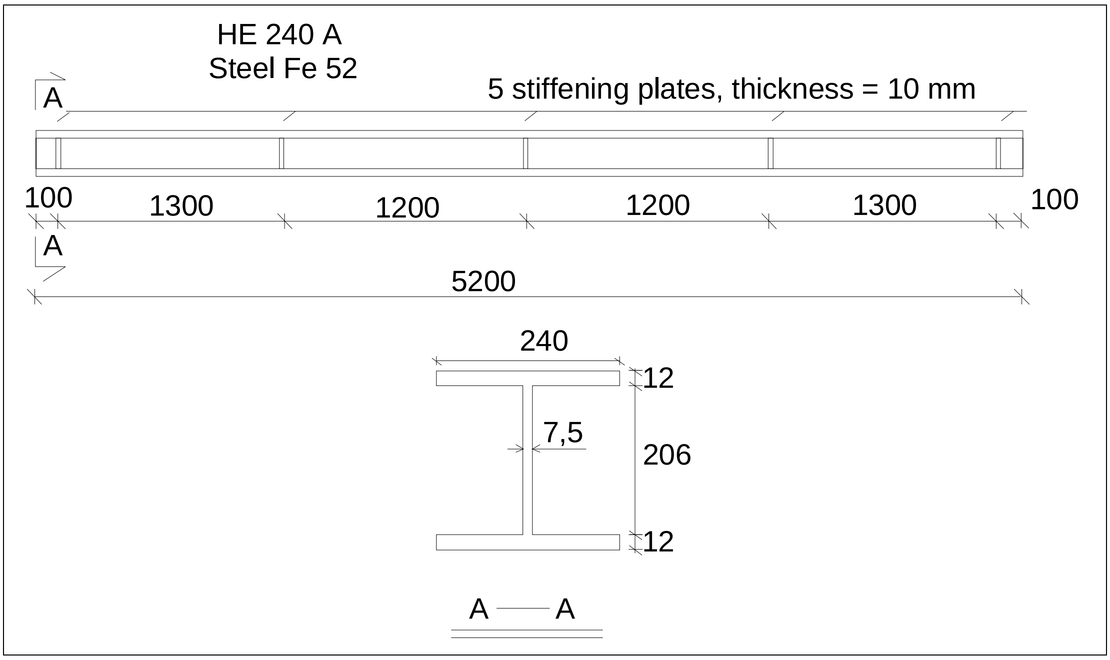

Fig. 3. End beam.

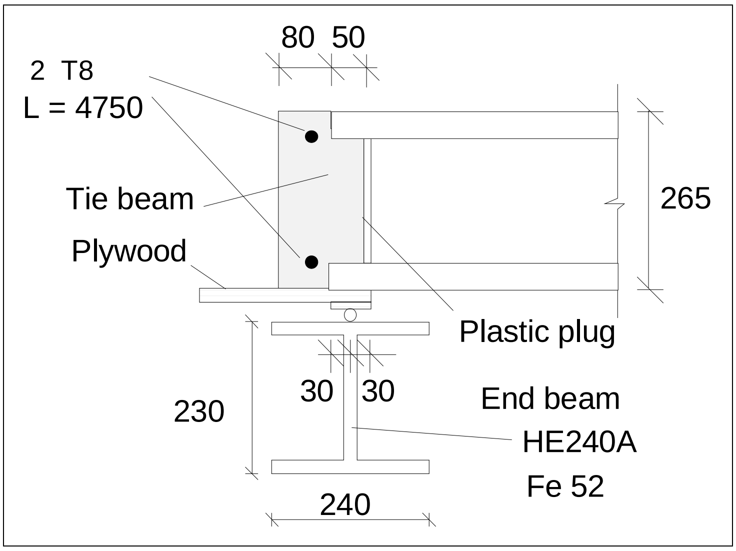

Fig. 4. Arrangements at end beam. T8 refers to a reinforcing bar, see 2.4.

2.3
Middle beam

The middle beam was a composite beam comprising a precast, prestressed concrete beam and a cast-in-situ component. The grade of the concrete was K60 in the lower, precast part and K30 in the upper part. See Figs 5 and 6 for the main characteristics of the beam.

<table>
<tr>
<td></td>
<td>
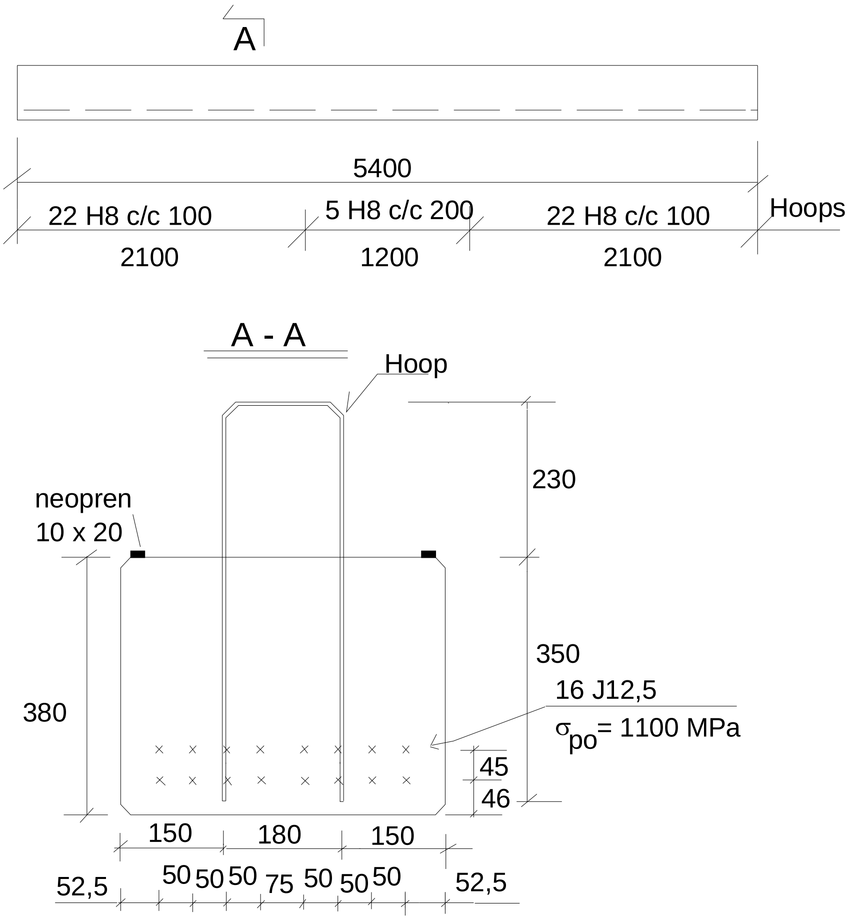

Fig. 5. Middle beam. Main reinforcements and hoops. H8 and J12,5 refer to rebar hoops and prestressing strands with diameter 8 and 12,5 mm, respectively, see 9.1.
</td>
</tr>
<tr>
<td>2.4
Arrangements at middle beam</td>
<td>
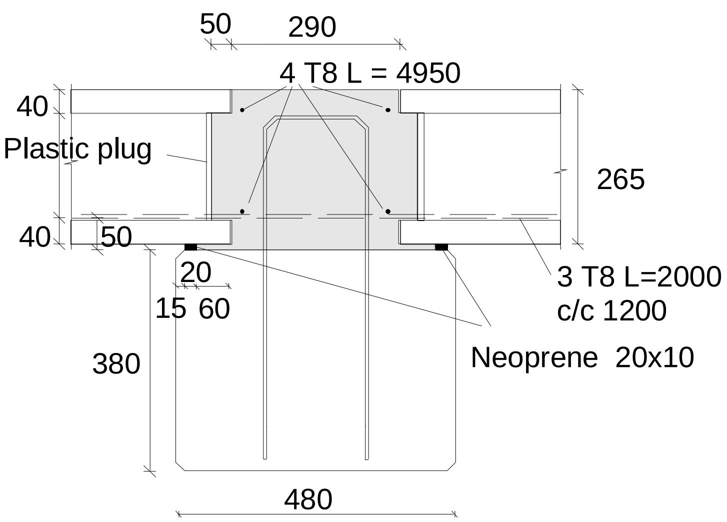

Fig. 6. Middle beam. Section along hollow cores.

T8: Hot rolled, weldable rebar A500HW, ϕ = 8 mm, in longitudinal joints between adjacent slabs, see 9.1.
</td>
</tr>
</table>

2.5
Slabs

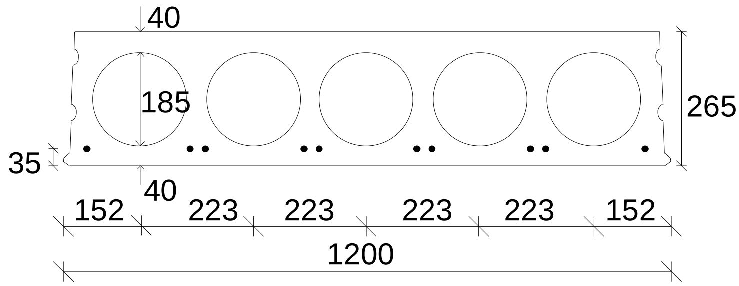

Fig. 7. Nominal geometry of slab units.

- Extruded by Partek Betoniteollisuus Oy, Hyrylä factory 8.11.1993 and 11.11.1993
- 10 lower strands J12,5 initial prestress 950 MPa

J12,5: seven indented wires, ϕ =12,5 mm, A_p = 93 mm^2

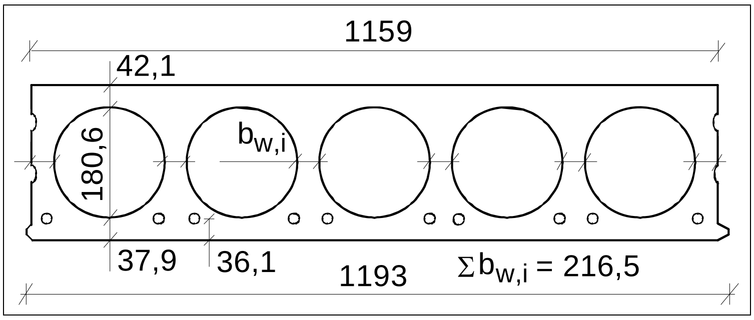

Fig. 8. Floor test. Mean of most relevant measured geometrical characteristics of slabs 1–8.

Max measured bond slips: 2,5 , 2,2 and 1,9 mm in slab 4; 2,3 mm in slabs 1 and 6, 1,9 and 1,8 mm in slab 7

Measured weight of slab units = 4,09 kN/m

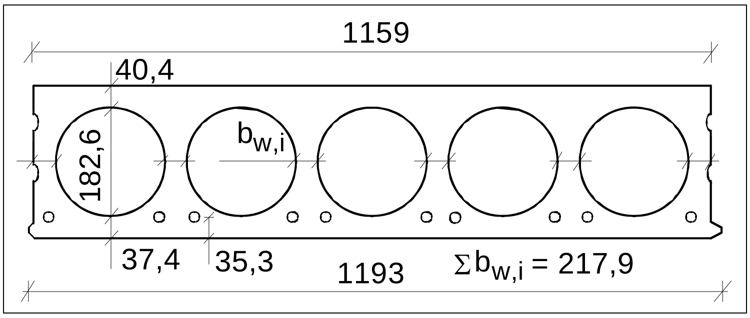

Fig. 9. Reference tests. Mean of most relevant measured geometrical characteristics of slabs 9 and 10.

Max measured bond slips: 2,3, 1,7and 1,4 mm in slab 10; 1,7, 1,5 and 1,4 mm in slab 9

Measured weight of slab units = 4,11 kN/m

There were 10 slabs cast on the same bed. Three of them were cast on the 8th of November, seven on the 11th of November. Since the expected failure mode was failure of the outermost slabs, the slabs were arranged as shown in Fig. 10. In this way, one slab from the both casting days remained for the reference tests.

	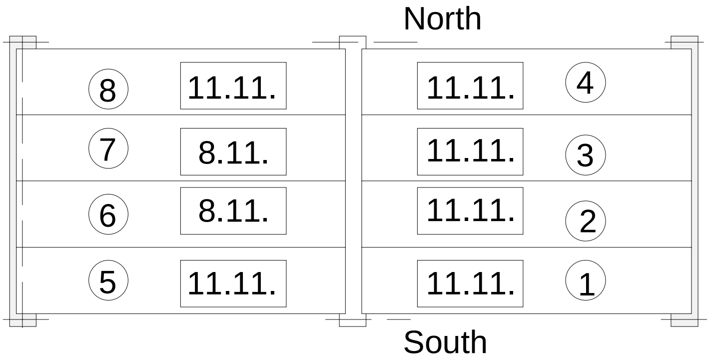 *Fig. 10.Floor test. Position of slabs cast on November 8 and 11.*
2.6 Temporary supports	Temporary supports below beams (Yes/No) - No
2.7 Loading arrangements	There were two separate, manually controlled hydraulic circuits, one for actuators P_1 and the other for actuators P_2, see Fig. 14. Attempts were made to keep $P_1 \approx P_2$ to generate two uniform line loads on the floor. The primary spreader beams on the top of the floor were slightly shorter than 0,6 m. There was gypsum mortar between the primary spreader beams and the top surface of the floor. The friction between the secondary and primary spreader beams was eliminated by teflon plates (beams spreading loads P_2) and by a roller bearing (beams spreading load P_1).

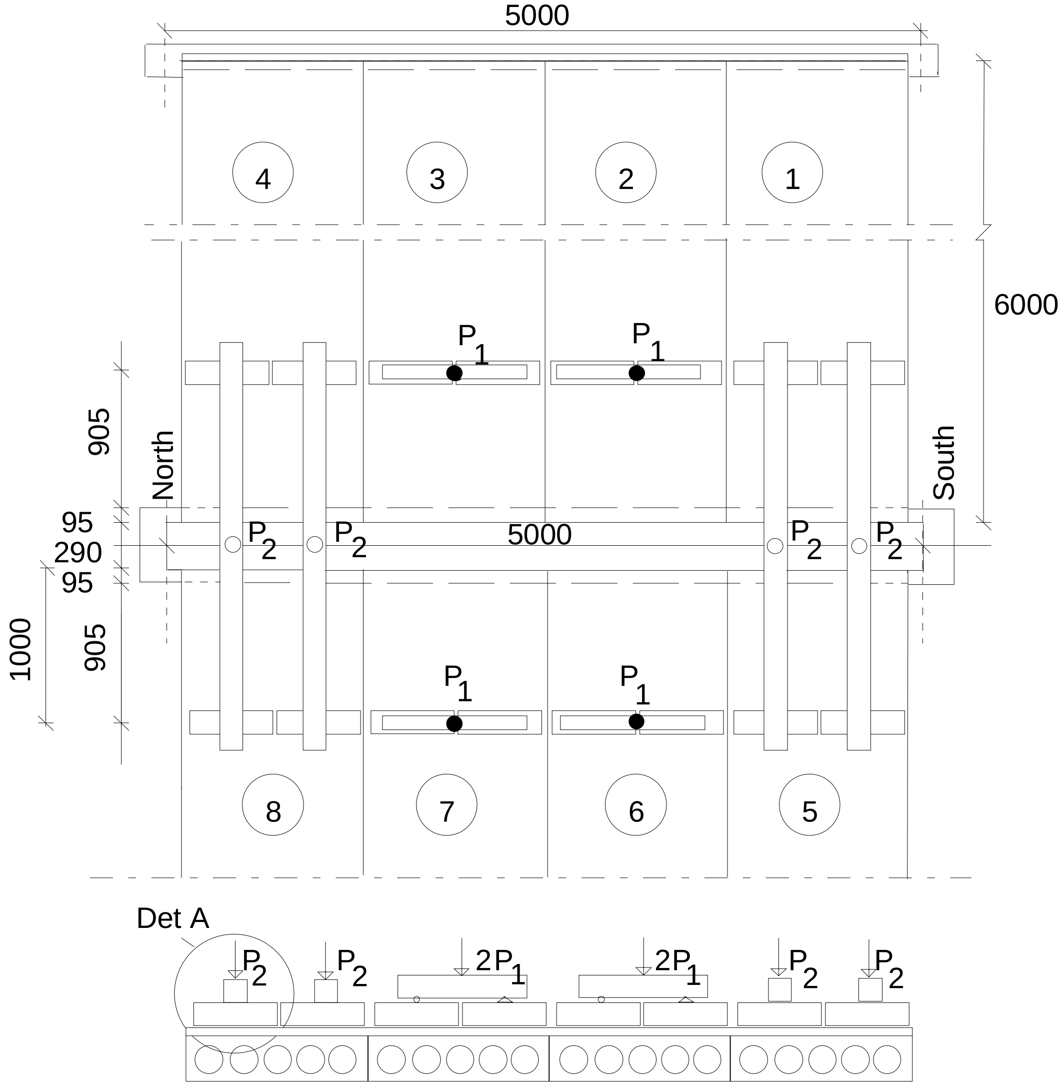

Fig. 11. Plan. P_1 and P_2 refer to vertical actuator forces. For det A, see Fig. 12.

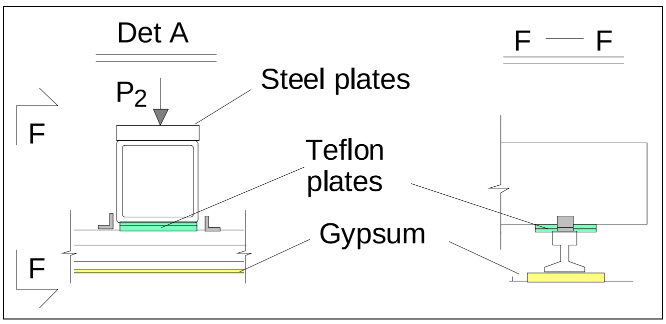

Fig. 12. Detail A, see the figure above.

3	**Measurements**
3.1 Support reactions	

	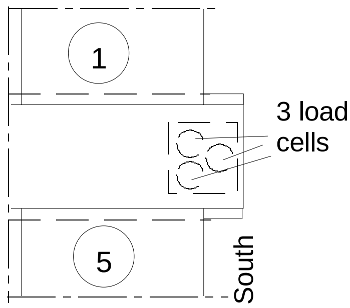 *Fig. 13. Load cells below the South end of the middle beam.*
3.2 Vertical displacement	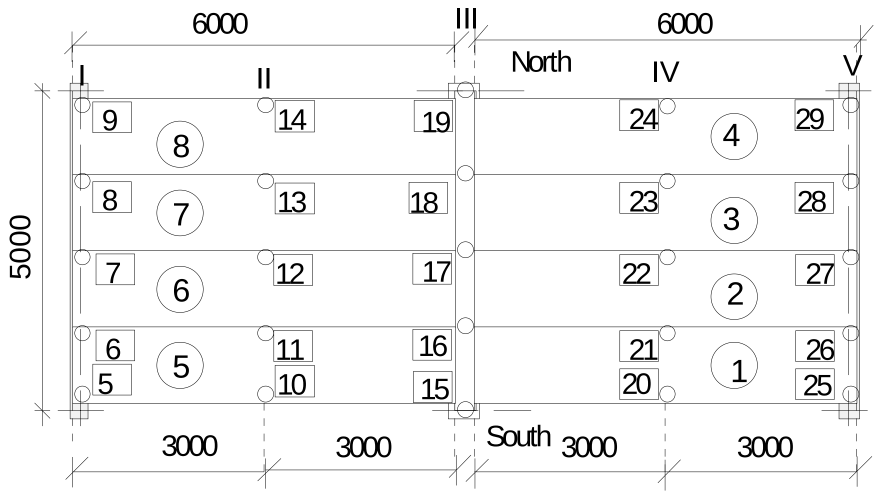 *Fig. 14. Location of transducers 5 … 29 for measuring vertical deflection.*
3.3 Average strain	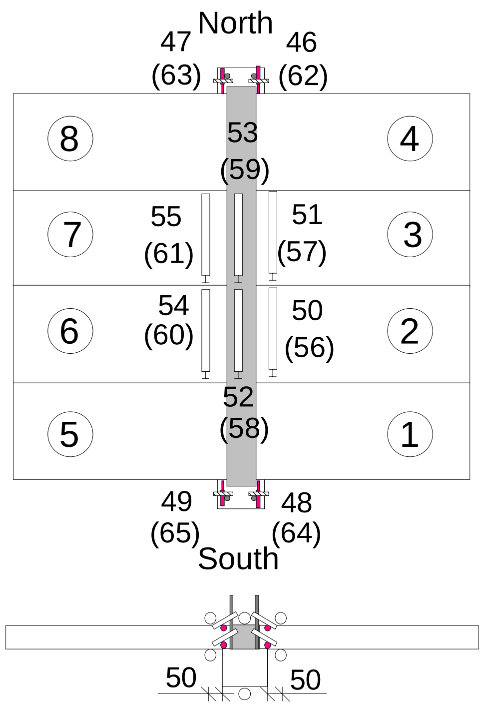 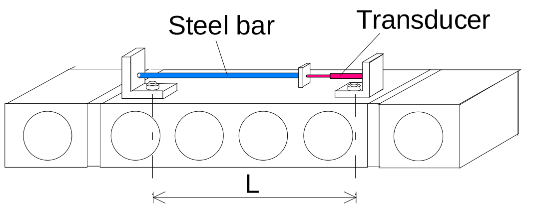 *Fig. 15. Apparatus for measuring average strain. L =1120mm and 1060 mm for the bottom and top side transducers, respectively.* *Fig. 16. Position of device (transducers 50–61) measuring average strain parallel to the beams. Transducers 46–49 and 62–65 measured the sliding of the outermost slabs along the beam. Numbers in parentheses refer to the bottom, others to the top side.*

3.4 Horizontal displacements	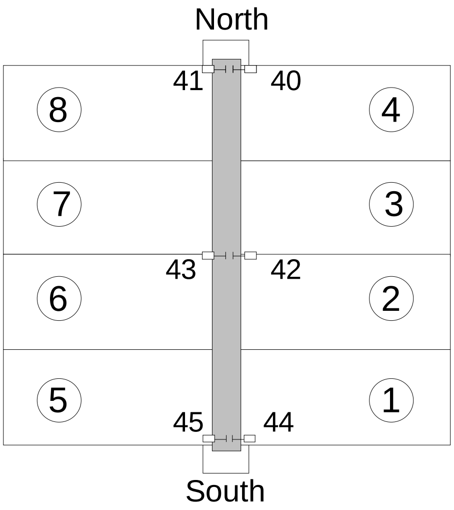 *Fig. 17. Transducers 40–45 measuring crack width on the top of the floor.*
3.5 Strain	-
4	**Special arrangements** -
5	**Loading strategy**
5.1 Load-time relationship	Date of the floor test was 14.12.1993 All measuring devices were zero-balanced when the actuator forces P_i were equal to zero but the weight of the loading equipment was on. The loading history is shown in Fig. 18. Note, that the number of load step, not the time, is given on the horizontal axis. The load test took 3,5 h but in the beginning there was a break of half an hour due to a system error in the data logger. In the following, the cyclic stage (steps 1–16) is called Stage I, the remaining part (steps 16–48) Stage II. 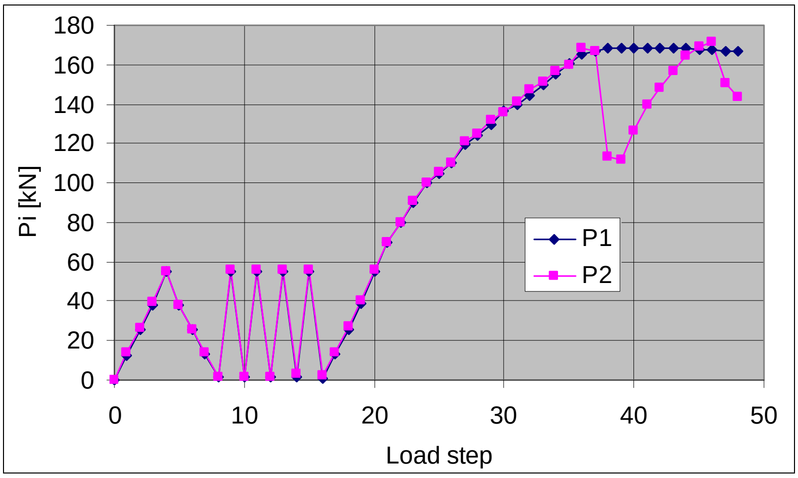 *Fig. 18. Development of actuator loads P_i.*

	The weight of loading equipment per actuator was 1,2 kN and 5,6 kN for actuators P_1 and P_2, respectively. Consequently, the imposed load per slab was $F_1 = P_1$ + 1,2 kN for slabs 2, 3, 6 and 7 $F_2 = P_2$ + 5,6 kN for slabs 1, 4, 5 and 8
5.2 After failure	-
6	**Observations during loading**

Stage I	The cast-in-situ concrete cracked vertically along ends of slabs 5, 7 and 8 at $P_1 = P_2$ = 55 kN.
Stage II	At $P_1 = P_2$ = 70 kN he cast-in-situ concrete cracked vertically along ends of slabs 1 and 4. At $P_1 = P_2$ = 80kN these cracks had grown together. At $P_1 = P_2$ = 90 kN similar cracks on the opposite side of the middle beam had also grown together. At $P_1 = P_2$ = 168 kN inclined shear cracks appeared in the outermost webs of slabs 1, 5 and 8 close to the ends of the middle beam. This was followed by a sudden drop of P_2. P_2 could still be increased to the previous value and beyond it. At $P_1 = P_2$ = 168 kN an inclined shear crack appeared in the outermost web of slab 4 close to the North end of the middle beam. At P_1 = 167,5 kN and P_2 = 171,2 kN slabs 5–8 failed in shear as shown in Fig. 19.
After failure	When the slabs were removed, it came out that the joint concrete had completely filled the space between the slab and the middle beam, the space under the slab end and the core fillings included.

7	**Cracks in concrete**
7.1 Cracks at service load	Not documented.
7.2 Cracks after failure	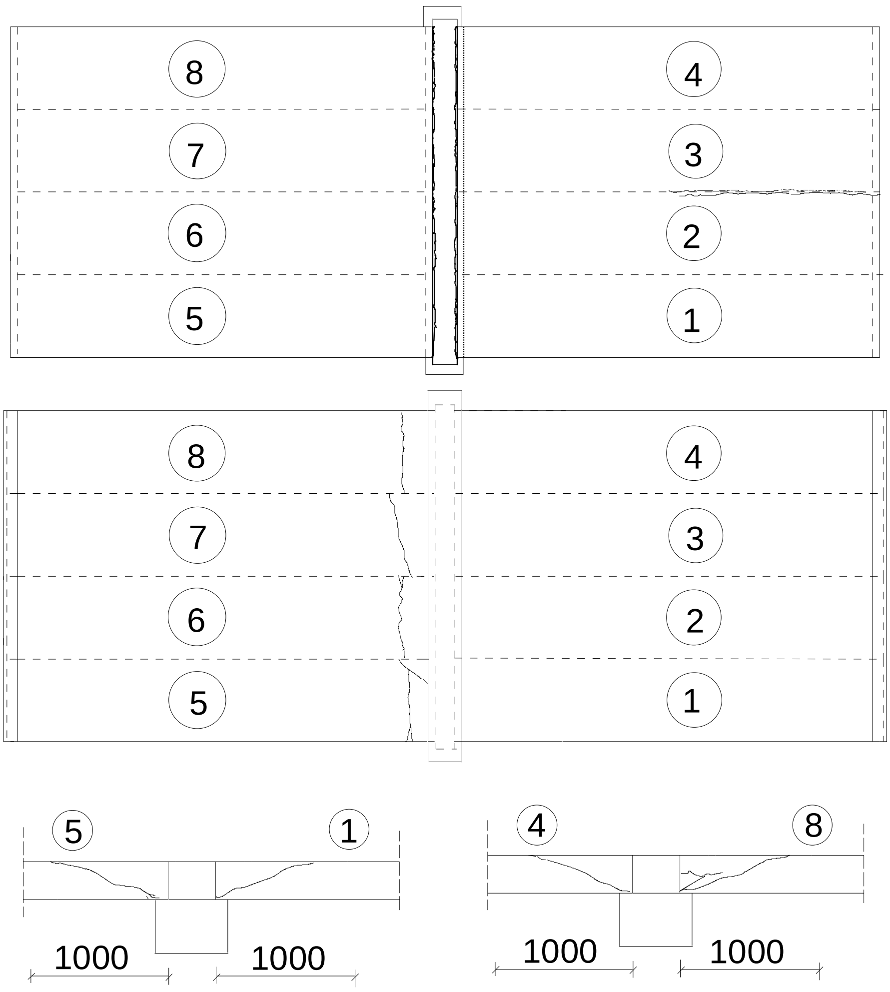 *Fig. 19. Cracks after failure on the top, at the bottom and in the longitudinal edges of the floor.*
8	**Observed shear resistance**
	The maximum measured support reaction is regarded as the indicator of failure. The failure took place at P_1 = 167,5 kN, P_2 = 171,2 kN or F_1 = 168,7 kN, F_2 = 176,8 kN. Fig. 20 shows the relationship between the measured support reaction below the South end of the middle beam and the sum of actuator loads on half floor. The ratio of the reaction to the load is shown in Fig. 21 and in a larger scale in Fig. 22. Based on Fig. 22 it is justified to assume that at failure the support reaction due to the line load is equal to 0,874 times the line load. Assuming simply supported slabs gives the theoretical ratio of 0,85.

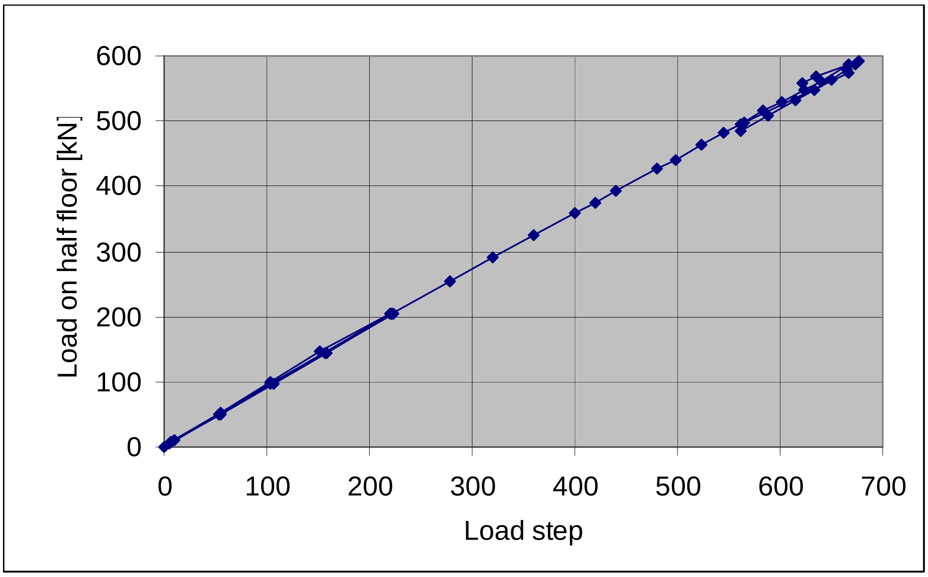

Fig. 20. Support reaction measured below South end of the middle beam vs. load on half floor = 2(P_1 + P_2).

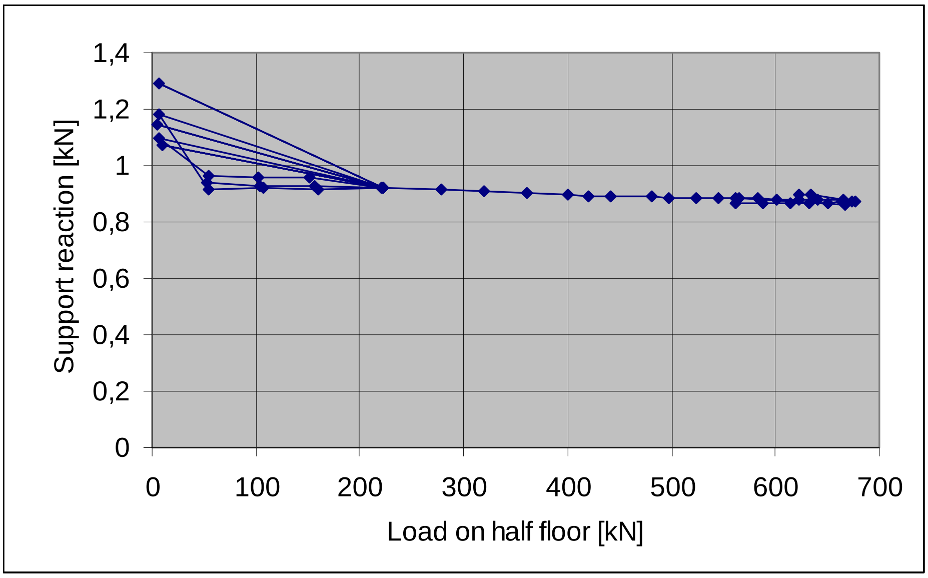

Fig. 21. Ratio of measured support reaction (below South end of the middle beam) to actuator loads on half floor.

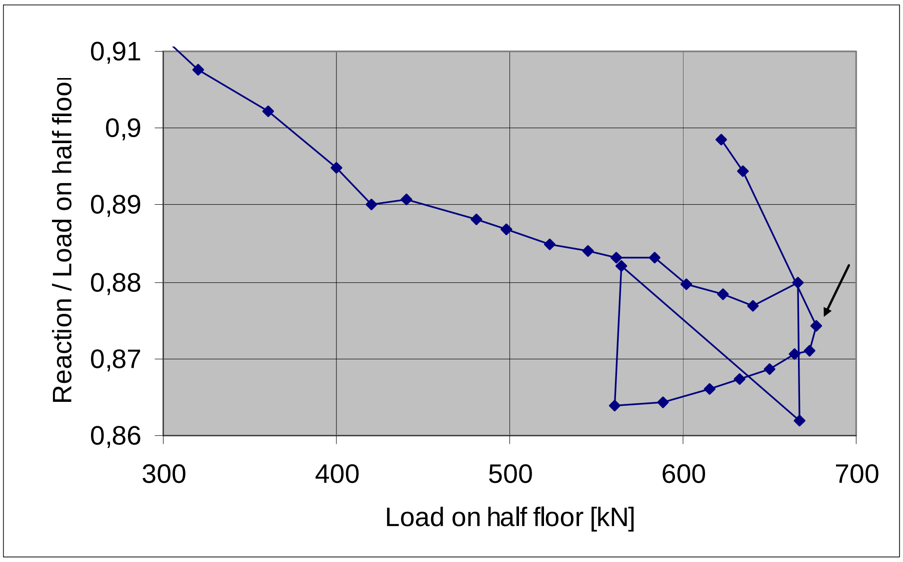

Fig. 22. A part of the previous figure in a large scale. The point corresponding to the highest support reaction has been indicated by an arrow.

The observed shear resistance of one slab end (support reaction of slab end at failure) due to different load components is given by

$$V_{obs} = V_{g,sl} + V_{g,jc} + V_{eq} + V_p$$

where $V_{g,sl}$, $V_{g,jc}$, V_{eq} and V_p are shear forces due to the self-weight of slab unit, weight of joint concrete, weight of loading equipment and actuator forces P_1, and P_2, respectively.

It is concluded that the maximum support reaction due to the imposed load on the failed slabs has been V_p = 0,874 x (actuator loads on half floor) / 4 = 0,874x(167,5 + 171,2) /2 = 148,0 kN. In the same way, the support reaction due to the weight of the loading equipment has been 0,874x(1,2+5,6)/2 = 2,97 kN. $V_{g,jc}$ is calculated from the nominal geometry of the joints and measured density of the grout. When calculating $V_{g,sl}$, the measured weight of the slabs is used. The values of the shear force components are given in Table 1 below.

Table 1. Components of shear resistance due to different loads.

Action	Load	Shear force kN/slab
Weight of slab unit	4,09 kN/m	12,3
Weight of joint concrete	0,17 kN/m	0,5
Loading equipment	(1,2+5,6)/2 kN/slab	3,0
Actuator loads	(199,7+200,5) /2 kN /slab	148,0

The observed shear resistance $\boldsymbol{V_{obs}}$ **= 163,8 kN** (shear force at support) is obtained for one slab unit with width = 1,2 m. The shear force per unit width is $\boldsymbol{v_{obs}}$ **= 136,5 kN/m.**

9 Material properties

9.1
Strength of steel:

Component	$R_{eH}/R_{p0,2}$ MPa	R_m MPa	Note
Strands J12,5	1630	1860	Nominal (no yielding in test)
Reinforcement Txy	500		Nominal value for reinforcing bars A500HW, no yielding in test
End beams	≈ 350		Nominal value for Fe 52, no yielding in test

9.2
Strength of slab concrete, floor test

#	Cores	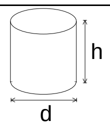	*h* mm	*d* mm	Date of test	Note
6			50	50	23.12.1993 (+9 d)[1)]	Upper flange of slabs 1, 2 and 5, two cores from each vertically drilled Tested as drilled[2)] Density = 2445 kg/m^3
Mean strength [MPa]			62,5			
St.deviation [MPa]			7,0			

9.3
Strength of slab concrete, reference tests

#	Cores	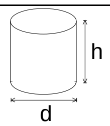	*h* mm	*d* mm	Date of test	Note
6			50	50	23.12.1993 (+9 d)[1)]	Upper flange of slab 9, vertically drilled Tested as drilled[2)] Density = 2462 kg/m^3
Mean strength [MPa]			70,8			
St.deviation [MPa]			4,3			

#	Cores	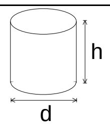	*h* mm	*d* mm	Date of test	Note
6			50	50	23.12.1993 (+9 d)[1)]	Upper flange of slab 10, vertically drilled Tested as drilled[2)] Density = 2453 kg/m^3
Mean strength [MPa]			68,0			
St.deviation [MPa]			8,1			

9.4
Strength of grout in joints and tie beams

#	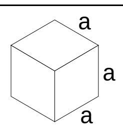	*a* mm	Date of test	Note
3		150	14.12.1993 (+0 d)[1)]	Kept in laboratory in the same conditions as the floor specimen Density = 2177 kg/m^3
Mean strength [MPa]		33,8		
St.deviation [MPa]		-		

9.5
Strength of concrete in upper part of middle beam

#	Cores	(cylinder sketch: h, d)	*h* mm	*d* mm	Date of test	Note
6			75	75	23.12.1993 (+9 d)[1)]	Upper surface of beam, vertically drilled Tested as drilled[2)] Density = 2217 kg/m^3
Mean strength [MPa]			35,2			
St.deviation [MPa]			2,8			

9.6 Strength of concrete in lower part of middle beam

#	Cores	(cylinder sketch: h, d)	*h* mm	*d* mm	Date of test	Note
6			75	75	23.12.1993 (+9 d)[1)]	Upper surface of beam, vertically drilled Tested as drilled[2)] Density = 2450 kg/m^3
Mean strength [MPa]			74,0			
St.deviation [MPa]			5,5			

1) Date of material test minus date of structural test (floor test or reference test)
2) After drilling, kept in a closed plastic bag until compression

10

Measured displacements

Note that the last two points on each curve represent the post failure situation.

10.1
Deflections

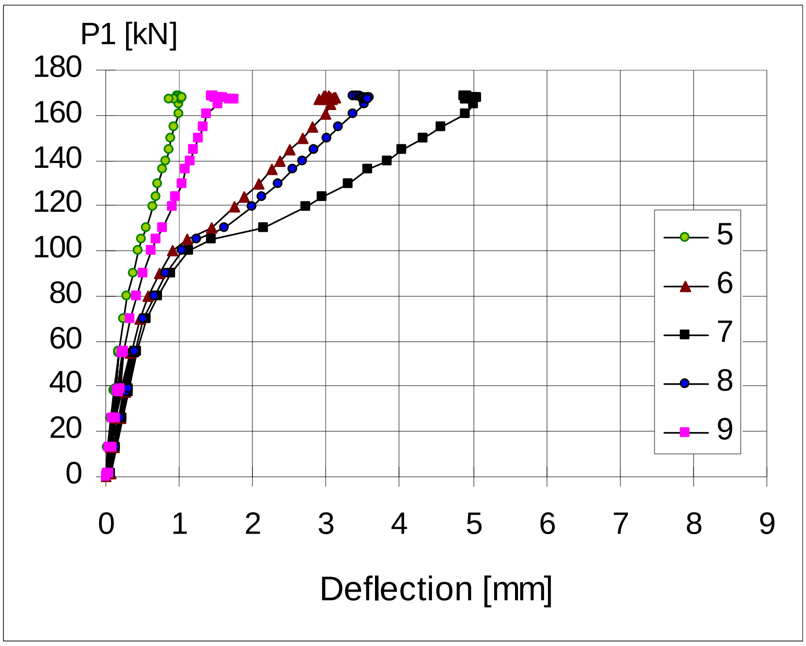

Fig. 23. Deflection on line I, Western end beam.

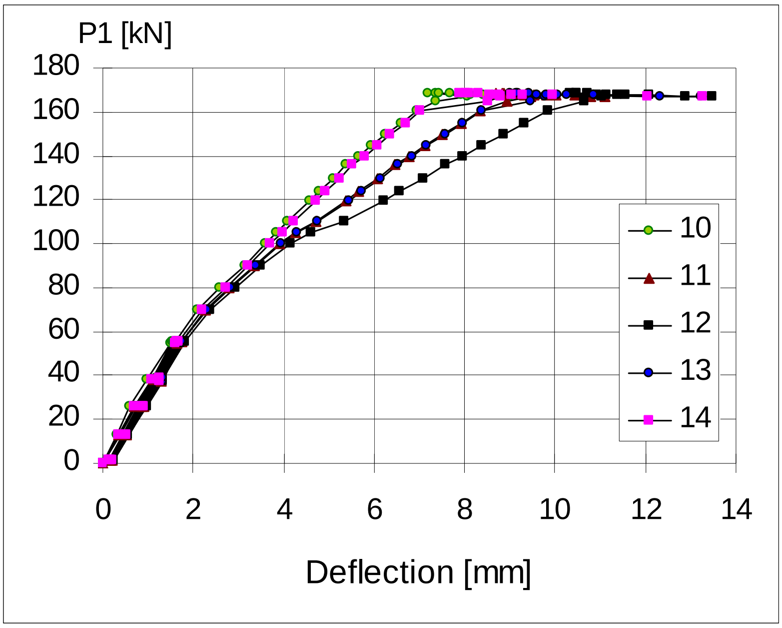

Fig. 24. Deflection on line II.

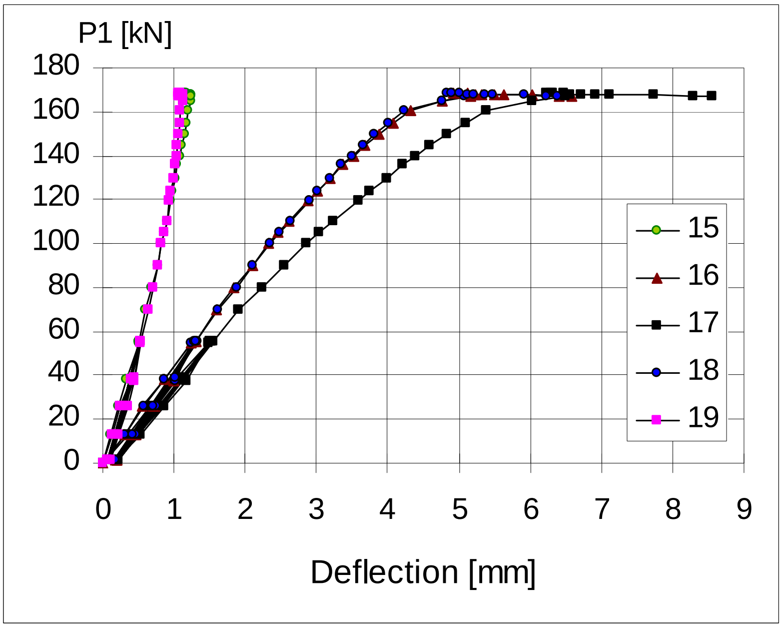

Fig. 25. Deflection on line III, middle beam.

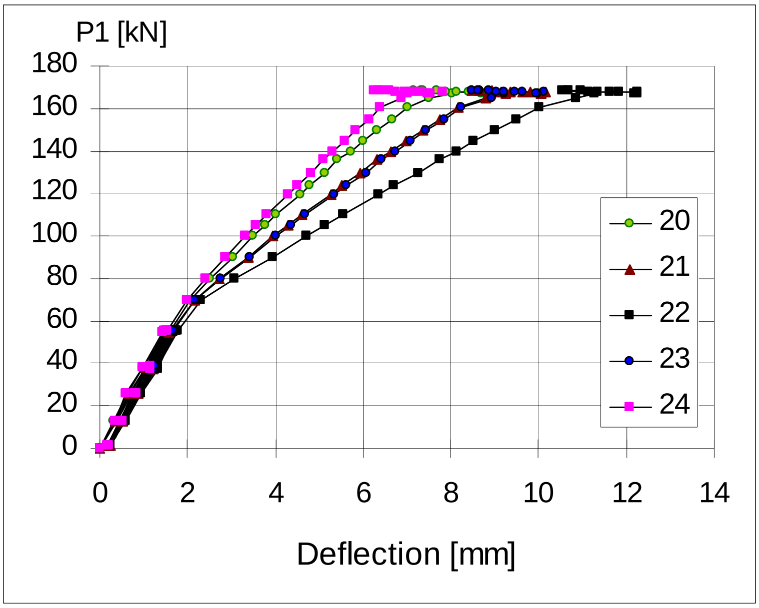

Fig. 26. Deflection on line IV.

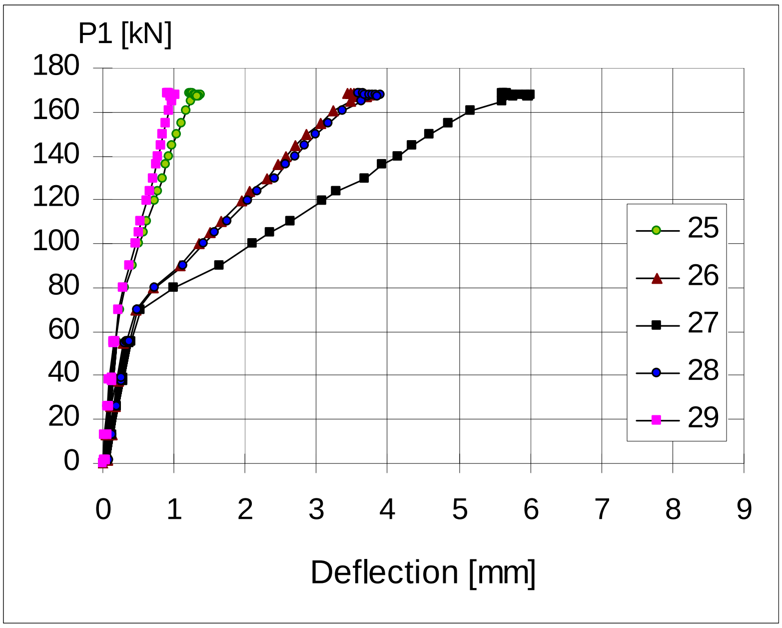

Fig. 27. Deflection on line V, Eastern end beam.

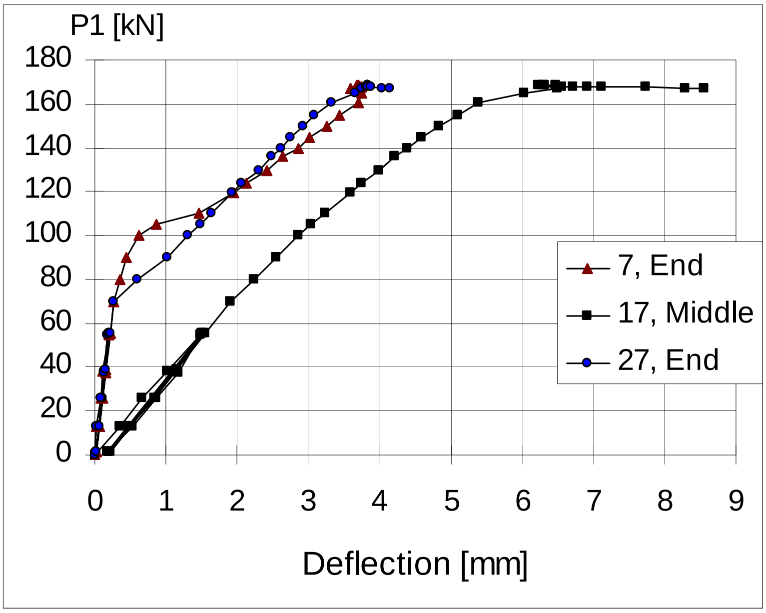

Fig. 28. Net deflection of mid-point of beams (rigid body motion = settlement of beam supports has been eliminated).

The last measured net deflection of the middle beam at highest load level before failure was 7,7 mm. This is 3,8–4 mm higher than the net deflection of the end beams.

10.2
Crack width

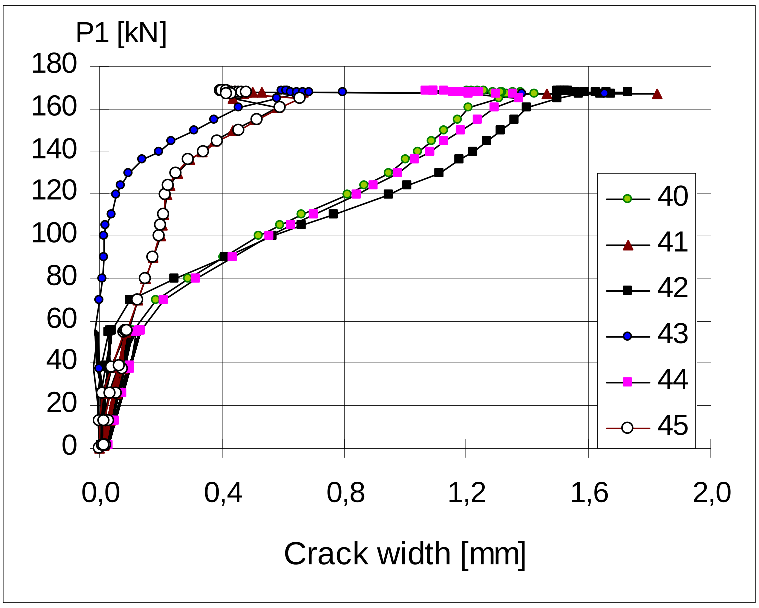

Fig. 29. Differential displacement (≈ crack width) measured by transducers 40–45.

10.3
Average strain (actually differential displacement between slab edges)

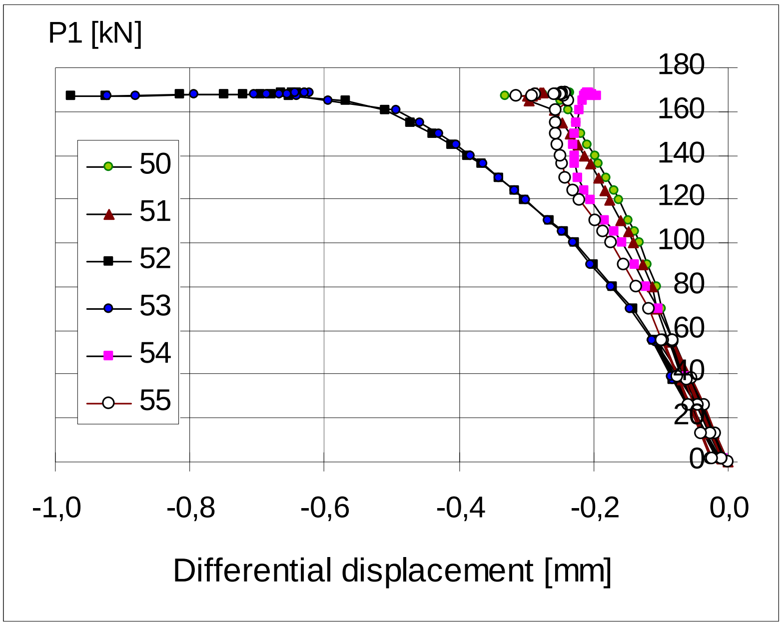

Fig. 30. Differential displacement at top surface of floor measured by transducers 50–55.

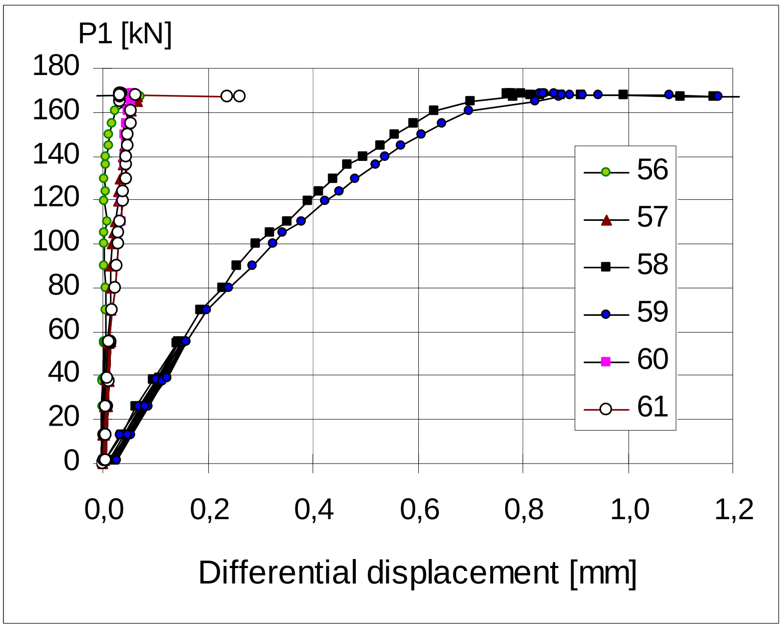

Fig. 31. Differential displacement at soffit measured by transducers 56–61.

<table>
<tr><td>10.4
Shear displacement between slab edge and middle beam</td><td>In Figs 32 and 33 the differential displacements measured by transducers 46–49 and 62–65 are shown. A negative sign means that the slab edge is coming closer to the fixing point of the transducer.

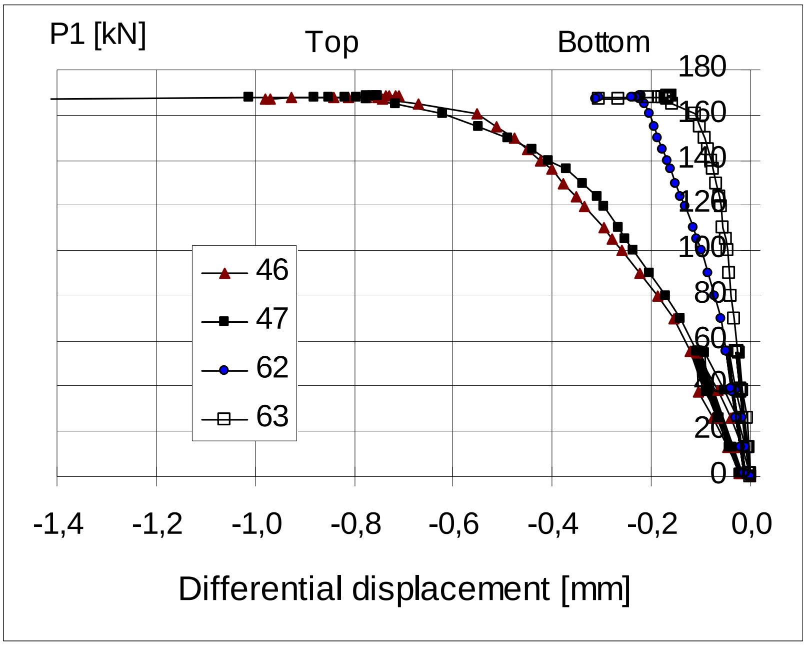

Fig. 32. North end of middle beam. Differential displacement between edge of slab and middle beam.

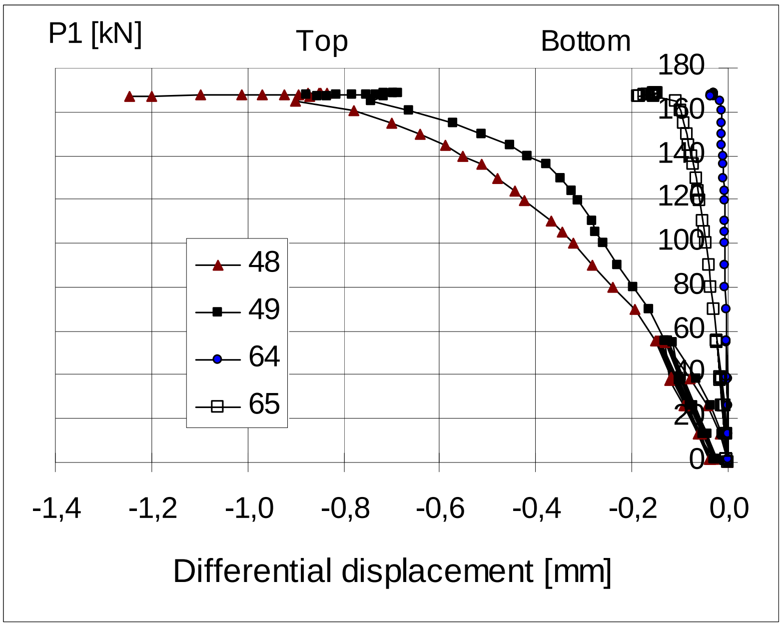

Fig. 33. South end of middle beam. Differential displacement between edge of slab and middle beam.</td></tr>
<tr><td>10.5</td><td>Strain
-</td></tr>
</table>

11 Reference tests

Both ends of slabs 9 and 10 were loaded in shear as shown in Fig. 34. The tests were performed after the floor test (21.12.1993).

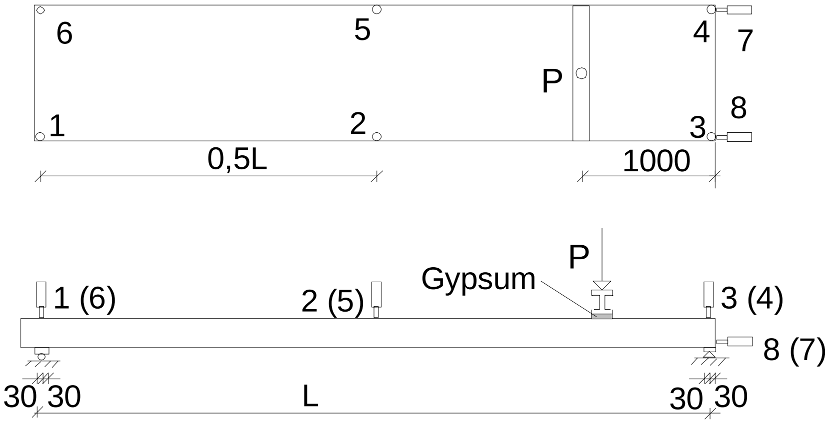

Fig. 34. Layout of reference tests. Transducers 2 and 5 are in the mid-span. For L, see Table 2. The slip of the outermost strands was measured by transducers 7 and 8.

The load-deflection relationship for the mid-point of the slabs is shown in Fig. 35 and the failure load in Table 2. The measured self-weight of the slabs = 4,11 kN/m has been used when calculating the shear resistance. Virtually no slip of the outermost strands was observed. For the failure mode, see also Appendix A.

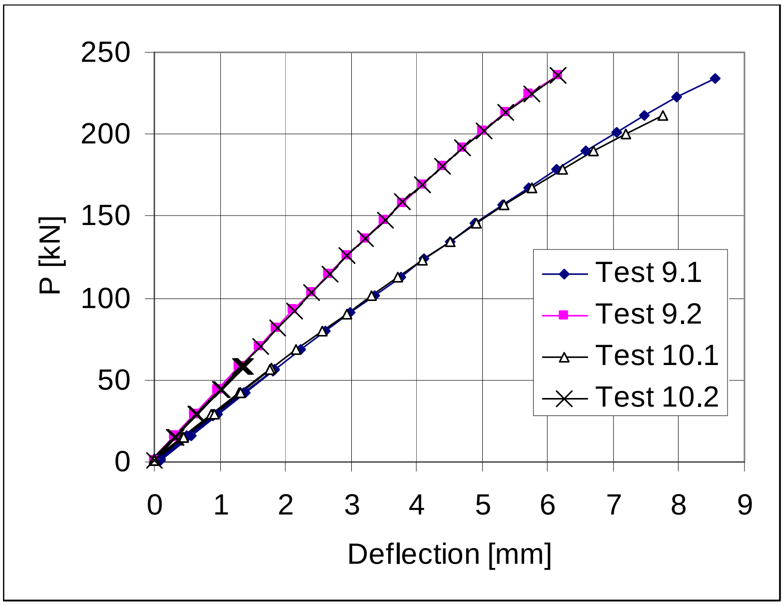

Fig. 35. Net mid-point deflection of slabs. Rigid body motion (= settlement of supports) has been eliminated.

Table 2. Span L, ultimate load P_u, shear force due to self weight V_g, shear force due to imposed load V_P, ultimate shear force V_u and failure mode in reference tests. The weight of the loading equipment = 1,4 kN is included in P_u.

Slab	L mm	P_u kN	V_g kN	V_P kN	V_u kN	Failure mode
9,1	5936	240,4	12,19	201,1	213,3	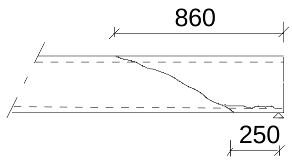
9.2	5000	256,4	10,3	206,7	217,0	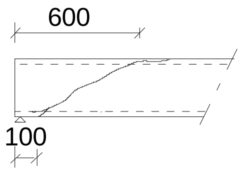
10.1	5935	219,4	12,2	183,5	195,7	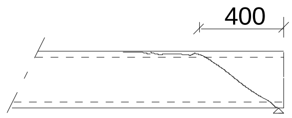
10.2	5000	257,3	10,3	207,4	217,7	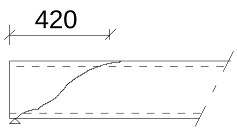
		Mean			210,9	

12 Comparison: floor test vs. reference tests

The observed shear resistance in the floor test was 163,8 kN per one slab unit or 136,5 kN/m. This is **65%** of the mean observed in the reference tests.

13 Discussion

1. The net deflection of the middle beam due to the imposed actuator loads only (deflection minus settlement of supports) was 7,7 mm or L/649 at the highest load level.
2. The shear resistance measured in the reference tests was of the same order as the mean of the observed values for similar slabs given in *Pajari, M. Resistance of prestressed hollow core slab against web shear failure. VTT Research Notes 2292, Espoo 2005*.
3. Before failure, the net deflection of the end beams was 3,8–4 mm lower than that of the middle beam. This is a too small difference to cause considerable torsional stresses in the slabs.
4. The failure mode was a web shear failure of slabs on one side of the middle beam. Before failure there were diagonal cracks in all for slab edges next to the supports of the middle beam.

The failure behaviour of the slabs was similar to that in the other Finnish floor tests in which the slabs were supported close to the soffit of the middle beam.

APPENDIX A: PHOTOGRAPHS

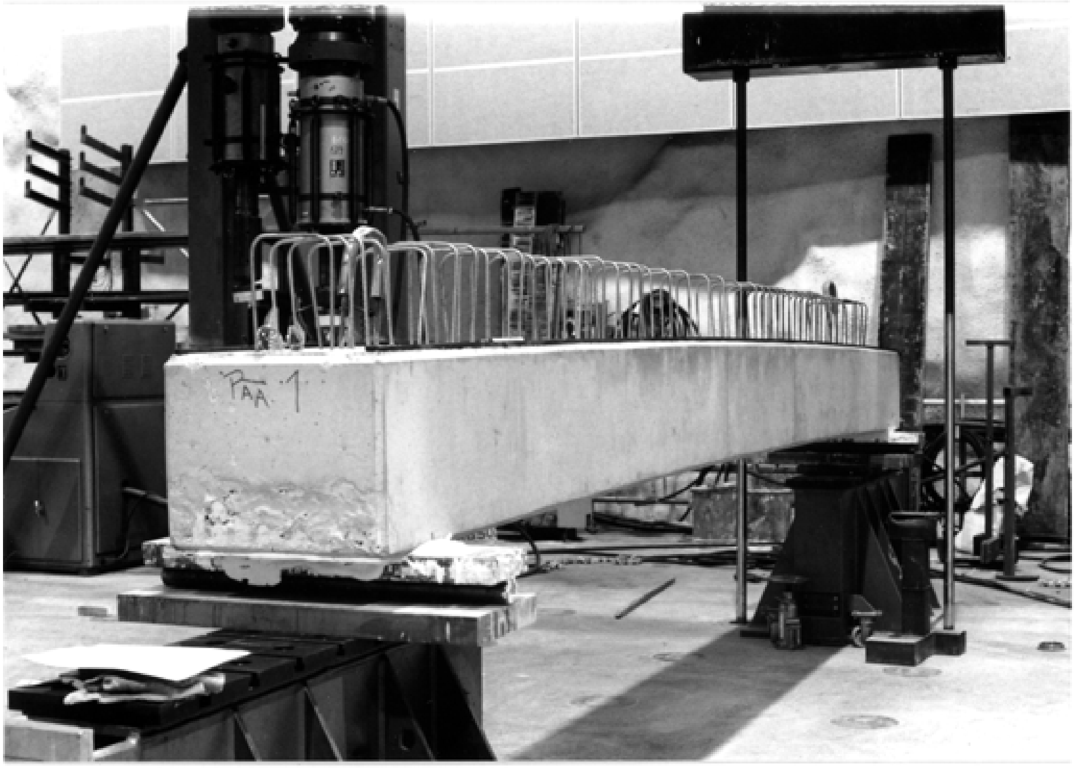

Fig. 1. The prestressed concrete middle beam on the supports.

Fig. 2. Cracking of the middle beam before the loading test.

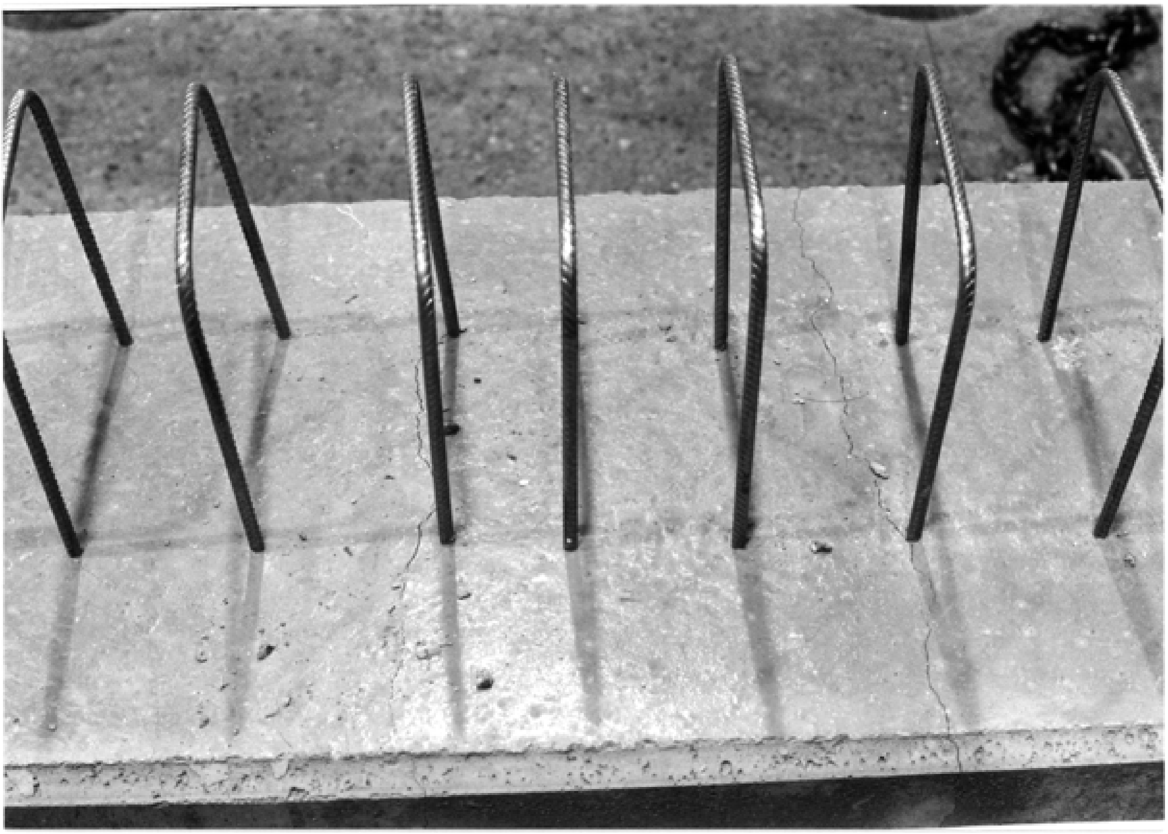

Fig. 3. The dowel reinforcement and top surface of the middle beam.

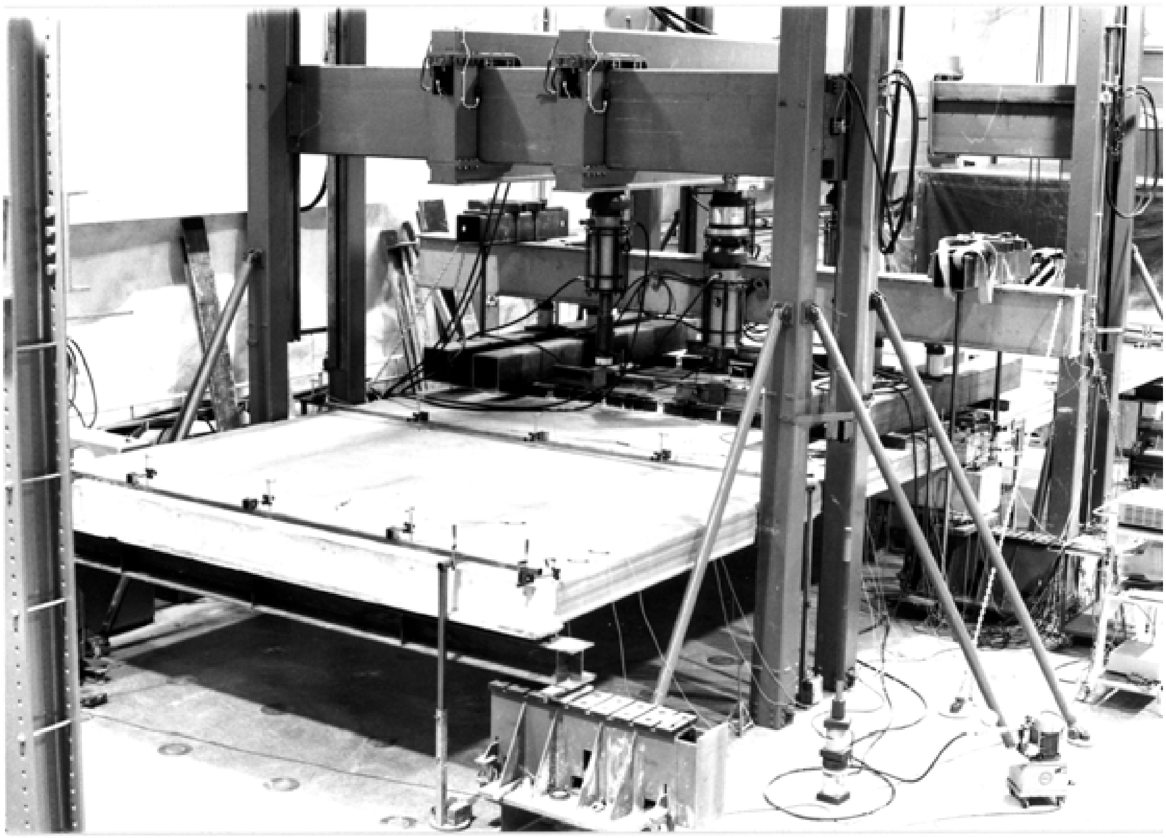

Fig. 4. The loading and measurement arrangement.

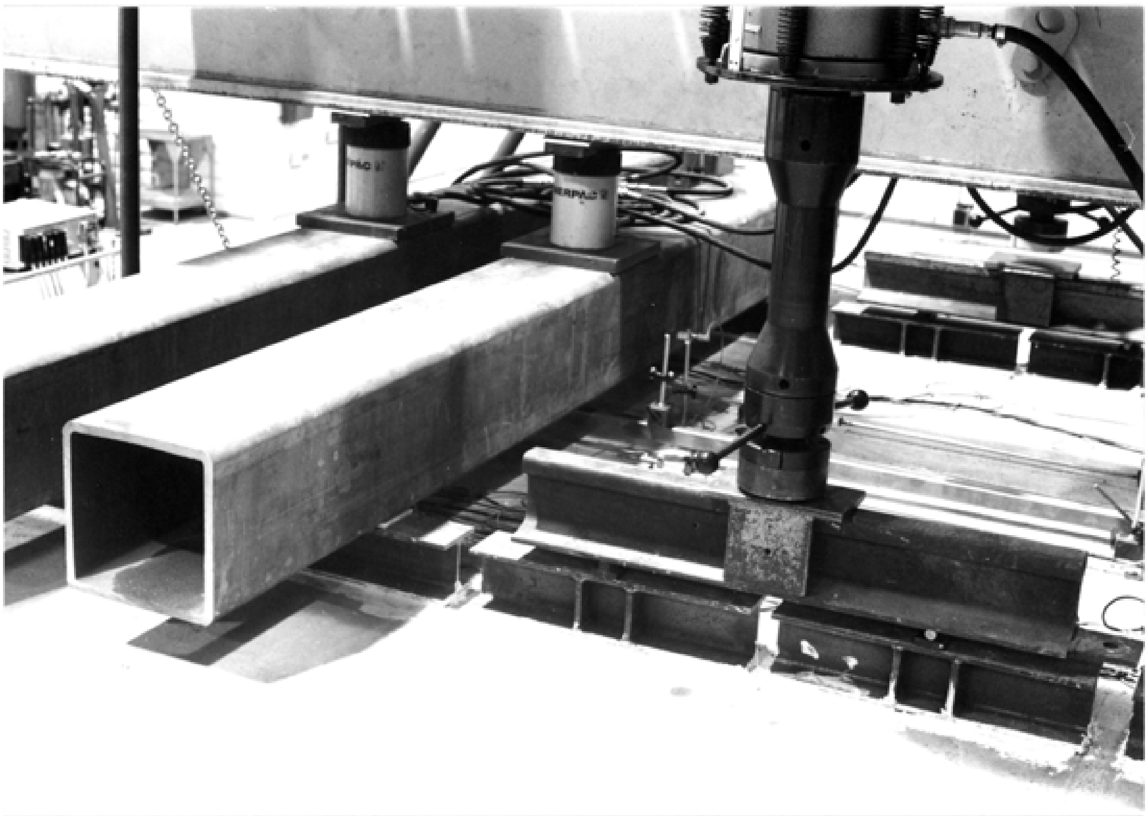

Fig. 5. Hydraulic jacks and spreader beams.

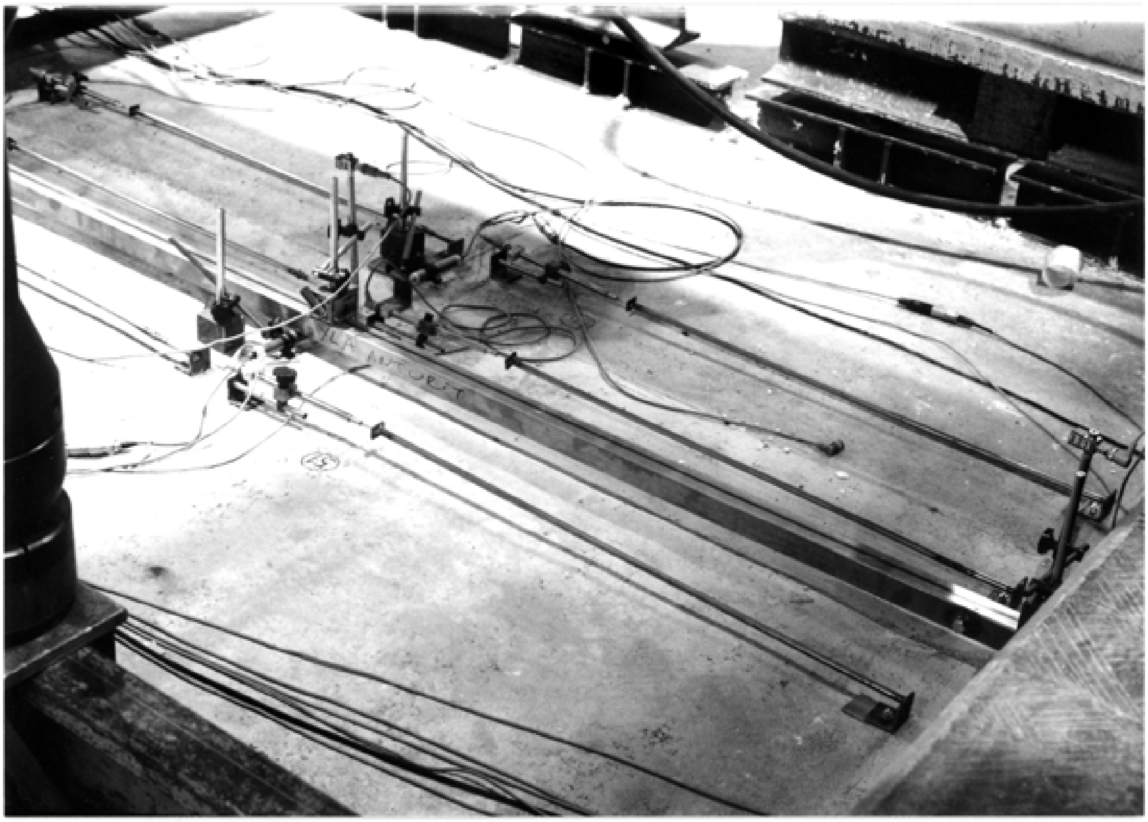

Fig. 6. Devices to measure the displacement differences between the middle beam and the ends of the slab units and between the edges of the slab units or between the corresponding points at the middle beam.

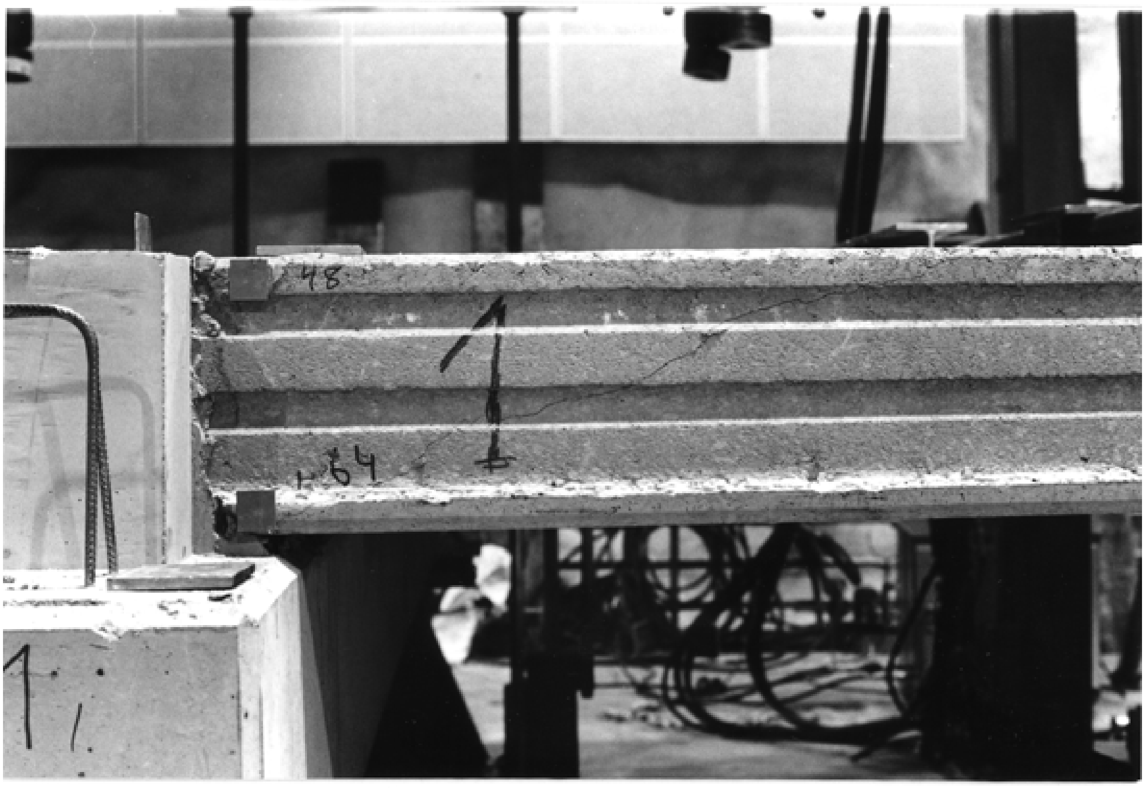

Fig. 7. The cracks in the longitudinal edge of the slab unit no 1, near the middle beam, at failure.

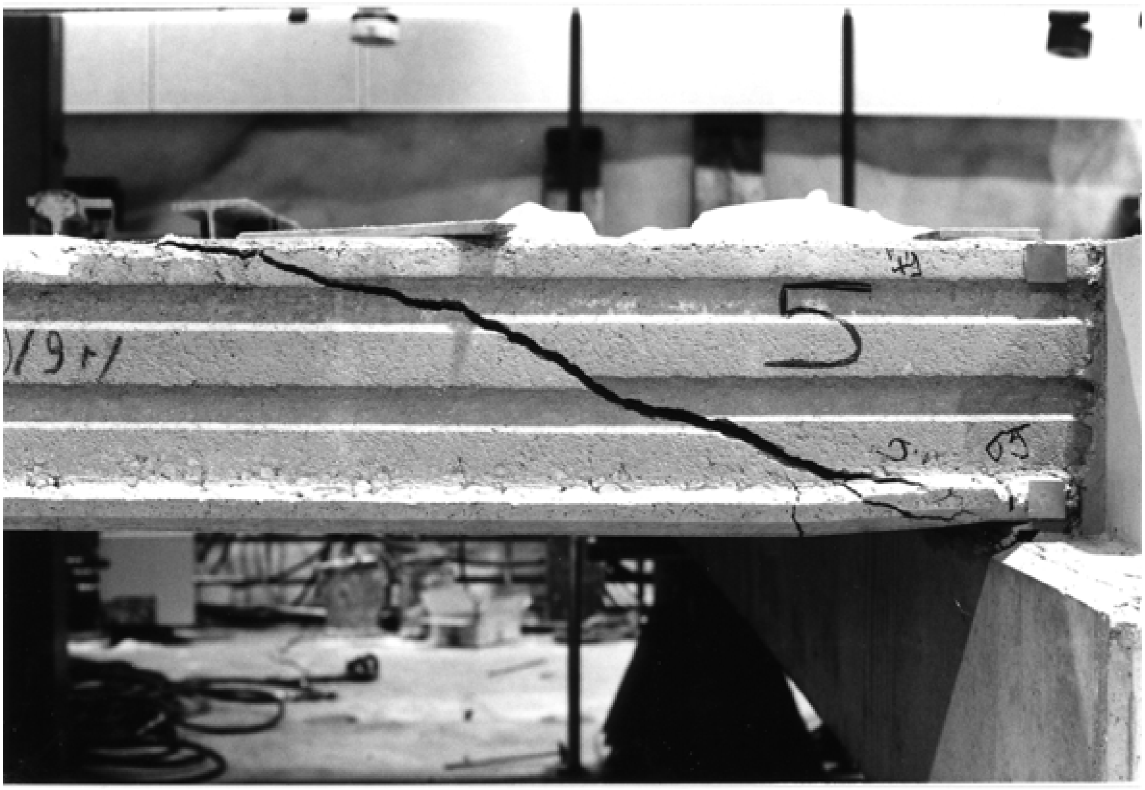

Fig. 8. The cracks in the longitudinal edge of the slab unit no 5, near the middle beam, at failure.

Fig. 9. The cracks in the longitudinal edge of the slab unit no 8, near the middle beam, at failure.

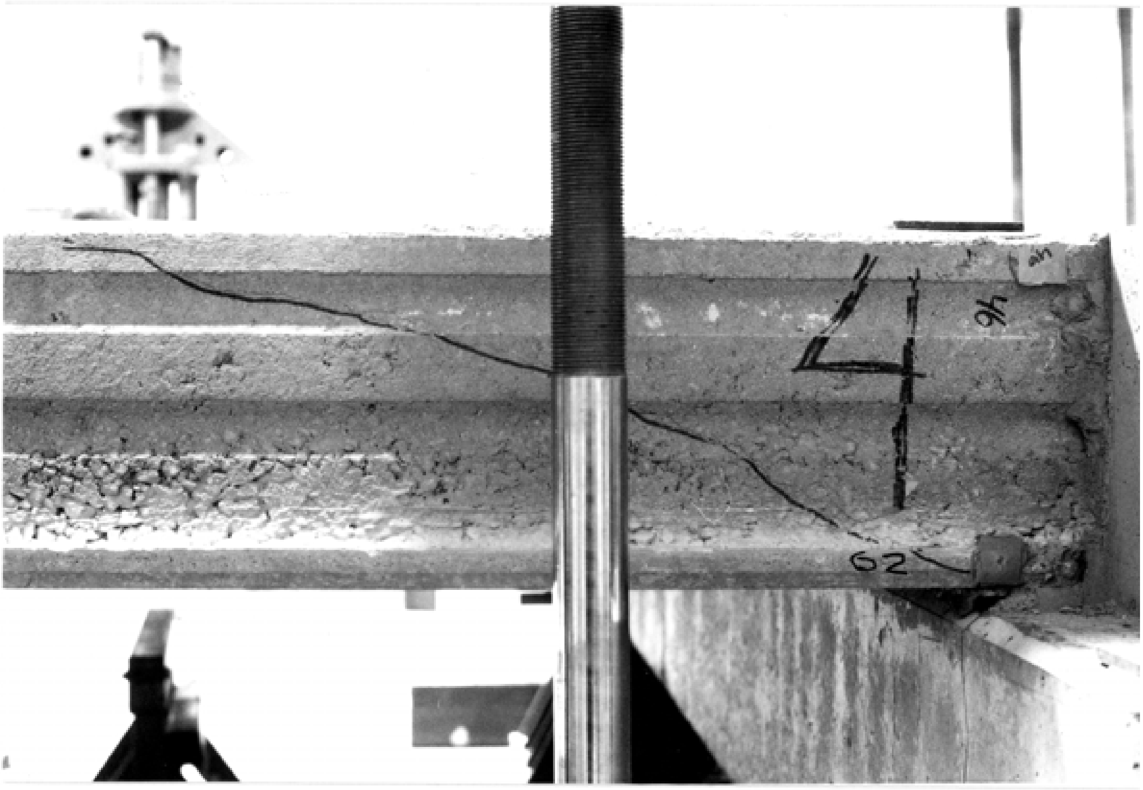

Fig. 10. The cracks in the longitudinal edge of the slab unit no 4, near the middle beam, at failure.

Fig. 11. Cracking of the joint between the cast in situ part of the middle beam and the ends of the slab units.

Fig. 12. The middle beam after the loading test, on the edge of the slab units no 1 - 4.

Fig. 13. The middle beam after the loading test, on the edge of the slab units no 5 - 8.

Fig. 14. The failure of the end 1 of the slab unit no 9 in the reference loading test.

Fig. 15. The failure of the end 2 of the slab unit no 9 in the reference loading test.

Fig. 16. The failure of the end 1 of the slab unit no 10 in the reference loading test.

Fig. 17. The failure of the end 2 of the slab unit no 10 in the reference loading test.

1	**General information**
1.1 Identification and aim	**VTT.PC.InvT_Cont.265.1994** **Last update 2.11.2010** PC265C (Internal identification) Aim of the test: To study the shear resistance of hollow core slabs supported on continuous beam.
1.2 Test type	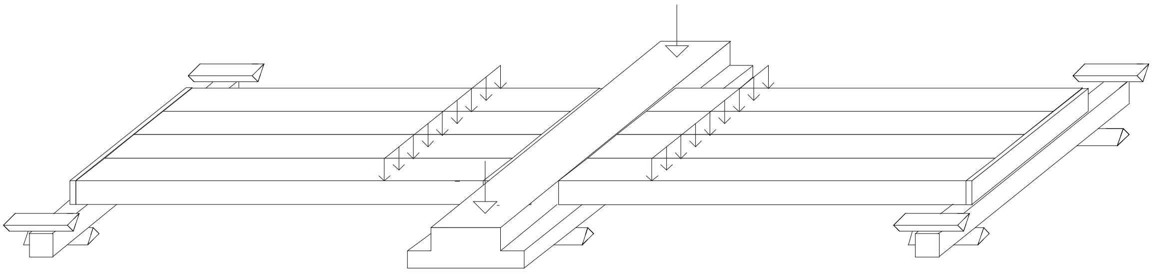 *Fig. 1. Illustration of test setup.*
1.3 Laboratory & date of test	VTT/FI 3.3.1994
1.4 Test report	Author(s): Pajari, M. Name: *Loading test for 265 mm hollow core floor supported on continuous beams* Ref. number: RTE5-IR-4/1994 Date: 29.4.1994 Availability: Public, available on request from VTT Expert Services, P.O. Box 1001, FI-02044 VTT. Financed by the Finnish Association of Building Industry RTT (supported by the Technology Development Centre of Finland); the Finnish Steel Work Association; the International prestressed Hollow core Association IPHA; KB Kristianstads Cementgjuteri, Sweden; Stombyggarna i Hudiksvall AB, Sweden and SBUF, Sweden
2	**Test specimen and loading** (see also Appendix A)
2.1 General plan	

	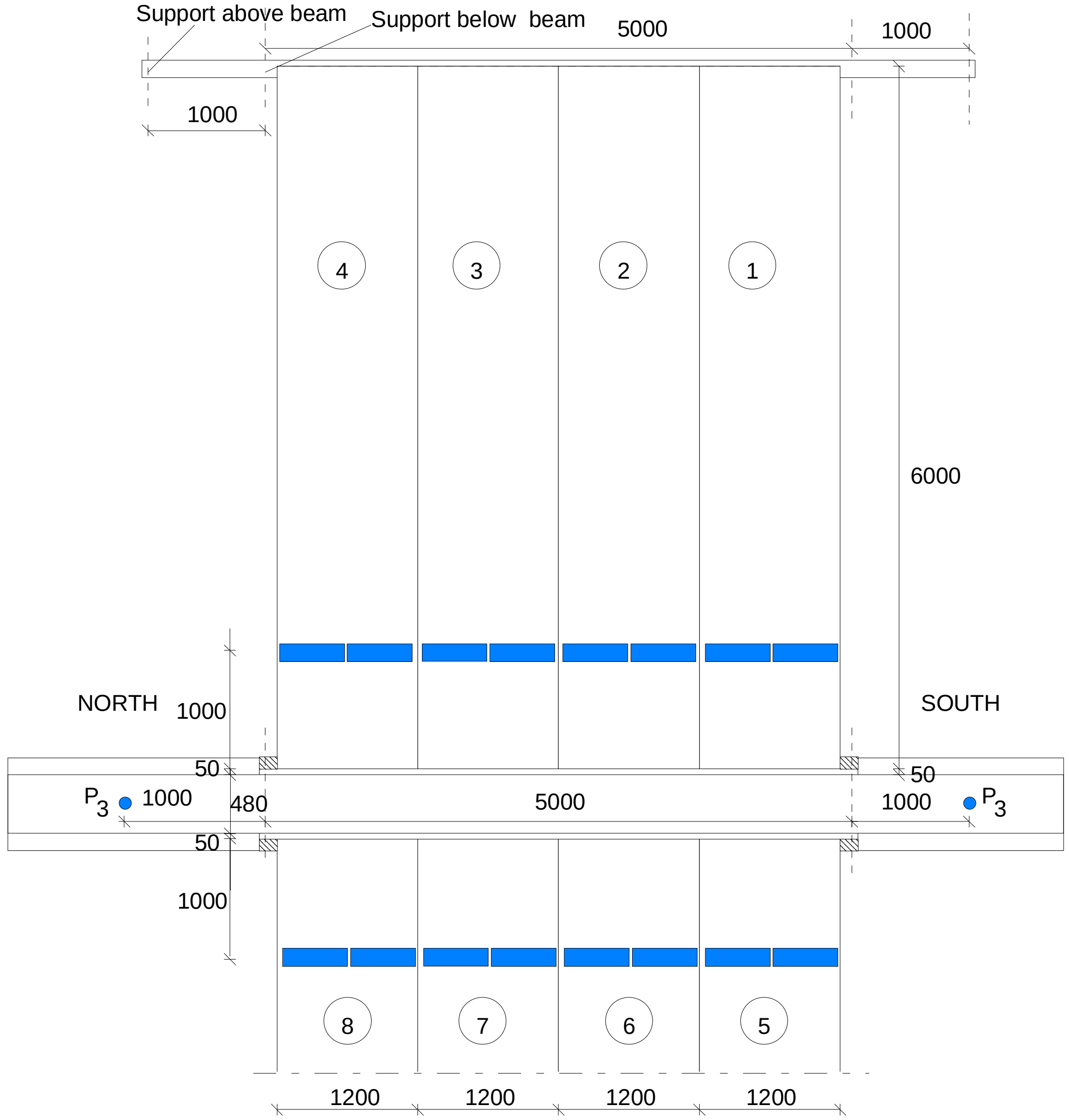 *Fig. 2. Plan.*
2.2 End beams	Box girders made of steel. Span = 5,0 m 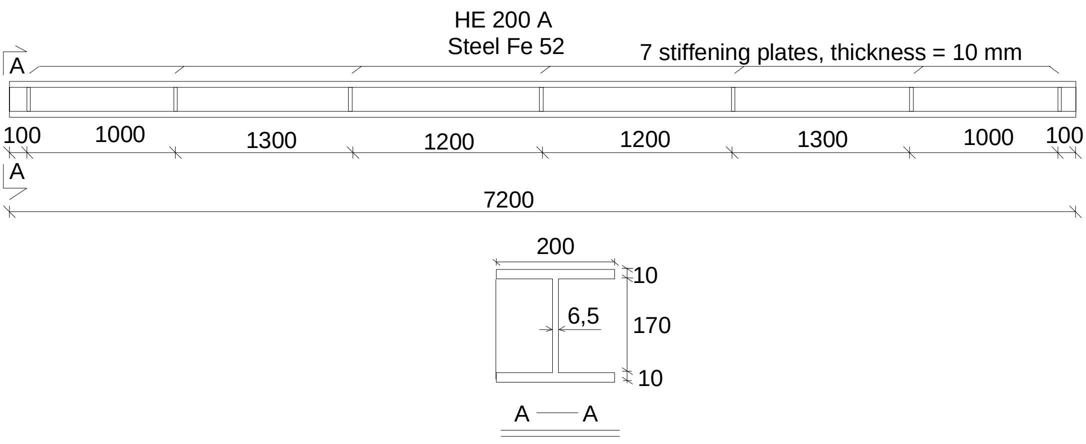 *Fig. 3. End beam.*

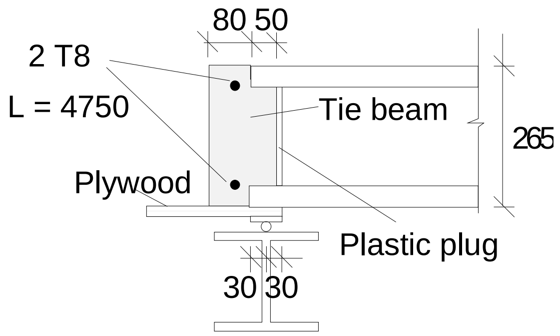

Fig. 4. Arrangements at end beam. T8 refers to a reinforcing bar, see 2.4.

2.3
Middle beam

The middle beam was a prestressed concrete beam provided with shear keys (indents) on both sides of the web. The grade of the concrete was K60. See Figs. 5, 6 and 8 for the dimensions of the cross-section.

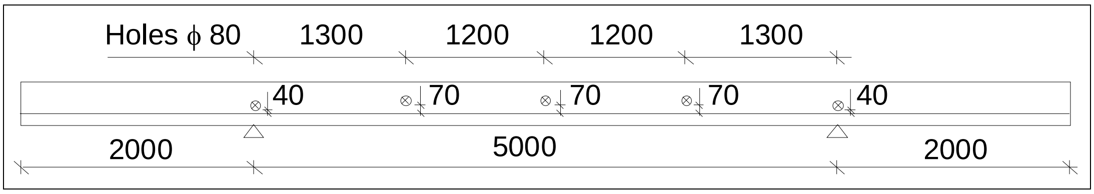

Fig. 5. Middle beam. Elevation.

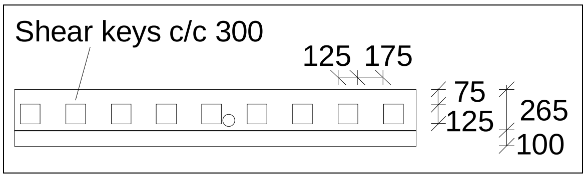

Fig. 6. Middle beam. Shear keys.

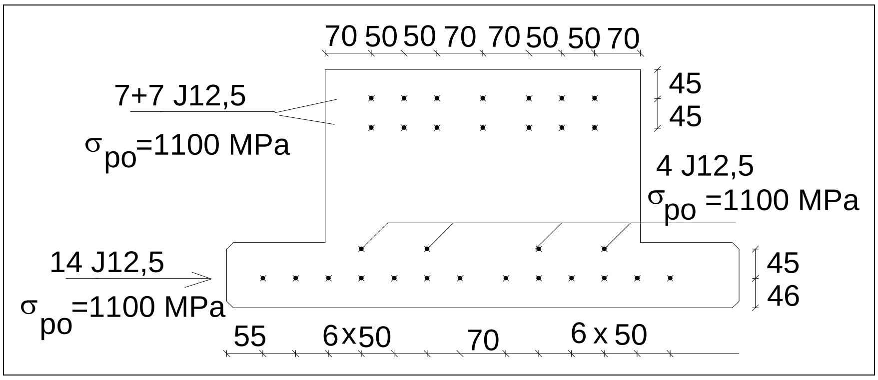

Fig. 7. Middle beam. Position of prestressing strands J12,5. For J12,5, see 9.1.

2.4
Arrangements at middle beam

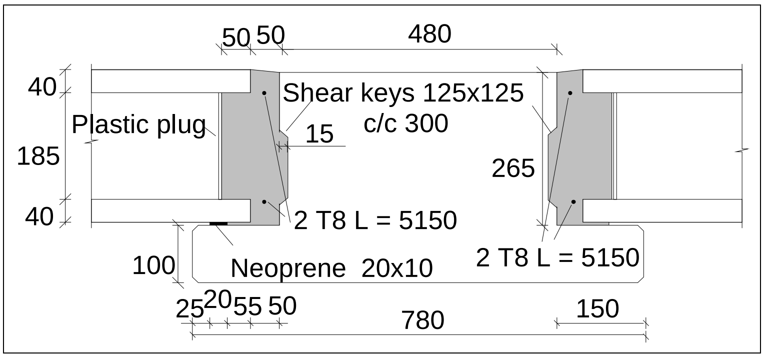

Fig. 8. Section along hollow cores.

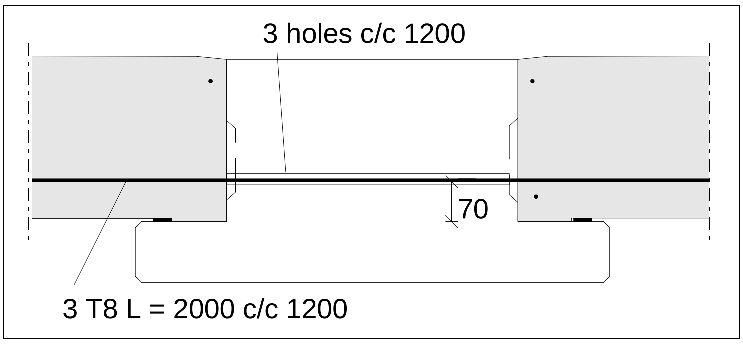

Fig. 9. Tie reinforcement in joints between adjacent slabs.

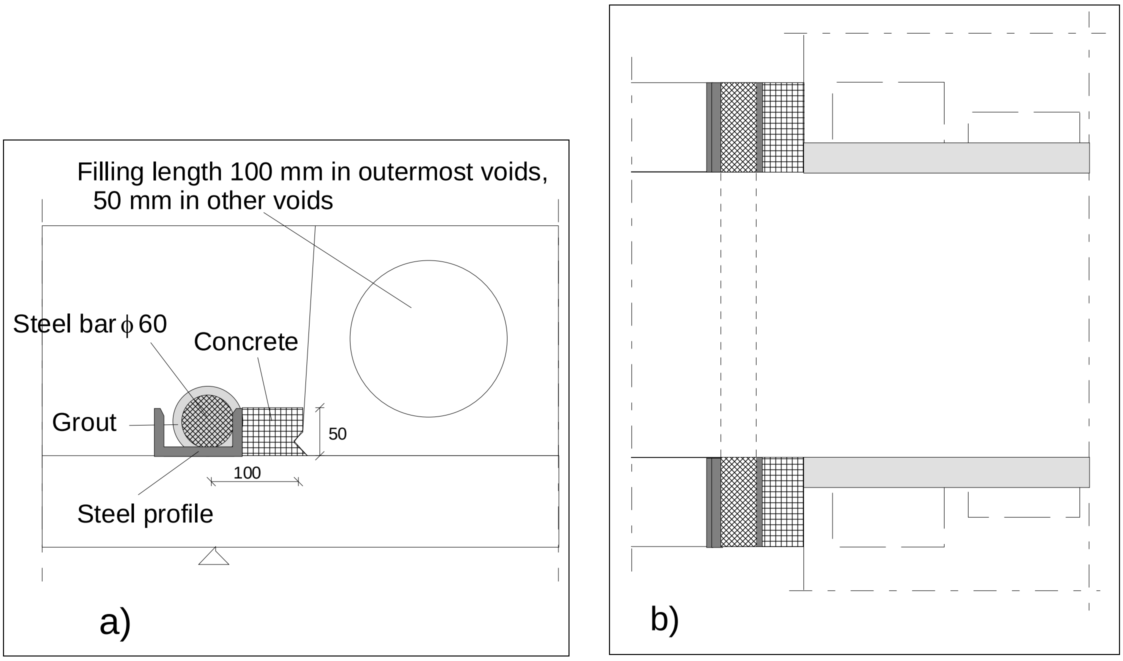

Fig. 10. To prevent sliding of slab edge along the middle beam (this is not possible if the continuous beam carries hollow core slabs on both sides of the continuous support), a steel bar penetrating the web and a steel profile were installed. The empty space around the bar in the hole as well as the gap between the U-profile and the slab edge were grouted. a) Elevation. b) Top view (see also Fig. 16). See Also Appendix A, Figs 5 and 7.

Txy: Hot rolled, weldable rebar A500HW, ϕ = xy mm, see 9.1.

2.5
Slabs

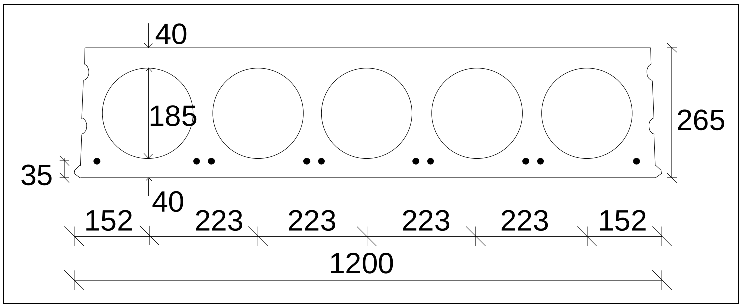

Fig. 11. Nominal geometry of slab units (in scale).

- Extruded by Partek Betoniteollisuus Oy, Hyrylä factory 21.1.1994
- 10 lower strands J12,5 initial prestress 950 MPa

J12,5: seven indented wires, ϕ =12,5 mm, A_p = 93 mm^2

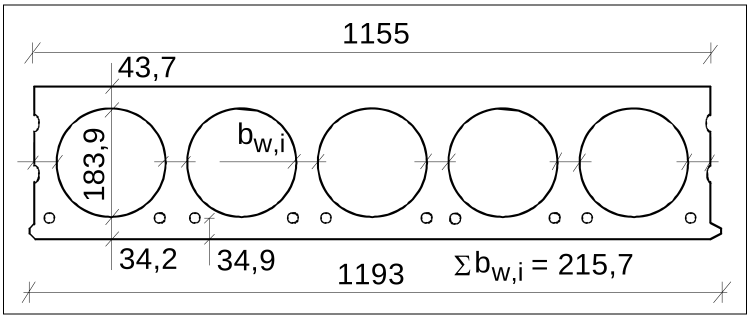

Max measured bond slips: 5,9 and 3,0 mm in slab 1; 3,3 and 2,5 mm in slab 6 and 2,2 mm in slab 7

Measured weight of slab units = 3,99 kN/m

Fig. 12. Floor test. Mean of most relevant measured geometrical characteristics of slabs 1–8.

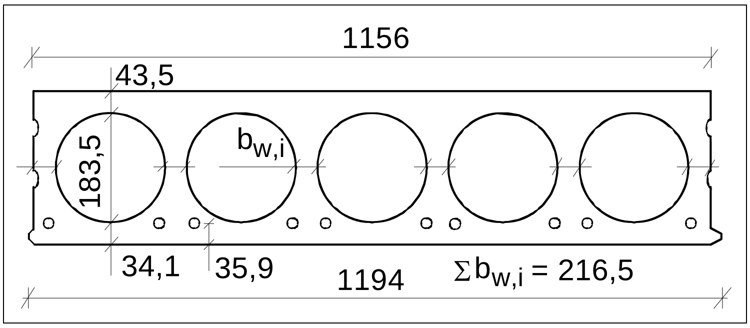

Max measured bond slips: 6,5, 4,0, 2,3 and 2,2 mm in slab 10 (1,3 mm in slab 9)

Measured weight of slab units = 4,01 kN/m

Fig. 13. Reference tests. Mean of most relevant measured geometrical characteristics of slab 9.

There were too large bond slips in strands at one end of slabs 1 and 6 (3,0–5,9 mm) and at both ends of slab 10. Slab 10 was rejected and the ends of slabs 1 and 6 with too high slip were placed on the end beams.

2.6
Temporary supports

Temporary supports below beams (Yes/No)
- No

2.7 Loading arrangements	There were three separate, manually controlled hydraulic circuits, one for actuators P_1 the other for actuators P_2, and the third for actuators P_3, see Fig. 14. Attempts were made to keep $P_1 \approx P_2$ to generate two uniform line loads on the floor. The aim of loads P_3 was to make the middle beam behave as one with clamped ends (no rotation at support) as far as possible. The primary spreader beams on the top of the floor were slightly shorter than 0,6 m. The friction between the secondary and primary spreader beams was eliminated by teflon plates (beams spreading loads P_2) and by a roller bearing (beams spreading load P_1). There was gypsum mortar between the primary spreader beams and the top surface of the floor. 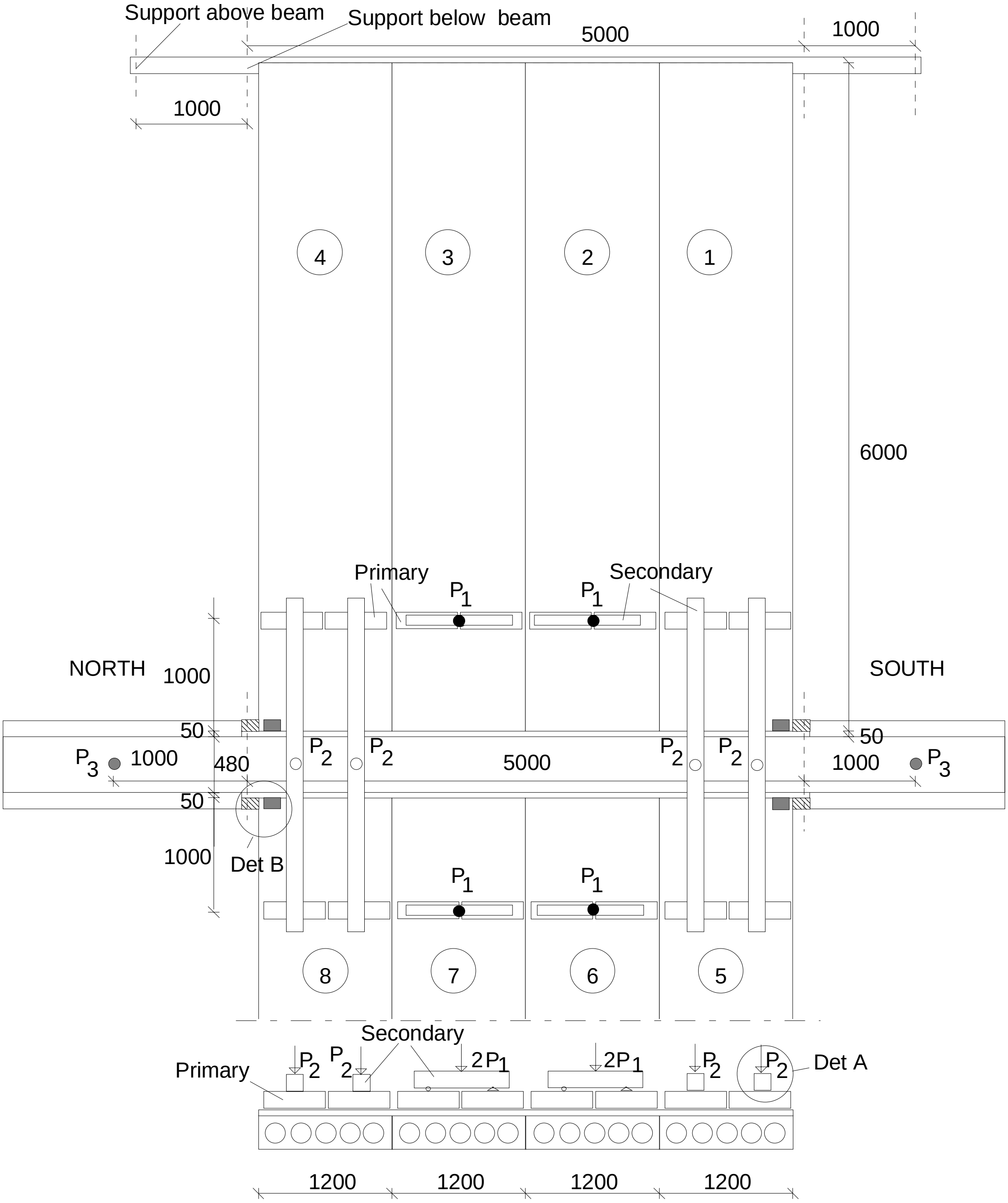 *Fig. 14. Plan. P_1, P_2 and P_3 refer to vertical actuator forces. For det A and det B, see Figs. 15 and 16.*

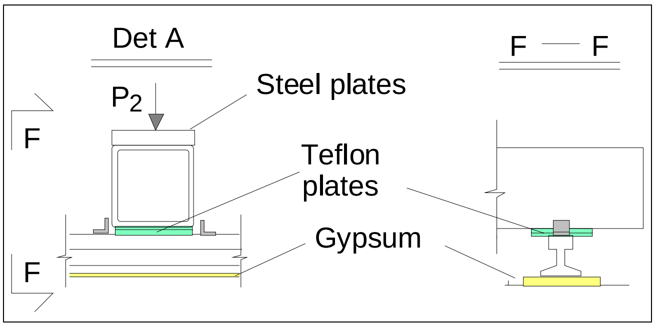

Fig. 15. Detail A, see the figure above.

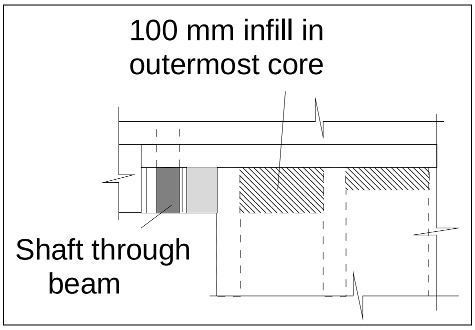

Fig. 16. Det B, see the figure above.

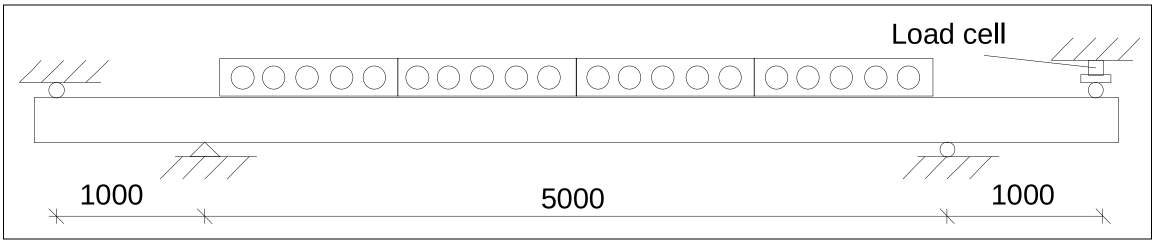

Fig. 17. Support conditions of end beams.

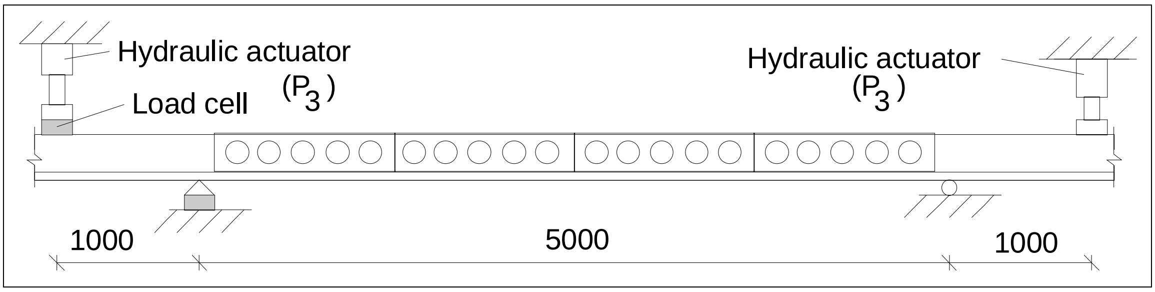

Fig. 18. Supports below and concentrated loads on middle beam.

3	**Measurements**
3.1 Support reactions	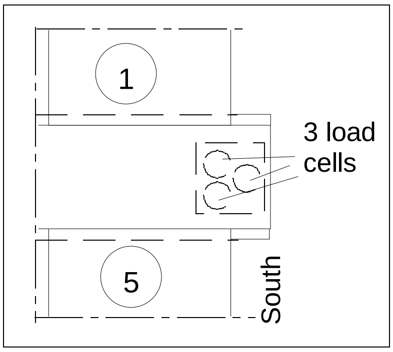 *Fig. 19. Load cells below the South end of the middle beam.*

3.2
Vertical displacement

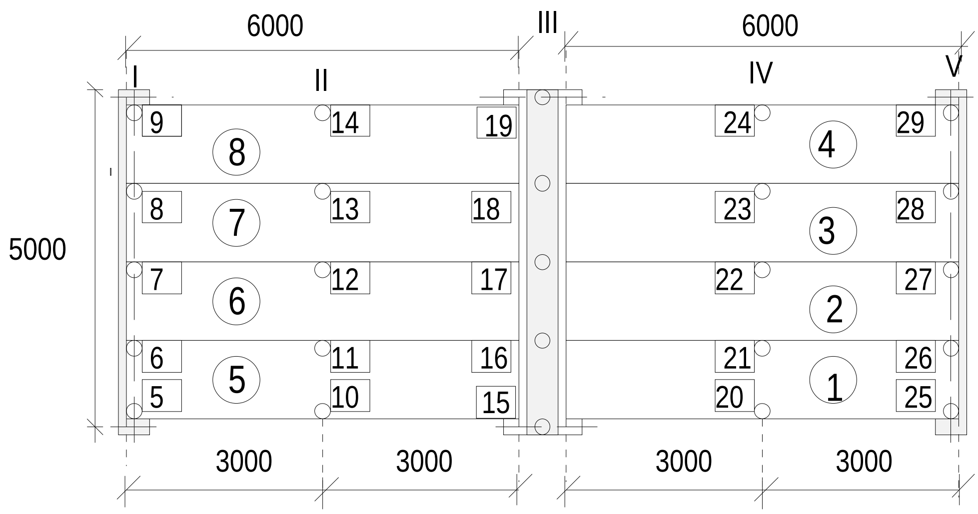

Fig. 20. Location of transducers 5 … 29 for measuring vertical deflection.

3.3
Average strain

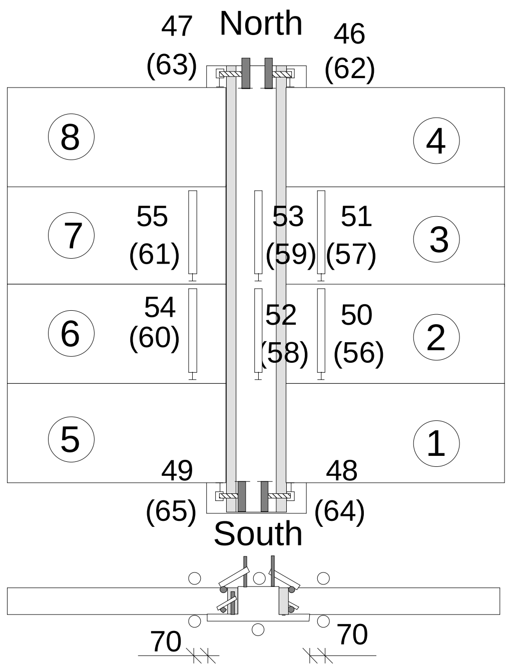

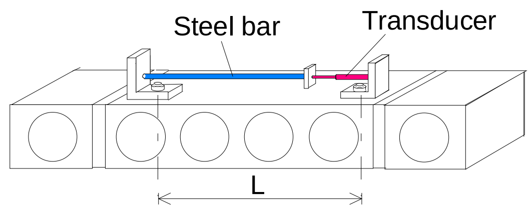

Fig. 21. Apparatus for measuring average strain. L =1120mm and 1060 mm for the bottom and top side transducers, respectively.

Fig. 22. Position of device (transducers 50–61) measuring average strain parallel to the beams. Transducers 46–49 and 62–65 measured the sliding of the outermost slabs along the beam. Numbers in parentheses refer to the soffit of the floor, others to the top side.

3.4
Horizontal. displacements

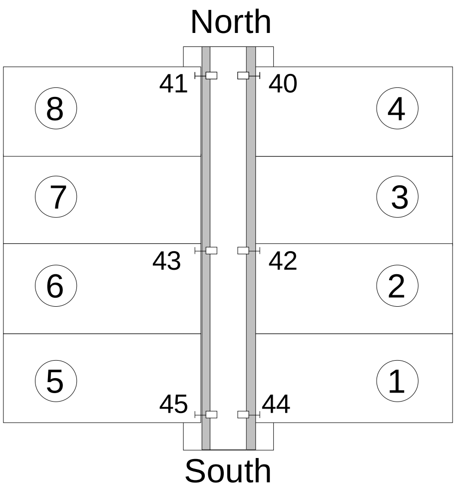

Fig. 23. Transducers 40–45 measuring crack width on the top of the floor.

3.5
Strain

-

4 **Special arrangements**

See 2.7 for the support conditions of the beams.

5 **Loading strategy**

5.1
Load-time relationship

Date of the floor test was 3.3.1994

All measuring devices were zero-balanced when the actuator forces P_i were equal to zero but the weight of the loading equipment was on.

The loading history is shown in Fig. 24. Note, that the number of load step, not the time, is given on the horizontal axis. The loading took 2 h 20 min.

In the following, the cyclic stage (steps 1–16) is called Stage I, the monotonous stage until P_3 = 450 kN Stage II and the final stage with constant P_3 until failure Stage III (steps 34–42).

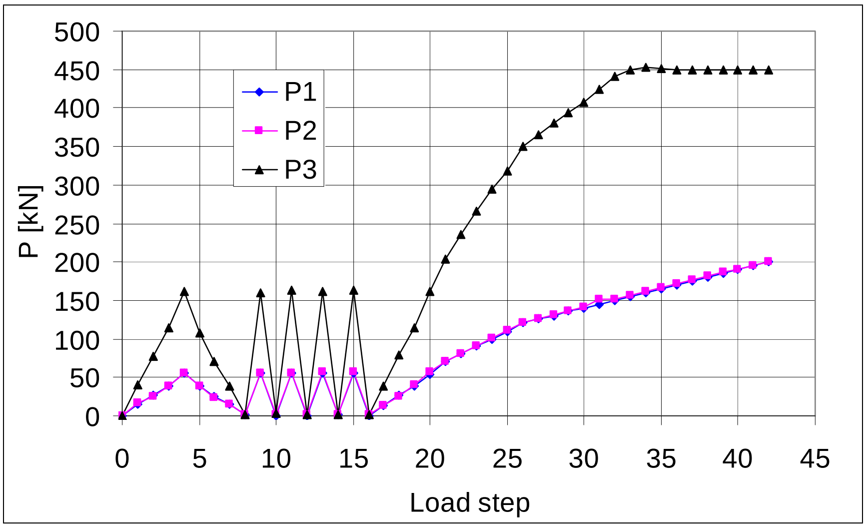

Fig. 24. Development of actuator loads P_i.

The weight of loading equipment per actuator was 1,2 kN and 5,6 kN for actuators P_1 and P_2, respectively. Consequently, the imposed load per slab was

$F_1 = P_1 + 1{,}2$ kN for slabs 2, 3, 6 and 7
$F_2 = P_2 + 5{,}6$ kN for slabs 1, 4, 5 and 8

The weight of the loading equipment below actuator loads P_3 was 0,5 kN and

$F_3 = P_3 + 0{,}5$ kN on the middle beam.

The bending moment between the supports of the middle beam followed closely the elastic bending moment distribution until $P_1 = P_2 = 160$ kN, $P_3 = 450$ kN. Thereafter P_3 was kept constant. The bending moment in the span was roughly equal but opposite to that at supports, see Fig. 25.

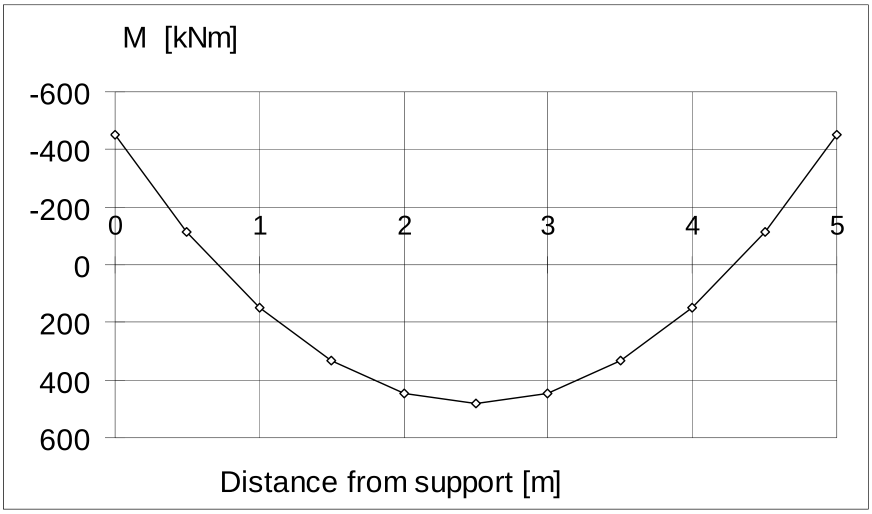

Fig. 25. Bending moment diagram of middle beam between supports at failure.

5.2 After failure	-

6 **Observations during loading**

Stage I	The vertical joints between the slab ends and the middle beam cracked, and at $P_1 = P_2 = 55$ kN these cracks had grown through the whole length of the joint.
Stage II	At $P_1 = P_2 = 110$ kN, the middle beam cracked in flexure at supports.
Stage III	At $P_1 = P_2 = 195$ kN it was observed that the outermost hollow core slabs 1, 4, 5 and 8 were cracked in flexure below the line loads. At $P_1 = P_2 = 200$ kN slabs 1–4 suddenly and simultaneously failed in shear, see Figs 26 & 27 and Appendix A, Figs 7–16. It was impossible to say where the first shear crack appeared.
After failure	When the slabs were removed, it came out that the joint concrete had completely filled the space between the slab and the middle beam, the space under the slab end included.

7	**Cracks in concrete**
7.1 Cracks at service load	Not documented.
7.2 Cracks after failure	 *Fig. 26. Cracks after failure on the top and at the edges of the floor specimen. The numbers refer to the actuator loads P_1.* 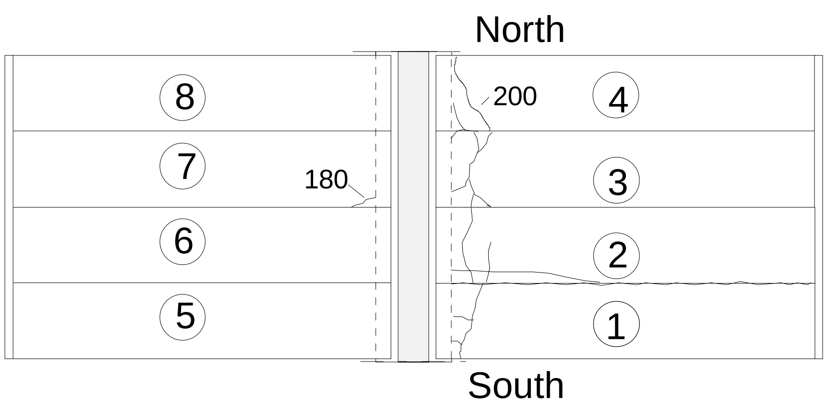 *Fig. 27. Cracks after failure in the soffit. The numbers refer to the actuator loads P_1.*

8	**Observed shear resistance**

The maximum measured support reaction is regarded as the indicator of failure. The failure took place at P_1 = 199,7 kN, P_2 = 200,5 kN or F_1 = 200,9 kN, F_2 = 206,1 kN.

Fig. 28 shows the relationship between the measured support reaction below the South end of the middle beam and the sum of actuator loads on half floor. The effect of the actuator forces P_3 have been subtracted from the measured support reaction, and it is not included in the load on the half floor, either.

The ratio of the reaction to the load is shown in Fig. 29 and in a larger scale in Fig. 30. Based on Fig. 30 it is justified to assume that at failure the support reaction due to the line load is 0,88 times the line load. Assuming simply supported slabs gives the theoretical ratio of 0,84.

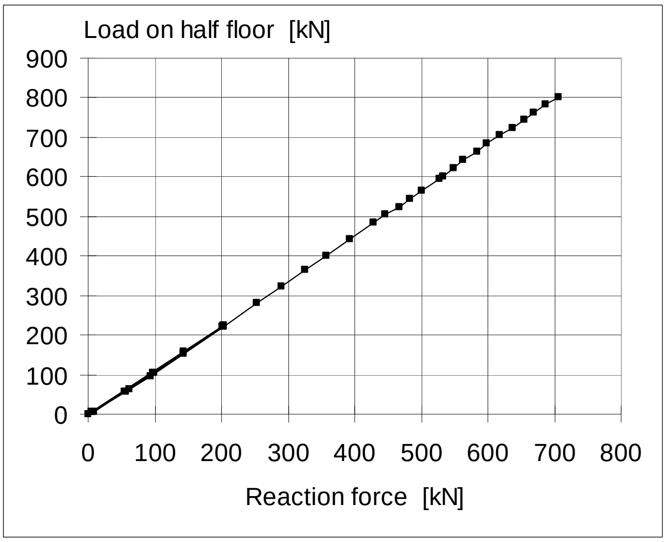

Fig. 28. Stage 1. Support reaction measured below South end of the middle beam vs. load on half floor = 2(P_1 + P_2).

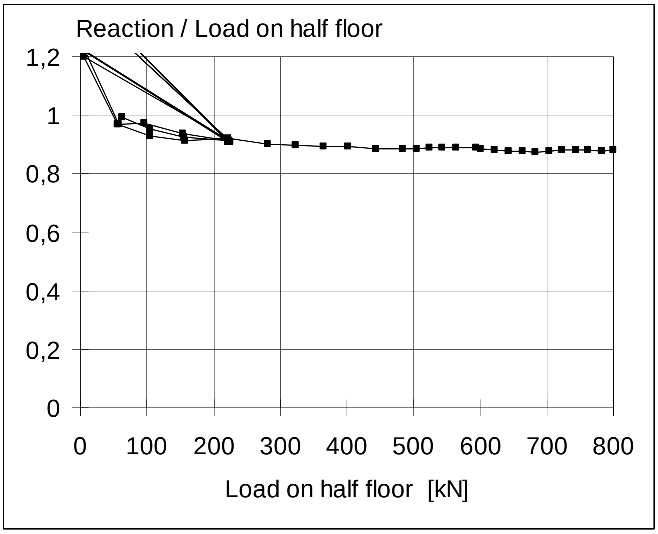

Fig. 29. Ratio of measured support reaction (below South end of the middle beam) to actuator loads on half floor.

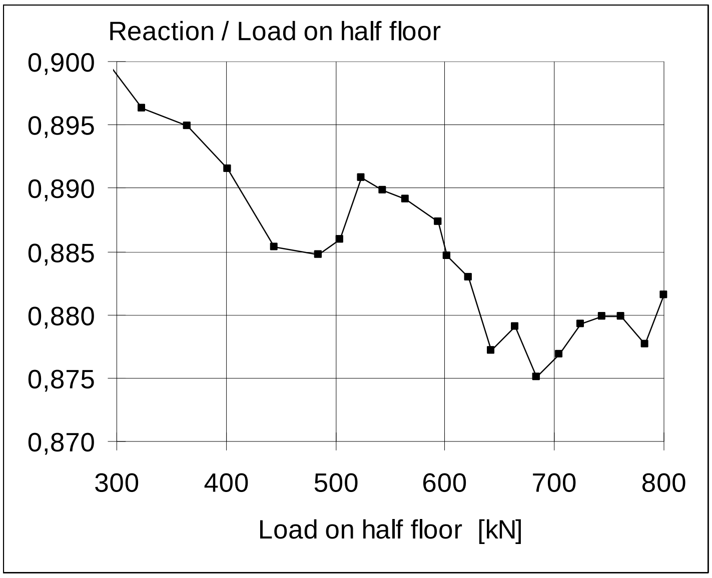

Fig. 30. A part of the previous figure in a large scale.

The observed shear resistance of one slab end (support reaction of slab end at failure) due to different load components is given by

$$V_{obs} = V_{g,sl} + V_{g,jc} + V_{eq} + V_p$$

where $V_{g,sl}$, $V_{g,jc}$, V_{eq} and V_p are shear forces due to the self-weight of slab unit, weight of joint concrete, weight of loading equipment and actuator forces P_1, and P_2, respectively.

It is concluded that the maximum support reaction due to the imposed load on the failed slabs has been V_p = 0,88 x (actuator loads on half floor) / 4 = 0,88 x(199,7 + 200,5) /2 = 176,09 kN. In the same way, the support reaction due to the weight of the loading equipment has been 0,88x(1,2+5,6)/2 = 2,99 kN. $V_{g,jc}$ is calculated from the nominal geometry of the joints and measured density of the grout. When calculating $V_{g,sl}$, the measured weight of the slabs is used. The values of the shear force components are given in Table 1 below.

Table 1. Components of shear resistance due to different loads.

Action	Load	Shear force kN/slab
Weight of slab unit	3,99 kN/m	11,8
Weight of joint concrete	0,17 kN/m	0,5
Loading equipment	(1,2+5,6)/2 kN/slab	3,0
Actuator loads	(199,7+200,5) /2 kN /slab	176,1

The observed shear resistance $\boldsymbol{V_{obs}}$ **= 191,4 kN** (shear force at support) is obtained for one slab unit with width = 1,2 m. The shear force per unit width is $\boldsymbol{v_{obs}}$ **= 159,5 kN/m.**

9 Material properties

9.1 Strength of steel

Component	$R_{eH}/R_{p0,2}$ MPa	R_m MPa	Note
Strands J12,5	1630	1860	Nominal (no yielding in test)
Reinforcement Txy	500		Nominal value for reinforcing bars, no yielding in test
End beams	≈ 350		Nominal value for Fe 52, no yielding in test

9.2 Strength of slab concrete, floor test

#	Cores	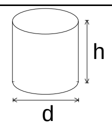	*h* mm	*d* mm	Date of test	Note
6			50	50	11.3.1994	Upper flange of slabs 1, 3 and 5, two cores from each
Mean strength [MPa]			73,4		(+8 d)[1)]	vertically drilled
St.deviation [MPa]			3,1			Tested as drilled[2)] Density = 2388 kg/m^3

9.3 Strength of slab concrete, reference tests

#	Cores	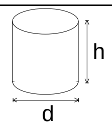	*h* mm	*d* mm	Date of test	Note
6			50	50	11.3.1994	Upper flange of slab 9,
Mean strength [MPa]			65,8		(+8 d)[1)]	vertically drilled
St.deviation [MPa]			2,1			Tested as drilled[2)] Density = 2382 kg/m^3

9.4 Strength of grout in joints and core filling

#	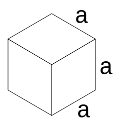	*a* mm	Date of test	Note
3		150	3.3.1994	Kept in laboratory in the same
Mean strength [MPa]		25,2	(+0 d)[1)]	conditions as the floor specimen
St.deviation [MPa]		-		Density = 2177 kg/m^3

9.5 Strength of concrete in middle beam

#	Cores	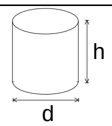	*h* mm	*d* mm	Date of test	Note
6			75	75	11.3.1994	Upper surface of beam,
Mean strength [MPa]			65,3		(+8 d)[1)]	vertically drilled
St.deviation [MPa]			3,1			Tested as drilled[2)] Density = 2425 kg/m^3

[1)] Date of material test minus date of structural test (floor test or reference test)
[2)] After drilling, kept in a closed plastic bag until compression

10	**Measured displacements**
10.1 Deflections	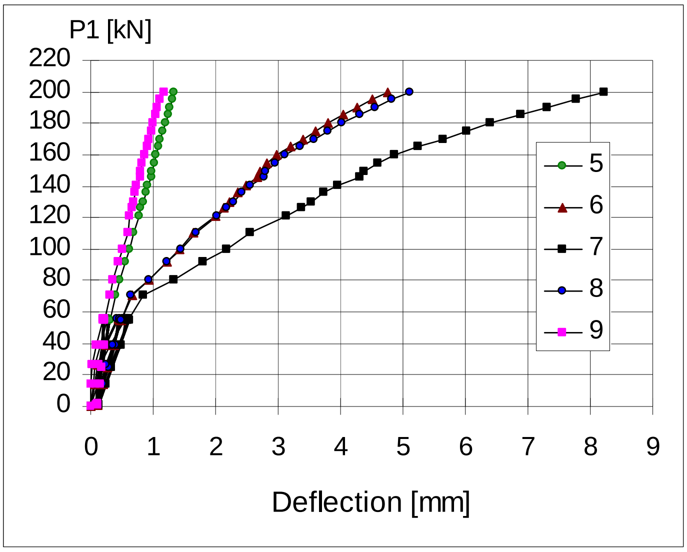 *Fig. 31. Deflection on line I, Western end beam.* 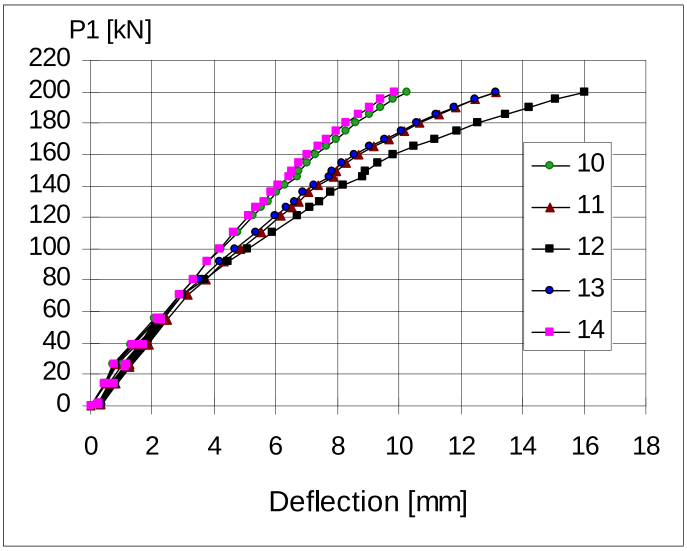 *Fig. 32. Deflection on line II.*

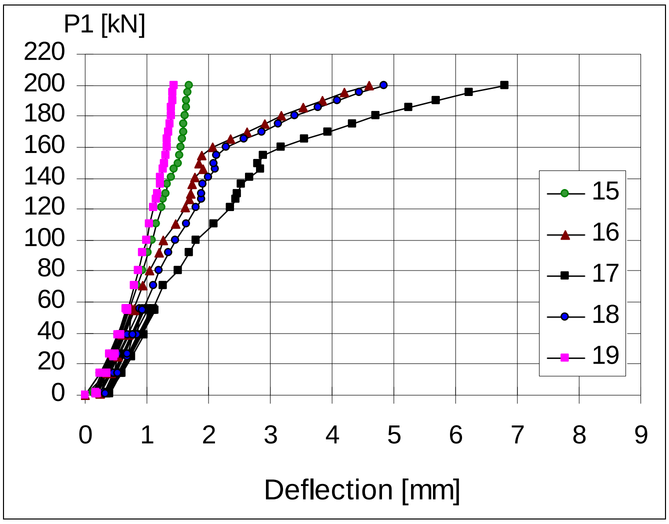

Fig. 33. Deflection on line III, middle beam.

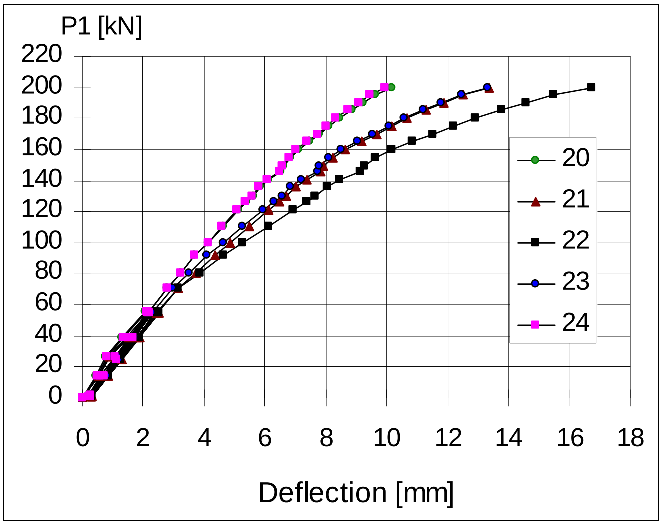

Fig. 34. Deflection on line IV.

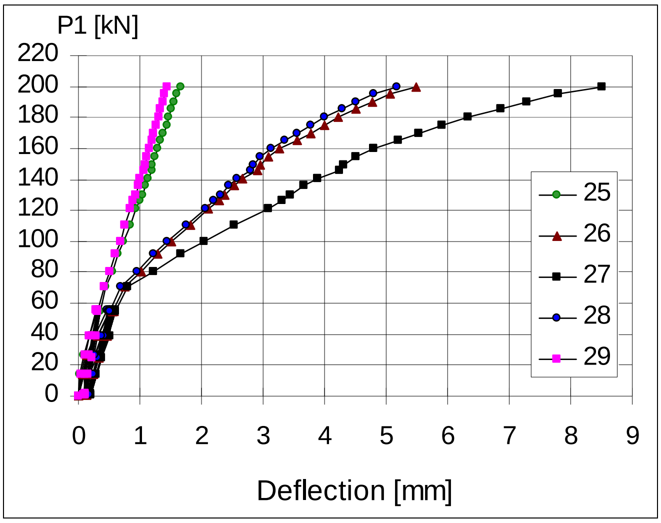

Fig. 35. Deflection on line V, Eastern end beam.

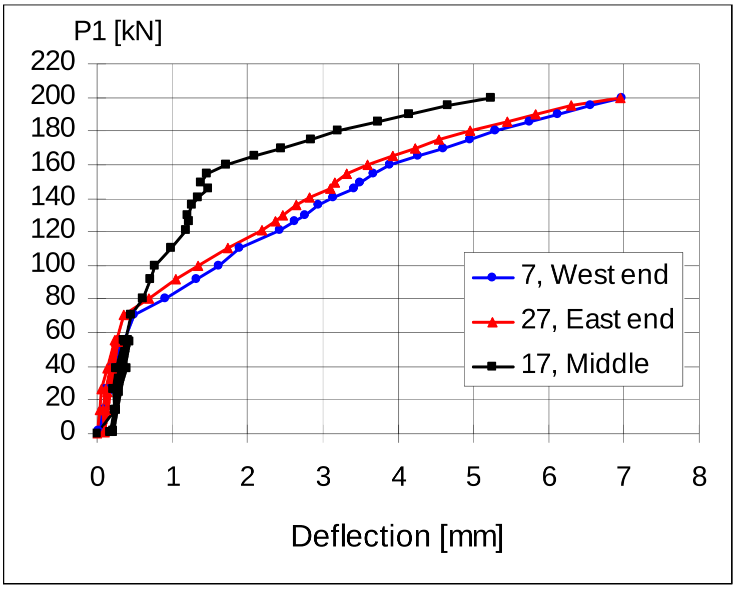

Fig. 36. Net deflection of mid-point of beams (rigid body motion = settlement of beam supports eliminated).

The last measured net deflection of the middle beam before failure was 5,2 mm. This was 1,7–1,8 mm lower than the net deflection of the end beams.

10.2
Crack width

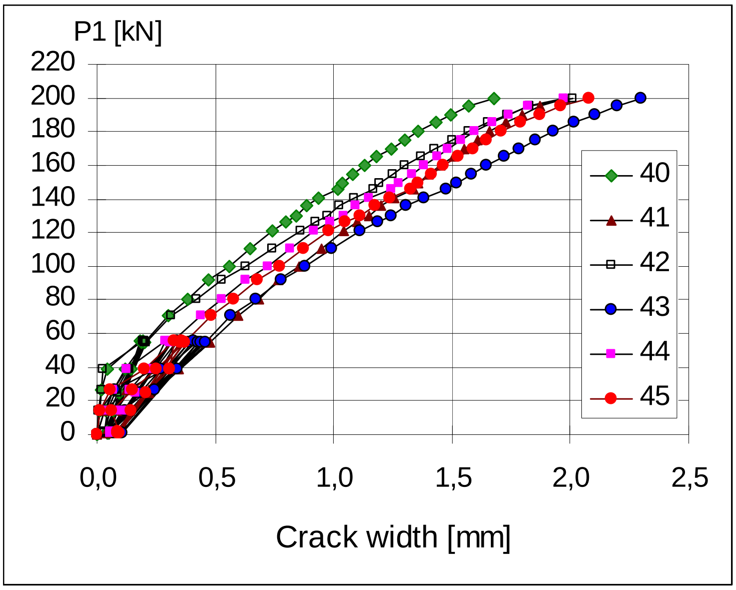

Fig. 37. Differential displacement (≈ crack width) measured by transducers 40–45.

10.3 Average strain (actually differential displacement between slab edges)	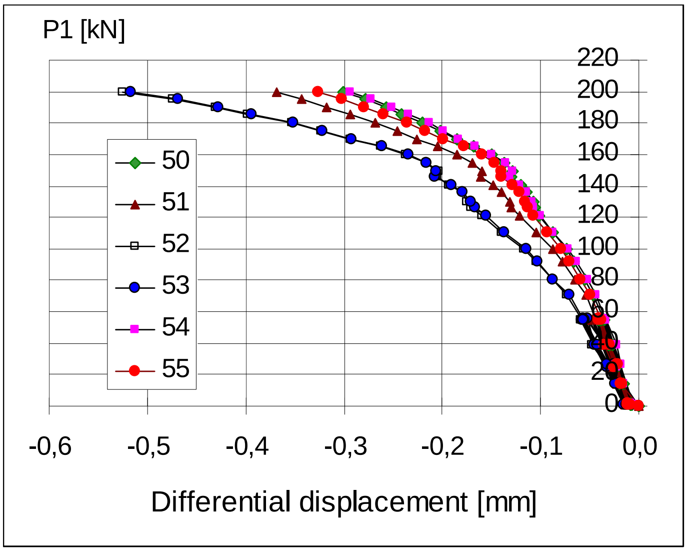 *Fig. 38. Differential displacement at top surface of floor measured by transducers 50–55.* 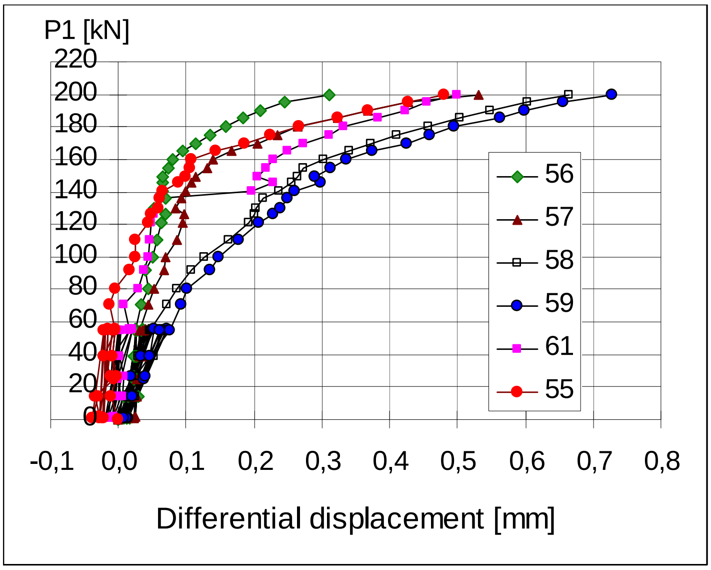 *Fig. 39. Differential displacement at soffit measured by transducers 56–61.*
10.4 Shear displacement between slab edge and middle beam	In Figs 41 and 42 the differential displacements measured by transducers 46–49 and 62–65 are shown. A negative sign means that the slab edge is coming closer to the fixing point of the transducer. Fig. 40 illustrates how the negative curvature and cracking due to negative bending moment at support result in positive values of measured differential displacements on the top edge of the slab.

	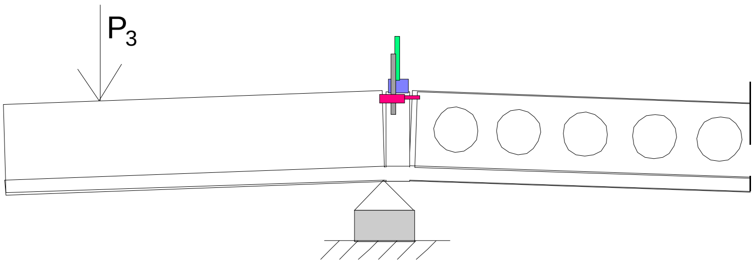 *Fig. 40. Measuring differential displacement on the top of the floor.* 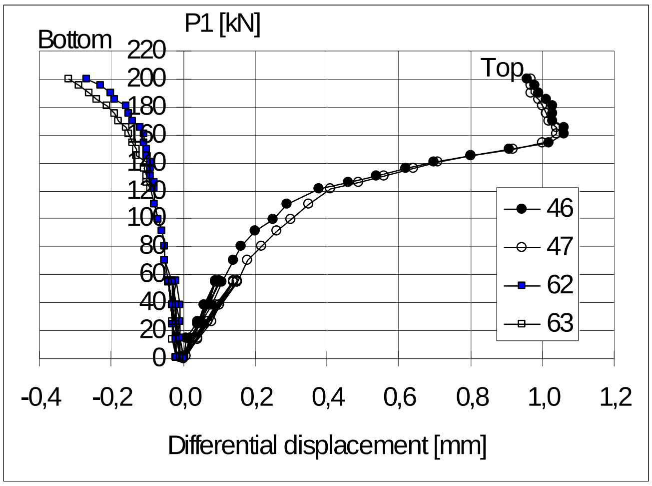 *Fig. 41. North end of middle beam. Differential displacement between edge of slab and middle beam.* 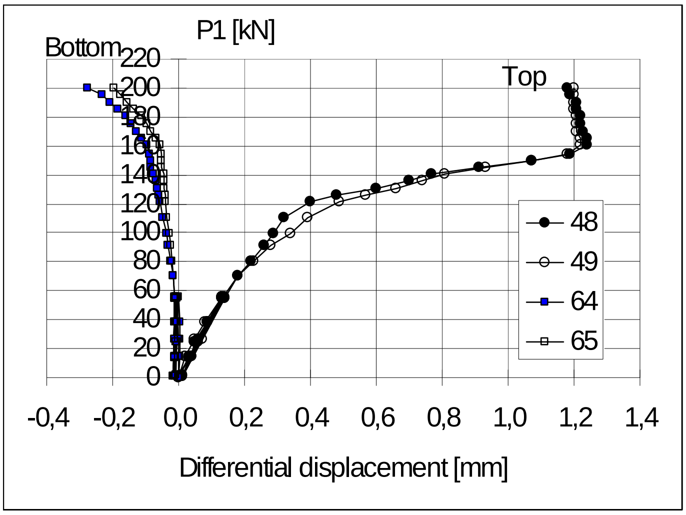 *Fig. 42. South end of middle beam. Differential displacement between edge of slab and middle beam.*
10.5	**Strain** -

11	Reference tests

Both ends of slab 9 were loadedin shear as shown in Fig. 43. The tests were performed after the floor test (3.3.1994) but before the cores were drilled and loaded (11.4.1994). The slip of the outermost strands was measured by transducers 7 and 8. No slip was observed before failure.

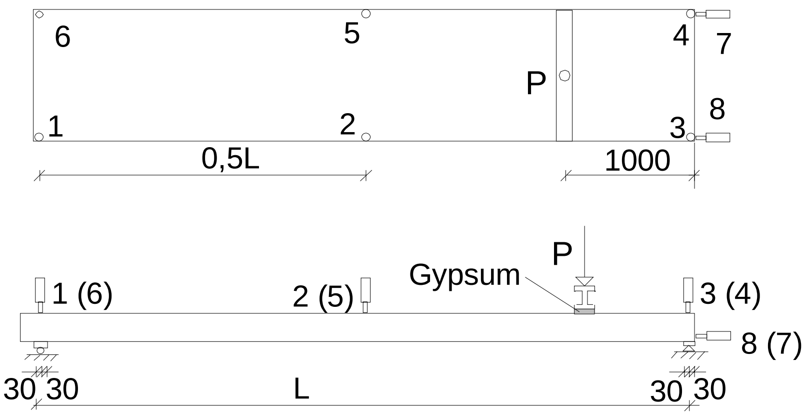

Fig. 43. Layout of reference tests. For L, see Table 2.

Table 2. Span L, ultimate load P_u, shear force due to self weight V_g, shear force due to imposed load V_u, ultimate shear force V_u and failure mode in reference tests. The weight of the loading equipment = 0,5 kN is included in P_u.

Slab	L mm	P_u kN	V_g kN	V_P kN	V_u kN	Failure mode
9.1	5936	211,0	11,9	176,5	188,4	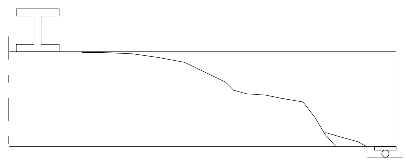 Shear tension failure
9.2	5000	237,1	9,6	191,1	200,7	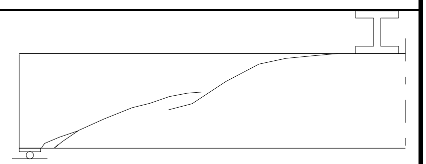 Shear tension failure
Mean					194,6	

12	**Comparison: floor test vs. reference tests**
	The observed shea191,4 kN per one slab unit or 159,5 kN/m. This is **98%** of the mean of the shear resistances observed in the reference tests.
13	**Discussion**
	1. The net deflection of the middle beam due to the imposed actuator loads only (deflection minus settlement of supports) was 5,2 mm or *L*/962 2. The shear resistance measured in the reference tests was of the same order as the mean of the observed values for similar slabs given in *Pajari, M. Resistance of prestressed hollow core slab against web shear failure. VTT Research Notes 2292, Espoo 2005*. 3. Before failure, the net deflection of the end beams was 1,7–1,8 mm greater than that of the middle beam. This is a too small difference to cause considerable torsional stresses in the slabs. 4. The failure mode was an abrupt web shear failure of slabs on one side of the middle beam. No shear cracks were observed before the failure. This is typical of the shear tests carried out on non-flexible supports and different from the behaviour of the other 19 Finnish floor tests reported elsewhere in this working paper. 5. Within the accuracy of the measurements, the shear resistance observed in the floor test was equal to the mean of the resistances observed in the reference tests. This is also different from the behaviour of the other 19 Finnish floor tests.

APPENDIX A: PHOTOGRAPHS

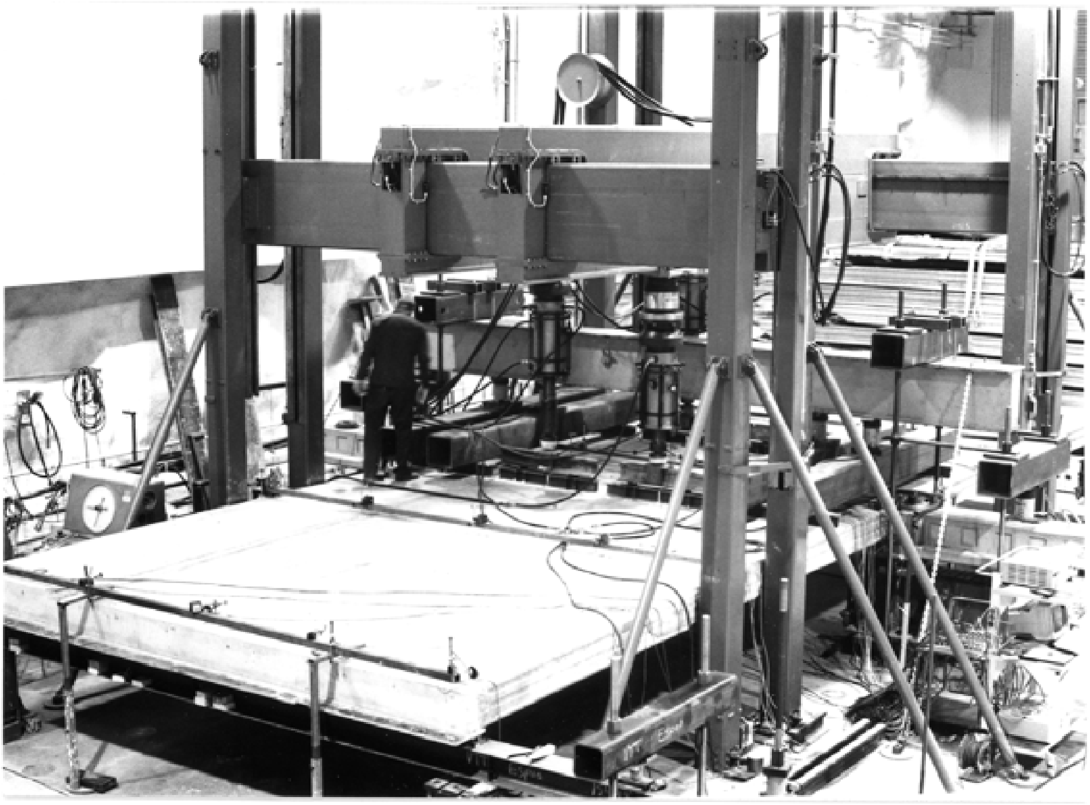

Fig. 1. Overview of test arrangements in floor test.

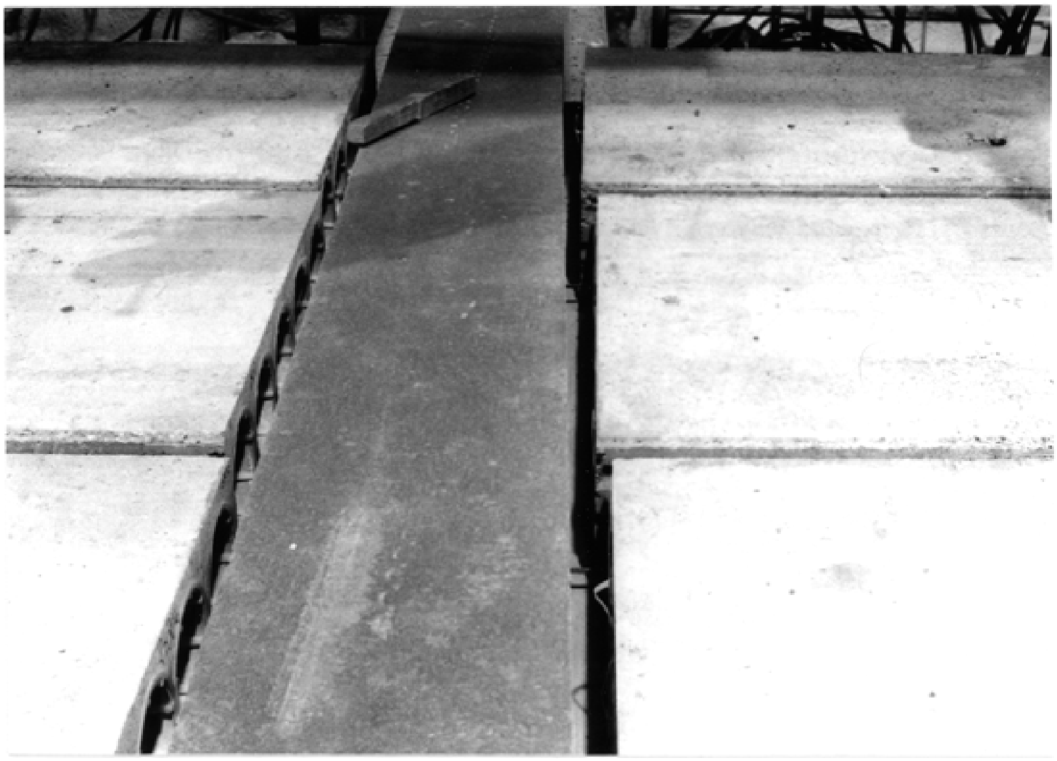

Fig. 2. Skew ends of slab units at middle beam.

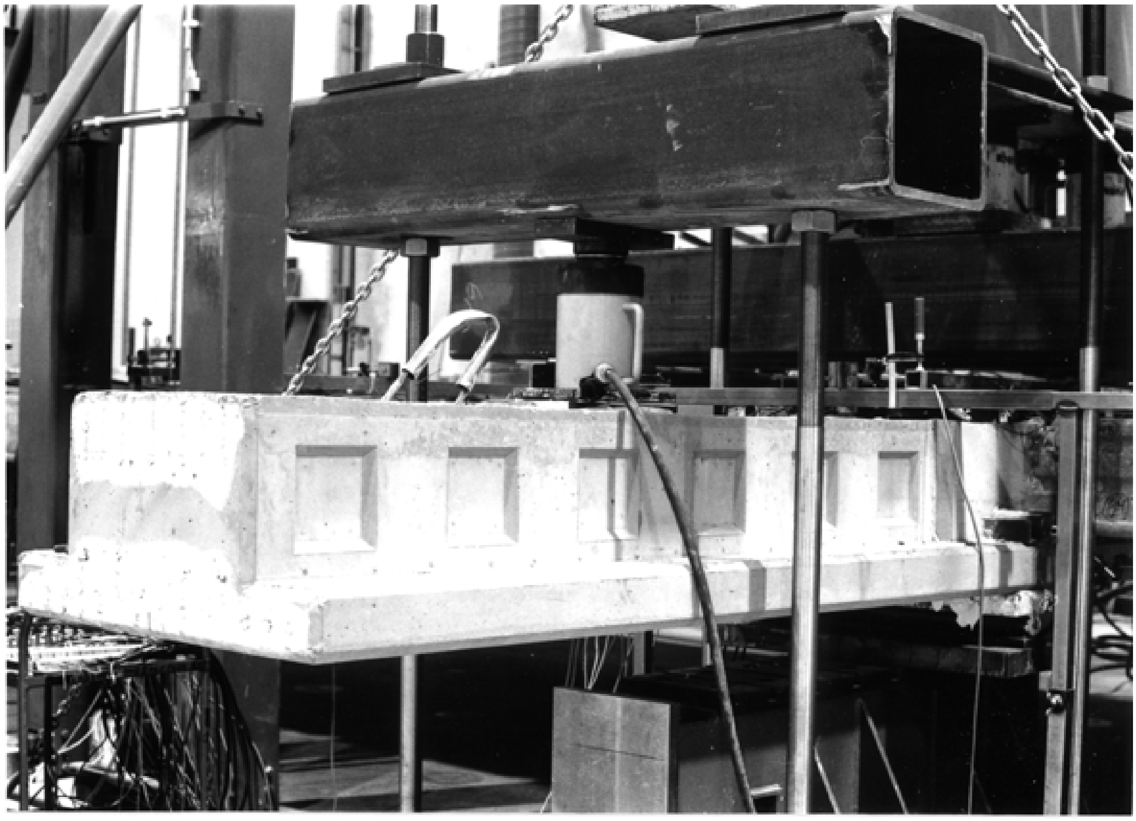

Fig. 3. Hydraulic actuator on end of middle beam.

Fig. 4. Support above end of end beam.

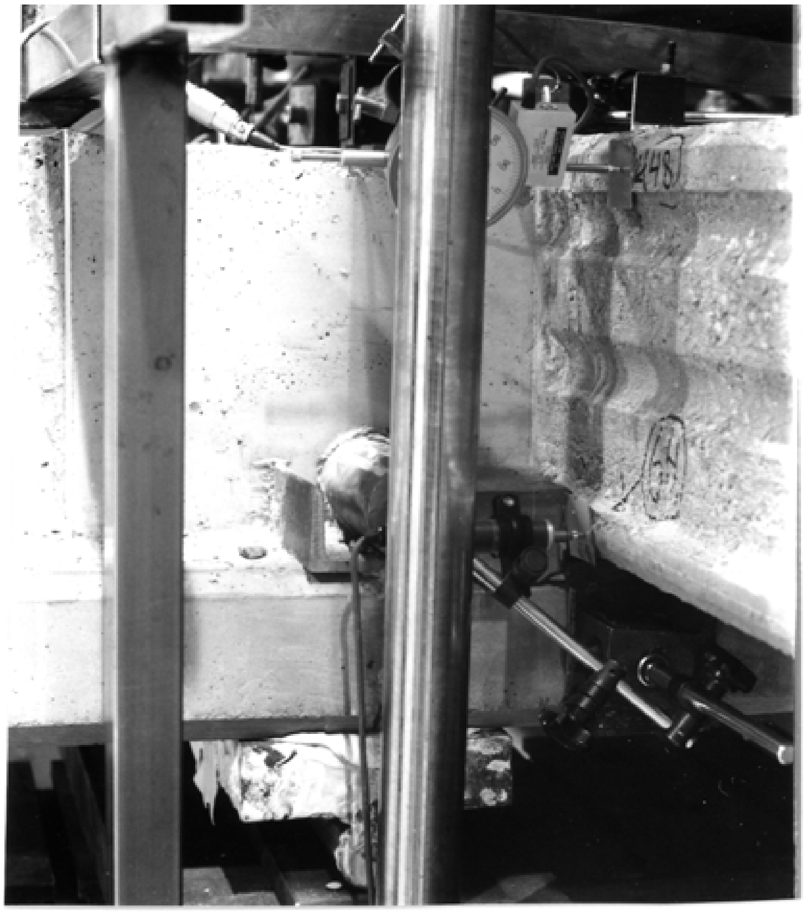

Fig. 5. Equipment for measuring transverse displacement of slab relative to middle beam.

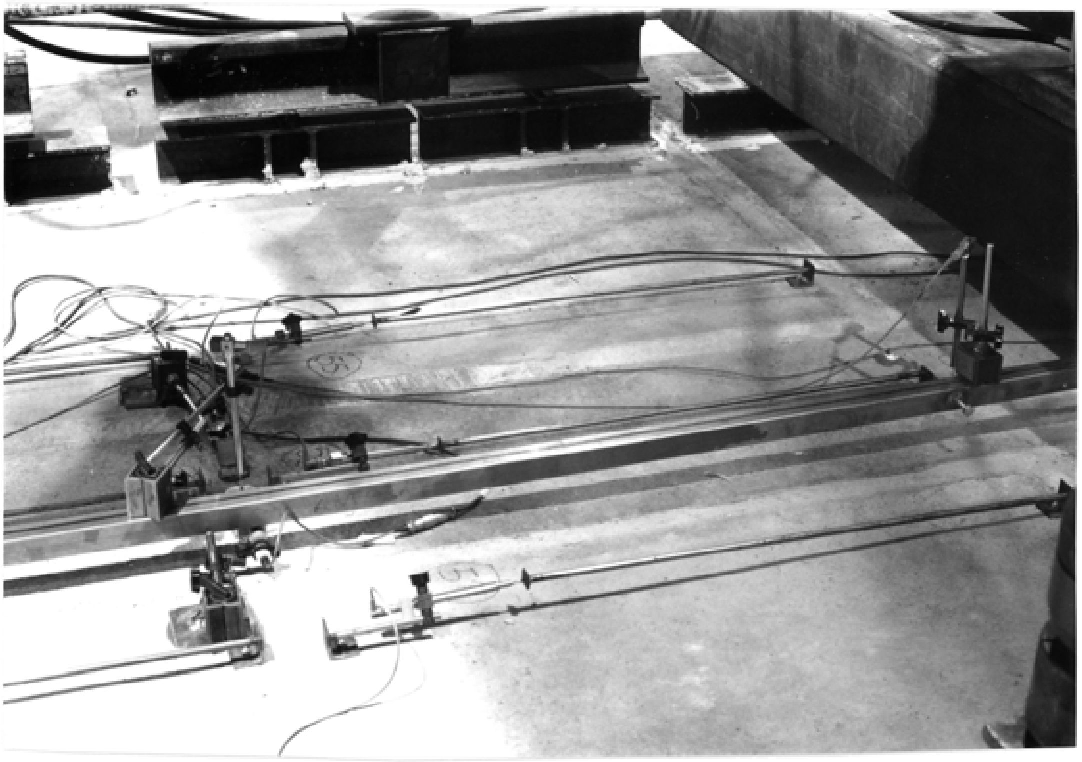

Fig. 6. Equipment for measuring transverse average strain of hollow core units and middle beam.

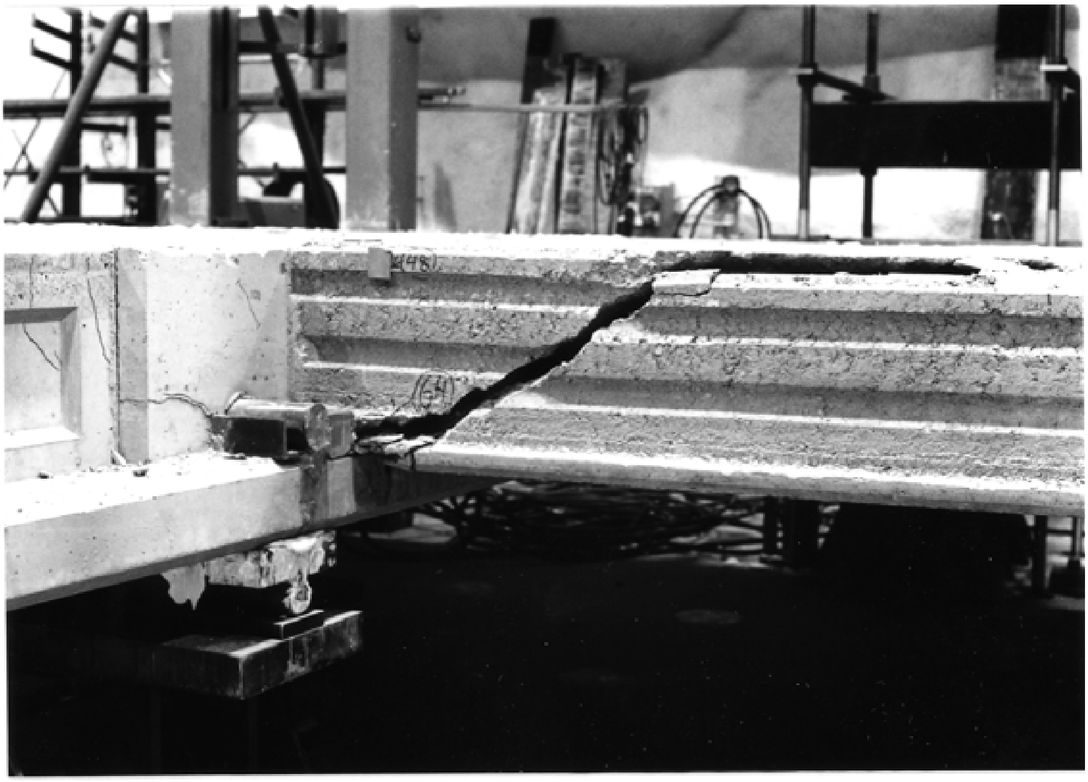

Fig. 7. Shear cracking of slab unit no 1. Note also the flexural cracks in the beam.

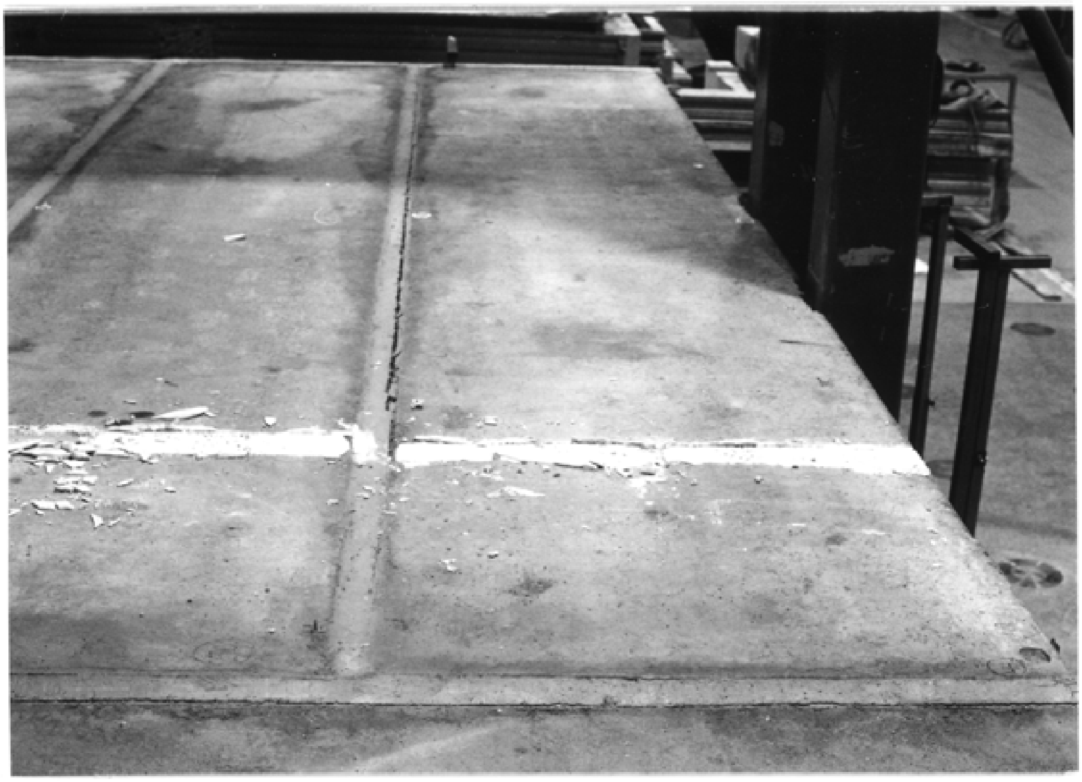

Fig. 8. Cracking pattern of slab unit no 1 seen from above.

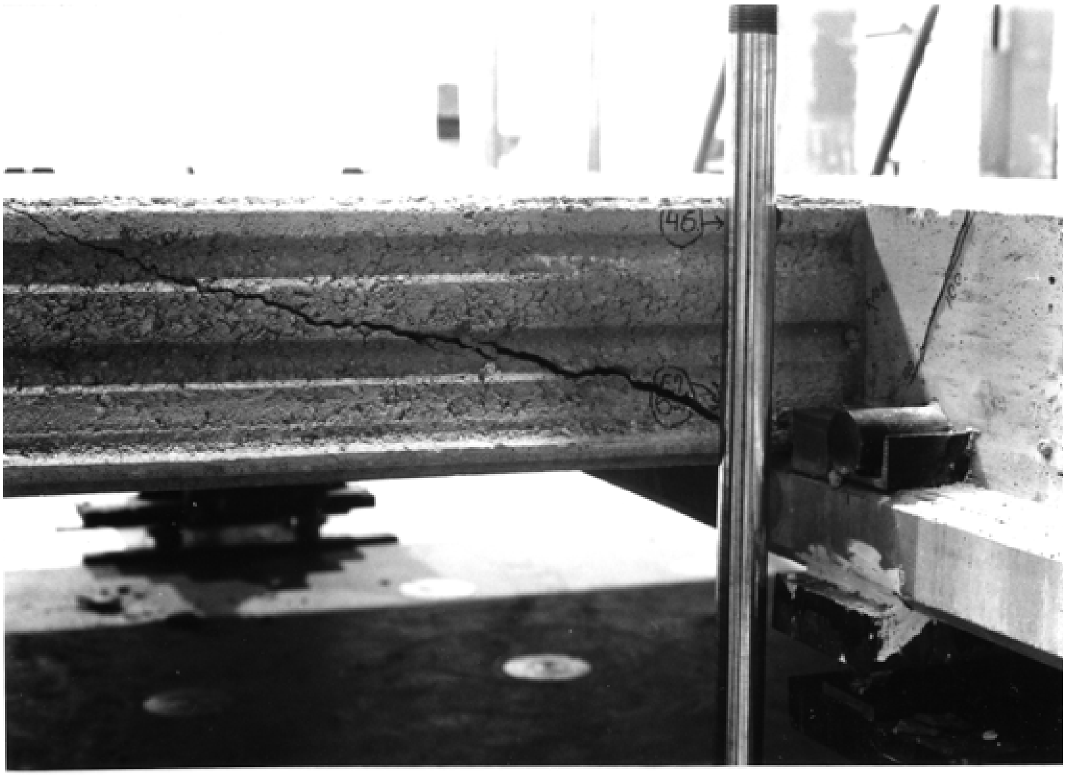

Fig. 9. Failure of slab unit no 4.

Fig. 10. Failure of slab units nos 1 - 4 seen from below.

Fig. 11. Cracks in the middle beam and along the joint between the slab ends and the beam.

Fig. 12. Reference test. Failure of slab unit no 9, end 1, edge 1.

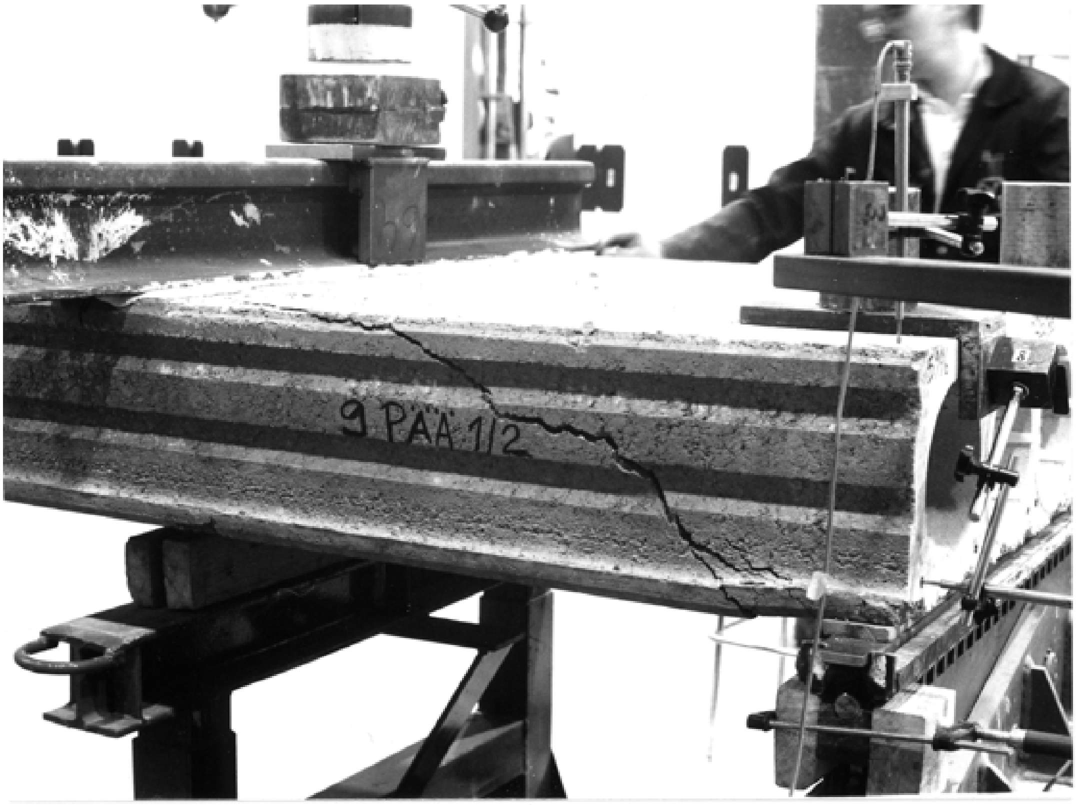

Fig. 13. Reference test. Failure of slab unit no 9, end 1, edge 2.

Fig. 14. Reference test. Failure of slab unit no 9, end 2, edge 1.

Fig. 15. Reference test. Failure of slab unit no 9, end 2, edge 2.

1	**General information**
1.1 Identification and aim	**TUT.CR.MEK.265.1994** **Last update 2.11.2010** MEK265 (Internal identification) Aim of the test: To study the interaction between the MEK beam and hollow core slabs.
1.2 Test type	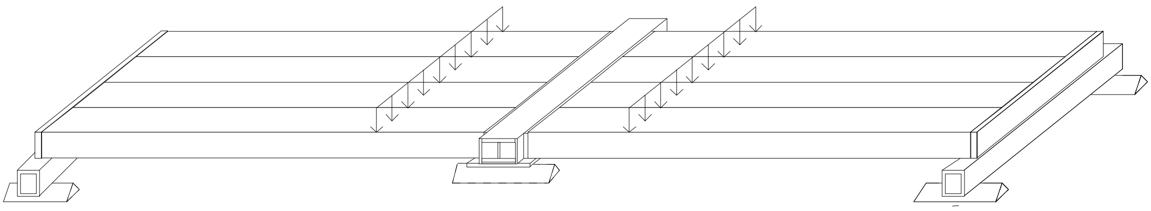 *Fig. 1. Illustration of test setup. MEK beam in the middle, steel beams (square tubes) at the ends.*
1.3 Laboratory & date of test	TUT/FI 15.4.1994
1.4 Test report	Author(s): Iso-Mustajärvi, Pertti Name: *MEK-liittopalkin ja ontelolaaston kuormituskoe (Load test on MEK composite beam and hollow core floor)* Ref. number: Tutkimusselostus N:o 253/94, Tampere University of Technology, Building Construction Date: 20.4.1994 Availability: Confidential, owner is Normek Oy, Hiomotie 10, FI-00380 Helsinki, Finland Note: Figures in this paper have partly been modified (e.g. translation of text) by M. Pajari
2	**Test specimen and loading**
2.1 General plan	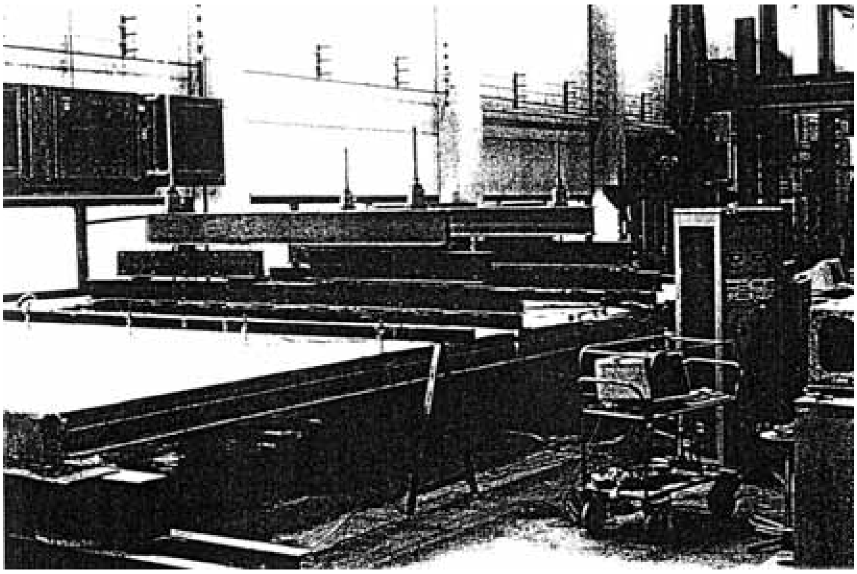 *Fig. 2. Overview.*

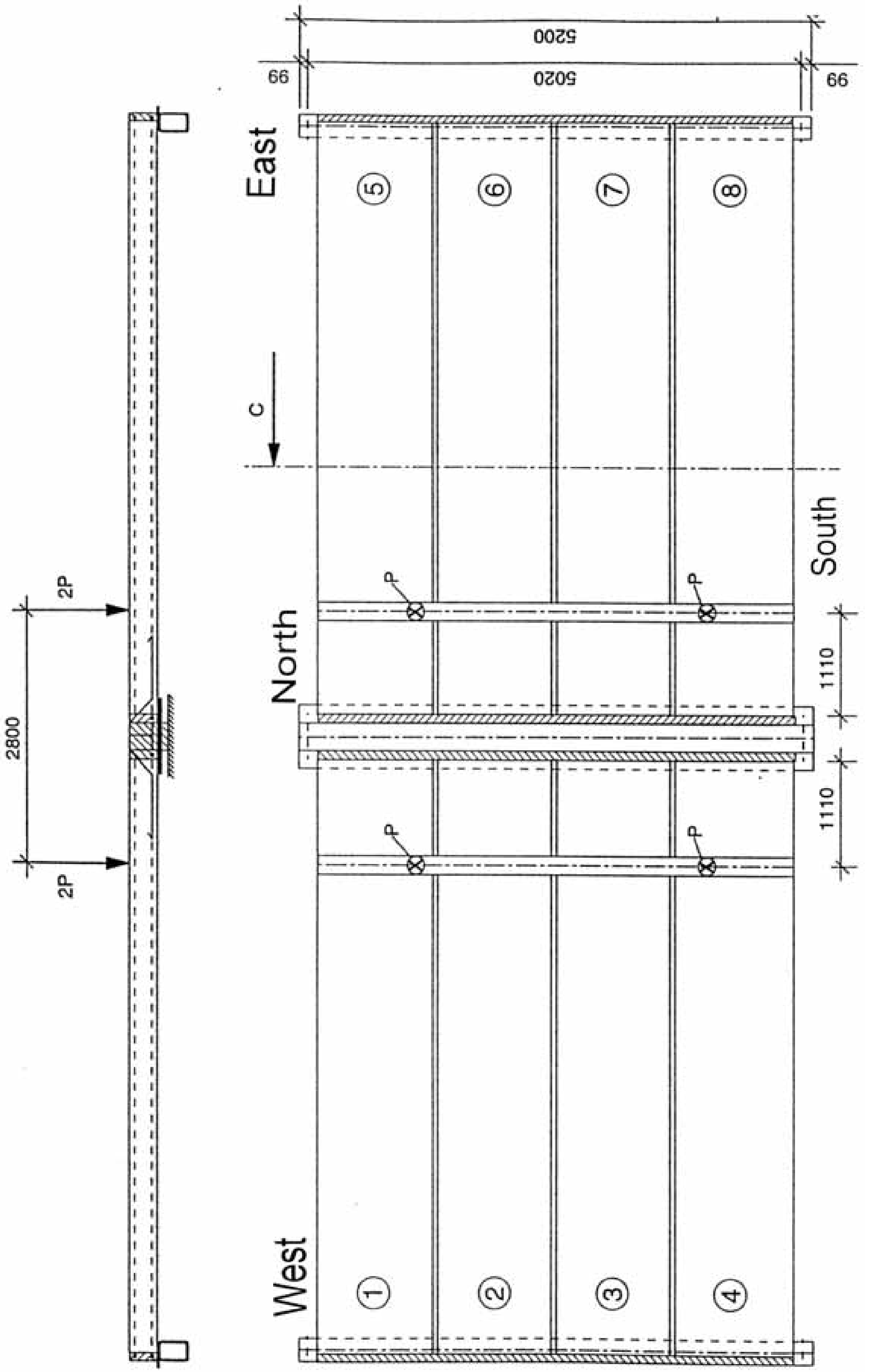
East
West
North
South
5200
5020
99
99
C
2P
2P
2800
P
P
P
P
1110
1110
5
6
7
8
1
2
3
4

Fig. 3. Plan.

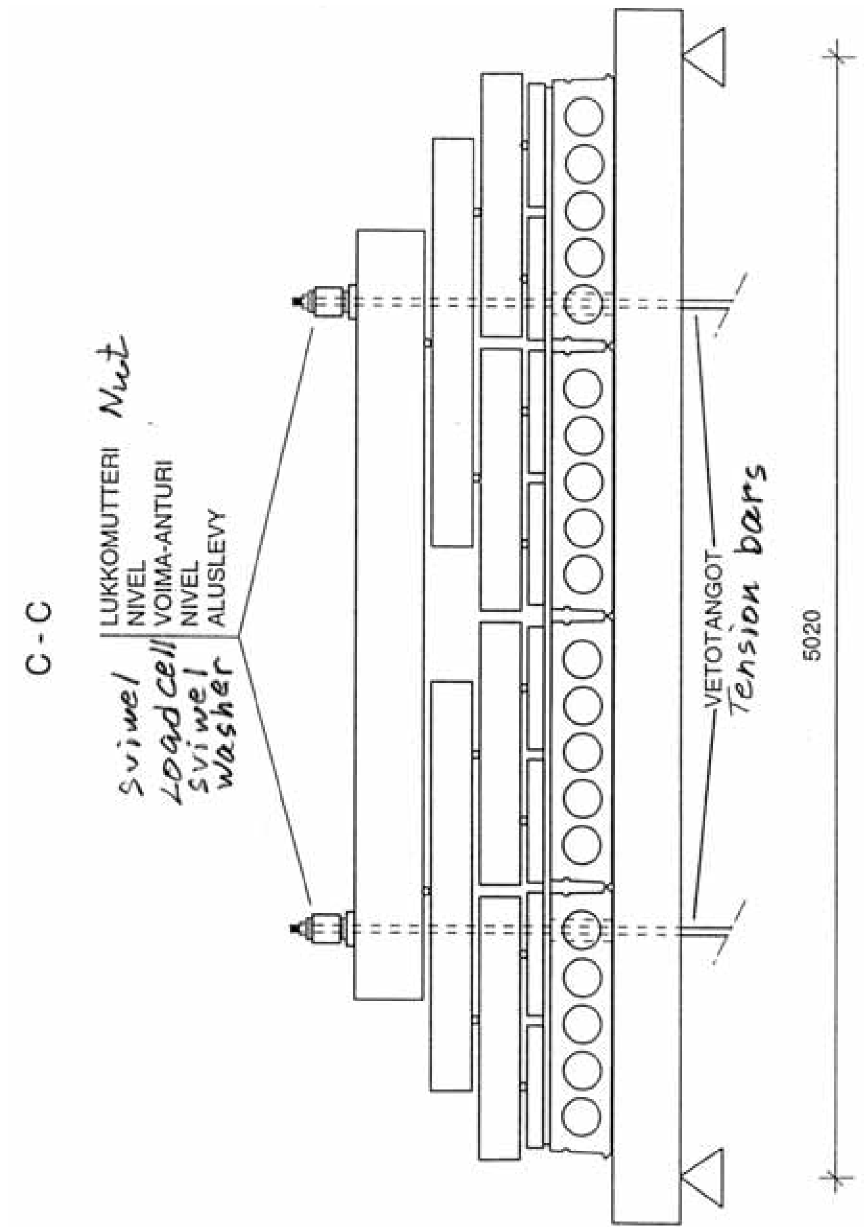

Fig. 4. Section C-C. Loading arrangements.

2.2
End beams

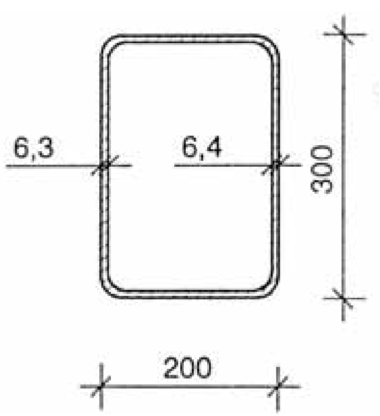

Fig. 5. End beam. Measured dimensions. Steel Fe 52D.

<table>
<tr>
<td></td>
<td>
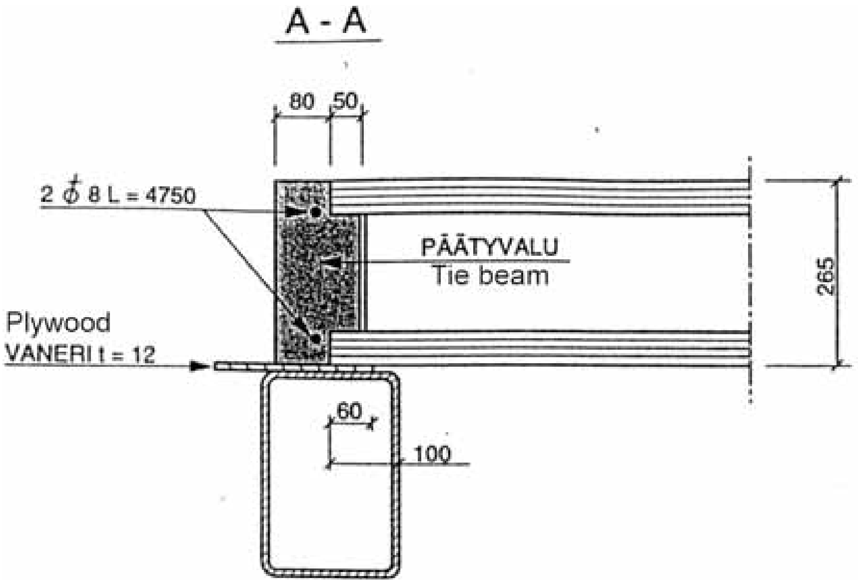

Fig. 6. End beam, section A-A. Measured dimensions. ϕ8 K 1200 refers to reinforcing bars T8 c/c 1200 where 8 is the thickness of the bar in mm.

Simply supported, span = 5,02 m, $f_y \approx$ 350 MPa (nominal f_y)
</td>
</tr>
<tr>
<td>2.3
Middle beam</td>
<td>
Simply supported, span = 5,02 m

The beam comprised a steel component, see Figs 7 and 8, which formed a composite beam with cast-in-situ concrete. The steel component was made of an I-beam, a horizontal plate (bottom flange) below the I-beam and two vertical zig-zag-shaped connector elements, welded to the I-beam and to the bottom plate. The cast-in-situ concrete, cast simultaneously with the grouting of the joints on the 31st of March 1994, filled the empty space between the slab ends laying on the bottom flange.

Concrete: K30, max aggregate size 8 mm

Structural steel: Fe52D

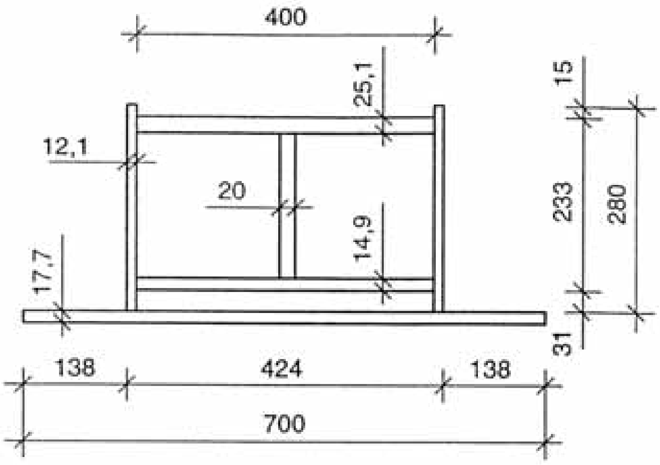

Fig. 7. Steel component of MEK beam. Cross-section.
</td>
</tr>
</table>

<table>
<tr>
<td></td>
<td>
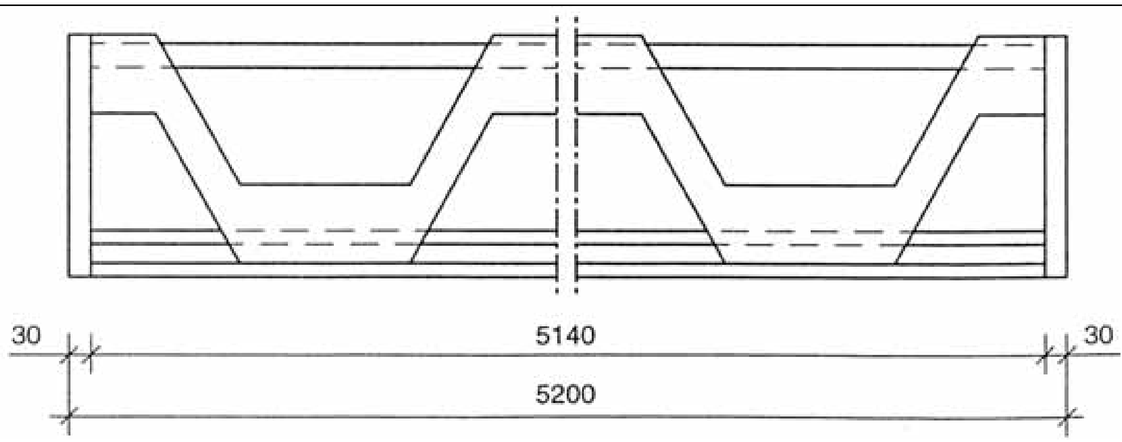

Fig. 8. Elevation. Note the zig-zag-shaped connector element.
</td>
</tr>
<tr>
<td>2.4
Arrangements at middle beam</td>
<td>
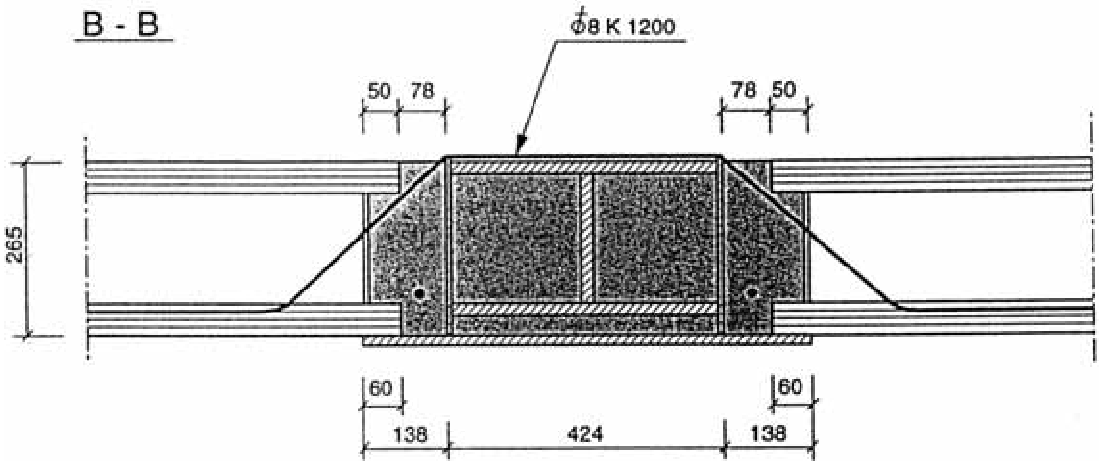

Fig. 9. Section B-B. ϕ8 K 1200 refers to reinforcing bars T8 c/c 1200 where 8 is the thickness in mm.
</td>
</tr>
<tr>
<td>2.5
Slabs</td>
<td>
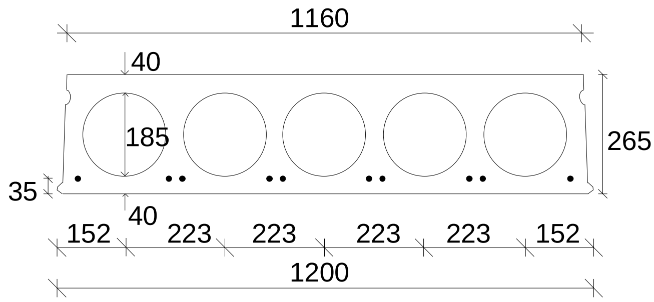

Fig. 10. Nominal geometry of slab units.

- Extruded by Parma Oy, 9 slab elements were delivered to laboratory 11.03.1994
- 10 lower strands J12,5; initial prestress not given in the report but 1100 MPa was a common value at that time

J12,5: seven indented wires, ϕ =12,5 mm, A_p = 93 mm^2
</td>
</tr>
<tr>
<td>2.6
Temporary supports</td>
<td>No temporary supports below beams.</td>
</tr>
</table>

2.7 Loading arrangements	See Figs 2–4. The idea was to create two line loads using four actuators. Two actuator forces loaded one primary spreader beam which distributed the load to two secondary beams. Each secondary beam distributed the load to two tertiary spreader beams and each tertiary beam to two quaternary spreader beams. The quaternary beams were 550 mm long steel tubes with square cross-section 80 mm x 80 mm x 5 mm. The top surface below these beams was evened out with gypsum and a soft wood fibre plate was placed onto the gypsum and below the beams. In this way, a linear line load was created by 8 quaternary spreader beams. The bearings below the primary, secondary and tertiary spreader beams were hinges which also allowed longitudinal displacement at one end of each spreader beam. The fixed hinges were placed symmetrically.
3	**Measurements**
3.1 Support reactions	There were load cells below the South end of the middle beam.

3.2 Vertical displacement	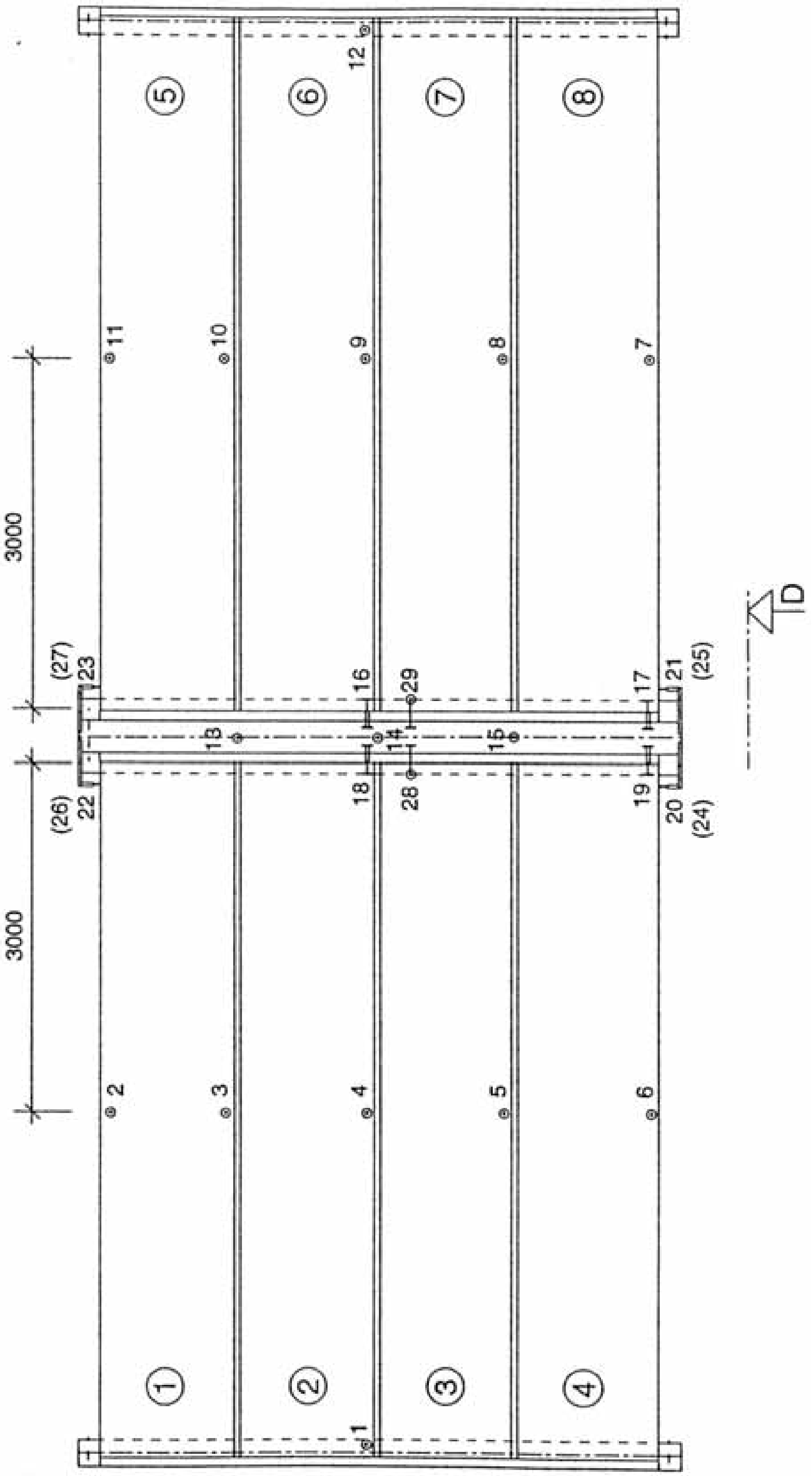 *Fig. 11. Location of transducers 1–15 for measuring vertical deflection and that of transducers 16–28 for measuring differential horizontal displacement.*

	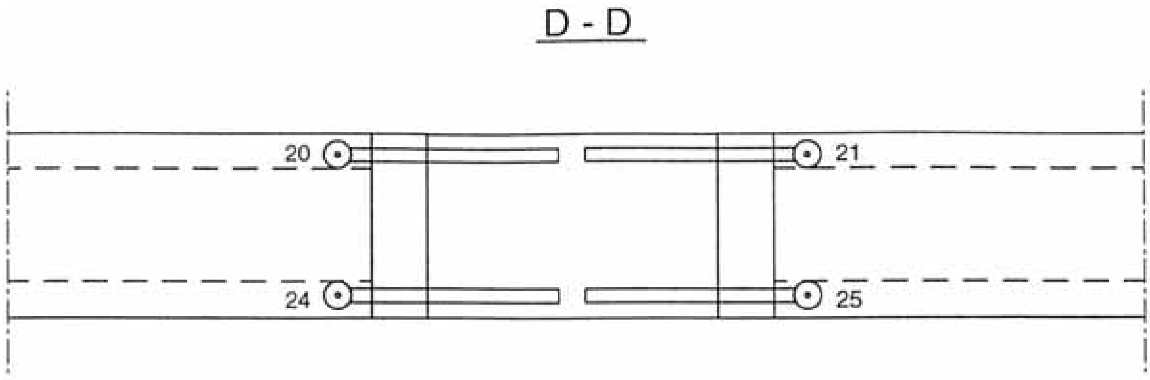 *Fig. 12. Section D-D.*
3.3 Average strain	-
3.4 Horizontal. displacements	See Fig. 11 for the position of the horizontal transducers 16–28.

3.5
Strain

The strains in the floor were measured by strain gauges placed as shown in Figs 13 and 14.

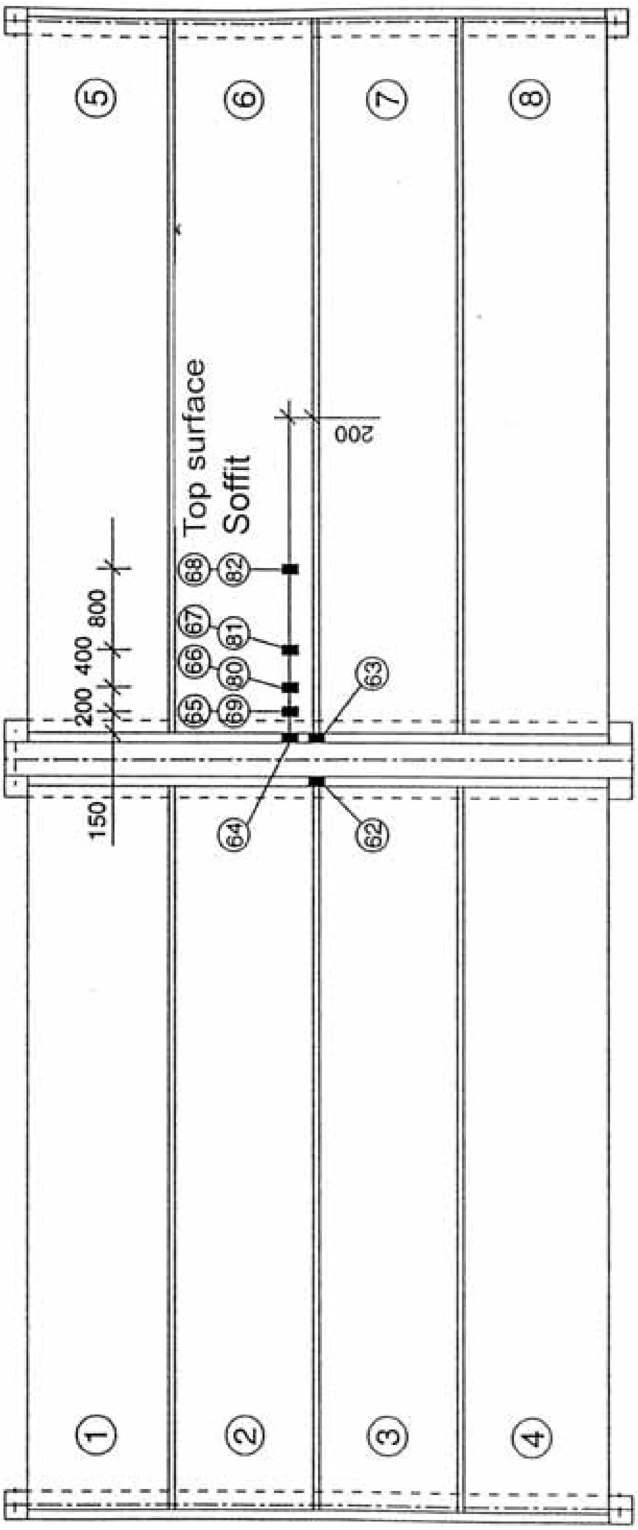

Fig. 13. Position of strain gauges 62 … 69 and 80 … 82.

	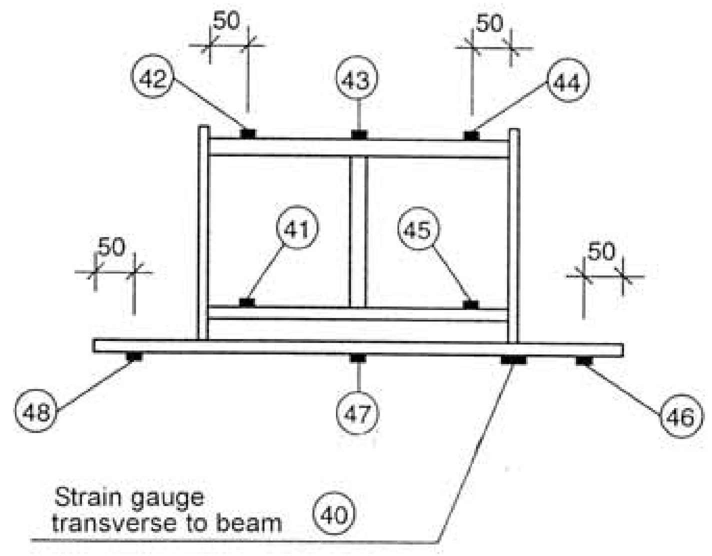 *Fig. 14. Location of strain gauges 40 … 48.*
4	**Special arrangements** - None …
5	**Loading strategy**
5.1 Load-time relationship	Date of the floor test was 15.4.1994. The support reaction, displacements and strains due to the installation of the slab elements, grouting and the weight of loading equipment are given in Sections 10.1 and 10.5. When the actuator forces *P* were equal to zero, all measuring devices were zero-balanced. Thereafter, each actuator force P was increased to 115 kN and reduced back to zero. This load cycle was repeated for four more times (5 cycles altogether) before increasing the actuator load monotonously to P = 324 kN which was the failure load. The cyclic and monotonous stages are called stage I and stage II, respectively.

	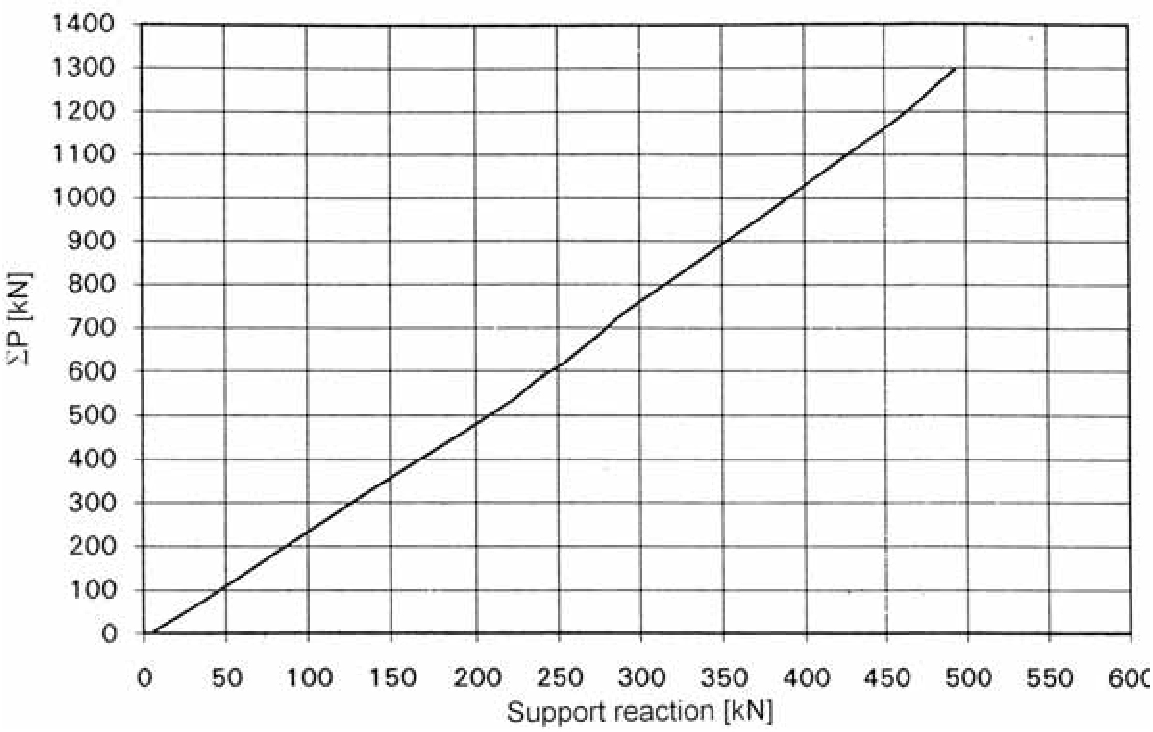 *Fig. 15. Support reaction below South end of MEK beam vs. sum of actuator forces P (= 4P).*
5.2 After failure	
6	**Observations during loading**

Stage I	At P = 91 kN, the first vertical cracks were observed in the tie beams at the ends of the floor. At P = 114 kN the joint concrete cracked along the slab ends next to the MEK beam 1,2 m from the edges of the floor.
Stage II	At P = 172 kN the crack on the East side of MEK beam extended over the whole length of the beam. On the West side the same was true at P = 302 kN. At P = 302 kN cracks also appeared between the joint concrete and the edges of MEK beam. These cracks were at the end of the beam and 1,2 m long. At P = 313 kN an inclined crack was observed at the end of slabs 4 and 8 close to the MEK beam. At P = 324 kN a new inclined crack appeared in slab 8. This crack was on the East side of the previous inclined crack and resulted in shear failure of the floor. The development of the cracks and the failure mode are illustrated in Figs 16–22.

7	**Cracks in concrete**
7.1 Cracks before failure	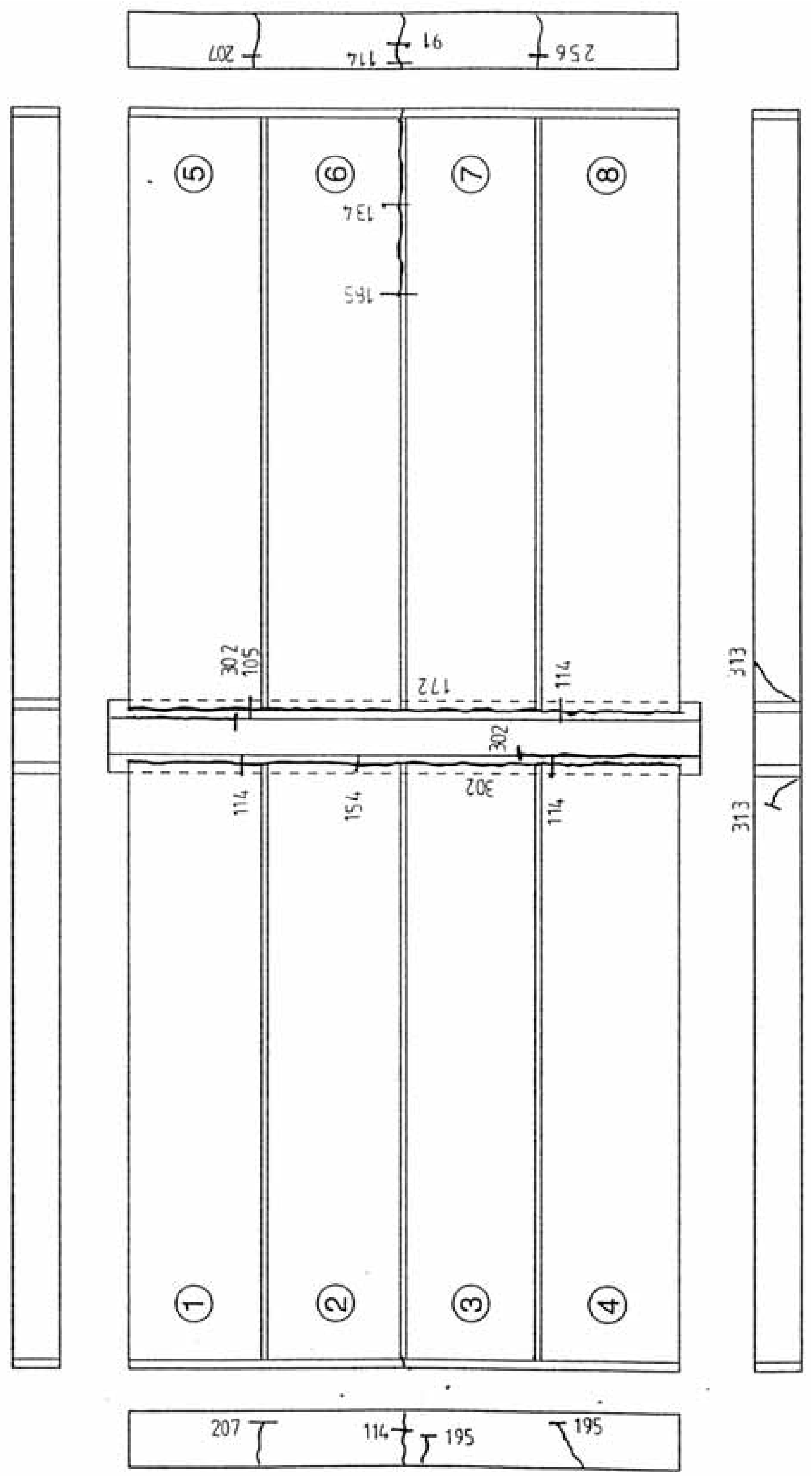 *Fig. 16. Cracks on the top surface and at the edges before failure. The numbers refer to the value of actuator load P.*

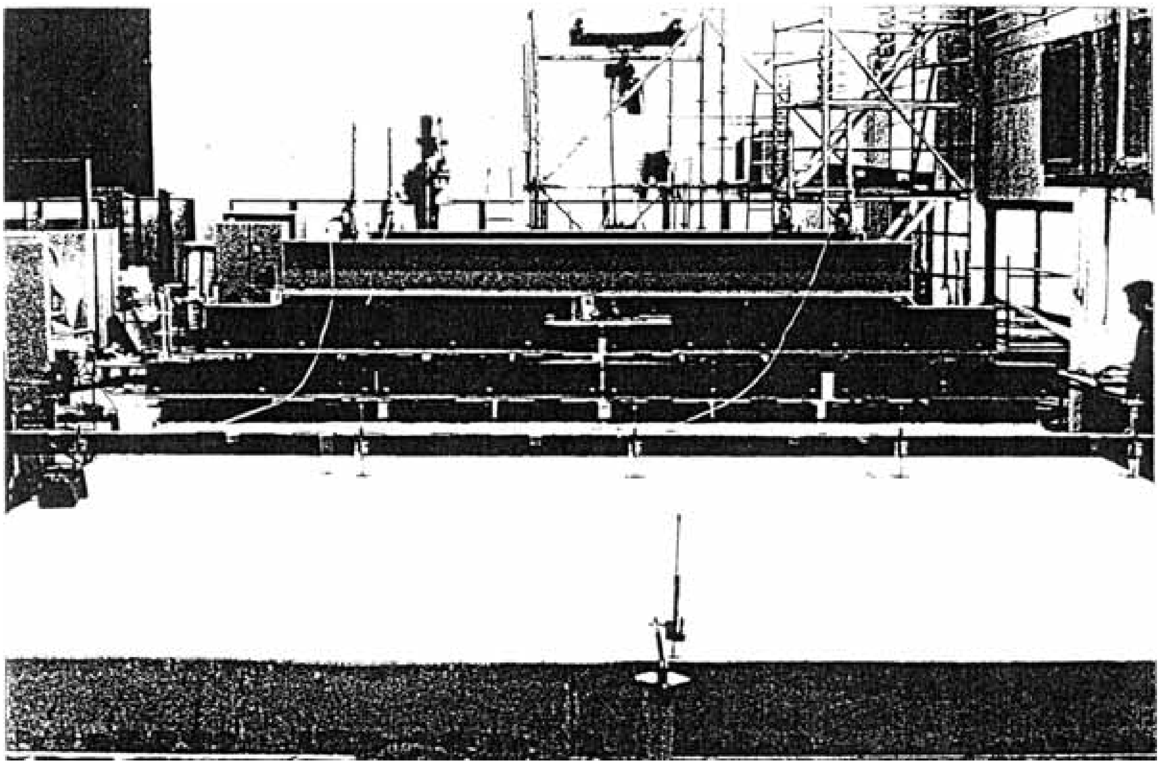

Fig. 17. Cracks in tie beam.

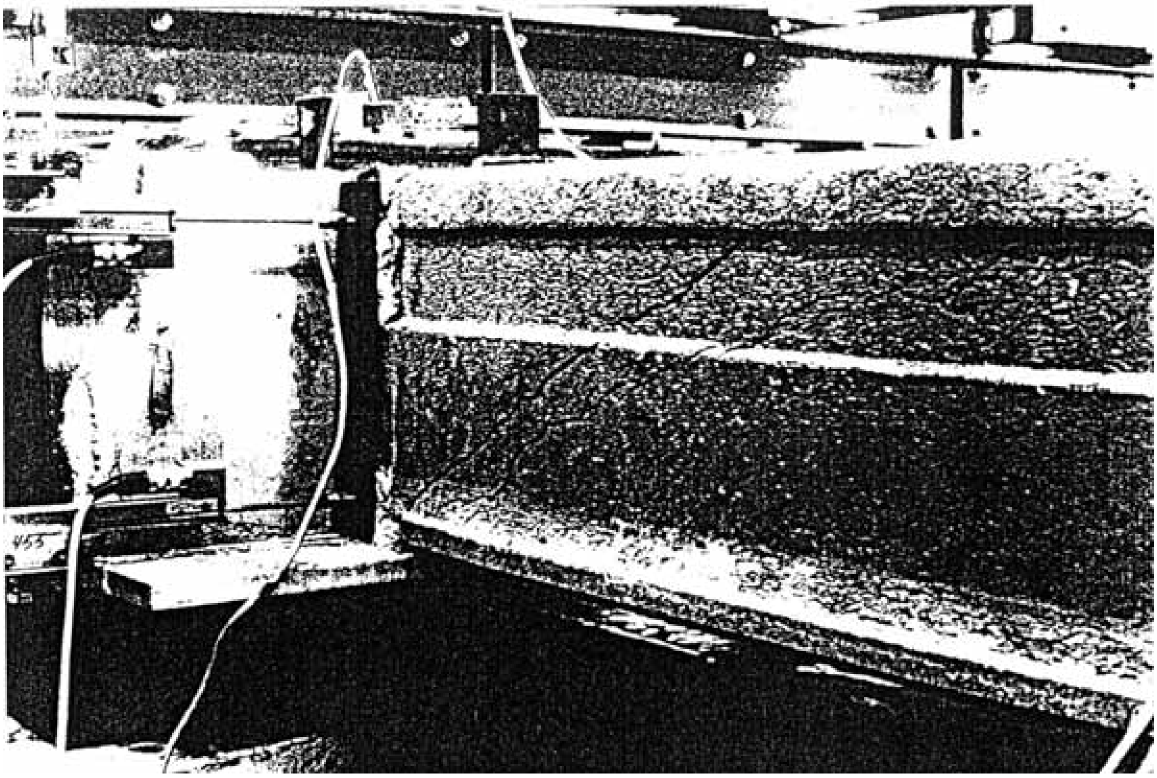

Fig. 18. Inclined cracks in slab 8. The final failure crack on the right.

<table>
<tr>
<td>7.2
Cracks after failure</td>
<td>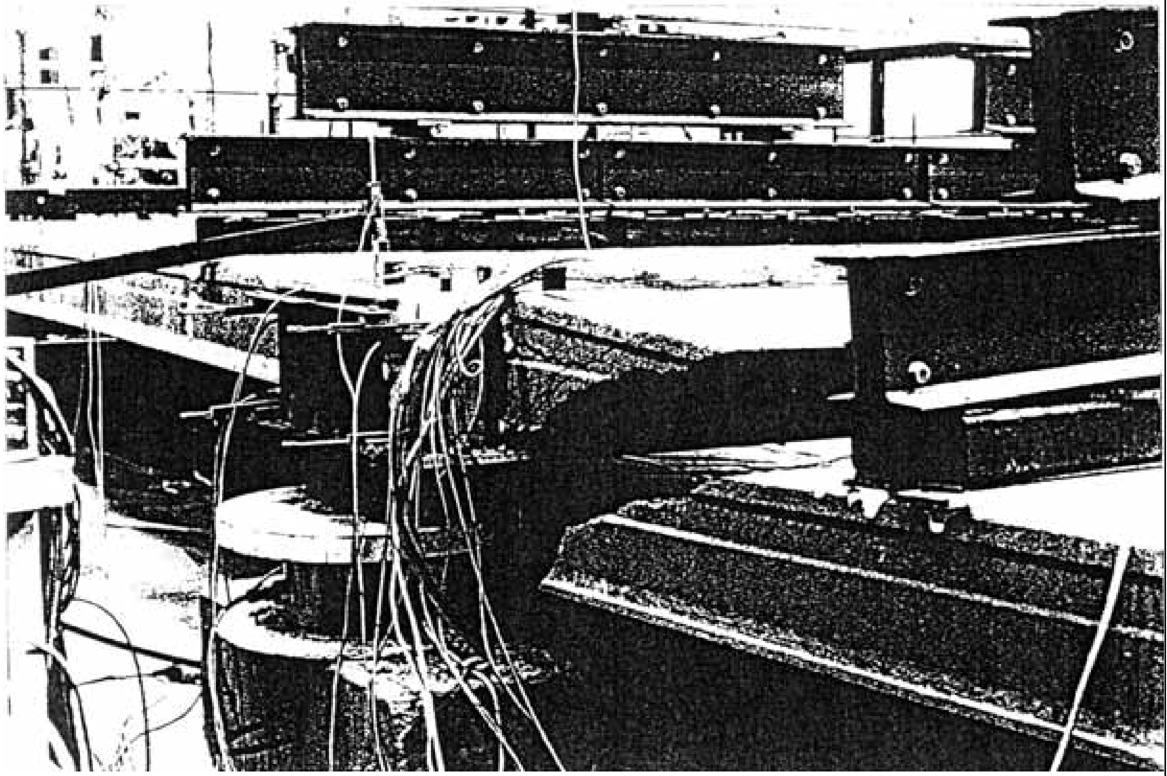
Fig. 19. Failure of slab 8.
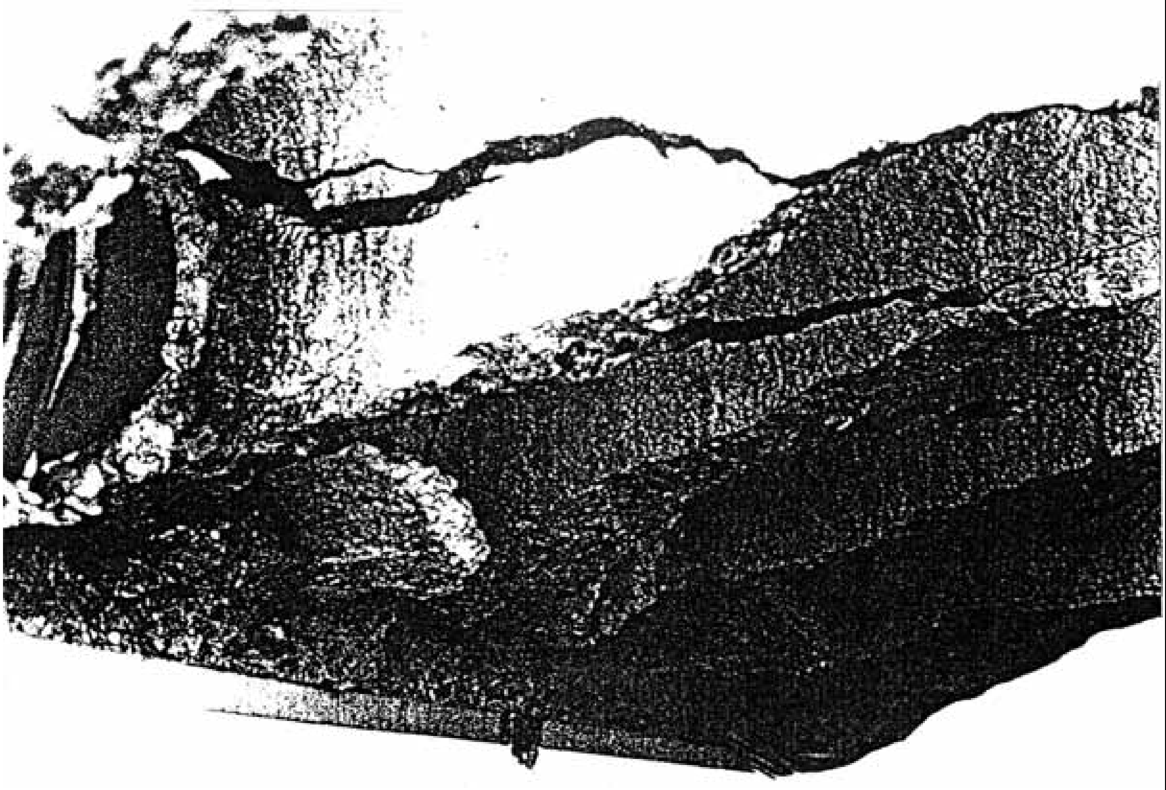
Fig. 20. Failure of slab 8.</td>
</tr>
</table>

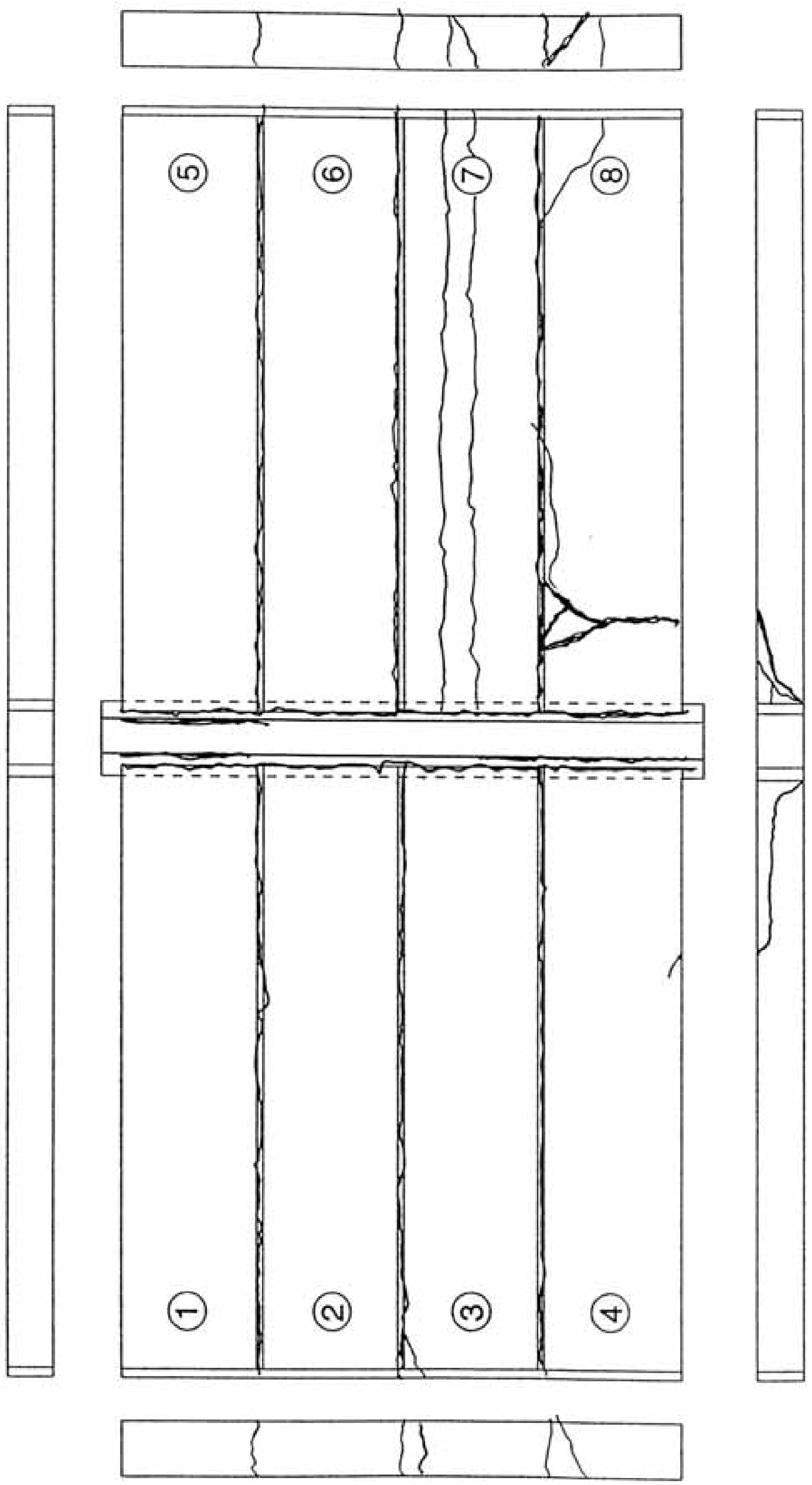

Fig. 21. Cracks after failure on the top and at the edges.

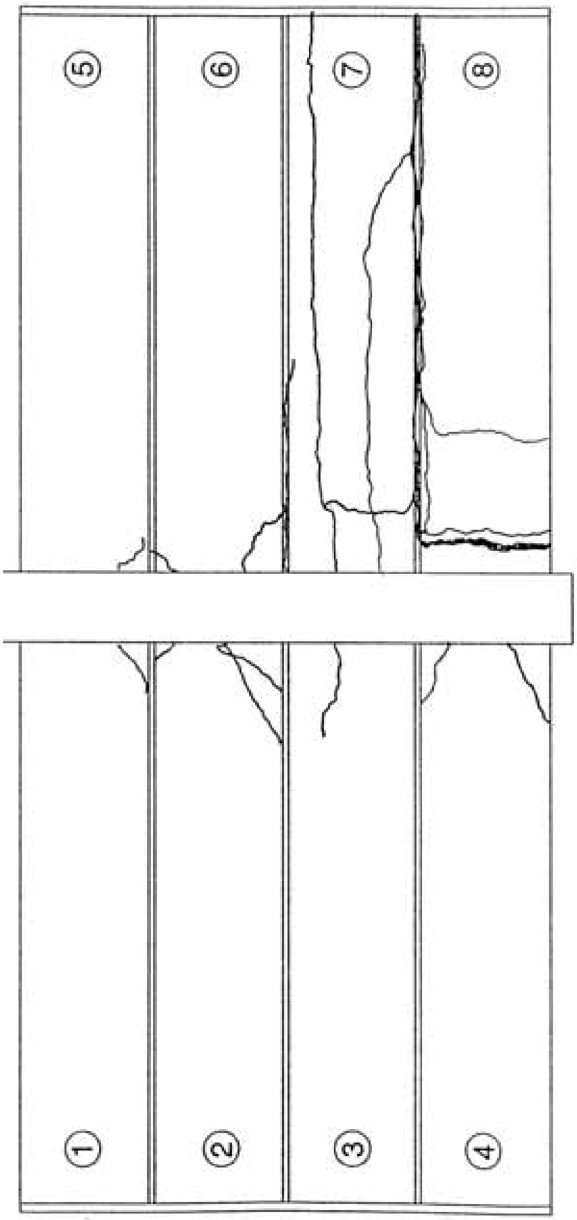

Fig. 22. Cracks after failure in the soffit.

8 Observed shear resistance

The shear resistance of one slab end (support reaction of slab end at failure) due to different load components is given by

$$V_{obs} = V_{g,sl} + V_{g,jc} + V_{eq} + V_P$$

where $V_{g,sl}$, $V_{g,jc}$, V_{eq} and V_P are shear forces due to the self-weight of slab unit, weight of joint concrete, weight of loading equipment and actuator forces P, respectively. In this case the support reaction due to the self weight of the floor and loading equipment was measured directly. Therefore, the weight of the components was not measured. The shear force at failure can be calculated from values given in Table 1 on the next page.

Table 1. Components of shear resistance due to different loads.

Action	Support reaction kN	Shear force kN
Weight of slab unit + Weight of joint concrete + Loading equipment	(65,53)/4	16,4
Actuator loads		131,8

The observed shear resistance V_{obs} **= 148,2 kN** (shear force at support) is obtained for one slab unit with width = 1,2 m. The shear force per unit width is v_{obs} **= 123,5 kN/m.**

9 **Material properties**

9.1 Strength of steel

Component	$R_{eH}/R_{p0,2}$ MPa	R_m MPa	Note
Bottom plate in MEK beam	354 350 358	513 501 518	
Other steel in beams (Fe52D)	≈ 350		Nominal value
Slab strands J12,5	≥ 1550	≥ 1770	Obviously no yielding before failure
Reinforcement T8	500		Nominal value for reinforcing bars (no yielding in test)

9.2 Strength of slab concrete

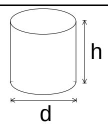

#	Cores		*h* mm	*d* mm	Date of test	Note
3			50	50	15.4.1994 (+0 d)[1)]	
Mean strength [MPa]			60,0			
St.deviation [MPa]						

9.3 Strength of slab concrete, reference tests

Not measured, assumed to be the same as that in the floor test.

9.4 Strength of grout in joints of slab units and in MEK beam

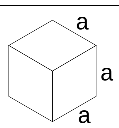

#		*a* mm	Date of test	Note
4		150	15.4.1994 (+0 d)[1)]	Kept in laboratory in the same conditions as the floor specimen
Mean strength [MPa]		33,3		
St.deviation [MPa]		0,96		

[1)] Date of material test minus date of structural test (floor test or reference test)

10 **Measured displacements**

In the following figures, *P* stands for the actuator load in one actuator. Only the monotonous loading stage after the cyclic stage is shown.

10.1
Deflections

Table 2. Support reaction below South end of MEK beam and deflection measured by transducers 13–15, both due to installation of hollow core slabs, grouting and loading equipment.

Reaction kN	13 [mm]	14 [mm]	15 [mm]	40 [0,001]	41 [0,001]	42 [0,001]
65,53	3,05	4,04	3,26	-0,491	0,129	-0,122

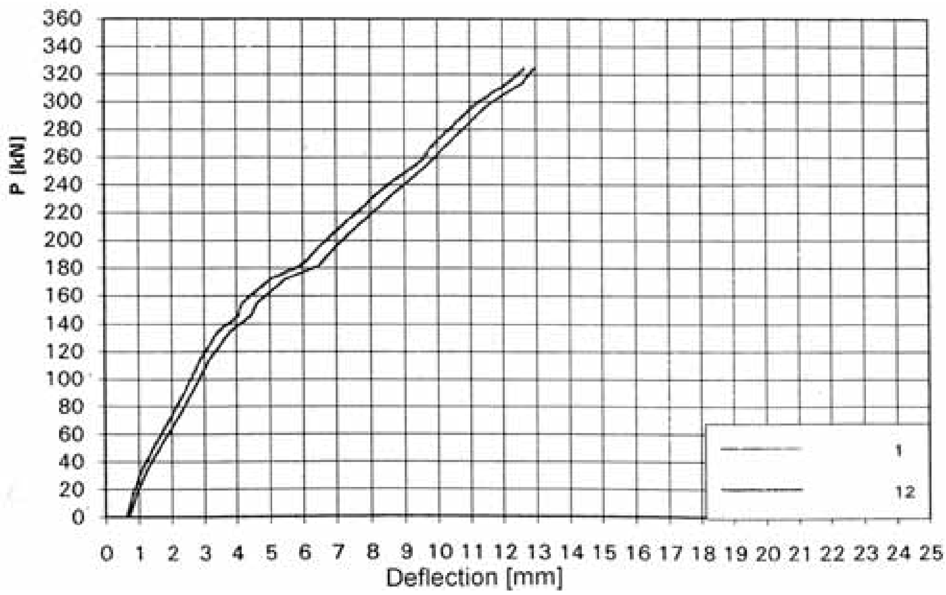

Fig. 23. Mid-point deflection of end beams.

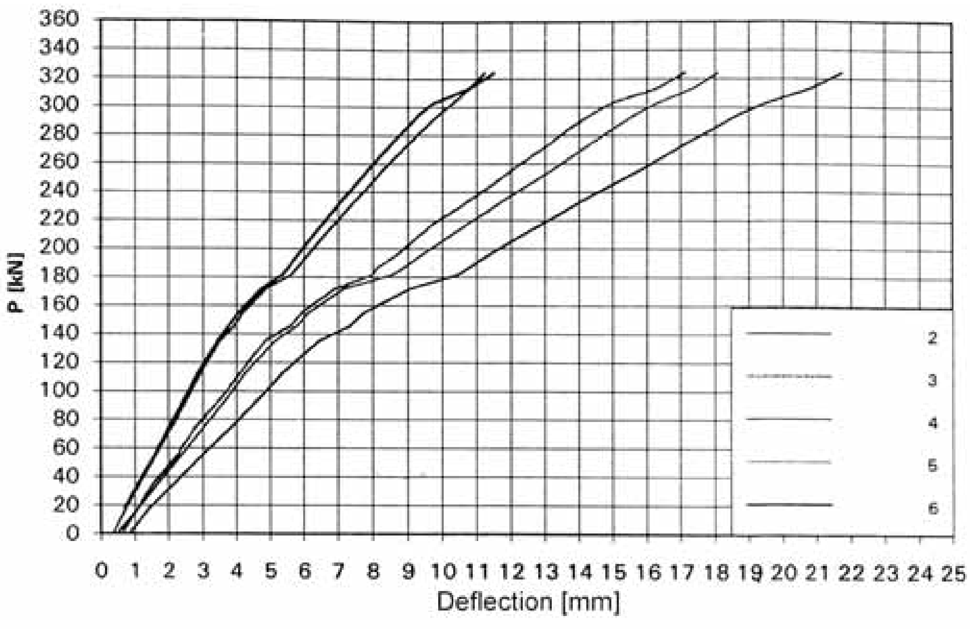

Fig. 24. Deflection of hollow core slabs, transducers 2–6.

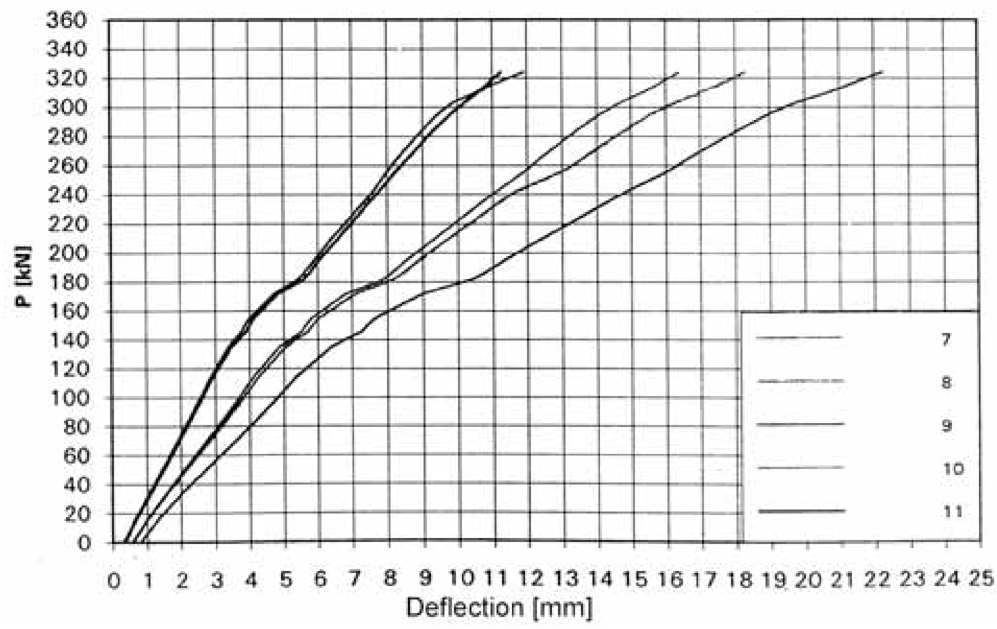

Fig. 25. Deflection of hollow core slabs, transducers 7–11.

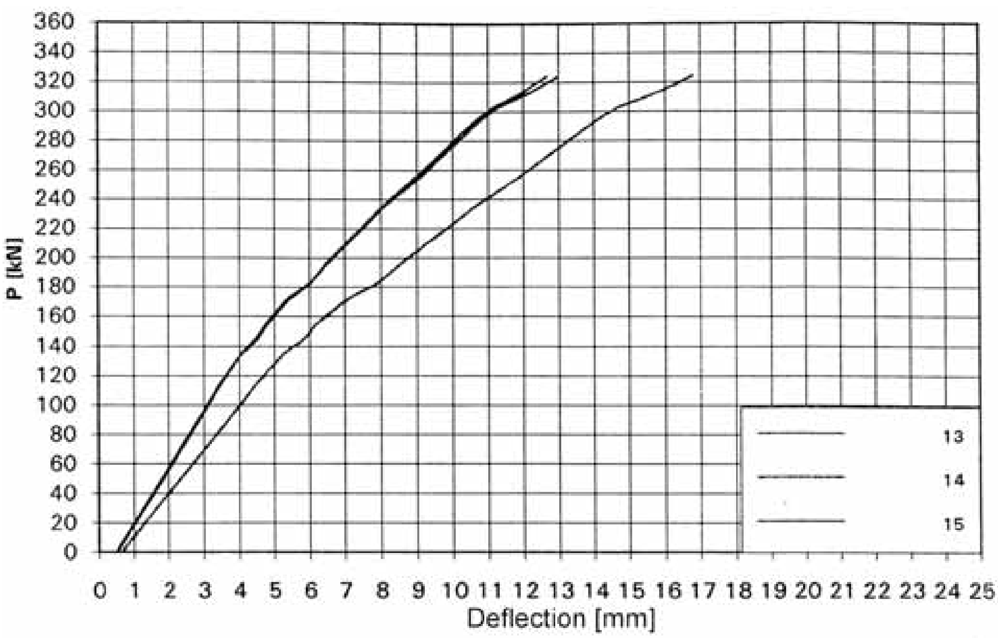

Fig. 26. Deflection of MEK beam, transducers 13–15.

<table>
<tr><td></td><td>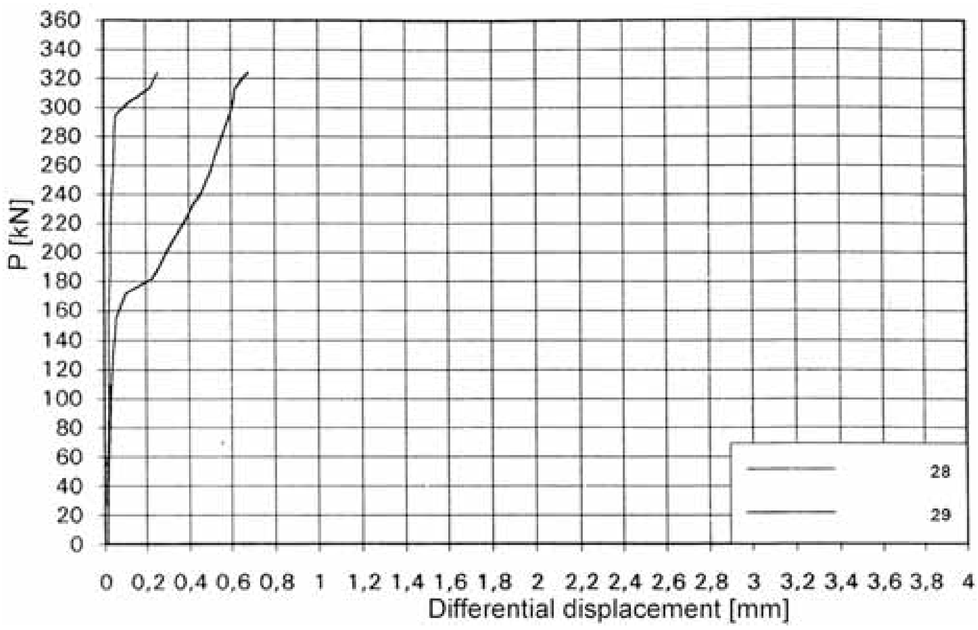

Fig. 27. Differential vertical displacement between MEK beam and slab end measured by gauges 28 and 29.</td></tr>
<tr><td>10.2
Crack width</td><td>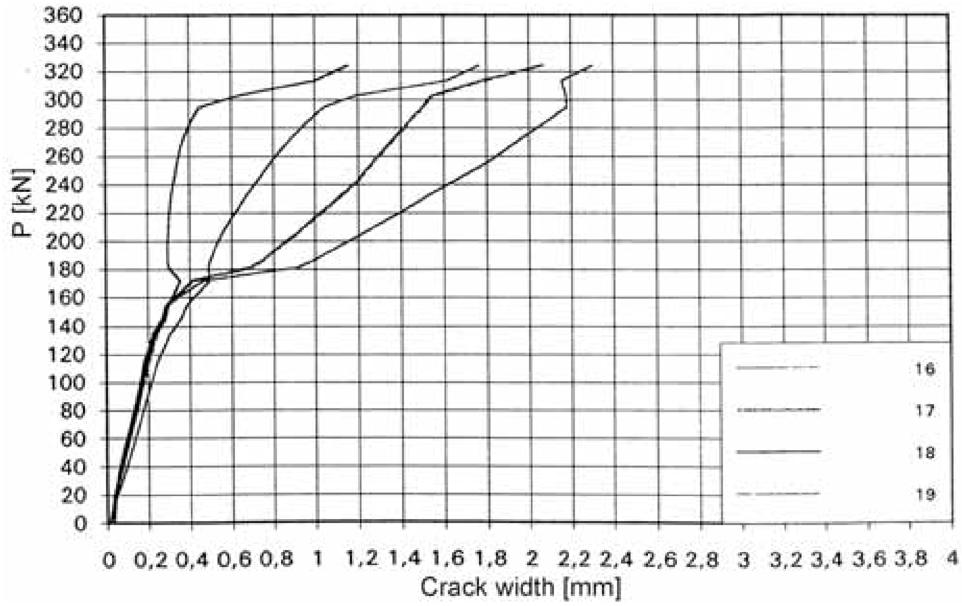

Fig. 28. Opening of joint (≈ crack width), transducers 16–19.</td></tr>
<tr><td>10.3
Average strain (actually differential displacement)</td><td>-</td></tr>
</table>

10.4 Shear displacement	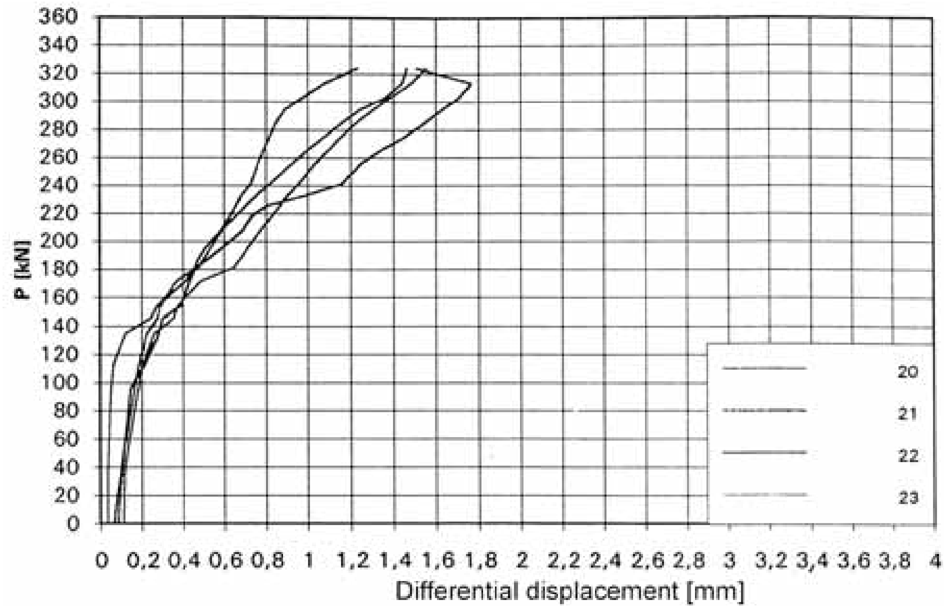 *Fig. 29. Southern end of middle beam. Differential displacement between edge of slab and middle beam. A positive value means that the slab is moving towards the end of the beam.* 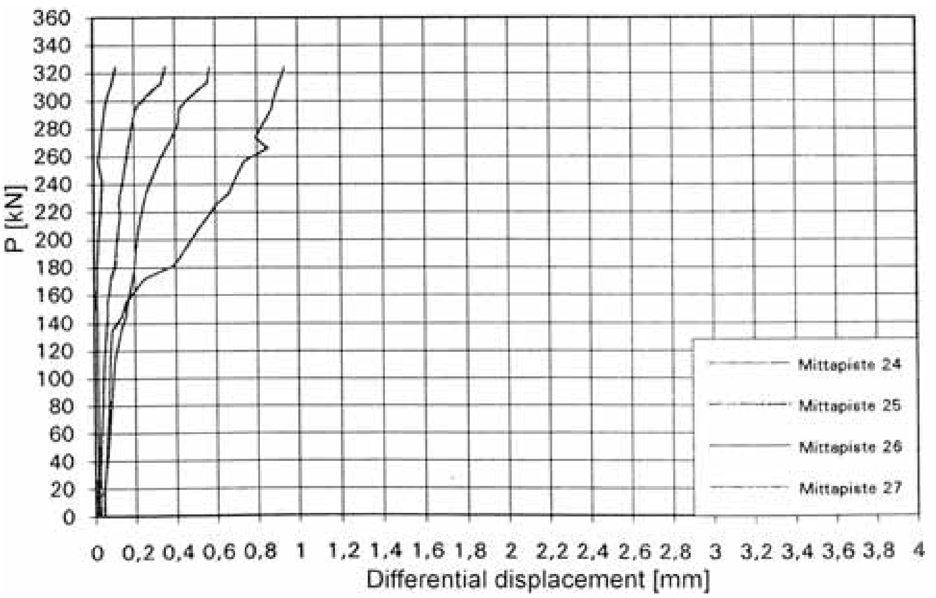 *Fig. 30. Northern end of middle beam. Differential displacement between edge of slab and middle beam. A positive value means that the slab is moving towards the end of the beam.*
10.5	**Strain** *Table 3. Strain in MEK beam due to installation of hollow core slabs, grouting and loading equipment measured by transducers 40–48.*

40 [0,001]	41 [0,001]	42 [0,001]	43 [0,001]	44 [0,001]	45 [0,001]	46 [0,001]	47 [0,001]	48 [0,001]
-0,491	0,129	-0,122	-0,177	-0,133	0,102	0,204	0,152	0,165

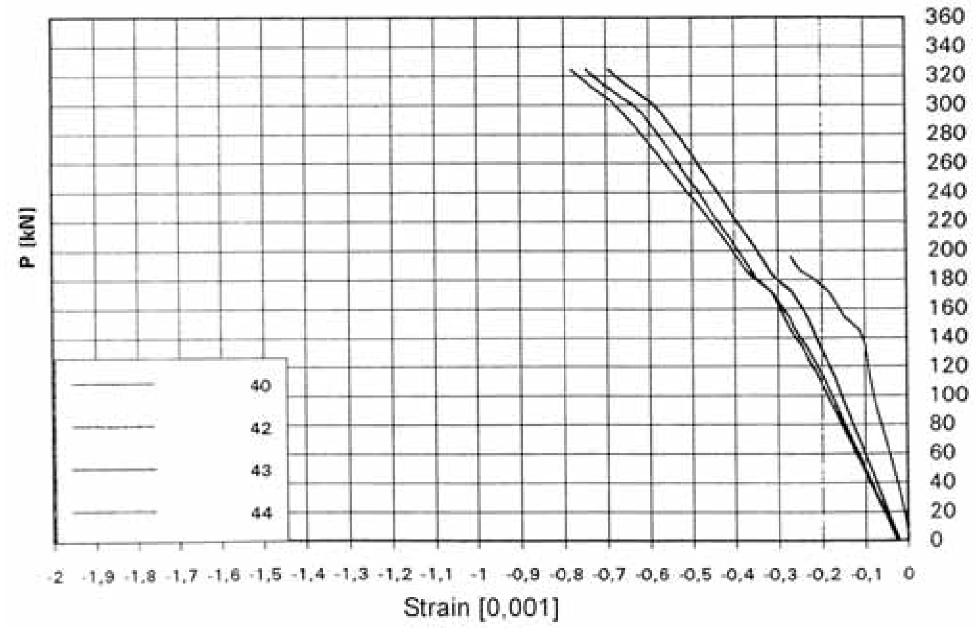

Fig. 31. Strain measured by gauges 40 (transverse to beam) and 42, 43 and 44 (parallel to beam).

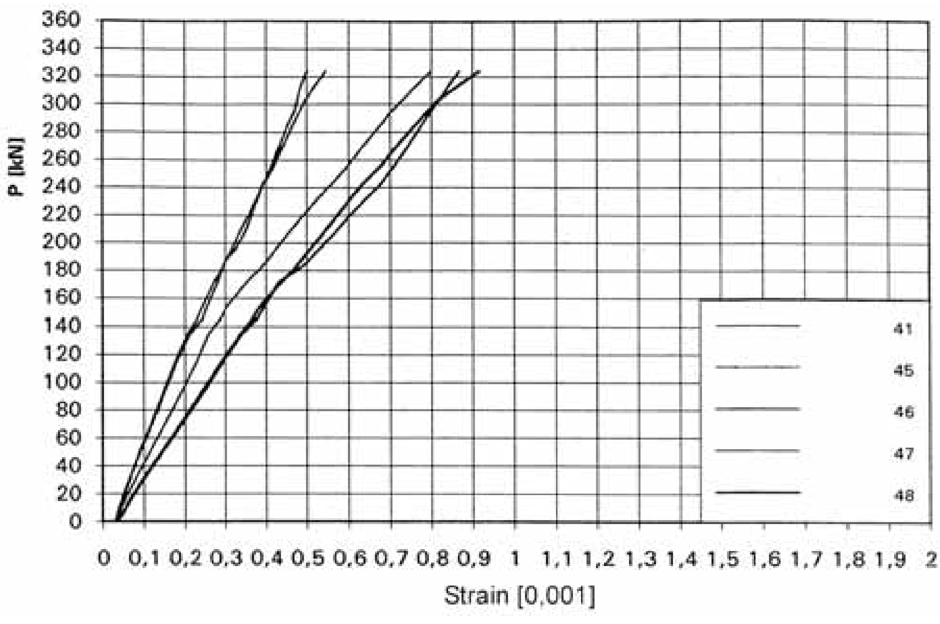

Fig. 32. Strain measured by gauges 41 and 45–48.

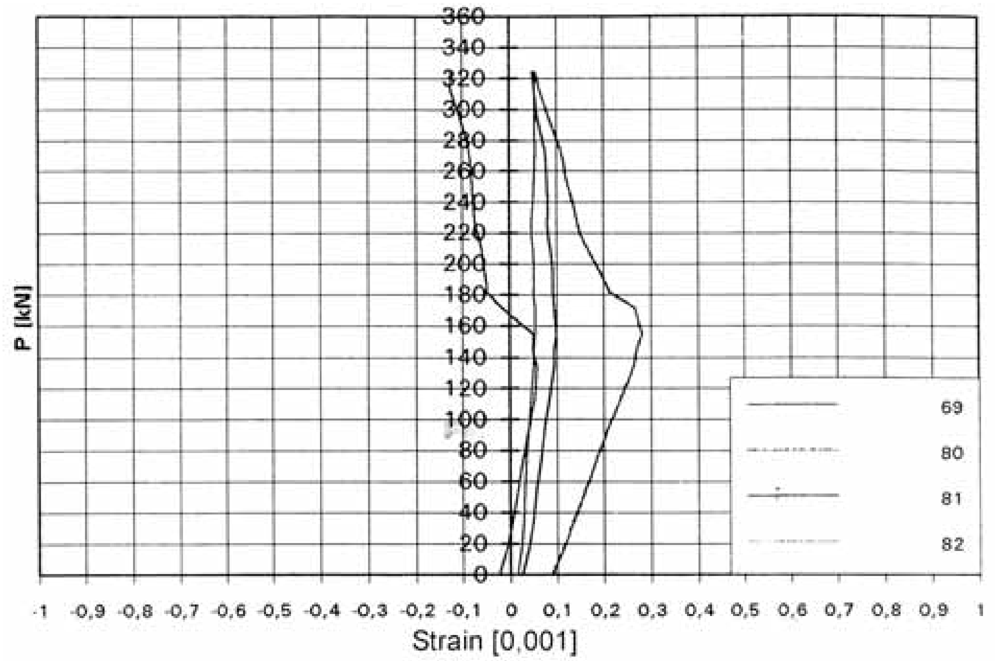

Fig. 33. Strain measured by gauges 69 and 80–82 in the soffit of hollow core slabs.

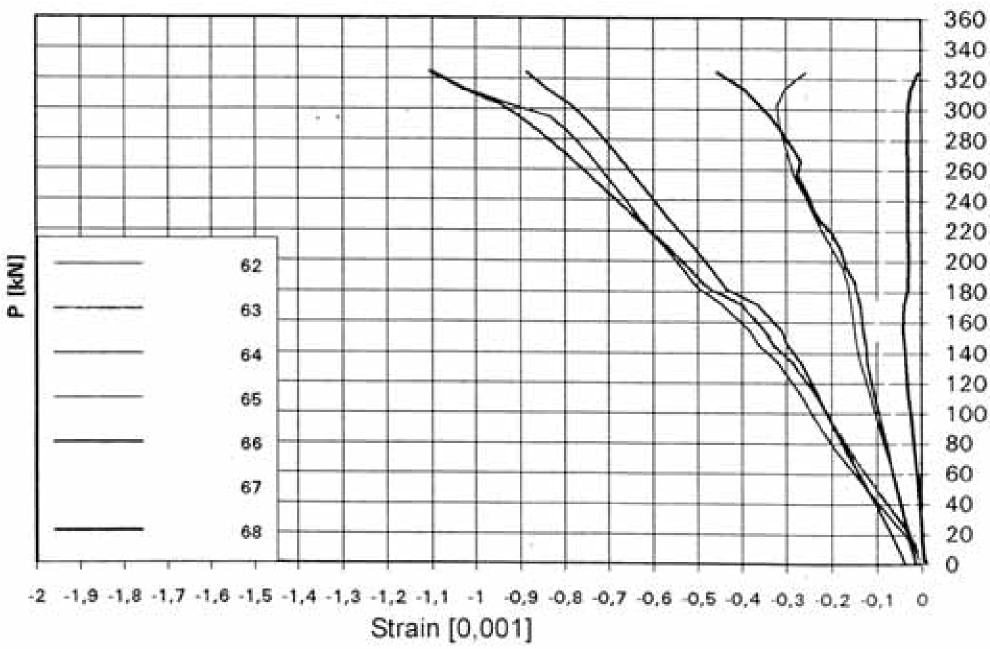

Fig. 34. Top surface of thee floor. Strain measured by gauges 62–68.

11 Reference tests

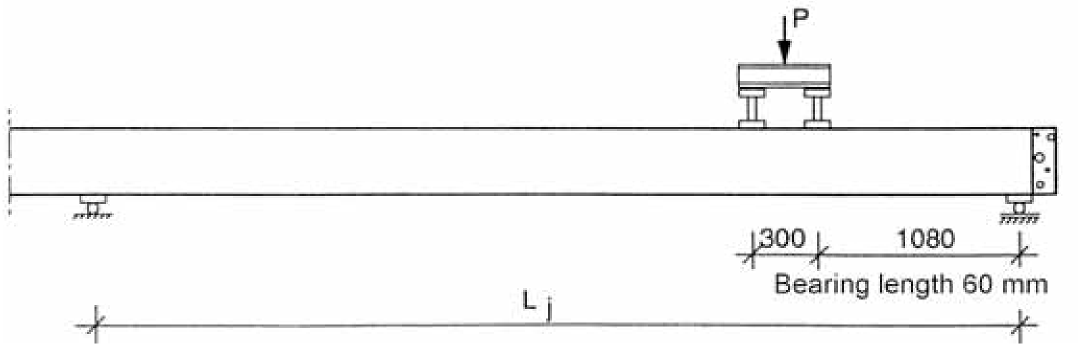

Fig. 35. Layout of reference test, slab 9. L_j = 5,93 m. Note the cast-in-situ concrete at the loaded end, cast on the 31st of March 1994, which filled 50 mm of the hollow cores.

Table 4. Reference test. Span of slab, sum of actuator force P_a at failure and weight of loading equipment P_{eq}, total shear force V_{obs} at failure and total shear force v_{obs} per unit width.

Test	Date	Span mm	P_a+P_{eq} kN	V_{obs} kN	v_{obs} kN/m	Note
R1	?	5930	230,7	223,2	186,0	Web shear failure

12 Comparison: floor test vs. reference tests

The observed shear resistance (support reaction) of the hollow core slab in the floor test was equal to 148,2 kN per one slab unit or 123,5 kN/m. This is **66%** of the shear resistance observed in the reference test.

13 Discussion

1. The deflection of the middle beam due to the imposed actuator loads only (deflection minus settlement of supports) was 16,7 mm or *L*/301.

2. The shear resistance measured in the reference tests was of the same order as the observed values for similar slabs given in *Pajari, M. Resistance of prestressed hollow core slab against a web shear failure. VTT Research Notes 2292, Espoo 2005*.

3. At failure load, the maximum difference in the mid-point deflection of the beams was 4,2 mm. Hence, the torsional stresses due to the different deflection of the middle beam and end beams had a minor effect on the failure of the slabs.

4. The failure mode was web shear failure of edge slab 8. The measured strains in the MEK beam show that the beam could not yield in longitudinal bending.

1	**General information**
1.1 Identification and aim	**VTT.RC.Rect-norm.265.1994** **Last update 2.11.2010** RC265N (Internal identification) Aim of the test: To study the shear resistance of hollow core slabs supported on the top of reinforced concrete beam.
1.2 Test type	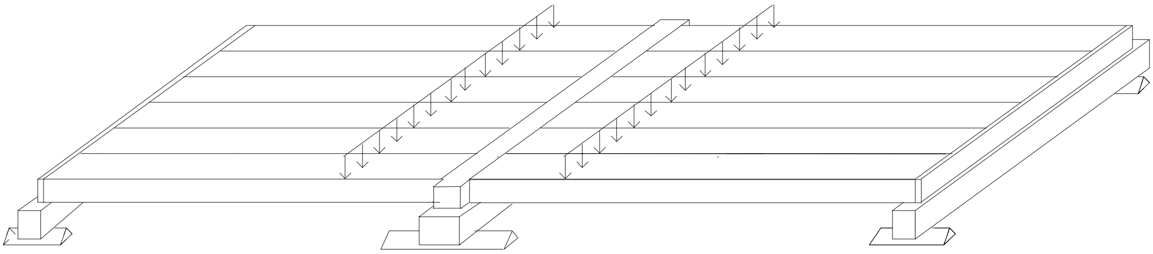 *Fig. 1. Illustration of test setup.*
1.3 Laboratory & date of test	VTT/FI 11.11.1994
1.4 Test report	Author(s): Pajari, M. Name: *Loading test for 265 mm hollow core floor supported on reinforced concrete beams* Ref. number: RTE-IR-7/1994 Date: 20.12.1994 Availability: Public, available on request from VTT Expert Services, P.O. Box 1001, FI-02044 VTT. Financed by the Finnish Association of Building Industry RTT (supported by the Technology Development Centre of Finland); the Finnish Steel Work Association, the International Prestressed Hollow Core Association IPHA; KB Kristianstads Cementgjuteri, Sweden, Stombyggarna i Hudisksvall, Sweden and SBUF, Sweden
2	**Test specimen and loading** (see also photographs in Appendix A)
2.1 General plan	

	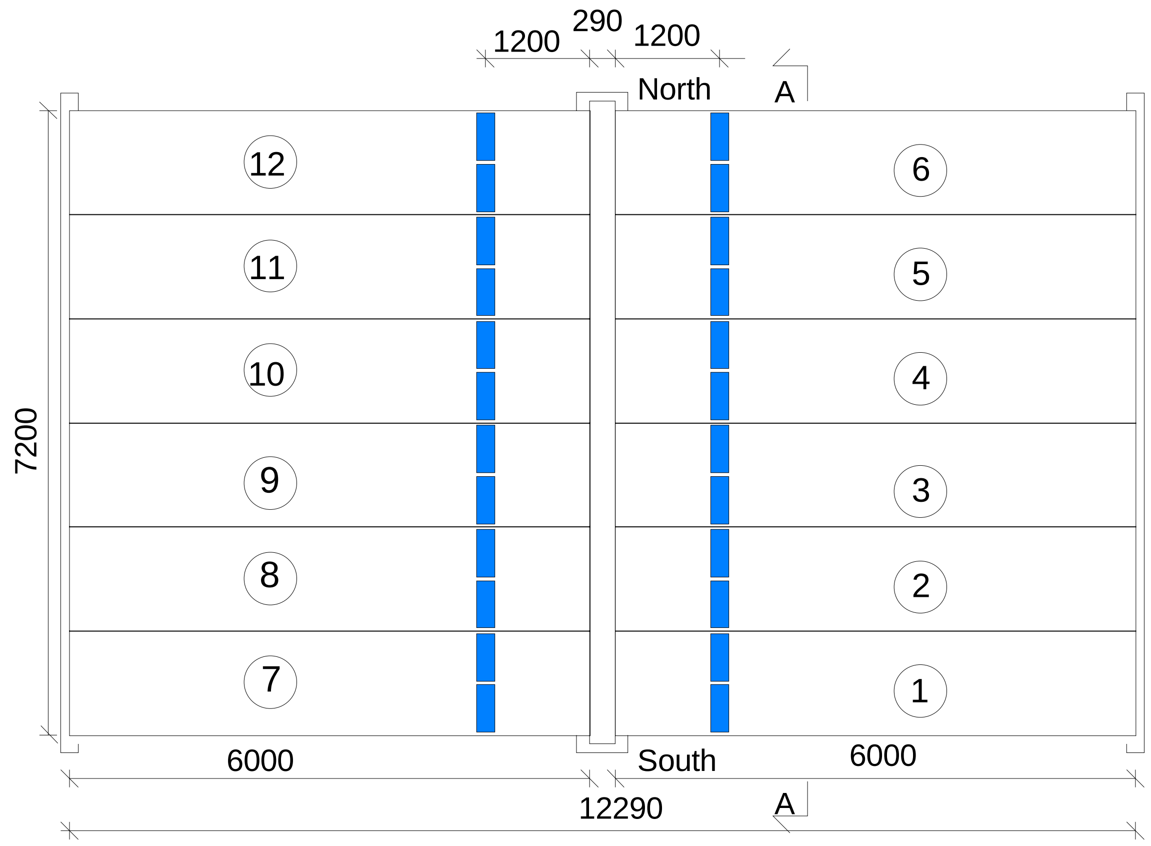 *Fig. 2. Plan.*
2.2 End beams	The length of the beam was 7,6 m. 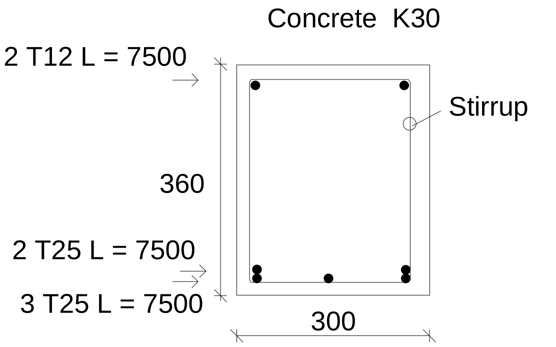 *Fig. 3. Section of end beam. TXY refers to rebars with thickness xy mm, see 9.1. The stirrups were 6 and 8 mm thick rebars in the middle and at the ends of the beams, respectively.* 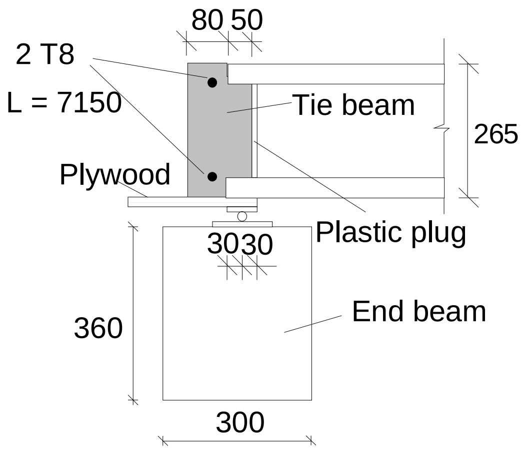 *Fig. 4. Arrangements at end beam. T8 refers to a reinforcing bar, see 9.1*
2.3 Middle beam	The middle beam was a reinforced concrete beam. The grade of the concrete was K60. See Figs 5 and 6. Txy refers to a reinforcing bar with diameter xy mm, see 9.1.

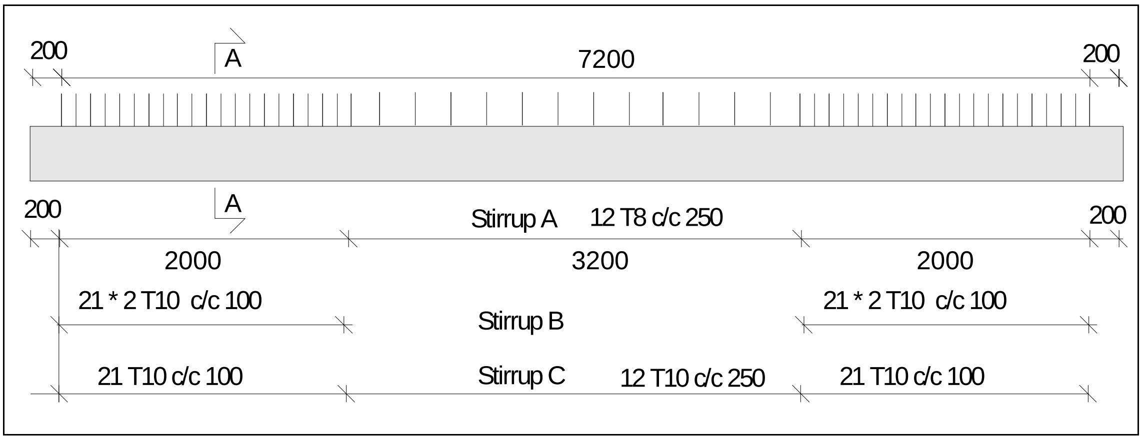

Fig. 5. Stirrups. Txy refers to a reinforcing bar with diameter xy mm, see 9.1. Stirrup A is a hoop (rounded rectangular) surrounding all longitudinal rebars shown in Fig. 6.

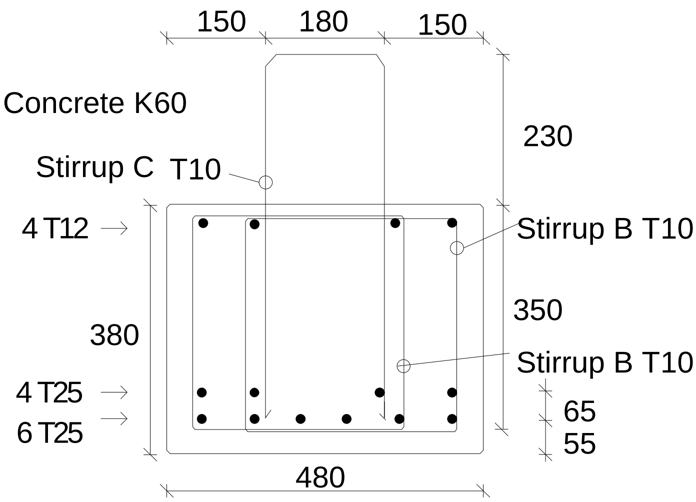

Fig. 6. Middle beam. For the material of Txy and stirrups see 9.1.

2.4
Arrangements at middle beam

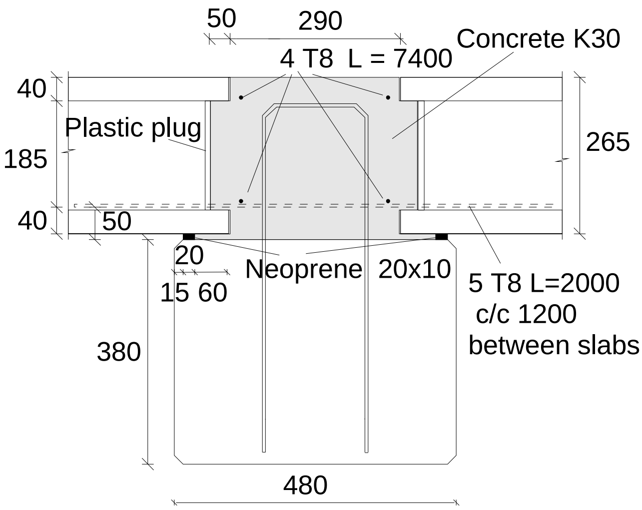

Fig. 7. Middle beam. Section along hollow cores. T8 refers to rebar A500HW, d = 8 mm, see 9.1.

<table>
<tr>
<td>2.5
Slabs</td>
<td>

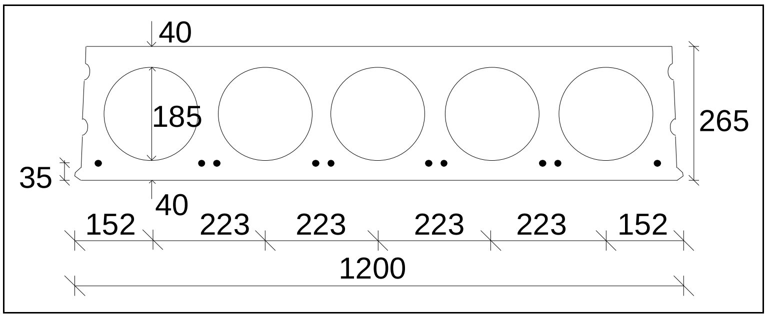

Fig. 8. Nominal geometry of slab units.

- Extruded by Partek Betoniteollisuus Oy, Hyrylä factory10.10.1994
- 10 lower strands J12,5

J12,5: seven indented wires, ϕ =12,5 mm, A_p = 93 mm^2, initial prestress = 950 MPa, see 9.1.

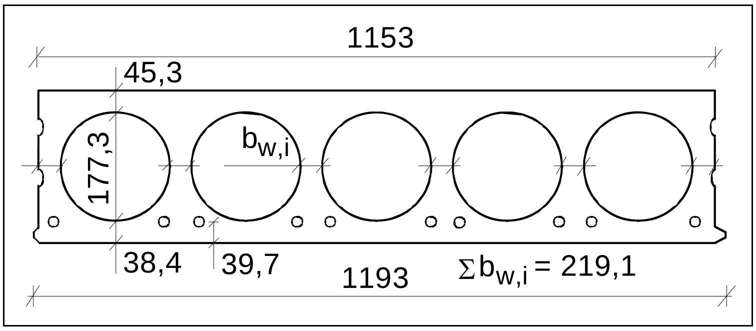

Max measured bond slips: 1,6 mm in slab 12; 1,4 and 1,3 mm in slab 5

Measured weight of slab units = 4,25 kN/m

Fig. 9. Floor test. Mean of most relevant measured geometrical characteristics of slabs 1–12.

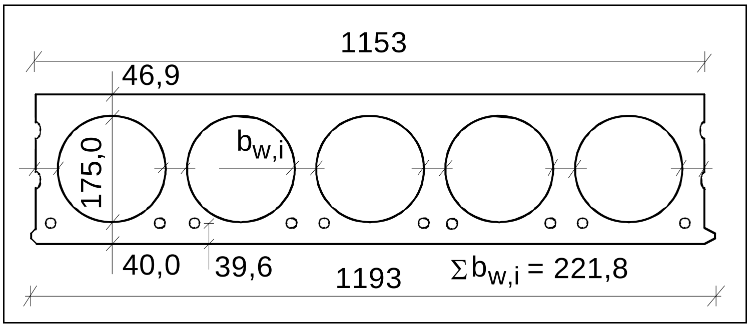

Max measured bond slips: 1,3 mm in slab 13 and 1,2 mm in slab 14,

Measured weight of slab units = 4,33 kN/m

Fig. 10. Reference tests. Mean of most relevant measured geometrical characteristics of slabs 13 and 14.

</td>
</tr>
<tr>
<td>2.6
Temporary supports</td>
<td>Temporary supports below beams (Yes/No)
- No</td>
</tr>
</table>

2.7 Loading arrangements	The loads *P*, see Fig. 11, were generated by 6 identical hydraulic actuators, each connected to the same hydraulic pressure. The actuator loads were spreaded with the aid of 6 primary, 12 secondary and 24 tertiary spreader beams to two transverse line loads on the slabs as shown in Figs 11–13. The reaction forces of the actuators were carried by a temporary steel frame which was fixed to the floor of the hall by tension bars. Four holes were drilled through the test floor for these bars. The position of the tension bars is shown in Fig. 11. After the test it came out that the holes had no effect on the failure mechanism. The tertiary spreader beams on the top of the floor were slightly shorter than 0,6 m. The friction between the teriary and secondary beams was eliminated by roller bearings and that between the secondary and primary spreader beams by teflon plates. There was gypsum mortar between the tertiary spreader beams and the top surface of the floor.

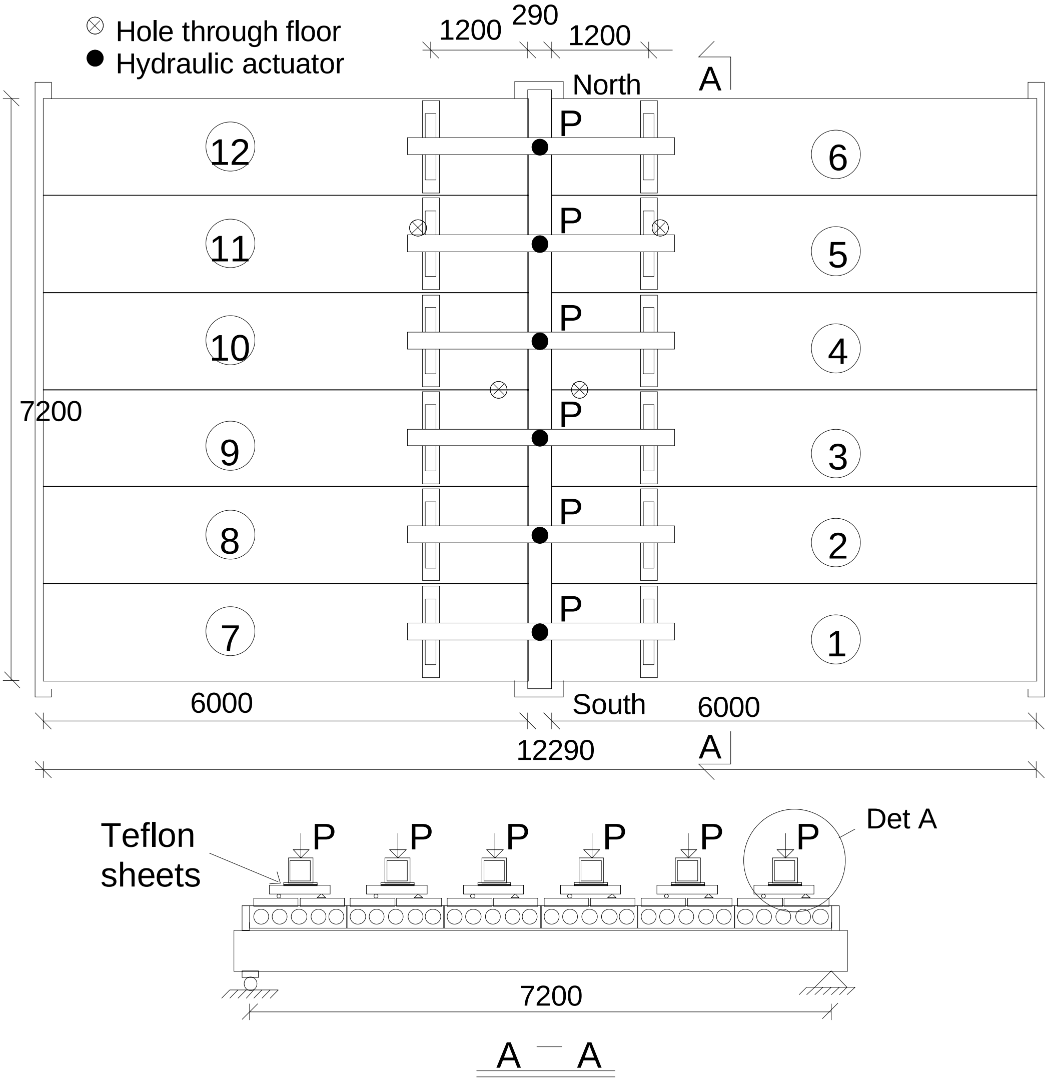

Fig. 11. Loading arrangements.

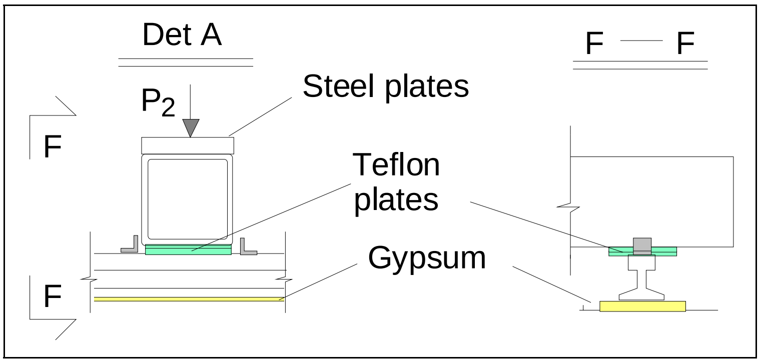

Fig. 12. Detail A, see the Fig. 11.

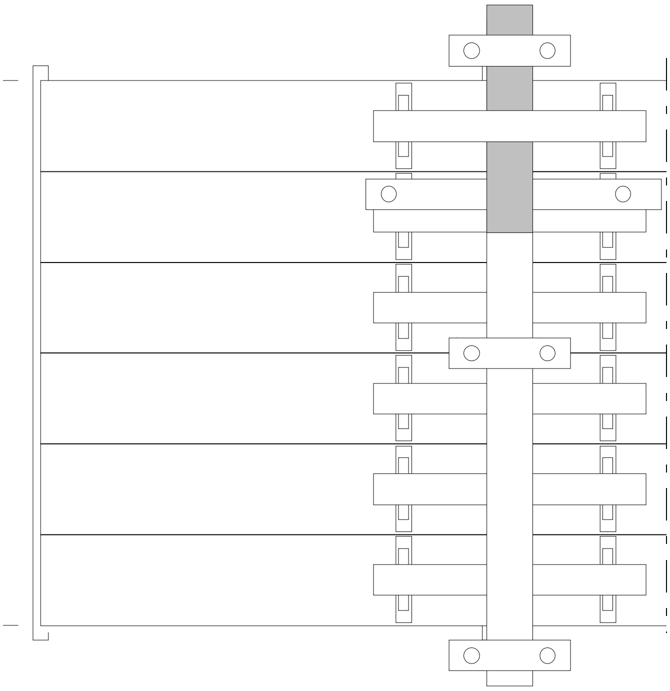

Fig. 13. Loading frame carrying the reaction of the actuators.

3 Measurements

3.1 Support reactions

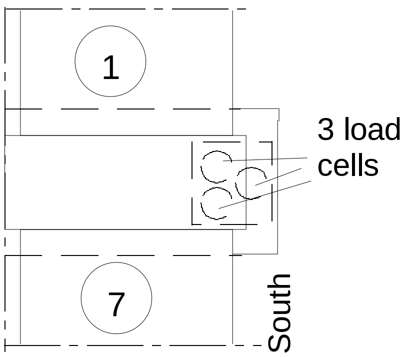

Fig. 14. Load cells below the South end of the middle beam.

3.2
Vertical displacement

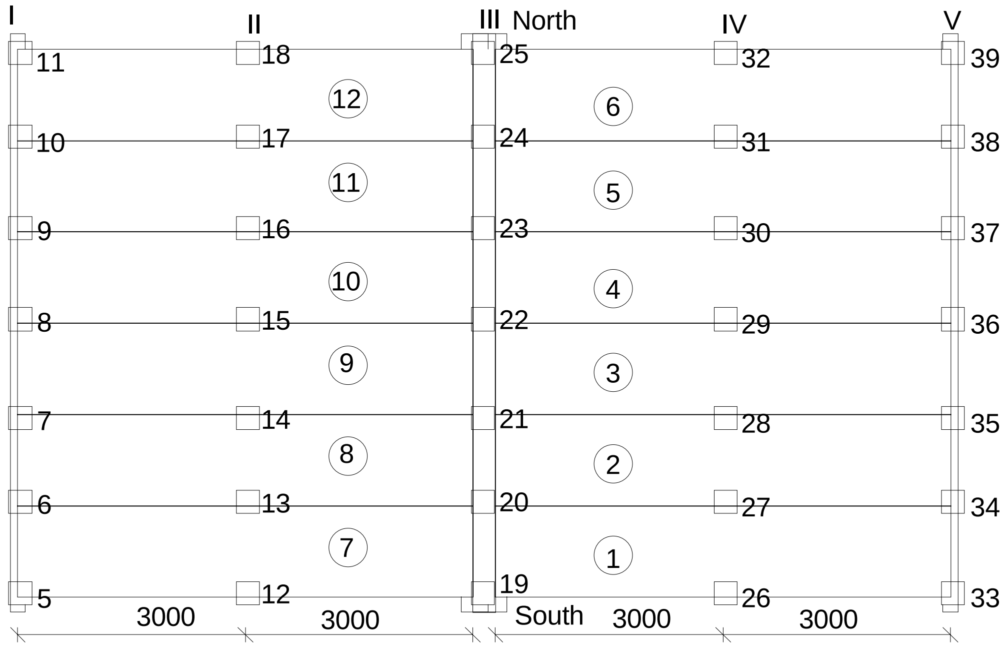

Fig. 15. Location of transducers 5 … 39 for measuring vertical deflection.

3.3
Average strain

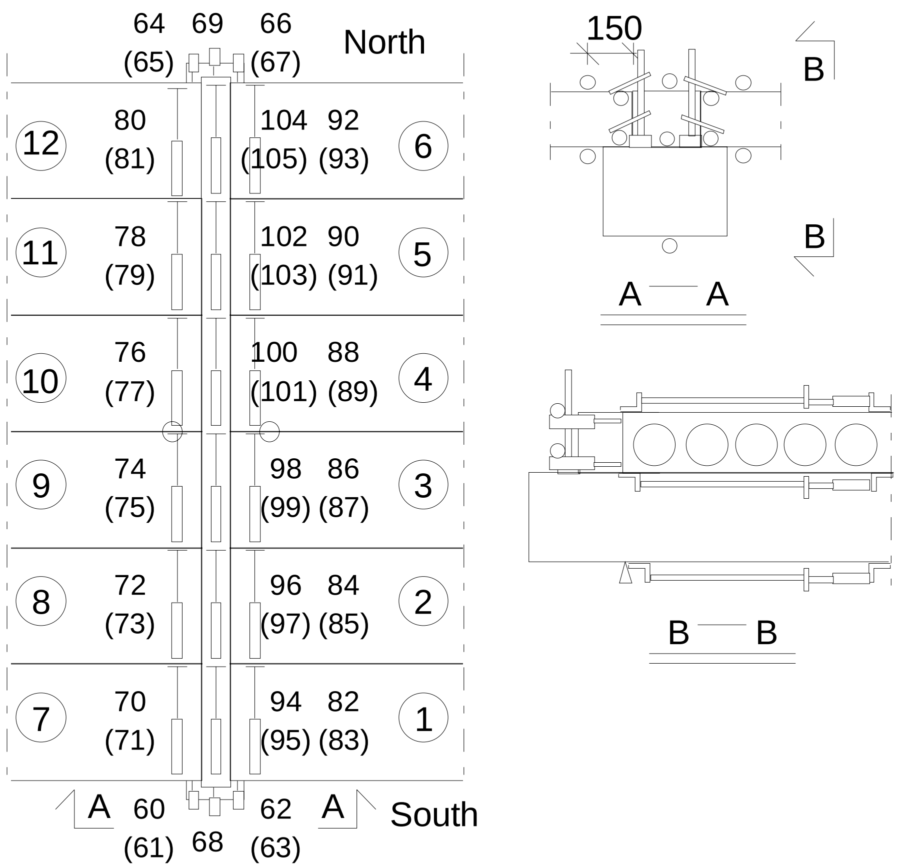

Fig. 16. Position of transducers measuring average strain parallel to the beam (70–105), displacement of the slab edges relative to the beam in beam's direction (60–67) and sliding of the upper part of the beam relative to the lower, precast part of the beam (68–69). Numbers in parentheses refer to the bottom, others to the top side.

	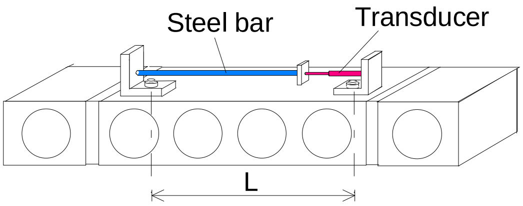 *Fig. 17. Apparatus for measuring average strain. L = 1120mm and 1060 mm for the bottom and top side transducers, respectively.*
3.4 Horizontal. displacements	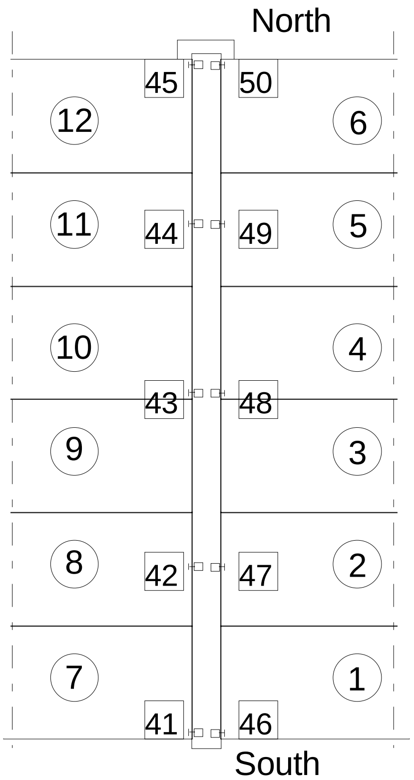 *Fig. 18. Transducers 41–50 measuring crack width on the top of the floor.*
3.5 Strain	-
4	**Special arrangements** -
5	**Loading strategy**
5.1 Load-time relationship	Date of the floor test was 11.10.1994. Before the onset of the loads, the middle beam and the end beams had cracked due to the dead weight. The mid-point deflection of the middle beam was 32 mm and that of the end beams of the same order. The maximum crack widths in the middle beam and end beams were 0,20 and 0,15 mm, respectively. All measuring devices were zero-balanced when the actuator forces *P* were equal to zero but the weight of the loading equipment was on.

	The loading history is shown in Fig. 19. Note, that the number of load step, not the time, is given on the horizontal axis. The load test took 2 h 35 min. In the following, the cyclic stage (steps 1–16) is called Stage I, the remaining part (steps 16–52) Stage II. 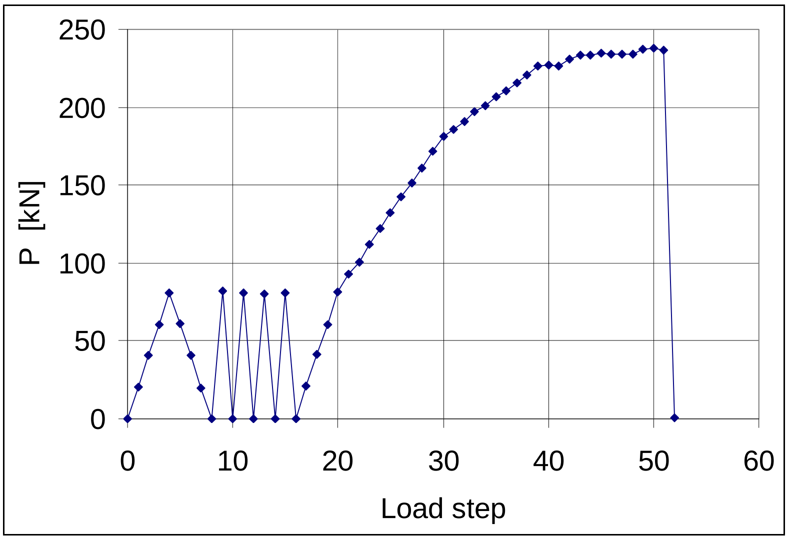 *Fig. 19. Development of actuator loads P_i.* The weight of loading equipment per one slab was 3,1 kN. Consequently, the imposed load per slab was $F = 0{,}5P + 3{,}1$ kN.
5.2 After failure	-
6	**Observations during loading**

Stage I	The cast-in-situ concrete in the upper part of the middle beam cracked vertically along the slab ends. At $P = 60$ kN the tie beams above the end beams started to crack. The maximum crack width in the middle beam was 0,25 mm.
Stage II	At P = 220 kN the first shear cracks were observed at the ends of slabs 1 and 7, at P = 225 kN in slab unit 12 and at P = 233 kN also in slab unit 6. At P = 238,2 kN slab 7 failed.
After failure	When removing the loading equipment, slab 8 was knocked with a hammer. The sound revealed that the slab end had cracked. This was confirmed when slab 7 had been removed. A diagonal shear crack was observed at the end of slab 8 close to the middle beam. When the slabs were removed, it came out that the joint concrete had completely filled the space between the slabs and the middle beam, the space under the slab end and the core fillings included. The concrete infill in the cores of slab units cracked along the slab ends on one side of the middle beam while on the other side it remained virtually uncracked, see Figs. 20 and 21 in App. A.

<table>
<tr><td></td><td>Three days after removal of the loads but when the loading equipment was still on, the deflection of the middle beam was 35 mm, i.e. only 3 mm more than the deflection before the test. Such a recovery is not possible after considerable yielding of the reinforcement in the concrete. This suggests that the softening behaviour observed in the load – deflection curve (see Fig. 29) is mainly attributable to effects other than the plastification of the reinforcement.</td></tr>
<tr><td>7</td><td>Cracks in concrete</td></tr>
<tr><td>7.1
Cracks at service load</td><td>See Fig. 20.</td></tr>
<tr><td>7.2
Cracks after failure</td><td>

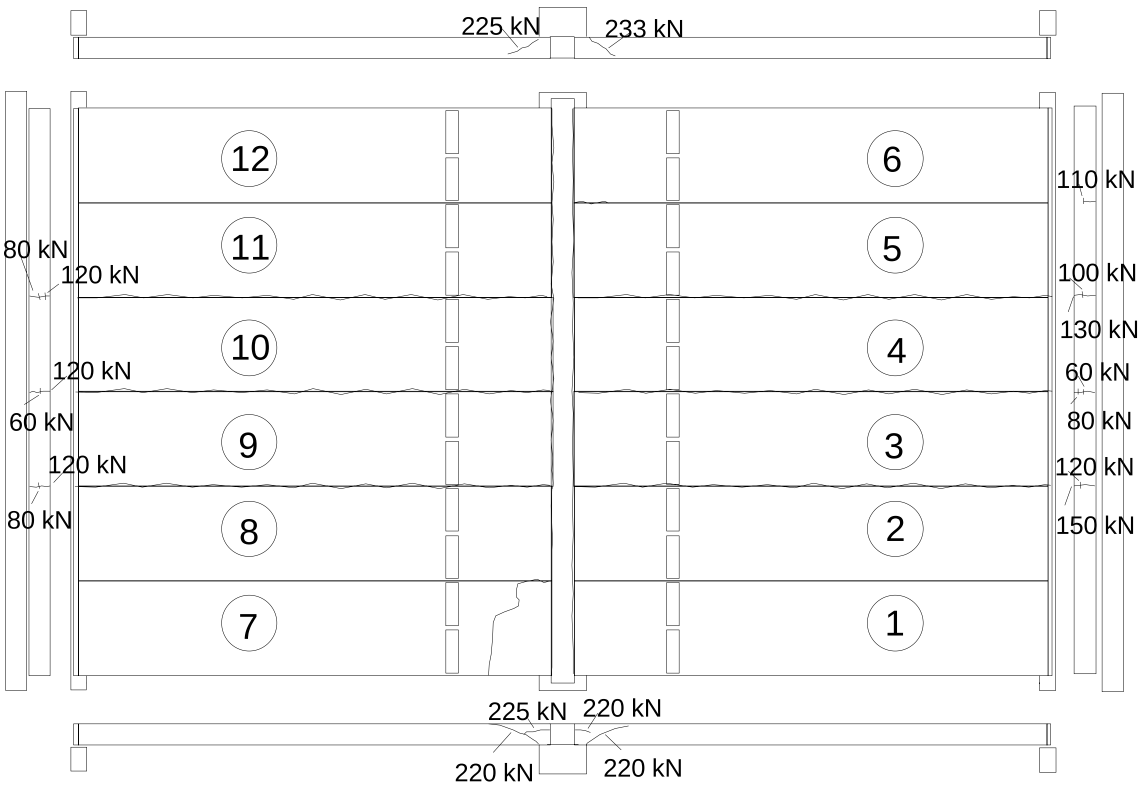

Fig. 20. Cracks after failure on the top and in the longitudinal edges of the floor. The force values refer to the load P at which the crack was observed.</td></tr>
<tr><td>8</td><td>Observed shear resistance</td></tr>
<tr><td></td><td>The maximum measured support reaction is regarded as the indicator of failure. The failure took place at P = 238,2 kN.

Fig. 21 shows the relationship between the measured support reaction below the South end of the middle beam and the sum of actuator loads on half floor.

The ratio of the reaction to the load is shown in Fig. 22 and in a larger scale in Fig. 23. Based on Fig. 23 it is justified to assume that at failure the support reaction due to the line load is equal to 0,765 times the line load. Assuming simply supported slabs gives the theoretical ratio of 0,800 ... 0,801.</td></tr>
</table>

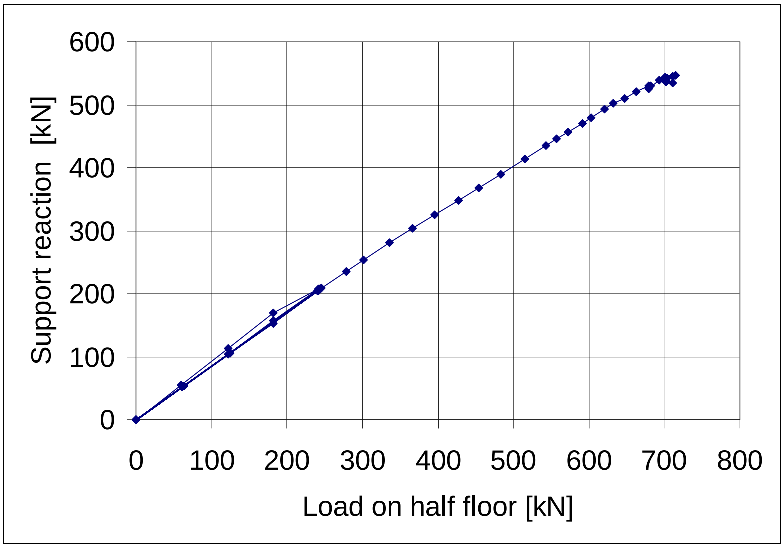

Fig. 21. Support reaction measured below South end of the middle beam vs. load on half floor (= 3P).

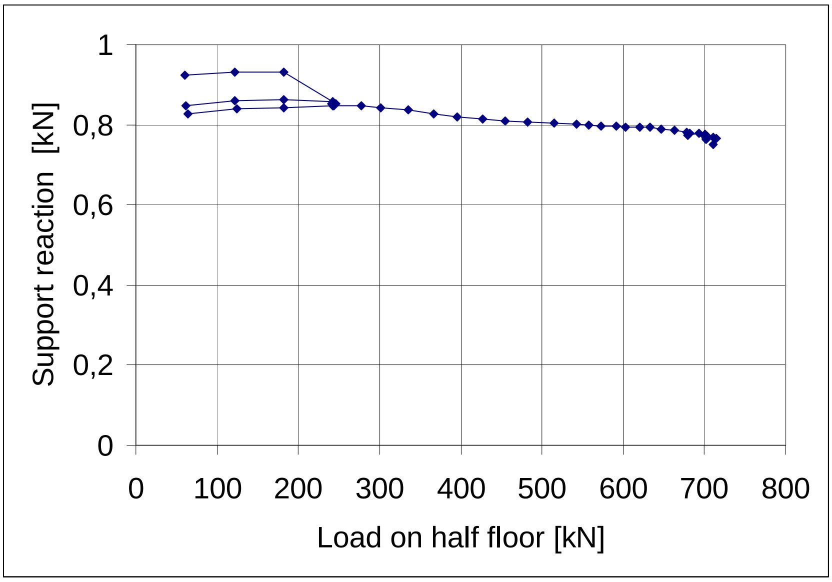

Fig. 22. Ratio of measured support reaction (below South end of the middle beam) to actuator loads on half floor. The points corresponding to load P $\approx$ 0 are not shown.

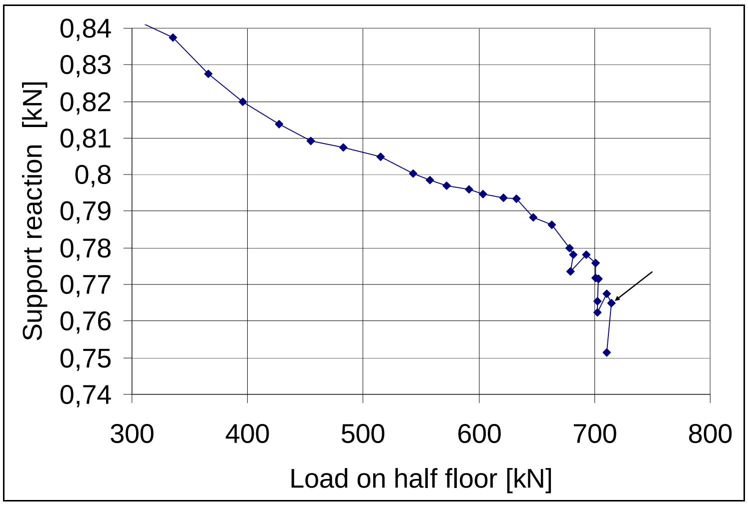

Fig. 23. A part of the previous figure in a large scale. The point corresponding to the highest support reaction has been indicated by an arrow.

The observed shear resistance of one slab end (support reaction of slab end at failure) due to different load components is given by

$$V_{obs} = V_{g,sl} + V_{g,jc} + V_{eq} + V_p$$

where $V_{g,sl}$, $V_{g,jc}$, V_{eq} and V_p are shear forces due to the self-weight of slab unit, weight of joint concrete, weight of loading equipment and actuator forces *P*, respectively.

It can be concluded that the maximum support reaction due to the imposed load on the failed slabs has been V_p = 0,765 x (actuator loads on half floor) / 6 = 0,765x3x238,2/6 = 91,11 kN. In the same way, the support reaction due to the weight of the loading equipment has been 0,765 x 3,1 = 2,37 kN. $V_{g,jc}$ is calculated from the nominal geometry of the joints and measured density of the grout. When calculating $V_{g,sl}$, the measured weight of the slabs is used. The values of the shear force components are given in Table 1 below.

Table 1. Components of shear resistance due to different loads.

Action	Load	Shear force kN/slab
Weight of slab unit	4,25 kN/m	12,75
Weight of joint concrete	0,14 kN/m	0,42
Loading equipment	3,1 kN/slab	2,37
Actuator loads	238,2 /2 kN /slab	91,11

The observed shear resistance $\boldsymbol{V_{obs}}$ **= 106,7 kN** (shear force at support) is obtained for one slab unit with width = 1,2 m. The shear force per unit width is $\boldsymbol{v_{obs}}$ **= 88,9 kN/m.**

9 Material properties

9.1 Strength of steel

Component	$R_{eH}/R_{p0,2}$ MPa	R_m MPa	Note
Strands J12,5	1630	1860	Nominal (no yielding in test)
Reinforcement Txy	500		Type A500 HW. Nominal value for reinforcing bars, no yielding in test

9.2
Strength of slab concrete, floor test

#	Cores	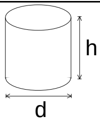	*h* mm	*d* mm	Date of test	Note
6			50	50	24.11.1994 (+13 d)[1]	Upper flange of slabs 1, 7 and 12, two cores from each, vertically drilled Tested as drilled[2] Density = 2378 kg/m^3
Mean strength [MPa]			67,2			
St.deviation [MPa]			1,7			

9.3
Strength of slab concrete, reference tests

#	Cores	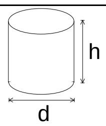	*h* mm	*d* mm	Date of test	Note
6			50	50	18.11.1994 (< 7 d)[1]	Upper flange of slab 13, vertically drilled Tested as drilled[2] Density = 2365 kg/m^3
Mean strength [MPa]			67,8			
St.deviation [MPa]			2,5			

#	Cores	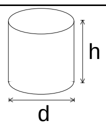	*h* mm	*d* mm	Date of test	Note
6			50	50	18.11.1994 (< 7 d)[1]	Upper flange of slab 14, vertically drilled Tested as drilled[2] Density = 2388 kg/m^3
Mean strength [MPa]			67,8			
St.deviation [MPa]			2,9			

9.4
Strength of grout in joints, tie beams and in the upper part of the middle beam

#	Cores	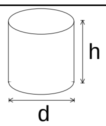	*h* mm	*d* mm	Date of test	Note
6			75	75	24.11.1994 (+13 d)[1]	Upper surface of middle beam, vertically drilled Tested as drilled[2] Density = 2177 kg/m^3
Mean strength [MPa]			25,3			
St.deviation [MPa]			1,3			

9.5
Strength of concrete in lower part of middle beam

#	Cores	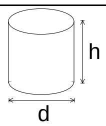	*h* mm	*d* mm	Date of test	Note
6			75	75	24.11.1994 (+13 d)[1]	Upper surface of beam, vertically drilled Tested as drilled[2] Density = 2412 kg/m^3
Mean strength [MPa]			63,6			
St.deviation [MPa]			4,0			

[1] Date of material test minus date of structural test (floor test or reference test)
[2] After drilling, kept in a closed plastic bag until compression

10	**Measured displacements**
10.1 Deflections	

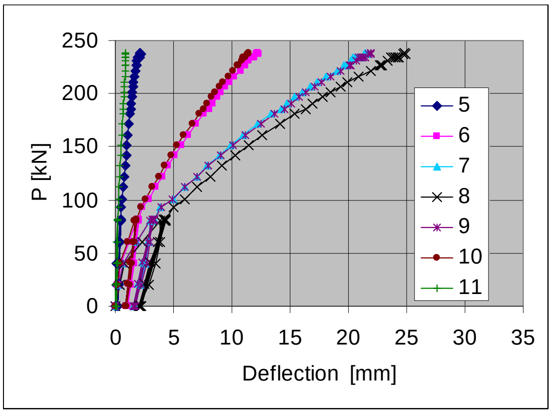

Fig. 24. Deflection on line I, Western end beam.

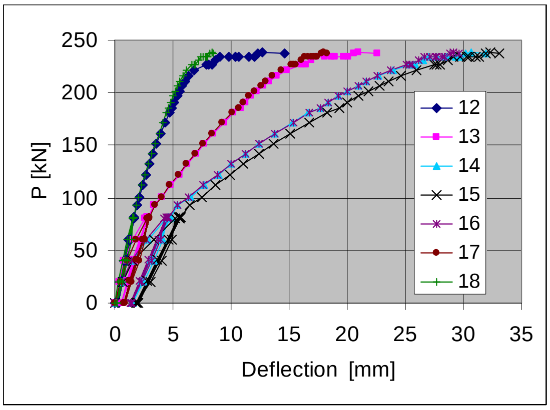

Fig. 25. Deflection on line II.

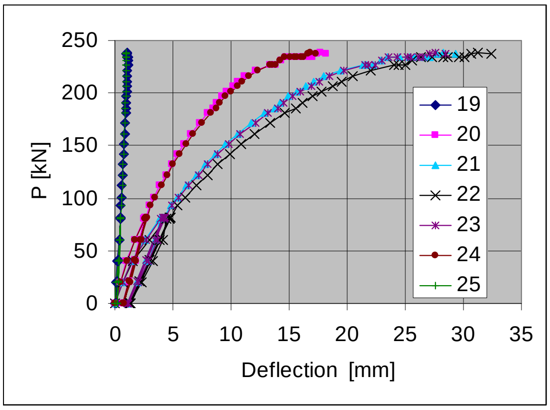

Fig. 26. Deflection on line III, middle beam.

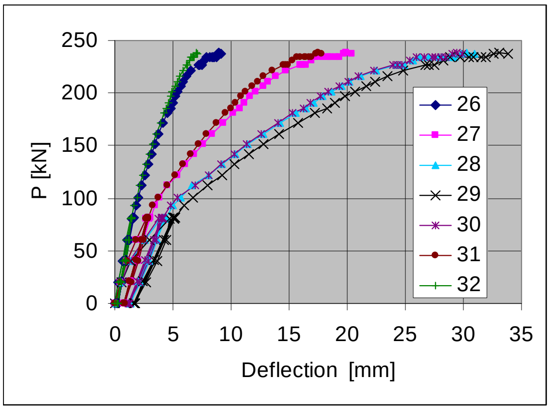

Fig. 27. Deflection on line IV.

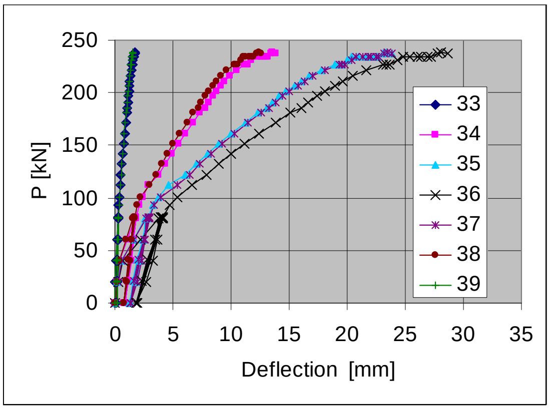

Fig. 28. Deflection on line V, Eastern end beam.

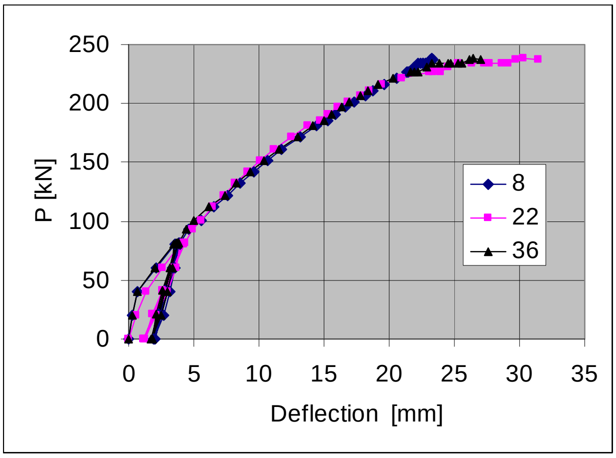

Fig. 29. Net deflection of mid-point of beams (rigid body motion = settlement of beam supports has been eliminated).

The last measured net deflection of the middle beam at highest load level before failure was 30,3 mm. This is 3,8–7 mm higher than the net deflection of the end beams. It is possible that the twist of the outermost slabs has affected the shear resistance.

10.2
Crack width

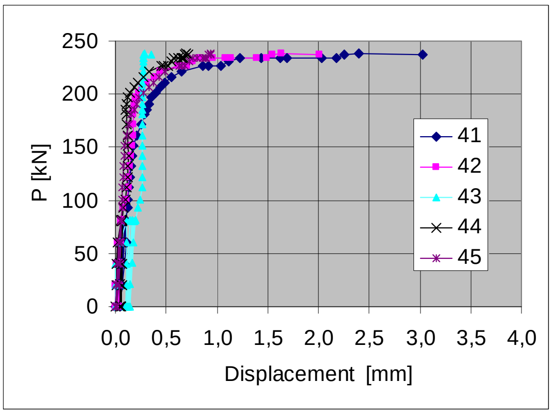

Fig. 30. Differential displacement (≈crack width) measured by transducers 41–45.

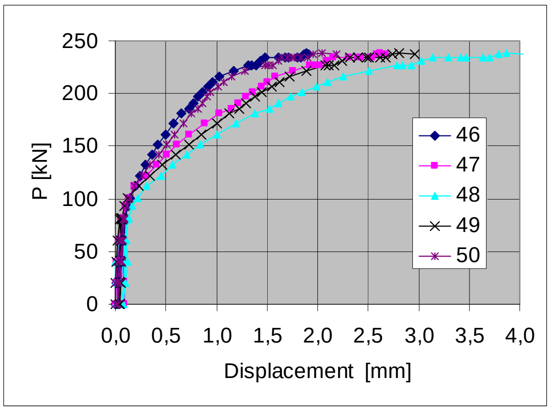

Fig. 31. Differential displacement (≈crack width) measured by transducers 46–50.

10.3
Average strain (actually differential displacement between slab edges)

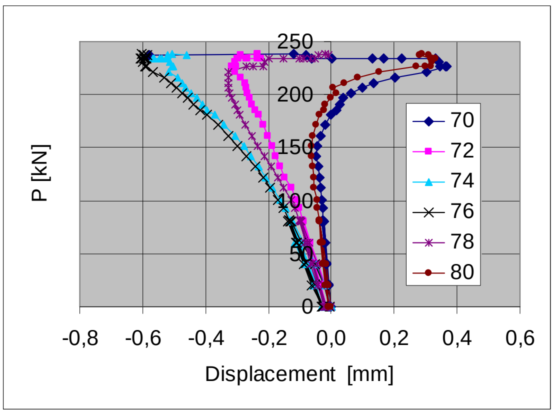

Fig. 32. Differential displacement at top surface of slabs 7–12 measured by transducers 70, 72,...,80.

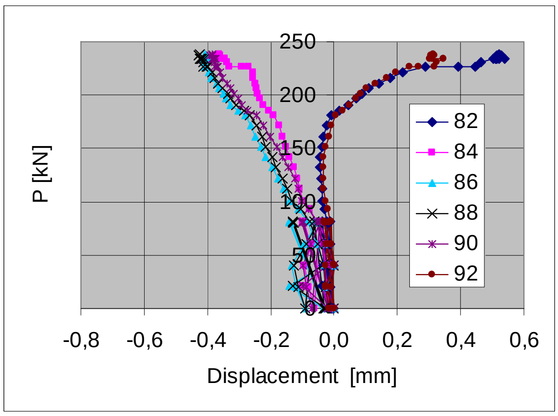

Fig. 33. Differential displacement at top surface of slabs 1–6 measured by transducers 82, 84,...,92

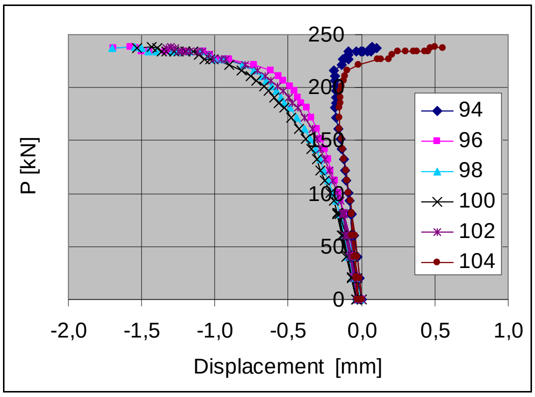

Fig. 34. Differential displacement at top surface of middle beam measured by transducers 94, 96,...,104.

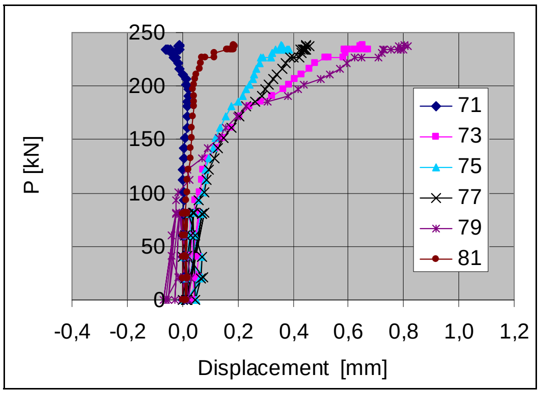

Fig. 35. Differential displacement at soffit of slabs 7–12 measured by transducers 71, 73,...,81.

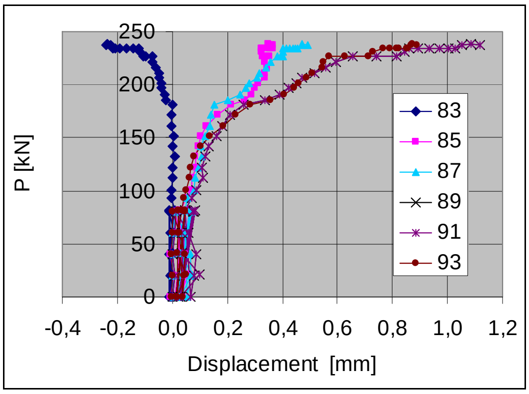

Fig. 36. Differential displacement at soffit of slabs 1–6 measured by transducers 83, 85,...,93.

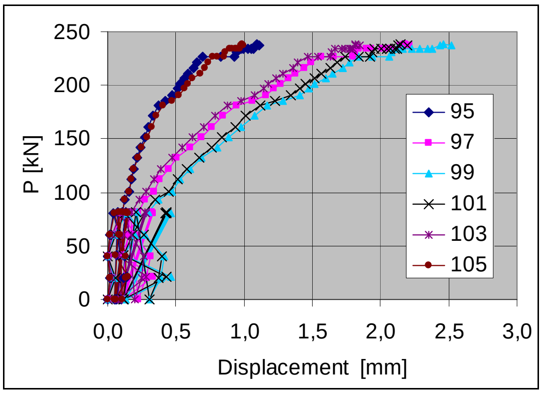

Fig. 37. Differential displacement at soffit of the middle beam measured by transducers 95, 97,...,105.

10.4
Shear displacement between slab edge and middle beam

In Figs 38 and 39 the differential displacements between the lower and upper part of the slab edges relative to the middle beam in beams's direction are shown. A negative sign means that the slab edge is approaching the end of the beam.

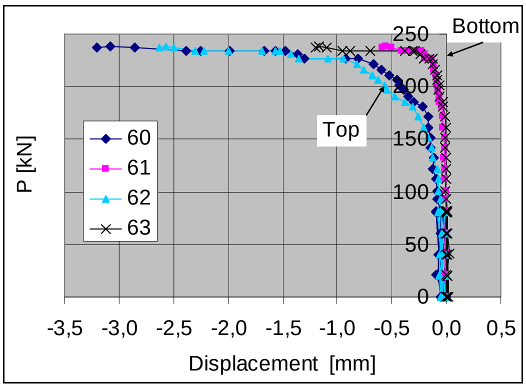

Fig. 38. South end of middle beam. Differential displacement measured by transducers 60–63.

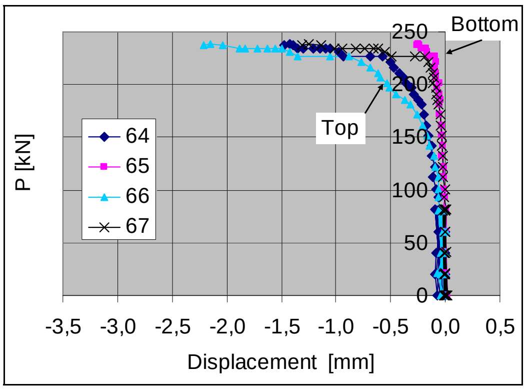

Fig. 39. North end of middle beam. Differential displacement measured by transducers 64–67.

	In Fig. 40 the longitudinal, differential displacements between the upper and lower part of the middle beam are shown. A negative sign means that the upper part is approaching the end of the lower part (moving outwards more than the lower part). 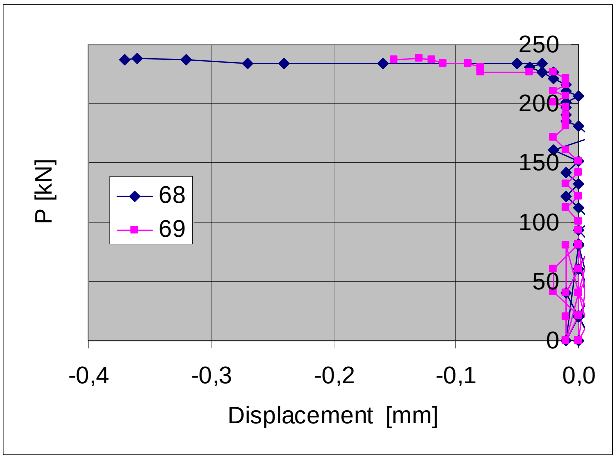 *Fig. 40. South end of middle beam. Differential displacement between upper and lower part of the middle beam at South end (transducer 68) and at North end (transducer 69).*
10.5	**Strain** **-**
11	**Reference tests**
	Slabs 13 and 14 were loaded in shear as shown in Fig. 41. The tests were performed after the floor test (11.11.1994) but before 18.11.1994. 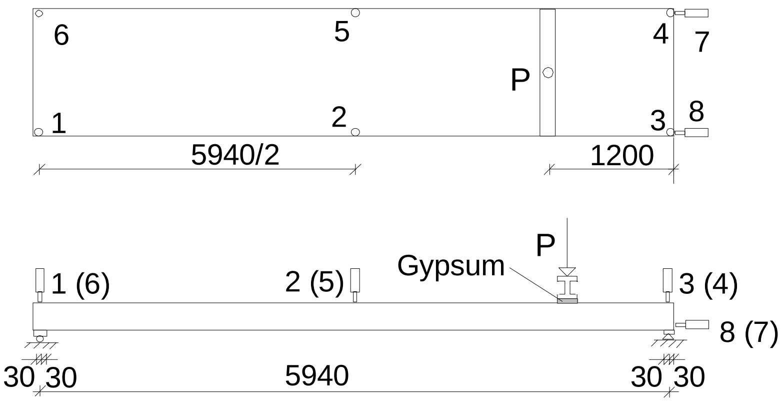 *Fig. 41. Layout of reference tests. The slippage of the outermost strands was measured by transducers 7 and 8.* The load-deflection relationship for the mid-point of the slabs is shown in Fig. 42. The change in the slope is attributable to flexural cracking below the load. Despite the cracking, the failure mode in both tests was tensile failure in the web. Virtually no slippage of the outermost strands occurred before failure.

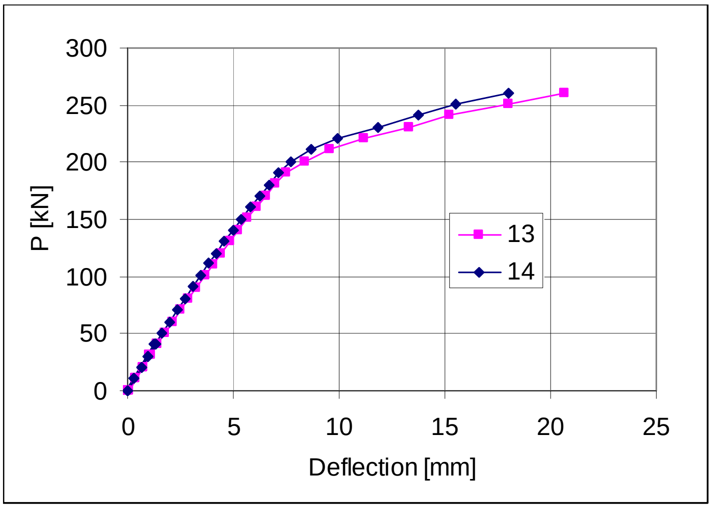

Fig. 42. Net mid-point deflection of slabs 13 and 14. Rigid body motion (= settlement of supports) has been eliminated.

The failure modes and failure loads are given in Table 2. The measured self-weight of the slabs = 4,33 kN/m has been used when calculating the shear resistance.

Table 2. Span L, ultimate load P_u, shear force due to self weight V_g, shear force due to imposed load V_P, ultimate shear force V_u and failure mode in reference tests. The weight of the loading equipment = 1,0 kN is included in P_u.

Slab	L mm	P_u kN	V_g kN	V_P kN	V_u kN	Failure mode
13	5940	264,9	12,86	212,7	225,6	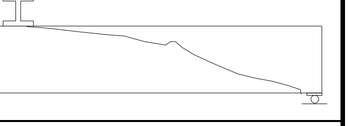
14	5940	266,5	12,86	214,0	226,9	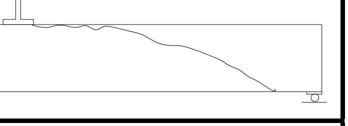
		Mean			226,2	

12	**Comparison: floor test vs. reference tests**
	The observed shear resistance in the floor test was 106,7 kN per one slab unit or 88,9 kN/m. This is **47%** of the mean of the shear resistances observed in the reference tests.
13	**Discussion**
	1. The net deflection of the middle beam due to the imposed actuator loads only (deflection minus settlement of supports) was 30,3 mm or *L*/238 at the highest load level. 2. The failure mode was a web shear failure of slab at the edge of the tested floor next to the middle beam. Before failure there were diagonal cracks in all four slab edges next to the supports of the middle beam. 3. The shear resistance measured in the reference tests was of the same order as the mean of the observed values for similar slabs given in *Pajari, M. Resistance of prestressed hollow core slab against web shear failure. VTT Research Notes 2292, Espoo 2005*. 4. Before failure, the net deflection of the end beams was 3,8–7 mm higher than the net deflection of the end beams. It is possible that the twist of the outermost slabs has affected the shear resistance. On the other hand, when the first diagonal cracks were observed at load *P* = 220 kN (92% of the failure load), the net deflection of the end beams was less than 1,0 mm smaller than that of the middle beam. 5. The failure behaviour of the slabs was similar to that in the other Finnish floor tests in which the slabs were supported close to the soffit of the middle beam.

APPENDIX A: PHOTOGRAPHS

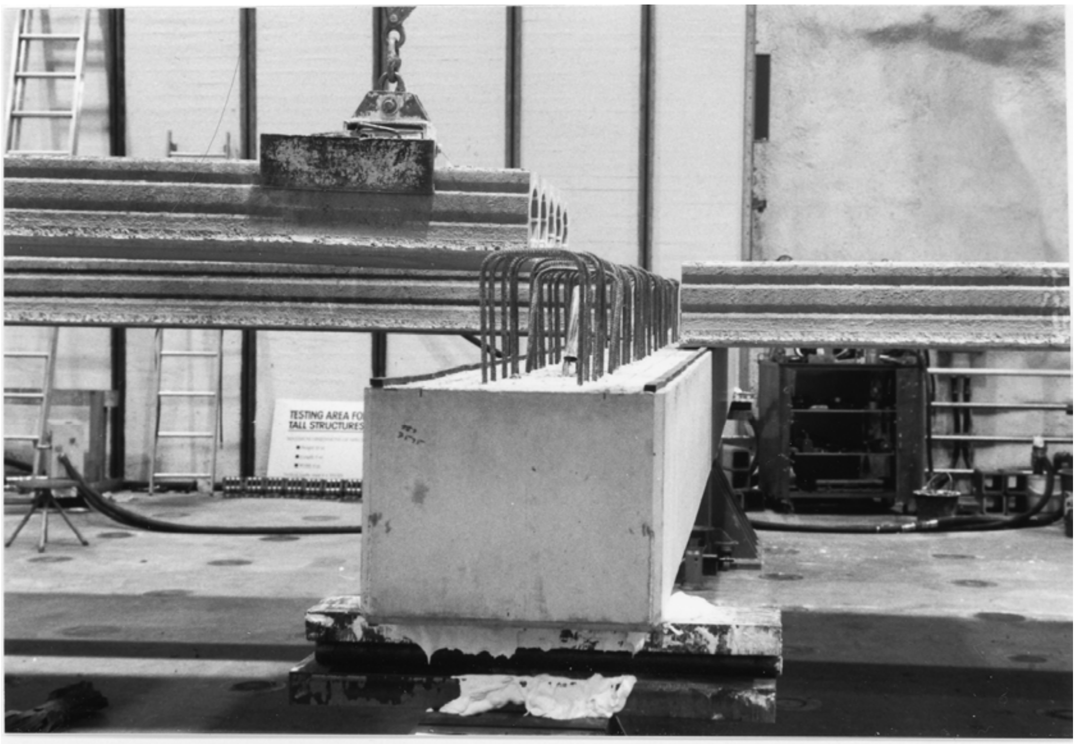

Fig. 1. Assembling specimen.

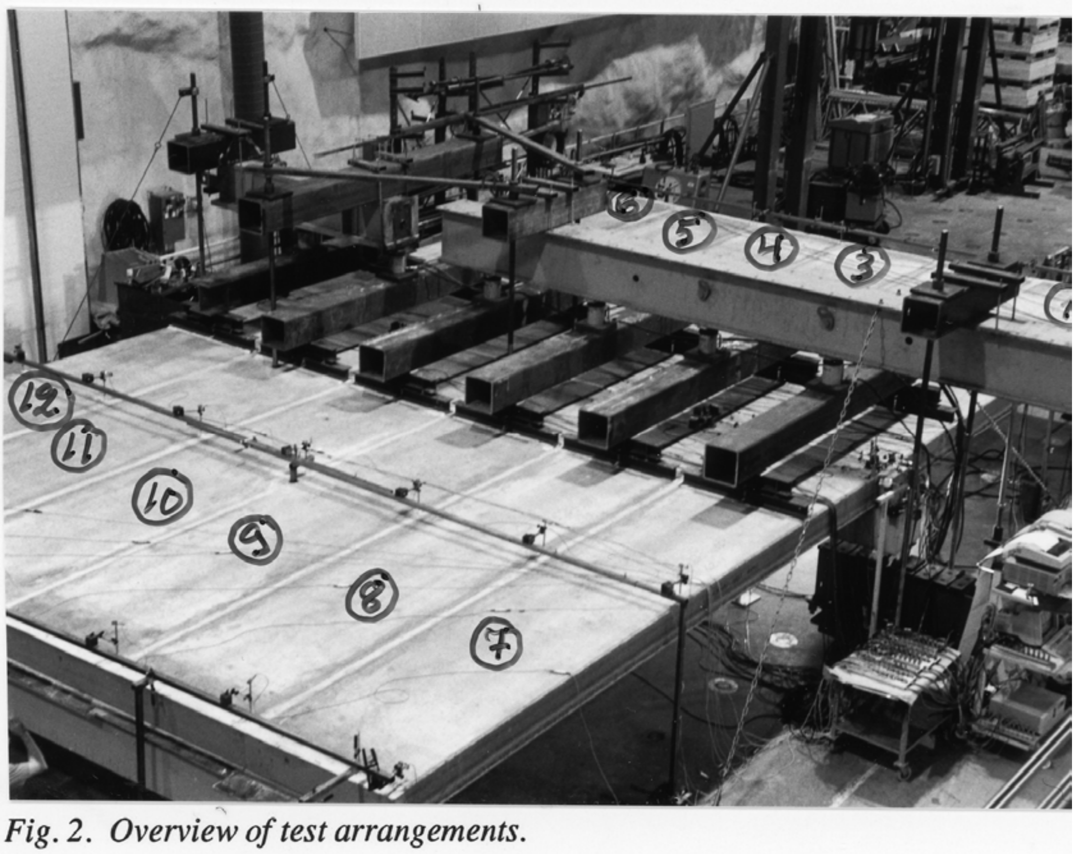

Fig. 2. Overview of test arrangements.

Fig. 3. Hydraulic actuator between the loading frame and a tertiary spreader beam. Note the teflon sheets.

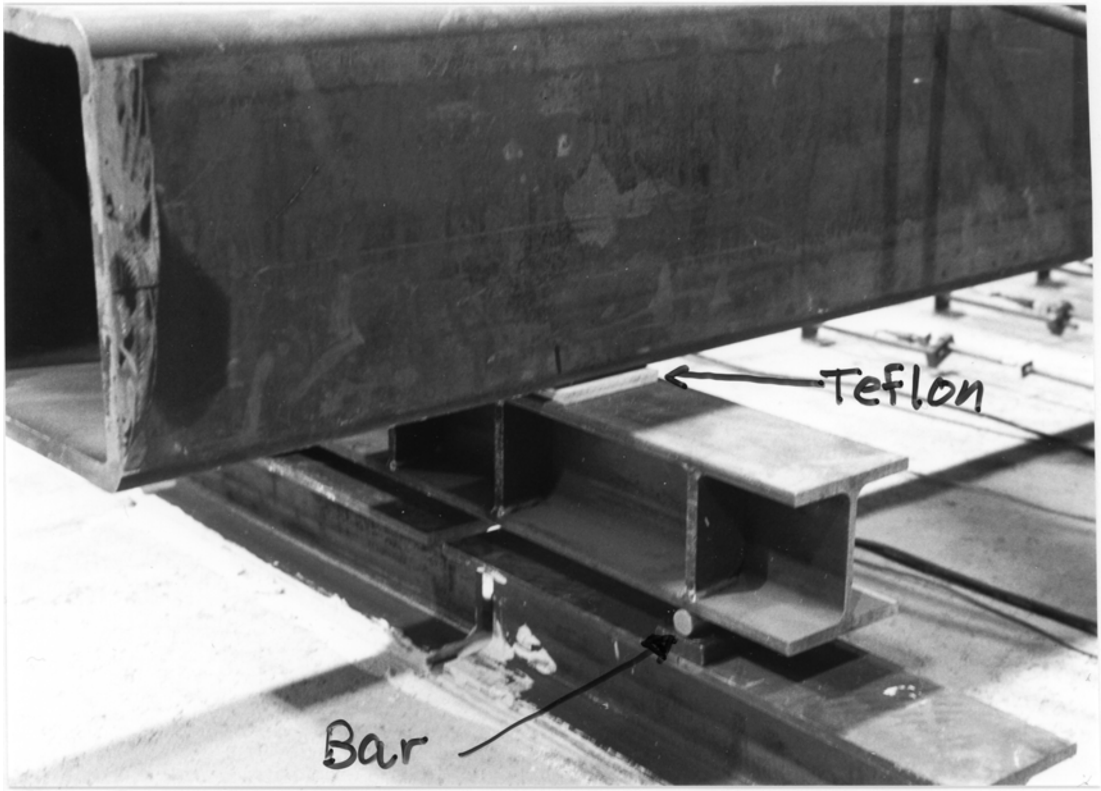

Fig. 4. Primary, secondary and tertiary spreader beam. Note the teflon sheets and the movable bar.

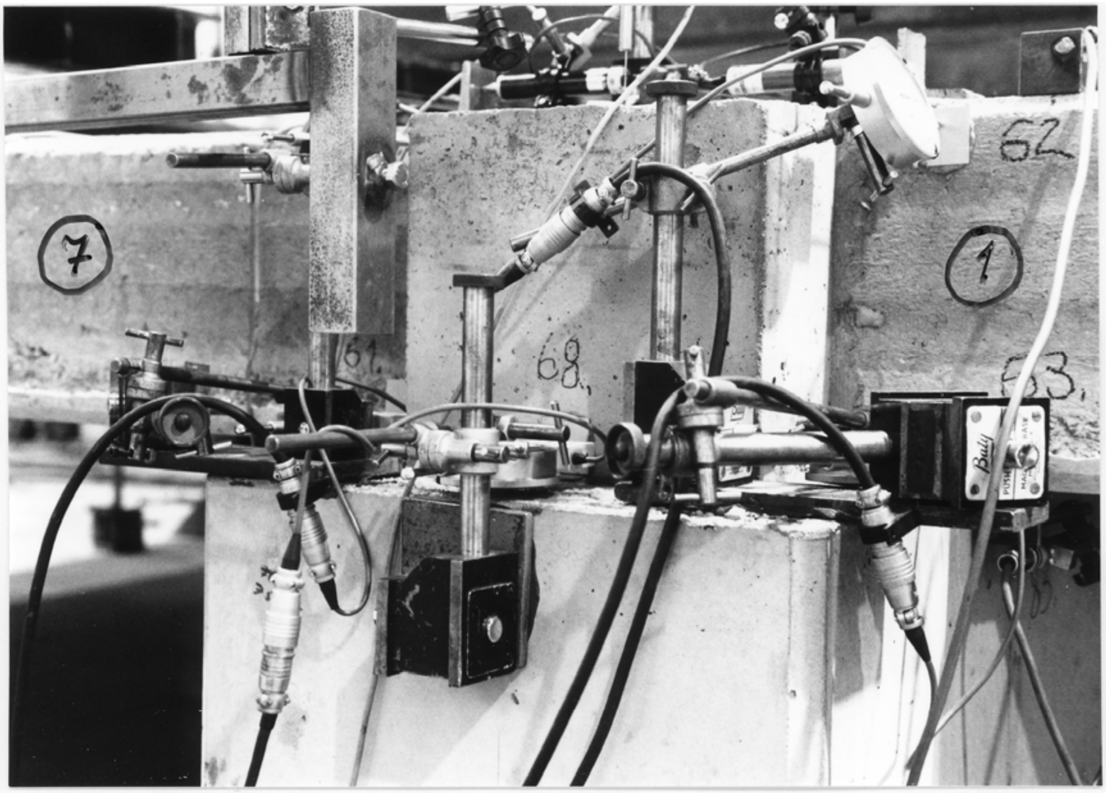

Fig. 5. Equipment for measuring transverse displacement of slabs and joint concrete relative to the middle beam.

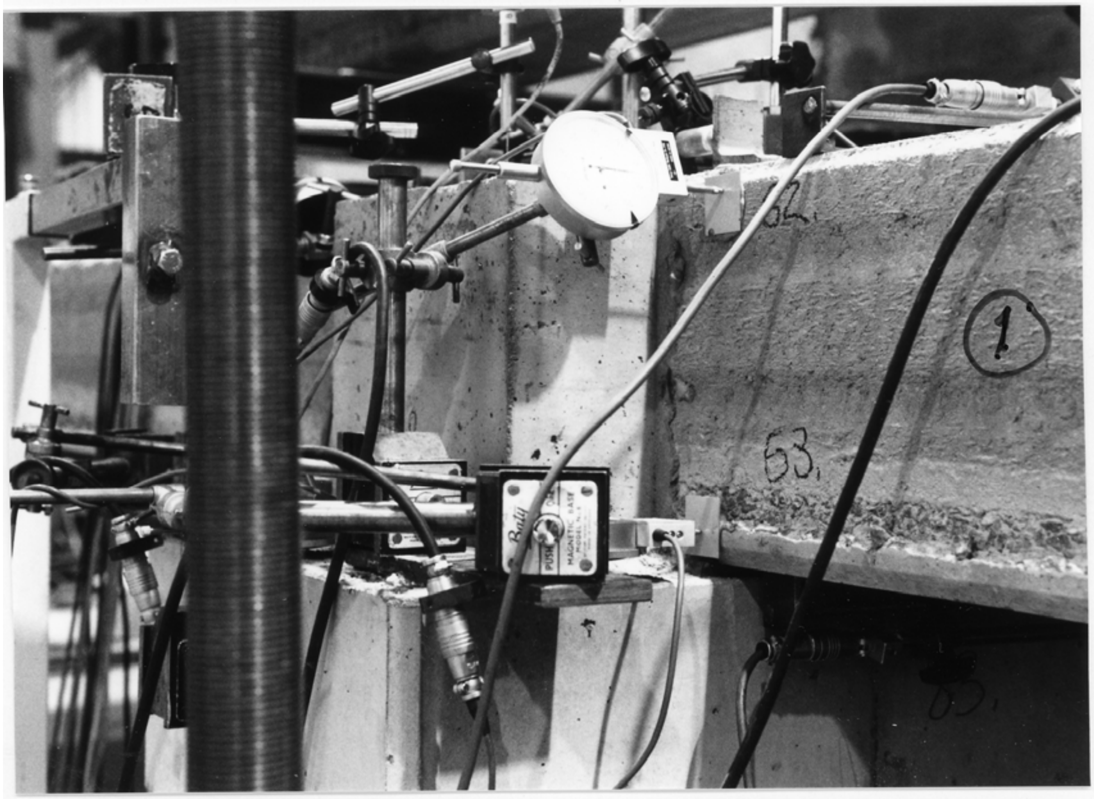

Fig. 6. The same as above.

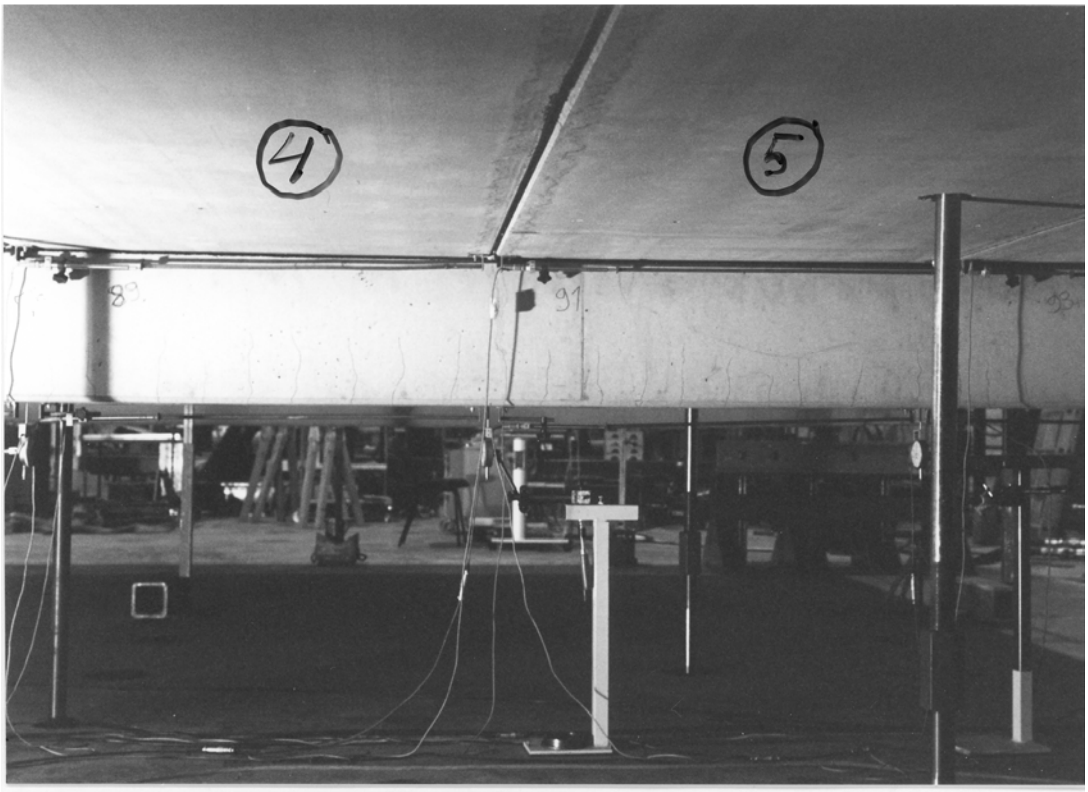

Fig. 7. Flexural cracking of the middle beam before loading.

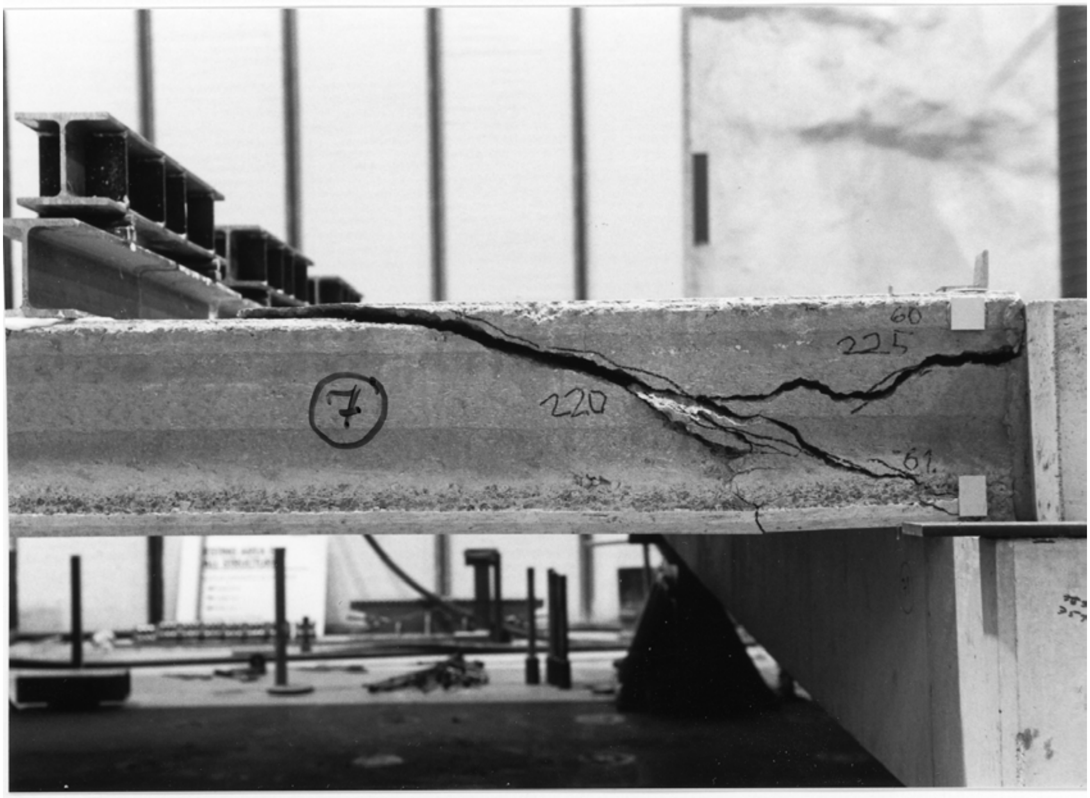

Fig. 8. Failure pattern of slab unit No. 7.

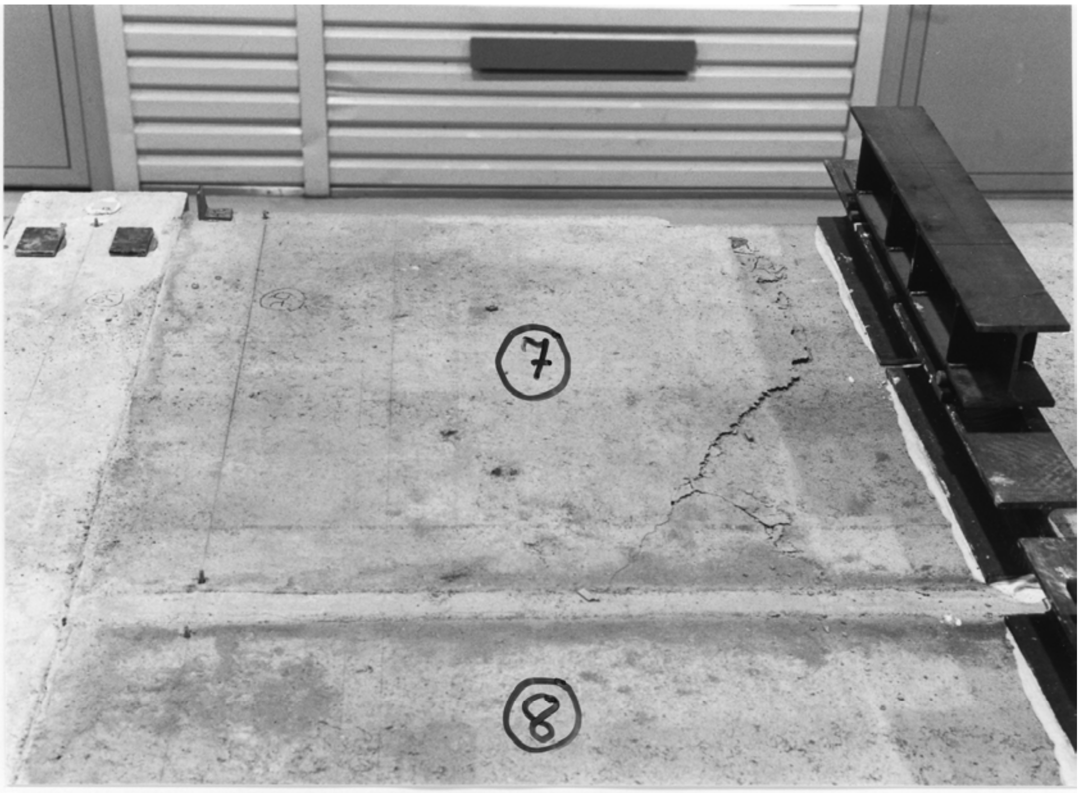

Fig. 9. Failure pattern of slab unit No. 7 seen from above.

Fig. 10. Cracking pattern of slab unit No. 1 after failure of slab unit No. 7.

Fig. 11. Cracking pattern of slab unit No. 12 after failure of slab unit No. 7.

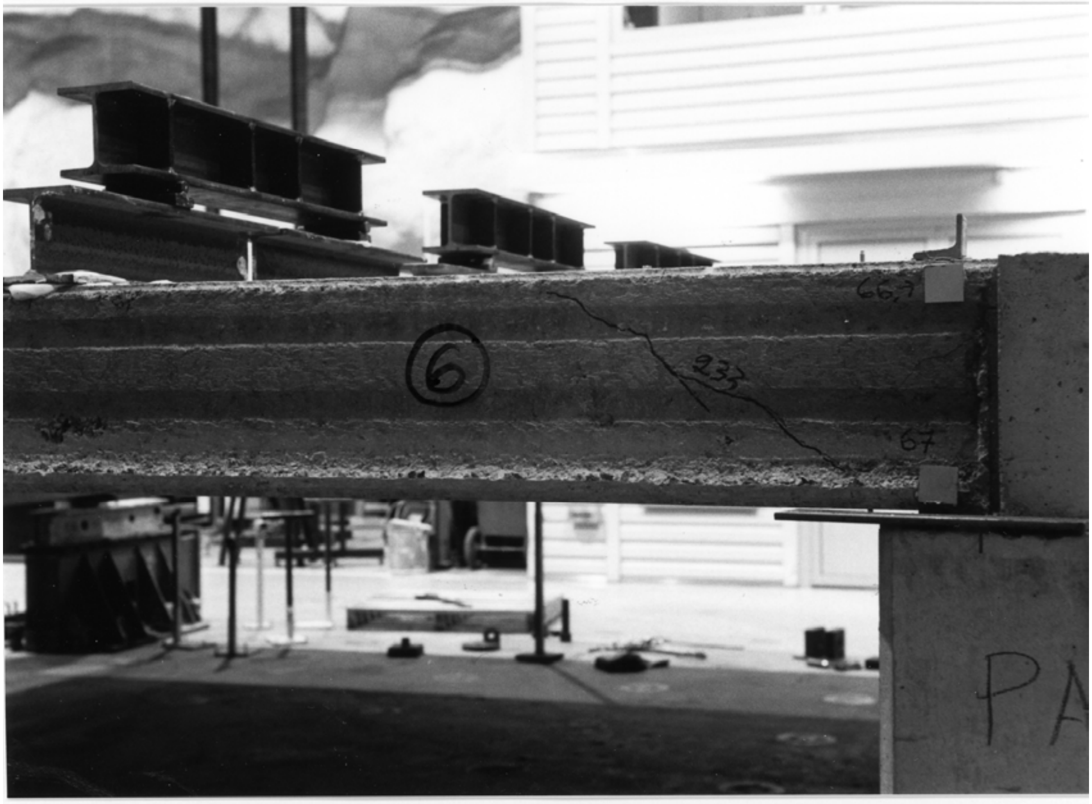

Fig. 12. Cracking pattern of slab unit No. 6 after failure of slab unit No. 7.

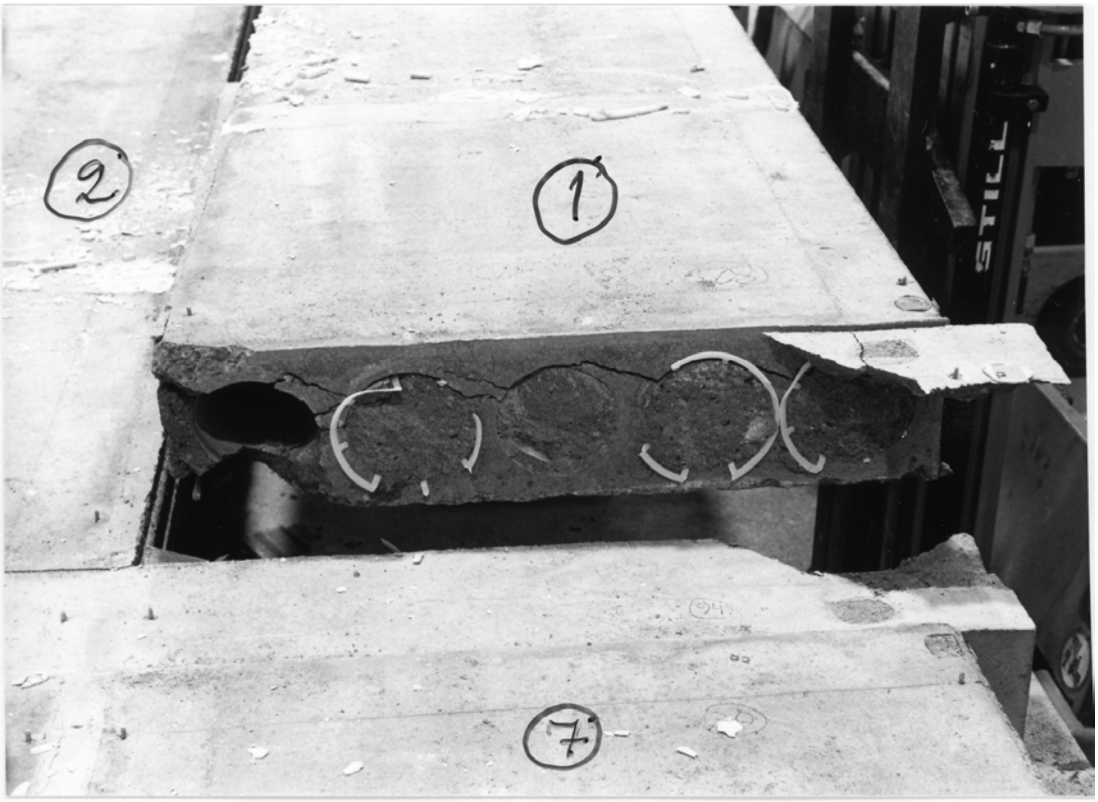

Fig. 13. Cracking pattern at end of slab unit No. 1.

Fig. 14. Cracks between the slab ends and joint concrete.

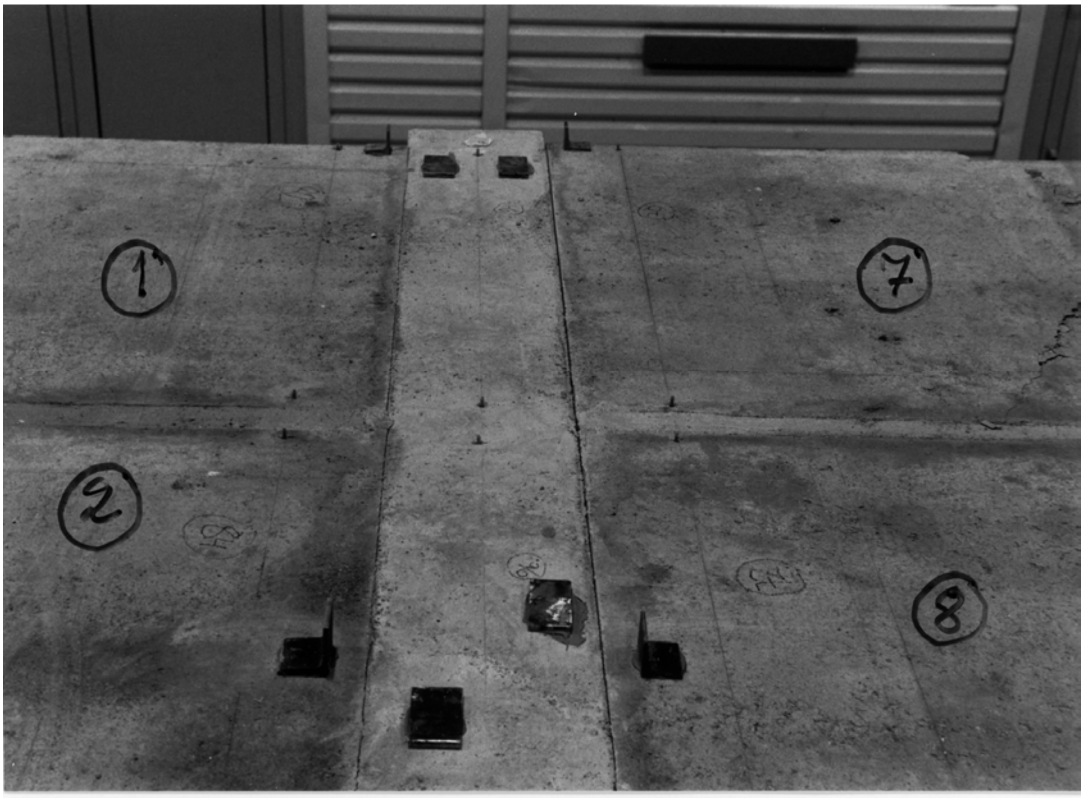

Fig. 15. Cracks between the slab ends and joint concrete.

Fig. 16. Cracking along joint between adjacent slab units.

Fig. 17. Cracking of slab unit No. 6.

Fig. 18. Typical cracking of concrete infill in the cores of slab unit No. 5.

Fig. 19. Middle beam after removal of slabs units. Side supporting slab units No. 5 and 6.

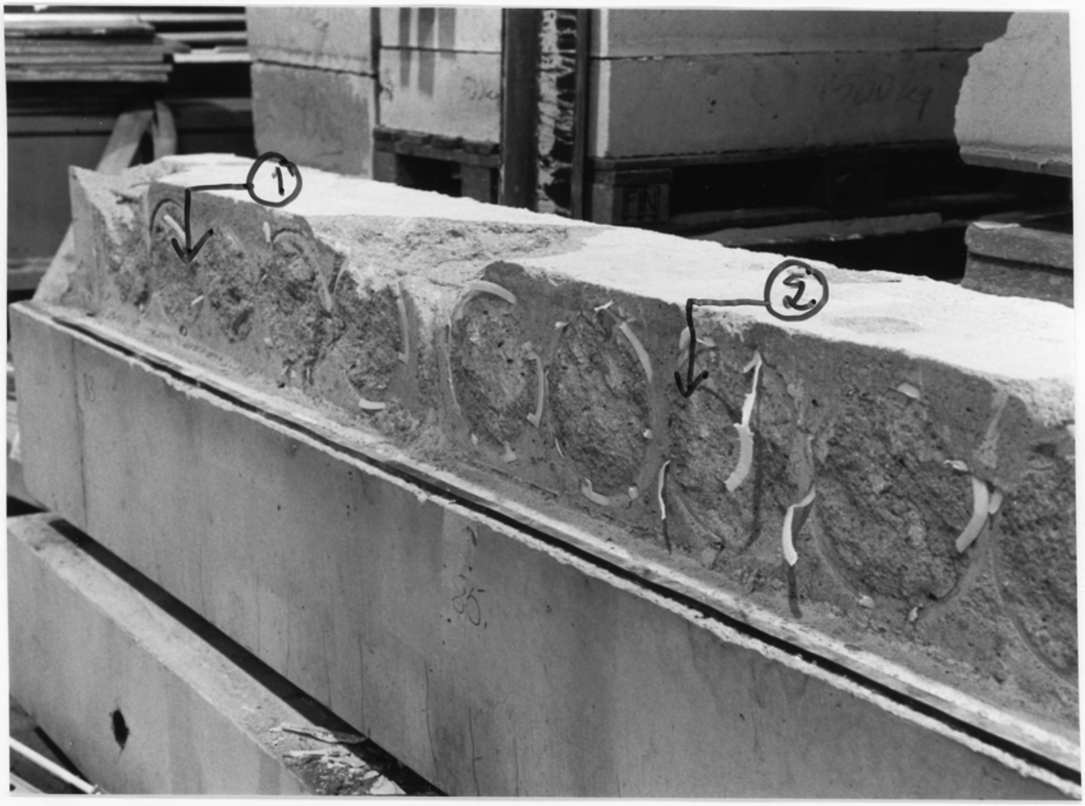

Fig. 20. Middle beam after removal of slab units. Side supporting slab units No. 1 and 2.

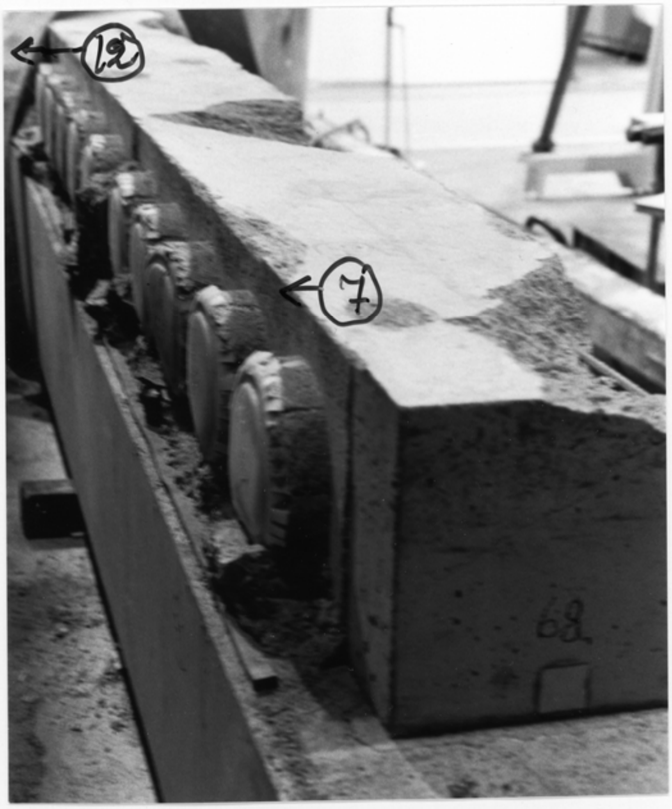

Fig. 21. Middle beam after removal of slab units. Side supporting slab units No. 7 - 12.

Fig. 22. Concrete infill below the slab ends. Note that the grout has properly filled the space. Note also the pores due to the air bubbles.

1	**General information**
1.1 Identification and aim	**VTT.CP.LBL.320.1998** **Last update 2.11.2010** LBL320 (Internal identification) Aim of the test: To quantify the interaction between the LBL beam and hollow core slabs.
1.2 Test type	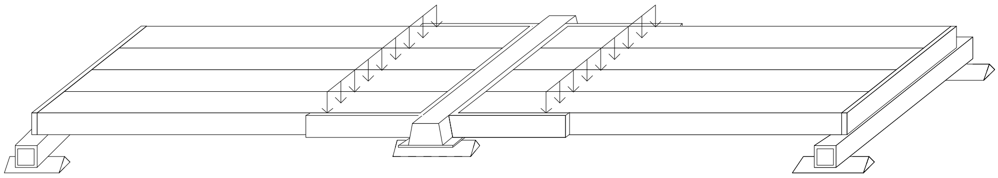 *Fig. 1. Overview on test arrangements. LBL beam in the middle, steel beams (square tubes) at the ends.*
1.3 Laboratory & date of test	VTT/FI 25.3.1998
1.4 Test report	Author(s): Pajari, M. Name: *Load test on hollow core floor* Ref. number: RTE30146/98 Date: 3.8.1998 Availability: Confidential, owner is Lujabetoni Oy, Harjamäentie 1, FI-71800 Siilinjärvi, Finland
2	**Test specimen and loading** (see also Appendices A and B) The tie beams at the ends of the slabs and the enlargements at the edges of the slab near the middle beam were cast and the joints grouted on the 16th of March 1998.

2.1
General plan

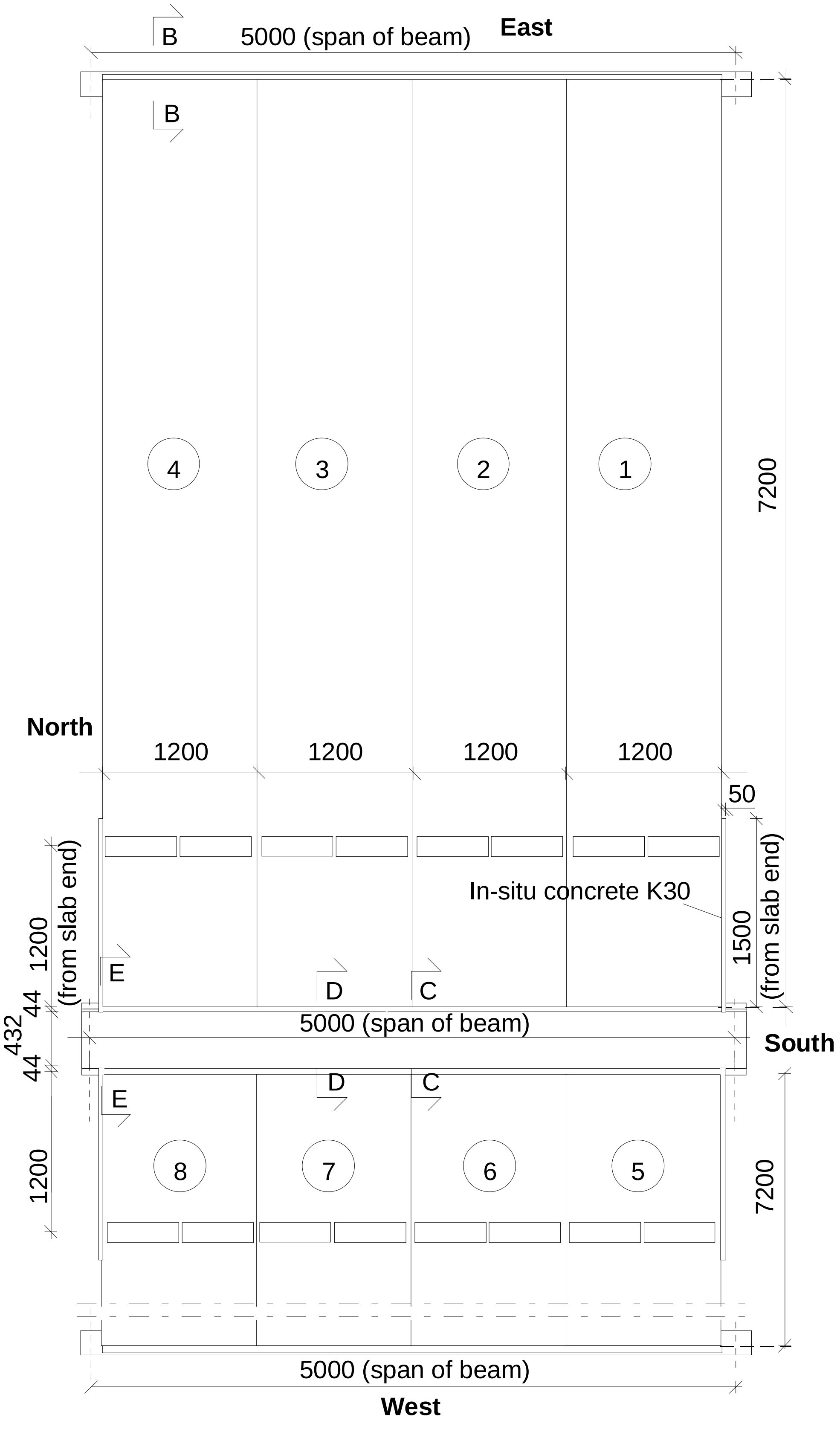

Fig. 2. Plan. For sections B-B, C-C, D-D and E-E see Figs 3, 4, 5 and 6.

2.2 End beams	See Fig. 3. Simply supported, span = 5,0 m, roller bearing below Northern end $f_y \approx 355$ MPa (nominal f_y), did not yield in the test. 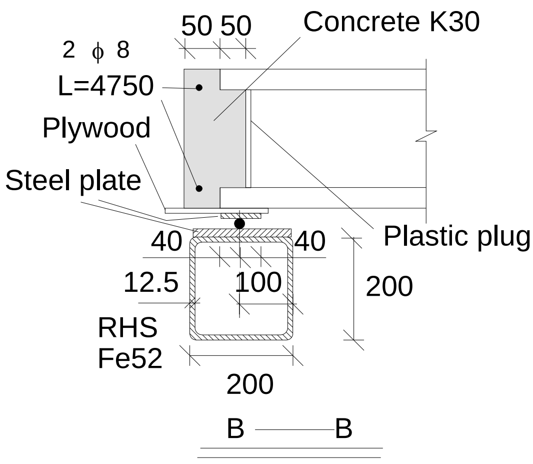 *Fig. 3. Arrangements at end beam (section B-B in Fig. 2). ϕ8 refers to a reinforcing bar T8 with diameter 8 mm.*
2.3 Middle beam	The beam, see illustration in Fig. 4 and App. A for more details, comprised - a prefabricated steel component with a bottom plate, two upper chords made of reinforcing bars and bent reinforcing bars welded both to the chords and to the bottom plate (lattice girders) as shown in App. A. - a precast and prestressed concrete component, see Fig 5 and App. A, provided with shear keys as shown in Fig. 4. 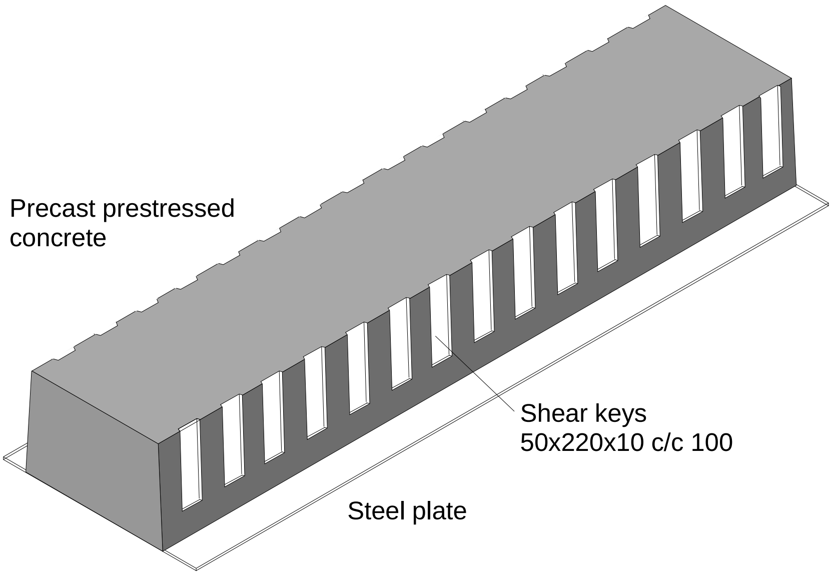 *Fig. 4. Illustration of LBL beam.* The prestressed part was cast by Lujabetoni Oy **Concrete**: K80, max aggregate size 16 mm, rapidly hardening cement

	Passive reinforcement and tendons in LBL beam: **Txy**: Hot rolled, weldable rebar A500HW, ϕ = xy mm **J12,9**: Prestressing strand, 7 wires, ϕ =12,9 mm, A_p = 100 mm^2, prestress = 1350 MPa, low relaxation (nominal value 2,5% at $\sigma = 0,7f_{pu}$) **Structural steel:** S355J0, $f_y \approx$ 355 MPa (nominal value) unless otherwise specified **Tie reinforcement across the beam**: A500HW, see above.
2.4 Arrangements at middle beam	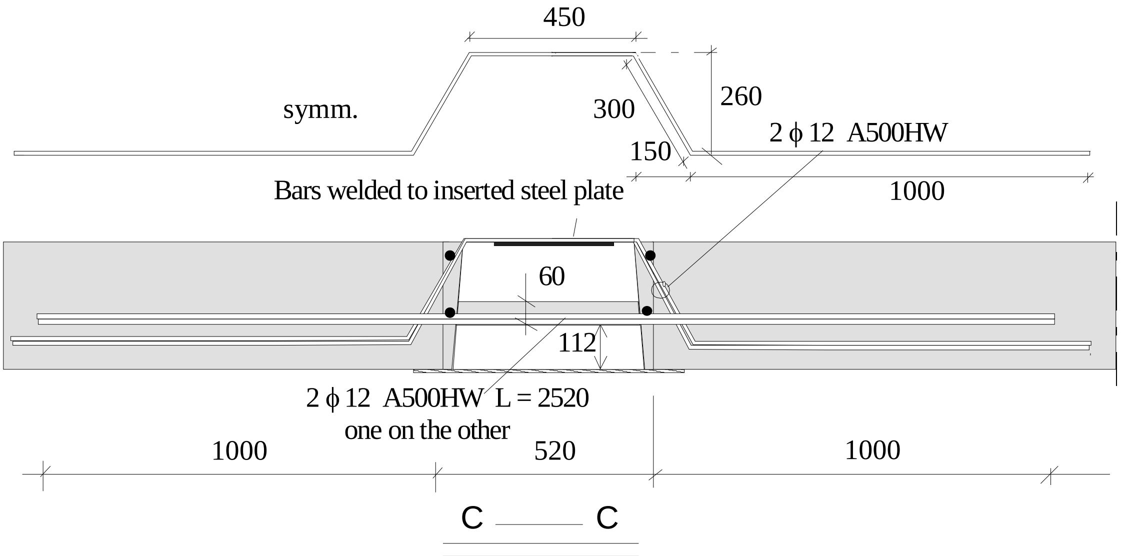 *Fig. 5. Suspension and tie reinforcement in joints between adjacent hollow core units (section C-C in Fig. 2). ϕ 12 refers to a reinforcing barT12 with diameter 12 mm.* 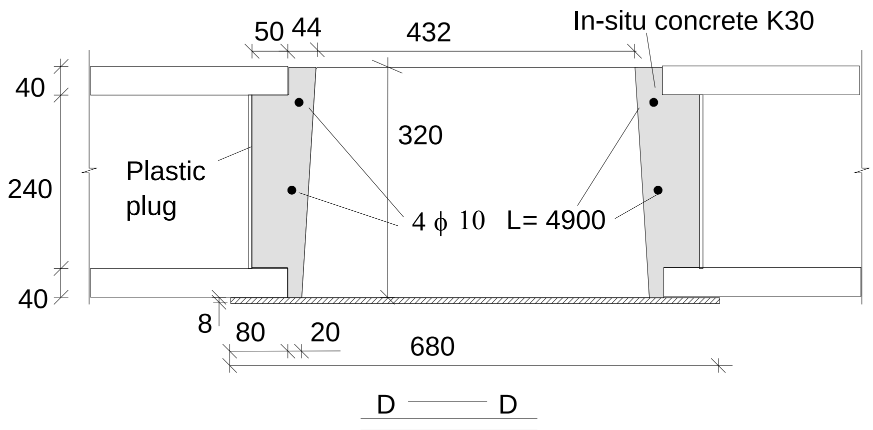 *Fig. 6. Arrangements at middle beam (section D-D in Fig. 2). ϕ10 refers to a reinforcing bar T10 with diameter 10 mm.*

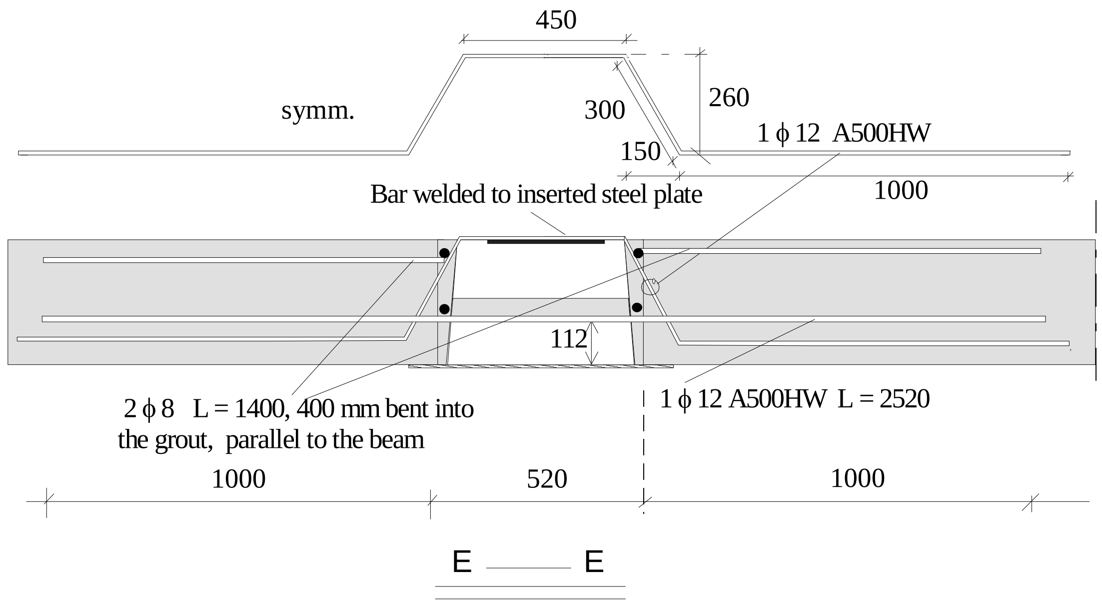

Fig. 7. Suspension and tie reinforcement at the outermost edges of the hollow core floor (section E-E in Fig. 2). ϕ8 and ϕ12 refer to reinforcing bars T8 and T12 with diameters 8 and 12 mm.

2.5
Slabs

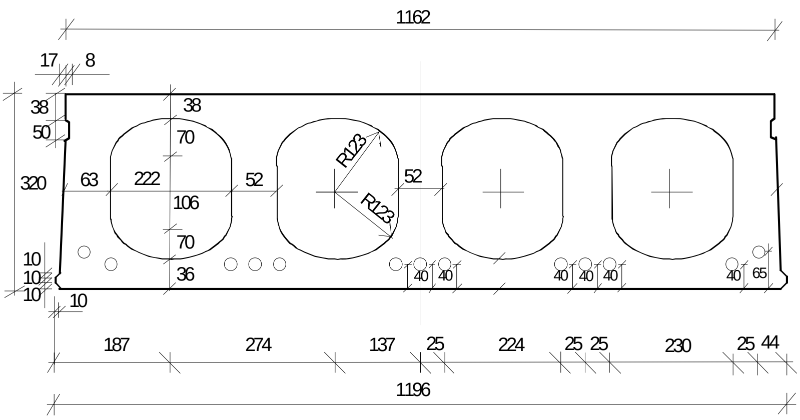

Fig. 8. Nominal geometry of slab units.

- Extruded by Lujabetoni Oy, Hämeenlinna factory 14.1.1998
- 13 lower strands J12,5, initial prestress 1100 MPa

J12,5: seven indented wires, ϕ =12,5 mm, A_p = 93 mm^2

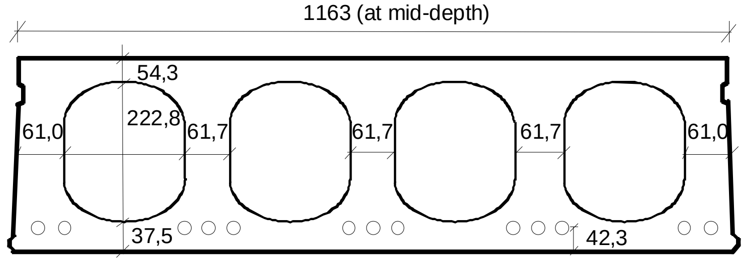

Fig. 9. Mean of most relevant measured geometrical characteristics.

Max measured bond slips:
2,5 and 2,1 mm in slab 8
2,4 mm in slab 6
2,2 and 2,1 mm in slabs 2 and 3

Measured weight of slab units = 5,13 kN/m

<table>
<tr><td>2.6
Temporary supports</td><td>No</td></tr>
<tr><td>2.7
Loading arrangements</td><td>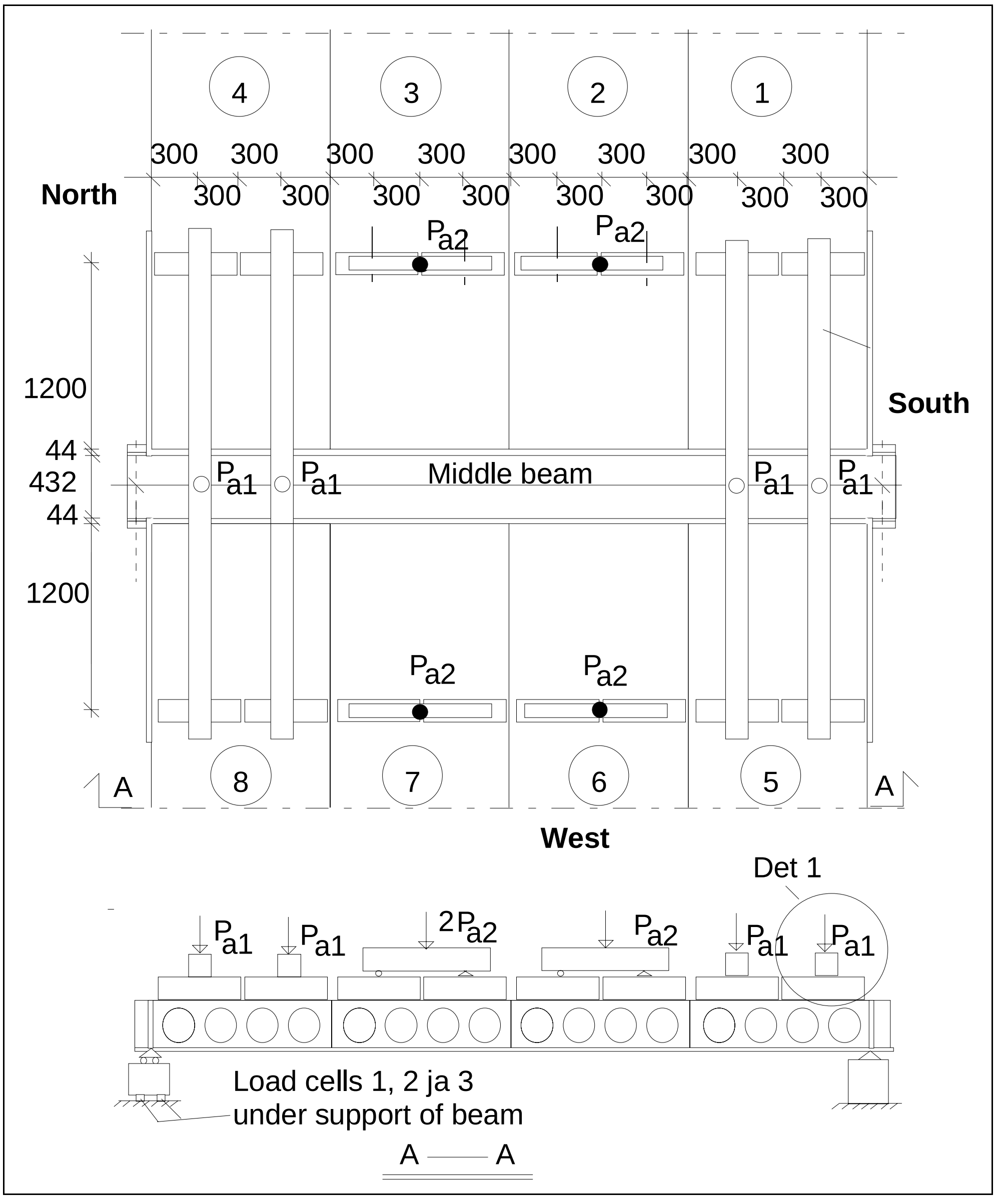

Fig. 10. Plan. P_{a1} and P_{a2} refer to vertical actuator forces.
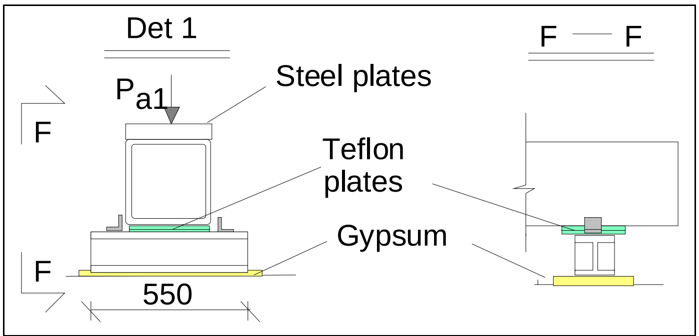

Fig. 11. Detail 1, see previous figure.</td></tr>
</table>

<table>
<tr><td>3</td><td>Measurements</td></tr>
<tr><td>3.1
Support reactions</td><td>
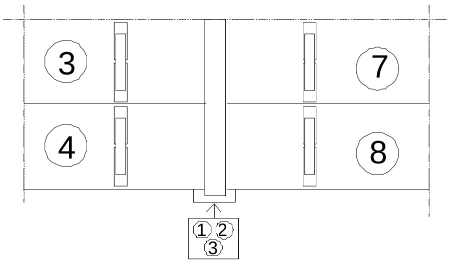

Fig. 12. Load cells below the Northern support of the middle beam.</td></tr>
<tr><td>3.2
Vertical displacement</td><td>
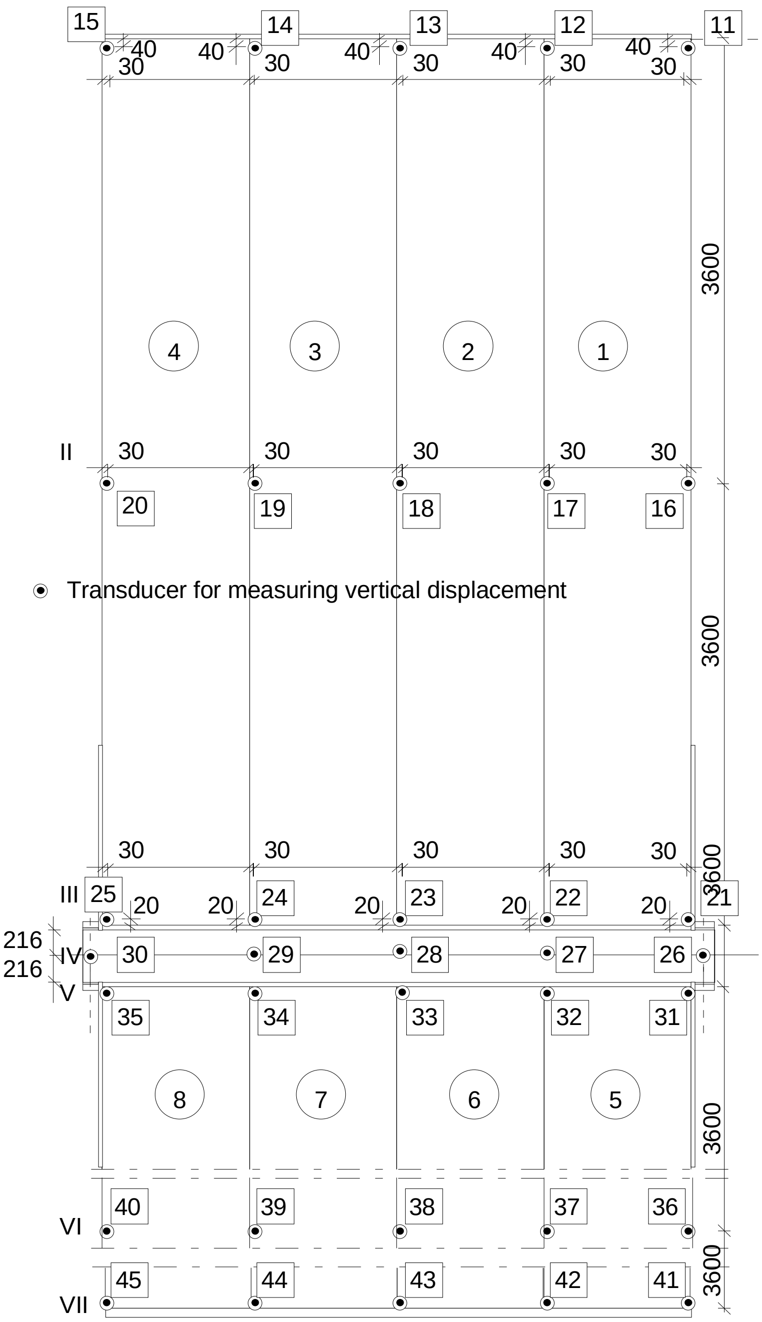

Fig. 13. Location of transducers 11 … 45 for measuring vertical deflection along lines I … VII.</td></tr>
</table>

<table>
<tr><td>3.3
Average strain</td><td>-</td></tr>
<tr><td>3.4
Horizontal displacements</td><td>
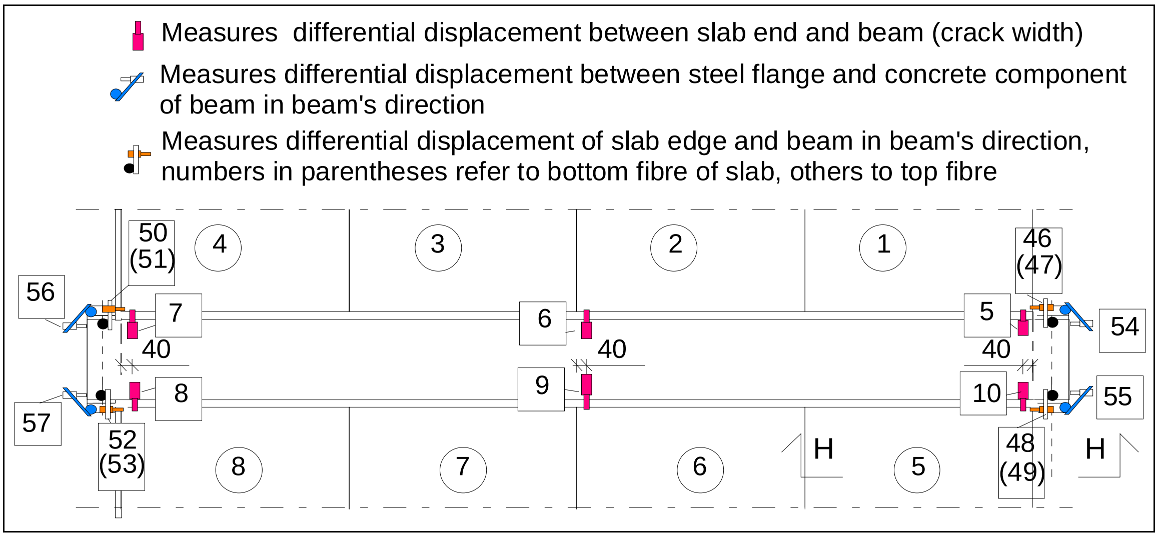

Fig. 14. Transducers measuring crack width (5–10), shear displacement at the ends of the middle beam (46–53) and differential displacement between bottom plate and concrete component of the middle beam. Transducers 47, 49, 51 and 53 are below transducers 46, 48, 50 and 52, respectively.

<table>
<tr><td>
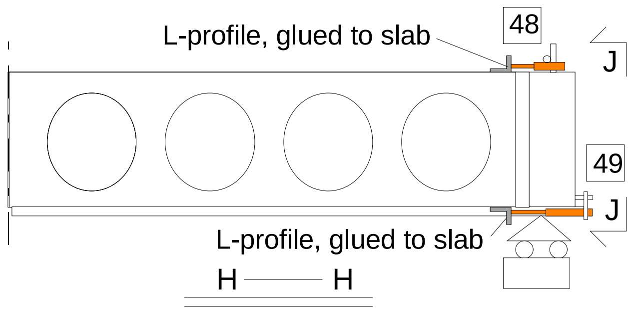

Fig. 15. Section H-H, see Fig. 15. Only transducers 48 and 49 shown.
</td><td>
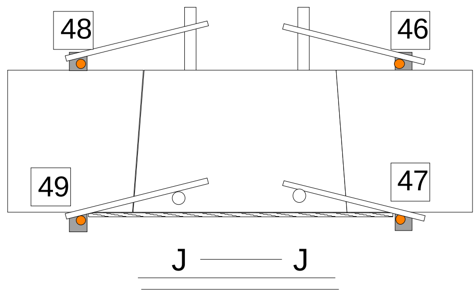

Fig. 16. Section J-J, see Fig. 16. Only transducers 46–49 shown.
</td></tr>
<tr><td>
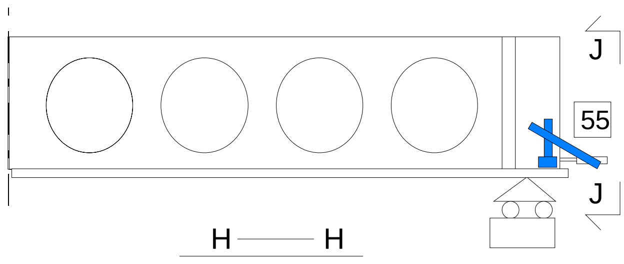

Fig. 17. Section H-H, see Fig. 15. Only transducers 55 is shown.
</td><td>
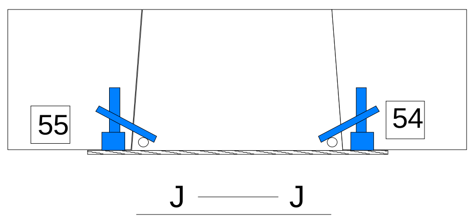

Fig. 18. Section J-J, see Fig. 18. Only transducers 54 and 55 shown.
</td></tr>
</table>
</td></tr>
<tr><td>3.5
Strain</td><td>-</td></tr>
</table>

4	**Special arrangements** -
5	**Loading strategy**
5.1 Load-time relationship	Date of test was 25.3.1998 All measuring devices were zero-balanced when the actuator forces P_{a1} and P_{a2} were equal to zero but the weight of the loading equipment and the self-weight of the structure were acting. The weight of the loading equipment below loads P_{a1} was equal to 5,6 kN and that below loads P_{a2} equal to 1,2 kN. To create two uniform line loads to the floor, attempts were made to keep P_{a2} equal to P_{a1} + 4,4 kN. The loading history for P_{a1} and P_{a2} is shown in Fig. 20 and the measured support reaction in Fig. 21. 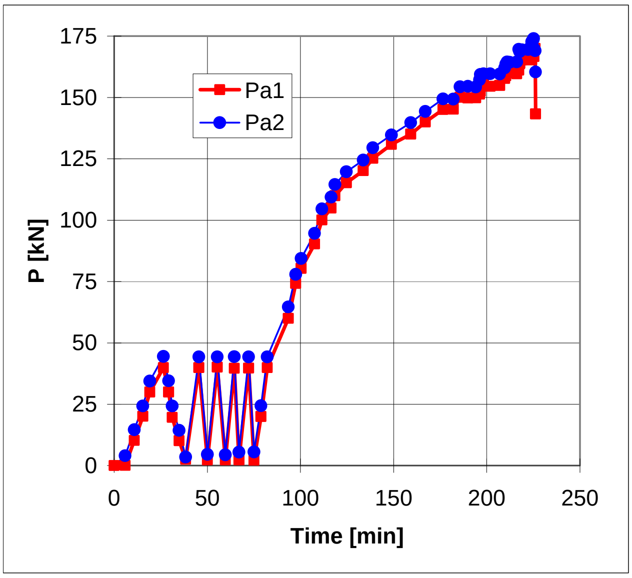 *Fig. 19. Actuator forces P_{a1} and P_{a2} vs. time.*

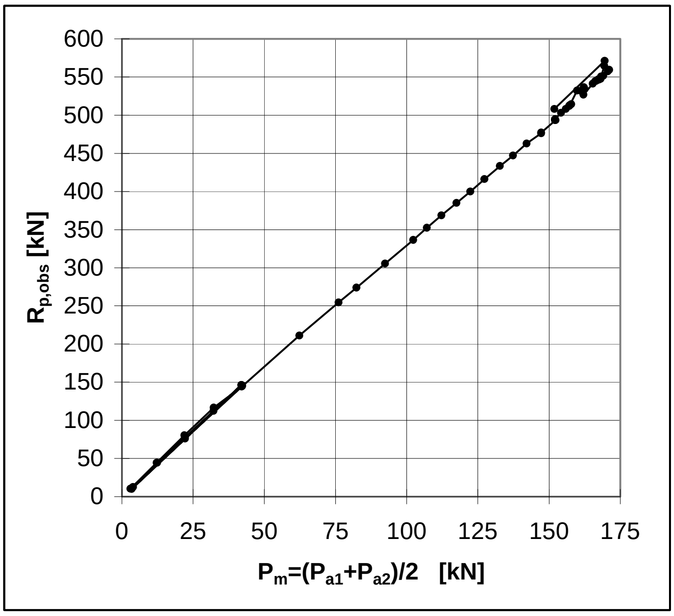

Fig. 20. Support reaction $R_{P,obs}$ below Northern end of middle beam. Note the slight increase in $R_{P,obs}$ despite the reduction of P_m at the end of the curve.

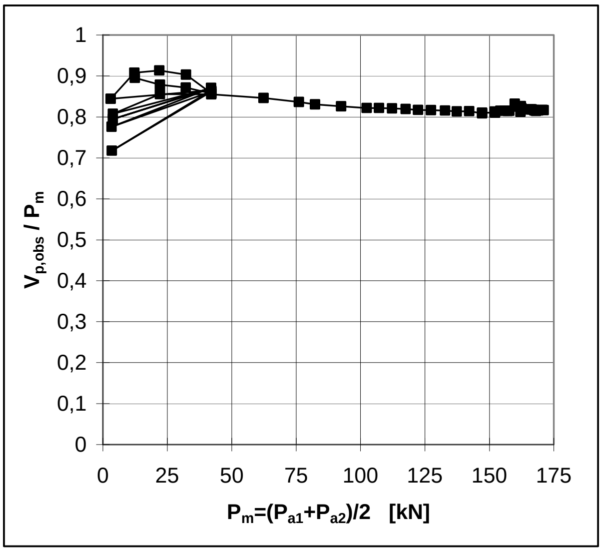

Fig. 21. Development of observed support reaction $V_{P,obs}$ per one slab as function of mean actuator force P_m.

5.2 After failure	-

6	**Observations during loading**	
	Stage I (Cyclic)	The joint concrete between the middle beam and the slab units started to crack along the slab ends.
	Stage II (Monotonous)	At P_{a1} = 70 kN the cracks in the joint concrete between the middle beam and the slab units were continuous. At P_{a1} = 80 kN the tie beams above the end beams started to crack. At P_{a1} = 115 kN flexural cracks were observed in slab unit 1 (see Fig. 23). At P_{a1} = 150 kN first shear cracks were observed in slab unit 5 and later in slab units 8, 1 and 4. At P_{a1} = 168,3 kN and P_{a2} = 174,0 kN a shear failure took place in slab units 5–8. The cracking pattern after failure is shown in Fig. 23 and in App. B. Figs 6–15.
	After failure	The concrete infill in the cores of slab units remained virtually uncracked as can be seen in App. B, Figs 16–17. The cracking took typically place along the surface of the core filling and along the slab ends.
7	**Cracks in concrete**	
7.1 Cracks at service load		
7.2 Cracks after failure		

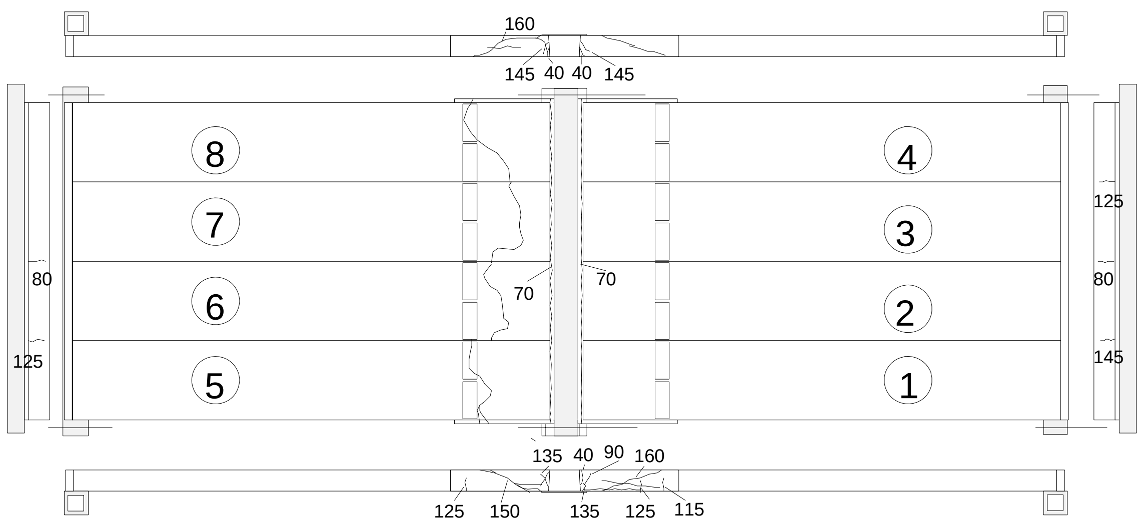

Fig. 22. Cracking pattern after failure at top surface and at edges of floor. The force values refer to the actuator force P_{a1}.

8	**Observed shear resistance**
	The ratio (measured support reaction below one end of the middle beam)/ (theoretical support reaction due to actuator forces on half floor) is shown in Fig. 23. The theoretical reaction is calculated assuming simply supported slabs. This comparison shows that the support reaction due to the actuator forces can be calculated accurately enough assuming simply supported slabs. However, the failure of the slab ends first at the South end of the middle beam resulted in reduction of support reaction below that end and increase at the North end while the symmetrically positioned actuator forces were reduced. Therefore, the measured support reaction under the maximum actuator forces, not the maximum measured support reaction, is regarded as the indicator of failure. See also Chapter 10, Fig. 29.

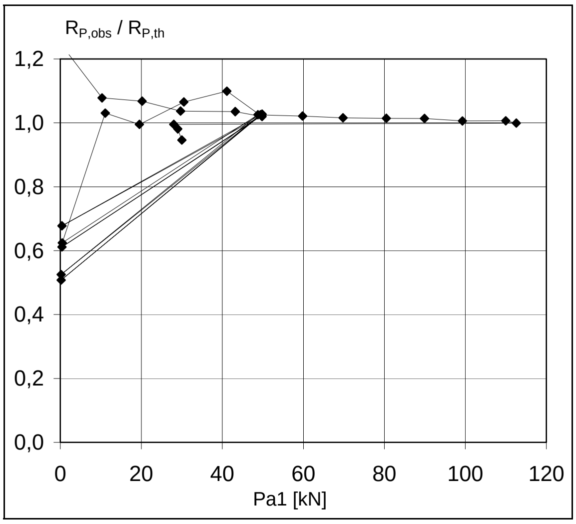

Fig. 23. Ratio of measured support reaction of the middle beam ($R_{p,obs}$) to theoretical support reaction ($R_{p,th}$) vs. actuator force P_{a1}. Only actuator loads P_{a1} and P_{a2} are taken into account in the support reaction.

Assuming simply supported slabs and calculating the support reaction of the actuator loads from equilibrium of forces, gives support reaction which is 83,7% of the actuator loads. On the other hand, just before the failure, the measured support reaction under the North end of the middle beam was 81,68% of the loads on half floor. Using this relationship for the weight of loading equipment, and assuming that the weight of the slabs and jointing concrete was distributed to both ends of the slab units as if the slabs were simply supported beams, the shear resistance of one slab end (support reaction of slab end at failure) due to different load components can be calculated as shown below.

Table. Components of shear resistance due to different loads.

Support reaction due to		
weight of slab unit ($V_{g,sl}$)	$\frac{3810+3750+3770+3760}{2\cdot 4}9{,}82$ N	18,5 kN
weight of cast-in-situ concrete ($V_{g,isc}$)	$\frac{2\cdot 0{,}52+3\cdot 0{,}75}{4}$ kN	0,8 kN
loading equipment (V_{eq})	$0{,}8168\frac{5{,}6+1{,}2}{2}$ kN	2,8 kN
actuator loads (V_p)	$0{,}8168\frac{168{,}3+174{,}0}{2}$ kN	139,8 kN

The shear resistance of one slab end due to imposed load

$V_{obs,imp}$ = V_p + V_{eq} = 139,8 kN + 2,78 kN = 142,6 kN

and the total shear resistance

V_{obs} = $V_{obs,imp}$ + $V_{g,sl}$ + $V_{g,isc}$ = 142,6 kN + 18,5 kN + 0,8 kN = 161,9 kN

are obtained.

The observed shear resistance **V_{obs} = 161,9 kN** (shear force at support) is obtained for one slab unit with width = 1,2 m. The shear force per unit width is **v_{obs} = 134,9 kN/m.**

9 Material properties

9.1
Strength of steel

Component	$R_{eH}/R_{p0,2}$ MPa	R_m MPa	Note
Bottom plate	≈ 355		Nominal (S355J0)
Lattice girders	500		Nominal (A500HW)
Slab strands J12,5	1570	1770	Nominal (no yielding in test)
Beam strands J12,9	1630	1860	Nominal (no yielding in test)
Reinforcement Txy	500		Nominal value for reinforcing bars A500H (no yielding in test)

9.2
Strength of slab concrete, floor test

#	Cores	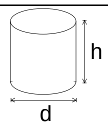	*h* mm	*d* mm	Date of test	Note
6			50	50	1.4.2009 (+7 d)[1)]	Upper flange of slab1 (11–13) and 5 (51 –53), vertically drilled Tested as drill2460 kg/m^3
Mean strength [MPa]			63,8			
St.deviation [MPa]			5,3			

9.3
Strength of slab concrete, reference tests

#	Cores	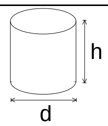	*h* mm	*d* mm	Date of test	Note
6			50	50	1.4.2009 (0 d)[1)]	Upper flange of slab 9 (91–93) and 10 (101 –103), vertically drilled Tested as drilled[2)] Density = 2480 kg/m^3
Mean strength [MPa]			61,8			
St.deviation [MPa]			2,4			

9.4
Strength of grout in longitudinal joints of slab units

#	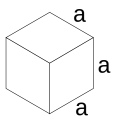	*a* mm	Date of test	Note
3		150	25.3.1998 (+0 d)[1)]	Kept in laboratory in the same conditions as the floor specimen Density = 2070 kg/m^3
Mean strength [MPa]		23,0		
St.deviation [MPa]		-		

9.5
Strength of concrete in LBL beam

#	Cores	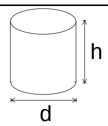	*h* mm	*d* mm	Date of test	Note
3			75	75	1.4.2009 (+7 d)[1)]	Upper flange, vertically drilled Tested as drilled[2)] Density = 2480 kg/m^3
Mean strength [MPa]			84,8			
St.deviation [MPa]			-			

[1)] Date of material test minus date of structural test (floor test or reference test)
[2)] After drilling, kept in a closed plastic bag until compression

10 **Measured displacements**

In the following Figs 26–32, V_p stands for the shear force of one slab end due to imposed actuator loads, more accurately 1/4 of the measured support reaction below the North end of the middle beam. On the other hand, in Fig. 33 the mean actuator force = (P_{a1}+P_{a2})/2 is used as load parameter.

Comparison between Figs 29 and 33 shows that the maximum load carrying capacity was achieved before the maximum support reaction below the North end was measured. This suggests that there was load transfer from the South to the North while the shear cracks propagated in the slab units.

10.1
Deflections

In Fig. 29 (middle beam) the net deflection (= measured deflection – rigid body motion due to settlement of supports) is given, other figures show the measured deflection.

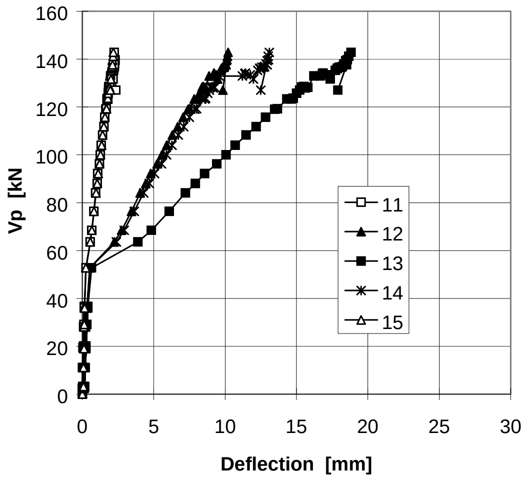

Fig. 24. Deflection on line I along end beam.

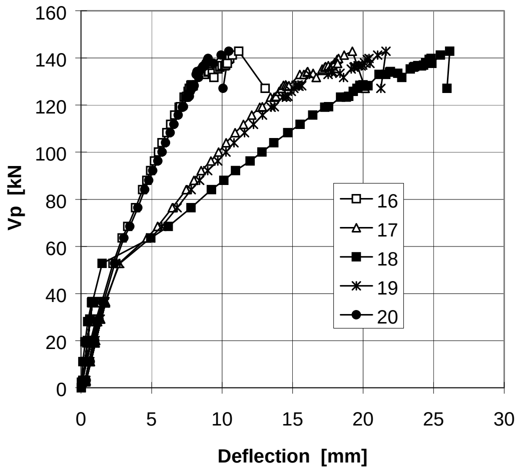

Fig. 25. Deflection on line II in the middle of slabs 1–4.

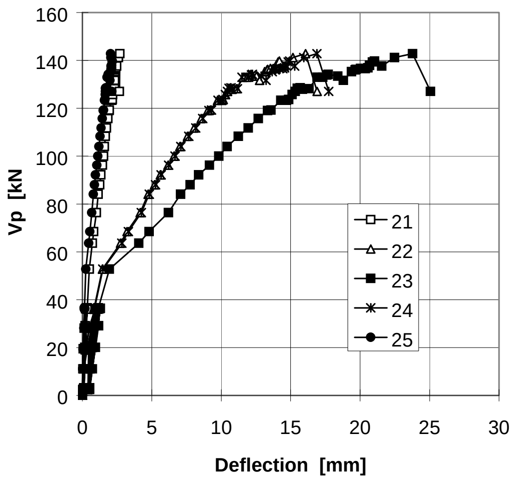

Fig. 26. Deflection on line III close to the line load, slabs 1–4.

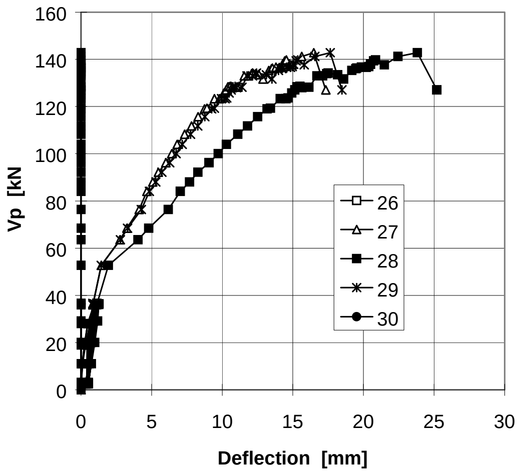

Fig. 27. Net deflection on line IV along the middle beam.

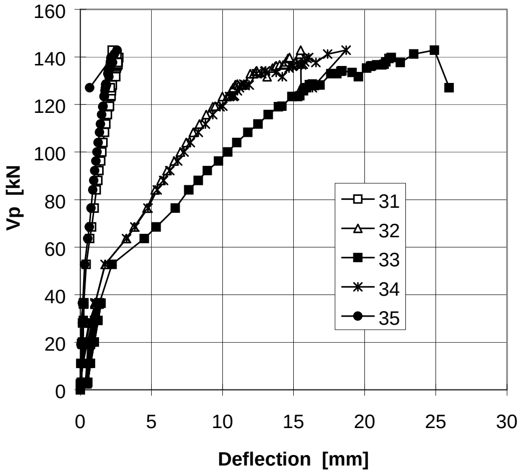

Fig. 28. Deflection on line V close to the line load, slabs 5–8.

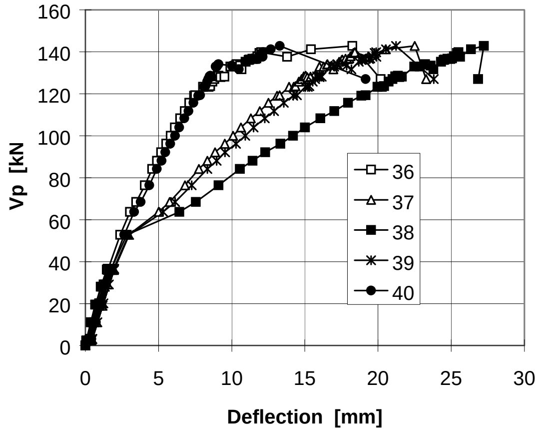

Fig. 29. Deflection on line VI in the middle of slabs 5–8.

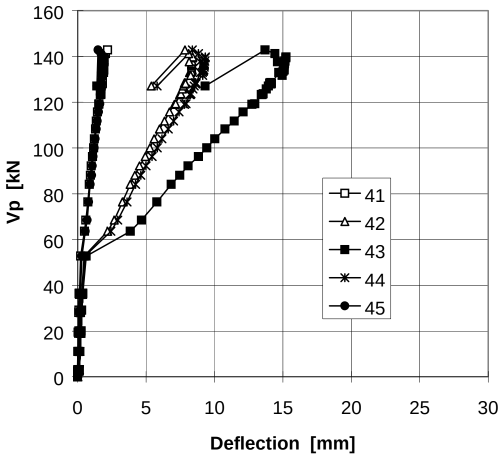

Fig. 30. Deflection on line VII along end beam, slabs 5–8.

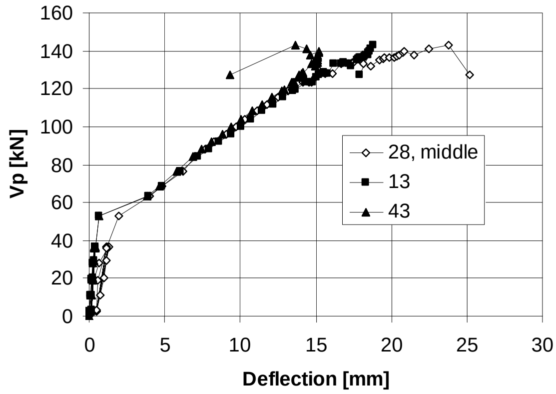

Fig. 31. Net deflection of midpoint of middle beam (28) and those of end beams (13, 43). (Settlement of supports eliminated.)

10.2
Crack width

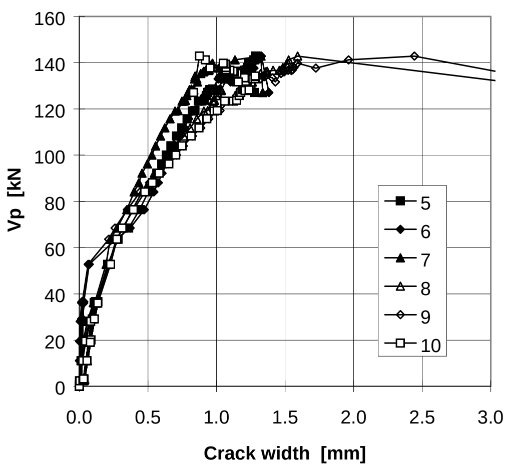

Fig. 32. Differential displacement (≈ crack width) measured by transducers 5–10.

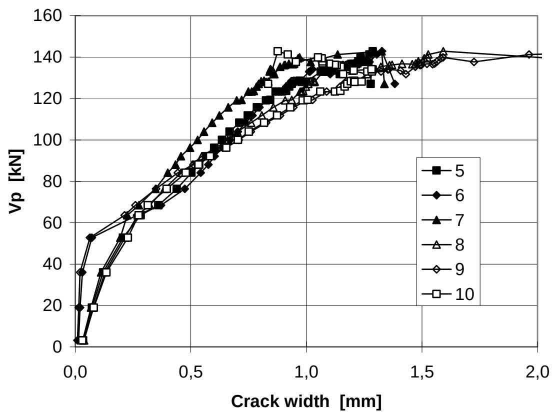

Fig. 33. Same as previous figure but the cyclic loading phase is not shown.

10.3 Average strain (actually differential displacement)	-
10.4 Shear displacement	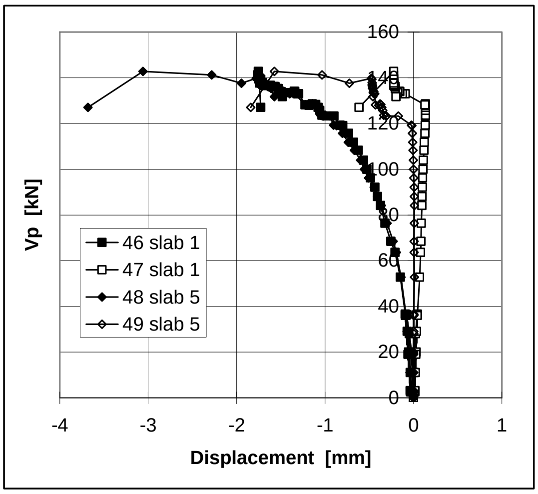 *Fig. 34. Southern end of middle beam. Differential displacement between edge of slab and middle beam. A negative value means that the slab is moving towards the end of the beam.* 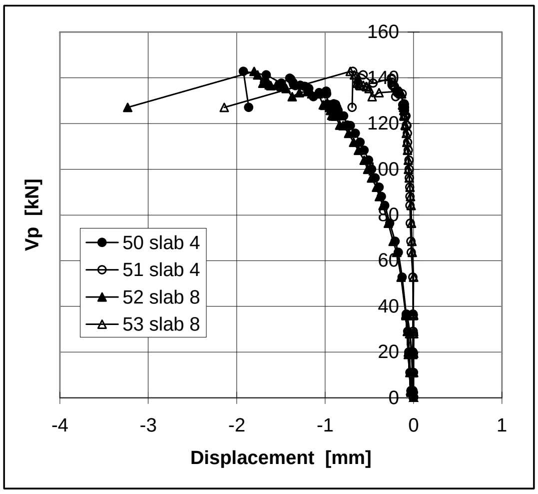 *Fig. 35. Northern end of middle beam. Differential displacement between edge of slab and middle beam. A negative value means that the slab is moving towards the end of the beam.* 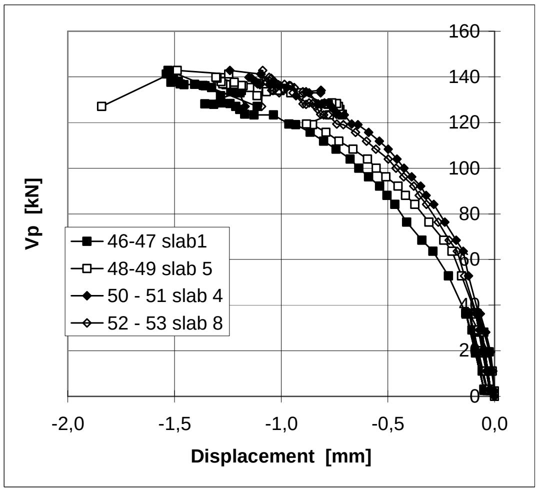 *Fig. 36. Shear displacement = differential displacement at upper edge – differential displacement at lower edge of slab.*

10.5 Relative displacement between bottom flange and concrete component of middle beam

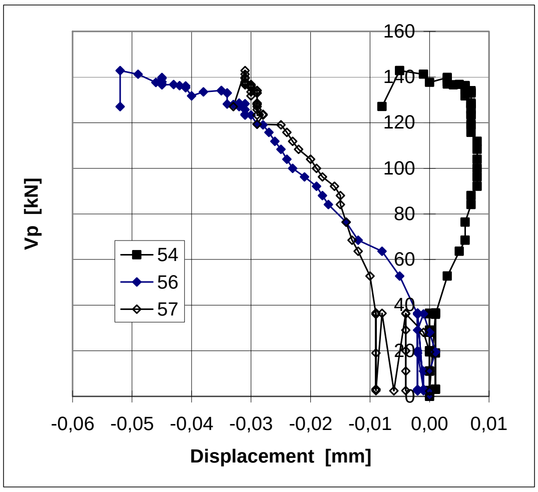

Fig. 37. Differential displacement measured by transducers 54, 56 and 57.

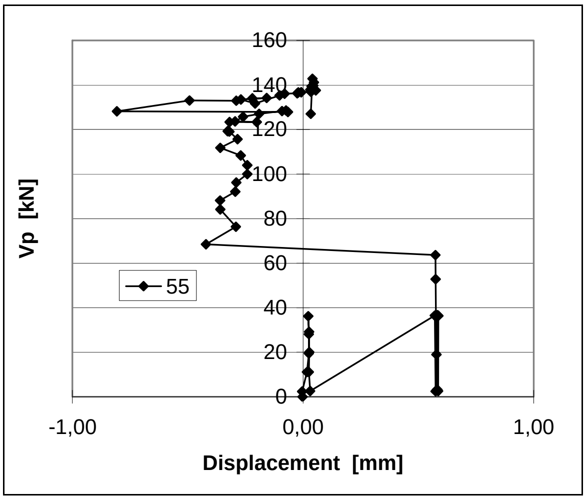

Fig. 38. Differential displacement measured by transducer 55 (obviously incorrect).

11 Reference tests

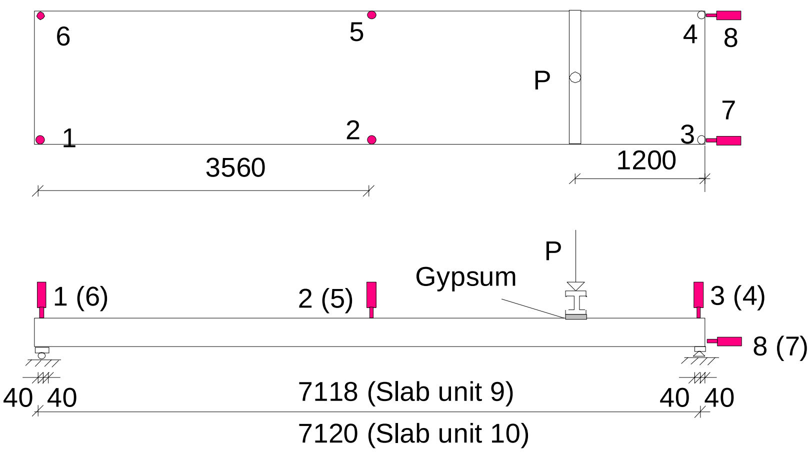

Fig. 39. Layout of reference test. a) Plan. b) Elevation. The displacements were measured by transducers 1–6, the bond slip of the outermost strands by transducers 7 and 8.

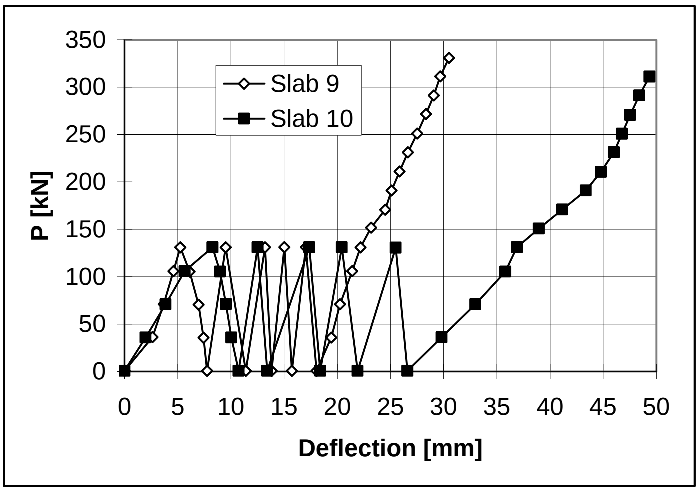

Fig. 40. Actuator force – time relationship. R1 : Slab 9; R2:Slab 10.

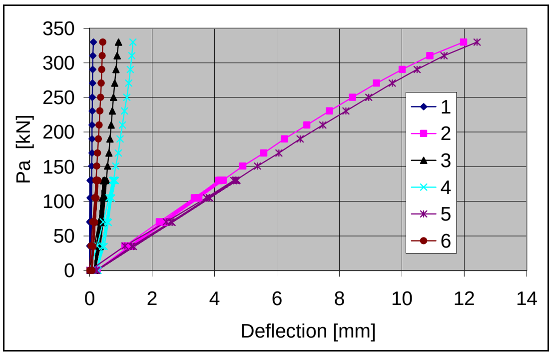

R1

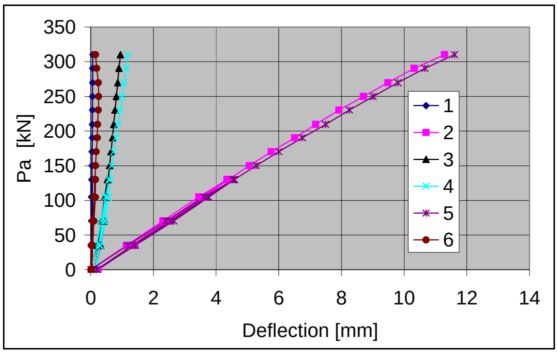

R2

Fig. 41. Displacements measured by transducers 1–6. P_a is the actuator force.

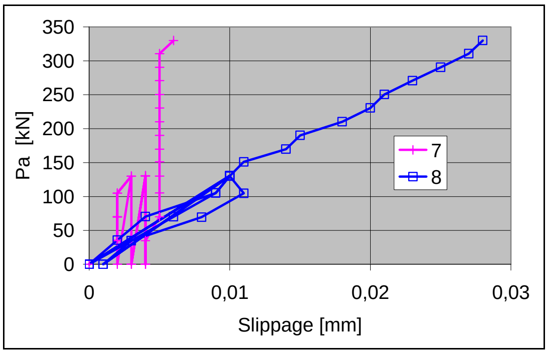

R1

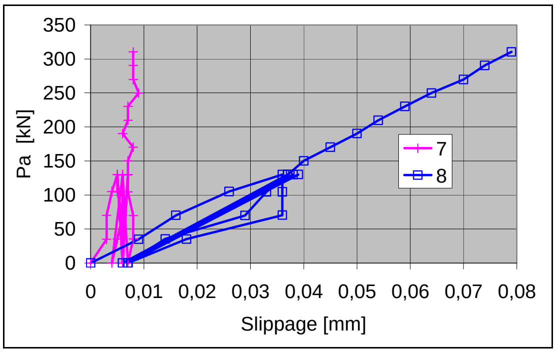

R2

Fig. 42. Slippage of outermost strands measured by transducers 7–8. P_a is the actuator force.

Table. Reference tests. Span of slab, shear force V_g at support due to the self weight of the slab, actuator force P_a at failure, weight of loading equipment P_{eq}, total shear force V_{obs} at failure and total shear force v_{obs} per unit width.

Test	Date	Span mm	V_g kN	P_a kN	P_{eq} kN	V_{obs} kN	v_{obs} kN/m	Note
R1	1.4.1998	7118	18,5	332,0	0,8	297,1	250,6	Web shear failure
R2	1.4.1998	7120	18,4	328,0	0,8	293,6	244,7	Web shear failure
Mean						**295,3**	**246,1**	

12 Comparison: floor test vs. reference tests

The observed shear resistance (support reaction) of the hollow core slab in the floor test was equal to 161,9 kN per one slab unit or 134,9 kN/m. This is **55%** of the mean of the shear resistances observed in the reference tests.

13 Discussion

1. At maximum load, the net deflection of the middle beam due to the imposed actuator loads (deflection minus settlement of supports) was 20,9 mm or *L*/240, i.e. rather small. It was 4,5–7,5 mm greater than that of the end beams. See Fig. 33 for the difference. Hence, the torsional stresses due to the different deflection of the middle beam and end beams may have had a minor effect on the failure of the slabs.

2. The shear resistance measured in the reference tests was typical of the similar slabs produced in Finland, see *Pajari, M. Resistance of prestressed hollow core slab against a web shear failure. VTT Research Notes 2292, Espoo 2005*.

3. The bond between the cast-in-situ concrete and the edges of the hollow cores was weak. This can be seen in the photographs in App. B in which the hardened hollow core fillings remained almost intact in most cases.

4. The sliding of the edge slabs along the middle beam was negligible before 85% of the failure load was achieved. At failure the differential displacement between the bottom flange of the beam and the soffit of the edge slabs was of the order of 0,2 … 0,5 mm. This reduced the negative effects of the transverse actions in the slab and had a positive effect on the shear resistance.

5. The transverse shear deformation of the edge slabs was considerable which can be seen in Figs 47–49.

6. The failure mode was web shear failure of edge slabs. The LBL beam seemed to recover completely after the failure.

APPENDIX A: STEEL COMPONENT OF LBL BEAM

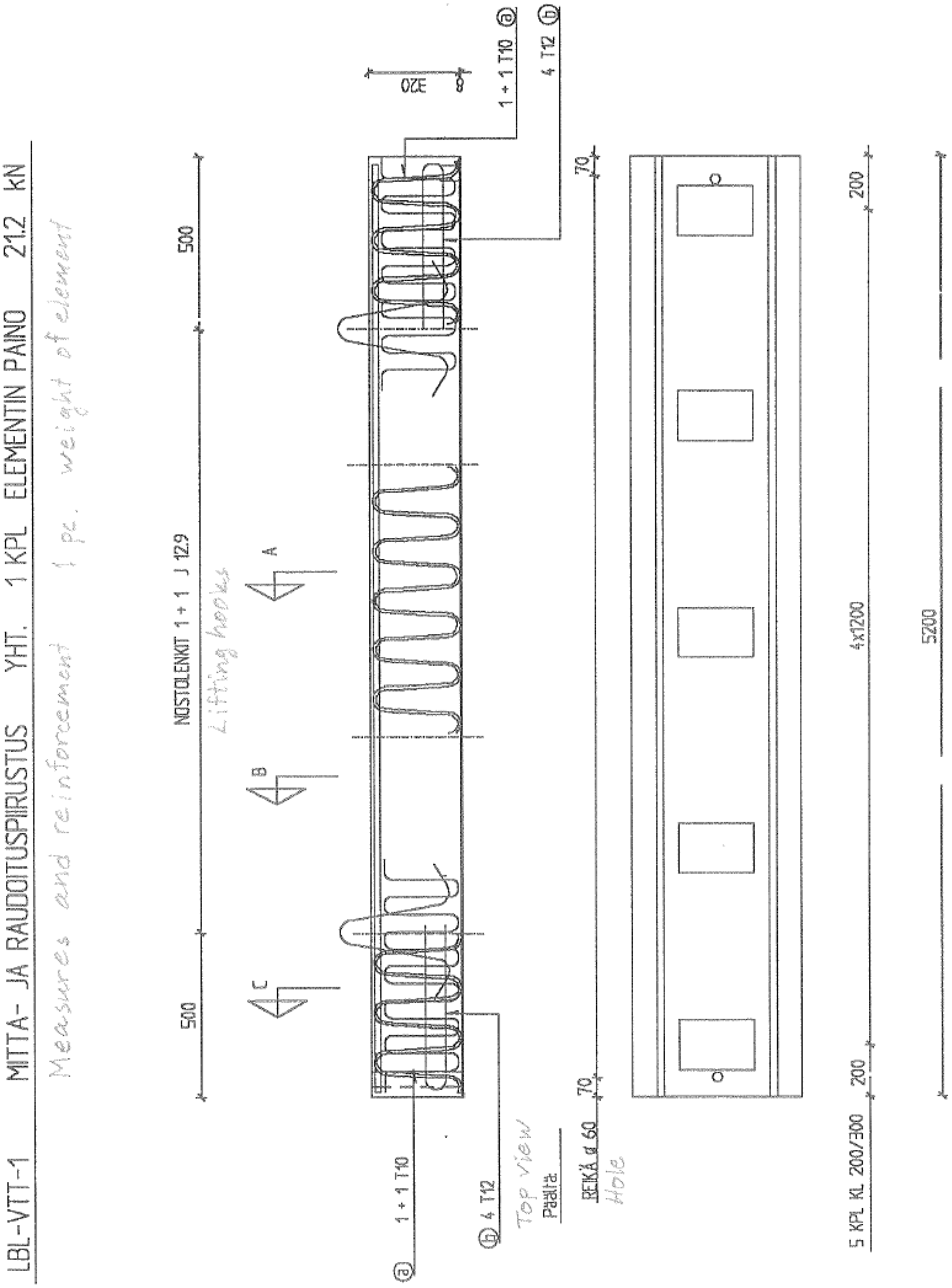

Fig. 1. Steel component of LBL beam. Elevation (lattice girders) and plan (bottom plate). See Fig. 2 for sections A, B and C.

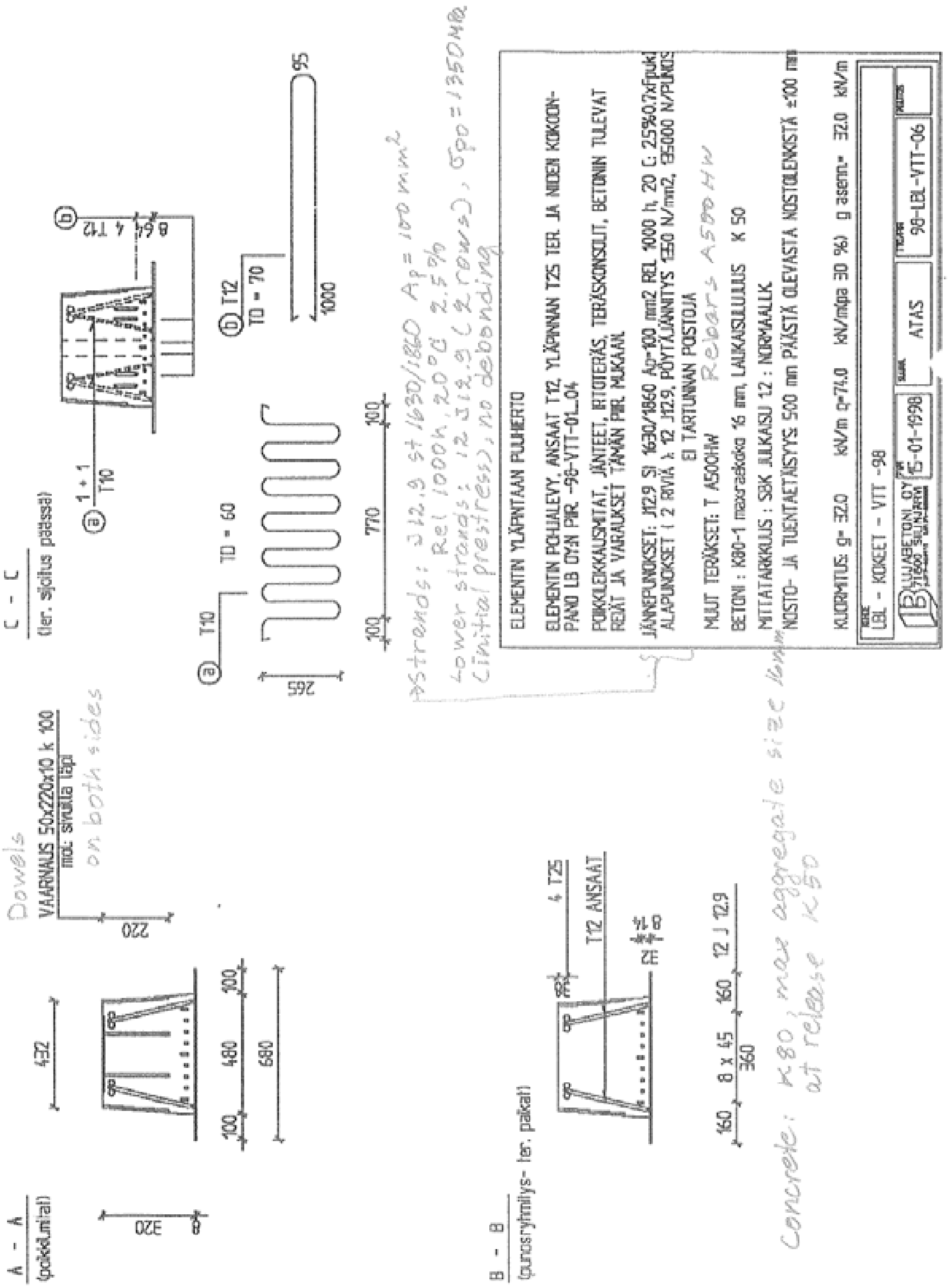

Fig. 2. Sections A, B and C, see Fig. 1.

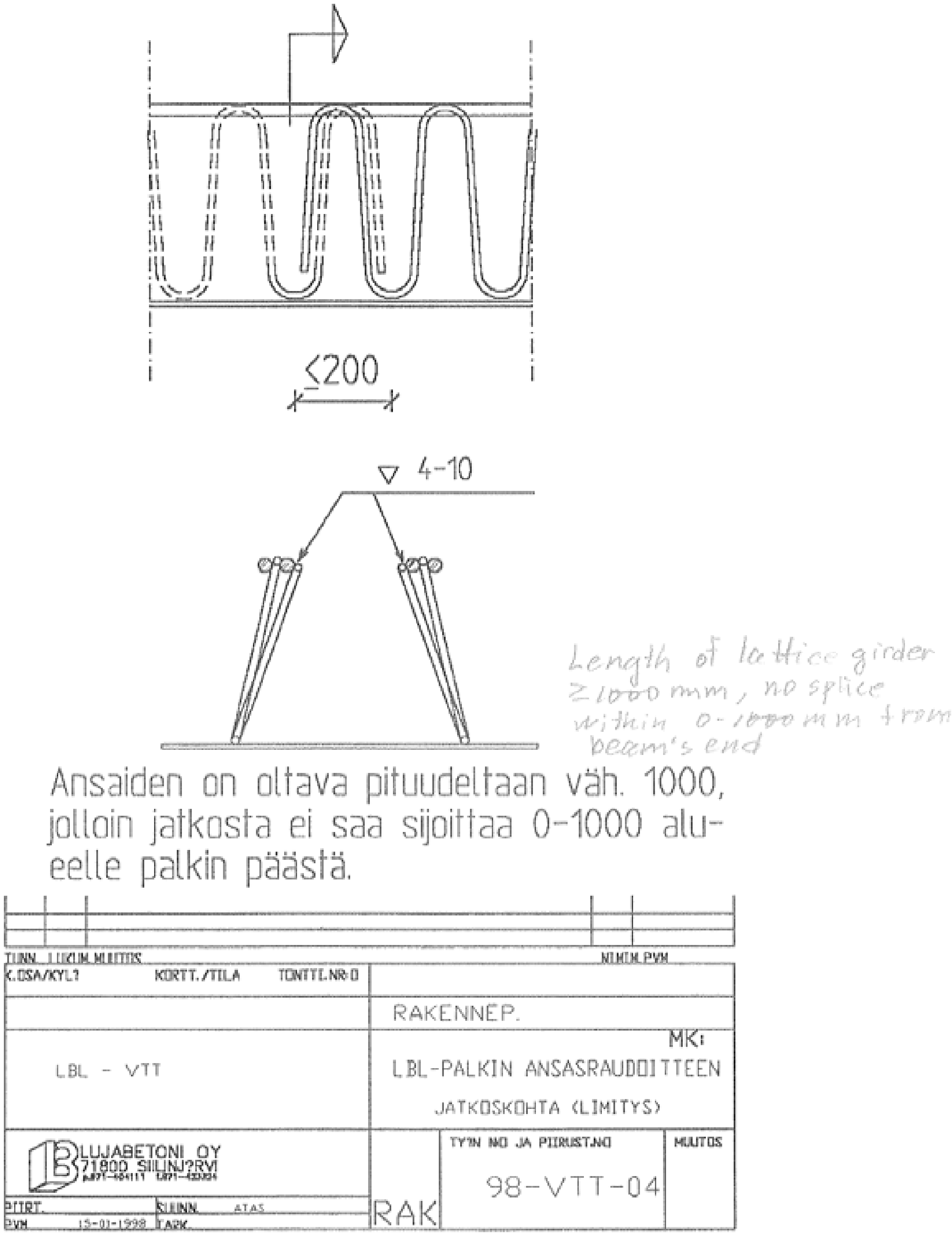

Fig. 3. Splicing of lattice girders.

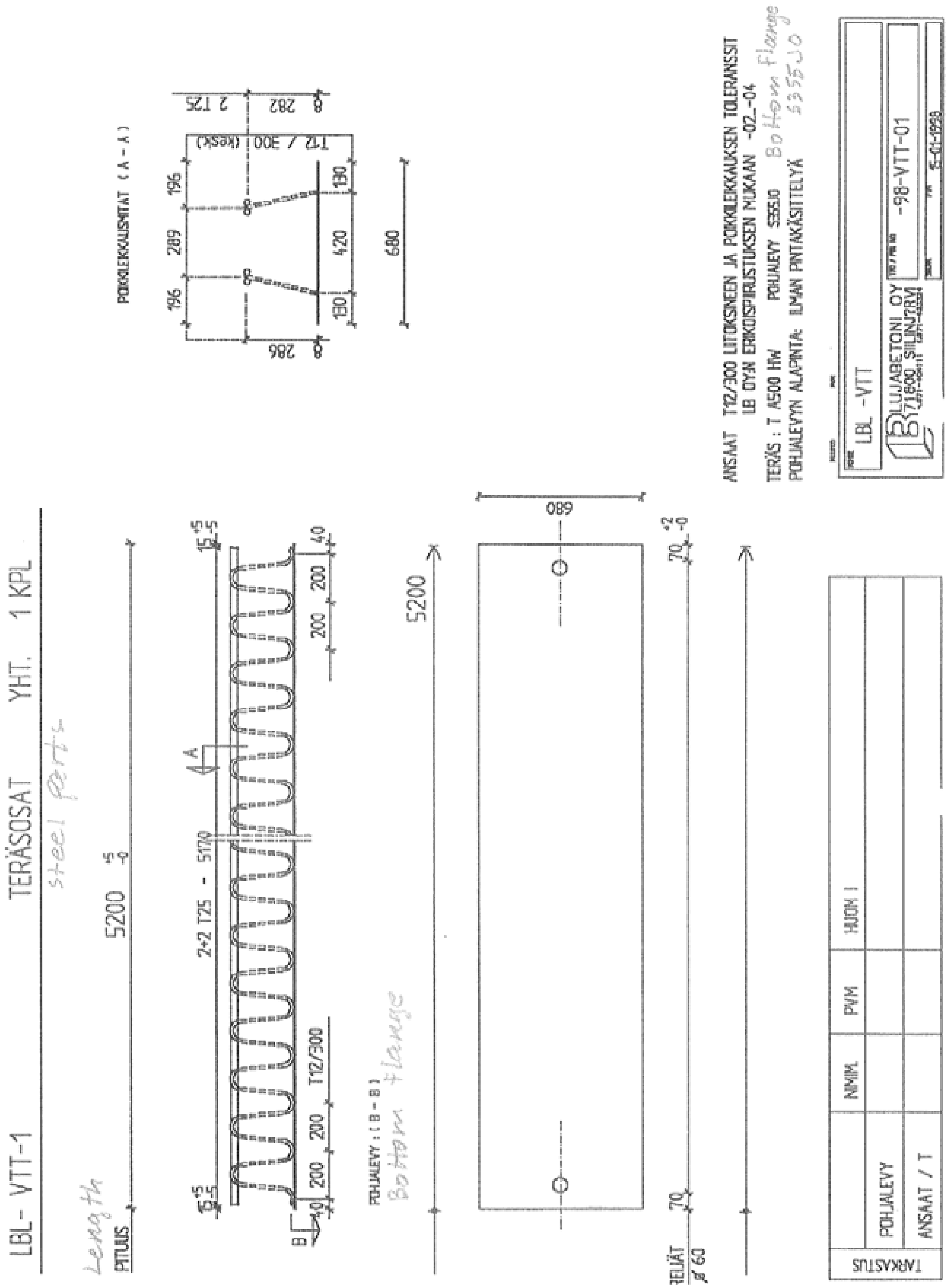

Fig. 4. Bottom flange and position of lattice girders.

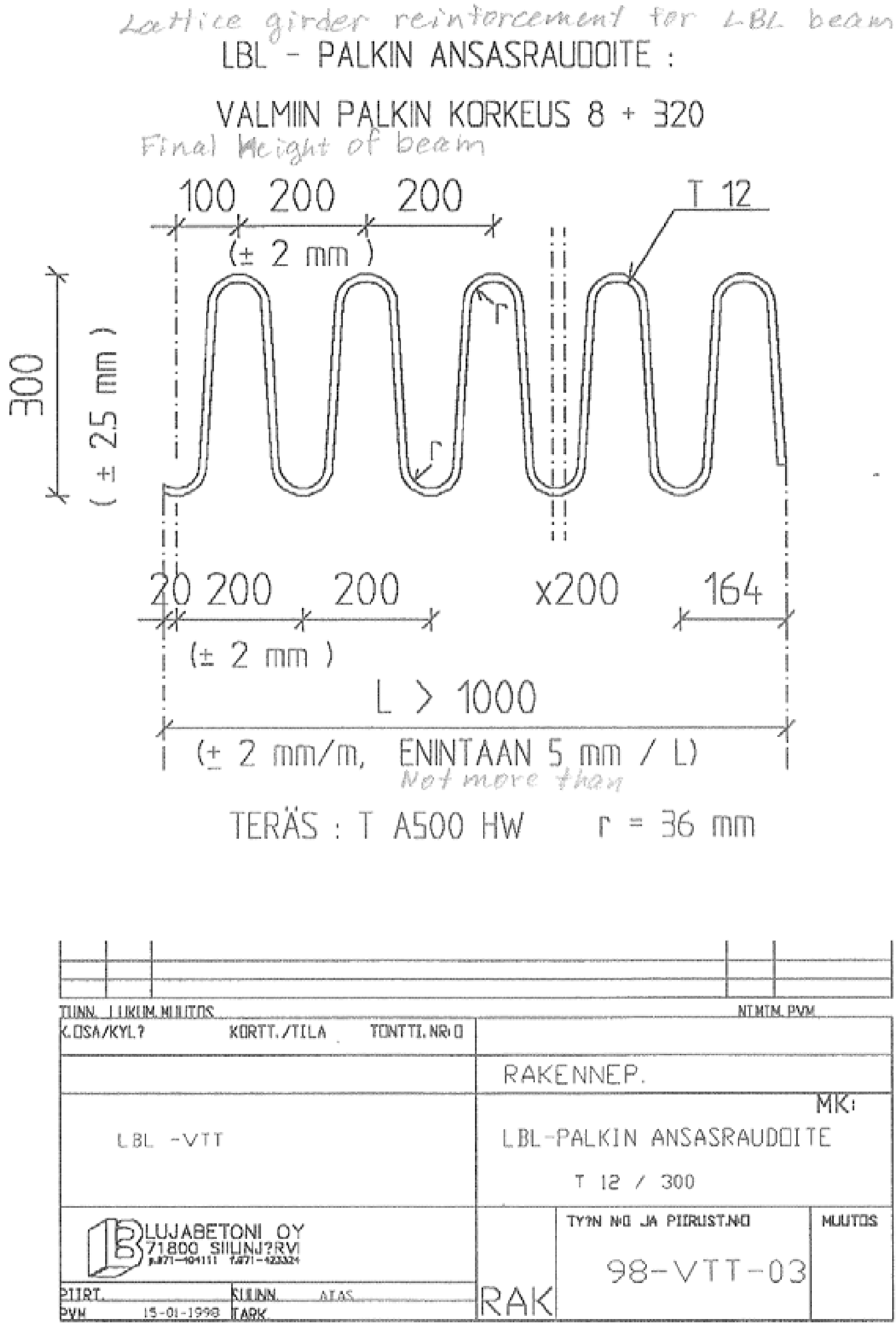

Fig. 5. Design of lattice girders.

APPENDIX B: PHOTOGRAPHS

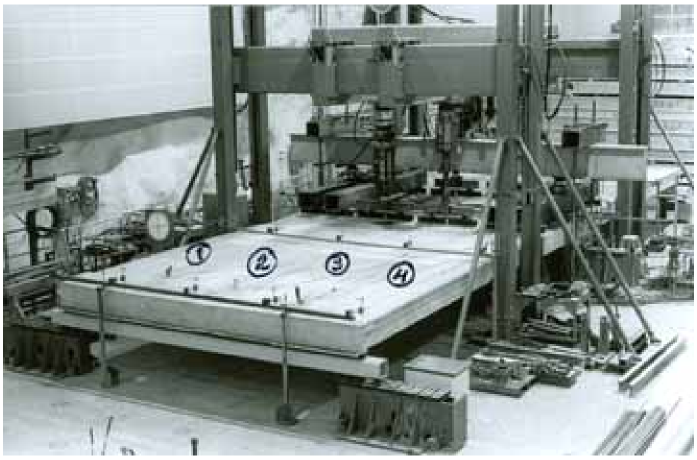

Fig. 1. Overview.

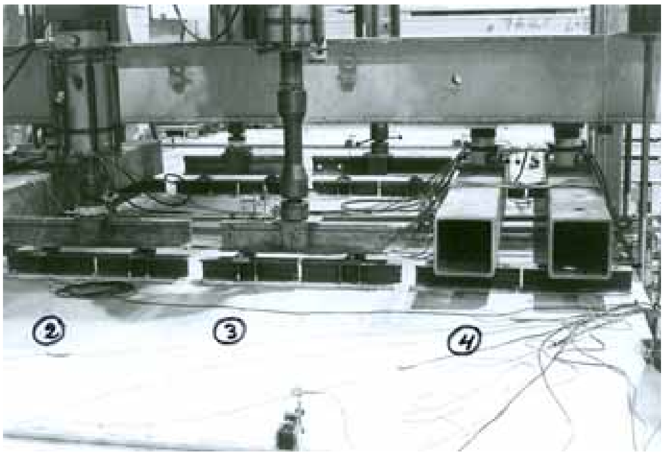

Fig. 2. Loading equipment.

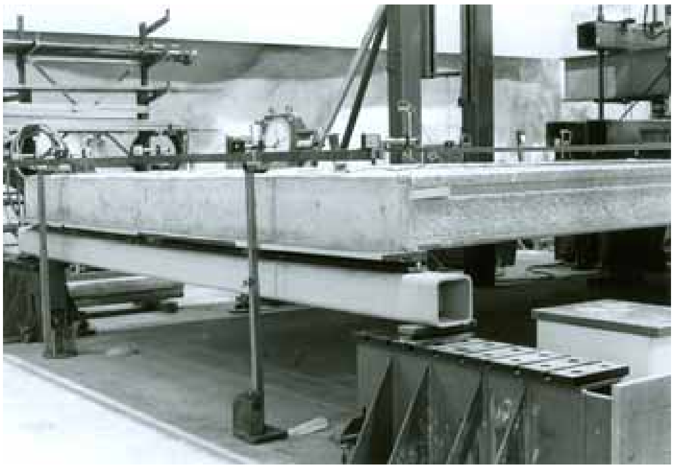

Fig. 3. Arrangements at end beams.

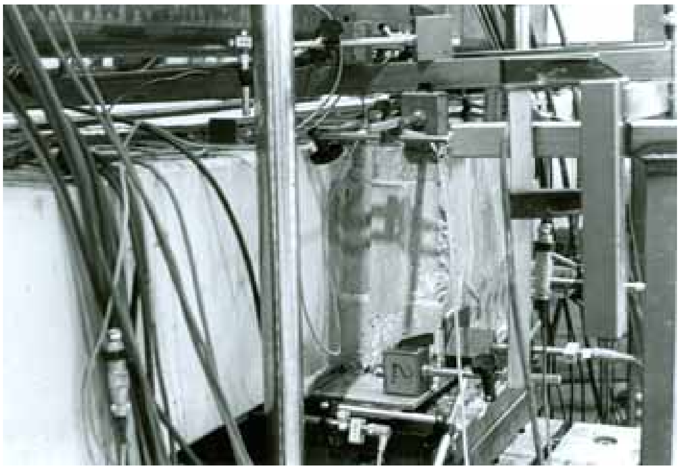

Fig. 4. Transducers at the end of middle beam.

Fig. 5. Failure pattern of slab unit 5.

Fig. 6. Detail of slab unit 5 after failure.

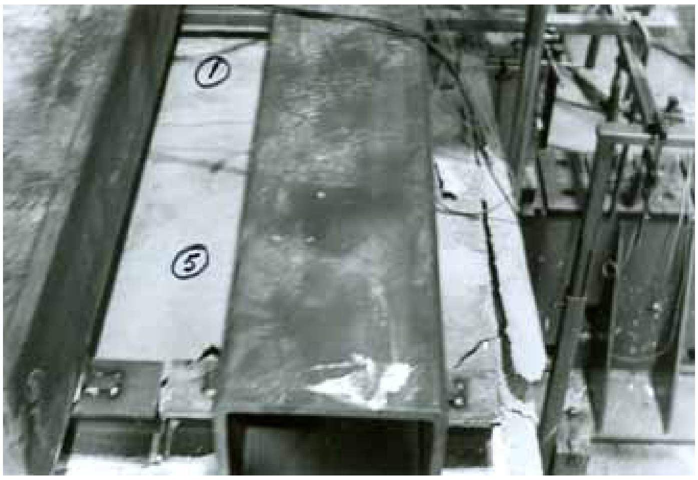

Fig. 7. Slab unit 5 seen from above after failure.

Fig. 8. Failure pattern of slab unit 8.

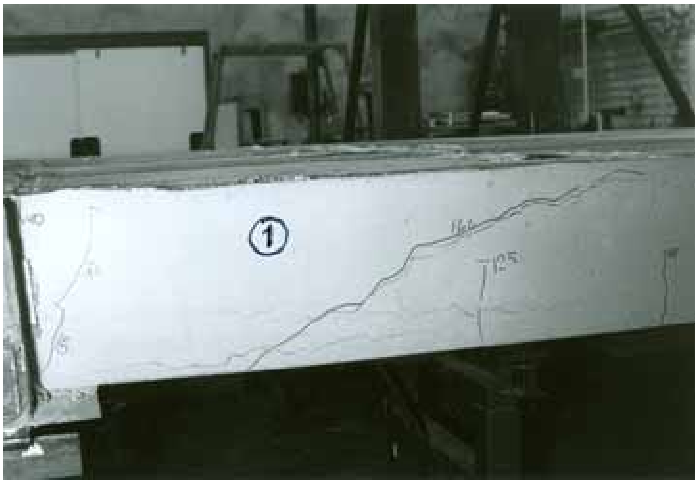

Fig. 9. Cracking pattern of slab unit 1 after failure of slab units 5–8.

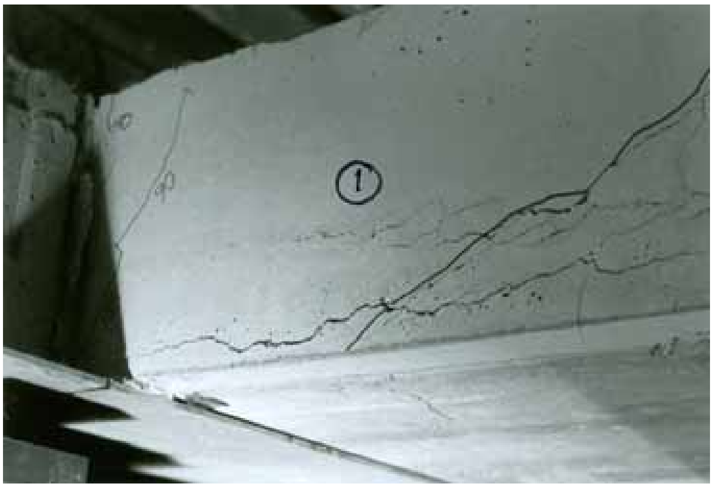

Fig. 10. Detail of slab unit 1. Note the transverse crack in the soffit.

Fig. 11. Cracking pattern of slab unit 4 after failure of slab units 5–8.

Fig. 12. Failure pattern of slab units 5–8 seen from above.

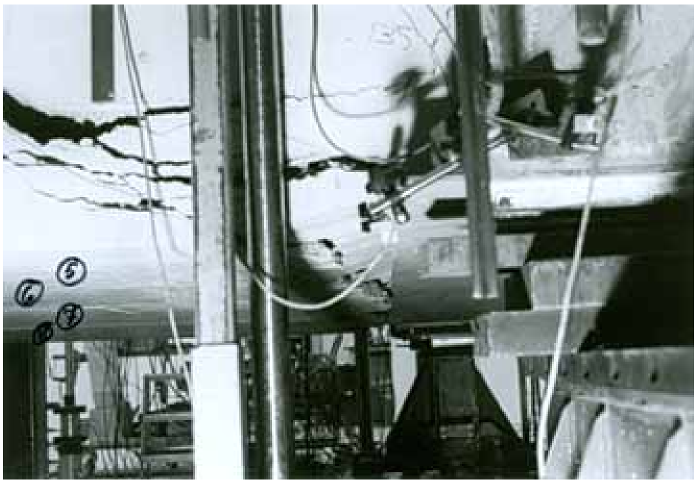

Fig. 13. Failure pattern of slab units 5–8 seen from below.

Fig. 14. Failure pattern of slab units 5–7 seen from below.

Fig. 15. Edge of middle beam after removing slab units 1–4.

Fig. 16. Edge of middle beam after removing slab units 5–8.

Fig. 17. Detail of middle beam after removing slab units.

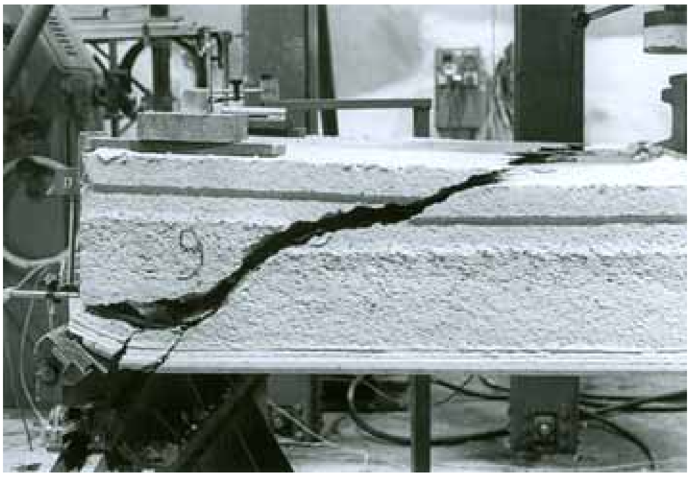

Fig. 18. Failure pattern of slab unit 9 in reference test.

Fig. 19. Failure pattern of slab unit 9 in reference test.

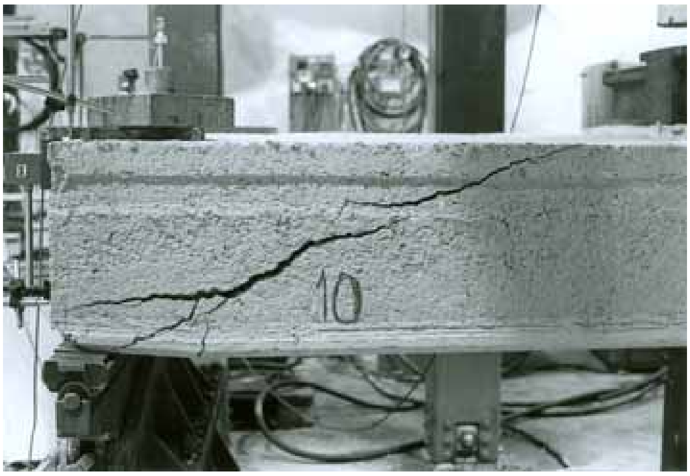

Fig. 20. Failure pattern of slab unit 10 in reference test.

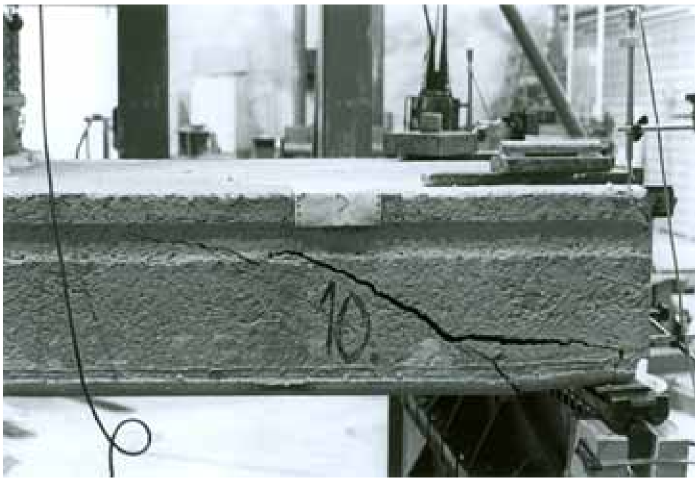

Fig. 21. Failure pattern of slab unit 10 in reference test.

1	**General information**
1.1 Identification and aim	**VTT.CR.Delta.400.1999** **Last update 2.11.2010** DE400 (Internal identification) Aim of the test To quantify the interaction between the Delta beam and 400 mm thick hollow core slabs.
1.2 Test type	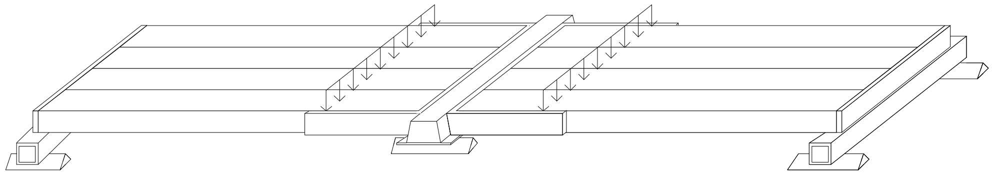 *Fig. 1. Overview of test arrangements. Delta beam in the middle, steel beams at the ends.*
1.3 Laboratory & date of test	VTT/FI 2.12.1999
1.4 Test report	Author(s) Pajari, M. Name *Load test on hollow core floor* Ref. number RTE47/00 Date 29.3.2000 Availability Confidential, owner is Peikko Group Oy, P.O. Box 104, FI-15101 Lahti, Finland
2	**Test specimen and loading** (see also Appendices A)

2.1
General plan

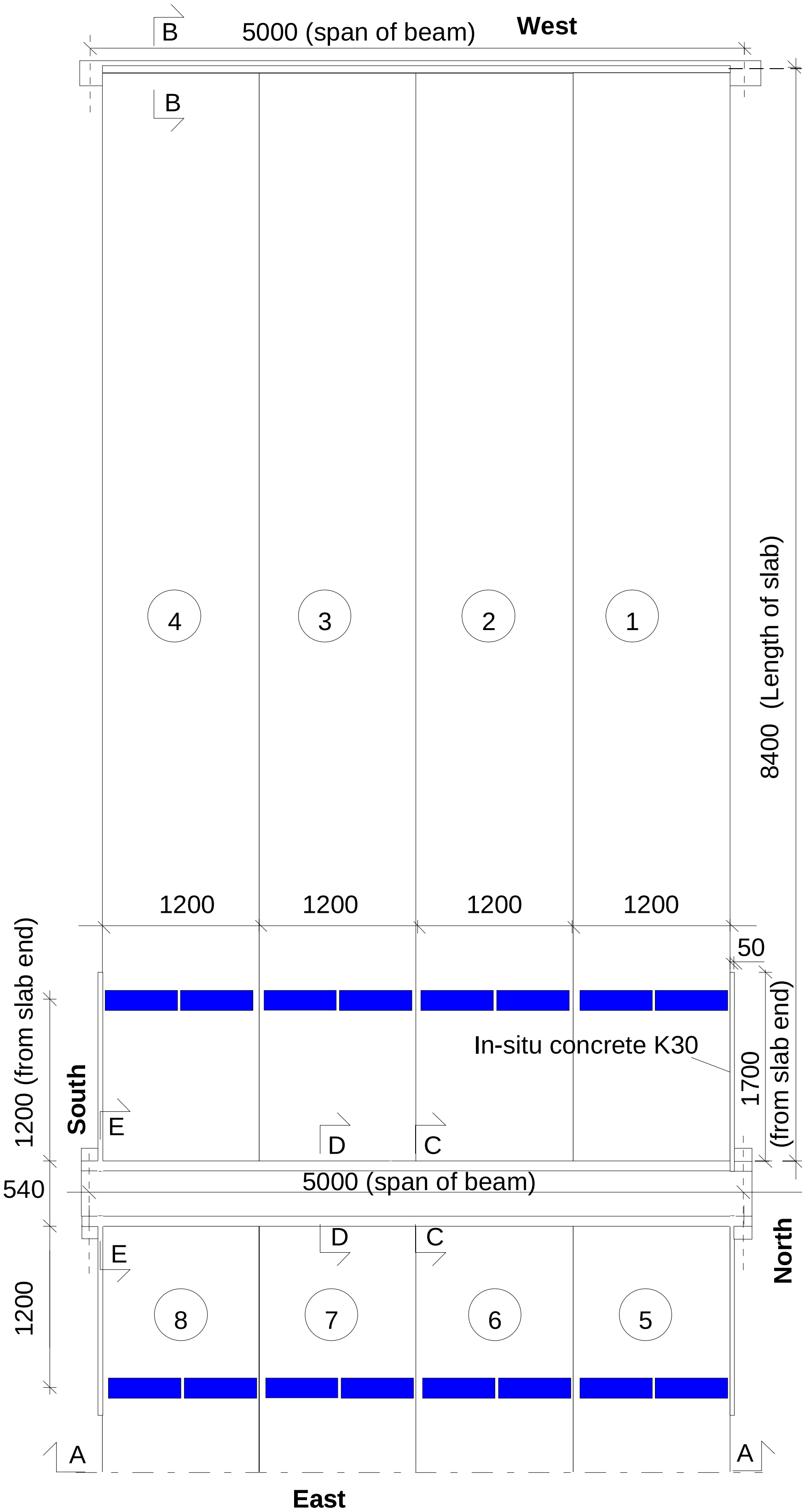

Fig. 2. Plan.

2.2
End beams

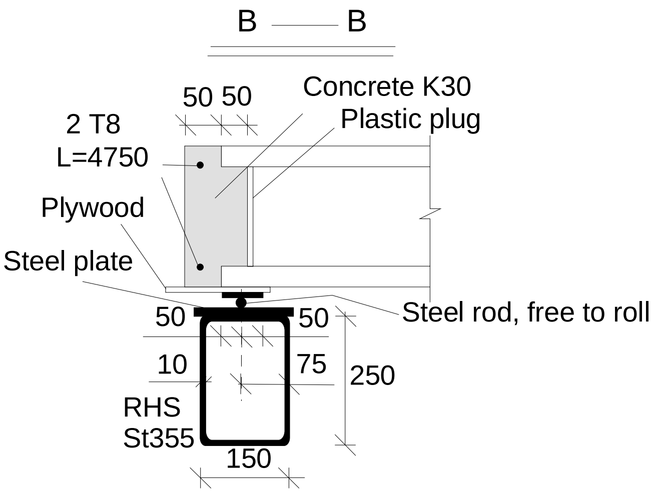

Fig. 3. Arrangements at end beam. T8 refers to a reinforcing bar A500HW with diameter 8 mm, see 2.3.

Simply supported, span = 5,0 m
$f_y \approx$ 355 MPa (nominal f_y), did not yield in the test.

2.3
Middle beam

The beam, see Fig. 4 and App. A, comprised

- a steel box girder with inclined, perforated webs
- a concrete component, cast by VTT in laboratory on the 19th of November 1999, which filled the empty space between the slab ends laying on the bottom flangee of the beam.

Concrete: K30

Reinforcement:
Txy: Hot rolled, weldable rebar A500HW, diameter = xy mm

Structural steel in Delta beam: Raex 420, $f_y \approx$ 420 MPa (nominal f_y) unless otherwise specified

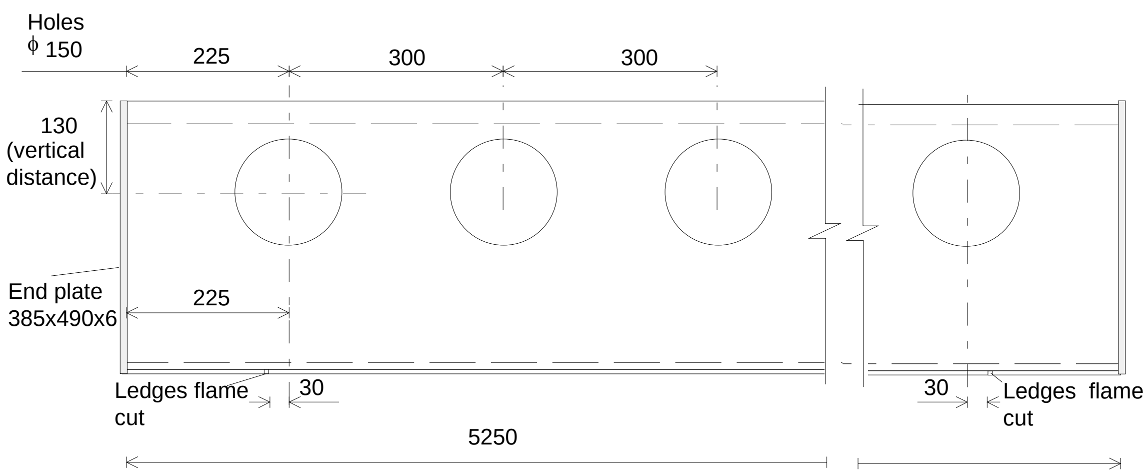

Fig. 4. Delta beam. The diameter of the holes was 150 mm.

	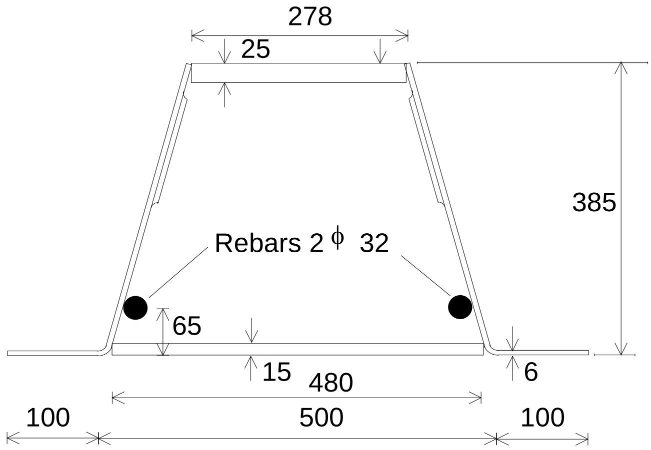 *Fig. 5. Cross-section of Delta beam. The rebars were welded to the webs of the beam.*
2.4 Arrangements at middle beam	- Simply supported, span = 5,0 m, roller bearing at one end C —— C Rebar T12 L = 3800 in each longitudinal joint between adjacent slab units 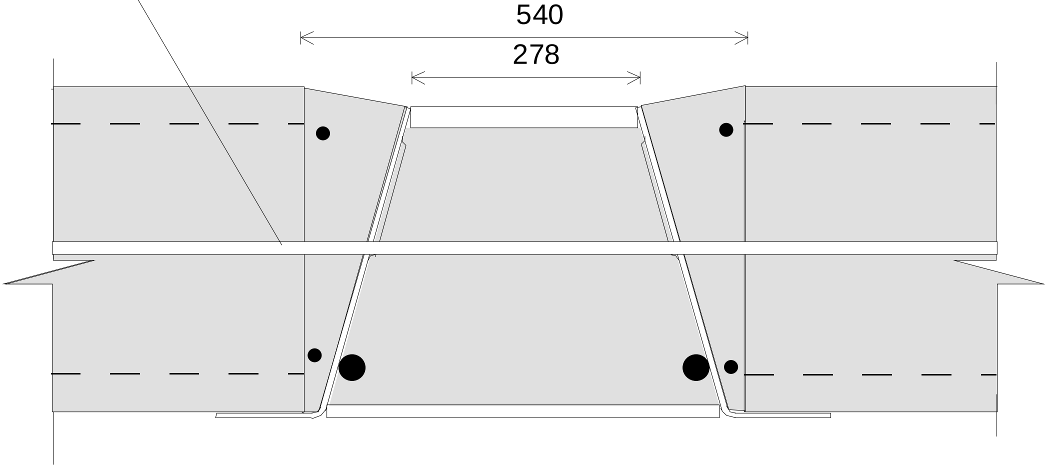 *Fig. 6. Section along joint between adjacent slab units, see Fig. 2.*

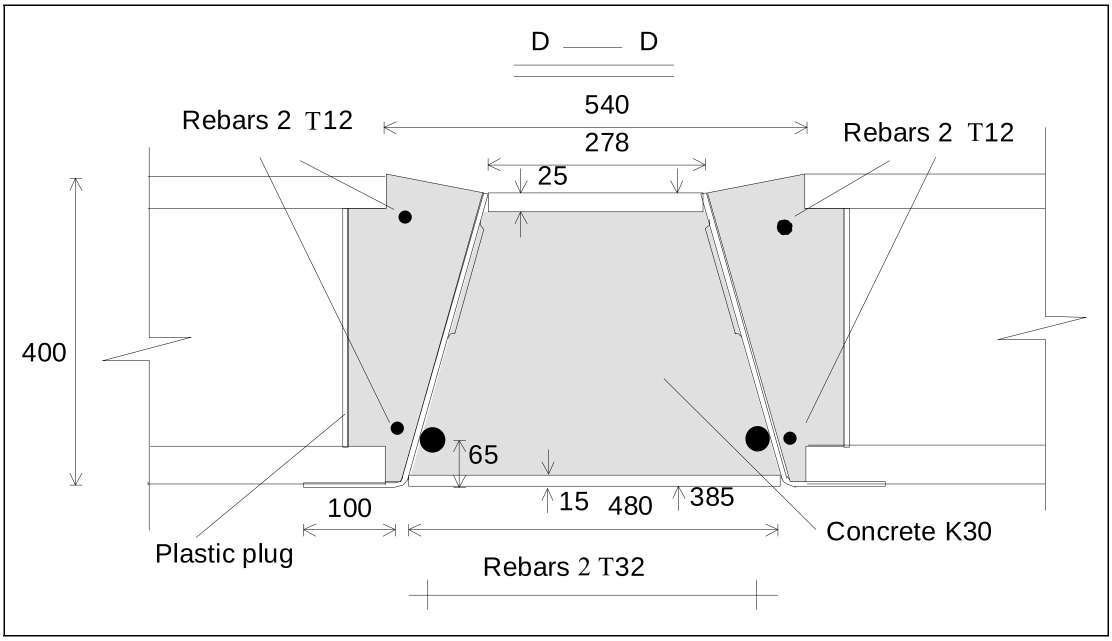

Fig. 7. Section along hollow cores, see Fig. 2.

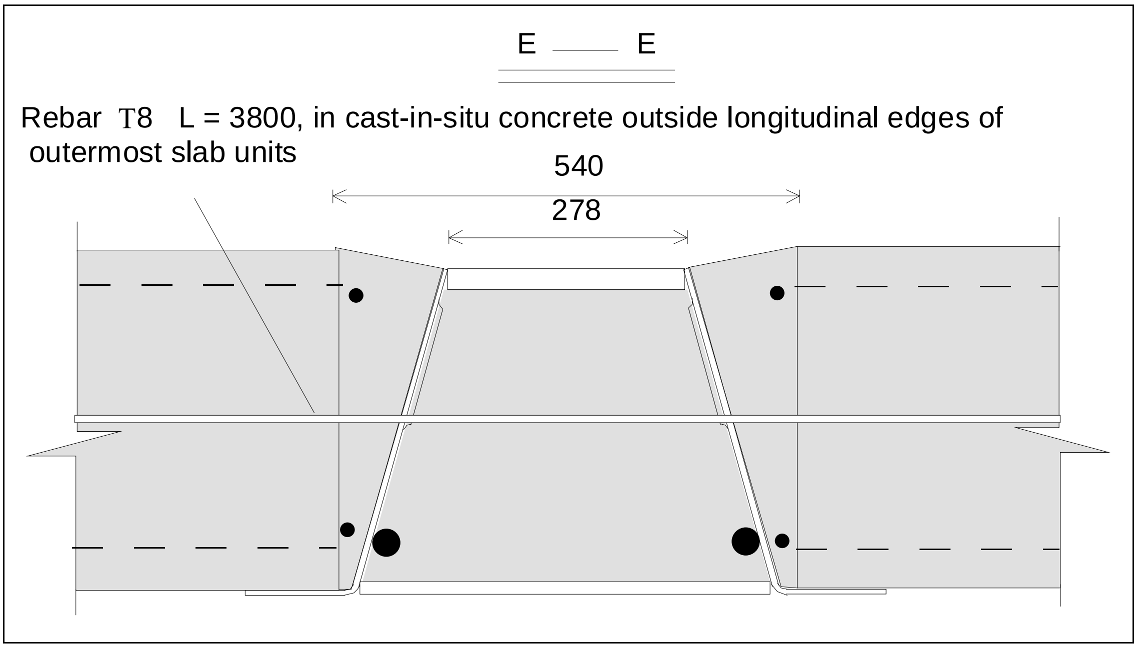

Fig. 8. Section along outer edge of floor specimen, see Fig. 2.

2.5
Slabs

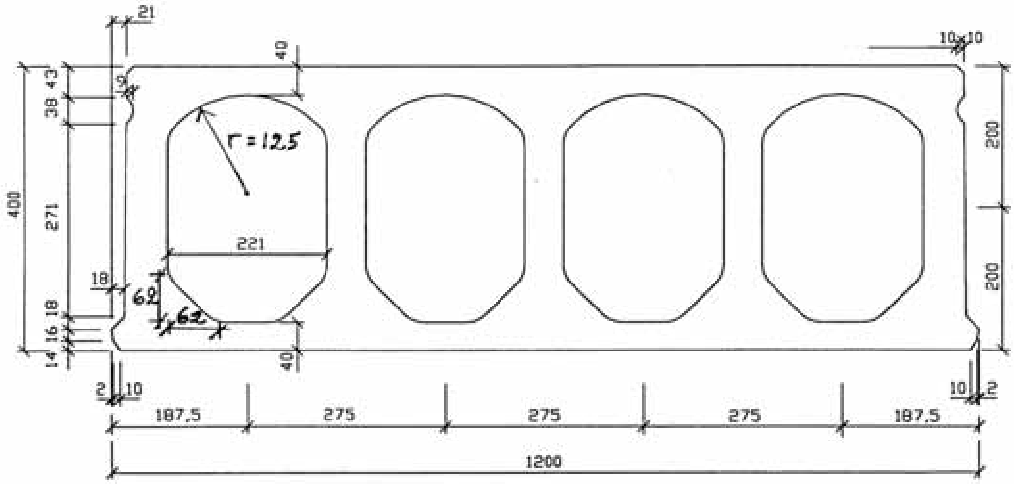

Fig. 9. Nominal geometry of slab units (in scale).

- Extruded by Parma Betonila Oy, Hyrylä factory 29.10.1999
- 13 lower strands J12,5; initial prestress 1000 MPa

J12,5: seven indented wires, ϕ =12,5 mm, A_p = 93 mm^2

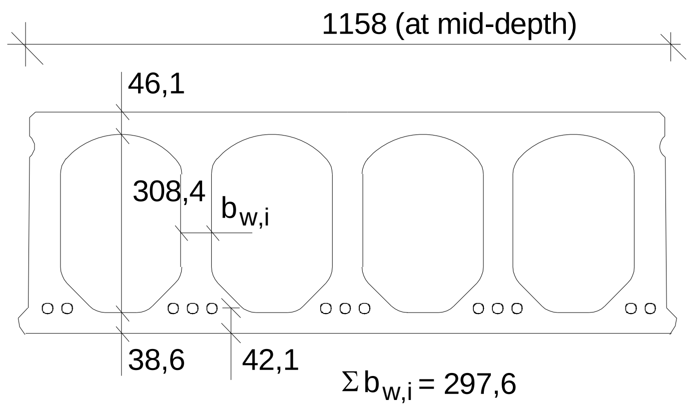

Max measured bond slips:
1,9 in slab 7; 1,8 in slab 8;
1,7 in slabs 2, 4, and 7

Measured weight of slab units = 5,39 kN/m

Fig. 10. Mean of most relevant measured geometrical characteristics.

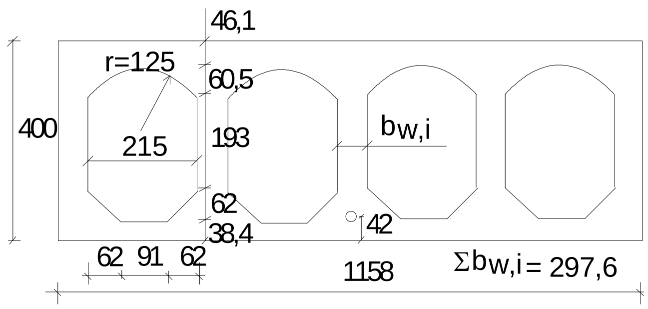

Fig. 11. Cross-sectional geometry based on nominal and measured geometry.

2.6
Temporary supports

No temporary supports below beams.

2.7 Loading arrangements	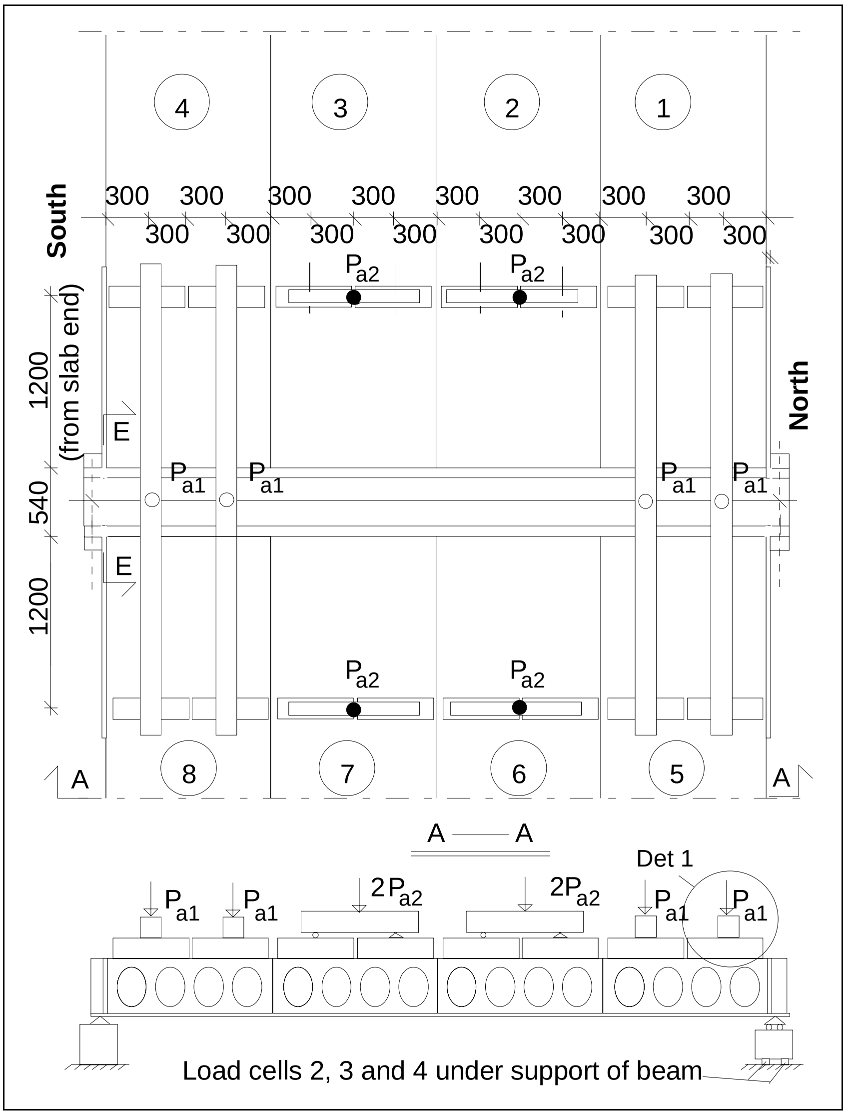 *Fig. 12. Plan. P_{a1} and P_{a2} refer to vertical actuator forces.* 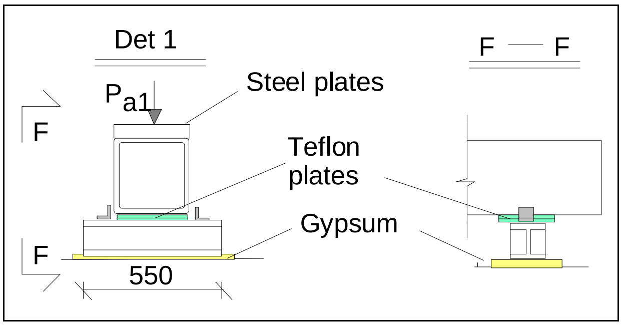 *Fig. 13. Detail 1, see previous figure.*

3	**Measurements**
3.1 Support reactions	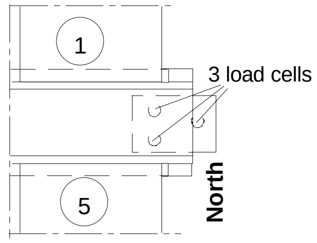 *Fig. 14. Load cells below the Northern support of the middle beam.*
3.2 Vertical displacement	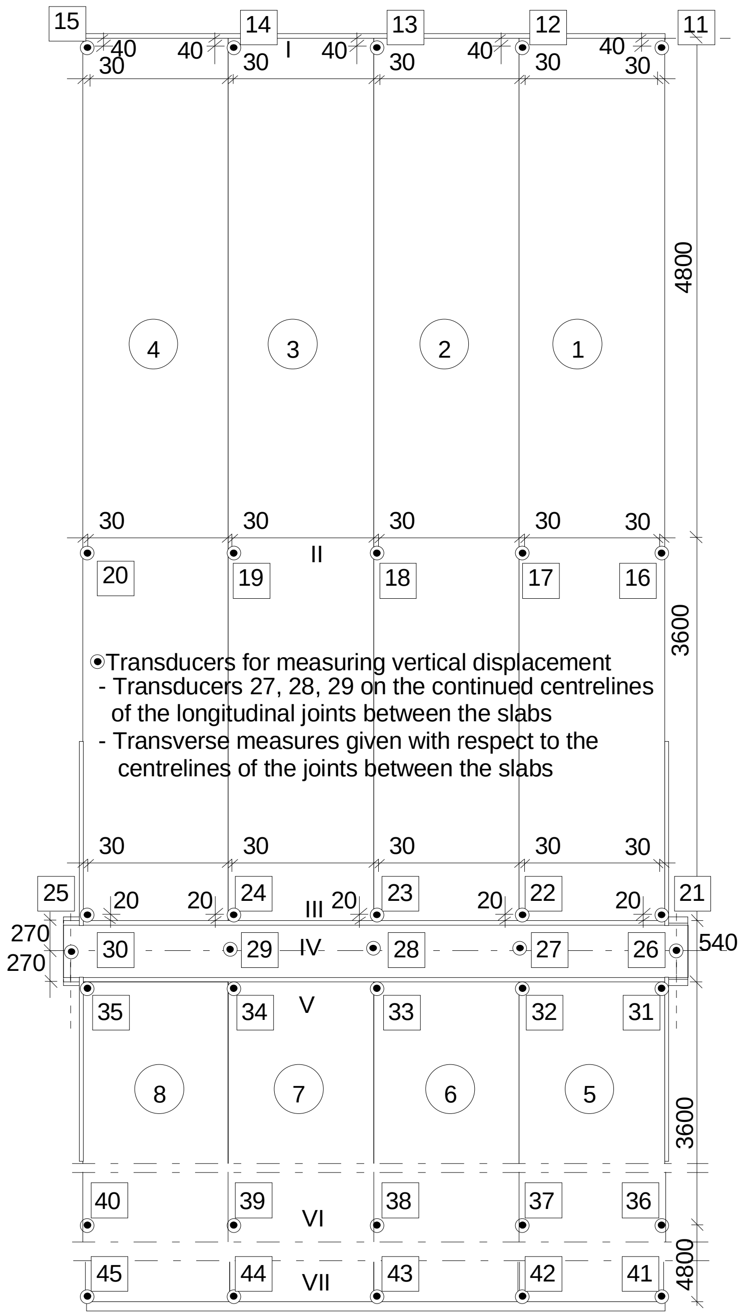 *Fig. 15. Location of transducers 11 … 45 for measuring deflection along lines I … VII.*

3.3 Average strain	Not measured
3.4 Horizontal. displacements	Measures differential displacement between slab end and beam (crack width) Measures differential displacement between slab edge and beam in beam's direction, numbers in parentheses refer to the soffit of the floor, others to the top 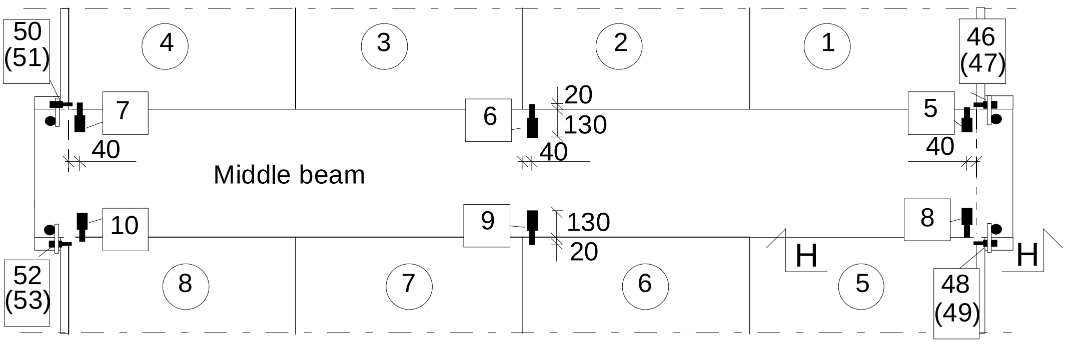 *Fig. 16. Transducers measuring crack width (5–10) and shear displacement at the ends of the middle beam (46–53). Transducers 47, 49, 51 and 53 are below transducers 46, 48, 50 and 52, respectively.* 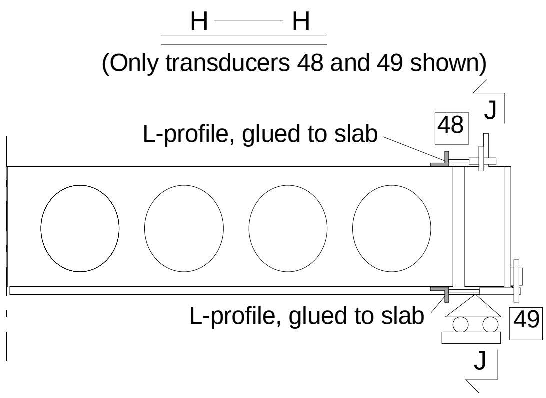 *Fig. 17. Section H-H, see Fig. 20.* 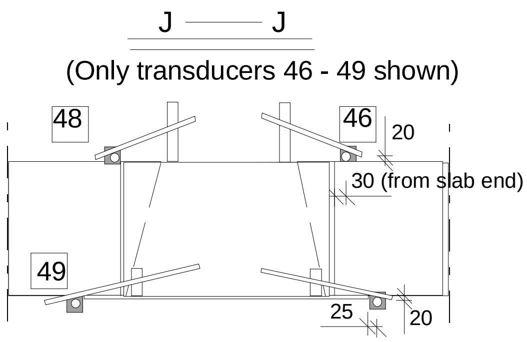 *Fig. 18. Section J-J, see Fig. 21.*

3.5 Strain and differential vertical displacement	The strain was measured using strain gauges at mid-span of the middle beam. Their position is shown in Fig. 19 The contact between the soffit of the slabs and the ledges of the middle beam was monitored by two transducers shown in Fig. 19. 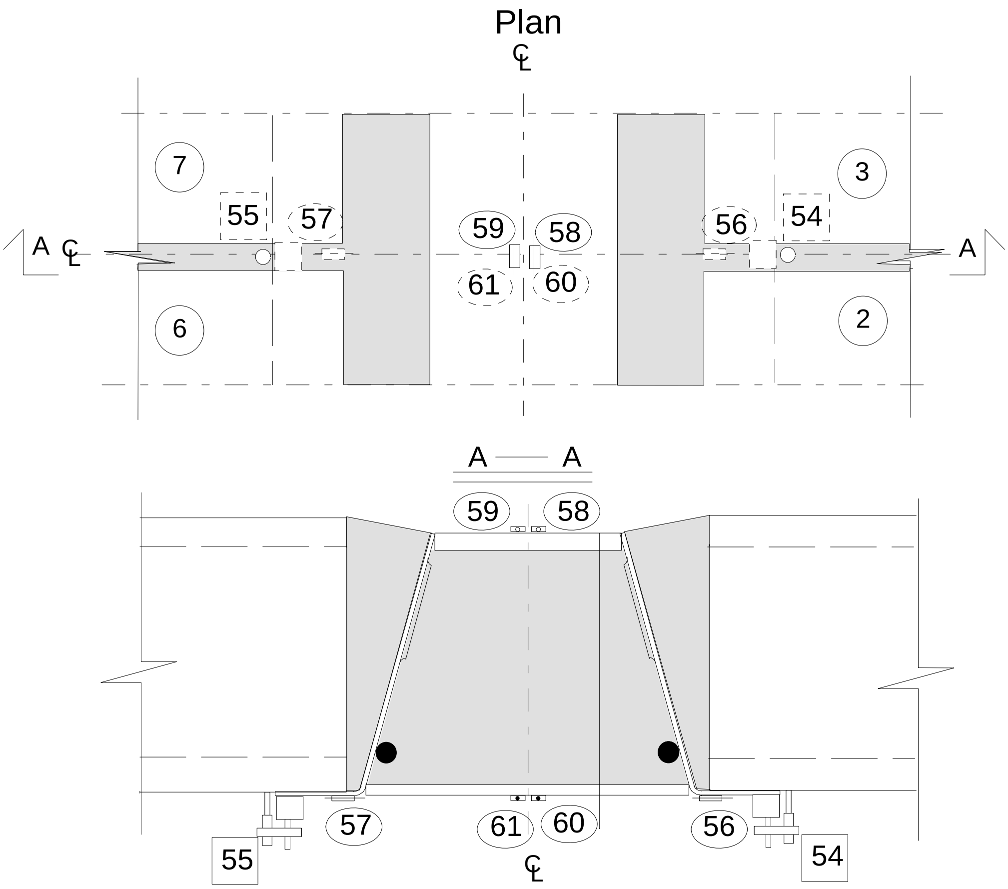 *Fig. 19.* Horizontal strain gauges 56–61 and transducers 54–55 for measuring differential vertical displacement.

4	**Special arrangements** - None
5	**Loading strategy**
5.1 Load-time relationship	Date of the floor test was 2.12.1999. The loading took 2 h 35 min. The actuator loads at different time steps are given in Fig. 20. 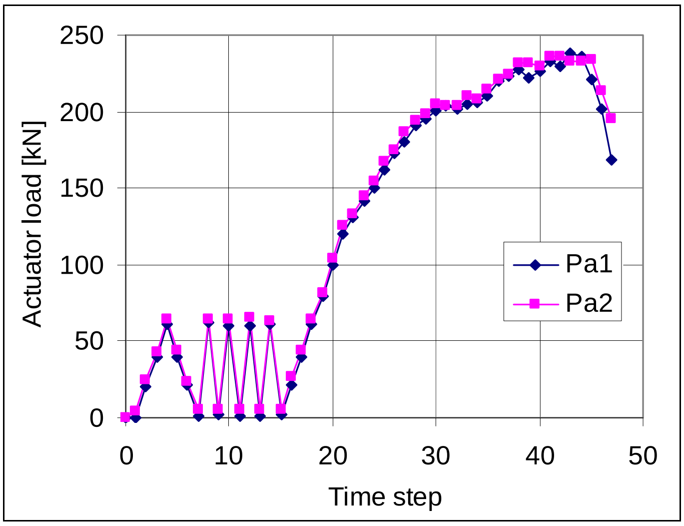 *Fig. 20. Actuator forces P_{a1} and P_{a2} at different time steps.*
5.2 After failure	

6 **Observations during loading**

Before test	Some longitudinal cracks along the strands were discovered in the soffit of the slabs before the test, see Fig. 22. They were below the webs (strands) of the hollow core units, parallel to the strands and obviously caused by the transfer of the prestressing force. Their width was less than 0,1 mm before the test, but it grew when the floor was loaded. They were obviously caused by the release of the prestressing force.
Stage I	The joint concrete started to crack along the web of the Delta beam, see Fig. 23. In Figs 22 and 23 as well as in all figures in App. A presenting cracking, the numbers refer to the value of P_{a1} in kN when the crack was first observed.
Stage II	At P_{a1} = 80 kN the tie beams at both ends of the specimen cracked vertically. There were also continuous, visible cracks between the joint concrete and the Delta beam, see Fig. 21. From P_{a1} = 80 kN on, an increasing number of inclined cracks were observed in the corners of the outermost slab units close to the ends of the Delta beam. At P_{a1} = 200 kN, diagonal shear cracks were observed in the corners of slab units 1 and 5, see App. 1, Figs 8 and 9. These cracks grew in width and length until at P_{a1} = 238 kN, P_{a2} = 233 kN slab units 5–8 failed in shear between the line load and the middle beam. The failure mode is illustrated in Fig. 23 and in App. A, Figs 8–24.
After failure	The joint between the slab ends and Delta beam opened along the webs of the beam. The joint concrete as well as the interface between the joint concrete and the slab ends remained virtually uncracked, see Fig. 21 and App. A, Figs 23–28. 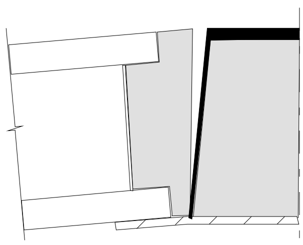 *Fig. 21. Cracking mode between joint concrete and Delta beam.* The ledge of the Delta beam was in tight contact with the bottom surface of the slab units until failure. After the failure, the collapsing slab units deformed the ledges as shown in App. 1, Figs 14–16 and 25–28.

7	**Cracks in concrete**
7.1 Cracks at service load	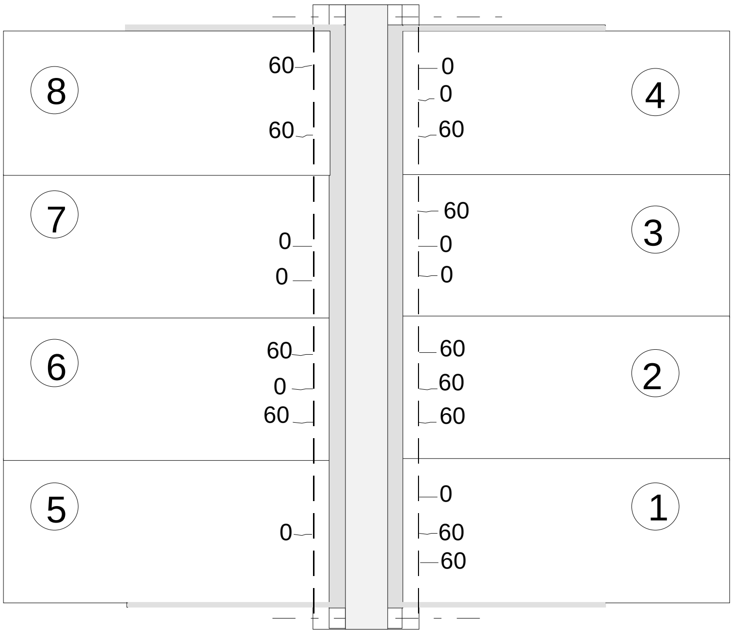 *Fig. 22. Cracks in the soffit at service load (P_{ai} = 60 kN). The initial cracks observed before loading are indicated with 0. The figures give the value of the actuator force at which the crack was observed.*
7.2 Cracks after failure	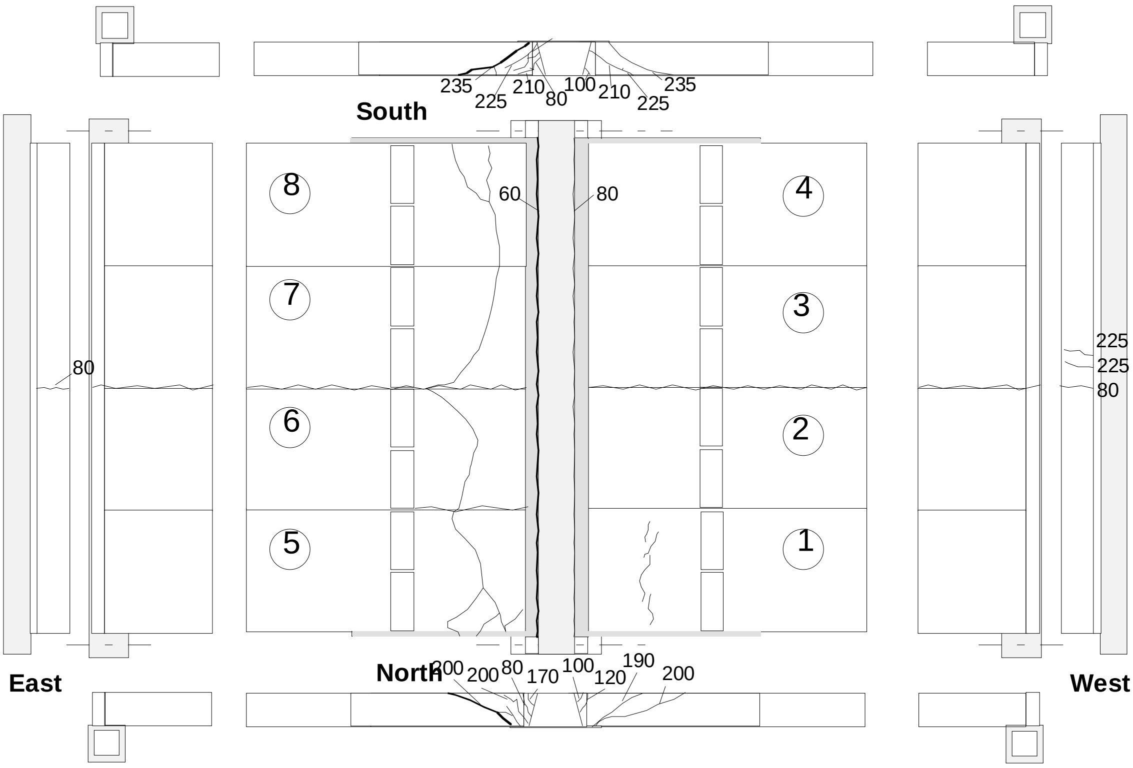 *Fig. 23. Cracks after failure on the top and at the edges.*

8	**Observed shear resistance**
	In Fig. 24 the reaction force under one end of the Delta beam, measured by load cells 2–4, is shown as a function of the load on half floor. The relationship is slightly nonlinear. 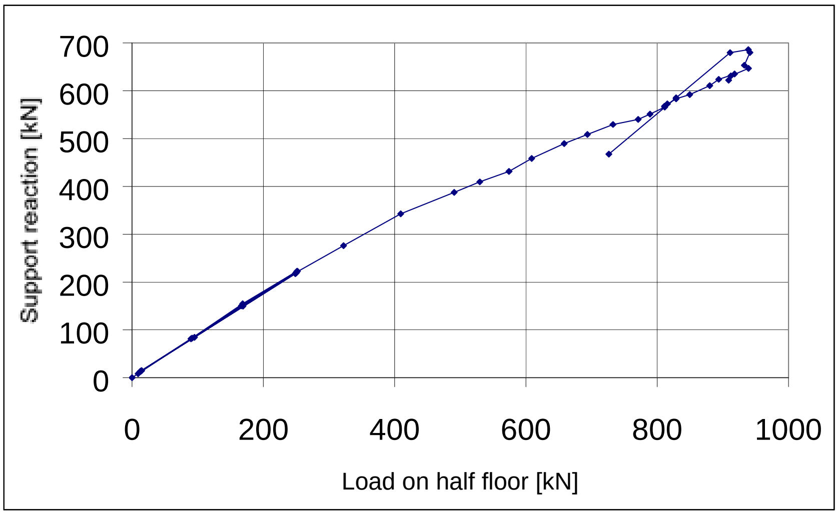 *Fig. 24. Reaction force under support 1 of middle beam vs. load on half floor (=2P_{a1} +2P_{a2}).* Fig. 25 illustrates the ratio of measured support reaction of one slab end V_p due to the actuator loads (= one fourth of measured support reaction under one end of Delta beam) to the imposed loads on one slab unit (= (4xP_{a1}+4xP_{a2})/8) as a function of P_{a1}. The dashed line in Fig. 25 indicates what the response for a simply supported slab would have been. 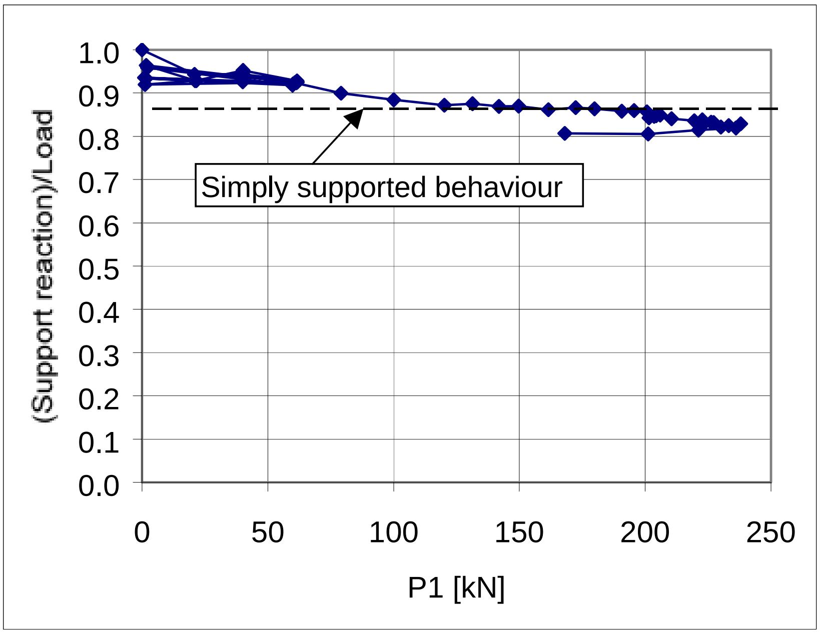 *Fig. 25. Ratio of measured support reaction of a half floor to the load on the half floor. Only imposed load considered.*

Assuming simply supported slabs and calculating the support reaction of the actuator loads from equilibrium of forces gives a support reaction which is 86,1% of the actuator loads. On the other hand, just before the failure, the measured support reaction under end 2 of the Delta beam was 82,9% of the loads on half floor. Using this relationship also for the weight of loading equipment, and assuming that the weight of the slabs and cast-in-situ concrete was distributed to both ends of the slab units as if the slabs were simply supported beams, the shear resistance of one slab end (support reaction of slab end at failure) due to different load components can be calculated as shown in Table 2.

Table 2. Components of shear resistance due to different loads.

Support reaction due to		
weight of slab unit ($V_{g,sl}$)	$\frac{4600+4630+4590+4630}{2\cdot 4}9,82$ kN	22,65 kN
weight of cast-in-situ concrete ($V_{g,isc}$)	$\frac{2\cdot 0,72+3\cdot 1,4}{4}$ kN	1,4 kN
loading equipment (V_{eq})	$0,8291\frac{5,6+1,2}{2}$ kN	2,82 kN
actuator loads (V_p)	$\frac{354,6+263,2+162,7}{4}$ kN	195,1 kN

The shear resistance of one slab end due to imposed load

$$V_{u,imp} = V_p + V_{eq} = 195,1 \text{ kN} + 2,8 \text{ kN} = 197,9 \text{ kN}$$

and the total shear resistance

$$V_u = V_{u,imp} + V_{g,sl} + V_{g,isc} = 197,9 \text{ kN} + 22,7 \text{ kN} + 1,4 \text{ kN} = 222,0 \text{ kN}$$

are obtained.

The strong deviation of the support reaction from the simply supported behaviour of the slab units at P_{a1} < 100 kN cannot be explained by the negative bending moment carried by the tie reinforcement penetrating the Delta beam. The bending moment corresponding to the yield stress 500 MPa of the tie reinforcement is of the order of 37 kNm per floor and 37/4 = 9,3 kNm per slab unit. This increases the support reaction of one slab unit at the Delta beam by 1,1 kN which is far too small to explain the behaviour. It is more likely that the extra support moment is due to the joint concrete. The tie reinforcement obviously helps in mobilizing vertical friction, dowel action and aggregate interlocking along the inclined webs of the Delta beam, particularly in the web holes. With increasing crack width along the Delta beam these effects fade out.

At P_{a1} = 200 kN diagonal shear cracks at the ends of slab units 1 and 5 started to change the load-carrying mechanism of these slab units. The loads were more and more transferred to the neighbouring slab units and less directly to the beam. As a result, the support reactions of the Delta beam became different in such a way that the reaction force at the North end was smaller than that at the opposite end. This effect can be seen in Fig. 25 when P_{a1} is greater than 200 kN.

9 Material properties

9.1 Strength of steel

Component	$R_{eH}/R_{p0,2}$ MPa	R_m MPa	Note
Delta beam	≈ 420		Nominal (Raex 420)
Slab strands J12,5	1630	1860	Nominal (no yielding in test)
Reinforcement Txy	500		Nominal value for reinforcing bars (no yielding in test)

9.2 Strength of slab concrete, floor test

#	Cores	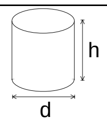	*h* mm	*d* mm	Date of test	Note
6			50	50	10.12.1999	Upper flange of slabs 5 and 6,
Mean strength [MPa]			68,6		(+8 d)[1)]	vertically drilled. Tested as drilled[2)]
St.deviation [MPa]			2,6			Density = 2448 kg/m³

9.3 Strength of slab concrete, reference tests

#	Cores	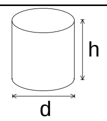	*h* mm	*d* mm	Date of test	Note
6			50	50	10.12.1999	Upper flange of slab9, vertic-
Mean strength [MPa]			67,3		(+2 d)[1)]	ally drilled. Tested as drilled[2)]
St.deviation [MPa]			1,7			Density = 2445 kg/m³

9.4 Strength of concrete in Delta beam and joints

#	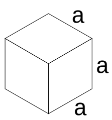		*a* mm	Date of test	Note
6			150	2.12.1999	Kept in laboratory in the same
Mean strength [MPa]			28,8	(+0 d)[1)]	conditions as the floor specimen
St.deviation [MPa]			0,8		Density = 2212 kg/m³

[1)] Date of material test minus date of structural test (floor test or reference test)
[2)] After drilling, kept in a closed plastic bag until compression

10 **Measured displacements**

In the following figures, V_p stands for the average shear force of one slab end due to imposed actuator loads, calculated assuming simply supported slabs.

10.1
Deflections

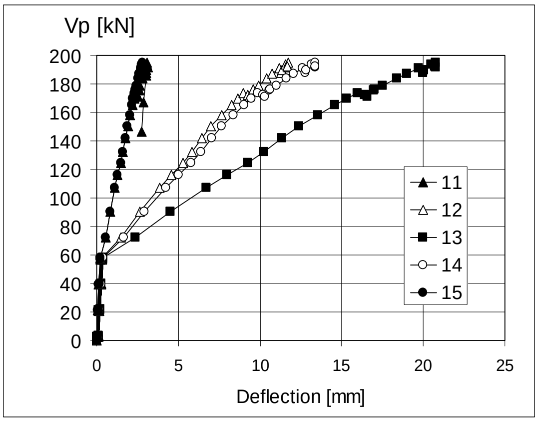

Fig. 26. Deflection on line I along Western end beam.

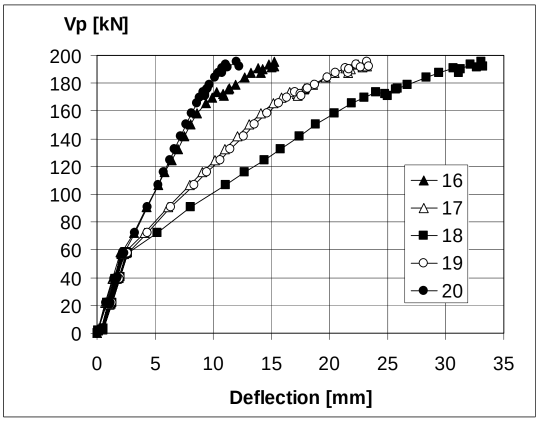

Fig. 27. Deflection on line II in the middle of slabs 1–4.

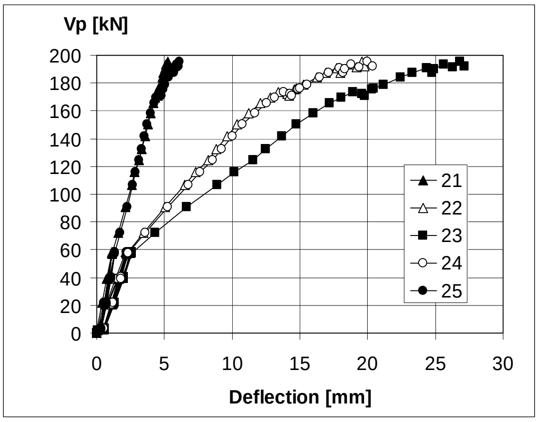

Fig. 28. Deflection on line III close to the Delta beam, slabs 1–4.

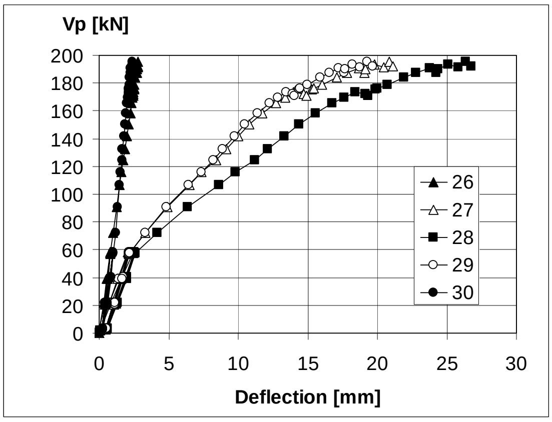

Fig. 29. Deflection on line IV along the middle beam.

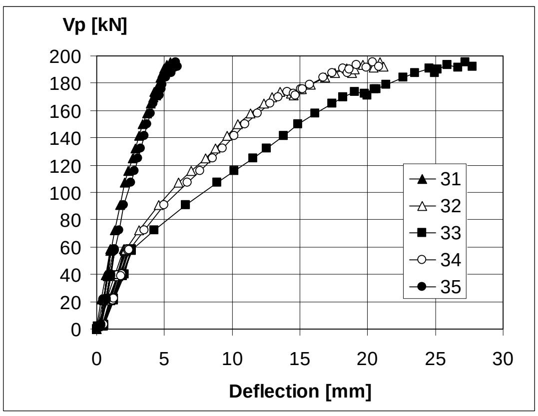

Fig. 30. Deflection on line V close to the Delta beam, slabs 5–8.

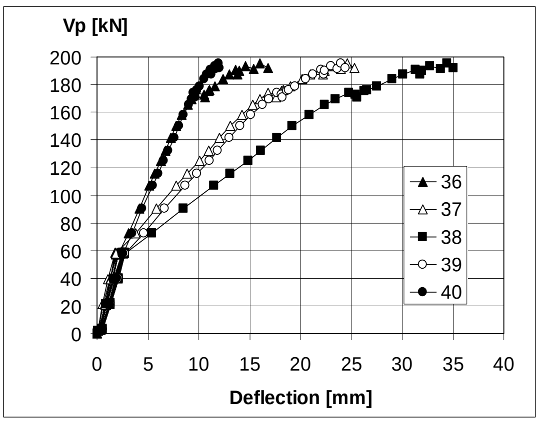

Fig. 31. Deflection on line VI in the middle of slabs 5–8.

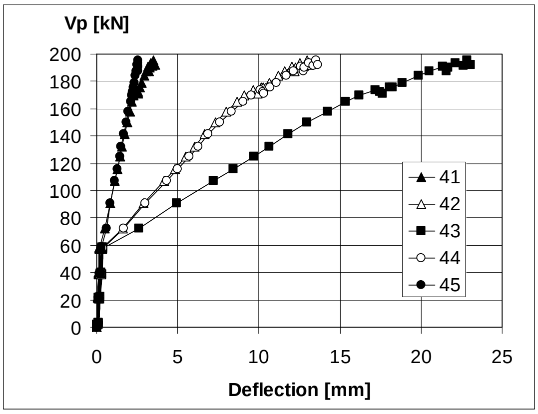

Fig. 32. Deflection on line VII along Eastern end beam, slabs 5–8.

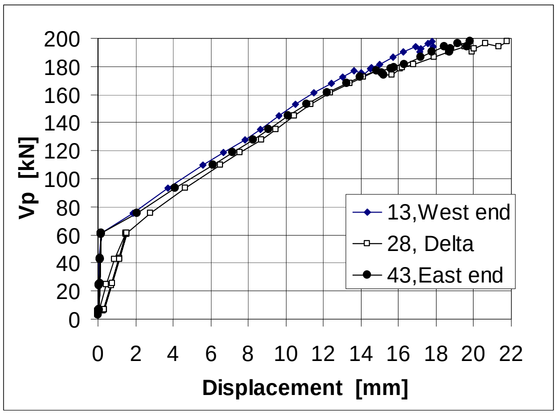

Fig. 33. Net deflection of midpoint of middle beam (28) and those of end beams (13, 43). (Settlement of supports eliminated.)

10.2
Crack width

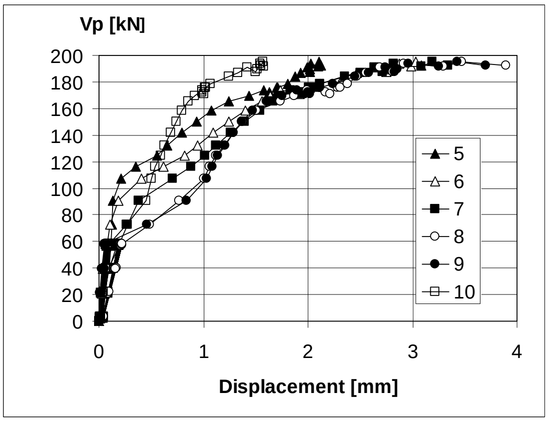

Fig. 34. Differential displacement (≈crack width) measured by transducers 5–10.

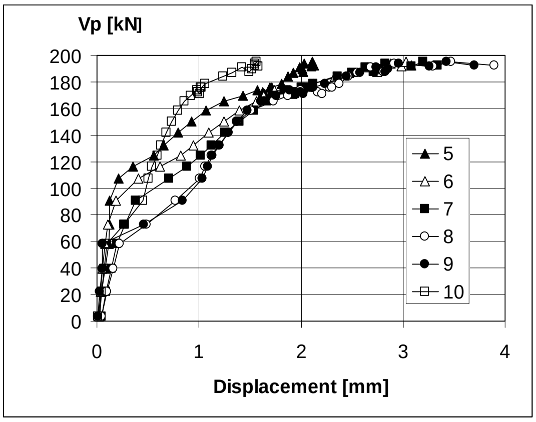

Fig. 35. Same as previous figure but the cyclic loading phase is not shown.

10.3
Opening of gap between slab and ledge of Delta beam

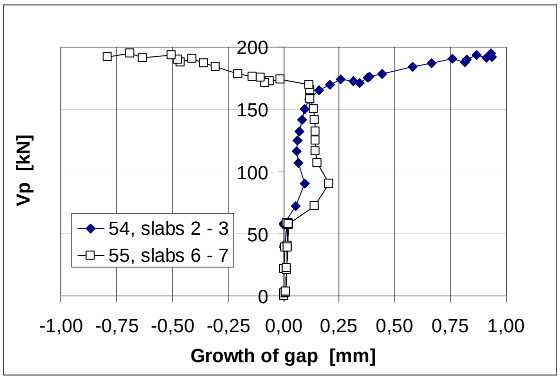

Fig. 36.

10.4 Shear displacement

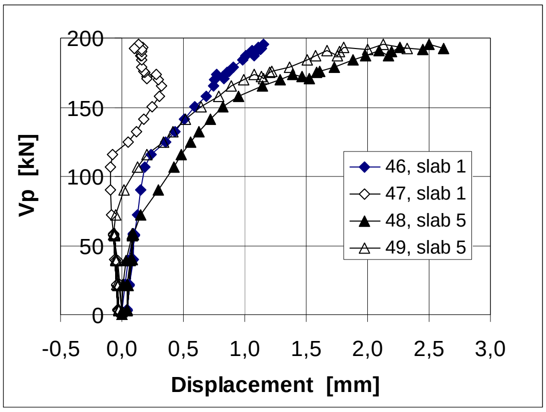

Fig. 37. Northern end of middle beam. Differential displacement between edge of slab and middle beam. A negative value means that the slab is moving towards the end of the beam.

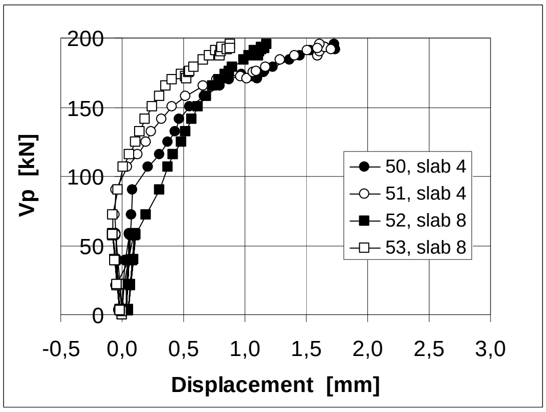

Fig. 38. Southern end of middle beam. Differential displacement between edge of slab and middle beam. A negative value means that the slab is moving towards the end of the beam.

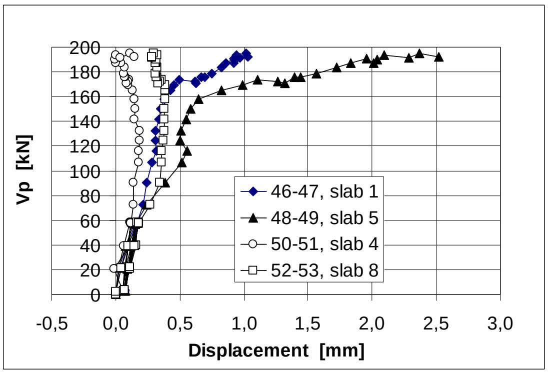

Fig. 39. Shear displacement = differential displacement at upper edge – differential displacement at lower edge of slab.

10.5 Strain

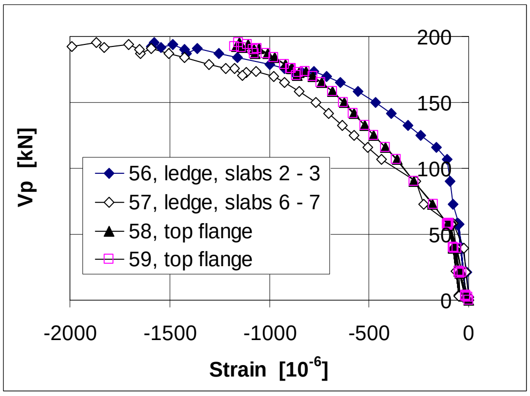

Fig. 40. Strain measured by gauges 56–59.

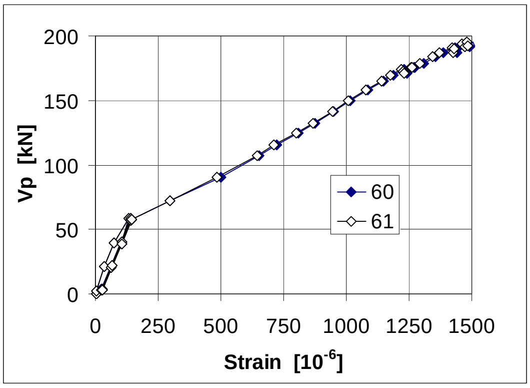

Fig. 41. Strain measured by gauges 60 and 61 parallel to Delta beam.

11 Reference tests

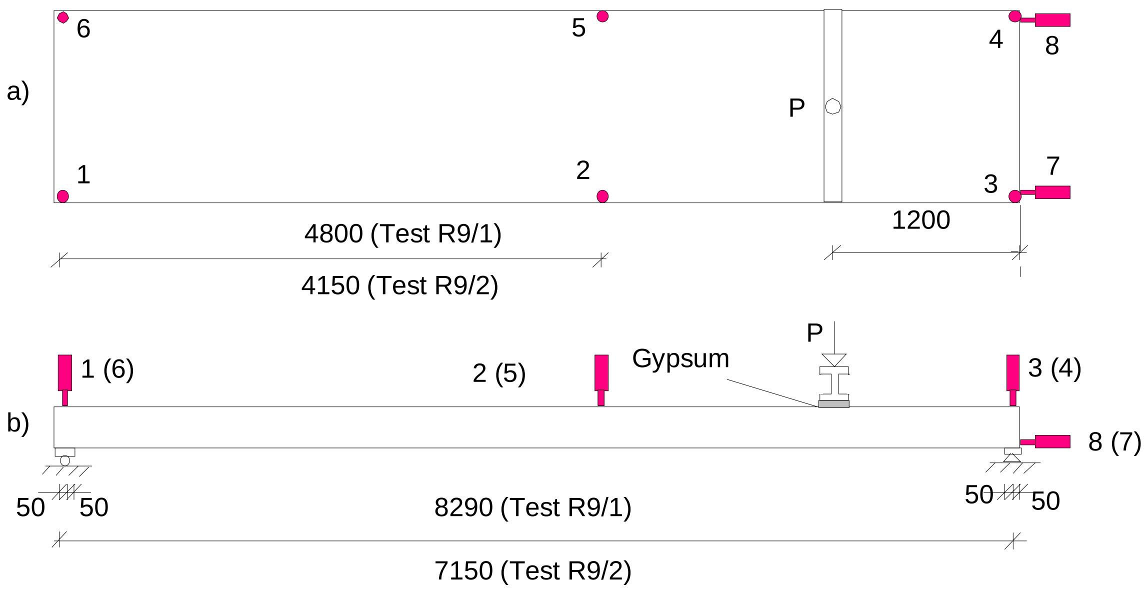

Fig. 42. Loading arrangements and position of transducers for measuring displacement (1–6) and slip of strand (7 and 8). a) Plan. b) Elevation.

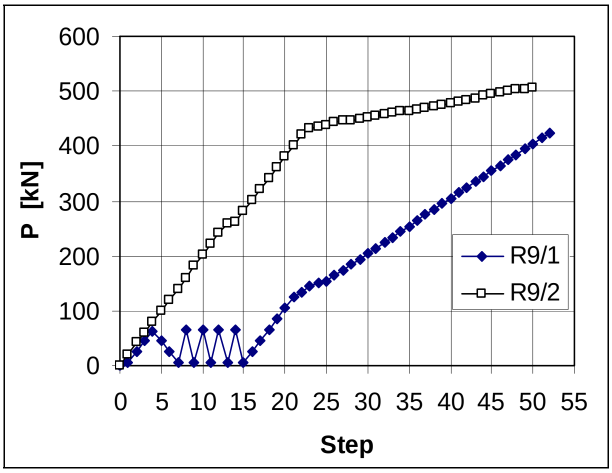

Fig. 43. Actuator force – time relationship.

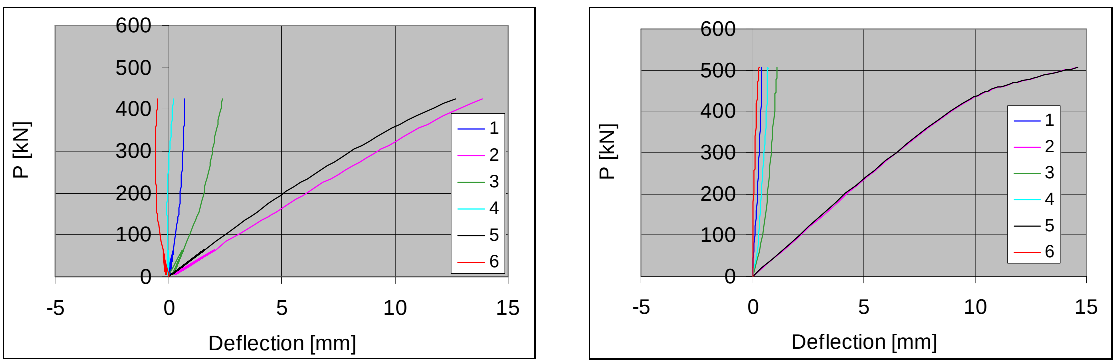

R9/1 R9/2

Fig. 44. Displacements measured by transducers 1–6. P is the actuator force.

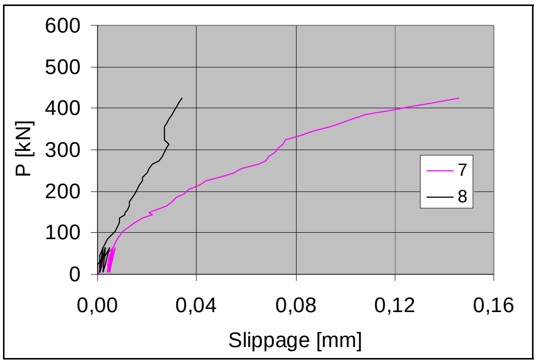

R9/1

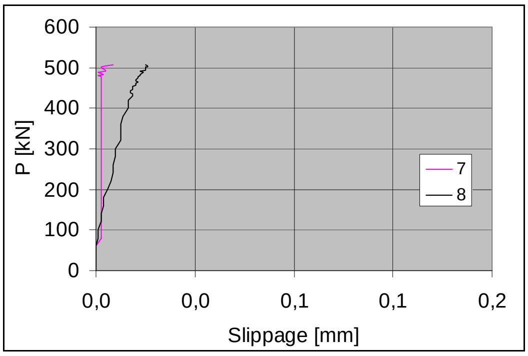

R9/1

Fig. 45. Slippage of outermost strands measured by transducers 7–8. P is the actuator force.

Table. Reference tests. Span of slab, shear force V_g at support due to the self weight of the slab, actuator force P at failure, weight of loading equipment P_{eq}, total shear force V_{obs} at failure and total shear force v_{obs} per unit width.

Test	Date	Span mm	V_g kN	P kN	P_{eq} kN	V_{obs} kN	v_{obs} kN/m	Note
R9/1	8.12.1999	8290	21,9	432,0	0,7	394,6	328,8	Web shear failure
R9/2	8.12.1999	7150	18,9	506,3	0,7	444,4	370,3	Web shear failure
				Mean		**419,5**	**349,6**	

12 **Comparison: floor test vs. reference tests**

The observed shear resistance (support reaction) of the hollow core slab in the floor test was equal to 222,0 kN per one slab unit or 185,0 kN/m. This is **53%** of the mean of the shear resistances observed in the reference tests.

13 **Discussion**

1. The net deflection of the middle beam due to the imposed actuator loads only (deflection minus settlement of supports) was 24,0 mm or *L*/208.
2. The shear resistance measured in the reference tests was of the same order as the mean of the observed values for similar slabs given in *Pajari, M. Resistance of prestressed hollow core slab against web shear failure. VTT Research Notes 2292, Espoo 2005*.
3. The maximum difference in the net mid-point deflection of the beams was 4,0 mm. Hence, the torsional stresses due to the different deflection of the middle beam and end beams had a negligible effect on the failure of the slabs.
4. The edge slabs slided 0,13 … 0,23 mm along the beam before failure. This reduced the negative effects of the transverse actions in the slab and had a positive effect on the shear resistance.
5. The failure mode was web shear failure of edge slabs. The plastic deformation of the ledges of Delta beam was considerable on the failed side. Otherwise the Delta beam seemed to recover completely after the failure.

APPENDIX A: PHOTOGRAPHS

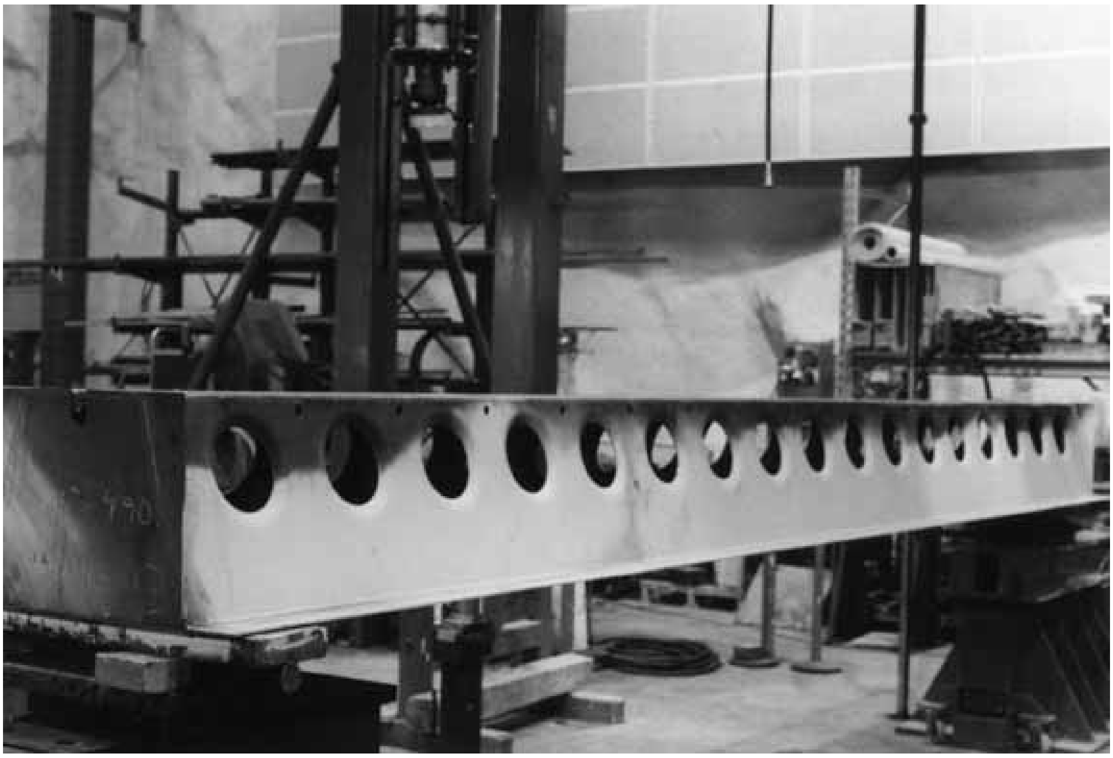

Fig. 1. Delta-beam (middle beam in floor test).

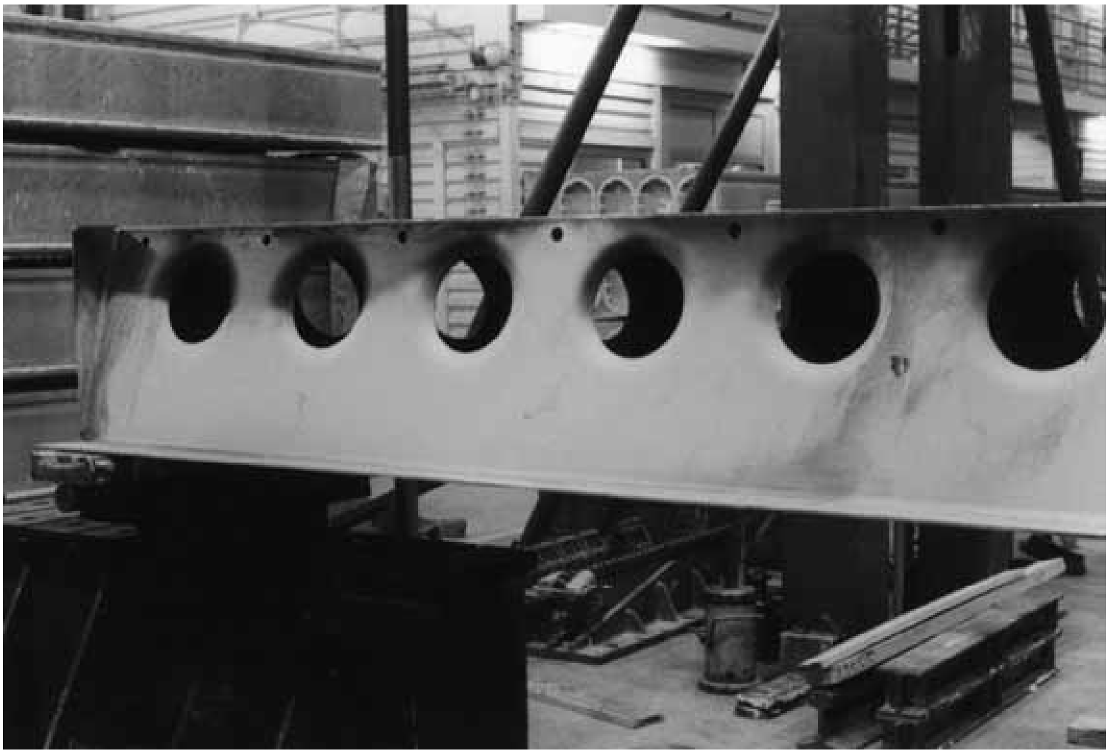

Fig. 2. Detail of Delta-beam.

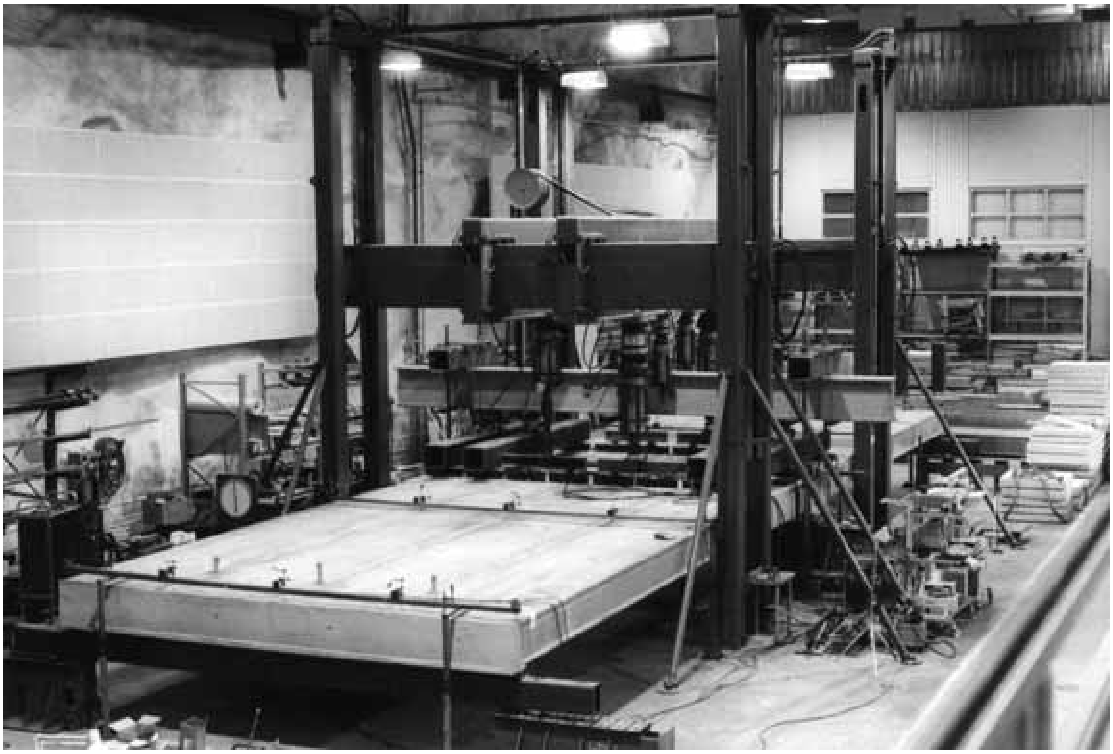

Fig. 3. Overview of test arrangements.

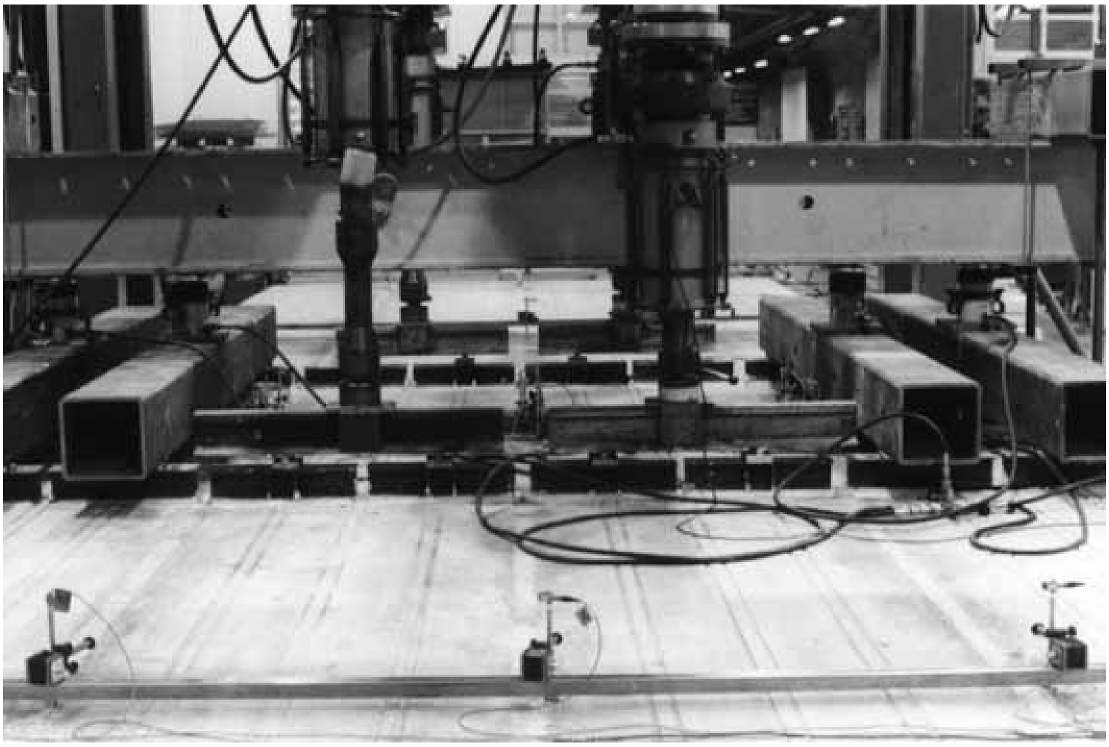

Fig. 4. Loading arrangements.

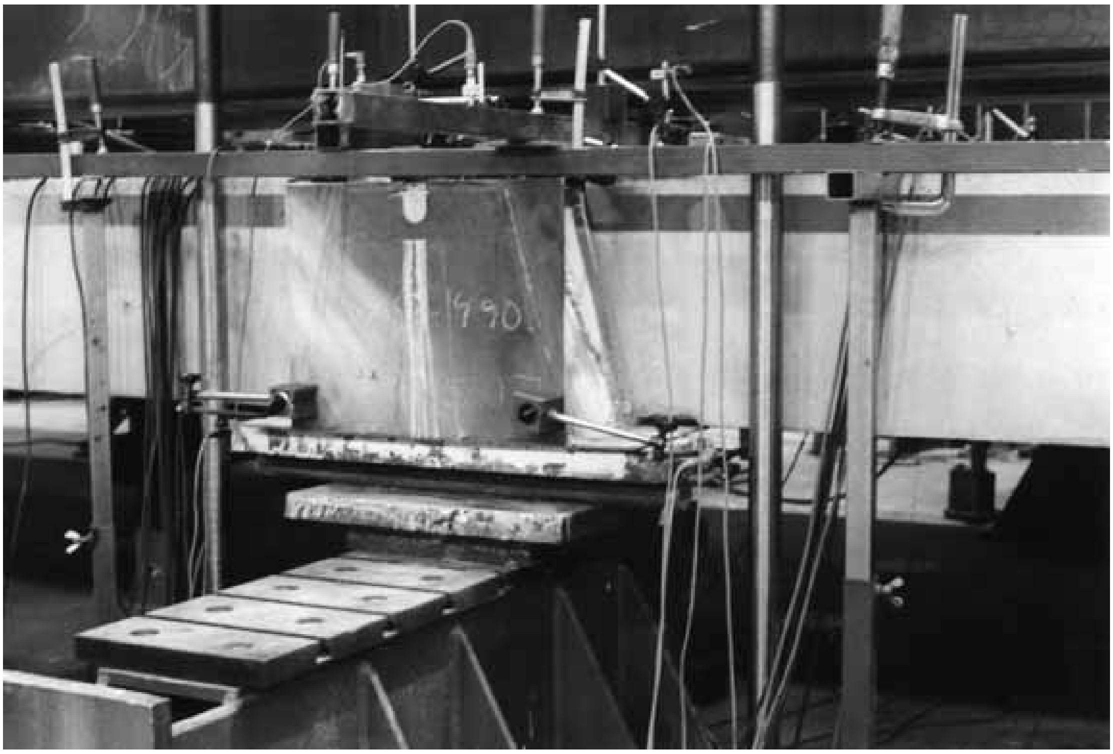

Fig. 5. Arrangements at support of middle beam.

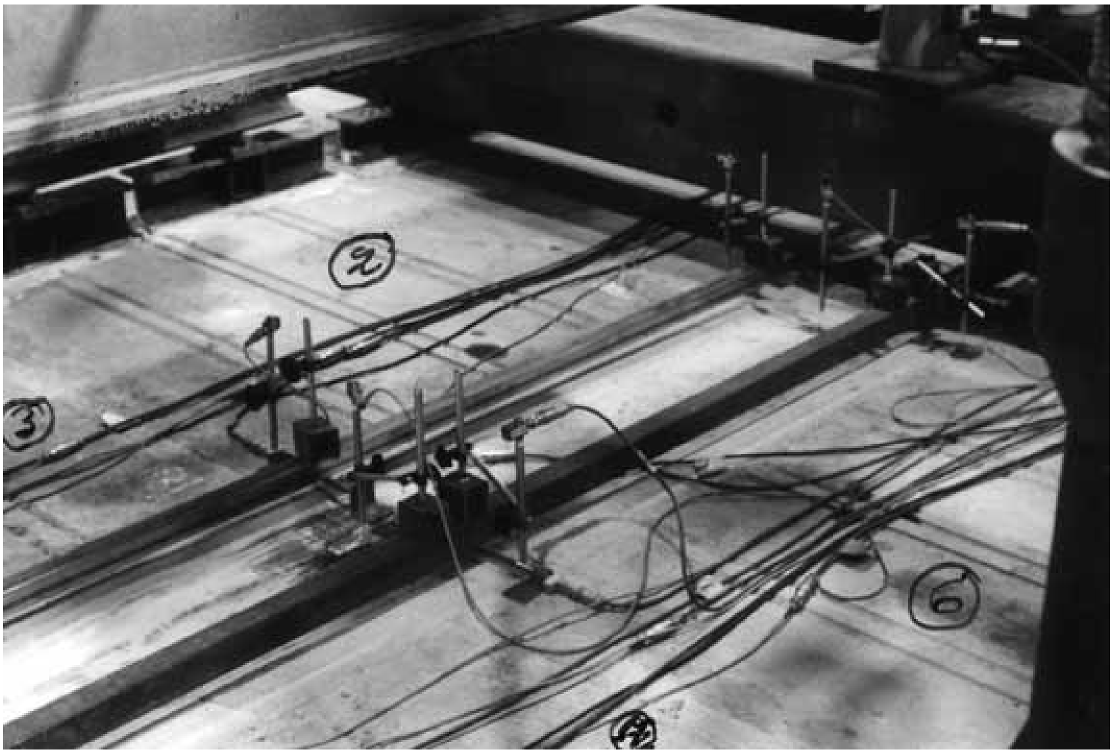

Fig. 6. Measuring equipment on slab units 2, 3, 6 and 7.

Fig. 7. Arrangements at support of end beam.

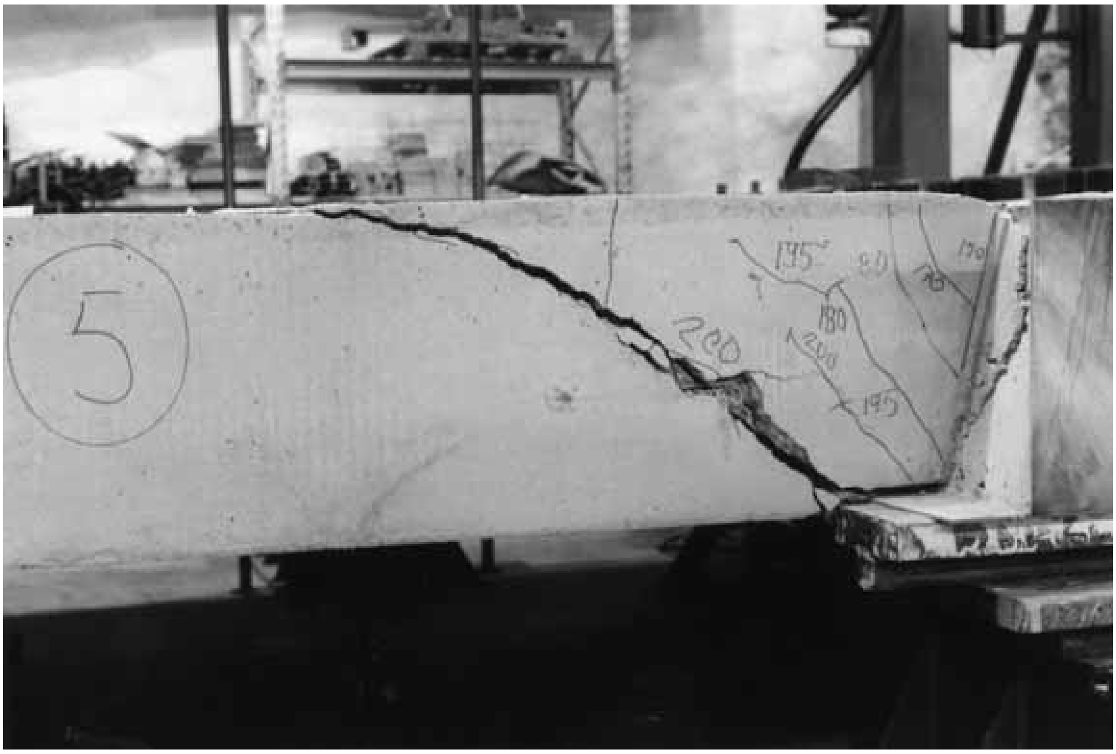

Fig. 8. Failure pattern of slab unit 5.

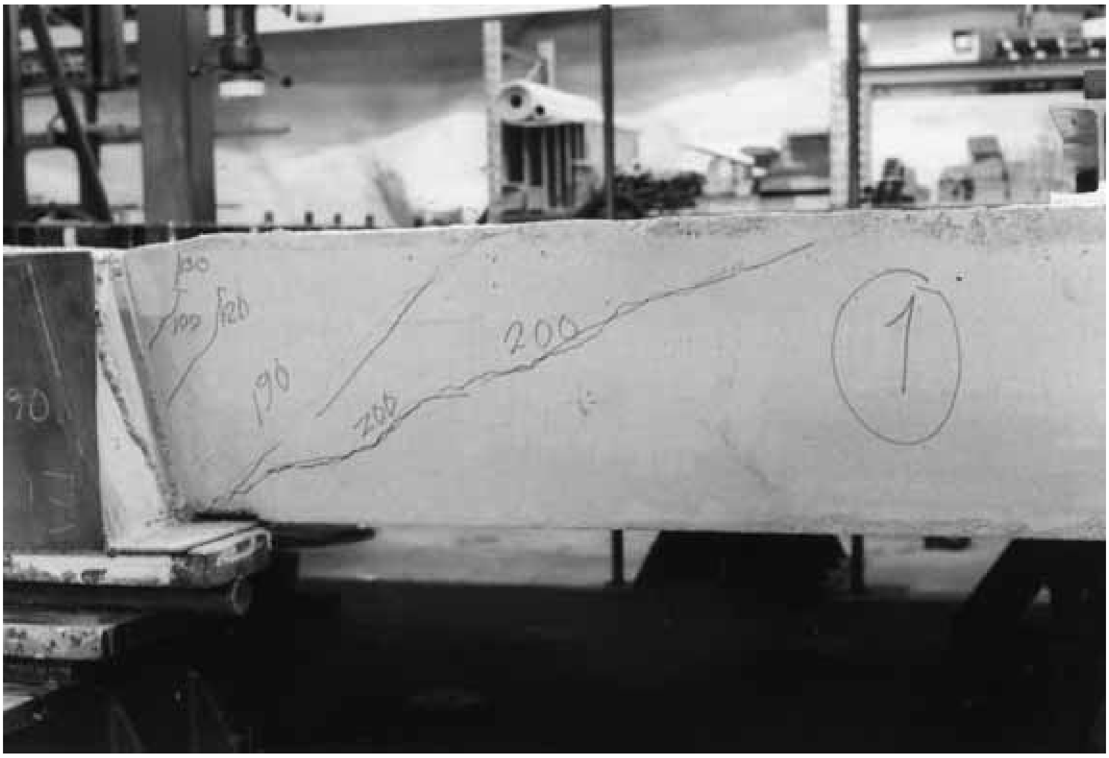

Fig. 9. Failure pattern of slab unit 1.

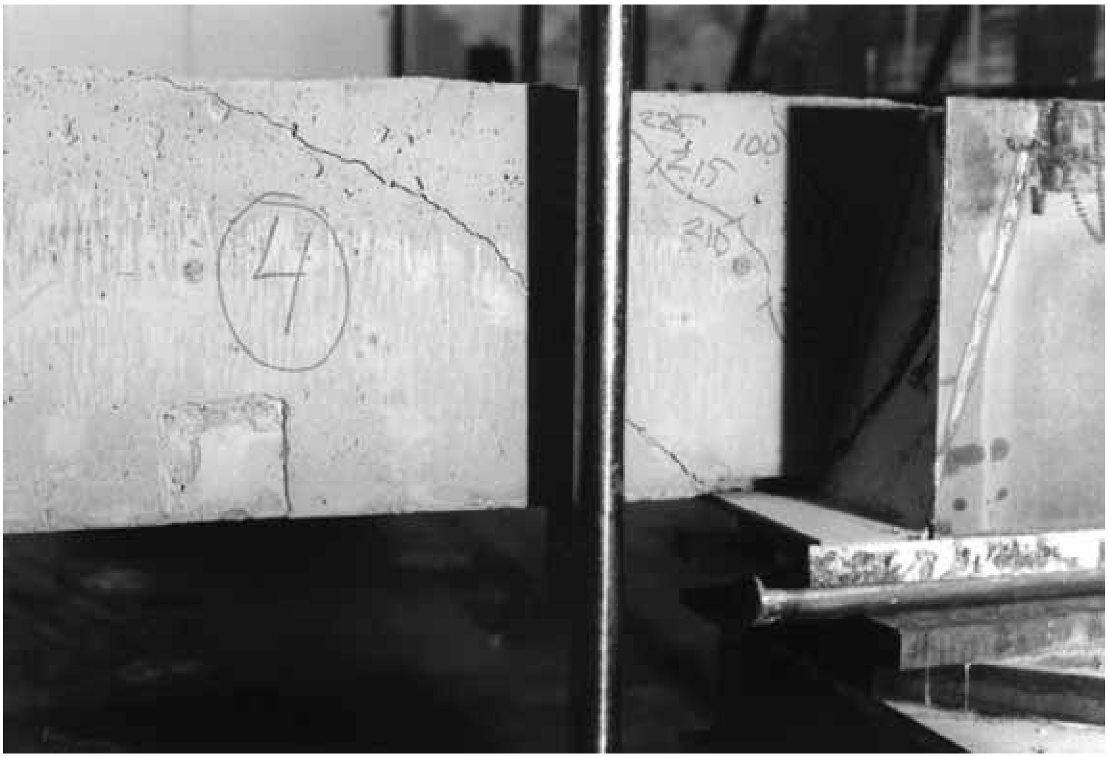

Fig. 10. Failure pattern of slab unit 4.

Fig. 11. Failure pattern of slab unit 8.

Fig. 12. Cracking pattern of tie beam between slab units 2 and 3 at failure of the floor.

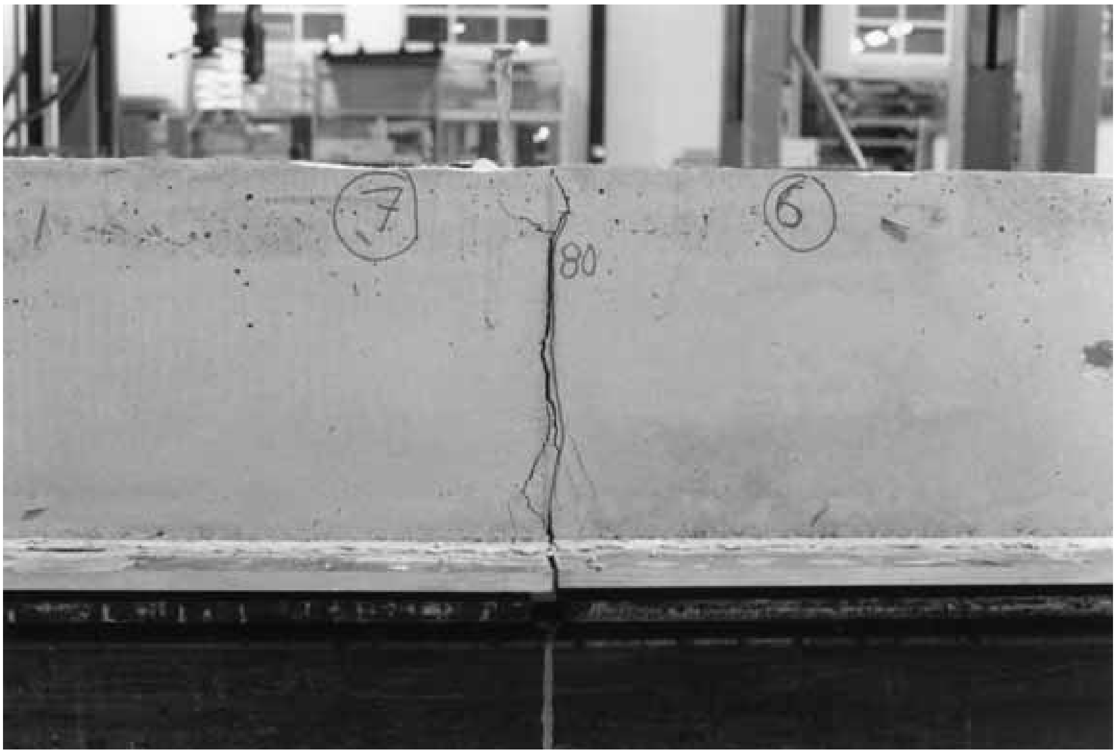

Fig. 13. Cracking pattern of tie beam at end of slab units 6 and 7 at failure of the floor.

Fig. 14. Deformation of ledge of Delta-beam under slab units 5–8 after failure of the floor.

Fig. 15. Deformation of ledge of Delta-beam under slab units 5–8 after failure of the floor.

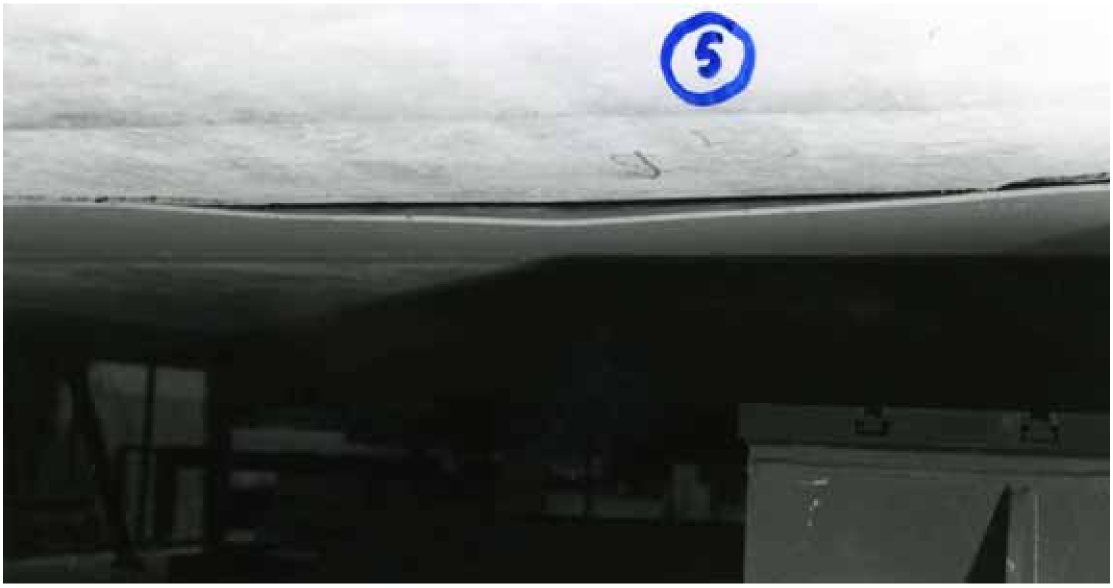

Fig. 16. Deformation of ledge of Delta-beam under slab unit 5 after failure of the floor.

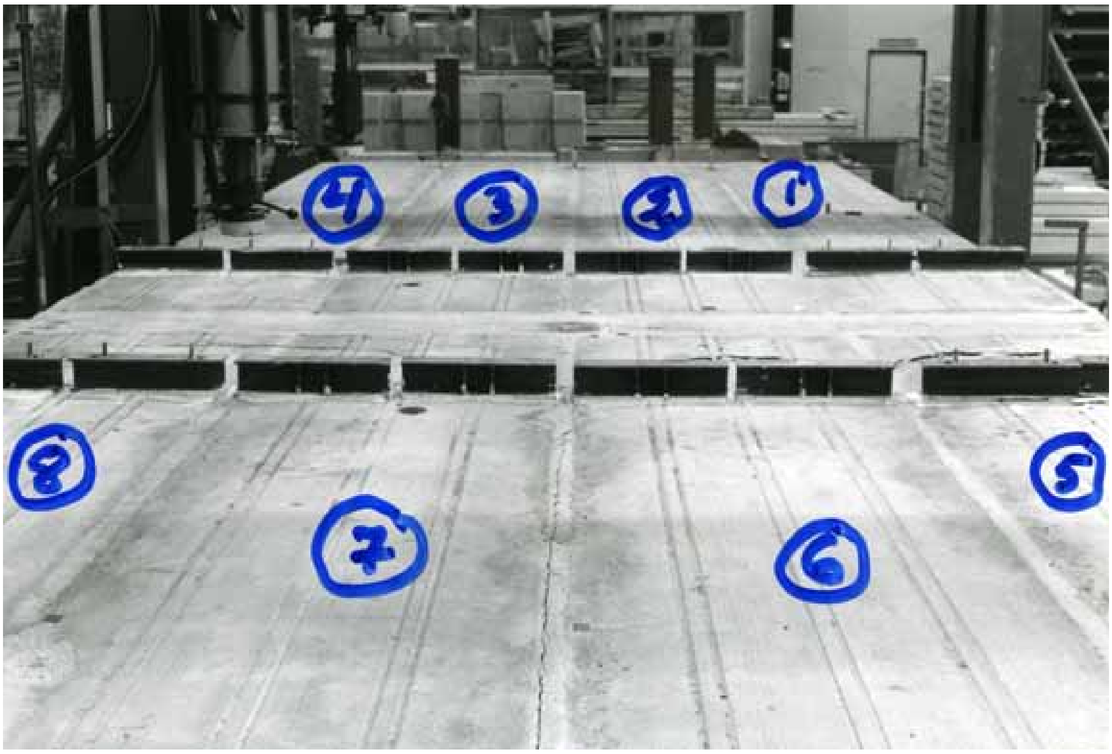

Fig. 17. Top surface of the floor after removal of loads.

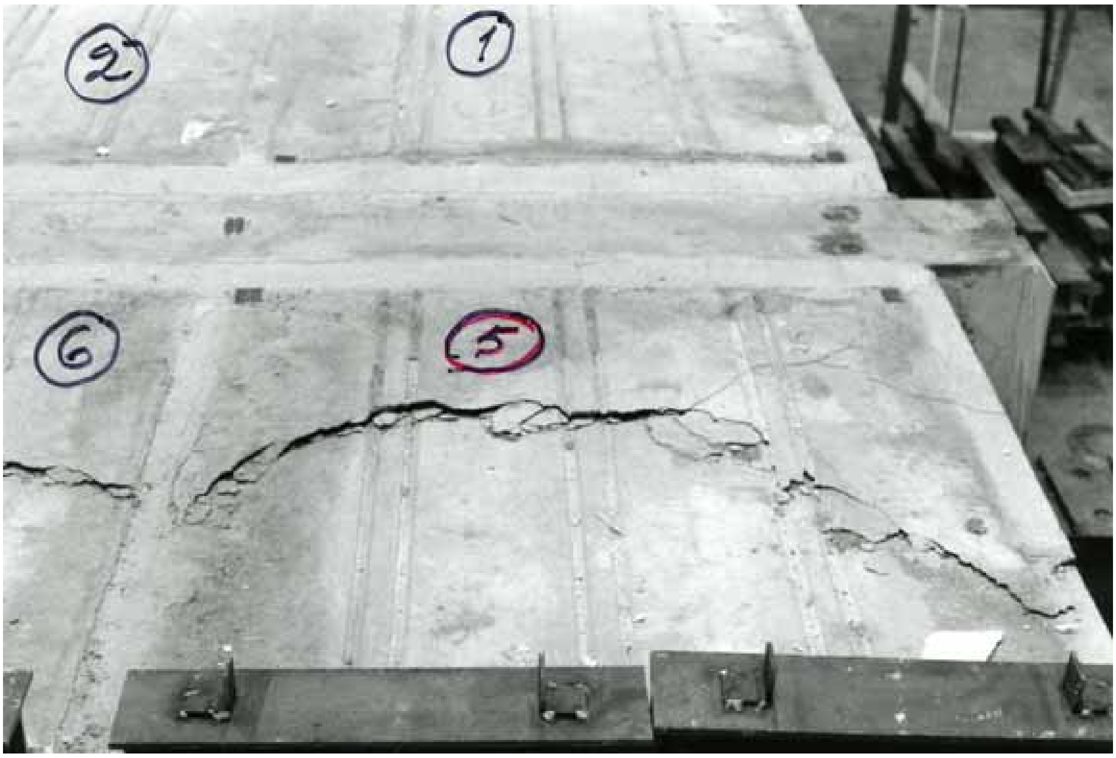

Fig. 18. Top surface of slab unit 5 after failure.

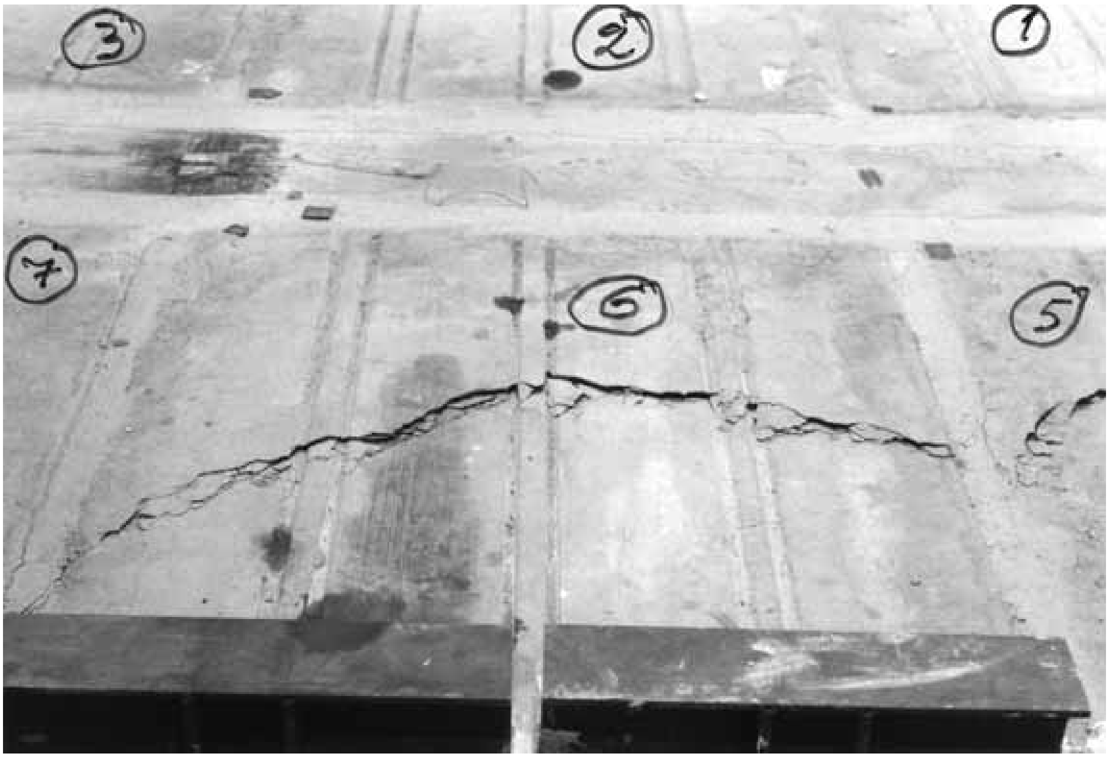

Fig. 19. Top surface of slab unit 6 after failure.

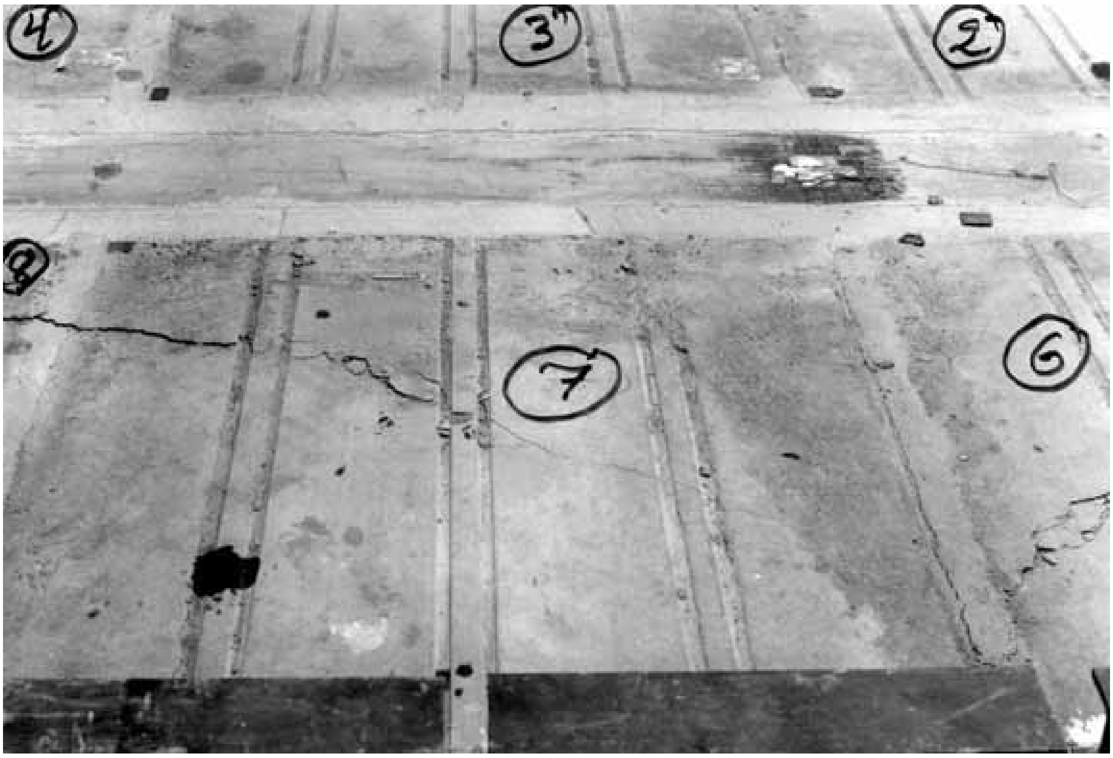

Fig. 20. Top surface of slab unit 7 after failure.

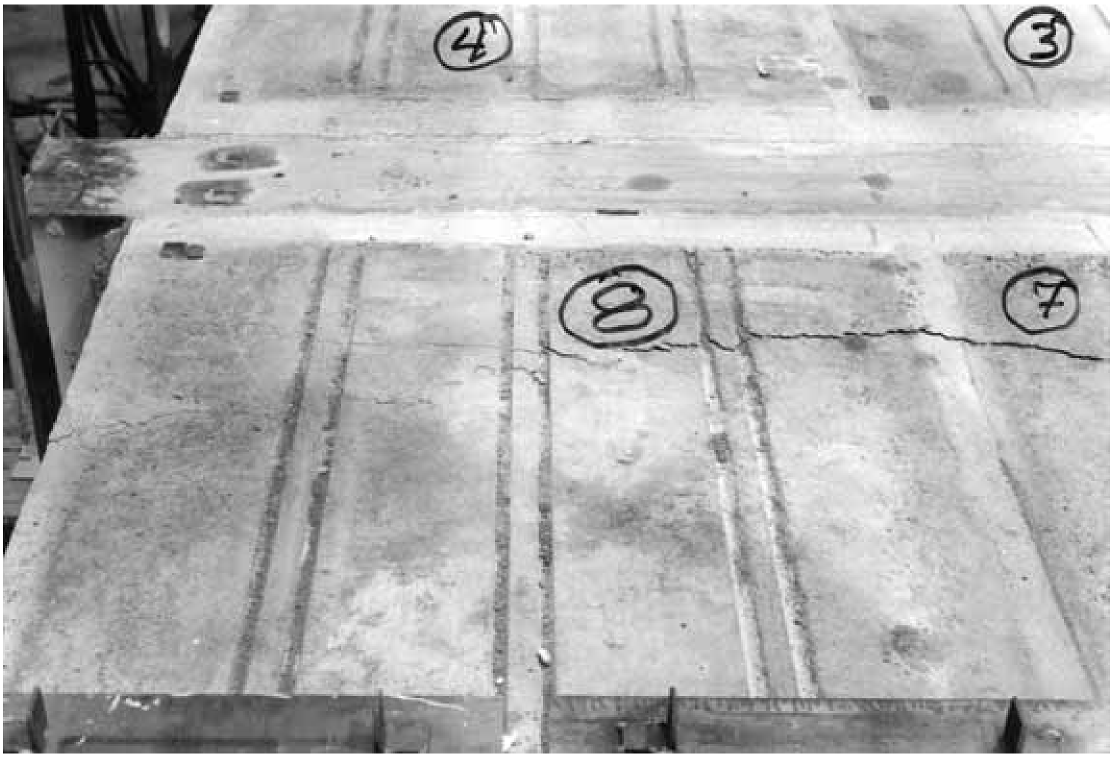

Fig. 21. Top surface of slab unit 8 after failure.

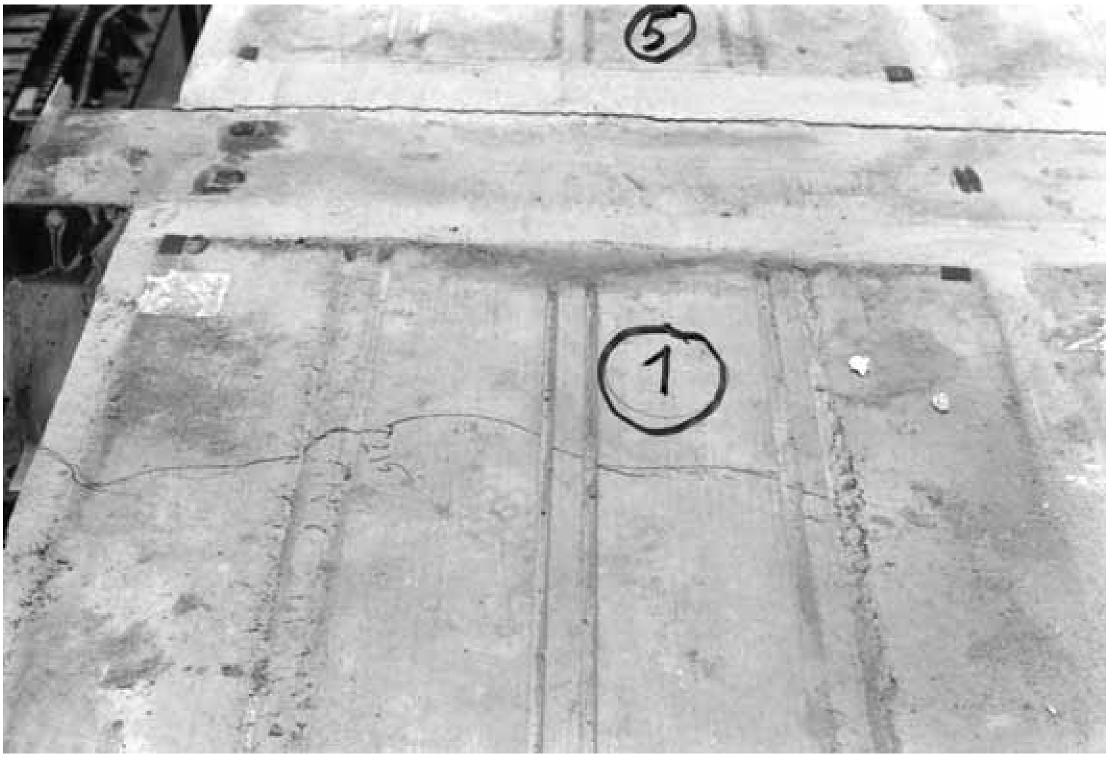

Fig. 22. Top surface of slab unit 1 after failure.

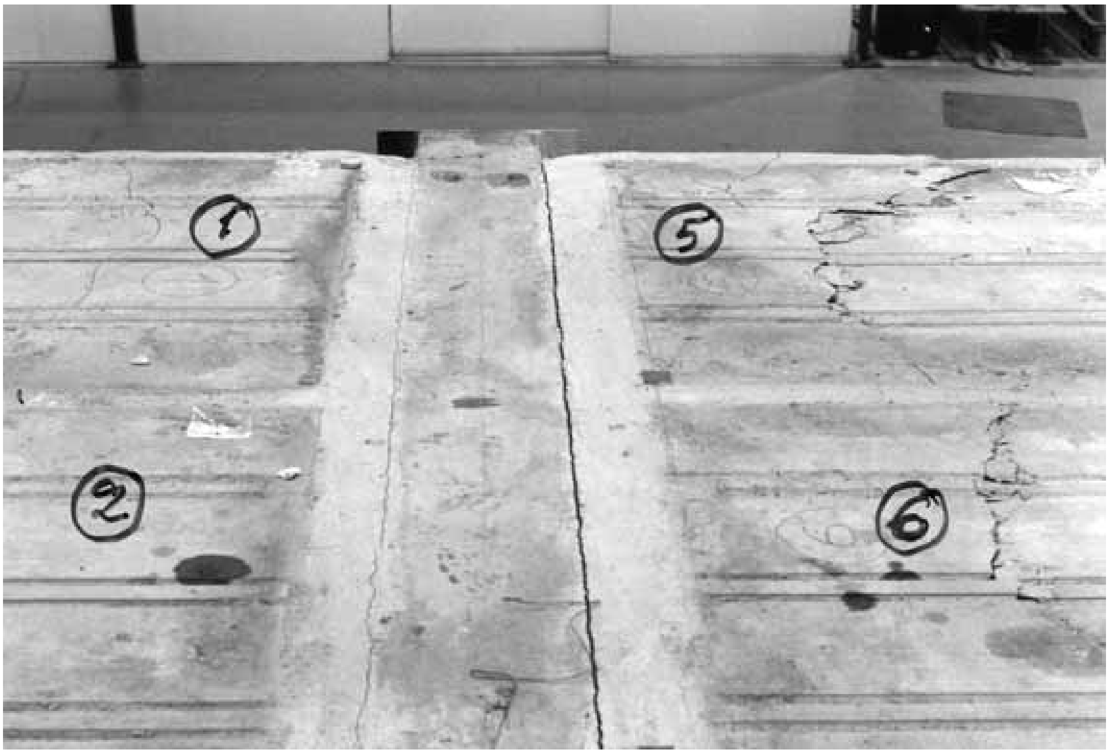

Fig. 23. Cracks along middle beam.

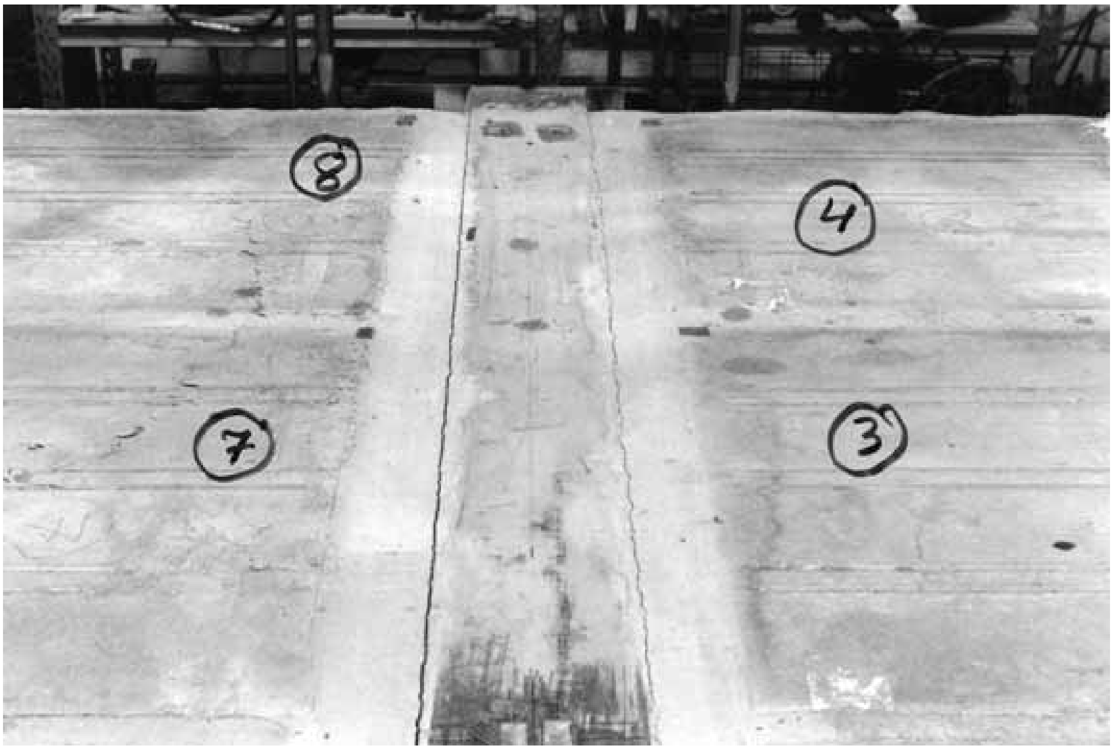

Fig. 24. Cracks along middle beam.

Fig. 25. Joint concrete between slab unit 5–8 and midde beam after removal of slab units.

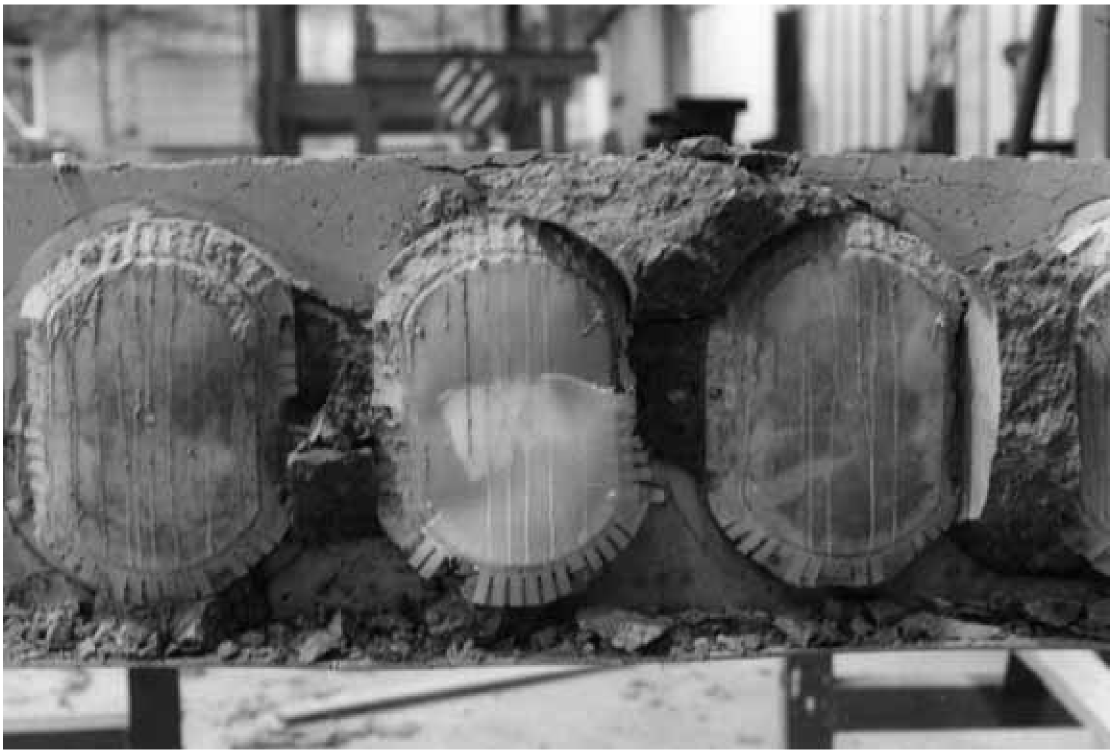

Fig. 26. Detail of the joint concrete after failure.

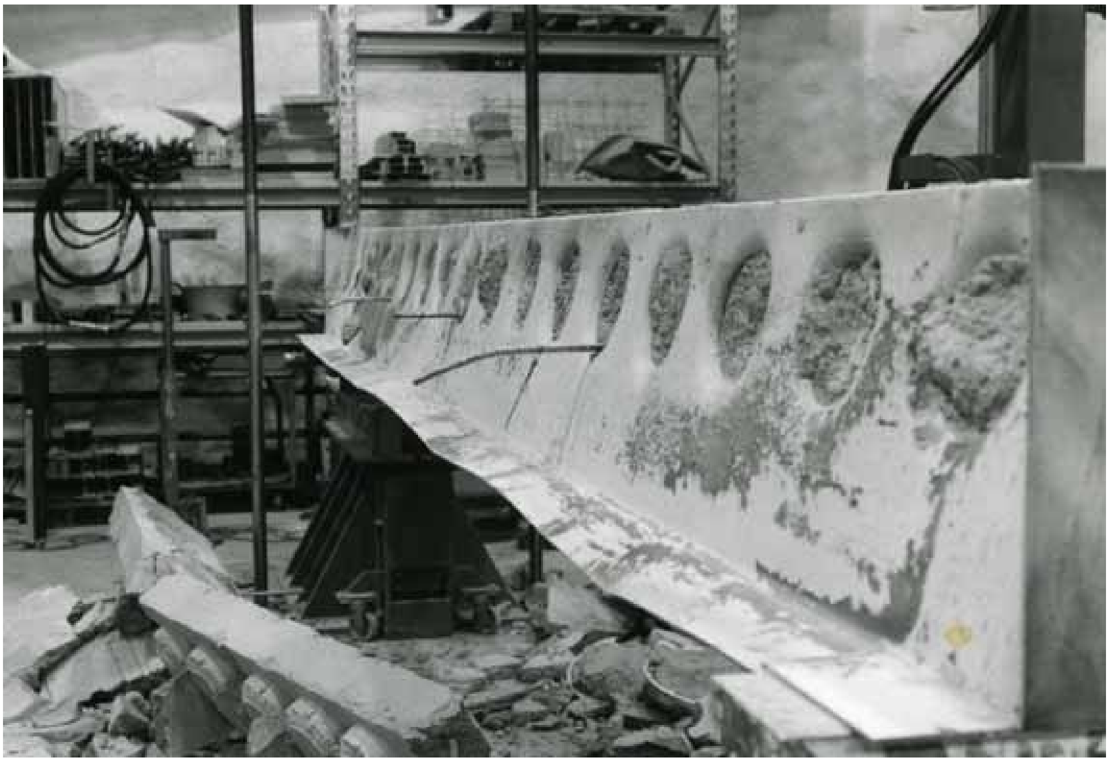

Fig. 27. Web and deformed ledge of middle beam after removal of slab units and joint concrete. The tie bars penetrating the beam have been flame-cut after the test.

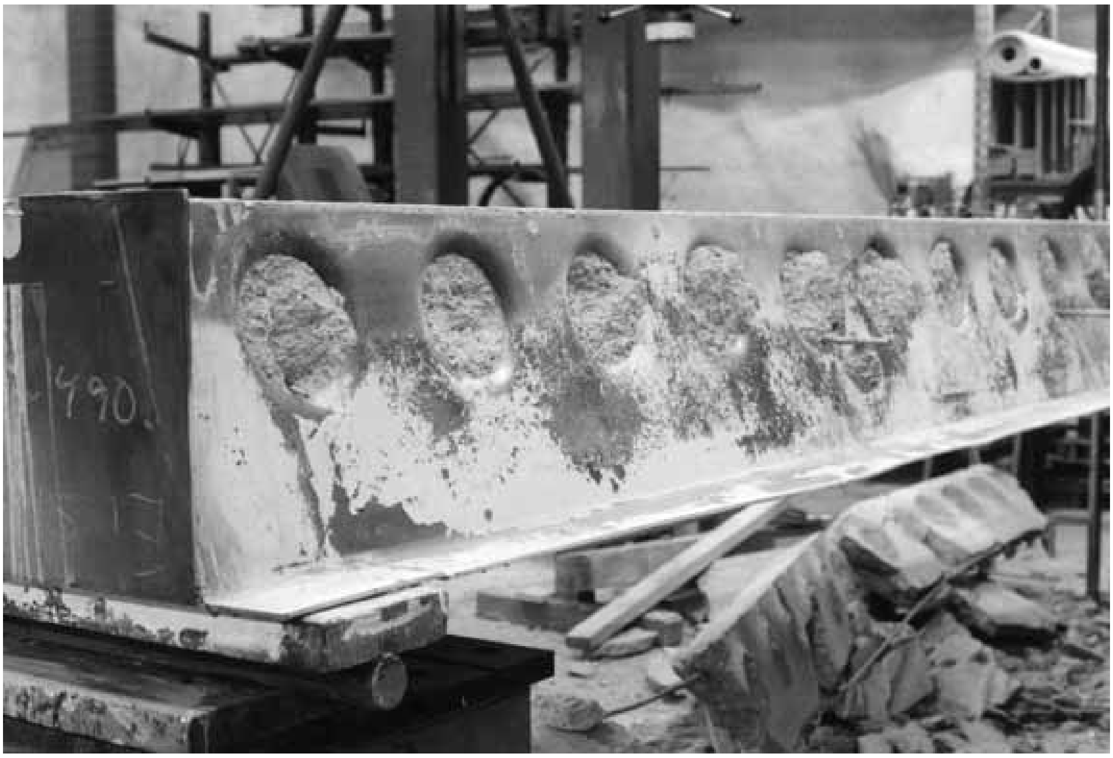

Fig. 28. Detail of middle beam after failure.

Fig. 29. Reference test R9/1. Failure pattern.

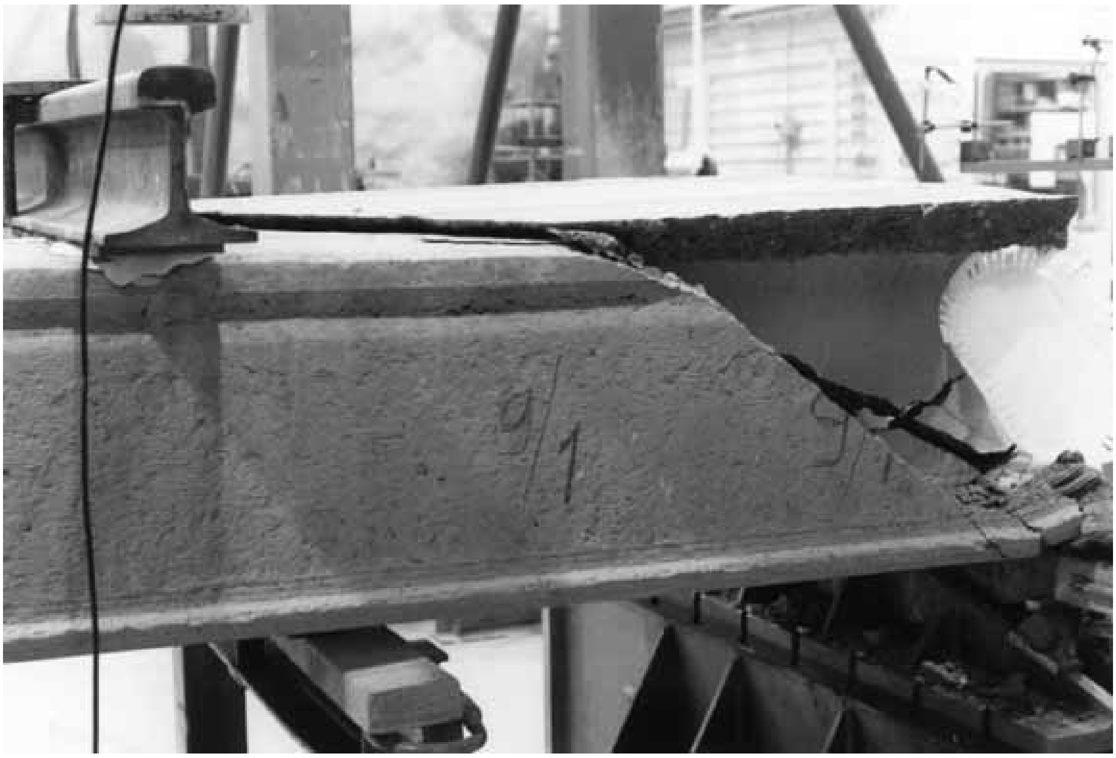

Fig. 30. Reference test R9/1. Failure pattern.

Fig. 31. Reference test R9/2. Failure pattern.

Fig. 32. Reference test R9/2. Failure pattern.

1	**General information**
1.1 Identification and aim	**VTT.CP.Super.320.2002** **Last update 2.11.2010** SUP320 (Internal identification) Aim of the test There were essential differences between Super beam and beams in previous floor test. A test was needed to quantify the interaction between the Super beam and hollow core slabs.
1.2 Test type	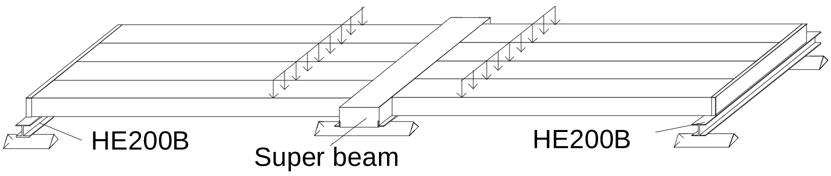 *Fig. 1. Illustration of test setup.*
1.3 Laboratory & date of test	VTT/FI 17.1.2002
1.4 Test report	Author(s) Pajari, M. Name *Load test on hollow core floor* Ref. number RTE868/02 Date 3.4.2002 Availability Confidential, owner is Betset Oy, P.O. Box 14, FI-43701 Kyyjärvi, Finland
2	**Test specimen and loading** (see also Appendices A and B)

2.1 General plan	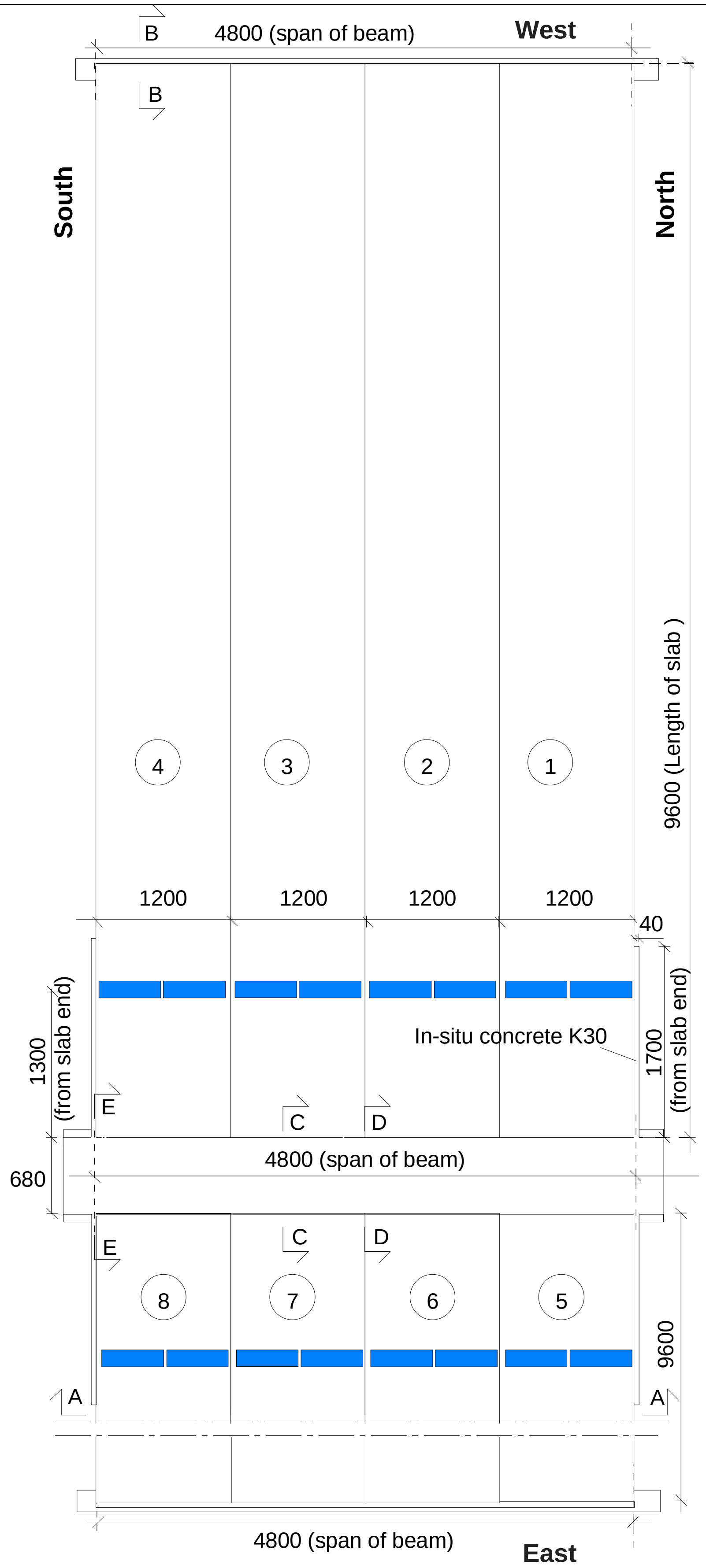 *Fig. 2. Plan.*

2.2 End beams	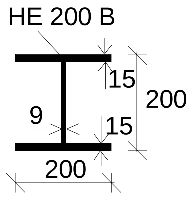 *Fig. 3. End beam.* 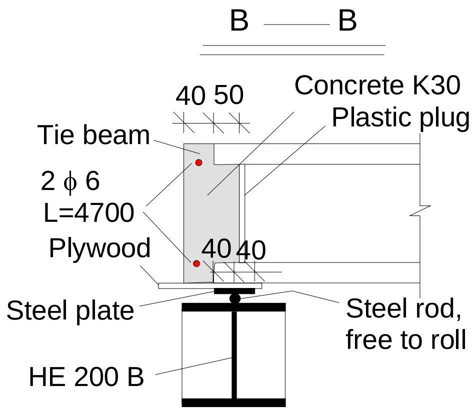 *Fig. 4. Arrangements at end beam. ϕ6 refers to a reinforcing bar TW6, see 2.3.* Simply supported, span = 4,8 m, roller bearing below Southern end $f_y \approx$ 355 MPa (nominal f_y), did not yield in the test.
2.3 Middle beam	The beam, see Fig. 5 and App. A, comprised - a prefabricated part with two L-shaped steel profiles, a folded and perforated steel plate welded to these profiles and a precast and prestressed concrete slab with ribbed reinforcement - a cast-in-situ part of concrete which filled the empty space between the slab ends laying on the L-profiles. - Lower, prestressed part cast by Betset Oy, 13.12.2001 - Upper part cast by VTT in laboratory, 4.1.2002 **Concrete**: K80 in the prefabricated part, K40 in the upper part **Passive reinforcement and tendons in Super beam:** **TWxy**: Hot rolled, weldable rebar A500HW, ϕ = xy mm **J12,9**: Prestressing strand, 7 wires, ϕ =12,9 mm, A_p = 100 mm^2, prestress = 1380 MPa **Kz**: Cold formed rebar B500K, ϕ = z mm **Structural steel:** S355J2G3, $f_y \approx$ 355 MPa (nominal f_y) unless otherwise specified **Tie reinforcement**: Straight, nonprestressed prestressing strands across the middle beam and in the longitudinal joints of the slabs or outside the outer slabs, see Figs 7- 9. **J12,5**: 7 indented wires, ϕ =12,5 mm, A_p = 93 mm^2 **J9,3**: 7 indented wires, ϕ =9,3 mm, A_p = 52 mm^2

Fig. 5. Middle beam.

2.4
Arrangements at middle beam

- Simply supported, span = 4,8 m, roller bearing at both ends

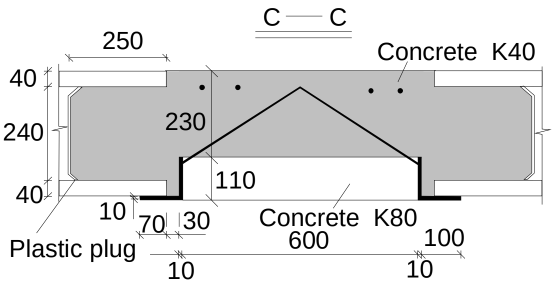

Fig. 6. Section along hollow cores, see Fig. 2.

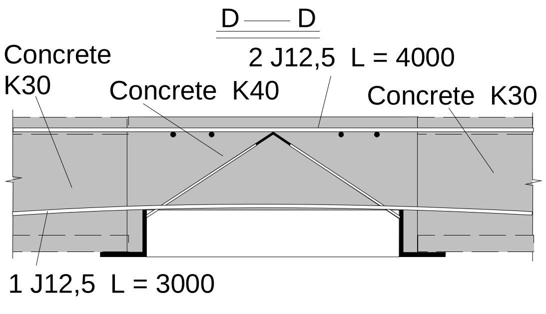

Fig. 7. Section along joint between adjacent slab units, see Fig. 2.

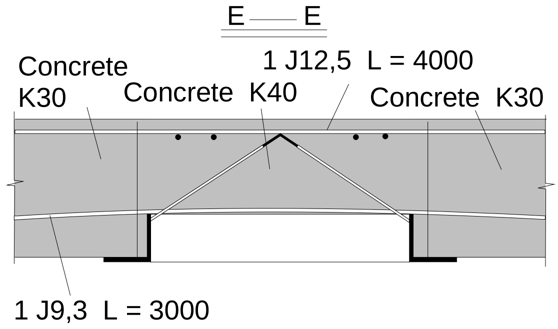

Fig. 8. Section along outer edge of floor specimen, see Fig. 2.

Fig. 9. Tie reinforcement across middle beam.

2.5
Slabs

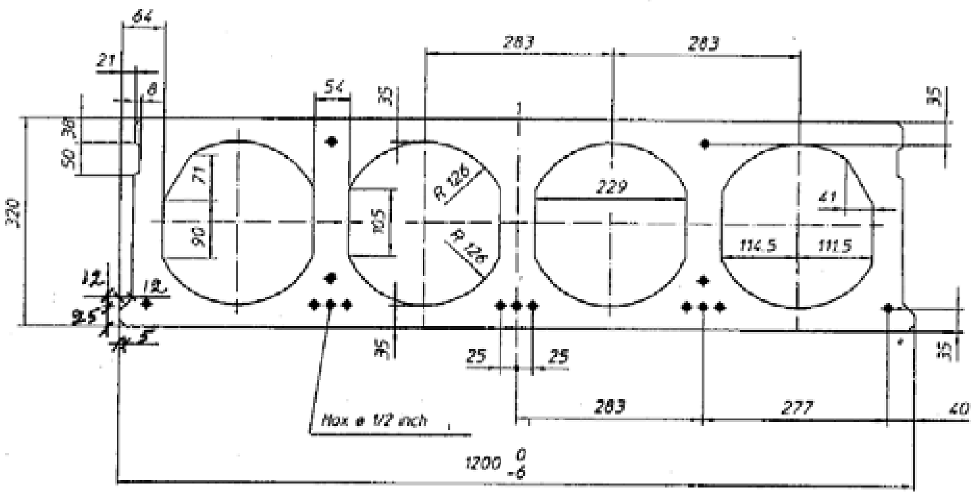

Fig. 10. Nominal geometry of slab units (in scale).

- Extruded by Betset Oy, Kyyjärvi factory 21.11.2001
- 13 lower strands J12,5 initial prestress 1000 MPa
- 2 upper strands J12,5 initial prestress 900 MPa

J12,5: seven indented wires, ϕ =12,5 mm, A_p = 93 mm^2

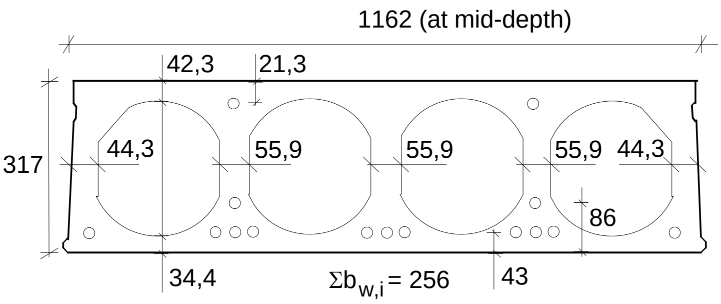

Fig. 11. Mean of most relevant measured geometrical characteristics.

Max measured bond slips: 2,5; 2,4; 2,3 and 2x2,1 mm, all in slab unit 6.

Measured weight of slab units = 4,40 kN/m

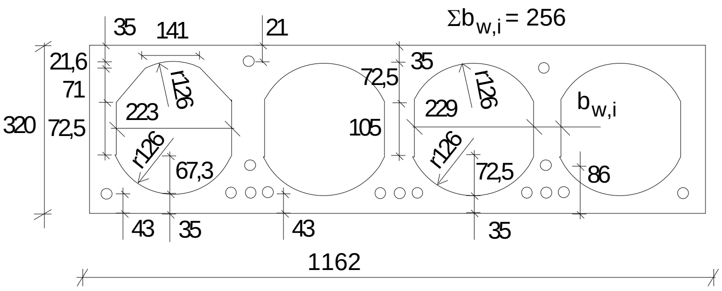

Fig. 12. Geometry for calculation of cross-sectional characteristics.

2.6
Temporary supports

There were temporary supports at mid-span of all three beams during erection, see Fig. 13. They carried the weight of the slabs and cast-in-situ concrete as well as the weight of the loading equipment, and were removed during the first stage of the floor test.

Fig. 13. Temporary support below mid-point of middle beam.

2.7 Loading arrangements	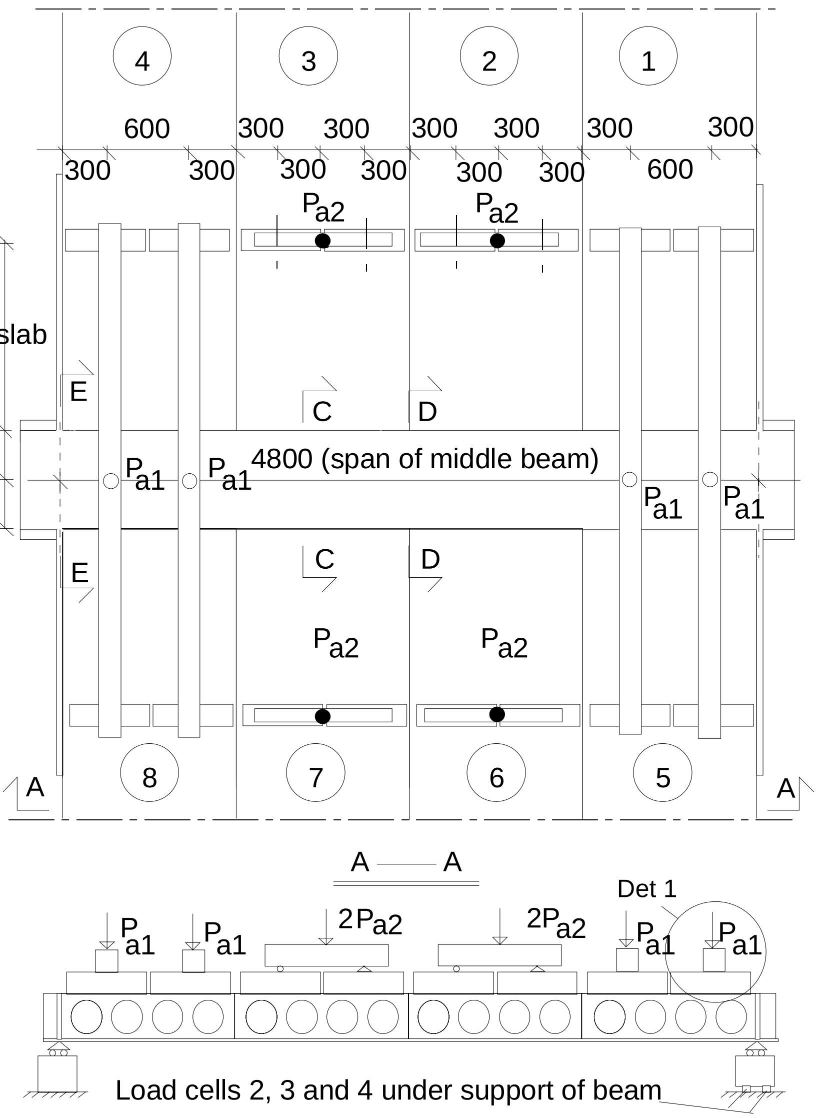 *Fig. 14. Plan. P_{a1} and P_{a2} refer to vertical actuator forces.* 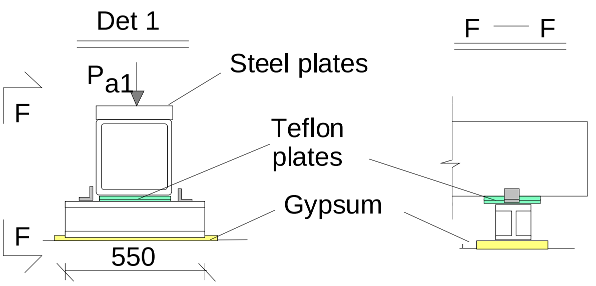 *Fig. 15. Detail 1, see previous figure.*

3	**Measurements**
3.1 Support reactions	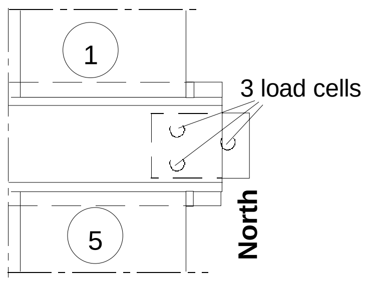 *Fig. 16. Load cells below the Northern support of the middle beam.*
3.2 Vertical displacement	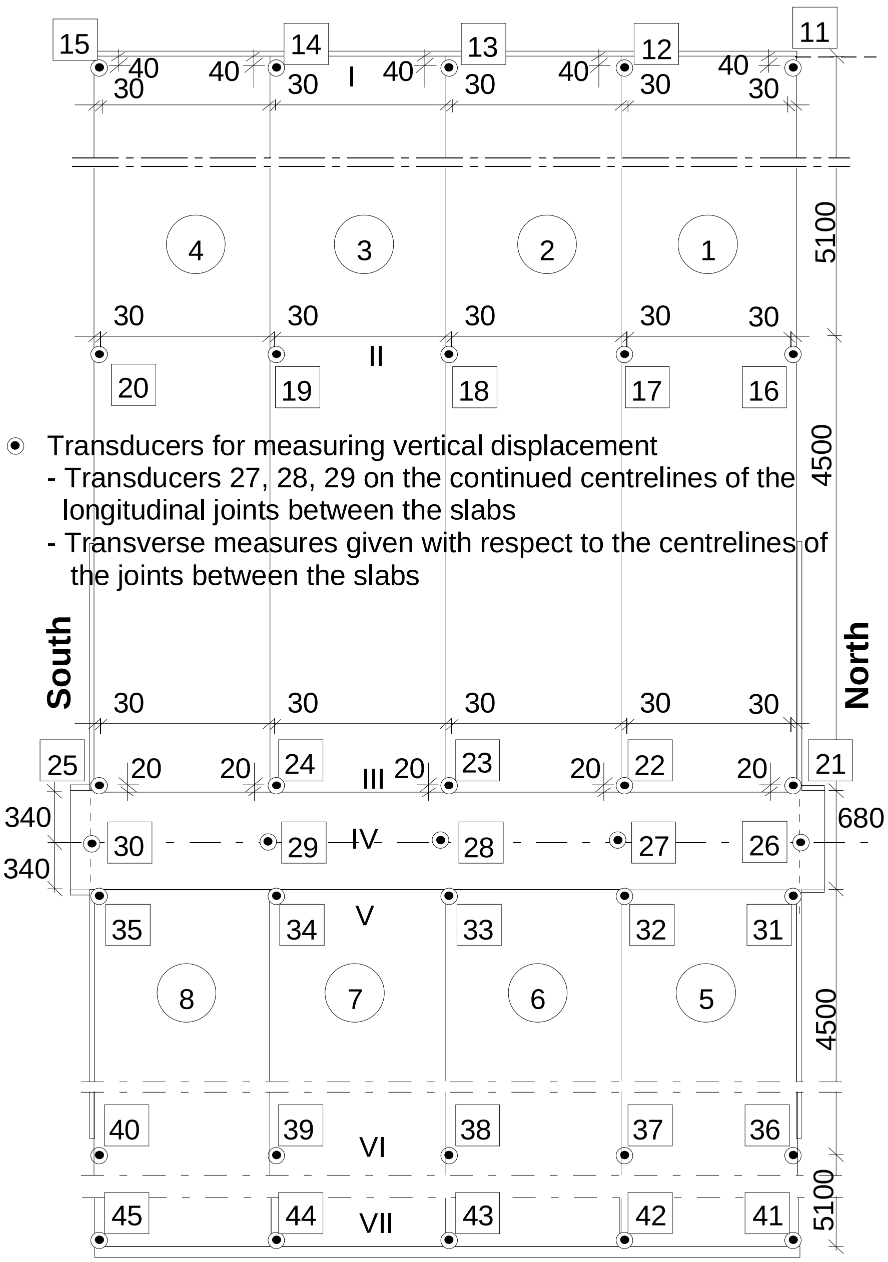 *Fig. 17. Location of transducers 11 … 45 for measuring vertical deflection along lines I … VII.*

3.3
Average strain

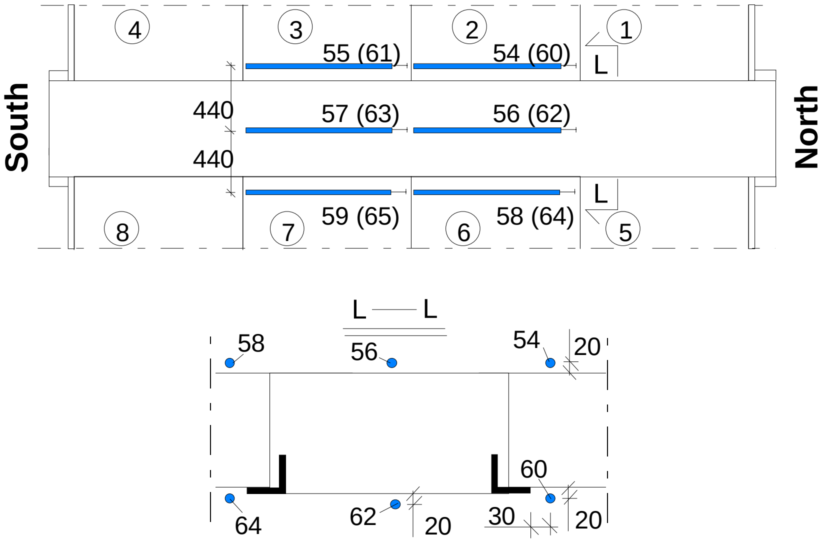

Fig. 18. Position of device (transducers 54–65) measuring average strain parallel to the beams. Numbers in parentheses refer to the soffit of the floor, others to the top.

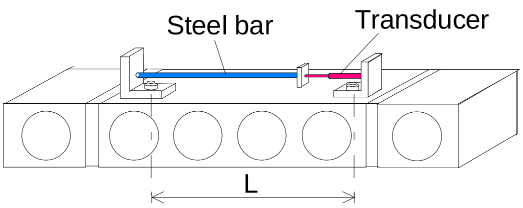

Fig. 19. Apparatus for measuring average strain. L =1040 mm and 1150 mm for the top and soffit transducers (54–59 and 60–65), respectively.

3.4
Horizontal.
displacements

Measures differential displacement between slab end and beam (crack width)

Measures differential displacement between slab edge and beam in beam's direction, numbers in parentheses refer to the soffit of the floor, others to the top

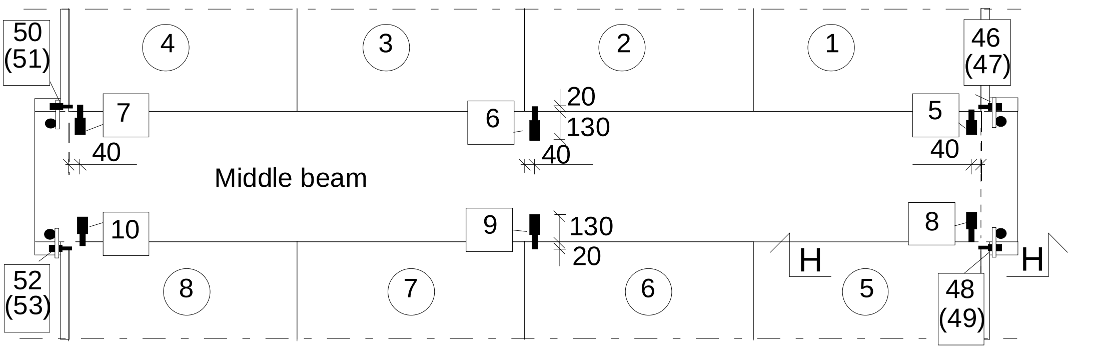

Fig. 20. Transducers measuring crack width (5–10) and shear displacement at the ends of the middle beam (46–53). Transducers 47, 49, 51 and 53 are below transducers 46, 48, 50 and 52, respectively.

<table>
<tr><td></td><td>
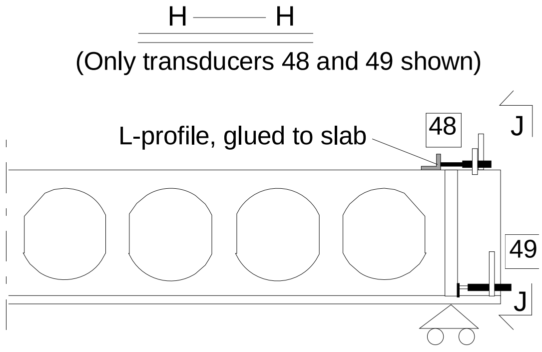

Fig. 21. Section H-H, see Fig. 20.

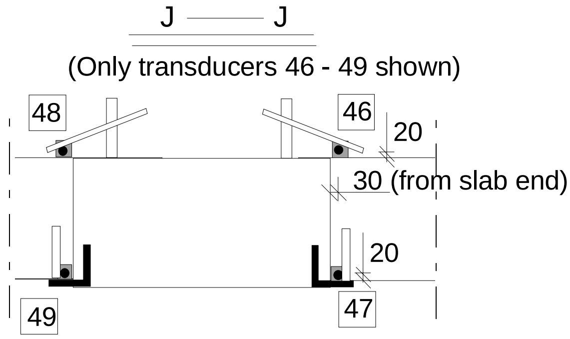

Fig. 22. Section J-J, see Fig. 21.
</td></tr>
<tr><td>3.5
Strain</td><td>
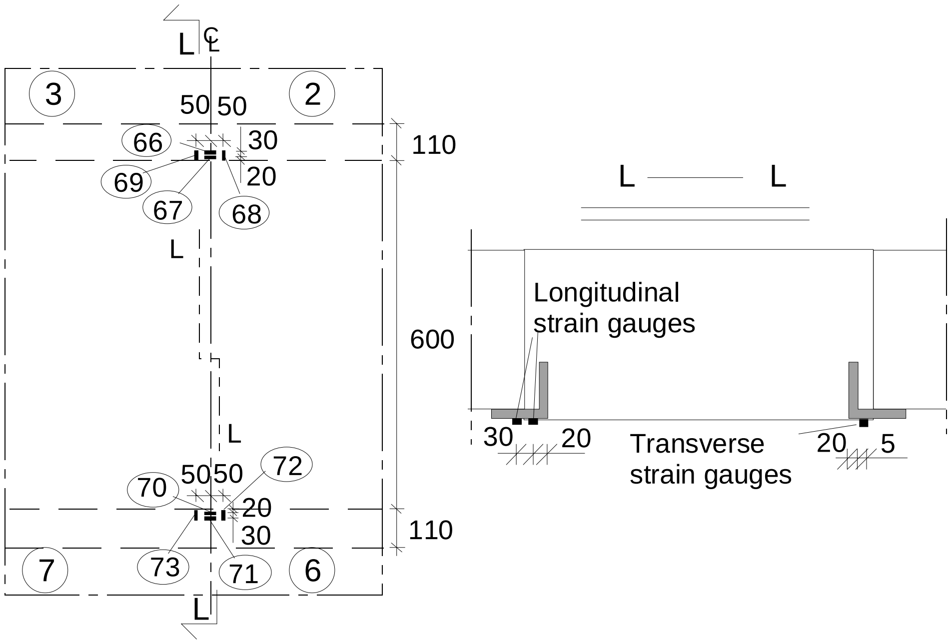

Fig. 23. Position of strain gauges 66–73 at mid-section of middle beam.
</td></tr>
<tr><td>4</td><td>Special arrangements</td></tr>
<tr><td>5</td><td>Loading strategy</td></tr>
<tr><td>5.1
Load-time relationship</td><td>
Date of test was 17.1.2001

Before removal of the temporary supports and when the actuator forces P_{ai} were equal to zero but the weight of the loading equipment was on, all measuring devices were zero-balanced. Thereafter, the temporary supports were removed. Fig 24 shows the effect of this operation to the support reaction of the middle beam. The loading history is shown in Fig. 25.
</td></tr>
</table>

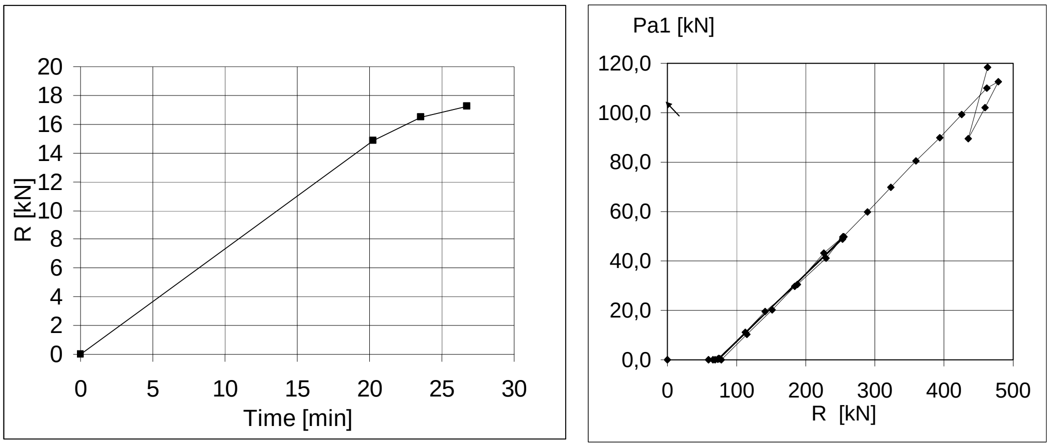

a) b)

Fig. 24. Development of support reaction R below Northern end of middle beam a) When removing the temporary supports. b) Later as function of P_{a1}.

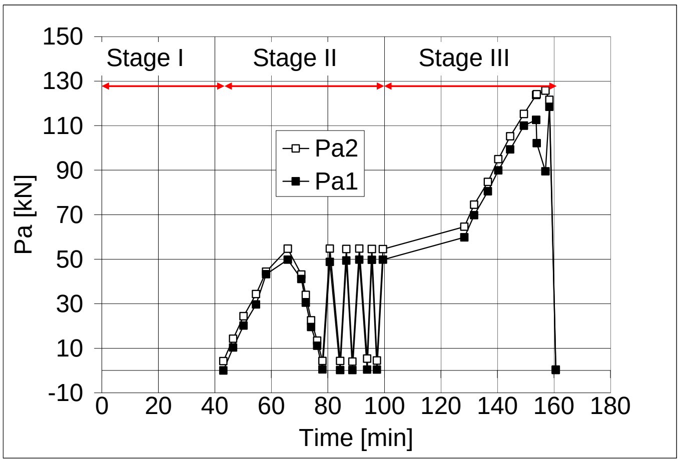

Fig. 25. Actuator forces P_{a1} and P_{a2} vs. time.

5.2
After failure

6 **Observations during loading**

Stage I	Some longitudinal cracks along the strands were discovered in the soffit of the slabs, see Fig. 30. Their width was of the order of 0,08 … 0,10 mm. They were obviously caused by the release of the prestressing force.
Stage II	The interface between the cast-in-situ concrete and slab ends cracked along slabs 1–4 at P_{a1} = 30 kN and along slabs 5–8 at P_{a1} = 50 kN. The tie beams at the ends of the floor specimen failed between slabs 2 and 3 at P_{a1} = 30 kN and between slabs 6 and 7 at P_{a1} = 50 kN. P_{ai} = 50 kN corresponds to the expected service load when the shear resistance of the slabs was assumed to be critical in the design. At the end of Stage II, some cracks in the soffit had increased in length and their maximum width was of the order of 0,10–0,12 mm , see Fig. 30.

		Stage III	*At* P_{a1} = 115 kN an inclined crack was observed outside slab 1 at Northern support of middle beam and soon after that a similar crack appeared outside slab 5. At P_{a1} = 120 kN, similar cracks appeared outside slabs 4 and 8, see Figs 8–11 in App. B. The next aimed load step P_{a1} = 120 kN, P_{a2} = 124,4 kN could not be achieved because new inclined cracks appeared below the previous ones in slabs 1 and 5 Consequently, slab 1, followed by slabs 4 and 5 failed in shear. The highest support reaction was obtained at load combination P_{a1} = 112,6 kN, *At* P_{a2} = 123,7 kN.
		After failure	When demolishing the test specimen it was observed that all core fillings were not perfect. Due to the cracking mechanism, see Fig. 26, the core fillings could be measured, see Figs 27–29 and App. B, Figs 22–25. 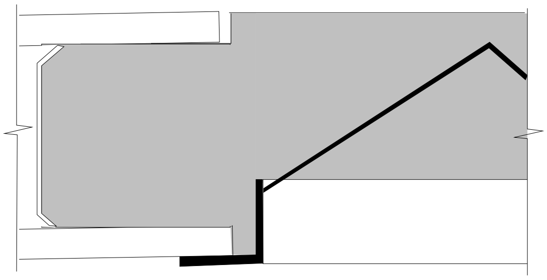 *Fig. 26. Cracking took typically place along the surface of the core filling.*  *Fig. 27. Super beam after removal of slab units.*

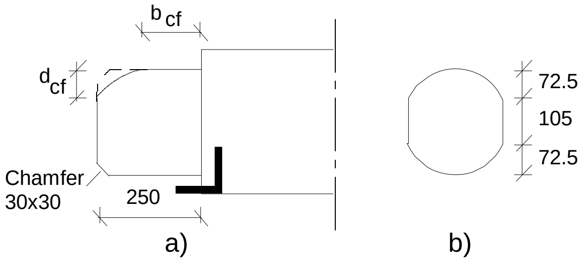

Fig. 28. a) Core filling seen in the beams's direction. b) Nominal dimensions of a hollow core.

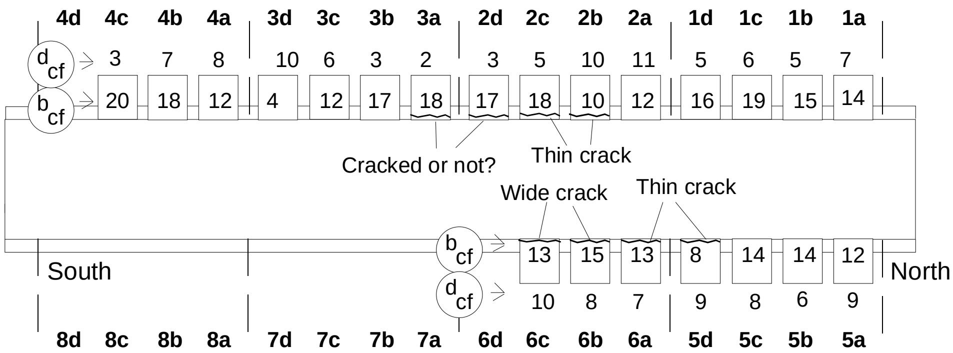

Fig. 29. Core fillings seen from above after removal of slabs. The core fillings are identified by the number of the slab and letters a–d. d_{cf} and b_{cf}, see Fig. 42, are given in centimetres.

7 Cracks in concrete

7.1 Cracks at service load

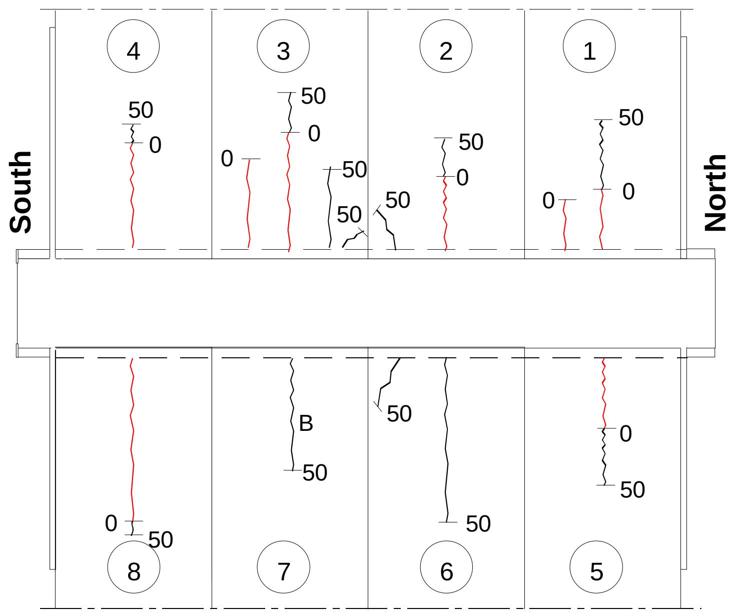

Fig. 30. Cracks in the soffit at service load (P_{ai} = 50 kN). The initial cracks observed before loading are indicated with red colour. The figures give the value of the actuator force at which the crack was observed.

7.2 Cracks after failure	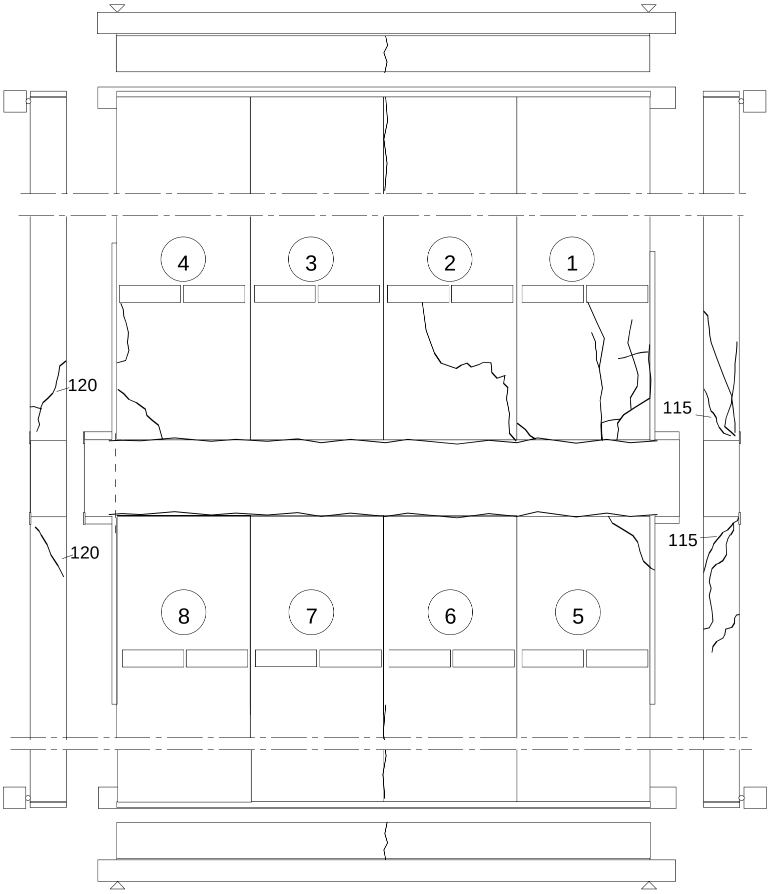 *Fig. 31. Cracks after failure on the top and at the edges.* 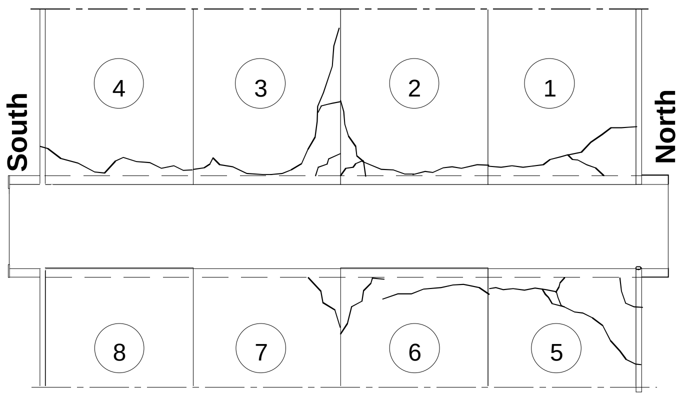 *Fig. 32. Cracks after failure in the soffit.*
8	**Observed shear resistance**
	The ratio (measured support reaction below one end of the middle beam)/ (theoretical support reaction due to actuator forces on half floor) is shown in Fig. 33. The theoretical reaction is calculated assuming simply supported slabs. This comparison shows that the support reaction due to the actuator forces can be calculated accurately enough assuming simply supported slabs. However, the failure of the slab ends at the North end of the middle beam resulted in reduction of support reaction below that end while the actuator force could still slightly be increased. The maximum support reaction is regarded as the indicator of failure.

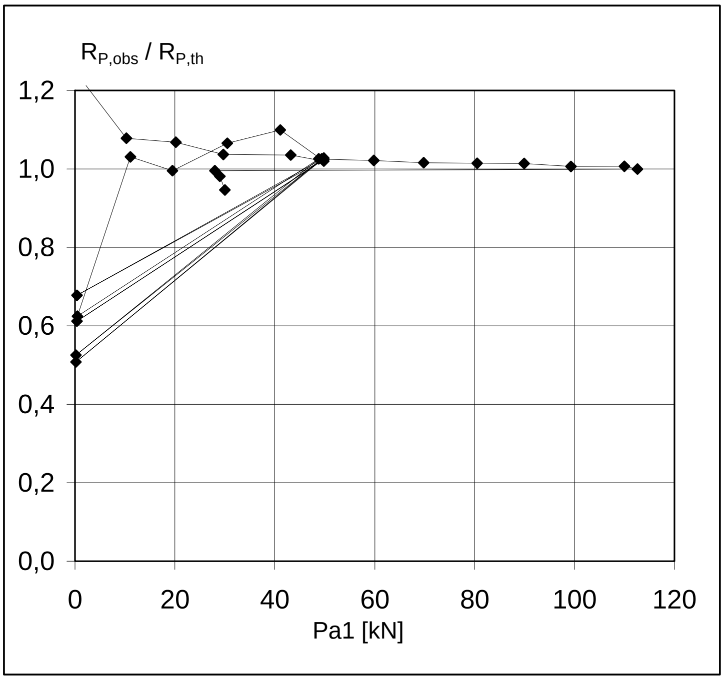

Fig. 33. Ratio of measured support reaction of the middle beam ($R_{p,obs}$) to theoretical support reaction ($R_{p,th}$) vs. actuator force P_{a1}. Only actuator loads P_{a1} and P_{a2} are taken into account in the support reaction.

The shear resistance of one slab end (support reaction of slab end at failure) due to different load components is given by

$$V_{obs} = V_{g,sl} + V_{g,jc} + V_{eq} + V_a$$

where $V_{g,sl}$, $V_{g,jc}$, V_{eq} and V_a are shear forces due to the self-weight of slab unit, weight of joint concrete, weight of loading equipment and actuator forces P_{ai}, respectively. All components of the shear force are calculated assuming that the slabs behave as simply supported beams. For V_{eq} and V_a this means that $V_{eq} = 0{,}8677 \times P_{eq}$ and $V_a = 0{,}8677 \times (P_{a1} + P_{a2})/2$. $V_{g,jc}$ is calculated from the nominal geometry of the joints and density of the concrete, other components of the shear force are calculated from measured loads and weights. The values for the components of the shear force are given in Table below.

Table. Components of shear resistance due to different loads.

Action	Load	Shear force kN
Weight of slab unit	4,40 kN/m	20,97
Weight of joint concrete	0,212 kN/m	1,01
Loading equipment	(1,2+5,6)/2 kN	2,95
Actuator loads	(112,6+123,7)/2 kN	102,52

The observed shear resistance $\boldsymbol{V_{obs}}$ **= 127,5 kN** (shear force at support) is obtained for one slab unit with width = 1,2 m. The shear force per unit width is $\boldsymbol{v_{obs}}$ **= 106,2 kN/m**

9	**Material properties**

9.1
Strength of steel

Component	$R_{eH}/R_{p\,0,2}$ MPa	R_m MPa	Note
L-profiles	≈ 355		Nominal (S355J2G3)
Folded plate	≈ 355		Nominal (S355J2G3)
Tie strands J12,5 and J9,3	1630	1860	Nominal (no yielding in test)
Slab strands J12,5	1630	1860	Nominal (no yielding in test)
Beam strands J12,9	1630	1860	Nominal (no yielding in test)
Reinforcement Txy and Kz	500		Nominal value for reinforcing bars (no yielding in test)

9.2
Strength of slab concrete, floor test

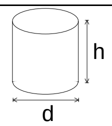

#	Cores		*h* mm	*d* mm	Date of test	Note
6			50	50	25.01.2002 (+8 d)[1)]	Upper flange of slabs 5 and 6, vertically drilled, tested as drilled[2)], density =2328 kg/m^3
Mean strength [MPa]			62,1			
St.deviation [MPa]			4,6			

9.3
Strength of slab concrete, reference tests

Not measured, assumed to be the same as that in the floor test

9.4
Strength of grout in longitudinal joints of slab units

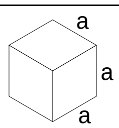

#		*a* mm	Date of test	Note
6		150	17.1.2002 (+0 d)[1)]	Kept in laboratory in the same conditions as the floor specimen density = 2152 kg/m^3
Mean strength [MPa]		21,4		
St.deviation [MPa]		0,90		

9.5
Strength of concrete in the upper part of the beam and in the core filling

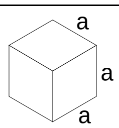

#		*a* mm	Date of test	Note
6		150	17.1.2002 (+0 d)[1)]	Kept in laboratory in the same conditions as the floor specimen density = 2178 kg/m^3
Mean strength [MPa]		33,3		
St.deviation [MPa]		0,30		

[1)] Date of material test minus date of structural test (floor test or reference test)
[2)] After drilling, kept in a closed plastic bag until compression

10 **Measured displacements**

In the following figures, V_a stands for the shear force of one slab end due to imposed actuator loads, calculated assuming simply supported slabs. Note that the last three points on each curve represent the post failure situation for which the real shear force has been lower than that shown in the figures. This note is based on the measured support reaction, see Fig. 25.b.

10.1
Deflections

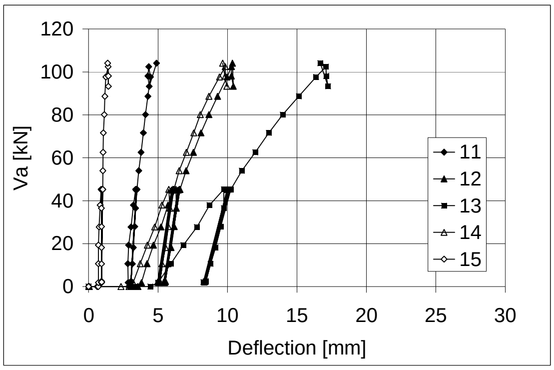

Fig. 34. Deflection on line I along western end beam.

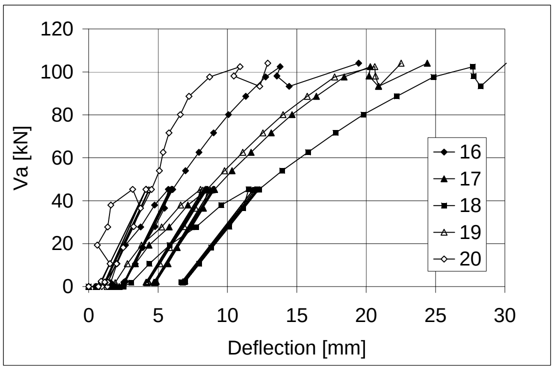

Fig. 35. Deflection on line II in the middle of slabs 1–4.

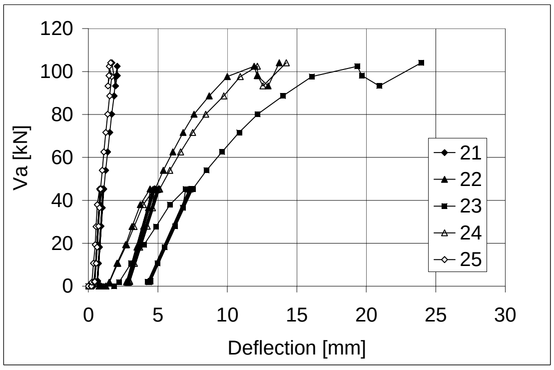

Fig. 36. Deflection on line III close to the line load, slabs 1–4.

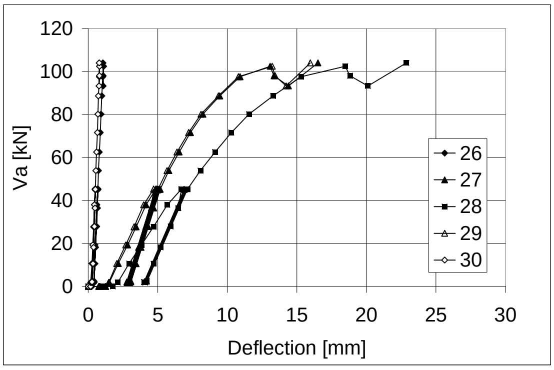

Fig. 37. Deflection on line IV along the middle beam.

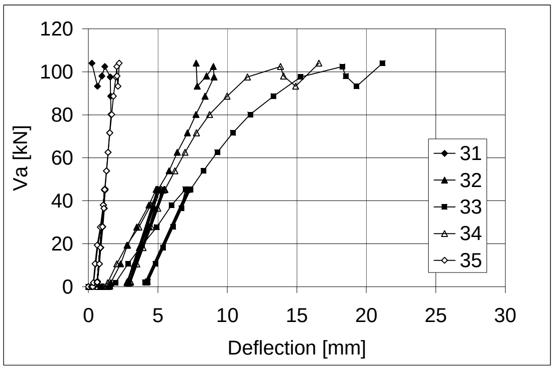

Fig. 38. Deflection on line V close to the line load, slabs 5–8.

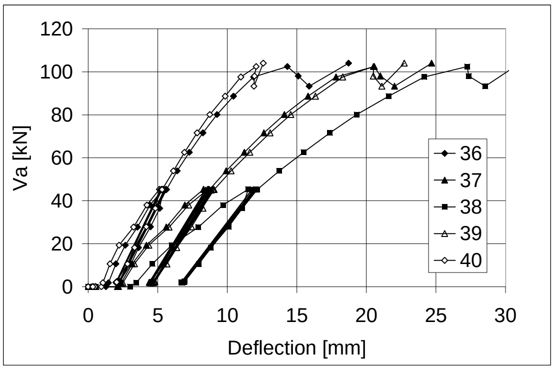

Fig. 39. Deflection on line VI in the middle of slabs 5–8.

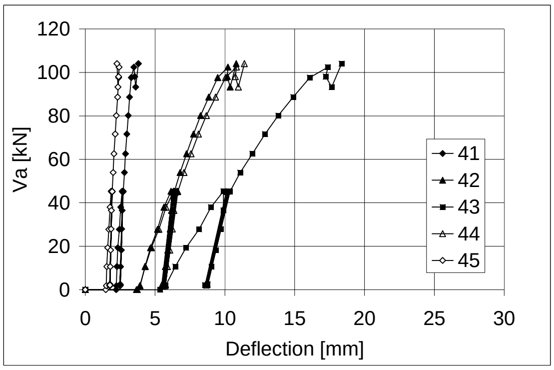

Fig. 40. Deflection on line VII along end beam, slabs 5–8.

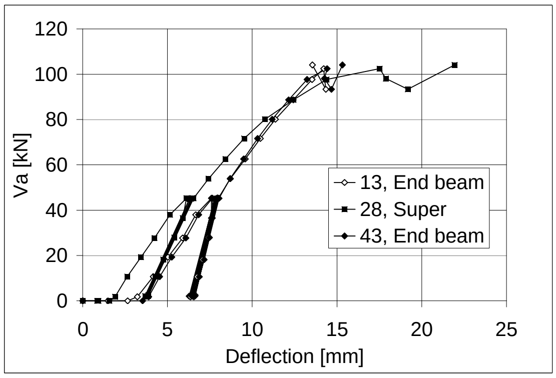

Fig. 41. Net deflection of midpoint of middle beam (28) and those of end beams (13, 43). (Settlement of supports eliminated.)

10.2
Crack width

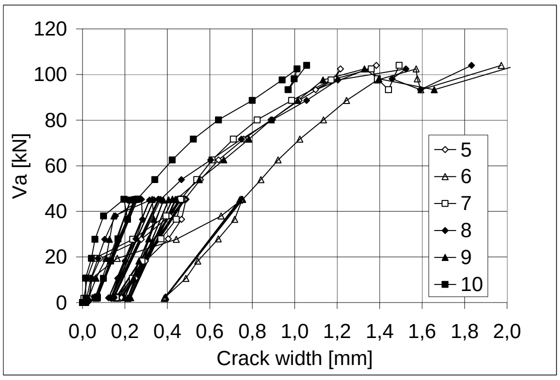

Fig. 42. Differential displacement (≈ crack width) measured by transducers 5–10.

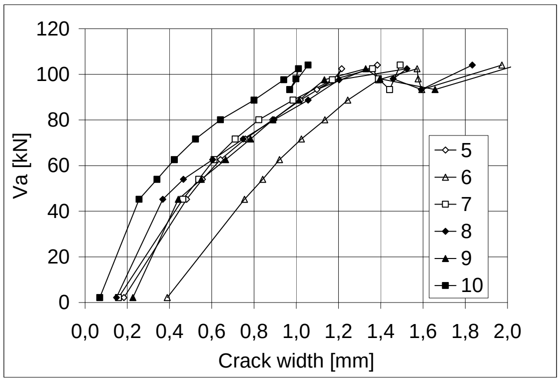

Fig. 43. Same as previous figure but the cyclic loading phase is not shown.

10.3
Average strain (actually differential displacement)

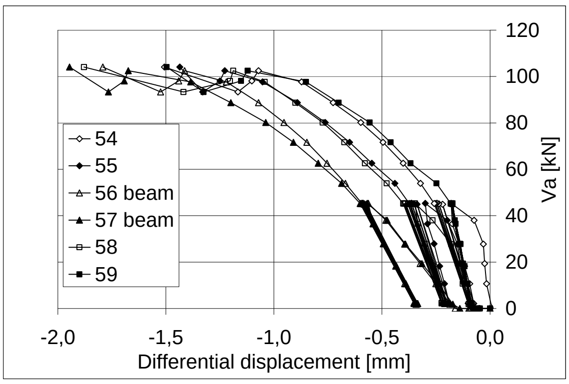

Fig. 44. Differential displacement at top surface of floor measured by transducers 54–59.

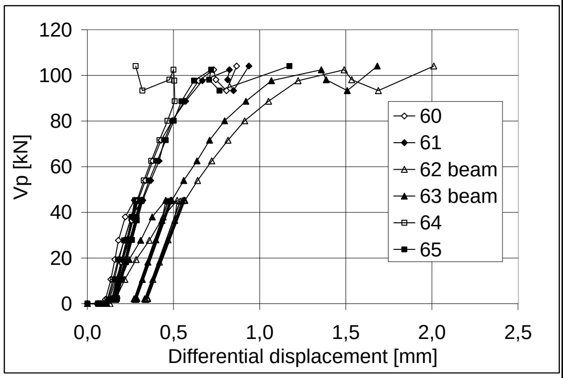

Fig. 45. Differential displacement at soffit measured by transducers 60–65.

10.4 Shear displacement

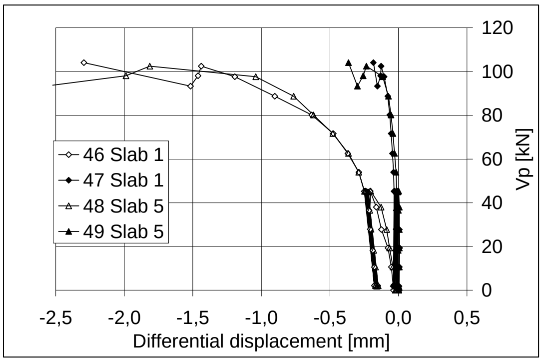

Fig. 46. Northern end of middle beam. Differential displacement between edge of slab and middle beam. A negative value means that the slab is moving towards the end of the beam.

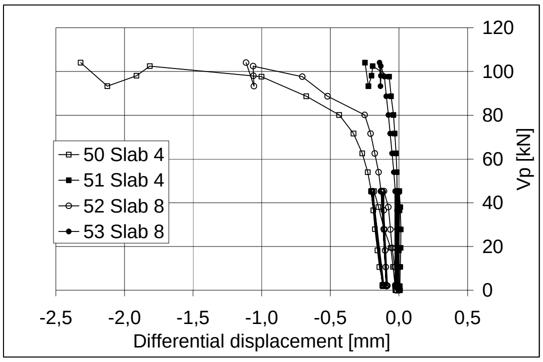

Fig. 47. Southern end of middle beam. Differential displacement between edge of slab and middle beam. A negative value means that the slab is moving towards the end of the beam.

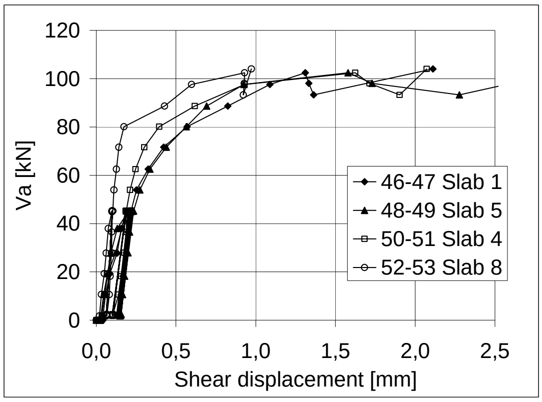

Fig. 48. Shear displacement = differential displacement at upper edge – differential displacement at lower edge of slab.

10.5 Strain

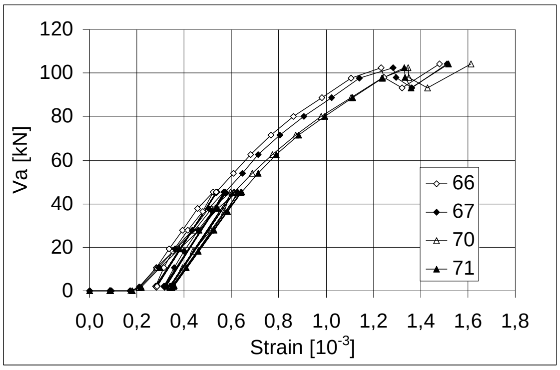

Fig. 49. Strain measured by gauges 66, 67, 70 and 71.

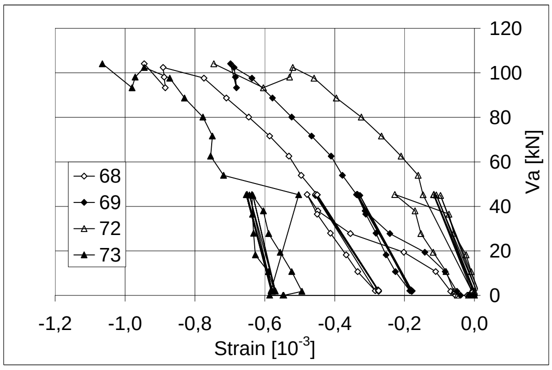

Fig. 50. Strain measured by gauges 68, 69, 72 and 73.

11	Reference tests

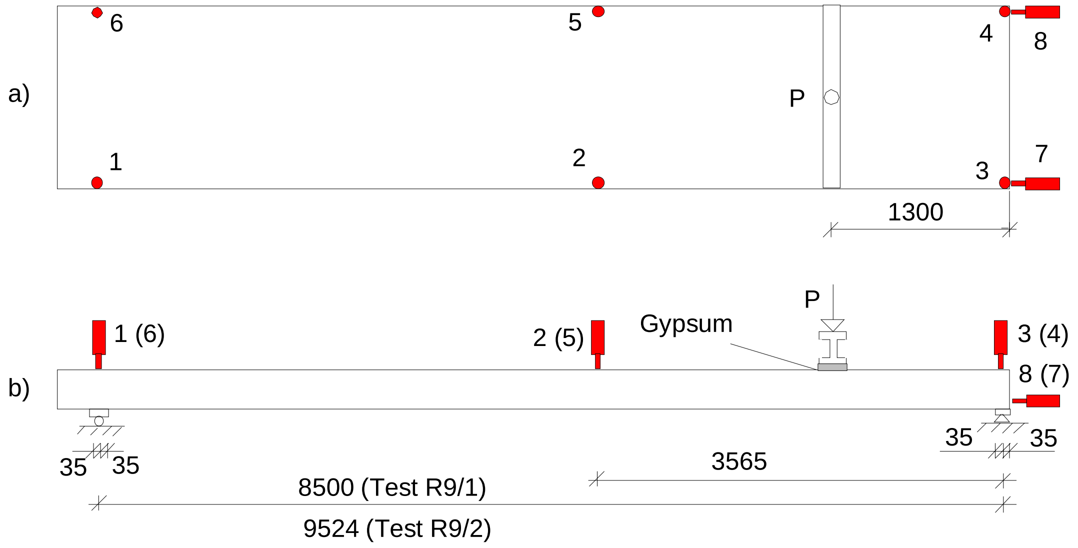

Fig. 51. Layout of reference test. a) Plan. b) Elevation. Test R9/2 was carried out first.

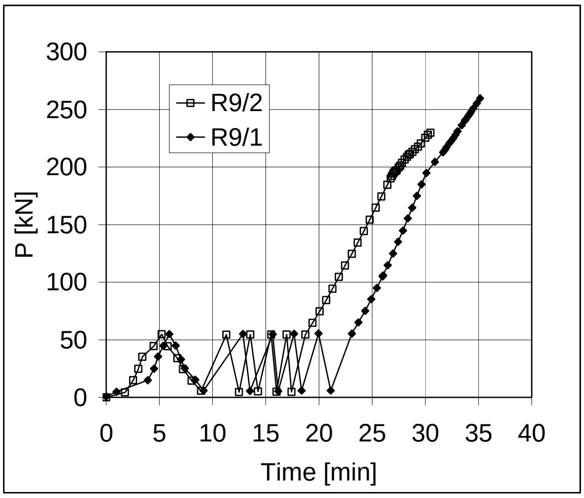

Fig. 52. Actuator force – time relationship.

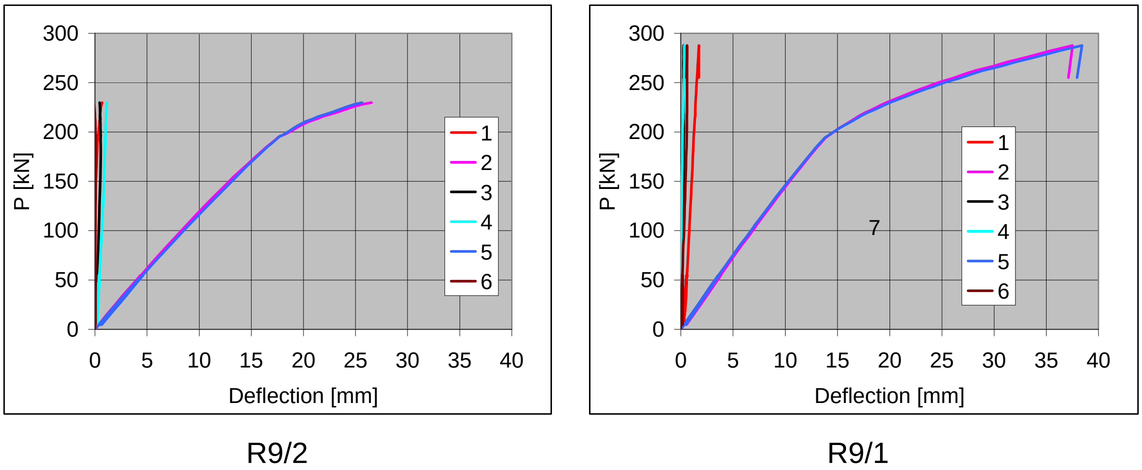

Fig. 53. Displacements measured by transducers 1–6. P is the actuator force.

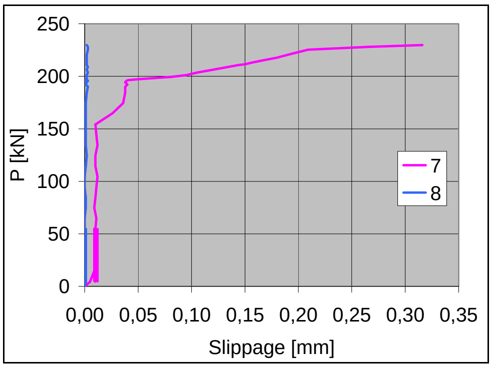

R9/2

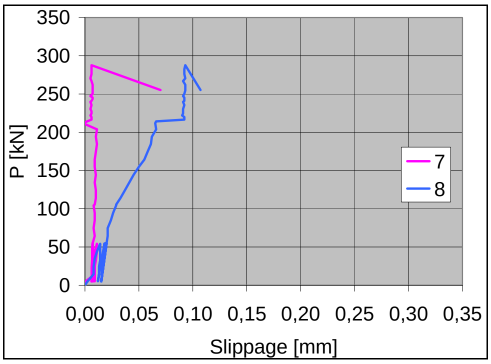

R9/1

Fig. 54. Slippage of outermost strands measured by transducers 7–8. P is the actuator force.

Table. Reference tests. Span of slab, shear force V_g at support due to the self weight of the slab, actuator force P_a at failure, weight of loading equipment P_{eq}, total shear force V_{obs} at failure and total shear force v_{obs} per unit width.

Test	Date	Span mm	V_g kN	P_a kN	P_{eq} kN	V_{obs} kN	v_{obs} kN/m	Note
R9/2	24.1.2002	9519	21,2	230,7	0,7	221,3	184,4	Web shear failure
R9/1	24.1.2002	8500	19,0	288,3	0,7	264,4	220,3	Flexural shear failure
					Mean	**242,8**	**202,4**	

12 Comparison: floor test vs. reference tests

The observed shear resistance (support reaction) of the hollow core slab in the floor test was equal to 127,5 kN per one slab unit or 106,3 kN/m. This is **53%** of the mean of the shear resistances observed in the reference tests.

13 Discussion

1. The net deflection of the middle beam due to the removed temporary supports and imposed actuator loads (deflection minus settlement of supports) was 17,5 mm or *L*/274, i.e. rather small. It was 3,1–3,3 mm greater than that of the end beams.
2. The net deflection of the middle beam due to the imposed actuator loads only (deflection minus settlement of supports) was 15,9 mm or *L*/300.
3. The shear resistance measured in the reference tests was 10% lower than the mean of the observed values for similar slabs given in *Pajari, M. Resistance of prestressed hollow core slab against web shear failure. VTT Research Notes 2292, Espoo 2005.*
4. The maximum difference in the net mid-point deflection of the beams was less than 3,3 mm. Hence, the torsional stresses due to the different deflection of the middle beam and end beams had a negligible effect on the failure of the slabs.
5. The bond between the cast-in-situ concrete and the edges of the hollow cores was weak.
6. The edge slabs slided 0,13 … 0,23 mm along the beam before failure. This reduced the negative effects of the transverse actions in the slab and had a positive effect on the shear resistance.
7. The transverse shear deformation of the edge slabs was considerable which can be seen in Figs 47–49.
8. The failure mode was web shear failure of edge slabs. The Super beam seemed to recover completely after the failure even though it obviously had cracked in flexure.

APPENDIX A: DETAILS OF SUPER BEAM

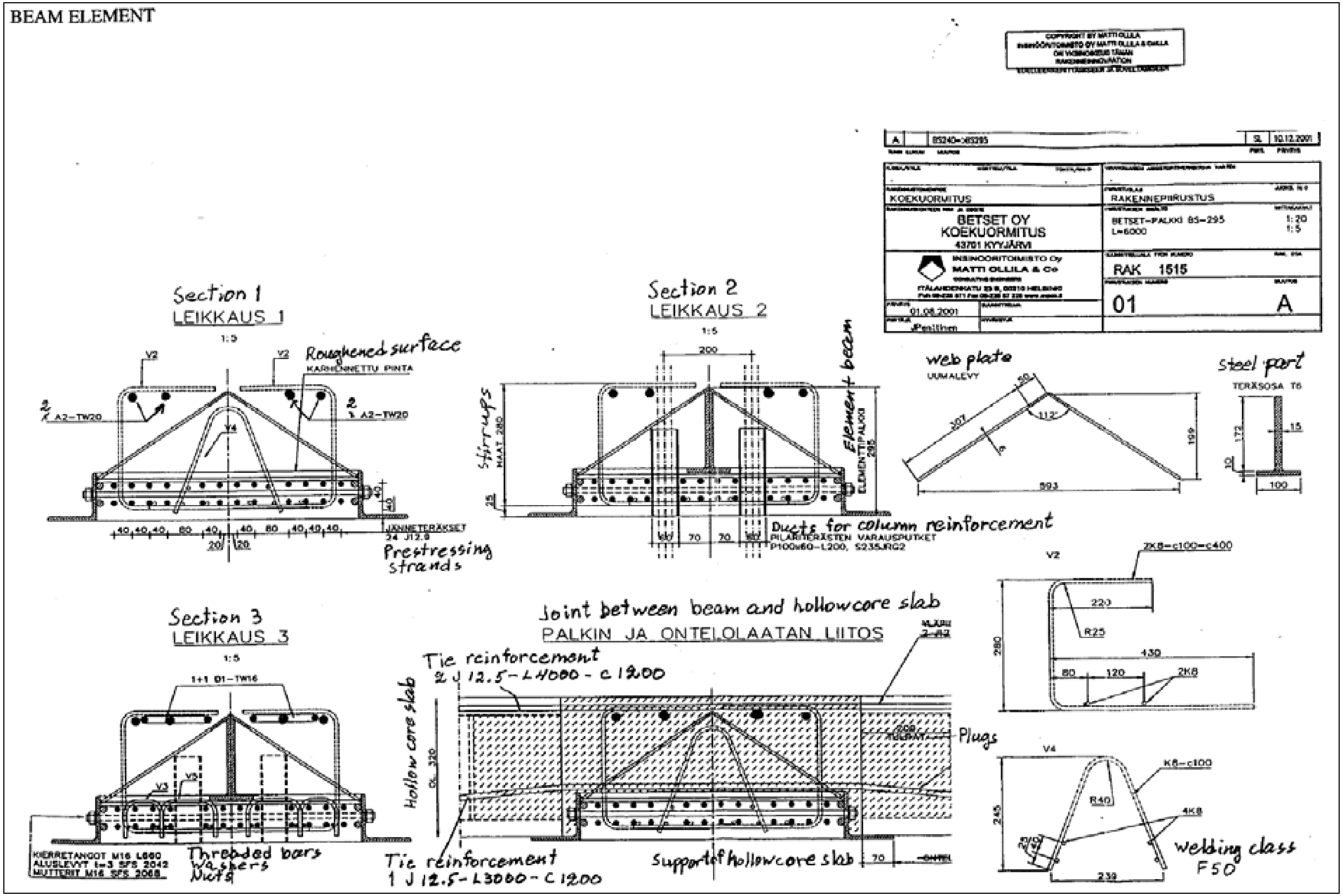

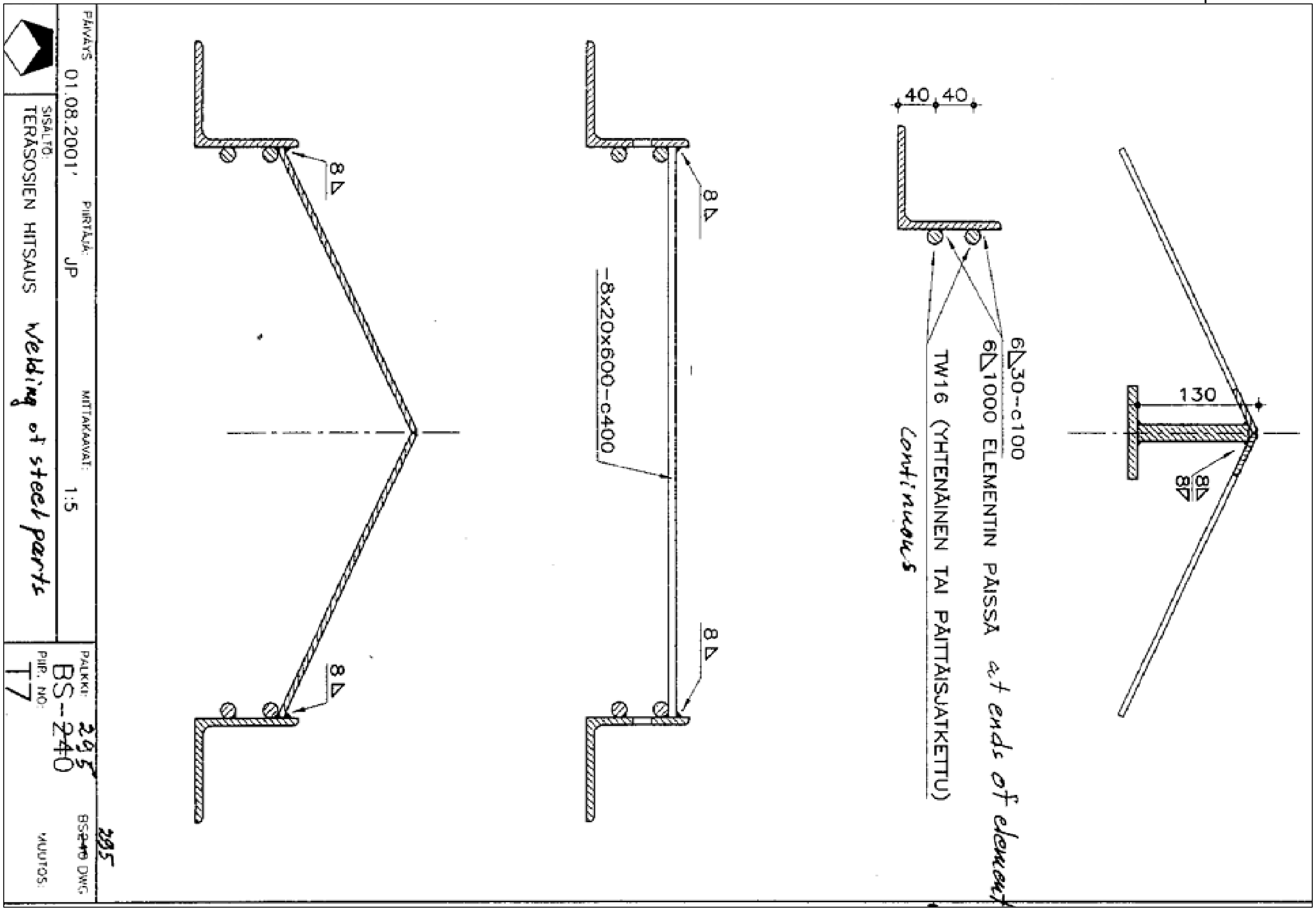
PÄIVÄYS
01.08.2001
SISÄLTÖ:
TERÄSOSIEN HITSAUS
Welding of steel parts
PIIRTÄJÄ:
JP
MITTAKAAVAT:
1:5
PALKKI:
BS-240
295
PIIR. NO:
T7
BS240 DWG
295
MUUTOS:
8
8
8
8
-8x20x600-c400
40
40
6△30-c100
6△1000 ELEMENTIN PÄISSÄ
at ends of element
TW16 (YHTENÄINEN TAI PÄITTÄISJATKETTU)
continuous
130
8
8

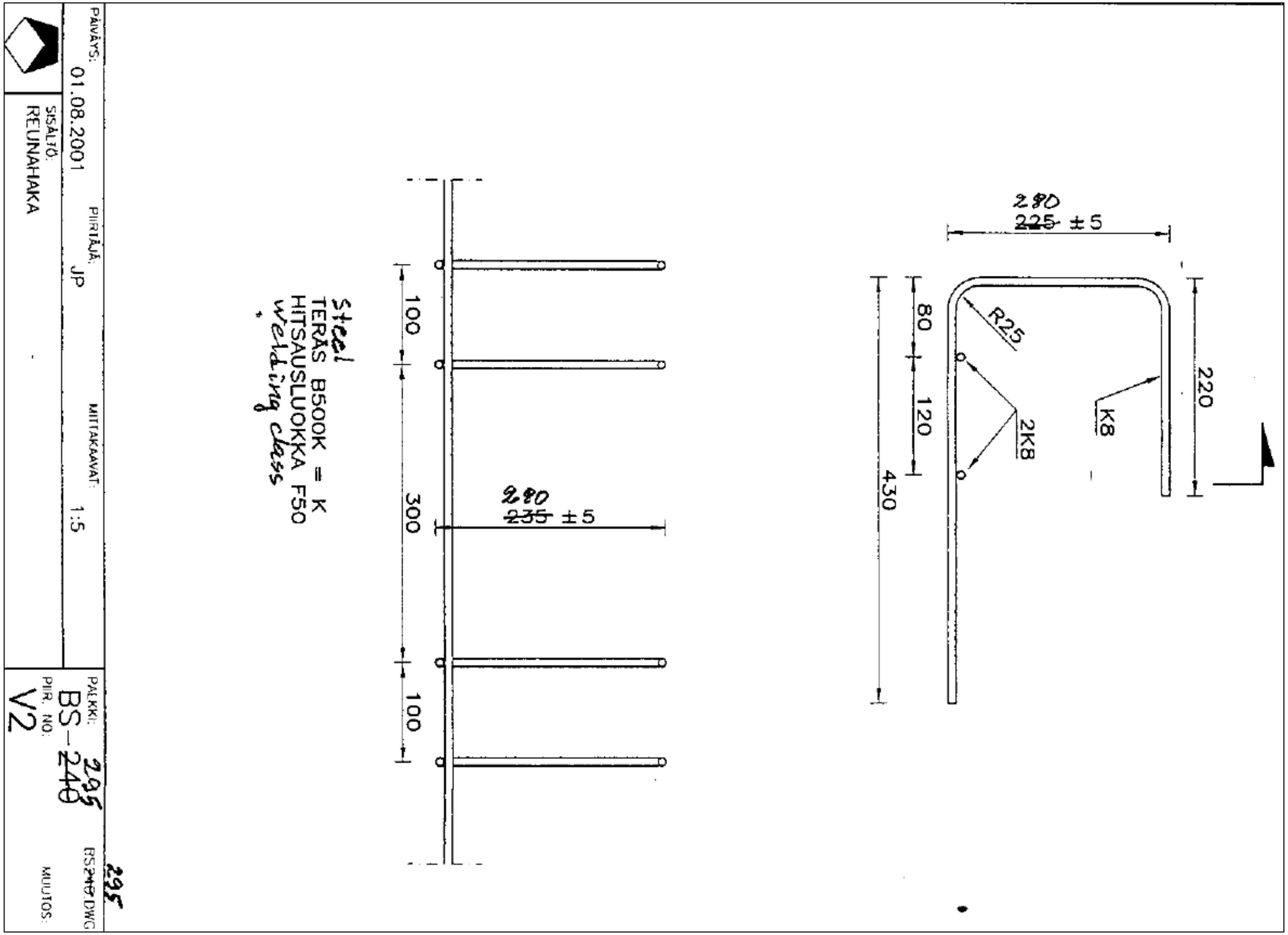
PÄIVÄYS:
01.08.2001
SISÄLTÖ:
REUNAHAKA
PIIRTÄJÄ:
JP
MITTAKAAVAT:
1:5
PALKKI:
BS-~~240~~ 295
PIIR. NO:
V2
BS~~240~~.DWG 295
MUUTOS:
steel
TERÄS B500K = K
HITSAUSLUOKKA F50
welding class
100
300
100
~~235~~ 280 ±5
~~225~~ 280 ±5
80
120
430
220
R25
2K8
K8

APPENDIX B: PHOTOGRAPHS

Fig. 1. Tie reinforcement at the edge of the floor.

Fig. 2. Overview on arrangements.

Fig. 3. Loading arrangements.

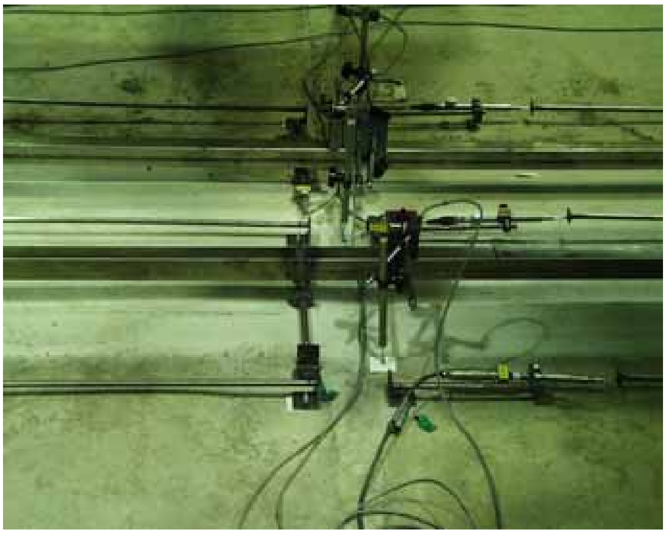

Fig. 4. Transducers measuring average strain in beam's direction.

Fig. 5. Arrangements at end beam.

Fig. 6. Transducers measuring sliding of slabs along middle beam.

Fig. 7. Arrangements for line loads.

Fig. 8. Failure of slab 5.

Fig. 9. Failure of slab 1.

Fig. 10. Diagonal crack in slab 8 after failure.

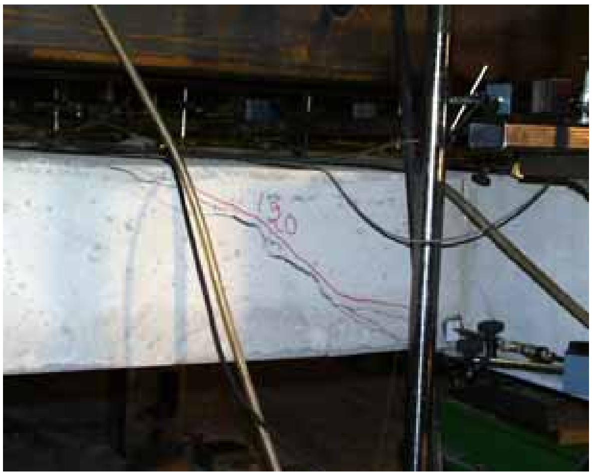

Fig. 11. Failure of slab 4.

Fig. 12. Vertical cracking of end beam between slabs 6 and 7.

Fig. 13. Wide crack along the western edge of middle beam next to slab 2.

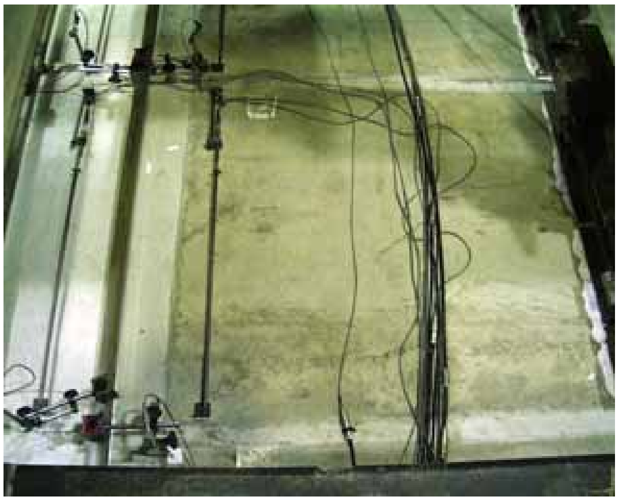

Fig. 14. Failure cracks in slab 2.

Fig. 15. Cracks in slab 4 after failure.

Fig. 16. Cracks in slabs 2–4 after failure.

Fig. 17. Cracks in slab 5 after failure.

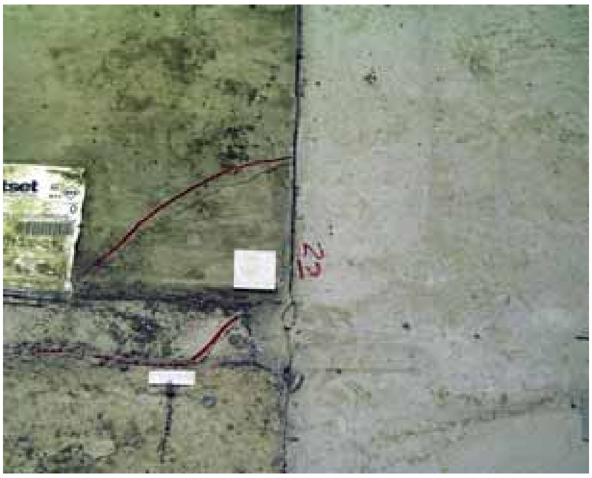

Fig. 18. Cracks in slab 1 after failure.

Fig. 19. Soffit of slabs 3 and 4 after failure.

Fig. 20. Soffit of slabs 1–2 after failure.

Fig. 21. *Failed ends of slabs 3–4 after failure.*

Fig. 22. Western side of middle beam. Note the bond failure along the vertical interface of the cast-in-situ concrete and the precast beam as well as the intact core fillings.

Fig. 23. Eastern side of middle beam after demolition.

Fig. 24. Western side of middle beam after demolition.

Fig. 25. Intact core fillings after failure. Note the geometric imperfections at the end.

Fig. 26. Web shear failure in reference test R9/2.

Fig. 27. Web shear failure in reference test R9/2.

Fig. 28. Flexural shear failure in reference test R9/1.

Fig. 29. Flexural shear failure in reference test R9/1.

1	**General information**
1.1 Identification and aim	**TUT.CP.LB.320.2002** **Last update 2.11.2010** LB320 (Internal identification) Aim of the test: To quantify the interaction between LB beam and hollow core slabs.
1.2 Test type	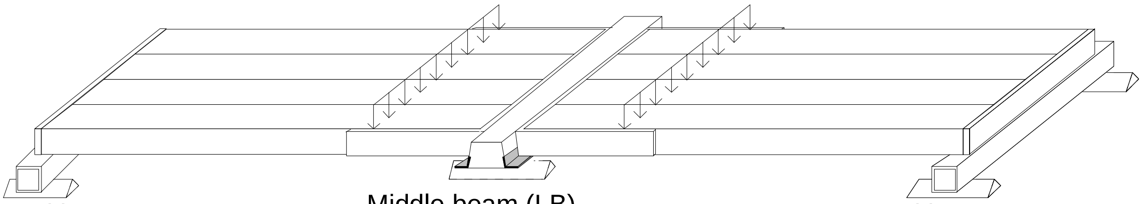 *Fig. 1. Overview on test arrangements. LB beam in the middle, steel beams (square tubes) at the ends.*
1.3 Laboratory & date of test	TUT/FI (Tampere University of Technology) 19.6.2002
1.4 Test report	Author(s): Suonio, M., Taskinen A. Name: *LUJABEAM-palkin (LB) laatastokoe (Test on hollow core floor with LUJABEAM (LB), in Finnish)* Ref. number: - Date: 28.8.2002 Availability: Confidential, owner is Lujabetoni Oy Harjamäentie 1 FI-71800 Siilinjärvi Finland
2	**Test specimen and loading** (see also Appendices A)

2.1
General plan

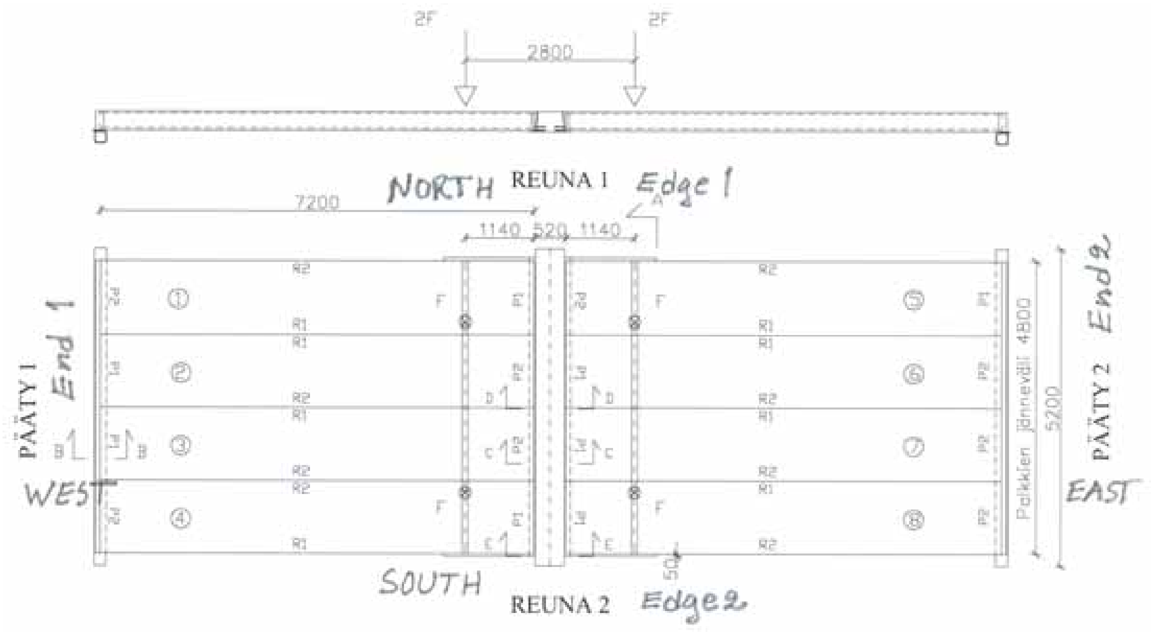

Fig. 2. Plan. Span of beams 4,8 m.

2.2
End beams

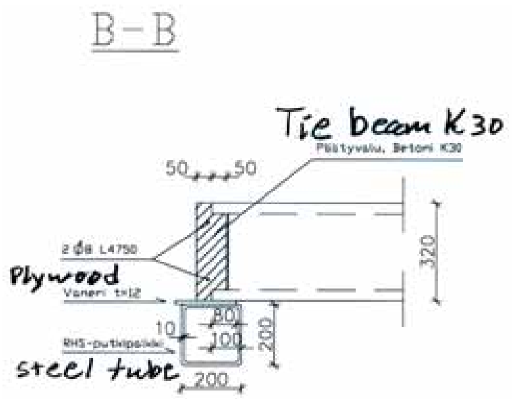

Fig. 3. Arrangements at end beam. ϕ8 refers to a reinforcing bar T8, see 2.3.

2.3
Middle beam

The beam, see Figs 4–7, comprised a precast and prestressed concrete component provided with shear keys and two L-shaped steel ledges.

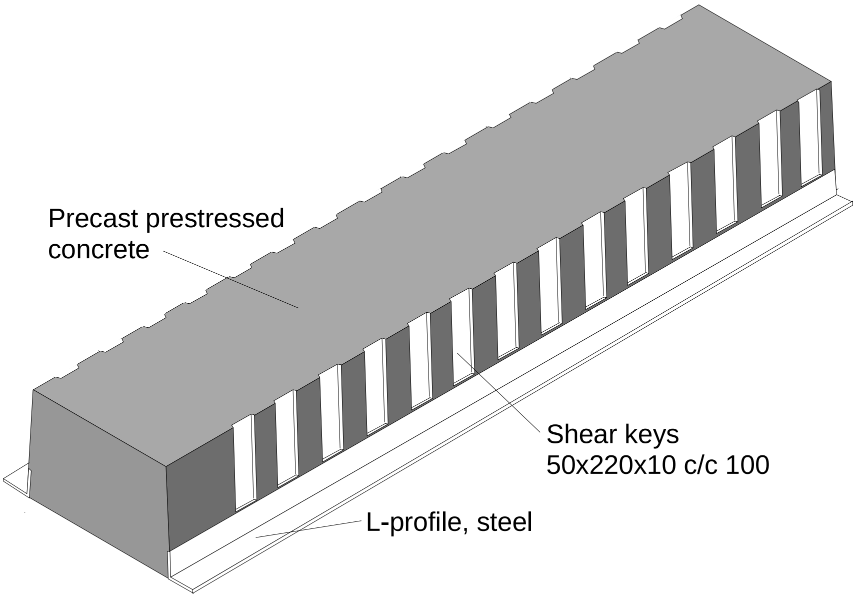

Fig. 4. Illustration of LB beam.

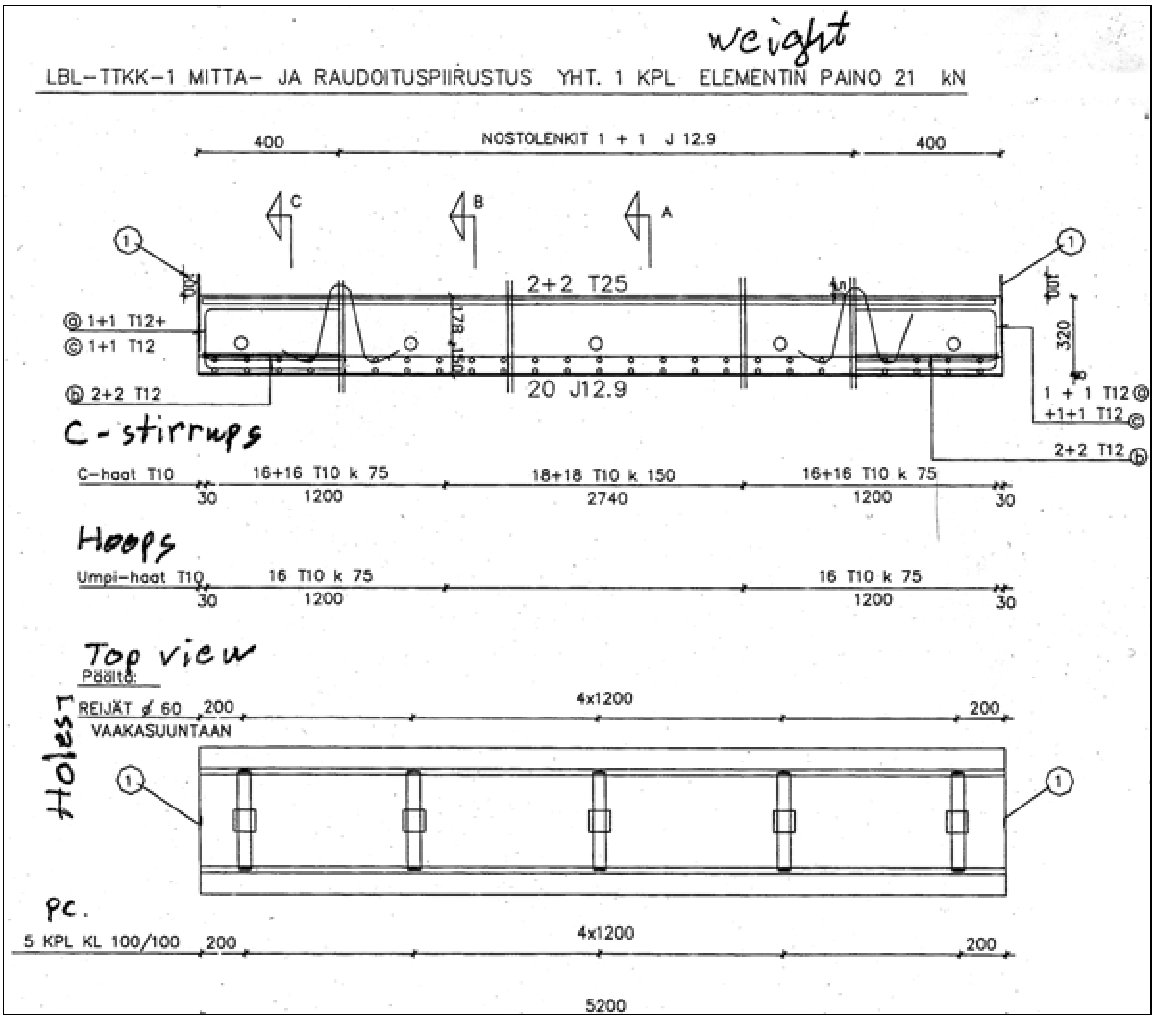

Fig. 5. Design of LB beam. Txy refers to reinforcing bar A500HW with diameter xy, see 2.3.

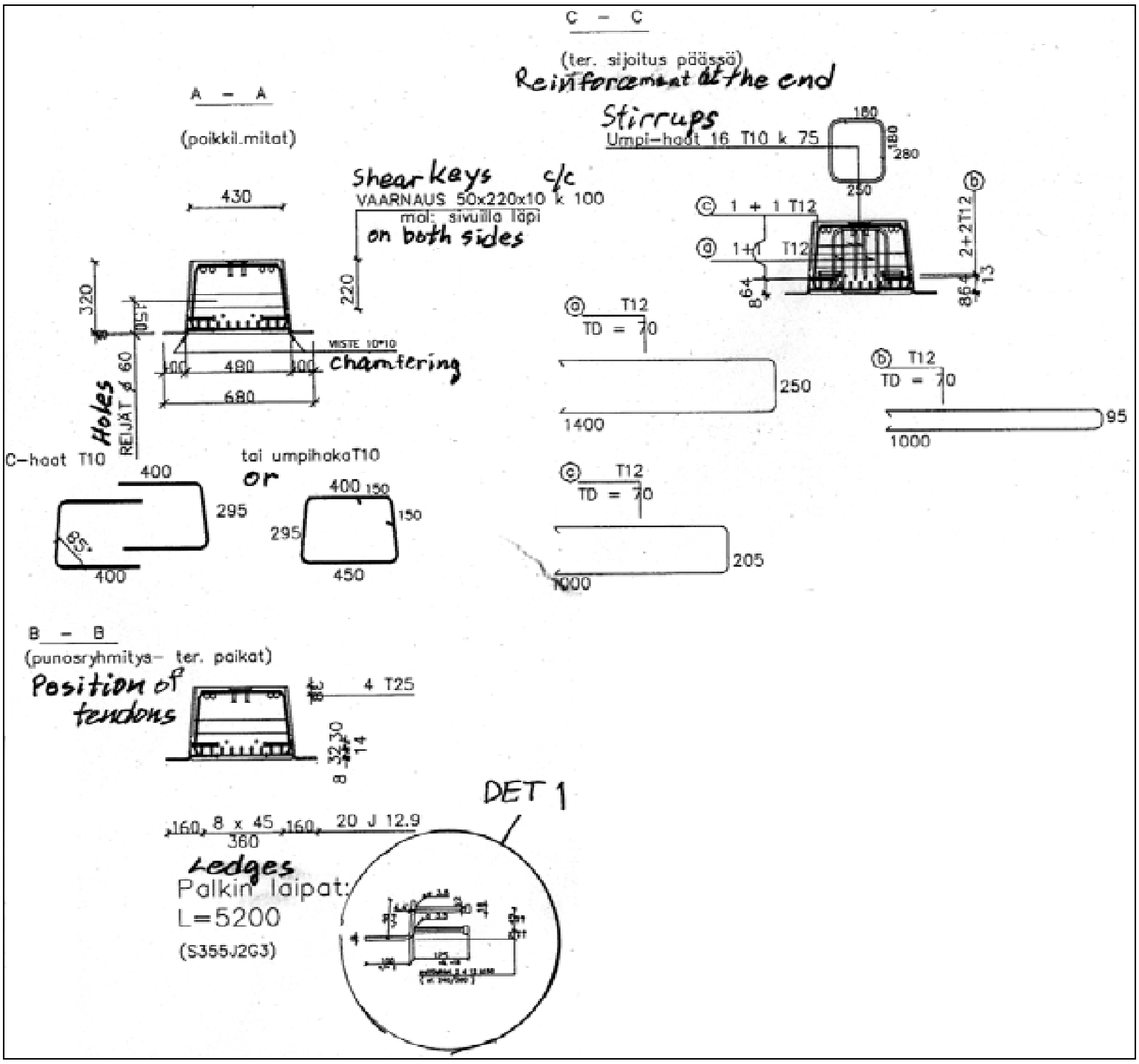

Fig. 6. Sections A-A, B-B and C-C. Txy refers to reinforcing bar A500HW, see 2.3.

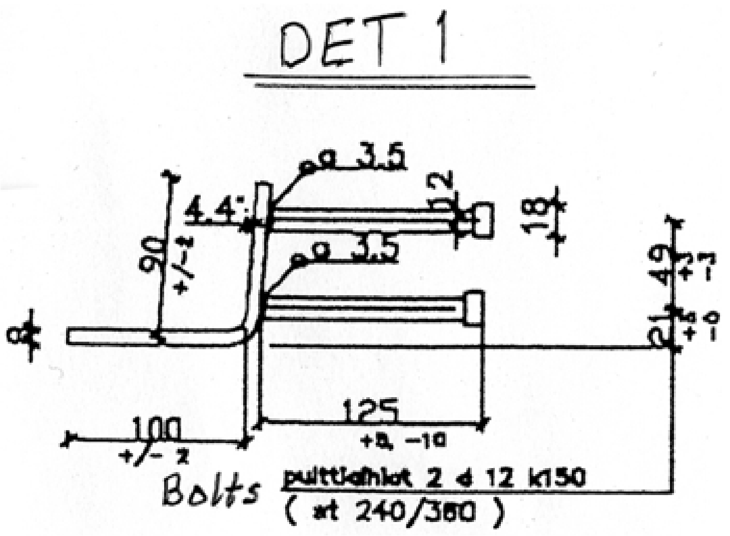

Fig. 7. Detail 1. Design of ledges.

	The prestressed part was cast by Lujabetoni Oy in their Siilinjärvi factory 25.4.2002 **Concrete**: K80, max aggregate size 16 mm, rapidly hardening cement **Passive reinforcement and tendons in LBL beam:** **Txy**: Hot rolled, weldable rebar A500HW, ϕ = xy mm **J12,9**: Prestressing strand, 7 wires, ϕ =12,9 mm, A_p = 100 mm^2, prestress = 1250 MPa, low relaxation (nominal value 2,5% at $\sigma = 0{,}7f_{pu}$) **Structural steel:** S355J2G3, $f_y \approx$ 355 MPa (nominal value) unless otherwise specified
2.4 Arrangements at middle beam	- Simply supported, span = 4,8 m 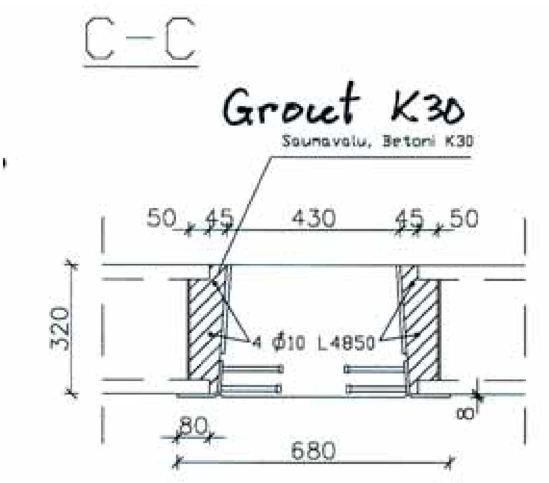 *Fig. 8. Section along hollow cores, see Fig. 2.* 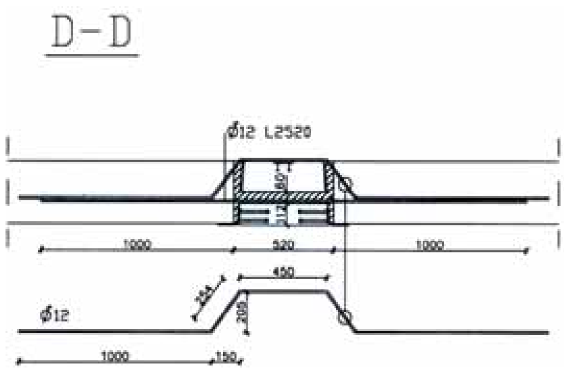 *Fig. 9. Section along joint between adjacent slab units, see Fig. 2. The rebars are made of A500 HW.* 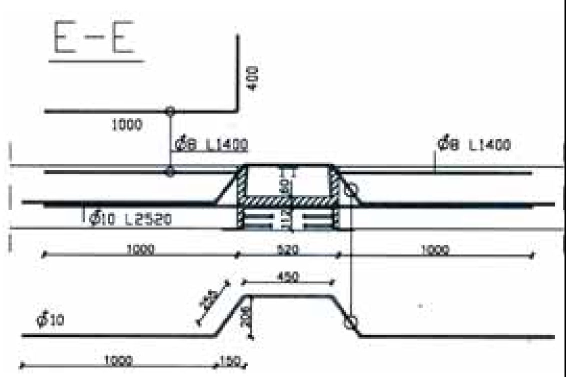 *Fig. 10. Section along outer edge of floor specimen, see Fig. 2. The rebars are made of A500 HW.*

<table>
<tr>
<td>2.5
Slabs</td>
<td>
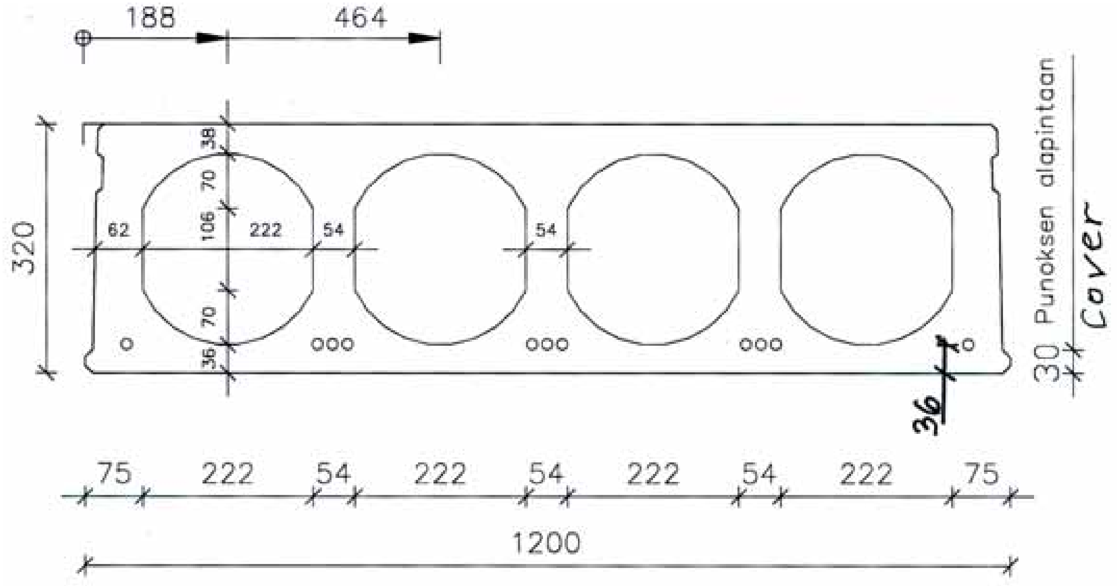

Fig. 11. Nominal geometry of slab units (in scale).

- Extruded by Lujabetoni Oy, Siilinjärvi factory, date not given in the report
- 11 lower strands J12,5 initial prestress 1100 MPa

J12,5: seven indented wires, ϕ =12,5 mm, A_p = 93 mm^2

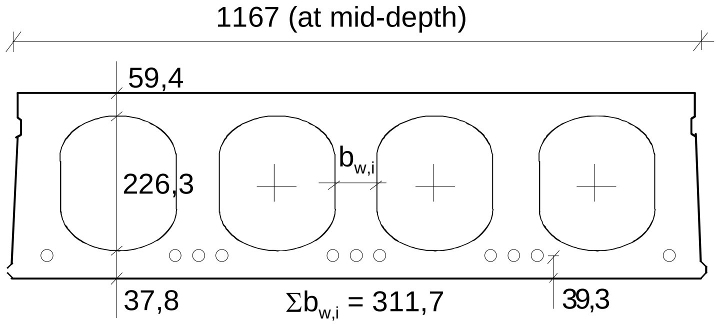

Max measured bond slips: 1,9 mm in slab unit 4, 1,8 mm in slab units 1 and 6, 1,7 in slab units 4, 5, 8 and 2 x 1,7 in slab unit 6

Measured weight of slab units = 5,33 kN/m

Fig. 12. Mean of most relevant measured geometrical characteristics.
</td>
</tr>
<tr>
<td>2.6
Temporary supports</td>
<td>There were no temporary supports below beams.</td>
</tr>
</table>

2.7 Loading arrangements	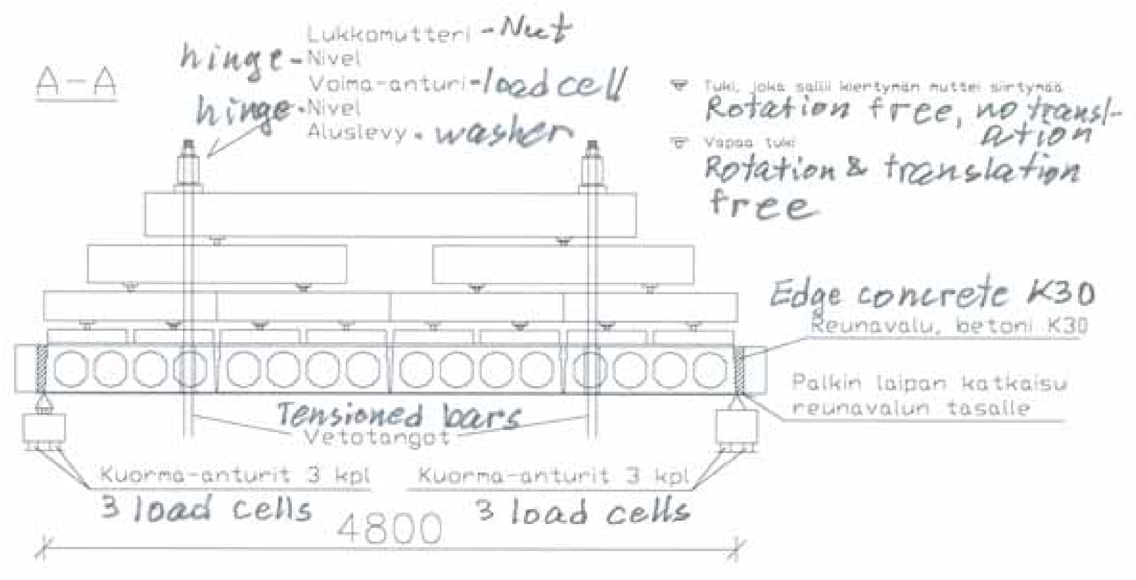 *Fig. 13. Section A-A in Fig. 2. Palkin laipan katkaisu reunavalun tasalle = the ledge of the beam was cut along the edge concrete.*
3	**Measurements**
3.1 Support reactions	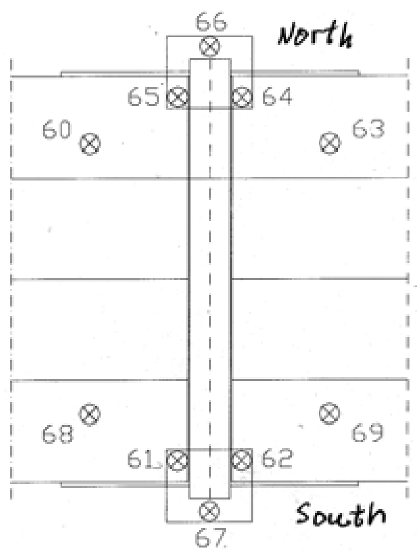 *Fig. 14. Load cells 60, 63, 68 and 69 measuring the force in the tension bars, see also Fig.13. Load cells 61, 62, 67 and 64–66 below the supports of the LB beam.*

<table>
<tr>
<td>3.2
Vertical displacement</td>
<td>
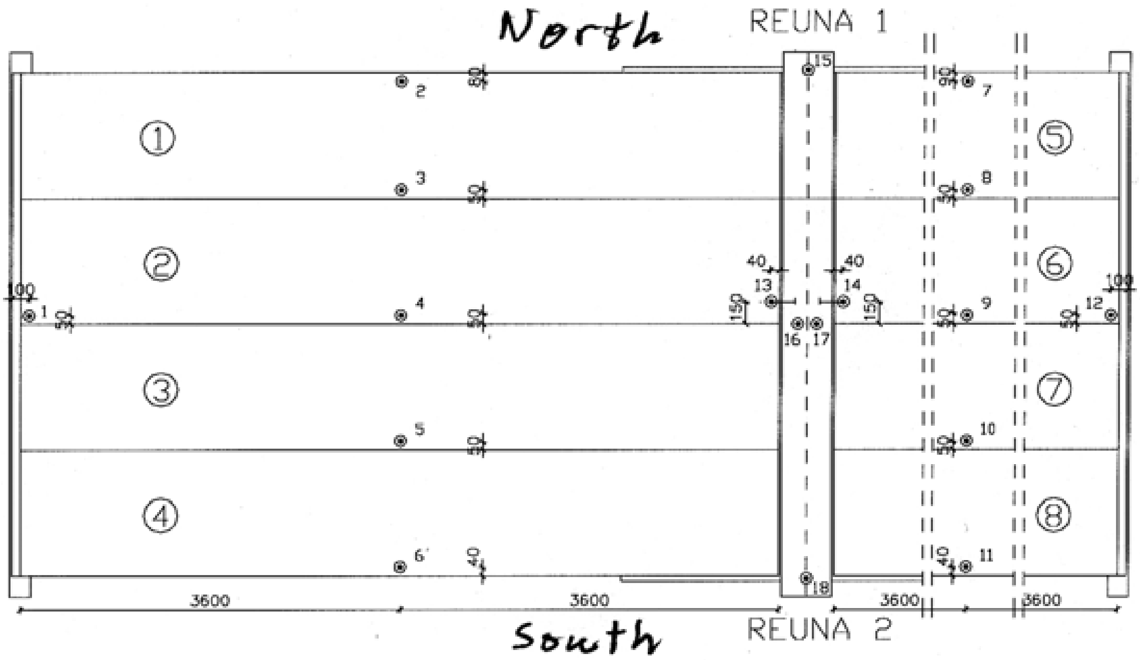

Fig. 15. Location of transducers 1–18 for measuring vertical deflection of floor.
</td>
</tr>
<tr>
<td>3.3
Average strain in mid-span and crack width along edges of middle beam</td>
<td>
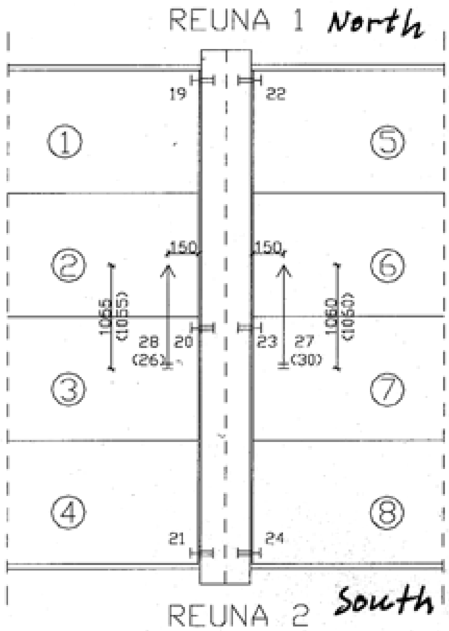

Fig. 16. Position of device (transducers 26, 27, 28 and 30) measuring average strain parallel to the beams. Numbers in parentheses refer to the soffit of the floor, others to the top. Position of transducers 19–24 for measuring crack width between LB beam and ends of hollow core slabs.
</td>
</tr>
</table>

3.4 Horizontal. displacements	*See 3.3*
3.5 Strain	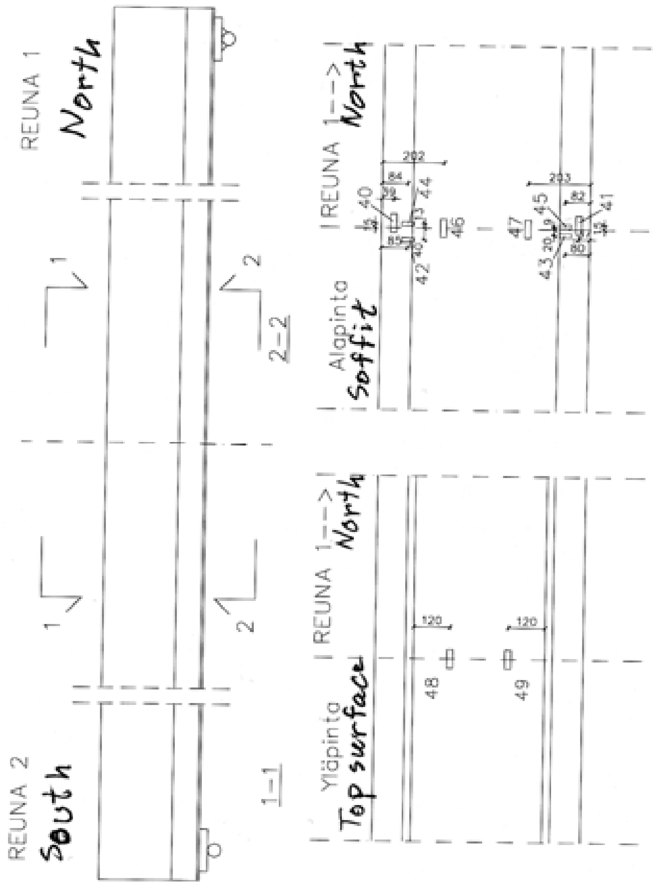 *Fig. 17. Strain gauges 40, 41, 46–49 measuring longitudinal strain of beam and strain gauges 42–45 measuring transverse strain of ledges.*
4	**Special arrangements** On top of the end beams shims were placed to simulate the camber of the middle beam in such a way that when the hollow core slabs were installed, all corners of the end beams touched the supporting beams. All cast-in-situ concrete (K30, max aggregate size 8 mm) was taken from the same batch. The date of casting was 4.6.2002. The ledges of the LB.beam were flame-cut along the outer edges of the outermost hollow core slabs and holes for the tension bars were drilled through the hollow cores.

5 Loading strategy

5.1
Load-time relationship

Date of the floor test was 19.6.2002.

Before starting, all measuring devices were zero-balanced. The loading history is shown in Fig. 18.

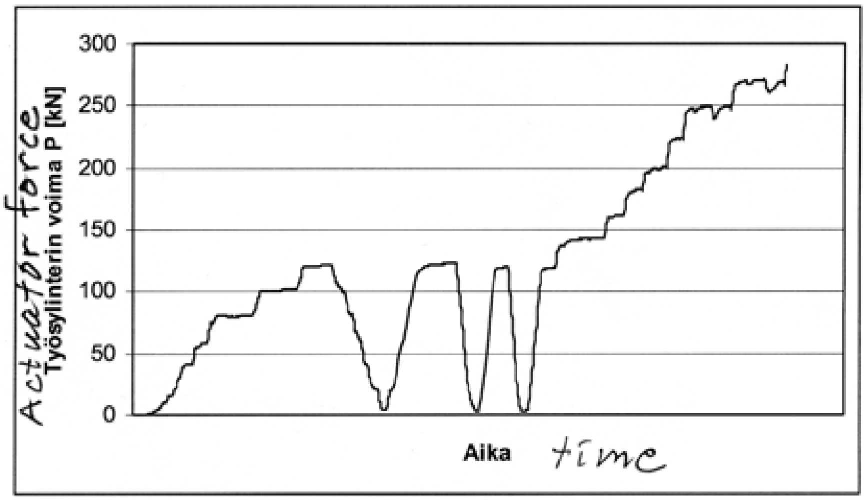

Fig. 18. Actuator force P vs. time.

6 Observations during loading

In the figures below, *P* refers to the force in the hydraulic actuators.

Stage I (Cyclic)	At *P* = 75 kN the joint concrete between the middle beam and the slab units started to crack along the slab ends, and at *P* = 80 kN there was a continuous crack in the joint concrete on both sides of the beam along the whole length of the beam. At *P* = 100 kN the cast-in-situ concrete cracked along the outer edge of slabs 1 and 5 and along the edge of slab 8. At *P* = 120 kN first vertical cracks were observed in the tie beams above the end beams of the test specimens.
Stage II (Monotonous)	At *P* = 140 kN the cast-in-situ concrete (edge concrete) cracked along the outer edge of slab 8. At *P* = 240 kN the joint concrete cracked along the edges of the middle beam in the mid-span of the beam. At *P* = 260 kN a longitudinal crack was observed in slab 4, see Fig. 20. At *P* = 283,4 a web shear failure took place in slab 8. The cracking pattern after failure is shown in Figs 20–21 (top surface and edges) and in Fig. 19 (soffit after failure).
After failure	See App. A, Figs 3–7. LB beam seemed intact after demolishing the slabs.

7	**Cracks in concrete**
7.1 Cracks at service load	See Fig. 20
7.2 Cracks after failure	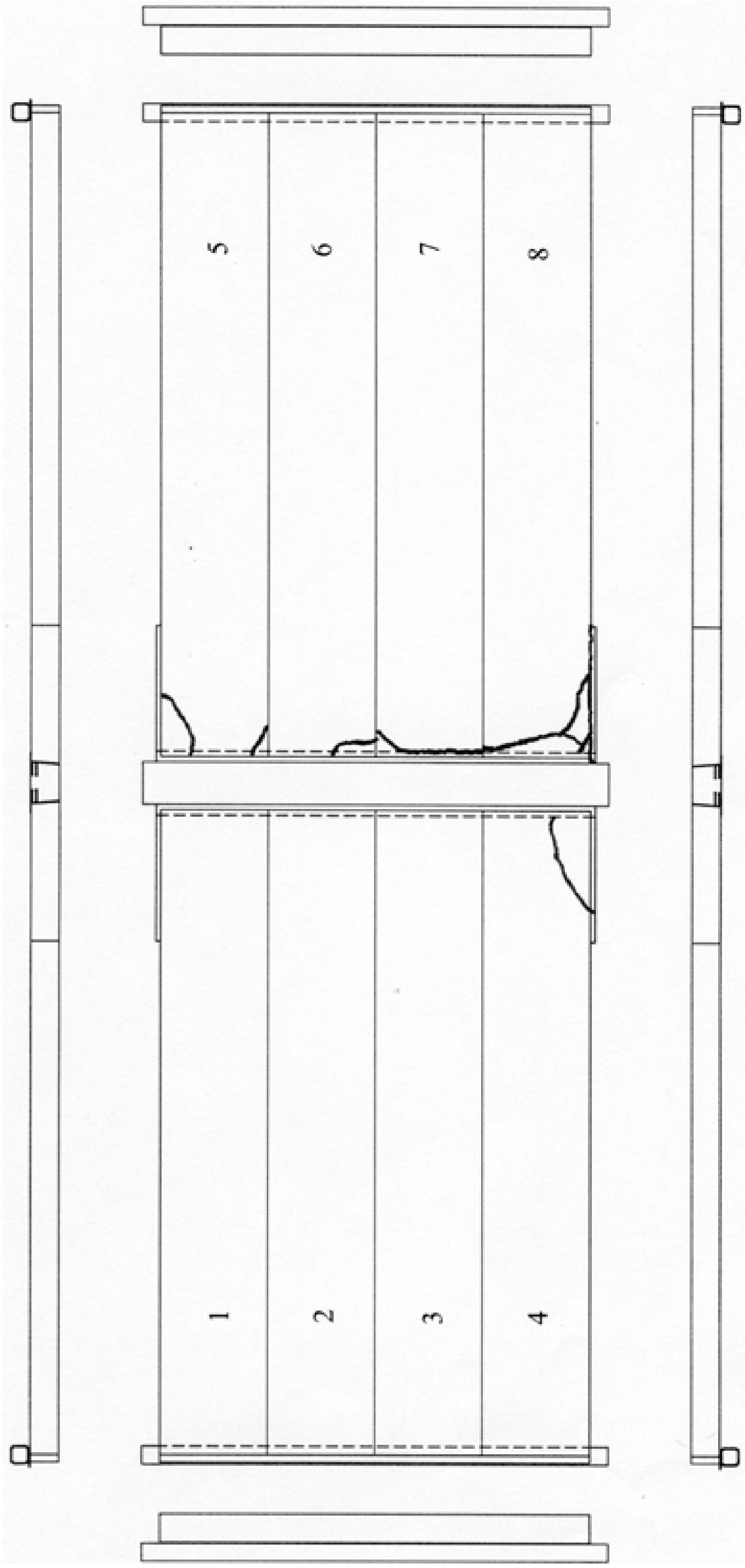 *Fig. 19. Cracks in the soffit after failure.*

	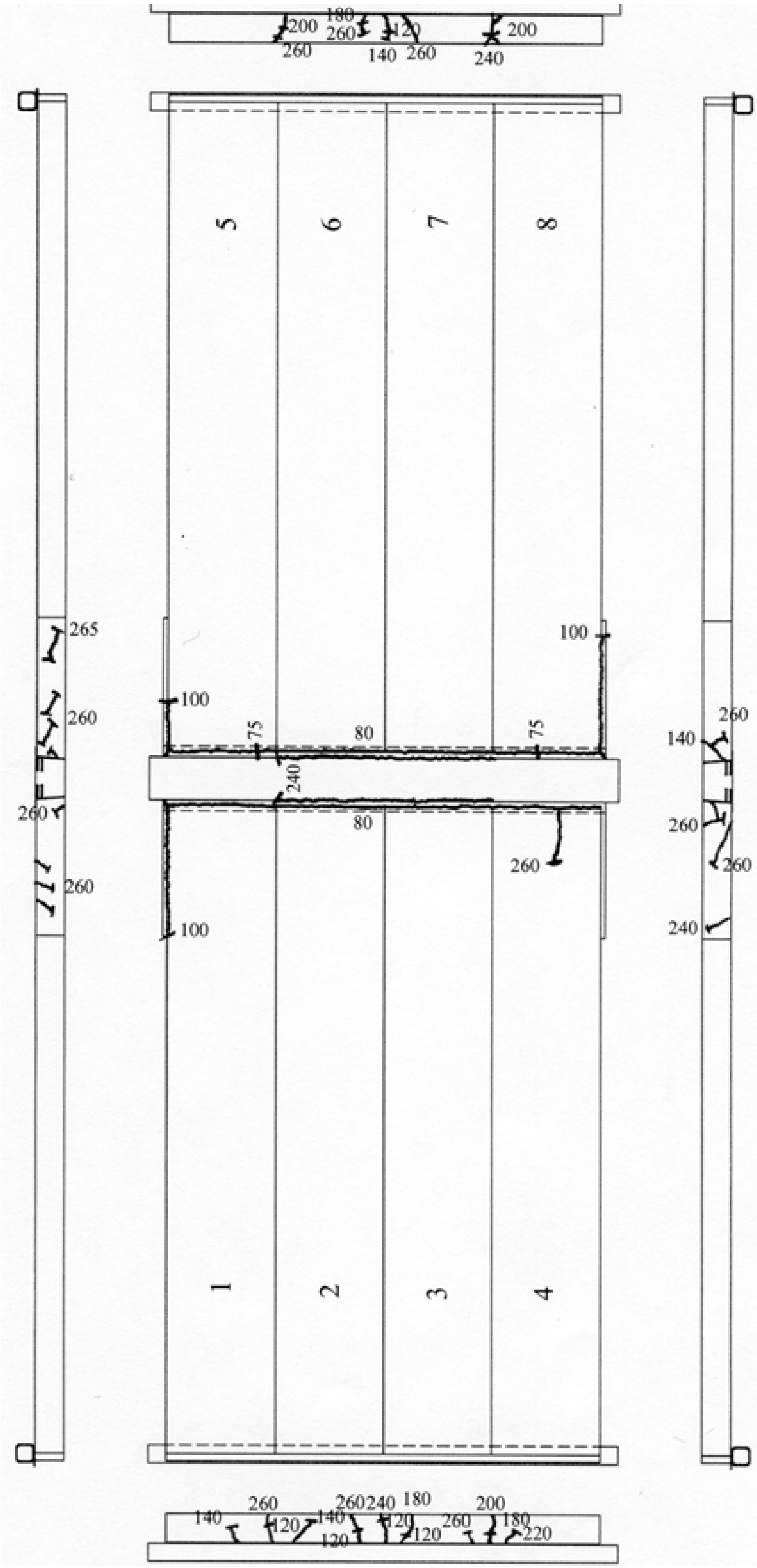 *Fig. 20. Cracks on the top and at the edges of the floor at load P = 260 kN. The numbers give the value of actuator load P when the crack appeared.*

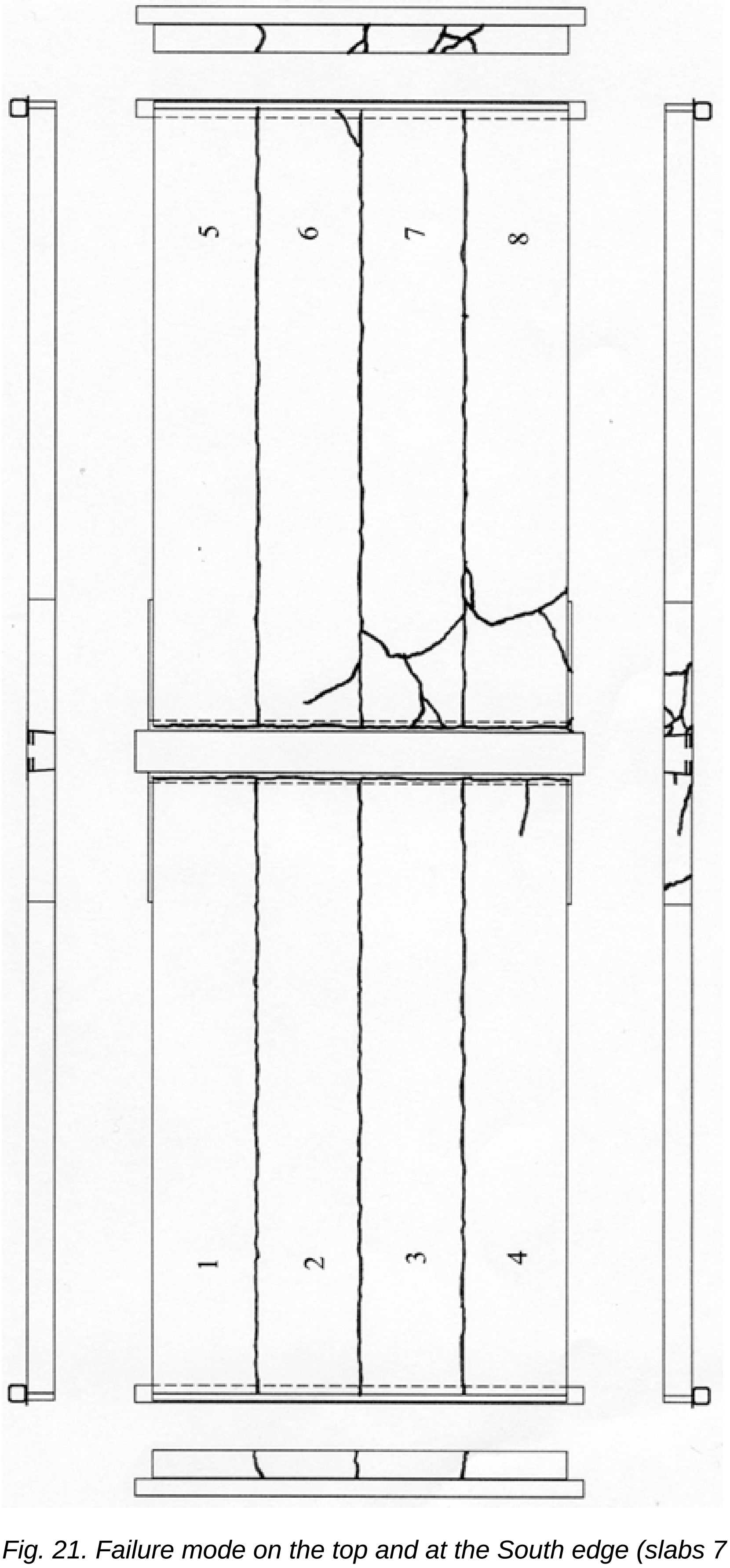

Fig. 21. Failure mode on the top and at the South edge (slabs 7 and 8).

8	**Observed shear resistance**

The ratio (measured support reaction below one end of the middle beam)/ (load due to actuator forces on half floor) is shown in Fig. 22 and the ratio (measured support reaction below one end of the middle beam) / (theoretical support reaction due to actuator forces on half floor) in Fig. 23. The theoretical reaction is calculated assuming simply supported slabs, which means that the support reaction force is 84,2% of 2*P*. The measured shear force is 89,4% of 2*P* before failure. This comparison shows that the support reaction due to the actuator forces cannot be calculated accurately enough assuming simply supported slabs.

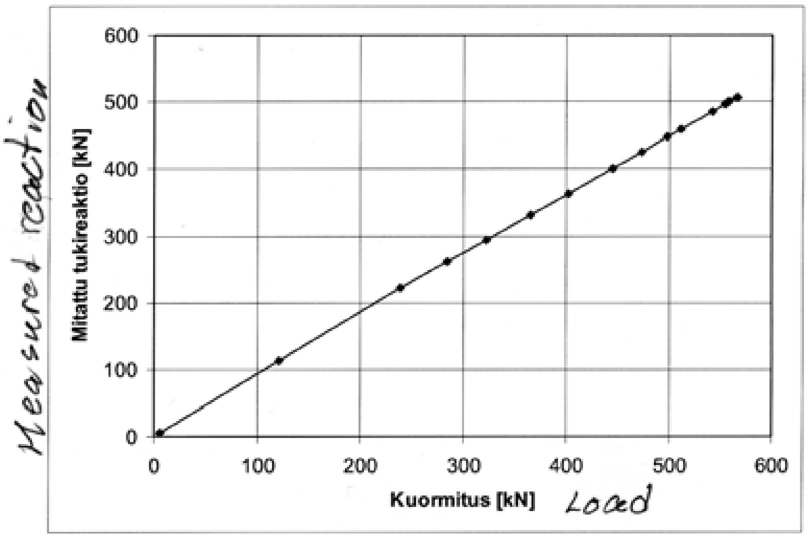

Fig. 22. Measured support reaction of the middle beam vs. actuator forces 2P. Only actuator loads are taken into account in the support reaction.

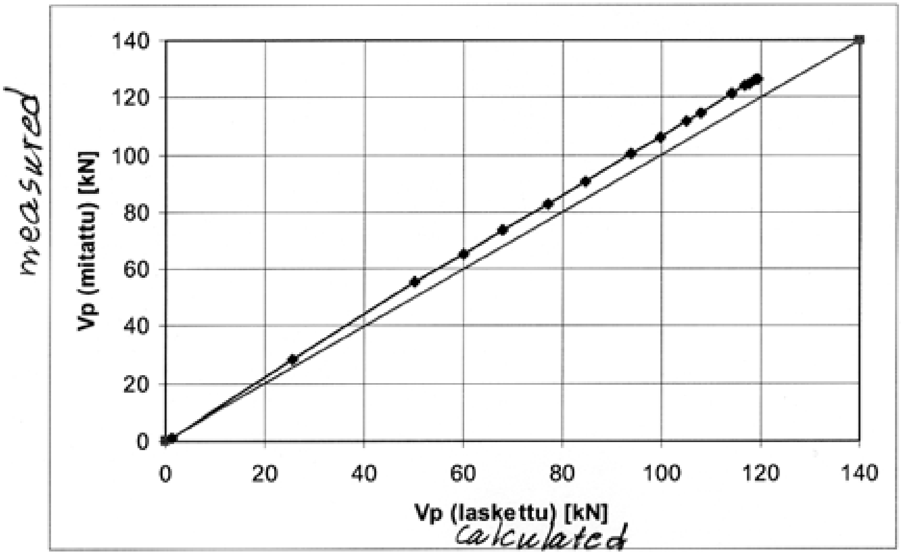

Fig. 23. Measured support reaction of one slab vs. theoretical support reaction due to actuator forces.

The shear resistance of one slab end (support reaction of slab end at failure) due to different load components is given by

$$V_{obs} = V_{g,sl} + V_{g,jc} + V_{eq} + V_P$$

where $V_{g,sl}$, $V_{g,jc}$, V_{eq} and V_P are shear forces due to the self-weight of slab unit, weight of joint concrete, weight of loading equipment and actuator forces P, respectively.

V_P is calculated from the measured support reactions below the middle beam. $V_{g,sl}$ and $V_{g,jc}$ are calculated assuming that the slabs behave as simply supported beams, but V_{eq} is obtained from $V_{eq} = 0{,}8938 \times F_{eq}$ because the measured support proved to be 89,38% of the imposed line load on one slab unit. The values for the components of the shear force are given in Table below.

Table 1. Components of shear resistance due to different loads.

Action	Load	Shear force kN
Weight of slab unit		18,9
Weight of joint concrete		0,8
Loading equipment		2,8
Actuator loads	(283,4)/2 kN	126,7

The observed shear resistance $\boldsymbol{V_{obs}}$ **= 149,2 kN** (shear force at support) is obtained for one slab unit with width = 1,2 m. The shear force per unit width is $\boldsymbol{v_{obs}}$ **= 124,3 kN/m**

9 **Material properties**

9.1
Strength of steel

Component	$R_{eH}/R_{p0,2}$ MPa	R_m MPa	Note
L-profiles	≈ 355		Nominal (S355J2G3C)
Slab strands J12,5	1570	1770	Nominal (no yielding in test)
Beam strands J12,9	1630	1860	Nominal (no yielding in test)
Reinforcement A500HW (Txy)	500		Nominal value for reinforcing bars (no yielding in test)

9.2
Strength of slab concrete, floor test

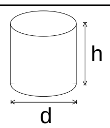

#	Cores		*h* mm	*d* mm	Date of test	Note
6			50	50	? 2)	Upper flange of slab 8, vertically drilled Tested as drilled2)
Mean strength [MPa]			65,7			
St.deviation [MPa]			6,48			

9.3
Strength of slab concrete, reference tests

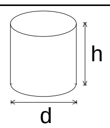

#	Cores		*h* mm	*d* mm	Date of test	Note
3			50	50	? 2)	Upper flange of slab, vertically drilled Tested as drilled2)
Mean strength [MPa]			72,9			
St.deviation [MPa]			-			

9.4
Strength of grout in joints

#	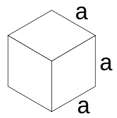	*a* mm	Date of test	Note
6		150	19.6.2002 (+0 d)[1)]	Kept in laboratory in the same conditions as the floor specimen
Mean strength [MPa]		36,2		
St.deviation [MPa]		0,26		

9.5
Strength of concrete in middle beam

#	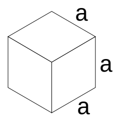	*a* mm	Date of test	Note
6		100	19.6.2002 (+0 d)[1)]	Kept in laboratory in the same conditions as the floor specimen
Mean strength [MPa]		90,1		
St.deviation [MPa]		2,85		

[1)] Date of material test minus date of structural test (floor test or reference test)
[2)] Date is not given in the report, but it is very likely 19.–22.6.2002

10
Measured displacements

In the following figures, *P* stands for the actuator load.

10.1
Deflections

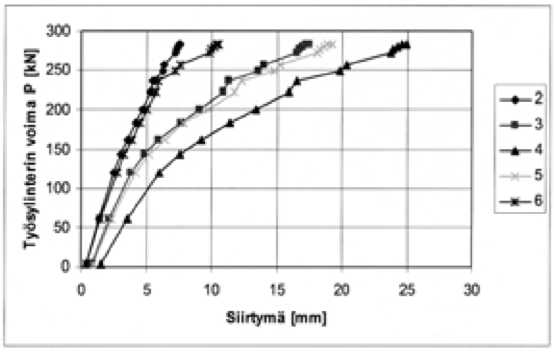

Fig. 24. Deflection in mid-span of slabs 1–4 measured by transducers 2–6.

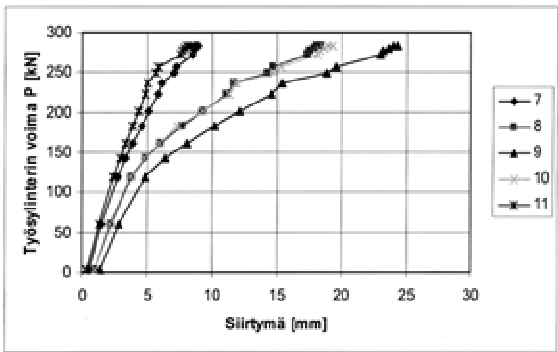

Fig. 25. Deflection in mid-span of slabs 5–8 measured by transducers 7–11.

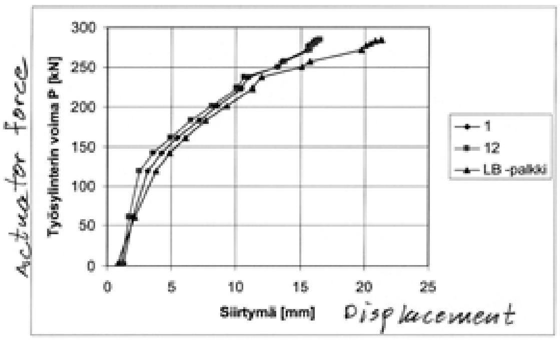

Fig. 26. Net deflection of midpoint of LB beam and those of end beams (1, 12). Settlement of supports is eliminated from deflection of LB beam.)

10.2 Crack width	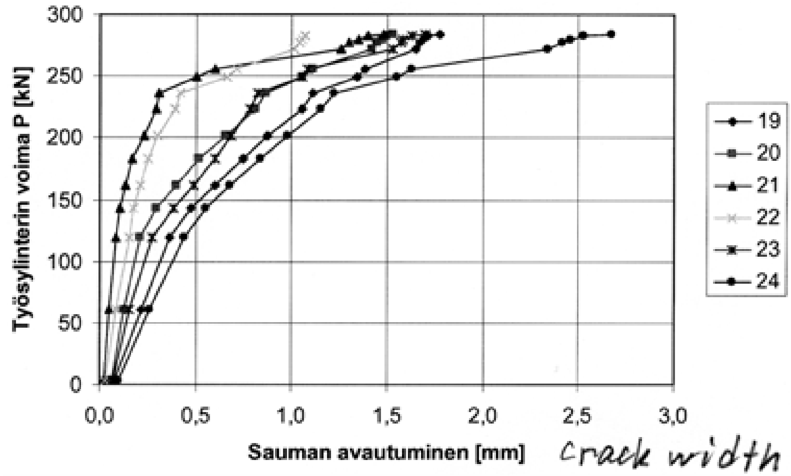 *Fig. 27. Differential displacement (≈ crack width) measured by transducers 19–24.*
10.3 Average strain (actually differential displacement)	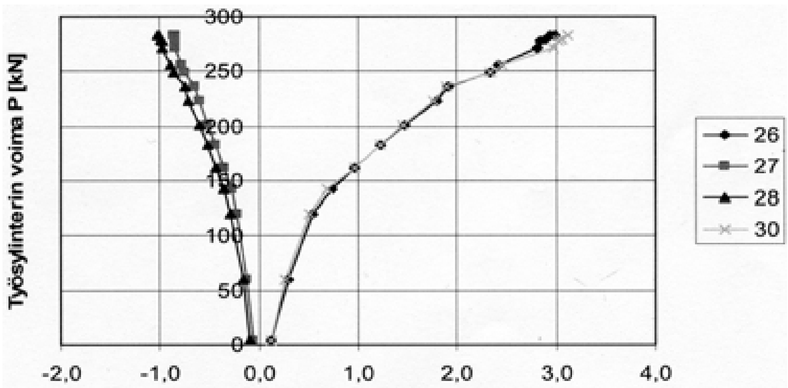 *Fig. 28. Differential displacement at top and bottom surface of floor measured by transducers 26, 27, 28 and 30.*
10.4 Differential displacement	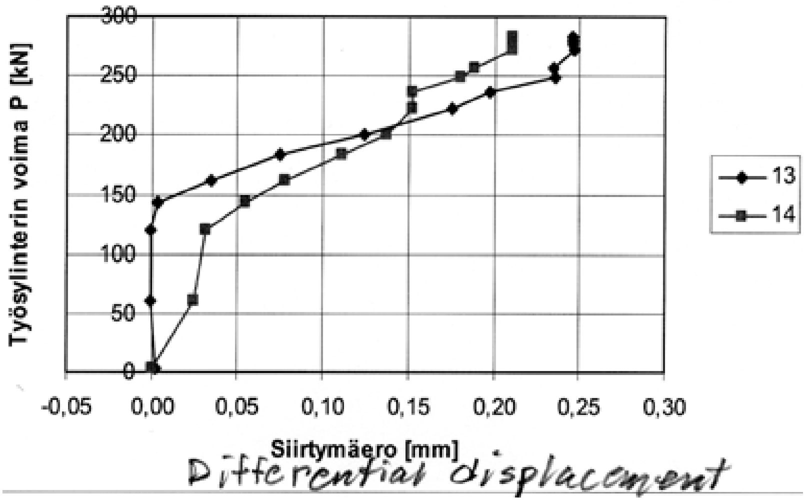 *Fig. 29. Differential vertical displacement between top surface of LB beam and the end of hollow core slabs measured by transducers 13 and 14. A positive value means that the slab end deflects more than the beam.*

10.5	Strain

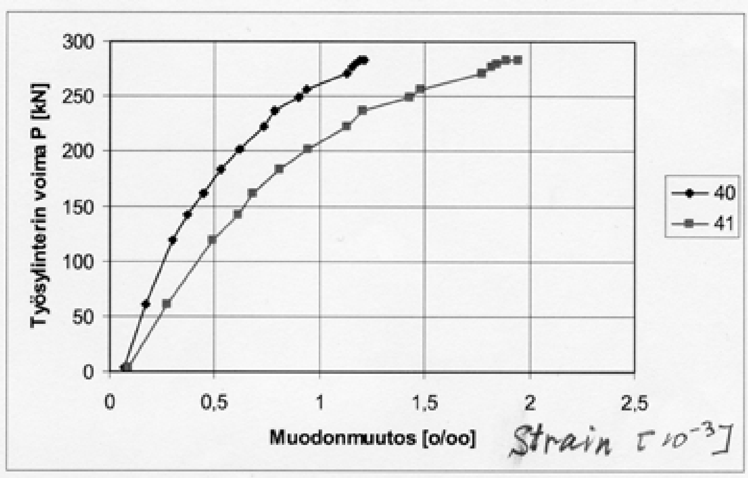

Kuvaaja 2.9. LB –palkin laipan pitkittäinen muodonmuutos.

Fig. 30. Longitudinal strain in ledges measured by gauges 40 and 41.

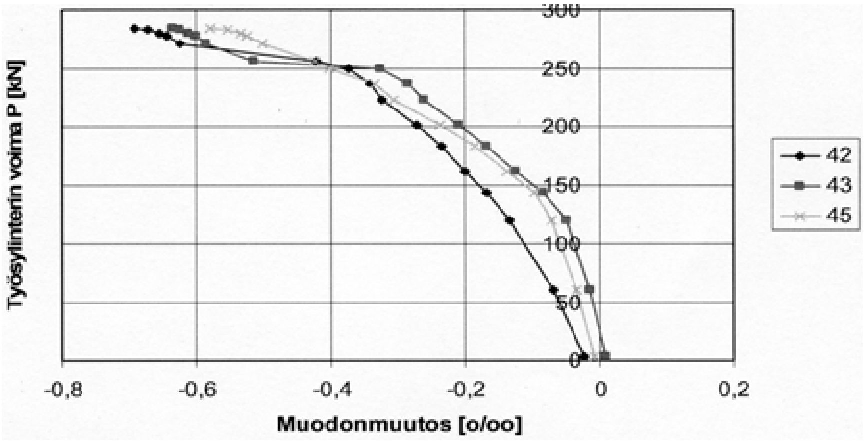

Fig. 31. Transverse strain in ledges measured by gauges 42, 43 and 45. The strain measured by gauge 44 is not shown because it was clearly erroneous.

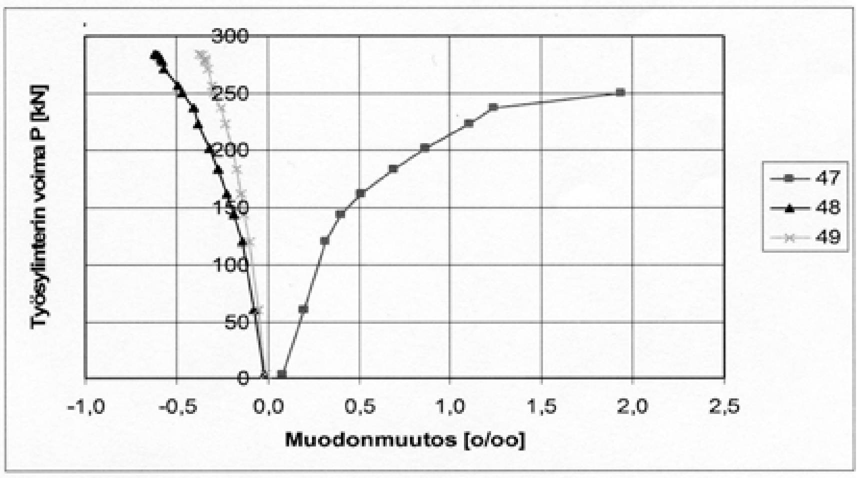

Fig. 32. Longitudinal concrete strain in LB beam measured by gauges 47, 48 and 49. The strain measured by gauge 46 is not shown because it was clearly erroneous.

11	Reference tests
	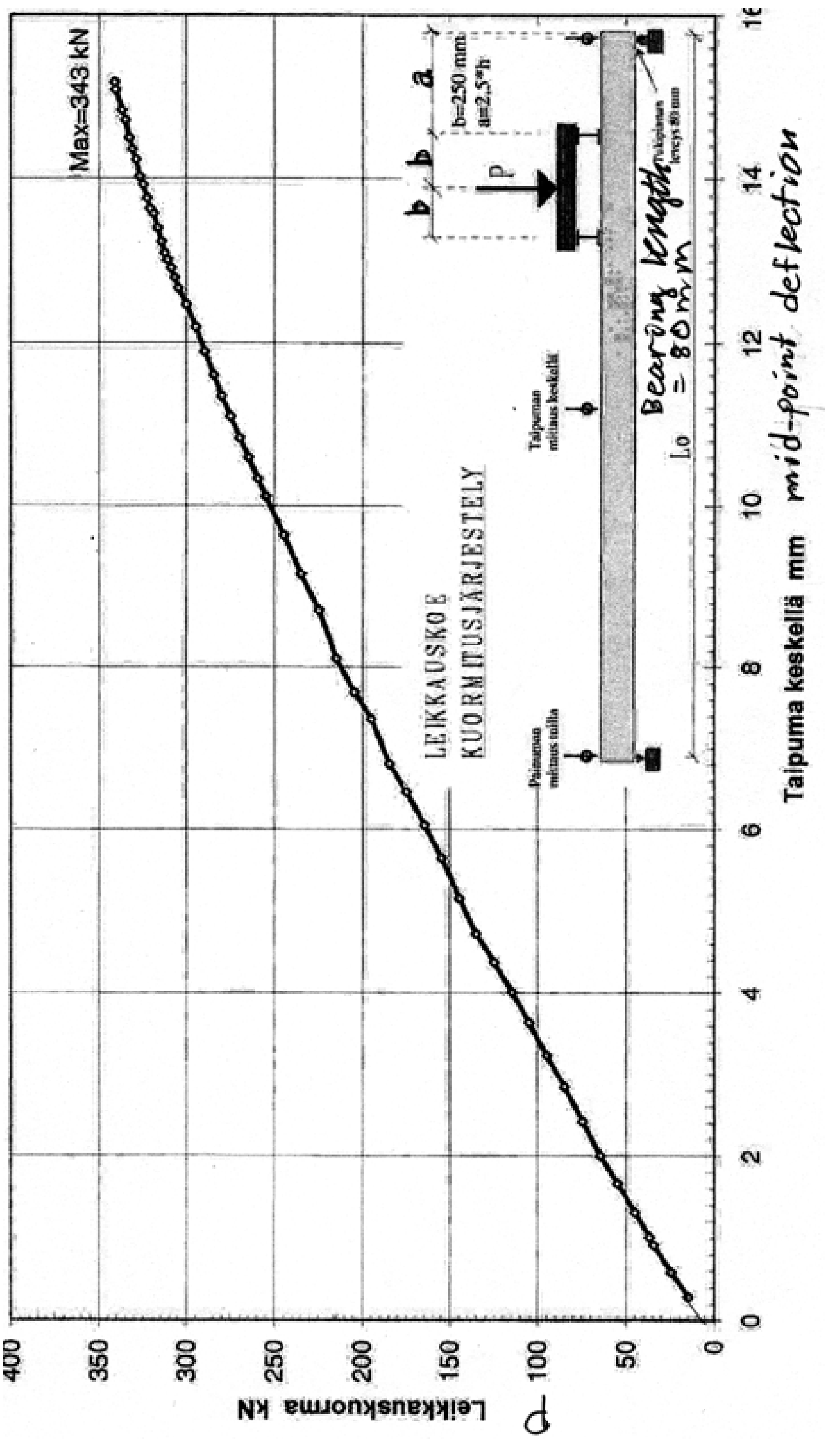 *Fig. 33. Layout of reference test and load – mid-point deflection curve.* *See also App. A, Fig. 8.*

Table 2. Reference test. Span of slab, shear force V_g at support due to the self weight of the slab, actuator force P_a at failure + weight of loading equipment P_{eq}, total shear force V_{obs} at failure and total shear force v_{obs} per unit width.

Test	Date	Span mm	V_g kN	P_a+P_{eq} kN	V_{obs} kN	v_{obs} kN/m	Note
R1	17.6.2002	7120	20,9	343,0	313,3	261,1	Web shear failure (flexural shear failure)

App. A, Fig. 8 shows that the lower end of the inclined failure crack is at a distance of 500 mm from the support. At this distance, assuming the losses of prestress equal to 10% and the transfer length of the prestressing force equal to 600–800 mm, the axial stress in the soffit = -2,9 … -0,1 MPa is obtained. This suggests that the failure mode could not be initiated by a flexural crack. Hence, the failure mode has been web shear failure rather than flexural shear failure.

12 Comparison: floor test vs. reference tests

The observed shear resistance (support reaction) of the hollow core slab in the floor test was equal to 149,2 kN per one slab unit or 124,3 kN/m. This is **48%** of the shear resistance observed in the reference test. Note that in this case the sheared end of the reference slab was provided with cast-in-situ concrete simulating the grouting outside the beam end in floor test, see App. A, Fig. 8.

13 Discussion

1. The net deflection of the middle beam due to the imposed actuator loads only (deflection minus settlement of supports) was 21,3 mm or *L*/225.

2. The shear resistance measured in the reference test was a bit higher than the mean of the observed values for similar slabs given in *Pajari, M. Resistance of prestressed hollow core slab against a web shear failure. VTT Research Notes 2292, Espoo 2005*. This may be attributable to the cast-in-situ concrete at the sheared end in the reference test.

3. The maximum difference in the net mid-point deflection of the beams was of the order of 5–6 mm. An estimated value is given because the settlement of the supports of the end beams was not measured. Hence, the torsional stresses due to the different deflection of the middle beam and end beams had a negligible effect on the failure of the slabs.

4. The failure mode was web shear failure of edge slabs close to the supports of the middle beam (LB beam). The LB beam seemed to recover completely after the failure.

APPENDIX A: PHOTOGRAPHS

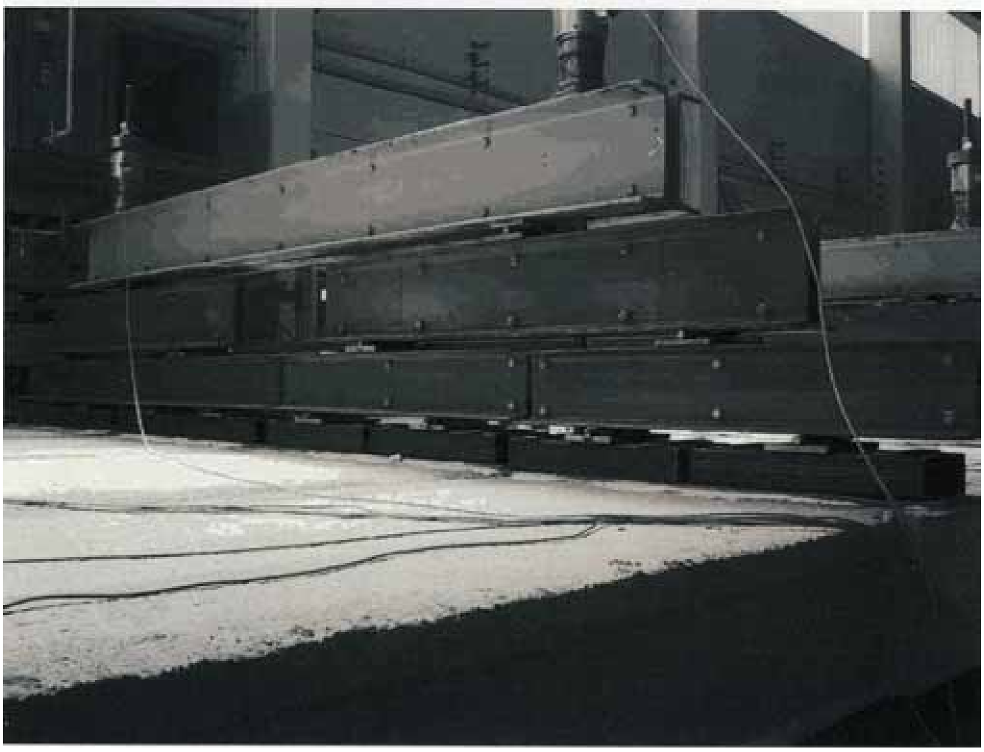

Fig. 1. Loading arrangements.

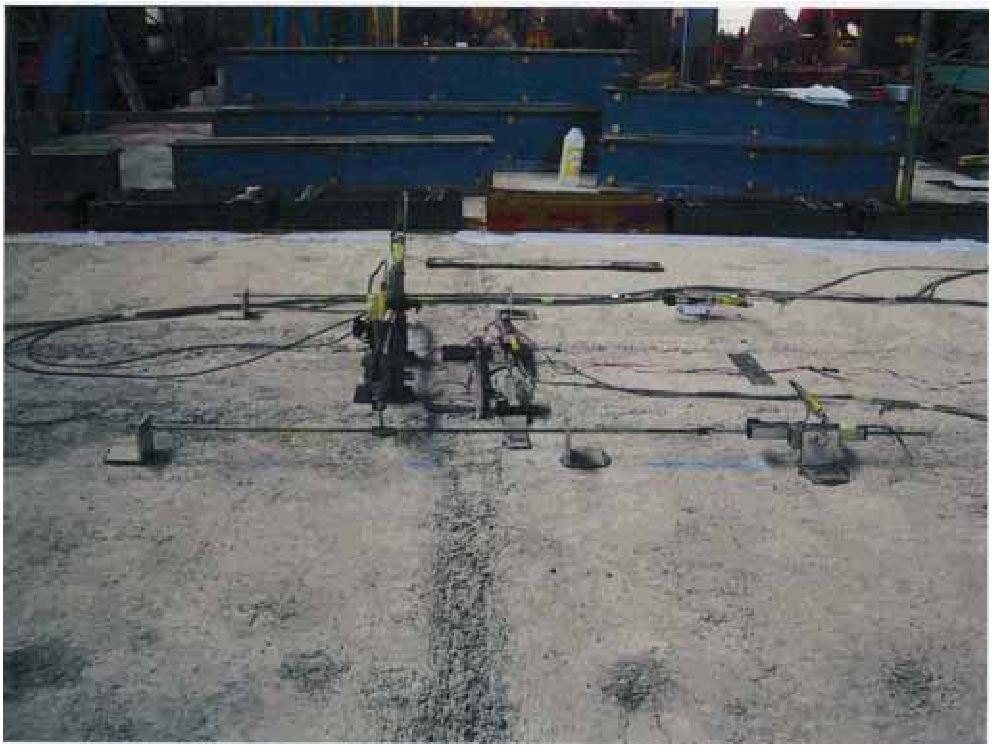

Fig. 2. Equipment for measuring average strain in hollow core slab.

Fig. 3. A step between LB beam and slab 4.

Fig. 4. Failure in slab 8.

Fig. 5. Soffit after failure. Slab 6 in the front, slabs 7 and 8 in the rear.

Fig. 6. Slab 8 after failure. The loose top part has been removed.

Fig. 7. Slab 8 after failure. All loose concrete material has been removed.

Fig. 8. Failure mode in reference test.

1	**General information**
1.1 Identification and aim	**VTT.S.WQ.500.2005** **Last update 2.11.2010** WQ500 (Internal identification) Aim of the test: To study the shear resistance of 500 mm slab supported on steel beams.
1.2 Test type	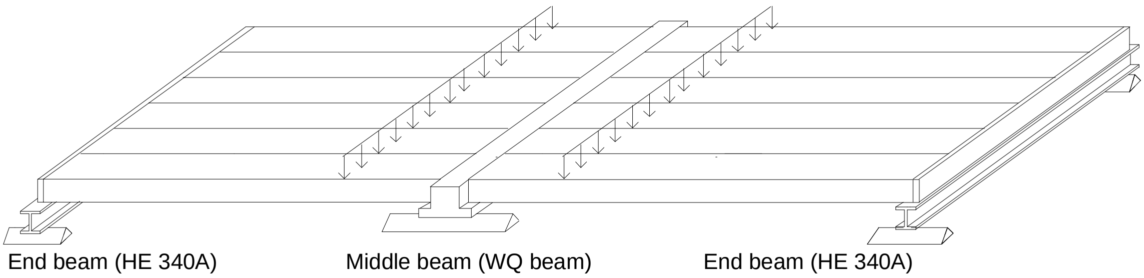 *Fig. 1. Illustration of test setup. The end beams were hot-rolled steel beams.*
1.3 Laboratory & date of test	VTT/FI 16.8.2005
1.4 Test report	Author(s): Pajari, M. Name: *Load test on hollow core slab floor with steel beams* Ref. number: RTE3405/05 Date: 14.12.2005 Availability: Available at www.rakennusteollisuus.fi
2	**Test specimen and loading**

2.1 General plan	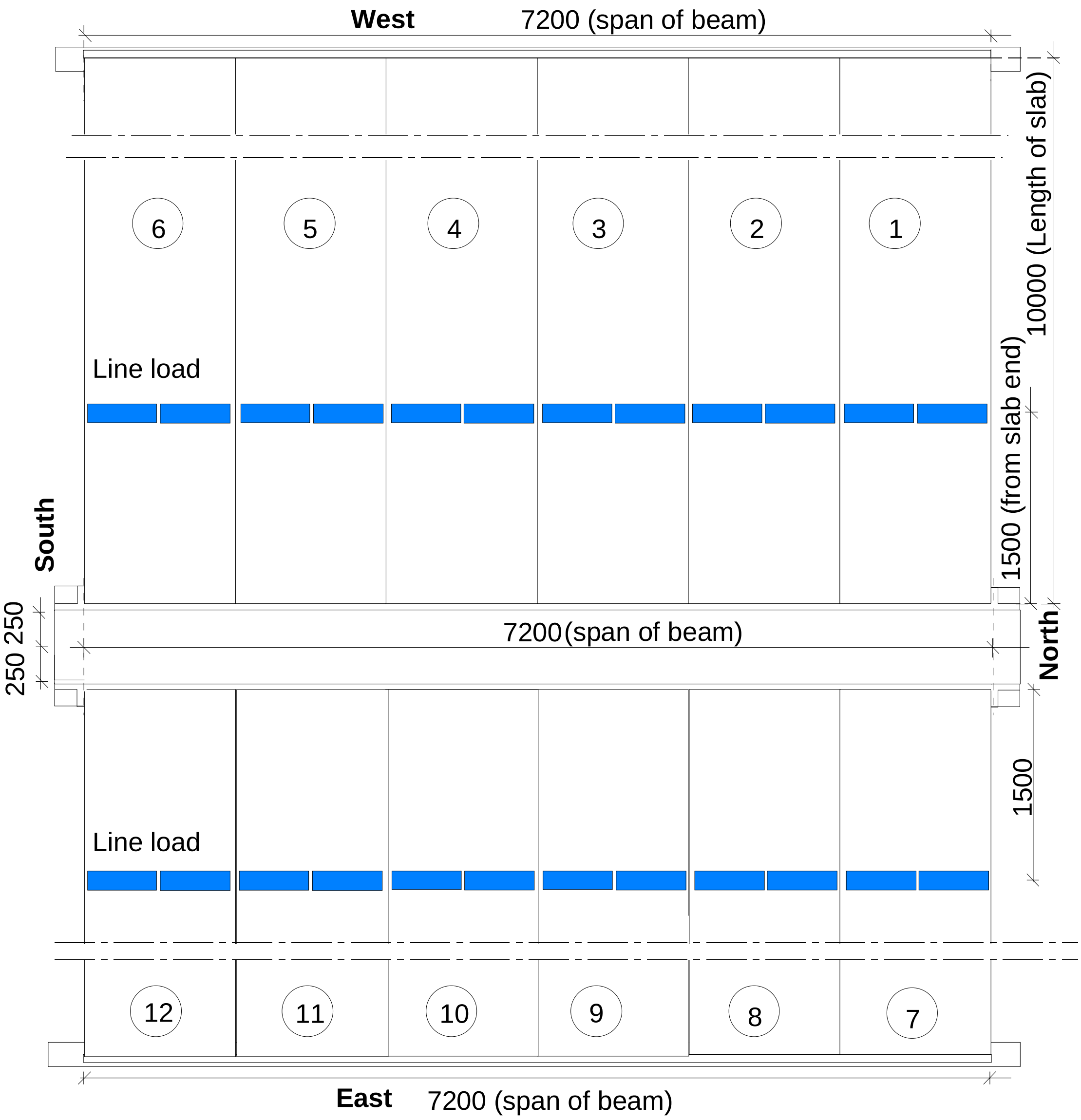 *Fig. 2. Plan.*

2.2
End beams

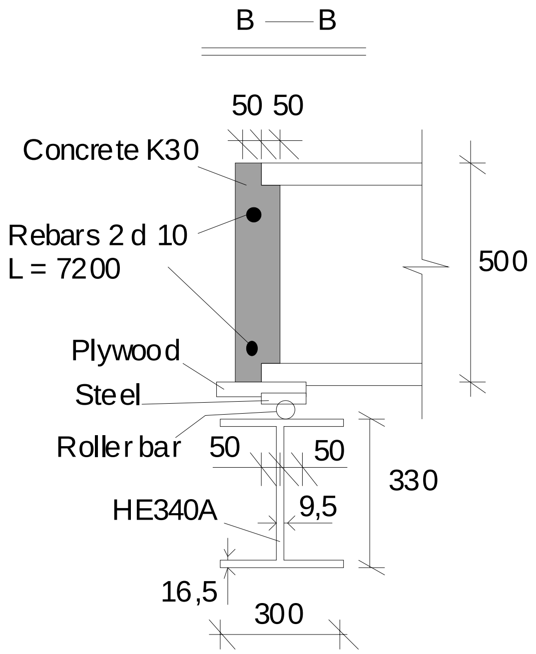

Simply supported, span = 7,2 m, roller bearing below one end

Fig. 3. Arrangements at end beam.

2.3
Middle beam

- Manufactured by PPTH Oy and transported to VTT Research Hall 1 23.5.2005
- Simply supported, span = 7,2 m, roller bearing at one end

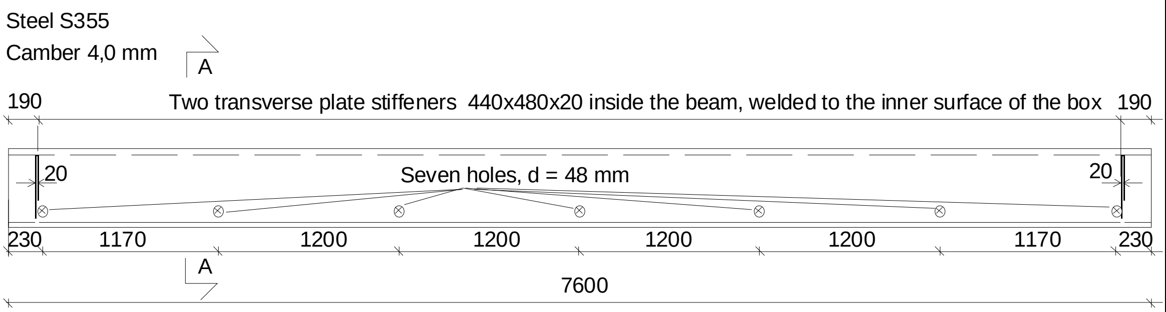

Fig. 4. Middle beam. Elevation.

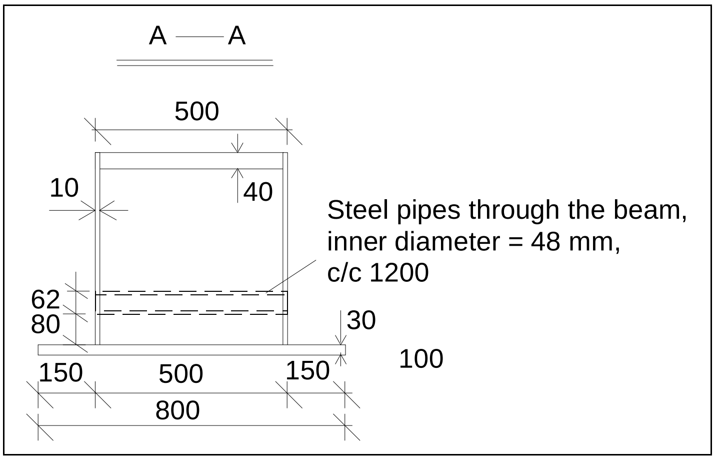

Fig. 5. Cross-sectional geometry.

2.4
Arrangements at middle beam

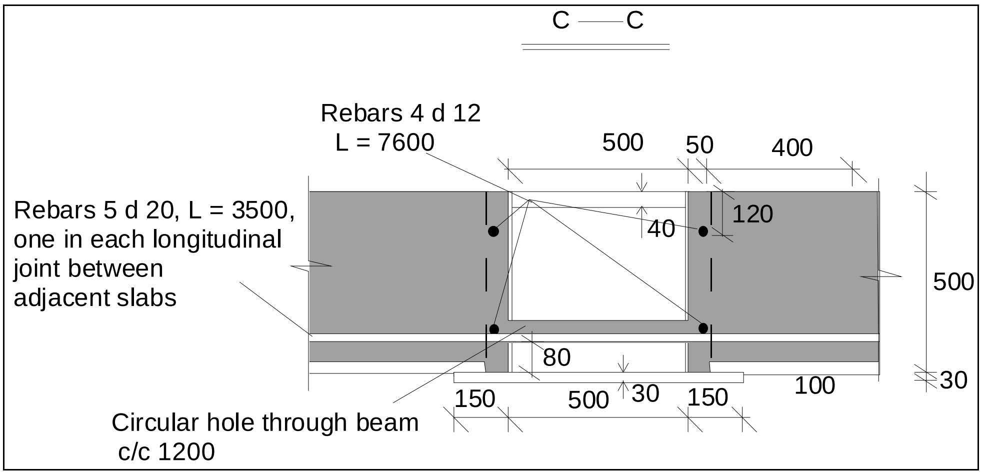

Fig. 6. Section C-C (see Fig. 13) along a joint between adjacent hollow core units.

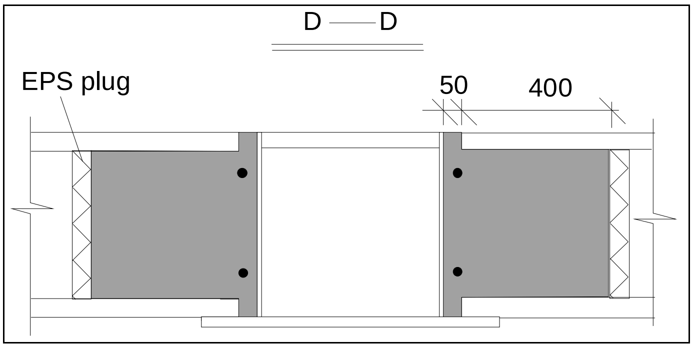

Fig. 7. Section D-D (see Fig. 13) along hollow cores. Plugs made of expanded polystyrene.

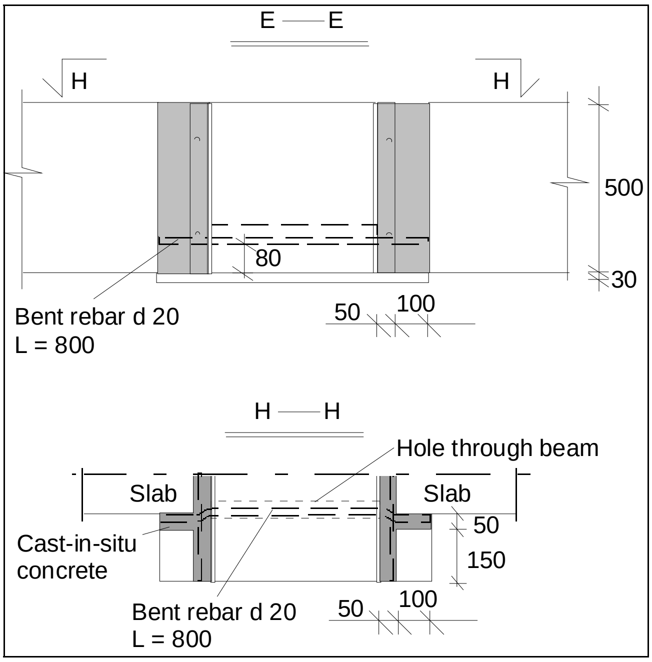

Fig. 8. Tie reinforcement in the cast-in-situ concrete outside the edge of the outermost slabs (section E-E in Fig. 13). See also App. A, Fig. 9.

Tie reinforcement: Horizontal rebars A500HW through the beam and parallel to the beam.

<table>
<tr><td>2.5
Slabs</td><td>
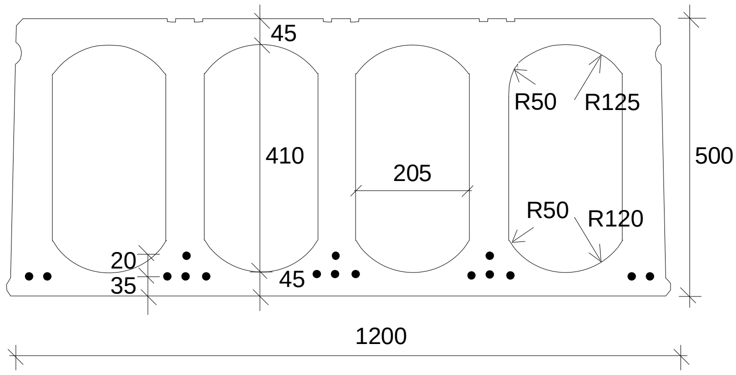

Fig. 9. Nominal geometry of slab units (in scale).

- Extruded by Parma Oy, Hyrylä factory 28.4.2005
- Strands: 16 J 12,5, A_p = 93 mm^2/strand, initial prestress = 1050 MPa

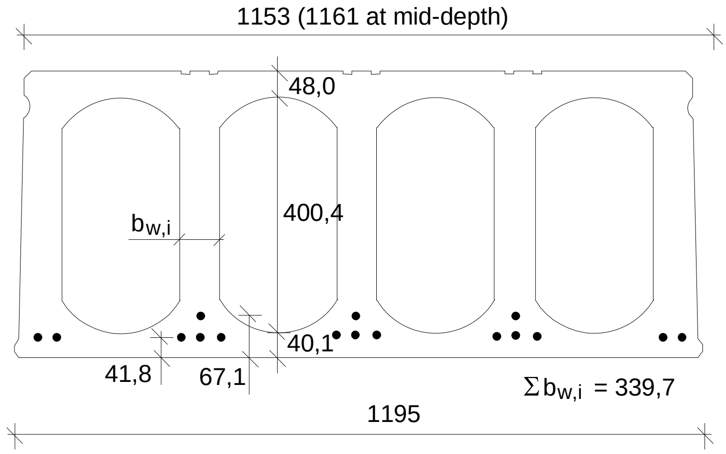

Fig. 10. Most relevant measured geometrical properties.

Max measured bond slippage: 1,9 mm (in slab 11);

2x1,7 mm (in slabs 10 and 11);

2x1,6 mm (in slabs 3 and 8)

- Measured weight = 6,49 kN/m
</td></tr>
<tr><td>2.6
Temporary supports</td><td>No</td></tr>
<tr><td>2.7
Loading arrangements</td><td>
An auxiliary loading frame was built above the test floor. It was tied by tension bars to the floor of the research hall, see Figs 11 and 12. Six tension bars penetrated the floor through the hollow cores outside the line loads, the rest were outside the test specimen.

The loads were generated by 12 actuators. See Fig. 13 for the position of the actuators. Taking into account the weight of the loading equipment P_{eq} = 6,14 kN/slab unit, the following relationship can be written for the line load on one slab:

$$F = P_a + 6{,}14 \text{ kN} \qquad (1)$$

P_a is the load in the actuator. The line loads were applied to the slab units by 24 tertiary steel beams of the type HE 120 A (a hot-rolled I-beam with depth = 114 mm, width = 120 mm and thickness of flange = 8 mm), each 550 mm in length. The top surface of the slabs under these beams was evened out by gypsum. On the top of the tertiary beams, secondary spreader beams were placed, each on two bearings. On the top of the secondary beams, primary spreader beams were installed. The friction between the primary and secondary spreader beams was eliminated with teflon sheets, and that
</td></tr>
</table>

between the secondary and tertiary spreader beams with a freely rolling circular steel bar, see Figs 14–16 The drifting of the primary spreader beams was prevented by the friction at the upper and lower end of the actuators. The upper end of each actuator was provided with a swivel (ball bearing).

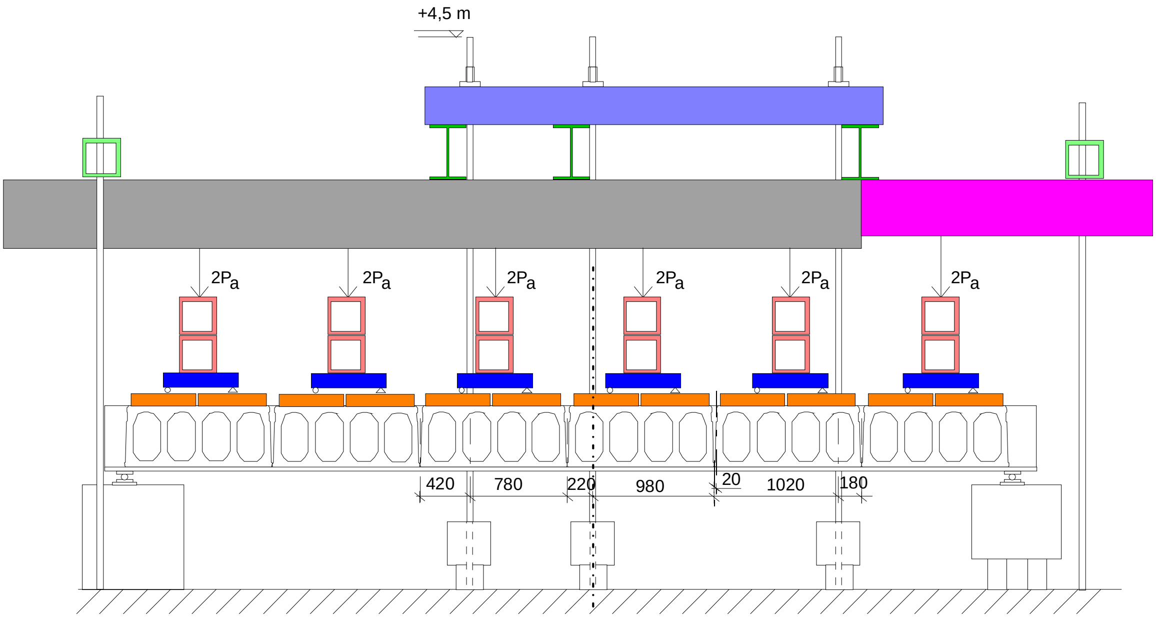

Fig. 11. Auxiliary loading frame. Elevation. North edge on the right.

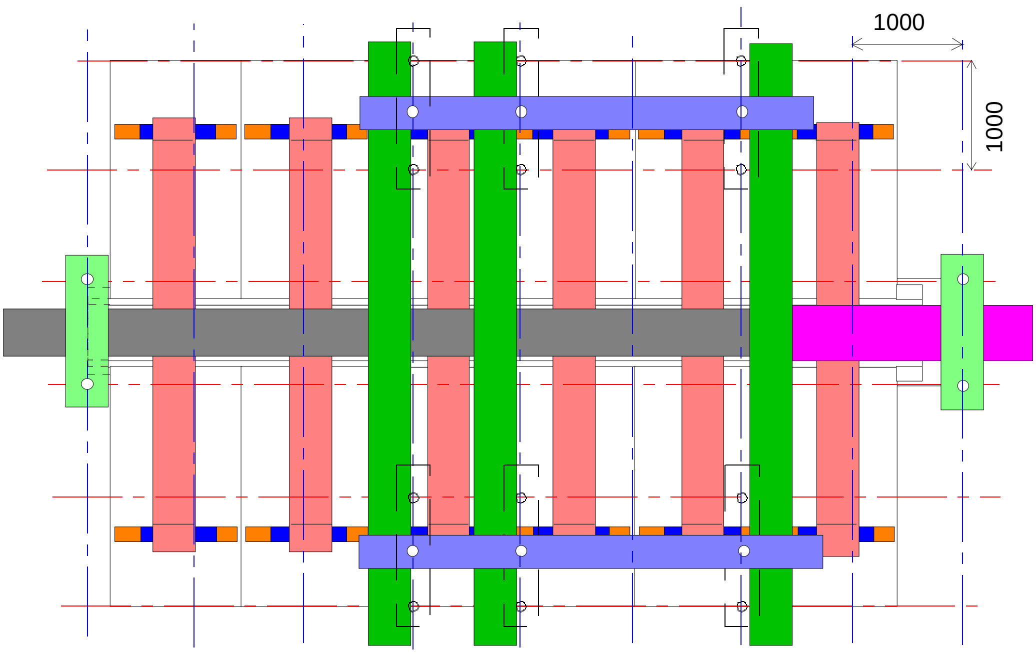

Fig. 12. Auxiliary loading frame. Plan. The position of the tension bars is indicated by white circles above the blue and green beams. North edge on the right.

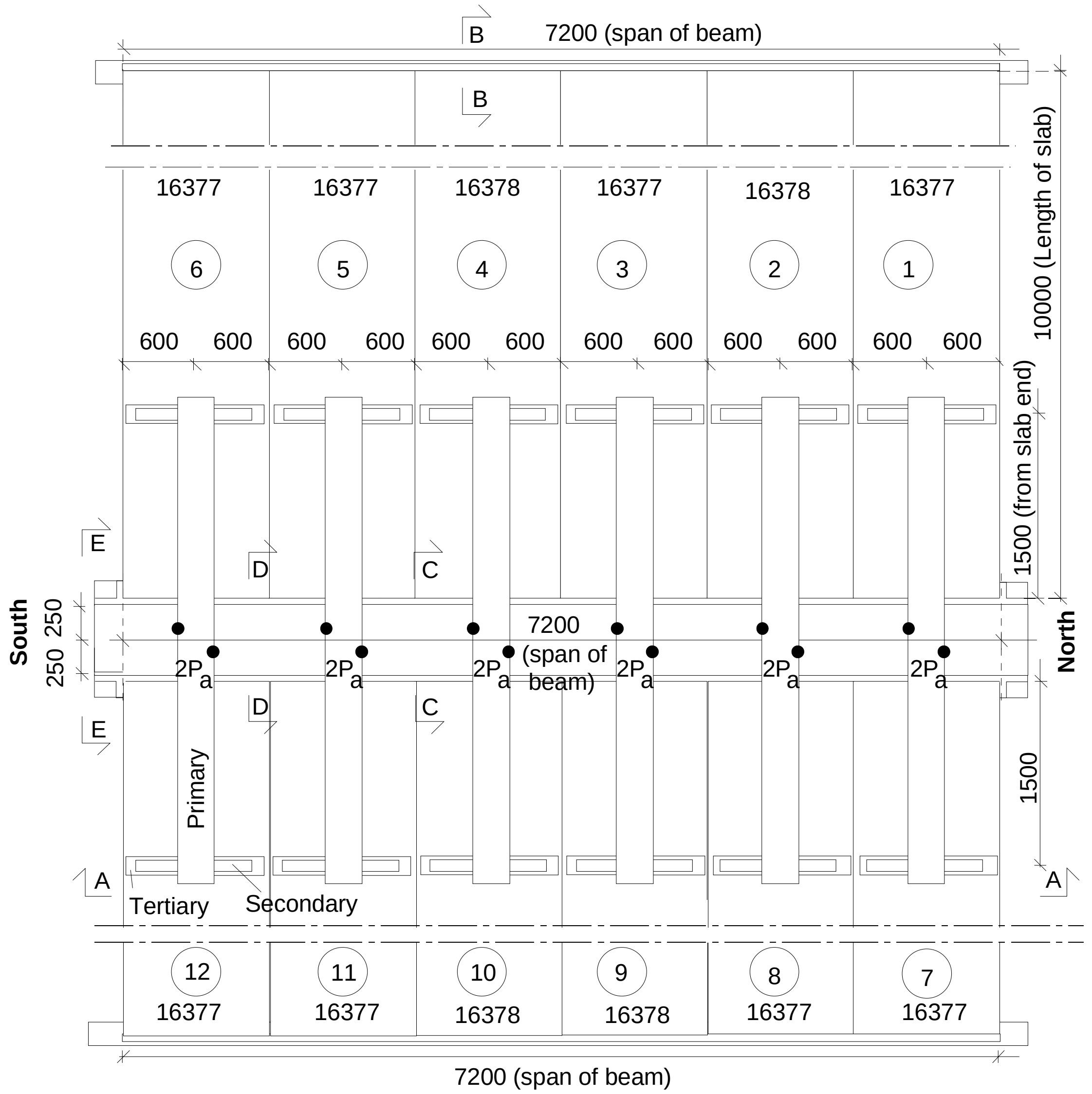

Fig. 13. Loading arrangements. The slabs are from two casting lots: 16377 and 16378. The position of the actuator loads is indicated by black circles above the middle beam.

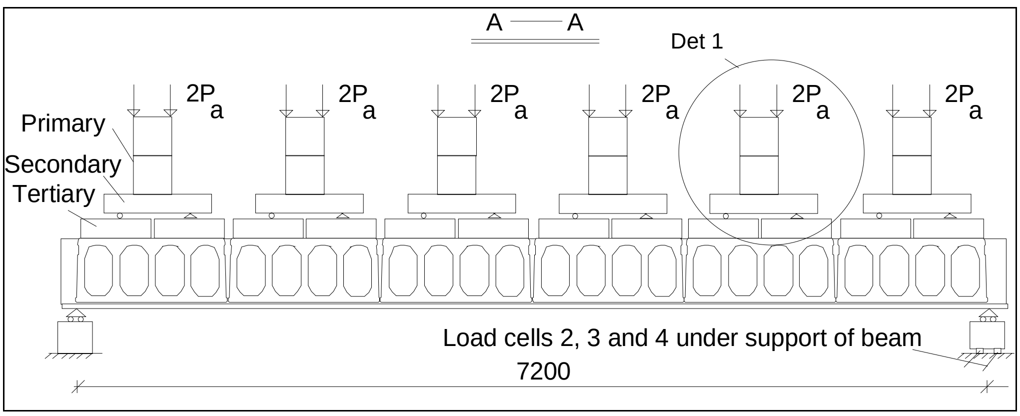

Fig. 14. Section A-A, see Fig. 13.

	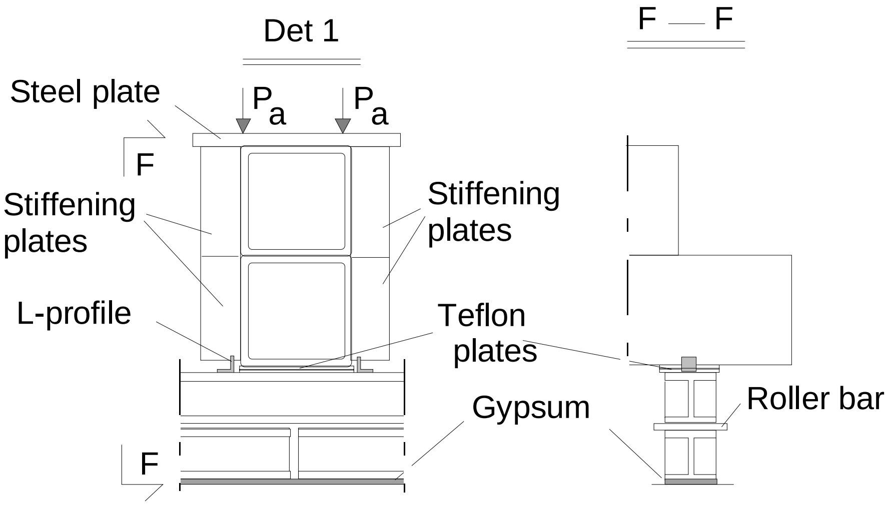 *Fig. 15. Detail 1, see Fig. 14.*
3	**Measurements**
3.1 Support reactions	Below one end of the middle beam, the support reaction due to the actuator loads was measured by three load cells as shown in Figs 14 and 16. 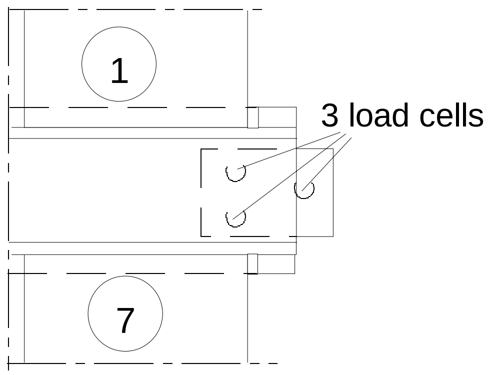 *Fig. 16. Load cells below the Northern support of the middle beam.*

3.2 Vertical displacement	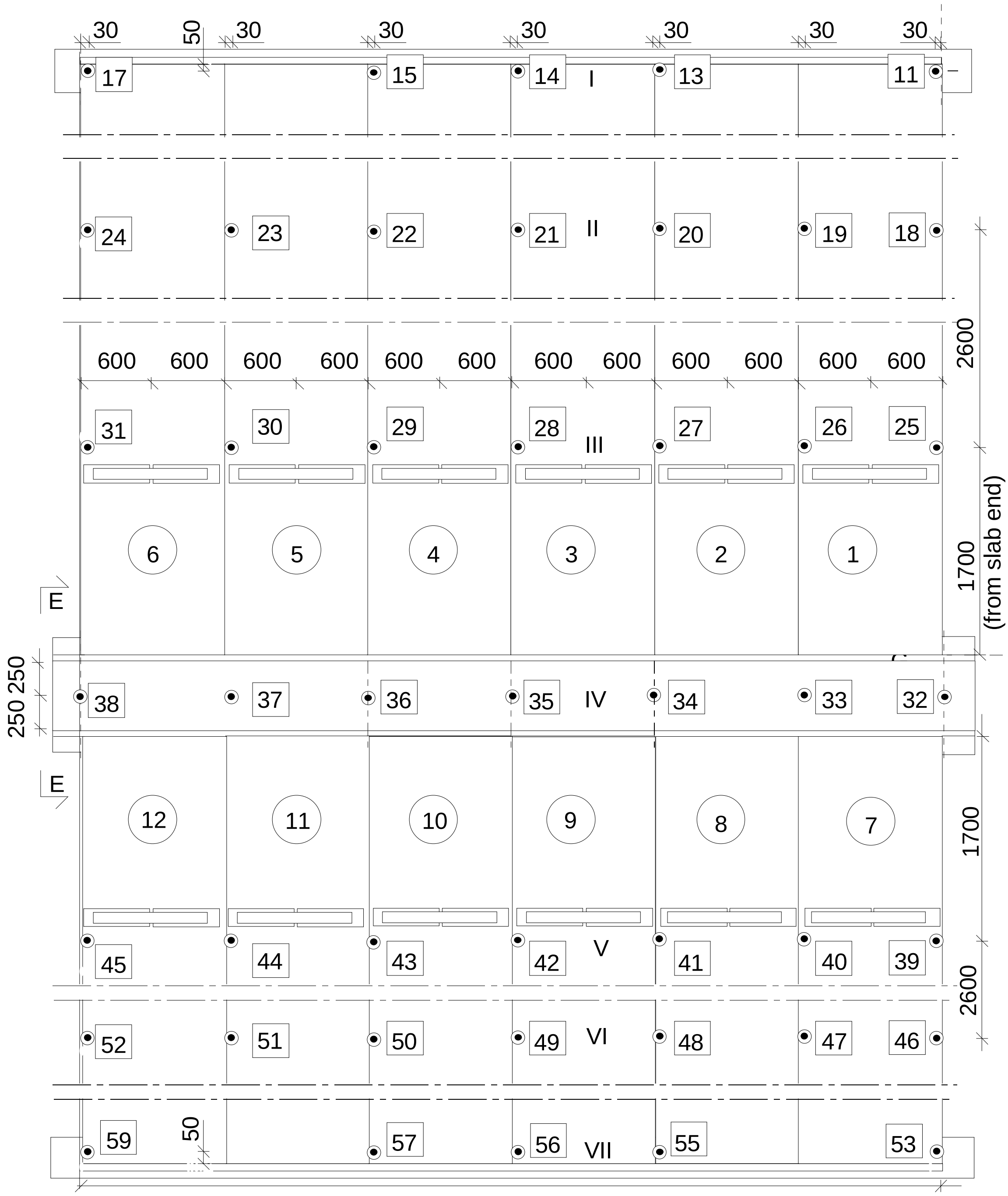 *Fig. 17. Location of transducers 11 … 59 for measuring vertical deflection along lines I … VII.*

3.3–3.4
Average strain and horizontal displacements

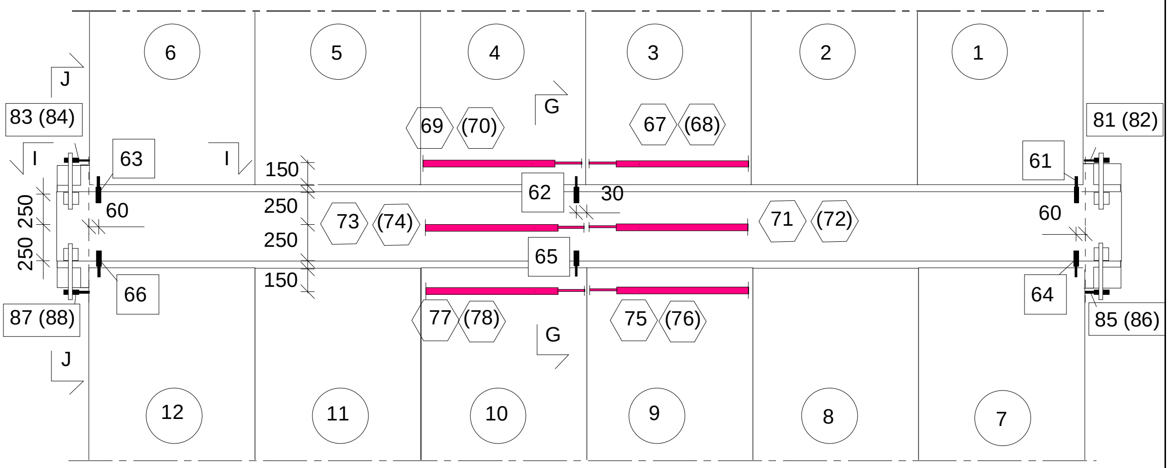

Fig. 18. Position of transducers 61-66, 67–78 and 81–88 measuring crack width, average strain parallel to the beams and displacement of the slab edges relative to the beam, respectively.

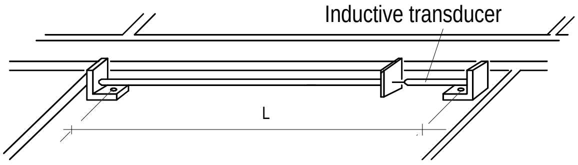

Fig. 19. Apparatus for measuring average strain. L =1100 mm.

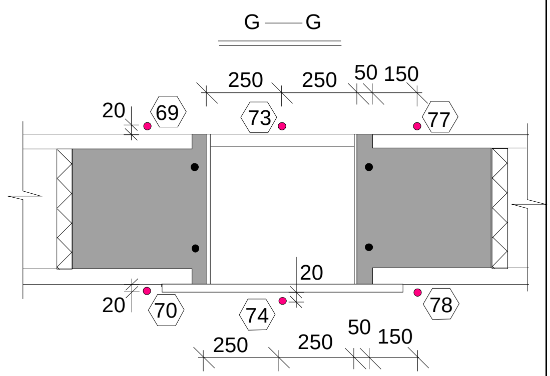

Fig. 20. Section G-G, see Fig. 18.

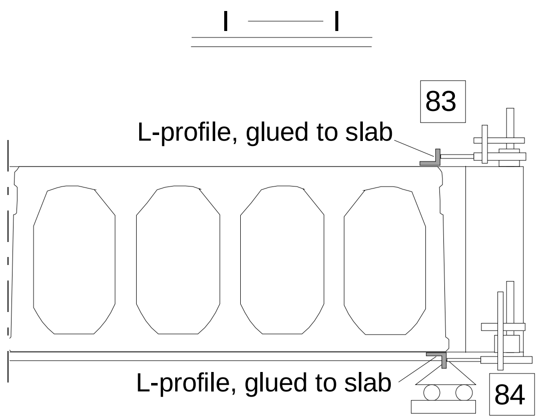

Fig. 21. Section I-I, see Fig. 18.

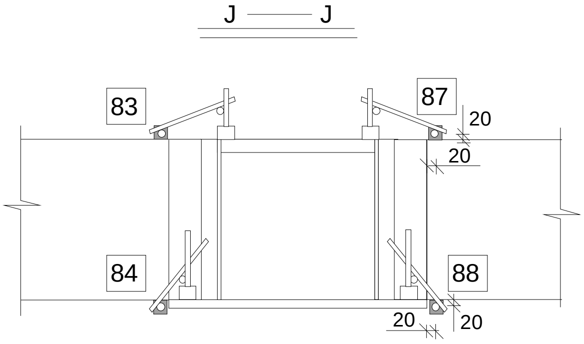

Fig. 22. Section J-J, see Fig. 18.

4 **Special arrangements**

- None

5 **Loading strategy**

5.1
Load-time relationship

The loads were applied in two stages: Stage I (cyclic) and Stage II (monotonous) as shown in Fig. 23.

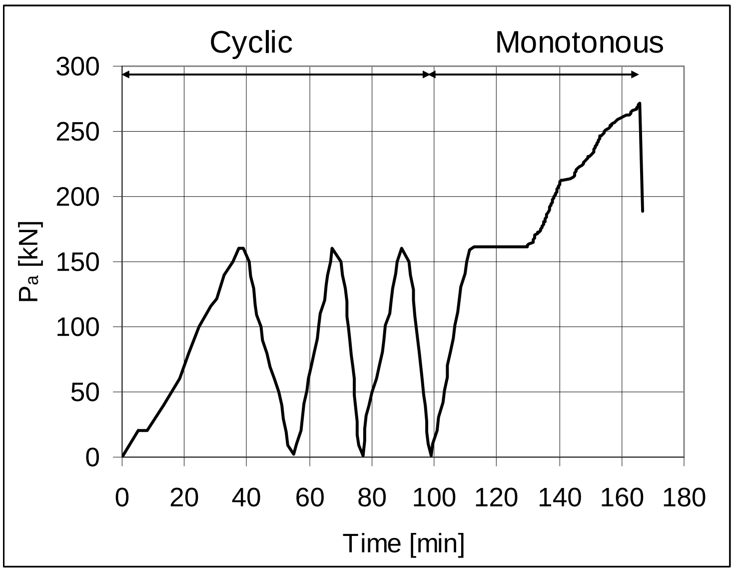

Fig. 23. Actuator force P_a vs. time.

Date of test: 16.8.2005

5.2
After failure

-

6 **Observations during loading** (see also the photographs in App. A)

Before loading	All measuring devices were zero-balanced when the actuator forces P_a were equal to zero but the weight of the loading equipment was on. The cracks in the slabs were visually inspected and found to be the same as those observed before the slabs were installed. They are shown in Fig. 32 in which the initial cracks in the cast-in-situ concrete are also indicated. The maximum crack width in the soffit of the slabs was of the order of 0,06–0,08 mm. The initial longitudinal crack on the top of slab 12 was above the midmost web. It was not deep. As can be seen later, the initial cracks on the top of slabs 3, 4, 9 and 12 did not affect the failure.
Cycling loading	P_a = 160 kN corresponds to the shear force due to the expected service load when the shear resistance of the slabs is supposed to be prevailing in the design.

	During the cyclic stage, the vertical interface between the cast-in-situ concrete of the middle beam and the sawn slab ends gradually cracked. At P_a = 109 kN, during the first load increase, the soffit of slab 10 cracked over the whole slab length, see Fig. 32 and App. A, Fig. 24. This crack may have been initiated near the 50 mm hole drilled for the vertical tension bars through the floor. When the load was last time at the expected service level (P_a = 160 kN), the soffit of the slabs between the line loads and the middle beam was inspected visually. The visible cracks are shown in Fig. 32. There were some new cracks along the strands and some initial cracks had grown in length. The maximum crack width in these cracks was of the order of 0,08 … 0,10 mm. No difference between the widths in the initial and new cracks could be observed. The width of the long longitudinal crack observed at P_a = 109 kN in the soffit of slab 10 was of the order of 1,0 mm.
P_a = 213 kN	An inclined crack was observed in slab 7 next to the middle beam.
P_a = 257 -259 kN	A similar crack was observed in slabs 1 and 12.
P_a = 272 kN	The crack in slab 12 grew in width and resulted in an abrupt shear failure. See Fig. 33 for all cracks and App. A, Figs 25–27 for the shear cracks in slabs 1, 7 and 12.

Observations after failure

When slab 12 failed, the loads on it were transferred to slab 11 over the longitudinal joint. The strength of this joint and the elastic energy stored in the loading frame made the floor fail in a complicated manner illustrated in Fig. 33 and in App. A, Figs 26–33. Despite the complexity of the crack pattern after the test, the origin of the failure was the shear crack in slab 12 next to the middle beam.

<u>About core filling</u>

After the test, the concrete filling of the slab ends next to the middle beam was investigated. In all hollow cores there was an empty space above the infill in the upper outer corner as shown in App. A, Figs 48–50. This was observed first after the end of slab 12 and the cast-in-situ concrete around it was broken during demolition. Fig. 24 shows the average geometry of the core infill for slabs 1 and 12. To illustrate the scatter, the geometry of the core infill for the individual cores is shown with dashed lines for slab 1.

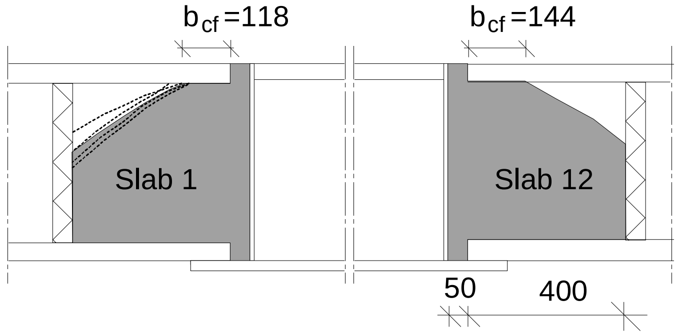

Fig. 24. a) Void filling seen in the beams's direction. On the left: average infill in the cores measured from slab 1 and the measured infill in the individual cores shown with dashed lines. On the right: average measured infill in the cores of slab 12.

The dimensions of the core infill for slab 1 were measured using a method shown in Fig. 25. The length of incomplete core filling was measured with a tape measure and subtracted from 400 mm to get b_{cf}, the length of the "complete" infill. Due to the vertical dimension of the measuring tape, the zone of complete infill includes both the zone of 100 % filling and the zone where the open space above the infill was less than 10 mm in depth. The same 10 mm tolerance was also applied when measuring b_{cf} for slab 12. As illustrated in Fig. 26, the open space above the infill, which is 10 mm or a bit more in depth, does not weaken the performance of the core infill against transverse shear.

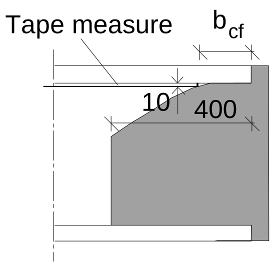

Fig. 25. Measuring the length of complete infill using a tape measure.

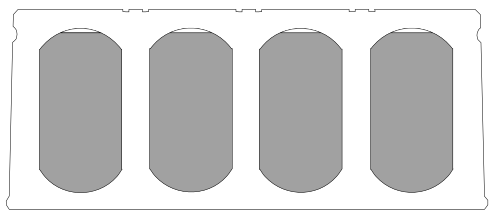

Fig. 26. Incomplete core infill with 10 mm gap above it.

It is obvious that the incomplete infill shown in Fig. 26 and a 100% infill are equally effective in eliminating the transverse deformation of the webs. This justifies the measuring method.

Fig. 50 in App. A shows how the pressure of the grout moved the EPS plug, glued with polyurethane to the concrete, forward along the core. There was a risk of collapse of the plug. For this reason, a more efficient vibration when compacting the grout could not be a solution for a better filling.

When demolishing the floor it was observed that the weakest average core infill was in slab 1. The hollow cores in slab 12 were slightly more effectively filled than in some slabs and slightly less effectively filled than in other slabs. In this sense the core filling in slab 12 was representative to the whole floor.

Observations on support conditions of slabs

The soffit of the slab units was not in complete contact with the middle beam when the slabs were installed and grouted, see Fig. 27. There were two reasons for this phenomenon. Firstly, the middle beam was stiffer than the end beams and had a precamber of 4 mm while the end beams were straight and deflected downwards due to their self weight. Due to these effects the slab ends were laying on non-parallel supports. Secondly, the soffit of the slabs was not completely planar but slightly curved downwards in transverse direction. Fig. 28 illustrates the typical joint between the outermost slabs and the ledge of the WQ beam. This gap was partly filled with the cement paste, and where wide enough, was also filled with the grout including aggregate. This is shown in App. A, Figs 53–59. At the support of the beam, the source of the grout below the slab was either the edge grouting as shown in Fig. 28 and App. A, Figs 41 and 44–47, or end grouting.

After the test, the maximum gap width δ_{max} was measured for the outermost slabs where possible. The results are given in the caption of Fig. 29.

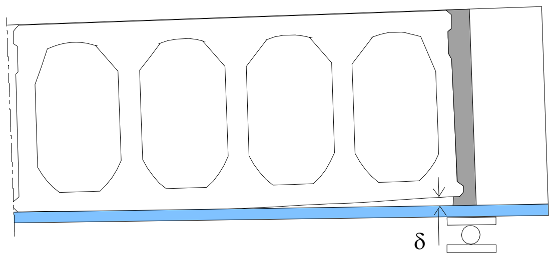

Fig. 27. Typical gap between slab and beam flange. δ_{max} = 1,3 mm, 3,8 mm and 5,5 mm for slabs 1, 6 and 7, respectively. For slab 12 the gap could not be measured after the failure.

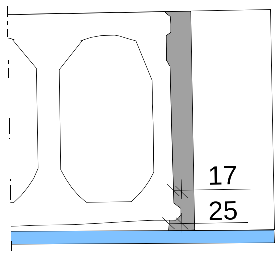

Fig. 28. Concrete cast outside the outermost edges of slabs intruded below the slab to some extent.

Fig. 29 shows the horizontal dimensions of a relatively thick grouting below the corners of the slab. These were measured using a steel wire which was 1 mm thick. Slab 1 was not checked because the wire was too thick for the gap. Slab 12 could not be measured because the concrete broken in the failure had filled the gap.

A direct contact between the soffit of the slab end and the ledge of the beam or grout on the ledge represents a favourable support condition. In this test also other mechanisms to transmit the support reaction of the slab to the beam may have been present.

The slab units were saw-cut but there was 10 mm deep zone at the bottom of the slab cross-section, which was not sawn but broken, see App. A, Fig. 52. The rough surface of this zone could work as a dowel, see Fig. 30. Even more important may have been the fact that the reinforced cast-in-situ concrete formed a beam which with the aid of the concrete in the cores may have transmitted the loads from the slabs to the bottom flange of the beam. This load-carrying mechanism may have been effective enough to transmit the loads even without any contact between the flange of the beam and the precast slab unit as shown in Fig. 31.

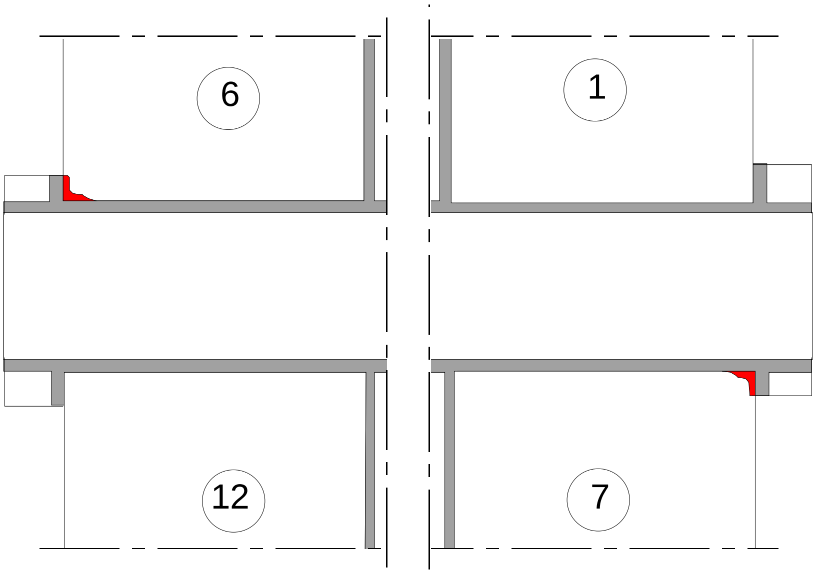

Fig. 29. The space between slab and the flange of the beam was partly filled with the jointing concrete. The filled areas were measured for slabs 6 and 7. They are drawn in scale and shown in red color.

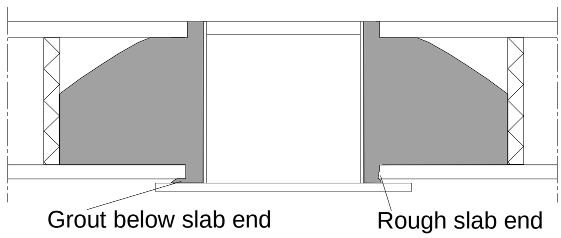

Fig. 30. Details affecting the transmission of support reaction between slab and beam. On the left: Grout below slab end. On the right: Rough slab end.

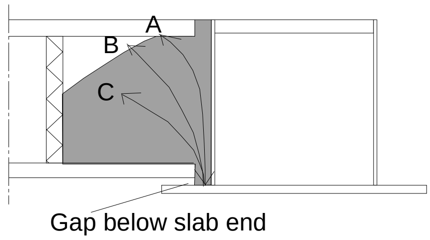

Fig. 31. Possible load-carrying mechanisms through cast-in-situ concrete when precast slab unit and ledge of beam are not in contact.

7	**Cracks in concrete**
7.1 Cracks at service load	

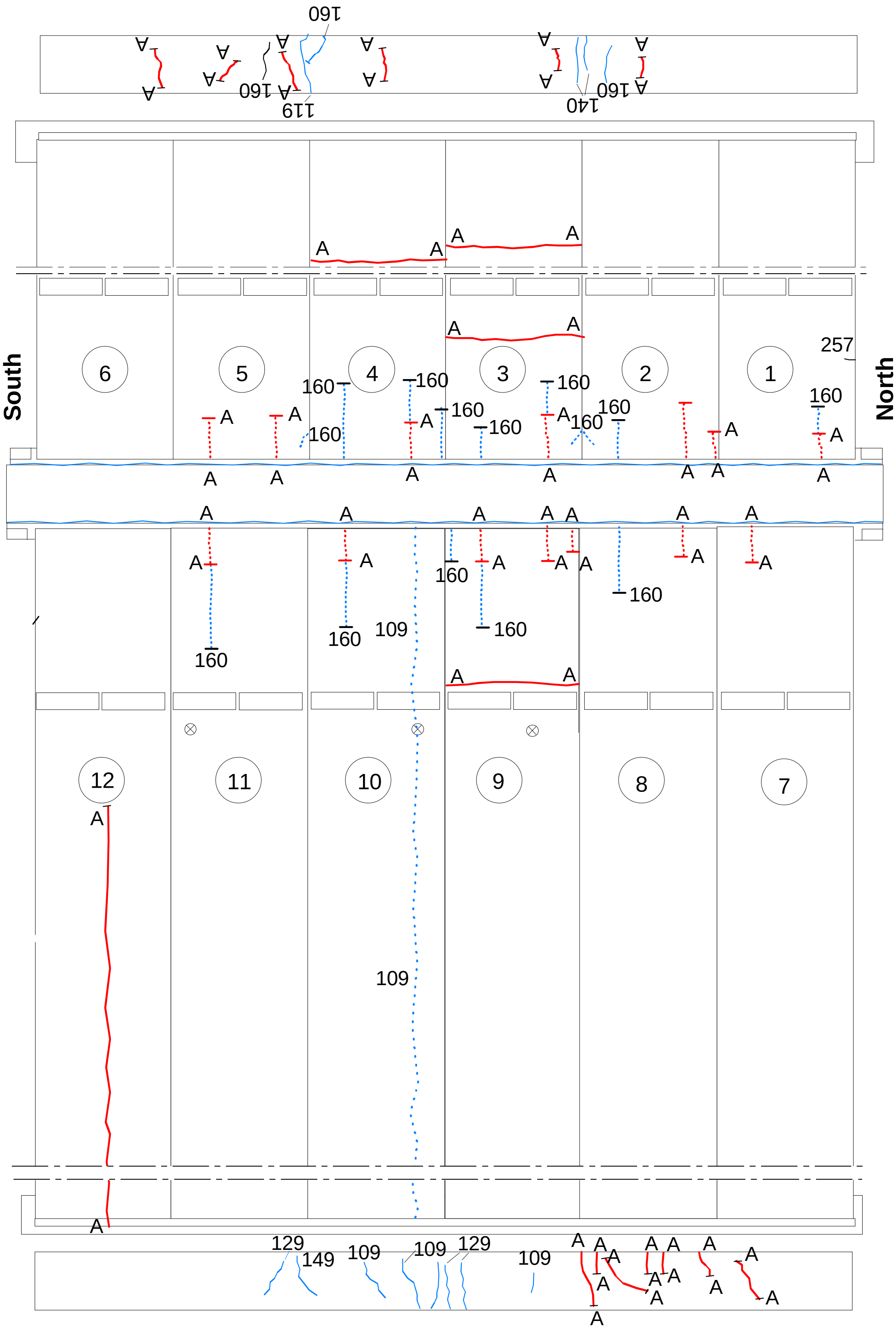

Fig. 32. Cracks at service load (P_a = 140 kN). The initial cracks observed before loading are indicated with red colour and letter A. A dashed line indicates a crack in the soffit. The numbers give the value of the actuator force at which the crack (other than initial crack) was observed.

7.2 Cracks after failure	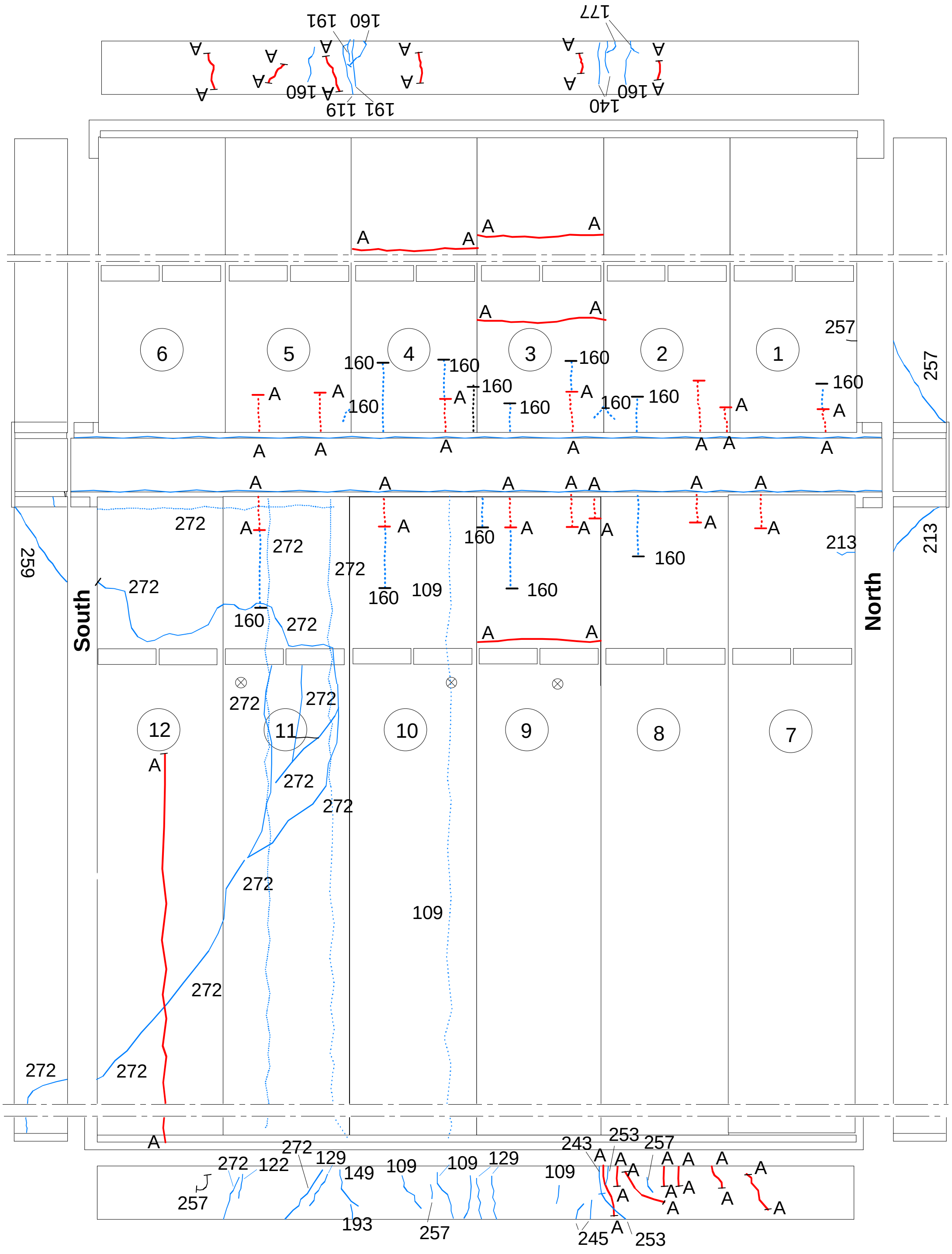 *Fig. 33. Cracks after failure. The initial cracks are indicated with red colour and letter A. A dashed line indicates a crack in the soffit. The numbers give the value of the actuator force at which the crack was observed.*

8	**Observed shear resistance**
	The ratio (measured support reaction below one end of the middle beam) / (actuator forces on half floor) is shown in Fig. 34 and in a larger scale in Fig. 35.

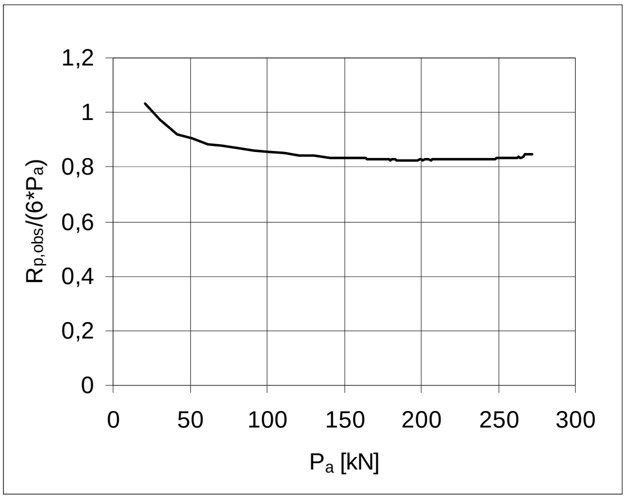

Fig. 34. Ratio of measured support reaction of the middle beam ($R_{p,obs}$) to actuator loads on half floor.

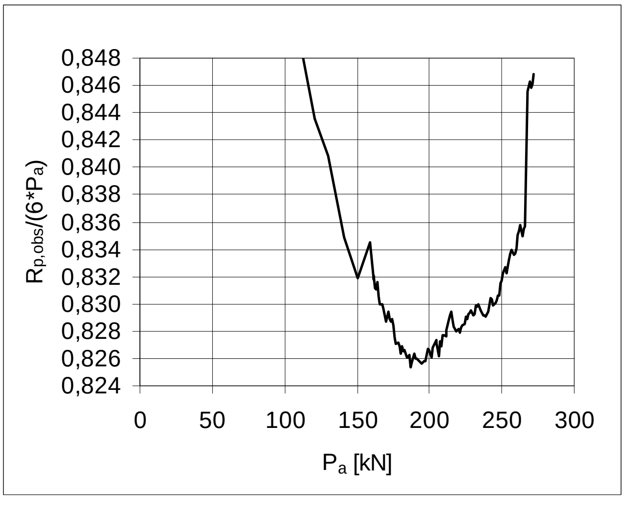

Fig. 35. A detail of the previous figure in a larger scale.

The shear resistance of one slab end (support reaction of slab end at failure) due to different load components is given by

$V_{obs} = V_{g,sl} + V_{g,jc} + V_{eq} + V_p$

where $V_{g,sl}$, $V_{g,jc}$, V_{eq} and V_p are shear forces due to the self-weight of slab unit, weight of joint concrete, weight of loading equipment and actuator forces P_a, respectively. $V_{g,sl}$ and $V_{g,jc}$, are calculated assuming that the slabs behave as simply supported beams. $V_{g,jc}$ is calculated from the nominal geometry of the joints and density of the concrete, other components of the shear force from measured loads and weights. For V_{eq} and V_p the relationship given in Fig. 35 is applied. This means that $V_{eq} = 0{,}847 \times P_{eq}$ and $V_p = 0{,}847 \times P_a$. The values for the components of the shear force are given in the Table on the next page.

Table. Components of shear resistance due to different loads.

Action	Load	Shear force kN
Weight of slab unit	6,49 kN/m	32,13
Weight of joint concrete	0,39 kN/m	1,93
Loading equipment	6,14 kN	5,20
Actuator loads	272,00 kN	230,38

The observed shear resistance V_{obs} = 269,6 kN (shear force at support) is obtained for one slab. The shear force per unit width is 224,7 kN/m.

9 **Material properties**

9.1
Strength of steel

Middle beam	Thickness mm	Strength R_e[1)] MPa
Top flange	40	388
Bottom flange	30	388
Web	10	407

1) Measured yield strength according to certificate of compliance

Component	$R_{eH}/R_{p0,2}$ MPa	R_m MPa	Note
End beam	≈350		Nominal (no yielding)
Strands J12,5	1630	1860	Nominal (no yielding)
Reinforcement	500		Nominal (A500HW,no yielding)

9.2
Strength of slab concrete, floor test

#	Cores	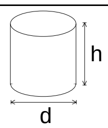	h mm	d mm	Date of test	Note
6			50	50	30.8.2005 (+14 d)[1)]	Upper flange of slabs 9 vertically drilled, tested as drilled[2)], density = 2363 kg/m^3
Mean strength [MPa]			82,0			
St.deviation [MPa]			1,1			

9.2
Strength of slab concrete, floor test

#	Cores	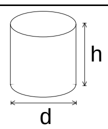	h mm	d mm	Date of test	Note
6			50	50	30.8.2005 (+14 d)[1)]	Upper flange of slabs 12 vertically drilled, tested as drilled[2)], density = 2363 kg/m^3
Mean strength [MPa]			84,4			
St.deviation [MPa]			2,1			

9.3
Strength of slab concrete, reference test

#	Cores	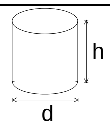	*h* mm	*d* mm	Date of test	From
6			50	50	30.8.2005 (+1 d)[1]	Upper flange of slab 13, vertically drilled, tested as drilled[2], density = 2430 kg/m^3
Mean strength [MPa]			86,8			
St.deviation [MPa]			4,2			

9.4
Strength of grout

#	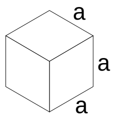	*a* mm	Date of test	Note
6		150	16.8.2005 (+0 d)[1]	Kept in laboratory in the same conditions as the floor specimen Density =2195 kg/m^3
Mean strength [MPa]		31,3		
St.deviation [MPa]		1,3		

[1] Date of material test minus date of test (floor test or reference test)
[2] kept in a closed plastic bag after drilling until compression

10 Measured displacements

In the following figures, P_a is the actuator force.

10.1 Deflections

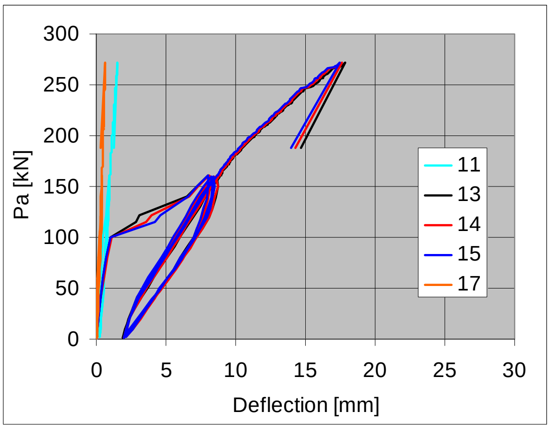

Fig. 36. Deflection on line I along Western end beam.

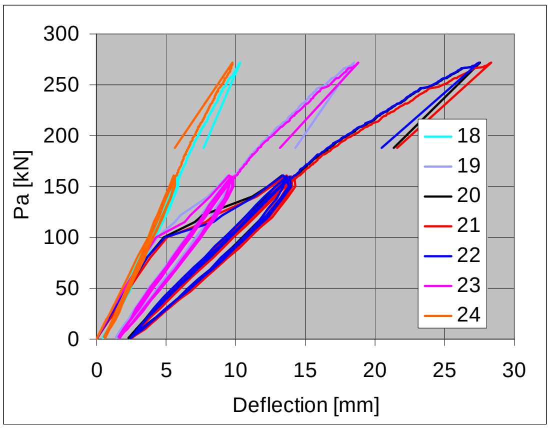

Fig. 37. Deflection on line II in the middle of slabs 1–6.

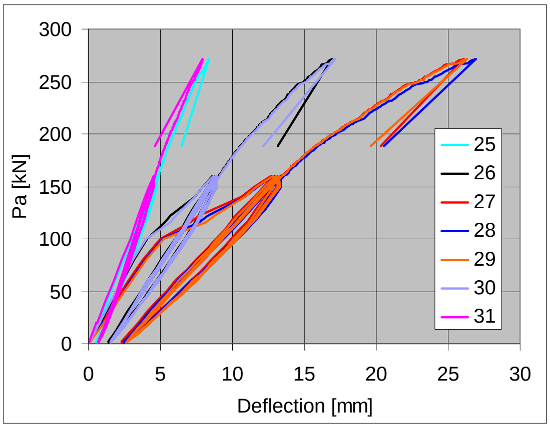

Fig. 38. Deflection on line III close to the line load, slabs 1–6.

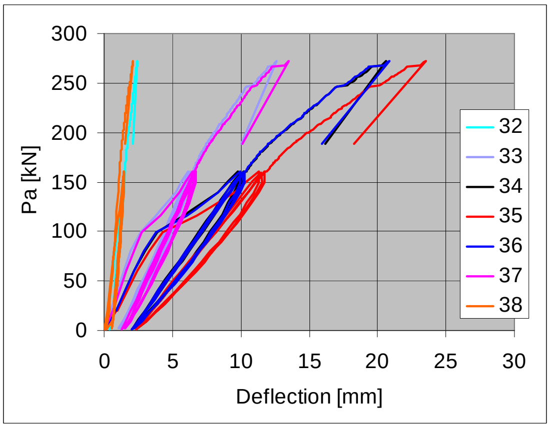

Fig. 39. Deflection on line IV along the middle beam.

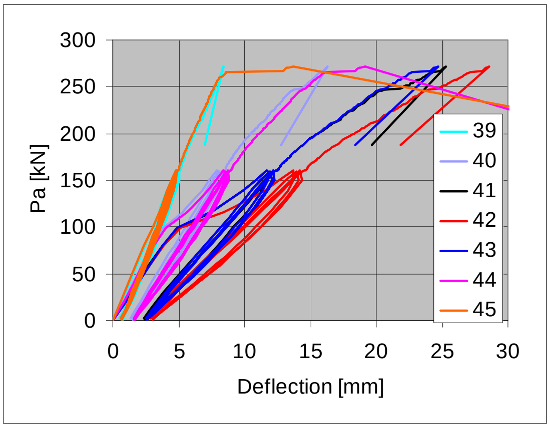

Fig. 40. Deflection on line V close to the line load, slabs 7–12.

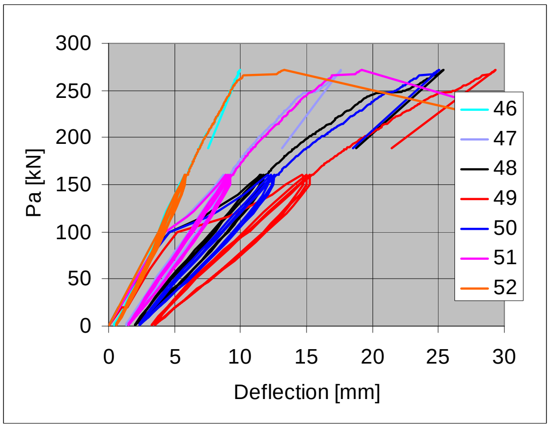

Fig. 41. Deflection on line VI in the middle of slabs 7–12.

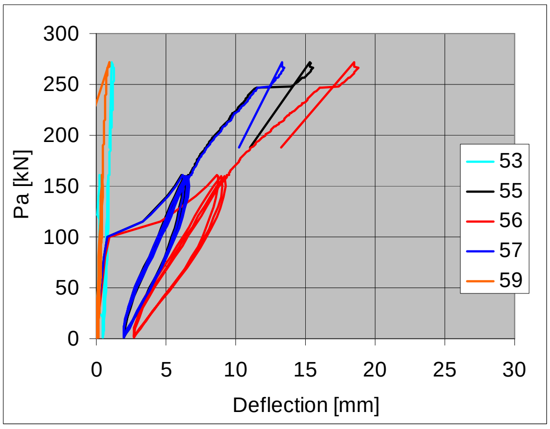

Fig. 42. Deflection on line VII along Eastern end beam, slabs 7–12.

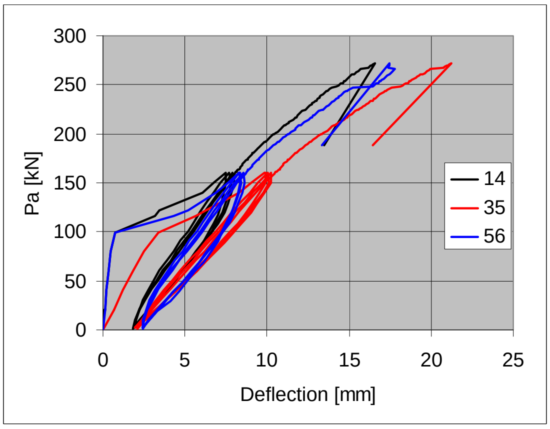

Fig. 43. Net deflection of midpoint of middle beam (35) and those of end beams (14, 56) (Rigid body motion due to settlement of supports eliminated).

10.2
Crack width

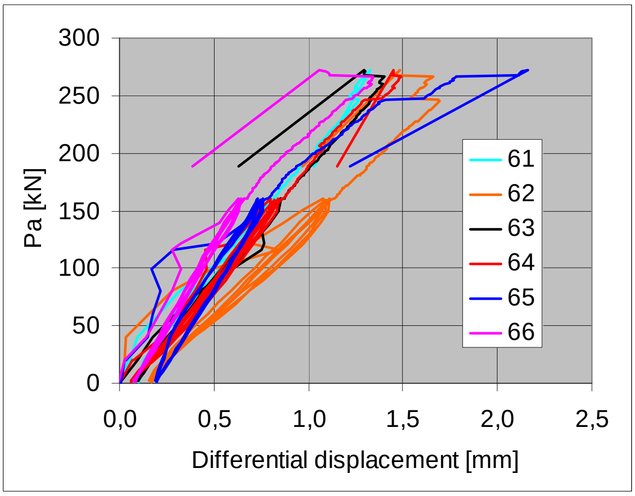

Fig. 44. Differential displacement parallel to the slab between the middle beam and the slabs (≈ crack width). See Fig. 18 for the location of the transducers.

10.3
Average strain

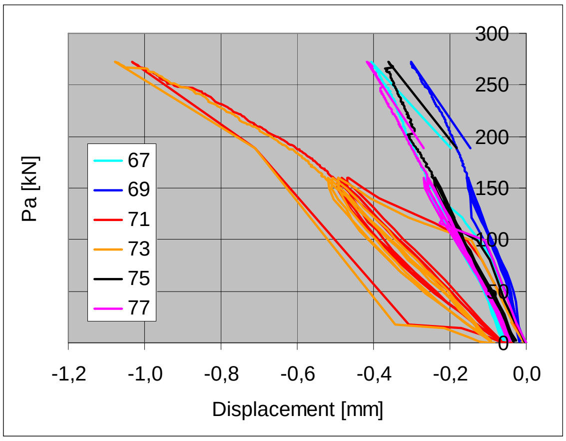

Fig. 45. Differential displacement at top surface of floor measured by transducers 57, 59, 61, 63, 65 and 67.

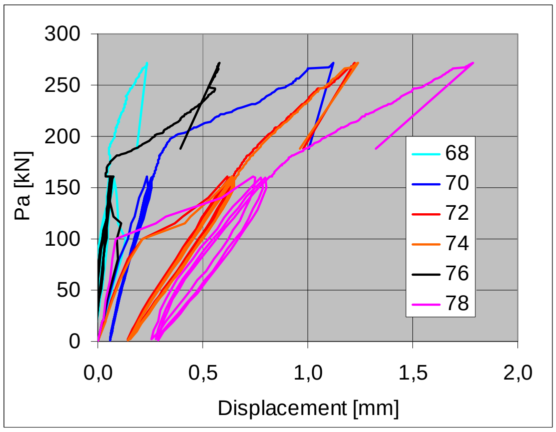

Fig. 46. Differential displacement at soffit of floor measured by transducers 58, 60, 62, 64, 66 and 68.

10.4
Shear displacement

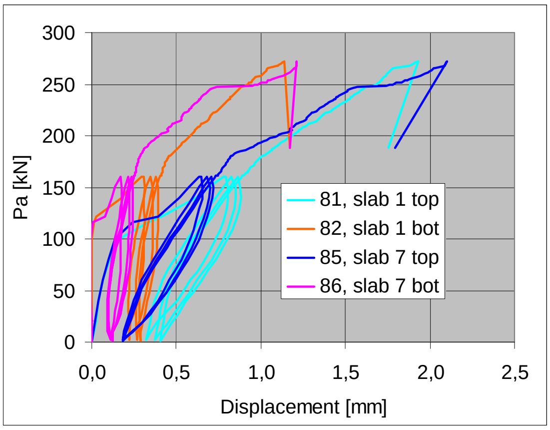

Fig. 47. Northern end of middle beam. Differential displacement between edge of slab and middle beam. A positive value means that the slab is moving towards the end of the beam.

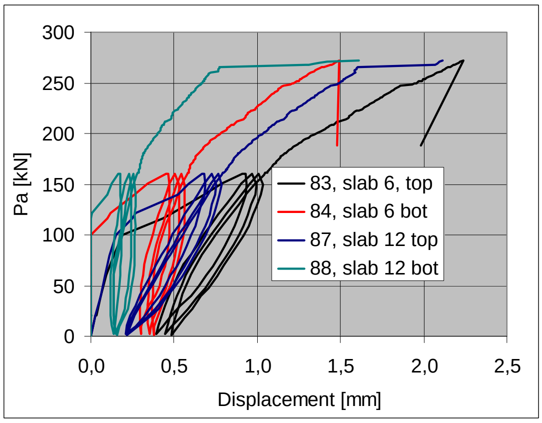

Fig. 48. Southern end of middle beam. Differential displacement between edge of slab and middle beam. A positive value means that the slab is moving towards the end of the beam.

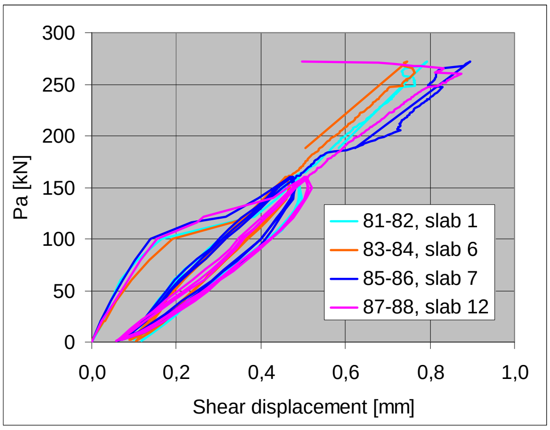

Fig. 49. Differential displacement between top and bottom edge of slabs 1, 6, 7 and 12.

11	**Reference tests**
	One end of slab 13 was loaded in shear as shown in Fig. 50. Test slab 13 was taken from the same casting lot as slab 12 which failed in the floor test. In the reference test the span of the slab was 9900 mm. At actuator load P_a = 250 kN (V_p = 427 kN) a flexural crack was observed below the line load. A web shear failure took place at P_a = 362,5 kN. No remarkable slippage of the strands was observed before the failure. The loading strategy is shown in Fig. 51. The failure mode is shown in Fig. 52and in App. A, Figs 62 and 63. The aim was to load both ends of slab 13. This was not possible because the other slab end deteriorated in the first test. The measured displacements are given in Fig. 53. The shear resistance 650,7 kN observed in the test is higher than the average value for normal production. 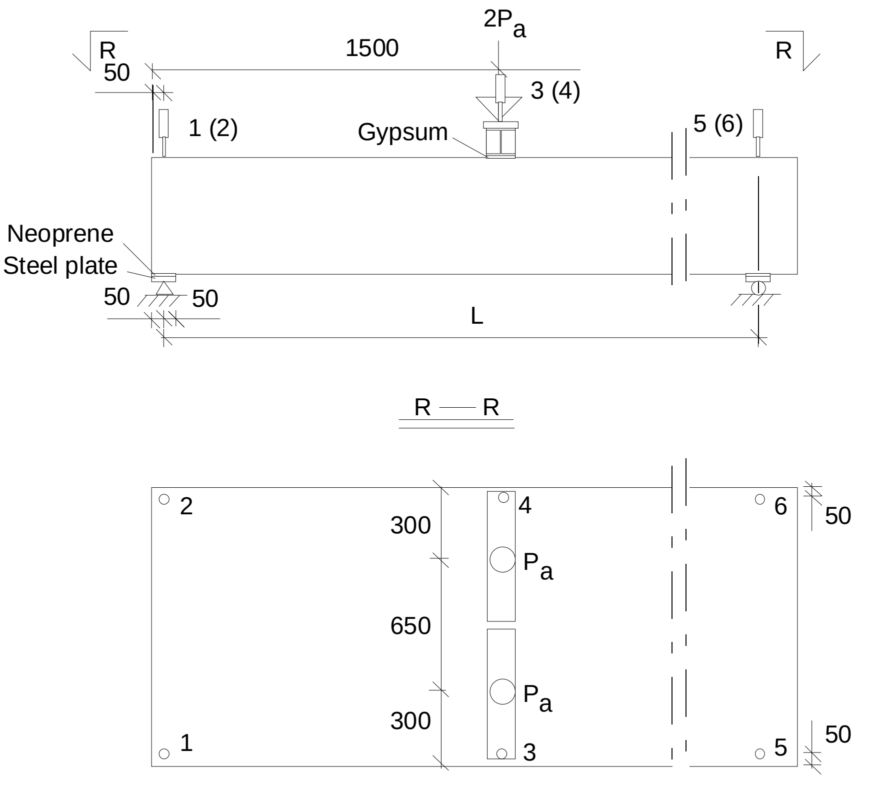 *Fig. 50. Layout of reference test. For L, see the next table.*

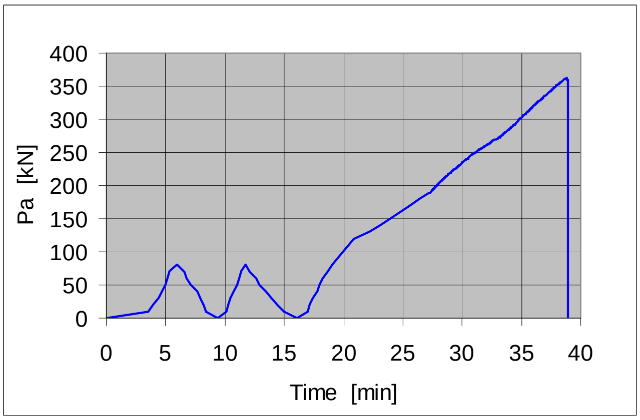

Fig. 51. Actuator force – time relationship.

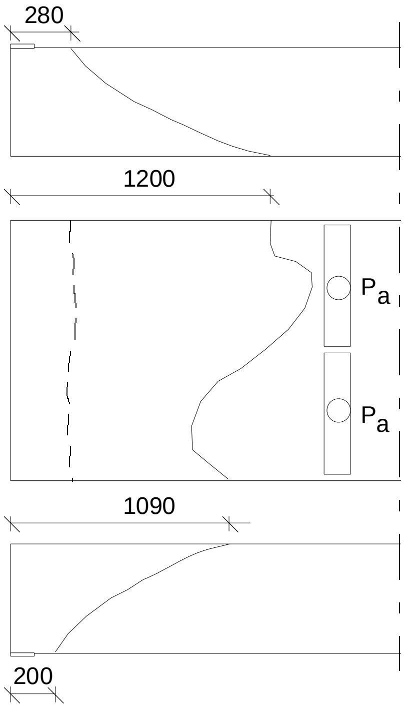

Fig. 52. Failure mode

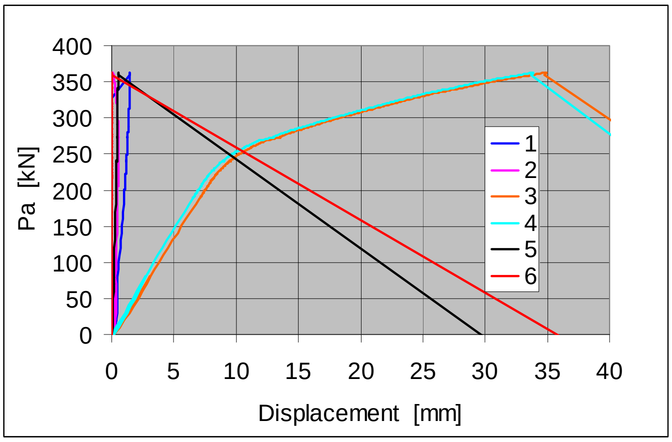

Fig. 53. Displacements measured by transducers 1–6.

Table. Span of slab L, shear force V_g at support due to the self weight of the slab, actuator force P_a at failure, weight of loading equipment P_{eq}, shear force V_p due to imposed load at failure, total shear force V_{obs} at failure and total shear force v_{obs} per unit width.

Test	Date	L mm	V_g kN	P_a kN	P_{eq} kN	V_{pa+eq} kN	V_{obs} kN	v_{obs} kN/m
R1	29.8.2005	9900	31,63	362,5	0,29	619,06	650,7	542,2

12	**Comparison: floor test vs. reference tests**
	The observed shear resistance (support reaction) of the hollow core slab in the floor test was equal to 269,6 kN per one slab unit or 224,7 kN/m. This is **41%** of the shear resistance observed in the reference test.
13	**Discussion**
	1. At failure, the net deflection of the middle beam due to the imposed actuator load (deflection minus settlement of supports) was 21,2 mm or *L*/340, i.e. rather small. 2. The shear resistance measured in the reference test was considerably higher than the mean of observed values for similar slabs given in *Pajari, M. Resistance of prestressed hollow core slab against web shear failure. VTT Research Notes 2292, Espoo 2005*. 3. The shear resistance observed in the floor test was 41% of that in the reference test. 4. The core fillings in the floor tests were not perfect. This may have affected the shear resistance. 5. The torsional stresses due to the different deflection of the middle beam and end beams had a negligible effect on the failure of the slabs because the maximum difference in the net mid-point deflection was less than 4,7 mm. 6. The bond between the smooth edges of the middle beam and the grout was weak. 7. The bond between the soffit of the slab and the grout below it was also weak. Due to the weak bond, the edge slabs slided along the beam before failure. This reduced the negative effects of the transverse actions in the slab and had a positive effect on the shear resistance

APPENDIX A: PHOTOGRAPHS

Fig. 1. WQ beam.

Fig. 2. Initial crack in slab 1.

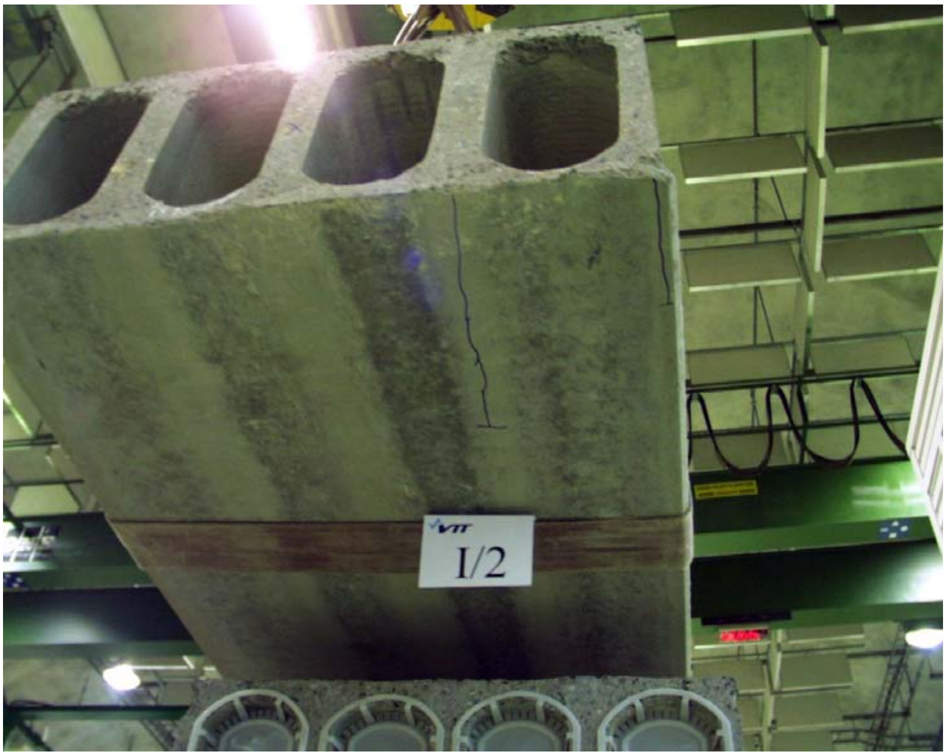

Fig. 3. Initial cracks in slab 2.

Fig. 4. Initial crack in slab 3.

Fig. 5. Initial crack in slab 4.

Fig. 6. Initial cracks in slab 5.

Fig. 7. Initial crack in slab 7.

Fig. 8. Initial crack in slab 8.

Fig. 9. Initial cracks in slab 9.

Fig. 10. Initial crack in slab 11.

Fig. 11. Slabs 1,2,6,7,8 and 12 in their final position.

Fig. 12. Slab 12 on WQ beam and a tie bar 20 mm.

Fig. 13. A short, bent tie bar, outer edge of slab 1.

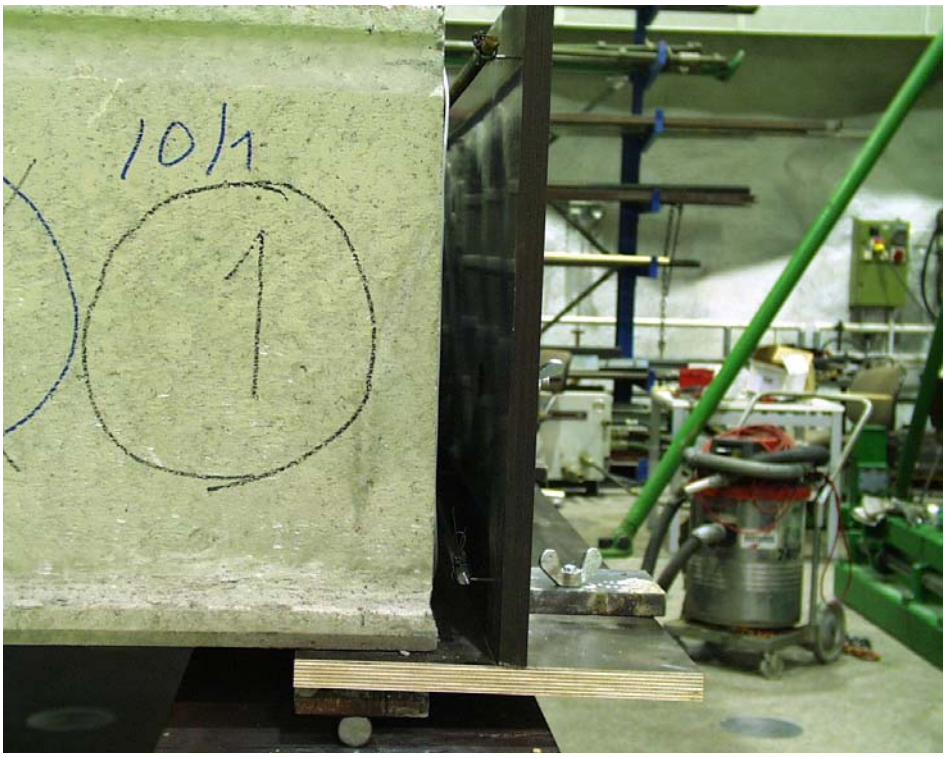

Fig. 14. Support conditions above end beam.

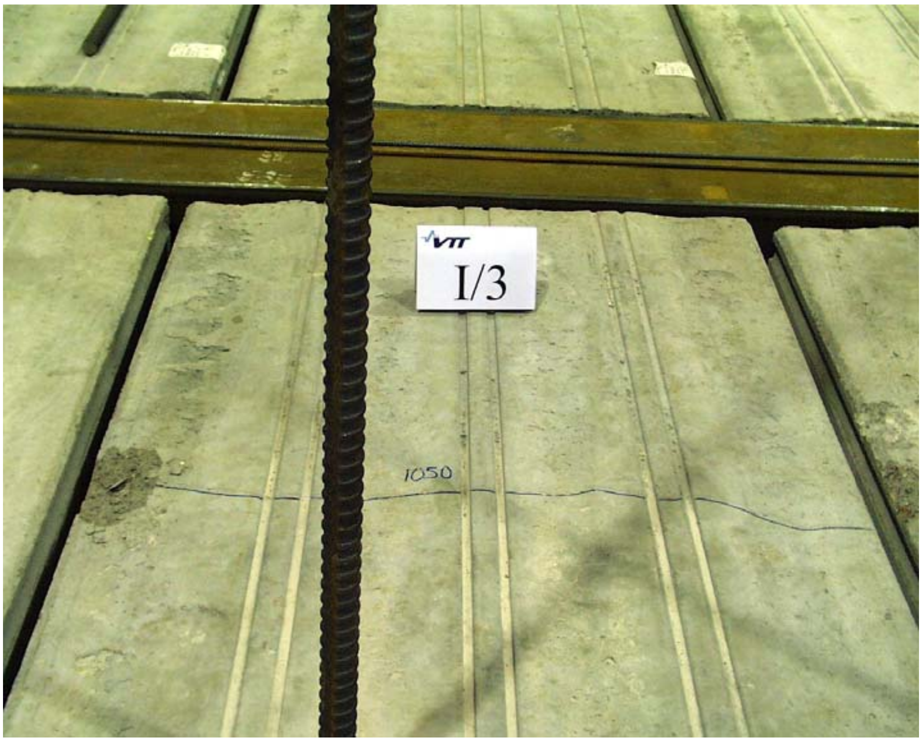

Fig. 15. Initial bending crack in slab 3 at a distance of 1050 mm from slab end.

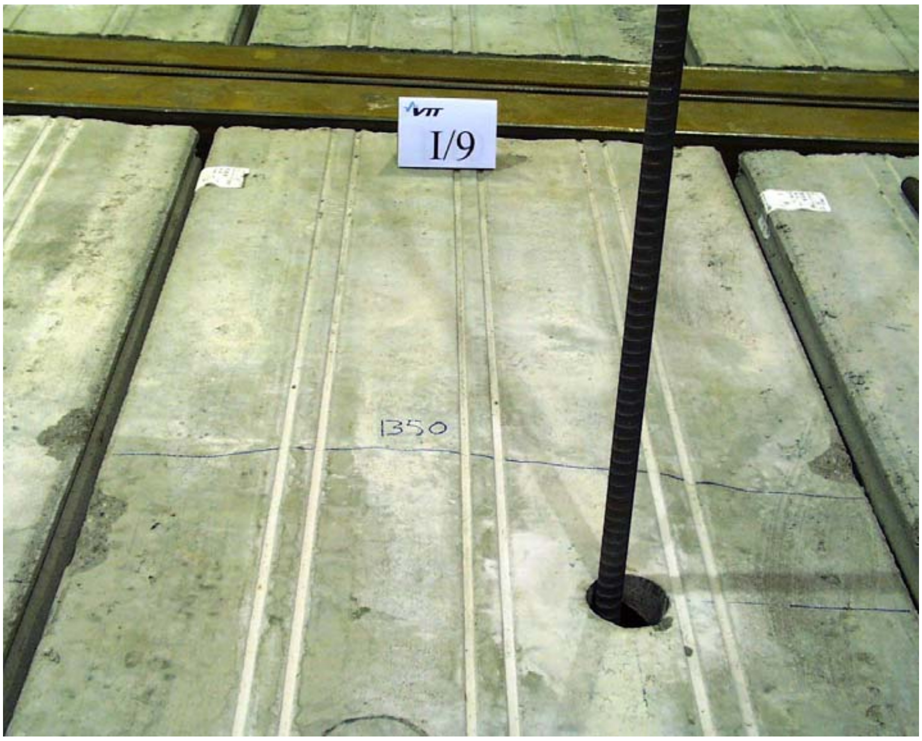

Fig. 16. Initial bending crack in slab 9 at a distance of 1350 mm from slab end.

Fig. 17. Overview on test arrangements.

Fig. 18. View on the loading frame and spreader beams.

Fig. 19. Actuators above primary spreader beams.

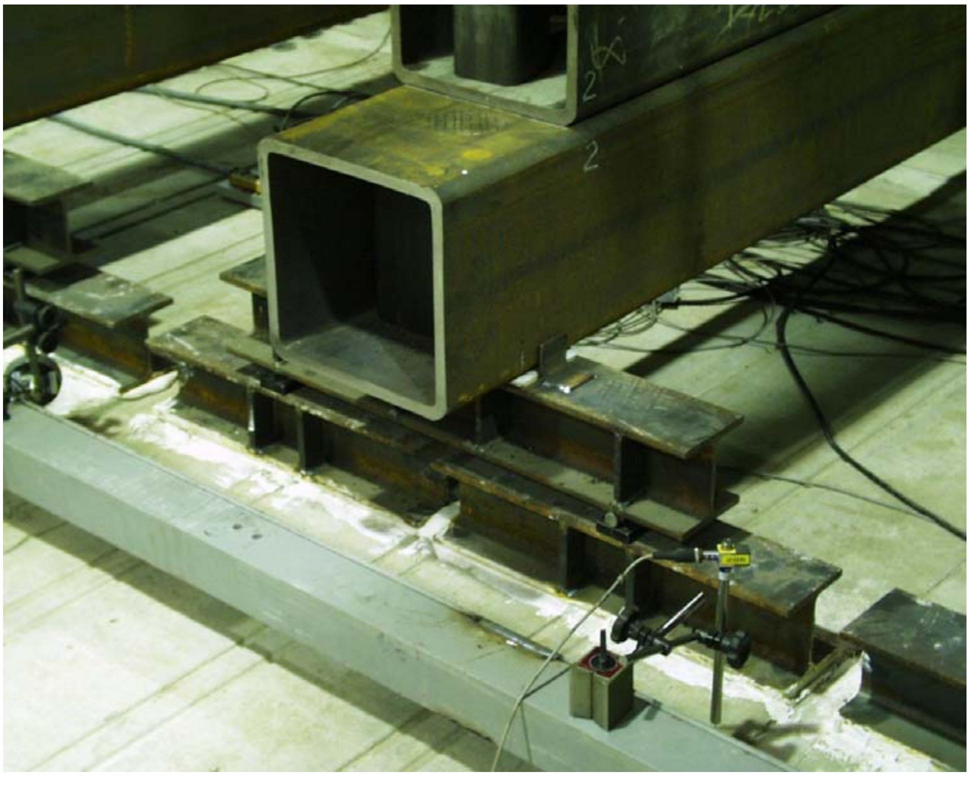

Fig. 20. Arrangements between spreader beams. Note the white teflon sheets between the primary and secondary spreader beams.

Fig. 21. Three orange load cells below one support of WQ beam.

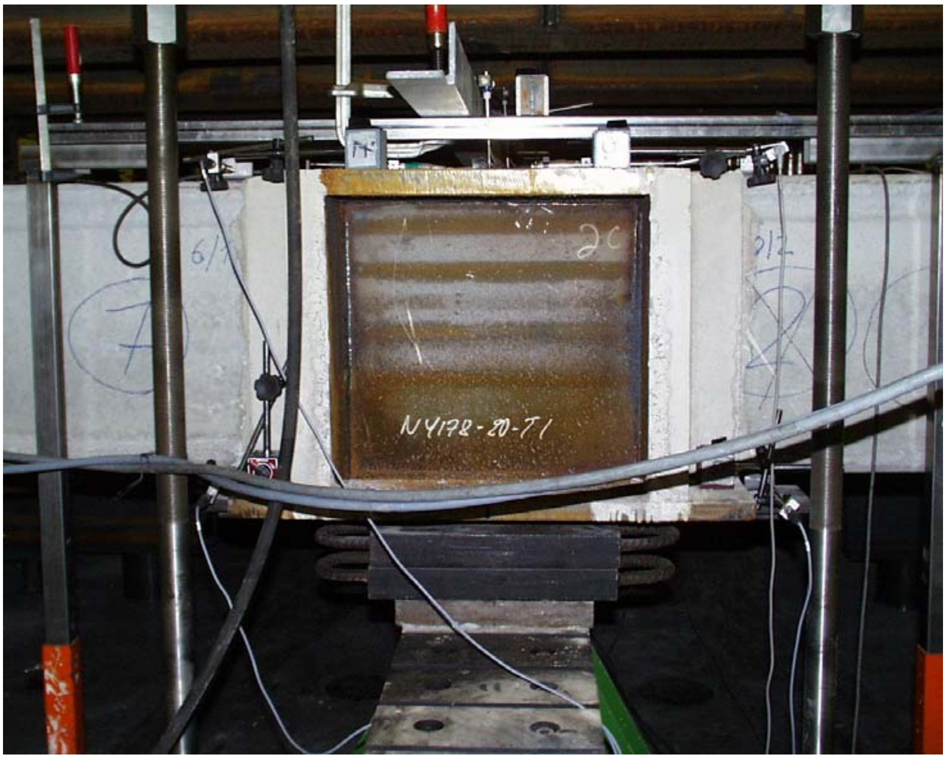

Fig. 22. North end of WQ beam before loading.

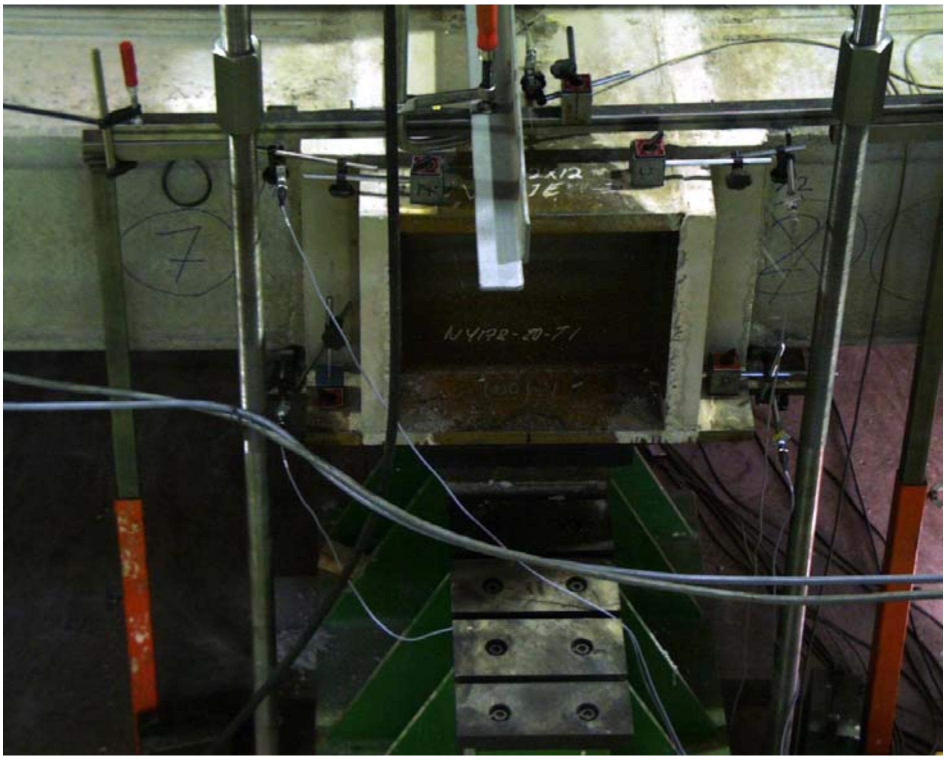

Fig. 23. North end of WQ beam before loading.

Fig. 24. Longitudinal crack in the soffit of slab 10 at P_a = 160 kN. The cracking took place at P_a = 109 kN.

Fig. 25. Inclined crack in slab 7 at P_a = 213 kN.

Fig. 26. Failure of slab 12 at P_a = 272 kN.

Fig. 27. Failure of slab 12 at P_a = 272 kN.

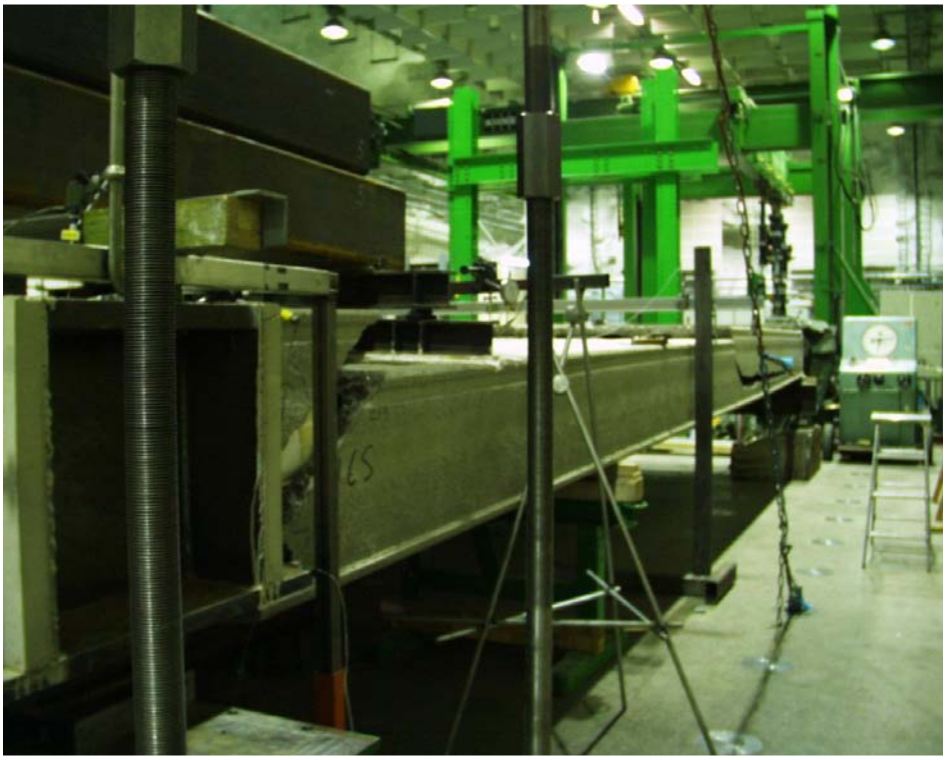

Fig. 28. Failure of slab 12 at P_a = 272 kN.

Fig. 29. Failure of slab 12 at P_a = 272 kN.

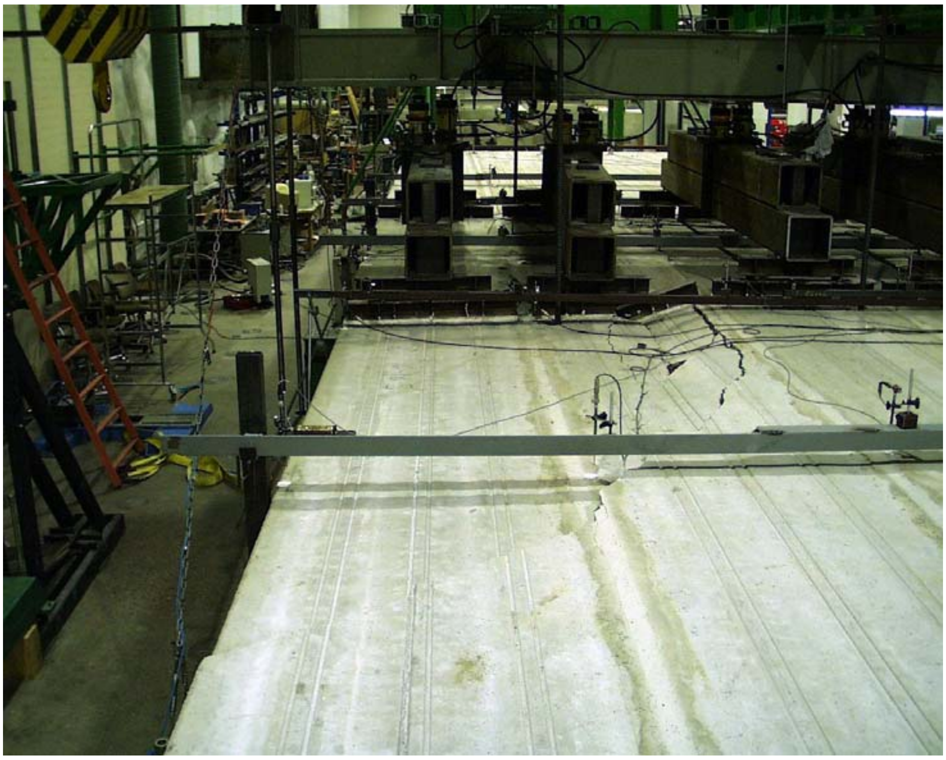

Fig. 30. Failure of slabs 11 and 12 at P_a = 272 kN.

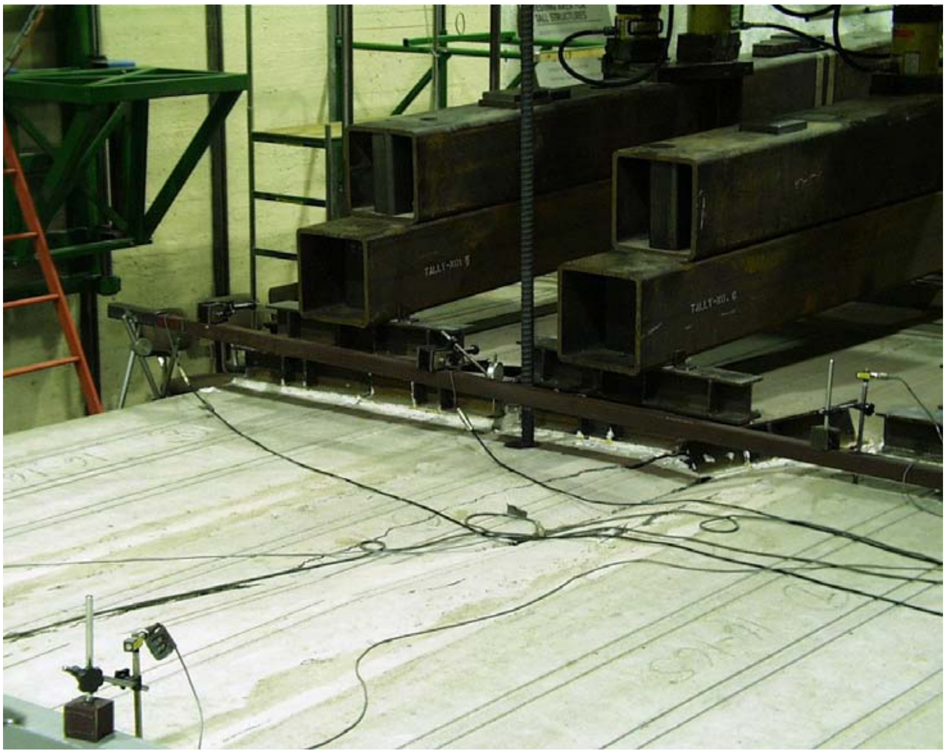

Fig. 31. Failure of slabs 11 and 12 at P_a = 272 kN.

Fig. 32. Slabs 11 and 12 after removing the loading equipment.

Fig. 33. Slabs 11 and 12 after removing the loading equipment.

Fig. 34. Slab 7 after test. Cracks in tie beam. The read line and capital A indicate an initial crack.

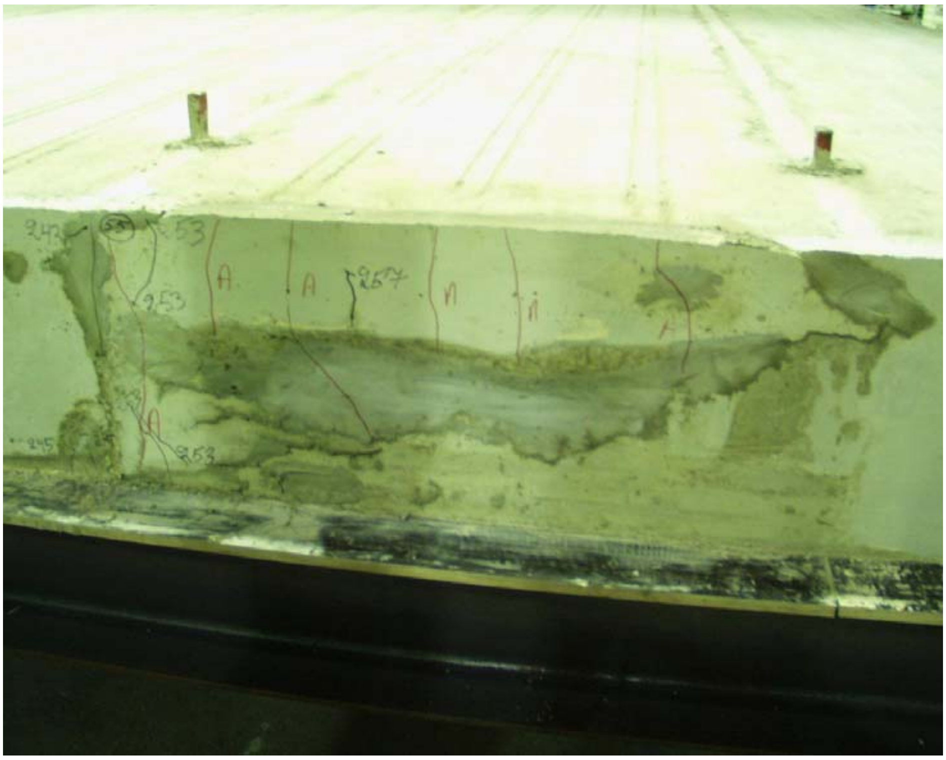

Fig. 35. Slab 8 after test. Cracks in tie beam. The read line and capital A indicate an initial crack. The nonuniform colour is due to a mortar treatment carried out after demolding.

Fig. 36. Slab 9 after test. Cracks in tie beam.

Fig. 37. Slab 10 after test. Cracks in tie beam.

Fig. 38. Slab 11 after test. Cracks in tie beam.

Fig. 39. Slab 12 after test. Cracks in tie beam.

Fig. 40. Slab 1 after test.

Fig. 41. Slab 1 after test.

Fig. 42. Slab 6 after test.

Fig. 43. Slab 12 after test.

Fig. 44. Slab 1 after test.

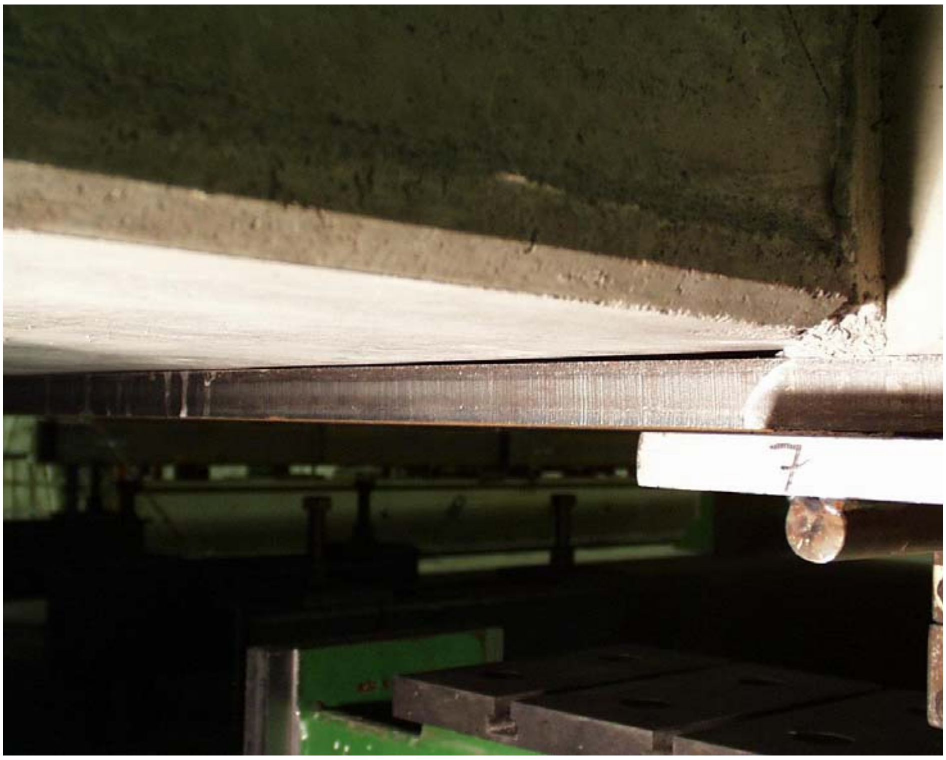

Fig. 45. Slab 7 after test.

Fig. 46. Slab 7 after test.

Fig. 47. Slab 6 after test.

Fig. 48. Failure surface at end of slab 1. Note the incomplete filling of the cores.

Fig. 49. Concrete filling taken from one core of slab 12.

Fig. 50. Concrete filling in one core of slab 2. Note that the polystyrene plug is inclined due to the casting pressure. Consequently, the length of the filling at the bottom is greater than 400 mm.

Fig. 51. Failure surface of slabs 11 and 12.

Fig. 52. Rough surface at slab end below even, saw-cut surface.

Fig. 53. Changes in colour on the flange below slab 1 due to the concrete or cement paste intruding into the gap between the soffit of the slab and the steel flange. See also the vertical stripes along the vertical edge of the flange.

Fig. 54. Thin layers of grout as well as changes in colour on the flange below slab 1 due to the grout intruding into the gap between the soffit of the slab and the steel flange.

Fig. 55. Thin layers of grout as well as changes in colour on the flange below slab 1 due to the grout intruding into the gap between the soffit of the slab and the steel flange.

Fig. 56. Thin layers of grout as well as changes in colour on the flange below slab 1 due to the grout intruding into the gap between the soffit of the slab and the steel flange.

Fig. 57. A detail of grout below slab 6.

Fig. 58. Grout below slab 5.

Fig. 59. Steel flange below slab 7. No clear sign of grout can be seen below the slab and above the flange.

Fig. 60. Overview on arrangements in reference test.

Fig. 61. Loading arrangements in reference test.

Fig. 62. Failure pattern in reference test. South edge.

Fig. 63. Failure pattern in reference test. North edge.

<table>
<tr><td>1</td><td>General information</td></tr>
<tr><td>1.1
Identification and aim</td><td>VTT.PC.InvT.500.2006   Last update 2.11.2010
PC500   (Internal identification)
Aim of the test   To study the shear resistance of 500 mm slab supported on concrete beams.</td></tr>
<tr><td>1.2 Test type</td><td>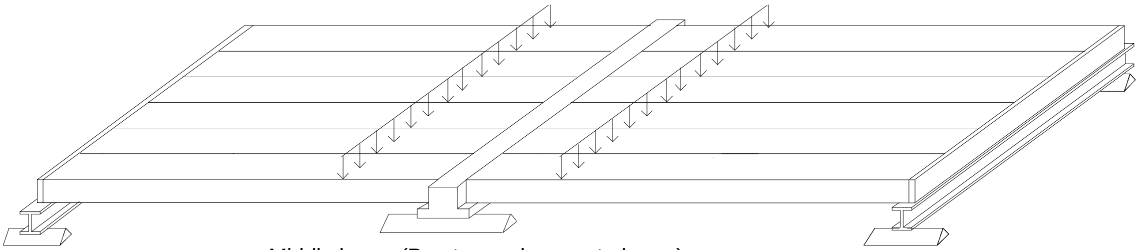

Fig. 1. Illustration of test setup. The end beams were hot-rolled steel beams.</td></tr>
<tr><td>1.3 Laboratory & date of test</td><td>VTT/FI   29.9.2005</td></tr>
<tr><td>1.4 Test report</td><td>Author(s)   Pajari, M.
Name   Load test on hollow core slab floor with concrete beam
Ref. number   VTT-S-2303-06
Date   9.3.2006
Availability   Available at www.rakennusteollisuus.fi</td></tr>
<tr><td>2</td><td>Test specimen and loading</td></tr>
</table>

2.1
General plan

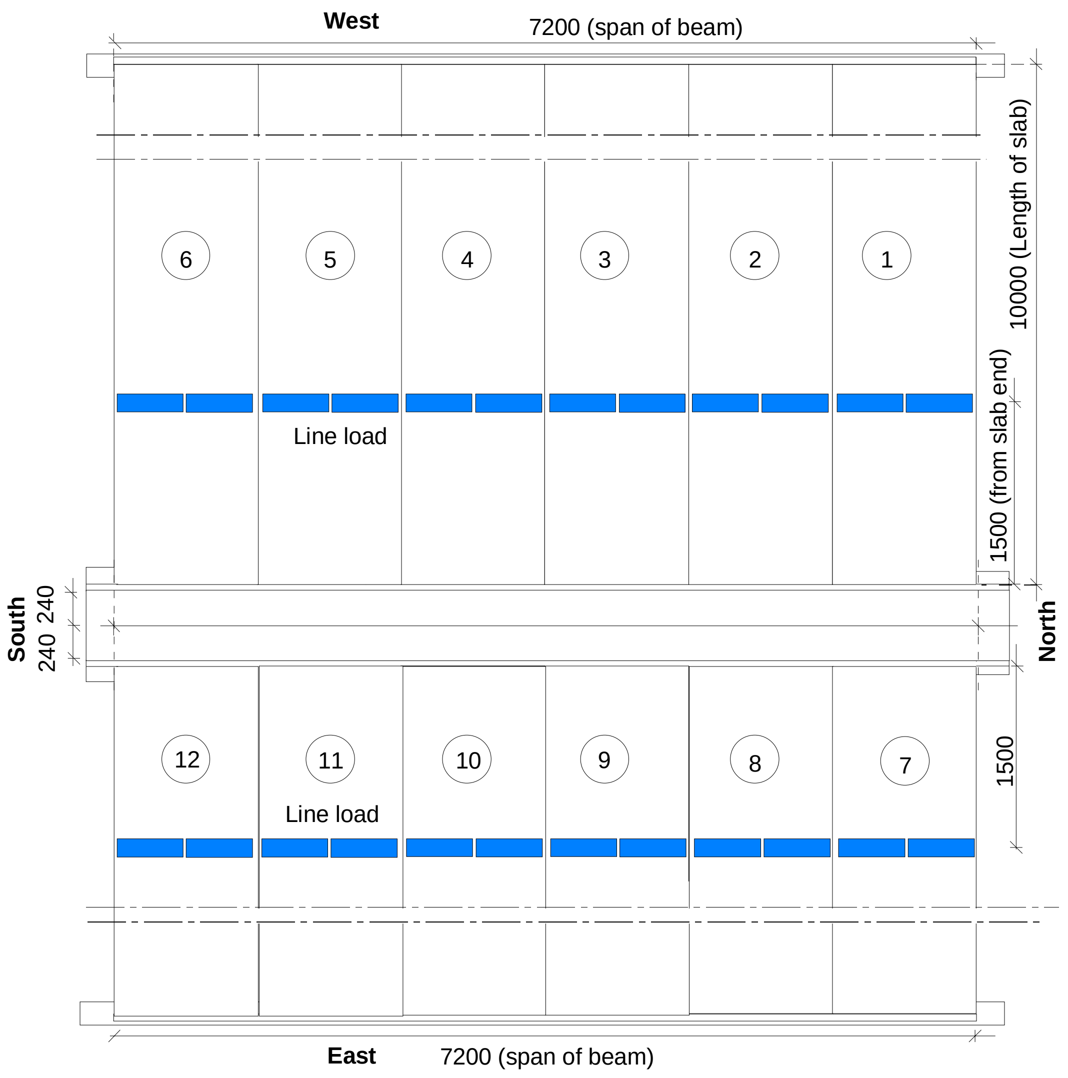

Fig. 2. Plan.

2.2
End beams

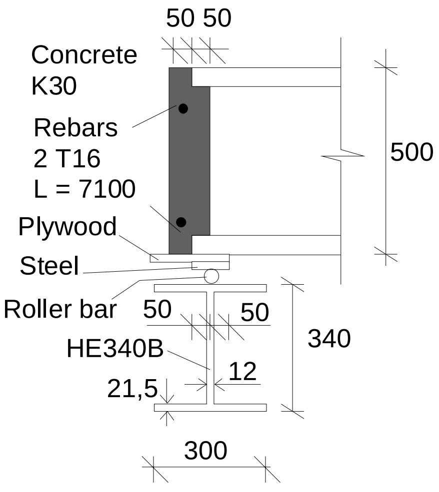

Fig. 3. Arrangements at end beam.

Simply supported, span = 7,2 m, roller bearing below Northern end
$f_y \approx$ 355 MPa (nominal f_y), did not yield in the test.

2.3
Middle beam

- Cast by Betonimestarit Oy, 4.8.2005
- Concrete K80
- Simply supported, span = 7,2 m, roller bearing at both ends

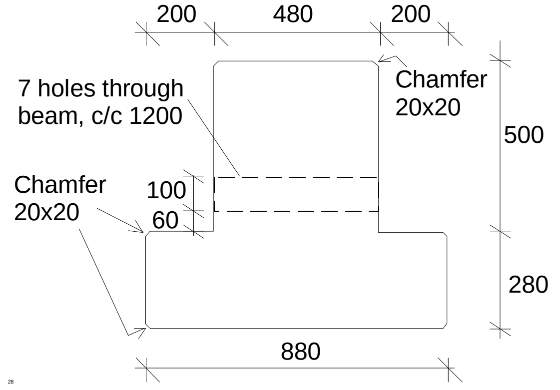

Fig. 4. Cross-sectional geometry.

Fig. 5. Longitudinal reinforcement. J12,5 refers to a prestressing strand; A1 and A2 to ribbed reinforcing bars, see below.

J12,5: Prestressing strand ϕ =12,5 mm, A_p = 93 mm^2, σ_{p0} = 1300 MPa, nominal strength $f_{p0,2}/f_p$ = 1630/1860 MPa, did not yield in the test

A1: Rebar A500HW, ϕ 12 mm, L = 7500 mm, nominal yield strength f_y = 500 MPa, did not yield in the test

A2: Rebar A500HW, ϕ 25 mm, L = 7500 mm, nominal yield strength f_y = 500 MPa, did not yield in the test

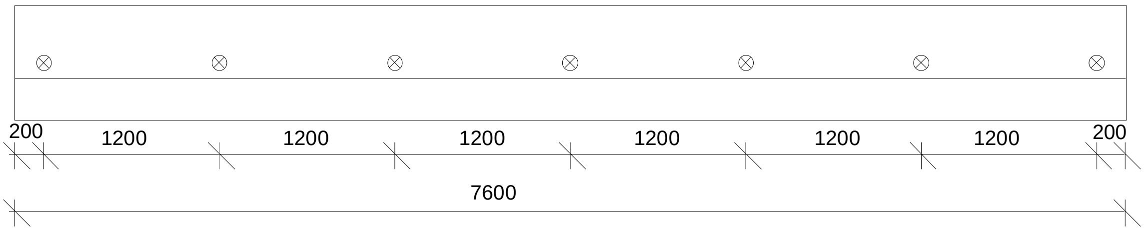

Fig. 6. Middle beam. Elevation.

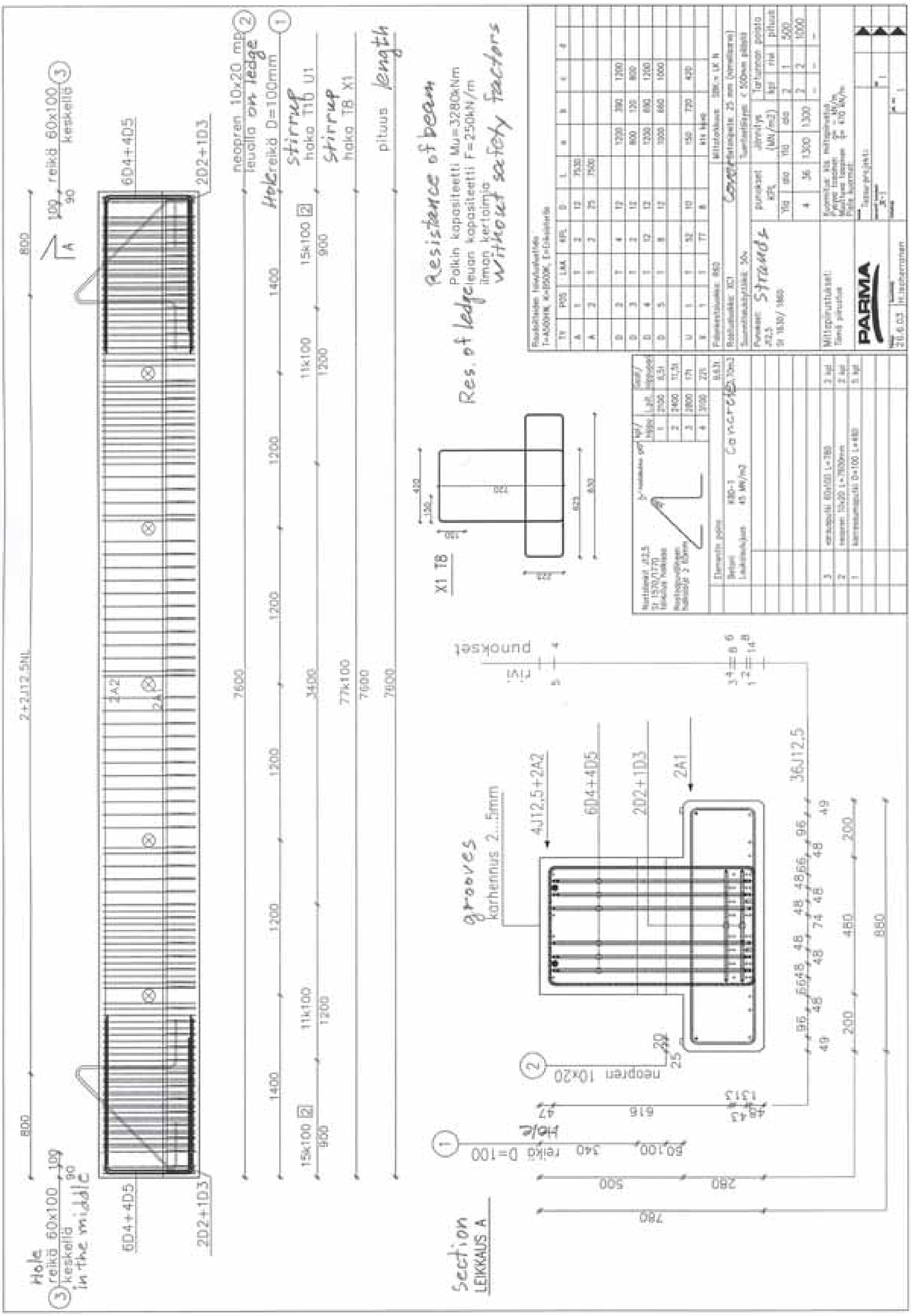

Fig. 7. Middle beam.

2.4
Arrangements at middle beam

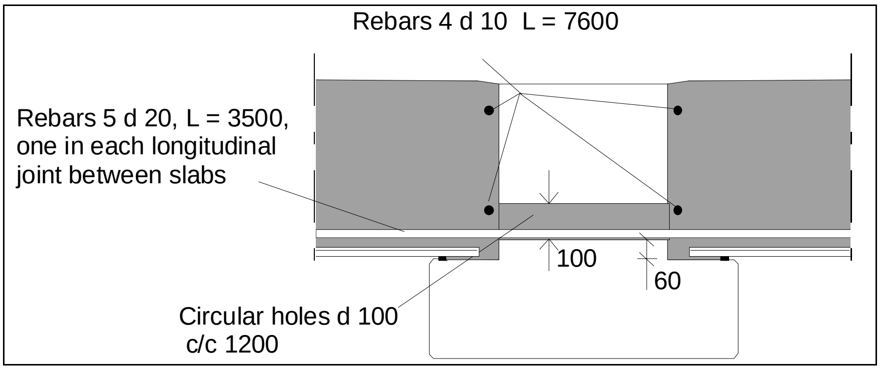

Fig. 8. Section along a joint between adjacent hollow core units.

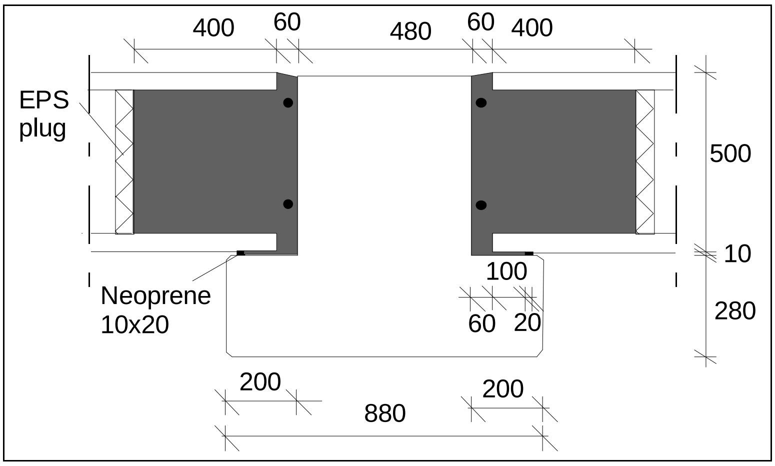

Fig. 9. Section along hollow cores. Plugs made of expanded polystyrene.

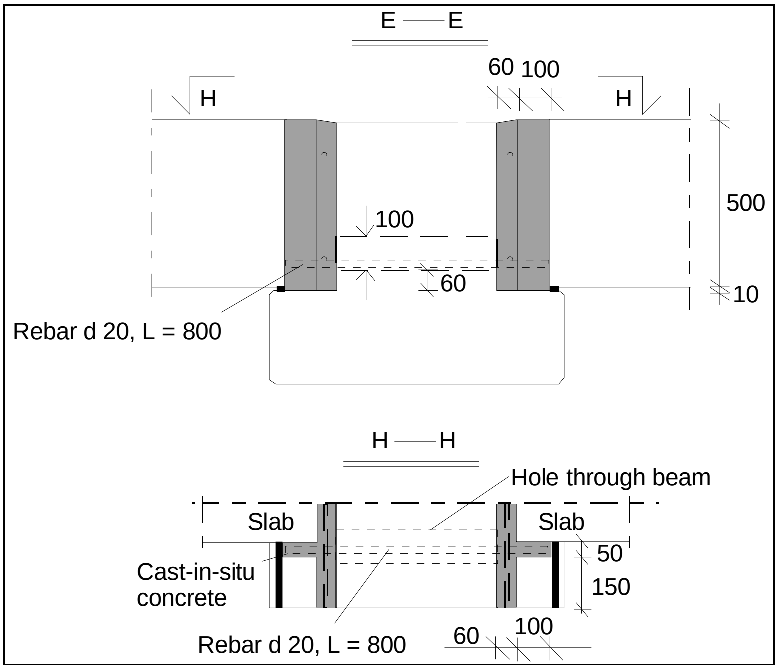

Fig. 10. Tie reinforcement in the cast-in-situ concrete outside the edge of the outermost slabs (section E-E in Fig. 15). See also App. A, Fig. 9.

Tie reinforcement: Straight horizontal rebars A500HW through the beam and parallel to the beam, nominal yield strength f_y = 500 MPa

2.5
Slabs

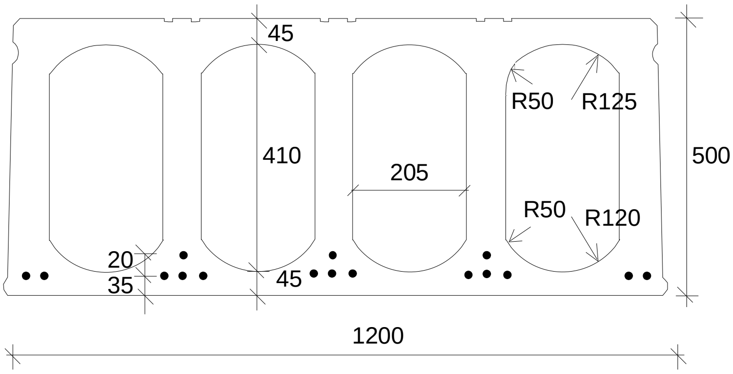

Fig. 11. Nominal geometry of slab units (in scale).

- Extruded by Parma Oy, Hyrylä factory 28.4.2005

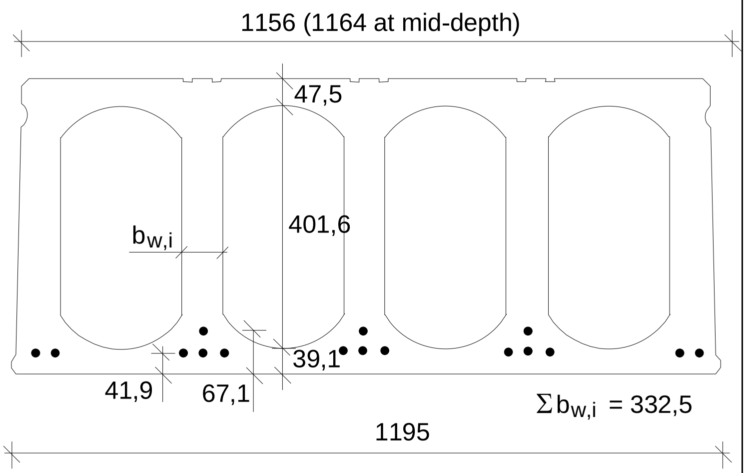

Fig. 12. Most relevant measured geometrical properties (average values).

In slabs 1–2, 5–8 and 12, one strand below the second web in the bottom layer was weakly bonded. Its slippage in all slab ends was 1,8–3,8 mm.

In other strands the max measured slippage was:
2,1 mm in slab 11
2 x 1,9 mm (in slab 5);
3 x 1,8 mm in slabs 2, 7 & 8

- Measured weight = 6,54 kN/m

2.6
Temporary supports

No

2.7
Loading arrangements

An auxiliary loading frame was built above the test floor. It was tied by tension bars to the floor of the research hall, see Figs 13 and 14. Six tension bars penetrated the floor through the hollow cores outside the line loads, the rest were outside the test specimen.

The loads were generated by 12 actuators. Taking into account the weight of the loading equipment P_{eq} = 6,22 kN / slab unit, the following relationship can be written for the line load on one slab:

$$F = P_a + 6{,}22 \text{ Kn} \qquad (1)$$

P_a is the load in the actuator. The line loads were applied to the slab units by 24 tertiary steel beams of the type HE 120 A (a hot-rolled I-beam with depth = 114 mm, width = 120 mm and thickness of flange = 8 mm), each 550 mm in length. The top surface of the slabs under these beams was evened out by gypsum. On the top of the tertiary beams, secondary spreader beams were placed, each on two bearings. On the top of the secondary beams, primary spreader beams were placed. The friction between the primary and secondary spreader beams was eliminated with teflon sheets, and that between the secondary and tertiary spreader beams with a freely rolling circular steel bar, see Figs 15–17. The drifting of the primary spreader beams was prevented by the friction at the upper and lower end of the actuators. The upper end of each actuator was provided with a swivel (ball bearing).

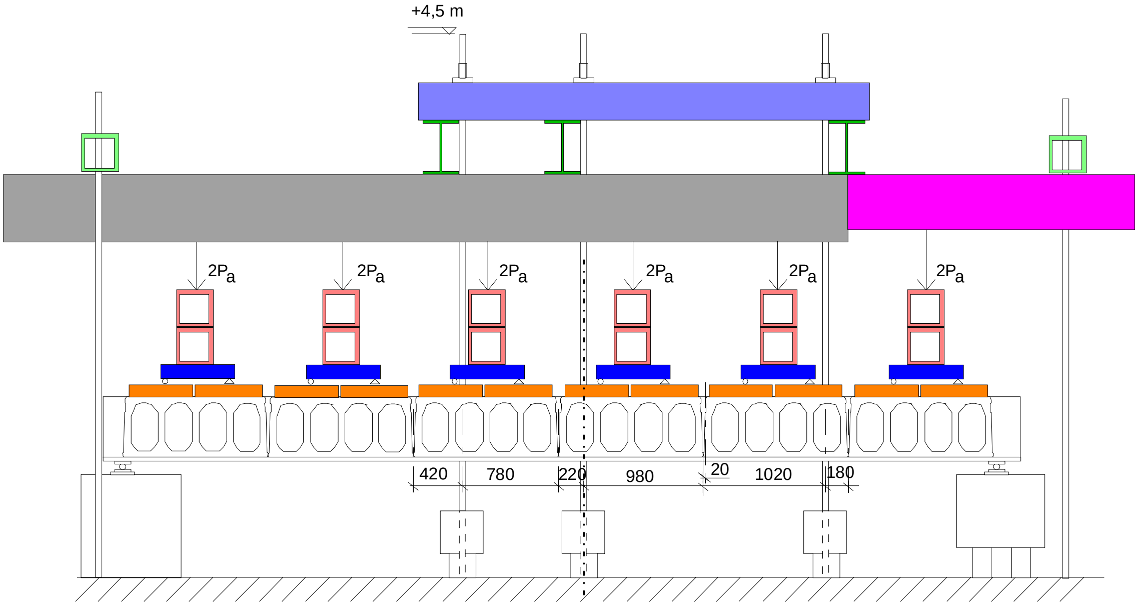

Fig. 13. Auxiliary loading frame. Elevation.

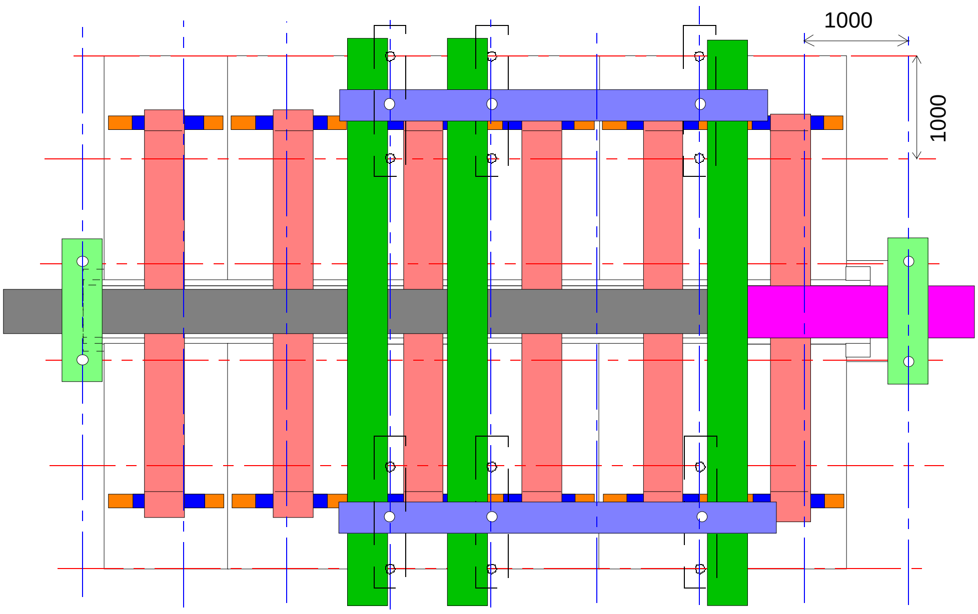

Fig. 14. Auxiliary loading frame. Plan. The position of the tension bars is indicated by white circles above the blue and green beams.

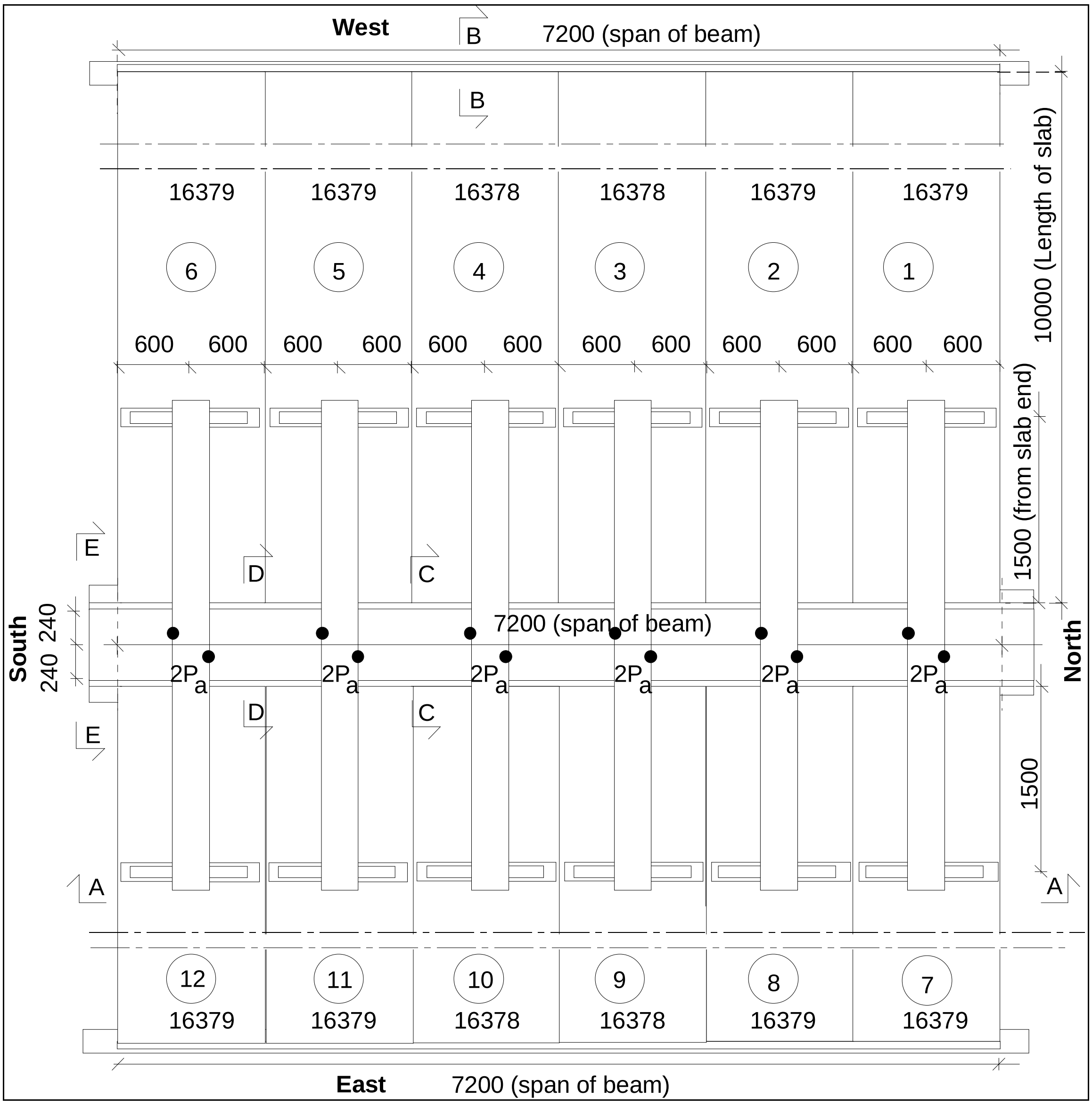

Fig. 15. Loading arrangements. The slabs are from two casting lots: 16377 and 16378. The position of the actuator loads is indicated by black circles above the middle beam.

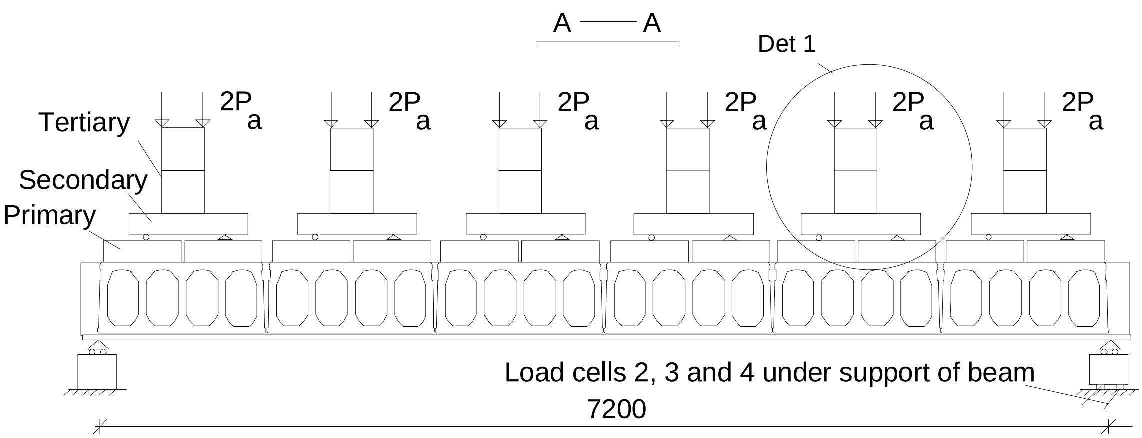

Fig. 16. Section A-A, see Fig. 15.

	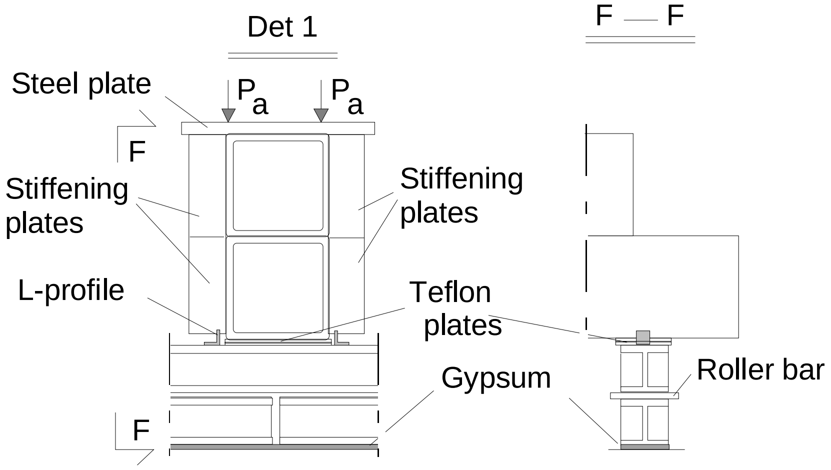 *Fig. 17. Detail 1, see Fig. 16.*
3	**Measurements**
3.1 Support reactions	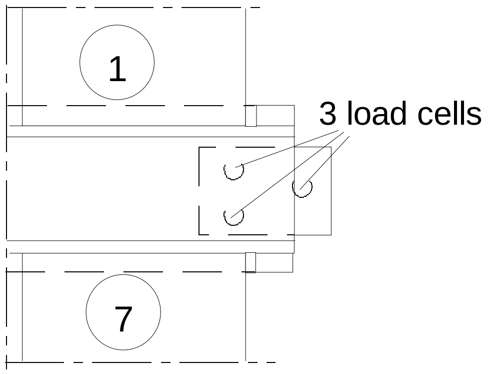 *Fig. 18. Load cells below the Northern support of the middle beam.*

3.2 Vertical displacement	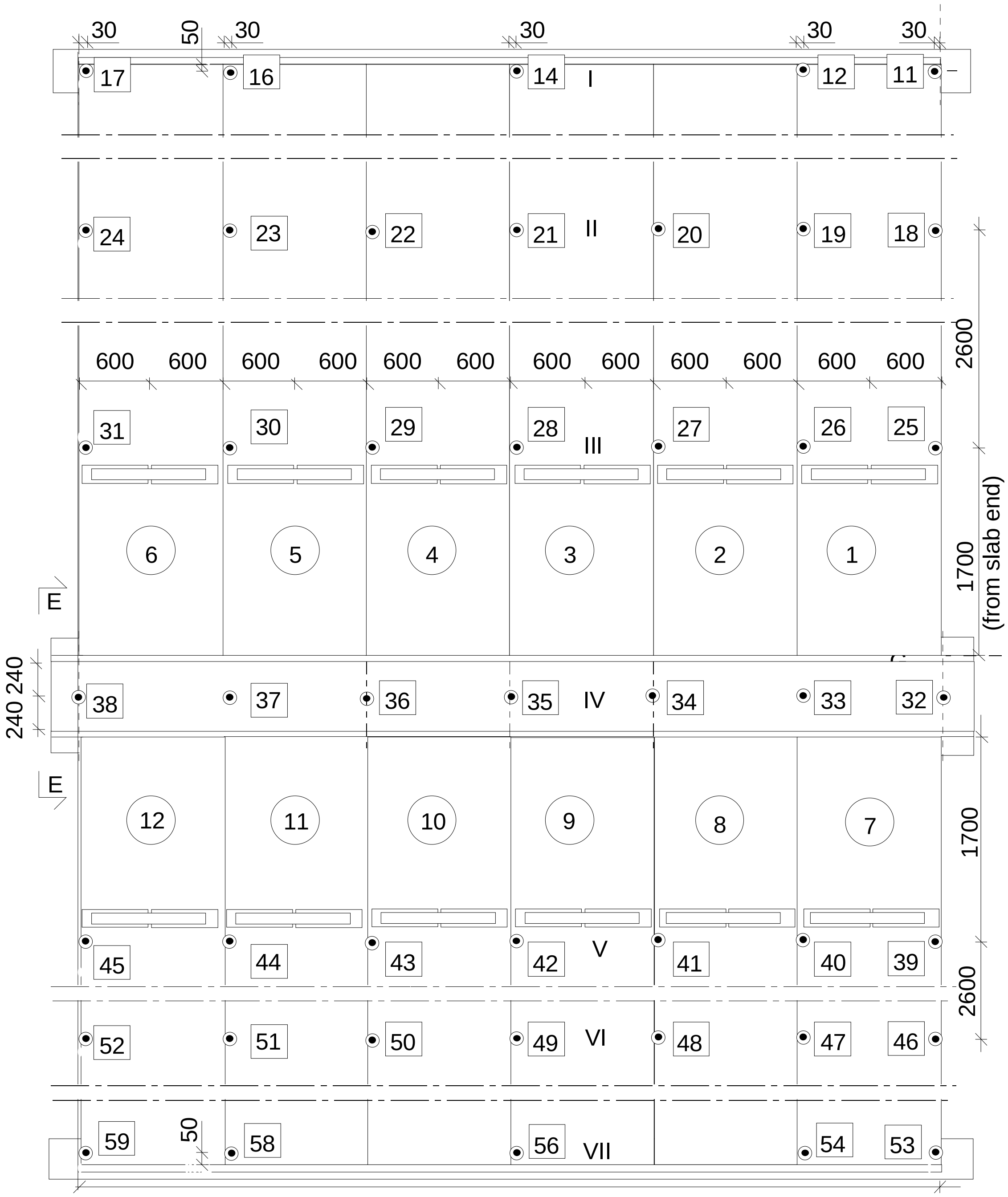 *Fig. 19. Location of transducers 11 … 59 for measuring vertical deflection along lines I … VII.*

3.3
Average strain

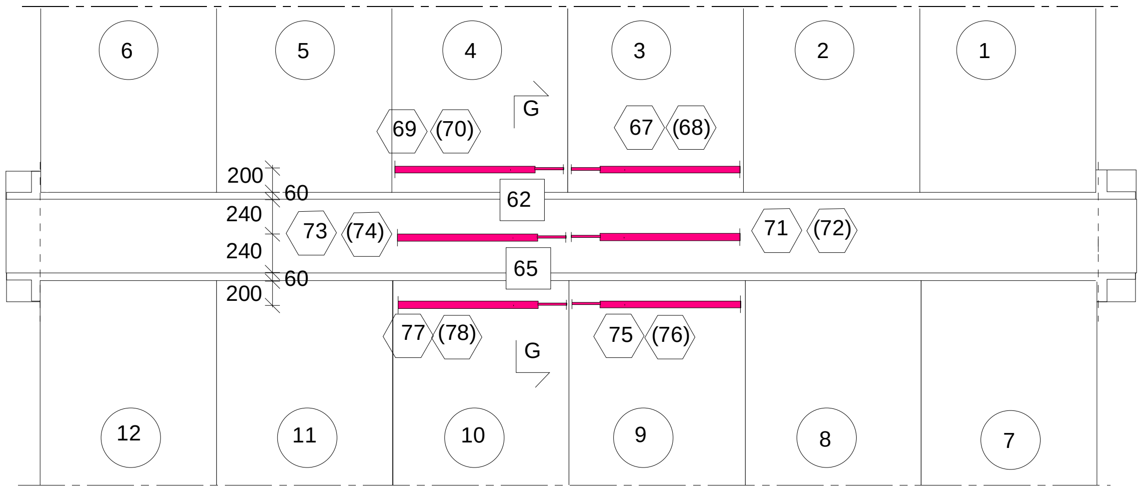

Fig. 20. Position of device (transducers 67–78) measuring average strain parallel to the beams.

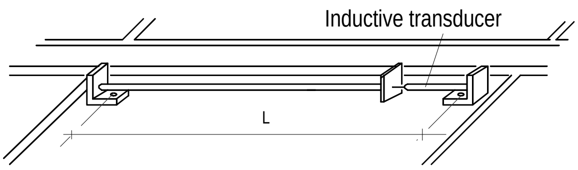

Fig. 21. Apparatus for measuring average strain. L = 1100 mm.

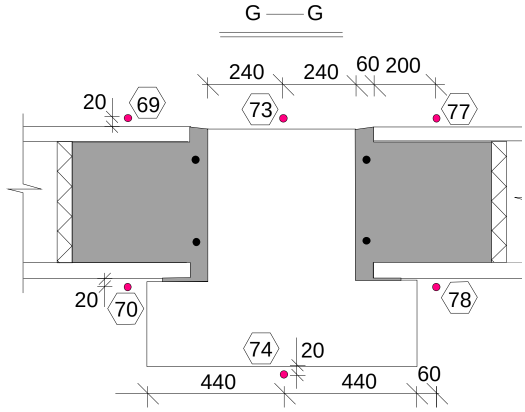

Fig. 22. Section G-G, see Fig. 20.

3.4
Horizontal displacements

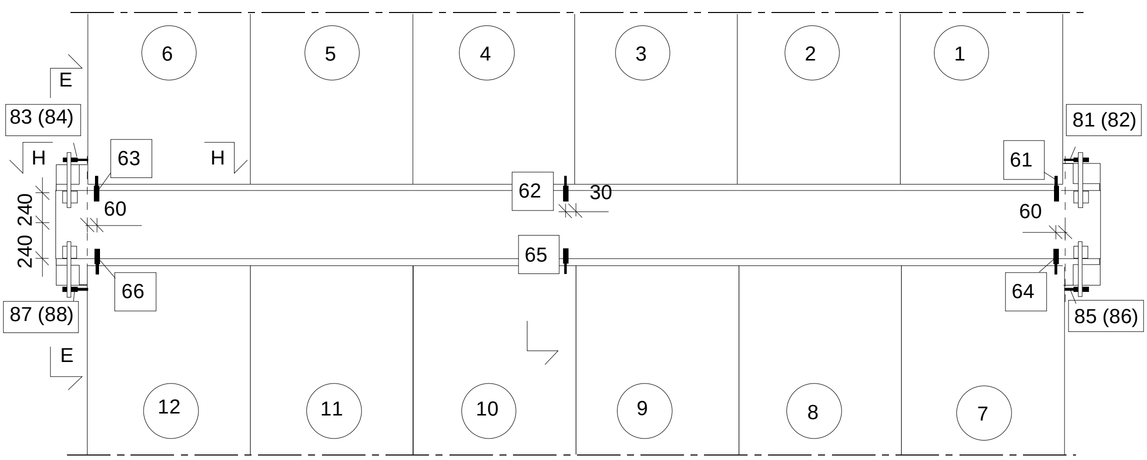

Fig. 23. Transducers measuring crack width (61–66) and shear displacement at the ends of the middle beam (81–88). Transducers 82, 84, 86 and 88 are below transducers 81, 83, 85 and 87, respectively.

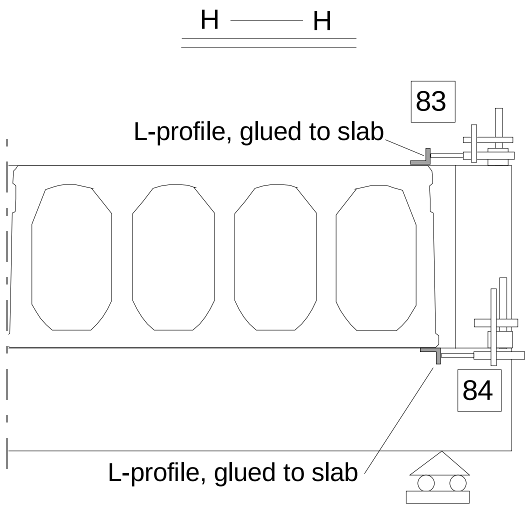

Fig. 24. Section H-H, see Fig. 23.

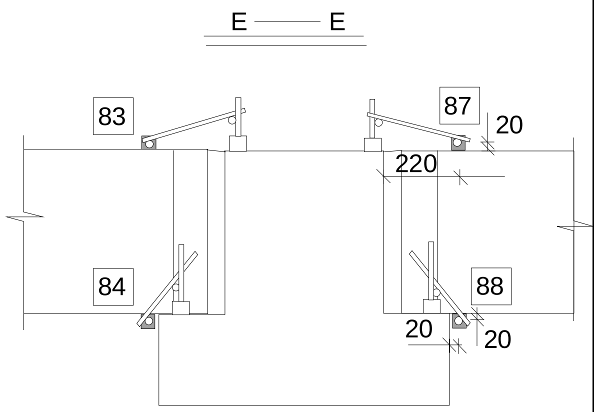

Fig. 25. Section J-J, see Fig. 23.

4 Special arrangements

- None

5 Loading strategy

5.1
Load-time relationship

The loads were applied in two stages: Stage I and Stage II as shown in Fig. 26: Stage II represents the post-failure loading. Measured results are given only for Stage I.

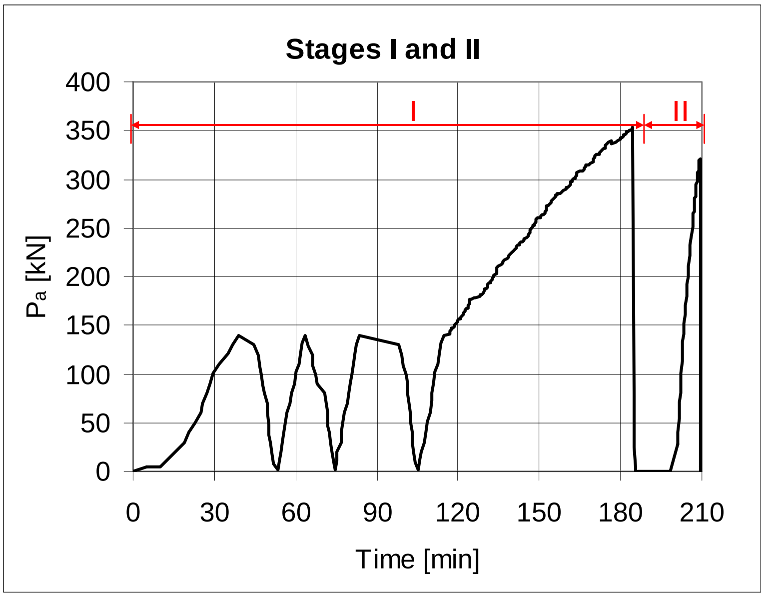

Fig. 26. Actuator force P_a vs. time.

Date of test 29.9.2005

5.2 After failure	-
6	**Observations during loading** (see also the photographs in App. A)

Before loading	All measuring devices were zero-balanced when the actuator forces P_a were equal to zero but the weight of the loading equipment was on. The cracks in the slabs were visually inspected and found to be the same as those observed before the slabs were installed. They are shown in Fig. 27 in which the initial cracks in the cast-in-situ concrete are also indicated. The maximum crack width in the soffit of the slabs was of the order of 0,06–0,08 mm. As can be seen later, the initial cracks on the top of slabs 3 and 12 did not affect the failure. P_a = 140 kN corresponds to the shear force due to the expected service load when the shear resistance of the slabs is supposed to be prevailing in the design.
Cycling loading	The interface between the joint concrete and the sawn slab ends gradually cracked vertically on both sides of the middle beam. At P_a = 140 kN (3rd cycle) the soffit of the floor was inspected visually. The observed cracks are shown in Fig. 27. There were diagonal cracks in the corners of slabs 4, 5 and 11, and some initial cracks had grown in length. The maximum width of these cracks was of the order of 0,08–0,10 mm.
P_a = 199 kN	A sudden increase in deflection was observed in the Western part of the test floor. Simultaneously a vertical crack was observed in the Western tie beam between slabs 4 and 5.
P_a = 308 kN	An inclined shear crack appeared in slab 1 next to the middle beam.
P_a = 353 kN	Additional inclined shear cracks appeared in slabs 1 (next to the previous crack) and in slab 7. Since slabs 1 and 7 seemed unable to carry more load, the loads were quickly reduced to prevent the possible collapse of the loading equipment. Soon after the unloading, the test floor was reloaded (Stage II) to check, whether the load before the unloading was really the failure load. This proved to be the case. In stage II the maximum actuator load was P_a = 321,5 kN. The cracks observed after the failure are shown in Fig. 28.
After failure	When removing the slabs, it came out that the bond between the slab ends and the underlying grout was weak, see App. A, Figs 27–30.

7	**Cracks in concrete**
7.1 Cracks at service load	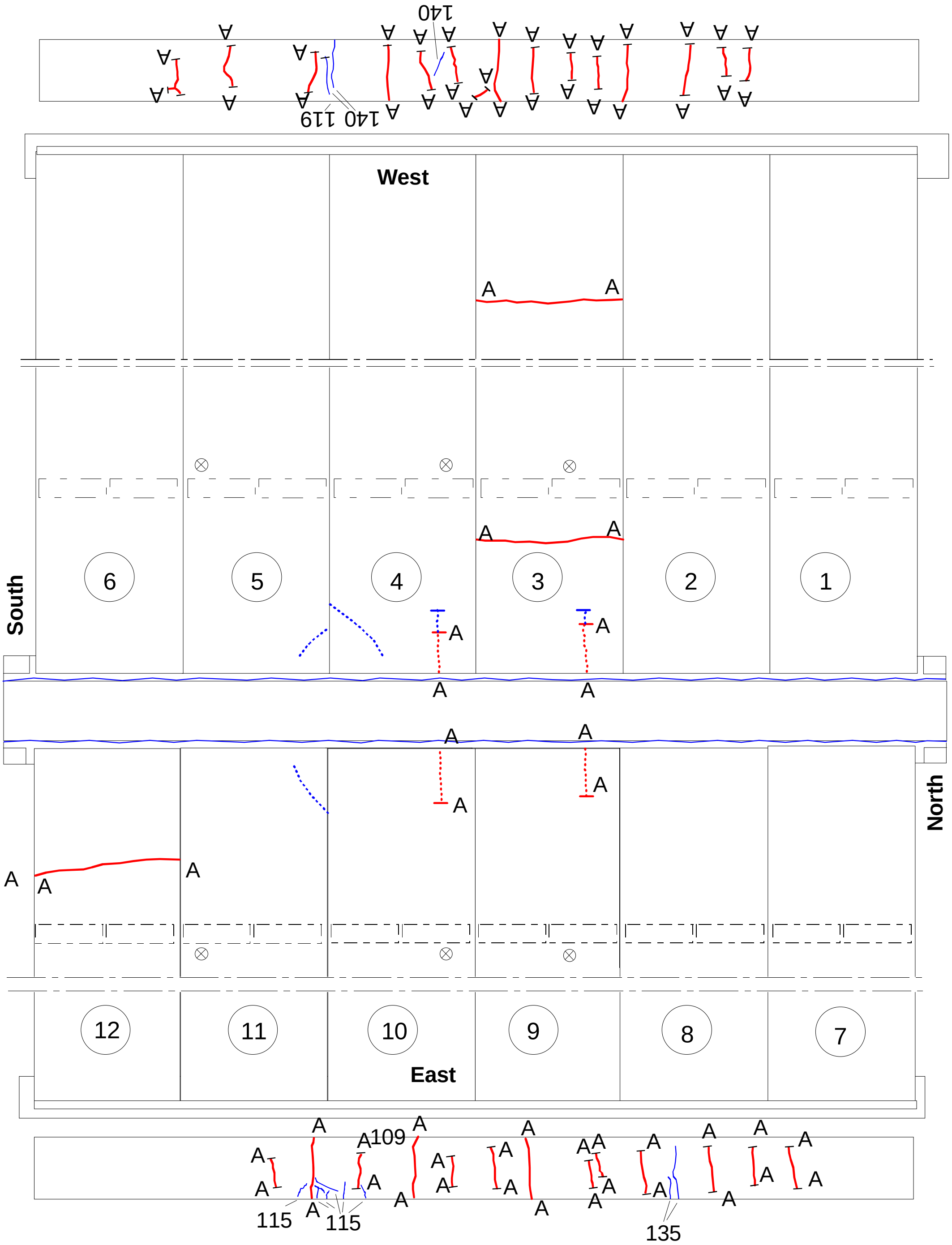 *Fig. 27. Cracks at service load (P_{ai} = 140 kN). The initial cracks observed before loading are indicated with red colour and letter A. A dashed line indicates a crack in the soffit. The figures give the value of the actuator force at which the crack (other than initial crack) was observed.*

7.2
Cracks after failure

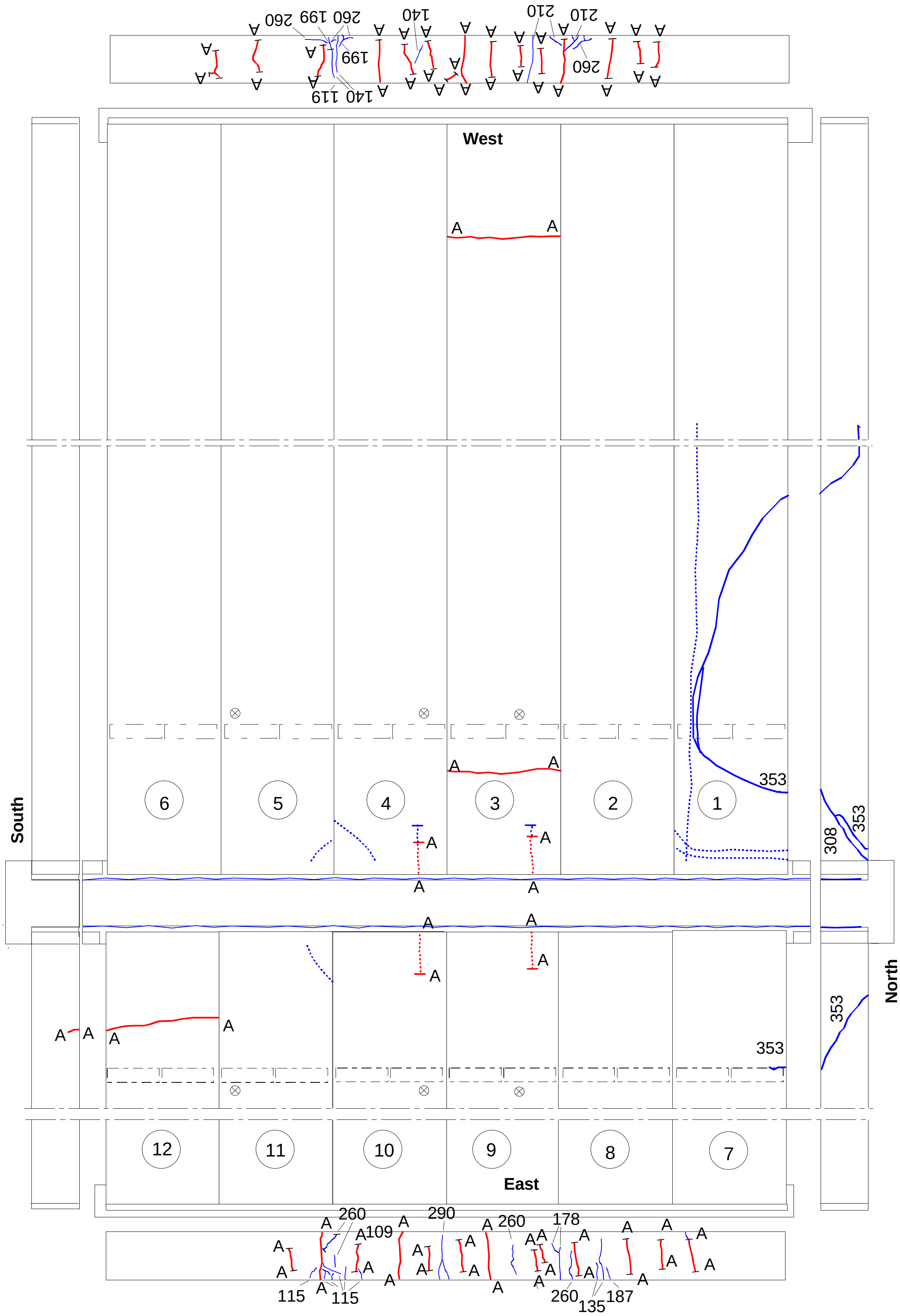

Fig. 28. Cracks after failure. The initial cracks are indicated with red colour and letter A. A dashed line indicates a crack in the soffit. The figures give the value of the actuator force at which the crack was observed.

8 Observed shear resistance

The ratio (measured support reaction below one end of the middle beam)/ (actuator forces on half floor) is shown in Fig. 29 and in a larger scale in Fig. 30.

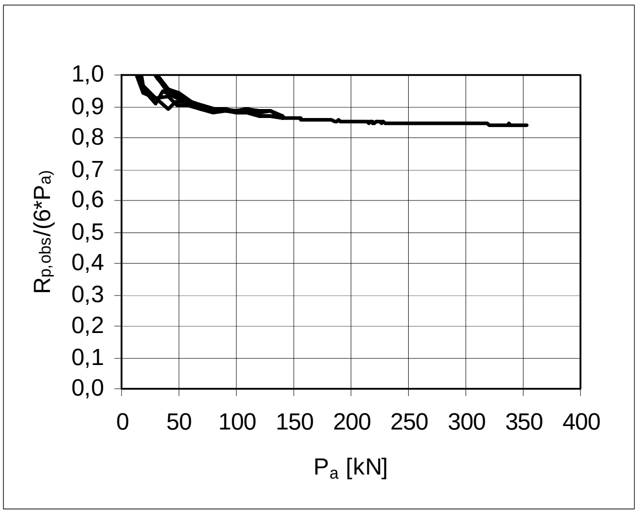

Fig. 29. Ratio of measured support reaction of the middle beam ($R_{p,obs}$) to actuator loads on half floor.

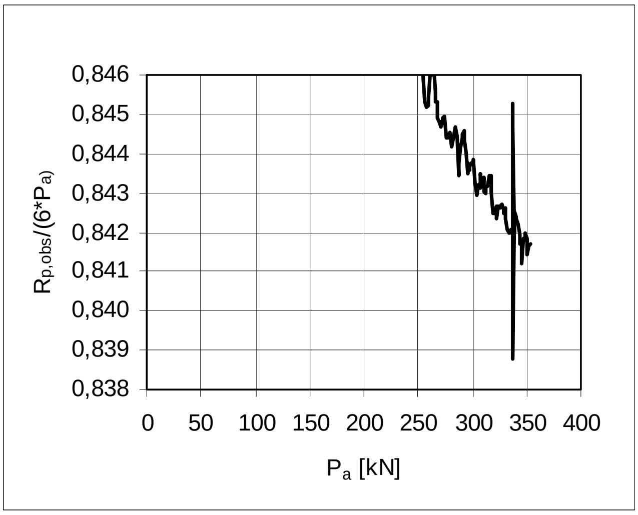

Fig. 30. A detail of the previous figure in a larger scale.

The shear resistance of one slab end (support reaction of slab end at failure) due to different load components is given by

$$V_{obs} = V_{g,sl} + V_{g,jc} + V_{eq} + V_p$$

where $V_{g,sl}$, $V_{g,jc}$, V_{eq} and V_p are shear forces due to the self-weight of slab unit, weight of joint concrete, weight of loading equipment and actuator forces P_a, respectively. $V_{g,jc}$ is calculated from the nominal geometry of the joints and density of the concrete, $V_{g,sl}$ *from* measured average weight of slabs, both assuming that the slabs behave as simply supported beams. For V_{eq} and V_p the relation to the load is taken from the measured support reaction at failure, in other words, $V_{eq} = 0{,}842 \times P_{eq}$ and $V_p = 0{,}842 \times P_a$. The values for the components of the shear force are given in Table on the next page.

Table. Components of shear resistance due to different loads.

Action	Load	Shear force kN
Weight of slab unit	6,54 kN/m	32,05
Weight of joint concrete	0,39 kN/m	1,91
Loading equipment	6,22 kN / slab	5,24
Actuator loads	353,0 kN / slab	297,20

The observed shear resistance V_{obs} = 336,4 kN (shear force at support) is obtained for one slab width = 1,2 m. The shear force per unit width is 280,3 kN/m

9 **Material properties**

9.1
Strength of steel

Component	$R_{eH}/R_{p0,2}$ MPa	R_m MPa	Note
End beam	≈350		Nominal (no yielding)
Slab strands	1630	1860	Nominal (no yielding)
Beam strands	1630	1860	Nominal (no yielding)
Reinforcement	500		Nominal (A500HW,no yielding)

9.2
Strength of slab concrete, floor test

#	Cores	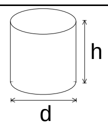	*h* mm	*d* mm	Date of test	Note
6			50	50	12.10.2005 (+13 d)[1)]	Upper flange of slab 1, vertically drilled, tested as drilled[2)], density = 2487 kg/m³
Mean strength [MPa]			85,4			
St.deviation [MPa]			1,72			

9.3
Strength of slab concrete, reference tests

#	Cores	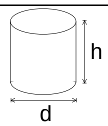	*h* mm	*d* mm	Date of test	From
6			50	50	12.9.2005 (+3 ... +4 d)[1)]	Upper flange of slab 13, vertically drilled, tested as drilled[2)], density = 2448 kg/m³
Mean strength [MPa]			89,2			
St.deviation [MPa]			2,84			

9.4
Strength of grout

#	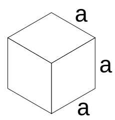	*a* mm	Date of test	Note
6		150	29.9.2005 (+0 d)[1)]	Kept in laboratory in the same conditions as the floor specimen Density = 2245 kg/m³
Mean strength [MPa]		46,6		
St.deviation [MPa]		0,97		

9.5
Strength of beam concrete

#	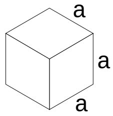	*a* mm	Date of test	Note
6		150	29.9.2005 (+0 d)[1)]	Kept in laboratory in the same conditions as the floor specimen Density = 2402 kg/m^3
Mean strength [MPa]		100,1		
St.deviation [MPa]		1,02		

[1)] Date of material test minus date of test (floor test or reference test)
[2)] kept in a closed plastic bag after drilling until compression

10 **Measured displacements**

In the following figures, P_a is the actuator force.

10.1
Deflections

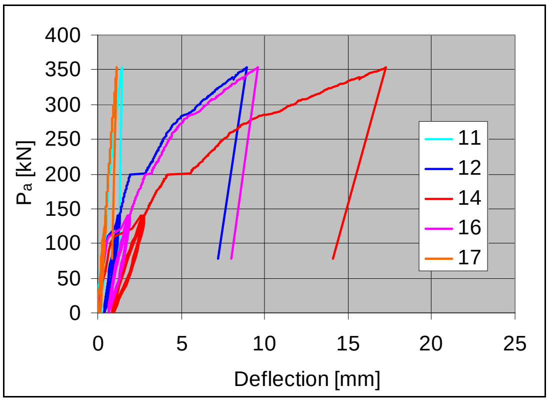

Fig. 31. Deflection on line I along Western end beam.

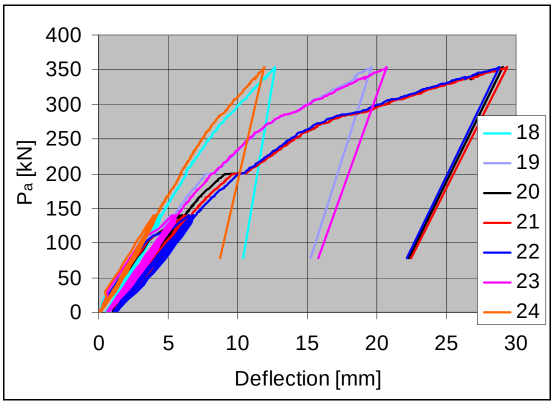

Fig. 32. Deflection on line II in the middle of slabs 1–6.

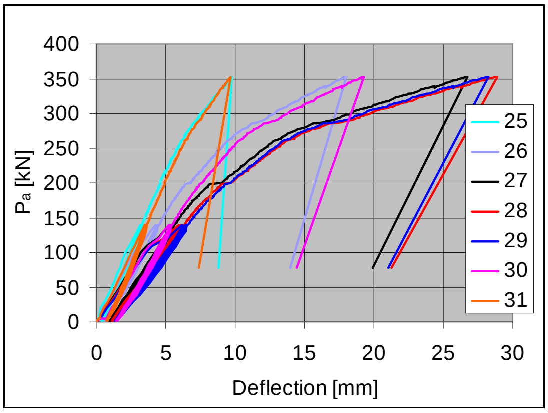

Fig. 33. Deflection on line III close to the line load, slabs 1–6.

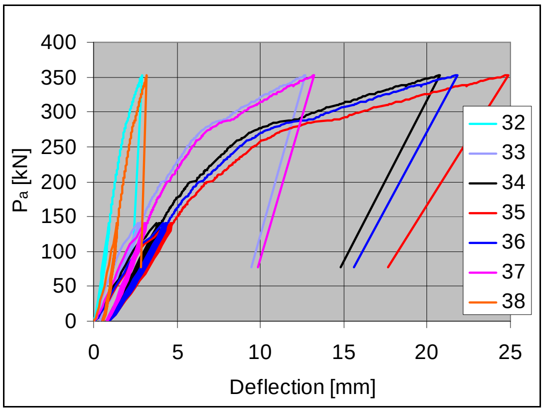

Fig. 34. Deflection on line IV along the middle beam.

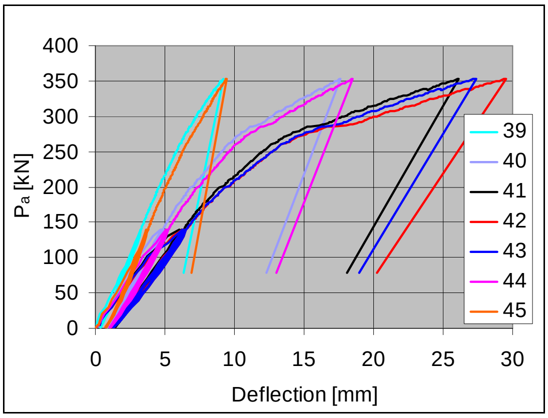

Fig. 35. Deflection on line V close to the line load, slabs 7–12.

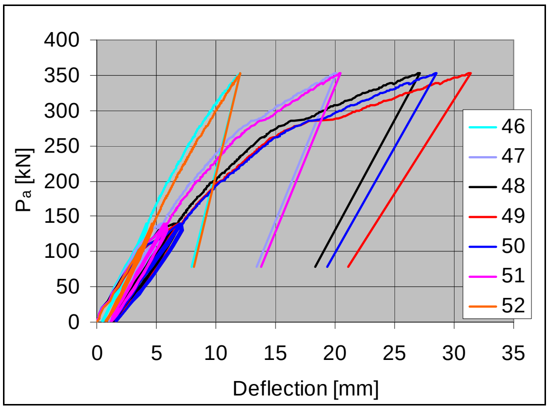

Fig. 36. Deflection on line VI in the middle of slabs 7–12.

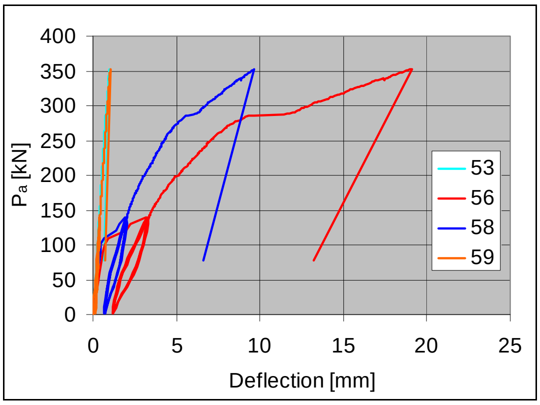

Fig. 37. Deflection on line VII along Eastern end beam, slabs 7–12.

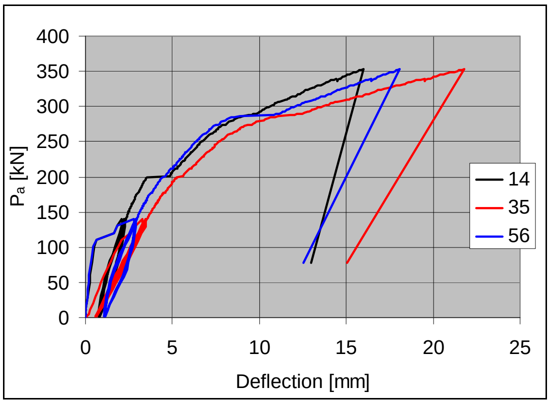

Fig. 38. Net deflection of midpoint of middle beam (35) and those of end beams (14, 56) (Rigid body motion due to settlement of supports eliminated).

10.2
Crack width

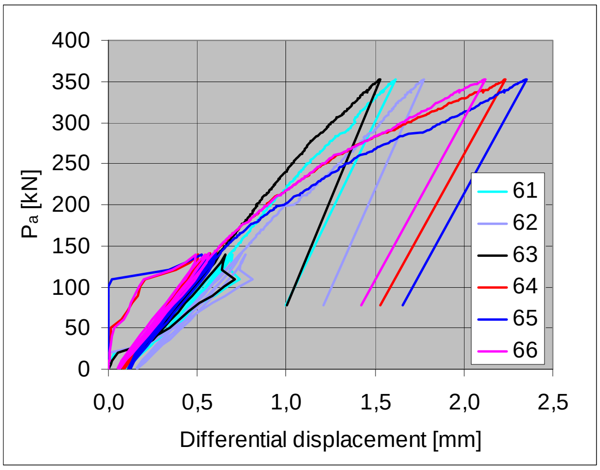

Fig. 39. Differential displacement parallel to the slab between the middle beam and the slabs (≈ crack width). See Fig. 23 for the location of the transducers.

10.3
Average strain

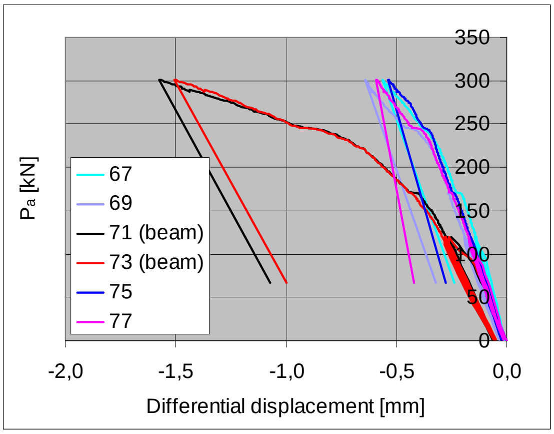

Fig. 40. Differential displacement at top surface of floor measured by transducers 57, 59, 61, 63, 65 and 67.

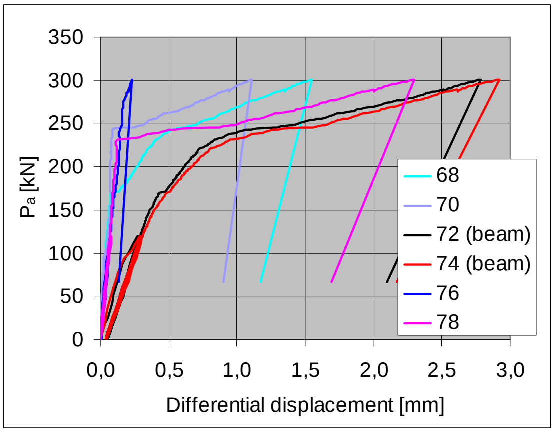

Fig. 41. Differential displacement at soffit of floor measured by transducers 58, 60, 62, 64, 66 and 68.

10.4
Shear displacement

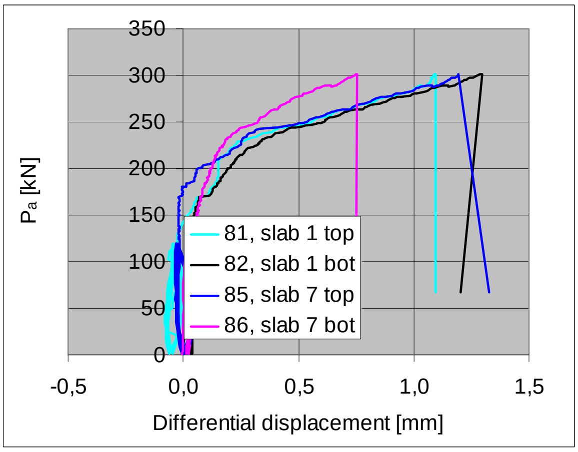

Fig. 42. Northern end of middle beam. Differential displacement between edge of slab and middle beam. A positive value means that the slab is moving towards the end of the beam.

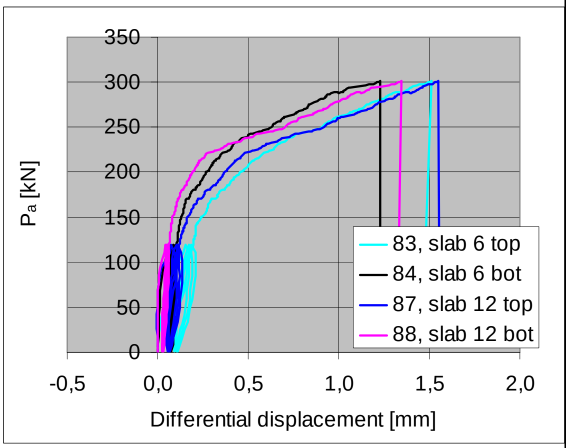

Fig. 43. Southern end of middle beam. Differential displacement between edge of slab and middle beam. A positive value means that the slab is moving towards the end of the beam.

11	**Reference tests**
	Both ends of slab 13 were loaded in shear as shown in Fig. 44.

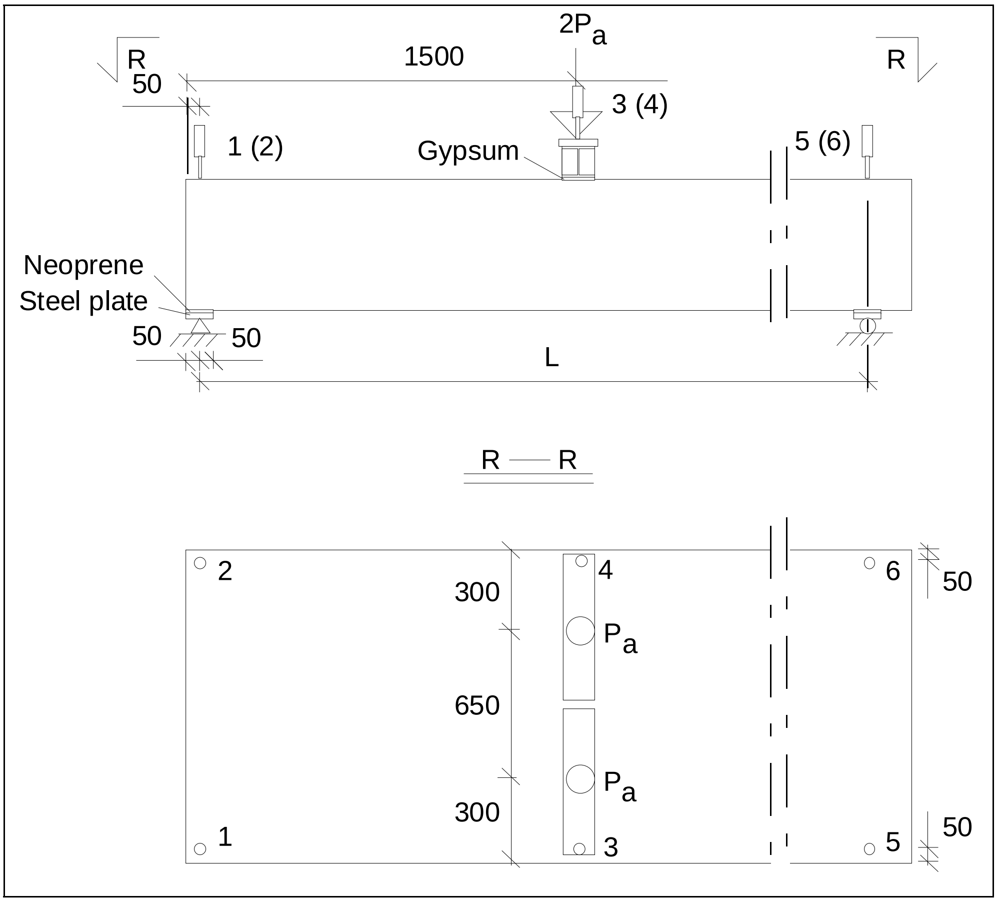

Fig. 44. Layout of reference test. For L, see the next table.

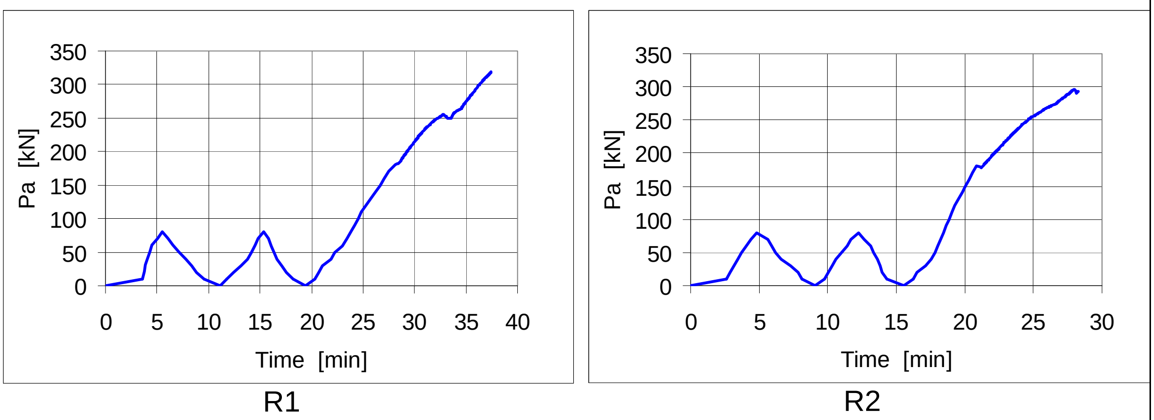

Fig. 45. Tests R1 and R2. Actuator force – time relationship.

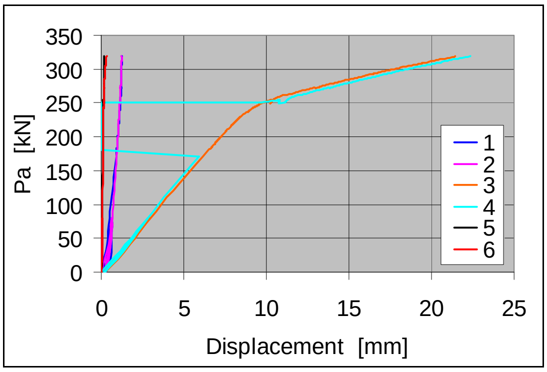

R1

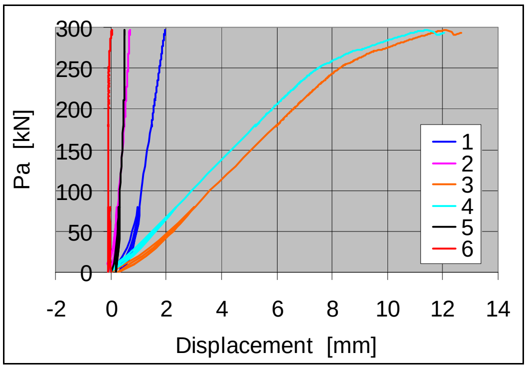

R2

Fig. 46. Tests R1 and R2. Displacements measured by transducers 1–6. In test R1, at P_a = 170 - 250 kN, transducer 4 was accidentaly disconnected from the data logger.

Table. Span of slab, shear force V_g at support due to the self weight of the slab, actuator force P_a at failure, weight of loading equipment P_{eq}, shear force V_{Pa+eq} due to imposed load (=actuator load and weight of loading equipment) at failure, total shear force V_{obs} at failure for one slab and total shear force v_{obs} per unit width.

Test	Date	Span mm	V_g kN	P_a kN	P_{eq} kN	V_{Pa+eq} kN	V_{obs} kN	v_{obs} kN/m
R1	7.9.2005	9867	32,02	318,7	0,29	544,00	576,02	480,0
R2	8.9.2005	8370	27,16	296,8	0,29	491,00	518,17	431,8
						Mean	547,1	455,9

12 Comparison: floor test vs. reference tests

The observed shear resistance (support reaction) of the hollow core slab in the floor test was equal to 336,4 kN per one slab unit or 280,3 kN/m. This is **61%** of the mean of the shear resistances observed in the reference tests.

13 Discussion

1. The net deflection of the middle beam due to the imposed actuator load (deflection minus settlement of supports) was 21,8 mm or *L*/330, i.e. rather small
2. The shear resistance measured in the reference tests was higher than the mean of observed values for similar slabs given in *Pajari, M. Resistance of prestressed hollow core slab against web shear failure. VTT Research Notes 2292, Espoo 2005*.
3. The torsional stresses due to the different deflection of the middle beam and end beams had a negligible effect on the failure of the slabs because the maximum difference in the net mid-point deflection was less than 5,8 mm
4. The bond between the smooth edges of the middle beam and the grout was weak.
5. The bond between the soffit of the slab and the grout below it was also weak.
6. Due to the weak bond, the edge slabs slided along the beam before failure. This reduced the negative effects of the transverse actions in the slab and had a positive effect on the shear resistance

APPENDIX A: PHOTOGRAPHS

Fig. 1. Failure mode in reference test R1.

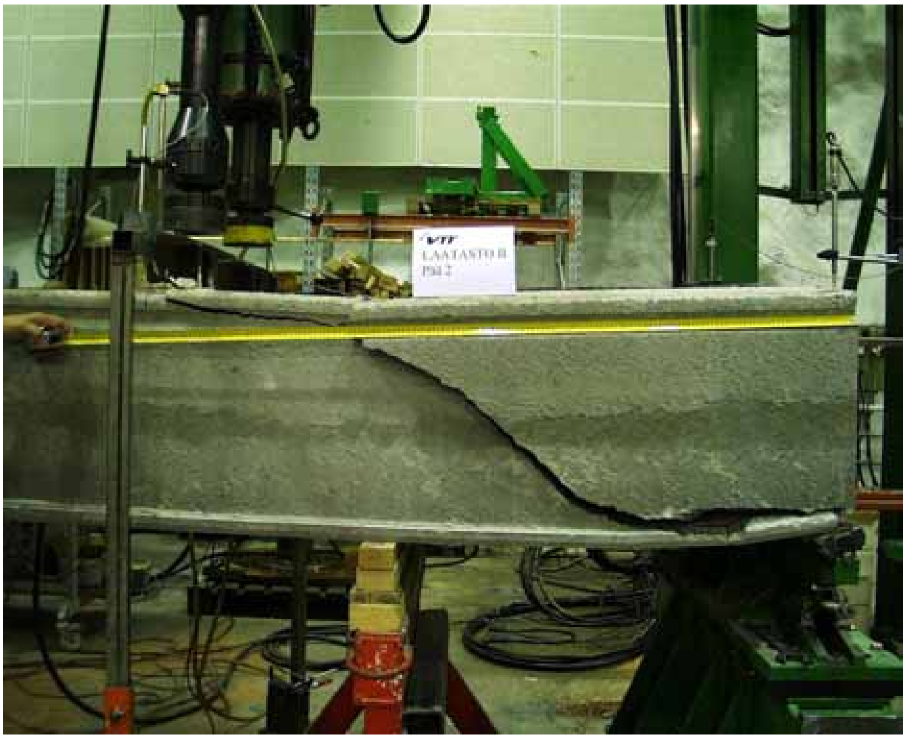

Fig. 2. Failure mode in reference test R2.

Fig. 3. Installing slabs on PC beam.

Fig. 4. Uneven surface of concrete beam due to air bubbles.

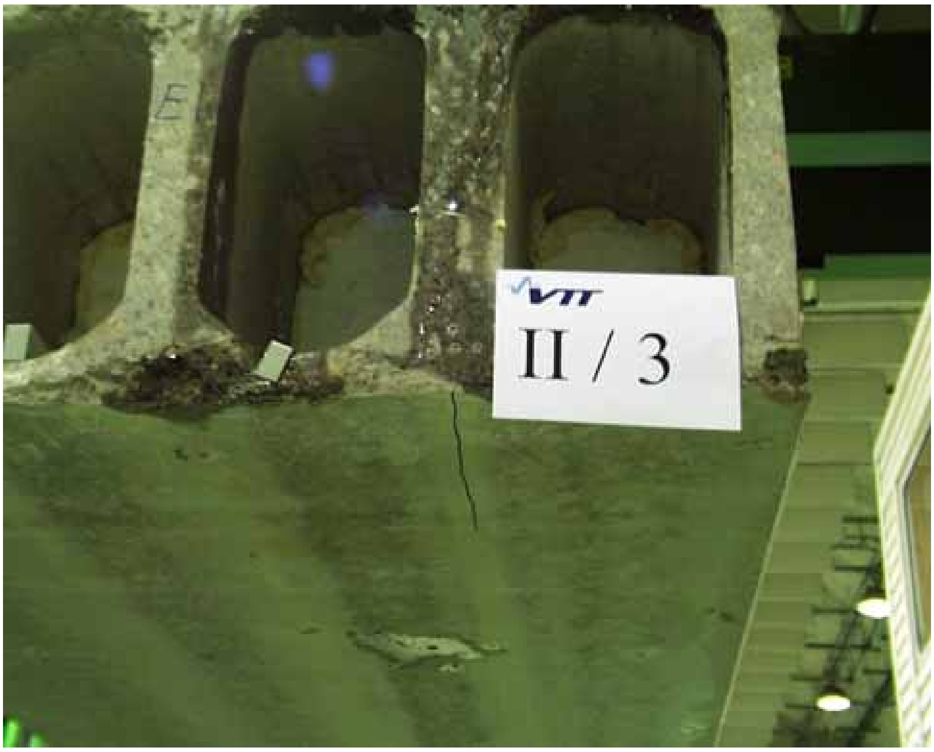

Fig. 5. Initial crack in slab 3.

Fig. 6. Initial crack in slab 4.

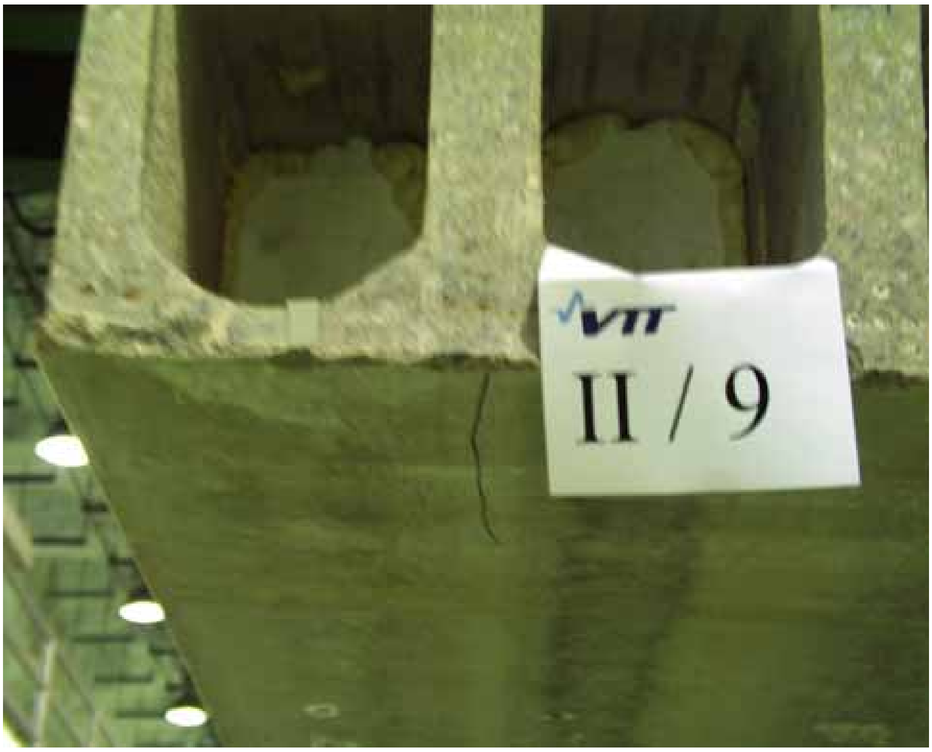

Fig. 7. Initial crack in slab 9.

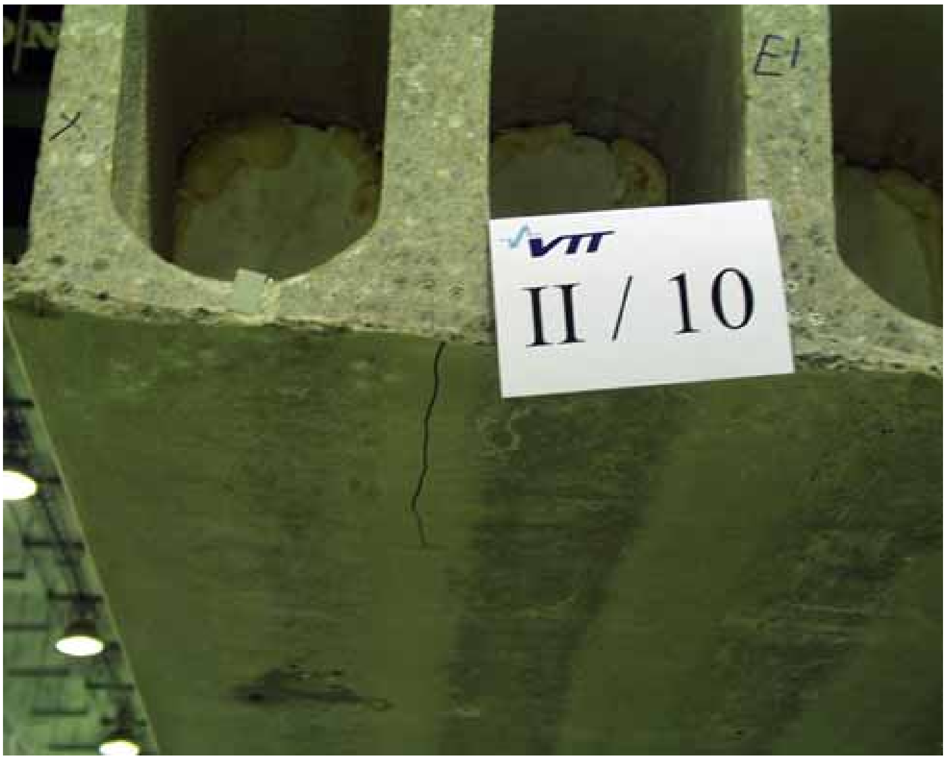

Fig. 8. Initial crack in slab 10.

Fig. 9. A short tie bar through beam at support.

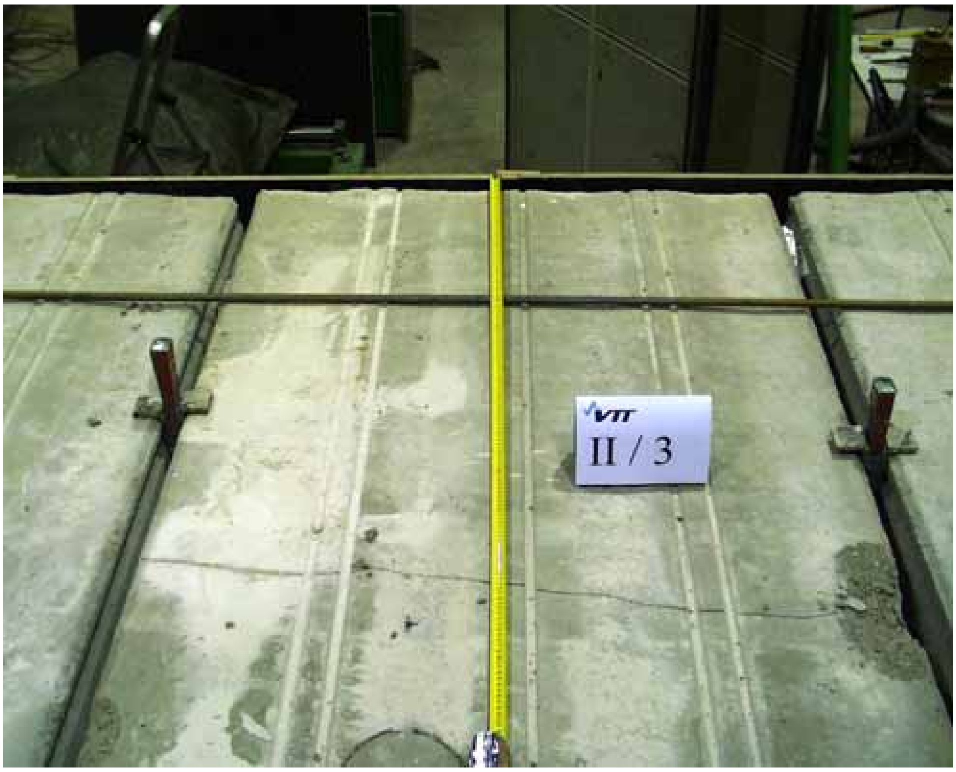

Fig. 10. Initial crack in slab 3.

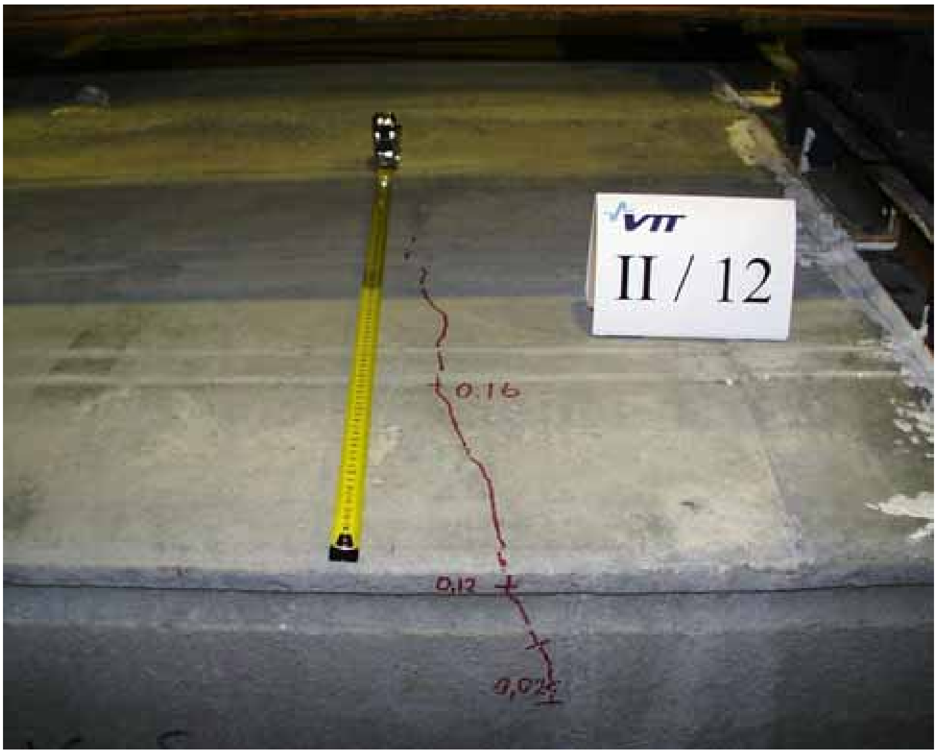

Fig. 11. Initial crack in slab 12.

Fig. 12. Initial crack in slab 12.

Fig. 13. Overview on test arrangements.

Fig. 14. Support arrangement at end beam.

Fig. 15. Shear crack at P_a = 308 kN. The black line drawn 200 mm below the shear crack is a misprint which does not refer to a crack.

Fig. 16. Shear crack in slab 7 at P_a = 353 kN.

Fig. 17. Failure in slab 1. Photographed after stage II. In stage I, the failure crack was the same but much thinner.

Fig. 18. Failure mode in slab 1.

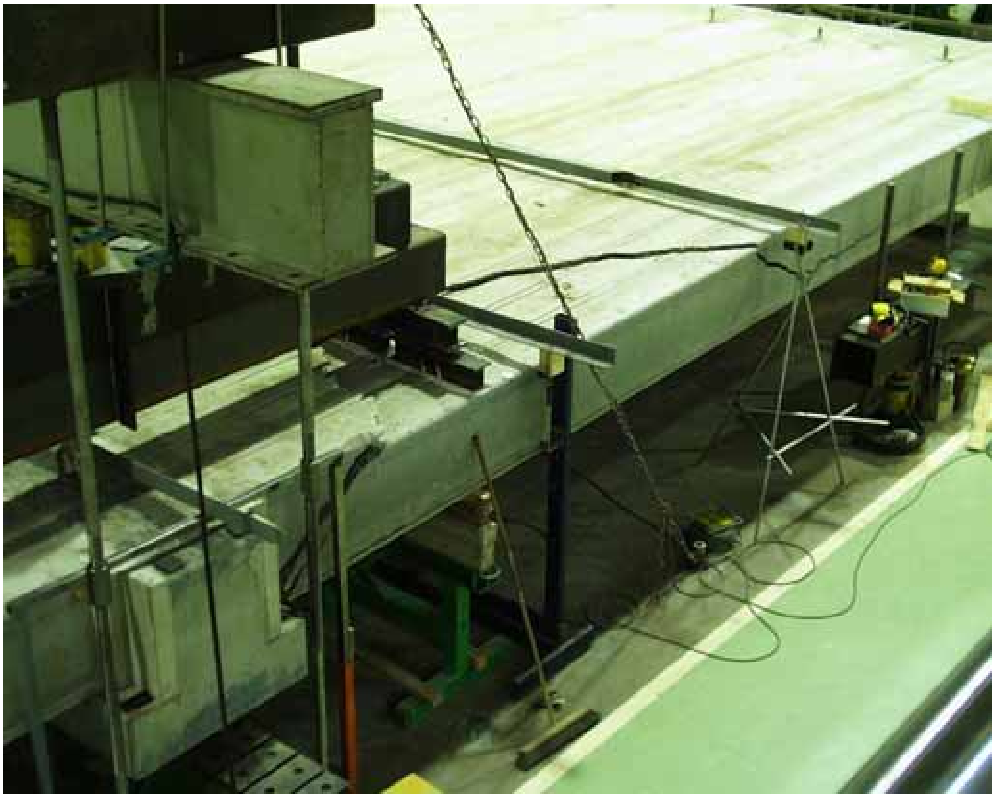

Fig. 19. Failure mode in slab 1.

Fig. 20. Cracks in soffit of slabs 4 and 5 after failure.

Fig. 21. Crack in soffit of slab 11 after failure.

Fig. 22. Failure mode.

Fig. 23. Core filling in slab 1.

Fig. 24. Grout at support after removal of slab. Note the perfect filling of the gap below the slab end.

Fig. 25. Perfect filling of hollow core. Note the lack of bond between the cast-in-situ and precast concrete.

Fig. 26. The only observed incomplete filling in hollow core.

Fig. 27. Cast-in-situ concrete below slab end. Good bond with slab, weaker bond with beam.

Fig. 28. Cast-in-situ concrete below slab end. Good bond with beam, weaker bond with slab.

Fig. 29. Vertical cracking at slab ends took place along the web ob the beam.

Fig. 30. Vertical cracking at slab ends took place along the web ob the beam.

1	**General information**
1.1 Identification and aim	**VTT.CR.Delta.500.2005** **Last update2.11.2010** DE500 (Internal identification) Aim of the test: To quantify the interaction between the Delta beam and 500 mm thick hollow core slabs.
1.2 Test type	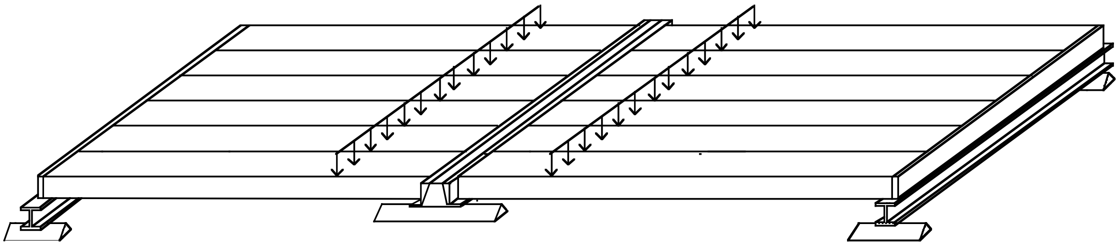 *Fig. 1. Illustration of test setup.*
1.3 Laboratory & date of test	VTT/FI 11.11.2005
1.4 Test report	Author(s): Pajari, M. Name: *Load test on hollow core slab floor with Delta beam* Ref. number: VTT-S-2555-06 Date: 10.8.2006 Availability: Confidential, owner is Peikko Finland Oy, P.O. Box 104, FI-15101 Lahti, Finland
2	**Test specimen and loading** (see also Appendices A and B)

2.1
General plan

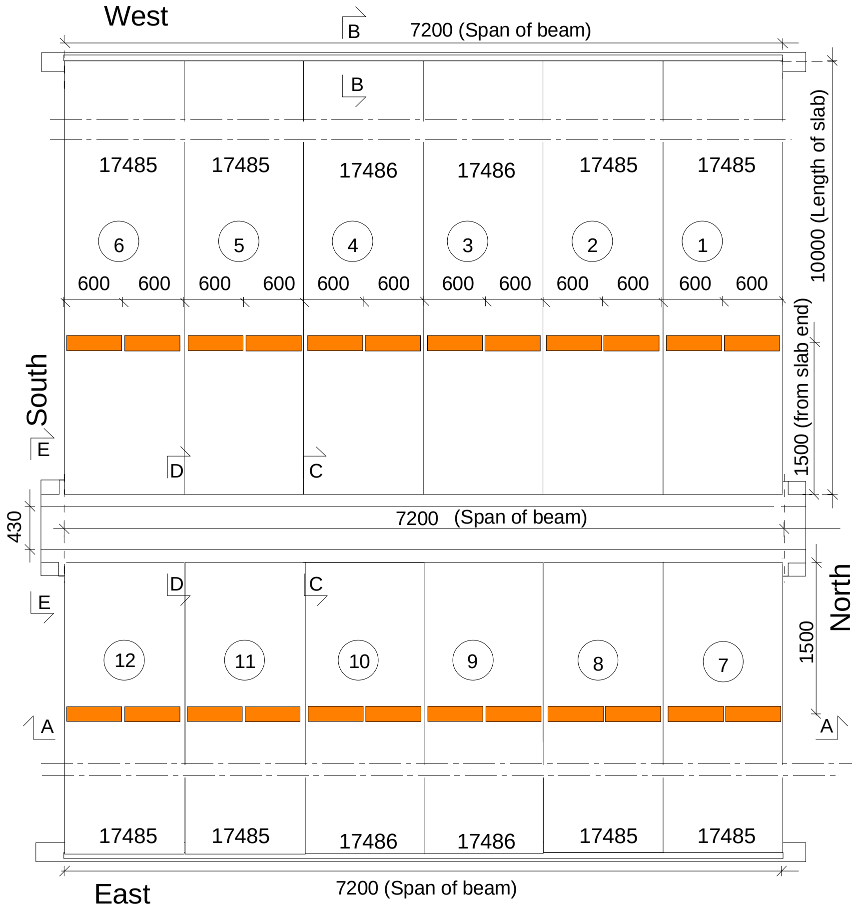

Fig. 2. Plan.

2.2
End beams

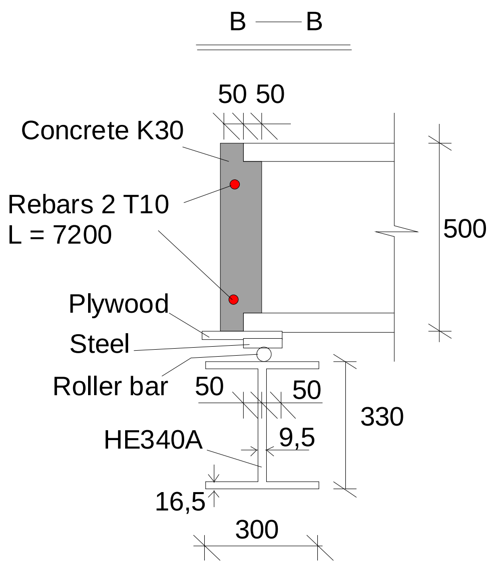

Fig. 3. Arrangements at end beam. T10 refers to a reinforcing bar A500HW with diameter 10 mm.

2.3 Middle beam	The beam, see Fig. 4 and App. B, comprised - a steel box girder with inclined, perforated webs - a concrete component filling the empty space between the slab ends laying on the bottom flange of the beam, cast by VTT in laboratory on the 27th of October 2005. **Concrete**: K30, max aggregate size 8 mm, consistency S4/16–21 cm **Structural steel in Delta beam:** S355

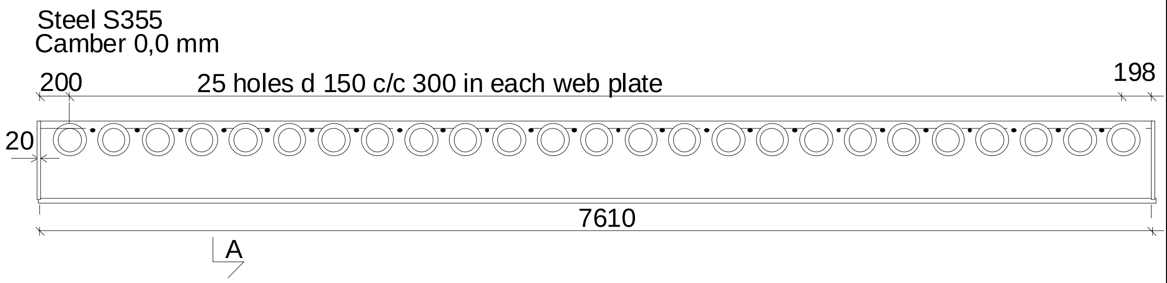

Fig. 4. Delta beam. The beam was provided with end plates, 20 mm in thickness.

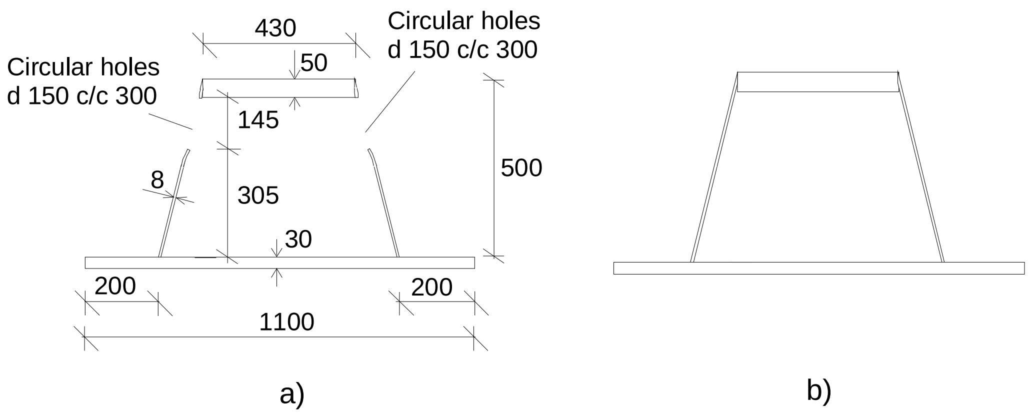

Fig. 5. Cross-section A-A of Delta beam. a) At web hole. b) Between web holes.

2.4 Arrangements at middle beam	- Simply supported, span = 7,2 m, roller bearing at South end **Rebars Txy**: Hot rolled, weldable rebar A500HW, diameter = xy mm

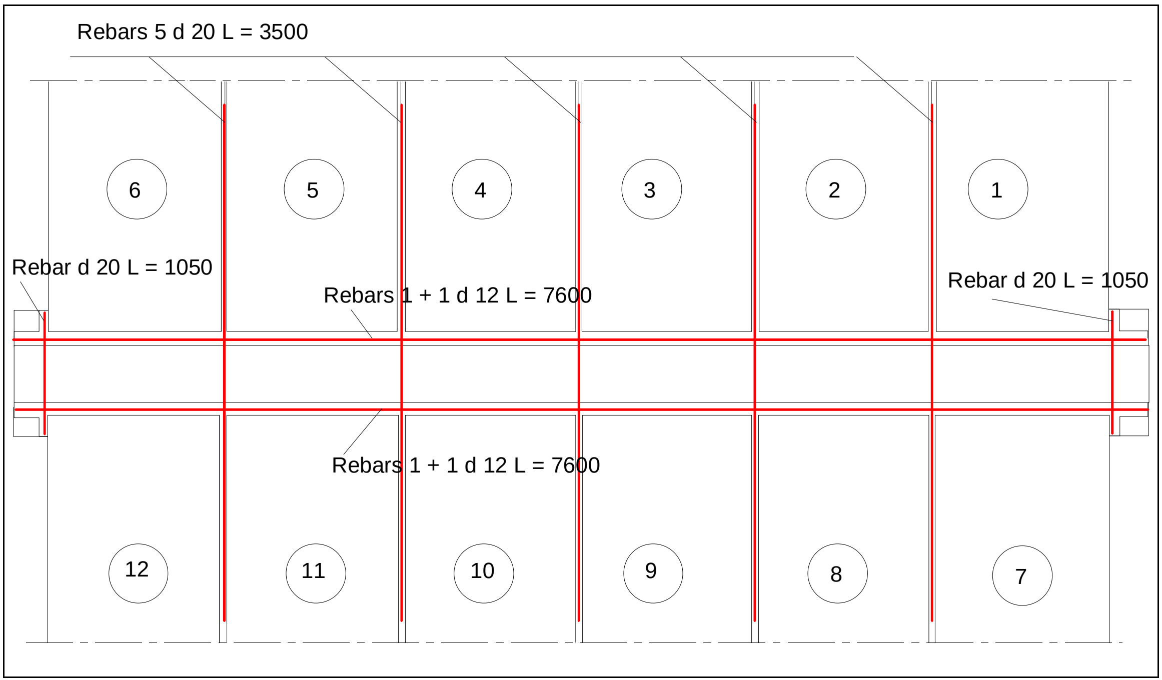

Fig. 6. Tie reinforcement across and along the middle beam.

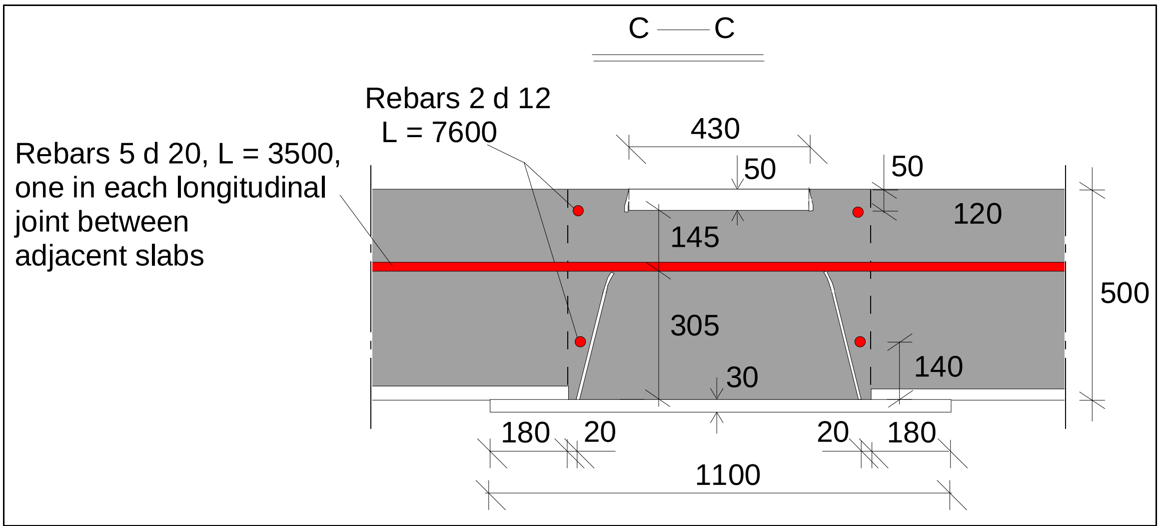

Fig. 7. Arrangements at middle beam, section C-C along a joint between adjacent hollow core units, see Fig. 2. Rebars are made of steel A500HW.

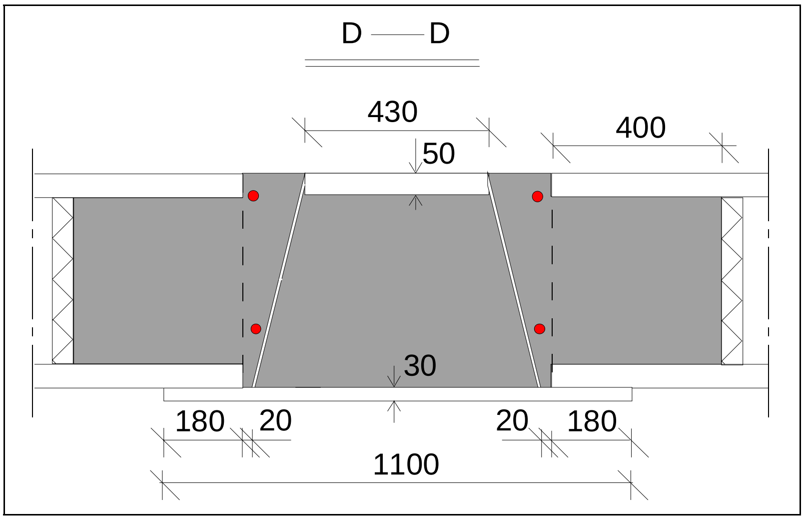

Fig. 8. Section D-D along hollow cores, see Fig. 2.

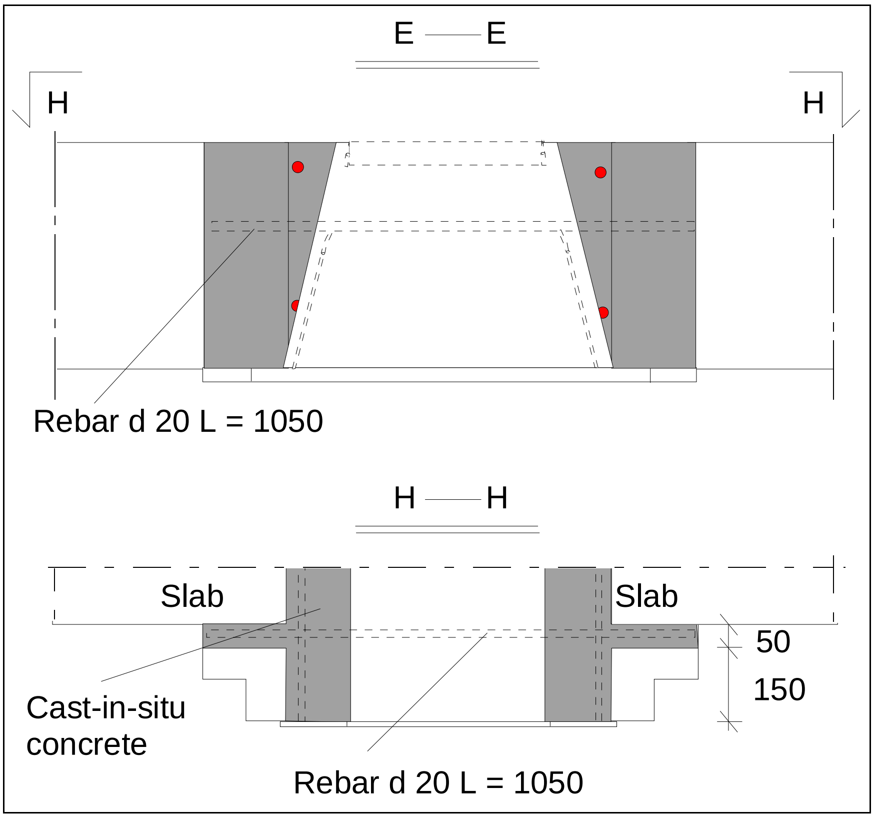

Fig. 9. Tie reinforcement in the cast-in-situ concrete outside the longitudinal edge of the outermost slabs (section E-E in Fig. 2). See also App. A, Fig. 3. Rebars are made of steel A500HW.

2.5 Slabs	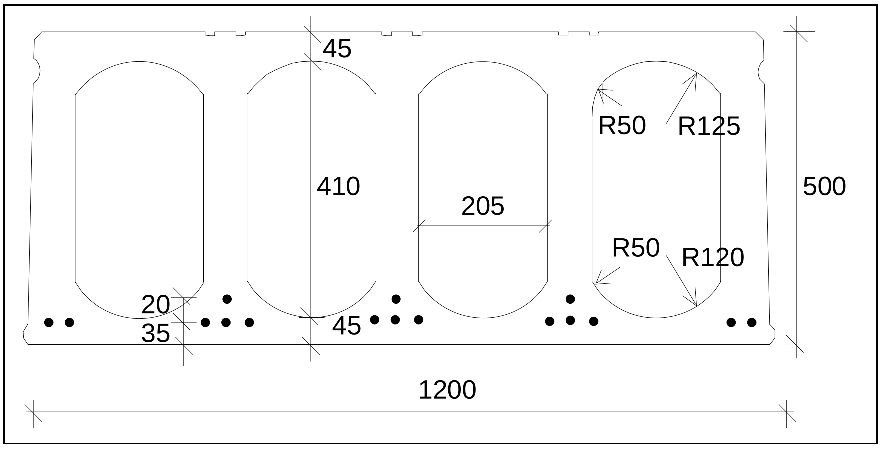 *Fig. 10. Nominal geometry of slab section. For more detailed data see Fig. 11.* 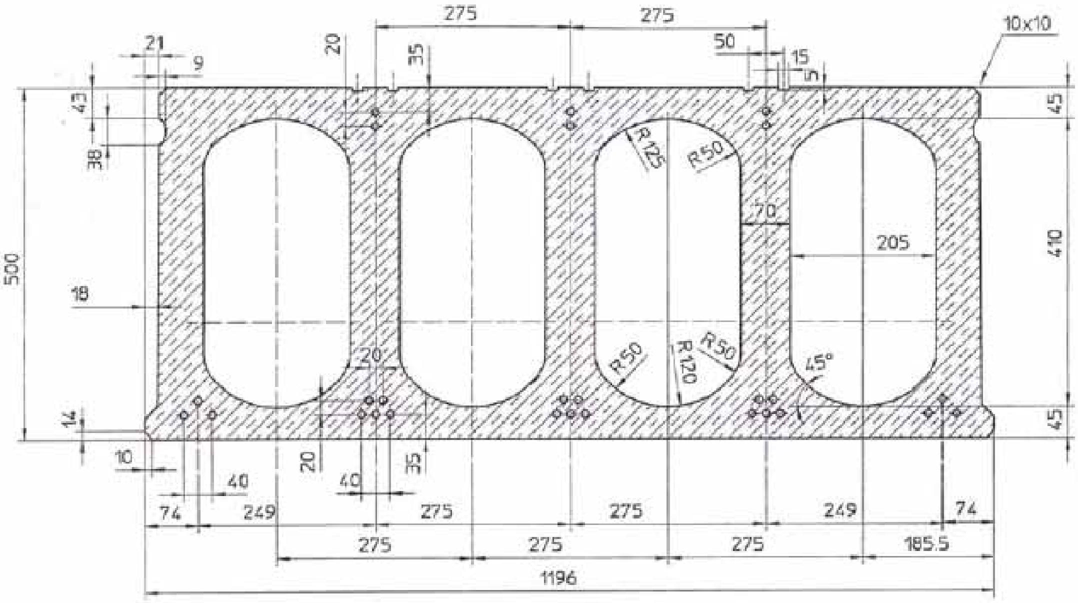 *Fig. 11. Nominal geometry of concrete section (in scale). (The number and position of strands were different in the present test, see Fig. 10.)* - Extruded by Parma Oy, Hyrylä factory 15.9.2005 - 16 lower strands J12,5 initial prestress 1050 MPa - No upper strands **J12,5**: seven indented wires, ϕ =12,5 mm, A_p = 93 mm^2

	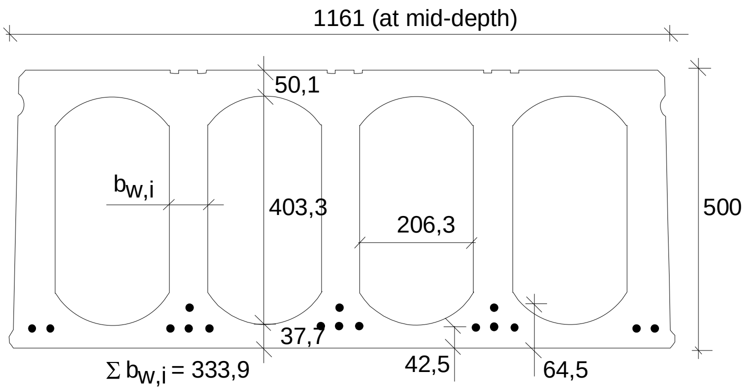 Max measured bond slips: 1,7 in slab unit 8; 1,6 in slab unit 11; 1,5 in slab units 6, 8 and 11 Measured weight of slab units = 6,43 kN/m *Fig. 12. Mean of most relevant measured geometrical characteristics.*
2.6 Temporary supports	No
2.7 Loading arrangements	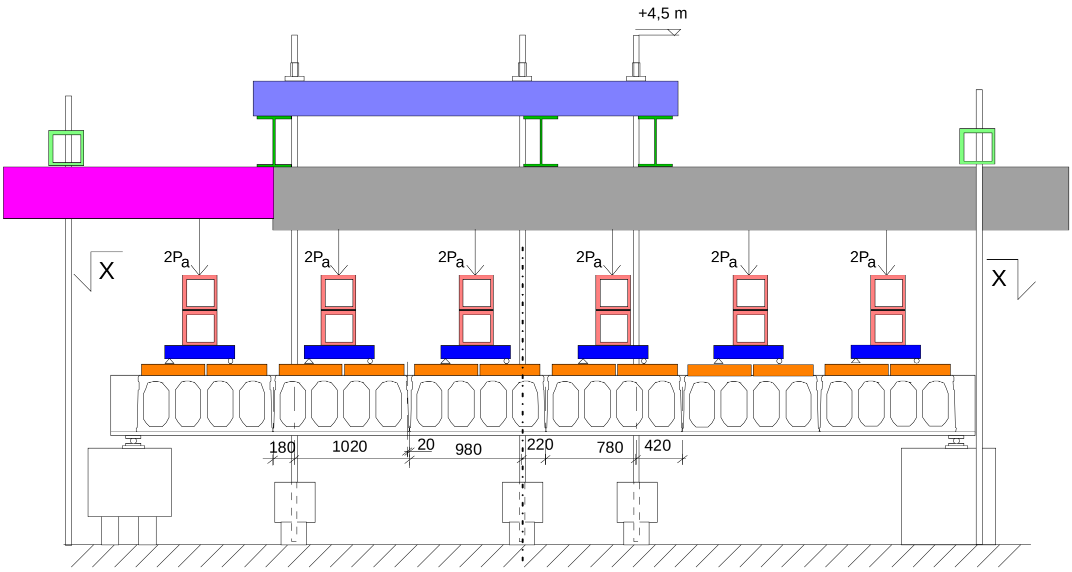 *Fig. 13. Auxiliary loading frame, fixed to the floor of the hall by tension bars, six of which penetrated the hollow core floor.*

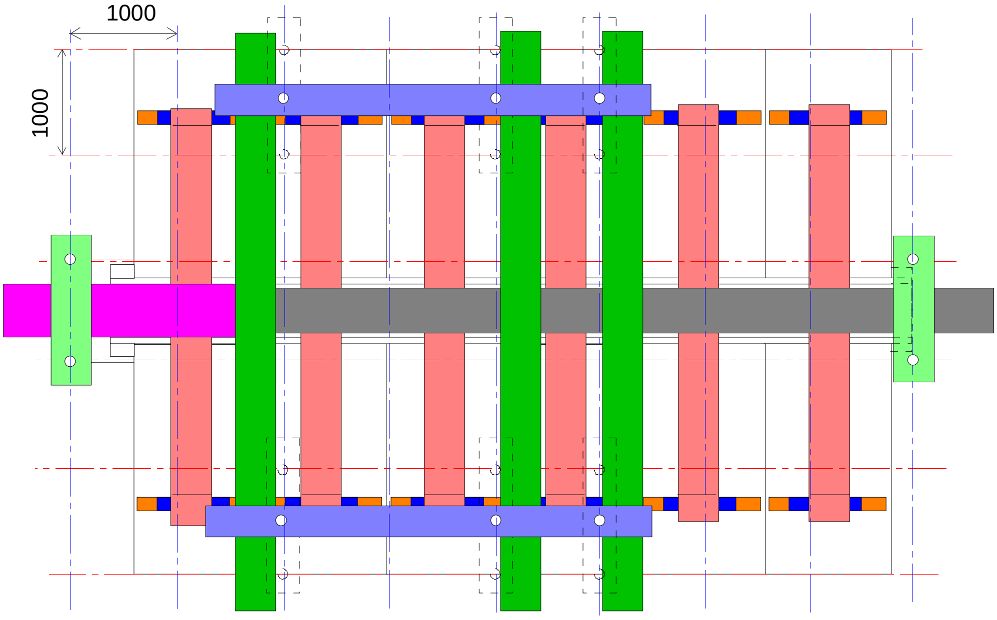

Fig. 14. Auxiliary loading frame, plan.

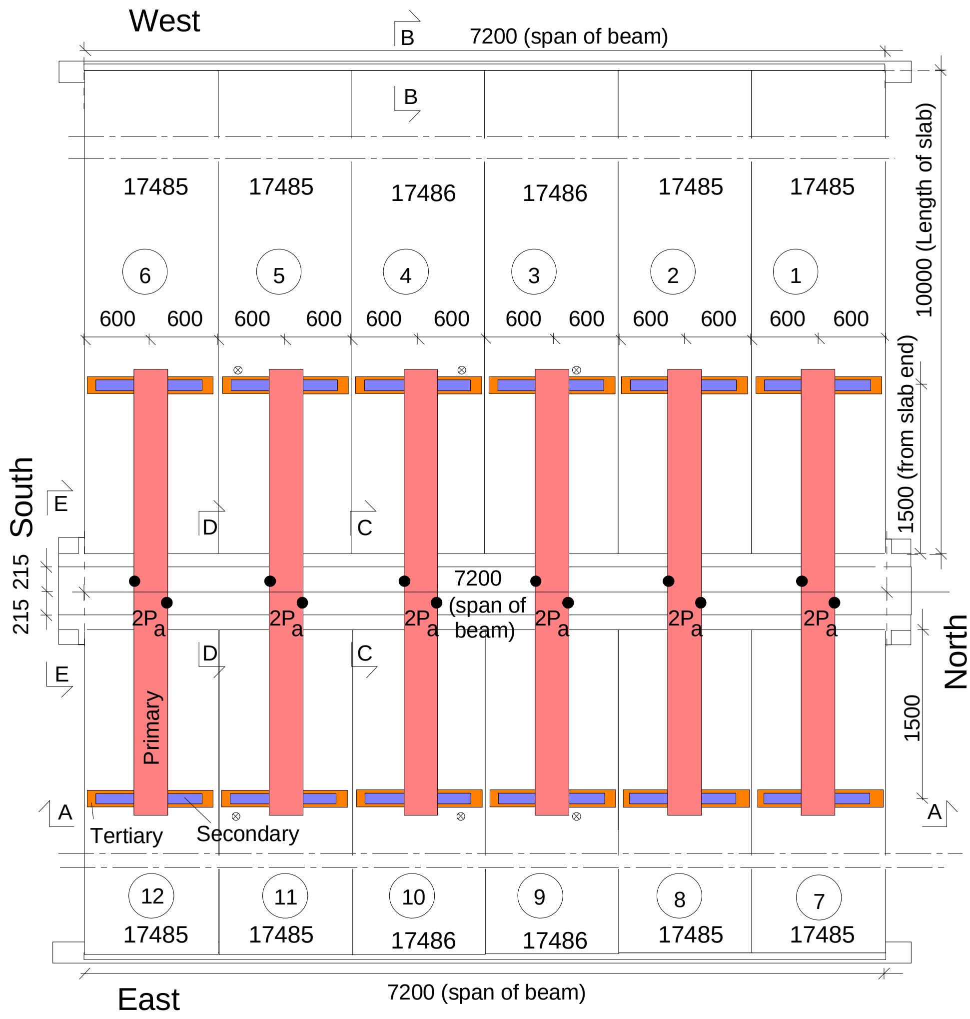

Fig. 15. Loading arrangements. Section X-X in Fig. 13. The slabs were from two casting lots: 17485 and 17486.

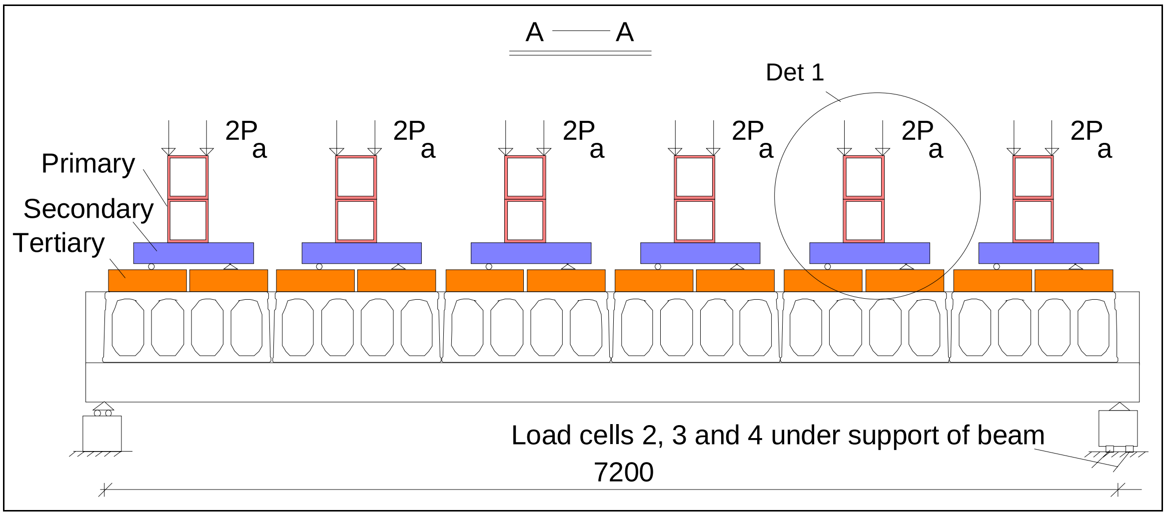

Fig. 16. Section A-A. P_a refers to vertical actuator force.

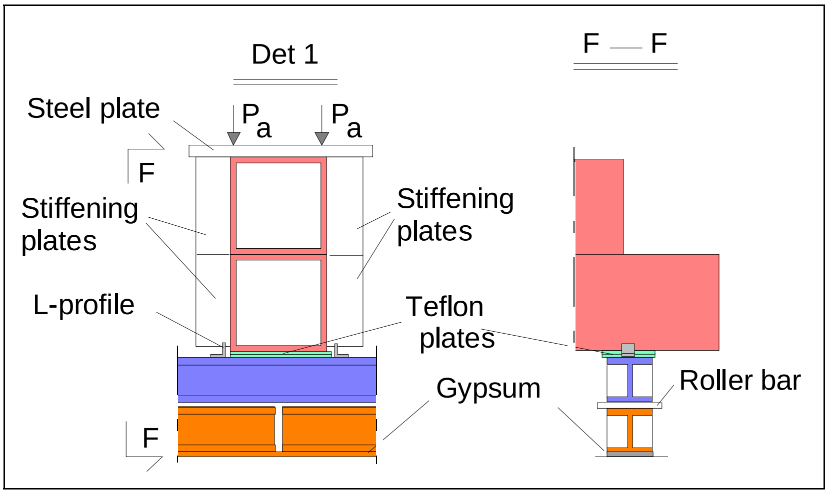

Fig. 17. Detail 1, see previous figure. The stiffening plates are below the loads P_a.

3 Measurements

3.1 Support reactions

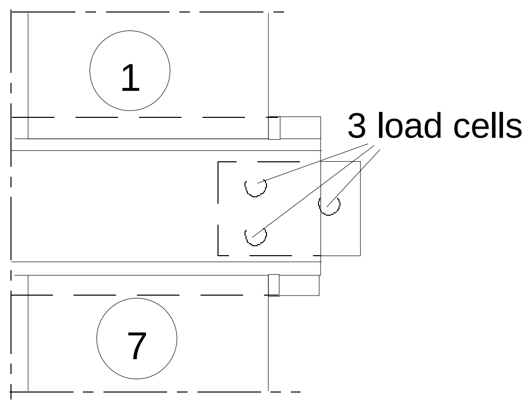

Fig. 18. Load cells below the Northern support of the middle beam.

3.2
Vertical displacement

Fig. 19. Location of transducers 11 … 45 for measuring vertical deflection along lines I … VII.

3.3
Average strain and

3.4
Horizontal. displacements

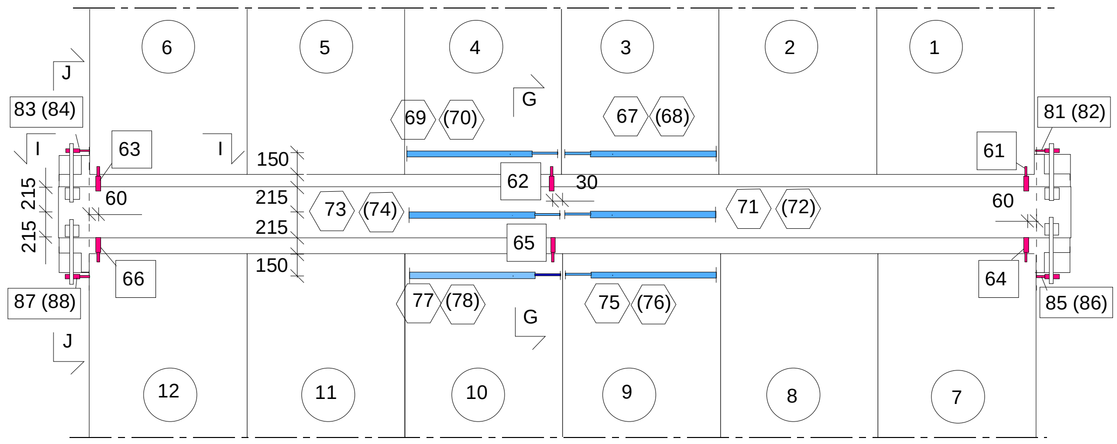

Fig. 20. Position of device (transducers 67–78) measuring average strain parallel to the beams, position of transducers 61–66 measuring crack width and position of transducers 81–88 measuring measuring shear displacement of the slab ends. Numbers in parentheses refer to the soffit of the floor, others to the top.

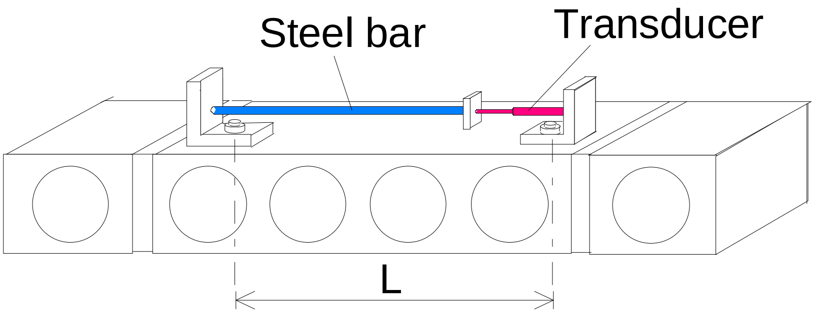

Fig. 21. Apparatus for measuring average strain. L = 1100 mm.

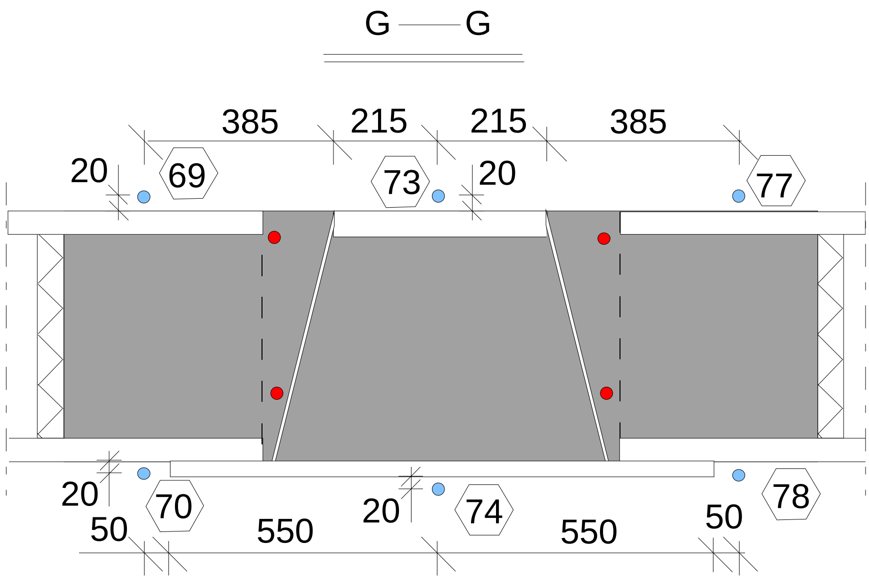

Fig. 22. Section G-G along hollow cores.

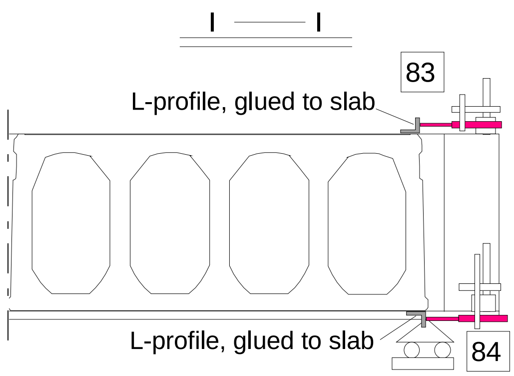

Fig. 23. Section I-I.

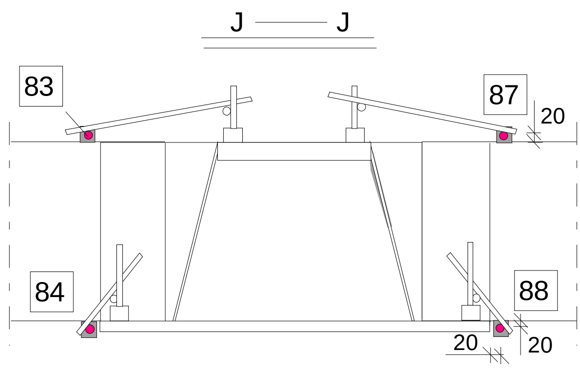

Fig. 24. Section J-J.

3.5
Strain

4	**Special arrangements** None
5	**Loading strategy**
5.1 Load-time relationship	Date of the floor test was 11.11.2005 Before test all measuring devices were zero-balanced. The loading history is shown in Fig. 25. It comprised the following stages: - Stage I: cyclic loading with three cycles up to P_a = 160 kN and back to zero - Stage II: monotonous loading close to failure followed by unloading which was necessary due to the restricted stroke of the actuators - Stage III: after shimming of actuators, monotonous loading until failure. P_a = 160 kN corresponds to the shear force due to the expected service load when the shear resistance of the slab is supposed to be critical in the design. 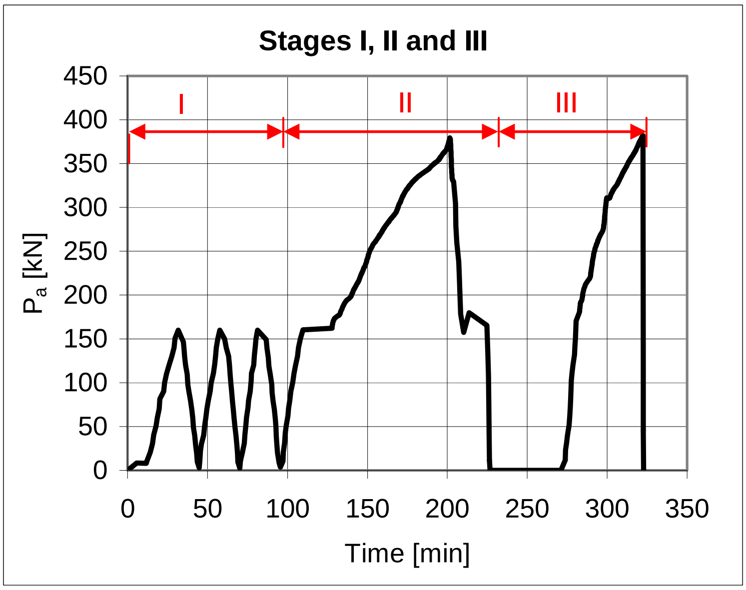 *Fig. 25. Actuator force P_a vs. time.*
5.2 After failure	-

6	**Observations during loading**

Before test	No longitudinal cracks along the strands were discovered in the soffit of the slabs.
Stage I	During stage I, the joint concrete gradually cracked along the webs of the middle beam. Here the first visible cracks were observed at P_a = 88 kN. At the same load new vertical cracks were also observed both in the Western and Eastern tie beam. The number of the new cracks in the tie beams increased with increasing load.
Stage II	At P_a = 160 kN during stage II, the soffit of the slabs between the line loads and the middle beam was inspected visually. The observed visible cracks are shown in Fig. 26. They were all below the webs of the slabs. When increasing P_a beyond 160 kN, new vertical cracks appeared in the tie beams. At P_a = 334 kN an inclined crack was observed in slab 7 accompanied by a new inclined crack at P_a = 336 kN. At P_a = 337 kN an inclined crack, similar to the two shear cracks in slab 7, was observed in slab 1. Simultaneously, a sudden increase in the deflection, as well as a new vertical crack in the tie beam between slabs 4 and 5, were observed in the Western part of the test floor. Despite these shear cracks on opposite sides of the middle beam, the actuator loads could still be increased until the maximum stroke of the actuators was achieved at P_a = 379 kN. After this, short prefacricated steel tubes were placed close to the actuators to keep the floor in deflected position when unloading and shimming the actuators.
Stage III	After completing the shimming in stage III, the floor was reloaded. A new inclined crack in slab 1 resulting in shear failure was observed at P_a = 382,4 kN The cracks after the failure are shown in Fig. 28. The initial crack on the top surface of slab 9 did not contribute to the failure as can be concluded from the crack pattern.
After failure	When demolishing the test specimen it was observed that that the core fillings were perfect, see App. A, Fig. 22. Delta beam seemed to recover completely after the test. The slabs were placed directly on the bottom flange of the Delta beam. Due to the uneven surfaces of the slab soffit and the steel flange, there were thin gaps between the slab and the flange of the beam. When demolishing the floor it came out that these gaps were filled with grout (thicker gaps) or with cement paste (thinner gaps), see App. A, Fig. 23.

7	**Cracks in concrete**
7.0 Cracks before test	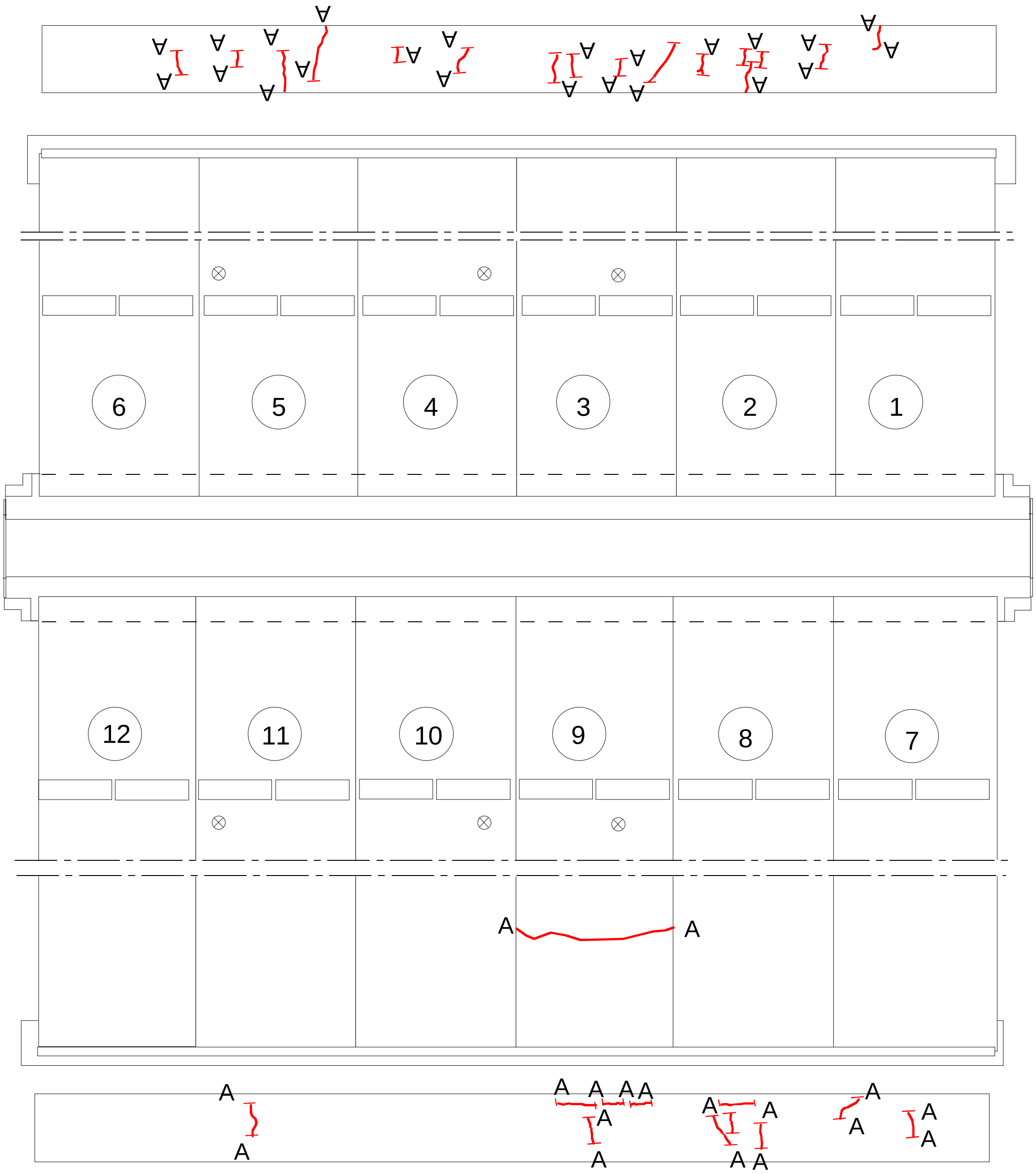 *Fig. 26. Initial cracks.*

7.1
Cracks at service load

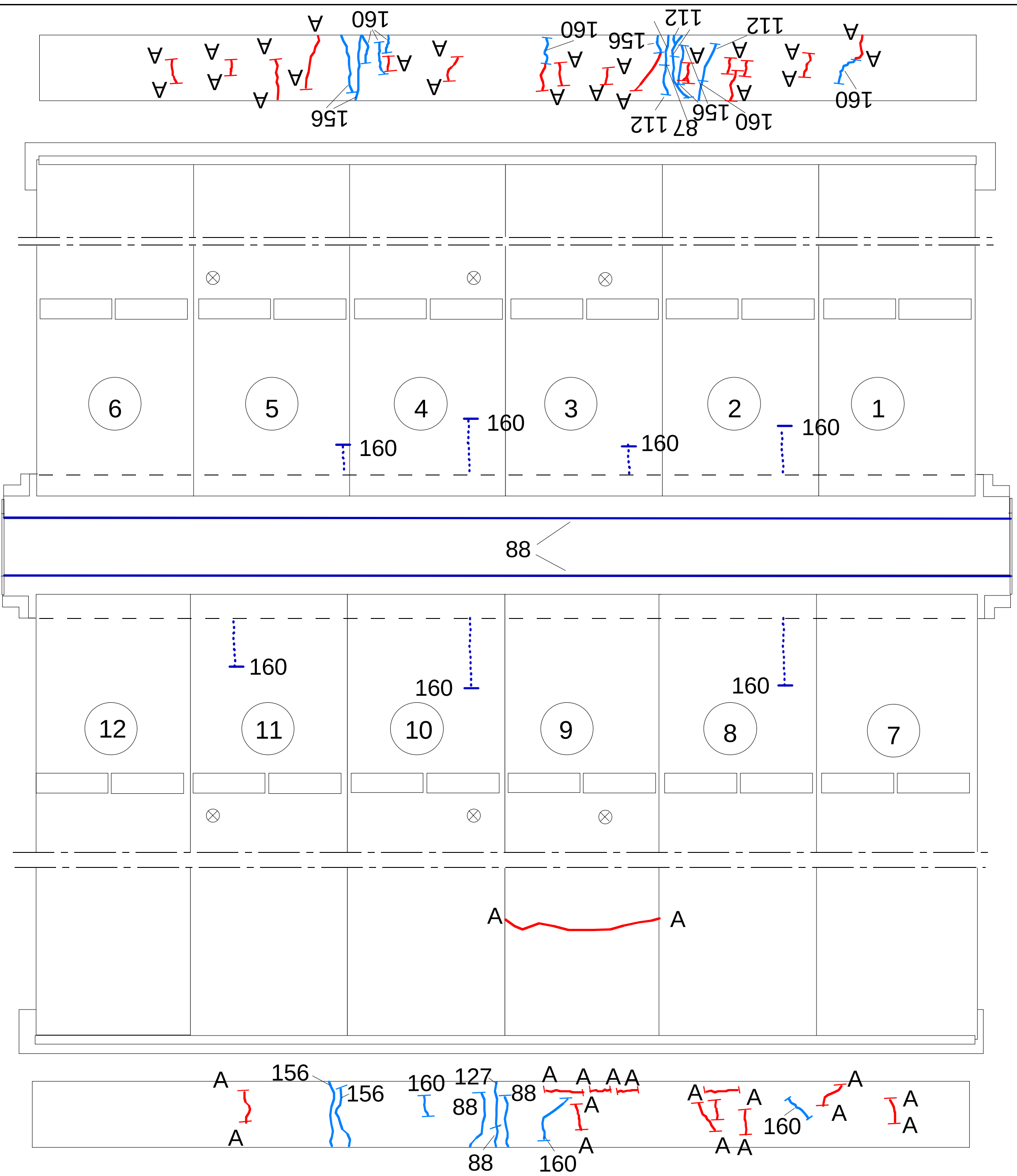

Fig. 27. Cracks at P_a = 160 kN. The dashed lines indicate thin ($\approx$0,1 mm) cracks in the soffit.

7.2 Cracks after failure	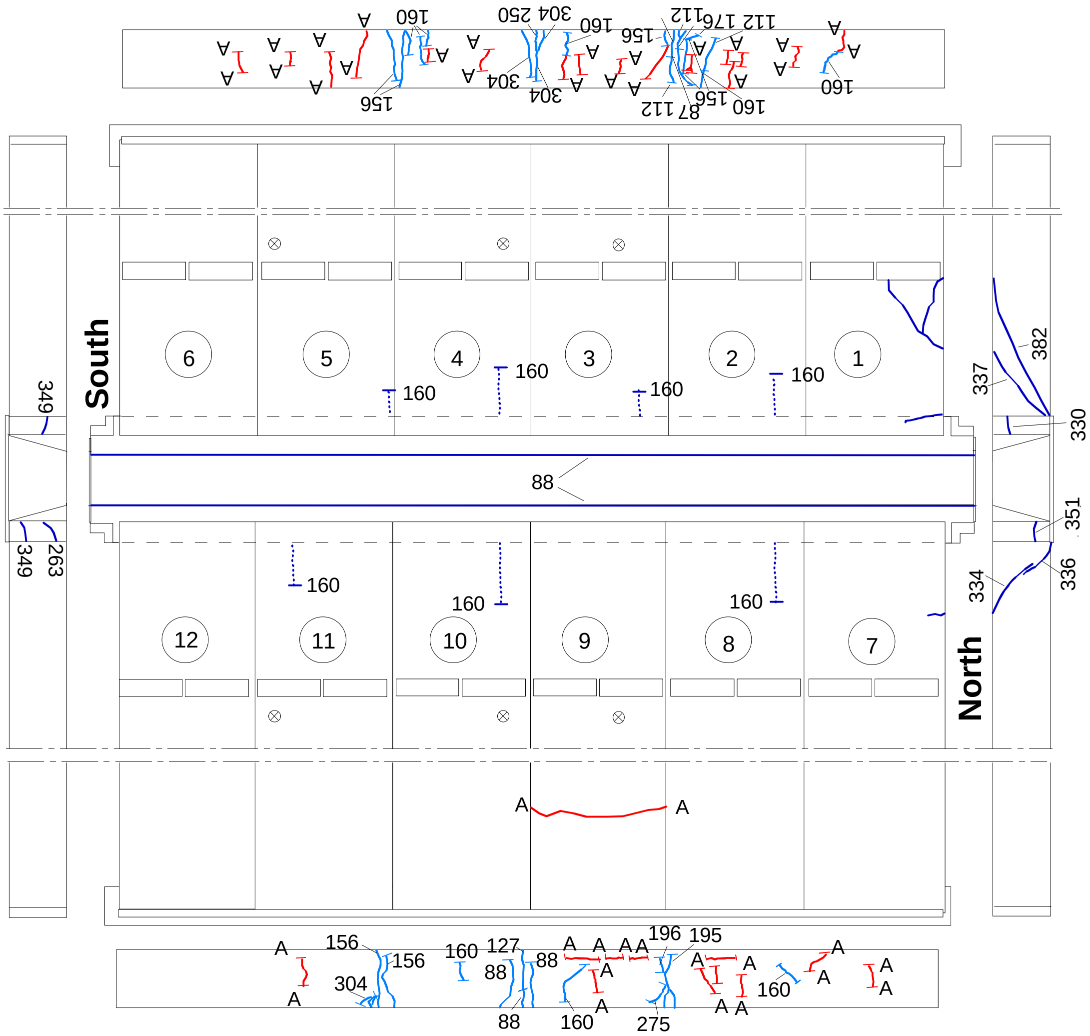 *Fig. 28. Cracks until Pa = 160 kN in the soffit (dashed lines) and after failure on the top and at the edges of the slabs.*

8 Observed shear resistance

In Fig. 29 the reaction force $R_{p,obs}$ at one end of the middle beam, measured by three load cells, vs. actuator load P_a is shown. The relationship is slightly nonlinear indicating some hysteresis in the cyclic stage.

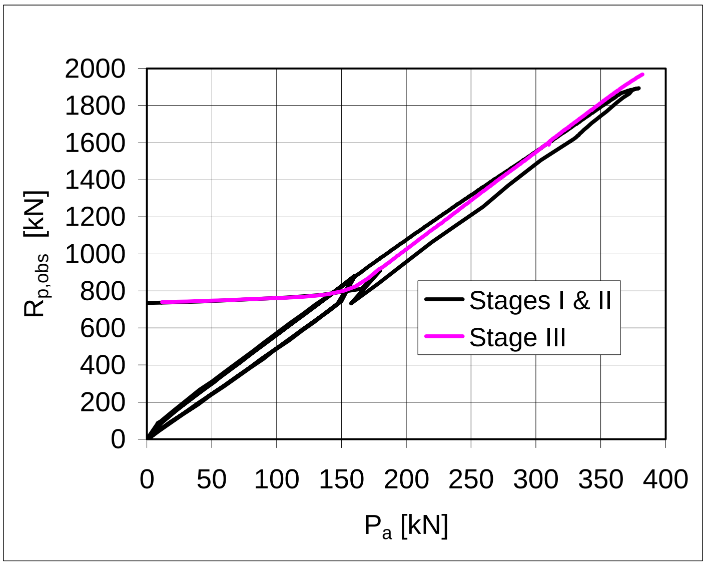

Fig. 29. Measured reaction force $R_{p,obs}$ at one end support of middle beam vs. actuator load P_a. $R_{p,obs}$ includes only the reaction due to the actuator loads P_a.

Figs 30 and 31 illustrate the ratio of measured support reaction $R_{p,obs}$ to the theoretical support reaction $R_{p,th}$ calculated from six actuator loads assuming simply supported slabs. Thus $R_{p,th}$ is equal to (9900–1450)/9900×6×P_a = 0,8535×6×P_a. Before failure the maximum difference is -0,59%, i.e. $R_{p,th}$ is less than 1% smaller than the measured support reaction. The assumption of simply supported slabs is accurate enough to justify the calculation of the experimental shear resistance based on it.

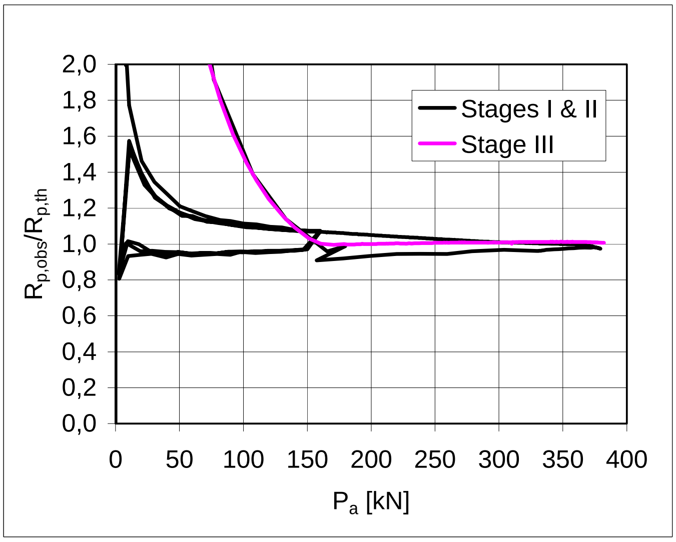

Fig. 30. Ratio of measured support reaction of the middle beam ($R_{p,obs}$) to theoretical support reaction ($R_{p,th}$) vs. actuator force P_a. Only actuator loads P_a are taken into account in the support reaction.

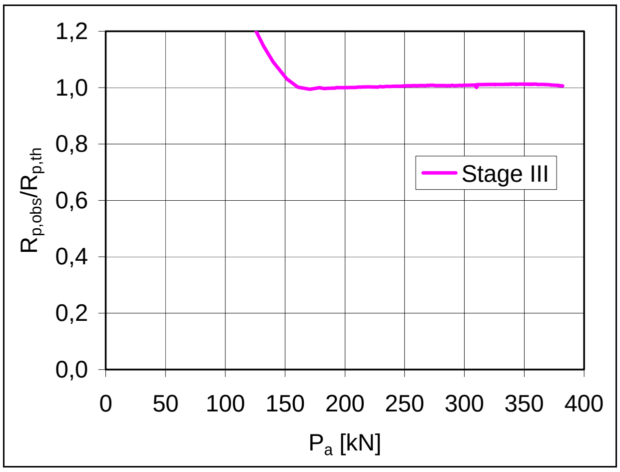

Fig. 31. As Fig. 27 but only stage III is shown.

The shear resistance of one slab end (support reaction of slab end at failure) due to different load components is given by

$$V_{obs} = V_{g,sl} + V_{g,jc} + V_{eq} + V_p$$

where $V_{g,sl}$, $V_{g,jc}$, V_{eq} and V_p are shear forces due to the self-weight of slab unit, weight of joint concrete, weight of loading equipment and actuator forces P_a, respectively. All components of the shear force are calculated assuming that the slabs behave as simply supported beams. For V_{eq} and V_p this means that $V_{eq} = 0{,}8535{\times}P_e$ and $V_p = 0{,}8535{\times}P_a$. $V_{g,jc}$ is calculated from the nominal geometry of the joints and density of the concrete, other components of the shear force are calculated from measured loads and weights. The values for the components of the shear force are given in Table 1.

Table 1. Components of shear resistance due to different loads.

Action	Load	Shear force	
			kN
Weight of slab unit	6,53 kN/m	$V_{g,sl}$	32,19
Weight of joint concrete	0,39 kN/m	$V_{g,jc}$	1,92
Loading equipment	6,22 kN	V_{eq}	5,33
Actuator loads	382,1 kN	V_p	327,46

The observed shear resistance $\boldsymbol{V_{obs}}$ **= 366,9 kN** (shear force at support) is obtained for one slab unit and the shear force per unit width is v_{obs} = **305,8 kN**.

9 Material properties

9.1
Strength of steel:

Component	$R_{eH}/R_{p0,2}$ MPa	R_m MPa	Note
Delta beam	≈ 355		Nominal (S355J2G3)
Slab strands J12,5	1630	1860	Nominal (no yielding in test)
Reinforcement Txy (A500HW)	500		Nominal value for reinforcing bars (no yielding in test)

9.2
Strength of slab concrete, floor test

#	Cores		*h* mm	*d* mm	Date of test	Note
6			50	50	15.11.2005 (+4 d)[1)]	Upper flange of slab 1, vertically drilled, tested as drilled[2)], density = 2468 kg/m^3
Mean strength [MPa]			70,5			
St.deviation [MPa]			3,32			

9.3
Strength of slab concrete, reference tests

#	Cores		*h* mm	*d* mm	Date of test	Note
6			50	50	23.11.2005 (+1-2 d)[1)]	Upper flange of slab 13, vertically drilled, tested as drilled[2)], density = 2463 kg/m^3
Mean strength [MPa]			75,9			
St.deviation [MPa]			3,34			

9.4
Strength of cast-in-situ concrete

#		*a* mm	Date of test	Note
6		150	11.11.2005 (+0 d)[1)]	Kept in laboratory in the same conditions as the floor specimen density = 2197 kg/m^3
Mean strength [MPa]		28,8		
St.deviation [MPa]		0,93		

[1)] Date of material test minus date of structural test (floor test or reference test)
[2)] After drilling, kept in a closed plastic bag until compression

10

Measured displacements

In the following figures, V_P stands for the shear force of one slab end due to imposed actuator loads, calculated assuming simply supported slabs.

10.1
Deflections

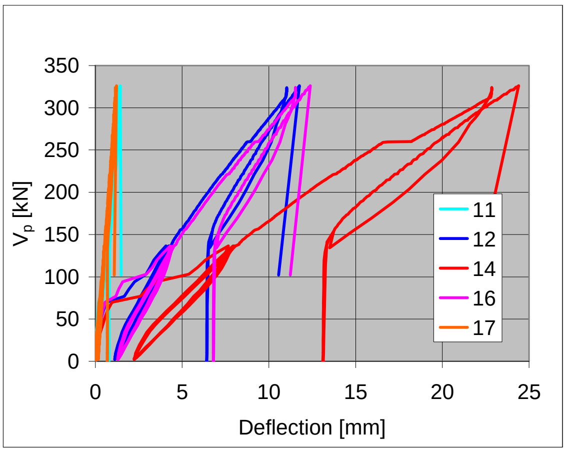

Fig. 32. Deflection on line I along Western end beam.

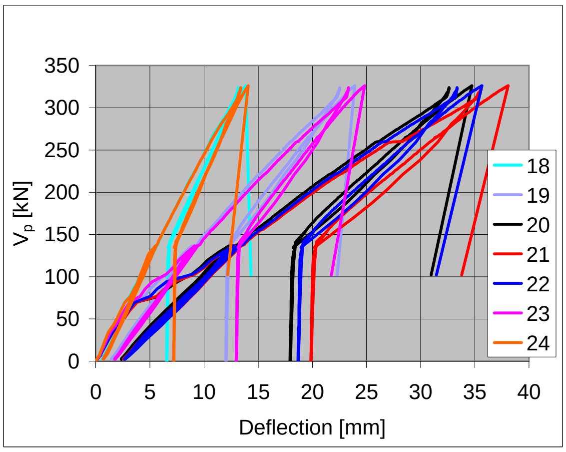

Fig. 33. Deflection on line II in the middle of slabs 1–6.

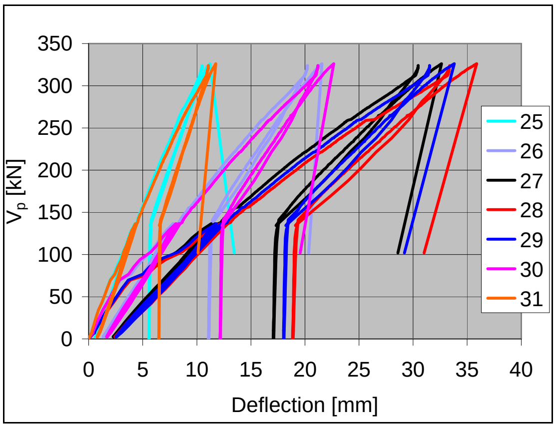

Fig. 34. Deflection on line III close to the line load, slabs 1–6.

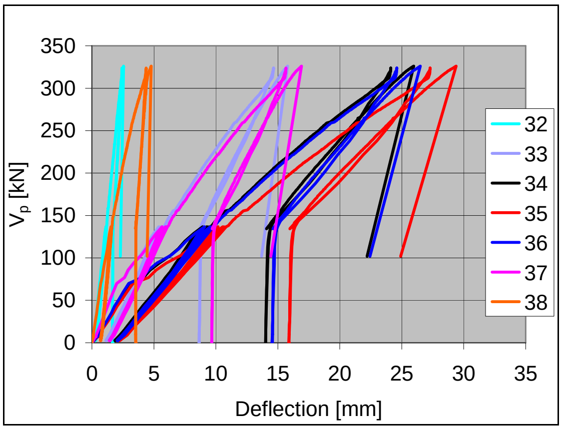

Fig. 35. Deflection on line IV along the middle beam.

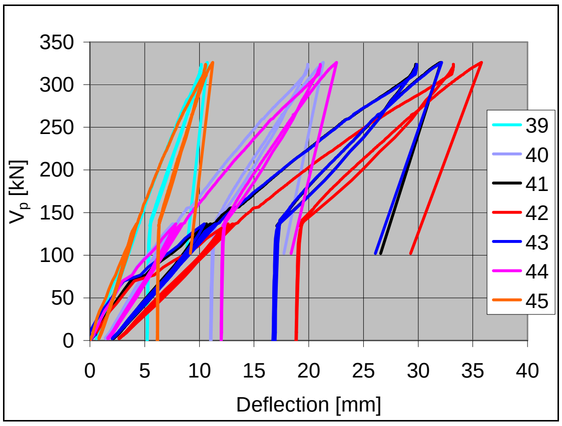

Fig. 36. Deflection on line V close to the line load, slabs 7–12.

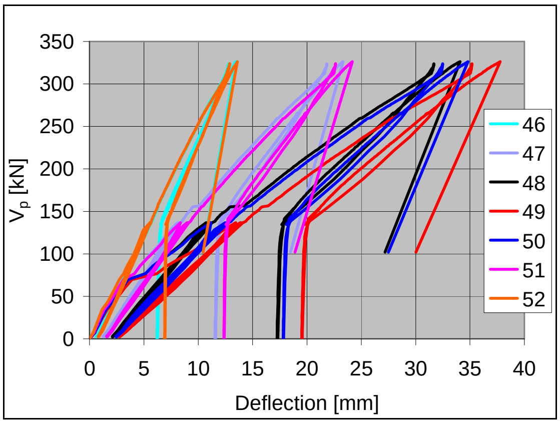

Fig. 37. Deflection on line VI in the middle of slabs 7–12.

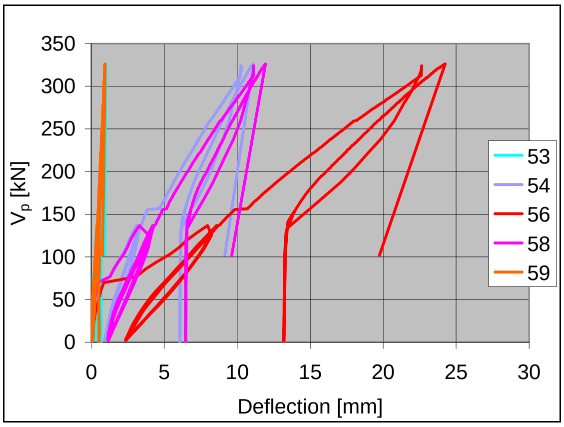

Fig. 38. Deflection on line VII along end beam, slabs 7–12.

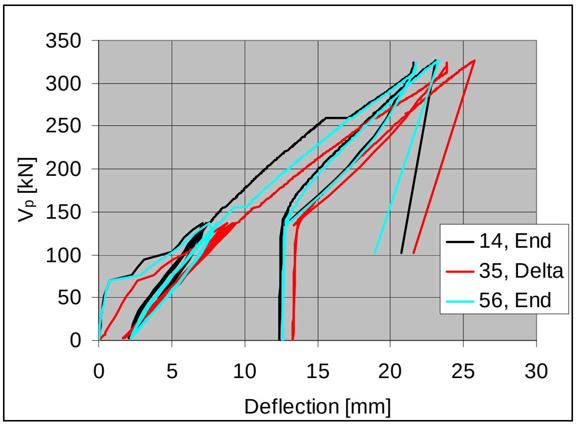

Fig. 39. Net deflection of midpoint of middle beam (35) and those of end beams (14, 56). Settlement of supports eliminated.

10.2
Crack width

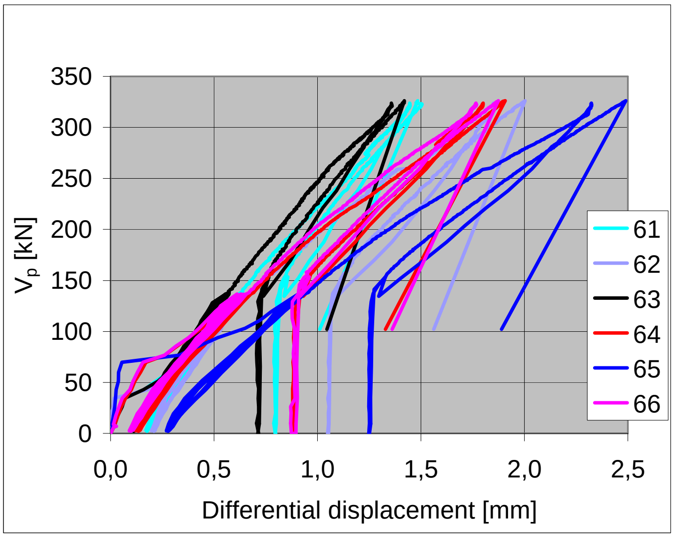

Fig. 40. Differential displacement (≈ crack width) measured by transducers 61–66.

10.3
Average strain

Transducers 67–78 shown in Figs 20–22 measured the differential displacement between two points fixed to the test floor in order to determine the strains in beam's direction. Figs 41–42 depict the results.

The differential displacement divided by the mutual distance of the two fixing points represents the average strain between those points. Assuming linear variation for the strain in vertical direction, the average strain at any depth between the measured top and bottom values can be calculated from the measured results. The average strain at the top and bottom fibre of the slabs and of the middle beam obtained in this way are shown in Figs 43–45 and in Figs 46–48 at service load and at failure load, respectively.

Assuming parabolic curvature due to the uniformly distributed load on the beam and having the span of the beam equal to 7,2 m, the maximum strain within each of the slabs 3, 4, 9 and 10 is 4% higher than the average strain measured between the edges of the slab. In this way, the maximum strain is obtained from the average strains by multiplying the latter by 1,04.

- On the top, the strains in the slabs were essentially smaller than those in the beam. This can be explained by the low transverse shear stiffness of the slabs. The scatter of the slab strains on the top was small.

- At the bottom, the strains in the slabs were also essentially smaller than those in the beam at the same level. The support reaction of the slabs was partly carried by the inclined webs of the middle beam. The interaction between the soffit of the slabs and the bottom flange of the beam was too weak to make the strains compatible. The tie reinforcement also tried to keep the transverse strain of the slab ends as small as possible. This can clearly be seen in Fig. 45. At V_p = 7 kN some kind of slippage took place

- At V_p = 137 kN the strain in the soffit of the slabs had a large scatter. At V_p = 326 kN the strain at the bottom of slab 9 was very small when compared with that of the other slabs. In slabs 3, 4 and 10 the scatter in the measured strains was relatively small. In slab 9, the strain at the bottom was much smaller than in the other slabs.

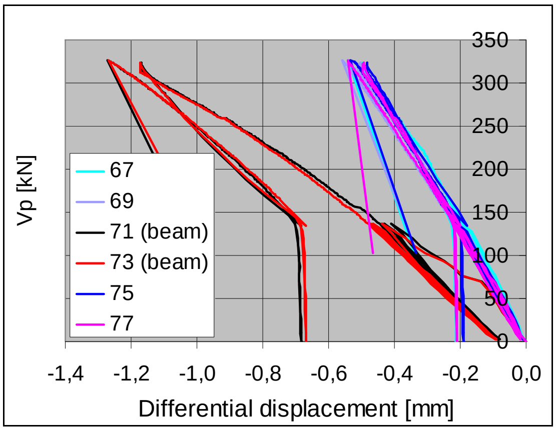

Fig. 41. Differential displacement at top surface of floor measured by transducers 67, 69, 71, 73, 75 and 77.

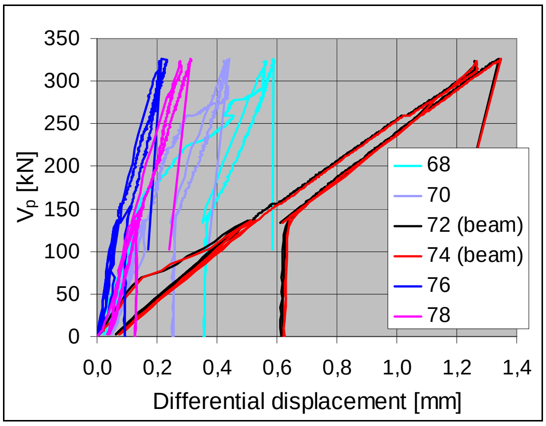

Fig. 42. Differential displacement at soffit of floor measured by transducers 68, 70, 72, 74, 76 and 78.

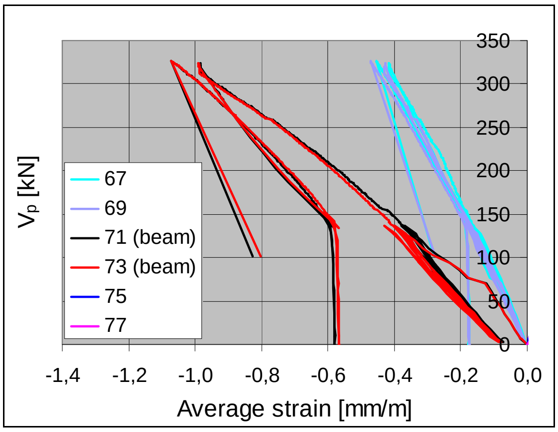

Fig. 43. Top fibre of floor. Average strain calculated from the differential displacements shown in Figs 41–42.

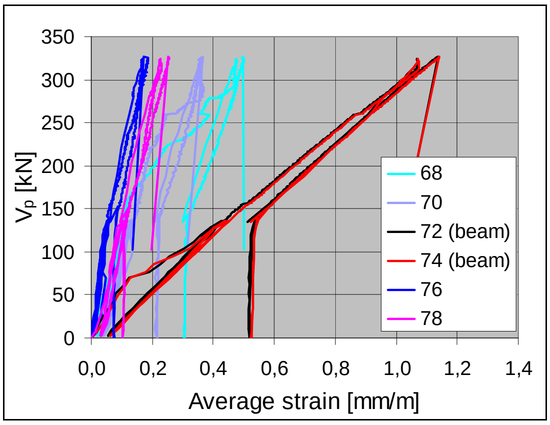

Fig. 44. Bottom fibre of floor. Average strain calculated from the differential displacements shown in Figs 41–42.

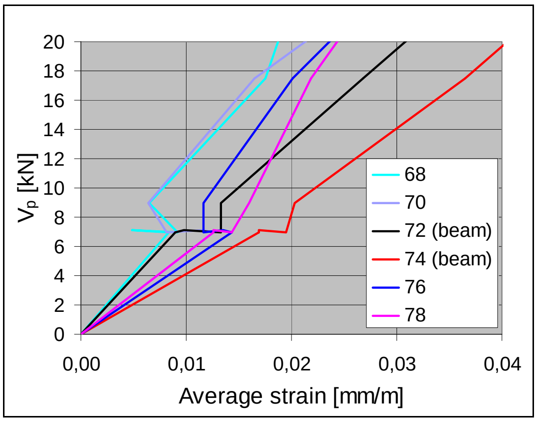

Fig. 45 Bottom fibre of floor. Initial part of the previous figure.

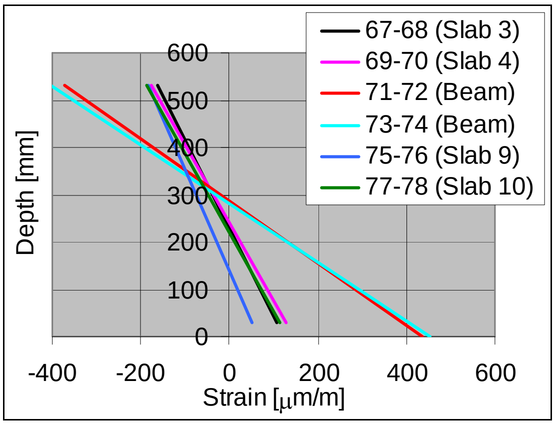

Fig. 46. Average strain of slabs 3, 4, 9 and 10 as well as that of the middle beam at estimated service load P_a = 160 kN (V_p = 137 kN).

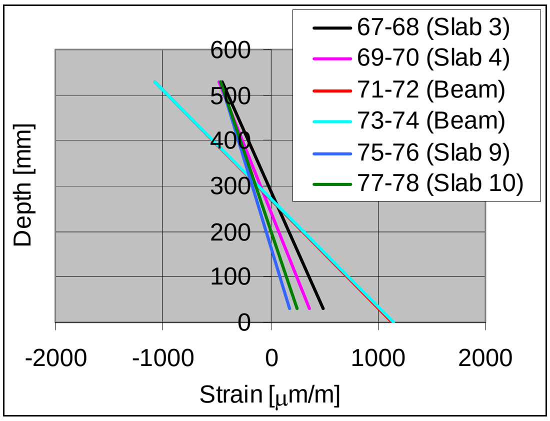

Fig. 47. Average strain of slabs 3, 4, 9 and 10 as well as that of the middle beam at failure load P_a =382 kN (V_p = 326 kN).

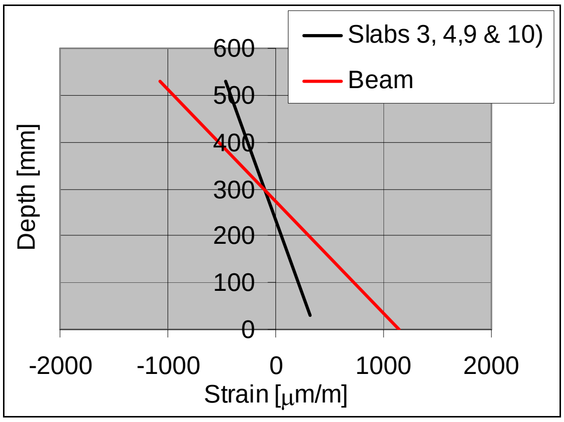

Fig. 48. Mean of average strains measured for slabs 3, 4, 9 and 10 as well as mean of average strains measured for the middle beam at failure load P_a = 382 kN (V_p = 326 kN).

10.4
Shear displacement

A positive value means that the slab is moving towards the end of the beam. The measured curves do not look logical, and there may have been some mess in numbering the transducers. There are two puzzles:

- why do the upper flange of slab 1 and lower flange of slab 7 in Fig. 49 move together and vice versa?
- why does the upper flange move less than the lower flange in Fig. 51 and partly in Fig. 49?

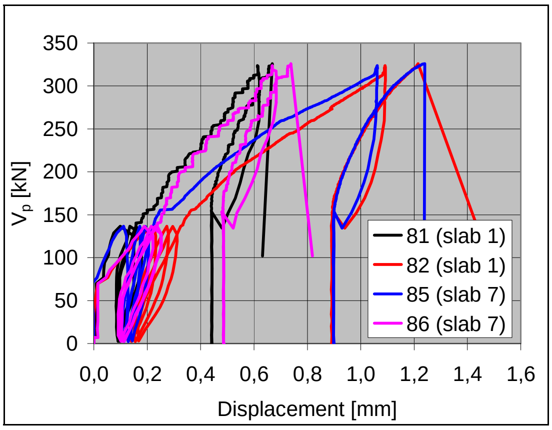

Fig. 49. North end of middle beam. Differential displacement between edge of slab and middle beam in beam's direction.

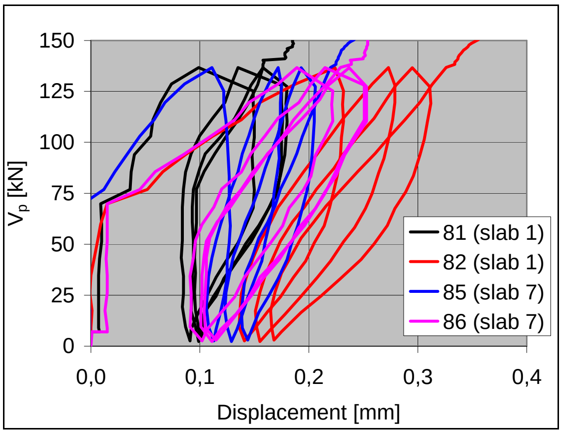

Fig. 50. Same as previous figure, but only the initial part of the curves is shown.

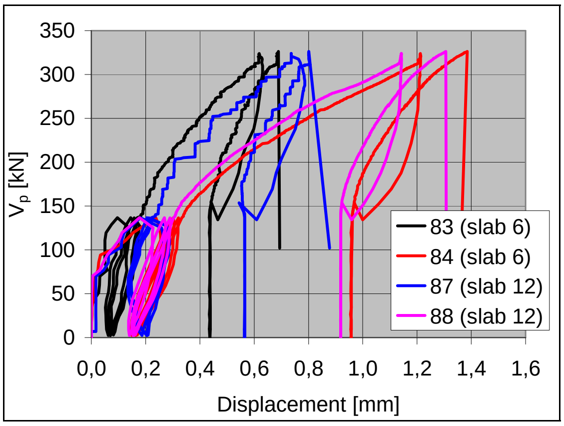

Fig. 51. South end of middle beam. Differential displacement between edge of slab and middle beam in beam's direction.

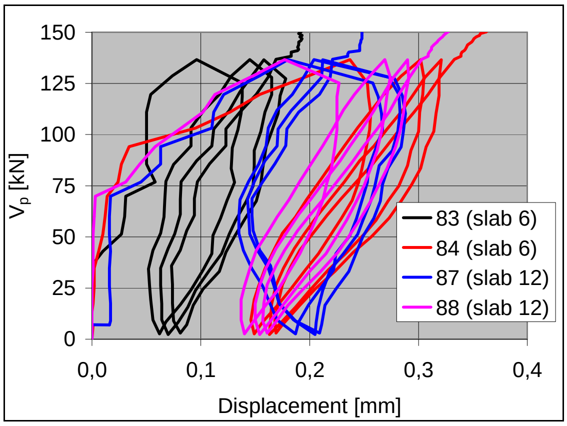

Fig. 52. Same as previous figure, but only the initial part of the curves is shown.

10.5 Strain

-

11 Reference tests

Slab 13 was taken from the same casting lot 17485 as four other slabs in the floor test.

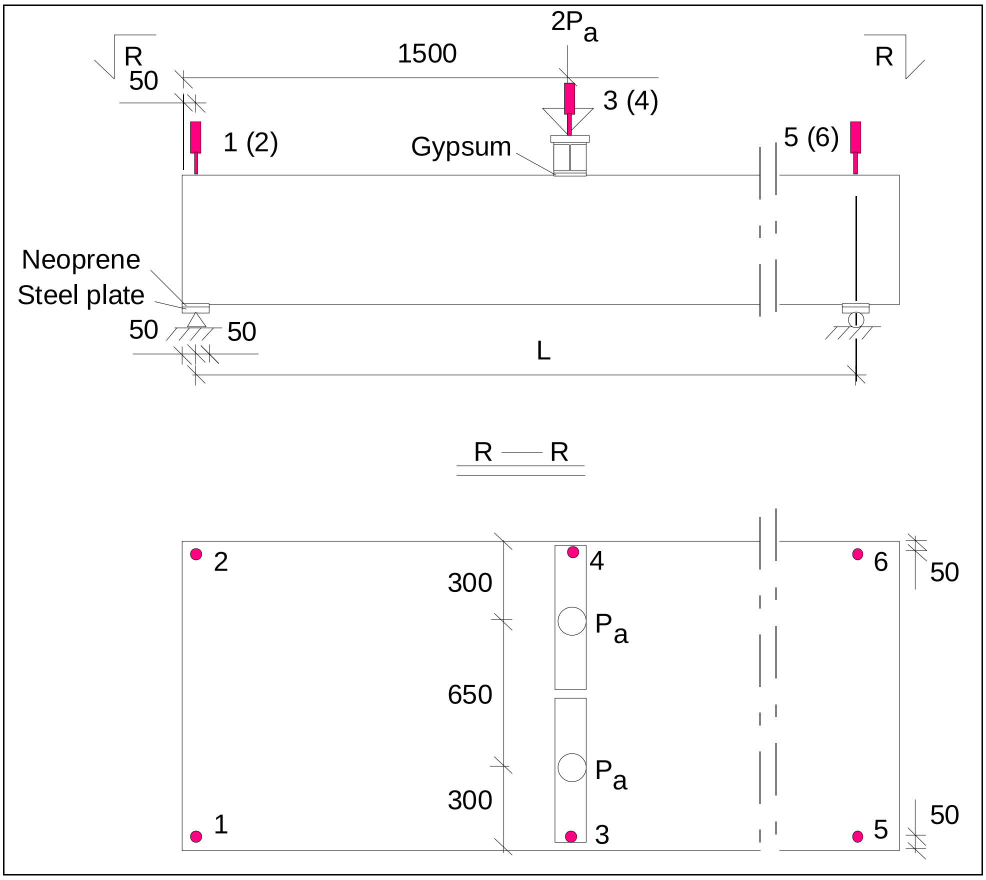

Fig. 53. Layout of reference tests. For L, see Table 3. Test R1 was carried out first.

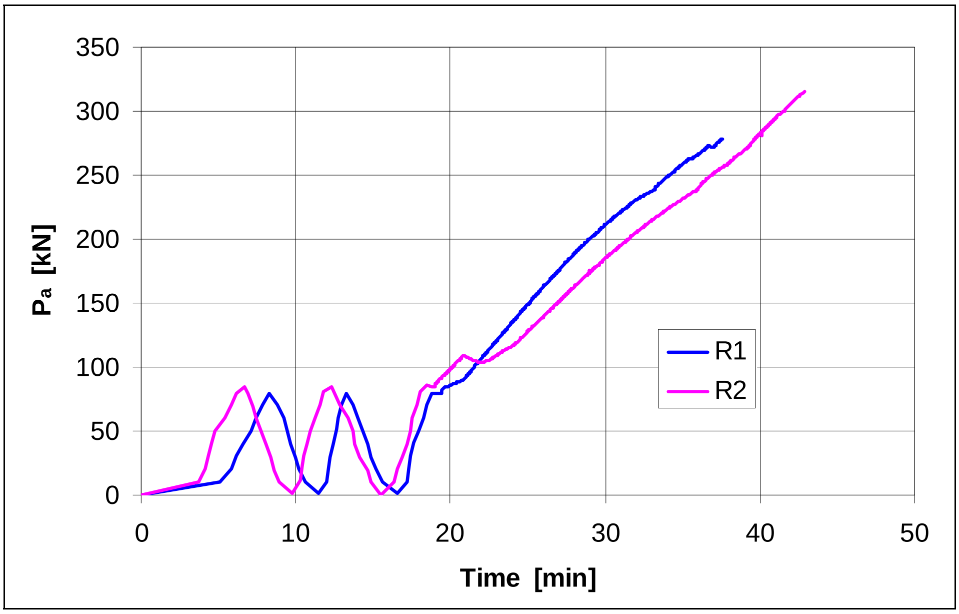

Fig. 54. Actuator force – time relationship.

In both reference tests flexural cracks were observed below the loads before the shear tension failure took place in the webs close to the support. No visible slippage of the strands was observed before the failure. The failure modes are illustrated in Fig. 56 and in App. A, Figs 38–41.

The time dependence of the load and measured load – deflection relationship are shown in Figs 55.

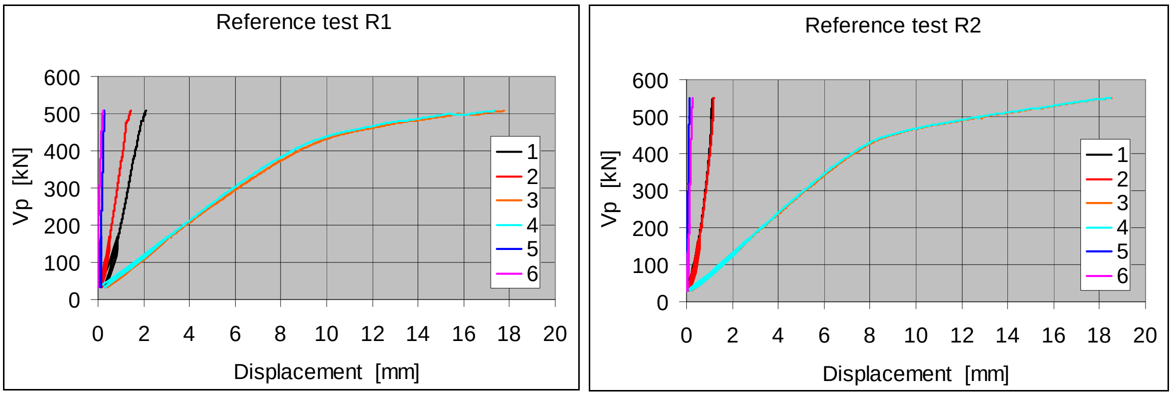

Fig. 55. Vertical displecements measured by transducers 1–6. V_P is the support reaction due to actuator forces P_a.

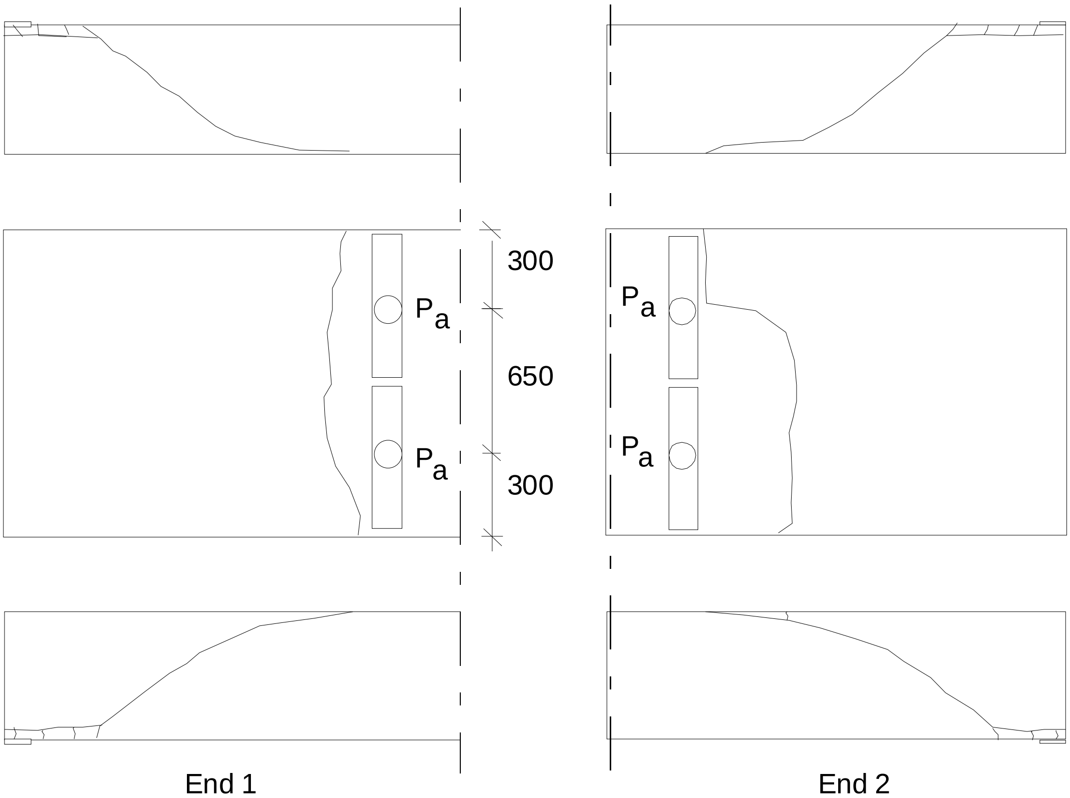

Fig. 56. Failure mode in tests R1 (End 1) and R2 (End 2).

Table 2. Span of slab, shear force V_g at support due to the self weight of the slab, actuator force P_a at failure, weight of loading equipment P_{eq}, shear force V_p due to imposed load at failure, total shear force V_{obs} at failure and total shear force v_{obs} per unit width.

Test	Date	Span mm	V_g kN	P_a kN	P_{eq} kN	V_{obs} kN	v_{obs} kN/m	Note
R1	21.12.2005	9900	32,1	278,5	0,29	507,8	396,4	Web shear failure
R2	22.12.2005	8420	28,1	315,0	0,29	550,9	435,7	Web shear failure
				Mean		529,4	**441,1**	

12	**Comparison: floor test vs. reference tests**
	The observed shear resistance (support reaction) of the hollow core slab in the floor test was equal to 366,9 kN per one slab unit or 305,8 kN/m. This is **69%** of the mean of the shear resistances observed in the reference tests.
13	**Discussion**
	1. The net deflection of the middle beam due to the imposed actuator loads only (deflection minus settlement of supports) was 25,7 mm or *L*/280, i.e. rather small. It was 2,4–2,6 mm greater than that of the end beams. Hence, the torsional stresses due to the different deflection of the middle beam and end beams had a negligible effect on the failure of the slabs. 2. The shear resistance measured in the reference tests was of the same order as the observed values for similar slabs given in *Pajari, M. Resistance of prestressed hollow core slab against a web shear failure. VTT Research Notes 2292, Espoo 2005*. 3. The observed shear resistance in the floor test was 69% of that in reference tests. 4. The edge slabs slided 0,6 … 1,4 mm along the beam before failure.This reduced the negative effects of the transverse actions in the slab and had a positive effect on the shear resistance. 5. The failure mode was web shear failure of edge slabs. The Delta beam seemed to recover completely after the failure.

APPENDIX A: PHOTOGRAPHS

Note: In Figs. 23–33 the cracks marked with red colour and letter A refer to initial cracks which existed before the onset of the loading.

Fig. 1. Delta beam as installed.

Fig. 2. Delta beam as installed.

Fig. 3. Slab placed on Delta beam.

Fig. 4. Tie reinforcement at support of beam.

Fig. 5. End of middle beam (Delta beam) after grouting.

Fig. 6. Overview on test arrangements.

Fig. 7. Loading equipment.

Fig. 8. Longitudinal view on the loading equipment.

Fig. 9. Actuators on the primary spreader beam and below the temporary loading frame.

Fig. 10. Arrangements at end beam.

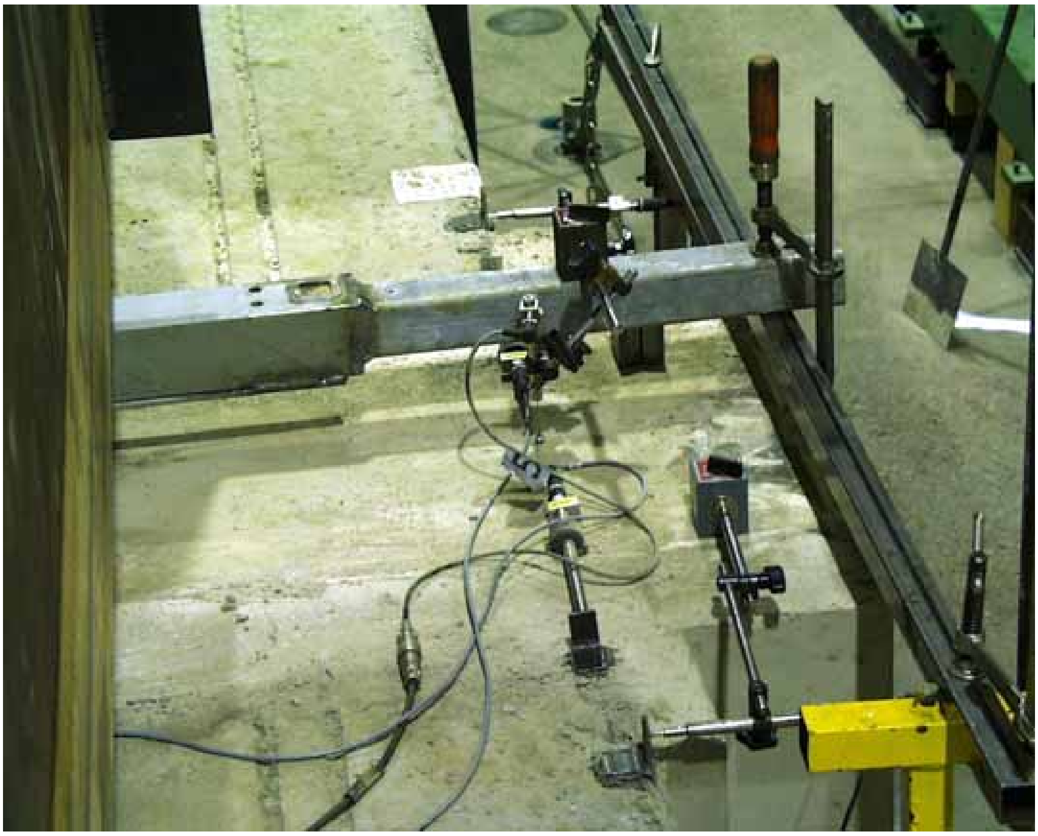

Fig. 11. Transducers at end of middle beam.

Fig. 12. Transducer, fixed to the bottom flange of the middle beam, measuring sliding of slab along beam.

Fig. 13. Bottom flange of middle beam supporting slabs.

Fig. 14. Equipment for measuring average transverse strain of the soffit.

Fig. 15. Initial crack in slab 3 close to end beam.

Fig. 16. Shear cracks in slab 7 at P_a = 336 kN.

Fig. 17. Shear crack in slab 1 at P_a = 337 kN.

Fig. 18. Shear cracks in slab 1 after failure at P_a = 382 kN.

Fig. 19. Shear cracks in slab 1 after removing the loading equipment.

Fig. 20. Failure pattern on the top of slab 1 after removing the loading equipment and drilling the cores.

Fig. 21. Slab 1 after removing slabs 2–6 and 8–12.

Fig. 22. Perfect filling in a hollow core of slab 1.

Fig. 23. Cast-in-situ concrete after removing the slabs. Note the grout layer between the slab and the flange of the beam.

Fig. 24. Western end beam. Cracks in cast in-situ concrete at the end of slabs 1 and 2.

Fig. 25. Western end beam. Cracks in cast in-situ concrete at the end of slabs 1 and 2.

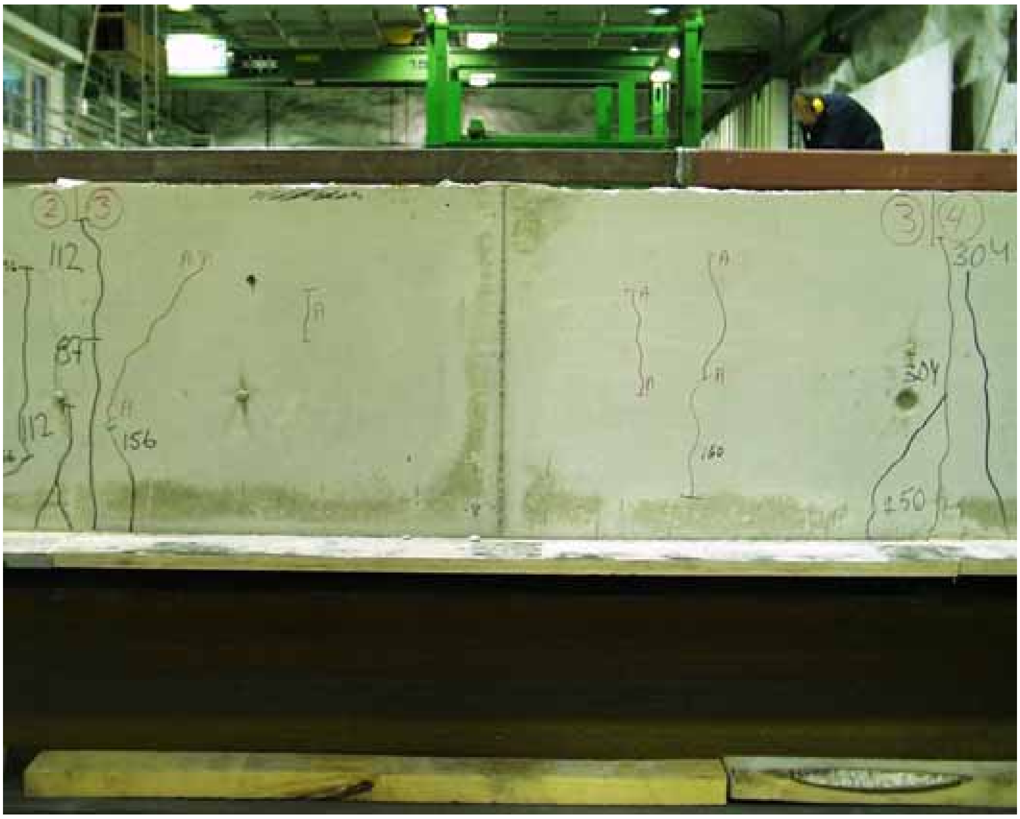

Fig. 26. Western end beam. Cracks in cast in-situ concrete at the end of slabs 2–4.

Fig. 27. Western end beam. Cracks in cast in-situ concrete at the end of slabs 3–5.

Fig. 28. Western end beam. Cracks in cast in-situ concrete at the end of slabs 4–6.

Fig. 29. Western end beam. Cracks in cast in-situ concrete at the end of slabs 5 and 6.

Fig. 30. Eastern end beam. Cracks in cast in-situ concrete at the end of slabs 7–9.

Fig. 31. Eastern end beam. Cracks in cast in-situ concrete at the end of slabs 7–8.

Fig. 32. Eastern end beam. Cracks in cast in-situ concrete at the end of slabs 8–9.

Fig. 33. Eastern end beam. Cracks in cast in-situ concrete at the end of slabs 9–11.

Fig. 34. Eastern end beam. Cracks in cast in-situ concrete at the end of slabs 10–12.

Fig. 35. Eastern end beam. No crack in cast in-situ concrete at the end of slab 12.

Fig. 36. Arrangements in reference test R1.

Fig. 37. Arrangements in reference test R1.

Fig. 38. Failure in reference test R1.

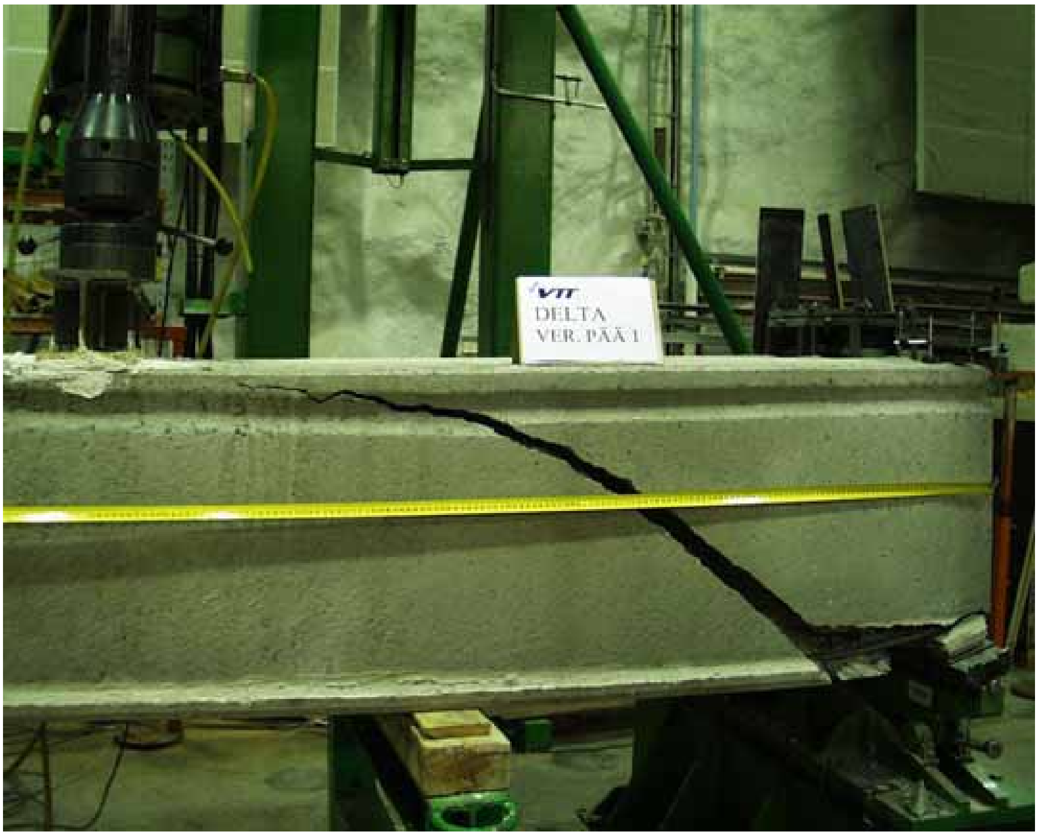

Fig. 39. Failure in reference test R1.

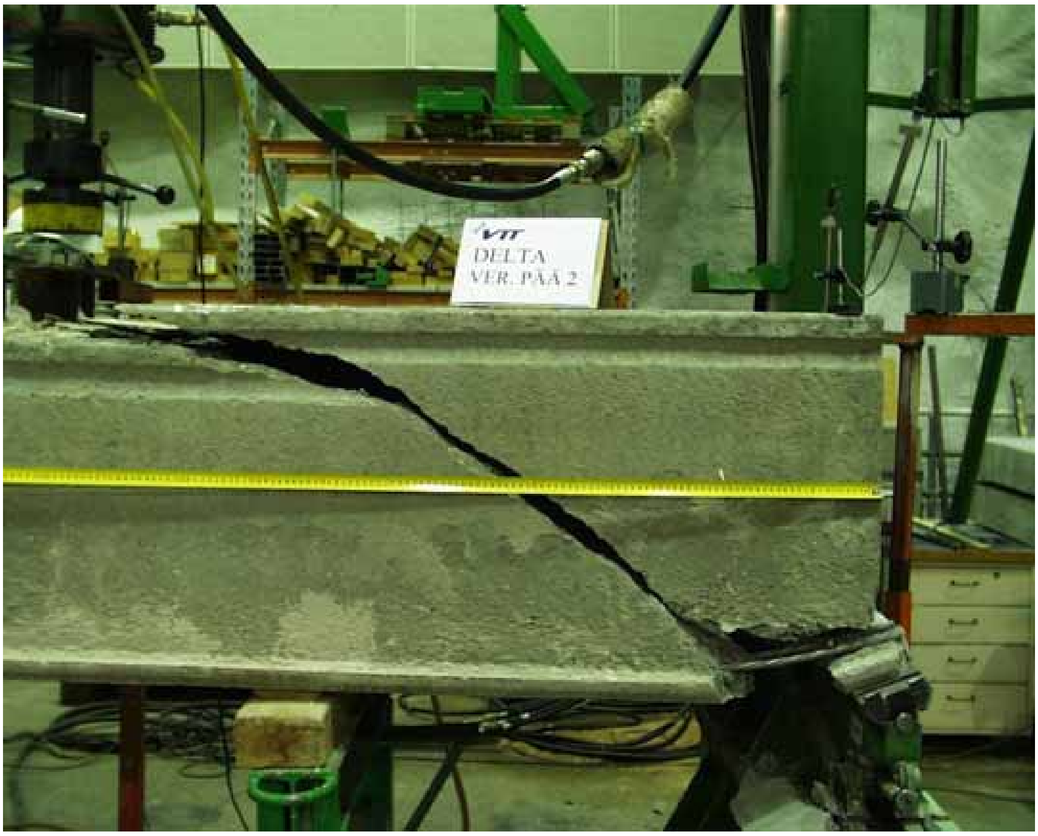

Fig. 40. Failure in reference test R2.

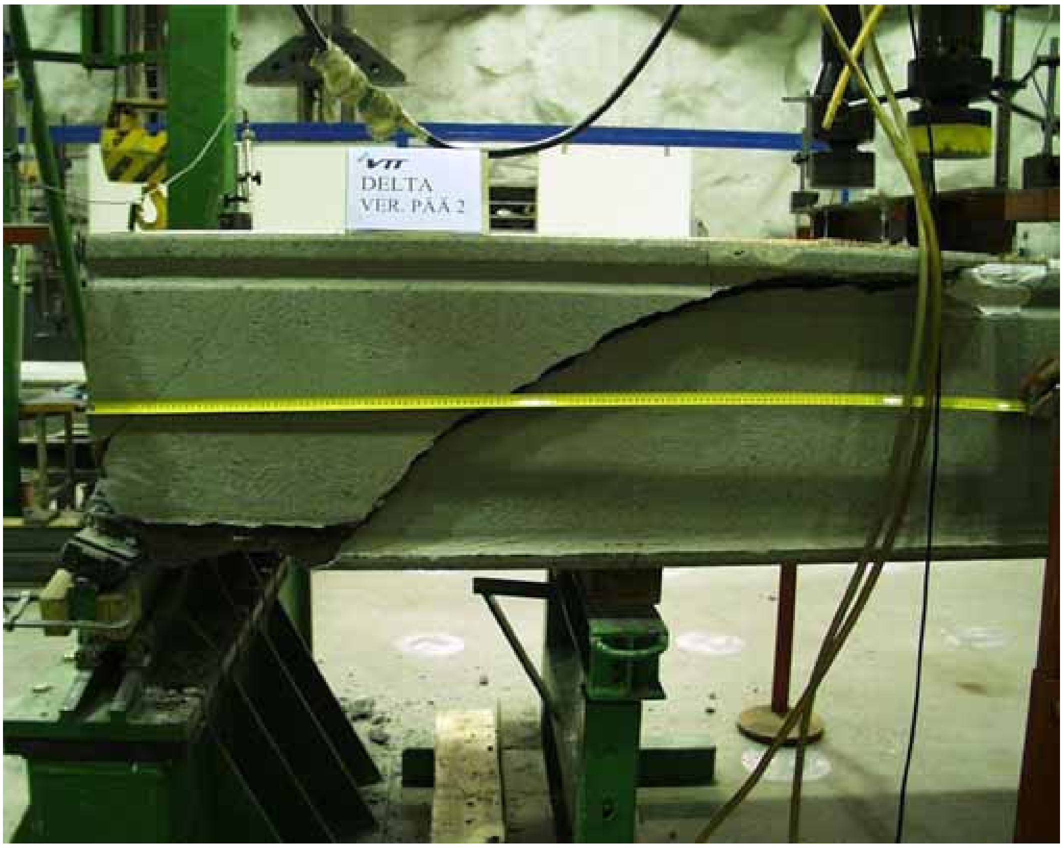

‘

Fig. 41. Failure in reference test R2.

APPENDIX B: DELTA BEAM

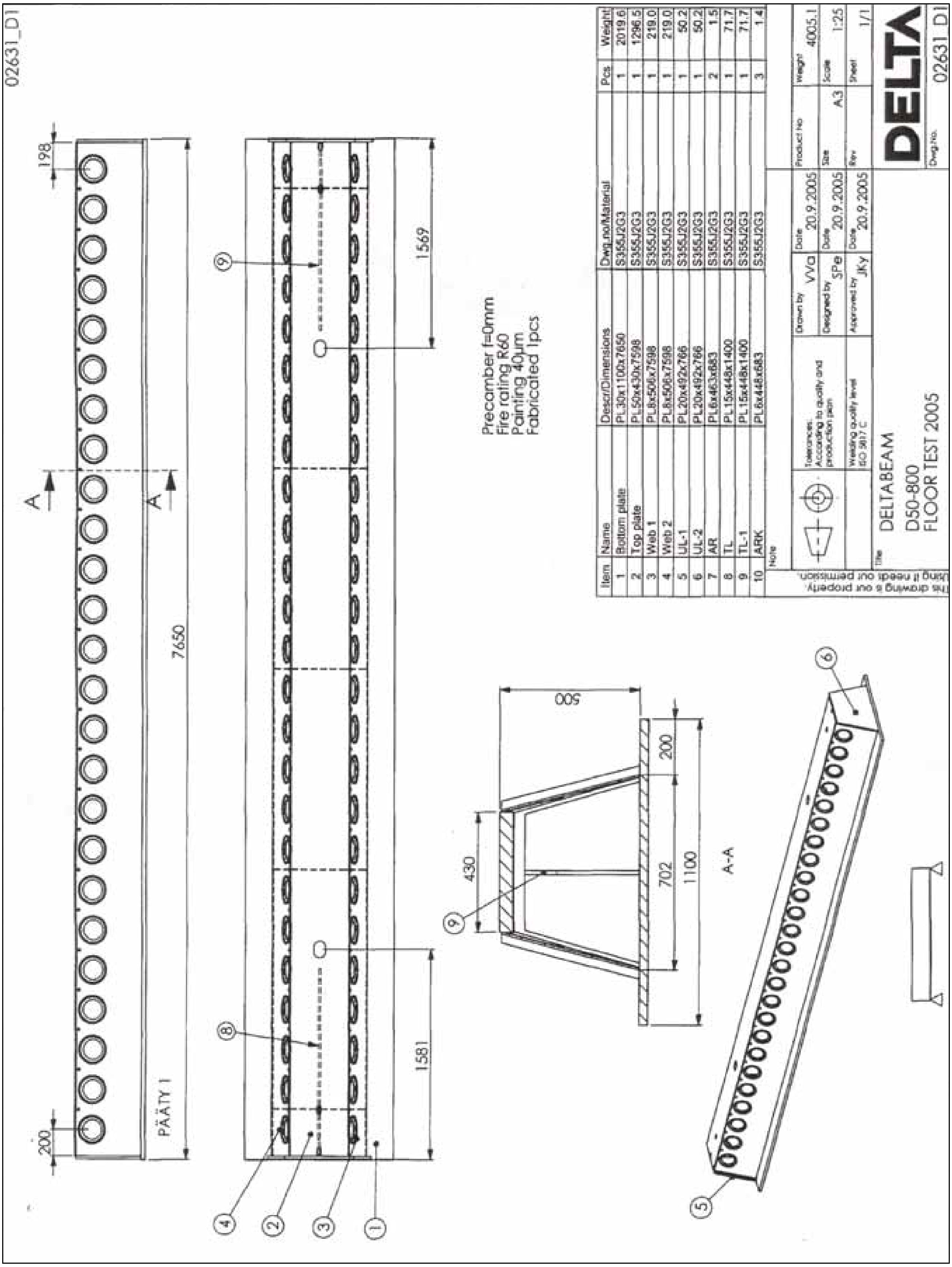

Fig. 1. Delta beam.

1	**General information**
1.1 Identification and aim	**VTT.PC.InvT.400.2006** **Last update 2.11.2010** PC400U (Internal identification) Aim of the test: In test VTT.PC.InvT.400.1993 the edges of the beam were provided with square indents which, after grouting, served as dowels between the slab ends and the beam. In the present test the indents were missing and the longitudinal tie reinforcement was placed near to the mid-depth of the slabs. It was anticipated that these changes would enhance the shear resistance of the slabs.
1.2 Test type	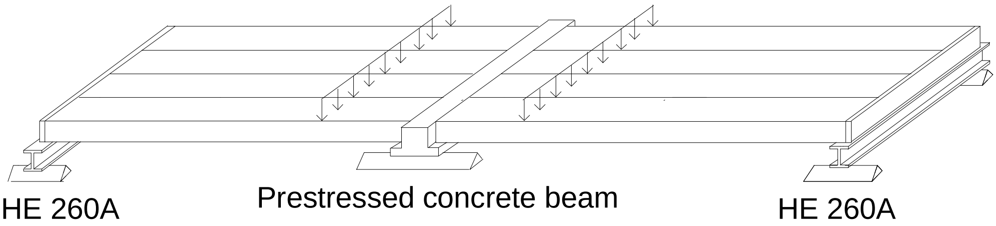 *Fig. 1. Illustration of test setup.*
1.3 Laboratory & date of test	VTT/FI 31.5.2006
1.4 Test report	Author(s): Pajari, M. Name: *Load test on hollow core slab floor with prestressed concrete beam* Ref. number: VTT-S-07331-06 Date: 27.12.2006 Availability: Available at www.rakennusteollisuus.fi
2	**Test specimen and loading**

2.1
General plan

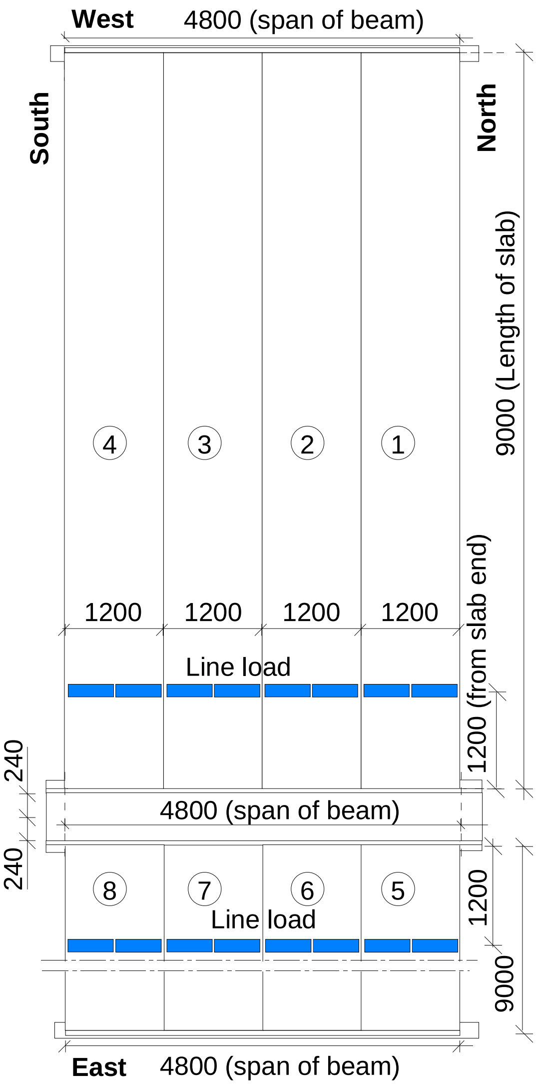

Fig. 2. Plan.

2.2
End beams

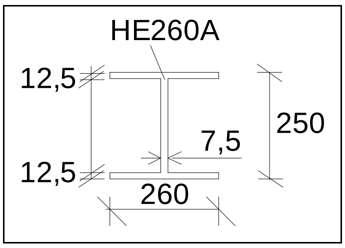

Fig. 3. End beam made of steel.

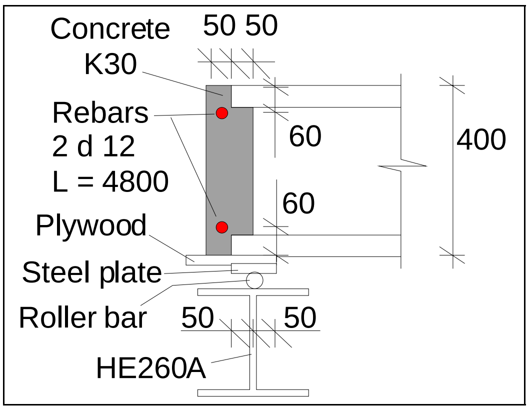

Fig. 4. Arrangements at end beam.

Simply supported, span = 4,8 m, roller bearing below Northern end
$f_y \approx$ 355 MPa (nominal f_y), did not yield in the test.

2.3
Middle beam

- Cast by Parma Oy, 13.4.2006
- Simply supported, span = 4,8 m, roller bearing at both ends

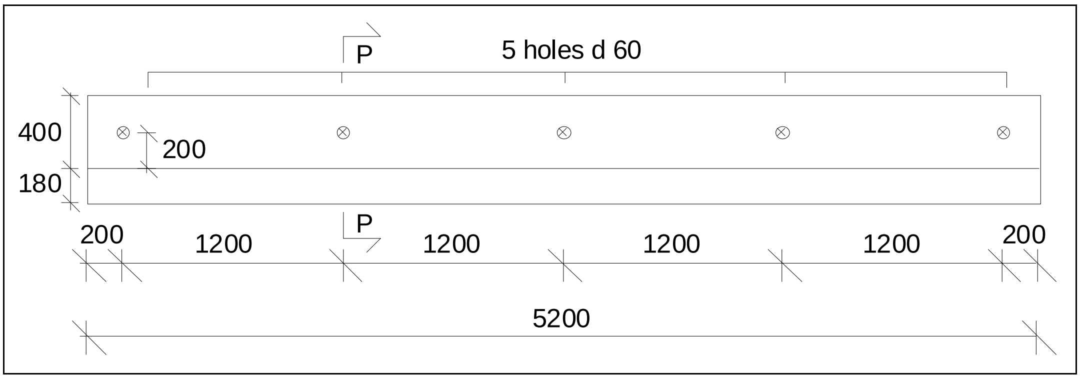

Fig. 5. Middle beam. Elevation.

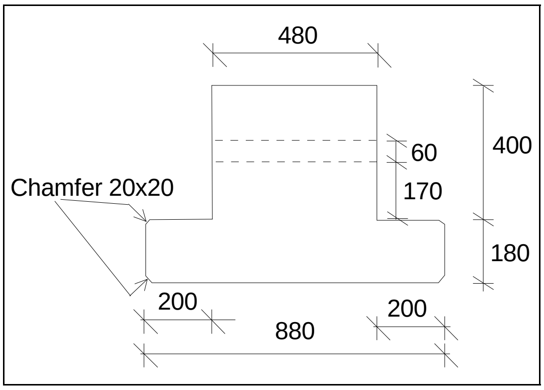

Fig. 6. Cross-sectional geometry.

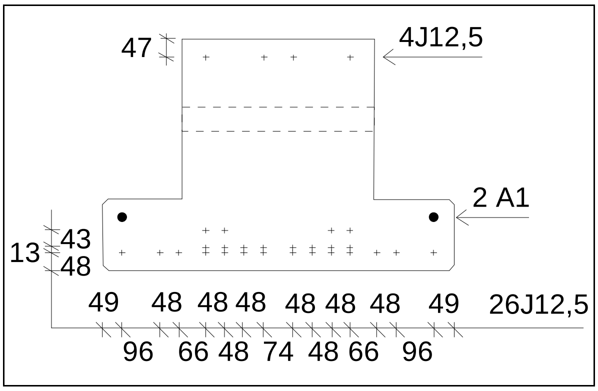

Fig. 7. Main reinforcement.

Concrete: K80

J12,5: Prestressing strand ϕ =12,5 mm, A_p = 93 mm^2, σ_{p0} = 1300 MPa, nominal strength $f_{p0,2}/f_p$ = 1630/1860 MPa, did not yield in the test

A1: Rebar A500HW, ϕ 12 mm, L = 5130 mm, nominal yield strength f_y = 500 MPa, did not yield in the test

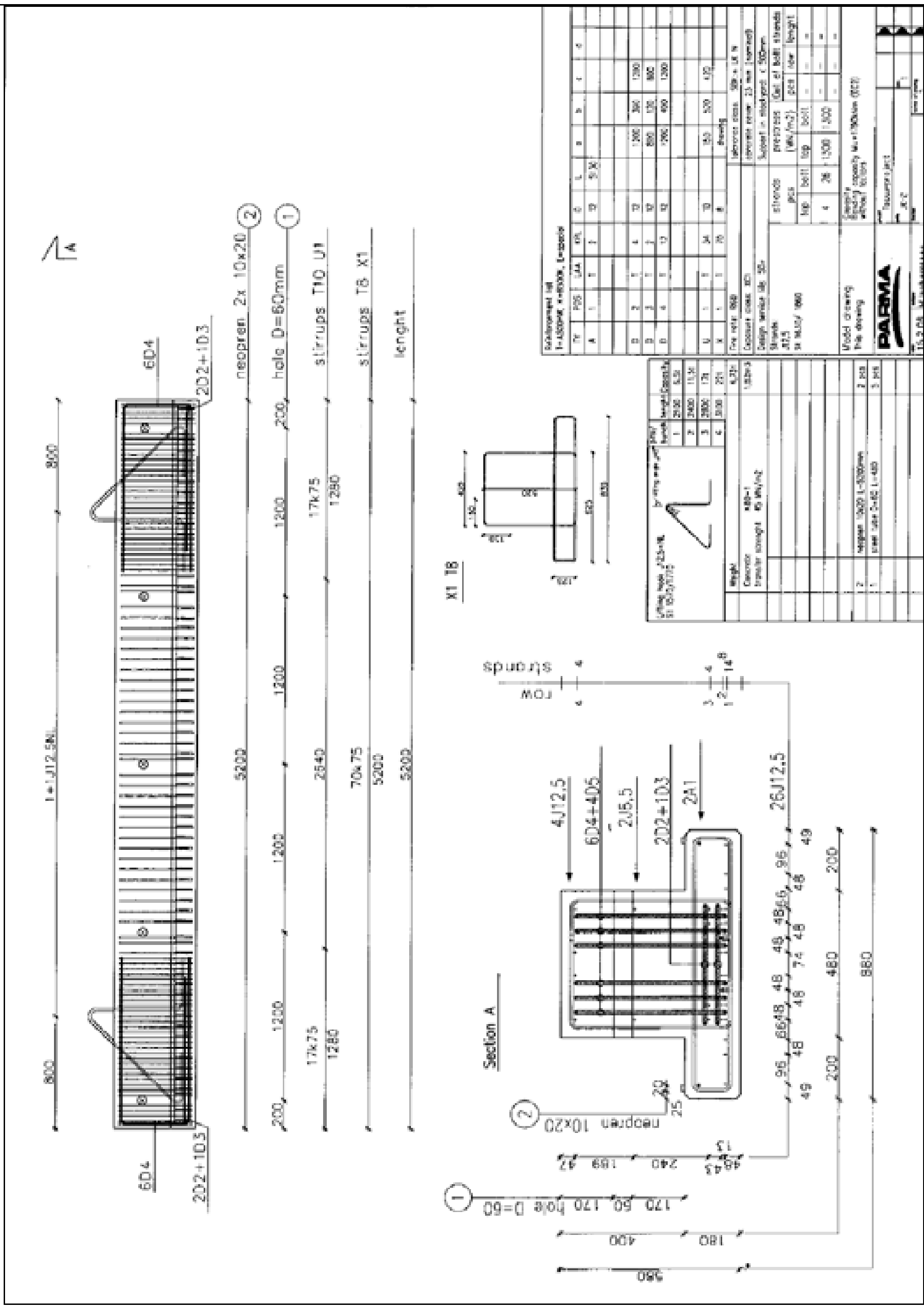

Fig. 8. Middle beam.

2.4
Arrangements at middle beam

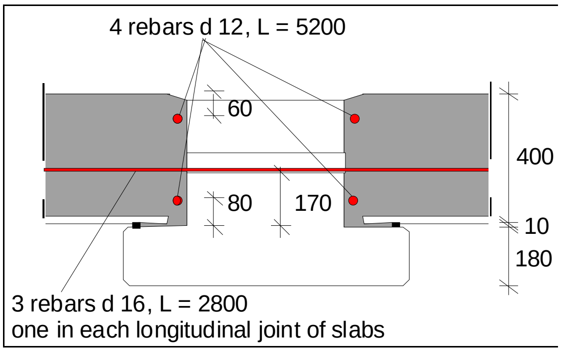

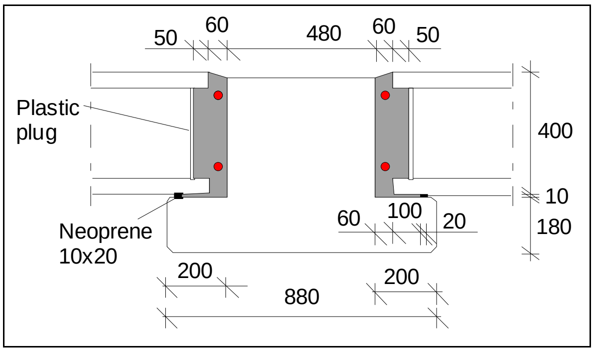

Fig. 9. Section along joint between adjacent slab units.

Fig. 10. Section along hollow cores.

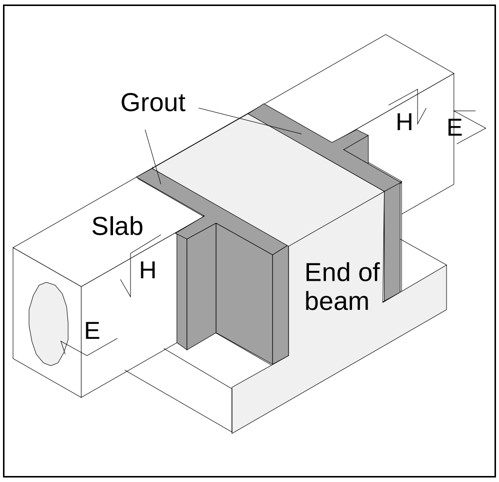

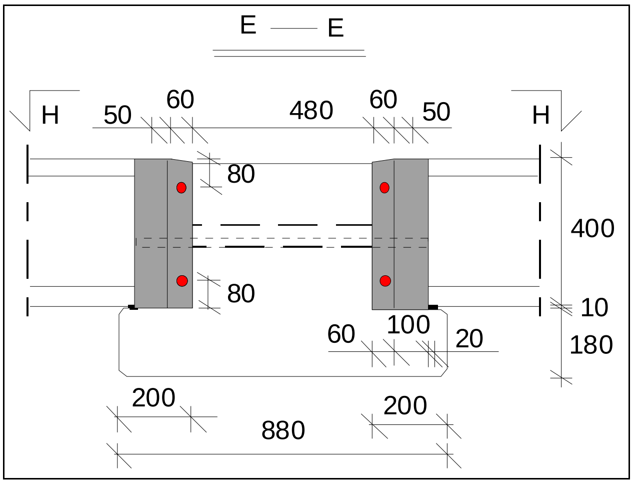

Fig. 11. Cast-in-situ concrete (grout) outside hollow core slabs.

Fig. 12. Section E-E, see Fig. 11.

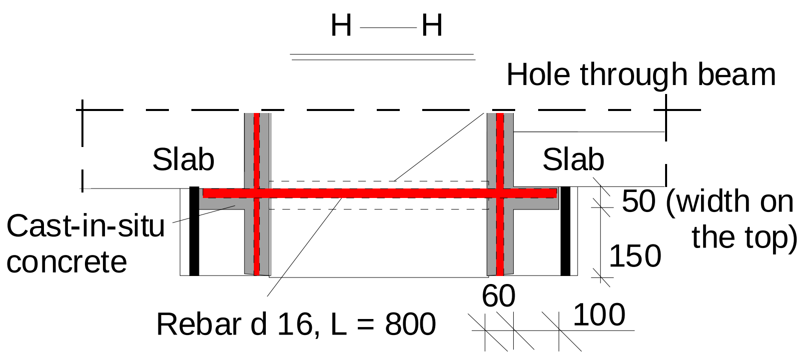

Fig. 13. Section H-H, see Fig. 11.

Tie reinforcement: Straight horizontal rebars A500HW through the beam and parallel to the beam, nominal yield strength f_y = 500 MPa

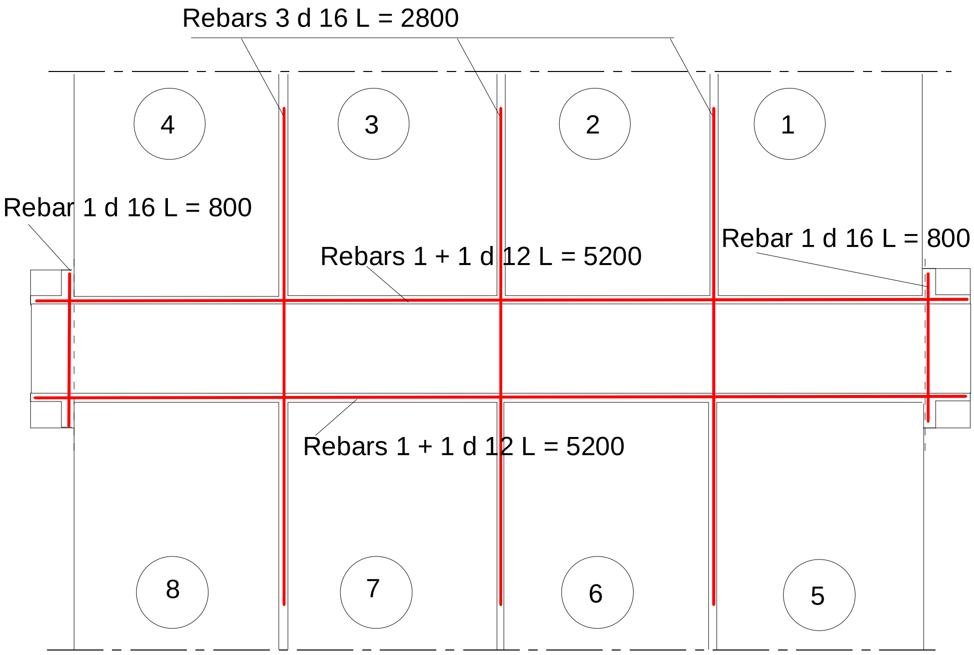

Fig. 14. Overview on tie reinforcement at middle beam. d xy refers to a reinforcing bar A500HW with diameter xy mm. For the vertical position of the bars, see Figs 9 and 12.

2.5
Slabs

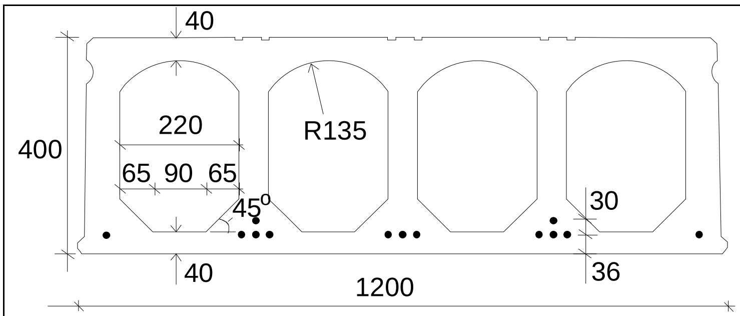

Fig. 15. Nominal geometry of slab units (in scale).

- Extruded by Parma Oy, Hyrylä factory 16.3.2006
- Measured weight = 5,65 kN/m

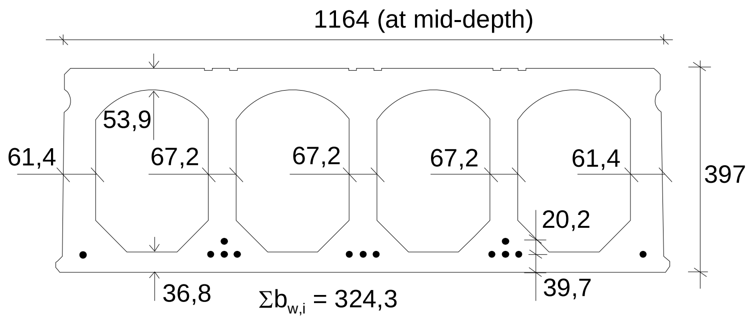

Max measured bond slippage: 3x2,0 mm (in slabs 1, 3 and 6; 3x1,9 mm (in slabs 1, 4 and 7)

Fig. 16. Most relevant measured geometrical properties.

2.6 Temporary supports	No
2.7 Loading arrangements	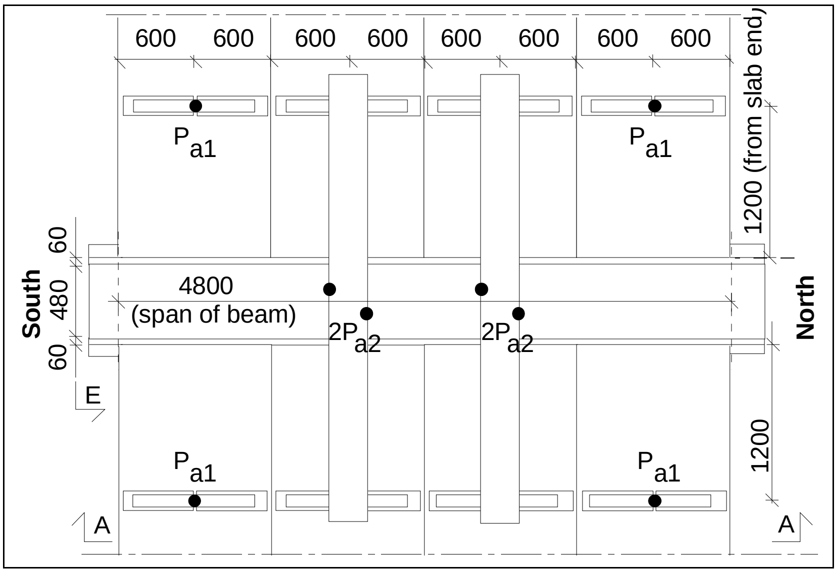 *Fig. 17. Plan. P_{a1} and P_{a2} refer to vertical actuator forces.* 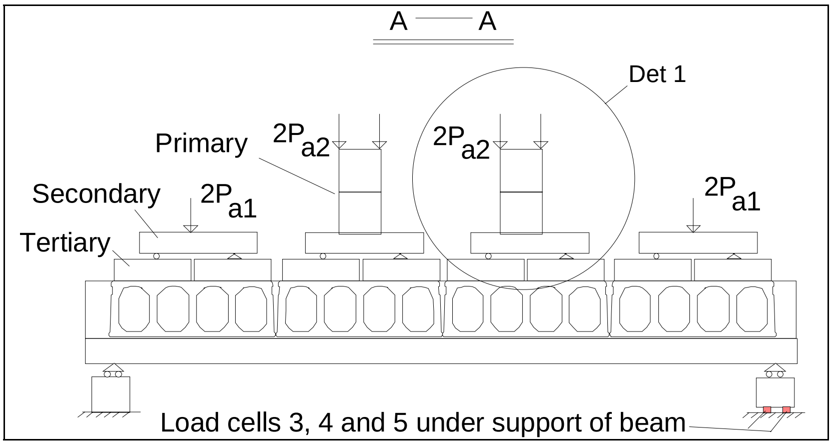 *Fig. 18. Section A-A, see Fig. 17.* 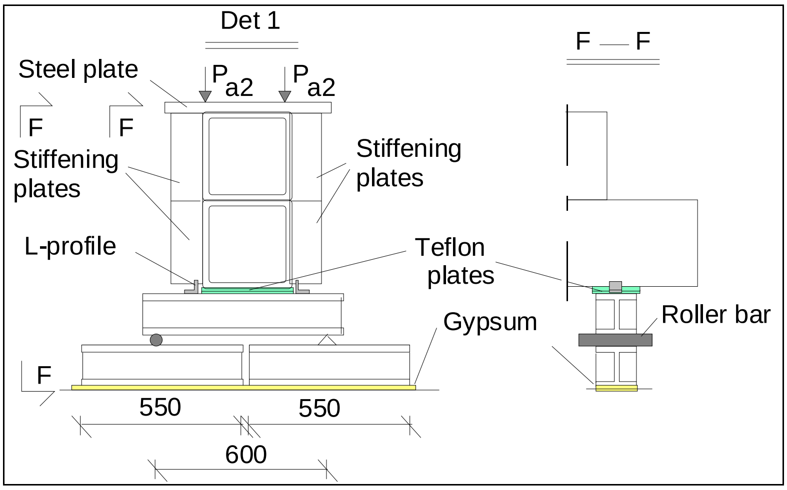 *Fig. 19. Detail 1, see previous figure.*

<table>
<tr><td>3</td><td>Measurements</td></tr>
<tr><td>3.1
Support reactions</td><td>
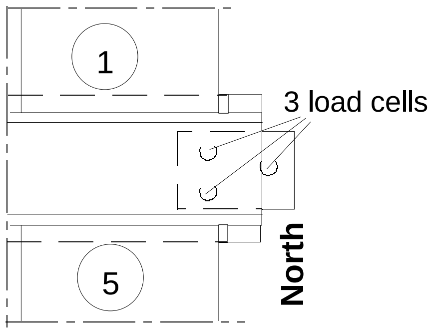

Fig. 20. Load cells below the Northern support of the middle beam.
</td></tr>
<tr><td>3.2
Vertical displacement</td><td>
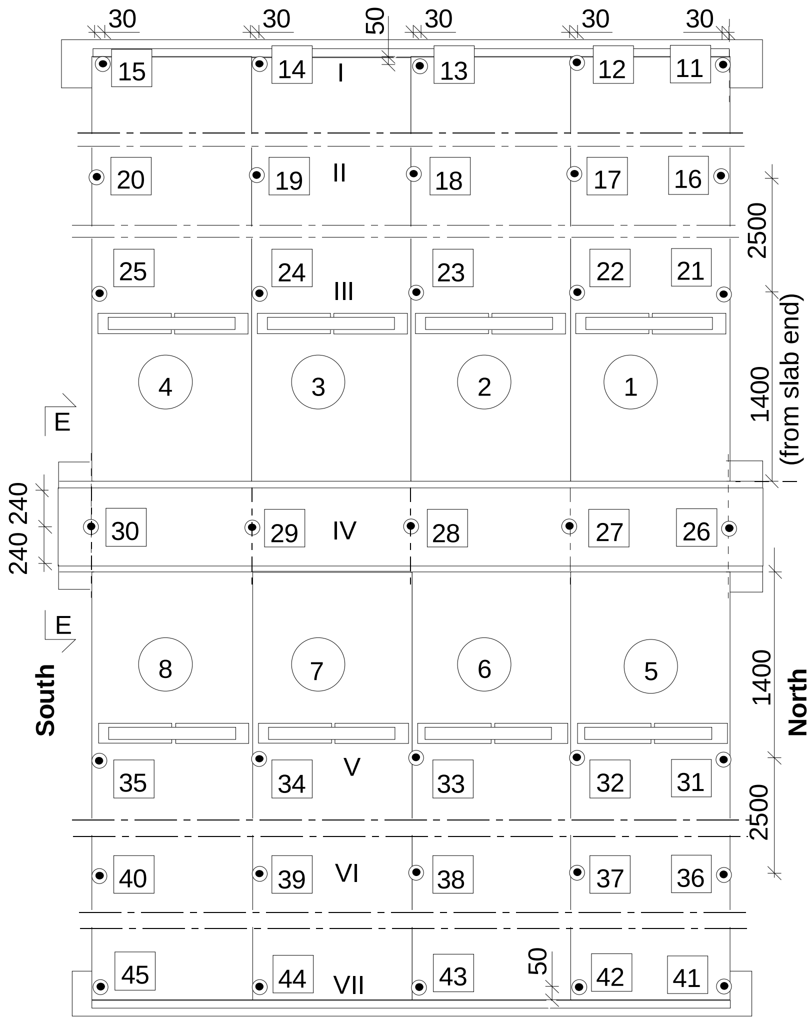

Fig. 21. Location of transducer 11 … 45 for measuring vertical deflection along lines I … VII.
</td></tr>
</table>

3.3
Average strain

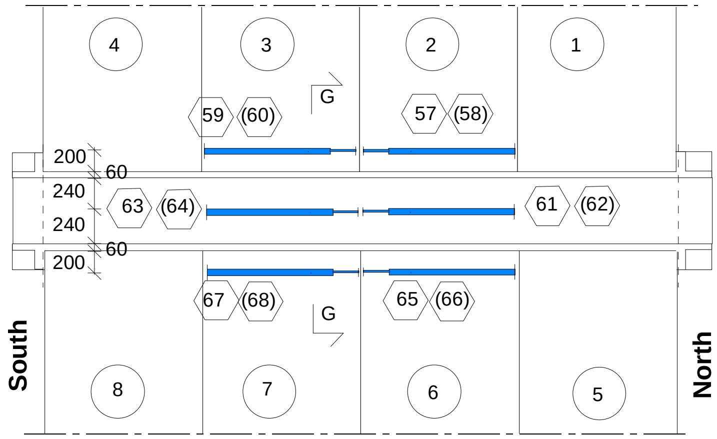

Fig. 22. Position of device (transducers 57–68) measuring average strain parallel to the beams.

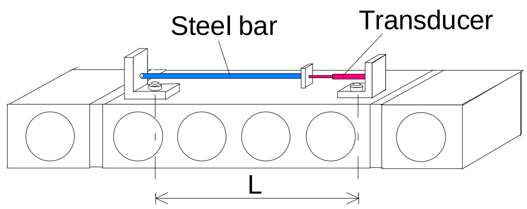

Fig. 23. Apparatus for measuring average strain. L =1100 mm.

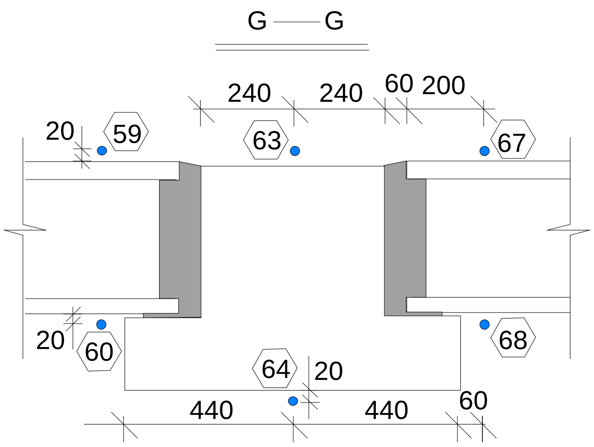

Fig. 24. Section G-G, see Fig. 22.

3.4
Horizontal.
displacements

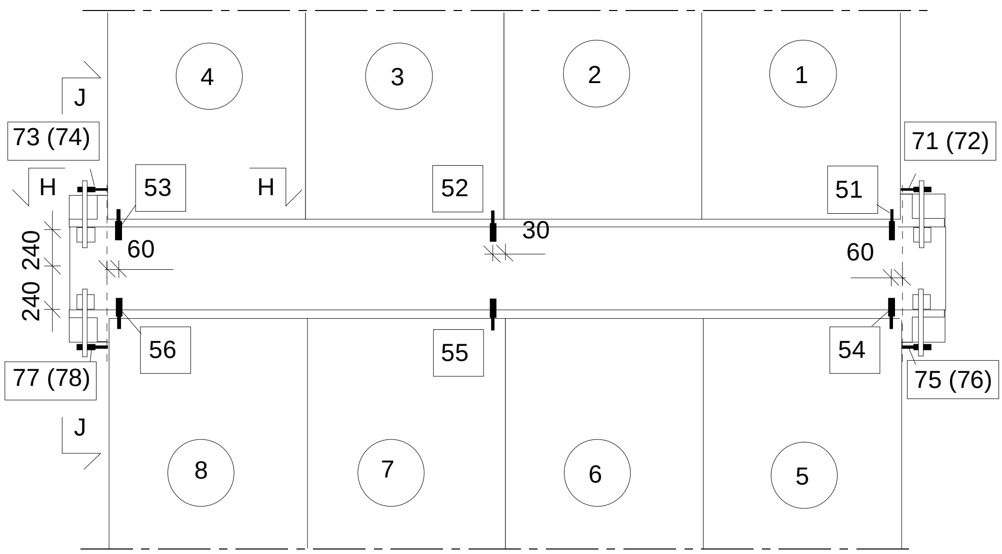

Fig. 25. Transducers measuring crack width (51–56) and shear displacement at the ends of the middle beam (71–78). Transducers 72, 74, 76 and 78 are below transducers 71, 73, 75 and 77, respectively.

	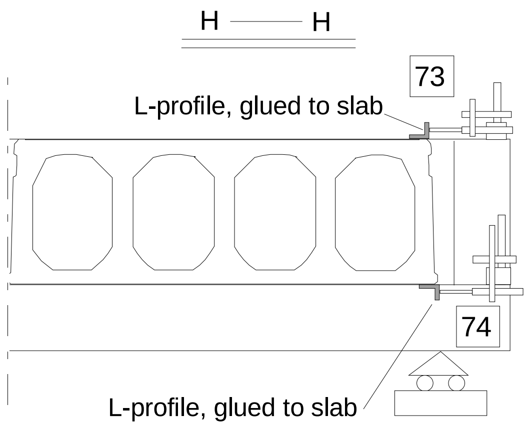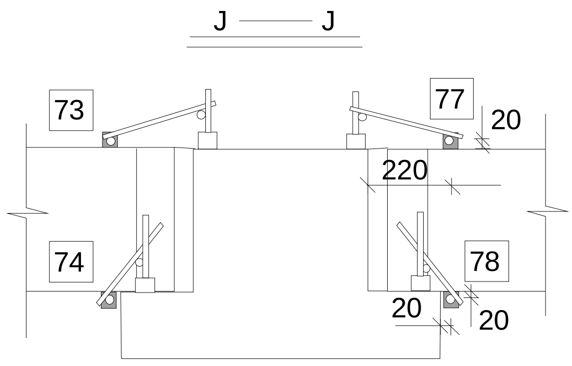*Fig. 27. Section J-J, see Fig. 25.* *Fig. 26. Section H-H, see Fig. 25.*
4	**Special arrangements** - None
5	**Loading strategy**
5.1 Load-time relationship	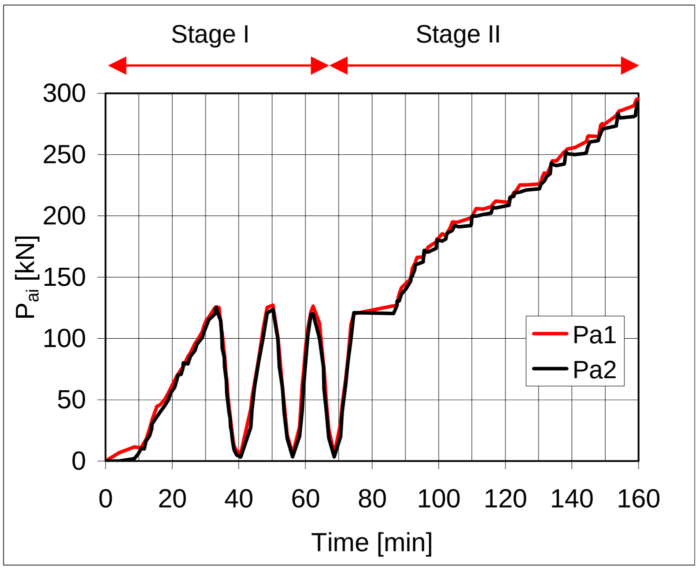*Fig. 28. Actuator forces $P_{a1\ and}\ P_{a2}$ vs. time.* Date of test 31.5.2006
5.2 After failure	-

6	**Observations during loading**	
	Before loading	All measuring devices were zero-balanced when the actuator forces P_{ai} were equal to zero but the weight of the loading equipment was on. The loading history is shown in Fig. 28. P_{ai} = 125 kN corresponds to the shear force due to the expected service load when the shear resistance of the slabs is supposed to be prevailing in the design.
	Stage I	The joint concrete gradually cracked along the webs of the middle beam on the Eastern side (slabs 5–8). Here the first visible cracks were observed at P_{a1} = 38 kN. On the opposite (Eastern) side of the middle beam, a similar crack was observed at P_{a1} = 70 kN.
	P_{a1} = 125 kN during stage II	The soffit of the slabs between the line loads and the middle beam was inspected visually. The observed two visible cracks are shown in Fig. 29. They were both below the webs of the slabs.
	P_{a1} = 189 – 200 kN	New vertical cracks were observed both in the Western and Eastern tie beam. Both the number and the length of the cracks in the tie beams (= concrete connecting the slab ends above the supporting end beams, see Fig. 30) increased with increasing load.
	P_{a1} = 295,1 kN and P_{a2} = 292,2 kN	The floor suddenly failed in shear on the Eastern side of the middle beam, see App., Figs 12–14 and 20–23. In slabs 5–8 an inclined crack appeared between the middle beam and the line load so rapidly that it was impossible to say, which slab failed first. The cracks after the failure are shown in Fig. 30. The joint between the grout and middle beam cracked neatly along the smooth edges of the middle beam as shown in App. A, Figs 24 an 25.

7	**Cracks in concrete**
7.1 Cracks at service load	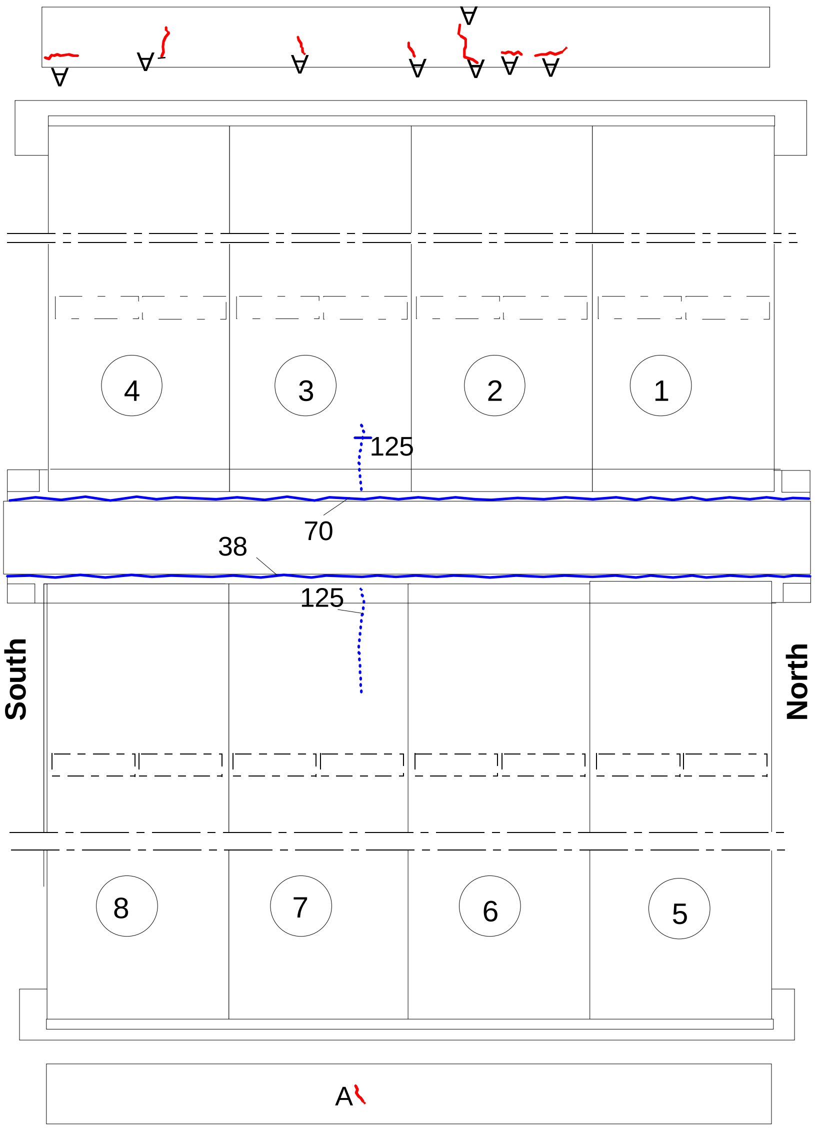 *Fig. 29. Cracks at service load (P_{ai} = 125 kN). The initial cracks observed before loading are indicated with red colour and letter A. A dashed line indicates a crack in the soffit. The figures give the value of the actuator force at which the crack (other than initial crack) was observed.*

7.2 Cracks after failure	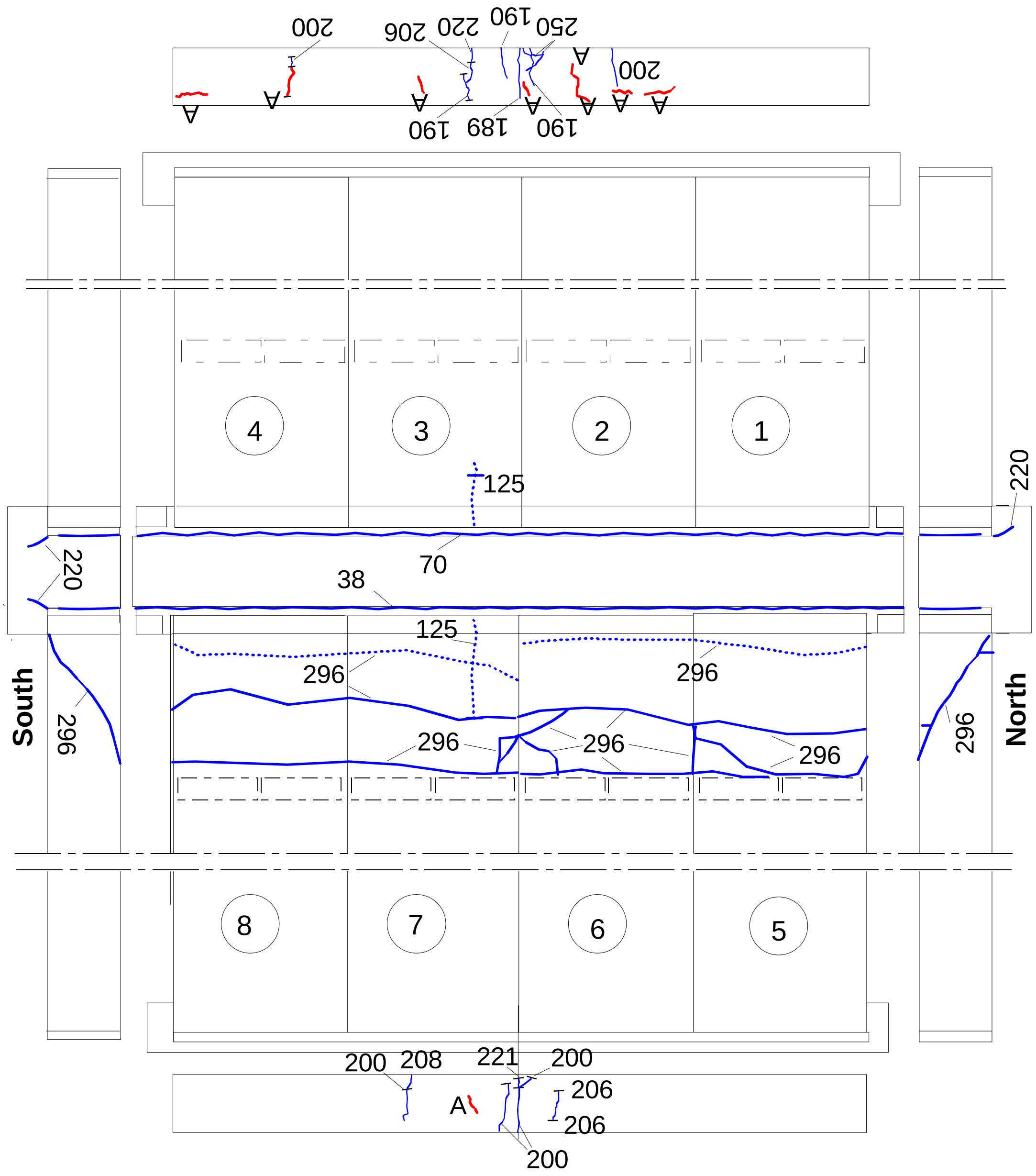 *Fig. 30. Cracks after failure. The initial cracks are indicated with red colour and letter A. A dashed line indicates a crack in the soffit. The figures give the value of the actuator force at which the crack was observed.*

8	**Observed shear resistance**

The ratio (measured support reaction below one end of the middle beam) / (load on half floor) is shown in Fig. 31.

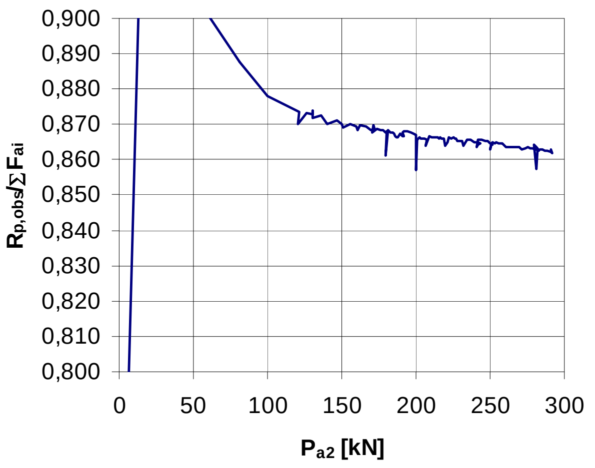

Fig. 31. Ratio of measured support reaction of the middle beam ($R_{p,obs}$) to load on half floor vs. actuator force P_{a2}. Only actuator loads P_{ai} are taken into account in the support reaction.

The shear resistance of one slab end (support reaction of slab end at failure) due to different load components is given by

$$V_{obs} = V_{g,sl} + V_{g,jc} + V_{eq} + V_p$$

where $V_{g,sl}$, $V_{g,jc}$, V_{eq} and V_p are shear forces due to the self-weight of slab unit, weight of joint concrete, weight of loading equipment and actuator forces P_{ai}, respectively. The components of the shear force due to the self-weight are calculated assuming that the slabs behave as simply supported beams. For V_{eq} and V_p the relation is $V_{eq} = 0,8619 \times P_e$ and $V_p = 0,8619 \times (P_{a1} + P_{a2})/2$ at failure. $V_{g,jc}$ is calculated from the nominal geometry of the joints and density of the concrete, other components of the shear force are calculated from measured loads and weights. The values for the components of the shear force are given in Table below.

Table. Components of shear resistance due to different loads.

Action	Load	Shear force kN
Weight of slab unit	5,65 kN/m	25,00
Weight of joint concrete	0,302 kN/m	1,34
Loading equipment	(0,66+6,22)/2 kN	2,96
Actuator loads	(295,1+292,2)/2 kN	253,10

The observed shear resistance V_{obs} = 282,4 kN (shear force at support) is obtained for one slab unit wit width = 1,2 m. The shear force per unit width is 235,3 kN/m.

9	**Material properties**

9.1 Strength of steel

Component	$R_{eH}/R_{p0,2}$ MPa	R_m MPa	Note
End beam	≈350		Nominal (no yielding)
Slab strands	1630	1860	Nominal (no yielding)
Beam strands	1630	1860	Nominal (no yielding)
Reinforcement	500		Nominal (A500HW,no yielding)

9.2 Strength of slab concrete, floor test

#	Cores	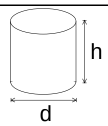	*h* mm	*d* mm	Date of test	Note
6			50	50	1.6.2006 (+1 d)[1)]	Upper flange of slab 5, vertically drilled, tested as drilled[2)], density = 2386 kg/m^3
Mean strength [MPa]			55,3			
St.deviation [MPa]			1,33			

9.3 Strength of slab concrete, reference tests

#	Cores	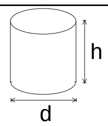	*h* mm	*d* mm	Date of test	From
6			50	50	9.6.2006 (+1 d)[1)]	Upper flange of slab 9, vertically drilled, tested as drilled[2)], density = 2387 kg/m^3
Mean strength [MPa]			58,9			
St.deviation [MPa]			0,87			

9.4 Strength of grout

#	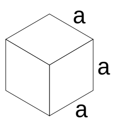	*a* mm	Date of test	Note
6		150	31.5.2006 (+0 d)[1)]	Kept in laboratory in the same conditions as the floor specimen density = 2196 kg/m^3
Mean strength [MPa]		33,7		
St.deviation [MPa]		0,37		

9.5 Strength of beam concrete

#	Cores	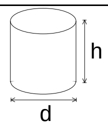	*h* mm	*d* mm	Date of test	From
6			100	100	1.6.2006 (+1 d)[1)] 2378	Upper part, vertically drilled Tested as drilled[2)] Density = 2378 kg/m^3
Mean strength [MPa]			72,0			
St.deviation [MPa]			1,84			

1) Date of material test minus date of test (floor test or reference test)
2) kept in a closed plastic bag after drilling until compression

10 **Measured displacements**

In the following figures, V_p stands for the shear force of one slab end due to imposed actuator loads, calculated assuming simply supported slabs.

10.1 Deflections

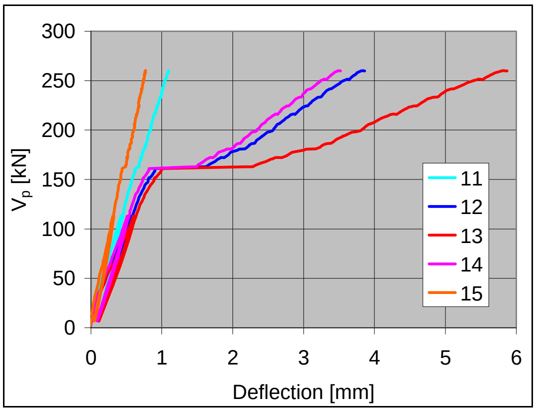

Fig. 32. Deflection on line I along western end beam vs. support reaction V_p of one slab due to actuator loads.

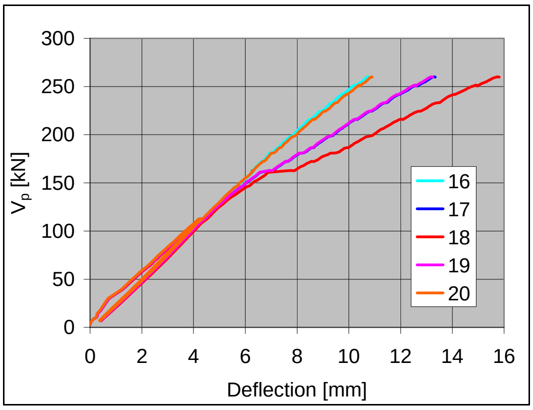

Fig. 33. Deflection on line II in the middle of slabs 1–4.

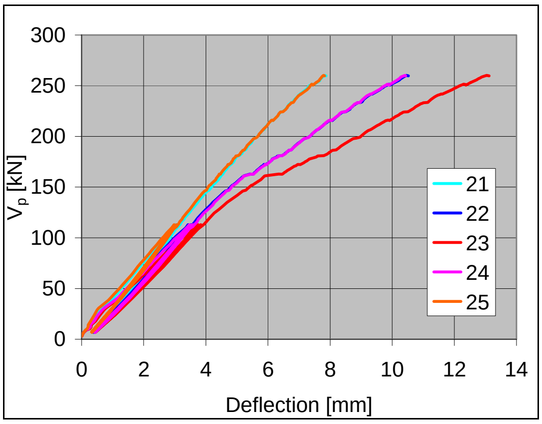

Fig. 34. Deflection on line III close to the line load, slabs 1–4.

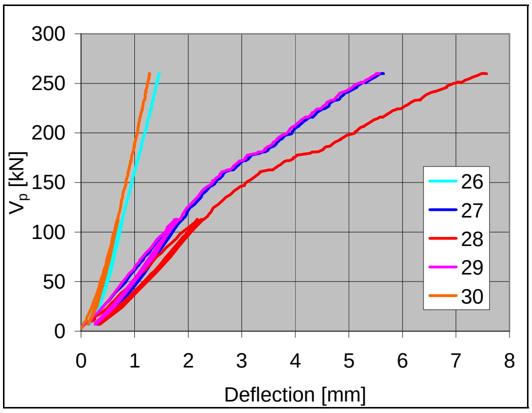

Fig. 35. Deflection on line IV along the middle beam.

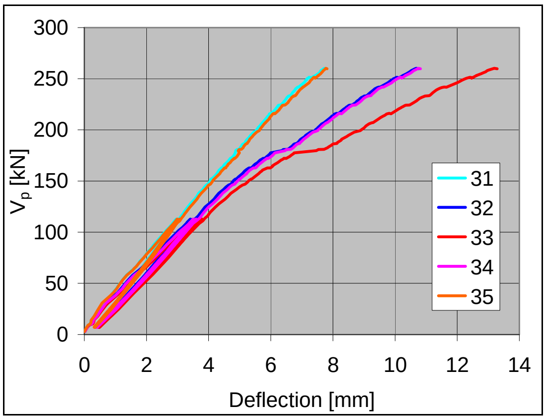

Fig. 36. Deflection on line V close to the line load, slabs 5–8.

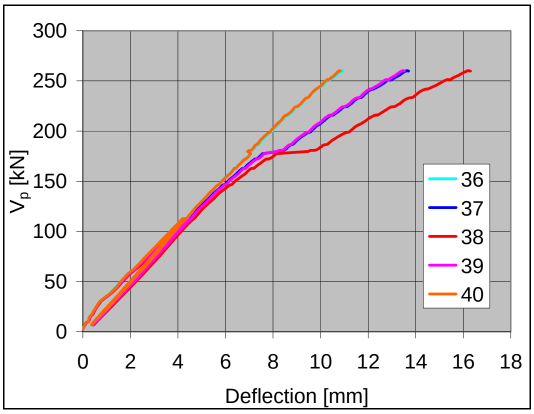

Fig. 37. Deflection on line VI in the middle of slabs 5–8.

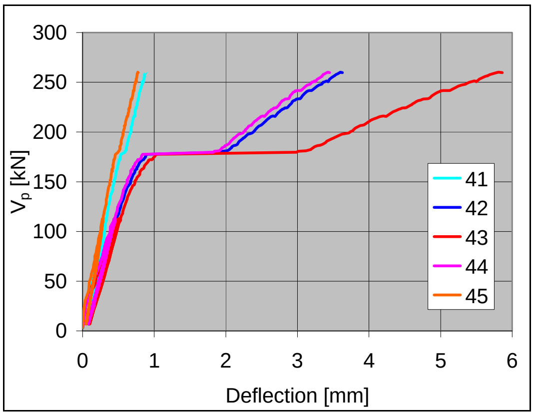

Fig. 38. Deflection on line VII along end beam, slabs 5–8.

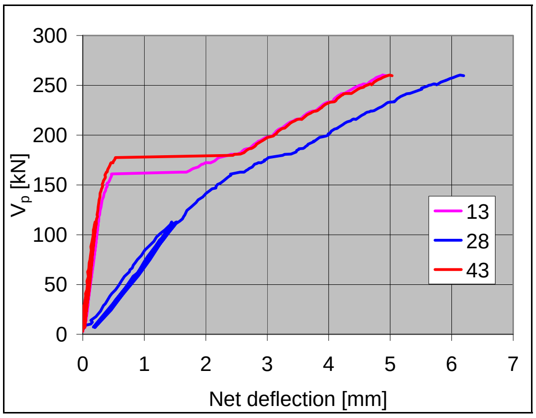

Fig. 39. Net deflection of midpoint of middle beam (28) and those of end beams (13, 43).

10.2
Crack width

Fig. 40. Differential displacement parallel to the slab between the middle beam and the slabs (≈ crack width). See Fig. 25 for the location of the transducers. Transducer 56 has given erroneus results because the crack width equal to 2,0 mm was not visually observed during the cyclic stage

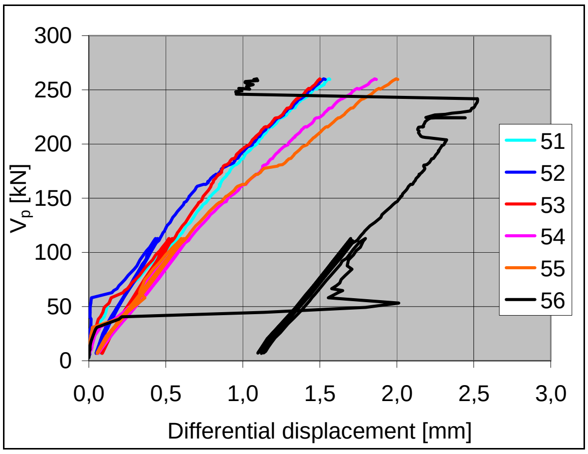

10.3
Average strain

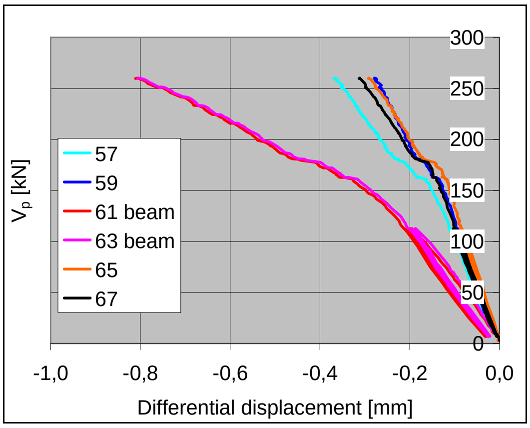

Fig. 41. Differential displacement at top surface of floor measured by transducers 57, 59, 61, 63, 65 and 67.

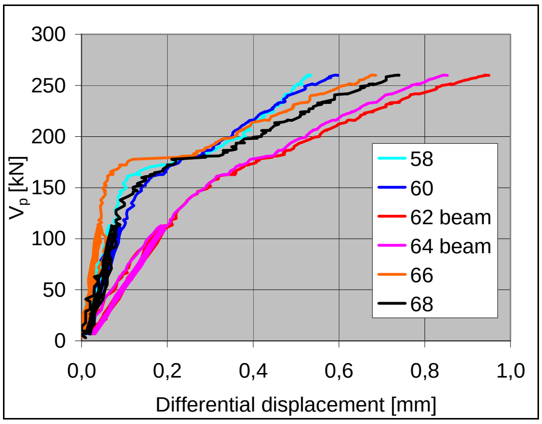

Fig. 42. Differential displacement at soffit of floor measured by transducers 58, 60, 62, 64, 66 and 68.

10.4
Shear displacement

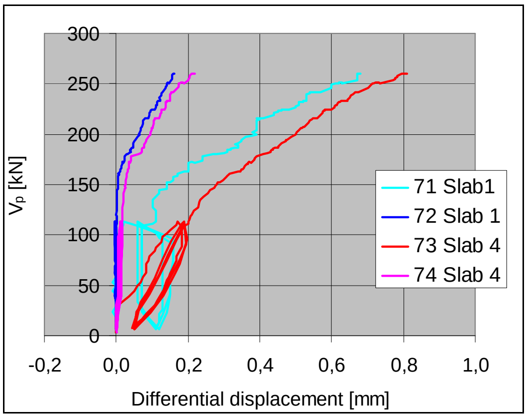

Fig. 43. Northern end of middle beam. Differential displacement between edge of slab and middle beam. A positive value means that the slab is moving towards the end of the beam.

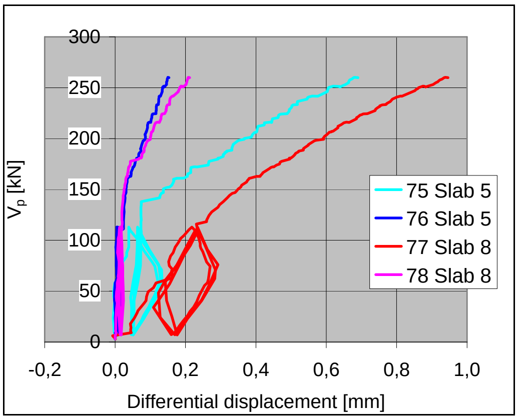

Fig. 44. Southern end of middle beam. Differential displacement between edge of slab and middle beam. A positive value means that the slab is moving towards the end of the beam.

11 **Reference tests**

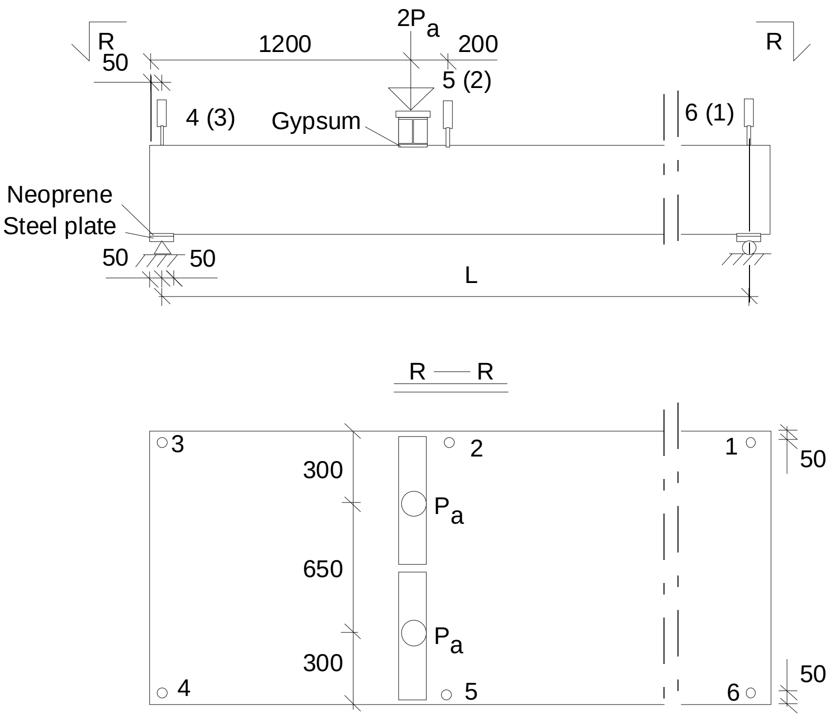

Fig. 45. Layout of reference test. For L, see the next table.

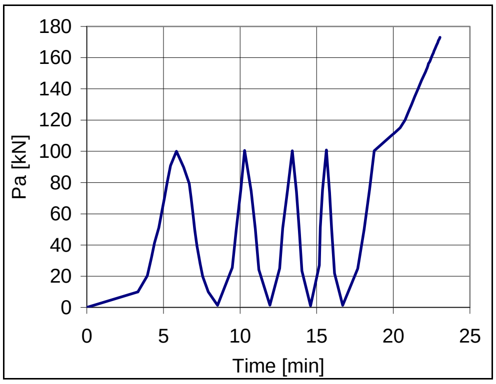

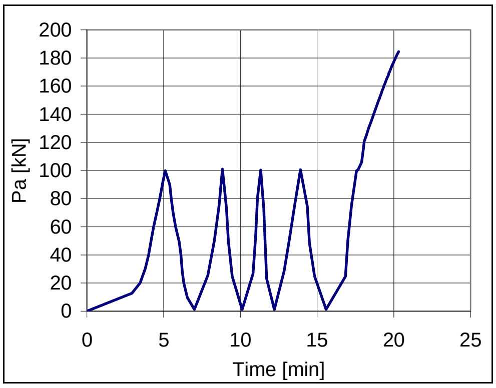

Fig. 46. Tests R1 and R2. Actuator force – time relationship.

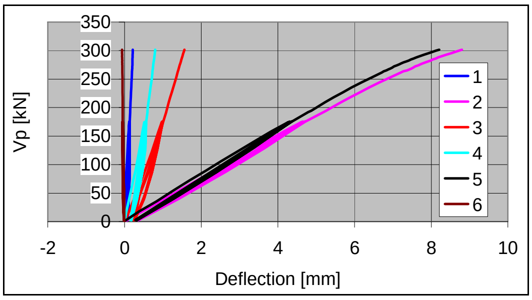

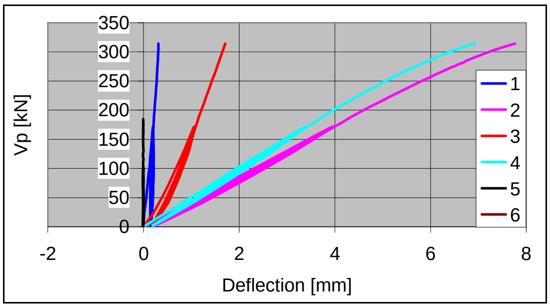

Fig. 47. Tests R1 and R2. Displacements measured by transducers 1–6. V_p is the shear force due to the actuator force P_a.

Table. Span of slab, shear force V_g at support due to self weight of slab, actuator force P_a at failure, weight of loading equipment P_{eq}, shear force V_p due to imposed load at failure, total shear force V_{obs} at failure and total shear force v_{obs} per unit width.

Test	Date	Span mm	V_g kN	P_a kN	P_{eq} kN	V_p kN	V_{obs} kN	v_{obs} kN/m
R1	June 9, 2006	8894	25,2	173,9	0,29	303,1	328,3	273,6
R2	June 9, 2006	7700	21,9	185,1	0,29	315,2	337,0	280,9
						Mean	332,7	277,2

12	**Comparison: floor test vs. reference tests**
	The observed shear resistance (support reaction) of the hollow core slab in the floor test was equal to 282,4 kN per one slab unit or 235,3 kN/m. This is **85%** of the mean of the shear resistances observed in the reference tests.
13	**Discussion**
	1. The net deflection of the middle beam due to the imposed actuator load (deflection minus settlement of supports) was 6,2 mm or *L*/774, i.e. very small 2. The shear resistance measured in the reference tests was a bit lower than the mean of observed values for similar slabs given in *Pajari, M. Resistance of prestressed hollow core slab against web shear failure. VTT Research Notes 2292, Espoo 2005*. 3. The torsional stresses due to the different deflection of the middle beam and end beams had a negligible effect on the failure of the slabs because the maximum difference in the net mid-point deflection was less than 1,3 mm 4. The bond between the smooth edges of the middle beam and the grout was weak. 5. The bond between the soffit of the slab and the grout below it was also weak. 6. The position of the tie reinforcement 170 mm above the slab soffit was favourable. 7. Due to the weak bond and position of the tie reinforcement, the edge slabs did slide 0,17 … 0,21 mm along the beam before failure, see Figs 43 and 44. This reduced the negative effects of the transverse actions in the slab and had a positive effect on the shear resistance 8. The transverse shear deformation of the edge slabs was considerable which can be seen from the relative displacement between the top flange and bottom flange, see Figs 43 and 44. At failure, the transverse horizontal displacement of the top flange was 0,52 … 0,67 mm greater than that of the bottom flange 9. The observed shear resistance was considerably higher than that in previous test VTT.PC.InvT.400.1993. This can be explained by the improvements in the middle beam, i.e. by elimination of indents at the edges of the beam and by the higher position of longitudinal reinforcement.

APPENDIX A: PHOTOGRAPHS

Fig. 1. Slab installed on middle beam.

Fig. 2. Middle beam.

Fig. 3. Reinforcement at the end of middle beam. One rebar parallel to the beam on the top of the joint is still missing.

Fig. 4. Reinforcement at the end of middle beam. One rebar parallel to the beam on the top of the joint is still missing.

Fig. 5. Loading arrangements.

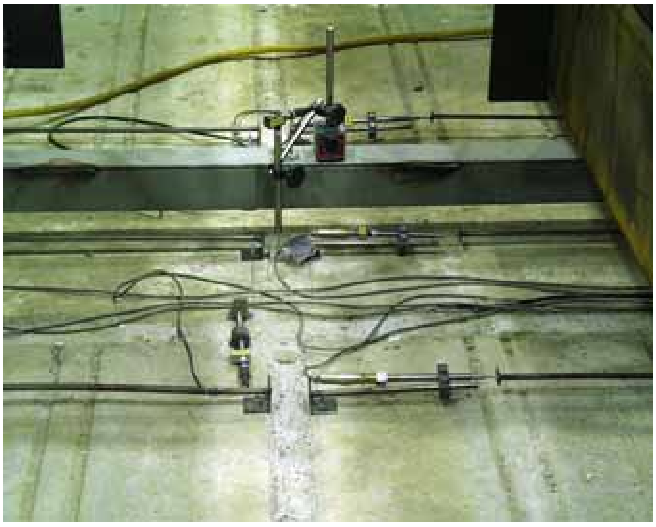

Fig. 6. Transducers measuring deflection and differential horizontal displacement in the middle of the test floor.

Fig. 7. Transducers measuring differential horizontal displacement at one end of the middle beam.

Fig. 8. Loading of slabs 2 and 6 with two actuators

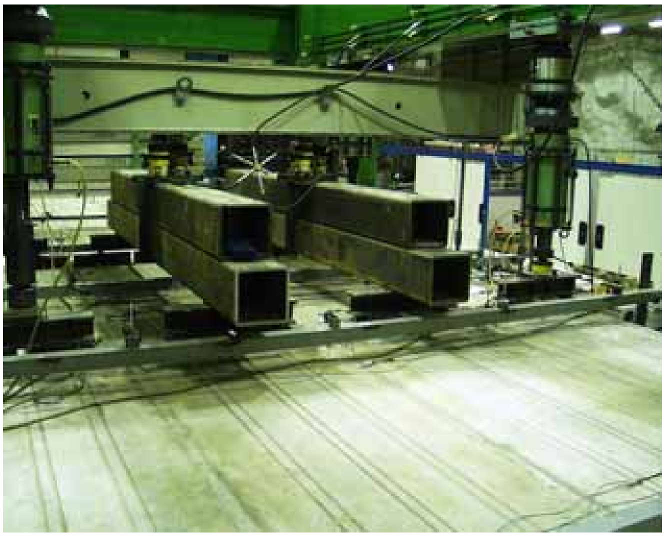

Fig. 9. Loading arrangements.

Fig. 10. Transducers at one end of middle beam

Fig. 11. An overview on test arrangements.

Fig. 12. Failure of slab 5.

Fig. 13. Failure of slab 8.

Fig. 14. Soffit of slabs 5–8 after failure.

Fig. 15. Cracks in Western tie beam after failure. Slabs 1–3.

Fig. 16. Cracks in Western tie beam after failure. Slabs 2–4.

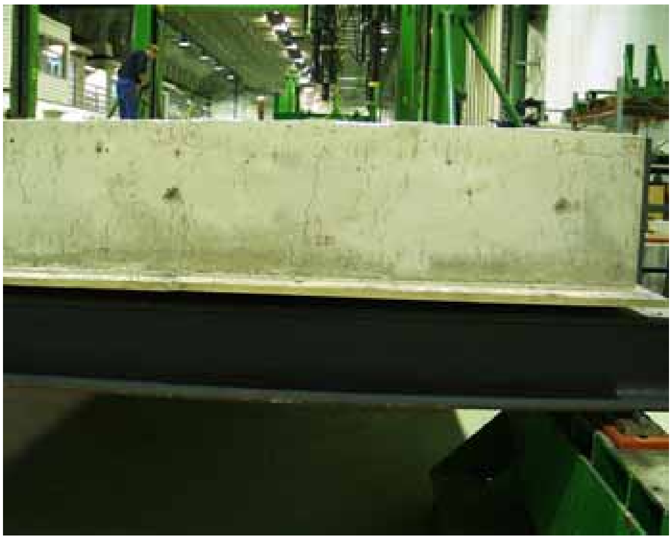

Fig. 17. Cracks in Western tie beam after failure. Slabs 3–4.

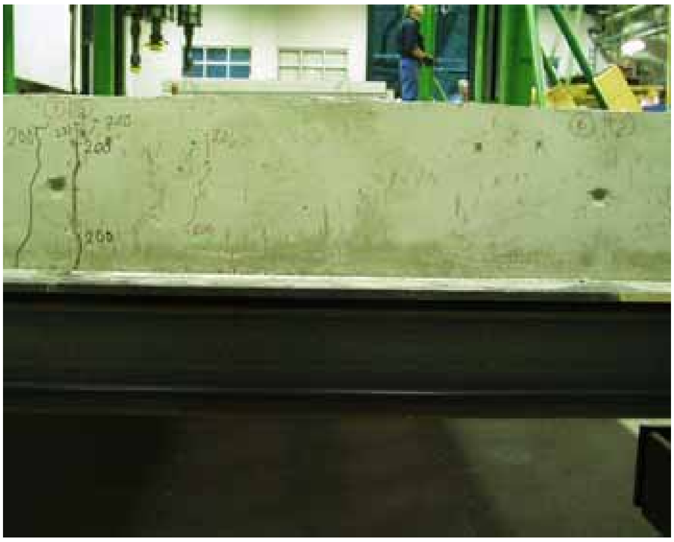

Fig. 18. Cracks in Eastern tie beam after failure. Slabs 5–7.

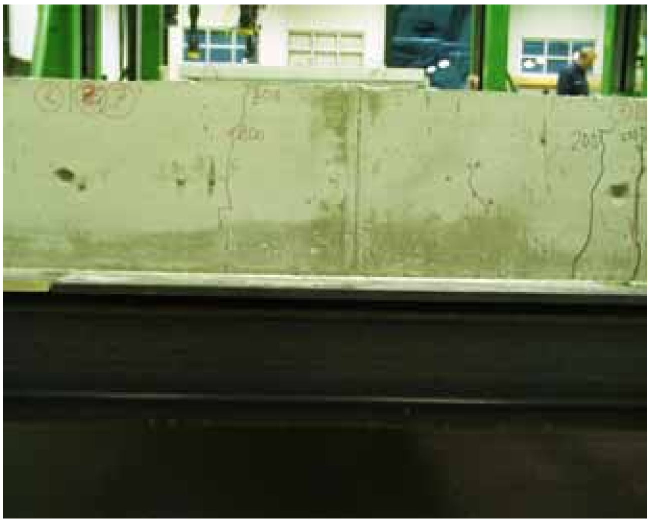

Fig. 19. Cracks in Eastern tie beam after failure. Slabs 7–8.

Fig. 20. Failure in slab 5.

Fig. 21. Failure in slabs 5–7.

Fig. 22. Failure in slabs 6–8.

Fig. 23. Failed ends of slabs 5–8.

Fig. 24. Western side of middle beam. Note the failure of the bond along the vertical interface of the cast-in-situ concrete and the precast beam as well as the perfect filling of the gap below the slab end.

Fig. 25. Western side of middle beam.

Fig. 26. Eastern side of middle beam.

Fig. 27. Overview on arrangements in reference tests. The actuators in the rear were not used.

Fig. 28. Reference test R1. Northern side of slab after failure.

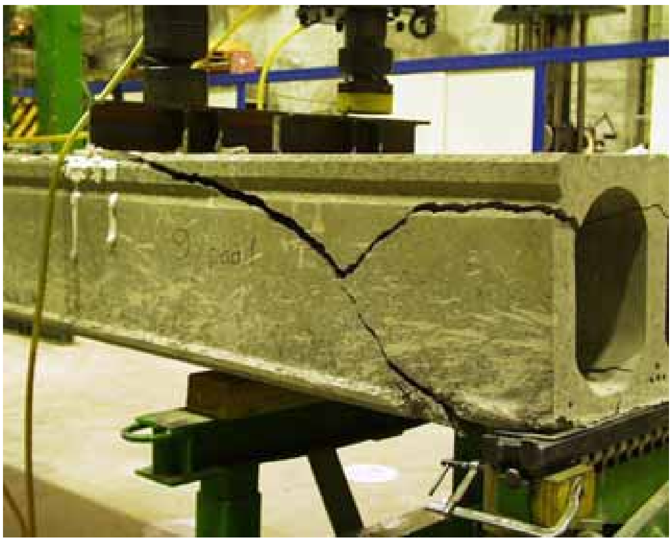

Fig. 29. Reference test R1. Southern side of slab after failure.

Fig. 30. Reference test R2. Northern side of slab after failure.

Fig. 31. Reference test R2. Southern side of slab after failure.

1	**General information**
1.1 Identification and aim	**VTT.CR.A-beam.320.2006** **Last update 2.11.2010** A320 (Internal identification) Aim of the test: To quantify the interaction between the A-beam and hollow core slabs.
1.2 Test type	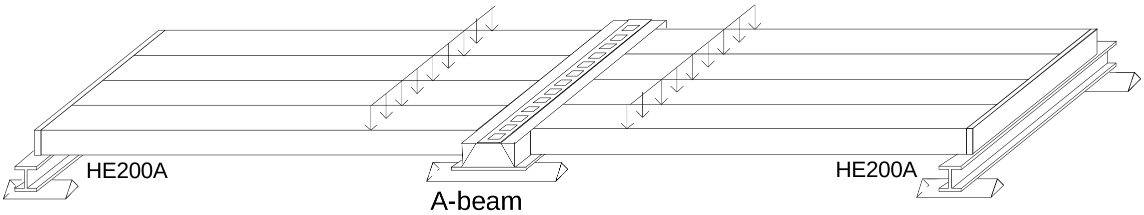 *Fig. 1. Illustration of test setup.*
1.3 Laboratory & date of test	VTT/FI 17.11.2006
1.4 Test report	Author(s): Pajari, M. Name: *Load test on hollow core slab floor with A-beam* Ref. number: RTE868/02 Date: 15.3.2007 Availability: Confidential, owner is Anstar Oy, Erstantie 2, FI-15540 Villähde, Finland www.anstar.fi
2	**Test specimen and loading** (see also Appendices A and B)

2.1
General plan

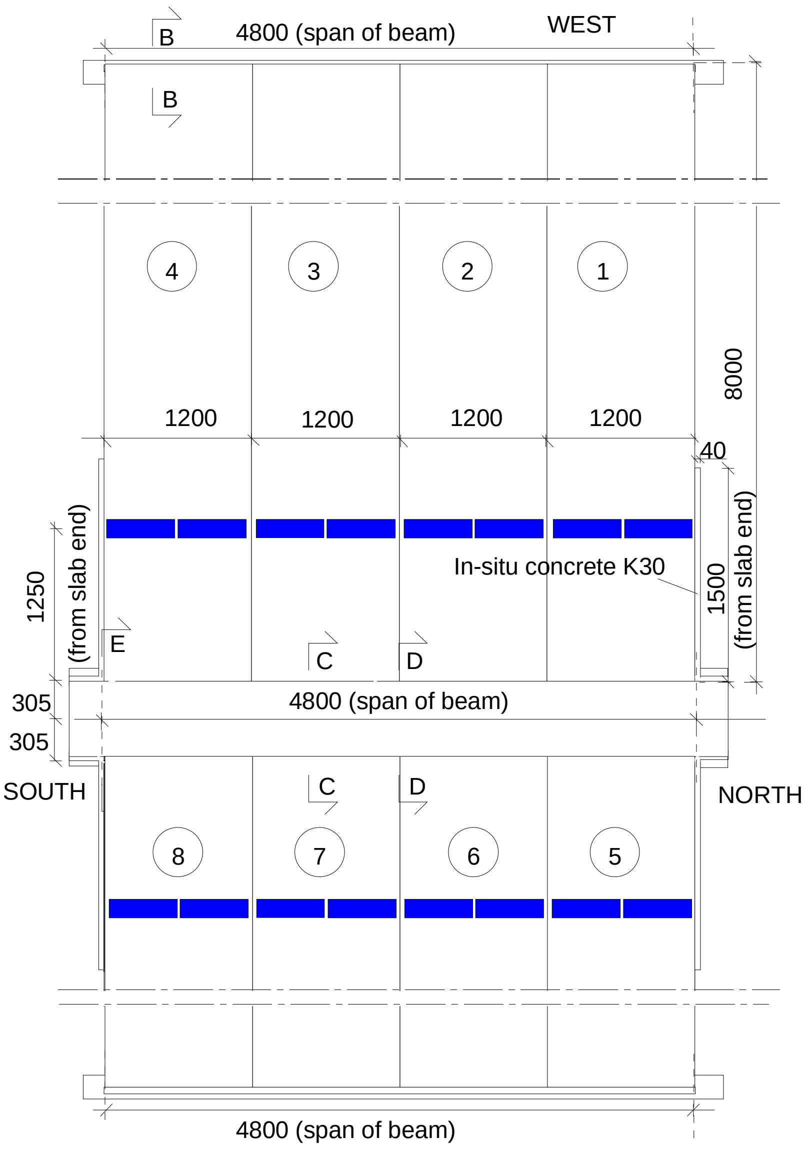

Fig. 2. Plan. Position of line loads shown in blue color.

2.2
End beams

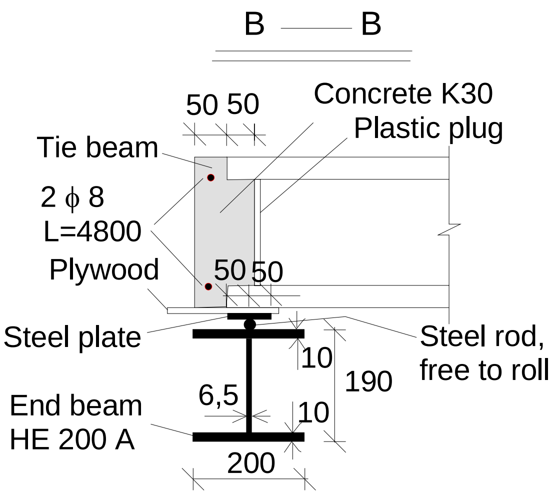

Fig. 3. Arrangements at end beam. ϕ8 refers to a reinforcing bar TW8, see 2.3.

	Simply supported, span = 4,8 m $f_y \approx$ 355 MPa (nominal f_y), did not yield in the test.
2.3 Middle beam	The beam, see Figs 4–9 and App. A, comprised - a prefabricated steel box girder with perforated top plate and lontitudinal rebars welded onto the top plate - a precast concrete component which filled the box girder - a cast-in-situ concrete component on the top of the box girder - The precast concrete cast by Anstar Oy - Upper part cast by VTT in laboratory together with the joint grouting, 6.11.2006 **Concrete**: K40 in the prefabricated part, K30 in the upper part **A-BEAM:** **End plates:** Raex 460 M (nominal $f_y \approx$ 460 MPa) **Other structural steel:** S355J2G3, $f_y \approx$ 355 MPa (nominal f_y) **Passive reinforcement in A-beam:** **Txy**: Hot rolled, weldable rebar A500HW, ϕ = xy mm **Tie reinforcement:** **Txy**: Hot rolled, weldable rebar A500HW, ϕ = xy mm, see Figs 4–8.  *Fig. 4. A-beam when one slab element has been installed.*

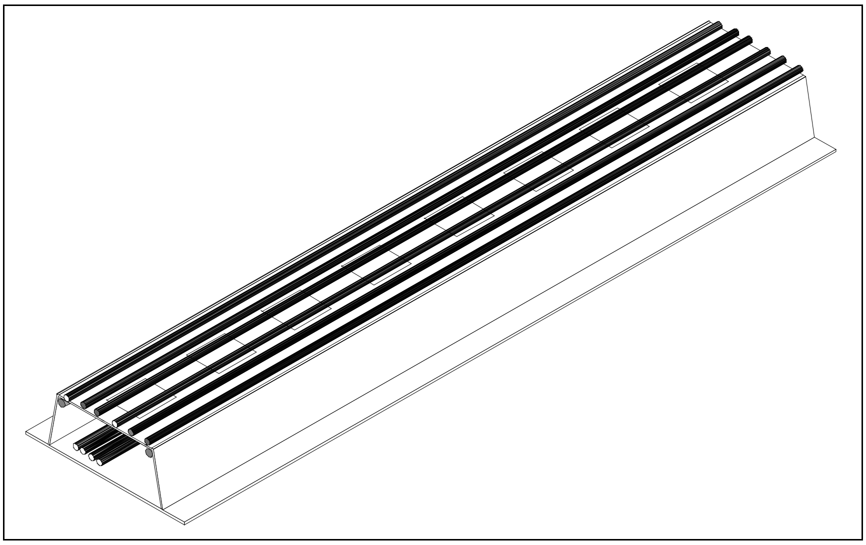

Fig. 5. Illustration of steel component of middle beam. End plates and hoop reinforcement not shown.

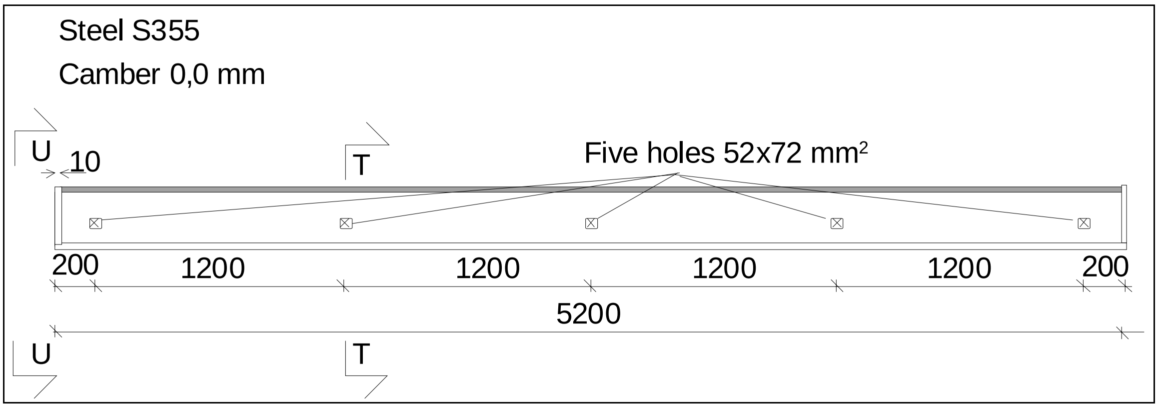

Fig. 6. A-beam. Elevation.

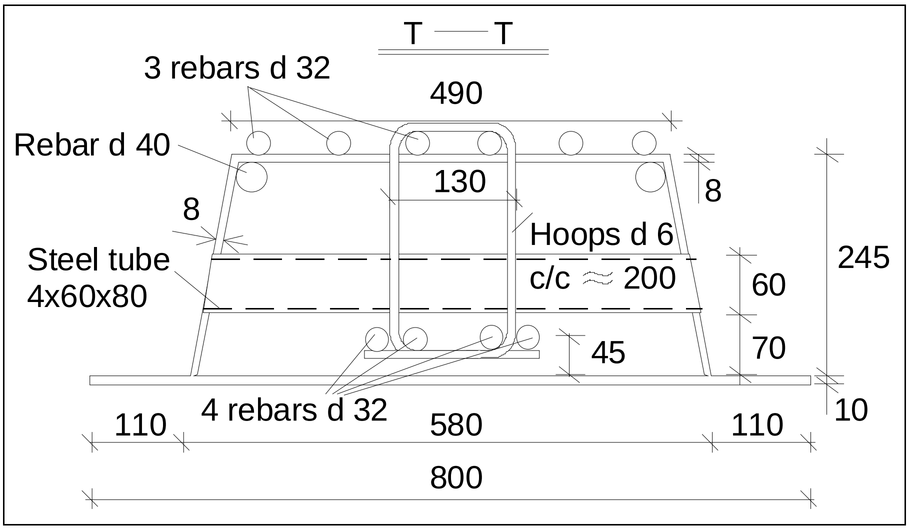

Fig. 7. A-beam. Section T-T. d xy refers to rebars Txy.

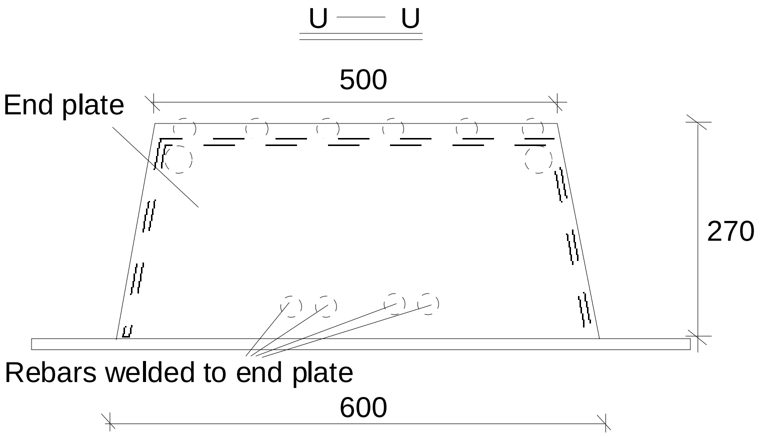

Fig. 8. A-beam. Section U-U.

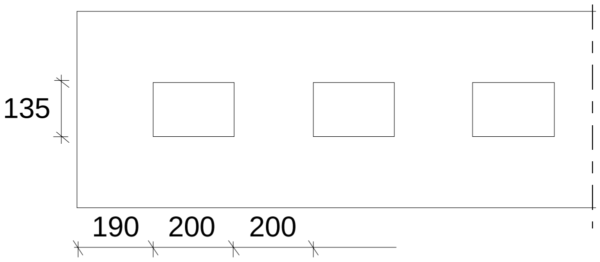

Fig. 9. A-beam. Holes in the top flange.

2.4 Arrangements at middle beam	- Simply supported, span = 4,8 m, roller bearing at North end

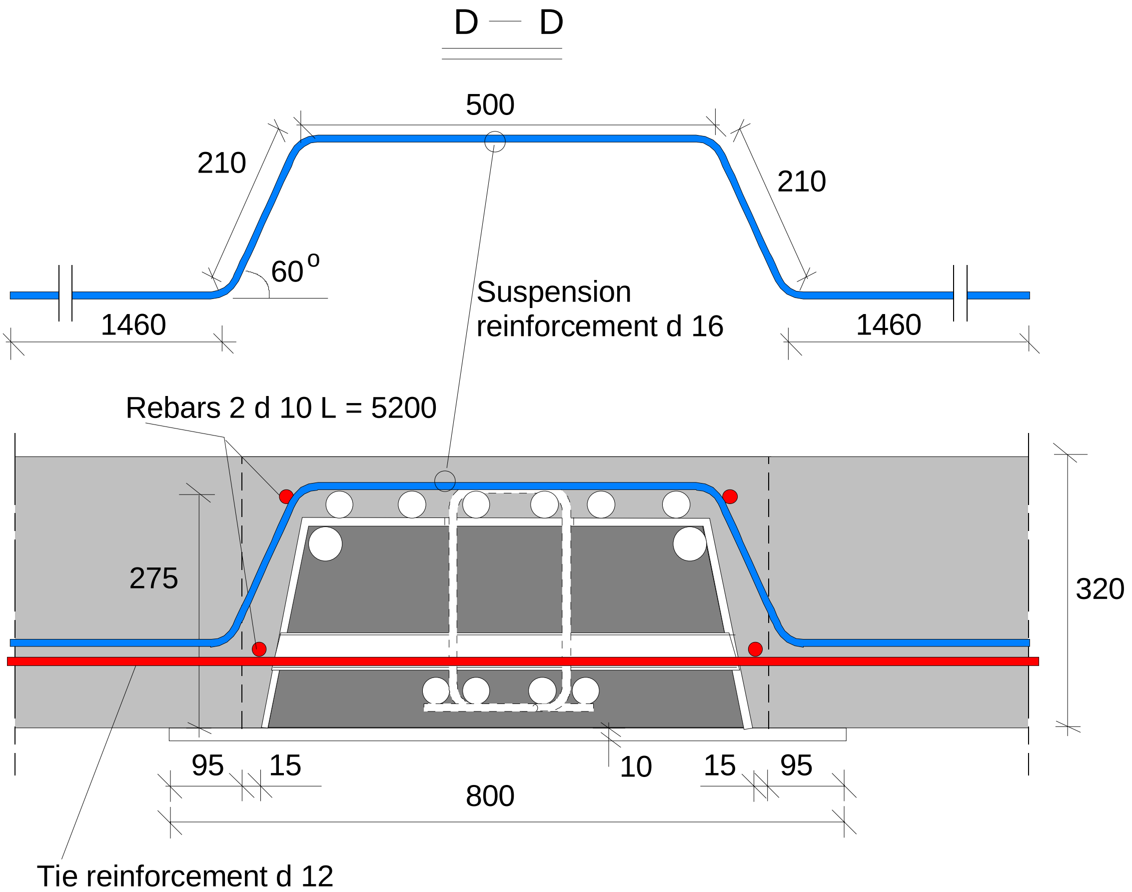

Fig. 10. Arrangements at middle beam, section D-D along a joint between adjacent hollow core units in Fig. 2. The suspension reinforcement along the edges of the floor was similar to that shown here but the length of the tails was 1260 mm instead of 1460 mm. d xy refers to rebar Txy, see 2.3.

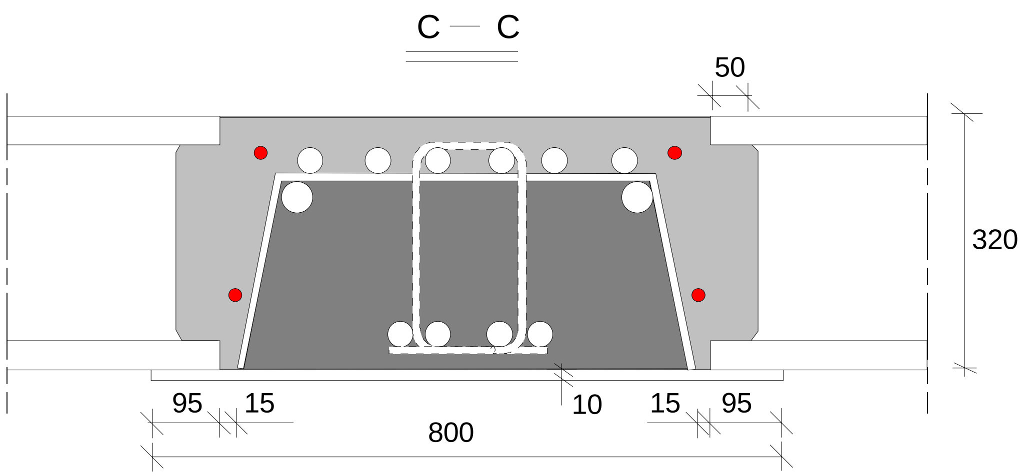

Fig. 11. Section C-C along hollow cores in Fig. 2.

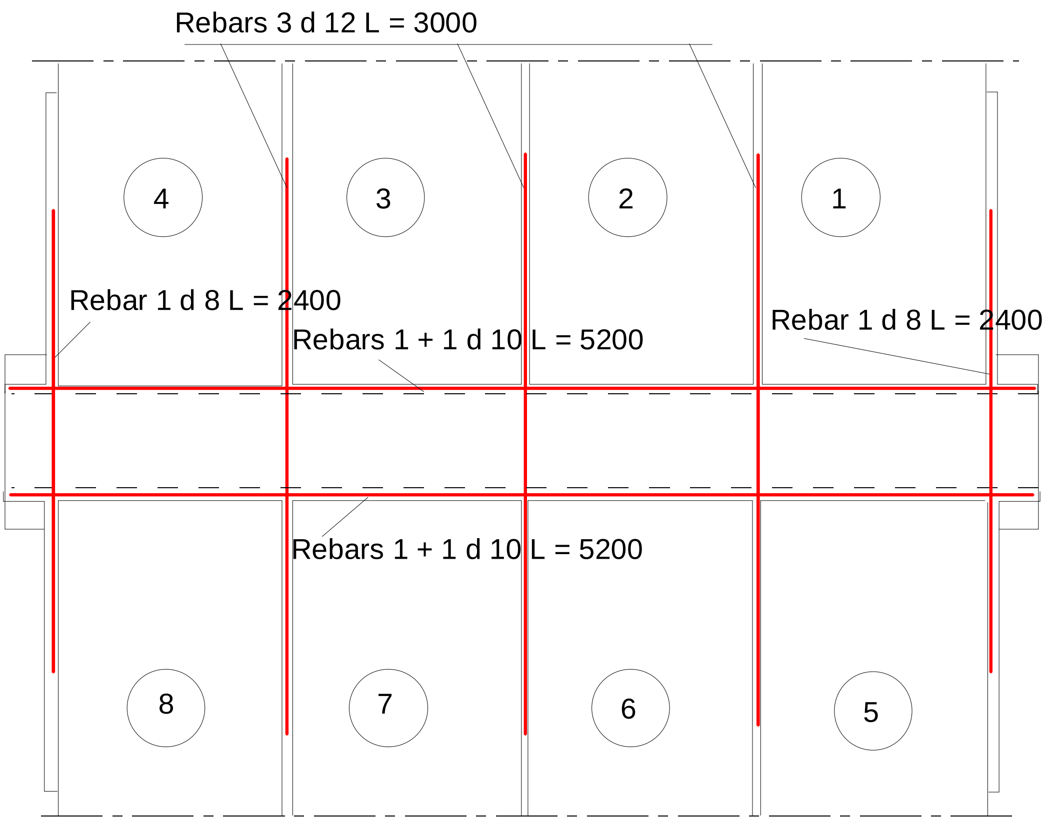

Fig. 12. Overview on tie reinforcement at middle beam. d xy refers to a reinforcing bar Txy, see 2.3.

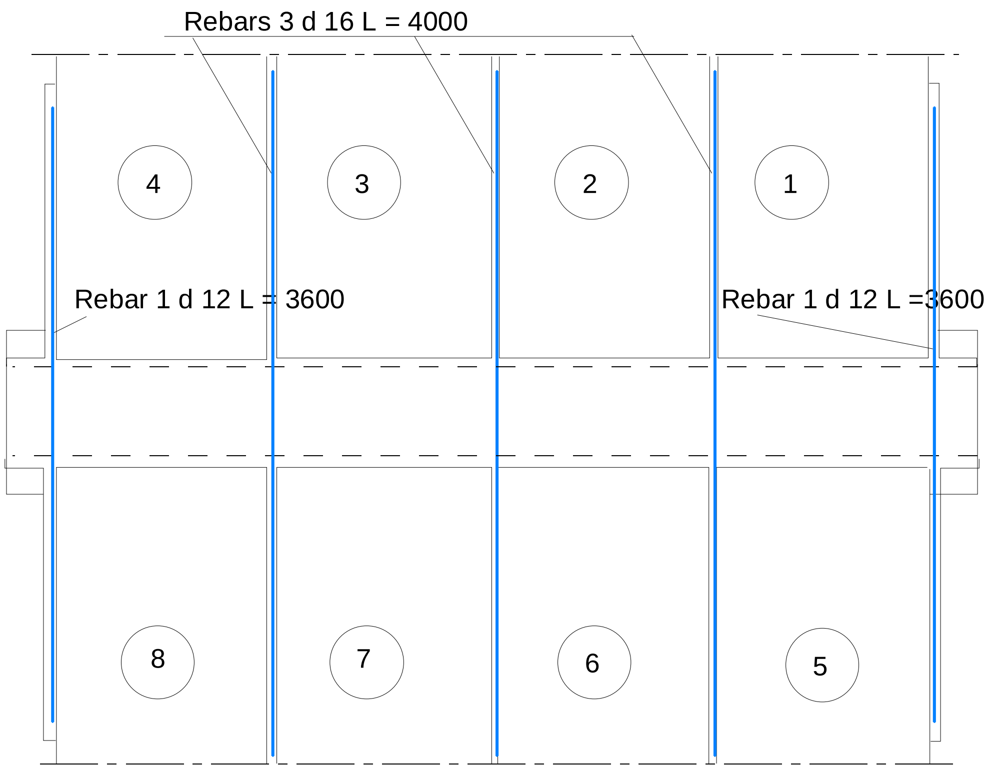

Fig. 13. Overview on suspension reinforcement at middle beam. d xy refers to a reinforcing bar Txy, see 2.3.

2.5 Slabs	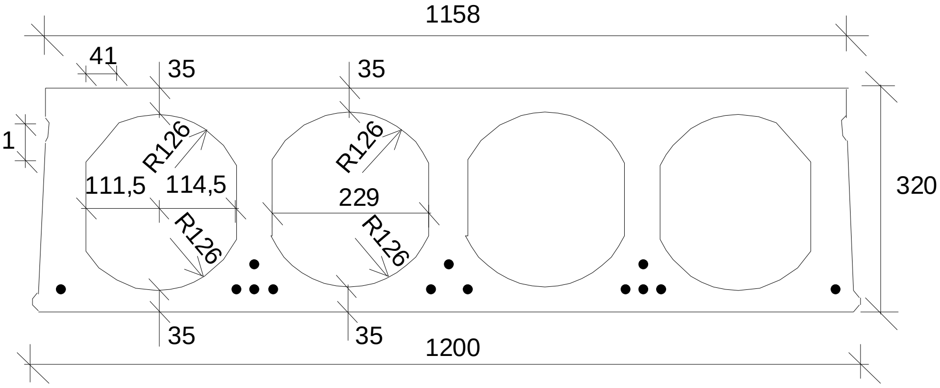 *Fig. 14. Illustration of nominal slab cross-section drawn in scale. Concrete K60.* - Extruded by Parma , Hyrylä factory 6.10.2006 - 13 lower strands J12,5 initial prestress 1000 MPa **J12,5**: seven indented wires, ϕ=12,5 mm, A_p = 93 mm^2 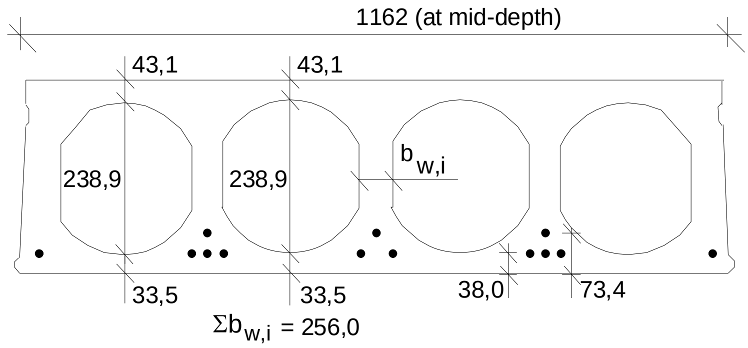 Max measured bond slips: 1,9 and 1,6 mm in slab unit 6, 2x1,4 mm in slab unit 8 Measured weight of slab units = 4,62 kN/m *Fig. 15. Mean of most relevant measured geometrical characteristics.*
2.6 Temporary supports	No

2.7
Loading arrangements

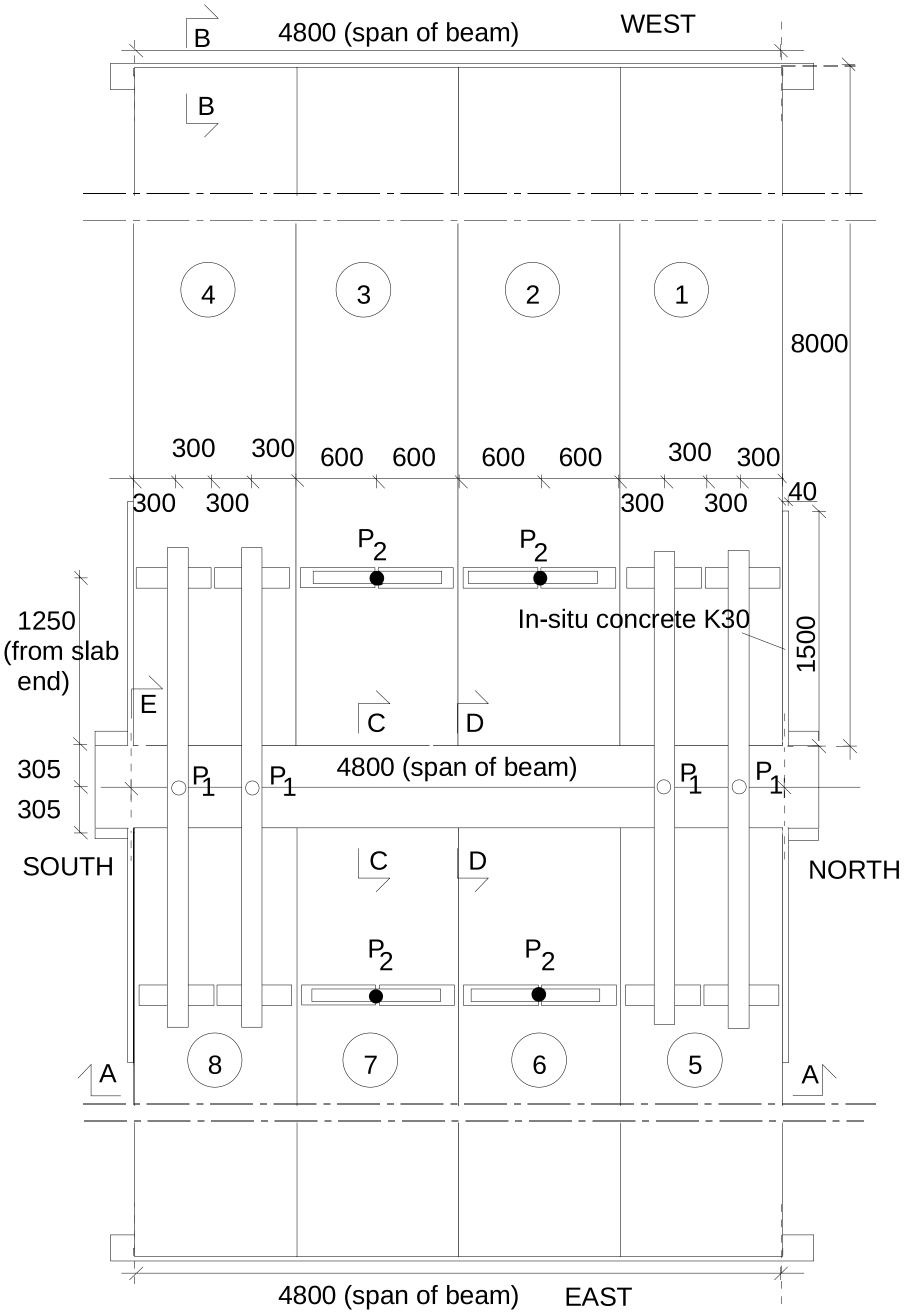

Fig. 16. Plan. P_1 =P_{a1} and P_2 =P_{a2} refer to vertical actuator forces.

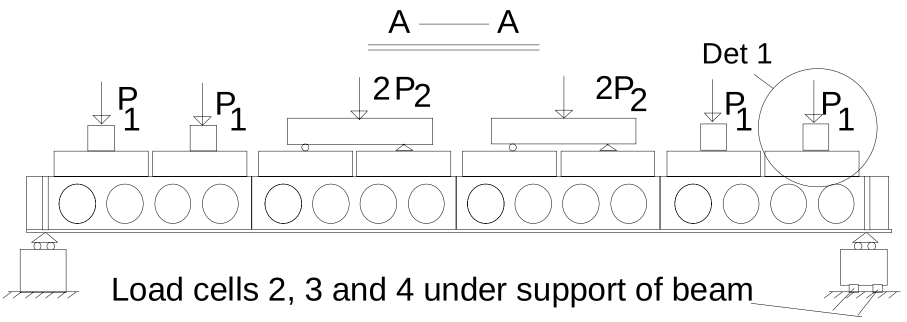

Fig. 17. Section A-A, see Fig. 17.

	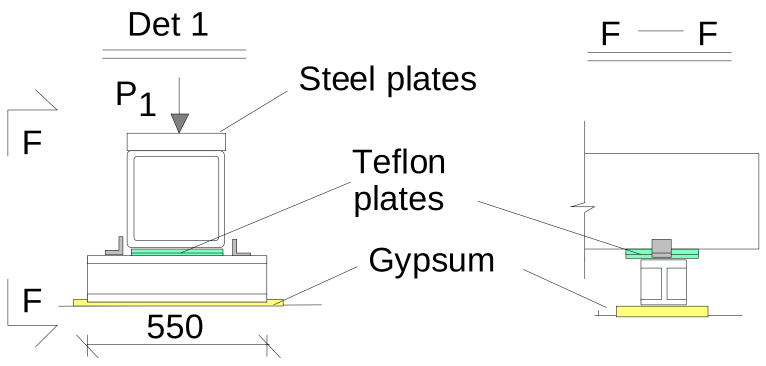 *Fig. 18. Detail 1, see Fig. 18.*
3	**Measurements**
3.1 Support reactions	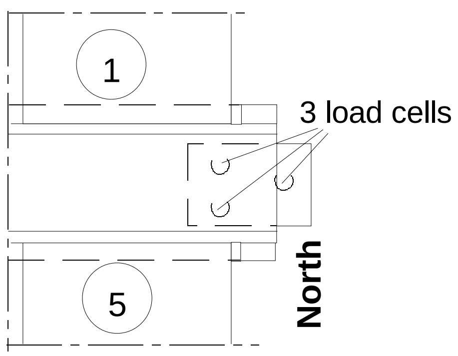 *Fig. 19. Load cells below the Northern support of the middle beam.*

<table>
<tr>
<td>3.2
Vertical displacement</td>
<td>
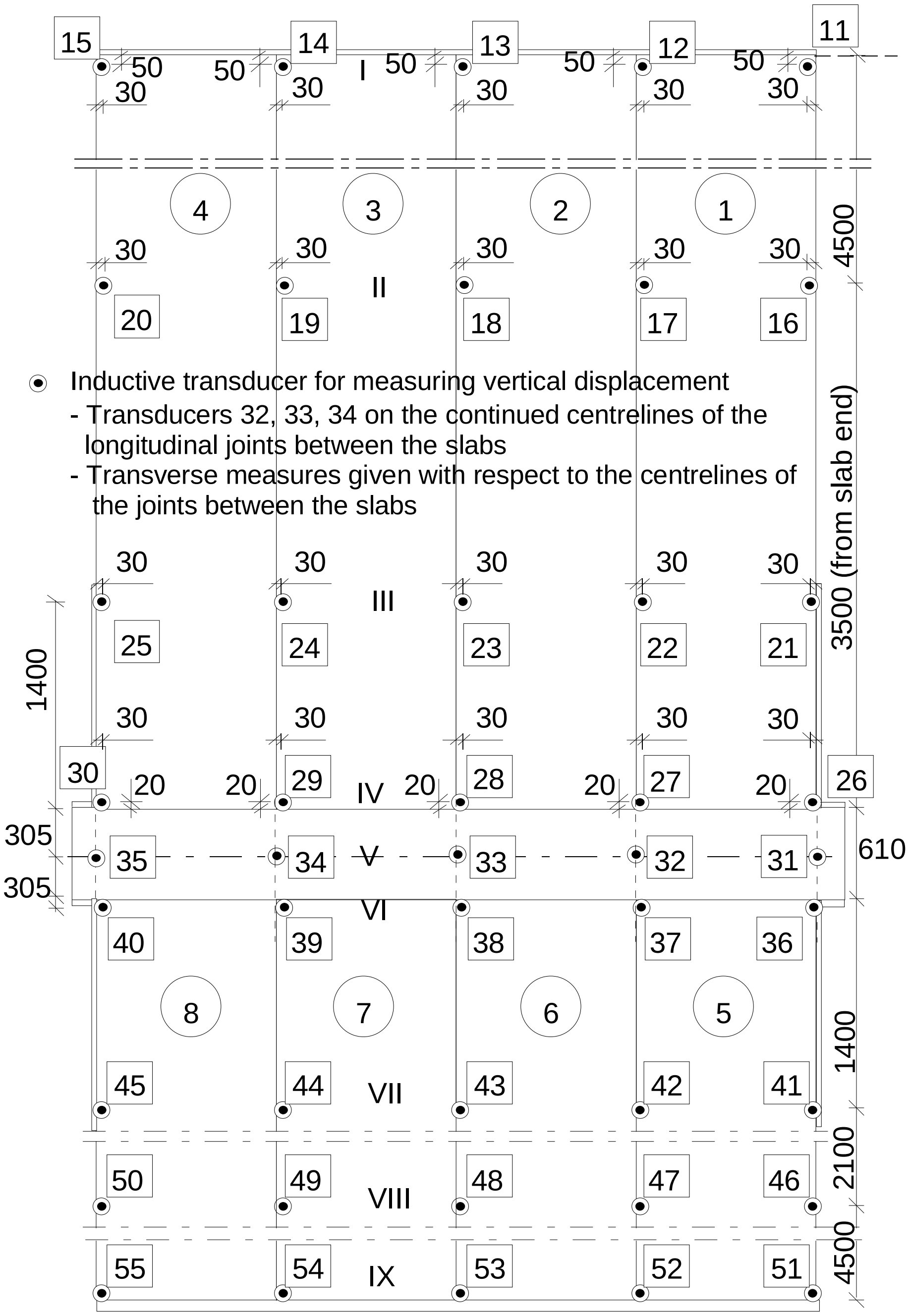

Fig. 20. Location and numbering of transducers 11–55 for measuring vertical displacement at lines I–IX.
</td>
</tr>
</table>

3.3
Average strain

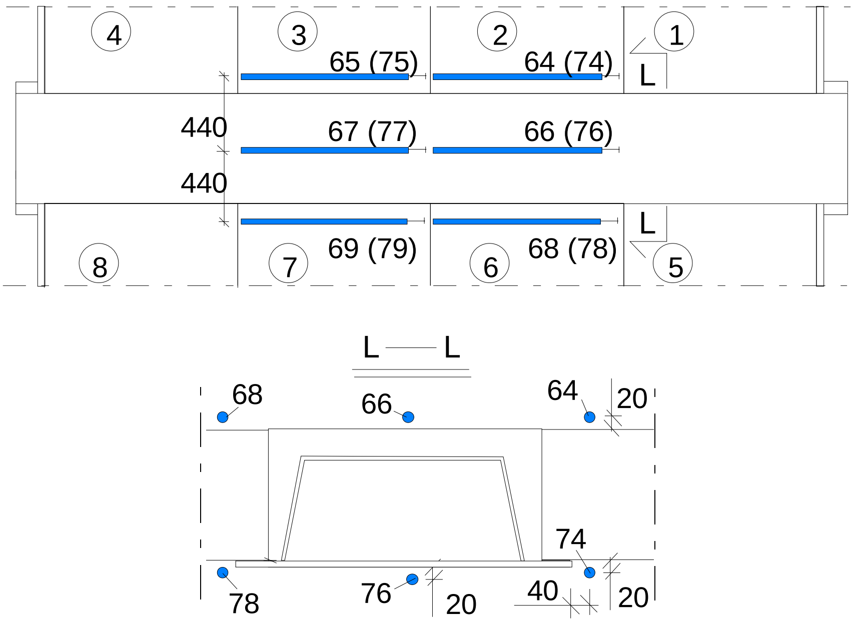

Fig. 21. Transducers measuring average strain in beam's direction. Numbers in parentheses refer to transducers below the floor.

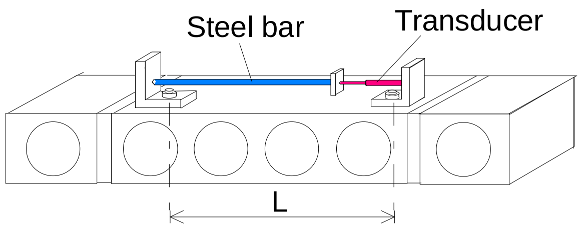

Fig. 22. Apparatus for measuring average strain. L =1100mm.

3.4
Horizontal. displacements

Measures differential displacement between slab end and beam (crack width)

Measures differential displacement between slab edge and beam in beam's direction

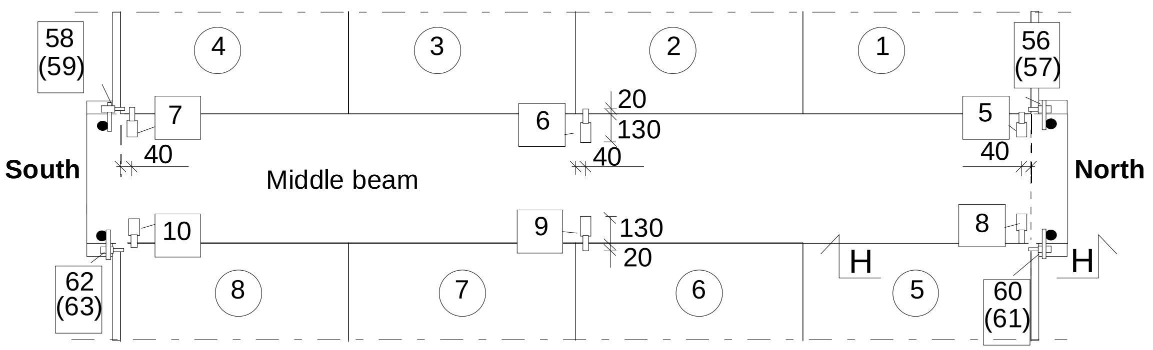

Fig. 23. Transducers measuring crack width (5–10) and shear displacement at the ends of the middle beam (56–63). Transducers 57, 59, 61 and 63 are below transducers 56, 58, 60 and 62, respectively.

	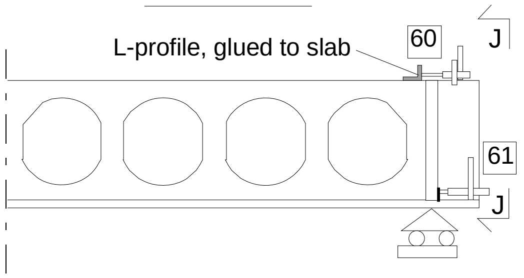 *Fig. 24. Section H-H, see Fig. 24.* 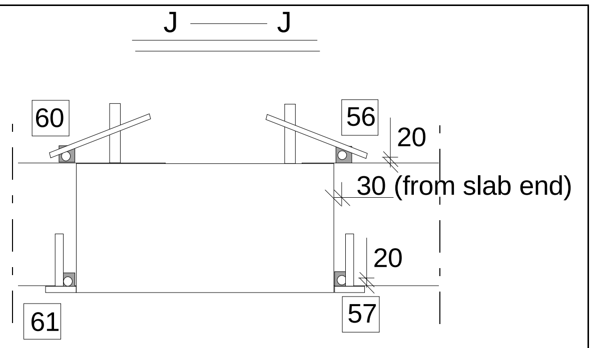 *Fig. 25. Section J-J, see Fig. 25.*
3.5 Strain	**-**
4	**Special arrangements** -
5	**Loading strategy**
5.1 Load-time relationship	Date of test was 17.11.2006 Before loading all measuring devices were zero-balanced. The loading history is shown in Fig. 27. 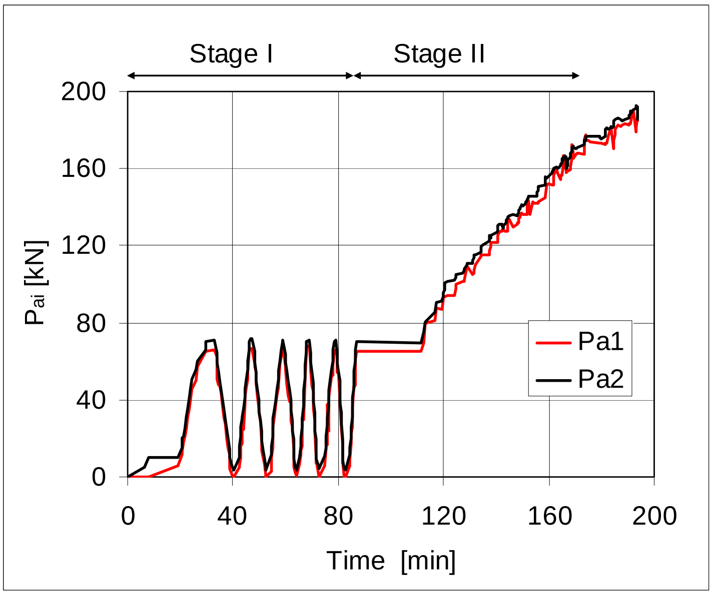 *Fig. 26. Actuator forces P_{a1} and P_{a2} vs. time.*

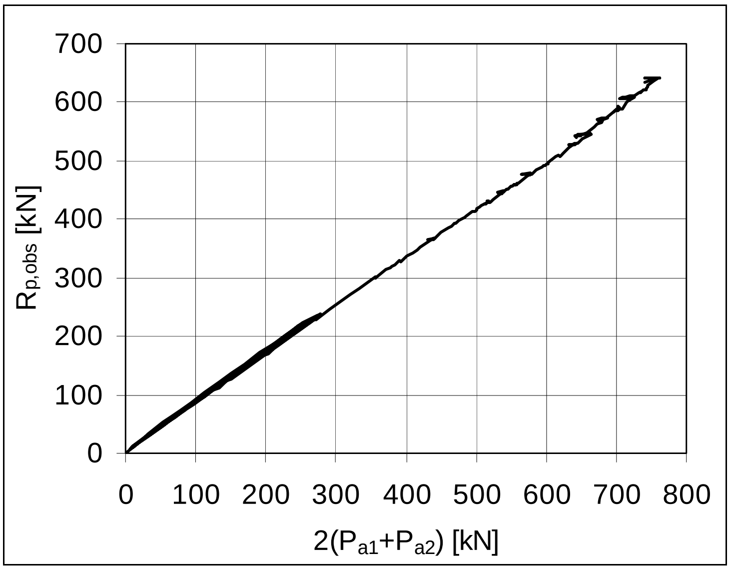

Fig. 27. Development of support reaction R below Northern end of middle beam as function of actuator loads $2(P_{a1} + P_{a2})$ on half floor.

5.2
After failure

-

6 **Observations during loading**

Before test	The soffit of the slabs next to the middle beam was visually inspected and some cracks along the strands were observed, see Fig. 29.
Stage I	The joint concrete at the middle beam gradually cracked along the ends of slabs 5–8. The first visible cracks were observed at P_{a2} = 38 kN. On the opposite (Western) side of the middle beam, a similar crack was observed at P_{a2} = 70 kN. The first flexural cracks in the tie beams above the end beams appeared at P_{a2} = 61 kN. Their number and length increased with increasing load, see Figs 29 and 30.
Stage II	At P_{a2} = 70 kN, the soffit of the slabs between the line loads and the middle beam was again inspected visually. The observed visible cracks are shown in Fig. 29. Most of them were below the webs with four strands, i.e. below the strands, but none below the midmost or outermost webs where the number of strands was only three or one per web, respectively, see. Fig. 14. With increasing load new inclined cracks gradually appeared in the cast-in-situ concrete at the outermost edges of the slabs next to the ends of the middle beam, see Fig. 30. Before failure there were such cracks in the corners of slabs 1, 4, 5 and 8. In slab 8 the cracks were particularly wide before failure as can be seen in App. B, Fig. 23. The tie beams at the ends of the floor also cracked in flexure. The first flexural cracks appeared in the middle of the beams at P_{a2} = 61 kN, i.e. during the cyclic load stage. Thereafter, the Eastern tie beam proved to be much stronger against cracking than the Western one. The Eastern tie beam was uncracked next to the joint between slabs 7 and 8 until failure. No reason for this nonsymmetrical behaviour could be detected.

		The failure mode was web shear failure in slabs 8 and 7, see Fig. 30 and App. B, Figs 26, 27, 36 and 39–42.
	After failure	When demolishing the test specimen it was observed that the core fillings were perfect. The slabs were placed on the ledge of the middle beam without any intermediate material. Due to the curved soffit of the slabs and uneven top surface of the ledge, small gaps remained somewhere between the soffit of the slab units and the underlying ledge of the middle beam, see e.g. App. B, Fig. 17. After demolishing the floor it was observed that cement paste or grout had gone into these gaps thus making the supporting ledge more even and able to distribute the support reaction to all webs. This is illustrated in App. B, Figs 43 and 44. When demolishing the floor it was observed that at the middle beam the cast-in-situ concrete had cracked vertically along the slab ends. This is illustrated in App. B, Figs 40–42.
7	**Cracks in concrete**	
7.1 Cracks at service load	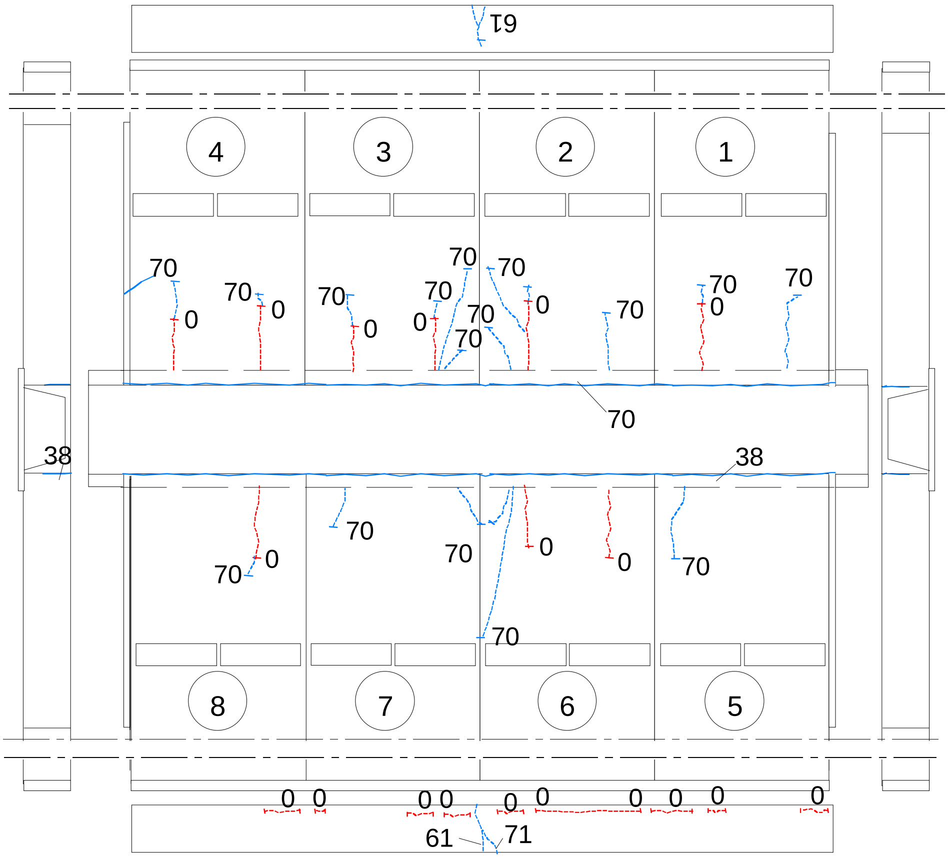 *Fig. 28. Cracks at service load (P_{ai} ≈ 70 kN). The initial cracks are indicated with red colour. A dashed line indicates a crack in the soffit. The figures give the value of the actuator force at which the crack was observed.*	

7.2
Cracks after failure

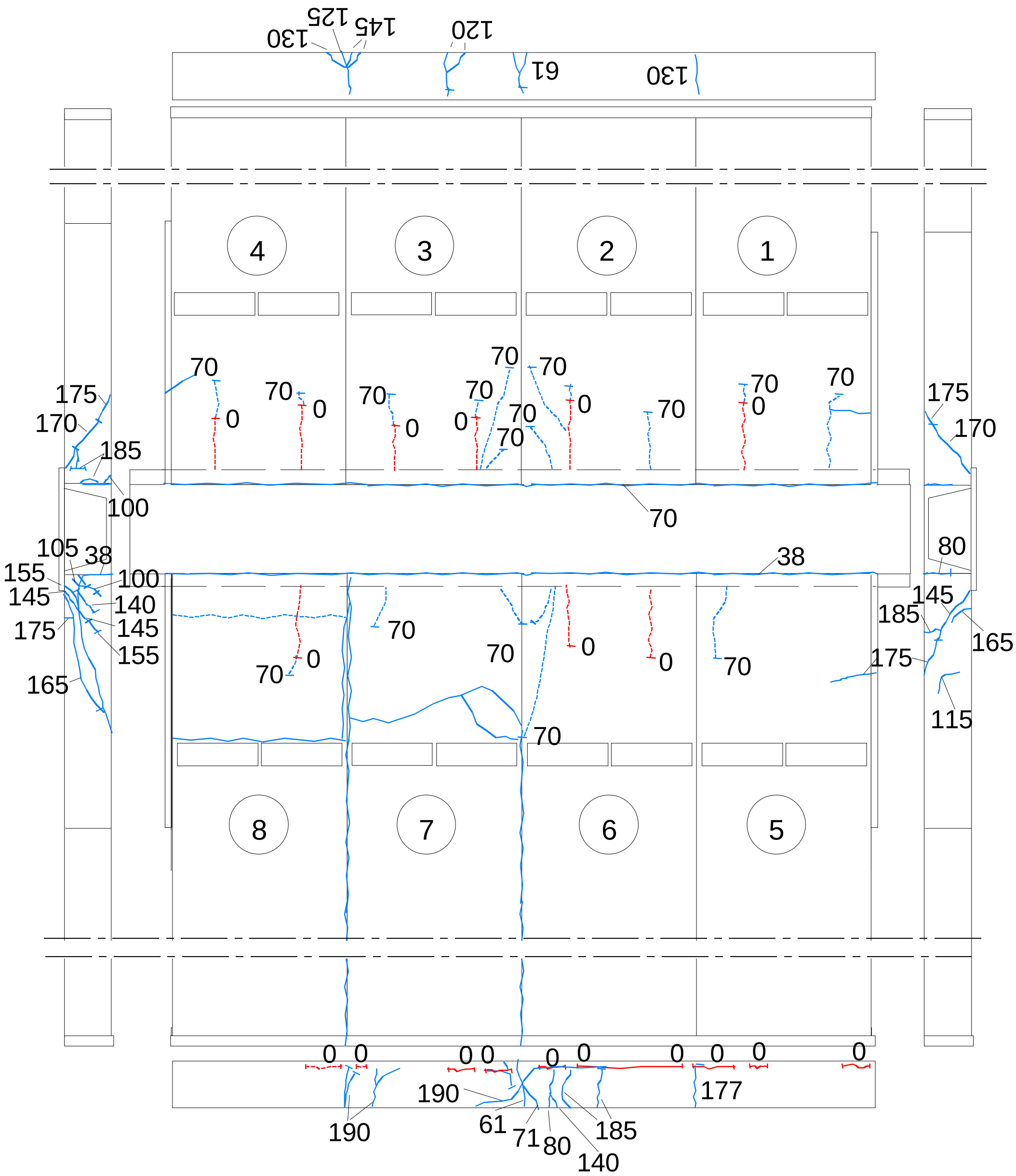

Fig. 29. Cracking pattern after the failure. The dashed lines illustrate the cracks in the soffit.

8 **Observed shear resistance**

The ratio (measured support reaction below one end of the middle beam)/ (theoretical support reaction due to actuator forces on half floor) is shown in Fig. 31. The theoretical reaction is calculated assuming simply supported slabs. This comparison shows that the support reaction due to the actuator forces can be calculated accurately enough assuming simply supported slabs. However, the failure of the slab ends at the North end of the middle beam resulted in reduction of support reaction below that end while the actuator force could still slightly be increased. The maximum support reaction is regarded as the indicator of failure.

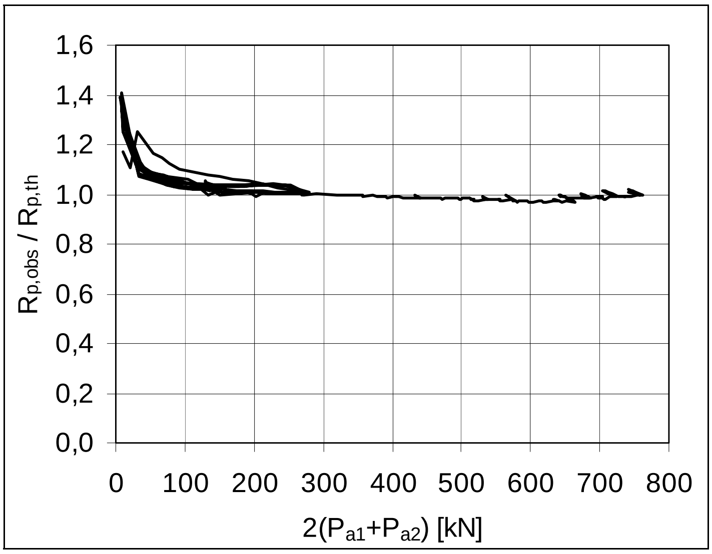

Fig. 30. Ratio of measured support reaction of the middle beam ($R_{p,obs}$) to theoretical support reaction ($R_{p,th}$) vs. actuator forces on half floor.

The theoretical support reaction $R_{p,th}$ is calculated from four actuator loads assuming simply supported slabs. Thus $R_{p,th}$ is equal to (7900–1200)/7900×4×P_{am} = 0,8481×4×P_{am}. where $P_{am} = (P_{a1} + P_{a2})/2$. Before failure the assumption of simply supported slabs is accurate enough to justify the calculation of the experimental shear resistance based on it.

The shear resistance of one slab end (support reaction of slab end at failure) due to different load components is given by

$$V_{obs} = V_{g,sl} + V_{g,jc} + V_{eq} + V_p \quad (1)$$

where $V_{g,sl}$, $V_{g,jc}$, V_{eq} and V_p are shear forces due to the self-weight of slab unit, weight of joint concrete, weight of loading equipment and actuator forces P_{ai}, respectively. All components of the shear force are calculated assuming that the slabs behave as simply supported beams. For V_{eq} and V_p this means that $V_{eq} = 0{,}8481 \times P_e$ and $V_p = 0{,}8481 \times (P_{a1}.+ P_{a2})/2$. $V_{g,jc}$ is calculated from the nominal geometry of the joints and density of the concrete, other components of the shear force are calculated from measured loads and weights. The values for the components of the shear force are given in Table 1.

Table 1. Components of shear resistance due to different loads.

Action	Load	Shear force kN
Weight of slab unit	4,62 kN/m	18,25
Weight of joint concrete	0,24 kN/m	0,95
Loading equipment	(0,66+5,70)/2 kN	2,70
Actuator loads	(190,6+190,1)/2 kN	161,44

The observed shear resistance V_{obs} = **183,3** kN (shear force at support) is obtained for one slab unit. The shear force per unit width is $\boldsymbol{v_{obs}}$ **= 152,8** kN/m

9 Material properties

9.1 Strength of steel

Component	$R_{eH}/R_{p0,2}$ MPa	R_m MPa	Note
A-Beam - End plates - Other structural steel	 ≈ 460 ≈ 355		 Nominal Raex 460 Nominal (S355J2G3)
End beams	≈ 355		(HEA 120)
Slab strands J12,5	1630	1860	Nominal (no yielding in test)
Reinforcement Txy	500		Nominal value for reinforcing bars (no yielding in test)

9.2 Strength of slab concrete, floor test

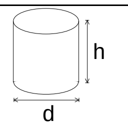

#	Cores		*h* mm	*d* mm	Date of test	Note
6			50	50	24.11.2006 (+7 d)[1)]	Upper flange of slab 7 (3 pc.) and slab 8 (3 pc.), vertically drilled, tested as drilled[2)] density = 2416 kg/m^3
Mean strength [MPa]			74,7			
St.deviation [MPa]			4,10			

9.3 Strength of slab concrete, reference tests

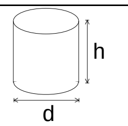

#	Cores		*h* mm	*d* mm	Date of test	Note
6			50	50	27.11.2006 (+3 d)[1)]	Upper flange of slab 9, vertically drilled, tested as drilled[2)], density =2416 kg/m^3
Mean strength [MPa]			79,7			
St.deviation [MPa]			3,96			

9.4 Strength of grout in longitudinal joints of slab units

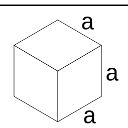

#		*a* mm	Date of test	Note
6		150	17.11.2006 (+0 d)[1)]	Kept in laboratory in the same conditions as the floor specimen density = 2183 kg/m^3
Mean strength [MPa]		25,0		
St.deviation [MPa]		0,72		

9.5 Strength of concrete inside the A-beam

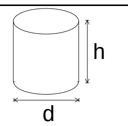

#	Cores		*h* mm	*d* mm	Date of test	Note
6			50	50	24.11.2006 (+7 d)[1)]	Vertically drilled through the holes of the top flange, tested as drilled[2)] density=2260 kg/m^3
Mean strength [MPa]			45,6			
St.deviation [MPa]			5,24			

1) Date of material test minus date of structural test (floor test or reference test)
2) After drilling, kept in a closed plastic bag until compression

10 Measured displacements

In the following figures, V_P stands for the shear force of one slab end due to imposed actuator loads, calculated assuming simply supported slabs.

10.1 Deflections

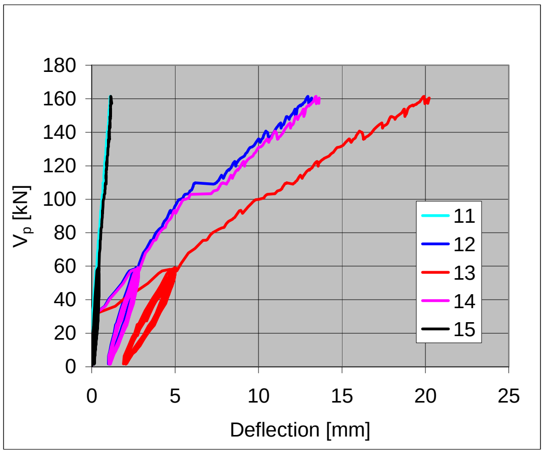

Fig. 31. Deflection on line I along Western end beam.

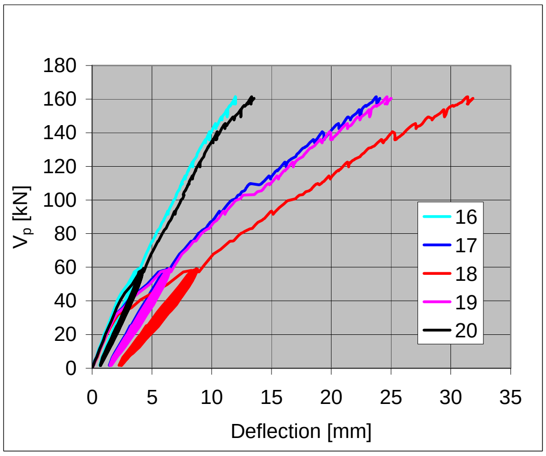

Fig. 32. Deflection on line II in the middle of slabs 1–4.

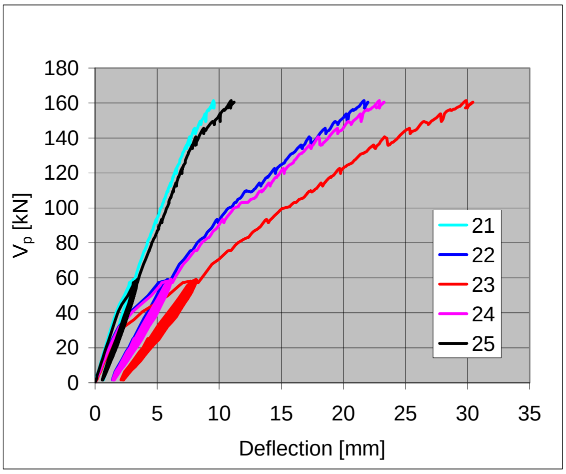

Fig. 33. Deflection on line III close to the line load, slabs 1–4.

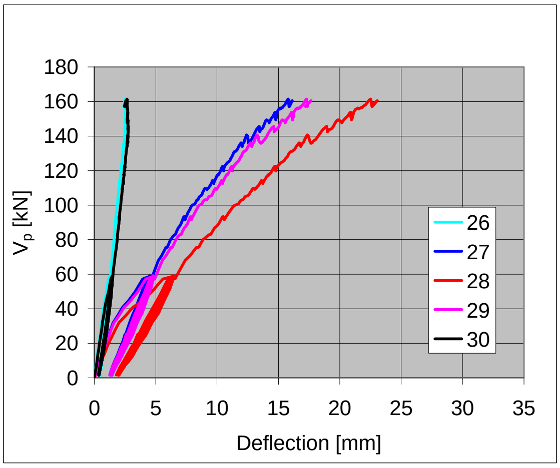

Fig. 34. Deflection on line IV next to the middle beam, slabs 1–4.

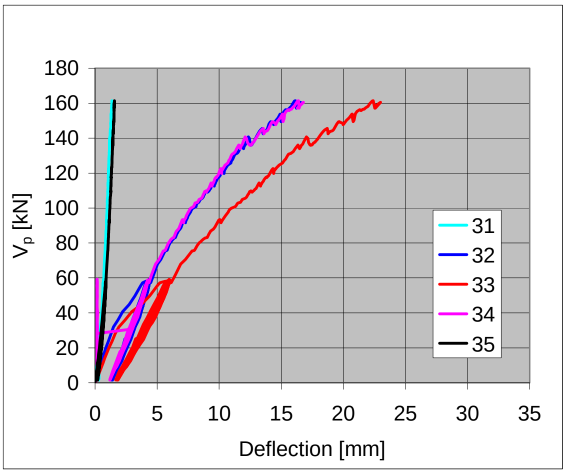

Fig. 35. Deflection on line V along the middle beam.

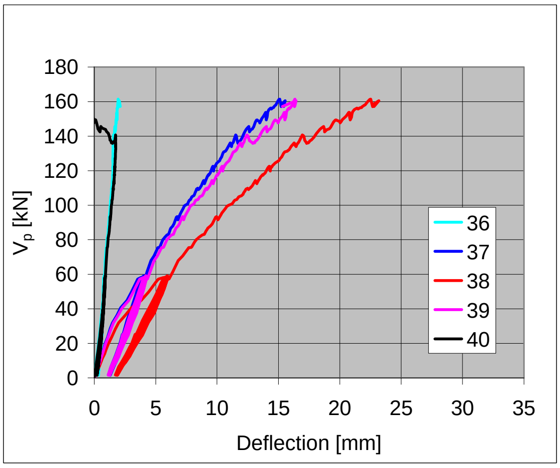

Fig. 36. Deflection on line VI next to the middle beam, slabs 5–8.

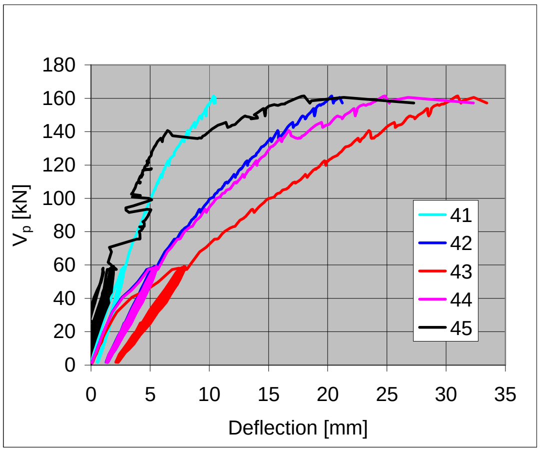

Fig. 37. Deflection on line VII next to the line loads, slabs 5–8.

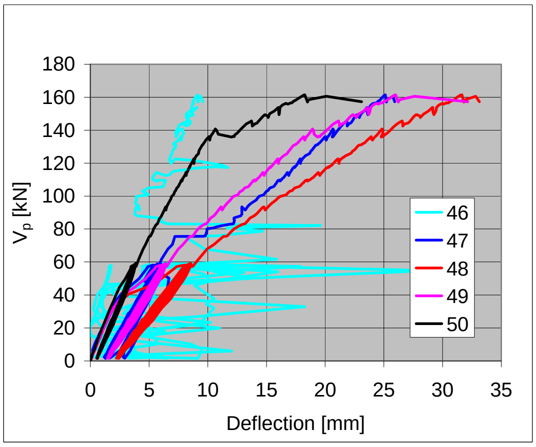

Fig. 38. Deflection on line VIII in the middle of slabs 5–8. Transducer 46 gave erroneous results.

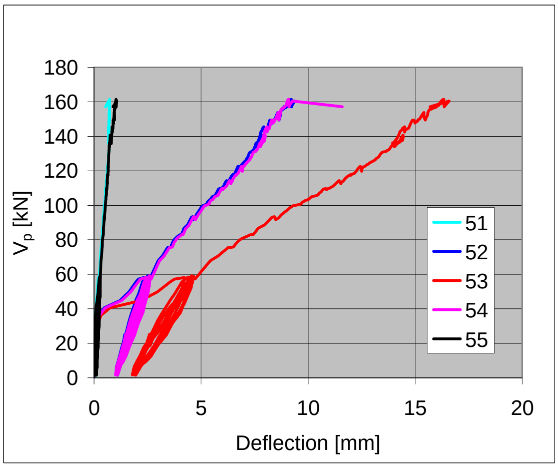

Fig. 39. Deflection on line IX along Eastern end beam, slabs 5–8.

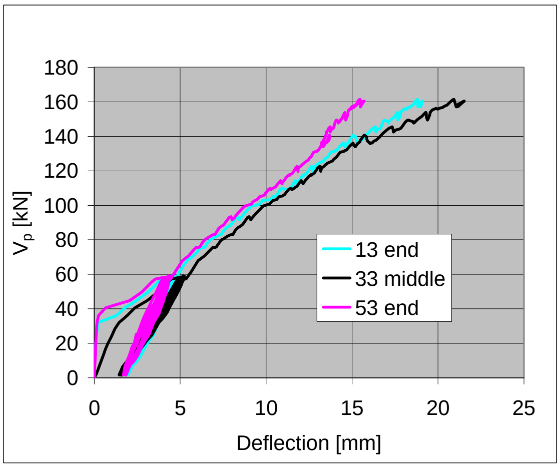

Fig. 40. Net deflection of midpoint of middle beam (33) and those of end beams (13, 53).

10.2
Crack width

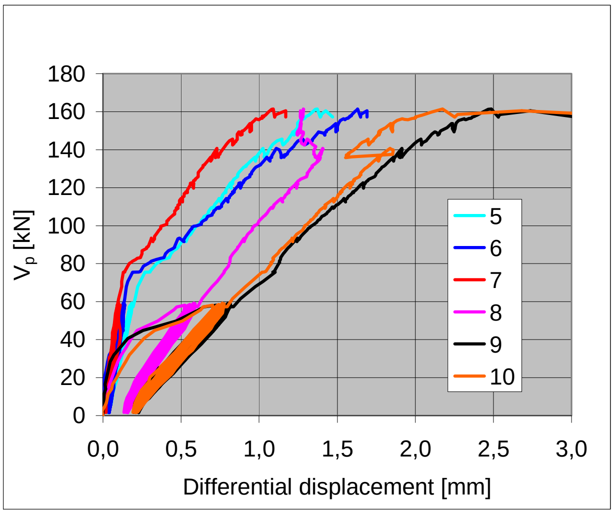

Fig. 41. Differential displacement parallel to the slab between the middle beam and the slabs (≈ crack width).

10.3
Average strain (actually differential displacement)

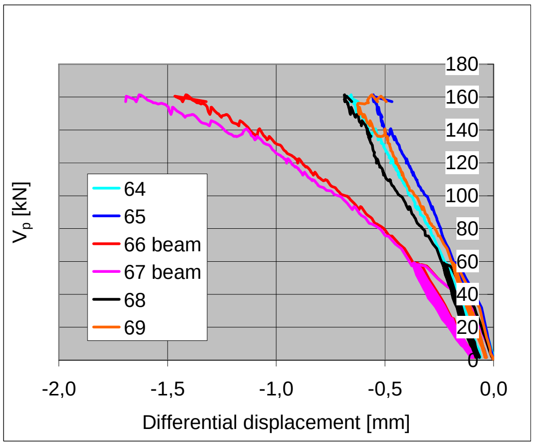

Fig. 42. Differential displacement at top surface of floor measured by transducers 64–69.

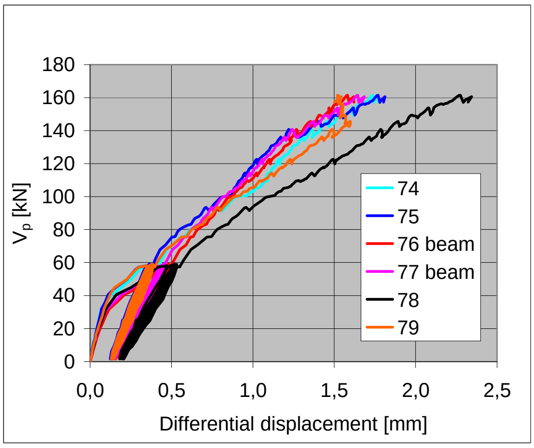

Fig. 43. Differential displacement at soffit of floor measured by transducers 74–79.

The differential displacement divided by the mutual distance of the two fixing points represents the average strain between those points. Assuming linearly changing strain in vertical direction, the average strain at any depth between the measured top and bottom values can be calculated from the measured results. The average strain at the top and bottom fibre of the slabs and the middle beam obtained in this way are shown in Figs 45–46.

Assuming parabolic curvature due to the uniformly distributed load on the beam, and having the span of the beam equal to 4,8 m, the maximum strain within each of the slabs 2, 3, 6 and 7 is 9% higher than the average strain measured between the edges of the slab. In this way, the maximum strain is obtained from the average strains by multiplying the latter by 1,09.

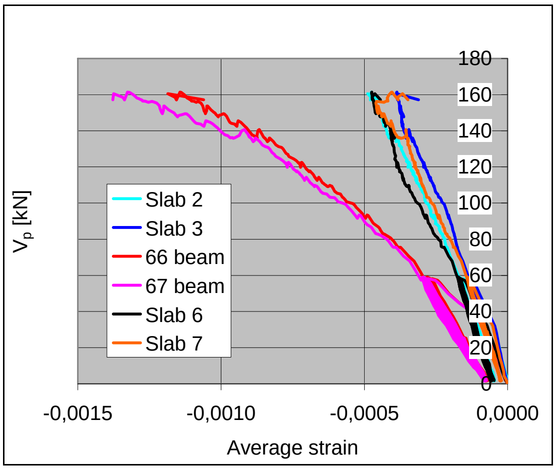

Fig. 44. Top fibre of floor. Average strain calculated from the differential displacements shown in Figs 41–42.

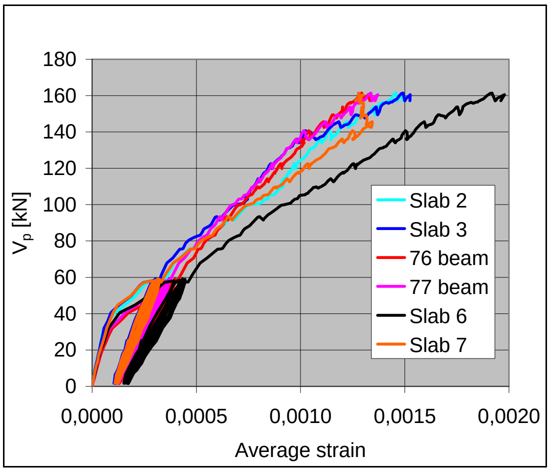

Fig. 45. Bottom fibre of floor. Average strain calculated from the differential displacements shown in Figs 41–42.

The variation of the average strain with the depth is illustrated in Figs 47 and 48 at the evaluated service load (V_p = 57 kN) and failure load, respectively. The mean of the average strain both for the slabs and for the beam is shown in Figs 49 and 50 at two load levels.

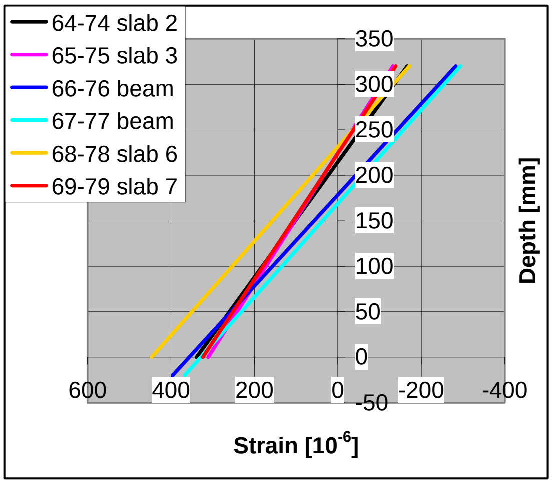

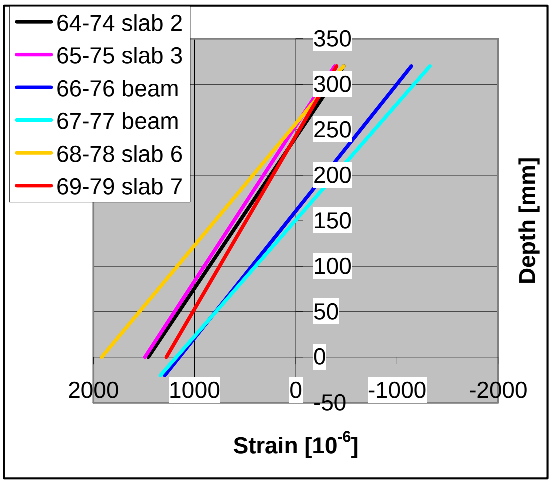

Fig. 46. Average strain of slabs 2, 3, 6 and 7 as well as that of the middle beam, all in beam's direction, at estimated service load (V_p = 57 kN).

Fig. 47. Average strain of slabs 2, 3, 6 and 7 as well as that of the middle beam, all in beam's direction, before failure at V_p = 161 kN.

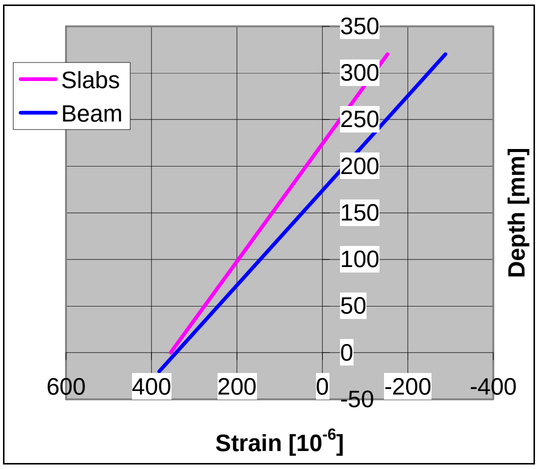

Fig. 48. Mean of average strains measured for slabs 2, 3, 6 and 7 as well as mean of average strains measured for the middle beam at estimated service load (Vp = 57 kN).

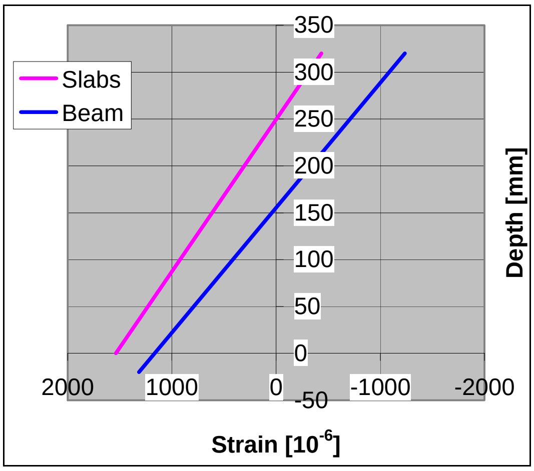

Fig. 49. Mean of average strains measured for slabs 2, 3, 6 and 7 as well as mean of average strains measured for the middle beam before failure at V_p = 161 kN.

Both at service load and at failure, the strains in the top of the slabs were essentially smaller than those in the beam. This can be explained by the low transverse shear stiffness of the slabs. The scatter of the slab strains on the top was small.

At service load, the strains in soffit of the slabs were on average of the same order as those in the beam at the same level. The friction force between the soffit of the slabs and the bottom flange of the beam was strong enough to make the strains compatible. This can clearly be seen in Fig. 49.

At failure load, the strain in the soffit of the slabs was greater than that in the beam. This may be explained by the weak interaction between the beam and the slabs and longitudinal cracking of the slabs, the first signs of which were observed already before loading and at service load, see Figs 29 and 35.

10.4 Shear displacement

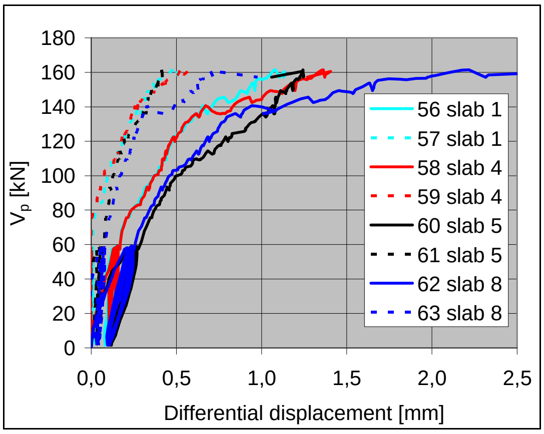

Fig. 50. Differential displacement between edge of slab and middle beam. A positive value means that the slab is moving towards the end of the beam. At V_P = 140 kN the end of slab 8 broke into pieces.

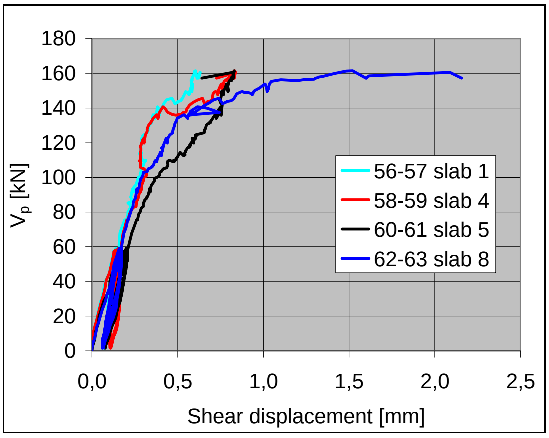

Fig. 51. Transverse shear displacement of slab end calculated from displacements shown in Fig. 51.

11	**Reference tests**

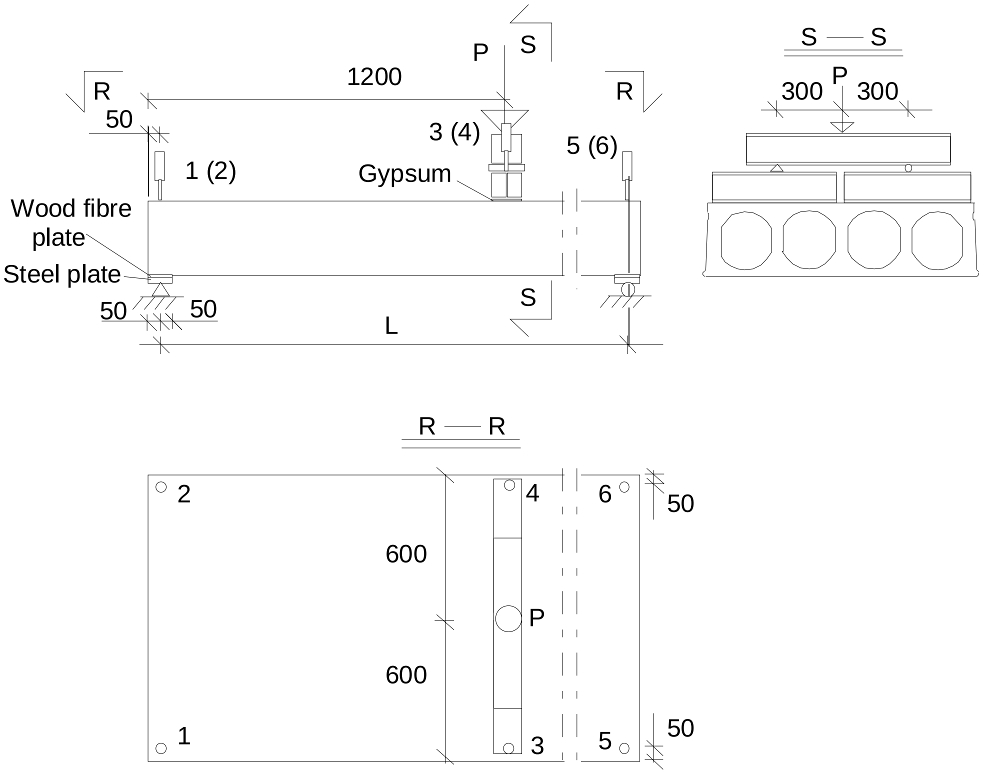

Fig. 52. Layout of reference test. For L see Table 2.

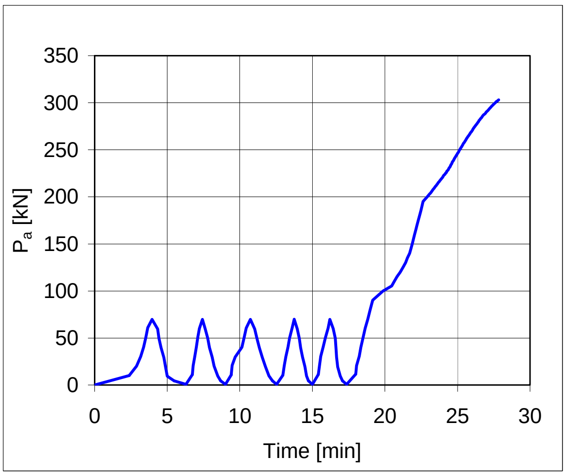

Fig. 53. Test R1. Actuator force – time relationship.

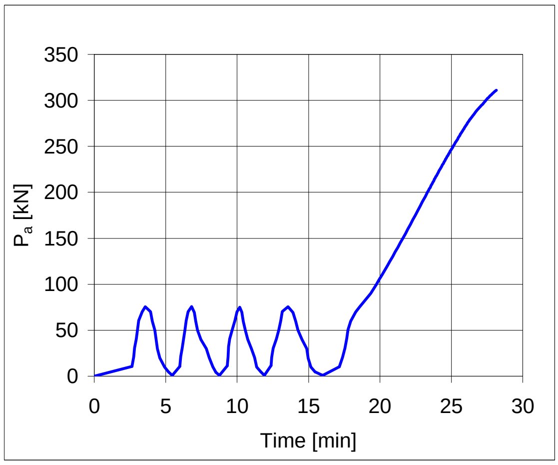

Fig. 54. Test R2. Actuator force – time relationship.

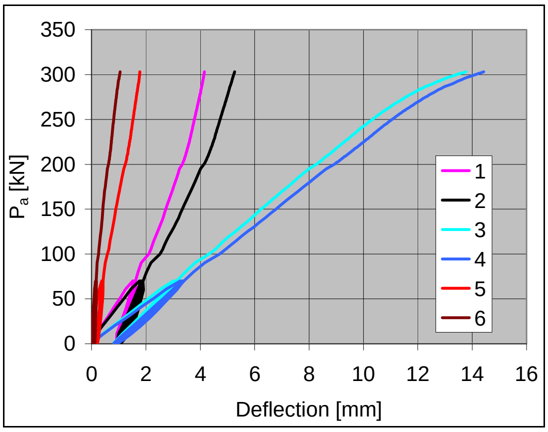

Fig. 55. Test R1. Displacements measured by transducers 1–6.

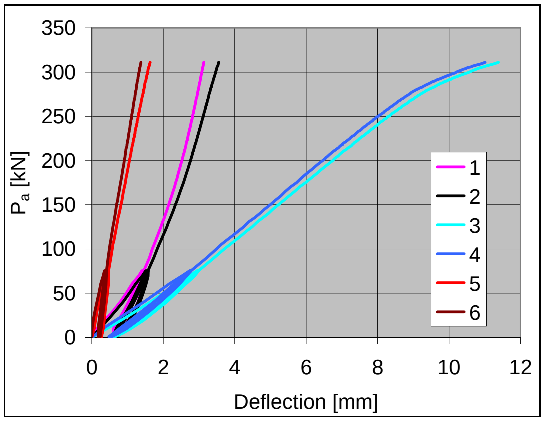

Fig. 56. Test R2. Displacements measured by transducers 1–6.

Table 2. Reference tests. Span of slab, shear force V_g at support due to the self weight of the slab, actuator force P_a at failure, weight of loading equipment P_{eq}, total shear force V_{obs} at failure and total shear force v_{obs} per unit width.

Test	Date	Span mm	V_g kN	P_a kN	P_{eq} kN	V_{obs} kN	v_{obs} kN/m	Note
R1	24.11.2006	7899	18,2	303,6	0,66	278,2	231,8	Web shear failure
R2	24.11.2006	6800	15,4	329,5	0,66	289,7	241,4	Flexural shear failure
				Mean		**283,9**	236,6	

12 Comparison: floor test vs. reference tests

The observed shear resistance (support reaction) of the hollow core slab in the floor test was equal to 183,3 kN per one slab unit or 152,8 kN/m. This is **65%** of the mean of the shear resistances observed in the reference tests.

13 Discussion

1. The net deflection of the middle beam due to the imposed actuator loads only (deflection minus settlement of supports) was 20,9 mm or *L*/230, i.e. rather small. It was 2,1–5,4 mm greater than that of the end beams. Hence, the torsional stresses due to the different deflection of the middle beam and end beams had a negligible effect on the failure of the slabs.
2. The shear resistance measured in the reference tests was of the same order as the mean of the observed values for similar slabs given in *Pajari, M. Resistance of prestressed hollow core slab against web shear failure. VTT Research Notes 2292, Espoo 2005*.
3. The edge slabs slided 0,4 … 0,5 mm along the beam before failure. This reduced the negative effects of the transverse actions in the slab and had a positive effect on the shear resistance.
4. The transverse shear deformation of the edge slabs was considerable which can be seen in Figs 51–52.
5. The failure mode was web shear failure of edge slabs. The A-beam seemed to recover completely after the failure.

APPENDIX A: A-BEAM

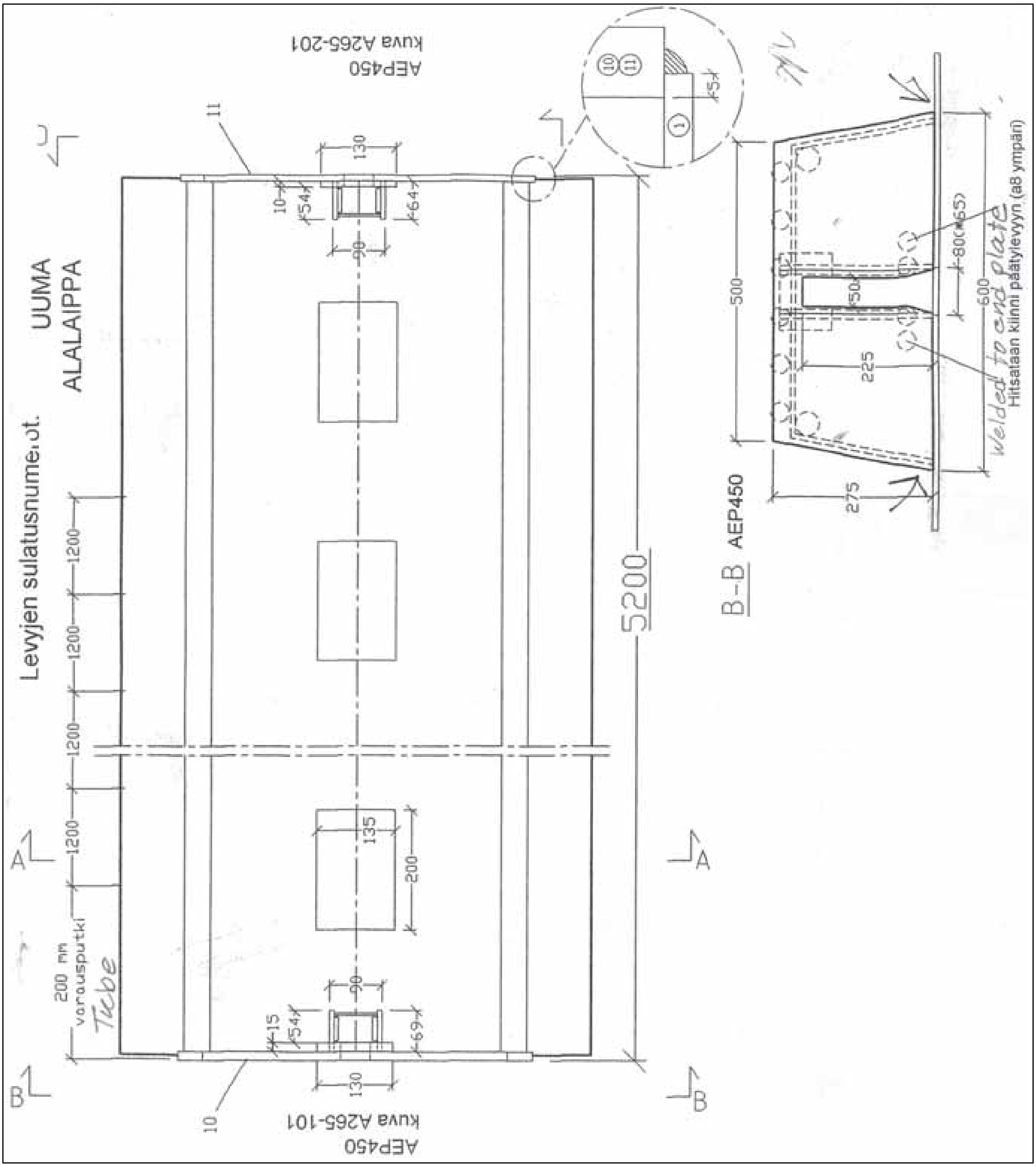

Fig. 1. Plan and section B-B.

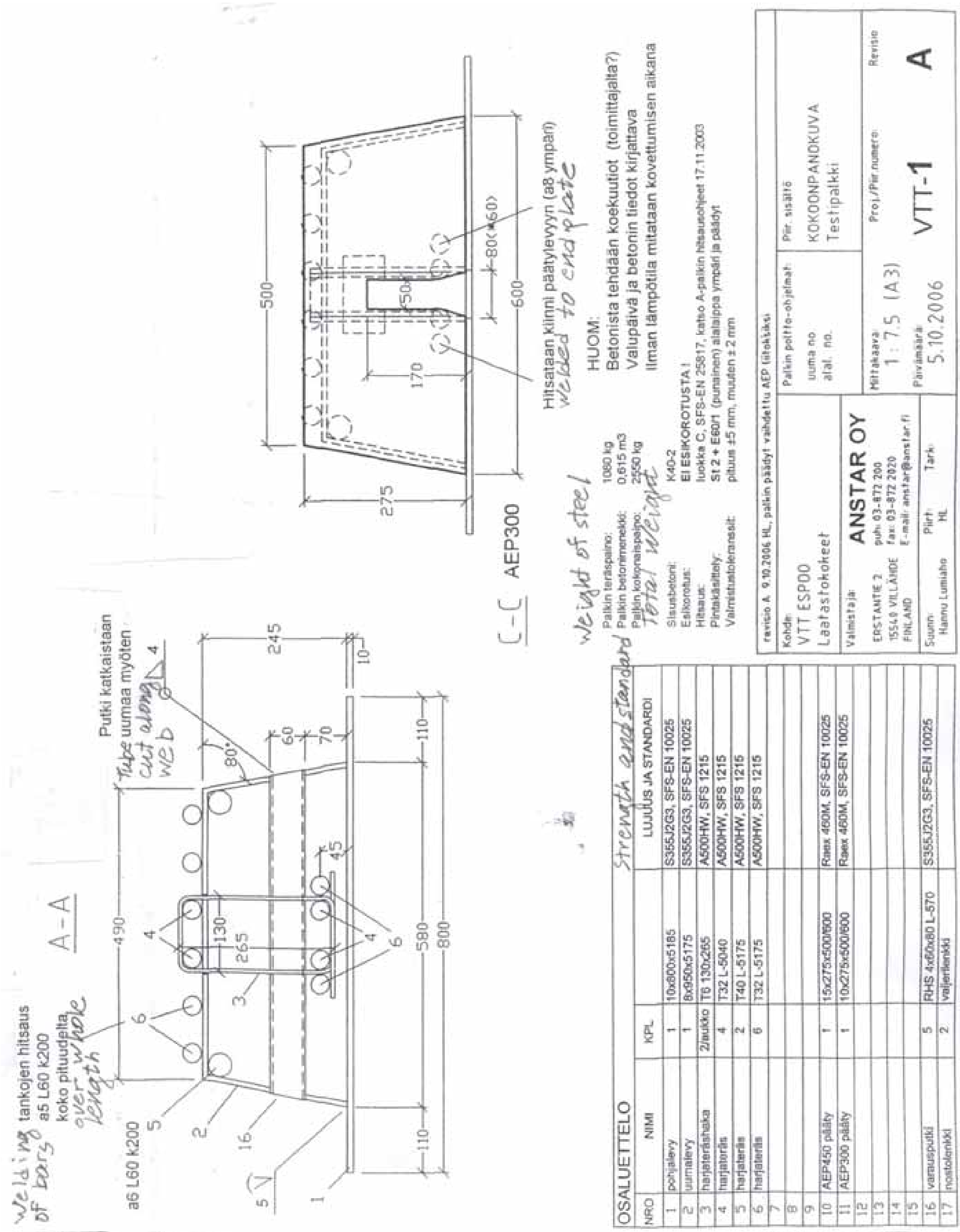

Fig. 2. Sections A-A and C-C and list of steel parts.

APPENDIX B: PHOTOGRAPHS

Fig. 1. A-beam.

Fig. 2. A-beam. Suspension bars temporarily stored on the top of the beam.

Fig. 3. Straight tie bar and bent suspension bar in their final position.

Fig. 4. Detail of the previous figure.

Fig. 5. Hollow core slabs temporarily supported on end beam.

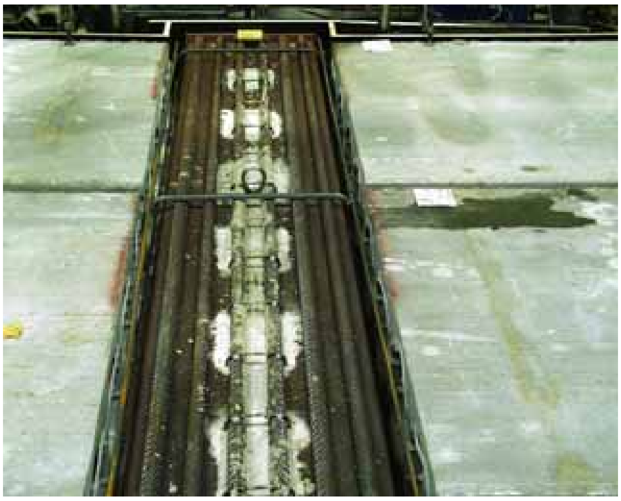

Fig. 6. Middle beam before grouting of joints.

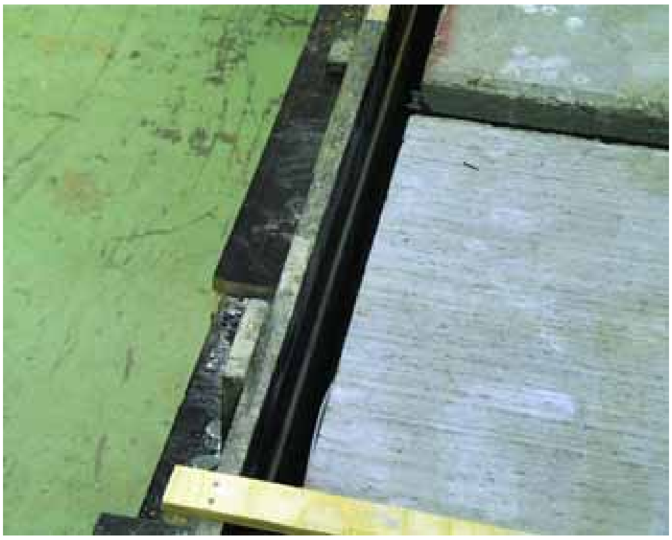

Fig. 7. End of floor before grouting.

Fig. 8. Test floor before grouting. Note the wedges in the joints to facilitate the demolishing of the floor after the test. To eliminate the contact between the floor and the loading frame, the outermost webs of the slabs were made thinner at the legs of the frame.

Fig. 9. Measuring devices at the end of the middle beam.

Fig. 10. Measuring devices at the end of the middle beam.

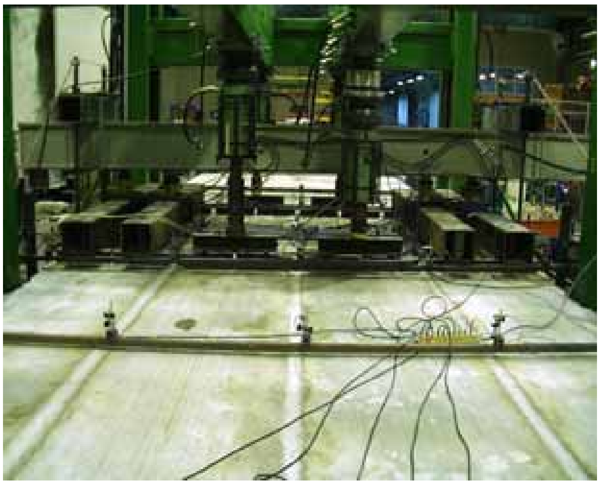

Fig. 11. View on the loading arrangements.

Fig. 12. Loading on outermost slabs.

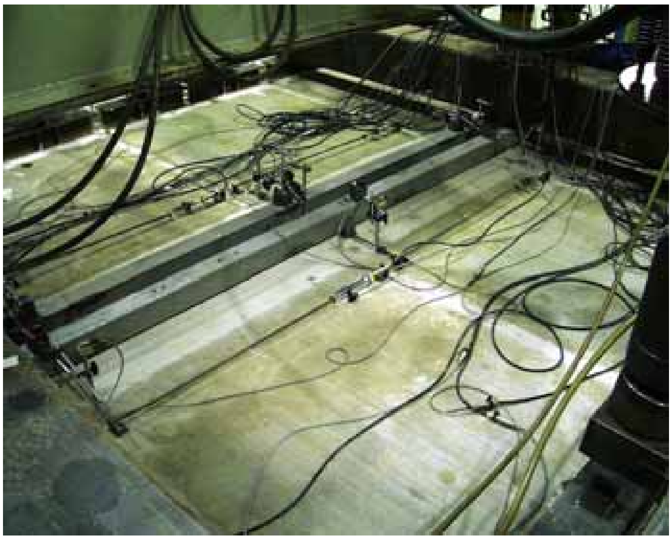

Fig. 13. Device for measuring strain parallel to the beams.

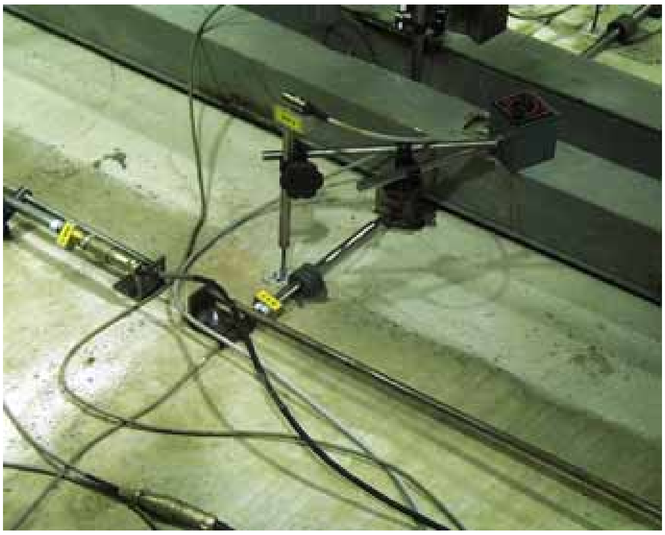

Fig. 14. Device for measuring crack width between slab end and middle beam.

Fig. 15. Arrangements at end beam.

Fig. 16. A general view on test arrangements.

Fig. 17. Gap between soffit of slab 1 and bottom flange of middle beam.

Fig. 18. Good contact between soffit of slab 4 and bottom flange of middle beam.

Fig. 19. Good contact between soffit of slab 5 and bottom flange of middle beam.

Fig. 20. Good contact between soffit of slab 8 and bottom flange of middle beam.

Fig. 21. Service load (P_{a2} = 70 kN). Cracks below soffit of slabs 2 and 3.

Fig. 22. Service load (P_{a2} = 70 kN). Cracks below soffit of slabs 6 and 7.

Fig. 23. P_{a2} = 155 kN. Wide cracks in slab 8.

Fig. 24. Cracks in slab 1 after failure.

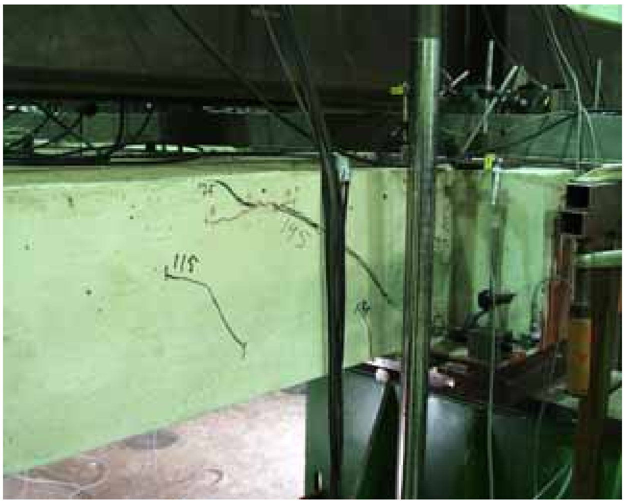

Fig. 25. Cracks in slab 5 after failure.

Fig. 26. Cracks in slab 8 after failure.

Fig. 27. Cracks in slab 8 after failure.

Fig. 28. Cracks in Western tie beam after failure. Slabs 1 and 2.

Fig. 29. Cracks in Western tie beam after failure. Slabs 2 and 3.

Fig. 30. Cracks in Western tie beam after failure. Slabs 3 and 4. The red colour and letter A refer to an initial crack.

Fig. 31. Cracks in Eastern tie beam after failure. Slabs 5 and 6. The red colour and letter A refer to an initial crack.

Fig. 32. Cracks in eastern tie beam after failure. Slabs 5, 6 and 7. The red colour and letter A refer to an initial crack.

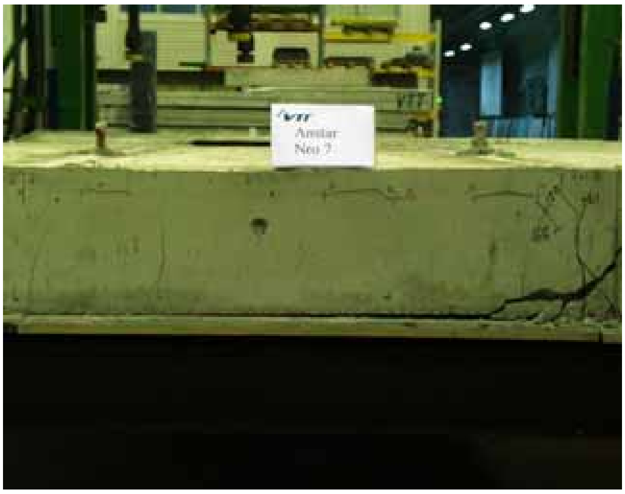

Fig. 33. Cracks in Eastern tie beam after failure. Slabs 6, 7 and 8. The red colour and letter A refer to an initial crack.

Fig. 34. Cracks in Eastern tie beam after failure. Slabs 7 and 8. The red colour and letter A refer to an initial crack.

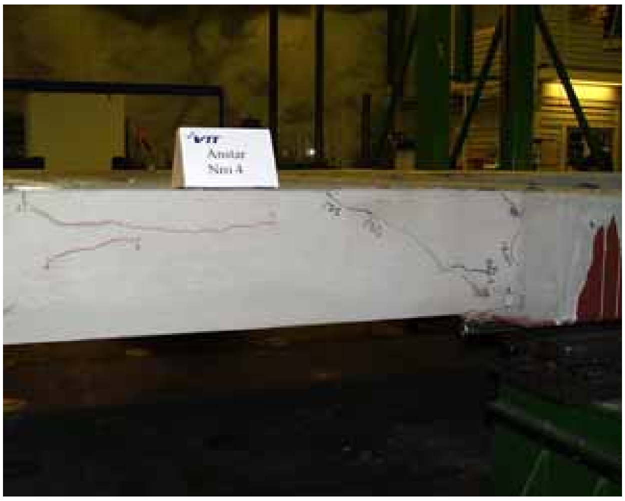

Fig. 35. Cracks in slab 4 after failure. The red colour and letter A refer to an initial crack.

Fig. 36. Cracks in slab 8 after failure.

Fig. 37. Cracks in slab 1 after failure. The red colour and letter A refer to an initial crack.

Fig. 38. Cracks in slab 5 after failure. The red colour and letter A refer to an initial crack.

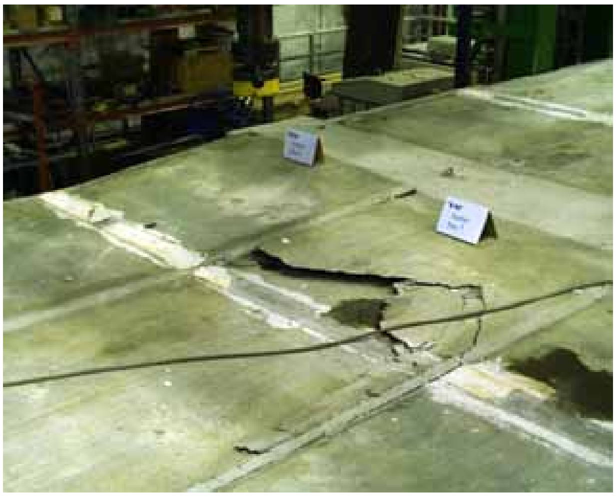

Fig. 39. Failed ends of slabs 7 and 8.

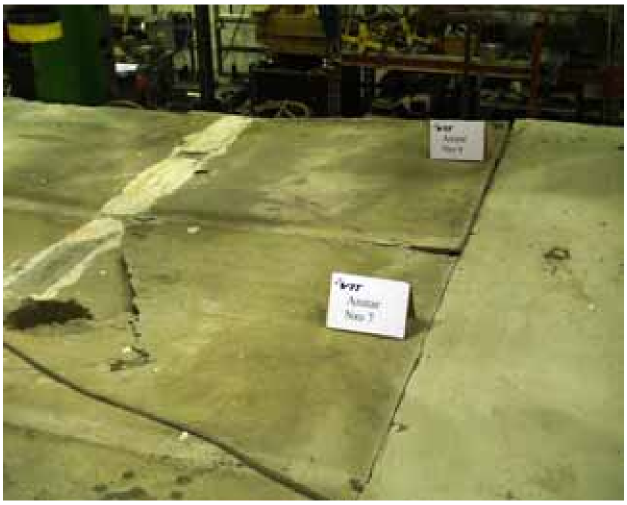

Fig. 40. Failed ends of slabs 7 and 8.

Fig. 41. Longitudinal cracking along joint between slabs 6 and 7.

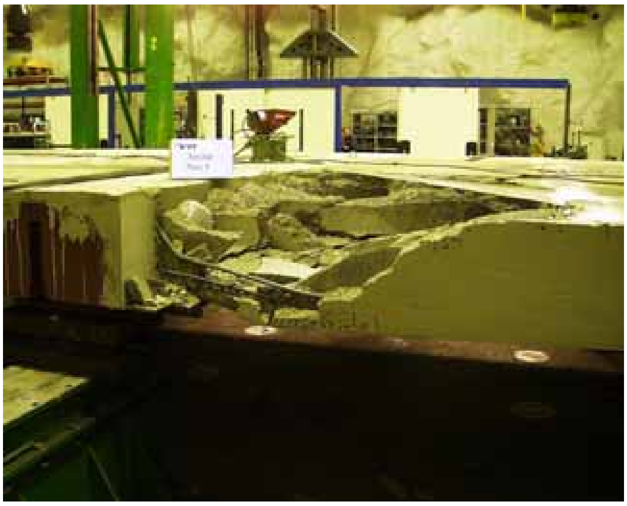

Fig. 42. End of slab 8 after removal of the top flange.

Fig. 43. A-beam after failure. The reinforcing bars have been cut after the test. Note the cement paste which has partly filled the gap between the soffit of slab 1 and the ledge of the beam.

Fig. 44. A-beam after failure. Note the cement paste which has partly filled the gap between the soffit of slab 1 and the ledge of the beam.

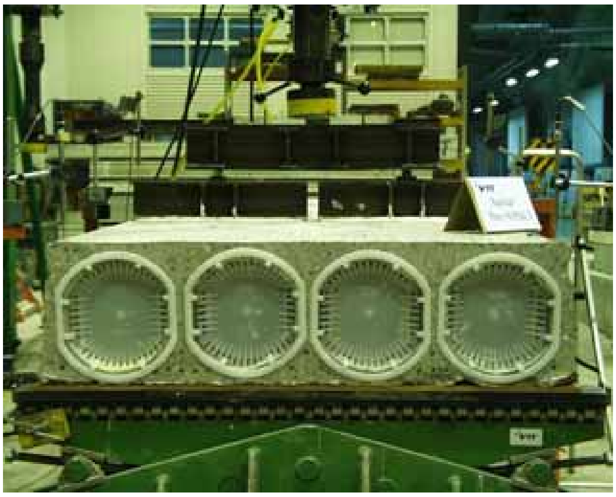

Fig. 45. Arrangements in reference tests.

Fig. 46. Reference test R1. Northern side of slab after failure.

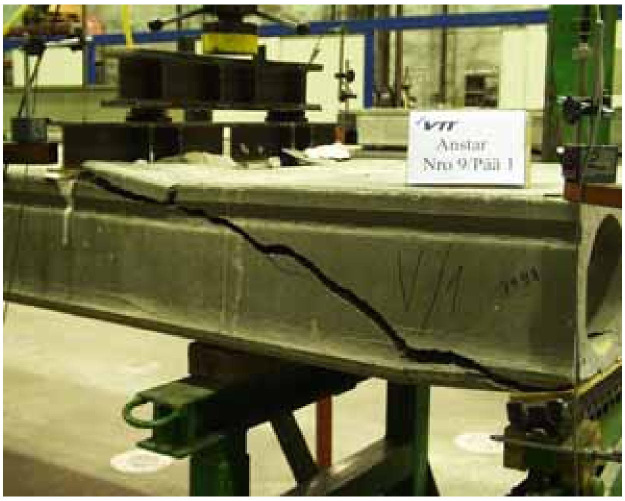

Fig. 47. Reference test R1. Southern side of slab after failure.

Fig. 48. Reference test R2. Northern side of slab after failure.

Fig. 49. Reference test R2. Southern side of slab after failure.

Arrangements and results of 20 full-scale load tests on floors, each made of eight to twelve prestressed hollow core slabs and three beams, are presented. The tests have been carried out by VTT Technical Research Centre of Finland and Tampere University of Technology.

ISBN 978-951-38-7495-7 (URL: http://www.vtt.fi/publications/index.jsp)
ISSN 1459-7683 (URL: http://www.vtt.fi/publications/index.jsp)